Cambridge Monographs on Applied and Computational Mathematics

The Theory of Composites

Graeme W. Milton

CAMBRIDGE

more information - www.cambridge.org/0521781256

This page intentionally left blank

Some of the greatest scientists, including Poisson, Faraday, Maxwell, Rayleigh, and Einstein, have contributed to the theory of composite materials. Mathematically, it is the study of partial differential equations with rapid oscillations in their coefficients. Although extensively studied for more than 100 years, an explosion of ideas in the last four decades (and particularly in the last two decades) has dramatically increased our understanding of the relationship between the properties of the constituent materials, the underlying microstructure of a composite, and the overall effective (electrical, thermal, elastic) moduli that govern the macroscopic behavior. This renaissance has been fueled by the technological need for improving our knowledge base of composites, by the advance of the underlying mathematical theory of homogenization, by the discovery of new variational principles, by the recognition of how important the subject is to solving structural optimization problems, and by the realization of the connection with the mathematical problem of quasiconvexification. This book surveys these exciting developments at the frontier of mathematics and presents many new results.

Graeme W. Milton is a Distinguished Professor in the Mathematics Department at the University of Utah. He has been awarded Sloan and Packard Fellowships and is on the editorial board of the *Archive for Rational Mechanics and Analysis.* He has published more than 70 papers on the theory of composite materials.

CAMBRIDGE MONOGRAPHS ON APPLIED AND COMPUTATIONAL MATHEMATICS

Series Editors
P. G. CIARLET, A. ISERLES, R. V. KOHN, M. H. WRIGHT

6 The Theory of Composites

The *Cambridge Monographs on Applied and Computational Mathematics* reflects the crucial role of mathematical and computational techniques in contemporary science. The series publishes expositions on all aspects of applicable and numerical mathematics, with an emphasis on new developments in this fast-moving area of research.

State-of-the-art methods and algorithms as well as modern mathematical descriptions of physical and mechanical ideas are presented in a manner suited to graduate research students and professionals alike. Sound pedagogical presentation is a prerequisite. It is intended that books in the series will serve to inform a new generation of researchers.

Also in this series:

A Practical Guide to Pseudospectral Methods, *Bengt Fornberg*

Dynamical Systems and Numerical Analysis, *A. M. Stuart and A. R. Humphries*

Level Set Methods and Fast Marching Methods, *J. A. Sethian*

The Numerical Solution of Integral Equations of the Second Kind, *Kendall E. Atkinson*

Orthogonal Rational Functions, *Adhemar Bultheel, Pablo González-Vera, Erik Hendiksen, and Olav Njåstad*

The Theory of Composites

GRAEME W. MILTON
University of Utah

PUBLISHED BY THE PRESS SYNDICATE OF THE UNIVERSITY OF CAMBRIDGE
The Pitt Building, Trumpington Street, Cambridge, United Kingdom

CAMBRIDGE UNIVERSITY PRESS
The Edinburgh Building, Cambridge CB2 2RU, UK
40 West 20th Street, New York, NY 10011-4211, USA
477 Williamstown Road, Port Melbourne, VIC 3207, Australia
Ruiz de Alarcón 13, 28014 Madrid, Spain
Dock House, The Waterfront, Cape Town 8001, South Africa

http://www.cambridge.org

First published in printed format 2002

ISBN 0-511-04092-X eBook (netLibrary)
ISBN 0-521-78125-6 hardback

To John, Winsome, and John

Contents

List of figures **xix**

Preface **xxiii**
References xxvi

1 Introduction **1**
1.1 What are composites, and why study them? 1
1.2 What makes composites useful? 2
1.3 The effective tensors of composites 5
1.4 Homogenization from an intuitive viewpoint 7
1.5 Periodic homogenization 8
1.6 Homogenization in random media 11
1.7 Homogenization in the settings of G-, H-, and Γ-convergence 12
References 14

2 Some equations of interest and numerical approaches to solving them **19**
2.1 The conductivity and related equations 19
2.2 Magnetotransport and convection enhanced diffusion 21
2.3 The elasticity equations 22
2.4 Thermoelectric, piezoelectric, and similar coupled equations 28
2.5 Thermoelasticity and poroelasticity 30
2.6 Pyroelectric equations and their relation to conductivity and magnetotransport equations in fibrous composites 33
2.7 The equivalence between elasticity in fibrous composites and two-dimensional piezoelectricity and thermoelasticity 35
2.8 Numerical methods for finding effective tensors 38
References 40

Sections or chapters marked with a dagger (†) can be skipped on a first reading of the book. They contain material that is not central to the book, or they include more advanced or more technical subject matter. However, they also sometimes address topics that are at the forefront of current research.

3	**Duality transformations in two-dimensional media**	**47**
3.1	Duality transformations for conductivity	47
3.2	Phase interchange identities for two-phase media	49
3.3	The conductivity of two-dimensional polycrystals	50
3.4	Duality transformations for pyroelectricity	51
3.5	Duality transformations for elasticity	51
3.6	Duality transformations for other elastic media	53
3.7	The effective shear modulus of incompressible two-dimensional polycrystals and symmetric materials	55
	References	57
4	**Translations and equivalent media**	**59**
4.1	Translations applied to conductivity	59
4.2	A formula for the Hall coefficient in two-dimensional polycrystals	60
4.3	A formula for the Hall coefficient in two-phase, two-dimensional media†	61
4.4	Inhomogeneous translations for three-dimensional conductivity	65
4.5	Translations for elasticity	66
4.6	A proof that the Young's modulus of a metal plate with holes does not depend on the Poisson's ratio of the metal	67
4.7	The elastic moduli of certain two-dimensional polycrystals and symmetric materials	69
	References	70
5	**Some microstructure-independent exact relations**	**75**
5.1	The uniform field argument	75
5.2	The bulk modulus of polycrystals with cubic symmetry	76
5.3	The elastic moduli of a composite with a constant shear modulus	77
5.4	The thermal expansion tensor and constant of specific heat in a composite of two isotropic phases	79
5.5	The extension to nonlinear thermal expansion	81
5.6	The thermal expansion tensor and specific heat in composites of two anisotropic phases	82
5.7	Exact thermoelastic relations for polycrystals	83
5.8	The effective poroelastic moduli of two-phase media	84
5.9	The elastic moduli of two-phase fibrous composites	86
5.10	Exact relations for pyroelectric, conductivity, and magnetotransport equations	87
5.11	The bulk modulus of a suspension of elastic particles in a fluid	88
	References	89
6	**Exact relations for coupled equations**	**93**
6.1	The covariance property of the effective tensor	93
6.2	The reduction to uncoupled equations for two-phase composites with isotropic phases	95
6.3	Translations for coupled equations	97
6.4	Elasticity as a special case of coupled field equations	98
6.5	Equivalent coupled field problems in two dimensions	101

6.6 The two-dimensional equations as a system of first-order partial differential equations 103
6.7 The covariance property of the fundamental matrix 104
6.8 Linking special classes of antiplane and planar elasticity problems 105
6.9 Expressing the fields in each phase in terms of analytic functions† 106
References 110

7 Assemblages of spheres, ellipsoids, and other neutral inclusions 113
7.1 The coated sphere assemblage 113
7.2 Multicoated sphere assemblages 117
7.3 A phase interchange identity and inequality 118
7.4 Assemblages of spheres with varying radial and tangential conductivity 120
7.5 The conductivity of Schulgasser's sphere assemblage 121
7.6 The conductivity of an assemblage of spheres with an isotropic core and polycrystalline coating 123
7.7 Assemblages of ellipsoids and their associated Ricatti equations† 124
7.8 The conductivity of an assemblage of coated ellipsoids† 127
7.9 A solution of the elasticity equations in the coated ellipsoid assemblage† 130
7.10 Expressions for the depolarization factors† 132
7.11 Neutral coated inclusions 134
References 139

8 Tricks for generating other exactly solvable microgeometries 143
8.1 Modifying the material moduli so the field is not disturbed 143
8.2 Assemblages of coated spheres and coated ellipsoids with anisotropic cores 144
8.3 Making an affine coordinate transformation 145
8.4 The conductivity of an assemblage of coated ellipsoids with an anisotropic core and coating 148
8.5 Making a curvilinear coordinate transformation† 149
8.6 Quasiconformal mappings 152
8.7 Generating microgeometries from fields 153
References 155

9 Laminate materials 159
9.1 The history of laminates and why they are important 159
9.2 Elementary lamination formulas 159
9.3 Lamination formulas when the direction of lamination is arbitrary 164
9.4 Tartar's lamination formula for two-phase simple and coated laminates 165
9.5 Lamination formulas for elasticity, thermoelasticity, thermoelectricity, and piezoelectricity 167
9.6 The lamination formula for a coated laminate with anisotropic coating and anisotropic core 171
9.7 Reference transformations 172
9.8 Explicit formulas for the conductivity and elasticity tensors of a coated laminate 173
9.9 Ordinary differential laminates† 175
9.10 Partial differential laminates† 177
References 181

10 Approximations and asymptotic formulas 185
10.1 Polarizability of a dielectric inclusion 185
10.2 Dielectric constant of a dilute suspension of inclusions to the first order in the volume fraction 188
10.3 Dielectric constant of a suspension of well-separated spheres to the second order in the volume fraction 189
10.4 The Maxwell approximation formula 192
10.5 The effective medium approximation for the dielectric constant of an aggregate with spherical grains 195
10.6 Average field approximations† 198
10.7 The differential scheme for the effective conductivity of a suspension of spheres 201
10.8 The effective medium approximation as the attractor of a differential scheme 203
10.9 Approximation formulas for effective elastic moduli 204
10.10 Asymptotic approximation formulas 207
10.11 Critical exponents and universality 211
References 213

11 Wave propagation in the quasistatic limit 221
11.1 Electromagnetic wave propagation in the quasistatic limit 222
11.2 Electromagnetic signals can propagate faster in a composite than in the constituent phases 228
11.3 Elastic wave propagation in the quasistatic limit 230
11.4 The correspondence principle and the attenuation of sound in a bubbly fluid 233
11.5 Transformation to real equations 234
11.6 Correspondence with thermoelectricity in two dimensions 237
11.7 Resonance and localized resonance in composites† 238
References 242

12 Reformulating the problem of finding effective tensors 245
12.1 Resolving a periodic field into its three component fields: The Γ-operators 245
12.2 A wider class of partial differential equations with associated effective tensors† 248
12.3 A related Γ-operator 250
12.4 The equation satisfied by the polarization field 251
12.5 The effective tensor of dilute suspensions of aligned ellipsoids 252
12.6 Expressions for the action of the Γ-operators in real space 257
12.7 A framework for defining effective tensors in a more general context 260
12.8 Various solutions for the fields and effective tensor 261
12.9 The duality principle 262
12.10 The effective tensor of the adjoint equation 263
12.11 Magnetotransport and its equivalence to thermoelectricity in two dimensions 264
References 267

13 Variational principles and inequalities **271**
13.1 Classical variational principles and inequalities 271
13.2 Monotonicity of the effective tensor 274
13.3 Null Lagrangians 274
13.4 Variational principles for problems with a complex or other non-self-adjoint tensor 276
13.5 Hashin-Shtrikman variational principles and inequalities 278
13.6 Relation between the Hashin-Shtrikman and classical variational inequalities† 281
13.7 Variational inequalities for nonlinear media 282
References 286

14 Series expansions for the fields and effective tensors **291**
14.1 Expanding the formulas for the effective tensors and fields in power series 291
14.2 The series expansion in a composite to second order 292
14.3 Thermoelastic composites for which the third and higher order terms in the expansion vanish 294
14.4 A large class of exactly solvable materials with complex moduli† 295
14.5 Reducing the dimensionality of the problem† 297
14.6 Convergence of the expansions and the existence and uniqueness of the fields and effective tensors 298
14.7 Convergence when $\boldsymbol{L}$ is not self-adjoint† 300
14.8 Extending the domain of convergence† 301
14.9 A series with a faster convergence rate 302
14.10 A related series that converges quickly 304
14.11 Numerical computation of the fields and effective tensor using series expansions 306
References 309

15 Correlation functions and how they enter series expansions† **313**
15.1 Expressing the third-order term of the series expansion in terms of correlation functions 313
15.2 The terms in the series expansion for random media 315
15.3 Correlation functions for penetrable spheres 319
15.4 Correlation functions for cell materials 320
15.5 Reduced correlation functions 323
15.6 Expansions for two-phase random composites with geometric isotropy 327
15.7 Series expansions for cell materials with geometric isotropy 333
References 335

16 Other perturbation solutions **341**
16.1 Effect of a small variation in the material moduli 341
16.2 Application to weakly coupled equations of thermoelectricity or piezoelectricity 342
16.3 Application to computing the effective Hall coefficient 344
16.4 The variance of the electric field in a two-phase conducting composite 344
16.5 Bounds on the conductivity tensor of a composite of two isotropic phases 346
16.6 The change in the effective tensor due to a shift in the phase boundary† 347

16.7 Perturbing the lamination directions in a multiple-rank laminate† 351
References 352

17 The general theory of exact relations and links between effective tensors 355
17.1 Links between effective tensors as exact relations: The idea of embedding 355
17.2 Necessary conditions for an exact relation 357
17.3 Sufficient conditions for an exact relation 359
17.4 An exact formula for the shear modulus of certain three-dimensional polycrystals 361
17.5 More exact relations for coupled equations† 362
17.6 Exact relations with limited statistical information 363
17.7 Additional necessary conditions for an exact relation† 365
References 367

18 Analytic properties 369
18.1 Analyticity of the effective dielectric constant of two-phase media 369
18.2 Analyticity of the effective tensor for problems involving many eigenvalues 370
18.3 Integral representations for the effective tensor for problems involving two eigenvalues 375
18.4 The correspondence between energy functions and microgeometries 381
18.5 The correspondence between effective conductivity functions and microgeometries in two dimensions† 383
18.6 Integral representations for problems involving more than two eigenvalues: The trajectory method 387
18.7 The lack of uniqueness in the choice of integral kernel: Constraints on the measure† 389
18.8 Integral representations for a broader class of composite problems† 391
References 391

19 Y-tensors 397
19.1 The Y-tensor in two-phase composites 397
19.2 The Y-tensor in multiphase composites 399
19.3 A formula for the effective thermoelastic tensor in terms of the elasticity Y-tensor 403
19.4 The Hilbert space setting for the Y-tensor problem† 406
19.5 The Y-tensor polarization problem† 408
19.6 Variational inequalities and principles for Y-tensors† 409
References 411

20 Y-tensors and effective tensors in electrical circuits† 413
20.1 The incidence matrix and the fields of potential drops and currents 413
20.2 The subdivision of bonds in an electrical circuit 415
20.3 The Y-tensor of the electrical circuit 417
20.4 The effective tensor of the passive network 418
20.5 The interpretation of the subspace $\mathcal{U}^{(1)}$ 419
20.6 The relation between the effective tensor and the Y-tensor in an electrical circuit 421
References 423

21 Bounds on the properties of composites 425
21.1 Why are bounds useful? 425
21.2 What are bounds? 426
21.3 The role of bounds in structural optimization: A model problem 429
References 433

22 Classical variational principle bounds 437
22.1 Multiphase conducting composites attaining energy bounds 437
22.2 Optimal bounds on the conductivity of isotropic polycrystals 439
22.3 Optimal bounds on the bulk modulus of isotropic polycrystals 441
22.4 The complete characterization of the set $G_f U e_0$ for n-phase composites and polycrystals 444
22.5 The G-closure in two dimensions of an arbitrary set of conducting materials 446
22.6 Bounds on complex effective tensors† 450
References 452

23 Bounds from the Hashin-Shtrikman variational inequalities 457
23.1 Bounds on the effective conductivity of an isotropic composite of n isotropic phases 457
23.2 Optimal bounds on the effective conductivity of an anisotropic composite of two isotropic phases 461
23.3 Bounds for two-phase, well-ordered materials 462
23.4 Bounds on the energy that involve only the volume fractions 465
23.5 Bounds on the effective tensor that involve only the volume fractions 468
23.6 Bounds for two-phase composites with non-well-ordered tensors† 474
23.7 Bounding the complex effective moduli of an isotropic composite of two isotropic phases† 476
23.8 Using quasiconformal mappings to obtain bounds 480
23.9 Optimal two-dimensional microgeometries: Reduction to a Dirichlet problem† 481
23.10 Bounds for cell polycrystals 487
References 490

24 Bounds using the compensated compactness or translation method 499
24.1 The translation bound and comparison bound 499
24.2 Upper bounds on the bulk modulus of two-phase composites and polycrystals in two dimensions 500
24.3 Allowing quasiconvex translations 503
24.4 A lower bound on the effective bulk modulus of a three-dimensional, two-phase composite 504
24.5 Using the idea of embedding to extend the translation method 505
24.6 Bounds on the conductivity tensor of a composite of two isotropic phases 506
24.7 The translation bounds as a corollary of the comparison bounds† 509
24.8 Embedding in a higher order tensorial problem: A lower bound on the conductivity tensor of a polycrystal 510
24.9 A geometric characterization of translations† 512
24.10 Translation bounds on the Y-tensor 516

24.11 Deriving the trace bounds† 518
24.12 Mixed bounds 519
24.13 Volume fraction independent bounds on the conductivity of a mixture of two isotropic phases 520
24.14 Bounds correlating different effective tensors 522
References 525

25 Choosing the translations and finding microgeometries that attain the bounds† 529
25.1 Other derivations of the translation bounds and their extension to nonlinear problems 529
25.2 Extremal translations 532
25.3 Attainability criteria for the comparison bounds 535
25.4 Isotropic polycrystals with minimum conductivity constructed from a fully anisotropic crystal 537
25.5 Attainability criteria for the translation bounds 541
25.6 Attainability criteria for the Hashin-Shtrikman-Hill bounds on the conductivity and bulk modulus 542
25.7 A general procedure for finding translations that generate optimal bounds on sums of energies 544
25.8 Translations for three-dimensional elasticity 547
References 550

26 Bounds incorporating three-point correlation functions† 553
26.1 A brief history of bounds incorporating correlation functions 553
26.2 Three-point bounds on the conductivity of a two-phase mixture 554
26.3 Three-point bounds on the elastic moduli of a two-phase mixture 557
26.4 Correlation function independent elasticity bounds: Improving the Hashin-Shtrikman-Hill-Walpole bounds 558
26.5 Using the translation method to improve the third-order bounds 560
26.6 Third-order bounds from cross-property bounds 561
26.7 General third-order bounds for a two-phase composite 562
26.8 Third-order bounds for two-phase composites with geometrical isotropy 564
References 564

27 Bounds using the analytic method 569
27.1 A brief history of bounds derived using the analytic method 569
27.2 A topological classification of rational conductivity functions 571
27.3 Bounds that incorporate a sequence of series expansion coefficients 573
27.4 Relation between the bounds and Padé approximants 578
27.5 Bounds incorporating known real or complex values of the function and series expansion coefficients 579
27.6 Numerical computation of the bounds† 583
27.7 Bounds for two-dimensional isotropic composites† 585
27.8 Bounds for symmetric materials† 588
27.9 Reducing the set of independent bounds 589

27.10 Proving elementary bounds using the method of variation of poles and residues 590
27.11 Proving the bounds using the method of variation of poles and zeros 592
References 596

28 Fractional linear transformations as a tool for generating bounds† 603
28.1 Eliminating the constraints imposed by known series expansion coefficients 603
28.2 Eliminating the constraints imposed by known real values of the function 607
28.3 An alternative approach that treats the components on a symmetric basis 610
28.4 The extension of the fractional linear transformations to matrix-valued analytic functions 614
References 617

29 The field equation recursion method† 619
29.1 Associations between operations on analytic functions and operations on subspace collections 619
29.2 Hints of a deeper connection between analytic functions and subspace collections 624
29.3 The field equation recursion method for two-phase composites 626
29.4 Representing the operators as infinite-dimensional matrices 631
29.5 The field equation recursion method for multiphase composites with isotropic components 633
29.6 Bounds on the energy function of a three-phase conducting composite 638
References 641

30 Properties of the G-closure and extremal families of composites 643
30.1 An equivalence between G-closure problems with and without prescribed volume fractions 643
30.2 Stability under lamination and the convexity properties of the G-closure 645
30.3 Characterizing the G-closure through minimums of sums of energies and complementary energies 647
30.4 Characterization of the G-closure by single energy minimizations 650
30.5 Extremal families of composites for elasticity: Proving that any positive-definite tensor can be realized as the effective elasticity tensor of a composite† 652
30.6 An extremal family of unimode materials for two-dimensional elasticity† 658
30.7 An extremal family of bimode materials for two-dimensional elasticity† 663
30.8 Extremal materials for three-dimensional elasticity 666
References 667

31 The bounding of effective moduli as a quasiconvexification problem 671
31.1 Quasiconvexification problems in elasticity theory 671
31.2 The independence of the quasiconvexified function on the shape and size of the region Ω 674
31.3 Replacing the affine boundary conditions with periodic boundary conditions 675

31.4 The equivalence of bounding the energy of multiphase linear composites and quasiconvexification 677
31.5 The link between the lamination closure and Λ-convexification 679
31.6 Quasiconvex hulls and rank-1 convex hulls 681
31.7 Laminate fields built from rank-1 incompatible matrices 683
31.8 Example of a rank-1 function that is not quasiconvex† 684
31.9 A composite with an elasticity tensor that cannot be mimicked by a multiple-rank laminate material† 690
References 695

Author index **699**

Subject index **711**

List of figures

1.1	A negative Poisson's ratio microstructure	3
1.2	A porous structure with a negative thermal expansion coefficient	4
1.3	A way to think about the function $\boldsymbol{\sigma}_\epsilon(\boldsymbol{x}) = \boldsymbol{\sigma}(\boldsymbol{x}, \boldsymbol{x}/\epsilon)$	9
3.1	Two-dimensional structures with conductivity $\sigma_* = \sqrt{\sigma_1\sigma_2}$	50
4.1	The idea of translation	60
4.2	Symmetrizing the conductivity tensor	63
4.3	Poisson's ratio of plates containing holes	68
5.1	Adjusting temperature and pressure so a bimetal strip does not bend	79
7.1	The coated sphere as a neutral inclusion	114
7.2	The Hashin coated sphere assemblage	114
7.3	The doubly coated sphere assemblage for a three-component material	118
7.4	The prototype sphere in the Schulgasser sphere assemblage	122
7.5	The coated elliptical cylinder assemblage	125
7.6	Inclusions that can and cannot be made neutral	136
7.7	Neutral inclusions with perfect interfaces and an insulating core	138
8.1	The stretched confocal coated ellipsoid assemblage	149
9.1	A three-dimensional, two-phase laminate	160
9.2	A two-dimensional, two-phase, second-rank laminate	160
9.3	Maxwell's third-rank coated laminate	166
9.4	Tree structure representing a finite-rank laminate	178
9.5	Approximation to a partial differential laminate	179
10.1	A material realizing the effective medium approximation	197
10.2	Conductivity of a fluid-filled porous medium of fused glass beads	202
10.3	Poisson's ratio of a checkerboard with dissimilar phases	208
10.4	Treating an assemblage of inclusions as a resistor network	209
11.1	Equivalence of lattices of coated cylinders and solid cylinders	241

12.1 Partitioning of space used to compute the action of $\mathbf{\Gamma}$ 258

16.1 Perturbation of the position of an interface 348

18.1 Second-rank laminates that mimic the conductivity function 383
18.2 The eigenvectors of $\boldsymbol{\sigma}_*$ can rotate as σ_1/σ_2 is varied 384

20.1 The Wheatstone bridge circuit 414

21.1 Values of the average current in a two-dimensional polycrystal 427
21.2 A model optimization problem 430

22.1 A polycrystal with the largest isotropic effective conductivity 441
22.2 Laminates in which either the strain or stress field equals $\boldsymbol{I}$ 443
22.3 Values of the average current in a multiphase composite 445
22.4 Construction of GU for two-dimensional conductivity 448

23.1 A three-phase assemblage attaining the Hashin-Shtrikman bounds 459
23.2 The stiffest isotropic two-phase material 472
23.3 Bounds on the complex bulk modulus 479
23.4 Solving a Dirichlet problem to find optimal structures 481
23.5 The periodic Vigdergauz microstructure 486
23.6 Sigmund's structures attaining the Hashin-Shtrikman bounds 486

24.1 Translations as ellipsoids in a cavity 514
24.2 Translations as planes that lie above a cut cylinder 515
24.3 Convexification of the cut cylinder 516

25.1 Ellipsoids corresponding to extremal translations 534

27.1 Bounds on the complex dielectric constant of a two-phase material 570
27.2 Different topological types of rational conductivity functions 573
27.3 Bounds on the conductivity of a cubic array of spheres 576

28.1 Action of the Y-transformation in the complex plane 613

29.1 Bounds on the complex conductivity of a three-phase composite 640

30.1 The characterization of G-closures by energy minimums 650
30.2 The Poisson's ratio of the herringbone laminate and bounds 653
30.3 A simple laminate is a bimode extremal material 655
30.4 A bimode material supporting a compressive stress 655
30.5 A bimode material supporting a shear stress 656
30.6 A unimode material approximating to the oblique box laminate 659
30.7 A unimode material approximating the herringbone laminate 661
30.8 A bimode material obtained by successive lamination 664
30.9 The diamond lattice of linkages 667

31.1 The relation between the various convexifications of a function 674
31.2 Why shape memory materials remember their shape 682

31.3 Building a field from gradients with no rank-1 connections 685
31.4 The infinite-rank cyclic laminate field corresponding to the previous figure 685
31.5 A field $\nabla \boldsymbol{u}$ that cannot be mimicked by a laminate field 687
31.6 Values of $\langle \nabla \boldsymbol{u} \rangle$ for a laminate field taking the seven specified values 688

Preface

This book is intended to be a self-contained introduction to the theory of composite materials, encompassing the electrical, thermal, magnetic, thermoelectric, mechanical, piezoelectric, poroelastic, and electromagnetic properties. It is intended not only for mathematicians, but also for physicists, geophysicists, material scientists, and electrical and mechanical engineers. Consequently, the results are not stated in the format of lemmas, propositions, and theorems. Instead, the focus is on explaining the central ideas and providing proofs that avoid unnecessary technicalities. The book is suitable as a textbook in an advanced-level graduate course, and also as a reference book for researchers working on composites or in related areas.

The field of composite materials is enormous. That's good, because it means that there are many avenues of research to explore. The drawback is that a single book cannot adequately cover the whole field. The main focus of this book is on the relation between the microstructure of composites and the effective moduli that govern their behavior. This choice reflects my research interests, and is also the starting point for many other avenues of research on composites. Topics not treated here include fatigue, fracture, and plastic yielding in composites, which are major factors in determining their strength (Sih and Tamuzs 1979; Sih and Chen 1981; Sih and Skudra 1985; Talreja 1994; Hull and Clyne 1996; Nemat-Nasser and Hori 1999); the propagation, localization, and scattering of waves in composites at wavelengths comparable to or smaller than the size of the inhomogeneities (Sheng 1990, 1995; Chew 1995) [of particular recent interest is the study of photonic band gap materials (Joannopoulos, Meade, and Winn 1995), which may lead to the development of new lasers and could be important in photonic circuitry]; flow in porous media, which has obvious applications to the management of oil and water reservoirs and to understanding the seepage of waste fluids (Scheidegger 1974; Sanchez-Palencia 1980); geometrical questions such as the microstructures of rocks (Pittman 1984) and dense random packings of hard spheres (Cargill III 1984; Torquato, Truskett, and Debenedetti 2000); and the many aspects of percolation theory (Kesten 1982; Stauffer and Aharony 1992; Grimmett 1999).

Other important topics, such as homogenization theory (discussed in chapter 1 on page 1), numerical methods for solving for the fields in composites, and hence for determining their effective moduli (discussed in section 2.8 on page 38), the nonlinear theory of composites (discussed in section 13.7 on page 282), structural optimization (discussed in section 21.3 on page 429), and quasiconvexification (discussed in chapter 31 on page 671) are not treated in the depth that they deserve. The reader is encouraged to refer to the references cited in those sections to gain a more complete understanding of these subjects.

The Contents gives a good indication of what topics the book covers. Briefly, the first chapter discusses the motivation for studying composites and outlines homogenization the-

ory from various viewpoints. The second chapter introduces some of the different equations considered in the book, and numerical methods for solving these equations are mentioned. Chapters 3 to 9 cover exact results for effective moduli, relations between (seemingly unconnected) effective moduli and microstructures for which at least some of the effective moduli can be exactly determined (such as coated sphere assemblages, laminates, and their generalizations). Chapter 10 discusses some of the many approximations that have been developed for estimating effective moduli and the asymptotic formulas that are valid in certain high-contrast materials. Chapter 11 shows how wave propagation in composites, at wavelengths much larger than the microstructure, can be treated by allowing the moduli, fields, and effective moduli to be complex, or alternatively by keeping everything real and doubling the size of the system of equations being considered.

Chapters 12 to 18 cover the general theory concerning effective tensors: the formulation as a problem in Hilbert space; various variational principles; convergent series expansions for the effective tensor in powers of the variation in the local tensor field; how (for random composites) the terms in the series expansion can be expressed in terms of correlation functions; other perturbation solutions for the effective tensor; the general theory of exact relations in composites; and, finally, the analytic properties of the effective tensor as a function of the tensors of the constituent tensors. These chapters (due to their generality) are harder to read than those in the first part of the book. The first part of chapter 12 is essential reading since it introduces some of the basic notation used in subsequent chapters. Also, chapter 13, on variational principles, should certainly be read, and will strengthen the reader's understanding of the material in chapter 12. Chapters 19 and 20 are optional. They introduce the Y-tensor, which in a multicomponent composite gives information about the average fields in each phase, and which in electrical circuits determines the response of the circuit. The theory of Y-tensors parallels that of effective tensors, and many bounds on effective tensors take a simpler form when expressed in terms of the Y-tensor.

Chapter 21 introduces the problem of bounding effective tensors and discusses its importance in optimal design problems. Chapters 22 to 26 describe variational methods for bounding effective tensors, including the Hashin-Shtrikman approach, the translation method (or compensated compactness) approach, and those approaches based on classical variational principles. Chapters 27 and 28 show how the analyticity properties of the effective tensor lead to large families of bounds, which usually are the simplest rational approximants of the function compatible with what is known about it. Chapter 29 outlines the parallel between operations on analytic functions and operations on subspace collections, and shows how this leads to bounds for multicomponent composites.

Chapter 30 discusses general properties and characterizations of the set of effective tensors obtained as the microstructure is varied over all configurations. The set of elastic tensors that can be made by mixing a sufficiently compliant isotropic material with a sufficiently stiff isotropic material is shown to coincide with the set of all positive-definite fourth-order tensors satisfying the symmetries of elasticity tensors. Chapter 31 shows how problems of bounding effective tensors are equivalent to quasiconvexification problems, and vice versa. Finally, by extending a famous example of Šverák, an example is given of a seven-phase composite whose effective elastic tensor cannot be mimicked by any (multiple-rank) laminate material.

There are many other related books that present the theory of composites from other perspectives. Those that are closest in their scope include the following. The report of Hashin (1972), the classic book of Christensen (1979), the books of Agarwal and Broutman (1990), Matthews and Rawlings (1994), and Hull and Clyne (1996), and the recent book of Nemat-Nasser and Hori (1999) cover the subject with an emphasis on the mechanical properties of

composites. The book of Zhikov, Kozlov, and Oleinik (1994) covers the subject from a rigorous mathematical perspective. The volume edited by Cherkaev and Kohn (1997) contains translations of many significant mathematical papers, which previously were only available in French or Russian. The books of Allaire (2001) and Cherkaev (2000) cover the subject with an emphasis on structural optimization. The book of Ball and James (2001) surveys many problems where microstructure plays an influential role in determining macroscopic behavior. The book of Beran (1968) covers the statistical theory, using an approach that is different from the one presented in chapter 15 on page 313. The book of Torquato (2001) covers many topics with an emphasis on the statistical aspects of composites. There are also many review papers, including Willis (1981), Hashin (1983), Torquato (1991), Bergman and Stroud (1992), and Markov (2000). Additionally, there are many books on homogenization theory and on quasiconvexification, which are referenced in chapters 1 on page 1 and 31 on page 671.

It is a great pleasure to thank those colleagues and friends who contributed in many ways to this book. I would like to thank Ross McPhedran, who introduced me to the subject of composite materials when I was an undergraduate at Sydney University. I am greatly indebted to Michael Fisher for his critical comments during my Ph.D., which have had a lasting impact. I am grateful to George Papanicolaou for encouraging me to write this book. When I started writing, more than 13 years ago, it was just meant to be one-third of a book and certainly was not intended to be more than 700 pages in length. But I found it difficult to resist the temptation to include topics that seemed to tie in closely with what I had already written, and to include new developments such as novel families of neutral inclusions and the associated exactly solvable assemblages (section 7.11 on page 134), the theory of partial differential laminates (section 9.10 on page 177), the general theory of exact relations in composites (chapter 17 on page 355), the optimal microstructures of Sigmund attaining the Hashin-Shtrikman bounds (section 23.9 on page 481), an approach for finding suitable quasiconvex functions for obtaining bounds (section 25.7 on page 544), and a composite with an effective tensor that cannot be mimicked by laminates (section 31.9 on page 690). John Willis and François Murat are especially thanked for their help in arranging my visits to the University of Bath, and to the Université Paris VI, where major portions of the text were written, and where (in Paris) the counterexample of 31.9 on page 690 was discovered. I am grateful to numerous people for their constructive comments on sections of the text, including Leonid Berlyand, Andrei Cherkaev, Gilles Francfort, Ken Golden, Zvi Hashin, Robert Kohn, Mordehai Milgrom, Vincenzo Nesi, Sergey Serkov, and Luc Tartar. I am thankful to Eleen Collins for typing most of the references into BIBTEX. I am most indebted to Nelson Beebe for the absolutely terrific job he did in developing the software for the book style and referencing style, for automating the conversion of references to BIBTEX, for solving many technical problems, and for spotting many errors. I am also grateful to Thilagavathi Murugesan for her substantial help in checking most of the equations, to Sergei Serkov for scanning many of the figures, and to Elise Oranges for the great copyediting job she did. Additionally, I wish to thank Bob Kohn for suggesting Cambridge University Press, and David Tranah and Alan Harvey at Cambridge University Press for their continued interest and helpful suggestions. I am grateful to my partner, John Patton, and my parents, John and Winsome Milton, for their continued support throughout the whole work. It is a pleasure to dedicate this book to them.

I am exceedingly thankful to the Packard Foundation for support from a Packard fellowship between 1988 and 1993. This generous award allowed me to spend more time on research and on writing this book. I am also pleased to thank the National Science Foundation for continued support, through grants DMS-9402763, DMS-9501025, DMS-9629692,

and DMS-9803748, and the Centre National de la Recherche Scientifique for supporting my visit to Université Pierre et Marie Curie in the fall of 1996.

While I hope that the derivations in the book are correct, and that work has been properly referenced, it is inevitable that there are still some errors and omissions. I would be grateful to learn about these. The Web site `http://www.math.utah.edu/books/tcbook` contains a list of known errors in the book, as well as the BIBTEX bibliographic database.

Salt Lake City, Utah *Graeme W. Milton*
October, 2001

References

Agarwal, B. D. and L. J. Broutman 1990. *Analysis and Performance of Fiber Composites* (Second ed.). Society of Plastic Engineers (SPE) Monographs. New York / London / Sydney, Australia: John Wiley and Sons. xviii + 449 pp. ISBN 0-471-51152-8. {*xxiv, xxvi*}

Allaire, G. 2001. *Shape Optimization by the Homogenization Method*. Berlin / Heidelberg / London / etc.: Springer-Verlag. 464 pp. ISBN 0-387-95298-5. {*xxv, xxvi, 426, 431, 433*}

Ball, J. M. and R. D. James 2001. *From Microscales to Macroscales in Materials*. In preparation. {*xxv, xxvi, 672, 695*}

Beran, M. J. 1968. *Statistical Continuum Theories*. New York: Interscience Publishers. xv + 424 pp. ISBN 0-470-06861-2. {*xxv, xxvi, 11, 15, 291, 309, 489, 491*}

Bergman, D. J. and D. Stroud 1992. Physical properties of macroscopically inhomogeneous media. In H. Ehrenreich and D. Turnbull (eds.), *Solid State Physics: Advances in Research and Applications*, pp. 147–269. New York: Academic Press. ISBN 0-12-607746-0. {*xxv, xxvi*}

Cargill III, G. S. 1984. Radial distribution functions and microgeometry of dense random packings of hard spheres. In D. L. Johnson and P. N. Sen (eds.), *Physics and Chemistry of Porous Media: Papers from a Symposium Held at Schlumberger-Doll Research, Oct. 24–25, 1983*, pp. 20–36. Woodbury, New York: American Institute of Physics. ISBN 0-88318-306-4. {*xxiii, xxvi*}

Cherkaev, A. and R. Kohn (eds.) 1997. *Topics in the Mathematical Modelling of Composite Materials*. Basel, Switzerland: Birkhäuser Verlag. xiv + 317 pp. ISBN 0-8176-3662-5. {*xxv, xxvi*}

Cherkaev, A. V. 2000. *Variational Methods for Structural Optimization*. Berlin / Heidelberg / London / etc.: Springer-Verlag. xxvi + 545 pp. ISBN 0-387-98462-3. {*xxv, xxvi, 352, 353, 426, 434, 666, 668*}

Chew, W. C. 1995. *Waves and Fields in Inhomogeneous Media*. IEEE Press Series on Electromagnetic Waves. Piscataway, New Jersey: IEEE Press. xx + 608 pp. ISBN 0-7803-1116-7. {*xxiii, xxvi*}

Christensen, R. M. 1979. *Mechanics of Composite Materials*. New York: Wiley-Interscience. xiv + 348 pp. ISBN 0-471-05167-5. {*xxiv, xxvi, 233, 243*}

In the chapter references, each entry is followed by a braced list of page numbers in small *italic* type, showing where in the book the entry is cited, or appears in the references.

Grimmett, G. 1999. *Percolation* (Second ed.). Berlin / Heidelberg / London / etc.: Springer-Verlag. xiv + 444 pp. ISBN 3-540-64902-6. {*xxiii, xxvii*}

Hashin, Z. 1972. Theory of fiber reinforced materials. NASA contractor report CR-1974, NASA, Washington, D.C. xv + 690 pp. {*xxiv, xxvii, 247, 268, 272, 287*}

Hashin, Z. 1983. Analysis of composite materials — A survey. *Journal of Applied Mechanics* 50:481–505. {*xxv, xxvii, 7, 16*}

Hull, D. and T. W. Clyne 1996. *An Introduction to Composite Materials* (Second ed.). Cambridge Solid State Science Series. Cambridge, United Kingdom: Cambridge University Press. xvi + 326 pp. ISBN 0-521-38190-8. {*xxiii, xxiv, xxvii*}

Joannopoulos, J. D., R. D. Meade, and J. N. Winn 1995. *Photonic Crystals: Molding the Flow of Light*. Princeton, New Jersey: Princeton University Press. ix + 184 pp. ISBN 0-691-03744-2. {*xxiii, xxvii*}

Kesten, H. 1982. *Percolation Theory for Mathematicians*. Basel, Switzerland: Birkhäuser Verlag. iv + 423 pp. ISBN 3-7643-3107-0. {*xxiii, xxvii*}

Markov, K. Z. 2000. Elementary micromechanics of heterogeneous media. In K. Markov and L. Preziosi (eds.), *Heterogeneous Media: Micromechanics Modeling Methods and Simulations*, Modeling and Simulation in Science, Engineering and Technology, pp. 1–162. Basel, Switzerland: Birkhäuser Verlag. ISBN 0-8176-4083-5. {*xxv, xxvii, 2, 16, 185, 217, 346, 353*}

Matthews, F. L. and R. D. Rawlings 1994. *Composite Materials: Engineering and Science*. London: Chapman and Hall. ix + 470 pp. ISBN 0-412-55960-9. {*xxiv, xxvii, 1, 16*}

Nemat-Nasser, S. and M. Hori 1999. *Micromechanics: Overall Properties of Heterogeneous Materials* (Second ed.). Amsterdam: Elsevier. xxiv + 786 pp. ISBN 0-444-50084-7. {*xxiii, xxiv, xxvii, 7, 17*}

Pittman, E. D. 1984. The pore geometries of reservoir rocks. In D. L. Johnson and P. N. Sen (eds.), *Physics and Chemistry of Porous Media: Papers from a Symposium Held at Schlumberger-Doll Research, Oct. 24–25, 1983*, pp. 1–19. Woodbury, New York: American Institute of Physics. ISBN 0-88318-306-4. {*xxiii, xxvii*}

Sanchez-Palencia, E. 1980. *Non-Homogeneous Media and Vibration Theory*. Berlin / Heidelberg / London / etc.: Springer-Verlag. ix + 398 pp. ISBN 0-540-10000-8. {*xxiii, xxvii, 8, 17, 221, 244*}

Scheidegger, A. E. 1974. *The Physics of Flow Through Porous Media* (Third ed.). Toronto, Canada: University of Toronto Press. xv + 353 pp. ISBN 0-8020-1849-1. {*xxiii, xxvii*}

Sheng, P. (ed.) 1990. *Scattering and Localization of Classical Waves in Random Media*. Singapore / Philadelphia / River Edge, New Jersey: World Scientific Publishing Co. 648 pp. ISBN 9971-50-539-8. {*xxiii, xxvii*}

Sheng, P. 1995. *Introduction to Wave Scattering, Localization, and Mesoscopic Phenomena*. New York: Academic Press. xi + 339 pp. ISBN 0-12-639845-3. {*xxiii, xxvii*}

Sih, G. C. and E. P. Chen 1981. *Cracks in Composite Materials: A Compilation of Stress Solutions for Composite Systems with Cracks*. The Hague, The Netherlands: Martinus Nijhoff Publishers. lxxxi + 538 pp. ISBN 90-247-2559-3. {*xxiii, xxvii*}

Sih, G. C. and A. M. Skudra (eds.) 1985. *Failure Mechanisms of Composites*. Amsterdam: North-Holland Publishing Co. xiii + 441 pp. ISBN 0-444-86879-8. {*xxiii, xxvii*}

Sih, G. C. and V. P. Tamuzs (eds.) 1979. *Fracture of Composite Materials*. Alphen aan den Rijn, The Netherlands: Sijthoff and Noordhoff. xvi + 413 pp. ISBN 90-286-0289-5. {*xxiii, xxviii*}

Stauffer, D. and A. Aharony 1992. *Introduction to Percolation Theory* (Second ed.). London: Taylor and Francis. x + 181 pp. ISBN 0-7484-0027-3. {*xxiii, xxviii*}

Talreja, R. (ed.) 1994. *Damage Mechanisms of Composite Materials*. Amsterdam: Elsevier. ix + 306 pp. ISBN 0-444-88852-7. {*xxiii, xxviii*}

Torquato, S. 1991. Random heterogeneous media: Microstructure and improved bounds on effective properties. *ASME Applied Mechanics Reviews* 44(2):37–76. {*xxv, xxviii, 331, 339, 425, 436, 553, 567*}

Torquato, S. 2001. *Random heterogeneous materials: microstructure and macroscopic properties*. Berlin / Heidelberg / London / etc.: Springer-Verlag. 712 pp. ISBN 0-387-95167-9. {*xxv, xxviii*}

Torquato, S., T. M. Truskett, and P. G. Debenedetti 2000. Is random close packing of spheres well defined? *Physical Review Letters* 84(10):2064–2067. {*xxiii, xxviii*}

Willis, J. R. 1981. Variational and related methods for the overall properties of composites. *Advances in Applied Mechanics* 21:1–78. {*xxv, xxviii, 185, 200, 220, 252, 255, 269, 291, 312*}

Zhikov, V. V., S. M. Kozlov, and O. A. Oleinik 1994. *Homogenization of Differential Operators and Integral Functionals*. Berlin / Heidelberg / London / etc.: Springer-Verlag. xi + 570 pp. ISBN 3-540-54809-2 (Berlin), 0-387-54809-2 (New York). {*xxv, xxviii, 8, 11, 13, 18, 47, 58, 200, 220*}

1

Introduction

1.1. What are composites, and why study them?

Composites are prevalent in both nature and among engineered materials. Common metals are composites. When one breaks a rod of metal the polycrystalline nature becomes evident in the roughness of the surface of the break. The American Museum of Natural History in New York has a wonderful meteorite collection. Some of the polished cross sections through these meteorites clearly show the individual metal crystals. Martensite, which is typical of a shape memory material, has a laminar-type structure comprised of alternating layers of the two variants of martensite. Some rocks, such as sandstone, are aggregates of grains; other rocks, such as granite, are aggregates of crystals. In porous rocks the pores are often filled with a fluid such as salt water or oil. The study of composites in a geological context is important to the oil industry and for the study of earthquakes. Construction materials such as wood and concrete are composites. Bone is a porous composite. Fiberglass and lightweight carbon fiber composites have found applications ranging from the aerospace industry to sports equipment.

Colloidal suspensions, emulsions, foams, slurries, and clays are all examples of composites. Clouds, fog, mist, and rain are composites of air and water. High-altitude clouds are composites of air and ice crystals. Suspensions of volcanic dust in the upper atmosphere are known to significantly perturb temperatures around the earth. Air itself is an inhomogeneous medium with fluctuations in density that cause the twinkling of stars. Sea ice is a composite of ice and brine pockets, and modeling of its properties is important in global climate prediction. Wool and cotton are composites of fiber and air. Ceramics are composites. Solid rocket propellant is a composite of aluminum particles in an oxidizing matrix. Even chocolate chip ice cream is a composite. Basically, composites are materials that have inhomogeneities on length scales that are much larger than the atomic scale (which allows us to use the equations of classical physics at the length scales of the inhomogeneities) but which are essentially (statistically) homogeneous at macroscopic length scales, or least at some intermediate length scales. An alloy, having disorder on the atomic scale, is excluded from consideration (except if it is one of the phases in a larger composite, in which case it is treated as a homogeneous material). The book of Matthews and Rawlings (1994) gives many examples of natural and man-made composites.

Why do we study composites? One obvious answer is their usefulness, which will be discussed in the next section. A second, equally important reason is that what we learn from the field of composites could have far-reaching implications in many fields of science. Significant progress in improving our understanding of how microscopic behavior influences

macroscopic behavior could impact our understanding of turbulence, of phase transitions involving many length scales, of how quantum behavior influences behavior on classical length scales, or, at the more extreme level, of how behavior on the Planck length scale, 10^{-33}cm, influences behavior on the atomic scale, 10^{-8}cm. While that may seem unlikely, it is hard to deny the impact that our understanding of classical physics had on the development of quantum mechanics. Therefore it is conceivable that a better understanding of classical questions involving multiple length scales could have large reverberations. A third compelling reason for studying composites is simply that there are many beautiful mathematical questions begging for answers. The solutions of some questions have already led to the development of new mathematical tools, and one can expect that the solution of the more challenging outstanding questions will open new mathematical frontiers.

The study of composites is a subject with a long history, which has attracted the interest of some of the greatest scientists. For example, Poisson (1826) constructed a theory of induced magnetism in which the body was assumed to be composed of conducting spheres embedded in a nonconducting material. Faraday (1839) proposed a model for dielectric materials that consisted of metallic globules separated by insulating material. Maxwell (1873) solved for the conductivity of a dilute suspension of conducting spheres in a conducting matrix. Rayleigh (1892) found a system of linear equations which, when solved, would give the effective conductivity of nondilute square arrays of cylinders or cubic lattices of spheres. Einstein (1905) calculated the effective shear viscosity of a suspension of rigid spheres in a fluid. The main historical developments are summarized in the articles of Landauer (1978) and Markov (2000).

1.2. What makes composites useful?

What gives composites their utility is that they often combine the attributes of the constituent materials. For example, suppose that one is given two isotropic conducting materials: a metal with high conductivity, and a plastic that is electrically insulating. If one places these two materials in alternating layers in a laminate, one obtains a highly anisotropic composite that has the conducting properties of the metal in directions parallel to the layers and the insulating properties of the plastic normal to the layers. Concrete is cheap and relatively light, but it breaks apart easily under tension. By contrast, steel is strong but expensive and heavy. By pouring the concrete around prestressed metal bars one obtains a composite, namely, reinforced concrete, that is cheap, relatively light, and strong. Wood is an example of a material that is strong in the fiber direction, but the fibers pull apart easily. By alternating layers of wood that are strong in the x_1 direction with layers of wood that are strong in the x_2 direction, one obtains a plywood that is strong in two directions, that is, in the (x_1, x_2)-plane.

By combining a compliant isotropic material that has low bulk and shear moduli with a stiff isotropic material that has high bulk and shear moduli, one can (with a judicious choice of microstructure) produce an elastically isotropic composite that effectively has the bulk modulus of the compliant phase and the shear modulus of the stiff phase. Such low-bulk and high-shear moduli materials are called negative Poisson's ratio materials: A rod of the material will expand laterally when stretched longitudinally. It was long a question of debate as to whether such materials could actually exist. Now their existence has been confirmed both experimentally and theoretically [see, for example, Lakes (1987) and Milton (1992) and references therein, and also section 30.5 on page 652]. A very simple two-dimensional microstructure that expands laterally when stretched longitudinally was designed and fabricated by Larsen, Sigmund, and Bouwstra (1997) and is illustrated in figure 1.1 on the facing page.

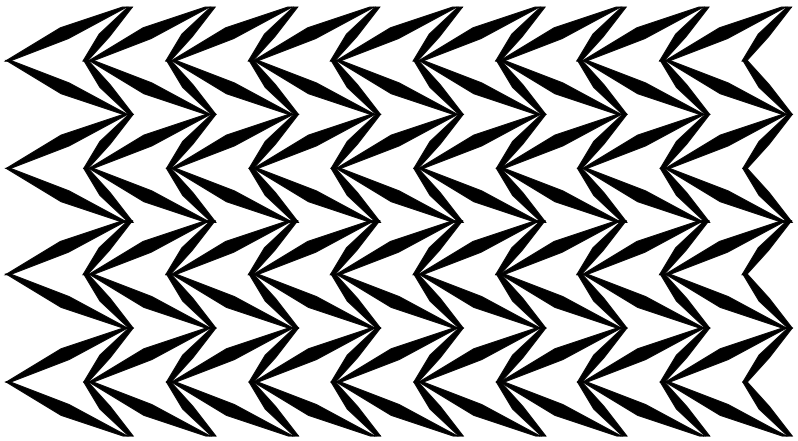

Figure 1.1. The two-dimensional microstructure of Larsen, Sigmund, and Bouwstra (1997), which will expand laterally when stretched longitudinally. Here the black region is relatively stiff and is surrounded by a void or very compliant material.

Sometimes the properties of a composite can be strikingly different from the properties of the constituent materials. To see this you can do the following experiment at home. Take a wine glass filled with air and strike it on the top (but not too hard) with a knife. It rings clearly. The same is true when it is filled with water. But add powdered Alka-Seltzer (or anything else that makes lots of bubbles) to the water and one just hears a thud. The acoustic properties of the bubbly fluid are quite different from those of either the air or the water. One application of this is to use a screen of bubbles to mask the engine or propeller noise of a submarine; as the oscillatory pressure in the sound wave compresses and decompresses each bubble, the water near each bubble is sheared, which dissipates the energy of the sound. The shear viscosity of the water is converted to the bulk viscosity of the bubbly fluid (Taylor 1954; see also section 11.4 on page 233). As another example, the beautiful red glass that one sees in some old church windows is a suspension of small gold particles in glass. The color arises not from any chemical effect but rather from the effective complex dielectric constant of the suspension at optical frequencies (Maxwell Garnett 1904). Opals consist of submicron spherical particles of silica arranged in a face-centered cubic array, diffracting light to create the brilliant colors that we see (Sanders 1964; Greer 1969). Similarly, the spines of a particular sea worm display a wonderful iridescence caused by light diffracting off a hexagonal array of fibers within each spine (Parker, McPhedran, McKenzie, Botten, and Nicorovici 2001).

By combining materials with positive thermal expansion coefficients it is possible to get a composite with a negative thermal expansion coefficient (Lakes 1996; Sigmund and Torquato 1996, 1997). This is most easily seen in a two-dimensional context. Following Lakes (1996) consider the structure of figure 1.2(b), where the cell walls consist of thin, stiff, curved metal strips with a low thermal expansion coefficient coated on the outside with a thick compliant strip of material with a high thermal expansion coefficient. As the composite is heated the strips become more tightly curved, as illustrated in figure 1.2(a) and consequently the material contracts, that is, it has a negative thermal expansion coefficient. Lakes also shows that it is possible to construct a porous composite with a significantly larger thermal expansion coefficient than either of the two phases. Bergman and Fel (1999) have shown that the

thermoelectric power factor in a two-phase composite can be greater than the thermoelectric power factors of both phases.

A composite of a piezoelectric material and an elastic material can have a dramatically larger electrical response to hydrostatic compression than either phase alone. For example, when a cylindrical rod of the piezoelectric material lead zirconate-titanate (PZT) is compressed longitudinally, an electric field is generated parallel to the axis of the rod. When it is compressed transversely an electric field is generated in the opposite direction. If the rod is immersed in a fluid and hydrostatic pressure is applied, then the rod is compressed both axially and transversely and the induced electric fields almost cancel out. This canceling is avoided if an array of such rods is embedded in a polymer matrix, which restricts the amount of transverse compression. The electric field generated in the composite can be measured and thus small variations in the fluid pressure can be detected. Such composites are useful in the design of piezoelectric hydrophones for detecting low-frequency underwater acoustic waves (Klicker, Biggers, and Newnham 1981; Avellaneda and Swart 1998). The performance is greatly enhanced by using a negative Poisson's ratio material in place of the polymer (Smith 1991; Gibiansky and Torquato 1997; Avellaneda and Swart 1998; Sigmund, Torquato, and Aksay 1998).

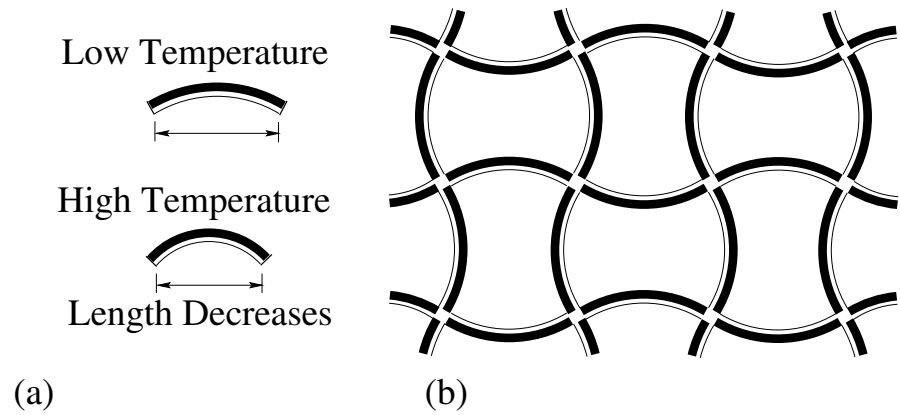

Figure 1.2. Two materials with positive thermal expansion coefficients can be combined in a porous structure to give a composite with a negative thermal expansion coefficient. The key observation, illustrated in (a), is that a thin, stiff, curved metal strip with low thermal expansion that is coated on the outside with a thick, compliant strip of material with high thermal expansion will, when heated, tighten its curvature and thereby reduce its length. By combining these elements as in (b), one obtains a porous structure with a negative thermal expansion coefficient. After Lakes (1996).

Composites can also exhibit product properties as defined by Albers (1973). A two-phase composite material exhibits a product property if the output from one phase acts as the input for the other phase. For example, following Albers (1973); Harshé, Dougherty and Newnham (1993a, 1993b); Avellaneda and Harshé (1994); and Nan (1994), consider a composite of the magnetostrictive material $CoFe_2O_4$ and the piezoelectric material Barium Titanate, $BaTiO_3$. An applied magnetic field generates a strain in the $CoFe_2O_4$ phase, which in turn generates a strain in the Barium Titanate phase, which thus produces an electric field. Thus the composite as a whole exhibits a magnetoelectric effect, where an applied magnetic effect generates an

electric field, although neither phase individually exhibits such an effect. As another example, consider a composite of a phase with a large thermal expansion coefficient combined with the piezoelectric material Barium Titanate. A temperature increase generates a strain in the first phase, which in turn causes the Barium Titanate to generate an electric field. Thus the composite as a whole exhibits a pyroelectric effect, where a temperature increase generates an electric field.

Sometimes it is advantageous to have composites with structure on a hierarchy of length scales. One sees such structural hierarchy in man-made structures such as the Eiffel tower and in biological structures such as bones and tendons (Lakes 1993). In this book we will come across many examples of optimal composites that have structural hierarchy. We will often explore the limits of what is possible by considering composites with structure on infinitely many length scales. These could be approximated by more realistic composites with structure on finitely many length scales.

It is hard to look into the future, but undoubtedly it will become increasingly possible to produce "designer composites," where the microstructure has been tailored to produce desirable properties. Obviously a better understanding of the link between the microstructure and the macroscopic properties will be essential in this endeavor.

1.3. The effective tensors of composites

At present, quantum mechanics and quantum field theory provide the best description of matter on atomic, or subatomic, length scales. Yet it is well beyond the capability of modern computers to make a full simulation of the quantum mechanical equations to analyze the behavior of macroscopic bodies. The wave function for the electrons alone is described by a function in a $3N$-dimensional space, where N is the number of electrons in the body. (The factor of three arises because each electron has three spatial degrees of freedom.) The situation becomes worse when one brings the protons and neutrons into the picture, allowing for interactions with the electromagnetic, strong, and weak fields. All of this complexity is avoided when we use the equations of macroscopic physics, which can be regarded as homogenized quantum mechanical equations.

The situation is quite similar in composite materials, where, instead of using the equations of classical physics at the microscopic level, we use homogenized or effective equations at the macroscopic level. For example, in the context of electrical conductivity in a periodic microgeometry the microscopic equations, in the absence of internal current sources, take the form

$$\boldsymbol{j}(\boldsymbol{x}) = \boldsymbol{\sigma}(\boldsymbol{x})\boldsymbol{e}(\boldsymbol{x}), \quad \nabla \cdot \boldsymbol{j} = 0, \quad \nabla \times \boldsymbol{e} = 0, \tag{1.1}$$

where $\boldsymbol{j}(\boldsymbol{x})$ is the current field, $\boldsymbol{e}(\boldsymbol{x}) = \nabla\phi(\boldsymbol{x})$ is the electric field, $-\phi(\boldsymbol{x})$ is the electrical potential, and $\boldsymbol{\sigma}(\boldsymbol{x})$ is the conductivity tensor field. The first equation in (1.1) is called the constitutive relation. It governs the relation between the fields $\boldsymbol{j}(\boldsymbol{x})$ and $\boldsymbol{e}(\boldsymbol{x})$, which satisfy the differential constraints imposed by the last two equations in (1.1). To avoid carrying around minus signs we will simply refer to $\phi(\boldsymbol{x})$ as the electrical potential, although it should be kept in mind that it is actually $-\phi(\boldsymbol{x})$, which is the electrical potential. All of these fields have rapid oscillations on the length scale of the microstructure, and possibly slow variations on a much larger length scale. At the macroscopic level the equations take the same basic form:

$$\boldsymbol{j}_0(\boldsymbol{x}) = \boldsymbol{\sigma}_*\boldsymbol{e}_0(\boldsymbol{x}), \quad \nabla \cdot \boldsymbol{j}_0 = 0, \quad \nabla \times \boldsymbol{e}_0 = 0, \tag{1.2}$$

where $\boldsymbol{j}_0(\boldsymbol{x})$ and $\boldsymbol{e}_0(\boldsymbol{x})$ are local averages of $\boldsymbol{j}$ and $\boldsymbol{e}$ over a cube centered at $\boldsymbol{x}$, having size

large compared with the microstructure (we will make this more precise in subsequent sections). These averaged fields have the oscillations on the length scale of the microstructure smoothed out, but they retain slow variations. The first equation is the effective constitutive relation. The tensor field $\boldsymbol{\sigma}_*$ appearing in it is called the effective conductivity tensor of the medium because on a macroscopic length scale the composite behaves exactly like a homogeneous medium with conductivity $\boldsymbol{\sigma}_*$, which only has variations on the macroscopic scale. It is defined through the solution to a cell problem. One looks for pairs of *periodic fields* $\boldsymbol{j}(\boldsymbol{x})$ and $\boldsymbol{e}(\boldsymbol{x})$, which solve the conductivity equations in the periodic microgeometry. The relation

$$\langle \boldsymbol{j} \rangle = \boldsymbol{\sigma}_* \langle \boldsymbol{e} \rangle$$

between the volume averages $\langle \boldsymbol{j} \rangle$ and $\langle \boldsymbol{e} \rangle$ of each pair $\boldsymbol{j}$ and $\boldsymbol{e}$; when evaluated for sufficiently many pairs, it serves to define the effective tensor $\boldsymbol{\sigma}_*$. Thus the problem of solving (1.1) is decoupled into the problem of solving the macroscopic equations (1.2) and the problem of solving the microscopic cell problem. This decoupling makes numerical solutions much easier, and also allows one to intuitively think of the medium as effectively a homogeneous medium with conductivity $\boldsymbol{\sigma}_*$.

The effective tensor $\boldsymbol{\sigma}_*$ is not just a simple local average of $\boldsymbol{\sigma}(\boldsymbol{x})$ but instead depends on it nonlinearly. The problem of determining $\boldsymbol{\sigma}_*$ from $\boldsymbol{\sigma}(\boldsymbol{x})$ is a nontrivial problem, even when only two isotropic conducting materials are present, that is, when $\boldsymbol{\sigma}(\boldsymbol{x})$ only takes the two values $\sigma_1 \boldsymbol{I}$ and $\sigma_2 \boldsymbol{I}$, in which $\boldsymbol{I}$ is the identity tensor and σ_1 and σ_2 are both positive. One might hope that if the two constituent materials were sufficiently "well mixed" there would be a universal mean-field formula giving $\boldsymbol{\sigma}_*$ in terms of σ_1, σ_2 and the volume fractions occupied by the materials. However, this is not the case. In the mixing of materials there is nothing equivalent to the Gibbs distribution in statistical physics. The probabilities of different configurations are highly dependent on the process by which the composite is formed (of which one typically has limited knowledge). An approximation for $\boldsymbol{\sigma}_*$ that works well for one class of materials will fail for another class of materials. The main focus of this book is how the behavior of tensor fields, such as $\boldsymbol{\sigma}(\boldsymbol{x})$, on the microscopic scale influence the behavior of the associated effective tensors, such as $\boldsymbol{\sigma}_*$, on the macroscopic scale.

It may happen that the equations on a macroscopic scale take a different form than the equations on the microscopic scale. For example, in a porous medium, and for low flow rates, the Stokes equations describe the fluid flow on the microscopic level whereas Darcy's law (which says that the fluid velocity is a linear function of the pressure gradient) describes the fluid flow on the macroscopic level. We do not investigate such equations in this book. We instead focus on sets of equations that have the same form on the microscopic and macroscopic levels, consisting of fields linked by a constitutive equation, and satisfying appropriate differential constraints. In the conductivity example, the constitutive equation is the relation $\boldsymbol{j} = \boldsymbol{\sigma}\boldsymbol{e}$, and the fields $\boldsymbol{j}$ and $\boldsymbol{e}$ satisfy the differential constraints that $\nabla \cdot \boldsymbol{j} = 0$ and $\nabla \times \boldsymbol{e} = 0$.

We now endeavor to clarify the concepts of homogenization and effective tensors from various different viewpoints. For simplicity we confine our attention to the conductivity problem. The extension to the various other physical equations described in the next chapter is straightforward. The descriptions given here are sketchy, and are not meant to be a substitute for the many books on homogenization. On the other hand, a deep understanding of homogenization theory is not necessary for following the rest of the book, so don't worry if you can't understand some of the approaches outlined here.

1.4. Homogenization from an intuitive viewpoint

Homogenization from an intuitive viewpoint is described in the review article of Hashin (1983) and in the book of Nemat-Nasser and Hori (1999). We need to introduce three length scales:

- The microscale is characterized by lengths less than ℓ_1, which must be chosen greater than the maximum size of inhomogeneities in the microstructure.
- The mesoscale, which is some intermediate length scale, is characterized by some length ℓ_2, at which the composite appears "statistically homogeneous," and at which the macroscopic fields have a slow variation. It is a convenient length scale for carrying out the mathematical analysis.
- The macroscale is characterized by lengths greater than ℓ_3, which must be chosen less than the relevant dimensions of the body Σ being examined and less than the scale of variations in the macroscopic structure of the composite.

It is assumed that these three length scales are well-separated:

$$\ell_1 \ll \ell_2 \ll \ell_3.$$

Inside the composite is a potential ϕ and an associated field $\nabla\phi$ satisfying the elliptic equation

$$\nabla \cdot \boldsymbol{\sigma} \nabla \phi = \rho \ \text{ within } \Sigma, \tag{1.3}$$

and subject to, say, the Dirichlet boundary condition $\phi(\boldsymbol{x}) = \psi(\boldsymbol{x})$ at the boundary of the body Σ, where $\psi(\boldsymbol{x})$ is some prescribed potential. The length scales have been defined so that the conductivity tensor field $\boldsymbol{\sigma}(\boldsymbol{x})$ has variations on the microscale and possibly on the macroscale, but no significant variations on the mesoscale. It is assumed that the source term $\rho(x)$ and the prescribed values of $\psi(\boldsymbol{x})$ at the boundary of the body have variations only on the macroscale, that is, only on length scales greater than ℓ_3.

On the mesoscale we introduce the smoothing operation of local averaging. Let $\Omega(\boldsymbol{x})$ denote a mesosized cubic window of side ℓ_2 and volume $|\Omega| = \ell_2^3$ centered at the point $\boldsymbol{x}$. Given a field $\boldsymbol{P}$, we define

$$\langle \boldsymbol{P} \rangle_\Omega(\boldsymbol{x}) = \frac{1}{|\Omega|} \int_{\Omega(\boldsymbol{x})} \boldsymbol{P}(\boldsymbol{x}')d\boldsymbol{x}' = \frac{1}{|\Omega|} \int_{\Omega(0)} \boldsymbol{P}(\boldsymbol{x}+\boldsymbol{y})d\boldsymbol{y} \tag{1.4}$$

as the average of $\boldsymbol{P}$ over the window, where $\boldsymbol{y} = \boldsymbol{x}' - \boldsymbol{x}$. Suppose, for example, that we have a curl free field $\boldsymbol{e}(\boldsymbol{x})$. Since the locally averaged field $\langle \boldsymbol{e} \rangle_\Omega(\boldsymbol{x})$ is an average over a set of fields $\boldsymbol{e}(\boldsymbol{x}+\boldsymbol{y})$ parameterized by $\boldsymbol{y}$, each of which is a translation of $\boldsymbol{e}(\boldsymbol{x})$ and therefore curl free, it follows that $\langle \boldsymbol{e} \rangle_\Omega(\boldsymbol{x})$ is also curl free. Thus local averaging preserves the differential constraints on the fields. The locally averaged field is defined by (1.4) only within a region Σ' inside Σ consisting of all points $\boldsymbol{x}$ such that $\Omega(\boldsymbol{x})$ lies entirely inside Σ. Since $\ell_2 \ll \ell_3$, the boundary of Σ' will be close to the boundary of Σ and the locally averaged fields will have some smooth extension to the boundary of Σ (we are not trying to be too precise here).

The basic idea behind homogenization is that when the three length scales are well-separated the elliptic equation decouples into an equation on the macroscopic scale and a set of equations on the mesoscale. The expectation is that on the macroscopic scale the local average $\langle \phi \rangle_\Omega$ of the potential ϕ satisfies

$$\nabla \cdot \boldsymbol{\sigma}_* \nabla \langle \phi \rangle_\Omega = \rho \ \text{ within } \Sigma, \quad \langle \phi \rangle_\Omega = \psi \ \text{ on } \partial\Sigma,$$

for some appropriate choice of the effective conductivity tensor field $\boldsymbol{\sigma}_*(\boldsymbol{x})$, which only has variations on the macroscale, and which only depends on values of $\boldsymbol{\sigma}$ within the window $\Omega(\boldsymbol{x})$, and not on ρ or ψ. Now, since the effective tensor $\boldsymbol{\sigma}_*(\boldsymbol{x})$ only has variations on the macroscopic scale, we only need calculate it at a set of representative sample points (avoiding those points where $\Omega(\boldsymbol{x})$ intersects the boundary of Σ) and then smoothly interpolate the function between these points and to the boundary of Σ. Then, because $\boldsymbol{\sigma}_*(\boldsymbol{x})$ only depends on $\boldsymbol{\sigma}$ within the window, we can calculate it at each representative sample point by considering a periodic medium obtained by periodically extending the material within the box $\Omega(\boldsymbol{x})$ and looking for solutions of the conductivity equation (1.3) with $\rho = 0$ and $\nabla\phi$ being periodic. The effective tensor is obtained through the relation between the average fields,

$$\langle \boldsymbol{\sigma}\nabla\phi\rangle_\Omega = \boldsymbol{\sigma}_*\langle\nabla\phi\rangle_\Omega, \tag{1.5}$$

within this periodic medium. This relation defines the effective tensor at each representative sample point.

The decoupling of the equations means that we can replace the composite that has rapid oscillations in its moduli by an effective material with a slowly varying effective tensor field $\boldsymbol{\sigma}_*(\boldsymbol{x})$ without changing the local averages of the fields. The idea is that this approximation should be good when the scales are well-separated, and exact in the limit as ℓ_2/ℓ_1 and ℓ_3/ℓ_2 approach infinity.

Incidentally, notice that when $\rho = 0$ any solution to the conductivity equations (1.3) remains a solution when $\boldsymbol{\sigma}(\boldsymbol{x})$ is replaced by $\boldsymbol{\sigma}'(\boldsymbol{x}) = \lambda\boldsymbol{\sigma}(\boldsymbol{x})$. It then follows from (1.5) that this medium with conductivity $\boldsymbol{\sigma}'$ will have effective conductivity $\boldsymbol{\sigma}'_* = \lambda\boldsymbol{\sigma}_*$. In other words, the effective conductivity has the homogeneity property that

$$\boldsymbol{\sigma}'_* = \lambda\boldsymbol{\sigma}_* \text{ when } \boldsymbol{\sigma}' = \lambda\boldsymbol{\sigma}. \tag{1.6}$$

1.5. Periodic homogenization

The intuitive viewpoint, while making good physical sense, needs some mathematical justification. A partial justification of the intuitive viewpoint is provided in the context of periodic homogenization. Periodic homogenization is described in the books of Bensoussan, Lions, and Papanicolaou (1978); Sanchez-Palencia (1980); Bakhvalov and Panasenko (1989); Persson, Persson, Svanstedt, and Wyller (1993); and Zhikov, Kozlov, and Oleinik (1994). The two-scale and multiscale treatments of Nguetseng (1989), Allaire (1992), and Allaire and Briane (1996), provide a rigorous basis for the method. One considers a sequence of problems, parameterized by a variable ϵ that, roughly speaking, corresponds to the size of the microstructure, and one examines what happens in the limit as ϵ tends to zero. The conductivity tensor field and the potential are assumed to be functions of both the variable $\boldsymbol{x}$, called the macroscopic or slow variable, and the variable $\boldsymbol{y} = \boldsymbol{x}/\epsilon$, called the microscopic or fast variable. Roughly speaking, the dependence of the fields on $\boldsymbol{x}$ captures their macroscopic variation while the dependence on $\boldsymbol{y}$ captures their microscopic or local variation.

In each problem the body Σ is filled by a material with conductivity tensor

$$\boldsymbol{\sigma}_\epsilon(\boldsymbol{x}) = \boldsymbol{\sigma}(\boldsymbol{x}, \boldsymbol{x}/\epsilon), \tag{1.7}$$

where for fixed $\boldsymbol{x}$, $\boldsymbol{\sigma}(\boldsymbol{x}, \boldsymbol{y})$ is periodic in the variable $\boldsymbol{y}$, say, with a square unit cell of side length h independent of $\boldsymbol{x}$. When ϵ is very small this means that $\boldsymbol{\sigma}_\epsilon(\boldsymbol{x})$ is almost periodic in $\boldsymbol{x}$ on the microscale, that is, on length scales of the order of h/ϵ. Some insight into the

geometrical interpretation of this can be gained by considering the case when $\boldsymbol{x}$ and $\boldsymbol{y}$ are one-dimensional variables. Then, as sketched in figure 1.3, $\boldsymbol{\sigma}(\boldsymbol{x}, \boldsymbol{y})$ is defined on a cylinder and $\boldsymbol{\sigma}_\epsilon(\boldsymbol{x})$ represents the values of $\boldsymbol{\sigma}(\boldsymbol{x}, \boldsymbol{y})$ along a tightly wound spiral on the cylinder, which gets tighter as $\epsilon \to 0$. (This geometrical interpretation was communicated to me by Luc Tartar.)

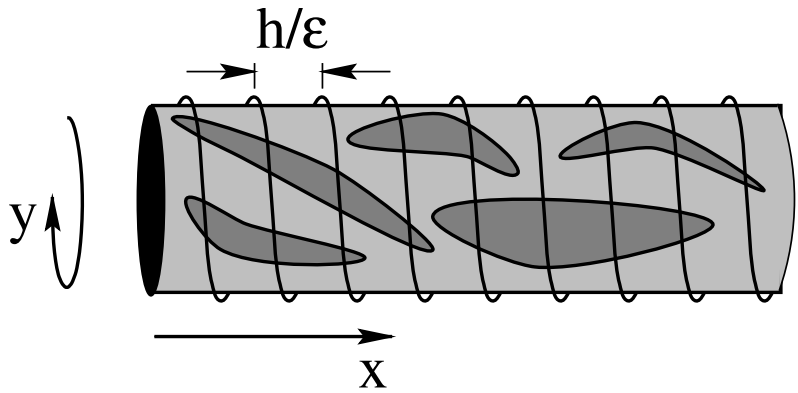

Figure 1.3. When $\boldsymbol{x}$ and $\boldsymbol{y}$ are one-dimensional, the function $\boldsymbol{\sigma}(\boldsymbol{x}, \boldsymbol{y})$ can be regarded as lying on the surface of a cylinder of circumference h. As illustrated here, the function $\boldsymbol{\sigma}(\boldsymbol{x}, \boldsymbol{y})$ could, for example, take two different values, one value in the darker shaded region and a different value in the lighter shaded region. The function $\boldsymbol{\sigma}_\epsilon(\boldsymbol{x}) = \boldsymbol{\sigma}(\boldsymbol{x}, \boldsymbol{x}/\epsilon)$ represents the values of the function along a tightly wound spiral on the cylinder.

To obtain the right homogenized equations one has to be careful. This is illustrated by the following example. Consider a connected cubic network of thin conducting rods, which is diagonally displaced from a second connected cubic network of conducting rods, with a different effective tensor, so that the two networks do not touch each other. The surrounding material is assumed to be nonconducting. It is clear that the electrical potential field on the second network is independent of the potential field on the first network, and thus one would expect the homogenized equations to be a pair of uncoupled conductivity equations, one for each network. If there are suitably thin bridges linking the two networks, then Khruslov (1978), Briane (1998), and Briane and Mazliak (1998) have shown that the homogenized equations are coupled.

Some restrictions of the conductivity field $\boldsymbol{\sigma}_\epsilon(\boldsymbol{x})$ are needed to avoid such strange homogenized equations. For simplicity we assume that $\boldsymbol{\sigma}_\epsilon(\boldsymbol{x})$ is a symmetric matrix-valued function satisfying the ellipticity condition

$$\alpha \boldsymbol{I} \leq \boldsymbol{\sigma}_\epsilon(\boldsymbol{x}) \leq \beta \boldsymbol{I} \quad \text{for all } \epsilon \text{ and } \boldsymbol{x}, \tag{1.8}$$

for some positive α and β independent of both ϵ and $\boldsymbol{x}$. We then have a sequence of electrical potentials $\phi_\epsilon(\boldsymbol{x})$ satisfying the elliptic equations

$$\nabla \cdot \boldsymbol{\sigma}_\epsilon \nabla \phi_\epsilon = \rho \quad \text{within } \Sigma, \quad \phi_\epsilon = \psi \quad \text{on } \partial\Sigma, \tag{1.9}$$

where the source term $\rho(\boldsymbol{x})$ and the potential $\psi(\boldsymbol{x})$ at the boundary of Σ are prescribed and assumed to be independent of ϵ.

To solve for the potential in the limit $\epsilon \to 0$ one uses a multiple-scale analysis and looks for a solution of the form

$$\phi_\epsilon(\boldsymbol{x}) = \phi_0(\boldsymbol{x}, \boldsymbol{x}/\epsilon) + \epsilon\phi_1(\boldsymbol{x}, \boldsymbol{x}/\epsilon) + \epsilon^2\phi_2(\boldsymbol{x}, \boldsymbol{x}/\epsilon) + \cdots,$$

where for fixed $\boldsymbol{x}$ the functions $\phi_i(\boldsymbol{x}, \boldsymbol{y})$, $i = 0, 1, 2, \ldots$, are periodic functions of $\boldsymbol{y}$ with the same periodicity as $\boldsymbol{\sigma}(\boldsymbol{x}, \boldsymbol{y})$. By substituting this expansion and (1.7) into (1.9) and separating terms having coefficients sharing the same power of ϵ one obtains a series of equations. I will not go through the analysis, since it is contained in the above-cited books. One finds that $\phi_0(\boldsymbol{x}, \boldsymbol{y})$ depends only on $\boldsymbol{x}$, that is, $\phi_0(\boldsymbol{x}, \boldsymbol{y}) = \phi_0(\boldsymbol{x})$, where $\phi_0(\boldsymbol{x})$ satisfies

$$\nabla \cdot \boldsymbol{\sigma}_* \nabla\phi_0 = \rho \ \text{ within } \Sigma, \quad \phi_0 = \psi \ \text{ on } \partial\Sigma,$$

in which the effective conductivity tensor field $\boldsymbol{\sigma}_*(\boldsymbol{x})$ is obtained at each point $\boldsymbol{x}$ by solving the auxiliary "cell problem." Given an applied field $\boldsymbol{e}_0$, the cell problem consists of finding the function $\phi_1(\boldsymbol{e}_0; \boldsymbol{y})$ periodic in $\boldsymbol{y}$, which solves

$$\nabla_y \cdot \boldsymbol{\sigma}(\boldsymbol{x}, \boldsymbol{y})\nabla_y[\boldsymbol{e}_0 \cdot \boldsymbol{y} + \phi_1(\boldsymbol{e}_0; \boldsymbol{y})] = 0,$$

where $\nabla_y \cdot$ and ∇_y are the divergence and gradient with respect to $\boldsymbol{y}$, keeping $\boldsymbol{x}$ fixed. Once the cell problem is solved for a basis of applied fields $\boldsymbol{e}_0$, the effective tensor is obtained through the relation

$$\langle \boldsymbol{\sigma}(\boldsymbol{x}, \boldsymbol{y})\nabla_y[\boldsymbol{e}_0 \cdot \boldsymbol{y} + \phi_1(\boldsymbol{e}_0; \boldsymbol{y})]\rangle = \boldsymbol{\sigma}_*\langle \nabla_y[\boldsymbol{e}_0 \cdot \boldsymbol{y} + \phi_1(\boldsymbol{e}_0; \boldsymbol{y})]\rangle,$$

where the averages are over $\boldsymbol{y}$, keeping $\boldsymbol{x}$ fixed. Since ϕ_1 is periodic in $\boldsymbol{y}$, it follows that the average value of $\nabla_y\phi_1$ is zero. Therefore we can rewrite the relation as

$$\langle \boldsymbol{\sigma}(\boldsymbol{x}, \boldsymbol{y})\nabla_y[\boldsymbol{e}_0 \cdot \boldsymbol{y} + \phi_1(\boldsymbol{e}_0; \boldsymbol{y})]\rangle = \boldsymbol{\sigma}_*\boldsymbol{e}_0.$$

The next function appearing in the series expansion is found to be

$$\phi_1(\boldsymbol{x}, \boldsymbol{y}) = \phi_1(\nabla\phi_0(\boldsymbol{x}); \boldsymbol{y}).$$

Thus the solution of the cell problem not only gives the effective tensor $\boldsymbol{\sigma}_*$ needed to compute ϕ_0, but it also gives the leading correction ϕ_1 to the potential in the series expansion. The results of this multiple-scale analysis can be verified by more rigorous methods [see, for example, Bensoussan, Lions, and Papanicolaou (1978); Tartar (1978); Nguetseng (1989); Allaire (1992); Allaire and Briane (1996); and Murat and Tartar (1997)]. One can extend the analysis to higher powers in ϵ and thereby obtain a solution that captures the correct asymptotic behavior as $\epsilon \to 0$. A rigorous justification of the resulting higher order homogenized solutions has been provided by Bakhvalov and Panasenko (1989). Smyshlyaev and Cherednichenko (2000) show how the higher order homogenized solutions also can be justified variationally, by using an energy that depends on higher order gradients.

Notice that while the potential $\phi_\epsilon(\boldsymbol{x})$ converges to $\phi_0(\boldsymbol{x})$ as $\epsilon \to 0$, the electric field $\nabla\phi_\epsilon(\boldsymbol{x})$ does not converge to $\nabla\phi_0(\boldsymbol{x})$. Indeed, $\nabla\phi_\epsilon(\boldsymbol{x})$ has rapid oscillations on the microscale, whereas $\nabla\phi_0(\boldsymbol{x})$ does not. Nevertheless, there is convergence in a weak sense. A sequence of fields $\boldsymbol{e}_\epsilon(\boldsymbol{x})$ is said to weakly converge to $\boldsymbol{e}_0(\boldsymbol{x})$ if

$$\lim_{\epsilon\to 0} \int g(\boldsymbol{x})\boldsymbol{e}_\epsilon(\boldsymbol{x})d\boldsymbol{x} = \int g(\boldsymbol{x})\boldsymbol{e}_0(\boldsymbol{x})d\boldsymbol{x},$$

for all square integrable test functions $g(\boldsymbol{x})$. With this definition $\nabla\phi_\epsilon(\boldsymbol{x})$ converges weakly to $\nabla\phi_0(\boldsymbol{x})$. Roughly speaking, taking the weak limit of a sequence of functions smoothes out the rapid oscillations; the weak limit represents the locally averaged function. To clarify the concept of weak convergence, let us consider a simple mathematical example, which is not intended to have any deeper physical significance: For any vector $\boldsymbol{n} \neq 0$ the sequence of functions

$$f_\epsilon(\boldsymbol{x}) = \frac{2\cos^2(\boldsymbol{x}\cdot\boldsymbol{n}/\epsilon)}{|\boldsymbol{x}|^4+1}$$

converges weakly as $\epsilon \to 0$ to the function

$$f_0(\boldsymbol{x}) = \frac{1}{|\boldsymbol{x}|^4+1}.$$

Of course the assumption (1.8) is too strong since it excludes all composite materials with voids. The homogenization of such perforated structures, including cellular materials, is treated in the books of Oleinik, Shamaev, and Yosifian (1992); Zhikov, Kozlov, and Oleinik (1994); and Cioranescu and Saint Jean Paulin (1999).

1.6. Homogenization in random media

In random media the analog of periodicity is statistical homogeneity or stationarity. Homogenization in random media is described with varying degrees of rigor in the books of Beran (1968); Bensoussan, Lions, and Papanicolaou (1978); Bakhvalov and Panasenko (1989); and Zhikov, Kozlov, and Oleinik (1994), and in the papers of Kozlov (1978), Papanicolaou and Varadhan (1982), and Golden and Papanicolaou (1983).

The conductivity tensor field $\boldsymbol{\sigma}(\boldsymbol{x},\omega)$ is a function of both $\boldsymbol{x}$ and the particular microstructure realization ω in the ensemble being considered. It is stationary if, given any set of points $\boldsymbol{x}_1, \boldsymbol{x}_2, \ldots, \boldsymbol{x}_m$ and any vector $\boldsymbol{h}$, the joint distribution of the set of tensors

$$\boldsymbol{\sigma}(\boldsymbol{x}_1,\omega), \boldsymbol{\sigma}(\boldsymbol{x}_2,\omega), \ldots, \boldsymbol{\sigma}(\boldsymbol{x}_m,\omega)$$

and the joint distribution of the set of tensors

$$\boldsymbol{\sigma}(\boldsymbol{x}_1+\boldsymbol{h},\omega), \boldsymbol{\sigma}(\boldsymbol{x}_2+\boldsymbol{h},\omega), \ldots, \boldsymbol{\sigma}(\boldsymbol{x}_m+\boldsymbol{h},\omega)$$

are the same as ω varies over all realizations weighted according to a probability measure $\mathcal{P}(\omega)$. This stationarity will be guaranteed if $\mathcal{P}(\omega)$ is invariant under translations of the microstructure, that is, if, roughly speaking, a given microstructure and the translated microstructure have the same probability of occurring. The case of periodic homogenization, where $\boldsymbol{\sigma}(\boldsymbol{x})$ is periodic in $\boldsymbol{x}$, can be treated in this framework by letting the ensemble consist of $\boldsymbol{\sigma}(\boldsymbol{x})$ and all of its translates $\boldsymbol{\sigma}(\boldsymbol{x}+\boldsymbol{h})$ weighted with uniform probability density $\mathcal{P}$.

The equations of interest are now

$$\nabla\cdot\boldsymbol{\sigma}(\boldsymbol{x}/\epsilon,\omega)\nabla\phi_\epsilon(\boldsymbol{x},\omega) = \rho(\boldsymbol{x}), \quad \phi_\epsilon(\boldsymbol{x},\omega) = \psi(\boldsymbol{x}) \text{ on } \partial\Sigma,$$

as ω varies over all microstructure realizations. Here ϵ can be regarded as a (continuous or discrete) parameter that sets the scale of the microstructure but does not necessarily represent a characteristic length. The homogenized fields are defined by the limits

$$\begin{aligned}
\phi_0(\boldsymbol{x}) &= \lim_{\epsilon\to 0} E\{\phi_\epsilon(\boldsymbol{x},\omega)\},\\
\boldsymbol{e}_0(\boldsymbol{x}) &= \lim_{\epsilon\to 0} E\{\nabla\phi_\epsilon(\boldsymbol{x},\omega)\},\\
\boldsymbol{j}_0(\boldsymbol{x}) &= \lim_{\epsilon\to 0} E\{\boldsymbol{\sigma}(\boldsymbol{x}/\epsilon,\omega)\nabla\phi_\epsilon(\boldsymbol{x},\omega)\},
\end{aligned}$$

where $E\{\cdot\}$ denotes the expectation value, or ensemble average:

$$E\{f(\boldsymbol{x},\omega)\} \equiv \int f(\omega)\mathcal{P}(\omega)d\omega,$$

where the integration is over all realizations ω in the ensemble. The homogenized potential $\phi_0(\boldsymbol{x})$ satisfies the homogenized equation

$$\nabla\cdot\boldsymbol{\sigma}_*\nabla\phi_0 = \rho \ \text{ within } \Sigma, \quad \phi_0(\boldsymbol{x}) = \psi(\boldsymbol{x}) \ \text{ on } \partial\Sigma,$$

or, equivalently,

$$\boldsymbol{j}_0 = \boldsymbol{\sigma}_*\boldsymbol{e}_0, \quad \nabla\cdot\boldsymbol{j}_0 = \rho, \quad \boldsymbol{e}_0 = \nabla\phi_0, \quad \phi_0(\boldsymbol{x}) = \psi(\boldsymbol{x}) \ \text{ on } \partial\Sigma,$$

where the effective tensor $\boldsymbol{\sigma}_*$ is independent of $\boldsymbol{x}$ and ω and is determined by finding *stationary* potentials $\phi_1(\boldsymbol{x},\omega)$ that solve

$$\nabla\cdot\boldsymbol{\sigma}(\boldsymbol{x}/\epsilon,\omega)[\boldsymbol{e}_0+\nabla\phi_1(\boldsymbol{x},\omega)] = 0,$$

for various constant fields $\boldsymbol{e}_0$ (independent of $\boldsymbol{x}$ and ω), by calculating

$$\boldsymbol{j}_0 = E\{\boldsymbol{\sigma}(\boldsymbol{x}/\epsilon,\omega)[\boldsymbol{e}_0+\nabla\phi_\epsilon(\boldsymbol{x},\omega)]\},$$

which gives $\boldsymbol{\sigma}_*$ via the relation

$$\boldsymbol{j}_0 = \boldsymbol{\sigma}_*\boldsymbol{e}_0.$$

When ϵ is small the potential $\phi_0(\boldsymbol{x})$ is not just a good approximation to the expectation value of $\phi_\epsilon(\boldsymbol{x},\omega)$. Kozlov (1978) and Papanicolaou and Varadhan (1982) establish the stronger result that

$$\int_\Sigma E\{|\phi_\epsilon(\boldsymbol{x},\omega)-\phi_0(\boldsymbol{x})|^2\}d\boldsymbol{x} = 0,$$

which shows that when ϵ is sufficiently small $\phi_0(\boldsymbol{x})$ is almost everywhere a good approximation to nearly every field $\phi_\epsilon(\boldsymbol{x},\omega)$ in the ensemble.

Papanicolaou and Varadhan (1982) and Golden and Papanicolaou (1983) have established that this definition of the effective conductivity tensor is consistent with the more usual definition where a cubic sample of the composite is taken and then $\boldsymbol{\sigma}_*$ is obtained in an infinite volume limit as the size the cube tends to infinity.

1.7. Homogenization in the settings of G-, H-, and Γ-convergence

The sequences of microstructures associated with periodic homogenization and homogenization in random media are rather special. Each element in the sequence $\boldsymbol{\sigma}_\epsilon(\boldsymbol{x}) = \boldsymbol{\sigma}(\boldsymbol{x},\boldsymbol{x}/\epsilon)$ or the sequence $\boldsymbol{\sigma}_\epsilon(\boldsymbol{x},\omega) = \boldsymbol{\sigma}(\boldsymbol{x}/\epsilon,\omega)$ has oscillations in the microstructure on lengths of the order of ϵ. One might wonder if homogenization can be generalized in some way to essentially arbitrary sequences of tensor fields. The frameworks of G-, H-, and Γ-convergence provide such a generalization. Spagnolo (1968) first introduced G-convergence. It is associated with the convergence of Green's functions, which is what the G signifies. Murat and Tartar (Tartar 1978; Murat and Tartar 1985, 1997) introduced H-convergence (H for homogenization), which permits problems with nonsymmetric conductivity tensors to be treated. De Giorgi (1975) introduced Γ-convergence, which is an abstract notion of functional convergence, not just limited to homogenization. These approaches provide a rigorous justification

for the intuitive viewpoint of homogenization in a very general setting. They are described, for example, in the articles of De Giorgi (1984), Allaire (1997), and Murat and Tartar (1997); in the books of Buttazzo (1989), Dal Maso (1993), Zhikov, Kozlov, and Oleinik (1994), and Attouch (1984); and in the lecture notes of Raitums (1997). Allaire (1997), in particular, provides an excellent short summary of the different approaches.

To define G-, H-, and Γ-convergence consider a sequence of symmetric second-order tensor fields $\boldsymbol{\sigma}_\epsilon(\boldsymbol{x})$ such that (1.8) is satisfied for some choice of positive constants α and β. This sequence is said to G-converge to a symmetric tensor field $\boldsymbol{\sigma}_*(\boldsymbol{x})$ if and only if for any $\rho(\boldsymbol{x})$ (in an appropriate space) the potentials ϕ_ϵ that solve the Dirichlet problem

$$\nabla \cdot \boldsymbol{\sigma}_\epsilon \nabla \phi_\epsilon = \rho \ \text{ within } \Sigma, \quad \phi_\epsilon = 0 \ \text{ on } \partial\Sigma,$$

converge to a potential $\nabla\phi_0$ that satisfies

$$\nabla \cdot \boldsymbol{\sigma}_* \nabla \phi_0 = \rho \ \text{ within } \Sigma, \quad \phi_0 = 0 \ \text{ on } \partial\Sigma.$$

This definition is motivated by the theorem of Spagnolo (1968) that *any* sequence $\boldsymbol{\sigma}_\epsilon(\boldsymbol{x})$ satisfying (1.8) has a subsequence that G-converges to a tensor field $\boldsymbol{\sigma}_*(\boldsymbol{x})$. Roughly speaking, in those regions where $\boldsymbol{\sigma}_\epsilon(\boldsymbol{x})$ converges to a fixed tensor field, $\boldsymbol{\sigma}_*(\boldsymbol{x})$ equals that tensor field; whereas in those regions where $\boldsymbol{\sigma}_\epsilon(\boldsymbol{x})$ develops oscillations on finer and finer length scales, $\boldsymbol{\sigma}_*(\boldsymbol{x})$ equals the associated effective tensor. If in a subregion the value of $\boldsymbol{\sigma}_\epsilon(\boldsymbol{x})$ alternates between two different fixed values as ϵ is decreased, one chooses the subsequence so that only one of these fixed values is selected.

The sequence is said to H-converge to a symmetric tensor field $\boldsymbol{\sigma}_*(\boldsymbol{x})$ if and only if on each bounded domain Σ all pairs of sequences of square integrable vector fields $\boldsymbol{j}_\epsilon$ and $\boldsymbol{e}_\epsilon$ on Σ for which

- $\boldsymbol{j}_\epsilon = \boldsymbol{\sigma}_\epsilon \boldsymbol{e}_\epsilon$ is satisfied for all ϵ;
- $\nabla \cdot \boldsymbol{j}_\epsilon$ and $\nabla \times \boldsymbol{e}_\epsilon$ remain within compact sets in appropriate Hilbert spaces (which guarantees that $\nabla \cdot \boldsymbol{j}_\epsilon$ and $\nabla \times \boldsymbol{e}_\epsilon$ do not oscillate too much as $\epsilon \to 0$);
- $\boldsymbol{j}_\epsilon$ and $\boldsymbol{e}_\epsilon$ converge weakly as ϵ tends to zero;

have weak limits $\boldsymbol{j}_0$ and $\boldsymbol{e}_0$ satisfying

$$\boldsymbol{j}_0 = \boldsymbol{\sigma}_* \boldsymbol{e}_0.$$

Again, *any* sequence $\boldsymbol{\sigma}_\epsilon(\boldsymbol{x})$ satisfying (1.8) has a subsequence that H-converges to a tensor field $\boldsymbol{\sigma}_*(\boldsymbol{x})$ (Tartar 1978; Murat and Tartar 1985, 1997).

The definition of Γ-convergence is more abstract. In the current setting it is defined in terms of the quadratic form $(\nabla\phi_\epsilon) \cdot \boldsymbol{\sigma}_\epsilon \nabla\phi_\epsilon$, which physically represents the electrical power dissipation. The sequence $\boldsymbol{\sigma}_\epsilon$ is defined to Γ-converge to $\boldsymbol{\sigma}_*(\boldsymbol{x})$ if

- for any potential $\phi_0(\boldsymbol{x})$ and any sequence $\varphi_\epsilon(\boldsymbol{x})$ such that $\varphi_\epsilon(\boldsymbol{x})$ converges to $\phi_0(\boldsymbol{x})$, we have
$$\lim_{\epsilon \to 0} \int_\Sigma (\nabla\varphi_\epsilon) \cdot \boldsymbol{\sigma}_\epsilon \nabla\varphi_\epsilon \geq \int_\Sigma (\nabla\phi_0) \cdot \boldsymbol{\sigma}_* \nabla\phi_0;$$
- for any potential $\phi_0(\boldsymbol{x})$ there exists a sequence $\phi_\epsilon(\boldsymbol{x})$ that converges to $\phi_0(\boldsymbol{x})$ such that
$$\lim_{\epsilon \to 0} \int_\Sigma (\nabla\phi_\epsilon) \cdot \boldsymbol{\sigma}_\epsilon \nabla\phi_\epsilon = \int_\Sigma (\nabla\phi_0) \cdot \boldsymbol{\sigma}_* \nabla\phi_0.$$

Here $\varphi_\epsilon(\boldsymbol{x})$ should be regarded as a sequence of trial potentials, and the first inequality arises from variational principles for the effective tensor (see section 13.1 on page 271). The sequence φ_ϵ (called a Γ-realizing sequence) can be taken to be the solution of

$$\nabla \cdot \boldsymbol{\sigma}_\epsilon \nabla \phi_\epsilon = \nabla \cdot \boldsymbol{\sigma}_* \nabla \phi_0 \text{ within } \Sigma, \quad \phi_\epsilon = \phi_0 \text{ on } \partial\Sigma.$$

Once again, *any* sequence $\boldsymbol{\sigma}_\epsilon(\boldsymbol{x})$ satisfying (1.8) has a subsequence that Γ-converges to a tensor field $\boldsymbol{\sigma}_*(\boldsymbol{x})$ (Dal Maso 1993). One advantage of Γ-convergence is that it is not restricted to linear equations. Using it, Braides (1985) and Müller (1987) have found that the homogenized energy for nonlinear elasticity in a periodic material has to be computed from solutions in increasingly large blocks of unit cells, not just from the solutions in a single unit cell of periodicity, as in the linear case.

Various properties of G-, H-, and Γ-convergence have been established. For example, the field $\boldsymbol{\sigma}_*(\boldsymbol{x})$ inside a window Ω within Σ is unaffected by the values that the sequence $\boldsymbol{\sigma}_\epsilon$ takes outside the window. Also, $\boldsymbol{\sigma}_*(\boldsymbol{x})$ is independent of the source term $\rho(\boldsymbol{x})$.

References

Albers, W. 1973. Physical properties of composite materials. In *Proceedings of the Conference on in situ Composites, Sept. 5–8, 1972, Lakeville, Connecticut*, pp. 1–19. Washington, D.C.: National Academy of Sciences. Publication NMAB-308-III. {*4, 14*}

Allaire, G. 1992. Homogenization and two-scale convergence. *SIAM Journal on Mathematical Analysis* 23(6):1482–1518. {*8, 10, 14*}

Allaire, G. 1997. Mathematical approaches and methods. In U. Hornung (ed.), *Homogenization and Porous Media*, pp. 225–257. Berlin / Heidelberg / London / etc.: Springer-Verlag. ISBN 0-387-94786-8. {*13, 14*}

Allaire, G. and M. Briane 1996. Multiscale convergence and reiterated homogenisation. *Proceedings of the Royal Society of Edinburgh. Section A, Mathematical and Physical Sciences* 126(2):297–342. {*8, 10, 14*}

Attouch, H. 1984. *Variational Convergence for Functions and Operators*. Applicable Mathematics Series. London: Pitman Publishing Ltd. xiv + 423 pp. ISBN 0-273-08583-2. {*13, 14*}

Avellaneda, M. and G. Harshé 1994. Magnetoelectric effect in piezoelectric/magnetostrictive multilayer (2-2) composites. *Journal of Intelligent Material Systems and Structures* 5(4):501–513. {*4, 14, 30, 40*}

Avellaneda, M. and P. J. Swart 1998. Calculating the performance of 1-3 piezocomposites for hydrophone applications: An effective medium approach. *Journal of the Acoustical Society of America* 103:1449–1467. {*4, 14*}

Bakhvalov, N. S. and G. P. Panasenko 1989. *Homogenisation: Averaging Processes in Periodic Media. Mathematical Problems in the Mechanics of Composite Materials*. Norwell, Massachusetts / Dordrecht, The Netherlands: Kluwer Academic Publishers Group. xxxv + 366 pp. ISBN 0-7923-0049-1. {*8, 10, 11, 14*}

Bensoussan, A., J.-L. Lions, and G. Papanicolaou 1978. *Asymptotic Analysis for Periodic Structures*. Amsterdam: North-Holland Publishing Co. xxiv + 700 pp. ISBN 0-444-85172-0. {*8, 10, 11, 14, 221, 242*}

Beran, M. J. 1968. *Statistical Continuum Theories*. New York: Interscience Publishers. xv + 424 pp. ISBN 0-470-06861-2. {*xxv, xxvi, 11, 15, 291, 309, 489, 491*}

Bergman, D. J. and L. G. Fel 1999. Enhancement of thermoelectric power factor in composite thermoelectrics. *Journal of Applied Physics* 85(12):8205–8217. {*3, 15, 97, 110, 580, 597*}

Braides, A. 1985. Homogenization of some almost periodic coercive functional. *Rendiconti. Accademia Nazionale delle Scienze detta dei XL. Serie V. Memorie di Matematica. Parte I* 9(1):313–321. {*14, 15*}

Briane, M. 1998. Homogenization in some weakly connected domains. *Ricerche di Matematica (Napoli)* 47(1):51–94. {*9, 15*}

Briane, M. and L. Mazliak 1998. Homogenization of two randomly weakly connected materials. *Portugaliae Mathematica* 55(2):187–207. {*9, 15*}

Buttazzo, G. 1989. *Semicontinuity, Relaxation and Integral Representations in the Calculus of Variations*. Harlow, Essex, United Kingdom: Longman Scientific and Technical. iv + 222 pp. ISBN 0-582-01859-5. {*13, 15*}

Cioranescu, D. and J. Saint Jean Paulin 1999. *Homogenization of Reticulated Structures*. Berlin / Heidelberg / London / etc.: Springer-Verlag. xx + 346 pp. ISBN 0-387-98634-0. {*11, 15*}

Dal Maso, G. 1993. *An Introduction to* Γ*-Convergence*. Basel, Switzerland: Birkhäuser Verlag. xiv + 340 pp. ISBN 0-8176-3679-X. {*13–15*}

De Giorgi, E. 1975. Sulla convergenza di alcune successioni di integrali del tipo dell'area. *Rendiconti di Matematica (6)* 8:277–294. {*12, 15*}

De Giorgi, E. 1984. *G*-operators and Γ-convergence. In *Proceedings of the International Congress of Mathematicians (Warsaw, 1983)*, pp. 1175–1191. Warsaw, Poland: PWN. {*13, 15*}

Einstein, A. 1905. Eine neue Bestimmung der Moleküldimensionen. (German) [A new determination of molecular dimensions]. *Annalen der Physik* 19:289–306. English translation in (Stachel 1998, pp. 45–69). {*2, 15*}

Faraday, M. 1839. *Experimental Researches in Electricity*. London: Richard and John Edward Taylor. pars. 1669, 1670. {*2, 15*}

Gibiansky, L. V. and S. Torquato 1997. On the use of homogenization theory to design optimal piezocomposites for hydrophone applications. *Journal of the Mechanics and Physics of Solids* 45(5):689–708. {*4, 15*}

Golden, K. and G. Papanicolaou 1983. Bounds for effective parameters of heterogeneous media by analytic continuation. *Communications in Mathematical Physics* 90(4):473–491. {*11, 12, 15, 248, 268, 370, 376, 393, 571, 598, 603, 617*}

Greer, R. T. 1969. Submicron structure of amorphous opal. *Nature* 224:1199–1200. {*3, 15*}

Harshé, G., J. P. Dougherty, and R. E. Newnham 1993a, September. Theoretical modelling of 3-0/0-3 magnetoelectric composites. *International Journal of Applied Electromagnetics in Materials* 4(2):161–171. {*4, 15*}

Harshé, G., J. P. Dougherty, and R. E. Newnham 1993b, September. Theoretical modelling of multilayer magnetoelectric composites. *International Journal of Applied Electromagnetics in Materials* 4(2):145–159. {*4, 16*}

Hashin, Z. 1983. Analysis of composite materials — A survey. *Journal of Applied Mechanics* 50:481–505. {*xxv, xxvii, 7, 16*}

Khruslov, E. Y. 1978. Asymptotic behavior of the solutions of the second boundary value problem in the case of the refinement of the boundary of the domain. *Matematicheskii sbornik* 106(4):604–621. English translation in *Math. USSR Sbornik* 35:266–282 (1979). {*9, 16*}

Klicker, K. A., J. V. Biggers, and R. E. Newnham 1981. Composites of PZT and epoxy for hydrostatic transducer applications. *Journal of the American Ceramic Society* 64:5–9. {*4, 16*}

Kozlov, S. M. 1978. Averaging of random structures. *Doklady Akademii Nauk SSSR* 241 (5):1016–1019. English translation in *Soviet Math. Dokl.* 19(4):950–954 (1978). {*11, 12, 16*}

Lakes, R. 1987. Foam structures with a negative Poisson's ratio. *Science* 235:1038–1040. {*2, 16, 652, 668*}

Lakes, R. 1993. Materials with structural hierarchy. *Nature* 361:511–515. {*5, 16, 479, 494*}

Lakes, R. 1996. Cellular solid structures with unbounded thermal expansion. *Journal of Materials Science Letters* 15(6):475–477. {*3, 4, 16*}

Landauer, R. 1978. Electrical conductivity in inhomogeneous media. In J. C. Garland and D. B. Tanner (eds.), *Electrical Transport and Optical Properties of Inhomogeneous Media*, pp. 2–43. Woodbury, New York: American Institute of Physics. ISBN 0-88318-139-8. {*2, 16, 185, 193, 217*}

Larsen, U. D., O. Sigmund, and S. Bouwstra 1997. Design and fabrication of compliant micro-mechanisms and structures with negative Poisson's ratio. *Journal of Microelectromechanical Systems* 6:99–106. {*2, 3, 16, 653, 668*}

Markov, K. Z. 2000. Elementary micromechanics of heterogeneous media. In K. Markov and L. Preziosi (eds.), *Heterogeneous Media: Micromechanics Modeling Methods and Simulations*, Modeling and Simulation in Science, Engineering and Technology, pp. 1–162. Basel, Switzerland: Birkhäuser Verlag. ISBN 0-8176-4083-5. {*xxv, xxvii, 2, 16, 185, 217, 346, 353*}

Matthews, F. L. and R. D. Rawlings 1994. *Composite Materials: Engineering and Science*. London: Chapman and Hall. ix + 470 pp. ISBN 0-412-55960-9. {*xxiv, xxvii, 1, 16*}

Maxwell, J. C. 1873. *A Treatise on Electricity and Magnetism*. Oxford, United Kingdom: Clarendon Press. Article 314 (pp. 365–367). {*2, 16*}

Maxwell Garnett, J. C. 1904. Colours in metal glasses and in metallic films. *Philosophical Transactions of the Royal Society of London* 203:385–420. {*3, 16, 239, 243*}

Milton, G. W. 1992. Composite materials with Poisson's ratios close to -1. *Journal of the Mechanics and Physics of Solids* 40(5):1105–1137. {*2, 16, 653, 661, 668*}

Müller, S. 1987. Homogenization of nonconvex integral functionals and cellular elastic materials. *Archive for Rational Mechanics and Analysis* 99:189–212. {*14, 16*}

Murat, F. and L. Tartar 1985. Calcul des variations et homogénísation. (French) [Calculus of variation and homogenization]. In *Les méthodes de l'homogénéisation: théorie et applications en physique*, pp. 319–369. Paris: Eyrolles. English translation in *Topics in the Mathematical Modelling of Composite Materials*, pp. 139–173, ed. by A. Cherkaev and R. Kohn, ISBN 0-8176-3662-5. {*12, 13, 17, 347, 353, 429, 431, 432, 435, 444, 454, 462, 495, 499, 503, 506, 508, 521, 527, 529, 551*}

Murat, F. and L. Tartar 1997. H-convergence. In A. Cherkaev and R. Kohn (eds.), *Topics in the Mathematical Modelling of Composite Materials*, pp. 21–43. Basel, Switzerland: Birkhäuser Verlag. ISBN 0-8176-3662-5 (Boston), 3-7643-3662-5 (Basel). {*10, 12, 13, 17*}

Nan, C.-W. 1994. Magnetoelectric effect in composites of piezoelectric and piezomagnetic phases. *Physical Review B (Solid State)* 50:6082–6088. {*4, 17*}

Nemat-Nasser, S. and M. Hori 1999. *Micromechanics: Overall Properties of Heterogeneous Materials* (Second ed.). Amsterdam: Elsevier. xxiv + 786 pp. ISBN 0-444-50084-7. {*xxiii, xxiv, xxvii, 7, 17*}

Nguetseng, G. 1989. A general convergence result for a functional related to the theory of homogenization. *SIAM Journal on Mathematical Analysis* 20(3):608–623. {*8, 10, 17*}

Oleinik, O. A., A. S. Shamaev, and G. A. Yosifian 1992. *Mathematical Problems in Elasticity and Homogenization*. Amsterdam: North-Holland Publishing Co. xiii + 398 pp. ISBN 0-444-88441-6. {*11, 17, 101, 111*}

Papanicolaou, G. and S. Varadhan 1982. Boundary value problems with rapidly oscillating random coefficients. *Colloquia Mathematica Societatis János Bolyai* 27:835–873. {*11, 12, 17, 248, 269*}

Parker, A. R., R. C. McPhedran, D. R. McKenzie, L. C. Botten, and N. A. Nicorovici 2001. Photonic engineering: Aphrodite's iridescence. *Nature* 409(6816):36–37. {*3, 17*}

Persson, L.-E., L. Persson, N. Svanstedt, and J. Wyller 1993. *The Homogenization Method: An Introduction*. Lund, Sweden: Studentlitteratur. viii + 80 pp. ISBN 91-44-37661-8. {*8, 17*}

Poisson, S. D. 1826. Mémoire sur la théorie du magnétisme. *Mémoires de l'Académie royale des Sciences de l'Institut de France* 5:247–338. {*2, 17*}

Raitums, U. 1997. Lecture notes on G-convergence, convexification and optimal control problems for elliptic equations. Lecture Notes 39, Department of Mathematics, University of Jyväskylä, Jyväskylä, Finland. iii + 86 pp. {*13, 17*}

Rayleigh, L. 1892. On the influence of obstacles arranged in rectangular order upon the properties of a medium. *Philosophical Magazine* 34:481–502. {*2, 17, 39, 45*}

Sanchez-Palencia, E. 1980. *Non-Homogeneous Media and Vibration Theory*. Berlin / Heidelberg / London / etc.: Springer-Verlag. ix + 398 pp. ISBN 0-540-10000-8. {*xxiii, xxvii, 8, 17, 221, 244*}

Sanders, J. V. 1964. Colour of precious opal. *Nature* 204:1151–1153. {*3, 17*}

Sigmund, O. and S. Torquato 1996. Composites with extremal thermal expansion coefficients. *Applied Physics Letters* 69(21):3203–3205. {*3, 17*}

Sigmund, O. and S. Torquato 1997. Design of materials with extreme thermal expansion using a three-phase topology optimization method. *Journal of the Mechanics and Physics of Solids* 45(6):1037–1067. {*3, 18*}

Sigmund, O., S. Torquato, and I. A. Aksay 1998. On the design of 1-3 piezocomposites using topology optimization. *Journal of Materials Research* 13(4):1038–1048. {*4, 18*}

Smith, W. A. 1991. Optimizing electromechanical coupling in piezocomposites using polymers with negative Poisson's ratio. In B. R. McAvoy (ed.), *IEEE 1991 Ultrasonics Symposium Proceedings*, pp. 661–666. Piscataway, New Jersey: IEEE press. {*4, 18*}

Smyshlyaev, V. P. and K. D. Cherednichenko 2000. On rigorous derivation of strain gradient effects in the overall behaviour of heterogeneous media. *Journal of the Mechanics and Physics of Solids* 48(6/7):1325–1357. {*10, 18*}

Spagnolo, S. 1968. Sulla convergenza della soluzioni di equaziona paraboliche ed ellittiche. *Annali della Scuola Normale Superiore di Pisa. Serie III* 22:571–597. {*12, 13, 18*}

Stachel, J. (ed.) 1998. *Einstein's miraculous year: five papers that changed the face of physics*. Princeton, New Jersey: Princeton University Press. xv + 198 pp. With the assistance of Trevor Lipscombe, Alice Calaprice, and Sam Elworthy, and with a foreword by Roger Penrose. ISBN 0-691-05938-1. {*15, 18*}

Tartar, L. 1978. Quelques remarques sur l'homogénéisation. In H. Fujita (ed.), *Functional Analysis and Numerical Analysis*, pp. 469–481. Tokyo: Japan Society for the Promotion of Sciences. {*10, 12, 13, 18*}

Taylor, G. I. 1954. The two coefficients of viscosity for an incompressible fluid containing air bubbles. *Proceedings of the Royal Society of London. Series A, Mathematical and Physical Sciences* 226:34–39. {*3, 18, 234, 244*}

Zhikov, V. V., S. M. Kozlov, and O. A. Oleinik 1994. *Homogenization of Differential Operators and Integral Functionals*. Berlin / Heidelberg / London / etc.: Springer-Verlag. xi + 570 pp. ISBN 3-540-54809-2 (Berlin), 0-387-54809-2 (New York). {*xxv, xxviii, 8, 11, 13, 18, 47, 58, 200, 220*}

2

Some equations of interest and numerical approaches to solving them

2.1. The conductivity and related equations

The basic equations

$$\boldsymbol{j}(\boldsymbol{x}) = \boldsymbol{\sigma}(\boldsymbol{x})\boldsymbol{e}(\boldsymbol{x}), \qquad \nabla \cdot \boldsymbol{j} = 0, \qquad \nabla \times \boldsymbol{e} = 0, \tag{2.1}$$

which we will refer to generically as the conductivity equations, arise in many different physical problems: electrical conductivity, dielectrics [see Scaife (1989) for an excellent introduction to the theory of dielectric materials], magnetism, thermal conduction, diffusion, flow in porous media, and antiplane elasticity. In each of these contexts the vector fields $\boldsymbol{j}(\boldsymbol{x})$ and $\boldsymbol{e}(\boldsymbol{x})$ and the tensor $\boldsymbol{\sigma}(\boldsymbol{x})$ entering the constitutive relation have the interpretations given in the following table, which is adapted from a similar one of Batchelor (1974). In this table, for flow in porous media, the weighted fluid velocity is the (locally averaged) fluid velocity $\boldsymbol{v}(\boldsymbol{x})$ multiplied by the shear viscosity η_μ of the fluid, which is assumed to be constant.

Problem	$\boldsymbol{j}$	$\boldsymbol{e}$	$\boldsymbol{\sigma}$
Electrical conduction	Electrical current $\boldsymbol{j}$	Electric field $\boldsymbol{e}$	Electrical conductivity $\boldsymbol{\sigma}$
Dielectrics	Displacement field $\boldsymbol{d}$	Electric field $\boldsymbol{e}$	Electric permittivity ε
Magnetism	Magnetic induction $\boldsymbol{b}$	Magnetic field $\boldsymbol{h}$	Magnetic permeability $\boldsymbol{\mu}$
Thermal conduction	Heat current $\boldsymbol{q}$	Temperature gradient $-\nabla T$	Thermal conductivity $\boldsymbol{\kappa}$
Diffusion	Particle current	Concentration gradient $-\nabla c$	Diffusivity $\boldsymbol{D}$
Flow in porous media	Weighted fluid velocity $\eta_\mu \boldsymbol{v}$	Pressure gradient ∇P	Fluid permeability $\boldsymbol{k}$
Antiplane elasticity	Stress Vector (τ_{13}, τ_{23})	Vertical Displacement gradient ∇u_3	Shear matrix $\boldsymbol{\mu}$

With the exception of antiplane elasticity (which will be discussed in section 2.7 on page 35 below and for which only the two-dimensional setting is relevant) the three-dimensional equations reduce to two-dimensional ones when the microstructure and fields are inde-

pendent of x_3 and the off-diagonal components σ_{13} and σ_{23} of the tensor $\boldsymbol{\sigma}(\boldsymbol{x})$ are zero. Then the differential constraints on the fields $\boldsymbol{j}(\boldsymbol{x})$ and $\boldsymbol{e}(\boldsymbol{x})$ imply that

$$\frac{\partial j_1}{\partial x_1} + \frac{\partial j_2}{\partial x_2} = 0, \quad \frac{\partial e_2}{\partial x_1} - \frac{\partial e_1}{\partial x_2} = 0, \quad e_3 = \text{constant}.$$

The scalar component $j_3(x_1, x_2)$ is not subject to any differential constraints at all. Defining the two-dimensional fields

$$\boldsymbol{j}'(x_1, x_2) = (j_1(x_1, x_2), j_2(x_1, x_2)), \quad \boldsymbol{e}'(x_1, x_2) = (e_1(x_1, x_2), e_2(x_1, x_2)), \tag{2.2}$$

we see that these vector fields satisfy the two-dimensional conductivity equations

$$\boldsymbol{j}'(\boldsymbol{x}) = \boldsymbol{\sigma}'(\boldsymbol{x})\boldsymbol{e}'(\boldsymbol{x}), \qquad \nabla \cdot \boldsymbol{j}' = 0, \qquad \nabla \times \boldsymbol{e}' = 0,$$

where now $\boldsymbol{x}$ is the two-dimensional vector $\boldsymbol{x} = (x_1, x_2)$, $\nabla\cdot$ and $\nabla\times$ are the two-dimensional divergence and curl operators, and

$$\boldsymbol{\sigma}'(\boldsymbol{x}) = \begin{pmatrix} \sigma_{11}(\boldsymbol{x}) & \sigma_{12}(\boldsymbol{x}) \\ \sigma_{21}(\boldsymbol{x}) & \sigma_{22}(\boldsymbol{x}) \end{pmatrix}. \tag{2.3}$$

This dimension reduction to two-dimensional equations also arises in the analysis of the three-dimensional conductivity equations in thin films or plates of constant or variable thickness. Let us assume that the plate has surfaces at $x_3 = h/2$ and at $x_3 = -h/2$, where $h = h(x_1, x_2)$ has a slow variation with respect to x_1 and x_2 on length scales comparable with the plate thickness. Let us also assume that the conductivity tensor field $\boldsymbol{\sigma}(\boldsymbol{x})$ within the plate has a slow variation with respect to x_1 and x_2 but a possibly rapid variation with respect to x_3. For instance, the plate could be a laminate of several plates, each with a different conductivity. In the medium surrounding the plate $\boldsymbol{\sigma}(\boldsymbol{x})$ is assumed to take comparatively small values. For electric or thermal conductivity this means that the surrounding medium has to be a good electrical or thermal insulator, like air or asbestos, respectively (although asbestos is probably not the healthiest choice). For dielectric or magnetic materials it means that the plate material must have a high electric permittivity or magnetic permeability, since the surrounding medium can never have permittivity or permeability below that of free space. For diffusion or flow in porous media it means that the plate must be surrounded by a barrier to the diffusion of particles or to the flow of fluids.

At the upper and lower surfaces of the plate the vertical component j_3 of the current is negligible because it is approximately the normal component of the current at the plate surface. The two-dimensional current field

$$\boldsymbol{j}'(x_1, x_2) = \int_{-h/2}^{h/2} (j_1(x_1, x_2, x_3), j_2(x_1, x_2, x_3))dx_3$$

is then essentially divergence free because

$$\nabla \cdot \boldsymbol{j}' = \int_{-h/2}^{h/2} \left[\frac{\partial j_1}{\partial x_1} + \frac{\partial j_2}{\partial x_2} \right] dx_3 = -\int_{-h/2}^{h/2} \frac{\partial j_3}{\partial x_3} dx_3$$

$$= j_3(x_1, x_2, -h/2) - j_3(x_1, x_2, h/2) \approx 0.$$

It is convenient to make the additional simplifying assumption that the components σ_{13} and σ_{23} are zero. Then the component $e_3 = j_3/\sigma_{33}$ will also be negligibly small at the plate

surfaces. To a good approximation it can be treated as being zero throughout the plate, that is, the potential can be treated as being independent of x_3. Defining the two-dimensional curl free vector field

$$\boldsymbol{e}' = (e_1'(x_1, x_2), e_2'(x_1, x_2)) = (e_1(x_1, x_2, 0), e_2(x_1, x_2, 0)),$$

we have

$$\boldsymbol{e}(x_1, x_2, x_3) \approx (e_1'(x_1, x_2), e_2'(x_1, x_2), 0) \quad \text{for} \quad -h(x_1, x_2)/2 \leq x_3 \leq h(x_1, x_2)/2.$$

By substituting the constitutive relation back into the defining equation for $\boldsymbol{j}'$ and using the above approximation for $\boldsymbol{e}$, we see that

$$\boldsymbol{j}' \approx \boldsymbol{\sigma}'\boldsymbol{e}', \quad \text{where } \boldsymbol{\sigma}'(x_1, x_2) = \int_{-h/2}^{h/2} \begin{pmatrix} \sigma_{11} & \sigma_{12} \\ \sigma_{21} & \sigma_{22} \end{pmatrix} dx_3.$$

Therefore the fields $\boldsymbol{e}'(x_1, x_2)$ and $\boldsymbol{j}'(x_1, x_2)$ approximately satisfy the conductivity equations in a two-dimensional medium with conductivity tensor $\boldsymbol{\sigma}'(x_1, x_2)$.

2.2. Magnetotransport and convection enhanced diffusion

In the preceding examples the tensor $\boldsymbol{\sigma}$ entering the constitutive relation is symmetric. However, this need not always be the case. Consider first a three-dimensional homogeneous isotropic body through which a constant uniform electrical current $\boldsymbol{j}$ flows. Because the body is isotropic, $\boldsymbol{j}$ will be aligned parallel to the electric field $\boldsymbol{e}$. Now suppose that we apply a constant magnetic field $\boldsymbol{h}$. The charge carriers of charge q and velocity $\boldsymbol{v}$ will then feel a magnetic force proportional to $q\boldsymbol{v} \times \boldsymbol{h}$ that is perpendicular to both $\boldsymbol{v}$ and $\boldsymbol{h}$. Since $\boldsymbol{v}$ is on average parallel to $\boldsymbol{j}$, this force will on average be perpendicular to both $\boldsymbol{j}$ and $\boldsymbol{h}$. So if the direction of $\boldsymbol{j}$ is to be maintained, we need to apply an additional electric field perpendicular to both $\boldsymbol{j}$ and $\boldsymbol{h}$ to oppose this force. When the magnetic field is weak the relation between $\boldsymbol{e}$, $\boldsymbol{j}$, and $\boldsymbol{h}$ takes the form

$$\boldsymbol{e} = \alpha\boldsymbol{j} + R\boldsymbol{h} \times \boldsymbol{j}, \tag{2.4}$$

where α is the resistivity of the medium in the absence of any magnetic field and the coefficient R is called the Hall coefficient. We can rewrite this equation as $\boldsymbol{e} = \boldsymbol{\rho}\boldsymbol{j}$, where

$$\boldsymbol{\rho} = \begin{pmatrix} \alpha & -Rh_3 & Rh_2 \\ Rh_3 & \alpha & -Rh_1 \\ -Rh_2 & Rh_1 & \alpha \end{pmatrix}$$

is the resistivity tensor of the medium. More generally, in an inhomogeneous, possibly anisotropic body containing a possibly strong magnetic field $\boldsymbol{h}(\boldsymbol{x})$ [which may depend on $\boldsymbol{x}$ due to variations in the magnetic permeability $\mu(\boldsymbol{x})$], the equations of conduction take the form

$$\boldsymbol{e}(\boldsymbol{x}) = \boldsymbol{\rho}(\boldsymbol{x})\boldsymbol{j}(\boldsymbol{x}), \quad \nabla \cdot \boldsymbol{j} = 0, \quad \nabla \times \boldsymbol{e} = 0,$$

where at any given point $\boldsymbol{x}$ the resistivity tensor field $\boldsymbol{\rho}(\boldsymbol{x})$ has a symmetric part that is an even function of $\boldsymbol{h}(\boldsymbol{x})$ and a skew symmetric part that is an odd function of $\boldsymbol{h}(\boldsymbol{x})$ [see Landau and Lifshitz (1960)]. We can also write the constitutive relation in the equivalent form $\boldsymbol{j}(\boldsymbol{x}) = \boldsymbol{\sigma}(\boldsymbol{x})\boldsymbol{e}(\boldsymbol{x})$, where $\boldsymbol{\sigma} = \boldsymbol{\rho}^{-1}$ is the conductivity tensor. The resulting current field $\boldsymbol{j}(\boldsymbol{x})$ will itself generate some magnetic field. We assume that the current is small enough to allow us to ignore these contributions to $\boldsymbol{h}(\boldsymbol{x})$ and treat $\boldsymbol{h}(\boldsymbol{x})$ and hence $\boldsymbol{\rho}(\boldsymbol{x})$ as being fixed.

Nonsymmetric conductivity tensors also enter the equations describing convection enhanced diffusion [see, for example, Fannjiang and Papanicolaou (1994)]. The temperature T in a fluid satisfies the heat equation

$$\frac{\partial T}{\partial t} = D\Delta T + \boldsymbol{v} \cdot \nabla T,$$

where t is the time, D is the diffusivity that is assumed to be constant (independent of both $\boldsymbol{x}$ and t), and $\boldsymbol{v} \cdot \nabla T$ is the convective term, in which $\boldsymbol{v}(\boldsymbol{x})$ is the fluid velocity that is assumed to be stationary (independent of t). We assume that the flow is periodic, has zero average value, and is incompressible, that is, $\nabla \cdot \boldsymbol{v} = 0$. Then there exists a periodic antisymmetric matrix potential $\boldsymbol{H}(\boldsymbol{x})$ such that

$$\boldsymbol{v} = \nabla \cdot \boldsymbol{H}.$$

Consequently, the heat equation can be rewritten in the form

$$\frac{\partial T}{\partial t} = \nabla \cdot \boldsymbol{\sigma} \nabla T, \tag{2.5}$$

with a conductivity tensor

$$\boldsymbol{\sigma}(\boldsymbol{x}) = D\boldsymbol{I} + \boldsymbol{H}(\boldsymbol{x}),$$

which is not symmetric. Indeed, by substituting this expression for $\boldsymbol{\sigma}(\boldsymbol{x})$ into (2.5) we obtain the relation

$$\frac{\partial T}{\partial t} = D\Delta T + (\nabla \cdot \boldsymbol{H}) \cdot \nabla T + \mathrm{Tr}(\boldsymbol{H} \nabla \nabla T),$$

which is easily identified with the heat equation once one realizes that the trace[1] of $\boldsymbol{H}\nabla\nabla T$ vanishes because $\boldsymbol{H}$ is antisymmetric.

2.3. The elasticity equations

The books of Atkin and Fox (1980) and Fung (1965) provide good introductions to the theory of linear elasticity, and Timoshenko (1983) provides a historical account of the subject. [Atkin and Fox (1980) also provide an introduction to nonlinear elasticity that is easy to follow. More comprehensive treatments of nonlinear elasticity can be found, for example, in the excellent books of Antman (1995), Ciarlet (1988), Lurie (1990), Marsden and Hughes (1994), and Ogden (1984).] In an elastic body at equilibrium and in the absence of body forces, the equations of linear elasticity take the form

$$\boldsymbol{\tau}(\boldsymbol{x}) = \boldsymbol{\mathcal{C}}(\boldsymbol{x})\boldsymbol{\epsilon}(\boldsymbol{x}), \quad \nabla \cdot \boldsymbol{\tau} = 0, \quad \boldsymbol{\epsilon} = [\nabla \boldsymbol{u} + (\nabla \boldsymbol{u})^T]/2,$$

where $\boldsymbol{\tau}(\boldsymbol{x})$ is the stress field,[2] $\boldsymbol{\epsilon}(\boldsymbol{x})$ is the strain field that is the symmetrized gradient of the displacement field $\boldsymbol{u}(\boldsymbol{x})$ that measures the displacement of the body relative to its original stress free state (roughly speaking, neglecting thermal vibrations, an atom at $\boldsymbol{x}$ gets displaced to $\boldsymbol{x}' = \boldsymbol{x} + \boldsymbol{u}(\boldsymbol{x})$, where $\boldsymbol{u}(\boldsymbol{x})$ is in some sense small), and $\boldsymbol{\mathcal{C}}(\boldsymbol{x})$ is the elasticity tensor of the medium that relates the two fields through the constitutive relation. This constitutive relation is sometimes written in the equivalent form

$$\boldsymbol{\epsilon}(\boldsymbol{x}) = \boldsymbol{\mathcal{S}}(\boldsymbol{x})\boldsymbol{\tau}(\boldsymbol{x}),$$

[1] Throughout the text we use Tr to denote the trace of a matrix or operator

[2] Often $\boldsymbol{\sigma}(\boldsymbol{x})$ is used to represent the stress field, but we use $\boldsymbol{\tau}(\boldsymbol{x})$ because $\boldsymbol{\sigma}(\boldsymbol{x})$ denotes the conductivity tensor field.

where $\boldsymbol{\mathcal{S}} = \boldsymbol{\mathcal{C}}^{-1}$ is called the compliance tensor. The stress field has the following physical interpretation: Given the body in a stressed state, we can carve out a small cavity from inside the body and keep the remaining part of the body in the same elastic state by applying a force distribution $\boldsymbol{\tau}(\boldsymbol{x}) \cdot \boldsymbol{n}(\boldsymbol{x})$ to the surface of the cavity, where $\boldsymbol{n}(\boldsymbol{x})$ is the normal at the cavity surface pointing toward the cavity.

In Cartesian coordinates $\boldsymbol{\tau}(\boldsymbol{x})$ and $\boldsymbol{\epsilon}(\boldsymbol{x})$ are represented as $d \times d$ symmetric matrices. Alternatively, they are often represented as $d(d+1)/2$-dimensional vectors, where each element of the vector is related to a corresponding element of the matrix. For example, in three-dimensional elasticity the constitutive relation linking the stress and strain components can be written in the form

$$\begin{pmatrix} \tau_{11} \\ \tau_{22} \\ \tau_{33} \\ \sqrt{2}\tau_{23} \\ \sqrt{2}\tau_{13} \\ \sqrt{2}\tau_{12} \end{pmatrix} = \begin{pmatrix} C_{1111} & C_{1122} & C_{1133} & \sqrt{2}C_{1123} & \sqrt{2}C_{1113} & \sqrt{2}C_{1112} \\ C_{1122} & C_{2222} & C_{2233} & \sqrt{2}C_{2223} & \sqrt{2}C_{2213} & \sqrt{2}C_{2212} \\ C_{1133} & C_{2233} & C_{3333} & \sqrt{2}C_{3323} & \sqrt{2}C_{3313} & \sqrt{2}C_{3312} \\ \sqrt{2}C_{1123} & \sqrt{2}C_{2223} & \sqrt{2}C_{3323} & 2C_{2323} & 2C_{2313} & 2C_{2312} \\ \sqrt{2}C_{1113} & \sqrt{2}C_{2213} & \sqrt{2}C_{3313} & 2C_{2313} & 2C_{1313} & 2C_{1312} \\ \sqrt{2}C_{1112} & \sqrt{2}C_{2212} & \sqrt{2}C_{3312} & 2C_{2312} & 2C_{1312} & 2C_{1212} \end{pmatrix} \begin{pmatrix} \epsilon_{11} \\ \epsilon_{22} \\ \epsilon_{33} \\ \sqrt{2}\epsilon_{23} \\ \sqrt{2}\epsilon_{13} \\ \sqrt{2}\epsilon_{12} \end{pmatrix}. \tag{2.6}$$

Thus in this representation the elasticity tensor is represented by a symmetric 6×6 matrix. It has 21 independent elements. The above representation differs from the conventional engineering representation, which does not involve factors of $\sqrt{2}$. We prefer to introduce these factors because the matrix entering the constitutive relation is then symmetric and the scalar product of the vectors representing the stress and strain matrices $\boldsymbol{\tau}(\boldsymbol{x})$ and $\boldsymbol{\epsilon}(\boldsymbol{x})$ then has a direct physical interpretation as twice the elastic energy density stored in the body. The conventional engineering notation is associated with taking an orthogonal basis on the space of symmetric matrices, whereas the above representation is associated with taking an orthonormal basis on the space of symmetric matrices.[3] Other choices of basis give alternative representations.

When the body is locally isotropic, the relation between the stress and the strain can be written in various equivalent forms, including

$$\begin{aligned} \boldsymbol{\tau} &= 2\mu\boldsymbol{\epsilon} + (\kappa - 2\mu/d)\,\mathrm{Tr}(\boldsymbol{\epsilon})\boldsymbol{I} \\ &= 2\mu\boldsymbol{\epsilon} + \lambda\,\mathrm{Tr}(\boldsymbol{\epsilon})\boldsymbol{I}, \\ \boldsymbol{\epsilon} &= (1/2\mu)\boldsymbol{\tau} + (1/d^2\kappa - 1/2d\mu)\,\mathrm{Tr}(\boldsymbol{\tau})\boldsymbol{I} \\ &= (1/E)\boldsymbol{\tau} - (\nu/E)[\mathrm{Tr}(\boldsymbol{\tau})\boldsymbol{I} - \boldsymbol{\tau}], \end{aligned} \tag{2.7}$$

where $\mu(\boldsymbol{x})$ is the shear modulus, $\kappa(\boldsymbol{x})$ is the bulk modulus, $\lambda(\boldsymbol{x})$ is the Lame modulus, $E(\boldsymbol{x})$ is the Young's modulus, $\nu(\boldsymbol{x})$ is Poisson's ratio, and d is the dimensionality ($d = 2$ or $d = 3$). These parameters satisfy the relations

$$\lambda = \kappa - 2\mu/d, \quad E = 2d^2\kappa\mu/[2\mu + d(d-1)\kappa], \quad \nu = [d\kappa - 2\mu]/[2\mu + d(d-1)\kappa].$$

With the exception of the Lame modulus, they arise as natural constants in different physical experiments. The shear modulus measures the resistance of the material to shearing (i.e., to a strain $\boldsymbol{\epsilon}$ that has zero trace); the bulk modulus measures the resistance to compression (i.e.,

[3] Two matrices $\boldsymbol{A}$ and $\boldsymbol{B}$ are said to be orthogonal if the product $\boldsymbol{A}^T\boldsymbol{B}$ has zero trace and the norm of a matrix $\boldsymbol{A}$ can be taken to be the square root of the trace of $\boldsymbol{A}^T\boldsymbol{A}$.

to a strain $\boldsymbol{\epsilon}$ that is proportional to the identity); and the Young's modulus and Poisson's ratio measure, respectively, the longitudinal extension and ratio of lateral contraction to longitudinal extension under uniaxial loading (i.e., the response to a stress $\boldsymbol{\tau}$ that is a rank-1 tensor). The Lame modulus is sometimes mathematically convenient because of the way in which its introduction simplifies the constitutive relation, as in (2.7).

In two dimensions there is another way of rewriting the elasticity equations which involves a scalar potential rather than the vector-valued potential $\boldsymbol{u}$, provided that the elastic body is simply connected (but possibly inhomogeneous). Since $\nabla \cdot \boldsymbol{\tau} = 0$, we have

$$\frac{\partial \tau_{11}}{\partial x_1} + \frac{\partial \tau_{21}}{\partial x_2} = 0, \quad \frac{\partial \tau_{12}}{\partial x_1} + \frac{\partial \tau_{22}}{\partial x_2} = 0. \tag{2.8}$$

It follows that there exist potentials ψ_1 and ψ_2 such that

$$\tau_{11} = \frac{\partial \psi_1}{\partial x_2}, \quad \tau_{21} = -\frac{\partial \psi_1}{\partial x_1}, \quad \tau_{12} = \frac{\partial \psi_2}{\partial x_2}, \quad \tau_{22} = -\frac{\partial \psi_2}{\partial x_1}. \tag{2.9}$$

The symmetry of the stress field gives $\tau_{21} = \tau_{12}$, which implies that

$$\frac{\partial \psi_1}{\partial x_1} + \frac{\partial \psi_2}{\partial x_2} = 0.$$

Consequently there must exit a further potential $\phi(\boldsymbol{x})$ such that

$$\psi_1 = \frac{\partial \phi}{\partial x_2}, \quad \psi_2 = -\frac{\partial \phi}{\partial x_1}. \tag{2.10}$$

This potential is called the Airy stress function. By substituting (2.10) into (2.9), we see that

$$\boldsymbol{\tau} = \begin{pmatrix} \tau_{11} & \tau_{12} \\ \tau_{21} & \tau_{22} \end{pmatrix} = \begin{pmatrix} \phi_{,22} & -\phi_{,12} \\ -\phi_{,12} & \phi_{,11} \end{pmatrix} = \boldsymbol{\mathcal{R}}_\perp \begin{pmatrix} \phi_{,11} & \phi_{,12} \\ \phi_{,12} & \phi_{,22} \end{pmatrix} = \boldsymbol{\mathcal{R}}_\perp \nabla\nabla\phi, \tag{2.11}$$

in which $\boldsymbol{\mathcal{R}}_\perp$ is the fourth-order tensor whose action is to rotate a second-order tensor by 90°. It has Cartesian elements

$$\mathcal{R}^\perp_{ijk\ell} = \delta_{ij}\delta_{k\ell} - (\delta_{ik}\delta_{j\ell} + \delta_{i\ell}\delta_{jk})/2.$$

Conversely, if $\boldsymbol{\tau}(\boldsymbol{x})$ can be expressed in the form (2.11), then clearly $\nabla \cdot \boldsymbol{\tau} = 0$.

Now consider the strain tensor components

$$\epsilon_{11} = \partial u_1/\partial x_1, \quad \epsilon_{12} = (\partial u_1/\partial x_2 + \partial u_2/\partial x_1)/2, \quad \epsilon_{22} = \partial u_2/\partial x_2.$$

These clearly satisfy the differential constraint

$$\frac{\partial^2 \epsilon_{22}}{\partial x_1^2} - 2\frac{\partial^2 \epsilon_{12}}{\partial x_1 \partial x_2} + \frac{\partial^2 \epsilon_{11}}{\partial x_2^2} = \frac{\partial}{\partial x_1}\left[\frac{\partial \epsilon_{22}}{\partial x_1} - \frac{\partial \epsilon_{12}}{\partial x_2}\right] + \frac{\partial}{\partial x_2}\left[-\frac{\partial \epsilon_{12}}{\partial x_1} + \frac{\partial \epsilon_{11}}{\partial x_2}\right] = 0,$$

which can be rewritten in the equivalent form

$$\nabla \cdot (\nabla \cdot \boldsymbol{M}) = 0, \quad \text{where } \boldsymbol{M} = \boldsymbol{\mathcal{R}}_\perp \boldsymbol{\epsilon} = \begin{pmatrix} \epsilon_{22} & -\epsilon_{12} \\ -\epsilon_{12} & \epsilon_{11} \end{pmatrix}, \text{ and } \{\nabla \cdot \boldsymbol{M}\}_j = \sum_{i=1}^{d} \frac{\partial M_{ij}}{\partial x_i}.$$

Conversely, if this differential constraint is satisfied, and the body is simply connected, then there exists a potential $\boldsymbol{u}$ such that $\boldsymbol{\epsilon}$ is the symmetrized gradient of $\boldsymbol{u}$. [For the proof of this see, for example, Fung (1965), pages 99–103.] The two-dimensional elasticity equation can now be rewritten as

$$\boldsymbol{M} = \boldsymbol{\mathcal{D}}\nabla\nabla\phi, \quad \nabla \cdot (\nabla \cdot \boldsymbol{M}) = 0, \tag{2.12}$$

in which $\boldsymbol{\mathcal{D}}(\boldsymbol{x})$ is the fourth-order tensor field

$$\boldsymbol{\mathcal{D}}(\boldsymbol{x}) = \boldsymbol{\mathcal{R}}_\perp \boldsymbol{\mathcal{S}}(\boldsymbol{x}) \boldsymbol{\mathcal{R}}_\perp.$$

When the elasticity tensor field is locally isotropic, with two-dimensional bulk and shear moduli $\kappa(\boldsymbol{x})$ and $\mu(\boldsymbol{x})$, these equations reduce to

$$\nabla \cdot \{\nabla \cdot [(2/\mu)\nabla\nabla\phi]\} + \Delta[(1/\kappa - 1/\mu)\Delta\phi] = 0, \tag{2.13}$$

where $\Delta = \nabla \cdot \cdot \nabla$ is the Laplacian.

The two-dimensional equations of elasticity arise as special cases of the three-dimensional elasticity equations. For example, consider the equations of three-dimensional elasticity in a locally isotropic body with bulk modulus $\kappa(x_1, x_2)$ and shear modulus $\mu(x_1, x_2)$, which are independent of x_3. We will call such materials "fibrous composites" because they are an approximation to the important class of fiber-reinforced materials where one treats the fibers as being infinitely long, perfectly aligned, and with a constant cross section. Suppose that we are looking for solutions with $u_3 = 0$ and u_1 and u_2 independent of x_3, as may occur if a slab of the fibrous composite is confined between two fixed horizontal plates. Then the body is said to be in a plane strain state. The strain fields and hence the stress fields are independent of x_3. Consequently, the equilibrium relation $\nabla \cdot \boldsymbol{\tau} = 0$ reduces to the equations (2.8), and consequently the two-dimensional fields

$$\boldsymbol{\tau}' = \begin{pmatrix} \tau_{11} & \tau_{12} \\ \tau_{21} & \tau_{22} \end{pmatrix}, \quad \boldsymbol{\epsilon}' = \begin{pmatrix} \epsilon_{11} & \epsilon_{12} \\ \epsilon_{21} & \epsilon_{22} \end{pmatrix} = \begin{pmatrix} u_{1,1} & (u_{1,2} + u_{2,1})/2 \\ (u_{1,2} + u_{2,1})/2 & u_{2,2} \end{pmatrix} \tag{2.14}$$

satisfy the required differential constraints of two-dimensional stress and strain fields. The three-dimensional constitutive relation implies that

$$\boldsymbol{\tau}' = 2\mu\boldsymbol{\epsilon}' + (\kappa - 2\mu/3)\,\mathrm{Tr}(\boldsymbol{\epsilon}')\boldsymbol{I} = 2\mu'\boldsymbol{\epsilon}' + (\kappa' - \mu')\,\mathrm{Tr}(\boldsymbol{\epsilon}')\boldsymbol{I},$$

where

$$\mu' = \mu, \quad \kappa' = \kappa + \mu/3$$

are the shear and bulk moduli of the associated two-dimensional medium under plane strain conditions.

Alternatively we can look for solutions in this fibrous composite with $\sigma_{13} = \sigma_{23} = \sigma_{33} = 0$. Then the body is said to be in a plane stress state. Again the two-dimensional fields (2.14) satisfy the required differential constraints of two-dimensional stress and strain fields. The three-dimensional constitutive relation now implies that

$$\boldsymbol{\epsilon}'(\boldsymbol{x}) = (1/2\mu)\boldsymbol{\tau}' + (1/9\kappa - 1/6\mu)\,\mathrm{Tr}(\boldsymbol{\tau}')\boldsymbol{I} = (1/2\mu')\boldsymbol{\tau}' + (1/4\kappa' - 1/4\mu')\,\mathrm{Tr}(\boldsymbol{\tau}')\boldsymbol{I},$$

where

$$\mu' = \mu, \quad \kappa' = \frac{3}{1/\mu + 4/(3\kappa)} = \frac{9\kappa\mu}{3\kappa + 4\mu}$$

are the shear and bulk moduli of the associated two-dimensional medium under plane stress conditions. If the body under consideration is a flat slab with surfaces at $x_3 = h/2$ and at $x_3 = -h/2$, where the thickness h is independent of x_1 and x_2, then the constraint $\sigma_{13} = \sigma_{23} = \sigma_{33} = 0$ automatically ensures that the normal component of the stress vanishes at the slab surface. Therefore, plane stress solutions are appropriate for describing the stretching of slabs of constant thickness that have no loadings on their surfaces.

The analysis changes when the slab is a thin plate that is bent, rather than stretched. However the resulting plate equations are equivalent to those of two-dimensional elasticity [see Timoshenko and Woinowsky-Krieger (1959), Fung (1965), and Ciarlet (1997)]. Let us allow the plate to have variable thickness with surfaces at $x_3 = h/2$ and at $x_3 = -h/2$, where $h = h(x_1, x_2)$ has a slow variation with respect to x_1 and x_2 on scales comparable with the plate thickness. Let us also assume, for simplicity, that the elasticity tensor field $\boldsymbol{\mathcal{C}}(\boldsymbol{x})$ within the plate is locally isotropic with bulk modulus $\kappa(x_1, x_2)$ and shear modulus $\mu(x_1, x_2)$, which are independent of x_3 and which have a slow variation with respect to x_1 and x_2. One side of the plate is extended under bending while the other side of the plate is compressed. It is convenient to assume the existence of a neutral surface midway through the plate at $x_3 = 0$ that has no compression or extension. On this neutral surface

$$u_1 = u_2 = 0, \quad u_3 = u(x_1, x_2).$$

As in plate stretching, the dominant stress components in the plate are τ_{11}, τ_{12}, and τ_{22} because the remaining stress components τ_{13}, τ_{23}, and τ_{33} must be vanishingly small at the plate surfaces. (However, these remaining stress components cannot be ignored. As we will see, they determine the equilibrium equation for the bending moments.) The components $\epsilon_{13} = \tau_{13}/2\mu$, $\epsilon_{23} = \tau_{23}/2\mu$ of the strain are therefore small in comparison to the other strain components and to a first approximation we have

$$\frac{\partial u_1}{\partial x_3} = 2\epsilon_{13} - \frac{\partial u_3}{\partial x_1} \approx -\frac{\partial u}{\partial x_1}, \quad \frac{\partial u_2}{\partial x_3} = 2\epsilon_{23} - \frac{\partial u_3}{\partial x_2} \approx -\frac{\partial u}{\partial x_2}.$$

This implies that

$$u_1 \approx -x_3 \frac{\partial u}{\partial x_1}, \quad u_2 \approx -x_3 \frac{\partial u}{\partial x_2},$$

and consequently

$$\epsilon_{11} \approx -x_3 \frac{\partial^2 u}{\partial x_1^2}, \quad \epsilon_{12} \approx -x_3 \frac{\partial^2 u}{\partial x_1 \partial x_2}, \quad \epsilon_{22} \approx -x_3 \frac{\partial^2 u}{\partial x_2^2}.$$

Also, since τ_{33} is comparatively small, the remaining dominant strain component is

$$\epsilon_{33} \approx -\frac{3\kappa - 2\mu}{3\kappa + 4\mu}(\epsilon_{11} + \epsilon_{22}) \approx \frac{(3\kappa - 2\mu)x_3}{3\kappa + 4\mu}\left[\frac{\partial^2 u}{\partial x_1^2} + \frac{\partial^2 u}{\partial x_2^2}\right].$$

From the constitutive relation it follows that the dominant stress components are

$$\begin{aligned}
\tau_{11} &\approx -2\mu x_3 \frac{\partial^2 u}{\partial x_1^2} - \frac{(3\kappa - 2\mu)2\mu x_3}{3\kappa + 4\mu}\left[\frac{\partial^2 u}{\partial x_1^2} + \frac{\partial^2 u}{\partial x_2^2}\right], \\
\tau_{12} &\approx -2\mu x_3 \frac{\partial^2 u}{\partial x_1 \partial x_2}, \\
\tau_{22} &\approx -2\mu x_3 \frac{\partial^2 u}{\partial x_2^2} - \frac{(3\kappa - 2\mu)2\mu x_3}{3\kappa + 4\mu}\left[\frac{\partial^2 u}{\partial x_1^2} + \frac{\partial^2 u}{\partial x_2^2}\right].
\end{aligned} \tag{2.15}$$

Now consider the components of the stress field integrated through the plate:

$$\tau'_{ij}(x_1, x_2) = \int_{-h/2}^{h/2} \tau_{ij}(x_1, x_2, x_3) dx_3.$$

The integrals of the dominant stress components through the plate are clearly zero, being proportional to x_3. These integrals are therefore insufficient to describe the stress state of the plate. When a hole is made in the plate, one needs to apply not only forces independent of x_3 to the hole edge but also bending torques (which are forces proportional to x_3) to keep the remaining part of the plate in approximately the same stress state. In addition to the average components τ'_{ij} of the stress fields it is also necessary to keep track of the bending moments

$$M_{ij}(x_1, x_2) = \int_{-h/2}^{h/2} x_3 \tau_{ij}(x_1, x_2, x_3) dx_3, \quad \text{for } i, j = 1, 2,$$

which are components of a two-dimensional, second-order tensor field $\boldsymbol{M}(x_1, x_2)$. From the approximation formulas (2.15) for the dominant stress components we have the constitutive relation

$$\boldsymbol{M} \approx -(\mu h^3/6)\nabla\nabla u - \frac{(3\kappa - 2\mu)\mu h^3}{6(3\kappa + 4\mu)}[\mathrm{Tr}(\nabla\nabla u)]\boldsymbol{I}, \tag{2.16}$$

which relates the bending moment tensor $\boldsymbol{M}$ to the curvature tensor $\nabla\nabla u$ of the plate. (The eigenvectors of $\nabla\nabla u$ give the axes of principle curvature, and the reciprocals of the associated eigenvalues give the radii of curvature along those axes.)

It remains to find the equilibrium equation for the bending moment tensor. Since $\nabla \cdot \boldsymbol{\tau} = 0$, and because τ_{13} is zero at the plate surface, we have

$$\frac{\partial M_{11}}{\partial x_1} + \frac{\partial M_{12}}{\partial x_2} = \int_{-h/2}^{h/2} -x_3 \frac{\partial \tau_{13}}{\partial x_3} dx_3 = \tau'_{13} - [x_3 \tau_{13}]_{-h/2}^{h/2} = \tau'_{13},$$

and similarly we have

$$\frac{\partial M_{12}}{\partial x_1} + \frac{\partial M_{22}}{\partial x_2} = \tau'_{23}.$$

Also, integrating the equilibrium relation $\nabla \cdot \boldsymbol{\tau} = 0$ through the plate gives

$$\frac{\partial \tau'_{13}}{\partial x_1} + \frac{\partial \tau'_{23}}{\partial x_2} = -[\tau_{33}]_{-h/2}^{h/2} = 0,$$

and this implies that the bending moments satisfy the equilibrium equation

$$\frac{\partial^2 M_{11}}{\partial x_1^2} + 2\frac{\partial^2 M_{12}}{\partial x_1 \partial x_2} + \frac{\partial^2 M_{22}}{\partial x_2^2} = 0 \text{ or, equivalently, } \nabla \cdot \nabla \cdot \boldsymbol{M} = 0.$$

By substituting (2.16) into the equilibrium equation we see that u satisfies

$$\nabla \cdot [\nabla \cdot (h^3 \mu \nabla\nabla u)] + \Delta\{h^3[(3\kappa - 2\mu)\mu/(3\kappa + 4\mu)]\Delta \boldsymbol{u}\} = 0.$$

By comparing this with (2.13) we see that the equations of plate bending are equivalent to those of two-dimensional elasticity, as is well known. The Airy stress function, which in two-dimensional elasticity has only an indirect physical interpretation (as the potential for the stress field) now has a direct physical significance. In plate bending its role is played by the vertical displacement $u(x_1, x_2)$ of the neutral surface, which is an easily measured quantity.

2.4. Thermoelectric, piezoelectric, and similar coupled equations

In a conducting material the equations of electrical conductivity and thermal conductivity are idealized equations. In practice there is usually some coupling. Because flowing electrons carry some heat with them, an electrical current will be accompanied by a flow of heat even in the absence of a temperature gradient. There is a lot of confusion, particularly in the composite materials community, as to the appropriate form of the thermoelectric equations. Here I follow the treatment of Callen (1960), which strikes me as the correct approach [see also Ashcroft and Mermin (1976)].

The constitutive equations take the form

$$\begin{pmatrix} -\boldsymbol{j}_N \\ \boldsymbol{j}_U \end{pmatrix} = \begin{pmatrix} \boldsymbol{L}_{11} & \boldsymbol{L}_{12} \\ \boldsymbol{L}_{21} & \boldsymbol{L}_{22} \end{pmatrix} \begin{pmatrix} \nabla(\mu/T) \\ \nabla(1/T) \end{pmatrix} = \boldsymbol{\mathcal{L}} \begin{pmatrix} \nabla(\mu/T) \\ \nabla(1/T) \end{pmatrix}, \tag{2.17}$$

where $T(\boldsymbol{x})$ is the temperature field, μ is the electrochemical potential per particle, and $\boldsymbol{j}_N$ and $\boldsymbol{j}_U$ are current densities of the number of electrons and energy, respectively, which in a steady state flow satisfy the differential constraints

$$\nabla \cdot \boldsymbol{j}_N = 0, \qquad \nabla \cdot \boldsymbol{j}_U = 0, \tag{2.18}$$

which are implied by the conservation of the number of electrons and the conservation of energy. The electrochemical potential μ is the sum $\mu = \mu_e + \mu_c$ of two parts: an electrical part $\mu_e(\boldsymbol{x}) = e\phi(\boldsymbol{x})$, where e represents the absolute value of the charge on an electron and $-\phi(\boldsymbol{x})$ represents the electrostatic potential, and a chemical part $\mu_c(\boldsymbol{x})$, which is a function of the temperature $T(\boldsymbol{x})$, the electron concentration, and the type of material located at the point $\boldsymbol{x}$.

In the absence of magnetic fields, Onsager's principle (Lifshitz and Pitaevskii 1980) implies that the matrix $\boldsymbol{\mathcal{L}}(\boldsymbol{x})$ entering the constitutive relation (2.17) is symmetric, that is,

$$\boldsymbol{L}_{11} = \boldsymbol{L}_{11}^T, \quad \boldsymbol{L}_{22} = \boldsymbol{L}_{22}^T, \quad \boldsymbol{L}_{21} = \boldsymbol{L}_{12}^T.$$

When a magnetic field $\boldsymbol{h}$ is present the symmetric part of $\boldsymbol{\mathcal{L}}(\boldsymbol{x})$ is an even function of $\boldsymbol{h}$, while the antisymmetric part is an odd function of $\boldsymbol{h}$. In general, the coefficient matrix $\boldsymbol{\mathcal{L}}(\boldsymbol{x})$ also depends on T and μ. However, it is assumed that the variations in T and μ are sufficiently small to allow us to treat $\boldsymbol{\mathcal{L}}(\boldsymbol{x})$ as depending only on $\boldsymbol{x}$ [and $\boldsymbol{h}(\boldsymbol{x})$, if a magnetic field is present].

The preceding equations are sometimes rewritten in the equivalent form

$$\begin{pmatrix} \boldsymbol{j} \\ \boldsymbol{q}/T \end{pmatrix} = \begin{pmatrix} \boldsymbol{L}'_{11} & \boldsymbol{L}'_{12} \\ \boldsymbol{L}'_{21} & \boldsymbol{L}'_{22} \end{pmatrix} \begin{pmatrix} \nabla(\mu/e) \\ -\nabla T \end{pmatrix},$$

where

$$\boldsymbol{j} = -e\boldsymbol{j}_N, \quad \boldsymbol{q} = \boldsymbol{j}_U - \mu\boldsymbol{j}_N$$

are the electric and heat current densities and

$$\begin{aligned} \boldsymbol{L}'_{11} &= e^2\boldsymbol{L}_{11}/T, \quad \boldsymbol{L}'_{12} = e(\boldsymbol{L}_{12} + \mu\boldsymbol{L}_{11})/T^2, \\ \boldsymbol{L}'_{21} &= e(\boldsymbol{L}_{21} + \mu\boldsymbol{L}_{11})/T^2, \quad \boldsymbol{L}'_{22} = [\boldsymbol{L}_{22} + \mu(\boldsymbol{L}_{12} + \boldsymbol{L}_{21}) + \mu^2\boldsymbol{L}_{11}]/T^3. \end{aligned}$$

Again the matrix entering the constitutive relation is symmetric in the absence of a magnetic field. However, the disadvantage of this form of the equations is that the field $\boldsymbol{q}/T$, which is also called the entropy current density, is not divergence free since

$$\nabla \cdot (\boldsymbol{q}/T) = [\boldsymbol{j} \cdot (\nabla\mu/e)]/T - (\boldsymbol{q} \cdot \nabla T)/T^2.$$

For this reason we prefer to consider the thermoelectric equations in the form (2.17) and (2.18).

When the coupling is negligible, that is, when $\boldsymbol{L}'_{21}$ and $\boldsymbol{L}'_{12}$ are small, the thermoelectric constitutive equation decouples into the constitutive equations of electrical and heat conductivity:

$$\boldsymbol{j} = \boldsymbol{\sigma}\nabla(\mu/e), \quad \boldsymbol{q} = -\boldsymbol{\kappa}\nabla T,$$

where

$$\boldsymbol{\sigma}(\boldsymbol{x}) = \boldsymbol{L}'_{11}(\boldsymbol{x}), \quad \boldsymbol{\kappa}(\boldsymbol{x}) = T\boldsymbol{L}'_{22}(\boldsymbol{x})$$

are the electrical conductivity tensor field and heat conductivity tensor field. The electrical current density $\boldsymbol{j}$ is divergence free (because e is constant) and the heat current $\boldsymbol{q}$ will be divergence free when the electrochemical potential μ is constant. When μ is not constant, the equations of electrical conductivity need to be solved first; then the temperature field is found as the solutions of the equations

$$\boldsymbol{q} = -\boldsymbol{\kappa}\nabla T, \qquad \nabla \cdot \boldsymbol{q} = \boldsymbol{j} \cdot \nabla(\mu/e),$$

where the term $\boldsymbol{j} \cdot \nabla(\mu/e)$ represents the dissipation of electrical power into heat.

Notice that even in the absence of coupling the electrical current is driven not only by variations in the electrical potential $\phi(\boldsymbol{x})$ but also by variations in the chemical potential $\mu_c(\boldsymbol{x})$. One sees this most clearly at junctions between different semiconductors. Each semiconductor has a different chemical potential μ_c, which is dependent on the level of doping. In the absence of any applied currents the electrical potential adjusts itself so that the electrochemical potential $\mu = e\phi + \mu_c$ is independent of $\boldsymbol{x}$. At the junction between the semiconductors there will be a gradient in μ_c and hence an electric field $\boldsymbol{e} = \nabla\phi = -\nabla(\mu_c/e)$ but no associated current because μ is constant. Thus the conductivity equation $\boldsymbol{j} = \boldsymbol{\sigma}\nabla\phi$ is only an approximation valid when there are no significant spatial variations in $\mu_c(\boldsymbol{x})$ and when the coupling matrices $\boldsymbol{L}'_{21}$ and $\boldsymbol{L}'_{12}$ are negligible.

In piezoelectrics, such as Barium Titanate, $BaTiO_3$, applied strains generate electric and/or electric displacement fields (which is why piezoelectrics work as strain measuring devices) and conversely applied electric fields generate strains and/or stresses (which is why piezoelectrics generate ultrasonic sound when subject to an oscillating electric field). Mason (1950) and Ikeda (1996) give excellent accounts of the theory of piezoelectricity. The constitutive relation takes form

$$\begin{pmatrix} \boldsymbol{\epsilon} \\ \boldsymbol{d} \end{pmatrix} = \begin{pmatrix} \boldsymbol{\mathcal{S}} & \boldsymbol{\mathcal{D}} \\ \boldsymbol{\mathcal{D}}^T & \boldsymbol{\varepsilon} \end{pmatrix} \begin{pmatrix} \boldsymbol{\tau} \\ \boldsymbol{e} \end{pmatrix},$$

where $\boldsymbol{\mathcal{S}}(\boldsymbol{x})$ is the compliance tensor under short-circuit boundary conditions (i.e., with $\boldsymbol{e} = 0$), $\boldsymbol{\mathcal{D}}(\boldsymbol{x})$ is the piezoelectric stress coupling tensor, and $\boldsymbol{\varepsilon}(\boldsymbol{x})$ is the free-body dielectric tensor (i.e., with $\boldsymbol{\tau} = 0$). The strain field $\boldsymbol{\epsilon}$, electric displacement field $\boldsymbol{d}$, stress field $\boldsymbol{\tau}$, and electric field $\boldsymbol{e}$ satisfy the usual differential constraints:

$$\boldsymbol{\epsilon} = [\nabla\boldsymbol{u} + (\nabla\boldsymbol{u})^T]/2, \quad \nabla \cdot \boldsymbol{d} = 0,$$
$$\nabla \cdot \boldsymbol{\tau} = 0, \quad \nabla \times \boldsymbol{e} = 0.$$

Since the stresses and strains are symmetric matrices, $\boldsymbol{\mathcal{D}}$ is a third-order tensor that maps vectors to symmetric matrices. The only rotationally invariant third-order tensor with this property is the trivial tensor $\boldsymbol{\mathcal{D}} = 0$. Therefore there is no piezoelectric coupling in isotropic materials. Piezoelectric materials are necessarily anisotropic.

The constitutive relation can also be rewritten in either of the two equivalent forms

$$\begin{pmatrix} \boldsymbol{\tau} \\ \boldsymbol{d} \end{pmatrix} = \begin{pmatrix} \boldsymbol{\mathcal{S}}^{-1} & -\boldsymbol{\mathcal{S}}^{-1}\boldsymbol{\mathcal{D}} \\ \boldsymbol{\mathcal{D}}^T\boldsymbol{\mathcal{S}}^{-1} & \boldsymbol{\varepsilon} - \boldsymbol{\mathcal{D}}^T\boldsymbol{\mathcal{S}}^{-1}\boldsymbol{\mathcal{D}} \end{pmatrix} \begin{pmatrix} \boldsymbol{\epsilon} \\ \boldsymbol{e} \end{pmatrix}$$

or

$$\begin{pmatrix} -\boldsymbol{\tau} \\ \boldsymbol{d} \end{pmatrix} = \begin{pmatrix} -\boldsymbol{\mathcal{S}}^{-1} & \boldsymbol{\mathcal{S}}^{-1}\boldsymbol{\mathcal{D}} \\ \boldsymbol{\mathcal{D}}^T\boldsymbol{\mathcal{S}}^{-1} & \boldsymbol{\varepsilon} - \boldsymbol{\mathcal{D}}^T\boldsymbol{\mathcal{S}}^{-1}\boldsymbol{\mathcal{D}} \end{pmatrix} \begin{pmatrix} \boldsymbol{\epsilon} \\ \boldsymbol{e} \end{pmatrix}$$

to ensure that the fields on the right-hand side of the equation derive from gradients. The disadvantage of these forms of the constitutive equation is that the matrix entering the constitutive relation is either not symmetric or not positive-definite.

In magnetostrictive materials, such as $CoFe_2O_4$, the coupling is between elastic fields and magnetic fields and the constitutive relation takes the form

$$\begin{pmatrix} \boldsymbol{\epsilon} \\ \boldsymbol{b} \end{pmatrix} = \begin{pmatrix} \boldsymbol{\mathcal{S}} & \boldsymbol{\mathcal{Q}} \\ \boldsymbol{\mathcal{Q}}^T & \boldsymbol{\mu} \end{pmatrix} \begin{pmatrix} \boldsymbol{\tau} \\ \boldsymbol{h} \end{pmatrix},$$

where $\boldsymbol{\mathcal{S}}(\boldsymbol{x})$ is the compliance tensor with $\boldsymbol{h} = 0$, $\boldsymbol{\mathcal{Q}}$ is the third-order coupling tensor, and $\boldsymbol{\mu}(\boldsymbol{x})$ is the free-body magnetic permeability (with $\boldsymbol{\tau} = 0$). Again the fields satisfy the usual differential constraints:

$$\begin{aligned} \boldsymbol{\epsilon} = [\nabla \boldsymbol{u} + (\nabla \boldsymbol{u})^T]/2, \quad \nabla \cdot \boldsymbol{\tau} = 0, \\ \nabla \cdot \boldsymbol{b} = 0, \quad \nabla \times \boldsymbol{h} = 0. \end{aligned}$$

By combining a piezoelectric material and a magnetostrictive material together in a composite, we obtain a material where there is coupling between electric fields, magnetic fields, and elastic fields. In such materials the constitutive relation takes the form

$$\begin{pmatrix} \boldsymbol{\epsilon} \\ \boldsymbol{d} \\ \boldsymbol{b} \end{pmatrix} = \begin{pmatrix} \boldsymbol{\mathcal{S}} & \boldsymbol{\mathcal{D}} & \boldsymbol{\mathcal{Q}} \\ \boldsymbol{\mathcal{D}}^T & \boldsymbol{\varepsilon} & \boldsymbol{\beta} \\ \boldsymbol{\mathcal{Q}}^T & \boldsymbol{\beta}^T & \boldsymbol{\mu} \end{pmatrix} \begin{pmatrix} \boldsymbol{\tau} \\ \boldsymbol{e} \\ \boldsymbol{h} \end{pmatrix},$$

where $\boldsymbol{\beta}(\boldsymbol{x})$ is the second-order magnetoelectric coupling tensor [see, for example, Avellaneda and Harshé (1994)]. The effective tensor of a composite can have a nonzero effective magnetoelectric coupling tensor $\boldsymbol{\beta}_*$ even when $\boldsymbol{\beta}(\boldsymbol{x})$ is zero for all $\boldsymbol{x}$. This is the product property mentioned in section 1.2 on page 2.

2.5. Thermoelasticity and poroelasticity

In the linear approximation thermal expansion is governed by the equations

$$\boldsymbol{\epsilon}(\boldsymbol{x}) = \boldsymbol{\mathcal{S}}(\boldsymbol{x})\boldsymbol{\tau}(\boldsymbol{x}) + \boldsymbol{\alpha}(\boldsymbol{x})\theta, \tag{2.19}$$

where $\theta = T - T_0$ is the change in temperature T measured from some constant base temperature T_0, $\boldsymbol{\epsilon}(\boldsymbol{x})$ and $\boldsymbol{\tau}(\boldsymbol{x})$ are the strain and stress fields, $\boldsymbol{\mathcal{S}}(\boldsymbol{x})$ is the compliance tensor, and $\boldsymbol{\alpha}(\boldsymbol{x})$ is the symmetric second-order tensor of thermal expansion [see Fung (1965)]. The average fields $\langle \boldsymbol{\epsilon} \rangle$ and $\langle \boldsymbol{\tau} \rangle$ satisfy equations of the same form:

$$\langle \boldsymbol{\epsilon} \rangle = \boldsymbol{\mathcal{S}}_* \langle \boldsymbol{\tau} \rangle + \boldsymbol{\alpha}_* \theta, \tag{2.20}$$

which serve to define the effective compliance tensor $\boldsymbol{\mathcal{S}}_*$ and the effective thermal expansion tensor $\boldsymbol{\alpha}_*$.

The equation (2.19) of thermal expansion is insufficient to describe the total thermoelastic state of the composite. Within a linear theory the complete description is provided by the equations

$$\begin{pmatrix} \boldsymbol{\epsilon}(\boldsymbol{x}) \\ \varsigma(\boldsymbol{x}) \end{pmatrix} = \begin{pmatrix} \boldsymbol{\mathcal{S}}(\boldsymbol{x}) & \boldsymbol{\alpha}(\boldsymbol{x}) \\ \boldsymbol{\alpha}(\boldsymbol{x}) & c(\boldsymbol{x})/T_0 \end{pmatrix} \begin{pmatrix} \boldsymbol{\tau}(\boldsymbol{x}) \\ \theta \end{pmatrix}, \quad \text{with} \quad \begin{array}{c} \nabla \cdot \boldsymbol{\tau} = 0, \\ \boldsymbol{\epsilon} = [\nabla \boldsymbol{u} + (\nabla \boldsymbol{u})^T]/2, \end{array} \tag{2.21}$$

where $\varsigma(\boldsymbol{x})$ is the increase in entropy per unit volume over the entropy of the state where $\boldsymbol{\tau} = \theta = 0$, and $c(\boldsymbol{x})$ is specific heat per unit volume at constant stress. This specific heat measures the amount of additional heat energy or, more precisely, entropy that is stored in the material when the temperature is increased at constant stress.

Macroscopically, the average fields satisfy

$$\begin{pmatrix} \langle \boldsymbol{\epsilon} \rangle \\ \langle \varsigma \rangle \end{pmatrix} = \begin{pmatrix} \boldsymbol{\mathcal{S}}_* & \boldsymbol{\alpha}_* \\ \boldsymbol{\alpha}_* & c_*/T_0 \end{pmatrix} \begin{pmatrix} \langle \boldsymbol{\tau} \rangle \\ \theta \end{pmatrix}, \tag{2.22}$$

and this serves to define the effective elasticity tensor $\boldsymbol{\mathcal{S}}_*$, the effective tensor of thermal expansion $\boldsymbol{\alpha}_*$, and the effective constant of specific heat at constant stress c_*.

Because the entropy increment $\varsigma(\boldsymbol{x})$ does not satisfy any differential constraints, we need not consider it when solving the equations of thermal expansion for the stress and strain fields. Once the stress field is found, (2.21) implies that

$$\varsigma(\boldsymbol{x}) = \mathrm{Tr}[\boldsymbol{\alpha}(\boldsymbol{x})\boldsymbol{\tau}(\boldsymbol{x})] + \theta c(\boldsymbol{x})/T_0,$$

and by taking averages of this expression we find that

$$\mathrm{Tr}[\boldsymbol{\alpha}_* \langle \boldsymbol{\tau} \rangle] + \theta c_*/T_0 = \langle \mathrm{Tr}[\boldsymbol{\alpha}\boldsymbol{\tau}] \rangle + \theta \langle c \rangle / T_0, \tag{2.23}$$

which provides an equation for determining c_*.

The thermoelastic equations (2.21) and the relation (2.22) between the average fields can be manipulated into the equivalent forms

$$\begin{pmatrix} \boldsymbol{\tau}(\boldsymbol{x}) \\ -\varsigma(\boldsymbol{x}) \end{pmatrix} = \begin{pmatrix} \boldsymbol{\mathcal{C}}(\boldsymbol{x}) & \boldsymbol{A}(\boldsymbol{x}) \\ \boldsymbol{A}(\boldsymbol{x}) & -c_\epsilon(\boldsymbol{x})/T_0 \end{pmatrix} \begin{pmatrix} \boldsymbol{\epsilon}(\boldsymbol{x}) \\ \theta \end{pmatrix}, \quad \text{with} \quad \begin{array}{c} \nabla \cdot \boldsymbol{\tau} = 0, \\ \boldsymbol{\epsilon} = [\nabla \boldsymbol{u} + (\nabla \boldsymbol{u})^T]/2, \end{array} \tag{2.24}$$

and

$$\begin{pmatrix} \langle \boldsymbol{\tau} \rangle \\ -\langle \varsigma \rangle \end{pmatrix} = \begin{pmatrix} \boldsymbol{\mathcal{C}}_* & \boldsymbol{A}_* \\ \boldsymbol{A}_* & -c_{\epsilon *}/T_0 \end{pmatrix} \begin{pmatrix} \langle \boldsymbol{\epsilon} \rangle \\ \theta \end{pmatrix},$$

where $\boldsymbol{\mathcal{C}} = \boldsymbol{\mathcal{S}}^{-1}$ and $\boldsymbol{\mathcal{C}}_* = \boldsymbol{\mathcal{S}}_*^{-1}$ are the elasticity tensor field and effective elasticity tensor;

$$\boldsymbol{A}(\boldsymbol{x}) = -\boldsymbol{\mathcal{C}}(\boldsymbol{x})\boldsymbol{\alpha}(\boldsymbol{x}), \quad \boldsymbol{A}_* = -\boldsymbol{\mathcal{C}}_*\boldsymbol{\alpha}_*$$

are the thermal stress (eigenstress) tensor field and effective thermal stress tensor; and

$$c_\epsilon(\boldsymbol{x}) = c(\boldsymbol{x}) - T_0\,\mathrm{Tr}[\boldsymbol{\alpha}(\boldsymbol{x})\boldsymbol{\mathcal{C}}(\boldsymbol{x})\boldsymbol{\alpha}(\boldsymbol{x})] \text{ and } c_{\epsilon *} = c_* - T_0\,\mathrm{Tr}[\boldsymbol{\alpha}_*\boldsymbol{\mathcal{C}}_*\boldsymbol{\alpha}_*]$$

are the specific heat per unit volume at constant strain and the effective specific heat per unit volume at constant strain. Written in this form, the tensor entering the constitutive law is not

positive-semidefinite. However, by a slight modification it can be made positive-semidefinite. One rewrites the equations in the form

$$\begin{pmatrix} \boldsymbol{\tau}(\boldsymbol{x}) \\ -\tau'(\boldsymbol{x}) \end{pmatrix} = \begin{pmatrix} \boldsymbol{C}(\boldsymbol{x}) & \boldsymbol{A}(\boldsymbol{x}) \\ \boldsymbol{A}(\boldsymbol{x}) & -c'_\epsilon(\boldsymbol{x})/T_0 \end{pmatrix} \begin{pmatrix} \boldsymbol{\epsilon}(\boldsymbol{x}) \\ \theta \end{pmatrix},$$

where

$$\varsigma'(\boldsymbol{x}) = \varsigma(\boldsymbol{x}) - t\theta/T_0, \quad c'_\epsilon(\boldsymbol{x}) = c_\epsilon(\boldsymbol{x}) - t, \tag{2.25}$$

and t is an arbitrary constant. Thus these fields solve the thermoelastic equations in a medium having specific heat $c'_\epsilon(\boldsymbol{x})$. If we choose t sufficiently large, the matrix entering the new constitutive relation will be positive-definite. Moreover, by taking averages of the fields, one sees that this new medium will have the same effective tensor as the original medium, but with effective specific heat

$$c'_{\epsilon *} = c_{\epsilon *} - t. \tag{2.26}$$

It was observed by Biot (1956), Rice and Cleary (1976), and Norris (1992) that the equations of poroelasticity are mathematically equivalent to those of linear thermoelasticity. These equations are appropriate for describing the average fluid and solid displacement in a fluid-filled porous medium subject to external stress and variations in the fluid pressure. Burridge and Keller (1981) provide a rigorous justification for the equations using homogenization theory.

We consider a material with variations in its microstructure on two widely separated length scales, the smallest scale ℓ_1 being set by the pore size and the largest scale ℓ_3 being set by, say, the variation in material moduli, or by the variation in porosity $\phi(\boldsymbol{x})$. The pore geometry is described by the characteristic function

$$\begin{aligned} \chi(\boldsymbol{x}) &= 1 \ \text{ within the pores,} \\ &= 0 \ \text{ within the solid,} \end{aligned}$$

which, when averaged on an intermediate length scale ℓ_2 with $\ell_1 \ll \ell_2 \ll \ell_3$, defines the porosity,

$$\phi(\boldsymbol{x}) = \langle \chi \rangle_\Omega,$$

where the angular brackets $\langle\ \rangle_\Omega$ denote a local average, defined by (1.4), of the bracketed expression over a cube of side ℓ_2 centered at $\boldsymbol{x}$. The other fields that we consider are the fluid pressure p_f, which is constant; the confining stress

$$\boldsymbol{\tau}_c(\boldsymbol{x}) = \langle \boldsymbol{\tau} \rangle_\Omega,$$

which includes contributions from the stress $\boldsymbol{\tau}(\boldsymbol{x})$ in the solid and from the stress

$$\chi(\boldsymbol{x})\boldsymbol{\tau}(\boldsymbol{x}) = -p_f \chi(\boldsymbol{x}) \boldsymbol{I}$$

in the fluid-filled pores; the average solid and fluid displacements

$$\boldsymbol{u}_s(\boldsymbol{x}) = \frac{\langle (1-\chi)\boldsymbol{u} \rangle_\Omega}{1 - \phi(\boldsymbol{x})}, \qquad \boldsymbol{u}_f(\boldsymbol{x}) = \frac{\langle \chi \boldsymbol{u} \rangle_\Omega}{\phi(\boldsymbol{x})},$$

where $\boldsymbol{u}(\boldsymbol{x})$ is the microscopic displacement of fluid or solid; and the increment of fluid content

$$\zeta(\boldsymbol{x}) = \phi(\boldsymbol{x}) \nabla \cdot [\boldsymbol{u}_s(\boldsymbol{x}) - \boldsymbol{u}_f(\boldsymbol{x})],$$

which measures the net fluid flow per unit volume in or out of a region.

The constitutive relations take the form

$$\begin{pmatrix} \boldsymbol{\epsilon}_s(\boldsymbol{x}) \\ -\zeta(\boldsymbol{x}) \end{pmatrix} = \begin{pmatrix} \boldsymbol{\mathcal{S}}(\boldsymbol{x}) & \boldsymbol{\alpha}(\boldsymbol{x}) \\ \boldsymbol{\alpha}(\boldsymbol{x}) & c(\boldsymbol{x}) \end{pmatrix} \begin{pmatrix} \boldsymbol{\tau}_c(\boldsymbol{x}) \\ -p_f \end{pmatrix}, \tag{2.27}$$

where

$$\boldsymbol{\epsilon}_s = [\nabla \boldsymbol{u}_s + (\nabla \boldsymbol{u}_s)^T]/2, \quad \nabla \cdot \boldsymbol{\tau}_c = 0, \tag{2.28}$$

$\boldsymbol{\mathcal{S}}(\boldsymbol{x})$ is now the compliance tensor of the drained porous frame, $\boldsymbol{\alpha}(\boldsymbol{x})$ is now the tensor of fluid pressure induced expansion (at constant confining stress), and $c(\boldsymbol{x})$ is now the coefficient relating the increment of fluid content to the fluid pressure (again at constant confining stress).

On a length scale much larger than ℓ_3, the behavior is governed by the equations

$$\begin{pmatrix} \langle \boldsymbol{\epsilon}_s \rangle \\ -\langle \zeta \rangle \end{pmatrix} = \begin{pmatrix} \boldsymbol{\mathcal{S}}_* & \boldsymbol{\alpha}_* \\ \boldsymbol{\alpha}_* & c_* \end{pmatrix} \begin{pmatrix} \langle \boldsymbol{\tau}_c \rangle \\ -p_f \end{pmatrix},$$

which serve to define the effective moduli. These effective poroelastic moduli determine the speeds of acoustic waves in poroelastic media. One interesting feature is that acoustic waves can travel at three different speeds in an isotropic poroelastic medium. (By contrast, acoustic waves travel at two different speeds in an isotropic elastic medium, depending on whether it is a shear wave or a compressional wave.)

By comparing (2.27) and (2.28) with (2.21) it is clear that the equations of poroelasticity are mathematically analogous to the equations of thermal expansion. Consequently, any results pertaining to thermoelasticity immediately extend to poroelasticity, and vice versa. The equations of poroelasticity remain the subject of active research; see, for example, the recent Biot memorial issue on poroelasticity edited by Cheng, Detournay, and Abousleiman (eds.) (1998).

2.6. Pyroelectric equations and their relation to conductivity and magnetotransport equations in fibrous composites

What distinguishes the thermoelastic and poroelastic problems is that a constant field, namely, the temperature or pressure, enters the constitutive relation. We will refer to such problems as thermoelastic-type problems. The equations of pyroelectricity (Landau and Lifshitz 1960) fall into this category and take the form:

$$\boldsymbol{d}(\boldsymbol{x}) = \boldsymbol{\epsilon}(\boldsymbol{x})\boldsymbol{e}(\boldsymbol{x}) + \boldsymbol{\alpha}(\boldsymbol{x})\theta, \quad \nabla \cdot \boldsymbol{d} = 0, \quad \nabla \times \boldsymbol{e} = 0, \quad \theta = \text{constant}, \tag{2.29}$$

where $\boldsymbol{d}(\boldsymbol{x})$ and $\boldsymbol{e}(\boldsymbol{x})$ are the electric displacement and electric fields, $\boldsymbol{\epsilon}(\boldsymbol{x})$ is the dielectric tensor fields, θ is the constant temperature increment, and $\boldsymbol{\alpha}(\boldsymbol{x})\theta$ is the pyroelectric vector.

This type of equation also arises from the basic conductivity, elasticity, or coupled field equations in fibrous composites, that is, when the microstructure and hence the fields are independent of x_3. In section 2.1 on page 19 we saw how the three-dimensional conductivity equations reduce to two-dimensional conductivity equations in such a microgeometry when the off-diagonal components $\sigma_{13}(\boldsymbol{x})$ and $\sigma_{23}(\boldsymbol{x})$ of the conductivity tensor $\boldsymbol{\sigma}(\boldsymbol{x})$ are zero. When they are not zero, the constitutive relation can be expressed in the form

$$\begin{pmatrix} \boldsymbol{j}' \\ j_3 \end{pmatrix} = \begin{pmatrix} \boldsymbol{\sigma}' & \boldsymbol{\alpha} \\ \boldsymbol{\alpha}^T & \sigma_{33} \end{pmatrix} \begin{pmatrix} \boldsymbol{e}' \\ e_3 \end{pmatrix}, \tag{2.30}$$

where $\boldsymbol{j}'(\boldsymbol{x})$ and $\boldsymbol{e}'(\boldsymbol{x})$ are the two-dimensional divergence free and curl free fields defined by (2.2), $\boldsymbol{\sigma}'(\boldsymbol{x})$ is the two-dimensional conductivity tensor field defined by (2.3), and $\boldsymbol{\alpha}(\boldsymbol{x})$ (which we can think of as being like the tensor of thermal expansion) is the vector field

$$\boldsymbol{\alpha}(\boldsymbol{x}) = \begin{pmatrix} \sigma_{13}(\boldsymbol{x}) \\ \sigma_{23}(\boldsymbol{x}) \end{pmatrix}.$$

As mentioned earlier, the field component e_3 is constant (we can think of it as being like the temperature increment in the thermoelastic equations) while the field component $j_3(x_1, x_2)$ is not subject to any differential constraints (we can think of it as being like the entropy in the thermoelastic equations). Since $j_3(x_1, x_2)$ is not subject to any differential constraints, we can ignore it when solving the equations and instead focus on the reduced system,

$$\boldsymbol{j}'(\boldsymbol{x}) = \boldsymbol{\sigma}'(\boldsymbol{x})\boldsymbol{e}'(\boldsymbol{x}) + \boldsymbol{\alpha}(\boldsymbol{x})e_3, \quad \nabla \cdot \boldsymbol{j}' = 0, \quad \nabla \times \boldsymbol{e}' = 0, \quad e_3 = \text{constant}, \tag{2.31}$$

which is clearly mathematically equivalent to the pyroelectric equations (2.29).

Similar equations arise in certain magnetotransport problems in fibrous composites. Consider a locally isotropic conducting medium with a microstructure independent of x_3, which is subsequently subject to a constant magnetic field $\boldsymbol{h}$ applied perpendicular to the x_3-axis, say, with $h_2 = h_3 = 0$. The constitutive relation (2.4) can be rewritten in the equivalent form

$$\begin{pmatrix} \boldsymbol{j}' \\ j_3 \end{pmatrix} = \begin{pmatrix} \boldsymbol{\sigma}' & \boldsymbol{\alpha} \\ -\boldsymbol{\alpha}^T & \sigma_{33} \end{pmatrix} \begin{pmatrix} \boldsymbol{e}' \\ e_3 \end{pmatrix}, \tag{2.32}$$

where

$$\boldsymbol{\sigma}' = \begin{pmatrix} 1/\alpha & 0 \\ 0 & \alpha/(\alpha^2 + R^2 h_1^2) \end{pmatrix}, \quad \boldsymbol{\alpha} = \begin{pmatrix} 0 \\ Rh_1/(\alpha^2 + R^2 h_1^2) \end{pmatrix}, \quad \sigma_{33} = \alpha/(\alpha^2 + R^2 h_1^2). \tag{2.33}$$

Since $j_3(x_1, x_2)$ is not subject to any differential constraints, we arrive back at exactly the same system of reduced equations (2.31) as we would have obtained from the system of equations (2.30) with a symmetric conductivity matrix. A related conclusion was reached by Bergman and Strelniker (1998) and Strelniker and Bergman (2000) through quite different arguments. [See also Bergman and Strelniker (1994) and Tornow, Weiss, v. Klitzing, Eberl, Bergman, and Strelniker (1996), where these equations are solved for square arrays of cylinders and compared with experiments.]

It follows that if

$$\boldsymbol{\sigma}_* = \begin{pmatrix} \boldsymbol{\sigma}'_* & \boldsymbol{\alpha}_* \\ \boldsymbol{\alpha}_*^T & c_* \end{pmatrix}$$

is the effective conductivity tensor associated with equations (2.30), then

$$\boldsymbol{\sigma}_* = \begin{pmatrix} \boldsymbol{\sigma}'_* & \boldsymbol{\alpha}_* \\ -\boldsymbol{\alpha}_*^T & 2\langle\sigma_{33}\rangle - c_* \end{pmatrix}$$

will be the effective conductivity tensor associated with the equations (2.32). The effective constant of $2\langle\sigma_{33}\rangle - c_*$ arises because although $\boldsymbol{j}'$ and $\boldsymbol{e}'$ are the same for both problems, the average value of j_3,

$$\langle j_3\rangle = \langle \boldsymbol{\alpha}^T \boldsymbol{e}'\rangle + \langle\sigma_{33}\rangle\theta = \boldsymbol{\alpha}_*^T\langle \boldsymbol{e}'\rangle + c_*\theta, \tag{2.34}$$

in equations (2.30) differs from the average value of j_3,

$$\langle j_3\rangle = -\langle \boldsymbol{\alpha}^T \boldsymbol{e}'\rangle + \langle\sigma_{33}\rangle\theta = -\boldsymbol{\alpha}_*^T\langle \boldsymbol{e}'\rangle + (2\langle\sigma_{33}\rangle - c_*)\theta, \tag{2.35}$$

in equations (2.32).

Pyroelectric type equations also arise from the analysis of coupled equations when certain blocks of moduli are constant and of an appropriate form. For example, consider the following coupled field equations:

$$\begin{pmatrix} \boldsymbol{j}_1 \\ \boldsymbol{j}_2 \end{pmatrix} = \boldsymbol{L} \begin{pmatrix} \boldsymbol{e}_1 \\ \boldsymbol{e}_2 \end{pmatrix}, \quad \text{where } \nabla \cdot \boldsymbol{j}_1 = \nabla \cdot \boldsymbol{j}_2 = 0, \ \ \nabla \times \boldsymbol{e}_1 = \nabla \times \boldsymbol{e}_2 = 0,$$

with a tensor $\boldsymbol{L}(\boldsymbol{x})$ of the form

$$\boldsymbol{L}(\boldsymbol{x}) = \begin{pmatrix} \boldsymbol{\sigma}(\boldsymbol{x}) & c_1 \boldsymbol{I} \\ c_1 \boldsymbol{I} & c_2 \boldsymbol{I} \end{pmatrix},$$

where c_1 and c_2 are constants and $\boldsymbol{I}$ is the identity tensor. Since

$$\boldsymbol{j}_2(\boldsymbol{x}) = c_1 \boldsymbol{e}_1(\boldsymbol{x}) + c_2 \boldsymbol{e}_2(\boldsymbol{x})$$

is both divergence free and curl free, it must necessarily be a constant field. Using this equation to express $\boldsymbol{e}_2$ in terms of $\boldsymbol{j}_2$ and $\boldsymbol{e}_1$, and substituting the result into the formula for $\boldsymbol{j}_1$ implied by the constitutive relation, gives

$$\boldsymbol{j}_1 = [\boldsymbol{\sigma}(\boldsymbol{x}) - (c_1^2/c_2)\boldsymbol{I}]\boldsymbol{e}_1 + (c_1/c_2)\boldsymbol{j}_2.$$

Since $\boldsymbol{j}_2$ is a constant vector, while $\boldsymbol{j}_1$ and $\boldsymbol{e}_1$ are, respectively, divergence free and curl free, this is clearly a pyroelectric-type equation.

2.7. The equivalence between elasticity in fibrous composites and two-dimensional piezoelectricity and thermoelasticity

The relationship between three-dimensional elasticity in fibrous composites and two-dimensional piezoelectricity has been studied by Milton (1997), Chen and Lai (1997), and Chen (1998). Consider a lattice of aligned circular or square cylinders or, more generally, any microstructure that is invariant with respect to spatial translations in one direction. Let us choose our coordinate-ordinate system so that this direction is the x_3-axis. Then the elasticity tensor field $\boldsymbol{\mathcal{C}}(\boldsymbol{x})$ will depend only on the spatial coordinates x_1 and x_2, and not on x_3. The periodic stress and strain fields, being unique, must be similarly independent of x_3. Consequently, the differential constraints on the stress field $\boldsymbol{\tau}(\boldsymbol{x})$ imply that

$$\frac{\partial \tau_{11}}{\partial x_1} + \frac{\partial \tau_{12}}{\partial x_2} = 0, \quad \frac{\partial \tau_{12}}{\partial x_1} + \frac{\partial \tau_{22}}{\partial x_2} = 0, \quad \frac{\partial \tau_{13}}{\partial x_1} + \frac{\partial \tau_{23}}{\partial x_2} = 0. \tag{2.36}$$

Notice that the stress field component τ_{33} is not subject to any differential restrictions. Since the strain components do not depend on x_3, the displacement field (apart from overall rotations) must be of the form

$$\boldsymbol{u}(\boldsymbol{x}) = \boldsymbol{u}'(x_1, x_2) + x_3 \boldsymbol{v},$$

that is, it depends linearly on x_3 with a constant coefficient $\boldsymbol{v}$. In terms of $\boldsymbol{u}'$ and $\boldsymbol{v}$ the strain field components are

$$\begin{aligned} &\epsilon_{11} = \partial u_1'/\partial x_1, \qquad \epsilon_{12} = (\partial u_1'/\partial x_2 + \partial u_2'/\partial x_1)/2, \quad \epsilon_{22} = \partial u_2'/\partial x_2, \\ &\epsilon_{13} = (v_1 + \partial u_3'/\partial x_1)/2, \quad \epsilon_{23} = (v_2 + \partial u_3'/\partial x_2)/2, \quad \epsilon_{33} = v_3. \end{aligned} \tag{2.37}$$

In particular, this implies that the strain field component ϵ_{33} must be constant.

Now observe that the constitutive relation (2.6) for elasticity can be rewritten in the equivalent form:

$$\begin{pmatrix} \tau_{11} \\ \tau_{22} \\ \sqrt{2}\tau_{12} \\ e_1' \\ e_2' \\ \tau_{33} \end{pmatrix} = \begin{pmatrix} C_{1111} & C_{1122} & \sqrt{2}C_{1112} & \sqrt{2}C_{1123} & -\sqrt{2}C_{1113} & C_{1133} \\ C_{1122} & C_{2222} & \sqrt{2}C_{2212} & \sqrt{2}C_{2223} & -\sqrt{2}C_{2213} & C_{2233} \\ \sqrt{2}C_{1112} & \sqrt{2}C_{2212} & 2C_{1212} & 2C_{2312} & -2C_{1312} & \sqrt{2}C_{3312} \\ \sqrt{2}C_{1123} & \sqrt{2}C_{2223} & 2C_{2312} & 2C_{2323} & -2C_{2313} & \sqrt{2}C_{3323} \\ -\sqrt{2}C_{1113} & -\sqrt{2}C_{2213} & -2C_{1312} & -2C_{2313} & 2C_{1313} & -\sqrt{2}C_{3313} \\ C_{1133} & C_{2233} & \sqrt{2}C_{3312} & \sqrt{2}C_{3323} & -\sqrt{2}C_{3313} & C_{3333} \end{pmatrix} \begin{pmatrix} \epsilon_{11} \\ \epsilon_{22} \\ \sqrt{2}\epsilon_{12} \\ d_1' \\ d_2' \\ \epsilon_{33} \end{pmatrix} \tag{2.38}$$

where $e_1'(x_1, x_2)$, $e_2'(x_1, x_2)$, $d_1'(x_1, x_2)$, and $d_2'(x_1, x_2)$ are components of the fields

$$\boldsymbol{e}' = \begin{pmatrix} e_1' \\ e_2' \end{pmatrix} = \begin{pmatrix} \sqrt{2}\tau_{23} \\ -\sqrt{2}\tau_{13} \end{pmatrix}, \quad \boldsymbol{d}' = \begin{pmatrix} d_1' \\ d_2' \end{pmatrix} = \begin{pmatrix} \sqrt{2}\epsilon_{23} \\ -\sqrt{2}\epsilon_{13} \end{pmatrix}.$$

From the constraints (2.36) and (2.37) on the stress and strain components we see that

$$\frac{\partial e_1'}{\partial x_2} - \frac{\partial e_2'}{\partial x_1} = 0, \quad \frac{\partial d_1'}{\partial x_1} + \frac{\partial d_2'}{\partial x_2} = 0.$$

In other words, $\boldsymbol{e}'(x_1, x_2)$ and $\boldsymbol{d}'(x_1, x_2)$ are, respectively, curl free and divergence free fields. We can think of $\boldsymbol{e}'(\boldsymbol{x})$ as an "electric field" and $\boldsymbol{d}'(\boldsymbol{x})$ as an "electric displacement field."

Let us also introduce the two-dimensional stress field

$$\boldsymbol{\tau}' = \begin{pmatrix} \tau_{11} & \tau_{12} \\ \tau_{12} & \tau_{22} \end{pmatrix}, \tag{2.39}$$

which, according to (2.36), is divergence free, and let us introduce the two-dimensional strain field

$$\boldsymbol{\epsilon}' = \begin{pmatrix} \epsilon_{11} & \epsilon_{12} \\ \epsilon_{12} & \epsilon_{22} \end{pmatrix}, \tag{2.40}$$

which, according to (2.37), derives from the two-dimensional displacement field $\boldsymbol{u}'(x_1, x_2)$. These strain and stress fields can be represented by the three-component vectors

$$\boldsymbol{\epsilon}' = \begin{pmatrix} \epsilon_{11} \\ \epsilon_{22} \\ \sqrt{2}\epsilon_{12} \end{pmatrix}, \qquad \boldsymbol{\tau}' = \begin{pmatrix} \tau_{11} \\ \tau_{22} \\ \sqrt{2}\tau_{12} \end{pmatrix}.$$

In the case when there is no axial stretching, that is, when $\epsilon_{33} = 0$, the constitutive relation (2.38) implies that

$$\begin{pmatrix} \boldsymbol{\tau}'(\boldsymbol{x}) \\ \boldsymbol{e}'(\boldsymbol{x}) \end{pmatrix} = \boldsymbol{L}(\boldsymbol{x}) \begin{pmatrix} \boldsymbol{\epsilon}'(\boldsymbol{x}) \\ \boldsymbol{d}'(\boldsymbol{x}) \end{pmatrix},$$

where $\boldsymbol{L}(\boldsymbol{x}) = \boldsymbol{L}(x_1, x_2)$ is the 5×5 symmetric matrix

$$\boldsymbol{L} = \begin{pmatrix} C_{1111} & C_{1122} & \sqrt{2}C_{1112} & \sqrt{2}C_{1123} & -\sqrt{2}C_{1113} \\ C_{1122} & C_{2222} & \sqrt{2}C_{2212} & \sqrt{2}C_{2223} & -\sqrt{2}C_{2213} \\ \sqrt{2}C_{1112} & \sqrt{2}C_{2212} & 2C_{1212} & 2C_{2312} & -2C_{1312} \\ \sqrt{2}C_{1123} & \sqrt{2}C_{2223} & 2C_{2312} & 2C_{2323} & -2C_{2313} \\ -\sqrt{2}C_{1113} & -\sqrt{2}C_{2213} & -2C_{1312} & -2C_{2313} & 2C_{1313} \end{pmatrix}.$$

This matrix, being a principal submatrix of $\mathcal{C}(\boldsymbol{x})$, is positive-definite when the elasticity tensor $\mathcal{C}(\boldsymbol{x})$ is positive-definite. We have thus reduced the three-dimensional elasticity problem to an equivalent two-dimensional piezoelectric problem. From the effective tensor $\boldsymbol{L}_*$ of the two-dimensional piezoelectric problem we can recover most of the components $C^*_{ijk\ell}$ of the effective elasticity tensor $\mathcal{C}_*$ by using the identity

$$\boldsymbol{L}_* = \begin{pmatrix} C^*_{1111} & C^*_{1122} & \sqrt{2}C^*_{1112} & \sqrt{2}C^*_{1123} & -\sqrt{2}C^*_{1113} \\ C^*_{1122} & C^*_{2222} & \sqrt{2}C^*_{2212} & \sqrt{2}C^*_{2223} & -\sqrt{2}C^*_{2213} \\ \sqrt{2}C^*_{1112} & \sqrt{2}C^*_{2212} & 2C^*_{1212} & 2C^*_{2312} & -2C^*_{1312} \\ \sqrt{2}C^*_{1123} & \sqrt{2}C^*_{2223} & 2C^*_{2312} & 2C^*_{2323} & -2C^*_{2313} \\ -\sqrt{2}C^*_{1113} & -\sqrt{2}C^*_{2213} & -2C^*_{1312} & -2C^*_{2313} & 2C^*_{1313} \end{pmatrix}.$$

If in the process of solving the two-dimensional piezoelectric problem we keep track of the fields $\boldsymbol{\epsilon}'(\boldsymbol{x})$ and $\boldsymbol{d}'(\boldsymbol{x})$, for five linearly independent choices of the applied fields, then by averaging the formula

$$\tau_{33} = C_{1133}\epsilon_{11} + C_{2233}\epsilon_{22} + 2C_{3312}\epsilon_{12} + \sqrt{2}C_{3323}d'_1 - \sqrt{2}C_{3313}d'_2,$$

which yields the identity

$$\begin{aligned}\langle C_{1133}\epsilon_{11} + C_{2233}\epsilon_{22} + 2C_{3312}\epsilon_{12} + \sqrt{2}C_{3323}d'_1 - \sqrt{2}C_{3313}d'_2\rangle \\ = C^*_{1133}\langle\epsilon_{11}\rangle + C^*_{2233}\langle\epsilon_{22}\rangle + 2C^*_{3312}\langle\epsilon_{12}\rangle + \sqrt{2}C^*_{3323}\langle d'_1\rangle - \sqrt{2}C^*_{3313}\langle d'_2\rangle,\end{aligned}$$

we can recover all of the remaining elements of the effective elasticity tensor apart from C^*_{3333}. For two-phase composites, and some polycrystalline materials, it turns out that one can recover all elements of $\mathcal{C}^*$ from $\boldsymbol{L}_*$ (including C^*_{3333}) without keeping track of the fields $\boldsymbol{\epsilon}'(\boldsymbol{x})$ and $\boldsymbol{d}'(\boldsymbol{x})$; this will be discussed further in section 5.9 on page 86.

Sometimes the symmetry of the elastic material may be such that it is invariant under reflection in the (x_1, x_2)-plane, that is, invariant under the transformation $x_3 \to -x_3$, implying that all components of the elasticity tensor having an odd number of indices taking the value 3 are zero:

$$C_{1123} = C_{1113} = C_{2223} = C_{1123} = C_{2213} = C_{1312} = C_{2312} = C_{3313} = C_{3323} = 0. \quad (2.41)$$

In this case the two-dimensional piezoelectric problem decouples into a two-dimensional elastic problem (the plane strain problem):

$$\boldsymbol{\tau}' = \mathcal{C}'\boldsymbol{\epsilon}', \quad \text{where } \mathcal{C}' = \begin{pmatrix} C_{1111} & C_{1122} & \sqrt{2}C_{1112} \\ C_{1122} & C_{2222} & \sqrt{2}C_{2212} \\ \sqrt{2}C_{1112} & \sqrt{2}C_{2212} & 2C_{1212} \end{pmatrix},$$

and a two-dimensional dielectric problem (the antiplane elasticity problem):

$$\boldsymbol{d}' = \boldsymbol{\varepsilon}\boldsymbol{e}', \quad \text{where } \boldsymbol{\varepsilon} = \begin{pmatrix} 2C_{2323} & -2C_{2313} \\ -2C_{2313} & 2C_{1313} \end{pmatrix}^{-1}. \quad (2.42)$$

The equations for antiplane elasticity can be expressed alternatively in the form

$$\begin{pmatrix} \tau_{13} \\ \tau_{23} \end{pmatrix} = \boldsymbol{\mu}\begin{pmatrix} 2\epsilon_{13} \\ 2\epsilon_{23} \end{pmatrix}, \quad \text{where } \boldsymbol{\mu} = \begin{pmatrix} C_{1313} & C_{2313} \\ C_{2313} & C_{2323} \end{pmatrix},$$

in which the fields on the left and right of the constitutive relation are, respectively, divergence free and curl free. The shear matrix $\boldsymbol{\mu}(\boldsymbol{x})$ equals $\mu(\boldsymbol{x})\boldsymbol{I}$ when the material is locally isotropic with shear modulus $\mu(\boldsymbol{x})$. For more about antiplane elasticity see, for example, Milne-Thomson (1962) or Atkin and Fox (1980).

From the associated two-dimensional effective elasticity tensor $\boldsymbol{\mathcal{C}}'_*$ and effective shear matrix $\boldsymbol{\mu}_*$, and from the solution for the stress field $\boldsymbol{\epsilon}'(\boldsymbol{x})$ in the two-dimensional elasticity problem (with $\epsilon_{33} = 0$) for three different applied fields, we obtain all nonzero elements of the three-dimensional effective elasticity tensor apart from C^*_{3333} by using the identities

$$\boldsymbol{\mathcal{C}}'_* = \begin{pmatrix} C^*_{1111} & C^*_{1122} & \sqrt{2}C^*_{1112} \\ C^*_{1122} & C^*_{2222} & \sqrt{2}C^*_{2212} \\ \sqrt{2}C^*_{1112} & \sqrt{2}C^*_{2212} & 2C^*_{1212} \end{pmatrix}, \quad \boldsymbol{\mu}_* = \begin{pmatrix} C^*_{1313} & C^*_{2313} \\ C^*_{2313} & C^*_{2323} \end{pmatrix}, \tag{2.43}$$

and

$$\langle C_{1133}\epsilon_{11} + C_{2233}\epsilon_{22} + 2C_{3312}\epsilon_{12}\rangle = C^*_{1133}\langle\epsilon_{11}\rangle + C^*_{2233}\langle\epsilon_{22}\rangle + 2C^*_{3312}\langle\epsilon_{12}\rangle.$$

To recover C^*_{3333} one needs to take nonzero values for the constant ϵ_{33}. From (2.38) and (2.41), the constitutive relation relating the two-dimensional stress and strain fields takes the same basic form:

$$\begin{pmatrix} \boldsymbol{\tau}' \\ \tau_{33} \end{pmatrix} = \begin{pmatrix} \boldsymbol{\mathcal{C}}' & \boldsymbol{A} \\ \boldsymbol{A}^T & C_{3333} \end{pmatrix} \begin{pmatrix} \boldsymbol{\epsilon}' \\ \epsilon_{33} \end{pmatrix}, \quad \text{where } \boldsymbol{A}(\boldsymbol{x}) = \begin{pmatrix} C_{1133}(\boldsymbol{x}) \\ C_{2233}(\boldsymbol{x}) \\ \sqrt{2}C_{1233}(\boldsymbol{x}) \end{pmatrix}, \tag{2.44}$$

as the constitutive relation for thermoelasticity in a two-dimensional medium, with the constant field ϵ_{33} playing the role of the temperature increment θ and $-\tau_{33}$ playing the role of the entropy ς. This connection is made more apparent if we use the representation where $\boldsymbol{\tau}'$ and $\boldsymbol{\epsilon}'$ are represented by 2×2 matrices as in (2.39) and (2.40). Then the constitutive relation takes exactly the same form,

$$\begin{pmatrix} \boldsymbol{\tau}' \\ \tau_{33} \end{pmatrix} = \begin{pmatrix} \boldsymbol{\mathcal{C}}' & \boldsymbol{A} \\ \boldsymbol{A} & C_{3333} \end{pmatrix} \begin{pmatrix} \boldsymbol{\epsilon}' \\ \epsilon_{33} \end{pmatrix}, \quad \text{where } \boldsymbol{A}(\boldsymbol{x}) = \begin{pmatrix} C_{1133}(\boldsymbol{x}) & C_{1233}(\boldsymbol{x}) \\ C_{1233}(\boldsymbol{x}) & C_{2233}(\boldsymbol{x}) \end{pmatrix}, \tag{2.45}$$

as the thermoelastic constitutive relation (2.24). The elements C^*_{1133}, C^*_{1233}, and C^*_{2233} of the effective elasticity tensor then can be identified with the elements of the effective tensor of thermal stress

$$\boldsymbol{A}_* = \begin{pmatrix} C^*_{1133} & C^*_{1233} \\ C^*_{1233} & C^*_{2233} \end{pmatrix} \tag{2.46}$$

associated with the two-dimensional thermoelastic medium. The constant C^*_{3333} can be obtained from the effective constant of specific heat at constant strain in the associated two-dimensional thermoelastic medium, with, say, $T_0 = 1$.

2.8. Numerical methods for finding effective tensors

Many numerical methods for calculating effective tensors have been developed. Ideally, a whole book should be written about this important subject, and it is difficult to do it justice here. This section is intended only as a brief introduction, and the interested reader is encouraged to refer to the papers referenced. The reader should also bear in mind that sometimes

results are reported which give worse estimates than previous work, and in which errors occur well before the last digit given in the result.

For the dielectric constant of periodic arrays of aligned circular cylinders and periodic lattices of spheres Rayleigh (1892) developed an approach based on matching coefficients in the multipole expansions, in cylindrical or spherical harmonics, of the electrical potential around a given cylinder or sphere. Once computers became sufficiently powerful, this method provided accurate solutions for the effective dielectric constant (Doyle 1978; McKenzie, McPhedran, and Derrick 1978; McPhedran and McKenzie 1978; Perrins, McKenzie, and McPhedran 1979). An alternative approach of Zuzovsky and Brenner (1977) was shown by Sangani and Acrivos (1983) to yield exactly the same set of equations for the multipole coefficients. Rayleigh's method failed to give accurate answers only when the cylinders or spheres were close to touching and had a very high or very low dielectric constant compared with the surrounding matrix. The extension of the method to other inclusion shapes, such as to arrays of aligned elliptical cylinders (Yardley, McPhedran, Nicorovici, and Botten 1999), requires care to ensure convergence. To calculate the elastic moduli of cubic lattices of spheres Sangani and Lu (1987) matched coefficients in the expansion of the displacement field around a given sphere in spherical harmonics. McPhedran and Movchan (1994) extended Rayleigh's method to planar elasticity. Lam (1986) applied it to calculate the dynamic magnetic permeability of cubic lattices of conducting magnetic spheres, including the effects of eddy currents, that is, the magnetic fields generated by induced electrical currents.

Bergman (1979) showed how the dielectric constant of a cubic array of spheres could be obtained from calculations of the electrostatic resonances. This approach was extended to elasticity by Kantor and Bergman (1982). McPhedran and Milton (1981), Sangani and Yao (1988a, 1988b), Helsing (1994), and Tokarzewski and Telega (1997) show how the calculation of high-order bounds can give accurate results for the effective conductivity of periodic arrays of spheres or aligned cylinders containing from one to as many as 16 randomly placed inclusions in the unit cell. Bonnecaze and Brady (1990, 1991) have developed another method that includes both near-field and far-field interactions to compute the effective dielectric properties of both periodic and random suspensions of spheres.

In a dielectric material, where only two isotropic phases are present, the fields within each phase are generated by the uniform applied field and by the polarization charges on the interfaces between the phases. Thus the density of polarization charges on the interfaces should satisfy an integral equation. One can then use the fast multipole method (Rokhlin 1985; Greengard and Rokhlin 1987; Carrier, Greengard, and Rokhlin 1988) to solve the resulting boundary integral equation. This is a fast way of computing the field due to a set of charges. Also, integrals over the interface around any inclusion can be computed by using the trapezoidal rule, which provides superalgebraic convergence. By this means the fields and effective coefficients in two-dimensional, two-phase microstructures have been computed with unparalleled accuracy and efficiency (Greengard and Moura 1994; Helsing 1998). Boundary integral equation methods have also been developed for two-phase composites containing anisotropic conducting materials (Helsing 1995b, 1995c; Helsing and Samuelsson 1995); for planar elasticity, with both isotropic and isotropic phases (Eischen and Torquato 1993; Helsing 1995a; Helsing, Milton, and Movchan 1997); and for three-dimensional elasticity (Nunan and Keller 1984). The fast multipole method has also been utilized to accelerate the solution of the planar elasticity equations (Greengard and Helsing 1998; Helsing 2000), yielding results for the effective elastic moduli of incredible accuracy. Not so much progress has been made for three-dimensional composites. However, a suitable three-dimensional fast multipole method is now available (Cheng, Greengard, and Rokhlin 1999).

To calculate the conductivity of a plate out of which randomly centered holes have been cut Garboczi, Thorpe, DeVries, and Day (1991) treated the plate as a two-dimensional resistor network [which is equivalent to solving the conductivity equations using a finite difference scheme, as explained, for example, by Hornung (1997)]. They then successively simplified the network using the $Y - \Delta$ algorithm of Frank and Lobb (1988) and thereby obtained the effective conductivity. For planar elasticity Day, Snyder, Garboczi, and Thorpe (1992) and Snyder, Garboczi, and Day (1992) treated a plate with circular inclusions as a spring network which they then solved. Finite element methods [see, for example, Davis (1992) and Helsing and Samuelsson (1995)] and multigrid methods (Eyre and Milton 1999) have also been used. Hou and Wu (1997) used a multiscale finite element method to simulate solving the homogenization problem directly.

Another approach to obtaining the effective conductivity has been developed and applied by Schwartz and Banavar (1989a, 1989b); Kim and Torquato (1990, 1991, 1992, 1993); McCarthy (1990, 1993); and Torquato, Kim, and Cule (1999). The approach uses the equivalence between the conductivity equations and the diffusion equations. Reasonable estimates of the effective diffusion coefficient and hence of the effective dielectric constant are obtained from the long-time behavior of the Brownian motion of a diffusing particle. The simulation time is reduced by letting the particle make jumps with the time being updated using a known first-passage time distribution.

Algorithms have been developed for treating high-contrast media with inclusions that have sharp corners or which are nearly touching (Milton, McPhedran, and McKenzie 1981; Helsing 1996, 1998; Cheng and Greengard 1997, 1998). For periodic composites, Fourier-based methods have been used with varying degrees of success (Nemat-Nasser, Iwakuma, and Hejazi 1982; Iwakuma and Nemat-Nasser 1983; Tao, Chen, and Sheng 1990; Bergman and Dunn 1992; Moulinec and Suquet 1994, 1998; Liu and Wu 1997; Eyre and Milton 1999; Ma, Zhang, Tam, and Sheng 2000; Michel, Moulinec and Suquet 2000, 2001). One advantage of these methods is that they can make use of the fast Fourier transform. They are best suited to problems where the moduli vary smoothly over the unit cell. We will return in section 14.11 on page 306 to discuss those Fourier methods associated with series expansions for the effective tensor.

References

Antman, S. S. 1995. *Nonlinear Problems of Elasticity*. Berlin / Heidelberg / London / etc.: Springer-Verlag. xviii + 750 pp. ISBN 0-387-94199-1. {*22, 40*}

Ashcroft, N. W. and N. D. Mermin 1976. *Solid State Physics*. Philadelphia: Saunders College. xxi + 826 pp. ISBN 0-03-083993-9 (College edition), 0-03-049346-3 (International edition). {*28, 40, 223, 224, 242*}

Atkin, R. J. and N. Fox 1980. *An Introduction to the Theory of Elasticity*. Harlow, Essex, United Kingdom: Longman Scientific and Technical. vii + 245 pp. ISBN 0-582-44283-4. {*22, 38, 40*}

Avellaneda, M. and G. Harshé 1994. Magnetoelectric effect in piezoelectric/magnetostrictive multilayer (2-2) composites. *Journal of Intelligent Material Systems and Structures* 5(4):501–513. {*4, 14, 30, 40*}

Batchelor, G. K. 1974. Transport properties of two-phase materials with random structure. *Annual Review of Fluid Mechanics* 6:227–255. {*19, 40*}

Bergman, D. J. 1979. The dielectric constant of a simple cubic array of identical spheres. *Journal of Physics C: Solid State Physics* 12:4947–4960. {*39, 40, 239, 242, 377, 380, 392*}

Bergman, D. J. and K.-J. Dunn 1992. Bulk effective dielectric constant of a composite with a periodic microgeometry. *Physical Review B (Solid State)* 45(23):13262–13271. {*40, 41*}

Bergman, D. J. and Y. M. Strelniker 1994. Calculation of strong-field magnetoresistance in some periodic composites. *Physical Review B (Solid State)* 49(23):16256–16268. {*34, 41*}

Bergman, D. J. and Y. M. Strelniker 1998. Duality transformation in a three dimensional conducting medium with two dimensional heterogeneity and an in-plane magnetic field. *Physical Review Letters* 80(15):3356–3359. {*34, 41, 51, 57*}

Biot, M. A. 1956. Thermoelasticity and irreversible thermodynamics. *Journal of Applied Physics* 27:240–253. {*32, 41*}

Bonnecaze, R. T. and J. F. Brady 1990. A method for determining the effective conductivity of dispersions of particles. *Proceedings of the Royal Society of London. Series A, Mathematical and Physical Sciences* 430:285–313. {*39, 41*}

Bonnecaze, R. T. and J. F. Brady 1991. The effective conductivity of random suspensions of spherical particles. *Proceedings of the Royal Society of London. Series A, Mathematical and Physical Sciences* 432:445–465. {*39, 41, 555, 565*}

Burridge, R. and J. B. Keller 1981. Poroelasticity equations derived from microstructure. *Journal of the Acoustical Society of America* 70:1140–1146. {*32, 41*}

Callen, H. B. 1960. *Thermodynamics: An Introduction to the Physical Theories of Equilibrium Thermostatics and Irreversible Thermodynamics*, pp. 293–302. New York / London / Sydney, Australia: John Wiley and Sons. {*28, 41*}

Carrier, J., L. Greengard, and V. Rokhlin 1988. A fast adaptive multipole algorithm for particle simulations. *SIAM Journal on Scientific and Statistical Computing* 9(4):669–686. {*39, 41*}

Chen, T. 1998. Further correspondences between plane piezoelectricity and generalized plane strain in elasticity. *Proceedings of the Royal Society of London. Series A, Mathematical and Physical Sciences* 454:873–884. {*35, 41*}

Chen, T. and D. Lai 1997. An exact correspondence between plane piezoelectricity and generalized plane strain in elasticity. *Proceedings of the Royal Society of London. Series A, Mathematical and Physical Sciences* 453:2689–2713. {*35, 41, 66, 71*}

Cheng, A. H.-D., E. Detournay, and Y. Abousleiman (eds.) 1998. Poroelasticity, Maurice A. Biot Memorial Issue. *International Journal of Solids and Structures* 35(34–35): 4513–5031. {*33, 41*}

Cheng, H. and L. Greengard 1997. On the numerical evaluation of electrostatic fields in dense random dispersions of cylinders. *Journal of Computational Physics* 136(2):629–639. {*40, 41, 210, 214*}

Cheng, H. and L. Greengard 1998. A method of images for the evaluation of electrostatic fields in systems of closely spaced conducting cylinders. *SIAM Journal on Applied Mathematics* 58(1):122–141. {*40, 41, 210, 214*}

Cheng, H., L. Greengard, and V. Rokhlin 1999. A fast adaptive multipole algorithm in three dimensions. *Journal of Computational Physics* 155(2):468–498. {*39, 42*}

Ciarlet, P. G. 1988. *Mathematical Elasticity. Volume I. Three-Dimensional Elasticity.* Amsterdam: North-Holland Publishing Co. xlii + 451 pp. ISBN 0-444-70259-8. {*22, 42*}

Ciarlet, P. G. 1997. *Mathematical Elasticity. Volume II. Theory of Plates.* Amsterdam: North-Holland Publishing Co. lxiv + 497 pp. ISBN 0-444-82570-3. {*26, 42*}

Davis, L. C. 1992. Calculating the elastic properties of composite materials. In *Advanced Composites: Design, Materials and Processing Technologies*, pp. 267–272. Materials Park, Ohio: ASM International. {*40, 42*}

Day, A. R., K. A. Snyder, E. J. Garboczi, and M. F. Thorpe 1992. The elastic moduli of a sheet containing circular holes. *Journal of the Mechanics and Physics of Solids* 40(5): 1031–1051. {*40, 42, 66, 68, 71*}

Doyle, W. T. 1978. The clausius-mossotti problem for cubic arrays of spheres. *Journal of Applied Physics* 49:795–797. {*39, 42*}

Eischen, J. W. and S. Torquato 1993. Determining elastic behavior of composites by the boundary element method. *Journal of Applied Physics* 74:159–170. {*39, 42, 558, 565*}

Eyre, D. J. and G. W. Milton 1999. A fast numerical scheme for computing the response of composites using grid refinement. *The European Physical Journal. Applied Physics* 6(1):41–47. {*40, 42, 303, 308, 310*}

Fannjiang, A. and G. Papanicolaou 1994. Convection enhanced diffusion for periodic flows. *SIAM Journal on Applied Mathematics* 54(2):333–408. {*22, 42, 265, 267, 277, 278, 287*}

Frank, D. J. and C. J. Lobb 1988. Highly efficient algorithm for percolative transport studies in two dimensions. *Physical Review B (Solid State)* 37(1):302–307. {*40, 42, 212, 215*}

Fung, Y. C. 1965. *Foundations of Solid Mechanics*. Upper Saddle River, New Jersey: Prentice-Hall. xiv + 525 pp. {*22, 25, 26, 30, 42*}

Garboczi, E. J., M. F. Thorpe, M. S. DeVries, and A. R. Day 1991. Universal conductivity curve for a plane containing random holes. *Physical Review A (Atomic, Molecular, and Optical Physics)* 43(12):6473–6482. {*40, 42*}

Greengard, L. and J. Helsing 1998. On the numerical evaluation of elastostatic fields in locally isotropic two-dimensional composites. *Journal of the Mechanics and Physics of Solids* 46(8):1441–1462. {*39, 42*}

Greengard, L. and M. Moura 1994. On the numerical evaluation of electrostatic fields in composite materials. *Acta Numerica* 3:379–410. Cambridge, United Kingdom: Cambridge University Press. {*39, 42, 188, 215*}

Greengard, L. and V. Rokhlin 1987. A fast algorithm for particle simulations. *Journal of Computational Physics* 73(2):325–348. {*39, 42*}

Helsing, J. 1994. Fast and accurate calculations of structural parameters for suspensions. *Proceedings of the Royal Society of London. Series A, Mathematical and Physical Sciences* 445:127–140. {*39, 42, 210, 216, 571, 598*}

Helsing, J. 1995c. A Nyström algorithm for electrostatics of an anisotropic composite. *Journal of Mathematical Physics* 36(6):2941–2950. {*39, 43*}

Helsing, J. 1995a. An integral equation method for elastostatics of periodic composites. *Journal of the Mechanics and Physics of Solids* 43(6):815–828. {*39, 43*}

Helsing, J. 1995b. An integral equation method for electrostatics of anisotropic composites. *Proceedings of the Royal Society of London. Series A, Mathematical and Physical Sciences* 450(1939):343–350. {*39, 43*}

Helsing, J. 1996. Thin bridges in isotropic electrostatics. *Journal of Computational Physics* 127(1):142–151. {*40, 43, 210, 216*}

Helsing, J. 1998. A high-order accurate algorithm for electrostatics of overlapping disks. *Journal of Statistical Physics* 90(5–6):1461–1473. {*39, 40, 43, 155, 156, 320, 337, 586, 598*}

Helsing, J. 2000. Fast and accurate numerical solution to an elastostatic problem involving ten thousand randomly oriented cracks. *International Journal of Fracture* 100(4):321–327. {*39, 43*}

Helsing, J., G. W. Milton, and A. B. Movchan 1997. Duality relations, correspondences and numerical results for planar elastic composites. *Journal of the Mechanics and Physics of Solids* 45(4):565–590. {*39, 43, 51, 53, 55, 57, 70, 72, 105, 106, 111*}

Helsing, J. and K. Samuelsson 1995. Electrostatics of anisotropic inclusions in anisotropic media. *Journal of Applied Physics* 78(4):2498–2503. {*39, 40, 43*}

Hornung, U. 1997. Introduction. In U. Hornung (ed.), *Homogenization and Porous Media*, pp. 1–25. Berlin / Heidelberg / London / etc.: Springer-Verlag. ISBN 0-387-94786-8. {*40, 43*}

Hou, T. Y. and X.-H. Wu 1997. A multiscale finite element method for elliptic problems in composite materials and porous media. *Journal of Computational Physics* 134(1): 169–189. {*40, 43*}

Ikeda, T. 1996. *Fundamentals of Piezoelectricity* (Corrected paperback ed.). Oxford, United Kingdom: Oxford University Press. xi + 263 pp. ISBN 0-19-856460-0. {*29, 43*}

Iwakuma, T. and S. Nemat-Nasser 1983. Composites with periodic microstructure. *Computers and Structures* 16(1–4):13–19. {*40, 43*}

Kantor, Y. and D. J. Bergman 1982. Elastostatic resonances- a new approach to the calculation of the effective elastic constants of composites. *Journal of the Mechanics and Physics of Solids* 30:355–376. {*39, 43, 370, 371, 393*}

Kim, I. C. and S. Torquato 1990. Determination of the effective conductivity of heterogeneous media by Brownian motion simulation. *Journal of Applied Physics* 68(8):3892–3903. {*40, 43, 586, 598*}

Kim, I. C. and S. Torquato 1991. Effective conductivity of suspensions of hard spheres by Brownian motion simulation. *Journal of Applied Physics* 69(4):2280–2289. {*40, 43, 555, 566*}

Kim, I. C. and S. Torquato 1992. Effective conductivity of suspensions of overlapping spheres. *Journal of Applied Physics* 71(6):2727–2735. {*40, 43, 554, 555, 566*}

Kim, I. C. and S. Torquato 1993. Effective conductivity of composites containing spheroidal inclusions: Comparison of simulations with theory. *Journal of Applied Physics* 74(3):1844–1854. {*40, 44, 465, 493*}

Lam, J. 1986. Magnetic permeability of a simple cubic lattice of conducting magnetic spheres. *Journal of Applied Physics* 60:4230–4235. {*39, 44*}

Landau, L. D. and E. M. Lifshitz 1960. *Electrodynamics of Continuous Media*. New York: Pergamon. 417 pp. {*21, 33, 44*}

Lifshitz, E. M. and L. P. Pitaevskii 1980. *Statistical Physics* (Third ed.). New York: Pergamon. xvii + 544 pp. ISBN 0-08-023039-3. {*28, 44, 61, 72*}

Liu, C. and H. Wu 1997. Computation of the effective dielectric constant of two-component, three-dimensional mixtures using a simple pole expansion method. *Journal of Applied Physics* 82(1):345–350. {*40, 44, 377, 394*}

Lurie, A. I. 1990. *Nonlinear Theory of Elasticity*. Amsterdam: North-Holland Publishing Co. xiv + 617 pp. ISBN 0-444-87439-9. {*22, 44*}

Ma, H., B. Zhang, W. Y. Tam, and P. Sheng 2000. Dielectric-constant evaluation from microstructures. *Physical Review B (Solid State)* 61(2):962–966. {*40, 44, 377, 394*}

Marsden, J. E. and T. J. R. Hughes 1994. *Mathematical Foundations of Elasticity*. New York: Dover Publications, Inc. xviii + 556 pp. ISBN 0-486-67865-2. {*22, 44*}

Mason, W. P. 1950. *Piezoelectric Crystals and their Applications to Ultrasonics*. New York: Van Nostrand Reinhold. xi + 508 pp. {*29, 44*}

McCarthy, J. F. 1990. Effective permeability of sandstone-shale reservoirs by a random walk method. *Journal of Physics A: Mathematical and General* 23:L445–L451. {*40, 44*}

McCarthy, J. F. 1993. Continuous-time random walks on random media. *Journal of Physics A: Mathematical and General* 26(11):2495–2503. {*40, 44*}

McKenzie, D. R., R. C. McPhedran, and G. H. Derrick 1978. The conductivity of lattices of spheres. II. The body centred and face centred cubic lattices. *Proceedings of the Royal Society of London. Series A, Mathematical and Physical Sciences* 362:211–232. {*39, 44*}

McPhedran, R. C. and D. R. McKenzie 1978. The conductivity of lattices of spheres. I. The simple cubic lattice. *Proceedings of the Royal Society of London. Series A, Mathematical and Physical Sciences* 359:45–63. {*39, 44*}

McPhedran, R. C. and G. W. Milton 1981. Bounds and exact theories for the transport properties of inhomogeneous media. *Applied Physics A* 26:207–220. {*39, 44, 317, 331, 333, 337, 571, 575–577, 583, 599*}

McPhedran, R. C. and A. B. Movchan 1994. The Rayleigh multipole method for linear elasticity. *Journal of the Mechanics and Physics of Solids* 42(5):711–727. {*39, 44, 210, 217*}

Michel, J. C., H. Moulinec, and P. Suquet 2000. A computational method based on augmented Lagrangians and fast Fourier transforms for composites with high contrast. *Computer Modeling in Engineering and Sciences* 1(2):79–88. {*40, 44, 309, 311*}

Michel, J. C., H. Moulinec, and P. Suquet 2001. A computational scheme for linear and nonlinear composites with arbitrary phase contrast. *International Journal Numerical Methods in Engineering* 52(1–2):139–160. {*40, 45, 298, 303, 308, 309, 311*}

Milne-Thomson, L. M. 1962. *Antiplane Elastic Systems*. Berlin / Heidelberg / London / etc.: Springer-Verlag. viii + 265 pp. {*38, 45*}

Milton, G. W. 1997. Composites: A myriad of microstructure independent relations. In T. Tatsumi, E. Watanabe, and T. Kambe (eds.), *Theoretical and Applied Mechanics 1996: Proceedings of the XIXth International Congress of Theoretical and Applied Mechanics, Kyoto, Japan, 25–31 August 1996*, pp. 443–459. Amsterdam: Elsevier. ISBN 0-444-82446-4. {*35, 45, 81, 91*}

Milton, G. W., R. C. McPhedran, and D. R. McKenzie 1981. Transport properties of arrays of intersecting cylinders. *Applied Physics* 25:23–30. {*40, 45, 571, 599*}

Moulinec, H. and P. Suquet 1994. A fast numerical method for computing the linear and non-linear properties of composites. *Comptes Rendus des Séances de l'Académie des Sciences. Série II* 318:1417–1423. {*40, 45, 306, 311*}

Moulinec, H. and P. Suquet 1998. A numerical method for computing the overall response of non-linear composites with complex microstructure. *Computer Methods in Applied Mechanics and Engineering* 157(1–2):69–94. {*40, 45, 306, 308, 311*}

Nemat-Nasser, S., T. Iwakuma, and M. Hejazi 1982. On composites with periodic structure. *Mechanics of Materials: An International Journal* 1:239–267. {*40, 45*}

Norris, A. 1992, February 1. On the correspondence between poroelasticity and thermoelasticity. *Journal of Applied Physics* 71(3):1138–1141. {*32, 45, 85, 91*}

Nunan, K. C. and J. B. Keller 1984. Effective elasticity tensor of a periodic composite. *Journal of the Mechanics and Physics of Solids* 32(4):259–280. {*39, 45, 210, 218*}

Ogden, R. W. 1984. *Nonlinear Elastic Deformations*. Mathematics and its Applications. Chichester, United Kingdom: Ellis Horwood Ltd. xv + 532 pp. ISBN 0-85312-273-3. {*22, 45*}

Perrins, W. T., D. R. McKenzie, and R. C. McPhedran 1979. Transport properties of regular arrays of cylinders. *Proceedings of the Royal Society of London. Series A, Mathematical and Physical Sciences* 369(1737):207–225. {*39, 45, 116, 141*}

Rayleigh, L. 1892. On the influence of obstacles arranged in rectangular order upon the properties of a medium. *Philosophical Magazine* 34:481–502. {*2, 17, 39, 45*}

Rice, J. R. and M. P. Cleary 1976. Some basic stress diffusion solutions for fluid saturated elastic porous media with compressible constituents. *Reviews of Geophysics and Space Physics* 14:227–241. {*32, 45*}

Rokhlin, V. 1985. Rapid solution of integral equations of classical potential theory. *Journal of Computational Physics* 60:187–207. {*39, 45*}

Sangani, A. S. and A. Acrivos 1983. The effective conductivity of a periodic array of spheres. *Proceedings of the Royal Society of London. Series A, Mathematical and Physical Sciences* 386(1791):263–275. {*39, 45*}

Sangani, A. S. and W. Lu 1987. Elastic coefficients of composites containing spherical inclusions in a periodic array. *Journal of the Mechanics and Physics of Solids* 35(1): 1–21. {*39, 45*}

Sangani, A. S. and C. Yao 1988a. Bulk thermal conductivity of composites with spherical inclusions. *Journal of Applied Physics* 63(5):1334–1341. {*39, 46, 331, 338, 571, 575, 600*}

Sangani, A. S. and C. Yao 1988b. Transport processes in random arrays of cylinders. I Thermal conduction. *Physics of Fluids* 31(9):2426–2434. {*39, 46, 333, 338, 571, 575, 600*}

Scaife, B. K. P. 1989. *Principles of Dielectrics*. Oxford, United Kingdom: Oxford University Press. xxxii + 384 pp. ISBN 0-19-851380-1. {*19, 46, 193, 219*}

Schwartz, L. M. and J. R. Banavar 1989a. Calculation of electrical transport in continuum systems by diffusion simulation. *Physica A* 157:230–234. {*40, 46*}

Schwartz, L. M. and J. R. Banavar 1989b. Transport properties of disordered continuum systems. *Physical Review B (Solid State)* 39:11965–11969. {*40, 46*}

Snyder, K. A., E. J. Garboczi, and A. R. Day 1992. The elastic moduli of simple two-dimensional isotropic composites: Computer simulation and effective medium theory. *Journal of Applied Physics* 72(12):5948–5955. {*40, 46*}

Strelniker, Y. M. and D. J. Bergman 2000. Exact relations between magnetoresistivity tensor components of conducting composites with a columnar microstructure. *Physical Review B (Solid State)* 61(9):6288–6297. {*34, 46, 51, 58*}

Tao, R., Z. Chen, and P. Sheng 1990. First-principles Fourier approach for the calculation of the effective dielectric constant of periodic composites. *Physical Review B (Solid State)* 41(4):2417–2420. {*40, 46*}

Timoshenko, S. 1983. *History of Strength of Materials*. New York: Dover Publications, Inc. x + 452 pp. ISBN 0-486-61187-6. {*22, 46*}

Timoshenko, S. and S. Woinowsky-Krieger 1959. *Theory of Plates and Shells* (Second ed.). New York: McGraw-Hill. xiv + 580 pp. ISBN 0-07-064779-8. {*26, 46*}

Tokarzewski, S. and J. J. Telega 1997. *S*-continued fraction method for the investigation of a complex dielectric constant of two-components composite. *Acta Applicandae Mathematicae* 49(1):55–83. {*39, 46, 575, 577, 600*}

Tornow, M., D. Weiss, K. v. Klitzing, K. Eberl, D. J. Bergman, and Y. M. Strelniker 1996. Anisotropic magnetoresistance of a classical antidot array. *Physical Review Letters* 77 (1):147–150. {*34, 46*}

Torquato, S., I. C. Kim, and D. Cule 1999. Effective conductivity, dielectric constant, and diffusion coefficient of digitized composite media via first-passage-time equations. *Journal of Applied Physics* 85(3):1560–1571. {*40, 46, 207, 219, 586, 600*}

Yardley, J. G., R. C. McPhedran, N. A. Nicorovici, and L. C. Botten 1999. Addition formulae and the Rayleigh identity for arrays of elliptical cylinders. *Physical Review E (Statistical Physics, Plasmas, Fluids, and Related Interdisciplinary Topics)* 60:6068–6080. {*39, 46*}

Zuzovsky, M. and H. Brenner 1977. Effective conductivities of composite materials composed of cubic arrangements of spherical particles embedded in an isotropic matrix. *Zeitschrift für Angewandte Mathematik und Physik = Journal of Applied Mathematics and Physics* 28(6):979–992. {*39, 46*}

3

Duality transformations in two-dimensional media

3.1. Duality transformations for conductivity

Duality transformations were first applied to conductivity problems by Keller (1963), who obtained an identity relating the transverse effective conductivity of a square array of non-conducting cylinders with the transverse effective conductivity for the same array of perfectly conducting cylinders. Subsequently, Keller (1964) generalized this result to other two-dimensional microgeometries of two isotropic phases. He obtained a phase interchange identity relating the effective conductivity with that obtained when the conductivities of the phases are swapped. Matheron (1967) noticed that if a macroscopically isotropic two-dimensional multiphase medium with local conductivity $\sigma(\boldsymbol{x})\boldsymbol{I}$ could not be statistically distinguished from a medium with conductivity $\sigma'(\boldsymbol{x})\boldsymbol{I} = c\boldsymbol{I}/\sigma(\boldsymbol{x})$ for some choice of the constant c, then the medium has effective conductivity $\boldsymbol{\sigma}_* = \sqrt{c}\boldsymbol{I}$. A checkerboard is one example of such a medium. Independently, Dykhne (1970) realized that a checkerboard with squares having conductivities σ_1 and σ_2 would have effective conductivity $\sqrt{\sigma_1\sigma_2}\boldsymbol{I}$. Dykhne also used duality relations to obtain an exact formula for the effective conductivity of a macroscopically isotropic two-dimensional polycrystal. Schulgasser (1977) showed that this exact formula was a corollary of Keller's phase interchange identity because each crystal could be replaced by a laminate of two isotropic phases. Mendelson (1975) obtained the most general form of the duality relation that is valid for any two-dimensional conducting medium, with possibly anisotropic local conductivity and possibly anisotropic effective conductivity [see also Nevard and Keller (1985), the proof of Tartar in Francfort and Murat (1987), Theorem 4, and section 1.5 of Zhikov, Kozlov, and Oleinik (1994).]. Levy and Kohn (1998) extended these duality relations to nonlinear conducting media.

Keller's original analysis was based on the equations satisfied by the harmonic conjugates of the electrical potentials in each phase. Here we follow the more general approach of Dykhne (1970) [see also Dykhne and Kaganova (1997)], who derived the duality relations by noting that a two-dimensional divergence free field when rotated pointwise by 90° produces a curl free field, and vice versa.

Consider conduction in a two-dimensional media, governed by the equations

$$\boldsymbol{j}(\boldsymbol{x}) = \boldsymbol{\sigma}(\boldsymbol{x})\boldsymbol{e}(\boldsymbol{x}), \qquad \nabla \cdot \boldsymbol{j} = 0, \qquad \nabla \times \boldsymbol{e} = 0. \tag{3.1}$$

The key to understanding duality is the observation that pointwise rotations of fields by 90° convert curl free fields to divergence free fields, and vice versa. Thus if we introduce the matrix

$$\boldsymbol{R}_\perp = \begin{pmatrix} 0 & 1 \\ -1 & 0 \end{pmatrix},$$

for a 90° rotation, then the fields

$$\boldsymbol{j}'(\boldsymbol{x}) \equiv \boldsymbol{R}_\perp \boldsymbol{e}(\boldsymbol{x}), \qquad \boldsymbol{e}'(\boldsymbol{x}) \equiv \boldsymbol{R}_\perp \boldsymbol{j}(\boldsymbol{x}) \tag{3.2}$$

satisfy

$$\nabla \cdot \boldsymbol{j}'(\boldsymbol{x}) = 0, \qquad \nabla \times \boldsymbol{e}'(\boldsymbol{x}) = 0.$$

The proof of this is trivial. Indeed we have

$$\frac{\partial j_1'}{\partial x_1} + \frac{\partial j_2'}{\partial x_2} = \frac{\partial e_2}{\partial x_1} - \frac{\partial e_1}{\partial x_2} = 0,$$
$$\frac{\partial e_2'}{\partial x_1} - \frac{\partial e_1'}{\partial x_2} = -\frac{\partial j_1}{\partial x_1} - \frac{\partial j_2}{\partial x_2} = 0.$$

Now how are the fields $\boldsymbol{j}'(\boldsymbol{x})$ and $\boldsymbol{e}'(\boldsymbol{x})$ related? From their defining equations and from the constitutive relation $\boldsymbol{j} = \boldsymbol{\sigma e}$ it is clear that

$$\boldsymbol{j}'(\boldsymbol{x}) = \boldsymbol{\sigma}'(\boldsymbol{x})\boldsymbol{e}'(\boldsymbol{x}),$$

where

$$\boldsymbol{\sigma}'(\boldsymbol{x}) \equiv \boldsymbol{R}_\perp[\boldsymbol{\sigma}(\boldsymbol{x})]^{-1}\boldsymbol{R}_\perp^T \tag{3.3}$$

and $\boldsymbol{R}_\perp^T = -\boldsymbol{R}_\perp$ is the transpose of $\boldsymbol{R}_\perp$. In other words, $\boldsymbol{j}'(\boldsymbol{x})$ and $\boldsymbol{e}'(\boldsymbol{x})$ solve the conductivity equations in a dual material with conductivity tensor $\boldsymbol{\sigma}'(\boldsymbol{x})$ given by (3.3). That is quite unexpected. Indeed, the media with tensors $\boldsymbol{\sigma}$ and $\boldsymbol{\sigma}'$ can be radically different. For example, for an isotropic conductivity tensor field $\boldsymbol{\sigma}(\boldsymbol{x}) = \sigma(\boldsymbol{x})\boldsymbol{I}$ we have $\boldsymbol{\sigma}'(\boldsymbol{x}) = \boldsymbol{I}/\sigma(\boldsymbol{x})$. So regions that originally had high conductivity now have low conductivity in the dual material.

Due to this isomorphism we can link the effective conductivity tensor $\boldsymbol{\sigma}_*'$ of the dual material with the effective tensor $\boldsymbol{\sigma}_*$ of the original material. Taking averages over $\boldsymbol{x}$ of (3.2) gives

$$\langle \boldsymbol{j}' \rangle = \boldsymbol{R}_\perp \langle \boldsymbol{e} \rangle, \quad \langle \boldsymbol{e}' \rangle = \boldsymbol{R}_\perp \langle \boldsymbol{j} \rangle.$$

From this and from the linear relation $\langle \boldsymbol{j} \rangle = \boldsymbol{\sigma}_* \langle \boldsymbol{e} \rangle$ defining the effective tensor $\boldsymbol{\sigma}_*$ it follows that $\langle \boldsymbol{j}' \rangle$ and $\langle \boldsymbol{e}' \rangle$ are linearly related through the equation

$$\langle \boldsymbol{j}' \rangle = \boldsymbol{R}_\perp (\boldsymbol{\sigma}_*)^{-1} \boldsymbol{R}_\perp^T \langle \boldsymbol{e}' \rangle.$$

But the effective tensor $\boldsymbol{\sigma}_*'$ by definition governs this linear relation between $\langle \boldsymbol{j}' \rangle$ and $\langle \boldsymbol{e}' \rangle$, and so we make the identification

$$\boldsymbol{\sigma}_*' = \boldsymbol{R}_\perp (\boldsymbol{\sigma}_*)^{-1} \boldsymbol{R}_\perp^T. \tag{3.4}$$

Thus under the duality transformation the effective tensor $\boldsymbol{\sigma}_*$ is transformed in exactly the same way as the local conductivity tensor $\boldsymbol{\sigma}(\boldsymbol{x})$. That the conductivity and effective conductivity of the dual material are in general given by (3.3) and (3.4) was noted by Mendelson (1975).

A straightforward matrix computation shows that we can rewrite the duality transformation as simply

$$\boldsymbol{\sigma}'(\boldsymbol{x}) = [\boldsymbol{\sigma}(\boldsymbol{x})]^T / \det \boldsymbol{\sigma}(\boldsymbol{x}), \qquad \boldsymbol{\sigma}_*' = [\boldsymbol{\sigma}_*]^T / \det \boldsymbol{\sigma}_*. \tag{3.5}$$

In particular, as applied to composites with both locally isotropic conductivity, $\boldsymbol{\sigma}(\boldsymbol{x}) = \sigma(\boldsymbol{x})\boldsymbol{I}$, and isotropic effective conductivity, $\boldsymbol{\sigma}_* = \sigma_*\boldsymbol{I}$, this result implies Keller's relation that

$$\boldsymbol{\sigma}_*' = \boldsymbol{I}/\sigma_* \text{ when } \boldsymbol{\sigma}'(\boldsymbol{x}) = \boldsymbol{I}/\sigma(\boldsymbol{x}). \tag{3.6}$$

Thus if we replace the conductivity by its reciprocal, the effective conductivity is replaced by its reciprocal.

Let us now examine some of the applications of the duality transformation.

3.2. Phase interchange identities for two-phase media

Consider a two-phase material with a locally isotropic conductivity tensor of the form

$$\boldsymbol{\sigma}(\boldsymbol{x}) = \chi_1(\boldsymbol{x})\sigma_1\boldsymbol{I} + \chi_2(\boldsymbol{x})\sigma_2\boldsymbol{I},$$

where χ_1 and χ_2 are the characteristic functions

$$\begin{aligned}\chi_1(\boldsymbol{x}) = 1 - \chi_2(\boldsymbol{x}) &= 1 \text{ in phase 1,}\\ &= 0 \text{ in phase 2,}\end{aligned} \tag{3.7}$$

describing the geometry of the composite. If we consider $\boldsymbol{\sigma}_*$ as a function of σ_1 and σ_2, then (3.5) implies that

$$\boldsymbol{\sigma}_*(1/\sigma_1, 1/\sigma_2) = \boldsymbol{\sigma}_*(\sigma_1, \sigma_2)/\det\boldsymbol{\sigma}_*(\sigma_1, \sigma_2). \tag{3.8}$$

Now, from the homogeneity of this function [see (1.6)], it follows that

$$\boldsymbol{\sigma}_*(1/\sigma_1, 1/\sigma_2) = \boldsymbol{\sigma}_*(\sigma_2, \sigma_1)/\sigma_1\sigma_2.$$

Substituting this back into (3.8) gives the formula of Keller (1964) for the effective tensor when the phases are interchanged:

$$\boldsymbol{\sigma}_*(\sigma_2, \sigma_1) = \sigma_1\sigma_2\boldsymbol{\sigma}_*(\sigma_1, \sigma_2)/\det\boldsymbol{\sigma}_*(\sigma_1, \sigma_2). \tag{3.9}$$

Flaherty and Keller (1973) recognized that an analogous relation holds for the mathematically equivalent problem of antiplane elasticity. Dykhne (1970) realized that for a particular class of microgeometries, now called symmetric materials, the geometry is invariant under phase interchange, and we have $\boldsymbol{\sigma}_*(\sigma_2, \sigma_1) = \boldsymbol{\sigma}_*(\sigma_1, \sigma_2)$, which together with (3.9) implies that

$$\det\boldsymbol{\sigma}_*(\sigma_1, \sigma_2) = \sigma_1\sigma_2. \tag{3.10}$$

A checkerboard, as illustrated in figure 3.1(a), is an example of such a material; because it has square symmetry $\boldsymbol{\sigma}_*$ is proportional to the identity tensor $\boldsymbol{I}$ and by virtue of (3.10) is known exactly:

$$\boldsymbol{\sigma}_*(\sigma_1, \sigma_2) = \sqrt{\sigma_1\sigma_2}\boldsymbol{I}. \tag{3.11}$$

What luck! We have obtained a precise formula for the effective conductivity $\boldsymbol{\sigma}_*$ without having to solve for the fields $\boldsymbol{j}(\boldsymbol{x})$ and $\boldsymbol{e}(\boldsymbol{x})$. Using complex analysis Berdichevskii (1985) has obtained closed-form solutions for the fields and has directly verified Dykhne's result. A way to produce symmetric materials with a random microgeometry is to fill all space with cells, of arbitrary and perhaps varying shape distributed in a periodic or statistically homogeneous fashion, and assign each cell in a completely random uncorrelated way (for instance by the toss of a coin) as phase 1 with probability $p_1 = 1/2$ or otherwise as phase 2. Materials produced in this way, generalized to allow for any probability $p_1 \in (0, 1)$, are called cell materials.

Schulgasser (1992), inspired by one of Escher's prints, noticed that there are some anisotropic two-dimensional microstructures, such as the one illustrated in figure 3.1(b), for which

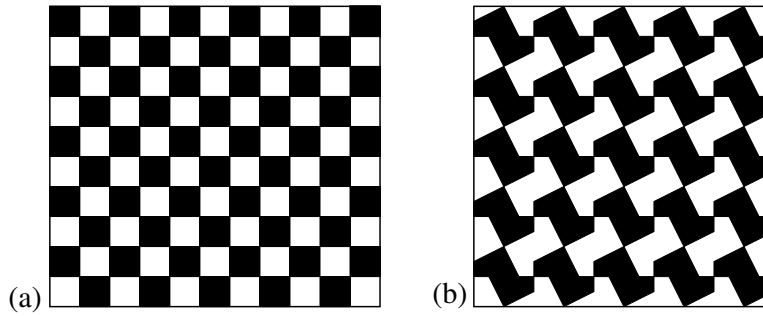

Figure 3.1. A checkerboard, as shown in (a), or any isotropically conducting microstructure that remains invariant under the interchange of the two phases, necessarily has effective conductivity $\sigma_* = \sqrt{\sigma_1\sigma_2}$. If the microstructure is not isotropic but is such that interchanging the phases produces the same effect as rotating the structure by 90°, as in (b), then the effective conductivity is isotropic and given by the same formula.

interchanging the phases produces the same effect as rotating the microstructure by 90°. For such microstructures

$$\boldsymbol{\sigma}_*(\sigma_2, \sigma_1) = \boldsymbol{R}_\perp \boldsymbol{\sigma}_*(\sigma_1, \sigma_2)\boldsymbol{R}_\perp^T,$$

which, together with the phase interchange identity (3.9), implies that the effective conductivity tensor is necessarily isotropic and given by (3.11), even though the microstructure is anisotropic.

3.3. The conductivity of two-dimensional polycrystals

Dykhne (1970) realized that the duality formula also gives an explicit formula for the effective conductivity tensor of an isotropic two-dimensional polycrystal. A polycrystal is a granular aggregate where the grains are crystallites solidified in different orientations from a homogeneous melt. In a polycrystal the local conductivity tensor $\boldsymbol{\sigma}(\boldsymbol{x})$ takes the form

$$\boldsymbol{\sigma}(\boldsymbol{x}) = \boldsymbol{R}(\boldsymbol{x})\boldsymbol{\sigma}_0\boldsymbol{R}^T(\boldsymbol{x}),$$

where $\boldsymbol{R}(\boldsymbol{x})$ is a rotation matrix, giving the orientation of the crystal at each point $\boldsymbol{x}$,

$$\boldsymbol{\sigma}_0 \equiv \begin{pmatrix} \lambda_1 & 0 \\ 0 & \lambda_2 \end{pmatrix},$$

represents the conductivity tensor of the pure crystal from which the polycrystal is formed, and λ_1 and λ_2 are the principal conductivities (eigenvalues) of that crystal. Although in practice $\boldsymbol{R}(\boldsymbol{x})$ will be essentially piecewise constant with discontinuities at grain boundaries, nothing prevents us from considering geometries where $\boldsymbol{R}(\boldsymbol{x})$ has a smooth variation with $\boldsymbol{x}$.

The conductivity tensor of the polycrystal has the special property that

$$\det \boldsymbol{\sigma}(\boldsymbol{x}) = \det \boldsymbol{\sigma}_0 = \lambda_1\lambda_2$$

is independent of $\boldsymbol{x}$. Thus the conductivity tensor

$$\boldsymbol{\sigma}'(\boldsymbol{x}) = \boldsymbol{\sigma}(\boldsymbol{x})/\lambda_1\lambda_2$$

of the dual material is the same as the conductivity tensor of the original polycrystal, aside from the factor of $1/\lambda_1\lambda_2$. Now whenever the local conductivity tensor is multiplied by a constant factor then, by homogeneity, the effective tensor is also multiplied by this same factor. But (3.5) says that the effective tensor is multiplied by the factor $1/\det \boldsymbol{\sigma}_*$. Equating these two factors gives the result

$$\det \boldsymbol{\sigma}_* = \lambda_1\lambda_2. \tag{3.12}$$

In particular, if the polycrystal is macroscopically isotropic in the sense that $\boldsymbol{\sigma}_*$ is proportional to the identity tensor, then $\boldsymbol{\sigma}_*$ is completely determined,

$$\boldsymbol{\sigma}_* = \sqrt{\lambda_1\lambda_2}\, \boldsymbol{I},$$

and is independent of the precise details of the polycrystalline microstructure. Schulgasser (1977) showed that this result for polycrystals is a corollary of the result for two-phase symmetric materials. (With negligible change to the overall effective conductivity, each grain in the polycrystal can be replaced by a laminate of equal portions of two appropriately chosen isotropic phases, where the layer thickness is chosen to be much smaller than the grain size and the laminate has the same effective conductivity as the crystal grain.)

3.4. Duality transformations for pyroelectricity

These duality transformations directly extend to the two-dimensional pyroelectric equations

$$\boldsymbol{d}(\boldsymbol{x}) = \boldsymbol{\epsilon}(\boldsymbol{x})\boldsymbol{e}(\boldsymbol{x}) + \boldsymbol{\alpha}(\boldsymbol{x})\theta, \quad \nabla \cdot \boldsymbol{d} = 0, \quad \nabla \times \boldsymbol{e} = 0, \quad \theta = \text{constant}.$$

The fields

$$\boldsymbol{d}'(\boldsymbol{x}) \equiv \boldsymbol{R}_\perp \boldsymbol{e}(\boldsymbol{x}), \qquad \boldsymbol{e}'(\boldsymbol{x}) \equiv \boldsymbol{R}_\perp \boldsymbol{d}(\boldsymbol{x})$$

satisfy the pyroelectric equations

$$\boldsymbol{d}'(\boldsymbol{x}) = \boldsymbol{\epsilon}'(\boldsymbol{x})\boldsymbol{e}'(\boldsymbol{x}) + \boldsymbol{\alpha}'(\boldsymbol{x})\theta, \quad \nabla \cdot \boldsymbol{d}' = 0, \quad \nabla \times \boldsymbol{e}' = 0, \quad \theta = \text{constant},$$

in a new dual pyroelectric medium with tensors

$$\boldsymbol{\epsilon}'(\boldsymbol{x}) = [\boldsymbol{\epsilon}(\boldsymbol{x})]^T / \det \boldsymbol{\epsilon}(\boldsymbol{x}), \quad \boldsymbol{\alpha}'(\boldsymbol{x}) = -\boldsymbol{R}_\perp [\boldsymbol{\epsilon}(\boldsymbol{x})]^{-1} \boldsymbol{\alpha}(\boldsymbol{x}).$$

By taking averages of the fields, we see that the effective tensors of this dual medium are related to the effective tensors of the original medium via the transformations

$$\boldsymbol{\epsilon}'_* = [\boldsymbol{\epsilon}_*]^T / \det \boldsymbol{\epsilon}_*, \quad \boldsymbol{\alpha}'_* = -\boldsymbol{R}_\perp [\boldsymbol{\epsilon}_*]^{-1} \boldsymbol{\alpha}_*.$$

This duality transformation was obtained by Bergman and Strelniker (1998) and Strelniker and Bergman (2000), who instead of considering pyroelectricity analyzed the equivalent magnetotransport problem; see section 2.6 on page 33.

3.5. Duality transformations for elasticity

Elasticity duality transformations were first derived by Berdichevskii (1983) for incompressible media. Following Helsing, Milton, and Movchan (1997), let us instead first consider a two-dimensional medium that is locally orthotropic, having the crystal axes aligned with the

coordinate axes, and which is locally rigid with respect to shears with $\tau_{11} = \tau_{22} = 0$ and $\tau_{12} \neq 0$. The constitutive relation in such a medium takes the special form

$$\begin{pmatrix} \epsilon_{11} \\ \epsilon_{22} \\ \sqrt{2}\epsilon_{12} \end{pmatrix} = \begin{pmatrix} S_{1111} & S_{1122} & 0 \\ S_{1122} & S_{2222} & 0 \\ 0 & 0 & 0 \end{pmatrix} \begin{pmatrix} \tau_{11} \\ \tau_{22} \\ \sqrt{2}\tau_{12} \end{pmatrix},$$

where the moduli S_{1111}, S_{1122}, and S_{2222} of the compliance tensor depend on $\boldsymbol{x}$. This constitutive relation imposes the differential constraint $\epsilon_{12} = 0$ on the stress component ϵ_{12}, and it imposes no constraint on the strain component τ_{12}. The remaining stress and strain components are linked through the reduced constitutive relation

$$\begin{pmatrix} \epsilon_{11} \\ \epsilon_{22} \end{pmatrix} = \boldsymbol{S}_r \begin{pmatrix} \tau_{11} \\ \tau_{22} \end{pmatrix}, \quad \text{where } \boldsymbol{S}_r(\boldsymbol{x}) = \begin{pmatrix} S_{1111}(\boldsymbol{x}) & S_{1122}(\boldsymbol{x}) \\ S_{1122}(\boldsymbol{x}) & S_{2222}(\boldsymbol{x}) \end{pmatrix}.$$

The associated effective tensor $\boldsymbol{S}_{r*}$, which governs the relation between the average fields,

$$\begin{pmatrix} \langle \epsilon_{11} \rangle \\ \langle \epsilon_{22} \rangle \end{pmatrix} = \boldsymbol{S}_{r*} \begin{pmatrix} \langle \tau_{11} \rangle \\ \langle \tau_{22} \rangle \end{pmatrix},$$

determines the elements of the effective compliance tensor $\boldsymbol{S}_*$:

$$\boldsymbol{S}_* = \begin{pmatrix} \boldsymbol{S}_{r*} & 0 \\ 0 & 0 \end{pmatrix}.$$

Now we ask, what are the differential constraints on the stress and strain components that enter the reduced constitutive relation? Since $\epsilon_{12} = 0$, the infinitesimal strain compatibility relation

$$\frac{\partial^2 \epsilon_{11}}{\partial x_2^2} + \frac{\partial^2 \epsilon_{22}}{\partial x_1^2} - 2\frac{\partial^2 \epsilon_{12}}{\partial x_1 \partial x_2} = 0$$

reduces to

$$\frac{\partial^2 \epsilon_{11}}{\partial x_2^2} + \frac{\partial^2 \epsilon_{22}}{\partial x_1^2} = 0. \tag{3.13}$$

To eliminate the stress component τ_{12} from the differential restrictions

$$\frac{\partial \tau_{11}}{\partial x_1} + \frac{\partial \tau_{12}}{\partial x_2} = 0, \quad \frac{\partial \tau_{12}}{\partial x_1} + \frac{\partial \tau_{22}}{\partial x_2} = 0$$

on the stress field components, we take the derivative of the first equation with respect to x_1 and the derivative of the second equation with respect to x_2 and subtract them. This yields the differential constraint

$$\frac{\partial^2 \tau_{11}}{\partial x_1^2} - \frac{\partial^2 \tau_{22}}{\partial x_2^2} = 0. \tag{3.14}$$

Notice the similarity between the differential constraints (3.13) and (3.14). If we define new fields

$$\begin{pmatrix} \epsilon'_{11} \\ \epsilon'_{22} \end{pmatrix} = \boldsymbol{R}_\perp \begin{pmatrix} \tau_{11} \\ \tau_{22} \end{pmatrix} = \begin{pmatrix} \tau_{22} \\ -\tau_{11} \end{pmatrix},$$

$$\begin{pmatrix} \tau'_{11} \\ \tau'_{22} \end{pmatrix} = \boldsymbol{R}_\perp \begin{pmatrix} \epsilon_{11} \\ \epsilon_{22} \end{pmatrix} = \begin{pmatrix} \epsilon_{22} \\ -\epsilon_{11} \end{pmatrix},$$

then the pair $(\epsilon'_{11}, \epsilon'_{22})$ satisfies the same differential constraints as the pair $(\epsilon_{11}, \epsilon_{22})$ while the pair (τ'_{11}, τ'_{22}) satisfies the same differential constraints as the pair (τ_{11}, τ_{22}). These new fields are linked by the constitutive relation

$$\begin{pmatrix} \epsilon'_{11} \\ \epsilon'_{22} \end{pmatrix} = \boldsymbol{S}'_r \begin{pmatrix} \tau'_{11} \\ \tau'_{22} \end{pmatrix}, \quad \text{where } \boldsymbol{S}'_r(\boldsymbol{x}) = \boldsymbol{R}_\perp[\boldsymbol{S}_r(\boldsymbol{x})]\boldsymbol{R}_\perp^T = \boldsymbol{S}_r(\boldsymbol{x})/\det \boldsymbol{S}_r(\boldsymbol{x}).$$

Hence all of the duality results for the conductivity problem immediately extend to this elasticity problem. In particular, a medium with elasticity tensor

$$\boldsymbol{S}'(\boldsymbol{x}) = \boldsymbol{S}(\boldsymbol{x})/\det \boldsymbol{S}_r(\boldsymbol{x}) \tag{3.15}$$

will have effective tensor

$$\boldsymbol{S}'_* = \boldsymbol{S}_*/\det \boldsymbol{S}_{r*}. \tag{3.16}$$

It follows that if $\det \boldsymbol{S}_r(\boldsymbol{x})$ takes a value Δ independent of $\boldsymbol{x}$, then necessarily $\det \boldsymbol{S}_{r*}$ takes the same value:

$$\det \boldsymbol{S}_{r*} = \Delta \text{ when } \det \boldsymbol{S}_r(\boldsymbol{x}) = \Delta \text{ for all } \boldsymbol{x}. \tag{3.17}$$

Also, if the medium is two-phase with $\boldsymbol{S}_r(\boldsymbol{x})$ taking the form

$$\boldsymbol{S}_r(\boldsymbol{x}) = (\alpha_1\chi_1(\boldsymbol{x}) + \alpha_2\chi_2(\boldsymbol{x}))\boldsymbol{A} \tag{3.18}$$

for some choice of matrix $\boldsymbol{A}$ and constants α_1 and α_2, and we consider $\boldsymbol{S}_{r*}$ and $\boldsymbol{S}_*$ as functions $\boldsymbol{S}_{r*}(\alpha_1, \alpha_2)$ and $\boldsymbol{S}_*(\alpha_1, \alpha_2)$ of α_1 and α_2, then we have the relation

$$\boldsymbol{S}_*(\alpha_2, \alpha_1) = \frac{\alpha_1\alpha_2 \det \boldsymbol{A}}{\det \boldsymbol{S}_{r*}(\alpha_1, \alpha_2)}\boldsymbol{S}_*(\alpha_1, \alpha_2), \tag{3.19}$$

which gives the effective elasticity tensor when we interchange the phases.

If the geometry described by the characteristic function $\chi_1(\boldsymbol{x}) = 1 - \chi_2(\boldsymbol{x})$ is invariant under phase interchange (like a checkerboard), then (3.19) implies that

$$\det \boldsymbol{S}_{r*}(\alpha_1, \alpha_2) = \alpha_1\alpha_2 \det \boldsymbol{A}. \tag{3.20}$$

The duality relation (3.16) and the phase interchange identity (3.19) have been checked numerically for a periodic array of amoeba-shaped inclusions (Helsing, Milton, and Movchan 1997).

3.6. Duality transformations for other elastic media

These duality relations extend to media where the compliance tensor $\boldsymbol{S}(\boldsymbol{x})$ is locally rigid with respect to stresses proportional to a constant matrix $\boldsymbol{v}_1$, that is, for media such that

$$\boldsymbol{S}(\boldsymbol{x})\boldsymbol{v}_1 = 0 \text{ for all } \boldsymbol{x}. \tag{3.21}$$

One can assume without loss of generality (by rotating the coordinate system and multiplying $\boldsymbol{v}_1$ by a constant, if necessary) that $\boldsymbol{v}_1$ is diagonal and of the form

$$\boldsymbol{v}_1 = \begin{pmatrix} a_1 & 0 \\ 0 & a_2 \end{pmatrix} \text{ with } a_1^2 + a_2^2 = 1.$$

Let us introduce the matrices

$$\boldsymbol{v}_2 = \begin{pmatrix} a_2 & 0 \\ 0 & -a_1 \end{pmatrix}, \quad \boldsymbol{v}_3 = \frac{1}{\sqrt{2}} \begin{pmatrix} 0 & 1 \\ 1 & 0 \end{pmatrix},$$

which together with v_1 form an orthonormal basis on the space of symmetric matrices.

We expand the stress and strain fields in this basis with coefficients

$$\begin{aligned} \epsilon_1 &= a_1\epsilon_{11} + a_2\epsilon_{22}, \quad \epsilon_2 = a_2\epsilon_{11} - a_1\epsilon_{22}, \quad \epsilon_3 = \sqrt{2}\epsilon_{12}, \\ \tau_1 &= a_1\tau_{11} + a_2\tau_{22}, \quad \tau_2 = a_2\tau_{11} - a_1\tau_{22}, \quad \tau_3 = \sqrt{2}\epsilon_{12}, \end{aligned}$$

which enter the expansions

$$\boldsymbol{\epsilon}(\boldsymbol{x}) = \epsilon_1(\boldsymbol{x})\boldsymbol{v}_1 + \epsilon_2(\boldsymbol{x})\boldsymbol{v}_2 + \epsilon_3(\boldsymbol{x})\boldsymbol{v}_3, \quad \boldsymbol{\tau}(\boldsymbol{x}) = \tau_1(\boldsymbol{x})\boldsymbol{v}_1 + \tau_2(\boldsymbol{x})\boldsymbol{v}_2 + \tau_3(\boldsymbol{x})\boldsymbol{v}_3 \quad (3.22)$$

of the stress and strain fields in this basis. These coefficients are linked through the constitutive equation

$$\begin{pmatrix} \epsilon_1 \\ \epsilon_2 \\ \epsilon_3 \end{pmatrix} = \begin{pmatrix} 0 & 0 \\ 0 & \boldsymbol{S}_r \end{pmatrix} \begin{pmatrix} \tau_1 \\ \tau_2 \\ \tau_3 \end{pmatrix},$$

where

$$\boldsymbol{S}_r(\boldsymbol{x}) = \begin{pmatrix} S_{1111}(\boldsymbol{x}) + S_{2222}(\boldsymbol{x}) & \sqrt{2}S_{1112}(\boldsymbol{x})/a_2 \\ \sqrt{2}S_{1112}(\boldsymbol{x})/a_2 & 2S_{1212}(\boldsymbol{x}) \end{pmatrix}.$$

The reduced constitutive relation takes the form

$$\begin{pmatrix} \epsilon_2 \\ \epsilon_3 \end{pmatrix} = \boldsymbol{S}_r \begin{pmatrix} \tau_2 \\ \tau_3 \end{pmatrix}.$$

Similarly, the associated reduced effective tensor $\boldsymbol{S}_{r*}$, which governs the relation between the average values of these fields, through the equation

$$\begin{pmatrix} \langle\epsilon_2\rangle \\ \langle\epsilon_3\rangle \end{pmatrix} = \boldsymbol{S}_{r*} \begin{pmatrix} \langle\tau_2\rangle \\ \langle\tau_3\rangle \end{pmatrix},$$

has matrix elements

$$\boldsymbol{S}_{r*} = \begin{pmatrix} S^*_{1111} + S^*_{2222} & \sqrt{2}S^*_{1112}/a_2 \\ \sqrt{2}S^*_{1112}/a_2 & 2S^*_{1212} \end{pmatrix}.$$

The components of the strain and stress fields entering the reduced constitutive relation satisfy the differential constraints

$$\begin{aligned} \Big[a_1\frac{\partial^2}{\partial x_1^2} - a_2\frac{\partial^2}{\partial x_2^2}\Big]\epsilon_2 + \Big[\sqrt{2}\frac{\partial^2}{\partial x_1\partial x_2}\Big]\epsilon_3 &= 0, \\ \Big[\sqrt{2}\frac{\partial^2}{\partial x_1\partial x_2}\Big]\tau_2 - \Big[a_1\frac{\partial^2}{\partial x_1^2} - a_2\frac{\partial^2}{\partial x_2^2}\Big]\tau_3 &= 0. \end{aligned}$$

If we introduce new fields

$$\begin{aligned} \begin{pmatrix} \epsilon'_2 \\ \epsilon'_3 \end{pmatrix} &= \boldsymbol{R}_\perp \begin{pmatrix} \tau_2 \\ \tau_3 \end{pmatrix} = \begin{pmatrix} \tau_3 \\ -\tau_2 \end{pmatrix}, \\ \begin{pmatrix} \tau'_2 \\ \tau'_3 \end{pmatrix} &= \boldsymbol{R}_\perp \begin{pmatrix} \epsilon_2 \\ \epsilon_3 \end{pmatrix} = \begin{pmatrix} \epsilon_3 \\ -\epsilon_2 \end{pmatrix}, \end{aligned}$$

then the pair $(\epsilon_2', \epsilon_3')$ satisfies the same differential constraints as the pair (ϵ_2, ϵ_3) while the pair (τ_2', τ_3') satisfies the same differential constraints as the pair (τ_2, τ_3). Consequently, all of the duality results extend to this problem: A medium with compliance tensor (3.15) will have effective tensor (3.16); the identity (3.17) will hold when $\det \boldsymbol{S}_r(\boldsymbol{x})$ is constant; and when the material is two-phase with $\boldsymbol{S}_r(\boldsymbol{x})$ of the form (3.18), then (3.19) gives the effective elasticity tensor of the phase interchanged geometry and (3.20) will hold if the material is interchange invariant (Helsing, Milton, and Movchan 1997).

3.7. The effective shear modulus of incompressible two-dimensional polycrystals and symmetric materials

A beautiful application of these duality transformations is to (two-dimensional) polycrystals assembled from an incompressible crystal. The fourth-order compliance tensor of the polycrystal takes the form

$$\boldsymbol{S}(\boldsymbol{x}) = \boldsymbol{R}(\boldsymbol{x})\boldsymbol{R}(\boldsymbol{x})\boldsymbol{S}_0\boldsymbol{R}^T(\boldsymbol{x})\boldsymbol{R}^T(\boldsymbol{x}),$$

where $\boldsymbol{R}(\boldsymbol{x})$ is a rotation matrix, giving the orientation of the crystal at each point $\boldsymbol{x}$, and $\boldsymbol{S}_0$ is the compliance tensor of a single crystal. The single crystal incompressibility implies that

$$\boldsymbol{S}(\boldsymbol{x})\boldsymbol{I} = \boldsymbol{S}_0\boldsymbol{I} = 0.$$

Thus the condition (3.21) for applying duality transformations is satisfied with $\boldsymbol{v}_1 = \boldsymbol{I}/\sqrt{2}$. Since $\boldsymbol{I}$ is an eigenvector of $\boldsymbol{S}_0$, the remaining eigenvectors must be orthogonal to $\boldsymbol{I}$, that is, they must have zero trace and they therefore represent pure shears.

Let us choose our spatial coordinates so that one of these eigenvectors is a diagonal matrix, and let us choose $\boldsymbol{v}_2$ to be this matrix and $\boldsymbol{v}_3$ to be the remaining eigenvector. The condition that $\boldsymbol{v}_2$ is trace free and diagonal, and the condition that $\boldsymbol{v}_3$ is trace free and orthogonal to $\boldsymbol{v}_2$, implies that

$$\boldsymbol{v}_1 = \frac{1}{\sqrt{2}}\begin{pmatrix} 1 & 0 \\ 0 & 1 \end{pmatrix}, \quad \boldsymbol{v}_2 = \frac{1}{\sqrt{2}}\begin{pmatrix} 1 & 0 \\ 0 & -1 \end{pmatrix}, \quad \boldsymbol{v}_3 = \frac{1}{\sqrt{2}}\begin{pmatrix} 0 & 1 \\ 1 & 0 \end{pmatrix}.$$

Since these are eigenvectors, the matrix representing $\boldsymbol{S}_0$ in this basis must necessarily be diagonal and therefore can be expressed in the form

$$\boldsymbol{S}_0 = \begin{pmatrix} 0 & 0 & 0 \\ 0 & 1/(2\mu^{(1)}) & 0 \\ 0 & 0 & 1/(2\mu^{(2)}) \end{pmatrix}. \tag{3.23}$$

The constants $\mu^{(1)}$ and $\mu^{(2)}$ entering this formula are called the shear moduli of the single crystal with respect to the shears $\boldsymbol{v}_2$ and $\boldsymbol{v}_3$. When the shear stress $\boldsymbol{\tau} = \boldsymbol{v}_2$ (or the shear stress $\tau = \boldsymbol{v}_3$) is applied to the single crystal the strain field is exactly the same as in an isotropic medium that has shear modulus $\mu^{(1)}$ (respectively $\mu^{(2)}$). Notice that the compliance tensor $\boldsymbol{S}_0$ represents a crystal with square symmetry. Under the reflection $x_1 \to -x_1$ (or under the reflection $x_2 \to -x_2$) the basis $(\boldsymbol{v}_1, \boldsymbol{v}_2, \boldsymbol{v}_3)$ transforms to $(\boldsymbol{v}_1, \boldsymbol{v}_2, -\boldsymbol{v}_3)$ and $\boldsymbol{S}_0$ remains invariant; while if we interchange x_1 and x_2 (corresponding to a reflection about the line $x_1 = x_2$), the basis $(\boldsymbol{v}_1, \boldsymbol{v}_2, \boldsymbol{v}_3)$ transforms to $(\boldsymbol{v}_1, -\boldsymbol{v}_2, \boldsymbol{v}_3)$ and again $\boldsymbol{S}_0$ remains invariant. Thus any incompressible two-dimensional material necessarily has an elasticity tensor with square symmetry. In particular, the effective elasticity tensor of the polycrystal necessarily has square symmetry, irrespective of the symmetry of the microgeometry.

To obtain an expression for the compliance tensor $\boldsymbol{S}(\boldsymbol{x})$ in the basis $(\boldsymbol{v}_1, \boldsymbol{v}_2, \boldsymbol{v}_3)$ notice that the constitutive law $\boldsymbol{\epsilon} = \boldsymbol{S}\boldsymbol{\tau}$ can be rewritten as

$$\boldsymbol{R}^T(\boldsymbol{x})\boldsymbol{\tau}(\boldsymbol{x})\boldsymbol{R}(\boldsymbol{x}) = \boldsymbol{S}_0[\boldsymbol{R}^T(\boldsymbol{x})\boldsymbol{\tau}(\boldsymbol{x})\boldsymbol{R}(\boldsymbol{x})]. \tag{3.24}$$

To evaluate this in the basis $(\boldsymbol{v}_1, \boldsymbol{v}_2, \boldsymbol{v}_3)$ we need to compute the action of rotation on each basis element. Setting

$$\boldsymbol{R}(\boldsymbol{x}) = \begin{pmatrix} \cos\theta(\boldsymbol{x}) & \sin\theta(\boldsymbol{x}) \\ -\sin\theta(\boldsymbol{x}) & \cos\theta(\boldsymbol{x}) \end{pmatrix},$$

where $\theta(\boldsymbol{x})$ represents the angle of crystal orientation at each point $\boldsymbol{x}$, direct calculation shows that

$$\begin{aligned} \boldsymbol{R}^T(\boldsymbol{x})\boldsymbol{v}_1\boldsymbol{R}(\boldsymbol{x}) &= \boldsymbol{v}_1, \\ \boldsymbol{R}^T(\boldsymbol{x})\boldsymbol{v}_2\boldsymbol{R}(\boldsymbol{x}) &= \cos[2\theta(\boldsymbol{x})]\boldsymbol{v}_2 + \sin[2\theta(\boldsymbol{x})]\boldsymbol{v}_3, \\ \boldsymbol{R}^T(\boldsymbol{x})\boldsymbol{v}_3\boldsymbol{R}(\boldsymbol{x}) &= -\sin[2\theta(\boldsymbol{x})]\boldsymbol{v}_2 + \cos[2\theta(\boldsymbol{x})]\boldsymbol{v}_3. \end{aligned} \tag{3.25}$$

Substituting (3.22) and (3.23) into (3.24), using (3.25), and equating the coefficients of $\boldsymbol{v}_1$, $\boldsymbol{v}_2$, and $\boldsymbol{v}_3$ yields the constitutive relation

$$\begin{pmatrix} \epsilon_1 \\ \epsilon_2 \\ \epsilon_3 \end{pmatrix} = \begin{pmatrix} 0 & 0 \\ 0 & \boldsymbol{S}_r(\boldsymbol{x}) \end{pmatrix} \begin{pmatrix} \tau_1 \\ \tau_2 \\ \tau_3 \end{pmatrix}, \tag{3.26}$$

in which $\boldsymbol{S}_r(\boldsymbol{x})$ is the matrix

$$\boldsymbol{S}_r(\boldsymbol{x}) = \begin{pmatrix} \cos(2\theta) & \sin(2\theta) \\ -\sin(2\theta) & \cos(2\theta) \end{pmatrix} \begin{pmatrix} 1/2\mu^{(1)} & 0 \\ 0 & 1/2\mu^{(2)} \end{pmatrix} \begin{pmatrix} \cos(2\theta) & -\sin(2\theta) \\ \sin(2\theta) & \cos(2\theta) \end{pmatrix},$$

where $\theta = \theta(\boldsymbol{x})$ depends on $\boldsymbol{x}$. From the constitutive relation (3.26) we see that

$$\boldsymbol{S}(\boldsymbol{x}) = \begin{pmatrix} 0 & 0 \\ 0 & \boldsymbol{S}_r(\boldsymbol{x}) \end{pmatrix}$$

must be the matrix representing the compliance tensor in the basis $(\boldsymbol{v}_1, \boldsymbol{v}_2, \boldsymbol{v}_3)$.

Now observe that the determinant of $\boldsymbol{S}_r(\boldsymbol{x})$ takes a constant value

$$\Delta = 1/(4\mu^{(1)}\mu^{(2)}),$$

independent of $\boldsymbol{x}$. From the duality result (3.17) it follows that the effective tensor must share the same value of the determinant of the reduced matrix. In other words, the two effective shear moduli $\mu_*^{(1)}$ and $\mu_*^{(2)}$ of the polycrystal must be such that

$$\mu_*^{(1)}\mu_*^{(2)} = \mu^{(1)}\mu^{(2)}. \tag{3.27}$$

This result was first obtained by Lurie and Cherkaev (1984). In particular, if the polycrystal is elastically isotropic with shear modulus μ_*, then $\mu_*^{(1)} = \mu_*^{(2)} = \mu_*$ and (3.27) implies that

$$\mu_* = \sqrt{\mu^{(1)}\mu^{(2)}}.$$

Thus the planar effective shear modulus of an incompressible two-dimensional polycrystal is independent of the microstructure. We will see in section 4.7 on page 69 that this is true even when the crystal is compressible, so long as it has square symmetry.

Another interesting application of these duality transformations is to two-phase isotropic composites of two isotropic incompressible phases. In the basis $(\boldsymbol{v}_1, \boldsymbol{v}_2, \boldsymbol{v}_3)$ the matrices representing the compliance tensor $\boldsymbol{S}(\boldsymbol{x})$ and effective compliance tensor $\boldsymbol{S}_*$ take the form

$$\boldsymbol{S}(\boldsymbol{x}) = \begin{pmatrix} 0 & 0 & 0 \\ 0 & \chi_1(\boldsymbol{x})/2\mu_1 + \chi_2(\boldsymbol{x})/2\mu_2 & 0 \\ 0 & 0 & \chi_1(\boldsymbol{x})/2\mu_1 + \chi_2(\boldsymbol{x})/2\mu_2 \end{pmatrix},$$

$$\boldsymbol{S}_* = \begin{pmatrix} 0 & 0 & 0 \\ 0 & 1/2\mu_* & 0 \\ 0 & 0 & 1/2\mu_* \end{pmatrix},$$

where μ_1, μ_2, and μ_* are the shear moduli of the two phases and composite, and $\chi_1(\boldsymbol{x}) = 1 - \chi_2(\boldsymbol{x})$ is the characteristic function (3.7) representing the geometry of phase 1. If we consider the effective shear modulus as a function $\mu_*(\mu_1, \mu_2)$ of the shear moduli μ_1 and μ_2, the duality result (3.19) implies the phase interchange identity

$$\mu_*(\mu_2, \mu_1)\mu_*(\mu_1, \mu_2) = \mu_1\mu_2, \tag{3.28}$$

of Berdichevskii (1983). If the geometry is symmetric (i.e., phase interchange invariant) and elastically isotropic, then this identity yields an exact formula for the planar effective shear modulus:

$$\mu_*(\mu_1, \mu_2) = \sqrt{\mu_1\mu_2}.$$

References

Berdichevskii, V. L. 1983. *Variational Principles in Mechanics of Continuum Media*. Moscow: Nauka. 2 + 446 pp. {*51, 57*}

Berdichevskii, V. L. 1985. Heat conduction of checkerboard structures. *Vestnik Moskovskogo Universiteta. Seriya I. Matematika, Mekhanika* 40(4):56–63. {*49, 57, 143, 155*}

Bergman, D. J. and Y. M. Strelniker 1998. Duality transformation in a three dimensional conducting medium with two dimensional heterogeneity and an in-plane magnetic field. *Physical Review Letters* 80(15):3356–3359. {*34, 41, 51, 57*}

Dykhne, A. M. 1970. Conductivity of a two-dimensional two-phase system. *Zhurnal eksperimental'noi i teoreticheskoi fiziki / Akademiia Nauk SSSR* 59:110–115. English translation in *Soviet Physics JETP* 32:63–65 (1971). {*47, 49, 50, 57*}

Dykhne, A. M. and I. M. Kaganova 1997. The electrodynamics of polycrystals. *Physics Reports* 288:263–290. {*47, 57*}

Flaherty, J. E. and J. B. Keller 1973. Elastic behavior of composite media. *Communications on Pure and Applied Mathematics (New York)* 26:565–580. {*49, 57, 210, 215*}

Francfort, G. A. and F. Murat 1987. Optimal bounds for conduction in two-dimensional, two-phase, anisotropic media. In R. J. Knops and A. A. Lacey (eds.), *Non-Classical Continuum Mechanics: Proceedings of the London Mathematical Society Symposium, Durham, July 1986*, pp. 197–212. Cambridge, United Kingdom: Cambridge University Press. ISBN 0-521-34935-4. {*47, 57, 447, 453*}

Helsing, J., G. W. Milton, and A. B. Movchan 1997. Duality relations, correspondences and numerical results for planar elastic composites. *Journal of the Mechanics and Physics of Solids* 45(4):565–590. {*39, 43, 51, 53, 55, 57, 70, 72, 105, 106, 111*}

Keller, J. B. 1963. Conductivity of a medium containing a dense array of perfectly conducting spheres or cylinders or nonconducting cylinders. *Journal of Applied Physics* 34(4):991–993. {*47, 58, 208, 210, 216*}

Keller, J. B. 1964. A theorem on the conductivity of a composite medium. *Journal of Mathematical Physics* 5(4):548–549. {*47, 49, 58*}

Levy, O. and R. V. Kohn 1998. Duality relations for non-Ohmic composites, with applications to behavior near percolation. *Journal of Statistical Physics* 90(1/2):159–189. {*47, 58*}

Lurie, K. A. and A. V. Cherkaev 1984. *G*-closure of some particular sets of admissible material characteristics for the problem of bending of thin elastic plates. *Journal of Optimization Theory and Applications* 42(2):305–316. {*56, 58, 66, 70, 72*}

Matheron, G. 1967. *Eléments pour une théorie des milieux poreux. (French) [Elements for a Theory of Porous Media]*. Masson, France: Masson Editeur. 168 pp. {*47, 58*}

Mendelson, K. S. 1975. A theorem on the effective conductivity of a two-dimensional heterogeneous medium. *Journal of Applied Physics* 46(11):4740–4741. {*47, 48, 58*}

Nevard, J. and J. B. Keller 1985. Reciprocal relations for effective conductivities of anisotropic media. *Journal of Mathematical Physics* 26(11):2761–2765. {*47, 58*}

Schulgasser, K. 1977. Bounds on the conductivity of statistically isotropic polycrystals. *Journal of Physics C: Solid State Physics* 10:407–417. {*47, 51, 58, 438–440, 454, 589, 600*}

Schulgasser, K. 1992. A reciprocal theorem in two-dimensional heat transfer and its implications. *International Communications in Heat and Mass Transfer* 19:639–649. {*49, 58*}

Strelniker, Y. M. and D. J. Bergman 2000. Exact relations between magnetoresistivity tensor components of conducting composites with a columnar microstructure. *Physical Review B (Solid State)* 61(9):6288–6297. {*34, 46, 51, 58*}

Zhikov, V. V., S. M. Kozlov, and O. A. Oleinik 1994. *Homogenization of Differential Operators and Integral Functionals*. Berlin / Heidelberg / London / etc.: Springer-Verlag. xi + 570 pp. ISBN 3-540-54809-2 (Berlin), 0-387-54809-2 (New York). {*xxv, xxviii, 8, 11, 13, 18, 47, 58, 200, 220*}

4

Translations and equivalent media

There are sometimes certain tensors $\boldsymbol{T}$, called translations, such that if $\boldsymbol{T}$ is added to the local tensor field $\boldsymbol{L}(\boldsymbol{x})$, then the effective tensor will also be shifted by $\boldsymbol{T}$. We saw a trivial example of such a tensor in section 2.5 on page 30, where it was remarked that if the local specific heat is shifted by a constant $-t$, the effective specific heat would also be shifted by that same constant [see equations (2.25) and (2.26)]. Here we discuss other translations and show how they lead to useful predictions about effective moduli. We will see later, in section 13.3 on page 274, that such translations are connected with quadratic null Lagrangians, when $\boldsymbol{T}$ is self-adjoint, and, more generally, with weakly continuous bilinear functions when $\boldsymbol{T}$ is not necessarily self-adjoint. There is an extensive literature on the theory of such functions (see section 13.3 on page 274 for some references) and the examples of this section fall under the umbrella of the more general theory. In particular, it is easy to check that all of the constant translations $\boldsymbol{T}$ discussed here satisfy the necessary and sufficient algebraic condition given by Murat (1978), theorem 3; see also Tartar (1979).

4.1. Translations applied to conductivity

The duality transformation is clearly a discrete transformation. However, as we will now see, it is just one example of a continuous group of fractional linear transformations, each having the special property that the effective tensor undergoes the same transformation as the local conductivity tensor.

An important first step is to understand a subgroup of transformations that are translations. Following Dykhne (1970), suppose that we have a solution to the conductivity problem (3.1). Then, for any choice of the constant c, the fields

$$\boldsymbol{e}'(\boldsymbol{x}) \equiv \boldsymbol{e}(\boldsymbol{x}), \quad \boldsymbol{j}'(\boldsymbol{x}) \equiv \boldsymbol{j}(\boldsymbol{x}) + c\boldsymbol{R}_\perp \boldsymbol{e}(\boldsymbol{x}) = (\boldsymbol{\sigma}(\boldsymbol{x}) + c\boldsymbol{R}_\perp)\boldsymbol{e}'(\boldsymbol{x}) \tag{4.1}$$

clearly solve the equations of conductivity in a medium with conductivity tensor

$$\boldsymbol{\sigma}'(\boldsymbol{x}) = \boldsymbol{\sigma}(\boldsymbol{x}) + c\boldsymbol{R}_\perp,$$

called the translated medium, because the conductivity tensor field $\boldsymbol{\sigma}(\boldsymbol{x})$ is shifted (translated) by the constant tensor $c\boldsymbol{R}_\perp$. Moreover, by taking averages over $\boldsymbol{x}$ of (4.1), we see that

$$\langle \boldsymbol{j}'(\boldsymbol{x}) \rangle = \langle \boldsymbol{j}(\boldsymbol{x}) \rangle + c\boldsymbol{R}_\perp \langle \boldsymbol{e}(\boldsymbol{x}) \rangle = (\boldsymbol{\sigma}_* + c\boldsymbol{R}_\perp)\langle \boldsymbol{e}'(\boldsymbol{x}) \rangle,$$

which implies that the translated medium has effective tensor

$$\boldsymbol{\sigma}'_* = \boldsymbol{\sigma}_* + c\boldsymbol{R}_\perp. \tag{4.2}$$

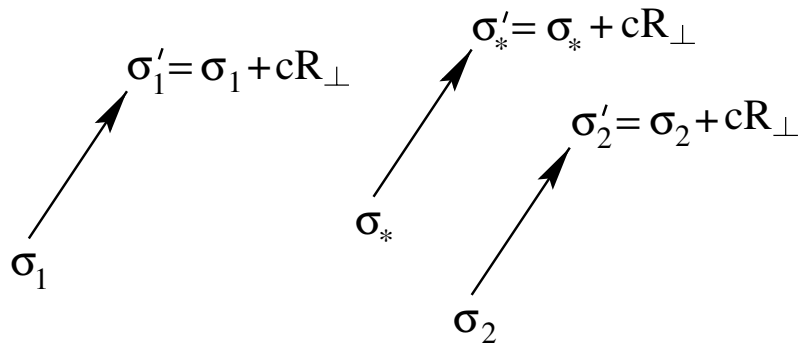

Figure 4.1. The idea of translation applied to a two-dimensional, two-phase conducting composite. When the component conductivity tensors $\boldsymbol{\sigma}_1$ and $\boldsymbol{\sigma}_2$ are translated in tensor space by $c\boldsymbol{R}_\perp$, the effective tensor $\boldsymbol{\sigma}_*$ is also translated in exactly the same way.

So the effective tensor translates in exactly the same way as the local conductivity tensor; see figure 4.1.

Similarly, by considering the relations between the fields

$$\boldsymbol{j}'(\boldsymbol{x}) = \boldsymbol{j}(\boldsymbol{x}), \qquad \boldsymbol{e}'(\boldsymbol{x}) = \boldsymbol{e}(\boldsymbol{x}) + c\boldsymbol{R}_\perp \boldsymbol{j}(\boldsymbol{x}),$$

we establish that when the inverse conductivity tensor field $[\boldsymbol{\sigma}(\boldsymbol{x})]^{-1}$ is translated to

$$[\boldsymbol{\sigma}'(\boldsymbol{x})]^{-1} = [\boldsymbol{\sigma}(\boldsymbol{x})]^{-1} + c\boldsymbol{R}_\perp \tag{4.3}$$

the inverse of the effective tensor undergoes the same translation:

$$(\boldsymbol{\sigma}'_*)^{-1} = (\boldsymbol{\sigma}_*)^{-1} + c\boldsymbol{R}_\perp. \tag{4.4}$$

More generally, we can combine translations of the conductivity tensor and inverse conductivity translations with homogeneity transformations. In this way Dykhne (1970) recognized that for any choice of parameters c_1, c_2, c_3, and c_4 a material with inverse conductivity tensor

$$[\boldsymbol{\sigma}'(\boldsymbol{x})]^{-1} = (c_3 + c_2c_4/c_1)[c_1\boldsymbol{\sigma}(\boldsymbol{x}) + c_2\boldsymbol{R}_\perp]^{-1} + (c_4/c_1)\boldsymbol{R}_\perp$$

or, equivalently, with tensor

$$\boldsymbol{\sigma}'(\boldsymbol{x}) = [c_1\boldsymbol{\sigma}(\boldsymbol{x}) + c_2\boldsymbol{R}_\perp][c_3\boldsymbol{I} + c_4\boldsymbol{R}_\perp\boldsymbol{\sigma}(\boldsymbol{x})]^{-1}, \tag{4.5}$$

would have effective tensor

$$\boldsymbol{\sigma}'_* = [c_1\boldsymbol{\sigma}_* + c_2\boldsymbol{R}_\perp][c_3\boldsymbol{I} + c_4\boldsymbol{R}_\perp\boldsymbol{\sigma}_*]^{-1}.$$

With the particular choice $c_1 = c_3 = 0, c_2 = c_4 = 1$ this transformation is precisely the duality transformation (3.3).

4.2. A formula for the Hall coefficient in two-dimensional polycrystals

Unlike the duality transformation, these fractional linear transformations (4.5) can change the symmetry of the tensor $\boldsymbol{\sigma}(\boldsymbol{x})$. The freedom in the choice of parameters c_1, c_2, c_3, and c_4 may

sometimes be used to advantage to map to an equivalent conductivity problem where $\boldsymbol{\sigma}(\boldsymbol{x})$ is not self-adjoint (due to the presence of a magnetic field) to a conductivity problems with a self-adjoint tensor field $\boldsymbol{\sigma}'(\boldsymbol{x})$ (in effect removing the complications due to the magnetic field).

From an experimental viewpoint it is desirable to express results in terms of the resistivity tensor field $\boldsymbol{\rho}(\boldsymbol{x}) = (\boldsymbol{\sigma}(\boldsymbol{x}))^{-1}$ and the effective resistivity tensor $\boldsymbol{\rho}_* = (\boldsymbol{\sigma}_*)^{-1}$, rather than in terms of the conductivity. For conduction in a polycrystal in the presence of a fixed magnetic field the local resistivity tensor field has the form

$$\boldsymbol{\rho}(\boldsymbol{x}) = \boldsymbol{R}(\boldsymbol{x})\boldsymbol{\rho}_0\boldsymbol{R}^T(\boldsymbol{x}), \qquad \boldsymbol{\rho}_0 \equiv \begin{pmatrix} \alpha_1 & \mu \\ -\mu & \alpha_2 \end{pmatrix}.$$

Onsager's principle (Lifshitz and Pitaevskii 1980) implies that μ will be an odd function of the magnetic field h applied perpendicular to the plane of conduction, while α_1 and α_2 will be even functions of h. At low magnetic fields μ is proportional to the magnetic field h,

$$\mu = Rh,$$

where the constant of proportionality R is called the Hall coefficient. In this section and in the subsequent one we will obtain formulas for μ_* or, equivalently, R in terms of other moduli.

Under the translation (4.3) the resistivity tensor field maps to

$$\boldsymbol{\rho}'(\boldsymbol{x}) = \boldsymbol{R}(\boldsymbol{x})\boldsymbol{\rho}_0'\boldsymbol{R}^T(\boldsymbol{x}), \qquad \boldsymbol{\rho}_0' \equiv \begin{pmatrix} \alpha_1 & c+\mu \\ -c-\mu & \alpha_2 \end{pmatrix}.$$

By selecting $c = -\mu$ we completely eliminate the antisymmetric part of the resistivity tensor field. Accordingly, the effective tensor $\boldsymbol{\rho}_*'$ must also be symmetric, of the form

$$\boldsymbol{\rho}_*' = \begin{pmatrix} \alpha_1^* & 0 \\ 0 & \alpha_2^* \end{pmatrix},$$

with $\alpha_1^*\alpha_2^* = \rho_1\rho_2$. It then follows directly from (4.4) that

$$\boldsymbol{\rho}_* = \begin{pmatrix} \alpha_1^* & \mu \\ -\mu & \alpha_2^* \end{pmatrix}.$$

In other words, the polycrystal tensor $\boldsymbol{\rho}_*$ and pure crystal tensor $\boldsymbol{\rho}_0$ share the same determinant, $\alpha_1\alpha_2 + \mu^2$, and Hall coefficient, R, irrespective of the crystal structure.

4.3. A formula for the Hall coefficient in two-phase, two-dimensional media†

As a second example of the usefulness of the transformation (4.5) in eliminating the skew part of the tensor field $\boldsymbol{\rho}(\boldsymbol{x})$, let us consider conduction in the presence of a magnetic field in a two-dimensional two-phase composite (Milton 1988). Although the ensuing analysis extends

†Throughout the book a dagger (†) is used to denote sections or chapters that can be skipped on a first reading of the book. These sections or chapters contain material that is not central to the book, or they include more advanced or more technical subject matter. However, they also sometimes address topics that are at the forefront of current research.

to the general case where both phases are anisotropic, let us assume, for simplicity, that the phases are isotropic. Then the local resistivity tensor takes the form

$$\boldsymbol{\rho}(\boldsymbol{x}) = \chi_1(\boldsymbol{x})\boldsymbol{\rho}_1 + \chi_2(\boldsymbol{x})\boldsymbol{\rho}_2,$$

where the characteristic functions χ_1 and χ_2 are defined by (3.7), and because of isotropy of the components, the tensors $\boldsymbol{\rho}_1$ and $\boldsymbol{\rho}_2$ have the form

$$\boldsymbol{\rho}_1 = \varrho_1\boldsymbol{I} + \mu_1\boldsymbol{R}_\perp, \quad \boldsymbol{\rho}_2 = \varrho_2\boldsymbol{I} + \mu_2\boldsymbol{R}_\perp.$$

Now the fractional linear transformation (4.5) maps the resistivity tensor field $\boldsymbol{\rho}(\boldsymbol{x})$ to

$$\boldsymbol{\rho}'(\boldsymbol{x}) = [c_3\boldsymbol{\rho}(\boldsymbol{x}) + c_4\boldsymbol{R}_\perp][c_1\boldsymbol{I} + c_2\boldsymbol{R}_\perp\boldsymbol{\rho}(\boldsymbol{x})]^{-1} \tag{4.6}$$

and maps the effective resistivity tensor $\boldsymbol{\rho}_*$ to

$$\boldsymbol{\rho}'_* = [c_3\boldsymbol{\rho}_* + c_4\boldsymbol{R}_\perp][c_1\boldsymbol{I} + c_2\boldsymbol{R}_\perp\boldsymbol{\rho}_*]^{-1}.$$

Note that $\boldsymbol{R}_\perp$ has the same algebraic properties as the complex number i, satisfying

$$(\boldsymbol{R}_\perp)^2 = -\boldsymbol{I}.$$

Consequently, the usual tricks that give the inverse of a complex number can be applied to evaluate (4.6). For simplicity, and without loss of generality, we assume that

$$c_3 = c_2 = 1.$$

In effect this removes the trivial part of the transformation (4.6) that corresponds to multiplying the tensor by constant factor. Then, using the algebraic properties of $\boldsymbol{R}_\perp$ we have, for $j = 1$ or 2,

$$\begin{aligned}[c_1\boldsymbol{I} + \boldsymbol{R}_\perp\boldsymbol{\rho}_j]^{-1} &= [(c_1-\mu_j)\boldsymbol{I} - \varrho_j\boldsymbol{R}_\perp]\{[(c_1-\mu_j)\boldsymbol{I} + \varrho_j\boldsymbol{R}_\perp][(c_1-\mu_j)\boldsymbol{I} - \varrho_j\boldsymbol{R}_\perp]\}^{-1}\\ &= [(c_1-\mu_j)\boldsymbol{I} - \varrho_j\boldsymbol{R}_\perp]/[(c_1-\mu_j)^2 + (\varrho_j)^2].\end{aligned}$$

It follows from this analysis that the fractional linear transformation (4.5) preserves isotropy and maps $\boldsymbol{\rho}(\boldsymbol{x})$ to the tensor field

$$\boldsymbol{\rho}'(\boldsymbol{x}) = \chi_1(\boldsymbol{x})\boldsymbol{\rho}'_1 + \chi_2(\boldsymbol{x})\boldsymbol{\rho}'_2,$$

where

$$\boldsymbol{\rho}'_1 = \varrho'_1\boldsymbol{I} + \mu'_1\boldsymbol{R}_\perp, \quad \boldsymbol{\rho}'_2 = \varrho'_2\boldsymbol{I} + \mu'_2\boldsymbol{R}_\perp$$

and

$$\begin{aligned}\varrho'_j &= (c_4+c_1)\varrho_j/[(c_1-\mu_j)^2 + \varrho_j^2],\\ \mu'_j &= [(c_4+\mu_j)(c_1-\mu_j) - \varrho_j^2]/[(c_1-\mu_j)^2 + \varrho_j^2].\end{aligned} \tag{4.7}$$

Luc Tartar (private communication) drew my attention to a beautiful geometrical way of thinking about this transformation based on the fact that $\boldsymbol{R}_\perp$ has the same algebraic properties as the complex number i. We can represent the tensors $\boldsymbol{\rho}_1$ and $\boldsymbol{\rho}_2$ as points

$$\rho_1 = \varrho_1 + i\mu_1, \quad \rho_2 = \varrho_2 + i\mu_2$$

in the complex ρ-plane, and we can represent $\boldsymbol{\rho}_1'$ and $\boldsymbol{\rho}_2'$ as points

$$\rho_1' = \varrho_1' + i\mu_1', \quad \rho_2' = \varrho_2' + i\mu_2'$$

in the complex ρ'-plane. Then the transformation (4.6), with $c_3 = c_2 = 1$, is equivalent to the fractional linear transformation

$$\rho' = (\rho + ic_4)/(c_1 + i\rho),$$

which maps the complex ρ-plane to the complex ρ'-plane. The points ρ_1' and ρ_2' are the images of ρ_1 and ρ_2 under this mapping. The fractional linear transformation is special in that the imaginary axis gets mapped to itself, and circles or straight lines symmetric about the imaginary axis get mapped to circles or straight lines symmetric about the imaginary axis. Now consider a circle symmetric about the imaginary axis passing through the points ρ_1 and ρ_2, as illustrated in figure 4.2. One expects that it should be possible to find a fractional linear transformation that maps this circle to the real axis, that is, a transformation that maps the original problem to an equivalent one where the resistivity tensor is symmetric, in effect converting it to a problem where the magnetic field is absent.

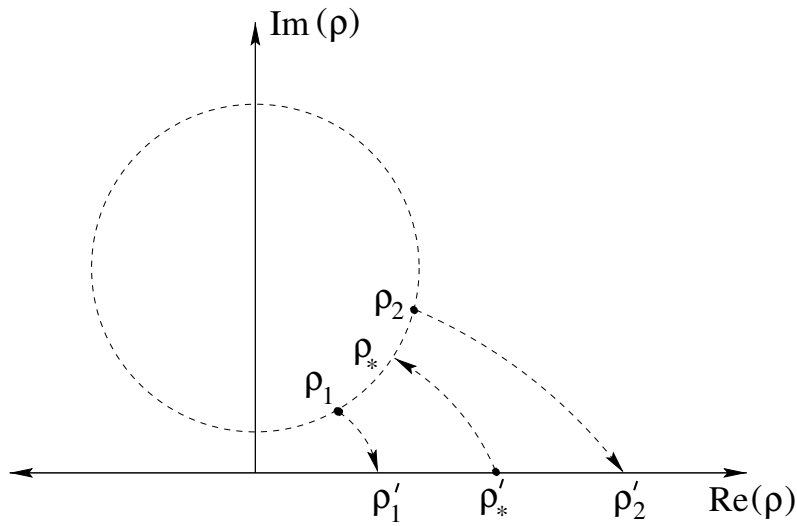

Figure 4.2. To find the fractional linear transformation of the required form that maps ρ_1 and ρ_2 to ρ_1' and ρ_2' on the real axis, one can look for a circle symmetric about the imaginary axis that passes through ρ_1 and ρ_2 and then find the appropriate fractional linear transformation that maps this circle to the real axis. When ρ_1' and ρ_2' are real ρ_*' is also real, and therefore the effective modulus ρ_* must lie on the circle for all isotropic microstructures. If a formula is available for ρ_*' given ρ_1' and ρ_2', then one can determine ρ_* through the inverse fractional linear transformation.

In other words, let us adjust the two free parameters c_1 and c_4 until the antisymmetric parts of the tensors $\boldsymbol{\rho}_1'$ and $\boldsymbol{\rho}_2'$ vanish, that is, until $\mu_1' = \mu_2' = 0$. From (4.7) this requires that c_1 and c_4 satisfy

$$\begin{aligned} c_1c_4 + (c_1 - c_4)\mu_1 &= \Delta_1, \\ c_1c_4 + (c_1 - c_4)\mu_2 &= \Delta_2, \end{aligned} \tag{4.8}$$

where Δ_1 and Δ_2 are the determinants

$$\Delta_1 \equiv \varrho_1^2 + \mu_1^2, \quad \Delta_2 \equiv \varrho_2^2 + \mu_2^2 \tag{4.9}$$

of the resistivity tensors $\boldsymbol{\rho}_1$ and $\boldsymbol{\rho}_2$. These equations are easily solved for c_1 and c_4, and it can be established that the solutions

$$\begin{aligned} c_1 &= \frac{(\Delta_2 - \Delta_1)}{2(\mu_2 - \mu_1)} \pm \frac{1}{2}\sqrt{\frac{(\Delta_2 - \Delta_1)^2}{(\mu_2 - \mu_1)^2} + \frac{4(\mu_2\Delta_1 - \mu_1\Delta_2)}{(\mu_2 - \mu_1)}}, \\ c_4 &= \frac{(\Delta_1 - \Delta_2)}{2(\mu_2 - \mu_1)} \pm \frac{1}{2}\sqrt{\frac{(\Delta_2 - \Delta_1)^2}{(\mu_2 - \mu_1)^2} + \frac{4(\mu_2\Delta_1 - \mu_1\Delta_2)}{(\mu_2 - \mu_1)}}, \end{aligned} \tag{4.10}$$

(where the same choice of $+$ or $-$ must be made in each equation) are real so long as ρ_1 and ρ_2 are both positive. With this choice of c_1 and c_4, the formulas (4.7) reduce to

$$\varrho_1' = \varrho_1/(c_1 - \mu_1), \quad \varrho_2' = \varrho_2/(c_1 - \mu_2), \quad \mu_1' = \mu_2' = 0. \tag{4.11}$$

It follows that the effective tensor $\boldsymbol{\rho}_*'$ must necessarily be symmetric because $\boldsymbol{\rho}_1'$ and $\boldsymbol{\rho}_2'$ are symmetric tensors. In particular, if the effective properties of the composite are isotropic, in the sense that $\boldsymbol{\rho}_*$ has the form

$$\boldsymbol{\rho}_* = \varrho_* \boldsymbol{I} + \mu_* \boldsymbol{R}_\perp,$$

then by analogy with (4.9) and (4.11) we have

$$c_1 c_4 + (c_1 - c_4)\mu_* = \Delta_*, \quad \text{where} \quad \Delta_* \equiv \varrho_*^2 + \mu_*^2, \tag{4.12}$$

and

$$\boldsymbol{\rho}_*' = \varrho_*' \boldsymbol{I} + \mu_*' \boldsymbol{R}_\perp, \quad \text{where} \quad \varrho_*' = \varrho_*/(c_1 - \mu_*), \quad \mu_*' = 0. \tag{4.13}$$

For (4.12) to be consistent with (4.8) the determinant

$$\det \begin{vmatrix} 1 & \mu_* & \Delta_* \\ 1 & \mu_1 & \Delta_1 \\ 1 & \mu_2 & \Delta_2 \end{vmatrix} = 0,$$

must vanish, or, equivalently, the identity

$$\frac{\mu_2 - \mu_*}{\mu_2 - \mu_1} = \frac{\Delta_2 - \Delta_*}{\Delta_2 - \Delta_1}, \tag{4.14}$$

must hold irrespective of the precise details of the microstructure.

We conclude that in the (Δ, μ)-plane the point (Δ_*, μ_*) representing the effective tensor $\boldsymbol{\rho}_*$ must lie on the straight line joining the points (Δ_1, μ_1) and (Δ_2, μ_2) that represent the tensors $\boldsymbol{\rho}_1$ and $\boldsymbol{\rho}_2$ of the components. This relation (Milton 1988; Dykhne and Ruzin 1994) is equivalent to saying that the point ρ_* in the complex plane must lie on the circle that is symmetric about the imaginary axis and which passes through the points ρ_1 and ρ_2; see figure 4.2 on the preceding page. It has been numerically verified by Christiansson (1997) and generalizes a relation

$$\frac{\mu_2 - \mu_*}{\mu_2 - \mu_1} \approx \frac{\varrho_2^2 - \varrho_*^2}{\varrho_2^2 - \varrho_1^2}$$

of Shklovskiĭ (1977) [see also Bergman (1983)], who assumed that the magnetic field h was small, that is, μ_1 and μ_2 were small compared with ϱ_1 and ϱ_1.

Moreover, the effective tensor $\boldsymbol{\rho}_*$ can be computed exactly if we know the effective conductivity function $\sigma_*(\sigma_1, \sigma_2)$ in the absence of a magnetic field. Indeed, when c_1 and c_4 are chosen so that $\mu_1' = \mu_2' = \mu_*' = 0$, (4.10) implies that

$$\varrho_*' = \frac{1}{\sigma_*(1/\varrho_1', 1/\varrho_2')} = \left[\sigma_*\Big(\frac{c_1-\mu_1}{\varrho_1}, \frac{c_1-\mu_2}{\varrho_2}\Big)\right]^{-1} = \sigma_*\Big(\frac{\varrho_1}{c_1-\mu_1}, \frac{\varrho_2}{c_1-\mu_2}\Big), \quad (4.15)$$

where we have used the duality relation (3.8) to obtain the last relation. Equating this expression for ϱ' with (4.13) and combining the result with (4.14) yields (after some algebra) expressions for ϱ_* and μ_* in terms of $\boldsymbol{\rho}_1$, $\boldsymbol{\rho}_2$ and the function $\sigma_*(\sigma_1, \sigma_2)$:

$$\varrho_* = \frac{1}{\varrho_*' + 1/\varrho_*'}\sqrt{\frac{(\Delta_2-\Delta_1)^2}{(\mu_2-\mu_1)^2} + \frac{4(\mu_2\Delta_1 - \mu_1\Delta_2)}{(\mu_2-\mu_1)}}, \qquad \mu_* = c_1 - \varrho_*/\varrho_*', \quad (4.16)$$

in which ϱ_*' is given by (4.15) and c_1 is given by (4.10), while Δ_1 and Δ_2 are given by (4.9). For example, we obtain the exact values of ϱ_* and μ_* for a checkerboard geometry by substituting

$$\varrho_*' = \sqrt{\frac{\varrho_1\varrho_2}{(c_1-\mu_1)(c_1-\mu_2)}}$$

back into (4.16).

4.4. Inhomogeneous translations for three-dimensional conductivity

So far we have been considering translations of the two-dimensional conductivity tensor field $\boldsymbol{\sigma}(\boldsymbol{x})$ or the associated resistivity field $\boldsymbol{\rho}(\boldsymbol{x})$ by a constant translation $c\boldsymbol{R}_\perp$. In three-dimensional conductivity we can translate the conductivity tensor field $\boldsymbol{\sigma}(\boldsymbol{x})$ by any periodic divergence free antisymmetric matrix-valued field $\boldsymbol{A}(\boldsymbol{x})$. (A matrix-valued field is divergence free if each column is a divergence free vector field.) The essential observation to make is that if $\boldsymbol{e}(\boldsymbol{x})$ is curl free, then the vector field $\boldsymbol{A}(\boldsymbol{x})\boldsymbol{e}(\boldsymbol{x})$ is divergence free:

$$\frac{\partial A_{ik}e_k}{\partial x_i} = \frac{\partial A_{ik}}{\partial x_i}e_k + A_{ik}\frac{\partial e_k}{\partial x_i} = \tfrac{1}{2}A_{ik}\left[\frac{\partial e_k}{\partial x_i} - \frac{\partial e_i}{\partial x_k}\right] = 0,$$

where summation over the repeated indices i and k is implied. Also, the antisymmetry of $\boldsymbol{A}(\boldsymbol{x})$ implies that each row of $\boldsymbol{A}(\boldsymbol{x})$ is divergence free. Consequently we have

$$\langle A_{ik}e_k\rangle = \langle A_{ik}\rangle\langle e_k\rangle,$$

as can be seen by integrating by parts. In particular, suppose that the field $\boldsymbol{e}(\boldsymbol{x})$ solves the conductivity equations (3.1) in the three-dimensional material $\boldsymbol{\sigma}(\boldsymbol{x})$. Then the fields

$$\boldsymbol{e}'(\boldsymbol{x}) = \boldsymbol{e}(\boldsymbol{x}), \quad \boldsymbol{j}'(\boldsymbol{x}) = \boldsymbol{j}(\boldsymbol{x}) + \boldsymbol{A}(\boldsymbol{x})\boldsymbol{e}(\boldsymbol{x}) \quad (4.17)$$

solve the conductivity equations in a medium with tensor

$$\boldsymbol{\sigma}'(\boldsymbol{x}) = \boldsymbol{\sigma}(\boldsymbol{x}) + \boldsymbol{A}(\boldsymbol{x}).$$

By taking averages of the fields in (4.17) we deduce that this new translated material has effective tensor

$$\boldsymbol{\sigma}'_* = \boldsymbol{\sigma}_* + \langle \boldsymbol{A} \rangle.$$

In particular, we conclude that when the conductivity tensor field $\boldsymbol{\sigma}(\boldsymbol{x})$ is translated by any constant antisymmetric tensor, the effective tensor $\boldsymbol{\sigma}_*$ of the medium is translated in exactly the same fashion (Stroud and Bergman 1984). However, the same does not hold true for the resistivity tensor since $\boldsymbol{A}$ acting on an arbitrary divergence free field does not produce a curl free field. Such translations of the resistivity tensor are only valid in two dimensions.

4.5. Translations for elasticity

A translation for two-dimensional linear elasticity was found by Lurie and Cherkaev (1984) in the context of the plate equation. Their work remained relatively unnoticed until Day, Snyder, Garboczi, and Thorpe (1992) numerically discovered that the effective Young's modulus of a metal plate with holes depends only on the Young's modulus of the metal and not at all on its Poisson's ratio. I realized that this could be proved using the translation of Lurie and Cherkaev. Our subsequent joint paper (Cherkaev, Lurie, and Milton 1992) received considerable attention, and for isotropic planar composites of isotropic components, the result that when $-1/\kappa(\boldsymbol{x})$ and $1/\mu(\boldsymbol{x})$ are shifted by given constant the moduli $-1/\kappa_*$ and $1/\mu_*$ undergo the same shift has become known as the CLM theorem, although it really stems back to the earlier paper of Lurie and Cherkaev. The theorem was linked by Thorpe and Jasiuk (1992) to certain invariance properties of the stress in two-phase bodies and composites that had been discovered by Dundurs (1967b, 1970). Dundurs had generalized a result of Michell (1899), who found that the stress in a homogeneous body is independent of the Poisson's ratio provided that the body is singly connected, or the tractions over each hole give no net force [see also Dundurs (1967a)]. Dundurs and Markenscoff (1993) and Chen (1995) [see also He (1998)] found that the stress in an inhomogeneous body is also invariant for shifts in the moduli that depend linearly on $\boldsymbol{x}$. Stress invariance results were extended to anisotropic inhomogeneous planar elastic bodies by Moran and Gosz (1994), to planar piezoelectric bodies by Chen (1995) [see also Chen and Lai (1997)], and to planar Cosserat elastic bodies by Ostoja-Starzewski and Jasiuk (1995).

The key property of the translation $\boldsymbol{R}_\perp$, essential for deriving (4.2), is that it maps the fields on the right-hand side of the constitutive equation, in this case curl free fields, to fields of the same type as those on the left-hand side of the constitutive equation, namely, divergence free fields. In two-dimensional elasticity, there is a fourth-order tensor that acts in a similar way to map stress fields to strain fields.

Let $\boldsymbol{\epsilon}(\boldsymbol{x})$ and $\boldsymbol{\tau}(\boldsymbol{x})$ be strain and stress fields that solve the two-dimensional equations of elasticity,

$$\boldsymbol{\epsilon}(\boldsymbol{x}) = \boldsymbol{\mathcal{S}}(\boldsymbol{x})\boldsymbol{\tau}(\boldsymbol{x}), \quad \nabla \cdot \boldsymbol{\tau}(\boldsymbol{x}) = 0, \quad \boldsymbol{\epsilon}(\boldsymbol{x}) = [\nabla \boldsymbol{u}(\boldsymbol{x}) + (\nabla \boldsymbol{u}(\boldsymbol{x}))^T]/2, \tag{4.18}$$

where $\boldsymbol{\mathcal{S}}(\boldsymbol{x})$ is the fourth-order compliance tensor. By definition, the effective compliance tensor, $\boldsymbol{\mathcal{S}}_*$, governs the linear relation between the averages of these fields:

$$\langle \boldsymbol{\epsilon}(\boldsymbol{x}) \rangle = \boldsymbol{\mathcal{S}}_* \langle \boldsymbol{\tau}(\boldsymbol{x}) \rangle,$$

Now suppose that we take the stress tensor field,

$$\boldsymbol{\tau} = \begin{pmatrix} \tau_{11} & \tau_{12} \\ \tau_{12} & \tau_{22} \end{pmatrix} = \begin{pmatrix} \phi_{,22} & -\phi_{,12} \\ -\phi_{,12} & \phi_{,11} \end{pmatrix},$$

which we have expressed in terms of the Airy stress function $\phi(\boldsymbol{x})$ (see section 2.3 on page 22), and rotate it locally by 90° at each point $\boldsymbol{x}$ to generate the field

$$\begin{aligned}\boldsymbol{\epsilon}' \equiv \boldsymbol{R}_\perp \boldsymbol{\tau} \boldsymbol{R}_\perp^T &= \begin{pmatrix} \tau_{22} & -\tau_{12} \\ -\tau_{12} & \tau_{11} \end{pmatrix} = \begin{pmatrix} \phi_{,11} & \phi_{,12} \\ \phi_{,12} & \phi_{,22} \end{pmatrix} = \nabla\nabla\phi \\ &= \begin{pmatrix} \tau_{22}+\tau_{11} & 0 \\ 0 & \tau_{11}+\tau_{22} \end{pmatrix} - \begin{pmatrix} \tau_{11} & \tau_{12} \\ \tau_{12} & \tau_{22} \end{pmatrix} \\ &= \mathrm{Tr}(\boldsymbol{\tau})\boldsymbol{I} - \boldsymbol{\tau}. \end{aligned} \tag{4.19}$$

Thus we have

$$\boldsymbol{\epsilon}'(\boldsymbol{x}) = [\nabla \boldsymbol{u}'(\boldsymbol{x}) + (\nabla \boldsymbol{u}'(\boldsymbol{x}))^T]/2, \quad \text{where } \boldsymbol{u}' = \nabla\phi.$$

In other words, $\boldsymbol{\epsilon}'(\boldsymbol{x})$ can be treated as a strain field that derives from a "displacement field" $\boldsymbol{u}'(\boldsymbol{x})$. So we see that 90° rotations convert stresses into strains in the same way that for the conductivity problem they convert curl free fields into divergence free fields.

Clearly a 90° rotation acting on a second-order field is a linear operation and can be represented by a fourth-order tensor $\boldsymbol{\mathcal{R}}_\perp$. According to (4.19), the action of $\boldsymbol{\mathcal{R}}_\perp$ on $\boldsymbol{\tau}(\boldsymbol{x})$ is simply given by

$$\boldsymbol{\mathcal{R}}_\perp \boldsymbol{\tau} = \mathrm{Tr}(\boldsymbol{\tau})\boldsymbol{I} - \boldsymbol{\tau}, \tag{4.20}$$

and by applying the same arguments as in the conductivity problem it is clear that for any constant c the strain field $\boldsymbol{\epsilon} + c\boldsymbol{\epsilon}'$ and the stress field $\boldsymbol{\tau}$ solve the elasticity equations in a material with compliance tensor

$$\boldsymbol{\mathcal{S}}'(\boldsymbol{x}) = \boldsymbol{\mathcal{S}}(\boldsymbol{x}) + c\boldsymbol{\mathcal{R}}_\perp. \tag{4.21}$$

Consequently this material will have effective compliance tensor

$$\boldsymbol{\mathcal{S}}'_* = \boldsymbol{\mathcal{S}}_* + c\boldsymbol{\mathcal{R}}_\perp. \tag{4.22}$$

That one can translate the compliance tensor by a multiple of $\boldsymbol{\mathcal{R}}_\perp$ and produce a similar translation of the effective compliance tensor is tied with the fact that the quadratic form $Q(\boldsymbol{\tau}) = \boldsymbol{\tau} \cdot \boldsymbol{\mathcal{R}}_\perp \boldsymbol{\tau} = 2 \det \boldsymbol{\tau}$ is a null Lagrangian satisfying $\langle Q(\boldsymbol{\tau})\rangle = Q(\langle \boldsymbol{\tau}\rangle)$ for all periodic 2×2 symmetric matrix-valued functions $\boldsymbol{\tau}$ satisfying $\nabla \cdot \boldsymbol{\tau} = 0$. The explanation of this connection requires the variational principle for the effective compliance tensor and therefore will not be given until section 13.3 on page 274.

4.6. A proof that the Young's modulus of a metal plate with holes does not depend on the Poisson's ratio of the metal

For locally isotropic materials the constitutive relation takes the form

$$\boldsymbol{\epsilon} = (1/E)\boldsymbol{\tau} - (\nu/E)[\mathrm{Tr}(\boldsymbol{\tau})\boldsymbol{I} - \boldsymbol{\tau}],$$

where $E = E(\boldsymbol{x})$ and $\nu = \nu(\boldsymbol{x})$ are the Young's modulus and Poisson's ratio. In view of (4.21) and (4.20), the constitutive relation in the translated medium is

$$\boldsymbol{\epsilon}' = (1/E)\boldsymbol{\tau} - (\nu/E - c)[\mathrm{Tr}(\boldsymbol{\tau})\boldsymbol{I} - \boldsymbol{\tau}] = (1/E')\boldsymbol{\tau} - (\nu'/E')[\mathrm{Tr}(\boldsymbol{\tau})\boldsymbol{I} - \boldsymbol{\tau}],$$

where

$$E'(\boldsymbol{x}) = E(\boldsymbol{x}), \qquad \nu'(\boldsymbol{x}) = \nu(\boldsymbol{x}) - cE(\boldsymbol{x}) \tag{4.23}$$

are the moduli of the translated medium. So the Young's modulus remains unchanged, while the ratio of the Poisson's ratio to the Young's modulus is shifted uniformly by $-c$. Assuming for simplicity that the composite is isotropic, (4.22) implies that the effective Young's modulus E_* and Poisson's ratio ν_* transform in a similar fashion:

$$E'_* = E_*, \qquad \nu'_* = \nu_* - cE_*. \tag{4.24}$$

Expressed in terms of the two-dimensional bulk and shear moduli, this result implies that

$$-1/\kappa'_* = -1/\kappa_* - 2c, \quad 1/\mu'_* = 1/\mu_* - 2c$$

when

$$-1/\kappa'(\boldsymbol{x}) = -1/\kappa(\boldsymbol{x}) - 2c, \quad 1/\mu'(\boldsymbol{x}) = 1/\mu(\boldsymbol{x}) - 2c.$$

So $-1/\kappa'_*$ and $1/\mu_*$ undergo precisely the same shift as $-1/\kappa'(\boldsymbol{x})$ and $1/\mu(\boldsymbol{x})$.

A nice application of this result is to a metal plate with constant moduli E and ν that has a statistically isotropic distribution of holes punched into it. Under the translation (4.23) the holes remain holes (since the holes effectively correspond to a material with zero Young's modulus), while the Young's modulus E of the metal is unchanged and its Poisson's ratio is shifted from ν to $\nu - cE$. By dimensional analysis it is apparent that the ratio E_*/E can depend only on ν and on the geometry. But (4.24) implies that this ratio remains invariant as c and hence ν varies. We conclude that E_*/E depends only on the geometry, and is independent of ν, confirming what was first observed numerically by Day, Snyder, Garboczi, and Thorpe (1992). This independence does not extend to three-dimensional composites. However, Christensen (1993) has provided some evidence to show that E_*/E is relatively insensitive (but not absolutely insensitive) to ν for values of ν in the range $0 \le \nu \le 1/2$.

A more striking result was found by Day, Snyder, Garboczi, and Thorpe in their numerical simulations. When there are so many holes that the plate is about to fall apart, so that E_* is close to zero, they observed that the effective Poisson's ratio takes a universal value that is independent of both the Young's modulus and the Poisson's ratio of the plate; see figure 4.3. Following Thorpe and Jasiuk (1992), we can see how this is a corollary of (4.24). In the limit as E_* approaches zero, ν'_* must approach ν_*, implying that ν_* is also independent of ν in this limit. In fact, as follows from (4.24), the effective Poisson's ratio ν_* of a plate with

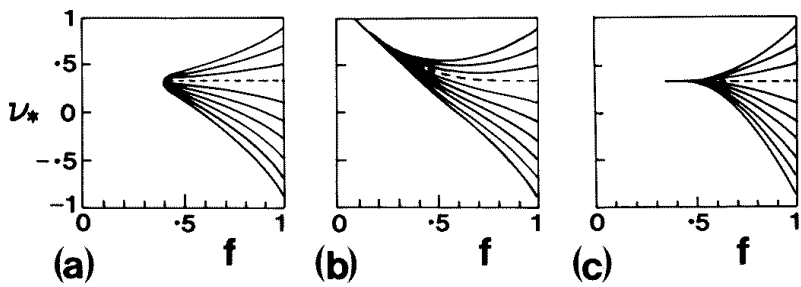

Figure 4.3. Plot of the effective Poisson's ratio ν_* against the volume fraction f occupied by the metal in a plate containing circular holes in (a) a triangular network, (b) a honeycomb network, and (c) a random arrangement. The different curves in each figure correspond to metals having different Poisson's ratios ν, given by the values at $f = 1$. The dashed line corresponds to $\nu = 1/3$. After Day, Snyder, Garboczi, and Thorpe (1992).

holes depends linearly on the Poisson's ratio ν of the plate, with a coefficient of E_*/E (Hu and Weng 2001). It is hard to make any such general statements about the variation of the Poisson's ratio with volume fraction when the holes are filled with a second rigid or elastic phase (Chen, Thorpe, and Davis 1995; Christiansson and Helsing 1996). Garboczi and Day (1995) suggested that the effective Poisson's ratio remains equal to 1/3 when both phases have a Poisson's ratio of 1/3, but Christiansson and Helsing (1996) disproved this.

If the plate has a anisotropic effective compliance tensor $\boldsymbol{\mathcal{S}}_*$, then it is convenient to introduce the defect compliance tensor, $\boldsymbol{\mathcal{H}} = \boldsymbol{\mathcal{S}}_* - \boldsymbol{\mathcal{S}}$, where

$$\{\boldsymbol{\mathcal{S}}\}_{ijk\ell} = [(1+\nu)/2E](\delta_{ik}\delta_{j\ell} + \delta_{i\ell}\delta_{jk}) - (\nu/E)\delta_{ij}\delta_{k\ell}$$

is the compliance tensor of the plate. By dimensional analysis $E\boldsymbol{\mathcal{H}}$ depends only on ν and on the geometry. But (4.21), (4.22), and (4.23) show that $E\boldsymbol{\mathcal{H}}$ remains invariant under translation, that is, as the Poisson's ratio of the plate is shifted from ν to $\nu - cE$. Zheng and Hwang (1996, 1997) concluded that $E\boldsymbol{\mathcal{H}}$ depends only on the geometry of the plate. A similar conclusion was reached by Movchan and Serkov (1997) for plates containing a dilute concentration of holes; see their theorem 4.2.

4.7. The elastic moduli of certain two-dimensional polycrystals and symmetric materials

One can sometimes use the translation (4.21) to map to an equivalent elasticity problem where one can apply the duality transformations discussed in sections 3.5 on page 51 and 3.6 on page 53. The condition is that there must exist a symmetric matrix $\boldsymbol{v}$ and a constant c such that

$$0 = \boldsymbol{\mathcal{S}}'(\boldsymbol{x})\boldsymbol{v} = \boldsymbol{\mathcal{S}}(\boldsymbol{x})\boldsymbol{v} + c\boldsymbol{\mathcal{R}}_\perp\boldsymbol{v} = 0. \tag{4.25}$$

This can be rewritten as

$$\boldsymbol{\mathcal{R}}_\perp^{-1}\boldsymbol{\mathcal{S}}(\boldsymbol{x})\boldsymbol{v} = -c\boldsymbol{v}.$$

In other words, $\boldsymbol{\mathcal{R}}_\perp^{-1}\boldsymbol{\mathcal{S}}(\boldsymbol{x})$ must have an eigenvector $\boldsymbol{v}$ and an associated eigenvalue $-c$ that are both independent of $\boldsymbol{x}$.

For example, consider a two-dimensional polycrystal manufactured from a crystal with square symmetry. In the basis

$$\boldsymbol{v}_1 = \frac{1}{\sqrt{2}}\begin{pmatrix} 1 & 0 \\ 0 & 1 \end{pmatrix}, \quad \boldsymbol{v}_2 = \frac{1}{\sqrt{2}}\begin{pmatrix} 1 & 0 \\ 0 & -1 \end{pmatrix}, \quad \boldsymbol{v}_3 = \frac{1}{\sqrt{2}}\begin{pmatrix} 0 & 1 \\ 1 & 0 \end{pmatrix} \tag{4.26}$$

the compliance tensor is represented by the 3×3 matrix

$$\boldsymbol{\mathcal{S}}(\boldsymbol{x}) = \begin{pmatrix} 1/2\kappa & 0 \\ 0 & \boldsymbol{\mathcal{S}}_r(\boldsymbol{x}) \end{pmatrix},$$

in which

$$\boldsymbol{\mathcal{S}}_r(\boldsymbol{x}) = \begin{pmatrix} \cos(2\theta) & \sin(2\theta) \\ -\sin(2\theta) & \cos(2\theta) \end{pmatrix}\begin{pmatrix} 1/2\mu^{(1)} & 0 \\ 0 & 1/2\mu^{(2)} \end{pmatrix}\begin{pmatrix} \cos(2\theta) & -\sin(2\theta) \\ \sin(2\theta) & \cos(2\theta) \end{pmatrix}.$$

Here $\mu^{(1)}$, $\mu^{(2)}$, and κ are the two shear moduli and bulk modulus of the single crystal, and $\theta = \theta(\boldsymbol{x})$ is the angle of orientation of the crystal at each point $\boldsymbol{x}$. Since a 90° rotation leaves

the matrix $\boldsymbol{v}_1$ invariant but changes the sign of $\boldsymbol{v}_2$ and $\boldsymbol{v}_3$, $\boldsymbol{\mathcal{R}}_\perp$ is represented in this basis by the diagonal matrix

$$\boldsymbol{\mathcal{R}}_\perp = \begin{pmatrix} 1 & 0 & 0 \\ 0 & -1 & 0 \\ 0 & 0 & -1 \end{pmatrix}.$$

Now the condition (4.25) is satisfied with $c = -1/(2\kappa)$ and $\boldsymbol{v} = \boldsymbol{v}_1$. By applying the duality result (3.27) to the translated medium we deduce that the effective compliance tensor $\boldsymbol{\mathcal{S}}_*$ associated with $\boldsymbol{\mathcal{S}}(\boldsymbol{x})$ necessarily has square symmetry with effective bulk modulus κ_* and effective shear moduli $\mu_*^{(1)}$ and $\mu_*^{(2)}$ satisfying the relations

$$\kappa_* = \kappa, \quad (1/\mu_*^{(1)} + 1/\kappa)(1/\mu_*^{(2)} + 1/\kappa) = (1/\mu^{(1)} + 1/\kappa)(1/\mu^{(2)} + 1/\kappa),$$

found by Lurie and Cherkaev (1984).

If the effective elasticity tensor of the polycrystal is isotropic, then this relation yields exact formulas for the effective bulk and shear moduli of the polycrystal:

$$\kappa_* = \kappa, \quad \mu_* = \mu_*^{(1)} = \mu_*^{(2)} = \frac{\kappa}{-1 + \sqrt{(1 + \kappa/\mu^{(1)})(1 + \kappa/\mu^{(2)})}}. \tag{4.27}$$

Now consider a two-phase composite comprised of two isotropic phases having the same bulk modulus κ. Again the condition (4.25) is satisfied with $c = -1/(2\kappa)$ and $\boldsymbol{v} = \boldsymbol{v}_1$. By applying the result (3.28) to the translated medium, one sees (Helsing, Milton, and Movchan 1997) that the effective shear modulus $\mu_*(\mu_1, \mu_2, \kappa)$ expressed as a function of the shear moduli μ_1 and μ_2 of the two phases and their common bulk modulus κ satisfies the phase interchange identity

$$[1/\kappa + 1/\mu_*(\mu_1, \mu_2, \kappa)][1/\kappa + 1/\mu_*(\mu_2, \mu_1, \kappa)] = (1/\kappa + 1/\mu_1)(1/\kappa + 1/\mu_2). \tag{4.28}$$

If the geometry is symmetric (i.e., phase interchange invariant) and elastically isotropic, then we obtain an exact result for the effective bulk and shear moduli of the structure

$$\kappa_* = \kappa, \quad \mu_* = \frac{\kappa}{-1 + \sqrt{(1 + \kappa/\mu_1)(1 + \kappa/\mu_2)}}.$$

Gibiansky and Torquato (1996) have derived phase interchange inequalities that generalize (4.28) when the two phases have unequal bulk moduli or when the composite is three-dimensional.

References

Bergman, D. J. 1983. Self-duality and the low field Hall effect in 2D and 3D metal-insulator composites. In G. Deutscher, R. Zallen, and J. Adler (eds.), *Percolation Structures and Processes*, pp. 297–321. Jerusalem: Israel Physical Society. ISBN 0-85274-477-3. {*65, 70, 344, 352*}

Chen, J., M. F. Thorpe, and L. C. Davis 1995. Elastic properties of rigid fiber-reinforced composites. *Journal of Applied Physics* 77:4349–4360. {*69, 70*}

Chen, T. 1995. Further results on invariant properties of the stress in plane elasticity and its extension to piezoelectricity. *Mechanics Research Communications* 22:251–256. {*66, 70*}

Chen, T. and D. Lai 1997. An exact correspondence between plane piezoelectricity and generalized plane strain in elasticity. *Proceedings of the Royal Society of London. Series A, Mathematical and Physical Sciences* 453:2689–2713. {*35, 41, 66, 71*}

Cherkaev, A. V., K. A. Lurie, and G. W. Milton 1992. Invariant properties of the stress in plane elasticity and equivalence classes of composites. *Proceedings of the Royal Society of London. Series A, Mathematical and Physical Sciences* 438(1904):519–529. {*66, 71*}

Christensen, R. M. 1993. Effective properties of composite materials containing voids. *Proceedings of the Royal Society of London. Series A, Mathematical and Physical Sciences* 440:461–473. {*68, 71*}

Christiansson, H. 1997. Hall effect in two-dimensional composites. *Physical Review B (Solid State)* 56(2):572–578. {*64, 71*}

Christiansson, H. and J. Helsing 1996. Poisson's ratio of fiber-reinforced composites. *Journal of Applied Physics* 79(10):7582–7585. {*69, 71*}

Day, A. R., K. A. Snyder, E. J. Garboczi, and M. F. Thorpe 1992. The elastic moduli of a sheet containing circular holes. *Journal of the Mechanics and Physics of Solids* 40(5): 1031–1051. {*40, 42, 66, 68, 71*}

Dundurs, J. 1967a. Dependence of stress on Poisson's ratio in plane elasticity. *International Journal of Solids and Structures* 3:1013–1021. {*66, 71*}

Dundurs, J. 1967b. Effect of elastic constants on stress in a composite under plane deformation. *Journal of Composite Materials* 1:310–322. {*66, 71*}

Dundurs, J. 1970. Some properties of elastic stresses in a composite. In A. C. Eringen (ed.), *Proceedings of the Sixth Annual Meeting of the Society of Engineering Science, Held at Princeton University, Princeton, New Jersey, November 11–13, 1968*, pp. 203–216. Langhorne, Pennsylvania: Gordon and Breach. ISBN 0-677-13780-X. {*66, 71*}

Dundurs, J. and X. Markenscoff 1993. Invariance of stresses under a change in elastic compliances. *Proceedings of the Royal Society of London. Series A, Mathematical and Physical Sciences* 443:289–300. {*66, 71*}

Dykhne, A. M. 1970. Anomalous plasma resistance in a strong magnetic field. *Zhurnal eksperimental'noi i teoreticheskoi fiziki / Akademiia Nauk SSSR* 59:641–647. English translation in *Soviet Physics JETP* 32:348–35 (1971). {*59, 60, 71*}

Dykhne, A. M. and I. M. Ruzin 1994. On the theory of the fractional quantum Hall effect: The two-phase model. *Physical Review B (Solid State)* 50:2369–2379. {*64, 71*}

Garboczi, E. J. and A. R. Day 1995. An algorithm for computing the effective linear elastic properties of heterogeneous materials: Three-dimensional results for composites with equal phase Poisson ratios. *Journal of the Mechanics and Physics of Solids* 43(9):1349–1362. {*69, 71*}

Gibiansky, L. V. and S. Torquato 1996. Phase-interchange relations for the elastic moduli of two-phase composites. *International Journal of Engineering Science* 34(7):739–760. {*70, 71*}

He, Q.-C. 1998. More on stress invariance conditions for the traction boundary value problem of plane linear elasticity. *International Journal of Solids and Structures* 35(26–27): 3519–3537. {*66, 71*}

Helsing, J., G. W. Milton, and A. B. Movchan 1997. Duality relations, correspondences and numerical results for planar elastic composites. *Journal of the Mechanics and Physics of Solids* 45(4):565–590. {*39, 43, 51, 53, 55, 57, 70, 72, 105, 106, 111*}

Hu, G. K. and G. J. Weng 2001. A new derivative on the shift property of effective elastic compliances for planar and three-dimensional composites. *Proceedings of the Royal Society of London. Series A, Mathematical and Physical Sciences* 457(2011):1675–1684. {*69, 72*}

Lifshitz, E. M. and L. P. Pitaevskii 1980. *Statistical Physics* (Third ed.). New York: Pergamon. xvii + 544 pp. ISBN 0-08-023039-3. {*28, 44, 61, 72*}

Lurie, K. A. and A. V. Cherkaev 1984. G-closure of some particular sets of admissible material characteristics for the problem of bending of thin elastic plates. *Journal of Optimization Theory and Applications* 42(2):305–316. {*56, 58, 66, 70, 72*}

Michell, J. H. 1899. On the direct determination of stress in an elastic solid, with application to the theory of plates. *Proceedings of the London Mathematical Society. Third Series* 31:100–125. {*66, 72*}

Milton, G. W. 1988. Classical Hall-effect in two-dimensional composites: a characterization of the set of realizable effective conductivity tensors. *Physical Review B (Solid State)* 38(16):11296–11303. {*61, 64, 72*}

Moran, B. and M. Gosz 1994. Stress invariance in plane anisotropic elasticity. *Modelling and Simulation in Materials Science and Engineering* 2:677–688. {*66, 72*}

Movchan, A. B. and S. K. Serkov 1997. The Pólya-Szegő matrices in asymptotic models of dilute composites. *European Journal of Applied Mathematics* 8(6):595–621. {*69, 72, 188, 218*}

Murat, F. 1978. Compacité par compensation. *Annali Scuola Normale Superiore-Pisa, Classe di Scienze, Serie IV.* 5(3):489–507. {*59, 72, 250, 269, 275, 276, 287*}

Ostoja-Starzewski, M. and I. Jasiuk 1995. Stress invariance in planar Cosserat elasticity. *Proceedings of the Royal Society of London. Series A, Mathematical and Physical Sciences* 451(1942):453–470. See erratum: *Proc. Roy. Soc. Lond. A* 452:1503 (1996). {*66, 72*}

Shklovskiĭ, B. I. 1977. Critical behavior of the Hall-coefficient near the percolation threshold. *Zhurnal eksperimental'noi i teoreticheskoi fiziki / Akademiia Nauk SSSR* 72:288–295. English translation in *Soviet Physics JETP* 45:152–156 (1977). {*65, 72*}

Stroud, D. and D. J. Bergman 1984. New exact results for the Hall-coefficient and magnetoresistance of inhomogeneous two-dimensional metals. *Physical Review B (Solid State)* 30:447–449. {*66, 72*}

Tartar, L. 1979. Compensated compactness and applications to partial differential equations. In R. J. Knops (ed.), *Nonlinear Analysis and Mechanics, Heriot-Watt Symposium, Volume IV*, pp. 136–212. London: Pitman Publishing Ltd. ISBN 0-8224-8461-7, 0-273-08461-5. {*59, 72, 275, 276, 288, 503, 527, 529, 552, 676, 677, 684, 698*}

Thorpe, M. F. and I. Jasiuk 1992, September 8. New results in the theory of elasticity for two-dimensional composites. *Proceedings of the Royal Society of London. Series A, Mathematical and Physical Sciences* 438(1904):531–544. {*66, 68, 72*}

Zheng, Q.-S. and K. C. Hwang 1996. Reduced dependence of defect compliance on matrix and inclusion elastic properties in two-dimensional elasticity. *Proceedings of the Royal*

Society of London. Series A, Mathematical and Physical Sciences 452(1954):2493–2507. {*69, 72*}

Zheng, Q.-S. and K. C. Hwang 1997. Two-dimensional elastic compliances of materials with holes and microcracks. *Proceedings of the Royal Society of London. Series A, Mathematical and Physical Sciences* 453(1957):353–364. {*69, 73*}

5

Some microstructure-independent exact relations

Typically the properties of a composite are microstructure-dependent. So it comes as a nice surprise to come across exact formulas for (or linking) effective moduli that are universally valid no matter how complicated the microstructure. Many exact relations stem from a very simple idea: Sometimes the medium and equations are such that an appropriate constant or uniform field provides a solution. The idea dates back to papers of Hill (1952, 1964) and Cribb (1968), and was subsequently generalized by Dvorak (1983, 1990) and Lurie, Cherkaev, and Fedorov (1984), among others. We will see that one gets a lot of mileage, in terms of applications, out of this simple idea.

5.1. The uniform field argument

Let us begin by considering the equations of conductivity in a composite. These have a simple solution when the conductivity tensor field $\boldsymbol{\sigma}(\boldsymbol{x})$ is such that there exist constant vectors $\boldsymbol{v}$ and $\boldsymbol{w}$ with

$$\boldsymbol{\sigma}(\boldsymbol{x})\boldsymbol{v} = \boldsymbol{w} \quad \text{for all } \boldsymbol{x}.$$

Then the current and electric fields,

$$\boldsymbol{j}(\boldsymbol{x}) = \boldsymbol{w}, \quad \boldsymbol{e}(\boldsymbol{x}) = \boldsymbol{v},$$

solve the equations

$$\boldsymbol{j}(\boldsymbol{x}) = \boldsymbol{\sigma}(\boldsymbol{x})\boldsymbol{e}(\boldsymbol{x}), \qquad \nabla \cdot \boldsymbol{j} = 0, \qquad \nabla \times \boldsymbol{e} = 0. \tag{5.1}$$

Since these fields are constant, and equal to their averages, it follows that the effective tensor $\boldsymbol{\sigma}_*$ necessarily satisfies

$$\boldsymbol{\sigma}_*\boldsymbol{v} = \boldsymbol{w}. \tag{5.2}$$

In particular, if it is a two-phase composite,

$$\boldsymbol{\sigma}(\boldsymbol{x}) = \chi_1(\boldsymbol{x})\boldsymbol{\sigma}_1 + \chi_2(\boldsymbol{x})\boldsymbol{\sigma}_2, \tag{5.3}$$

and there exists a $\boldsymbol{v} \neq 0$ such that

$$(\boldsymbol{\sigma}_1 - \boldsymbol{\sigma}_2)\boldsymbol{v} = 0,$$

then (5.2) implies that

$$(\boldsymbol{\sigma}_* - \boldsymbol{\sigma}_2)\boldsymbol{v} = 0.$$

In other words, $\boldsymbol{\sigma}_*$ must be such that the right nullspace of $(\boldsymbol{\sigma}_* - \boldsymbol{\sigma}_2)$ includes any right null vector of $(\boldsymbol{\sigma}_1 - \boldsymbol{\sigma}_2)$.

When the conductivity tensor field $\boldsymbol{\sigma}(\boldsymbol{x})$ is not symmetric and there exist vectors $\boldsymbol{v}'$ and $\boldsymbol{w}'$ such that

$$[\boldsymbol{\sigma}(\boldsymbol{x})]^T \boldsymbol{v}' = \boldsymbol{w}' \quad \text{for all } \boldsymbol{x},$$

then for any solutions $\boldsymbol{j}(\boldsymbol{x})$ and $\boldsymbol{e}(\boldsymbol{x})$ to the conductivity equations (5.1) we have

$$\begin{aligned} \boldsymbol{v}' \cdot \boldsymbol{\sigma}_* \langle \boldsymbol{e}(\boldsymbol{x}) \rangle &= \langle\, \boldsymbol{v}' \cdot \boldsymbol{j}(\boldsymbol{x}) \,\rangle = \langle\, \boldsymbol{v}' \cdot \boldsymbol{\sigma}(\boldsymbol{x}) \boldsymbol{e}(\boldsymbol{x}) \,\rangle \\ &= \langle\, ([\boldsymbol{\sigma}(\boldsymbol{x})]^T \boldsymbol{v}') \cdot \boldsymbol{e}(\boldsymbol{x}) \,\rangle = \boldsymbol{w}' \cdot \langle \boldsymbol{e}(\boldsymbol{x}) \rangle, \end{aligned}$$

which implies that

$$[\boldsymbol{\sigma}_*]^T \boldsymbol{v}' = \boldsymbol{w}'.$$

So, for example, in the two-phase composite of (5.3) the left nullspace of $(\boldsymbol{\sigma}_* - \boldsymbol{\sigma}_2)$ must include any left null vector of $(\boldsymbol{\sigma}_1 - \boldsymbol{\sigma}_2)$.

As Lurie, Cherkaev, and Fedorov (1984) noticed [see also Lurie and Cherkaev (1986)] similar considerations apply to the elasticity problem: If the elasticity tensor field $\boldsymbol{\mathcal{C}}(\boldsymbol{x})$ is such that there exist symmetric tensors $\boldsymbol{V}$ and $\boldsymbol{W}$ with

$$\boldsymbol{\mathcal{C}}(\boldsymbol{x}) \boldsymbol{V} = \boldsymbol{W} \quad \text{for all } \boldsymbol{x}, \tag{5.4}$$

then the effective tensor $\boldsymbol{\mathcal{C}}_*$ must satisfy

$$\boldsymbol{\mathcal{C}}_* \boldsymbol{V} = \boldsymbol{W}. \tag{5.5}$$

Let us apply these results to several elasticity problems.

5.2. The bulk modulus of polycrystals with cubic symmetry

In a polycrystal the elasticity tensor field takes the form

$$\boldsymbol{\mathcal{C}}(\boldsymbol{x}) = \boldsymbol{\mathcal{R}}(\boldsymbol{x}) \boldsymbol{\mathcal{C}}_0 [\boldsymbol{\mathcal{R}}(\boldsymbol{x})]^T,$$

where $\boldsymbol{\mathcal{C}}_0$ represents the elasticity tensor of the pure crystal and $\boldsymbol{\mathcal{R}}(\boldsymbol{x})$ is the fourth-order tensor field with Cartesian elements

$$\mathcal{R}_{ijk\ell}(\boldsymbol{x}) = R_{ik}(\boldsymbol{x}) R_{j\ell}(\boldsymbol{x}),$$

representing the action of a local rotation $\boldsymbol{R}(\boldsymbol{x})$ on $\boldsymbol{\mathcal{C}}_0$. If the pure crystal has cubic symmetry, then (within the approximation of linear elasticity) it responds isotropically to hydrostatic compression, contracting equally in all directions. Mathematically this means that the second-order identity $\boldsymbol{I}$ is an eigentensor of $\boldsymbol{\mathcal{C}}_0$, that is,

$$\boldsymbol{\mathcal{C}}_0 \boldsymbol{I} = d\kappa_0 \boldsymbol{I},$$

where d is the spatial dimension (2 or 3) and

$$\kappa_0 = \mathrm{Tr}(\boldsymbol{\mathcal{C}}_0 \boldsymbol{I})/d^2$$

is the bulk modulus of the pure crystal.

Since $\boldsymbol{I}$ commutes with rotations, $\mathcal{C}(\boldsymbol{x})$ satisfies

$$\mathcal{C}(\boldsymbol{x})\boldsymbol{I} = d\kappa_0\boldsymbol{I},$$

and (5.5) implies that

$$\mathcal{C}_*\boldsymbol{I} = d\kappa_0\boldsymbol{I}. \tag{5.6}$$

In particular, if the polycrystal is statistically isotropic, then (5.6) implies that its effective bulk modulus κ_* is exactly the same as the bulk modulus κ_0 of the pure crystal, as noted by Hill (1952)

5.3. The elastic moduli of a composite with a constant shear modulus

If the fluctuations in the tensor field $\mathcal{C}(\boldsymbol{x})$ are rank-1, that is, there exists a symmetric second-order tensor $\boldsymbol{A}$ such that the field $\mathcal{C}(\boldsymbol{x})$ has the form

$$\mathcal{C}(\boldsymbol{x}) = \alpha(\boldsymbol{x})\boldsymbol{A}\otimes\boldsymbol{A} + \mathcal{C}_0, \tag{5.7}$$

where $\mathcal{C}_0$ is a constant fourth-order elasticity tensor, then (5.4) is satisfied for any symmetric tensor $\boldsymbol{V}$ such that $\mathrm{Tr}(\boldsymbol{AV}) = 0$. Hence (5.5) is satisfied for any symmetric tensor $\boldsymbol{V}$ such that $\mathrm{Tr}(\boldsymbol{AV}) = 0$, which implies that $\mathcal{C}_* - \mathcal{C}_0$ is rank-1 of the form

$$\mathcal{C}_* = \alpha_*\boldsymbol{A}\otimes\boldsymbol{A} + \mathcal{C}_0. \tag{5.8}$$

Thus $\mathcal{C}_*$ is completely determined aside from the constant α_*. We can picture this in tensor space as follows: Take any straight line oriented in a rank-1 direction in the space of fourth-order elasticity tensors and suppose that the tensors $\mathcal{C}(\boldsymbol{x})$ lie along this line for all $\boldsymbol{x}$; then (5.8) implies that $\mathcal{C}_*$ also lies along the same straight line.

One beautiful application of this result is to locally isotropic composites with constant shear modulus. The local elasticity tensor takes the form

$$\mathcal{C}(\boldsymbol{x}) = \lambda(\boldsymbol{x})\boldsymbol{I}\otimes\boldsymbol{I} + 2\mu\mathcal{I},$$

where $\boldsymbol{I}$ and $\mathcal{I}$ are the second-order and fourth-order identity tensors, $\lambda(\boldsymbol{x})$ is the Lame modulus, and μ is the (constant) shear modulus. The Lame modulus can be expressed in terms of the bulk modulus $\kappa(\boldsymbol{x})$ through the equation

$$\lambda(\boldsymbol{x}) = \kappa(\boldsymbol{x}) - 2\mu/d.$$

From (5.8) we see that the effective tensor $\mathcal{C}_*$ necessarily has the form

$$\mathcal{C}_* = \lambda_*\boldsymbol{I}\otimes\boldsymbol{I} + 2\mu\mathcal{I}. \tag{5.9}$$

So, as Hill (1964) first noticed, the composite is always elastically isotropic with shear modulus μ, irrespective of whether the geometry is anisotropic or not; see also Francfort and Tartar (1991).

What is more remarkable is that λ_* can be computed exactly, independent of the microstructure. Let us suppose for simplicity that the microstructure is periodic. Following Hill (1963), we look for a solution of the elasticity equations with a periodic displacement field $\boldsymbol{u}(\boldsymbol{x})$ of the form

$$\boldsymbol{u}(\boldsymbol{x}) = \alpha\boldsymbol{x} + \nabla\varphi(\boldsymbol{x}),$$

where α is a constant and $\varphi(\boldsymbol{x})$ is a periodic scalar potential that needs to be chosen so the stress field has zero divergence. The associated strain and stress fields are

$$\boldsymbol{\epsilon}(\boldsymbol{x}) = \alpha \boldsymbol{I} + \nabla\nabla\varphi(\boldsymbol{x}), \tag{5.10}$$

$$\boldsymbol{\tau}(\boldsymbol{x}) = \lambda(\boldsymbol{x})[\mathrm{Tr}\,\boldsymbol{\epsilon}(\boldsymbol{x})]\boldsymbol{I} + 2\mu\boldsymbol{\epsilon}(\boldsymbol{x}) = \lambda(\boldsymbol{x})[d\alpha + \Delta\varphi(\boldsymbol{x})]\boldsymbol{I} + 2\mu[\alpha\boldsymbol{I} + \nabla\nabla\varphi(\boldsymbol{x})], \tag{5.11}$$

where $\Delta = \nabla \cdot \nabla$ denotes the Laplacian. The equilibrium equation for the stress field,

$$\nabla \cdot \boldsymbol{\tau}(\boldsymbol{x}) = \nabla\{d\lambda(\boldsymbol{x})\alpha + [\lambda(\boldsymbol{x}) + 2\mu]\Delta\varphi(\boldsymbol{x})\} = 0, \tag{5.12}$$

is satisfied when the bracketed expression in (5.12) reduces to a constant:

$$d\lambda(\boldsymbol{x})\alpha + [\lambda(\boldsymbol{x}) + 2\mu]\Delta\varphi(\boldsymbol{x}) = \beta - 2d\mu\alpha, \tag{5.13}$$

where β is arbitrary and the additional constant of $-2d\mu\alpha$ has been added to the right-hand side to simplify subsequent equations.

By solving (5.13) it is clear that $\varphi(\boldsymbol{x})$ must be chosen so that

$$\Delta\varphi(\boldsymbol{x}) = -d\alpha + \beta[\lambda(\boldsymbol{x}) + 2\mu]^{-1}. \tag{5.14}$$

Since $\nabla\varphi(\boldsymbol{x})$ is periodic, it follows, by a simple application of the divergence theorem within a unit cell, that

$$\langle \nabla\nabla\varphi(\boldsymbol{x}) \rangle = 0. \tag{5.15}$$

In particular, by taking the trace of this equation, we see that $\langle \Delta\varphi(\boldsymbol{x}) \rangle$ must vanish. So for (5.14) to have a solution for $\varphi(\boldsymbol{x})$ we must choose β such that

$$d\alpha/\beta = \langle\, (\lambda + 2\mu)^{-1} \rangle, \tag{5.16}$$

and this guarantees that a solution exists.

Fortunately we do not need to solve for $\varphi(\boldsymbol{x})$ to compute the effective Lame modulus λ_*. Indeed, by taking averages of the strain and stress fields in (5.10) and (5.11), and using (5.13) and (5.15) to simplify the resulting expressions, we see that

$$\langle \boldsymbol{\epsilon} \rangle = \alpha \boldsymbol{I}, \tag{5.17}$$

$$\langle \boldsymbol{\tau} \rangle = (\beta/\alpha - 2d\mu + 2\mu)\alpha \boldsymbol{I}. \tag{5.18}$$

With this choice (5.17) of average strain, the average stress is given from (5.9) by

$$\langle \boldsymbol{\tau} \rangle = (d\lambda_* + 2\mu)\alpha \boldsymbol{I},$$

and equating this with (5.18) gives

$$\lambda_* + 2\mu = \beta/(d\alpha).$$

Finally, by using (5.16) to eliminate $\beta/(d\alpha)$, we obtain Hill's formula,

$$(\lambda_* + 2\mu)^{-1} = \langle\, (\lambda + 2\mu)^{-1} \rangle. \tag{5.19}$$

This gives us an exact expression for λ_* and, in view of (5.9), an exact expression for $\boldsymbol{\mathcal{C}}_*$. Another result that follows from this analysis (D. L. Johnson, private communication) is that the hydrostatic component of the stress, $\mathrm{Tr}\,\boldsymbol{\tau}(\boldsymbol{x})$, is constant within each phase. Indeed, it follows from (5.11) and (5.14) that

$$\mathrm{Tr}\,\boldsymbol{\tau}(\boldsymbol{x}) = \beta[d\lambda(\boldsymbol{x}) + 2\mu]/[\lambda(\boldsymbol{x}) + 2\mu],$$

and so $\mathrm{Tr}\,\boldsymbol{\tau}(\boldsymbol{x})$ will be constant in any region where $\lambda(\boldsymbol{x})$ is constant.

5.4. The thermal expansion tensor and constant of specific heat in a composite of two isotropic phases

Another well-known example where the existence of a uniform field solution leads to a non-trivial relation amongst effective constants is in the problem of thermal expansion. In the linear approximation thermal expansion is governed by the equations

$$\boldsymbol{\epsilon}(\boldsymbol{x}) = \boldsymbol{\mathcal{S}}(\boldsymbol{x})\boldsymbol{\tau}(\boldsymbol{x}) + \boldsymbol{\alpha}(\boldsymbol{x})\theta, \tag{5.20}$$

where $\theta = T - T_0$ is the change in temperature T measured from some constant base temperature T_0, while $\boldsymbol{\epsilon}(\boldsymbol{x})$ and $\boldsymbol{\tau}(\boldsymbol{x})$ are the strain and stress fields, $\boldsymbol{\mathcal{S}}(\boldsymbol{x})$ is the compliance tensor, and $\boldsymbol{\alpha}(\boldsymbol{x})$ is the tensor of thermal expansion. The average fields $\langle\boldsymbol{\epsilon}\rangle$ and $\langle\boldsymbol{\tau}\rangle$ satisfy equations of the same form,

$$\langle\boldsymbol{\epsilon}\rangle = \boldsymbol{\mathcal{S}}_*\langle\boldsymbol{\tau}\rangle + \boldsymbol{\alpha}_*\theta, \tag{5.21}$$

which serve to define the effective compliance tensor $\boldsymbol{\mathcal{S}}_*$ and effective thermal expansion tensor $\boldsymbol{\alpha}_*$.

Following Cribb (1968), let us first give a physical argument that suggests why it is possible to find uniform fields that solve these equations when the composite has two isotropic phases. Consider, for simplicity, the model problem, sketched in figure 5.1, of a bimetal

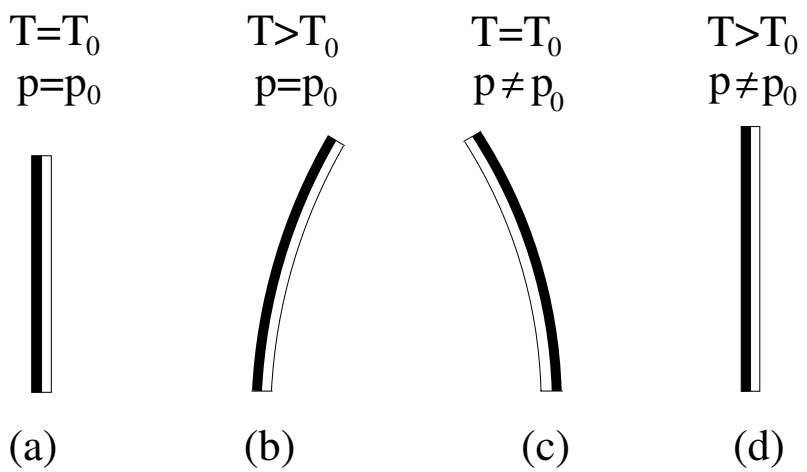

Figure 5.1. A bimetal strip (a) immersed in water at temperature T_0 and pressure p_0 will bend when heated, as in (b), and will bend when the pressure of the water is changed, as in (c). However, with the right combination of temperature increase and pressure change, as in (d), both metals will expand at exactly the same rate, and the strip will expand as if it was a homogeneous material. This argument extended to two-phase composites provides an exact relation between the effective thermal expansion coefficient and the effective bulk modulus.

strip that is immersed in water. [Incidentally, bimetal strips have an interesting origin. John Harrison invented them while developing a marine chronometer in his (ultimately successful) effort to win the longitudinal prize (Sobel 1995; Sobel and Andrewes 1998). The bimetal strip controlled the active length of a spring to minimize the influence of temperature on the clock speed.] It is clear that if the temperature of the water is raised, the bimetal strip will bend due to the mismatch in thermal expansion coefficients of the two metals. On the other

hand, if the temperature is held fixed while pressure in the water is changed, the bimetal strip will again bend due to the mismatch in bulk moduli of the two metals. Now one can imagine applying a judicious combination of temperature increase and pressure change such that both metals expand at exactly the same rate and no bending of the bimetal strip occurs. The strip expands as if it was a homogeneous material. Of course this argument should apply to composites and not just bimetal strips. By judiciously choosing the temperature increase and pressure change both phases will expand at exactly the same rate. Then the composite will expand uniformly at the same rate as the phases. This rate of expansion will be independent of the composite geometry, implying that the effective moduli must have some universal microstructure-independent relations.

Now for the mathematics. We look for a solution where the stress is a uniform hydrostatic compression,

$$\boldsymbol{\tau}(\boldsymbol{x}) = \langle \boldsymbol{\tau} \rangle = -p\boldsymbol{I} \quad \text{for all } \boldsymbol{x}, \tag{5.22}$$

where the pressure p is constant. Since the medium is locally isotropic, the thermal expansion is proportional to the identity tensor, that is, $\boldsymbol{\alpha}(\boldsymbol{x}) = \alpha(\boldsymbol{x})\boldsymbol{I}$, and the constitutive equation (5.20) implies that the strain field is

$$\boldsymbol{\epsilon}(\boldsymbol{x}) = [-p/d\kappa(\boldsymbol{x}) + \theta\alpha(\boldsymbol{x})]\boldsymbol{I}, \tag{5.23}$$

where $\kappa(\boldsymbol{x})$ is the local bulk modulus. In a two-phase medium the strain field given by (5.23) will be piecewise constant, taking the values

$$\boldsymbol{\epsilon}_1 = [-p/(d\kappa_1) + \theta\alpha_1]\boldsymbol{I}, \qquad \boldsymbol{\epsilon}_2 = [-p/(d\kappa_2) + \theta\alpha_2]\boldsymbol{I}, \tag{5.24}$$

in each phase. The requirement that the strain field be completely uniform,

$$\boldsymbol{\epsilon}_1 = \boldsymbol{\epsilon}_2 = \langle \boldsymbol{\epsilon} \rangle, \tag{5.25}$$

is, according to (5.24), satisfied for any given temperature change θ if we adjust the pressure p so that

$$p/\theta = \frac{d(\alpha_1 - \alpha_2)}{(1/\kappa_1 - 1/\kappa_2)}. \tag{5.26}$$

In other words, at this particular ratio of p/θ the equations (5.21) of thermal expansion are solved by constant fields $\boldsymbol{\tau}$ and $\boldsymbol{\epsilon}$. Substitution of the expressions (5.22) and (5.25) for the average fields $\langle \boldsymbol{\tau} \rangle$ and $\langle \boldsymbol{\epsilon} \rangle$ into (5.21) yields the exact formula of Rosen and Hashin (1970) for the effective thermal expansion tensor,

$$\boldsymbol{\alpha}_* = \frac{d(\alpha_1 - \alpha_2)\boldsymbol{\mathcal{S}}_*\boldsymbol{I} + (\alpha_2/\kappa_1 - \alpha_1/\kappa_2)\boldsymbol{I}}{1/\kappa_1 - 1/\kappa_2}, \tag{5.27}$$

which is true in any dimension d and for any composite of two isotropic phases. If the composite is also isotropic, then $\boldsymbol{\alpha}_* = \alpha_*\boldsymbol{I}$ and $\boldsymbol{\mathcal{S}}_*\boldsymbol{I} = \boldsymbol{I}/(d\kappa_*)$, where κ_* is the effective bulk modulus and α_* is the constant of effective thermal expansion. So (5.27) reduces to the formula of Levin (1967),

$$\alpha_* = \frac{\alpha_1(1/\kappa_* - 1/\kappa_2) - \alpha_2(1/\kappa_* - 1/\kappa_1)}{1/\kappa_1 - 1/\kappa_2}, \tag{5.28}$$

for the effective thermal expansion coefficient. This is an example of a cross-property relation, linking two different effective moduli.

When three phases are present it is generally impossible to adjust the pressure and temperature change so that all three phases expand at the same rate. Consequently there is no general exact relation linking the effective thermal expansion coefficient and effective bulk modulus of three-phase composites. Nevertheless, one can use measurements of the effective bulk modulus to bound the effective thermal expansion coefficient; see Rosen and Hashin (1970) and Gibiansky and Torquato (1997). Exact results for three-phase composites can be obtained if there is another way of influencing the expansion of the phases, perhaps through swelling due to an externally adjustable factor like humidity. Then it is possible to adjust the temperature change, humidity content, and external pressure in such a way that all three phases contract (or expand) by the same amount; see Schulgasser (1989) for a related analysis.

One can also obtain a formula for determining the constant of specific heat c_*. The relation (2.23) giving c_* must hold when $\boldsymbol{\tau}(\boldsymbol{x})$ is the uniform hydrostatic compression (5.22) and p/θ is given by (5.26). Upon making this substitution for the stress field, (2.23) implies that

$$\frac{c_* - \langle c\rangle}{\mathrm{Tr}(\boldsymbol{\alpha}_* - \langle\boldsymbol{\alpha}\rangle)T_0} = \frac{p}{\theta} = \frac{d(\alpha_1-\alpha_2)}{1/\kappa_1 - 1/\kappa_2},$$

which in view of (5.27) reduces to the exact expression

$$c_* = \langle c\rangle + \frac{d^2(\alpha_1-\alpha_2)^2}{(1/\kappa_1 - 1/\kappa_2)^2}\Big[\mathrm{Tr}(\boldsymbol{\mathcal{S}}_*\boldsymbol{I}) - \langle 1/\kappa\rangle\Big]T_0 \tag{5.29}$$

of Rosen and Hashin (1970) for the effective constant of specific heat at constant pressure, where $\mathrm{Tr}(\boldsymbol{\mathcal{S}}_*\boldsymbol{I})$ should be identified with $1/\kappa_*$ when the composite is isotropic.

5.5. The extension to nonlinear thermal expansion

These exact relations have a simple generalization to the nonlinear case as found by Berryman and myself [see Milton (1997)]. Suppose that the two phases are isotropic so that a block of phase 1 or phase 2 immersed in a fluid heat bath at temperature T and pressure p expands or contracts isotropically as T and p are varied. Let $\rho_1(T, p)$ and $\rho_2(T, p)$ denote the mass density of phase 1 or phase 2 relative to some base temperature T_0 and base pressure p_0; thus $1/\rho_1(T, p)$ and $1/\rho_2(T, p)$ measure the relative change in the volume of each phase as the temperature and pressure change from (T_0, p_0) to (T, p). According to this definition we have

$$\rho_1(T_0, p_0) = \rho_2(T_0, p_0) = 1.$$

So the two surfaces $\rho_1(T, p)$ and $\rho_2(T, p)$ intersect at $(T, p) = (T_0, p_0)$. Unless the surfaces are tangent at this point, they will intersect along a trajectory passing through (T_0, p_0). Along this trajectory $(T(h), p(h))$ parameterized by h both phases expand or contract at an equal rate.

Now suppose that a composite is manufactured at the base temperature T_0 and pressure p_0 with no internal residual stress. When this composite is placed in the heat bath at temperature T and pressure p there is no reason to suppose that the composite will expand or contract isotropically as T and p are varied. Indeed by considering the example of a bimetal strip it is clear that internal shear stresses and warping can occur. However, along the trajectory $(T(h), p(h))$ the composite will expand isotropically, and its density relative to its density at the base temperature and pressure will be

$$\rho_*(T(h), p(h)) = \rho_1(T(h), p(h)) = \rho_2(T(h), p(h)) \quad \text{for all } h. \tag{5.30}$$

This is the nonlinear generalization of the relation (5.28). To see the connection we rewrite (5.30) as

$$1/\rho_*(T(h),\, p(h)) = 1/\rho_1(T(h),\, p(h)) = 1/\rho_2(T(h),\, p(h)).$$

Differentiating this with respect to h gives

$$d\alpha_*\frac{dT(h)}{dh} - \frac{1}{\kappa_*}\frac{dp(h)}{dh} = d\alpha_1\frac{dT(h)}{dh} - \frac{1}{\kappa_1}\frac{dp(h)}{dh} = d\alpha_2\frac{dT(h)}{dh} - \frac{1}{\kappa_2}\frac{dp(h)}{dh}, \tag{5.31}$$

where

$$\alpha_a(T,\, p) = \frac{1}{d}\frac{\partial(1/\rho_a)}{\partial T}, \quad \kappa_a(T,\, p) = -\left\{\frac{\partial(1/\rho_a)}{\partial p}\right\}^{-1}, \quad a = 1, 2, \text{ or } *,$$

are the tangent bulk moduli and thermal expansion constants of the phases and composite along the trajectory. By eliminating dp/dh and dT/dh from the linear equations (5.31) we recover (5.28).

5.6. The thermal expansion tensor and specific heat in composites of two anisotropic phases

When the compliance tensor $\boldsymbol{\mathcal{S}}(\boldsymbol{x})$ and thermal expansion tensor $\boldsymbol{\alpha}(\boldsymbol{x})$ take constant values in each phase of a two-phase composite,

$$\boldsymbol{\mathcal{S}}(\boldsymbol{x}) = \boldsymbol{\mathcal{S}}_1\chi_1(\boldsymbol{x}) + \boldsymbol{\mathcal{S}}_2\chi_2(\boldsymbol{x}), \quad \boldsymbol{\alpha}(\boldsymbol{x}) = \boldsymbol{\alpha}_1\chi_1(\boldsymbol{x}) + \boldsymbol{\alpha}_2\chi_2(\boldsymbol{x}),$$

we can still derive an exact expression for the effective thermal expansion tensor $\boldsymbol{\alpha}_*$ in terms of the effective compliance tensor $\boldsymbol{\mathcal{S}}_*$, even when the tensors $\boldsymbol{\alpha}_1$, $\boldsymbol{\alpha}_2$, $\boldsymbol{\mathcal{S}}_1$, and $\boldsymbol{\mathcal{S}}_2$ are not isotropic. To do this we look for a constant stress field $\boldsymbol{\tau}$ and a constant strain field $\boldsymbol{\epsilon}$, not necessarily proportional to the identity tensor, which solve the constitutive equations in each phase, that is, they satisfy

$$\boldsymbol{\epsilon} = \boldsymbol{\mathcal{S}}_1\boldsymbol{\tau} + \boldsymbol{\alpha}_1\theta, \quad \boldsymbol{\epsilon} = \boldsymbol{\mathcal{S}}_2\boldsymbol{\tau} + \boldsymbol{\alpha}_2\theta. \tag{5.32}$$

Since the fields are constant, they can be equated with their average values and the effective constitutive law then implies that

$$\boldsymbol{\epsilon} = \boldsymbol{\mathcal{S}}_*\boldsymbol{\tau} + \boldsymbol{\alpha}_*\theta. \tag{5.33}$$

By eliminating $\boldsymbol{\epsilon}$ from (5.32) and (5.33) we see that

$$\boldsymbol{\tau} = \theta(\boldsymbol{\mathcal{S}}_1 - \boldsymbol{\mathcal{S}}_2)^{-1}(\boldsymbol{\alpha}_2 - \boldsymbol{\alpha}_1) = \theta(\boldsymbol{\mathcal{S}}_1 - \boldsymbol{\mathcal{S}}_*)^{-1}(\boldsymbol{\alpha}_* - \boldsymbol{\alpha}_1), \tag{5.34}$$

which provides the desired formula,

$$\boldsymbol{\alpha}_* = \boldsymbol{\alpha}_1 + (\boldsymbol{\mathcal{S}}_1 - \boldsymbol{\mathcal{S}}_*)(\boldsymbol{\mathcal{S}}_1 - \boldsymbol{\mathcal{S}}_2)^{-1}(\boldsymbol{\alpha}_2 - \boldsymbol{\alpha}_1), \tag{5.35}$$

for the thermal expansion tensor $\boldsymbol{\alpha}_*$ in terms of the effective compliance tensor $\boldsymbol{\mathcal{S}}_*$.

To obtain a formula for the effective specific heat c_* we first observe that with field $\boldsymbol{\tau}$ being constant, and given by (5.34), the constitutive law and effective constitutive law imply that

$$\begin{aligned} \varsigma(\boldsymbol{x}) &= \operatorname{Tr}[\boldsymbol{\alpha}(\boldsymbol{x})\boldsymbol{\tau}] + \theta c(\boldsymbol{x})/T_0 = \theta \operatorname{Tr}[\boldsymbol{\alpha}(\boldsymbol{x})(\boldsymbol{\mathcal{S}}_1 - \boldsymbol{\mathcal{S}}_2)^{-1}(\boldsymbol{\alpha}_2 - \boldsymbol{\alpha}_1)] + \theta c(\boldsymbol{x})/T_0, \\ \langle\varsigma\rangle &= \operatorname{Tr}[\boldsymbol{\alpha}_*\boldsymbol{\tau}] + \theta c_*/T_0 = \theta \operatorname{Tr}[\boldsymbol{\alpha}_*(\boldsymbol{\mathcal{S}}_1 - \boldsymbol{\mathcal{S}}_2)^{-1}(\boldsymbol{\alpha}_2 - \boldsymbol{\alpha}_1)] + \theta c_*/T_0. \end{aligned}$$

By averaging the first equation and equating it with the second, we obtain the desired formula,

$$c_* = f_1 c_1 + f_2 c_2 + \mathrm{Tr}[(f_1\boldsymbol{\alpha}_1 + f_2\boldsymbol{\alpha}_2 - \boldsymbol{\alpha}_*)(\boldsymbol{\mathcal{S}}_1 - \boldsymbol{\mathcal{S}}_2)^{-1}(\boldsymbol{\alpha}_2 - \boldsymbol{\alpha}_1)]T_0, \tag{5.36}$$

for the effective specific heat at constant pressure. These formulas (5.35) and (5.36) are due to Rosen and Hashin (1970).

5.7. Exact thermoelastic relations for polycrystals

In three-dimensional polycrystalline materials the local compliance tensor $\boldsymbol{\mathcal{S}}(\boldsymbol{x})$, thermal expansion tensor $\boldsymbol{\alpha}(\boldsymbol{x})$, and specific heat $c(\boldsymbol{x})$ take the forms

$$\boldsymbol{\mathcal{S}}(\boldsymbol{x}) = \boldsymbol{\mathcal{R}}(\boldsymbol{x})\boldsymbol{\mathcal{S}}_0[\boldsymbol{\mathcal{R}}(\boldsymbol{x})]^T, \quad \boldsymbol{\alpha}(\boldsymbol{x}) = \boldsymbol{R}(\boldsymbol{x})\boldsymbol{\alpha}_0[\boldsymbol{R}(\boldsymbol{x})]^T, \quad c(\boldsymbol{x}) = c_0,$$

in which $\boldsymbol{\mathcal{S}}_0$, $\boldsymbol{\alpha}_0$, and c_0 are the compliance tensor, thermal expansion tensor, and specific heat of the pure crystal, while the second-order tensor field $\boldsymbol{R}(\boldsymbol{x})$ and its associated fourth-order tensor $\boldsymbol{\mathcal{R}}(\boldsymbol{x}) = \boldsymbol{R}(\boldsymbol{x}) \otimes \boldsymbol{R}(\boldsymbol{x})$ represent the action of a local rotation on $\boldsymbol{\alpha}_0$ and $\boldsymbol{\mathcal{S}}_0$, respectively. To derive a relation between the different effective moduli we assume that the pure crystal is such that the second-order tensors $\boldsymbol{\mathcal{S}}_0\boldsymbol{I}$ and $\boldsymbol{\alpha}_0$ are both uniaxial with a common axis of symmetry. This is certainly ensured if the crystal has hexagonal, tetragonal, or trigonal symmetry. By taking this axis as a basis vector, $\boldsymbol{\mathcal{S}}_0\boldsymbol{I}$ and $\boldsymbol{\alpha}_0$ can be represented by diagonal matrices:

$$\boldsymbol{\mathcal{S}}_0\boldsymbol{I} = \begin{pmatrix} \mu_1 & 0 & 0 \\ 0 & \mu_2 & 0 \\ 0 & 0 & \mu_2 \end{pmatrix}, \quad \boldsymbol{\alpha}_0 = \begin{pmatrix} \lambda_1 & 0 & 0 \\ 0 & \lambda_2 & 0 \\ 0 & 0 & \lambda_2 \end{pmatrix}.$$

Under a combination of uniform hydrostatic compression $\boldsymbol{\tau} = -p\boldsymbol{I}$ and temperature increase θ, the strain in a sample of this pure crystal is

$$\boldsymbol{\epsilon}_0 = -p\boldsymbol{\mathcal{S}}_0\boldsymbol{I} + \theta\boldsymbol{\alpha}_0 = \begin{pmatrix} -p\mu_1 + \theta\lambda_1 & 0 & 0 \\ 0 & -p\mu_2 + \theta\lambda_2 & 0 \\ 0 & 0 & -p\mu_2 + \theta\lambda_2 \end{pmatrix}.$$

By a judicious choice of the ratio p/θ, namely,

$$p/\theta = \frac{\lambda_1 - \lambda_2}{\mu_1 - \mu_2},$$

we see that the strain in the pure crystal reduces to a multiple of the identity

$$\boldsymbol{\epsilon}_0 = \frac{\lambda_2\mu_1 - \lambda_1\mu_2}{\mu_1 - \mu_2}\theta\boldsymbol{I},$$

and thus represents a dilation.

Under this combination of pressure and temperature change, each crystal in the polycrystal undergoes the same uniform dilation in size, and so the polycrystal as a whole must dilate in size by this same factor. The effective constitutive law implies that

$$\begin{aligned} \langle\boldsymbol{\epsilon}\rangle &= \frac{\lambda_2\mu_1 - \lambda_1\mu_2}{\mu_1 - \mu_2}\boldsymbol{I}\theta \\ &= \boldsymbol{\mathcal{S}}_*\langle\boldsymbol{\tau}\rangle + \boldsymbol{\alpha}_*\theta = \Big[-\frac{\lambda_1 - \lambda_2}{\mu_1 - \mu_2}\boldsymbol{\mathcal{S}}_*\boldsymbol{I} + \boldsymbol{\alpha}_*\Big]\theta, \end{aligned}$$

which gives us the formula for the effective thermal expansion tensor in terms of the effective compliance tensor:

$$\boldsymbol{\alpha}_* = \frac{\lambda_1 - \lambda_2}{\mu_1 - \mu_2}\boldsymbol{\mathcal{S}}_*\boldsymbol{I} + \frac{\lambda_2\mu_1 - \lambda_1\mu_2}{\mu_1 - \mu_2}\boldsymbol{I}. \tag{5.37}$$

For macroscopically isotropic polycrystals this formula reduces to the relation

$$\alpha_* = \frac{\lambda_1 - \lambda_2}{d\kappa_*(\mu_1 - \mu_2)} + \frac{\lambda_2\mu_1 - \lambda_1\mu_2}{\mu_1 - \mu_2}, \tag{5.38}$$

relating the effective coefficient of thermal expansion α_* to of the effective bulk modulus κ_*. This relation (5.38) is due to Hashin (1984). Subsequently, Schulgasser (1987) saw that it could be generalized and obtained the formula (5.37).

The special combination of pressure and temperature change generates a uniform entropy field

$$\varsigma(\boldsymbol{x}) = \langle\varsigma\rangle = -p\,\mathrm{Tr}[\boldsymbol{\alpha}_0] + \theta c_0/T_0 = -p\,\mathrm{Tr}[\boldsymbol{\alpha}_*] + \theta c_*/T_0,$$

implying that

$$\frac{c_* - c_0}{\mathrm{Tr}(\boldsymbol{\alpha}_* - \boldsymbol{\alpha}_0)T_0} = \frac{p}{\theta} = \frac{\lambda_1 - \lambda_2}{\mu_1 - \mu_2}.$$

In other words, the effective specific at constant pressure must be given by the formula

$$c_* = c_0 + \frac{\lambda_1 - \lambda_2}{\mu_1 - \mu_2}\,\mathrm{Tr}(\boldsymbol{\alpha}_* - \boldsymbol{\alpha}_0)T_0.$$

5.8. The effective poroelastic moduli of two-phase media

Since the equations of thermoelasticity are equivalent to those of poroelasticity, all of the results that we have derived for thermoelastic media immediately extend to poroelastic media. The poroelastic equations take the form

$$\begin{pmatrix} \boldsymbol{\epsilon}_s(\boldsymbol{x}) \\ -\zeta(\boldsymbol{x}) \end{pmatrix} = \begin{pmatrix} \boldsymbol{\mathcal{S}}(\boldsymbol{x}) & \boldsymbol{\alpha}(\boldsymbol{x}) \\ \boldsymbol{\alpha}(\boldsymbol{x}) & c(\boldsymbol{x}) \end{pmatrix} \begin{pmatrix} \boldsymbol{\tau}_c(\boldsymbol{x}) \\ -p_f \end{pmatrix}, \tag{5.39}$$

where

$$\boldsymbol{\epsilon}_s = [\nabla\boldsymbol{u}_s + (\nabla\boldsymbol{u}_s)^T]/2, \quad \nabla\cdot\boldsymbol{\tau}_c = 0, \tag{5.40}$$

and, as explained in the introduction, $\boldsymbol{u}_s(\boldsymbol{x})$ is the average solid displacement, $\zeta(\boldsymbol{x})$ is the increment of fluid content, $\boldsymbol{\tau}_c(\boldsymbol{x})$ is the confining stress, p_f is the fluid pressure (which is constant), $\boldsymbol{\mathcal{S}}(\boldsymbol{x})$ is now the compliance tensor of the drained porous frame, $\boldsymbol{\alpha}(\boldsymbol{x})$ is now the tensor of fluid pressure induced expansion (at constant confining stress), and $c(\boldsymbol{x})$ is now the coefficient relating the increment of fluid content to the fluid pressure (again at constant confining stress). The macroscopic behavior is governed by the equations

$$\begin{pmatrix} \langle\boldsymbol{\epsilon}_s\rangle \\ -\langle\zeta\rangle \end{pmatrix} = \begin{pmatrix} \boldsymbol{\mathcal{S}}_* & \boldsymbol{\alpha}_* \\ \boldsymbol{\alpha}_* & c_* \end{pmatrix} \begin{pmatrix} \langle\boldsymbol{\tau}_c\rangle \\ -p_f \end{pmatrix},$$

which serve to define the effective moduli.

Because of the equivalence with the thermoelastic equations, the formulas (5.27) and (5.29) also apply to poroelastic media built from two isotropic porous phases once we set

$T_0 = 1$. In particular, let us consider a poroelastic solid where phase 1 is entirely solid and isotropic with poroelastic tensor

$$\mathcal{L}_1 = \begin{pmatrix} \mathcal{S}_1 & \boldsymbol{\alpha}_1 \\ \boldsymbol{\alpha}_1 & c_1 \end{pmatrix} = \begin{pmatrix} \mathcal{S}_1 & 0 \\ 0 & 0 \end{pmatrix},$$

where

$$\mathcal{S}_1 = \Big(\frac{1}{9\kappa_1} - \frac{1}{6\mu_1}\Big)\boldsymbol{I} \otimes \boldsymbol{I} + \frac{\mathcal{I}}{2\mu_1}$$

is the compliance tensor of the solid while κ_1 and μ_1 are its bulk and shear moduli.

Ultimately we want to take phase 2 as entirely liquid. However, to avoid infinite moduli let us suppose that phase 2 is itself a poroelastic media, comprised of a skeletal porous frame immersed in fluid with the frame occupying only an infinitesimal volume fraction and having the same bulk modulus as the fluid (and with pore structure being much smaller than the microstructure of the larger composite). When $\boldsymbol{\tau}_c = -p_f \boldsymbol{I}$, the average solid displacement $\boldsymbol{u}_s$ in phase 2 will exactly equal the average fluid displacement $\boldsymbol{u}_f$, implying that $\zeta = 0$ and $\boldsymbol{\epsilon}_s = -(p_f/3\kappa_f)\boldsymbol{I}$, where κ_f is the fluid (or frame) bulk modulus. Consequently in this phase the poroelastic tensor is

$$\mathcal{L}_2 = \begin{pmatrix} \mathcal{S}_2 & \boldsymbol{\alpha}_2 \\ \boldsymbol{\alpha}_2 & c_2 \end{pmatrix} = \begin{pmatrix} \mathcal{S}_2 & (1/3\kappa_f - 1/3\kappa_2)\boldsymbol{I} \\ (1/3\kappa_f - 1/3\kappa_2)\boldsymbol{I} & 1/\kappa_2 - 1/\kappa_f \end{pmatrix},$$

where

$$\mathcal{S}_2 = \Big(\frac{1}{9\kappa_2} - \frac{1}{6\mu_2}\Big)\boldsymbol{I} \otimes \boldsymbol{I} + \frac{\mathcal{I}}{2\mu_2}$$

is the effective elasticity tensor of the drained porous frame of phase 2, while κ_2 and μ_2 are its effective bulk and shear moduli.

In the limit as the volume fraction of the porous frame in phase 2 approaches zero, the effective moduli κ_2 and μ_2 approach zero. In this limit (5.27) and (5.29) reduce to

$$\boldsymbol{\alpha}_* = -\mathcal{S}_*\boldsymbol{I} + \frac{\boldsymbol{I}}{3\kappa_1}, \qquad c_* = \operatorname{Tr}(\mathcal{S}_*\boldsymbol{I}) - \frac{1}{\kappa_1} + \phi_*\Big(\frac{1}{\kappa_f} - \frac{1}{\kappa_1}\Big), \tag{5.41}$$

where $\mathcal{S}_*$ is the compliance tensor of the drained porous frame of the composite and ϕ_* is its porosity, that is, the volume fraction occupied by the pores. These formulas (5.41) for the poroelastic moduli of a fluid-filled porous solid are equivalent to those derived by Gassmann (1951). This equivalence was recognized by Berryman and Milton (1991) and Norris (1992), who also extended the formulas to composites of two poroelastic phases.

Following Brown and Korringa (1975) it is convenient (from an experimental perspective) to introduce three characteristic bulk moduli κ_*, κ_*^s, and κ_*^ϕ through the expressions

$$\frac{1}{\kappa_*} = -\frac{1}{V}\Big(\frac{\partial V}{\partial p_d}\Big)_{p_f}, \qquad \frac{1}{\kappa_*^s} = -\frac{1}{V}\Big(\frac{\partial V}{\partial p_f}\Big)_{p_d}, \qquad \frac{1}{\kappa_*^\phi} = -\frac{1}{V_\phi}\Big(\frac{\partial V_\phi}{\partial p_f}\Big)_{p_d},$$

where V is the total volume of a jacketed fluid-filled sample of the composite, $V_\phi = \phi V$ is the pore volume in that sample, $p = -\operatorname{Tr}(\boldsymbol{\tau}_c)/3$ is the external (confining) pressure applied to the outside of the jacket, p_f is the fluid pressure, and $p_d = p - p_f$ is the differential pressure. The definitions of these bulk moduli imply that

$$\operatorname{Tr}(\mathcal{S}_*\boldsymbol{I}) = \frac{1}{\kappa_*}, \qquad \operatorname{Tr}(\boldsymbol{\alpha}_*) = \Big(\frac{1}{\kappa_*^s} - \frac{1}{\kappa_*}\Big), \qquad c_* = \Big(\frac{1}{\kappa_*} - \frac{1}{\kappa_*^s}\Big) + \phi_*\Big(\frac{1}{\kappa_f} - \frac{1}{\kappa_*^\phi}\Big), \tag{5.42}$$

and it is evident by comparing (5.42) with (5.41) that the Gassman equations, when expressed in terms of these new moduli, reduce to

$$\kappa_*^s = \kappa_*^\phi = \kappa_1,$$

where κ_1 is the bulk modulus of the solid phase.

5.9. The elastic moduli of two-phase fibrous composites

Consider a two-phase elastic fibrous composite where the phase boundaries are independent of x_3 and the two phases have fixed orientation with elasticity tensors $\mathcal{C}_1$ and $\mathcal{C}_2$. We assume that these elasticity tensors are invariant under the reflection transformation $x_3 \to -x_3$, implying that their elements $C^1_{ijk\ell}$ and $C^2_{ijk\ell}$ are zero whenever an odd number of indices take the value 3, that is,

$$\begin{aligned} C^1_{1123} = C^1_{1113} = C^1_{2223} = C^1_{1123} = C^1_{2213} = C^1_{1312} = C^1_{2312} = C^1_{3313} = C^1_{3323} = 0, \\ C^2_{1123} = C^2_{1113} = C^2_{2223} = C^2_{1123} = C^2_{2213} = C^2_{1312} = C^2_{2312} = C^2_{3313} = C^2_{3323} = 0. \end{aligned}$$

The effective elasticity tensor $\mathcal{C}_*$ will also be invariant under this reflection transformation and so its elements $C^*_{ijk\ell}$ will vanish whenever an odd number of indices take the value 3.

We saw in section 2.7 on page 35 that for such a medium the three-dimensional elasticity equations decouple into a two-dimensional dielectric-type problem [the antiplane-strain problem (2.42)], and a two-dimensional thermoelastic-type problem [with a constitutive law given by (2.44)]. By applying uniform field arguments to the two-dimensional thermoelastic-type problem one obtains the formulas

$$\begin{aligned} \boldsymbol{A}_* &= \boldsymbol{A}_1 + (\mathcal{C}'_1 - \mathcal{C}'_*)(\mathcal{C}'_1 - \mathcal{C}'_2)^{-1}(\boldsymbol{A}_2 - \boldsymbol{A}_1), \\ C^*_{3333} &= f_1 C^1_{3333} + f_2 C^2_{3333} + \mathrm{Tr}[(f_1\boldsymbol{A}_1 + f_2\boldsymbol{A}_2 - \boldsymbol{A}_*)(\mathcal{C}'_1 - \mathcal{C}'_2)^{-1}(\boldsymbol{A}_2 - \boldsymbol{A}_1)], \end{aligned} \tag{5.43}$$

which are directly analogous to (5.35) and (5.36). In these formulas $\mathcal{C}'_1$, $\mathcal{C}'_2$, and $\mathcal{C}'_*$ are the two-dimensional, fourth-order elasticity tensors associated with the plane-strain problem while $\boldsymbol{A}_1$, $\boldsymbol{A}_2$, and $\boldsymbol{A}_*$ are the second-order coupling tensors. These can alternatively be represented by the matrices and vectors

$$\mathcal{C}'_i = \begin{pmatrix} C^i_{1111} & C^i_{1122} & \sqrt{2}C^i_{1112} \\ C^i_{1122} & C^i_{2222} & \sqrt{2}C^i_{2212} \\ \sqrt{2}C^i_{1112} & \sqrt{2}C^i_{2212} & 2C^i_{1212} \end{pmatrix}, \quad \boldsymbol{A}_i = \begin{pmatrix} C^i_{1133} \\ C^i_{2233} \\ \sqrt{2}C^i_{3312} \end{pmatrix} \quad \text{for } i = 1, 2, *,$$

in which case the second relation in (5.43) takes the form

$$C^*_{3333} = f_1 C^1_{3333} + f_2 C^2_{3333} + (f_1\boldsymbol{A}_1 + f_2\boldsymbol{A}_2 - \boldsymbol{A}_*) \cdot (\mathcal{C}'_1 - \mathcal{C}'_2)^{-1}(\boldsymbol{A}_2 - \boldsymbol{A}_1).$$

In other words, all of the elements of the three-dimensional effective elasticity tensor $\mathcal{C}_*$ can be determined once the effective tensor $\mathcal{C}'_*$ of the planar elasticity problem and the effective shear matrix $\boldsymbol{\mu}_*$ of the antiplane elasticity problem are determined.

In particular, suppose that both phases are elastically isotropic with bulk moduli κ_1 and κ_2 and shear moduli μ_1 and μ_2, and that the cylindrical microgeometry is transversely isotropic. Then the two-dimensional in-plane elasticity tensors and coupling tensors are

$$\mathcal{C}'_i = \kappa'_i \boldsymbol{I} \otimes \boldsymbol{I} + 2\mu'_i(\mathcal{I} - \boldsymbol{I} \otimes \boldsymbol{I}/2), \quad \boldsymbol{A}_i = \lambda_i \boldsymbol{I} \text{ for } i = 1, 2, *,$$

where

$$\begin{aligned}\mu_1' &= \mu_1, \quad \mu_2' = \mu_2\\ \kappa_1' &= \kappa_1 + \mu_1/3, \quad \kappa_2' = \kappa_2 + \mu_2/3,\\ \lambda_1 &= \kappa_1 - 2\mu_1/3, \quad \lambda_2 = \kappa_2 - 2\mu_2/3.\end{aligned}$$

Here κ_1', κ_2', μ_1', and μ_2' are the bulk and shear moduli of the phases in the associated two-dimensional medium under plane strain conditions, and κ_*' and μ_*' are the associated two-dimensional effective bulk and shear moduli, while λ_1 and λ_2 are the (three-dimensional) Lame moduli of the two phases. By direct analogy with (5.28) and (5.29) [replacing α by λ, $1/(d^2\kappa)$ by κ' and c/T_0 by C_{3333}] we have the relations

$$\begin{aligned}C_{1133}^* &= C_{3311}^* = C_{2233}^* = C_{3322}^* = \frac{\lambda_1(\kappa_*' - \kappa_2') - \lambda_2(\kappa_*' - \kappa_1')}{\kappa_1' - \kappa_2'},\\ C_{3333}^* &= \langle\lambda + 2\mu\rangle + \frac{(\lambda_1 - \lambda_2)^2}{(\kappa_1' - \kappa_2')^2}(\kappa_*' - \langle\kappa'\rangle),\end{aligned} \tag{5.44}$$

due to Hill (1964), linking the various effective moduli.

The only other nonzero elements of the effective elasticity tensor are the nonzero elements of the effective in-plane elasticity tensor $\boldsymbol{\mathcal{C}}_*'$, namely,

$$C_{1111}^* = C_{2222}^* = \kappa_*' + \mu_*', \quad C_{1122}^* = C_{1122}^* = \kappa_*' - \mu_*', \quad C_{1212}^* = \mu_*',$$

and the nonzero elements of the effective shear matrix $\boldsymbol{\mu}_*$,

$$C_{1313}^* = C_{2323}^* = \mu_{a*},$$

in which μ_{a*} is the effective axial shear modulus. Due to the equivalence between the equations of antiplane elasticity and two-dimensional conductivity it is given by the formulas

$$\mu_{a*} = \sigma_*(\mu_1, \mu_2),$$

in which $\sigma_*(\sigma_1, \sigma_2)$ is the transverse effective conductivity when phase 1 has conductivity σ_1 and phase 2 has conductivity σ_2. He (1999) has shown how these results can be extended to nonlinear elastic fibrous composites.

5.10. Exact relations for pyroelectric, conductivity, and magnetotransport equations

The equations of pyroelectricity

$$\boldsymbol{d}(\boldsymbol{x}) = \boldsymbol{\epsilon}(\boldsymbol{x})\boldsymbol{e}(\boldsymbol{x}) + \boldsymbol{\alpha}(\boldsymbol{x})\theta, \quad \nabla\cdot\boldsymbol{d} = 0, \quad \nabla\times\boldsymbol{e} = 0, \quad \theta = \text{constant},$$

have basically the same structure as the equations of thermal expansion, and by applying the same uniform field arguments one obtains the formula

$$\boldsymbol{\alpha}_* = \boldsymbol{\alpha}_1 + (\boldsymbol{\epsilon}_1 - \boldsymbol{\epsilon}_*)(\boldsymbol{\epsilon}_1 - \boldsymbol{\epsilon}_2)^{-1}(\boldsymbol{\alpha}_2 - \boldsymbol{\alpha}_1)$$

for the effective pyroelectric vector $\boldsymbol{\alpha}_*$ in a two-phase medium, in terms of the pyroelectric vectors $\boldsymbol{\alpha}_1$ and $\boldsymbol{\alpha}_2$ and dielectric tensors $\boldsymbol{\epsilon}_1$ and $\boldsymbol{\epsilon}_2$ of the two phases and the effective dielectric tensor $\boldsymbol{\epsilon}_*$ of the composite.

Similarly, for the conductivity equations (2.30) or magnetotransport equations (2.32) in a two-phase fibrous composite with microstructure independent of x_3, the effective conductivity tensors given respectively by (2.34) and (2.35) have components

$$\begin{aligned}\boldsymbol{\alpha}_* &= \boldsymbol{\alpha}_1 + (\boldsymbol{\sigma}'_1 - \boldsymbol{\sigma}'_*)(\boldsymbol{\sigma}'_1 - \boldsymbol{\sigma}'_2)^{-1}(\boldsymbol{\alpha}_2 - \boldsymbol{\alpha}_1),\\ c_* &= \langle \sigma_{33} \rangle + (f_1\boldsymbol{\alpha}_1 + f_2\boldsymbol{\alpha}_2 - \boldsymbol{\alpha}_*) \cdot (\boldsymbol{\sigma}'_1 - \boldsymbol{\sigma}'_2)^{-1}(\boldsymbol{\alpha}_2 - \boldsymbol{\alpha}_1),\end{aligned}$$

where the last equation follows from basically the same reasoning as led to (5.36). In particular it follows that the effective conductivity tensors are completely determined once one has calculated the two-dimensional effective conductivity tensor $\boldsymbol{\sigma}'_*$ associated with the diagonal conductivity tensor field $\boldsymbol{\sigma}'$ given by (2.33). Surprisingly, this seems not to have been previously observed, despite the many papers on magnetotransport.

5.11. The bulk modulus of a suspension of elastic particles in a fluid

You have probably noticed that the equation (2.21) describing thermoelasticity in two-phase composites differs from the examples discussed earlier in the chapter in the sense that fluctuations remain in the field $\boldsymbol{\varsigma}(\boldsymbol{x})$ even when the fields $\boldsymbol{\tau}(\boldsymbol{x})$, θ, and $\boldsymbol{\epsilon}(\boldsymbol{x})$ are uniform. These fluctuations do not matter as $\boldsymbol{\varsigma}(\boldsymbol{x})$ is not subject to any differential constraints. A similar situation occurs when a suspension of elastic particles in a fluid, with bulk modulus κ_0, is subject to hydrostatic compression.

Let us suppose that the elasticity tensor field takes the form

$$\boldsymbol{\mathcal{C}}(\boldsymbol{x}) = \chi_0\boldsymbol{\mathcal{C}}_0 + \sum_{a=1}^{n} \chi_a\boldsymbol{\mathcal{C}}_a,$$

where the characteristic functions

$$\begin{aligned}\chi_a(\boldsymbol{x}) &= 1 \text{ in phase } a,\\ &= 0 \text{ otherwise,}\end{aligned}$$

describe the geometry of the suspension and

$$\boldsymbol{\mathcal{C}}_0 = \kappa_0\boldsymbol{I} \otimes \boldsymbol{I}$$

represents the elasticity tensor of the fluid. Note that within the fluid the curl of the displacement field is not subject to any differential constraints. We assume that each of the n suspended phases consists of isolated particles surrounded by fluid.

Since the fluid can flow and accommodate any change in the shape of each particle, it follows that the elasticity equations will be satisfied with a uniform stress field

$$\boldsymbol{\tau}(\boldsymbol{x}) = -p\boldsymbol{I},$$

where p is the pressure. Inside each suspended phase the corresponding strain will be

$$\boldsymbol{\epsilon}_a = -p\boldsymbol{\mathcal{S}}_a\boldsymbol{I},$$

where $\boldsymbol{\mathcal{S}}_a = (\boldsymbol{\mathcal{C}}_a)^{-1}$ is the associated compliance tensor, while in the fluid the strain has trace

$$\operatorname{Tr}\boldsymbol{\epsilon}_0 = -p/\kappa_0,$$

where κ_0 is the fluid bulk modulus.

By taking averages of the strain we find that

$$\mathrm{Tr}\langle\boldsymbol{\epsilon}\rangle = -p\Big[f_0/\kappa_0 + \sum_{a=1}^{n} f_a \ \mathrm{Tr}(\boldsymbol{\mathcal{S}}_a\boldsymbol{I})\Big], \tag{5.45}$$

where $f_a = \langle\chi_a\rangle$ is the volume fraction occupied by phase a. Since the suspension is not resistant to shear, it behaves as a fluid with elasticity tensor

$$\boldsymbol{\mathcal{C}}_* = \kappa_*\boldsymbol{I}\otimes\boldsymbol{I},$$

where according to (5.45) its bulk modulus κ_* is given by

$$1/\kappa_* = f_0/\kappa_0 + \sum_{a=1}^{n} f_a \ \mathrm{Tr}(\boldsymbol{\mathcal{S}}_a\boldsymbol{I}).$$

For a suspension of isotropic phases this reduces to the harmonic mean average of the bulk moduli of the phases,

$$1/\kappa_* = \sum_{a=0}^{n} f_a/\kappa_a, \tag{5.46}$$

which is known as Wood's formula (Wood 1955).

Wood applied this result to calculate the phase velocity of sound c_s in water containing bubbles of gas. Assuming that the wavelength of the sound is sufficiently large compared to the inhomogeneities, and neglecting the shear viscosity of the water [which causes attenuation and dispersion of the waves (see section 11.4 on page 233)] we have

$$c_s = \sqrt{\kappa_*/\varrho_*},$$

where

$$\varrho_* = f_1\varrho_1 + f_2\varrho_2, \quad \kappa_* = (f_1/\kappa_1 + f_2/\kappa_2)^{-1}$$

are the effective density and effective bulk modulus [given by (5.46)] expressed in terms of the densities ϱ_1, ϱ_2; bulk moduli κ_1, κ_2; and volume fractions f_1, f_2 of the gas (phase 1) and the water (phase 2). Neglecting the density of the gas and treating the water as incompressible (i.e., taking the limit $\varrho_1 \to 0$ and $\kappa_2 \to \infty$) we obtain the estimate

$$c_s \approx \sqrt{\kappa_1/(f_1 f_2 \varrho_2)}.$$

This is dramatically less than either the speed of sound in the gas ($\sqrt{\kappa_1/\varrho_1}$) or the speed of sound in the water ($\sqrt{\kappa_2/\varrho_2}$), both of which approach infinity in the limit as $\varrho_1 \to 0$ and $\kappa_2 \to \infty$. The mixture transmits sound at much slower velocities than the pure phases.

References

Berryman, J. G. and G. W. Milton 1991. Exact results for generalized Gassman's equations in composite porous media with two constituents. *Geophysics* 56(12):1950–1960. {*85, 89*}

Brown, R. J. S. and J. Korringa 1975. On the dependence of the elastic properties of a porous rock on the compressibility of a pore fluid. *Geophysics* 40:608–616. {*85, 89*}

Cribb, J. L. 1968. Shrinkage and thermal expansion of a two phase material. *Nature* 220: 576–577. {*75, 79, 90*}

Dvorak, G. J. 1983. Metal matrix composites: Plasticity and fatigue. In Z. Hashin and C. Herakovich (eds.), *Mechanics of Composite Materials: Recent Advances: Proceedings of the IUTAM Symposium on Mechanics of Composite Materials, Virginia Polytechnic Institute and State University, Blacksburg, Virginia, USA, August 16–19, 1982*, pp. 73–91. New York: Pergamon. ISBN 0-08-029384-0. {*75, 90*}

Dvorak, G. J. 1990. On uniform fields in heterogeneous media. *Proceedings of the Royal Society of London. Series A, Mathematical and Physical Sciences* 431(1881):89–110. {*75, 90*}

Francfort, G. A. and L. Tartar 1991. Effective behavior of a mixture of isotropic materials with identical shear moduli. *Comptes rendus de l'Académie des sciences, Paris* 312: 301–307. {*77, 90*}

Gassmann, F. 1951. Über die elastizität poröser medien. (German) [On the elasticity of porous media]. *Vierteljahrsschrift der Naturforschenden Gesellschaft in Zürich* 96:1–23. {*85, 90*}

Gibiansky, L. V. and S. Torquato 1997. Thermal expansion of isotropic multiphase composites and polycrystals. *Journal of the Mechanics and Physics of Solids* 45(7):1223–1252. {*81, 90*}

Hashin, Z. 1984. Thermal expansion of polycrystalline aggregates: I. Exact analysis. *Journal of the Mechanics and Physics of Solids* 32:149–157. {*84, 90*}

He, Q.-C. 1999. Uniform strain fields and microstructure-independent relations in nonlinear elastic fibrous composites. *Journal of the Mechanics and Physics of Solids* 47(8): 1781–1793. {*87, 90*}

Hill, R. 1952. The elastic behavior of a crystalline aggregate. *Proceedings of the Physical Society, London, A* 65:349–354. {*75, 77, 90, 271, 273, 287, 442, 453*}

Hill, R. 1963. Elastic properties of reinforced solids: Some theoretical principles. *Journal of the Mechanics and Physics of Solids* 11:357–372. {*77, 90, 247, 268, 272, 287, 471, 473, 493*}

Hill, R. 1964. Theory of mechanical properties of fiber-strengthened materials: I. Elastic behavior. *Journal of the Mechanics and Physics of Solids* 12:199–212. {*75, 77, 87, 90, 471, 474, 493*}

Levin, V. M. 1967. Thermal expansion coefficients of heterogeneous materials. *Mekhanika Tverdogo Tela* 2(1):88–94. English translation in *Mechanics of Solids* 2(1):58–61 (1967). {*80, 90*}

Lurie, K. A. and A. V. Cherkaev 1986. Effective characteristics of composite materials and the optimal design of structural elements. *Uspekhi Mekhaniki = Advances in Mechanics* 9(2):3–81. English translation in *Topics in the Mathematical Modelling of Composite Materials*, pp. 175–258, ed. by A. Cherkaev and R. Kohn. ISBN 0-8176-3662-5. {*76, 90, 529, 551*}

Lurie, K. A., A. V. Cherkaev, and A. V. Fedorov 1984. On the existence of solutions to some problems of optimal design for bars and plates. *Journal of Optimization Theory and Applications* 42(2):247–281. {*75, 76, 90*}

Milton, G. W. 1997. Composites: A myriad of microstructure independent relations. In T. Tatsumi, E. Watanabe, and T. Kambe (eds.), *Theoretical and Applied Mechanics 1996: Proceedings of the XIXth International Congress of Theoretical and Applied Mechanics, Kyoto, Japan, 25–31 August 1996*, pp. 443–459. Amsterdam: Elsevier. ISBN 0-444-82446-4. {*35, 45, 81, 91*}

Norris, A. 1992, February 1. On the correspondence between poroelasticity and thermoelasticity. *Journal of Applied Physics* 71(3):1138–1141. {*32, 45, 85, 91*}

Rosen, B. W. and Z. Hashin 1970. Effective thermal expansion coefficients and specific heats of composite materials. *International Journal of Engineering Science* 8:157–173. {*80, 81, 83, 91*}

Schulgasser, K. 1987. Thermal expansion of polycrystalline aggregates with texture. *Journal of the Mechanics and Physics of Solids* 35:35–42. {*84, 91*}

Schulgasser, K. 1989. Thermal expansion of polycrystals. *Journal of Materials Science Letters* 8:228–229. {*81, 91*}

Sobel, D. 1995. *Longitude: The True Story of a Lone Genius Who Solved the Greatest Scientific Problem of His Time*. New York: Walker. viii + 184 pp. A biography of John Harrison, 1693–1776. ISBN 0-8027-1312-2. {*79, 91*}

Sobel, D. and W. J. H. Andrewes 1998. *The Illustrated Longitude*. New York: Walker. 216 pp. ISBN 0-8027-1344-0. {*79, 91*}

Wood, A. B. 1955. *A Textbook of Sound: Being an Account of the Physics of Vibrations with Special Reference to Recent Theoretical and Technical Developments* (Third revised ed.). London: G. Bell. xvi + 610 pp. {*89, 91*}

6

Exact relations for coupled equations

6.1. The covariance property of the effective tensor

Let us consider a problem with couplings. We suppose that there are m divergence free fields $\boldsymbol{j}_1(\boldsymbol{x}), \boldsymbol{j}_2(\boldsymbol{x}), \ldots, \boldsymbol{j}_m(\boldsymbol{x})$ and m curl free fields $\boldsymbol{e}_1(\boldsymbol{x}), \boldsymbol{e}_2(\boldsymbol{x}), \ldots, \boldsymbol{e}_m(\boldsymbol{x})$ that are linked through the constitutive relation

$$j_{i\alpha}(\boldsymbol{x}) = \sum_{j=1}^{d}\sum_{\beta=1}^{m} L_{i\alpha j\beta}(\boldsymbol{x}) e_{j\beta}(\boldsymbol{x}), \tag{6.1}$$

where α and β are field indices while i and j are space indices. This constitutive relation can be rewritten either in the form

$$\begin{pmatrix} \boldsymbol{j}_1 \\ \boldsymbol{j}_2 \\ \vdots \\ \boldsymbol{j}_m \end{pmatrix} = \begin{pmatrix} \boldsymbol{L}_{11} & \boldsymbol{L}_{12} & \ldots & \boldsymbol{L}_{1m} \\ \boldsymbol{L}_{21} & \boldsymbol{L}_{22} & \ldots & \boldsymbol{L}_{2m} \\ \vdots & \vdots & \ddots & \vdots \\ \boldsymbol{L}_{m1} & \boldsymbol{L}_{m2} & \ldots & \boldsymbol{L}_{mm} \end{pmatrix} \begin{pmatrix} \boldsymbol{e}_1 \\ \boldsymbol{e}_2 \\ \vdots \\ \boldsymbol{e}_m \end{pmatrix}, \tag{6.2}$$

where the ij-th element of the matrix $\boldsymbol{L}_{\alpha\beta}$ is $L_{i\alpha j\beta}$, or more concisely as

$$\boldsymbol{J}(\boldsymbol{x}) = \boldsymbol{\mathcal{L}}(\boldsymbol{x})\boldsymbol{E}(\boldsymbol{x}), \tag{6.3}$$

in which $\boldsymbol{J}(\boldsymbol{x})$, $\boldsymbol{\mathcal{L}}(\boldsymbol{x})$, and $\boldsymbol{E}(\boldsymbol{x})$ are identified with the terms in (6.2) in the obvious manner. The averages of the fields $\boldsymbol{J}$ and $\boldsymbol{E}$ are linked through the linear equation

$$\langle \boldsymbol{J} \rangle = \boldsymbol{\mathcal{L}}_* \langle \boldsymbol{E} \rangle, \tag{6.4}$$

which serves to define the effective tensor $\boldsymbol{\mathcal{L}}_*$.

We now note that any linear combination of divergence free fields is itself divergence free, and that any linear combination of curl free fields is curl free. This simple observation has profound consequences, as recognized by Straley (1981) and Milgrom and Shtrikman (1989). Suppose that $\boldsymbol{\mathcal{V}}$ and $\boldsymbol{\mathcal{W}}$ are a pair of nonsingular matrices of the form

$$\boldsymbol{\mathcal{V}} = \begin{pmatrix} v_{11}\boldsymbol{I} & v_{12}\boldsymbol{I} & \ldots & v_{1m}\boldsymbol{I} \\ v_{21}\boldsymbol{I} & v_{22}\boldsymbol{I} & \ldots & v_{2m}\boldsymbol{I} \\ \vdots & \vdots & \ddots & \vdots \\ v_{m1}\boldsymbol{I} & v_{m2}\boldsymbol{I} & \ldots & v_{mm}\boldsymbol{I} \end{pmatrix}, \quad \boldsymbol{\mathcal{W}} = \begin{pmatrix} w_{11}\boldsymbol{I} & w_{12}\boldsymbol{I} & \ldots & w_{1m}\boldsymbol{I} \\ w_{21}\boldsymbol{I} & w_{22}\boldsymbol{I} & \ldots & w_{2m}\boldsymbol{I} \\ \vdots & \vdots & \ddots & \vdots \\ w_{m1}\boldsymbol{I} & w_{m2}\boldsymbol{I} & \ldots & w_{mm}\boldsymbol{I} \end{pmatrix}. \tag{6.5}$$

Then the fields

$$\boldsymbol{E}'(\boldsymbol{x}) = \boldsymbol{\mathcal{V}}\boldsymbol{E}(\boldsymbol{x}), \quad \boldsymbol{J}'(\boldsymbol{x}) = \boldsymbol{\mathcal{W}}\boldsymbol{J}(\boldsymbol{x}) \tag{6.6}$$

have the forms

$$\boldsymbol{E}'(\boldsymbol{x}) = \begin{pmatrix} \boldsymbol{e}'_1(\boldsymbol{x}) \\ \boldsymbol{e}'_2(\boldsymbol{x}) \\ \vdots \\ \boldsymbol{e}'_m(\boldsymbol{x}) \end{pmatrix}, \qquad \boldsymbol{J}'(\boldsymbol{x}) = \begin{pmatrix} \boldsymbol{j}'_1(\boldsymbol{x}) \\ \boldsymbol{j}'_2(\boldsymbol{x}) \\ \vdots \\ \boldsymbol{j}'_m(\boldsymbol{x}) \end{pmatrix},$$

where

$$\nabla \times \boldsymbol{e}'_\alpha = 0, \qquad \nabla \cdot \boldsymbol{j}'_\alpha = 0, \quad \text{for } \alpha = 1, 2 \ldots, m.$$

The old constitutive relation (6.3), when expressed in terms of these new fields, becomes

$$\boldsymbol{J}'(\boldsymbol{x}) = \boldsymbol{\mathcal{L}}'(\boldsymbol{x})\boldsymbol{E}'(\boldsymbol{x}),$$

where

$$\boldsymbol{\mathcal{L}}'(\boldsymbol{x}) = \boldsymbol{\mathcal{W}}\boldsymbol{\mathcal{L}}(\boldsymbol{x})\boldsymbol{\mathcal{V}}^{-1}. \tag{6.7}$$

In other words, the new fields solve the coupled equations in a material with moduli $\boldsymbol{\mathcal{L}}'(\boldsymbol{x})$ given by (6.7). By taking averages over $\boldsymbol{x}$ of the relations (6.6) and using (6.4) we see that the averages of $\boldsymbol{J}'(\boldsymbol{x})$ and $\boldsymbol{E}'(\boldsymbol{x})$ are linked through the equations

$$\langle \boldsymbol{J}' \rangle = \boldsymbol{\mathcal{L}}'_* \langle \boldsymbol{E}' \rangle,$$

where

$$\boldsymbol{\mathcal{L}}'_* = \boldsymbol{\mathcal{W}}\boldsymbol{\mathcal{L}}_*\boldsymbol{\mathcal{V}}^{-1} \tag{6.8}$$

is the effective tensor of the new material. Thus the effective tensor $\boldsymbol{\mathcal{L}}_*$ undergoes exactly the same transformation as the local tensor $\boldsymbol{\mathcal{L}}(\boldsymbol{x})$.

To see the implications of this result more clearly let us consider an n-phase composite. Then the local tensor $\boldsymbol{\mathcal{L}}(\boldsymbol{x})$ takes the form

$$\boldsymbol{\mathcal{L}}(\boldsymbol{x}) = \sum_{a=1}^{n} \chi_a(\boldsymbol{x})\boldsymbol{\mathcal{L}}_a,$$

where the characteristic functions

$$\begin{aligned} \chi_a(\boldsymbol{x}) &= 1 \text{ in phase } a, \\ &= 0 \quad \text{otherwise,} \end{aligned}$$

represent the geometry of the composite. If we keep the geometry fixed and consider the effective tensor $\boldsymbol{\mathcal{L}}_*$ as a function of the tensors $\boldsymbol{\mathcal{L}}_a$, $a = 1, 2, \ldots, n$ representing the moduli of the phases, then (6.7) and (6.8) imply that this function satisfies

$$\boldsymbol{\mathcal{L}}_*(\boldsymbol{\mathcal{W}}\boldsymbol{\mathcal{L}}_1\boldsymbol{\mathcal{V}}^{-1}, \boldsymbol{\mathcal{W}}\boldsymbol{\mathcal{L}}_2\boldsymbol{\mathcal{V}}^{-1}, \ldots \boldsymbol{\mathcal{W}}\boldsymbol{\mathcal{L}}_n\boldsymbol{\mathcal{V}}^{-1}) = \boldsymbol{\mathcal{W}}\boldsymbol{\mathcal{L}}_*(\boldsymbol{\mathcal{L}}_1, \boldsymbol{\mathcal{L}}_2, \ldots \boldsymbol{\mathcal{L}}_n)\boldsymbol{\mathcal{V}}^{-1} \tag{6.9}$$

for all nonsingular matrices $\boldsymbol{\mathcal{W}}$ and $\boldsymbol{\mathcal{V}}$ of the form (6.5). This property, called covariance by Milgrom (1990) , is a generalization to coupled field problems of the homogeneity property of the effective conductivity function.

6.2. The reduction to uncoupled equations for two-phase composites with isotropic phases

These transformations have an important application when the tensor field $\mathcal{L}(\boldsymbol{x})$ is symmetric, positive-definite, and only two isotropic components are present in the composite. As Straley (1981) discovered, we can use them to reduce the coupled equations to a set of uncoupled equations. In effect this decoupling transformation simplifies the system of equations (6.1) to a set of independent conductivity problems.

The symmetry and rotational invariance (in the space indices) of the tensors $\mathcal{L}_1$ and $\mathcal{L}_2$ implies that they take the form

$$\mathcal{L}_a = \begin{pmatrix} L^a_{11}\boldsymbol{I} & L^a_{12}\boldsymbol{I} & \dots & L^a_{1m}\boldsymbol{I} \\ L^a_{12}\boldsymbol{I} & L^a_{22}\boldsymbol{I} & \dots & L^a_{2m}\boldsymbol{I} \\ \vdots & \vdots & \ddots & \vdots \\ L^a_{1m}\boldsymbol{I} & L^a_{2m}\boldsymbol{I} & \dots & L^a_{mm}\boldsymbol{I} \end{pmatrix} \quad \text{for } a = 1, 2. \tag{6.10}$$

To diagonalize these, following Milgrom and Shtrikman (1989), we select

$$\mathcal{W} = \mathcal{Q}(\mathcal{L}_2)^{-1/2}, \quad \mathcal{V}^{-1} = \mathcal{W}^T,$$

where $\mathcal{Q}$ is the orthogonal matrix (satisfying $\mathcal{Q}\mathcal{Q}^T = \boldsymbol{I}$) that diagonalizes $\mathcal{L}_2^{-1/2}\mathcal{L}_1\mathcal{L}_2^{-1/2}$. Under this transformation $\mathcal{L}_1$ and $\mathcal{L}_2$ are mapped to

$$\mathcal{L}'_1 = \begin{pmatrix} \lambda_1\boldsymbol{I} & 0 & \dots & 0 \\ 0 & \lambda_2\boldsymbol{I} & \dots & 0 \\ \vdots & \vdots & \ddots & \vdots \\ 0 & 0 & \dots & \lambda_m\boldsymbol{I} \end{pmatrix}, \quad \mathcal{L}'_2 = \begin{pmatrix} \boldsymbol{I} & 0 & \dots & 0 \\ 0 & \boldsymbol{I} & \dots & 0 \\ \vdots & \vdots & \ddots & \vdots \\ 0 & 0 & \dots & \boldsymbol{I} \end{pmatrix}.$$

So the coupling between the fields has been completely eliminated, and the equations reduce to a set of m uncoupled conductivity equations. This implies that the effective tensor $\mathcal{L}'_*$ necessarily has the form

$$\mathcal{L}'_* = \begin{pmatrix} \boldsymbol{\sigma}_*(\lambda_1) & 0 & \dots & 0 \\ 0 & \boldsymbol{\sigma}_*(\lambda_2) & \dots & 0 \\ \vdots & \vdots & \ddots & \vdots \\ 0 & 0 & \dots & \boldsymbol{\sigma}_*(\lambda_m) \end{pmatrix}, \tag{6.11}$$

where $\boldsymbol{\sigma}_*(\lambda)$ represents the effective conductivity tensor when phase 1 has conductivity tensor $\boldsymbol{\sigma}_1 = \lambda\boldsymbol{I}$ and phase 2 has conductivity tensor $\boldsymbol{\sigma}_2 = \boldsymbol{I}$. Thus if we know $\boldsymbol{\sigma}_*(\lambda)$ as a function of λ, we can determine $\mathcal{L}'_*$ and from (6.8) also determine

$$\mathcal{L}_* = (\mathcal{L}_2)^{1/2}\mathcal{Q}^T\mathcal{L}'_*\mathcal{Q}(\mathcal{L}_2)^{1/2}.$$

Milgrom and Shtrikman (1989) recognized that the original effective tensor $\mathcal{L}_*$ must satisfy some exact relations to have the form (6.11) after the transformation (6.8). In particular, because the matrices $\mathcal{L}'_1$, $\mathcal{L}'_2$, and $\mathcal{L}'_*$ commute, it follows that

$$\mathcal{L}_*(\mathcal{L}_2)^{-1}\mathcal{L}_1 - \mathcal{L}_1(\mathcal{L}_2)^{-1}\mathcal{L}_* = \mathcal{W}^{-1}[\mathcal{L}'_*(\mathcal{L}'_2)^{-1}\mathcal{L}'_1 - \mathcal{L}'_1(\mathcal{L}'_2)^{-1}\mathcal{L}'_*]\mathcal{V} = 0. \tag{6.12}$$

This gives us a set of linear relations that must be satisfied by the matrix elements of $\mathcal{L}_*$.

These exact relations can be cast in other equivalent forms. Let us assume that the microgeometry is isotropic so that $\mathcal{L}_1$, $\mathcal{L}_2$, and $\mathcal{L}_*$ all have the block structure (6.10). Then they can be represented by $m \times m$ matrices with elements L^a_{ij}, for $a = 1, 2, *$, which by an abuse of notation we also denote as $\mathcal{L}_1$, $\mathcal{L}_2$ and $\mathcal{L}_*$. Chen (1995, 1997) has shown that when the $m \times m$ matrix $(\mathcal{L}_2)^{-1}\mathcal{L}_1$ has nondegenerate eigenvalues (6.12) holds if and only if $\mathcal{L}_*$ can be expressed as the linear combination

$$\mathcal{L}_* = a_0\mathcal{L}_1 + a_1\mathcal{L}_2 + a_2\mathcal{L}_1(\mathcal{L}_2)^{-1}\mathcal{L}_1 + \cdots + a_{m-1}\mathcal{L}_1[(\mathcal{L}_2)^{-1}\mathcal{L}_1]^{m-2}, \tag{6.13}$$

where the scalar-valued coefficients $a_0, a_1, \ldots, a_{m-1}$ depend on the microgeometry and on the moduli of the tensors $\mathcal{L}_1$ and $\mathcal{L}_2$. Milgrom (1997), whose proof we now follow, rederived and generalized Chen's results, allowing for nonconsecutive powers in the expansion (6.13).

For simplicity, we will just consider the case of consecutive powers. One can easily check by substitution that (6.12) holds if $\mathcal{L}_*$ has the form (6.13). Conversely, to show that (6.12) implies (6.13) we choose a basis where the $m \times m$ matrix $\mathcal{A} = (\mathcal{L}_2)^{-1}\mathcal{L}_1$ is diagonal. Then (6.12), multiplied on the left by $(\mathcal{L}_2)^{-1}$, implies that $(\mathcal{L}_2)^{-1}\mathcal{L}_*$ is also diagonal. Setting $\mathcal{A} = \operatorname{diag}(\lambda_1, \lambda_2, \ldots, \lambda_m)$ we see that the $m \times m$ diagonal matrices $\boldsymbol{I}$, $\mathcal{A}$, $\mathcal{A}^2, \ldots, \mathcal{A}^{m-1}$ (regarded as vectors of length m) are independent because the Vandermonde determinant

$$\det \begin{vmatrix} 1 & \lambda_1 & \lambda_1^2 & \ldots & \lambda_1^{m-1} \\ 1 & \lambda_2 & \lambda_2^2 & \ldots & \lambda_2^{m-1} \\ \vdots & \vdots & \vdots & \ddots & \vdots \\ 1 & \lambda_m & \lambda_m^2 & \ldots & \lambda_m^{m-1} \end{vmatrix} = \prod_{i<j}(\lambda_j - \lambda_i)$$

is nonzero when the eigenvalues λ_i are all distinct. Therefore they form a basis for the m-dimensional space of $m \times m$ diagonal matrices. Any $m \times m$ diagonal matrix and in particular $(\mathcal{L}_2)^{-1}\mathcal{L}_*$ can be expressed as a linear combination of them, which implies (6.13). Both (6.12) and (6.13) express the fact that only m numbers are needed to determine all of the elements of the effective tensor $\mathcal{L}_*$.

When only two fields are present ($m = 2$) and the composite is isotropic, $\mathcal{L}_1$, $\mathcal{L}_2$, and $\mathcal{L}_*$ have the forms

$$\mathcal{L}_1 = \begin{pmatrix} \alpha_1\boldsymbol{I} & \beta_1\boldsymbol{I} \\ \beta_1\boldsymbol{I} & \gamma_1\boldsymbol{I} \end{pmatrix}, \quad \mathcal{L}_2 = \begin{pmatrix} \alpha_2\boldsymbol{I} & \beta_2\boldsymbol{I} \\ \beta_2\boldsymbol{I} & \gamma_2\boldsymbol{I} \end{pmatrix}, \quad \mathcal{L}_* = \begin{pmatrix} \alpha_*\boldsymbol{I} & \beta_*\boldsymbol{I} \\ \beta_*\boldsymbol{I} & \gamma_*\boldsymbol{I} \end{pmatrix}.$$

The condition (6.13) then implies that $\mathcal{L}_*$ must be a linear combination of $\mathcal{L}_1$ and $\mathcal{L}_2$. Thus the moduli must satisfy the relation

$$\det \begin{vmatrix} \alpha_* & \gamma_* & \beta_* \\ \alpha_1 & \gamma_1 & \beta_1 \\ \alpha_2 & \gamma_2 & \beta_2 \end{vmatrix} = 0 \tag{6.14}$$

of Milgrom and Shtrikman (1989).

In other words, if the diagonal elements α_* and γ_* of $\mathcal{L}_*$ have been determined through a set of experiments, then (6.14) provides a formula for obtaining the coupling β_*. [More generally, when $m \geq 3$, Milgrom (1997) has shown that (6.13) implies that any particular off-diagonal element of $\mathcal{L}_*$ can be expressed in terms of the m diagonal elements of $\mathcal{L}_*$ and the moduli of $\mathcal{L}_1$ and $\mathcal{L}_2$.] This has obvious applications to the effective thermoelectric coefficients of isotropic composites of two isotropic phases. Similar sorts of relations among piezoelectric moduli were found by Schulgasser (1992) and Benveniste (1994) for two-phase

fibrous composites and polycrystals with a columnar microstructure. Benveniste (1995b) extended these relations to the moduli of two-phase fibrous composites where one phase is piezoelectric and the other is magnetostrictive.

Associated with isotropic thermoelectric materials are two numbers (dependent on the three moduli) called the thermoelectric figure of merit and the thermoelectric power factor, which govern the performance and efficiency of practical thermoelectric devices such as heat pumps [see, for example, Harman and Honig (1967)]. Using the decoupling transformation, Bergman and Levy (1991) have shown that the thermoelectric figure of merit of any isotropic two-phase composite must be less than the thermoelectric figure of merit of at least one of the two phases. Subsequently, Bergman (1997) proved that the figure of merit in multiphase composites can never be greater than the largest figure of merit of any of the phases. His proof was based on an argument of Avellaneda and Olson (1993), who established that the largest electromechanical coupling factor of a piezoelectric composite cannot exceed the largest coupling factor of the phase with the strongest electromechanical coupling.

Also using the decoupling transformation, Bergman and Fel (1999) have shown that the thermoelectric power factor can be greater in a coated sphere assemblage than in either of the two phases. Moreover, once the definition of the thermoelectric power factor is adjusted to allow for anisotropy, they find (subject to some minor technical assumptions) that simple laminates of the two phases have the largest possible thermoelectric power factor compared to any other microstructure.

6.3. Translations for coupled equations

In section 2.5 on page 30 we already encountered the idea of translation, whereby the local conductivity or compliance tensor field undergoes a shift by a (possibly inhomogeneous) translation tensor field and the effective tensor undergoes precisely the same shift. For this property to hold the translation tensor involved in this shift cannot be arbitrary, but instead must have a special property: When applied to the field appearing on the right-hand side of the constitutive equation it must produce a field satisfying the same differential constraints as the field appearing on the left-hand side of the constitutive equation. In the context of the coupled equations (6.2) it is clear that in a three-dimensional medium any translation of the form

$$\boldsymbol{\mathcal{T}}(\boldsymbol{x}) = \begin{pmatrix} \boldsymbol{A}_{11}(\boldsymbol{x}) & \boldsymbol{A}_{12}(\boldsymbol{x}) & \dots & \boldsymbol{A}_{1m}(\boldsymbol{x}) \\ \boldsymbol{A}_{21}(\boldsymbol{x}) & \boldsymbol{A}_{22}(\boldsymbol{x}) & \dots & \boldsymbol{A}_{2m(\boldsymbol{x})} \\ \vdots & \vdots & \ddots & \vdots \\ \boldsymbol{A}_{m1}(\boldsymbol{x}) & \boldsymbol{A}_{m2}(\boldsymbol{x}) & \dots & \boldsymbol{A}_{mm}(\boldsymbol{x}) \end{pmatrix},$$

where

$$\nabla \cdot \boldsymbol{A}_{ij}(\boldsymbol{x}) = 0 \ \text{ and } \ \boldsymbol{A}_{ij}(\boldsymbol{x}) = -[\boldsymbol{A}_{ij}(\boldsymbol{x})]^T \ \text{ for all } i \text{ and } j, \tag{6.15}$$

has this property, because any divergence free antisymmetric matrix field $\boldsymbol{A}_{ij}(\boldsymbol{x})$ acting on a curl free field produces a divergence free field. Since the application of $\boldsymbol{\mathcal{T}}(\boldsymbol{x})$ to a vector of m curl free fields produces a vector of m divergence free fields, it follows that a medium with tensor

$$\boldsymbol{\mathcal{L}}'(\boldsymbol{x}) = \boldsymbol{\mathcal{L}}(\boldsymbol{x}) + \boldsymbol{\mathcal{T}}(\boldsymbol{x})$$

has an effective tensor

$$\boldsymbol{\mathcal{L}}'_* = \boldsymbol{\mathcal{L}}_* + \langle \boldsymbol{\mathcal{T}} \rangle.$$

If the tensor $\mathcal{L}$ is symmetric and we want this symmetry to be preserved under the translation, then we should choose a translation $\mathcal{T}$ that is itself symmetric, of the form

$$\mathcal{T}(\boldsymbol{x}) = \begin{pmatrix} 0 & \boldsymbol{A}_{12}(\boldsymbol{x}) & \dots & \boldsymbol{A}_{1m}(\boldsymbol{x}) \\ -\boldsymbol{A}_{12}(\boldsymbol{x}) & 0 & \dots & \boldsymbol{A}_{2m}(\boldsymbol{x}) \\ \vdots & \vdots & \ddots & \vdots \\ -\boldsymbol{A}_{1m}(\boldsymbol{x}) & -\boldsymbol{A}_{2m}(\boldsymbol{x}) & \dots & 0 \end{pmatrix},$$

where the blocks $\boldsymbol{A}_{ij}(\boldsymbol{x})$ satisfy (6.15). Sometimes such translations can be used to convert a problem where the matrix entering the constitutive law is not positive-definite to an equivalent problem where a strictly positive-definite matrix enters the constitutive law. We will see an application of this in the next section.

6.4. Elasticity as a special case of coupled field equations

Some of the preceding formulas could have been written in a more concise form by representing the fields $\boldsymbol{J}$ and $\boldsymbol{E}$ not as vectors but as $d \times m$ matrices, which respectively have the fields $\boldsymbol{j}_1, \boldsymbol{j}_2, \dots, \boldsymbol{j}_m$ and $\boldsymbol{e}_1, \boldsymbol{e}_2, \dots, \boldsymbol{e}_m$ as columns, while $\mathcal{L}(\boldsymbol{x})$ is represented as a tensor with elements $L_{i\alpha j\beta}(\boldsymbol{x})$. With this notation, the constitutive relation (6.1) governs the relation between the matrix elements $j_{i\alpha}$ of $\boldsymbol{J}(\boldsymbol{x})$ and the matrix elements $e_{j\beta}$ of $\boldsymbol{E}(\boldsymbol{x})$. The formulas (6.5) and (6.6) take the form

$$\boldsymbol{E}'(\boldsymbol{x}) = \mathcal{V}\boldsymbol{E}(\boldsymbol{x}) = \boldsymbol{E}(\boldsymbol{x})\boldsymbol{V}^T, \quad \boldsymbol{J}'(\boldsymbol{x}) = \mathcal{W}\boldsymbol{J}(\boldsymbol{x}) = \boldsymbol{J}(\boldsymbol{x})\boldsymbol{W}^T,$$

where $\boldsymbol{V}$ and $\boldsymbol{W}$ are $m \times m$ matrices with elements $v_{\alpha\beta}$ and $w_{\alpha\beta}$. Thus $\mathcal{V}$ and $\mathcal{W}$ act simply to multiply the matrix fields $\boldsymbol{E}$ and $\boldsymbol{J}$ on the right by $\boldsymbol{V}^T$ and $\boldsymbol{W}^T$. Also note that the fields $\boldsymbol{J}(\boldsymbol{x})$ and $\boldsymbol{E}(\boldsymbol{x})$ satisfy

$$\nabla \cdot \boldsymbol{J}(\boldsymbol{x}) = 0, \quad \nabla \times \boldsymbol{E}(\boldsymbol{x}) = 0, \tag{6.16}$$

where the divergence and curl act only on the first (space) index of the matrix.

By writing the elasticity equations in the form

$$\boldsymbol{\tau}(\boldsymbol{x}) = \mathcal{C}(\boldsymbol{x})\nabla\boldsymbol{u}(\boldsymbol{x}), \quad \text{where } \nabla \cdot \boldsymbol{\tau} = 0, \tag{6.17}$$

it is evident that elasticity equations are just a special case of the coupled field equations with d coupled fields, where $\boldsymbol{J}(\boldsymbol{x})$, $\boldsymbol{E}(\boldsymbol{x})$, and $\mathcal{L}(\boldsymbol{x})$ can be identified with the stress field $\boldsymbol{\tau}(\boldsymbol{x})$, displacement gradient $\nabla\boldsymbol{u}(\boldsymbol{x})$, and elasticity tensor field $\mathcal{C}(\boldsymbol{x})$, respectively. In particular, two-dimensional elasticity can be regarded as equivalent to a two-dimensional thermoelectric problem. The elasticity tensor field $\mathcal{C}(\boldsymbol{x})$, when regarded as a tensor field $\mathcal{L}(\boldsymbol{x})$ of a coupled field equation, is rather special. It is self-adjoint and positive-semidefinite rather than positive-definite, with its nullspace comprised of all antisymmetric matrices. We have

$$\mathcal{C}^T = \mathcal{C} \quad \text{and} \quad \mathcal{C}\boldsymbol{A} = 0 \text{ whenever } \boldsymbol{A}^T = -\boldsymbol{A},$$

implying that the matrix elements of $\mathcal{C}$ satisfy

$$C_{ijk\ell} = C_{k\ell ij}, \quad C_{ijk\ell} = C_{ij\ell k}, \quad C_{ijk\ell} = C_{jik\ell}.$$

Due to the last of these symmetry relations (which is a consequence of the first two), any matrix-valued field $\boldsymbol{\tau}(\boldsymbol{x})$ solving the equations (6.17) must necessarily be symmetric. Hence the symmetry of the stress field $\boldsymbol{\tau}(\boldsymbol{x})$ can be regarded as a consequence of the constitutive

relation; it is not necessary to impose it as an additional constraint on the field. (Conversely, from a physical viewpoint, the symmetry of the elasticity tensor can be regarded as being a consequence of the symmetry of the stress tensor field.)

Despite this mathematical equivalence between elasticity and coupled field problems, it is important to bear in mind that the tensors have different tensorial properties, that is, they transform differently under a rotation of the coordinate system. When the coordinate system is rotated from $\boldsymbol{x}$ to $\boldsymbol{x}' = \boldsymbol{R}\boldsymbol{x}$, where $\boldsymbol{R}$ is a rotation matrix, the matrix elements representing the coupled fields and moduli undergo the transformation

$$J_{i\alpha}(\boldsymbol{x}) \to \sum_{m=1}^{d} R_{mi} J_{m\alpha}(\boldsymbol{x}'), \quad E_{j\beta}(\boldsymbol{x}) \to \sum_{n=1}^{d} R_{nj} E_{n\beta}(\boldsymbol{x}'),$$
$$L_{i\alpha j\beta}(\boldsymbol{x}) \to \sum_{m,n=1}^{d} R_{mi} R_{nj} L_{m\alpha n\beta}(\boldsymbol{x}'),$$

whereas the matrix elements representing the elastic fields and moduli undergo the transformation

$$\tau_{ij}(\boldsymbol{x}) \to \sum_{m,n=1}^{d} R_{mi} R_{nj} \tau_{mn}(\boldsymbol{x}'), \qquad \epsilon_{k\ell}(\boldsymbol{x}) \to \sum_{o,p=1}^{d} R_{ok} R_{p\ell} \epsilon_{op}(\boldsymbol{x}'),$$
$$C_{ijk\ell}(\boldsymbol{x}) \to \sum_{m,n,o,p=1}^{d} R_{mi} R_{nj} R_{ok} R_{p\ell} C_{mnop}(\boldsymbol{x}').$$

Naturally the same transformation rules apply if we keep the coordinates fixed but globally rotate the material and the fields that it contains.

Now suppose that we are given an elasticity tensor field $\boldsymbol{\mathcal{C}}(\boldsymbol{x})$. If we change coordinates to $\boldsymbol{x}'$ and map the elasticity tensor field to the equivalent coupled field tensor $\boldsymbol{\mathcal{L}}(\boldsymbol{x})$ in these new coordinates and then change back to the original coordinates, we obtain a different coupled field problem than if we had mapped to the equivalent coupled field problem without changing coordinates. The two coupled field problems are however mathematically equivalent; their moduli are linked through a relation of the form (6.7).

Due to this difference in transformation under rotation, a two-dimensional elasticity tensor of an isotropic material does not usually map to an isotropic thermoelectric tensor, and conversely a thermoelectric tensor of an isotropic material does not usually map to an isotropic elasticity tensor. Also, a two-dimensional polycrystalline elastic material comprised of grains of a single crystal in different orientations does not correspond to a thermoelectric material constructed from a single crystal, but instead corresponds to a multiphase thermoelectric material where the number of phases is determined by the number of different grain orientations. Consequently, the correspondence between elasticity and coupled field problems is most useful when only a finite number of phases are present in the material, each with a fixed orientation.

It is possible to transform the elasticity problem into an equivalent coupled field problem where the matrix entering the constitutive law is symmetric and strictly positive-definite. To see this, let us consider three-dimensional elasticity and suppose that the elasticity tensor field is strictly positive-definite on the space of symmetric matrices, that is, there exists a constant $\alpha > 0$ such that

$$\boldsymbol{P}(\boldsymbol{x}) \cdot \boldsymbol{\mathcal{C}}(\boldsymbol{x}) \boldsymbol{P}(\boldsymbol{x}) \geq \alpha \boldsymbol{P}(\boldsymbol{x}) \cdot \boldsymbol{P}(\boldsymbol{x}),$$

for all $\boldsymbol{x}$, and for all $\boldsymbol{P}(\boldsymbol{x})$ with $\boldsymbol{P}(\boldsymbol{x}) = \boldsymbol{P}^T(\boldsymbol{x})$, where

$$\boldsymbol{P}(\boldsymbol{x}) \cdot \boldsymbol{\mathcal{C}}(\boldsymbol{x})\boldsymbol{P}(\boldsymbol{x}) \equiv \sum_{ijk\ell=1}^{d} P_{ij}(\boldsymbol{x})C_{ijk\ell}(\boldsymbol{x})P_{k\ell}(\boldsymbol{x}),$$
$$\boldsymbol{P}(\boldsymbol{x}) \cdot \boldsymbol{P}(\boldsymbol{x}) \equiv \sum_{ij} P_{ij}(\boldsymbol{x})P_{ij}(\boldsymbol{x}).$$

Now consider the following translation $\boldsymbol{\mathcal{T}}$, which acts on any matrix-valued field $\boldsymbol{P}(\boldsymbol{x})$ to produce the 3×3 matrix-valued field $\boldsymbol{P}'(\boldsymbol{x})$ with elements

$$\begin{pmatrix} P'_{11} \\ P'_{21} \\ P'_{31} \\ P'_{12} \\ P'_{22} \\ P'_{32} \\ P'_{13} \\ P'_{23} \\ P'_{33} \end{pmatrix} = \begin{pmatrix} 0 & 0 & 0 & 0 & 1 & 0 & 0 & 0 & 1 \\ 0 & 0 & 0 & -1 & 0 & 0 & 0 & 0 & 0 \\ 0 & 0 & 0 & 0 & 0 & 0 & -1 & 0 & 0 \\ 0 & -1 & 0 & 0 & 0 & 0 & 0 & 0 & 0 \\ 1 & 0 & 0 & 0 & 0 & 0 & 0 & 0 & 1 \\ 0 & 0 & 0 & 0 & 0 & 0 & 0 & -1 & 0 \\ 0 & 0 & -1 & 0 & 0 & 0 & 0 & 0 & 0 \\ 0 & 0 & 0 & 0 & 0 & -1 & 0 & 0 & 0 \\ 1 & 0 & 0 & 0 & 1 & 0 & 0 & 0 & 0 \end{pmatrix} \begin{pmatrix} P_{11} \\ P_{21} \\ P_{31} \\ P_{12} \\ P_{22} \\ P_{32} \\ P_{13} \\ P_{23} \\ P_{33} \end{pmatrix} = \begin{pmatrix} P_{22} + P_{33} \\ -P_{12} \\ -P_{13} \\ -P_{21} \\ P_{11} + P_{33} \\ -P_{23} \\ -P_{31} \\ -P_{32} \\ P_{11} + P_{22} \end{pmatrix}. \tag{6.18}$$

From this relation we see that $\boldsymbol{\mathcal{T}}$ acts on a matrix-valued field $\boldsymbol{P}(\boldsymbol{x})$ to produce the matrix-valued field

$$\boldsymbol{P}'(\boldsymbol{x}) = \boldsymbol{\mathcal{T}}\boldsymbol{P}(\boldsymbol{x}) = \boldsymbol{I}\ \mathrm{Tr}[\boldsymbol{P}(\boldsymbol{x})] - \boldsymbol{P}^T(\boldsymbol{x}),$$

implying that $\boldsymbol{\mathcal{T}}$ itself is a rotationally invariant fourth-order tensor with matrix elements

$$T_{ijk\ell} = \delta_{ij}\delta_{k\ell} - \delta_{i\ell}\delta_{jk}. \tag{6.19}$$

Moreover, because the 3×3 off-diagonal blocks of the matrix $\boldsymbol{\mathcal{T}}$ are antisymmetric matrices, it follows from the observation made in the previous section that the three columns of $\boldsymbol{P}'(\boldsymbol{x})$ will be divergence free vector fields whenever the columns of $\boldsymbol{P}(\boldsymbol{x})$ are curl free vector fields. In particular it follows that $\boldsymbol{\mathcal{T}}$ acting on the gradient of the displacement field produces a divergence free matrix-valued field

$$\boldsymbol{J}'(\boldsymbol{x}) = \boldsymbol{\mathcal{T}}\nabla\boldsymbol{u}(\boldsymbol{x}) \ \text{ satisfying } \nabla \cdot \boldsymbol{J}' = 0.$$

This can also be verified by direct computation:

$$\frac{\partial J'_{ij}(\boldsymbol{x})}{\partial x_i} = \frac{\partial}{\partial x_i}\Big[\delta_{ij}\frac{\partial u_k(\boldsymbol{x})}{\partial x_k} - \frac{\partial u_i(\boldsymbol{x})}{\partial x_j}\Big] = \frac{\partial^2 u_k(\boldsymbol{x})}{\partial x_j \partial x_k} - \frac{\partial^2 u_i(\boldsymbol{x})}{\partial x_i \partial x_j} = 0.$$

Consequently, in a medium with a coupled field tensor

$$\boldsymbol{\mathcal{L}} = \boldsymbol{\mathcal{C}} + c\boldsymbol{\mathcal{T}},$$

the differential constraints (6.16) are solved with fields

$$\boldsymbol{J}(\boldsymbol{x}) = \boldsymbol{\tau}(\boldsymbol{x}) + c\boldsymbol{J}'(\boldsymbol{x}), \quad \boldsymbol{E}(\boldsymbol{x}) = \nabla\boldsymbol{u}(\boldsymbol{x}),$$

and conversely from any solution to this coupled field problem we can generate solutions to the original elasticity problem with stress and displacement gradients

$$\boldsymbol{\tau}(\boldsymbol{x}) = \boldsymbol{J}(\boldsymbol{x}) - c\boldsymbol{\mathcal{T}}\boldsymbol{E}(\boldsymbol{x}), \quad \nabla\boldsymbol{u}(\boldsymbol{x}) = \boldsymbol{E}(\boldsymbol{x}),$$

where the symmetry of $\boldsymbol{\tau}(\boldsymbol{x})$ follows from the constitutive relation. By taking averages of these equations we see that the effective coupled field tensor is just a translation of the effective elastic tensor:

$$\boldsymbol{\mathcal{L}}_* = \boldsymbol{\mathcal{C}}_* + c\boldsymbol{\mathcal{T}}.$$

We still need to check that $\boldsymbol{\mathcal{L}}$ is self-adjoint and positive-definite, at least for some values of c. The self-adjointness of $\boldsymbol{\mathcal{L}}$ is an obvious consequence of the self-adjointness of $\boldsymbol{\mathcal{C}}$ and $\boldsymbol{\mathcal{T}}$. To examine the positive-definiteness we take an arbitrary matrix $\boldsymbol{P}$ and represent it as a sum of a hydrostatic part $p\boldsymbol{I}$ proportional to the identity matrix, a shear part $\boldsymbol{P}_s$ that is symmetric and trace free, and an antisymmetric part $\boldsymbol{P}_a$:

$$\boldsymbol{P} = p\boldsymbol{I} + \boldsymbol{P}_s + \boldsymbol{P}_a \qquad \text{with } \boldsymbol{P}_s = \boldsymbol{P}_s^T, \quad \operatorname{Tr}\boldsymbol{P}_s = 0, \quad \boldsymbol{P}_a = -\boldsymbol{P}_a^T,$$

in terms of which the quadratic form associated with $\boldsymbol{\mathcal{L}}$ is

$$\begin{aligned}\boldsymbol{P}\cdot\boldsymbol{\mathcal{L}}\boldsymbol{P} &= (p\boldsymbol{I}+\boldsymbol{P}_s)\cdot\boldsymbol{\mathcal{C}}(p\boldsymbol{I}+\boldsymbol{P}_s) + c(p\boldsymbol{I}+\boldsymbol{P}_s+\boldsymbol{P}_a)\cdot(2p\boldsymbol{I}-\boldsymbol{P}_s+\boldsymbol{P}_a)\\ &\geq \alpha(3p^2+\boldsymbol{P}_s\cdot\boldsymbol{P}_s) + c(6p^2-\boldsymbol{P}_s\cdot\boldsymbol{P}_s+\boldsymbol{P}_a\cdot\boldsymbol{P}_a)\\ &\geq 3(\alpha+2c)p^2 + (\alpha-c)\boldsymbol{P}_s\cdot\boldsymbol{P}_s + c\boldsymbol{P}_a\cdot\boldsymbol{P}_a. \qquad (6.20)\end{aligned}$$

This expression is clearly nonnegative provided c is chosen with

$$\alpha > c > 0,$$

and for such choices of c, $\boldsymbol{\mathcal{L}}$ is strictly positive-definite:

$$\boldsymbol{P}\cdot\boldsymbol{\mathcal{L}}\boldsymbol{P} \geq \alpha'(3p^2+\boldsymbol{P}_s\cdot\boldsymbol{P}_s+\boldsymbol{P}_a\cdot\boldsymbol{P}_a) = \alpha'\boldsymbol{P}\cdot\boldsymbol{P}, \quad \text{where } \alpha' \equiv \min\{c, \alpha-c\} > 0.$$

Thus we have succeeded in transforming the elasticity problem into an equivalent coupled field problem with a positive-definite tensor $\boldsymbol{\mathcal{L}}$. One consequence that follows from (6.20), with $\alpha > c > 0$, is the inequality

$$\langle\nabla\boldsymbol{u}\rangle\cdot\boldsymbol{\mathcal{L}}_*\langle\nabla\boldsymbol{u}\rangle \geq c\langle(\nabla\boldsymbol{u})_a\cdot(\nabla\boldsymbol{u})_a\rangle, \quad \text{where } (\nabla\boldsymbol{u}(\boldsymbol{x}))_a = [\nabla\boldsymbol{u}(\boldsymbol{x}) - (\nabla\boldsymbol{u}(\boldsymbol{x}))^T]/2,$$

which shows that the fluctuations in the antisymmetric part of $\nabla\boldsymbol{u}(\boldsymbol{x})$ are bounded. In the more general setting of minimizing sequences of fields, Bhattacharya (1991) has used $\boldsymbol{\mathcal{T}}$ to bound the fluctuations in the antisymmetric part of $\nabla\boldsymbol{u}(\boldsymbol{x})$ in terms of fluctuations of the symmetric part of $\nabla\boldsymbol{u}(\boldsymbol{x})$. Such bounds are called Korn-type inequalities and are important for establishing the existence of solutions to boundary value problems in elasticity; see Kondratiev and Oleinik (1988) and Oleinik, Shamaev, and Yosifian (1992) and references therein.

6.5. Equivalent coupled field problems in two dimensions

In two dimensions we can enlarge the class of equivalent problems. Specifically, because a local 90° rotation acting on a divergence free field produces a curl free field, and vice versa (see section 3.1 on page 47), we are free to add to the divergence free fields any linear combination of $\boldsymbol{R}_\perp$ acting on the curl free fields, and similarly we are free to add to the curl free

fields any linear combination of $\boldsymbol{R}_\perp$ acting on the divergence free fields. In other words, if we let $\boldsymbol{\mathcal{V}}$ and $\boldsymbol{\mathcal{W}}$ denote the $2m \times 2m$ matrices as given by (6.5), and we let $\widetilde{\boldsymbol{\mathcal{V}}}$, $\widetilde{\boldsymbol{\mathcal{W}}}$, and $\underline{\boldsymbol{R}}_\perp$ denote the $2m \times 2m$ matrices

$$\widetilde{\boldsymbol{\mathcal{V}}} = \begin{pmatrix} \tilde{v}_{11}\boldsymbol{I} & \tilde{v}_{12}\boldsymbol{I} & \dots & \tilde{v}_{1m}\boldsymbol{I} \\ \tilde{v}_{21}\boldsymbol{I} & \tilde{v}_{22}\boldsymbol{I} & \dots & \tilde{v}_{2m}\boldsymbol{I} \\ \vdots & \vdots & \ddots & \vdots \\ \tilde{v}_{m1}\boldsymbol{I} & \tilde{v}_{m2}\boldsymbol{I} & \dots & \tilde{v}_{mm}\boldsymbol{I} \end{pmatrix}, \quad \widetilde{\boldsymbol{\mathcal{W}}} = \begin{pmatrix} \tilde{w}_{11}\boldsymbol{I} & \tilde{w}_{12}\boldsymbol{I} & \dots & \tilde{w}_{1m}\boldsymbol{I} \\ \tilde{w}_{21}\boldsymbol{I} & \tilde{w}_{22}\boldsymbol{I} & \dots & \tilde{w}_{2m}\boldsymbol{I} \\ \vdots & \vdots & \ddots & \vdots \\ \tilde{w}_{m1}\boldsymbol{I} & \tilde{w}_{m2}\boldsymbol{I} & \dots & \tilde{w}_{mm}\boldsymbol{I} \end{pmatrix},$$

$$\underline{\boldsymbol{R}}_\perp = \begin{pmatrix} \boldsymbol{R}_\perp & 0 & \dots & 0 \\ 0 & \boldsymbol{R}_\perp & \dots & 0 \\ \vdots & \vdots & \ddots & \vdots \\ 0 & 0 & \dots & \boldsymbol{R}_\perp \end{pmatrix}, \quad \text{where } \boldsymbol{R}_\perp = \begin{pmatrix} 0 & 1 \\ -1 & 0 \end{pmatrix},$$

then the two sets of fields

$$\begin{aligned} \boldsymbol{E}'(\boldsymbol{x}) &= \boldsymbol{\mathcal{V}}\boldsymbol{E}(\boldsymbol{x}) + \widetilde{\boldsymbol{\mathcal{V}}}\underline{\boldsymbol{R}}_\perp \boldsymbol{J}(\boldsymbol{x}), \\ \boldsymbol{J}'(\boldsymbol{x}) &= \widetilde{\boldsymbol{\mathcal{W}}}\underline{\boldsymbol{R}}_\perp \boldsymbol{E}(\boldsymbol{x}) + \boldsymbol{\mathcal{W}}\boldsymbol{J}(\boldsymbol{x}) \end{aligned} \tag{6.21}$$

are curl free and divergence free, respectively. (The entries $\tilde{v}_{ij}$ and $\tilde{w}_{ij}$ of $\widetilde{\boldsymbol{\mathcal{V}}}$ and $\widetilde{\boldsymbol{\mathcal{W}}}$ can be arbitrary and unrelated to the entries v_{ij} and w_{ij} of $\boldsymbol{\mathcal{V}}$ and $\boldsymbol{\mathcal{W}}$.) These relations between the new fields and old fields can be rewritten as a single matrix equation:

$$\begin{pmatrix} \boldsymbol{E}' \\ \boldsymbol{J}' \end{pmatrix} = \boldsymbol{\mathcal{K}} \begin{pmatrix} \boldsymbol{E} \\ \boldsymbol{J} \end{pmatrix}, \quad \text{where } \boldsymbol{\mathcal{K}} = \begin{pmatrix} \boldsymbol{\mathcal{V}} & \widetilde{\boldsymbol{\mathcal{V}}}\underline{\boldsymbol{R}}_\perp \\ \widetilde{\boldsymbol{\mathcal{W}}}\underline{\boldsymbol{R}}_\perp & \widetilde{\boldsymbol{\mathcal{W}}} \end{pmatrix}. \tag{6.22}$$

We assume that the $4m \times 4m$ matrix $\boldsymbol{\mathcal{K}}$ entering this equation is nonsingular to ensure that the old fields can be recovered from the new fields.

Next we look for the constitutive relation between these new fields. The old constitutive relation $\boldsymbol{J}(\boldsymbol{x}) = \boldsymbol{\mathcal{L}}(\boldsymbol{x})\boldsymbol{E}(\boldsymbol{x})$ in conjunction with (6.21) implies that

$$\boldsymbol{J}'(\boldsymbol{x}) = [\boldsymbol{\mathcal{W}}\boldsymbol{\mathcal{L}}(\boldsymbol{x}) + \widetilde{\boldsymbol{\mathcal{W}}}\underline{\boldsymbol{R}}_\perp]\boldsymbol{E}(\boldsymbol{x}) = [\boldsymbol{\mathcal{W}}\boldsymbol{\mathcal{L}}(\boldsymbol{x}) + \widetilde{\boldsymbol{\mathcal{W}}}\underline{\boldsymbol{R}}_\perp][\boldsymbol{\mathcal{V}} + \widetilde{\boldsymbol{\mathcal{V}}}\underline{\boldsymbol{R}}_\perp\boldsymbol{\mathcal{L}}(\boldsymbol{x})]^{-1}\boldsymbol{E}'(\boldsymbol{x}), \tag{6.23}$$

where it has been assumed that the matrix $\boldsymbol{\mathcal{V}} + \widetilde{\boldsymbol{\mathcal{V}}}\underline{\boldsymbol{R}}_\perp\boldsymbol{\mathcal{L}}(\boldsymbol{x})$ is nonsingular for all $\boldsymbol{x}$. From (6.23) we see that the new sets of fields satisfy the constitutive relation

$$\boldsymbol{J}'(\boldsymbol{x}) = \boldsymbol{\mathcal{L}}'(\boldsymbol{x})\boldsymbol{E}'(\boldsymbol{x}),$$

in a medium with tensor

$$\boldsymbol{\mathcal{L}}'(\boldsymbol{x}) = [\boldsymbol{\mathcal{W}}\boldsymbol{\mathcal{L}}(\boldsymbol{x}) + \widetilde{\boldsymbol{\mathcal{W}}}\underline{\boldsymbol{R}}_\perp][\boldsymbol{\mathcal{V}} + \widetilde{\boldsymbol{\mathcal{V}}}\underline{\boldsymbol{R}}_\perp\boldsymbol{\mathcal{L}}(\boldsymbol{x})]^{-1}. \tag{6.24}$$

This transformation from $\boldsymbol{\mathcal{L}}(\boldsymbol{x})$ to $\boldsymbol{\mathcal{L}}'(\boldsymbol{x})$ is the generalization to coupled field problems of the fractional linear transformation (4.5).

Since the relation (6.21) between the new and old fields is linear, it immediately follows that the effective tensors in the two media are linked in the same way that the local tensor fields $\boldsymbol{\mathcal{L}}'(\boldsymbol{x})$ and $\boldsymbol{\mathcal{L}}(\boldsymbol{x})$ are linked:

$$\boldsymbol{\mathcal{L}}'_* = [\boldsymbol{\mathcal{W}}\boldsymbol{\mathcal{L}}_* + \widetilde{\boldsymbol{\mathcal{W}}}\underline{\boldsymbol{R}}_\perp][\boldsymbol{\mathcal{V}} + \widetilde{\boldsymbol{\mathcal{V}}}\underline{\boldsymbol{R}}_\perp\boldsymbol{\mathcal{L}}_*]^{-1}. \tag{6.25}$$

While this text was being written, Benveniste (1995a) independently recognized that the effective tensor $\boldsymbol{\mathcal{L}}_*$ would undergo the transformation (6.25) when the local tensor $\boldsymbol{\mathcal{L}}(\boldsymbol{x})$ underwent the transformation (6.24). He applied this result to obtain phase interchange identities for two-phase piezoelectric fibrous composites (i.e., with microgeometry independent of x_3); see also Chen (1995), who used a different approach to obtain exact results for the moduli of two-phase piezoelectric symmetric materials with columnar microstructure.

6.6. The two-dimensional equations as a system of first-order partial differential equations

The transformations (6.24) and (6.25) relating the tensor field $\boldsymbol{\mathcal{L}}'(\boldsymbol{x})$ with $\boldsymbol{\mathcal{L}}(\boldsymbol{x})$ and the effective tensor $\boldsymbol{\mathcal{L}}'_*$ with $\boldsymbol{\mathcal{L}}_*$ take an even simpler form when expressed in terms of certain matrices, known as fundamental matrices. These matrices arise when the governing equations are rewritten as a system of first-order partial differential equations for the potentials. For conductivity and related problems this form of the equations is well known; see, for example, chapter 2 of Bers (1958). The first-order form of the elasticity equations was introduced by Ingebrigtsen and Tonning (1969).

The differential constraints that $\boldsymbol{E}(\boldsymbol{x})$ is curl free and that $\boldsymbol{J}(\boldsymbol{x})$ is divergence free imply that there exist m-component potentials ϕ and ψ such that

$$\boldsymbol{E} = \nabla\phi, \quad \boldsymbol{J} = \underline{\boldsymbol{R}}_\perp \nabla\psi. \tag{6.26}$$

Substituting these expressions into the constitutive relation $\boldsymbol{J} = \boldsymbol{\mathcal{L}}\boldsymbol{E}$ gives the system of equations

$$\frac{\partial\psi}{\partial x_2} = \boldsymbol{L}^{11}\frac{\partial\phi}{\partial x_1} + \boldsymbol{L}^{12}\frac{\partial\phi}{\partial x_2},$$

$$-\frac{\partial\psi}{\partial x_1} = \boldsymbol{L}^{21}\frac{\partial\phi}{\partial x_1} + \boldsymbol{L}^{22}\frac{\partial\phi}{\partial x_2},$$

in which the $\boldsymbol{L}^{ij}$ are $m \times m$ matrices with elements

$$\{\boldsymbol{L}^{ij}(\boldsymbol{x})\}_{\alpha\beta} = L_{i\alpha j\beta}(\boldsymbol{x}).$$

Further algebraic manipulation of these equations yields a system of equations where the partial derivatives involving $\partial/\partial x_1$ are on the right-hand side, while the partial derivatives involving $\partial/\partial x_2$ are on the left-hand side:

$$\frac{\partial\boldsymbol{\eta}}{\partial x_2} = \boldsymbol{\mathcal{N}}(\boldsymbol{x})\frac{\partial\boldsymbol{\eta}}{\partial x_1}, \quad \text{where } \boldsymbol{\eta} = \begin{pmatrix}\phi\\ \psi\end{pmatrix}, \tag{6.27}$$

in which the $2m \times 2m$ matrix $\boldsymbol{\mathcal{N}}(\boldsymbol{x})$ entering this equation is given by

$$\boldsymbol{\mathcal{N}} = \begin{pmatrix} -(\boldsymbol{L}^{22})^{-1}\boldsymbol{L}^{21} & -(\boldsymbol{L}^{22})^{-1} \\ \boldsymbol{L}^{11} - \boldsymbol{L}^{12}(\boldsymbol{L}^{22})^{-1}\boldsymbol{L}^{21} & -\boldsymbol{L}^{12}(\boldsymbol{L}^{22})^{-1} \end{pmatrix}.$$

This matrix is called the fundamental matrix.

Similar manipulation of the effective equation leads to the relation

$$\langle\partial\boldsymbol{\eta}/\partial x_2\rangle = \boldsymbol{\mathcal{N}}_*\langle\partial\boldsymbol{\eta}/\partial x_1\rangle, \tag{6.28}$$

where

$$\boldsymbol{\mathcal{N}}_* = \begin{pmatrix} -(\boldsymbol{L}_*^{22})^{-1}\boldsymbol{L}_*^{21} & -(\boldsymbol{L}_*^{22})^{-1} \\ \boldsymbol{L}_*^{11} - \boldsymbol{L}_*^{12}(\boldsymbol{L}_*^{22})^{-1}\boldsymbol{L}_*^{21} & -\boldsymbol{L}_*^{12}(\boldsymbol{L}_*^{22})^{-1} \end{pmatrix}$$

is the effective fundamental matrix, in which the $\boldsymbol{L}_*^{ij}$ are $m \times m$ matrices with elements

$$\{\boldsymbol{L}_*^{ij}\}_{\alpha\beta} = L^*_{i\alpha j\beta}.$$

6.7. The covariance property of the fundamental matrix

The fields $\boldsymbol{E}'(\boldsymbol{x})$ and $\boldsymbol{J}'(\boldsymbol{x})$ defined by (6.22) being curl free and divergence free can be expressed in terms of potentials ϕ' and ψ' through the relations

$$\boldsymbol{E}' = \nabla\phi', \quad \boldsymbol{J}' = \underline{\boldsymbol{R}}_{\perp}\nabla\psi', \tag{6.29}$$

which are analogous to (6.26). By substituting (6.26) and (6.29) back into (6.22) we see that the potentials ϕ' and ψ' are related to the potentials ϕ and ψ through the equation

$$\begin{pmatrix} \phi' \\ \psi' \end{pmatrix} = \boldsymbol{\mathcal{M}} \begin{pmatrix} \phi \\ \psi \end{pmatrix}, \quad \text{where } \boldsymbol{\mathcal{M}} = \begin{pmatrix} \boldsymbol{\mathcal{V}} & -\widetilde{\boldsymbol{\mathcal{V}}} \\ \widetilde{\boldsymbol{\mathcal{W}}} & \boldsymbol{\mathcal{W}} \end{pmatrix}.$$

Hence the governing equation (6.27), when expressed in terms of the new potentials, becomes

$$\partial\boldsymbol{\eta}'/\partial x_2 = \boldsymbol{\mathcal{N}}'(\boldsymbol{x})\partial\boldsymbol{\eta}'/\partial x_1, \quad \text{where } \boldsymbol{\eta}' = \begin{pmatrix} \phi' \\ \psi' \end{pmatrix}, \tag{6.30}$$

in which the fundamental matrix is now

$$\boldsymbol{\mathcal{N}}'(\boldsymbol{x}) = \boldsymbol{\mathcal{M}}\boldsymbol{\mathcal{N}}(\boldsymbol{x})\boldsymbol{\mathcal{M}}^{-1}. \tag{6.31}$$

In other words, the fundamental matrix undergoes a similarity transformation. Similarly, the effective equation (6.28), when expressed in terms of the new potentials, becomes

$$\langle\partial\boldsymbol{\eta}'/\partial x_2\rangle = \boldsymbol{\mathcal{N}}'_*\langle\partial\boldsymbol{\eta}'/\partial x_1\rangle,$$

in which the effective fundamental matrix is now

$$\boldsymbol{\mathcal{N}}'_* = \boldsymbol{\mathcal{M}}\boldsymbol{\mathcal{N}}_*\boldsymbol{\mathcal{M}}^{-1}. \tag{6.32}$$

We are free to choose all of the matrix elements of $\boldsymbol{\mathcal{M}}$ subject only to the constraint that $\boldsymbol{\mathcal{M}}$ be kept nonsingular.

Now consider an n-phase composite where the fundamental matrix $\boldsymbol{\mathcal{N}}(\boldsymbol{x})$ takes the form

$$\boldsymbol{\mathcal{N}}(\boldsymbol{x}) = \sum_{a=1}^{n} \chi_a(\boldsymbol{x})\boldsymbol{\mathcal{N}}_a,$$

where the characteristic functions $\chi_a(\boldsymbol{x})$ represent the geometry of the composite. If we keep the geometry fixed and consider the effective fundamental matrix $\boldsymbol{\mathcal{N}}_*$ as a function of the tensors $\boldsymbol{\mathcal{N}}_a$, $a = 1, 2, \ldots, n$ representing the fundamental matrices of the phases, then (6.31) and (6.32) imply that this function satisfies the covariance relation

$$\boldsymbol{\mathcal{N}}_*(\boldsymbol{\mathcal{M}}\boldsymbol{\mathcal{N}}_1\boldsymbol{\mathcal{M}}^{-1}, \boldsymbol{\mathcal{M}}\boldsymbol{\mathcal{N}}_2\boldsymbol{\mathcal{M}}^{-1}, \ldots \boldsymbol{\mathcal{M}}\boldsymbol{\mathcal{N}}_n\boldsymbol{\mathcal{M}}^{-1}) = \boldsymbol{\mathcal{M}}\boldsymbol{\mathcal{N}}_*(\boldsymbol{\mathcal{N}}_1, \boldsymbol{\mathcal{N}}_2, \ldots \boldsymbol{\mathcal{N}}_n)\boldsymbol{\mathcal{M}}^{-1}$$

for all nonsingular choices of the $2m \times 2m$ matrix $\boldsymbol{\mathcal{M}}$. In other words, if the fundamental matrices of all of the phases undergo the same similarity transformation, then the effective fundamental matrix must also undergo this similarity transformation.

6.8. Linking special classes of antiplane and planar elasticity problems

One useful application of these transformations is to provide a link between certain planar elasticity problems and pairs of antiplane elasticity problems (Milton and Movchan 1995, 1998; Helsing, Milton, and Movchan 1997). This example is a little artificial in that it assumes a constant orientation of the phases, but it does show how the transformation can lead to unexpected connections.

Consider a simply connected, planar, locally orthotropic medium, with the axes of orthotropy aligned with the coordinate axes. The constitutive law takes the form

$$\begin{pmatrix} u_{1,1} \\ u_{2,2} \\ (u_{1,2}+u_{2,1})/\sqrt{2} \end{pmatrix} = \boldsymbol{S}\begin{pmatrix} \sigma_{11} \\ \sigma_{22} \\ \sqrt{2}\sigma_{21} \end{pmatrix}, \quad \boldsymbol{S} = \begin{pmatrix} s_1 & s_2 & 0 \\ s_2 & s_4 & 0 \\ 0 & 0 & s_6 \end{pmatrix},$$

and the equilibrium constraint $\nabla \cdot \sigma = 0$ implies that there exist stress potentials $\psi_1(\boldsymbol{x})$ and $\psi_2(\boldsymbol{x})$ such that

$$\begin{pmatrix} \sigma_{11} & \sigma_{12} \\ \sigma_{21} & \sigma_{22} \end{pmatrix} = \begin{pmatrix} \psi_{1,2} & \psi_{2,2} \\ -\psi_{1,1} & -\psi_{2,1} \end{pmatrix}.$$

We substitute these expressions back into the constitutive law and into the relation $\sigma_{12} = \sigma_{21}$, which are implied by symmetry of the stress field. Subsequent manipulating of the resulting four equations so that the terms involving derivatives with respect to x_2 appear on the left while terms involving derivatives with respect to x_1 appear on the right gives the fundamental form of the elasticity equations, $\partial\boldsymbol{\eta}/\partial x_2 = \boldsymbol{\mathcal{N}}\partial\boldsymbol{\eta}/\partial x_1$, where

$$\boldsymbol{\eta} = \begin{pmatrix} u_1 \\ u_2 \\ \psi_1 \\ \psi_2 \end{pmatrix}, \quad \boldsymbol{\mathcal{N}} = \begin{pmatrix} 0 & -1 & -2s_6 & 0 \\ s_2/s_1 & 0 & 0 & s_2^2/s_1 - s_4 \\ 1/s_1 & 0 & 0 & s_2/s_1 \\ 0 & 0 & -1 & 0 \end{pmatrix}.$$

The effective fundamental elasticity matrix $\boldsymbol{\mathcal{N}}_*$ governs the relation between the average fields, $\langle\partial\boldsymbol{\eta}/\partial x_2\rangle = \boldsymbol{\mathcal{N}}_*\langle\partial\boldsymbol{\eta}/\partial x_1\rangle$, and is related to the effective compliance matrix $\boldsymbol{S}_*$ in the same way that the fundamental elasticity matrix $\boldsymbol{\mathcal{N}}(\boldsymbol{x})$ is related to the local compliance matrix $\boldsymbol{S}(\boldsymbol{x})$.

For simplicity let us assume that the moduli are such that for all $\boldsymbol{x}$

$$\Delta(\boldsymbol{x}) = (s_2(\boldsymbol{x}) + s_6(\boldsymbol{x}))^2 - s_1(\boldsymbol{x})s_4(\boldsymbol{x}) > 0.$$

Then the eigenvalues of $\boldsymbol{\mathcal{N}}(\boldsymbol{x})$ at each point $\boldsymbol{x}$ are

$$\lambda_1 = -\lambda_2 = -i\alpha_1, \quad \lambda_3 = -\lambda_4 = -i\alpha_2,$$

where $\alpha_1(\boldsymbol{x})$ and $\alpha_2(\boldsymbol{x})$ are the two real positive roots of the polynomial

$$s_1(\boldsymbol{x})\alpha^4 - 2(s_2(\boldsymbol{x}) + s_6(\boldsymbol{x}))\alpha^2 + s_4(\boldsymbol{x}) = 0.$$

The corresponding eigenvectors are

$$\boldsymbol{v}_1 = \begin{pmatrix} -p_1 \\ i\alpha_1 p_2 \\ i\alpha_1 \\ 1 \end{pmatrix}, \ \boldsymbol{v}_2 = \begin{pmatrix} -p_1 \\ -i\alpha_1 p_2 \\ -i\alpha_1 \\ 1 \end{pmatrix}, \ \boldsymbol{v}_3^{(j)} = \begin{pmatrix} -p_2 \\ i\alpha_2 p_1 \\ i\alpha_2 \\ 1 \end{pmatrix}, \ \boldsymbol{v}_4^{(j)} = \begin{pmatrix} -p_2 \\ -i\alpha_2 p_1 \\ -i\alpha_2 \\ 1 \end{pmatrix},$$

in which

$$p_1(\boldsymbol{x}) = -s_6(\boldsymbol{x}) + \sqrt{\Delta(\boldsymbol{x})}, \qquad p_2(\boldsymbol{x}) = -s_6(\boldsymbol{x}) - \sqrt{\Delta(\boldsymbol{x})}.$$

Now suppose that p_1 and p_2 do not depend on $\boldsymbol{x}$. (This holds if and only if s_6 and Δ are both independent of $\boldsymbol{x}$.) Then $\boldsymbol{v}_1$ and $\boldsymbol{v}_2$ will span a two-dimensional space that does not depend on $\boldsymbol{x}$, and similarly $\boldsymbol{v}_3$ and $\boldsymbol{v}_4$ will span a two-dimensional space that does not depend on $\boldsymbol{x}$. Thus, with an appropriate choice of $\boldsymbol{\mathcal{M}}^{-1}$, the matrix $\boldsymbol{\mathcal{N}}'(\boldsymbol{x}) = \boldsymbol{\mathcal{M}}\boldsymbol{\mathcal{N}}(\boldsymbol{x})\boldsymbol{\mathcal{M}}^{-1}$ will be block-diagonal. Specifically, the choice

$$\boldsymbol{\mathcal{M}}^{-1} = \begin{pmatrix} -p_1 & 0 & 0 & -p_2 \\ 0 & p_2 & p_1 & 0 \\ 0 & 1 & 1 & 0 \\ 1 & 0 & 0 & 1 \end{pmatrix} \quad \text{gives} \quad \boldsymbol{\mathcal{N}}' = \begin{pmatrix} 0 & -1 & 0 & 0 \\ \alpha_1^2 & 0 & 0 & 0 \\ 0 & 0 & 0 & \alpha_2^2 \\ 0 & 0 & -1 & 0 \end{pmatrix}.$$

As a consequence, the equation $\partial\boldsymbol{\eta}'/\partial x_2 = \boldsymbol{N}'\partial\boldsymbol{\eta}'/\partial x_1$ decouples into a pair of equations that can be expressed in the forms

$$\begin{pmatrix} \partial\eta_2'/\partial x_2 \\ -\partial\eta_2'/\partial x_1 \end{pmatrix} = \boldsymbol{m}_1 \begin{pmatrix} \partial\eta_1'/\partial x_1 \\ \partial\eta_1'/\partial x_2 \end{pmatrix}, \quad \begin{pmatrix} \partial\eta_3'/\partial x_2 \\ -\partial\eta_3'/\partial x_1 \end{pmatrix} = \boldsymbol{m}_2 \begin{pmatrix} \partial\eta_4'/\partial x_1 \\ \partial\eta_4'/\partial x_2 \end{pmatrix},$$

where $\boldsymbol{m}_1(\boldsymbol{x})$ and $\boldsymbol{m}_2(\boldsymbol{x})$ are the 2×2 matrix-valued fields

$$\boldsymbol{m}_1 = \begin{pmatrix} \alpha_1^2 & 0 \\ 0 & 1 \end{pmatrix}, \quad \boldsymbol{m}_2 = \begin{pmatrix} \alpha_2^2 & 0 \\ 0 & 1 \end{pmatrix}.$$

These can be regarded as equations of antiplane elasticity in two different inhomogeneous anisotropic media, with $\boldsymbol{m}_1(\boldsymbol{x})$ and $\boldsymbol{m}_2(\boldsymbol{x})$ being the antiplane shear matrix fields of these media. In other words, when s_6 is constant and Δ is constant and positive, the original planar elasticity equations can be reduced to a pair of uncoupled antiplane elasticity equations. The uniform field argument implies that when s_6 is constant the effective compliance matrix $\boldsymbol{S}_*$ is necessarily orthotropic with its axes aligned with the coordinate axes having $s_{*6} = s_6$. From the effective antiplane shear matrices

$$\boldsymbol{m}_{*1} = \begin{pmatrix} \alpha_{*1}^2 & 0 \\ 0 & 1 \end{pmatrix}, \quad \boldsymbol{m}_{*2} = \begin{pmatrix} \alpha_{*2}^2 & 0 \\ 0 & 1 \end{pmatrix}$$

associated with $\boldsymbol{m}_1(\boldsymbol{x})$ and $\boldsymbol{m}_2(\boldsymbol{x})$ we can compute the remaining elements s_{*1}, s_{*2}, and s_{*4} of the effective compliance matrix $\boldsymbol{S}_*$ associated with $\boldsymbol{S}(\boldsymbol{x})$ by solving the three equations

$$(s_{*2} + s_{*6})^2 - s_{*1}s_{*4} = \Delta, \quad s_{*1}\alpha_{*j}^4 - 2(s_{*2} + s_{*6})\alpha_{*j}^2 + s_{*4} = 0, \quad j = 1, 2.$$

This correspondence between the moduli of the effective antiplane shear matrices and the moduli of the effective compliance tensor has been verified numerically (Helsing, Milton, and Movchan 1997). When s_6 is constant and Δ is constant and negative there is still a correspondence with antiplane elasticity. The original planar elasticity equations can then be reduced to a single viscoelastic antiplane problem, with a complex shear matrix field $\boldsymbol{m}(\boldsymbol{x})$.

6.9. Expressing the fields in each phase in terms of analytic functions†

Any potential that satisfies the two-dimensional harmonic equation can be expressed as the real part of an analytic function. In particular, the electrical potential in each isotropic phase

in a multiphase composite can be expressed as the real part of an analytic function. This representation is useful, for example, when one seeks a numerical or analytic solution of the conductivity equations. Similarly, the solutions of the elasticity equations in any two-dimensional homogeneous body can be expressed in terms of two analytic functions as noted by Muskhelishvili (1963) in the context of isotropic elasticity [see also Kolosov (1909), who introduced one of the analytic functions to solve certain elastostatic problems] and by Lekhnitskii (1968) in the context of anisotropic elasticity. Many two-dimensional elasticity problems have been solved through the use of this representation [see, for example, England (1971)]. It is well-known that the representation extends to the more general coupled equations (6.2) in two dimensions. We can express the fields in any homogeneous, possibly multiconnected, body in terms of a set of analytic functions. In particular we can express the field inside a single phase in a multiphase material in terms of a set of analytic functions.

To see this, let us assume that the fundamental matrix $\mathcal{N}$ is constant, real, and has distinct eigenvalues. Unfortunately this excludes elastically isotropic materials from consideration, but it has the advantage of simplifying the analysis. (If a set of eigenvalues are equal, then we can recover the relevant results by treating it as the limit of a sequence of problems where these eigenvalues are distinct but close.)

The eigenvalues are necessarily complex when the tensor $\mathcal{L}$ is positive-semidefinite. By eliminating the vector $\boldsymbol{v}$ from the relations

$$\mathcal{N}\begin{pmatrix}\boldsymbol{u}\\ \boldsymbol{v}\end{pmatrix}=\begin{pmatrix}-(\boldsymbol{L}^{22})^{-1}\boldsymbol{L}^{21}\boldsymbol{u}-(\boldsymbol{L}^{22})^{-1}\boldsymbol{v}\\ (\boldsymbol{L}^{11}-\boldsymbol{L}^{12}(\boldsymbol{L}^{22})^{-1}\boldsymbol{L}^{21})\boldsymbol{u}-\boldsymbol{L}^{12}(\boldsymbol{L}^{22})^{-1}\boldsymbol{v}\end{pmatrix}=\mu\begin{pmatrix}\boldsymbol{u}\\ \boldsymbol{v}\end{pmatrix},$$

defining an eigenvalue μ and an associated eigenvector, we arrive at the equation

$$[\boldsymbol{L}^{11}+\mu(\boldsymbol{L}^{12}+\boldsymbol{L}^{21})+\mu^2\boldsymbol{L}^{22}]\boldsymbol{u}=0, \tag{6.33}$$

which has a solution for $\boldsymbol{u}$ if and only if μ is a root of the characteristic polynomial

$$\det[\boldsymbol{L}^{11}+\mu(\boldsymbol{L}^{12}+\boldsymbol{L}^{21})+\mu^2\boldsymbol{L}^{22}]=0. \tag{6.34}$$

Now the positive-definiteness of the tensor $\mathcal{L}$ implies that the inequality

$$\boldsymbol{a}_1\boldsymbol{L}^{11}\boldsymbol{a}_1+\boldsymbol{a}_1\boldsymbol{L}^{12}\boldsymbol{a}_2+\boldsymbol{a}_2\boldsymbol{L}^{21}\boldsymbol{a}_1+\boldsymbol{a}_2\boldsymbol{L}^{22}\boldsymbol{a}_2>0$$

holds for all nonzero choices of the vectors $\boldsymbol{a}_1$ and $\boldsymbol{a}_2$. In particular, by setting $\boldsymbol{a}_2=\mu\boldsymbol{a}_1$ we see that the matrix entering the relation (6.34) is strictly positive-definite when μ is real, implying that μ must be complex for the equation to have a solution. Hence the eigenvalues of $\mathcal{N}$ are complex and because $\mathcal{N}$ is real they occur in complex conjugate pairs.

Since these eigenvalues by assumption are distinct, we can choose a complex-valued matrix $\mathcal{M}$ so that $\mathcal{N}'=\mathcal{M}\mathcal{N}\mathcal{M}^{-1}$ is diagonal of the form

$$\mathcal{N}'=\begin{pmatrix}\mu_1 & \dots & 0 & 0 & \dots & 0\\ \vdots & \ddots & \vdots & \vdots & \ddots & \vdots\\ 0 & \dots & \mu_m & 0 & \dots & 0\\ 0 & \dots & 0 & \overline{\mu}_1 & \dots & 0\\ \vdots & \ddots & \vdots & \vdots & \ddots & \vdots\\ 0 & \dots & 0 & 0 & \dots & \overline{\mu}_m\end{pmatrix},$$

in which $\overline{\mu}_\alpha$ is the complex conjugate of μ_α for $\alpha = 1, 2, \ldots, m$. The governing equation (6.30) now reduces to a set of $2m$ uncoupled equations:

$$\frac{\partial \phi'_\alpha}{\partial x_2} = \mu_\alpha \frac{\partial \phi'_\alpha}{\partial x_1}, \quad \frac{\partial \psi'_\alpha}{\partial x_2} = \overline{\mu}_\alpha \frac{\partial \psi'_\alpha}{\partial x_1},$$

which have the solutions

$$\phi'_\alpha = f_\alpha(x_1 + \mu_\alpha x_2), \quad \psi'_\alpha = g_\alpha(x_1 + \overline{\mu}_\alpha x_2),$$

involving m analytic functions $f_1(z), \ldots, f_m(z)$ and m analytic functions $g_1(z), \ldots, g_m(z)$.

Having established that the coupled equations in a homogeneous medium have a solution in terms of analytic functions, we can look for this solution directly without reference to the fundamental matrix. Accordingly, let us look for a solution with m curl free fields $\boldsymbol{e}_\beta(\boldsymbol{x})$ of the form

$$\boldsymbol{e}_\beta(\boldsymbol{x}) = u_\beta \nabla[f(\boldsymbol{c} \cdot \boldsymbol{x})] = u_\beta \boldsymbol{c} f'(\boldsymbol{c} \cdot \boldsymbol{x}), \tag{6.35}$$

where the amplitude factors u_β for $\beta = 1, 2, \ldots, m$ are a set of complex constants, dependent on $\boldsymbol{\mathcal{L}}$, $\boldsymbol{c} = (c_1, c_2)$ is a complex two-dimensional vector with complex numbers c_1 and c_2 as elements, f' is the derivative of the analytic function f, and

$$\boldsymbol{c} \cdot \boldsymbol{x} \equiv c_1 x_1 + c_2 x_2.$$

Notice that this scalar product does not represent the usual inner product of two complex vectors, in particular, $\boldsymbol{c} \cdot \boldsymbol{c}$ is not generally real.

From the constitutive relation (6.2) the associated current fields are

$$\boldsymbol{j}_\alpha(\boldsymbol{x}) = \sum_{\beta=1}^{m} \boldsymbol{L}_{\alpha\beta} \boldsymbol{c} u_\beta f'(\boldsymbol{c} \cdot \boldsymbol{x}).$$

Since these are divergence free, it follows that

$$\nabla \cdot \boldsymbol{j}_\alpha(\boldsymbol{x}) = \nabla \cdot [\sum_{\beta=1}^{m} \boldsymbol{L}_{\alpha\beta} \boldsymbol{c} u_\beta f'(\boldsymbol{c} \cdot \boldsymbol{x})] = \sum_{\beta=1}^{m} \boldsymbol{c} \cdot \boldsymbol{L}_{\alpha\beta} \boldsymbol{c} u_\beta f''(\boldsymbol{c} \cdot \boldsymbol{x}) = 0,$$

and this will be guaranteed provided that

$$\sum_{\beta=1}^{m} \boldsymbol{c} \cdot \boldsymbol{L}_{\alpha\beta} \boldsymbol{c} u_\beta = 0 \quad \text{for } \alpha = 1, 2, \ldots, m. \tag{6.36}$$

This gives us a set of m complex linear equations for the m complex amplitude factors u_β. The complex two-dimensional vector $\boldsymbol{c}$ should be chosen so that these equations have a nontrivial solution, that is, so that the determinant associated with the equations vanishes.

The positive-definiteness of the matrix $\boldsymbol{L}^{22}$ implies that (6.36) only has the trivial solution $u_1 = u_2 = \ldots = u_m$ when $c_1 = 0$. Therefore we can assume that c_1 is nonzero. Since we are free to multiply $\boldsymbol{c}$ by any nonzero complex number λ and in particular $\lambda = 1/c_1$ while redefining the function f to absorb the factor of $1/\lambda$, it follows that we can assume that $c_1 = 1$ without any loss of generality. Substituting

$$\boldsymbol{c} = \begin{pmatrix} 1 \\ \mu \end{pmatrix}$$

into (6.36) we obtain (6.33), which has a nontrivial solution if and only if μ is a root of the characteristic polynomial (6.34). For a given μ and $\boldsymbol{u}$ satisfying (6.33) the fields (6.35) represent a particular solution. Other choices for μ and $\boldsymbol{u}$ generate additional solutions. In particular, the pair $\overline{\mu}$ and $\overline{\boldsymbol{u}}$ will generate the solution

$$\boldsymbol{e}_\beta(\boldsymbol{x}) = \overline{u}_\beta \nabla[g(\overline{\boldsymbol{c}} \cdot \boldsymbol{x})] = \overline{u}_\beta \overline{\boldsymbol{c}} g'(\overline{\boldsymbol{c}} \cdot \boldsymbol{x}),$$

in which g is another analytic function with derivative g'. The most general solution will be a superposition of all possible solutions, which total $2m$ in number, corresponding to the $2m$ roots of the characteristic polynomial (which can be grouped into m complex conjugate pairs). If we are seeking real-valued fields, then the analytic function g associated with $\overline{\mu}$ and $\overline{\boldsymbol{u}}$ should be set equal to the analytic function f associated with μ and $\boldsymbol{u}$.

The form of the solution (6.35) closely resembles a wave solution. In particular, for the choice of analytic function $f(\boldsymbol{c} \cdot \boldsymbol{x}) = e^{i\boldsymbol{c}\cdot\boldsymbol{x}}$ the vector $\boldsymbol{c}$ can be interpreted as a complex wavevector. Accordingly, in the same way that wave solutions extend to three-dimensional problems, so too do solutions of the form (6.35) extend to three-dimensional coupled field problems. The three-dimensional complex vector $\boldsymbol{c}$ is taken so that the equations (6.36) have a solution for the m-dimensional vector $\boldsymbol{u}$.

In particular, solutions to the three-dimensional Laplace equation $\Delta\phi(\boldsymbol{x}) = 0$ can be generated in this manner. The following is a calculation that I did with François Murat, although I suspect that we were not the first. Making the substitution $\boldsymbol{L} = \boldsymbol{I}$, we see that (6.36) has a nontrivial solution when the components of the complex vector $\boldsymbol{c}$ are chosen with

$$c_1^2 + c_2^2 + c_3^2 = 0.$$

For example, we could take a real value of α between 0 and 2π and set

$$c_1 = 1, \quad c_2 = i\cos\alpha, \quad c_3 = i\sin\alpha,$$

where α is real and between 0 and 2π. Since $1/z$ is analytic for all $z \neq 0$, it follows that $1/(\boldsymbol{c} \cdot \boldsymbol{x})$ is a solution of the Laplace equation when $\boldsymbol{c} \cdot \boldsymbol{x} \neq 0$ and consequently so is

$$\phi(\boldsymbol{x}) = \int_0^{2\pi} \frac{d\alpha}{x_1 + ix_2\cos\alpha + ix_3\sin\alpha} \quad \text{for all } x_1 \neq 0.$$

To integrate this we introduce the complex variable $w = \rho e^{i\alpha}$. Then the integral becomes a contour integral

$$\begin{aligned}\phi(\boldsymbol{x}) &= \int_C \frac{dw}{iw[x_1 + ix_2(w + w^{-1})/2 + x_3(w - w^{-1})/2]} \\ &= \int_C \frac{2dw}{[ix_3 - x_2][w + i(r + x_1)/(ix_3 - x_2)][w - i(r - x_1)/(ix_3 - x_2)]}\end{aligned}$$

around the contour C representing the unit circle $|w| = 1$ in the complex w-plane, where $r = |\boldsymbol{x}|$. This integral can then be evaluated using the method of residues. Depending on the sign of x_1, either one pole or the other is inside the unit circle and we have

$$\begin{aligned}\phi(\boldsymbol{x}) &= 2\pi/r \text{ when } x_1 > 0 \\ &= -2\pi/r \text{ when } x_1 < 0.\end{aligned}$$

Thus there is a discontinuity in the potential across the plane $x_1 = 0$. On one side of the plane the potential is precisely the same as that generated from a single charge at the origin. Across

the other side the potential is the same as that generated from a single charge at the origin of the same magnitude but opposite sign. The discontinuity at the plane $x_1 = 0$ arises from the singularity of the function $1/(\boldsymbol{c} \cdot \boldsymbol{x})$ along the line $x_1 = 0, x_2 = -x_3 \tan\alpha$.

More generally, the potential in a region Ω where $\Delta\phi(\boldsymbol{x}) = 0$ can be treated as arising from source charges lying outside that region. The potential generated by each source charge can then be mimicked by a superposition of analytic functions, provided that there exists a plane which separates the source charge from the region Ω. In this way we see that analytic functions can be used to solve the three-dimensional Laplace equation in any *convex* domain. An extension of this result should have applications to boundary value problems in three-dimensional elasticity. Suppose that a convex domain contains a homogeneous anisotropic medium that does not have a closed form expression for its Green's function in real space. To generate a numerical solution one could use a superposition of a finite number of plane waves, but it would be better to use a superposition of analytic function solutions, since the wider choice of functions will allow for a better fit to the boundary data, particularly if the boundary data are almost singular.

References

Avellaneda, M. and T. Olson 1993, January. Effective medium theories and effective electromechanical coupling factors for piezoelectric composites. *Journal of Intelligent Material Systems and Structures* 4(1):82–88. {*97, 110, 163, 182*}

Benveniste, Y. 1994, October. Exact connections between polycrystal and crystal properties in two-dimensional polycrystalline aggregates. *Proceedings of the Royal Society of London. Series A, Mathematical and Physical Sciences* 447(1929):1–22. {*96, 110*}

Benveniste, Y. 1995a. Correspondence relations among equivalent classes of heterogeneous piezoelectric solids under anti-plane mechanical and in-plane electrical fields. *Journal of the Mechanics and Physics of Solids* 43(4):553–571. {*102, 110*}

Benveniste, Y. 1995b. Magnetoelectric effect in fibrous composites with piezoelectric and piezomagnetic phases. *Physical Review B (Solid State)* 51(22):16424–16427. {*97, 110*}

Bergman, D. J. 1997. Thermoelectric tensor and figure of merit for a composite medium: Some exact bounds. In *Sixteenth International Conference on Thermoelectrics: Proceedings ICT'97, August 26–29, 1977, Dresden, Germany*, pp. 401–403. Piscataway, New Jersey: IEEE Press. ISBN 0-7803-4057-4. {*97, 110*}

Bergman, D. J. and L. G. Fel 1999. Enhancement of thermoelectric power factor in composite thermoelectrics. *Journal of Applied Physics* 85(12):8205–8217. {*3, 15, 97, 110, 580, 597*}

Bergman, D. J. and O. Levy 1991, December 1. The thermoelectric properties of a composite medium. *Journal of Applied Physics* 70(11):6821–6833. {*97, 110*}

Bers, L. 1958. *Mathematical Aspects of Subsonic and Transonic Gas Dynamics*. New York / London / Sydney, Australia: John Wiley and Sons. xv + 164 pp. {*103, 110*}

Bhattacharya, K. 1991. Korn's inequality for sequences. *Proceedings of the Royal Society of London. Series A, Mathematical and Physical Sciences* 434(1891):479–484. {*101, 110*}

Chen, T. 1995. Exact moduli of phase interchange invariant composites with coupled fields. *Journal of Applied Physics* 78(12):7413–7415. {*96, 102, 110*}

Chen, T. 1997. Exact moduli and bounds of two-phase composites with coupled multifield linear responses. *Journal of the Mechanics and Physics of Solids* 45(3):385–398. {*96, 111*}

England, A. H. 1971. *Complex Variable Methods in Elasticity*. New York: Wiley-Interscience. x + 181 pp. ISBN 0-471-24160-1. {*107, 111*}

Harman, T. C. and J. M. Honig 1967. *Thermoelectric and Thermomagnetic Effects and Applications*. New York: McGraw-Hill. {*97, 111*}

Helsing, J., G. W. Milton, and A. B. Movchan 1997. Duality relations, correspondences and numerical results for planar elastic composites. *Journal of the Mechanics and Physics of Solids* 45(4):565–590. {*39, 43, 51, 53, 55, 57, 70, 72, 105, 106, 111*}

Ingebrigtsen, K. A. and A. Tonning 1969. Elastic surface waves in crystals. *Physical Review* 184(3):942–951. {*103, 111*}

Kolosov, G. V. 1909. *On One Application of the Theory of Functions of a Complex Variable to the Plane Problem of the Mathematical Theory of Elasticity*. Tartu, Estonia: Dorpat (Yuriev) University. {*107, 111*}

Kondratiev, V. A. and O. A. Oleinik 1988. Boundary value problems for a system in elasticity theory in unbounded domains. Korn inequalities. *Uspekhi Matematicheskikh Nauk = Russian Mathematical Surveys* 43(5):55–98. {*101, 111*}

Lekhnitskii, S. G. 1968. *Anisotropic Plates*. Langhorne, Pennsylvania: Gordon and Breach. xvi + 534 pp. ISBN 0-677-20670-4. {*107, 111*}

Milgrom, M. 1990. Linear response of general composite systems to many coupled fields. *Physical Review B (Solid State)* 41:12484–12494. {*94, 111*}

Milgrom, M. 1997. Some more exact results concerning multifield moduli of two-phase composites. *Journal of the Mechanics and Physics of Solids* 45(3):399–404. {*96, 111*}

Milgrom, M. and S. Shtrikman 1989. Linear response of two-phase composites with cross moduli: Exact universal relations. *Physical Review A (Atomic, Molecular, and Optical Physics)* 40:1568–1575. {*93, 95, 96, 111*}

Milton, G. W. and A. B. Movchan 1995. A correspondence between plane elasticity and the two-dimensional real and complex dielectric equations in anisotropic media. *Proceedings of the Royal Society of London. Series A, Mathematical and Physical Sciences* 450(1939):293–317. {*105, 111, 147, 156*}

Milton, G. W. and A. B. Movchan 1998. Mapping certain planar elasticity problems to antiplane ones. *European Journal of Mechanics, A, Solids.* 17(1):1–11. {*105, 111*}

Muskhelishvili, N. I. 1963. *Some Basic Problems of the Mathematical Theory of Elasticity: Fundamental Equations, Plane Theory of Elasticity, Torsion, and Bending*. Groningen, The Netherlands: P. Noordhoff. xxxi + 718 pp. {*107, 111*}

Oleinik, O. A., A. S. Shamaev, and G. A. Yosifian 1992. *Mathematical Problems in Elasticity and Homogenization*. Amsterdam: North-Holland Publishing Co. xiii + 398 pp. ISBN 0-444-88441-6. {*11, 17, 101, 111*}

Schulgasser, K. 1992. Relationships between the effective properties of transversely isotropic piezoelectric composites. *Journal of the Mechanics and Physics of Solids* 40(2): 473–479. {*96, 111*}

Straley, J. P. 1981. Thermoelectric properties of inhomogeneous materials. *Journal of Physics D: Applied Physics* 14:2101–2105. {*93, 95, 112*}

7

Assemblages of spheres, ellipsoids, and other neutral inclusions

Since the effective properties of a composite depend in a complicated way on the microstructure, it is useful to have realistic model composites for which the effective properties can be computed exactly. One such model, called the coated sphere assemblage, was introduced by Hashin (1962) as a model of a composite comprised of spherical grains of one phase embedded in a matrix of a second phase. This model and its generalizations are the subject of this chapter.

7.1. The coated sphere assemblage

Hashin (1962) found that the effective bulk modulus of the assemblage could be computed exactly for all volume fractions of the phases. Using a similar analysis, Hashin and Shtrikman (1962) found an exact expression for the effective conductivity of the assemblage. To see how their argument works, consider a coated sphere consisting of a spherical core of phase 1 of isotropic conductivity $\sigma_1 \boldsymbol{I}$ fitting snugly inside a concentric spherical shell of phase 2 of isotropic conductivity $\sigma_2 \boldsymbol{I}$, with a core radius r_c and exterior radius r_e. This coated sphere is inserted as an inclusion in an infinite matrix of conductivity $\sigma_0 \boldsymbol{I}$ within which a uniform current field flows from infinity. Suppose for the moment that $\sigma_1 > \sigma_2$. From a physical standpoint it is clear that when $\sigma_0 = \sigma_1$ the inclusion has lower conductivity than its surroundings and current will tend to flow around this obstacle. On the other hand, if $\sigma_0 = \sigma_2$, then the inclusion has higher conductivity and current will be attracted towards it. This suggests, but by no means proves, that there may be an intermediate value of σ_0 at which the current is neither attracted nor diverted around the inclusion but remains completely unperturbed in the exterior region. In other words, inserting this coated sphere into the matrix would not disturb the uniform current outside the sphere, as illustrated in figure 7.1 on the next page.

Since the equations of conductivity are local equations, we could continue to add similar coated spheres without disturbing the electric or current fields in the surrounding matrix. By adding coated spheres of various sizes ranging to the infinitesimal we could completely fill all space, aside from a set of measure zero, with a periodic assemblage of these coated spheres. In this way we obtain a two-phase composite. Each coated sphere in the assemblage is taken as a scaled version of the original prototype coated sphere, as illustrated in figure 7.2 on the following page. For simplicity, let us assume that the coated spheres do not overlap the boundary of the unit cell of periodicity. Then during the process of adding the coated spheres the flux of current and electrical potential at the boundary of the unit cell remains unaltered. Consequently, the effective conductivity does not change at any stage. At the end of the

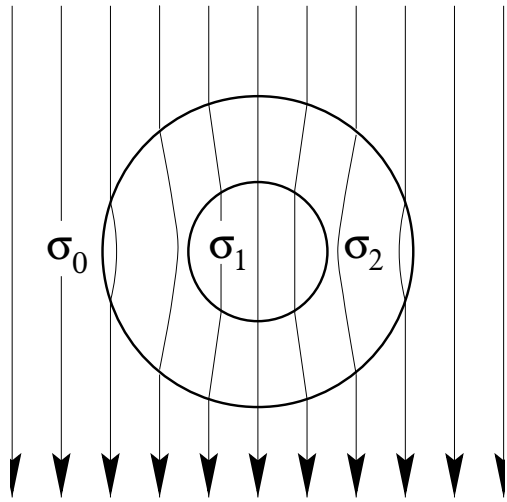

Figure 7.1. When the conductivity σ_0 of a medium is chosen appropriately one can insert a coated sphere, with core conductivity σ_1 and coating conductivity σ_2, into the medium without disturbing the surrounding uniform current field.

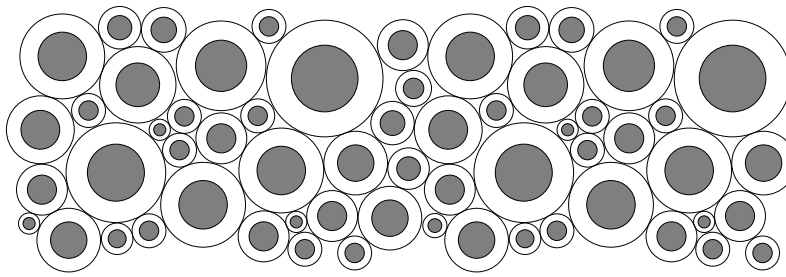

Figure 7.2. Cross section of the Hashin coated sphere assemblage. Each coated sphere is identical up to a scale factor to any other coated sphere in the assemblage. The figure is schematic in that the coated spheres should fill all space and in that the spheres are not necessarily centered on the cross-sectional plane.

construction procedure we can identify the initial conductivity $\sigma_0 \boldsymbol{I}$ with the final effective conductivity $\sigma_* \boldsymbol{I}$ of the sphere assemblage.

It remains to see if we can find this special value of $\sigma_0 = \sigma_*$. Accordingly, we consider a single coated sphere centered at the origin and look for a solution to the conductivity equations with a uniform field in the exterior region, denoted here by phase $*$, and traditionally called the effective medium. Using polar coordinates, we look for a solution with the electric potentials

$$\begin{aligned} \phi_1(\boldsymbol{x}) &= a_1 r \cos\theta \qquad \text{in the core,} \\ \phi_2(\boldsymbol{x}) &= (a_2 r + b_2/r^2)\cos\theta \quad \text{in the coating,} \\ \phi_*(\boldsymbol{x}) &= a_* r \cos\theta \quad \text{in the effective medium,} \end{aligned} \tag{7.1}$$

where $r = |\boldsymbol{x}|$ and θ measures the angle between the unit vector $\boldsymbol{v}$ representing the direction

of the applied field and $\boldsymbol{x}$. These potentials generate uniform electric and current fields

$$\begin{aligned}
\boldsymbol{e}_1 &= \nabla\phi_1 = a_1\boldsymbol{v} = a_1[\cos\theta\ \boldsymbol{v}_r - \sin\theta\ \boldsymbol{v}_\theta],\\
\boldsymbol{e}_* &= \nabla\phi_* = a_*\boldsymbol{v} = a_*[\cos\theta\ \boldsymbol{v}_r - \sin\theta\ \boldsymbol{v}_\theta],\\
\boldsymbol{j}_1 &= \sigma_1 a_1\boldsymbol{v} = \sigma_1 a_1[\cos\theta\ \boldsymbol{v}_r - \sin\theta\ \boldsymbol{v}_\theta],\\
\boldsymbol{j}_* &= \sigma_* a_*\boldsymbol{v} = \sigma_* a_*[\cos\theta\ \boldsymbol{v}_r - \sin\theta\ \boldsymbol{v}_\theta]
\end{aligned} \tag{7.2}$$

inside the core and effective medium, and a combination of uniform and dipolar fields,

$$\begin{aligned}
\boldsymbol{e}_2 &= \nabla\phi_2 = [a_2 - 2b_2/r^3]\cos\theta\ \boldsymbol{v}_r - [a_2 + b_2/r^3]\sin\theta\ \boldsymbol{v}_\theta,\\
\boldsymbol{j}_2 &= \boldsymbol{\sigma}_2\nabla\phi_2 = \sigma_2[a_2 - 2b_2/r^3]\cos\theta\ \boldsymbol{v}_r - \sigma_2[a_2 + b_2/r^3]\sin\theta\ \boldsymbol{v}_\theta
\end{aligned} \tag{7.3}$$

inside the shell, where $\boldsymbol{v}_r$ is the unit radial vector and $\boldsymbol{v}_\theta$ is the unit vector perpendicular to $\boldsymbol{v}_r$ lying in the plane containing $\boldsymbol{x}$ and $\boldsymbol{v}$, in terms of which $\boldsymbol{v} = \cos\theta\ \boldsymbol{v}_r - \sin\theta\ \boldsymbol{v}_\theta$.

Since these potentials satisfy Laplace's equation in each of the three regions, we only need to satisfy the required compatibility conditions at the interfaces. Substituting the conditions

$$a_1 = a_2 + b_2/r_c^3, \qquad a_* = a_2 + b_2/r_e^3 \tag{7.4}$$

for continuity of potential at r_c and r_e into the conditions

$$\sigma_1 a_1 = \sigma_2[a_2 - 2b_2/r_c^3], \quad \sigma_* a_* = \sigma_2[a_2 - 2b_2/r_e^3]$$

for continuity of the normal component of the flux $\boldsymbol{j}\cdot\boldsymbol{v}_r$, gives

$$\begin{aligned}
a_2 &= -b_2[\sigma_1 + 2\sigma_2]/[r_c^3(\sigma_1 - \sigma_2)] = -b_2[1 + 3\sigma_2/(\sigma_1 - \sigma_2)]/r_c^3,\\
a_2 &= -b_2[\sigma_* + 2\sigma_2]/[r_e^3(\sigma_* - \sigma_2)] = -b_2[1 + 3\sigma_2/(\sigma_* - \sigma_2)]/r_e^3.
\end{aligned} \tag{7.5}$$

Clearly these equations have a nontrivial solution for a_2 and b_2 if and only if the right-hand sides of (7.5) match, that is,

$$\frac{f_1\sigma_2}{\sigma_* - \sigma_2} = \frac{\sigma_2}{\sigma_1 - \sigma_2} + \frac{f_2}{3} \tag{7.6}$$

or, equivalently, if and only if σ_* is given by the Hashin-Shtrikman formula

$$\sigma_* = \sigma_2 + \frac{3f_1\sigma_2(\sigma_1 - \sigma_2)}{3\sigma_2 + f_2(\sigma_1 - \sigma_2)}, \tag{7.7}$$

where

$$f_1 = 1 - f_2 = r_c^3/r_e^3 \tag{7.8}$$

is the volume fraction occupied by phase 1 in the coated sphere. The remaining set of coated spheres inserted into the matrix is chosen to have the same ratio (7.8) of inner to outer radius to ensure that they too can be inserted without disturbing the field. Thus f_1 is the actual proportion of phase 1 in the resulting coated sphere assemblage and σ_* represents its effective conductivity.

It might be argued that such models are unrealistic. Clearly such periodic assemblages could never be built in practice because the construction of a single unit cell requires the addition of infinitely many coated spheres ranging to infinitesimal sizes. However, we could stop the construction process once, say, less than 1% of the effective medium remains. This remaining effective medium could then be replaced with phase 2 with typically little change

to the effective conductivity. Indeed (7.7) is easily extended to the two-dimensional case and the transverse effective conductivity σ_* of an assemblage of coated cylinders,

$$\sigma_* = \sigma_2 + \frac{2f_1\sigma_2(\sigma_1 - \sigma_2)}{2\sigma_2 + f_2(\sigma_1 - \sigma_2)}, \tag{7.9}$$

agrees remarkably well with the transverse conductivity of a hexagonal array of conducting cylinders in a conducting matrix over a wide range of volume fractions f_1 and conductivity ratios σ_1/σ_2. Such an array can be viewed as a hexagonal array of touching coated cylinders, comprised of a core of phase 1 and a coating of phase 2 surrounded by a remaining small fraction of phase 2 (occupying about 4% of the total area). The approximation (7.9) breaks down only when the ratio σ_1/σ_2 is large and the cylinders are close to touching. More accurate approximation formulas are provided by Perrins, McKenzie, and McPhedran (1979), among others.

We will see later, in sections 16.5 on page 346 and 23.1 on page 457, that the effective conductivity σ_* of any isotropic composite of phases 1 and 2 satisfies the bounds of Hashin and Shtrikman (1962):

$$\sigma_1 + \frac{df_2\sigma_1(\sigma_2 - \sigma_1)}{d\sigma_1 + f_1(\sigma_2 - \sigma_1)} \geq \sigma_* \geq \sigma_2 + \frac{df_1\sigma_2(\sigma_1 - \sigma_2)}{d\sigma_2 + f_2(\sigma_1 - \sigma_2)}, \tag{7.10}$$

where $d = 2$ or 3 is the dimensionality of the composite and it is assumed that the phases have been labeled so that $\sigma_1 > \sigma_2$. Thus the coated sphere and coated cylinder assemblages with phase 1 as core and phase 2 as coating attain the lower bound and the coated sphere, and coated cylinder assemblages with phase 2 as core and phase 1 as coating attain the upper bound. Thus they represent isotropic materials that, for fixed volume fractions f_1 and $f_2 = 1 - f_1$, have the minimum or maximum possible effective conductivity.

Following Hashin (1962) let us now find a formula for the effective bulk modulus of the coated sphere assemblage. The two components are assumed to be elastically isotropic. Again one considers a prototype coated sphere with a central core radius r_c of phase 1, with bulk and shear moduli κ_1 and μ_1, surrounded by a concentric coating radius r_e of phase 2, with bulk and shear moduli κ_2 and μ_2. The coated sphere is embedded in a stress free state in an effective medium with nonzero bulk and shear moduli κ_* and μ_*. The bulk modulus κ_* needs to be selected carefully so that there exists a solution to the elasticity equations with a purely hydrostatic constant stress field $\boldsymbol{\tau} = -p\boldsymbol{I}$ in the region outside the coated sphere. We look for a solution with a radial displacement field

$$\begin{aligned} \boldsymbol{u}_1(\boldsymbol{x}) &= (a_1 r)\boldsymbol{v}_r \qquad \text{in the core,} \\ \boldsymbol{u}_2(\boldsymbol{x}) &= (a_2 r + b_2/r^2)\boldsymbol{v}_r \qquad \text{in the coating,} \\ \boldsymbol{u}_3(\boldsymbol{x}) &= (a_3 r)\boldsymbol{v}_r \qquad \text{in the effective medium,} \end{aligned} \tag{7.11}$$

in which $\boldsymbol{v}_r$ is the unit vector in the radial direction. This displacement is simply a dilation in the core and effective medium, and consequently the stress and strain fields in these two regions are uniform and hydrostatic.

The conditions for continuity of the displacement field,

$$a_1 = a_2 + b_2/r_c^3, \qquad a_* = a_2 + b_2/r_e^3,$$

and the conditions for continuity of the radial stress $\boldsymbol{\tau} \cdot \boldsymbol{v}_r$,

$$\kappa_1 a_1 = \kappa_2 a_2 - 4\mu_2 b_2/3r_c^3, \qquad \kappa_* a_* = \kappa_2 a_2 - 4\mu_2 b_2/3r_e^3,$$

have a nonzero solution for the coefficients a_1, a_2, b_2, and a_* if and only if

$$\frac{f_1}{\kappa_* - \kappa_2} = \frac{1}{\kappa_1 - \kappa_2} + \frac{3f_2}{3\kappa_2 + 4\mu_2} \tag{7.12}$$

or, equivalently, if and only if

$$\kappa_* = \kappa_2 + \frac{f_1}{1/(\kappa_1 - \kappa_2) + f_2/(\kappa_2 + 4\mu_2/3)}. \tag{7.13}$$

Provided that the conditions (7.12) and (7.13) are fulfilled, the effective bulk modulus does not change as additional coated spheres are inserted in the effective medium. By applying the same reasoning as before we conclude that κ_* given by (7.12) or (7.13) represents the effective bulk modulus of the sphere assemblage. Prior to Hashin's work, Kerner (1956) proposed a formula equivalent to (7.13) as an approximation to the effective bulk modulus of a suspension of spherical inclusions of phase 1 in a matrix of phase 2.

Hashin (1985) has shown that these arguments apply even when the phases are nonlinear and the assemblage undergoes a finite elastic deformation under hydrostatic compression. The key point is the symmetry of the problem. Under hydrostatic compression each coated sphere remains spherical, and each will deform in proportion to its size. Therefore the deformation of the assemblage can be obtained from the deformation of a single coated sphere, which is easy to calculate numerically.

7.2. Multicoated sphere assemblages

It is clear from (7.2) that the field inside the core region of each coated sphere is uniform. Accordingly, we can treat it as an effective medium into which other families of coated spheres could be inserted. For example, suppose that we have three isotropic phases with conductivity tensors σ_1, σ_2, and σ_3. A coated sphere with a core of phase 1 of radius r_c and coating of phase 2 of radius r_e can, according to (7.7), be inserted into an effective medium of conductivity

$$\sigma_0 = \sigma_2 + \frac{3p_1\sigma_2}{p_2 - 3\sigma_2/(\sigma_2 - \sigma_1)}, \tag{7.14}$$

where $p_1 = 1 - p_2 = r_c^3/r_e^3$. Now consider an assemblage built from coated spheres each consisting of a core of the effective medium σ_0 surrounded by an outer shell of phase 3. According to (7.7), this assemblage has effective conductivity

$$\sigma_* = \sigma_3 + \frac{3(1 - f_3)\sigma_3}{f_3 - 3\sigma_3/(\sigma_3 - \sigma_0)}, \tag{7.15}$$

where f_3 is the volume fraction of component 3.

Now we can replace the cores of material 0 with coated spheres of phase 1 surrounded by phase 2. The easiest way to do this is to replace each core entirely by a single coated sphere, thereby generating a space filling assemblage of doubly coated spheres, as illustrated in figure 7.3 on the next page, each consisting of a core of phase 1 surrounded by a coating of phase 2 that is in turn surrounded by a coating of phase 3. By substituting (7.15) into (7.14)

we see that this doubly coated sphere assemblage has conductivity

$$\sigma_* = \sigma_3 + \cfrac{3(1-f_3)\sigma_3}{f_3 - \cfrac{3\sigma_3}{\sigma_3 - \sigma_2 - \cfrac{3f_1\sigma_2}{f_2 - \cfrac{3(1-f_3)\sigma_2}{\sigma_2 - \sigma_1}}}}, \tag{7.16}$$

where $f_1 = p_1(1-f_3)$, $f_2 = p_2(1-f_3)$, and f_3 are the volume fractions of the three phases in the composite. By repeating this construction procedure one can generate continued fraction expressions for the conductivity of assemblages of multicoated spheres (or cylinders) with an arbitrary number of coatings. The idea of considering multicoated sphere or cylinder assemblages is a natural one. It was proposed by Schulgasser (1977); see also Milton (1981a, 1981b), Lurie and Cherkaev (1985), and Milgrom (1989) among other papers.

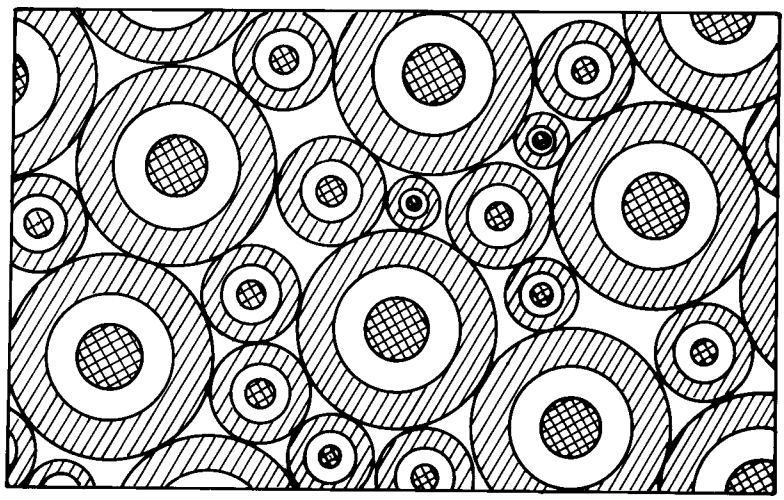

Figure 7.3. Cross section of the doubly coated sphere assemblage for a three-component material. The doubly coated spheres should be densely packed and so fill all space. Reprinted with permission from Milton (1981b). Copyright 1981, Springer-Verlag.

7.3. A phase interchange identity and inequality

For two-phase assemblages of multicoated spheres each with a core of phase 1 (or phase 2) surrounded by successive shells alternating between phase 1 and phase 2, the effective conductivity satisfies the phase interchange identity

$$\frac{\sigma_*(\sigma_1,\sigma_2)\sigma_*(\sigma_2,\sigma_1)}{\sigma_1\sigma_2} + \frac{\sigma_*(\sigma_1,\sigma_2)+\sigma_*(\sigma_2,\sigma_1)}{\sigma_1+\sigma_2} = 2, \tag{7.17}$$

which relates the effective conductivity $\sigma_*(\sigma_1,\sigma_2)$ of the assemblage to the effective conductivity $\sigma_*(\sigma_2,\sigma_1)$ when the phases are interchanged while keeping the microgeometry fixed. This is proved by induction (Milton 1981a).

We assume that (7.17) is satisfied for an assemblage of spheres with m coatings ; This is certainly true when $m = 0$, since then the assemblage consists purely of phase 1 or phase 2, and $\sigma_*(\sigma_1, \sigma_2)$ equals σ_1 or σ_2. Let $\sigma_0(\sigma_1, \sigma_2)$ denote its effective conductivity and suppose that we now coat each multicoated sphere in this assemblage with phase 2 to form an assemblage with effective conductivity $\sigma_*(\sigma_1, \sigma_2)$. The key step is to rewrite (7.17) applied to $\sigma_0(\sigma_1, \sigma_2)$ in the equivalent form

$$\frac{\sigma_2(2\sigma_1 + \sigma_2)}{\sigma_2 - \sigma_0(\sigma_1, \sigma_2)} + \frac{\sigma_1(2\sigma_2 + \sigma_1)}{\sigma_1 - \sigma_0(\sigma_2, \sigma_1)} = \sigma_1 + \sigma_2. \tag{7.18}$$

Now from our formula (7.6) for the effective tensor of a coated sphere assemblage we have

$$\frac{\sigma_2}{\sigma_2 - \sigma_0(\sigma_1, \sigma_2)} = \frac{p_1\sigma_2}{\sigma_2 - \sigma_*(\sigma_1, \sigma_2)} + \frac{p_2}{3}, \tag{7.19}$$

where $p_1 = 1 - p_2$ is the volume fraction occupied by the last coating in the composite.

Interchanging the roles of σ_1 and σ_2 in this expression gives

$$\frac{\sigma_1}{\sigma_1 - \sigma_0(\sigma_2, \sigma_1)} = \frac{p_1\sigma_1}{\sigma_1 - \sigma_*(\sigma_2, \sigma_1)} + \frac{p_2}{3}. \tag{7.20}$$

A direct substitution of (7.19) and (7.20) into (7.18) produces

$$\frac{\sigma_2(2\sigma_1 + \sigma_2)}{\sigma_2 - \sigma_*(\sigma_1, \sigma_2)} + \frac{\sigma_1(2\sigma_2 + \sigma_1)}{\sigma_1 - \sigma_*(\sigma_2, \sigma_1)} = \sigma_1 + \sigma_2,$$

thereby verifying that $\sigma_*(\sigma_1, \sigma_2)$ satisfies (7.17). Coating with phase 1 instead of phase 2 would have produced the same result because (7.18) is symmetric with respect to σ_1 and σ_2. Hence an assemblage with $m + 1$ coatings satisfies (7.17) and by induction the phase interchange relation must be true for assemblages with arbitrarily many coatings.

In particular, if the multicoated sphere is built from infinitesimally thin, equally spaced concentric layers, alternating between phase 1 and phase 2, then the function $\sigma_*(\sigma_1, \sigma_2)$ is symmetric in its arguments,

$$\sigma_*(\sigma_2, \sigma_1) = \sigma_*(\sigma_1, \sigma_2), \tag{7.21}$$

and by substituting this into (7.17) we obtain the formula of Schulgasser (1983),

$$\sigma_* = \frac{\sqrt{2\sigma_1\sigma_2(\sigma_1 + \sigma_2)^2 + \sigma_1^2\sigma_2^2} \; - \; \sigma_1\sigma_2}{\sigma_1 + \sigma_2}, \tag{7.22}$$

for the conductivity of this phase interchange invariant sphere assemblage. Unlike the formula (3.9), which implies that $\sqrt{\sigma_1\sigma_2}$ is the effective conductivity of any isotropic two-dimensional symmetric material (such as a checkerboard), (7.17) is not universally valid for isotropic three-dimensional symmetric materials. For example, if the symmetric material is biconnected (like a porous conducting rock filled with conducting fluid), then both $\sigma_*(\sigma_1, \sigma_2)$ and $\sigma_*(\sigma_2, \sigma_1)$ become asymptotically proportional to σ_1 in the limit as σ_1 tends to infinity, with σ_2 held fixed, and in this limit the left-hand side of (7.17) is proportional to σ_1/σ_2 and so is clearly greater than the right-hand side.

In fact, it has been established that the inequality

$$\frac{\sigma_*(\sigma_1, \sigma_2)\sigma_*(\sigma_2, \sigma_1)}{\sigma_1\sigma_2} + \frac{\sigma_*(\sigma_1, \sigma_2) + \sigma_*(\sigma_2, \sigma_1)}{\sigma_1 + \sigma_2} \geq 2 \tag{7.23}$$

is universally valid for two-phase materials with isotropic components and isotropic effective conductivity tensors. This phase interchange inequality was first conjectured by Milton (1981a). Avellaneda, Cherkaev, Lurie, and Milton (1988) proposed a proof, but there was an error in the published analysis [following equation (138)]. This error was corrected by Nesi (1991), who also derived interchange inequalities for multiphase media, and by Zhikov (1991). It follows from (7.23) and (7.21) that if the material is phase interchange invariant (like a three-dimensional checkerboard), then

$$\sigma_* \geq \frac{\sqrt{2\sigma_1\sigma_2(\sigma_1+\sigma_2)^2+\sigma_1^2\sigma_2^2}\ -\ \sigma_1\sigma_2}{\sigma_1+\sigma_2}, \tag{7.24}$$

with equality holding for the phase interchange invariant sphere assemblage.

Another phase interchange inequality that is universally valid for two-phase materials with isotropic components and isotropic effective conductivity tensors is the inequality of Schulgasser (1976),

$$\sigma_*(\sigma_1,\sigma_2)\sigma_*(\sigma_2,\sigma_1) \geq 1.$$

This turns out to be weaker than the inequality (7.23), given that $\sigma_*(\sigma_1,\sigma_2)$ satisfies the Hashin-Shtrikman bounds (7.10).

7.4. Assemblages of spheres with varying radial and tangential conductivity

Since we are able to find the effective conductivity of multicoated spheres with arbitrarily many coatings, it must naturally be possible to solve for the effective conductivity when the conductivity varies smoothly with the radius. Consider a radially symmetric spherical inclusion with radial conductivity $\lambda_n(r)$, tangential conductivity $\lambda_t(r)$, and exterior radius r_e. We want to find an effective medium with constant conductivity σ_* chosen so that inserting the spherical inclusion does not disturb a uniform field outside the inclusion.

The solution (7.1) suggests that we should try a potential of the form

$$\begin{aligned}\phi(\boldsymbol{x}) &= \varphi(r)r\cos\theta, \quad \text{for } r \leq r_e,\\ &= \varphi(r_e)r\cos\theta, \quad \text{for } r > r_e.\end{aligned} \tag{7.25}$$

We could of course absorb the factor r into $\varphi(r)$ but it is helpful, for later comparison with the results for ellipsoidal assemblages, to write the potential in the form (7.25). This potential generates an electric field

$$\begin{aligned}\boldsymbol{e} &= \nabla\phi = \frac{d}{dr}\Big(r\varphi(r)\Big)\cos\theta\ \boldsymbol{v}_r - \varphi(r)\sin\theta\ \boldsymbol{v}_\theta, \quad \text{for } r < r_e,\\ &= \varphi(r_e)[\cos\theta\ \boldsymbol{v}_r - \sin\theta\ \boldsymbol{v}_\theta], \quad \text{for } r > r_e,\end{aligned}$$

and a current field

$$\begin{aligned}\boldsymbol{j} &= \boldsymbol{\sigma}\nabla\phi = \lambda_n(r)\frac{d}{dr}\Big(r\varphi(r)\Big)\cos\theta\ \boldsymbol{v}_r - \lambda_t(r)\varphi(r)\sin\theta\ \boldsymbol{v}_\theta, \quad \text{for } r < r_e,\\ &= \varphi(r_e)[\lambda_n(r)\cos\theta\ \boldsymbol{v}_r - \lambda_t(r)\sin\theta\ \boldsymbol{v}_\theta], \quad \text{for } r > r_e,\end{aligned}$$

which has divergence

$$\begin{aligned}\nabla\cdot\boldsymbol{\sigma}\nabla\phi &= \left\{\frac{1}{r^2}\frac{d}{dr}\Big[r^2\lambda_n(r)\frac{d}{dr}\Big(r\varphi(r)\Big)\Big] - 2\frac{\lambda_t(r)\varphi(r)}{r}\right\}\cos\theta, \quad \text{for } r < r_e,\\ &= 0, \quad \text{for } r > r_e.\end{aligned}$$

Setting the divergence of the current to zero inside the sphere gives the second-order differential equation

$$\frac{d}{dr}\Big[r^2\lambda_n(r)\frac{d}{dr}\Big(r\varphi(r)\Big)\Big] = 2r\lambda_t(r)\varphi(r) \tag{7.26}$$

for $\varphi(r)$. Also, continuity of the normal component of the flux $\boldsymbol{j}\cdot\boldsymbol{v}_r$ through the exterior surface of the sphere implies that

$$\sigma_*\varphi(r_e) = \lambda_n(r_e)\Big[\frac{d}{dr}\Big(r\varphi(r)\Big)\Big]_{r=r_e}. \tag{7.27}$$

Now let us introduce for $r \le r_e$ the function

$$\sigma_*(r) \equiv \frac{\lambda_n(r)}{\varphi(r)}\frac{d}{dr}\Big(r\varphi(r)\Big), \tag{7.28}$$

which according to (7.27) represents the effective conductivity of an assemblage of spherical inclusions the prototype of which is formed by removing all material outside the radius r from the original sphere of radius r_e; all of the other spherical inclusions in the assemblage are scaled versions of this prototype. From the definition (7.28) of $\sigma_*(r)$ we have

$$\begin{aligned}\frac{d}{dr}\Big[r^2\lambda_n(r)\frac{d}{dr}\Big(r\varphi(r)\Big)\Big] &= r\varphi(r)\frac{d}{dr}\Big[r\sigma_*(r)\Big] + r\sigma_*(r)\frac{d}{dr}\Big(r\varphi(r)\Big)\\ &= r\varphi(r)\frac{d}{dr}\Big[r\sigma_*(r)\Big] + r\varphi(r)\frac{[\sigma_*(r)]^2}{\lambda_n(r)}.\end{aligned}$$

By substituting this into (7.26) and canceling out the common factor of $\varphi(r)$ we see that $\sigma_*(r)$ solves the Ricatti equation

$$\frac{d}{dr}\Big[r\sigma_*(r)\Big] + \frac{[\sigma_*(r)]^2}{\lambda_n(r)} = 2\lambda_t(r),$$

which is the continuum analog of the continued fraction expansion (7.16). Once the function $\sigma_*(r)$ has been found we can recover the potential $\varphi(r)$ from the formula

$$\log[r\varphi(r)] = \log[r_e\varphi(r_e)] - \int_r^{r_e} dr'\frac{\sigma_*(r')}{\lambda_n(r')},$$

implied by (7.28). This result, that $\sigma_*(r)$ satisfies a Ricatti equation, is due to Luc Tartar (private communication).

7.5. The conductivity of Schulgasser's sphere assemblage

The second-order differential equation (7.26) can be explicitly solved when $\lambda_n(r)$ and $\lambda_t(r)$ are constants independent of r. Physically this means that the spherical inclusion is formed from a single uniaxial crystal phase with the crystal axis directed radially outward, as illustrated in figure 7.4 on the following page. This polycrystalline composite is called a Schulgasser sphere assemblage because it was Schulgasser (1983) who realized that an exact expression could be obtained for its effective conductivity. Suppose that we set $\lambda_n(r) = \lambda_1$ and $\lambda_t(r) = \lambda_2$, where λ_1 and λ_2 denote the axial and transverse conductivity of the crystal phase. If we look for a solution of the form

$$\varphi(r) = r^{\alpha-1},$$

then (7.26) will be satisfied provided α is a root of the quadratic

$$\alpha^2\lambda_1 + \alpha\lambda_1 - 2\lambda_2 = 0. \tag{7.29}$$

Only the solution

$$\alpha = \tfrac{1}{2}[-1 + \sqrt{1 + 8(\lambda_2/\lambda_1)}\,]$$

gives an associated electric field that is square integrable. The effective conductivity is, from (7.27),

$$\sigma_* = \frac{\lambda_1}{\varphi(r_e)}\left[\frac{d}{dr}\Big(r\varphi(r)\Big)\right]_{r=r_e} = \alpha\lambda_1 = \frac{\lambda_1}{2}\Big[-1 + \sqrt{1 + 8(\lambda_2/\lambda_1)}\,\Big]. \tag{7.30}$$

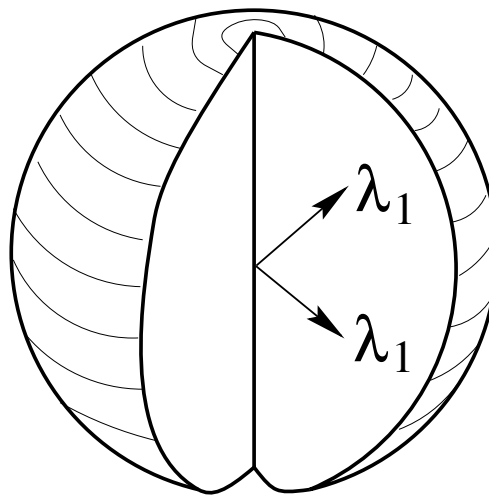

Figure 7.4. The prototype sphere in the Schulgasser sphere assemblage. The sphere has conductivity λ_1 in the radial direction and conductivity λ_2 in the tangential direction. When various sized spheres of this type are packed to fill all space the resulting composite has effective conductivity given by (7.30).

Following Schulgasser (1983) we can use this result as a check on the formula (7.22) for the effective conductivity of the phase interchange invariant sphere assemblage. In this material the concentric layers in each sphere are finely spaced, and we can homogenize the conductivity equations on an intermediate length scale with no change to the overall effective conductivity of the assemblage. In other words, the microstructure of the phase invariant sphere assemblage can be replaced locally by a uniaxial radially oriented crystalline material with radial and tangential conductivities

$$\lambda_1 = 2\sigma_1\sigma_2/(\sigma_1 + \sigma_2), \quad \lambda_2 = (\sigma_1 + \sigma_2)/2, \tag{7.31}$$

given by the lamination formula applied at volume fraction $f_1 = f_2 = 0.5$. By a simple substitution of (7.31) into (7.30) we recover the formula (7.22). We will see in section 24.8 on page 510 that the Schulgasser sphere assemblage has the lowest effective conductivity amongst all isotropic polycrystalline microgeometries. When $\lambda_2 > \lambda_1$ we can also derive this

result from the phase interchange inequality (7.23). Given any periodic isotropic microgeometry we replace each crystal grain by a laminate with finely spaced layers of equal proportions of two isotropic materials. The conductivities

$$\sigma_1 = \lambda_2 + \sqrt{\lambda_2^2 - \lambda_1\lambda_2}, \quad \sigma_2 = \lambda_2 - \sqrt{\lambda_2^2 - \lambda_1\lambda_2},$$

of these isotropic materials are chosen so that (7.31) is satisfied. Since the resulting composite is a symmetric material, $\sigma_*(\sigma_2, \sigma_1) = \sigma_*(\sigma_2, \sigma_1)$ and equation (7.23) implies the bound

$$\sigma_* \geq -\sigma_1\sigma_2/(\sigma_1 + \sigma_2) + \sqrt{[\sigma_1\sigma_2/(\sigma_1 + \sigma_2)]^2 + 2\sigma_1\sigma_2} = \frac{\lambda_1}{2}\Big[-1 + \sqrt{1 + 8(\lambda_2/\lambda_1)}\,\Big].$$

This establishes that the conductivity of the given microgeometry is greater than or equal to the conductivity of the Schulgasser sphere assemblage.

7.6. The conductivity of an assemblage of spheres with an isotropic core and polycrystalline coating

Let us extend Schulgasser's model slightly and allow a spherical isotropic core of conductivity σ_0 and radius r_c positioned at the center of the inclusion. In other words, we assume that the radial and tangential conductivity functions have the forms

$$\lambda_n(r) = \lambda_t(r) = \sigma_0 \ \text{ for } r < r_c, \qquad \lambda_n(r) = \lambda_1 \ \text{ and } \ \lambda_t(r) = \lambda_2 \ \text{ for } r_c < r < r_e.$$

Then inside the core and polycrystalline phase (7.26) is solved by

$$\begin{aligned} \varphi(r) &= a_1 && \text{for } r < r_c, \\ &= c_1 r^{\alpha_1 - 1} + c_2 r^{\alpha_2 - 1} && \text{for } r_c < r < r_e, \end{aligned}$$

where

$$\alpha_1 = \tfrac{1}{2}[-1 + \sqrt{1 + 8(\lambda_2/\lambda_1)}\,], \quad \alpha_2 = \tfrac{1}{2}[-1 - \sqrt{1 + 8(\lambda_2/\lambda_1)}\,]$$

are the roots of (7.29). The equations of continuity of radial flux and potential at r_c and r_e,

$$\begin{aligned} \lambda_1[c_1\alpha_1 r_c^{\alpha_1 - 1} + c_2\alpha_2 r_c^{\alpha_2 - 1}] &= \sigma_0 a_1 = \sigma_0[c_1 r_c^{\alpha_1 - 1} + c_2 r_c^{\alpha_2 - 1}], \\ \lambda_1[c_1\alpha_1 r_e^{\alpha_1 - 1} + c_2\alpha_2 r_e^{\alpha_2 - 1}] &= \sigma_*[c_1 r_e^{\alpha_1 - 1} + c_2 r_e^{\alpha_2 - 1}], \end{aligned}$$

imply that

$$\sigma_* = \alpha_1\lambda_1 + \frac{3Kf_0^K\lambda_1(\sigma_0 - \alpha_1\lambda_1)}{3K\lambda_1 + (\sigma_0 - \alpha_1\lambda_1)(1 - f_0^K)}, \tag{7.32}$$

where $f_0 = r_c^3/r_e^3$ is the volume fraction occupied by the core of phase 0 material and

$$K = \tfrac{1}{3}(\alpha_1 - \alpha_2) = \tfrac{1}{3}\sqrt{1 + 8(\lambda_2/\lambda_1)}. \tag{7.33}$$

When $\lambda_1 = \lambda_2 = \sigma_2$ we have $\alpha_1 = 1, \alpha_2 = 1 - d$, and $K = 1$, and so (7.32) reduces to the formula (7.7) for the conductivity of a coated sphere assemblage of two isotropic phases.

This example illustrates that the dependence of σ_* on the volume fraction f_0 need not be linear in the limit where f_0 is small. Indeed we see from (7.32) that the correction to σ_* due to the presence of a small fraction $f_0 \ll 1$ of core material is of order f_0^K. This has a simple physical interpretation. When $\lambda_1 \gg \lambda_2$ current prefers to flow toward the center of each sphere

and accordingly σ_* has a strong dependence on σ_0, whereas when $\lambda_1 \ll \lambda_2$ it is difficult for current to penetrate into the coated sphere because of the high resistivity in the radial direction and accordingly σ_* has a weak dependence on σ_0. These field concentration effects become more pronounced as the volume fraction of the core decreases, and this accounts for the f_0^K algebraic dependence of the correction to σ_* on f_0. When the core material is absent ($f_0 = 0$) the fields $\boldsymbol{e}(\boldsymbol{x})$ and $\boldsymbol{j}(\boldsymbol{x})$ become singular at the sphere center and either grow to infinity or damp to zero, depending on whether the ratio λ_1/λ_2 is greater or less than 1.

There is an obvious analogous microgeometry in two dimensions with effective conductivity

$$\sigma_* = \sqrt{\lambda_1\lambda_2} + \frac{2Kf_0^K\lambda_1(\sigma_0 - \sqrt{\lambda_1\lambda_2})}{2K\lambda_1 + (\sigma_0 - \sqrt{\lambda_1\lambda_2})(1 - f_0^K)}, \quad \text{where } K = \sqrt{\lambda_2/\lambda_1}. \tag{7.34}$$

Nesi (1996) has shown that this expression is in fact the lowest possible effective conductivity amongst all two-dimensional isotropic composites obtained by mixing a polycrystalline material with principal conductivities λ_1 and $\lambda_2 > \lambda_1$ with a proportion f_0 of isotropic material with conductivity $\sigma_0 \geq \sqrt{\lambda_1\lambda_2}$ (see section 23.8 on page 480).

One can generalize the two-dimensional Schulgasser model and allow the conductivity tensor in each circular inclusion to have a radially varying antisymmetric part. Avellaneda (1991) used such models for studying convection enhanced diffusion.

7.7. Assemblages of ellipsoids and their associated Ricatti equations†

Most of the above treatment can be generalized to assemblages of ellipsoids. I first introduced assemblages of coated elliptical cylinders in a paper originally submitted to *Nature* and later published in *Applied Physics Letters* (Milton 1980). Figure 7.5 on the next page shows an example of such an assemblage. The following analysis is based on some unpublished notes that I wrote in early 1980 while analyzing the conductivity of coated ellipsoidal assemblages of arbitrary eccentricity [the results of which were published in Milton (1981a)].

We need to introduce ellipsoidal coordinates ρ, μ, and ν, which are defined implicitly [see, for example, Kellogg (1953)] as the solution to the set of equations

$$\begin{aligned}
\frac{x_1^2}{c_1^2+\rho} + \frac{x_2^2}{c_2^2+\rho} + \frac{x_3^2}{c_3^2+\rho} &= 1 \quad \text{(confocal ellipsoids)},\\
\frac{x_1^2}{c_1^2+\mu} + \frac{x_2^2}{c_2^2+\mu} + \frac{x_3^2}{c_3^2+\mu} &= 1 \quad \text{(hyperboloids of one sheet)},\\
\frac{x_1^2}{c_1^2+\nu} + \frac{x_2^2}{c_2^2+\nu} + \frac{x_3^2}{c_3^2+\nu} &= 1 \quad \text{(hyperboloids of two sheets)},
\end{aligned} \tag{7.35}$$

subject to the restrictions

$$\rho > -c_1^2 > \mu > -c_2^2 > \nu > -c_3^2,$$

where c_1, c_2, and c_3 are fixed positive constants that determine the coordinate system. These equations can be solved explicitly for the Cartesian coordinates in terms of the ellipsoidal coordinates. For all permutations j, k, ℓ of 1, 2, 3 we have

$$x_j^2 = \frac{(c_j^2+\rho)(c_j^2+\mu)(c_j^2+\nu)}{(c_j^2-c_k^2)(c_j^2-c_\ell^2)}.$$

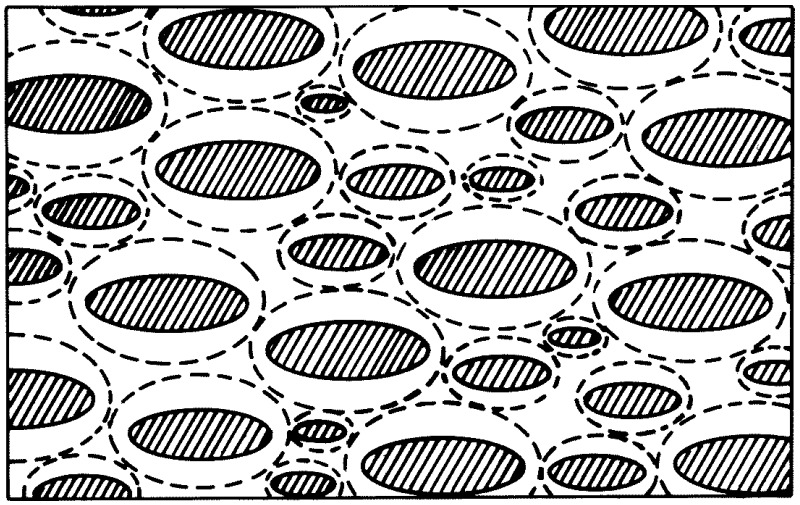

Figure 7.5. Cross section of the coated elliptical cylinder assemblage. The inner and outer boundaries of each coated ellipse are confocal and all are identical apart from a scale factor. Reprinted with permission from Milton (1981a). Copyright 1981, American Institute of Physics.

The coordinate ρ plays the role that the radius plays in spherical coordinates.

Our prototype ellipsoid is defined by the region $\rho < \rho_e$. Within the ellipsoid the conductivity depends only on the coordinate ρ but may take different values $\lambda_n(\rho)$ and $\lambda_t(\rho)$ in the directions normal and tangential to the elliptical surfaces of constant ρ. The ellipsoid is embedded in a medium with isotropic conductivity tensor $\lambda_1^* \boldsymbol{I}$, where the value of λ_1^* needs to be chosen so that the conductivity equations have a solution with a uniform field aligned in the x_1 direction in the region exterior to the ellipse. Once this is done it follows by the usual argument that λ_1^* represents the effective conductivity in the x_1 direction of an assemblage of aligned ellipsoids, each identical within a scale factor to the given prototype. Written in ellipsoidal coordinates the conductivity equations become

$$\begin{aligned} 0 = \nabla \cdot \boldsymbol{\sigma} \nabla \phi = & \frac{4\sqrt{g(\rho)}}{(\rho-\mu)(\rho-\nu)} \frac{\partial}{\partial \rho}\left[\lambda_n \sqrt{g(\rho)}\, \frac{\partial \phi}{\partial \rho}\right] \\ & + \frac{4\sqrt{g(\mu)}}{(\mu-\nu)(\mu-\rho)} \frac{\partial}{\partial \mu}\left[\lambda_t \sqrt{g(\mu)}\, \frac{\partial \phi}{\partial \mu}\right] + \frac{4\sqrt{g(\nu)}}{(\nu-\rho)(\nu-\mu)} \frac{\partial}{\partial \nu}\left[\lambda_t \sqrt{g(\nu)}\, \frac{\partial \phi}{\partial \nu}\right], \end{aligned} \tag{7.36}$$

where

$$g(t) = (c_1^2 + t)(c_2^2 + t)(c_3^2 + t). \tag{7.37}$$

The form of the potential (7.25) suggests that we should look for a solution of the form

$$\begin{aligned} \phi(\boldsymbol{x}) &= \varphi(\rho) x_1 \quad \text{for } \rho < \rho_e, \\ &= \varphi(\rho_e) x_1 \quad \text{for } \rho > \rho_e, \end{aligned} \tag{7.38}$$

corresponding to an external field aligned with the x_1-axis. Since the Laplacian of x_1 is zero,

(7.36) implies that

$$0 = \nabla \cdot \boldsymbol{\sigma} \nabla \phi - \varphi \lambda_t \nabla \cdot \nabla x_1 = \frac{4\sqrt{g(\rho)}}{(\rho-\mu)(\rho-\nu)} \frac{\partial}{\partial \rho}\left[\lambda_n \sqrt{g(\rho)}\left(x_1 \frac{d\varphi}{d\rho} + \varphi \frac{\partial x_1}{\partial \rho}\right)\right] - \frac{4\varphi\lambda_t\sqrt{g(\rho)}}{(\rho-\mu)(\rho-\nu)} \frac{\partial}{\partial \rho}\left[\sqrt{g(\rho)}\,\frac{\partial x_1}{\partial \rho}\right]. \tag{7.39}$$

We next eliminate x_1 from this equation, by first repeatedly substituting the identity

$$\frac{\partial x_1}{\partial \rho} = \frac{x_1}{2(c_1^2+\rho)}$$

into (7.39) and then dividing the resulting expression by x_1. This gives

$$\frac{d}{d\rho}\left[\lambda_n\sqrt{g(\rho)}\left(\frac{d\varphi}{d\rho} + \frac{\varphi}{2(c_1^2+\rho)}\right)\right] + \frac{\lambda_n\sqrt{g(\rho)}}{2(c_1^2+\rho)}\left(\frac{d\varphi}{d\rho} + \frac{\varphi}{2(c_1^2+\rho)}\right) = \varphi\lambda_t \frac{d}{d\rho}\left(\frac{\sqrt{g(\rho)}}{2(c_1^2+\rho)}\right) + \frac{\varphi\lambda_t}{2(c_1^2+\rho)}\left(\frac{\sqrt{g(\rho)}}{2(c_1^2+\rho)}\right),$$

which simplifies to the second-order differential equation

$$2\frac{d}{d\rho}\left[\lambda_n\sqrt{g(\rho)}\frac{d}{d\rho}\left(\varphi(\rho)\sqrt{c_1^2+\rho}\right)\right] = \varphi(\rho)\lambda_t \frac{d}{d\rho}\left[\sqrt{\frac{g(\rho)}{c_1^2+\rho}}\right], \tag{7.40}$$

where $g(\rho)$ is given by (7.37).

The continuity of the normal component of the current through the outer boundary of the ellipse,

$$\lambda_n(\rho)\left[\frac{d}{d\rho}\left(\varphi(\rho)\sqrt{c_1^2+\rho}\right)\right]_{\rho=\rho_e} = \lambda_1^*\left[\frac{d}{d\rho}\left(\varphi(\rho_e)\sqrt{c_1^2+\rho}\right)\right]_{\rho=\rho_e} = \lambda_1^* \frac{\varphi(\rho_e)}{2\sqrt{c_1^2+\rho_e}}, \tag{7.41}$$

allows us to determine the appropriate value of λ_1^* from the solution $\varphi(\rho)$ of the differential equation (7.40). If we define for $\rho < \rho_e$ the function $\lambda_1^*(\rho)$ via

$$\frac{d}{d\rho}\left(\varphi(\rho)\sqrt{c_1^2+\rho}\right) = \frac{\lambda_1^*(\rho)\varphi(\rho)}{2\lambda_n(\rho)\sqrt{c_1^2+\rho}}, \tag{7.42}$$

then (7.41) implies that $\lambda_1^*(\rho_e)$ can be identified with the effective conductivity λ_1^* in the x_1 direction of our original ellipsoid assemblage. More generally, $\lambda_1^*(\rho)$ represents the conductivity in the x_1 direction of an assemblage of ellipses the prototype of which is obtained by removing all material from the original ellipse outside the elliptical surface parameterized by ρ.

By substituting (7.42) into (7.40) we find that the second-order differential equation reduces to

$$(c_1^2+\rho)\left\{\frac{d}{d\rho}\left[2\lambda_1^*(\rho)h_1(\rho)\right] - 2\lambda_t(\rho)\frac{d}{d\rho}\left[h_1(\rho)\right]\right\} = h_1(\rho)\left\{\lambda_t(\rho) - \frac{[\lambda_1^*(\rho)]^2}{\lambda_n(\rho)}\right\}, \tag{7.43}$$

where

$$h_i(\rho) = \frac{\sqrt{g(\rho)}}{c_i^2+\rho} = \frac{\sqrt{(c_1^2+\rho)(c_2^2+\rho)(c_3^2+\rho)}}{c_i^2+\rho}, \qquad i = 1, 2, 3.$$

It is easy to see that when the conductivity has a constant value $\lambda_n(\rho) = \lambda_t(\rho) = \sigma_0$ independent of ρ then (7.43) has the expected solution $\lambda_1^*(\rho) = \sigma_0$. The differential equation can be rewritten as

$$\sqrt{g(\rho)}\left[\frac{d\sqrt{g(\rho)}}{d\rho}\right]^{-1}\frac{d\lambda_1^*}{d\rho} = \lambda_t - \lambda_1^* - k_1(\rho)\left[\lambda_t - 2\lambda_1^* + \frac{[\lambda_1^*(\rho)]^2}{\lambda_n}\right],$$

in which

$$k_i(\rho) = \frac{h_i(\rho)}{2}\left[\frac{d\sqrt{g(\rho)}}{d\rho}\right]^{-1} = \frac{h_i(\rho)}{h_1(\rho)+h_2(\rho)+h_3(\rho)}, \qquad i = 1, 2, 3. \tag{7.44}$$

Upon introducing the new variable

$$t = c + \log\sqrt{g(\rho)},$$

where c is an arbitrary constant, this differential equation further simplifies to the Ricatti equation

$$\frac{d\lambda_1^*}{dt} = \lambda_t - \lambda_1^*(t) - k_1(t)\left[\lambda_t - 2\lambda_1^* + \frac{[\lambda_1^*(t)]^2}{\lambda_n}\right]. \tag{7.45}$$

The effective conductivities $\lambda_2^*(t)$ and $\lambda_3^*(t)$ in the x_2 and x_3 directions similarly solve Ricatti equations, obtained by substituting 2 or 3 for the index 1 into (7.45) and (7.44). The coefficients $k_1(t)$, $k_2(t)$, and $k_3(t)$ are nonnegative and satisfy

$$k_1(t) + k_2(t) + k_3(t) = 1 \ \text{ for all } t. \tag{7.46}$$

The variable t has a natural interpretation. If t_1 and t_2 denote two values of t with $t_1 > t_2$, while ρ_1 and ρ_2 denote the corresponding values of ρ, then we have

$$t_1 - t_2 = -\log[\sqrt{g(\rho_2)}/\sqrt{g(\rho_1)}] = -\log f_r,$$

in which $f_r < 1$ is the volume fraction occupied by the ellipse with surface $\rho = \rho_2$ inside the larger ellipse with surface $\rho = \rho_1$.

7.8. The conductivity of an assemblage of coated ellipsoids†

As a particular example of an assemblage of elliptical inclusions let us consider an assemblage where the ellipsoids have a core of phase 1 with an isotropic conductivity tensor $\sigma_1\boldsymbol{I}$ surrounded by a coating of phase 2 with an isotropic conductivity tensor $\sigma_2\boldsymbol{I}$. The prototype ellipsoid has confocal elliptical interior and exterior surfaces, parameterized in ellipsoidal coordinates by $\rho = \rho_c$ and $\rho = \rho_e$.

In an isotropic material with $\lambda_n = \lambda_t$ independent of ρ, (7.40) reduces to

$$\frac{dq}{d\rho} = -\frac{q}{c_1^2+\rho}, \quad \text{where } q \equiv \frac{d\varphi}{d\rho}\sqrt{g(\rho)},$$

which has a solution in terms of elliptic integrals:

$$\varphi(\rho) = a + b\int_0^{\rho} \frac{d\rho}{\sqrt{(c_1^2+\rho)^3(c_2^2+\rho)(c_3^2+\rho)}},$$

where a and b are arbitrary constants. Accordingly, in our coated ellipsoid we look for a solution with uniform fields in the core and exterior regions of the forms

$$\varphi(\rho) = a_1 \quad \text{for } \rho \le \rho_c, \qquad \varphi(\rho) = a_* \quad \text{for } \rho > \rho_e,$$

$$\varphi(\rho) = a_2 + b_2\int_{\rho_c}^{\rho} \frac{d\rho}{\sqrt{(c_1^2+\rho)^3(c_2^2+\rho)(c_3^2+\rho)}} \quad \text{for } \rho_c < \rho \le \rho_e, \tag{7.47}$$

where, because the potential is continuous at ρ_c and ρ_e, we have

$$a_2 = a_1, \qquad a_* = a_1 + b_2\int_{\rho_c}^{\rho_e} \frac{d\rho}{\sqrt{(c_1^2+\rho)^3(c_2^2+\rho)(c_3^2+\rho)}}. \tag{7.48}$$

The continuity of the normal component of the current at ρ_e implies that (7.41) must hold with $\lambda_n = \lambda_t = \sigma_2$. A similar condition holds at the interface ρ_c. These conditions lead to the equations

$$a_1 = \frac{2b_2\sigma_2}{(\sigma_1-\sigma_2)\sqrt{g(\rho_c)}}, \quad a_* = \frac{2b_2\sigma_2}{(\lambda_1^*-\sigma_2)\sqrt{g(\rho_e)}}, \tag{7.49}$$

which when substituted in (7.48) directly give a formula for the conductivity λ_1^* of the ellipsoid assemblage in direction x_1. To express this formula in a convenient form we introduce the lengths

$$\ell_{cj} = \sqrt{c_j^2+\rho_c}, \quad \ell_{ej} = \sqrt{c_j^2+\rho_e}, \qquad j = 1, 2, 3, \tag{7.50}$$

which represent the semi-axis lengths of the core and exterior surfaces of the coated ellipsoid, the volume fraction

$$f_1 = \sqrt{g(\rho_c)/g(\rho_e)} = \ell_{c1}\ell_{c2}\ell_{c3}/\ell_{e1}\ell_{e2}\ell_{e3} \tag{7.51}$$

occupied by phase 1, and the depolarizing (or demagnetizing) factors

$$d_{cj} = d_j(\ell_{c1}, \ell_{c2}, \ell_{c3}), \quad d_{ej} = d_j(\ell_{e1}, \ell_{e2}, \ell_{e3}), \qquad j = 1, 2, 3, \tag{7.52}$$

where

$$d_j(\ell_1, \ell_2, \ell_3) = \frac{\ell_1\ell_2\ell_3}{2}\int_0^{\infty} \frac{dy}{(\ell_j^2+y)\sqrt{(\ell_1^2+y)(\ell_2^2+y)(\ell_3^2+y)}} \tag{7.53}$$

is the depolarization factor in direction $j = 1, 2$, or 3 of an ellipsoid with semi-axis lengths ℓ_1, ℓ_2, and ℓ_3. In terms of these depolarization factors we have

$$\begin{aligned}\int_{\rho_c}^{\rho_e} \frac{d\rho}{\sqrt{(c_1^2+\rho)^3(c_2^2+\rho)(c_3^2+\rho)}} &= \int_{\rho_c}^{\infty} \frac{d\rho}{\sqrt{(c_1^2+\rho)^3(c_2^2+\rho)(c_3^2+\rho)}} \\ &\quad - \int_{\rho_e}^{\infty} \frac{d\rho}{\sqrt{(c_1^2+\rho)^3(c_2^2+\rho)(c_3^2+\rho)}} \\ &= \frac{2d_{c1}}{\sqrt{g(\rho_c)}} - \frac{2d_{e1}}{\sqrt{g(\rho_e)}},\end{aligned}$$

and the formula for the conductivity of the ellipsoid assemblage in the x_1 direction implied by (7.48) and (7.49) becomes

$$\frac{f_1\sigma_2}{\lambda_1^* - \sigma_2} = \frac{\sigma_2}{\sigma_1 - \sigma_2} + d_{c1} - f_1 d_{e1}$$

or, equivalently,

$$\lambda_1^* = \sigma_2 + \frac{f_1\sigma_2(\sigma_1 - \sigma_2)}{\sigma_2 + (d_{c1} - f_1 d_{e1})(\sigma_1 - \sigma_2)}.$$

Of course the conductivities in the x_2 and x_3 directions are given by similar expressions, and taking these into account we obtain the formula

$$f_1\sigma_2(\boldsymbol{\sigma}_* - \sigma_2\boldsymbol{I})^{-1} = \sigma_2(\sigma_1 - \sigma_2)^{-1}\boldsymbol{I} + f_2\boldsymbol{M} \tag{7.54}$$

for the effective conductivity tensor

$$\boldsymbol{\sigma}_* = \begin{pmatrix} \lambda_1^* & 0 & 0 \\ 0 & \lambda_2^* & 0 \\ 0 & 0 & \lambda_3^* \end{pmatrix}$$

of the coated ellipsoid assemblage, where

$$\boldsymbol{M} = (\boldsymbol{D}_c - f_1\boldsymbol{D}_e)/f_2 \tag{7.55}$$

and

$$\boldsymbol{D}_c = \begin{pmatrix} d_{c1} & 0 & 0 \\ 0 & d_{c2} & 0 \\ 0 & 0 & d_{c3} \end{pmatrix}, \qquad \boldsymbol{D}_e = \begin{pmatrix} d_{e1} & 0 & 0 \\ 0 & d_{e2} & 0 \\ 0 & 0 & d_{e3} \end{pmatrix}$$

are the depolarization tensors of the core and exterior elliptical surfaces of the confocal coated ellipsoids. We will see later [equations (7.61) and (7.70)] that the matrix $\boldsymbol{M}$ has trace 1. That the effective conductivity tensor of the coated ellipsoid assemblage is given by (7.54), where $\mathrm{Tr}\boldsymbol{M} = 1$, and $\boldsymbol{M}$ is positive-semidefinite was established by Milton (1981a) [see also Bergman (1982)]. Tartar (1985) independently arrived at this same result, and moreover established that $\boldsymbol{M}$ ranges over all positive-semidefinite symmetric matrices satisfying $\mathrm{Tr}\boldsymbol{M} = 1$ as the shape of the coated ellipsoid is varied while keeping the volume fraction $f_1 = 1 - f_2$ fixed.

The two depolarization tensors $\boldsymbol{D}_c$ and $\boldsymbol{D}_e$ are not independent of each other because the core and exterior surfaces of the coated ellipse are confocal. Indeed, suppose that the semi-axis lengths ℓ_{cj}, $j = 1, 2, 3$ of the elliptical core and the volume fraction f_1 are known. Then from (7.37), (7.50), and (7.51) we have

$$\ell_{ej} = \sqrt{\ell_{cj}^2 + \alpha}, \quad j = 1, 2, 3, \tag{7.56}$$

where $\alpha = \rho_e - \rho_c$ is the positive root of the cubic equation

$$\alpha^3 + (\ell_{c1}^2 + \ell_{c2}^2 + \ell_{c3}^2)\alpha^2 + (\ell_{c1}^2\ell_{c2}^2 + \ell_{c2}^2\ell_{c3}^2 + \ell_{c3}^2\ell_{c1}^2)\alpha + (1 - f_1^2)(\ell_{c1}^2\ell_{c2}^2\ell_{c3}^2) = 0.$$

In other words, the semi-axis lengths ℓ_{ej}, $j = 1, 2, 3$ of the exterior surface of the coated ellipsoid, and hence the depolarization tensor $\boldsymbol{D}_e$, are completely determined in terms of the volume fraction f_1 and the semi-axis lengths of the elliptical core.

7.9. A solution of the elasticity equations in the coated ellipsoid assemblage†

We can use the solutions of the conductivity equations in the coated ellipsoid assemblage to construct a solution to the elasticity equations in the same geometry with a uniform and hydrostatic field inside the ellipsoid cores. This was first recognized by Grabovsky and Kohn (1995) using an indirect but powerful argument. Here we verify their result directly. Consider the prototype ellipsoid described in the previous section, and let $\phi_i(\boldsymbol{x})$ for $i = 1, 2$, and 3 denote the solution for the potential when the applied field is directed parallel to the x_i-axis, and adjusted in magnitude so that $\phi_i(\boldsymbol{x}) = x_i/(\sigma_1 - \sigma_2)$ inside the ellipsoid core.

The first claim is that these potentials are in fact components of a vector field $\boldsymbol{u}(\boldsymbol{x}) = (\phi_1(\boldsymbol{x}), \phi_2(\boldsymbol{x}), \phi_3(\boldsymbol{x}))$, which itself is the gradient of a scalar potential $\psi(\boldsymbol{x})$, that is, $\boldsymbol{u} = \nabla\psi$. Inside the ellipsoid coating (i.e., for $\rho_c < \rho \le \rho_e$) the potentials are given by the formulas

$$\phi_i(\boldsymbol{x}) = \frac{x_i}{\sigma_1 - \sigma_2} + \frac{x_i\sqrt{g(\rho_c)}}{2\sigma_2}\int_{\rho_c}^{\rho} \frac{d\rho}{(c_i^2+\rho)\sqrt{(c_1^2+\rho)(c_2^2+\rho)(c_3^2+\rho)}},$$

as follows from (7.38), (7.47), (7.48), and (7.49). Consequently, for $i \neq j$ we have

$$\frac{\partial\phi_i}{\partial x_j} - \frac{\partial\phi_j}{\partial x_i} = \left[\frac{x_i}{c_i^2+\rho}\frac{\partial\rho}{\partial x_j} - \frac{x_j}{c_j^2+\rho}\frac{\partial\rho}{\partial x_i}\right]\frac{\sqrt{g(\rho_c)}}{2\sigma_2\sqrt{(c_1^2+\rho)(c_2^2+\rho)(c_3^2+\rho)}}. \tag{7.57}$$

Also, differentiating the first formula in (7.35) with respect to x_i gives

$$\frac{\partial\rho}{\partial x_i} = \frac{2x_i}{c_i^2+\rho}\left[\frac{x_1^2}{(c_1^2+\rho)^2} + \frac{x_2^2}{(c_2^2+\rho)^2} + \frac{x_3^2}{(c_3^2+\rho)^2}\right]^{-1}. \tag{7.58}$$

By substituting this back into (7.57) we see that inside the ellipsoid coating $\nabla \times \boldsymbol{u} = 0$ or, equivalently, $\nabla\boldsymbol{u}$ is a symmetric matrix. Also, a direct computation shows that $\boldsymbol{u}$ is curl free inside the core and outside the ellipse. Finally, the continuity of the potential at $\rho = \rho_c$ and at $\rho = \rho_e$ implies the continuity of $\boldsymbol{u}$, and hence the tangential components of $\boldsymbol{u}$, across the boundaries of the core and ellipsoid. Therefore $\boldsymbol{u}(\boldsymbol{x})$ is the gradient of some potential $\psi(\boldsymbol{x})$.

The second claim is that

$$\mathrm{Tr}(\nabla\boldsymbol{u}) = \nabla\cdot\boldsymbol{u} = \Delta\psi = 3/(\sigma_1-\sigma_2) + 1/\sigma_2 = (\sigma_1+2\sigma_2)/\sigma_2(\sigma_1-\sigma_2), \tag{7.59}$$

for all $\boldsymbol{x}$ inside the ellipsoid coating. It is easy to prove that $\Delta\psi$ must be constant inside the coating; since the potential ϕ_i is harmonic for $i = 1, 2, 3$ it follows that

$$\nabla(\Delta\psi) = \Delta(\nabla\psi) = \Delta\boldsymbol{u} = (\Delta\phi_1, \Delta\phi_2, \Delta\phi_3) = 0, \tag{7.60}$$

implying that $\Delta\psi = \nabla\cdot\boldsymbol{u}$ is constant there. Also, as $\rho \to \rho_c$ we have

$$\frac{\partial\phi_i(\boldsymbol{x})}{\partial x_i} \to \frac{1}{\sigma_1-\sigma_2} + \frac{x_i}{2\sigma_2(c_i^2+\rho)}\frac{\partial\rho(\boldsymbol{x})}{\partial x_i}.$$

By making the substitution (7.58) and summing over i to get $\nabla\cdot\boldsymbol{u}$ we see that the value of the constant must be $3/(\sigma_1-\sigma_2) + 1/\sigma_2$. Incidentally, by taking the limit $\rho \to \rho_e$, applying a similar analysis, and using (7.59) one obtains the corollary that

$$\mathrm{Tr}\,\boldsymbol{M} = 1. \tag{7.61}$$

Now let us set $\sigma_2 = 1$ and define the strain field

$$\begin{aligned}\boldsymbol{\epsilon} = \nabla\boldsymbol{u} = [\nabla\boldsymbol{u} + (\nabla\boldsymbol{u})^T]/2 &= \boldsymbol{I}/(\sigma_1 - 1) \text{ in the core,}\\ &= \nabla\nabla\psi \text{ in the coating,}\\ &= \boldsymbol{\epsilon}_0 \text{ outside the ellipsoid,}\end{aligned} \tag{7.62}$$

where, as follows from (7.49), (7.51), and (7.54),

$$\boldsymbol{\epsilon}_0 = f_1(\boldsymbol{\sigma}_* - \boldsymbol{I})^{-1} = \boldsymbol{I}/(\sigma_1 - 1) + f_2\boldsymbol{M}.$$

Let us also define the stress field

$$\begin{aligned}\boldsymbol{\tau} &= (\kappa_1 - 2\mu_1/3)\boldsymbol{I}\,\mathrm{Tr}\,\boldsymbol{\epsilon} + 2\mu_1\boldsymbol{\epsilon} \text{ in the core,}\\ &= (\kappa_2 - 2\mu_2/3)\boldsymbol{I}\,\mathrm{Tr}\,\boldsymbol{\epsilon} + 2\mu_2\boldsymbol{\epsilon} \text{ in the coating,}\\ &= \boldsymbol{\tau}_0 \text{ outside the ellipsoid,}\end{aligned}$$

where κ_1, μ_1, and κ_2, μ_2 are the bulk and shear moduli of the core and coating, respectively, and $\boldsymbol{\tau}_0$ is a constant symmetric matrix to be determined from the conditions of stress compatibility. This stress is clearly symmetric and being constant in the core and outside the ellipsoid satisfies $\nabla\cdot\boldsymbol{\tau} = 0$ inside those regions. Inside the coating, where

$$\boldsymbol{\tau} = (\kappa_2 - 2\mu_2/3)\boldsymbol{I}\Delta\psi + 2\mu_2\nabla\nabla\psi = \frac{(\kappa_2 - 2\mu_2/3)(\sigma_1 + 2)\boldsymbol{I}}{(\sigma_1 - 1)} + 2\mu_2\nabla\nabla\psi,$$

it also has zero divergence because of the relations (7.60).

The continuity of the normal component of the current $\boldsymbol{\sigma}(\boldsymbol{x})\nabla\phi_i(\boldsymbol{x})$ across the core boundary implies the continuity of $\boldsymbol{n}\cdot\boldsymbol{\sigma}(\boldsymbol{x})\nabla\boldsymbol{u}$, where $\boldsymbol{n}$ is the normal to the interface. Therefore the hydrostatic stress

$$\boldsymbol{\tau} = 3\kappa_1\boldsymbol{I}/(\sigma_1 - 1)$$

inside the core will be compatible with the stress inside the coating, provided that we take

$$\sigma_1 = 1 + 9(\kappa_1 - \kappa_2)/(3\kappa_2 + 4\mu_2),$$

and with this value of σ_1 we have

$$\boldsymbol{\epsilon}_0 = (3\kappa_2 + 4\mu_2)\boldsymbol{I}/9(\kappa_1 - \kappa_2) + f_2\boldsymbol{M}. \tag{7.63}$$

Similarly the continuity of $\boldsymbol{n}\cdot\boldsymbol{\sigma}(\boldsymbol{x})\nabla\boldsymbol{u}$ across the outer boundary of the ellipsoid implies that the stress inside the coating will be compatible with the stress $\boldsymbol{\tau}_0$ outside the ellipsoid, provided that we take

$$\begin{aligned}\boldsymbol{\tau}_0 &= (\kappa_2 - 2\mu_2/3)(\sigma_1 + 2)\boldsymbol{I}/(\sigma_1 - 1) + 2\mu_2\boldsymbol{\sigma}_*\boldsymbol{\epsilon}_0\\ &= [\kappa_2(\kappa_1 + 4\mu_2/3)/(\kappa_1 - \kappa_2) + 4\mu_2 f_1/3]\boldsymbol{I} + 2\mu_2 f_2(\boldsymbol{M} - \boldsymbol{I}/3).\end{aligned} \tag{7.64}$$

Thus we have obtained a solution for the elasticity equations for the prototype ellipsoid, and by extension a solution for the elasticity equations with average strain $\boldsymbol{\epsilon}_0$ and average stress $\boldsymbol{\tau}_0$ in the associated coated ellipsoid assemblage. The effective elasticity tensor $\boldsymbol{\mathcal{C}}_*$ of the ellipsoid assemblage depends on how the coated ellipsoids are packed together but must be such that

$$\boldsymbol{\tau}_0 = \boldsymbol{\mathcal{C}}_*\boldsymbol{\epsilon}_0.$$

When the coated ellipsoids are coated spheres then $\boldsymbol{M} = \boldsymbol{I}/3$ and the elasticity tensor $\boldsymbol{\mathcal{C}}_*$ is isotropic with bulk modulus κ_* and shear modulus μ_*. We have $\boldsymbol{\tau}_0 = 3\kappa_*\boldsymbol{\epsilon}_0$ with

$$\begin{aligned}\kappa_* &= \frac{\kappa_2(\kappa_1 + 4\mu_2/3)/(\kappa_1 - \kappa_2) + 4\mu_2 f_1/3}{(\kappa_2 + 4\mu_2/3)/(\kappa_1 - \kappa_2) + f_2} \\ &= \kappa_2 + \frac{f_1}{1/(\kappa_1 - \kappa_2) + f_2/(\kappa_2 + 4\mu_2/3)},\end{aligned}$$

in agreement with (7.13).

Incidentally, in the two-dimensional context of a single coated confocal elliptical cylinder subject to a uniform applied field, Ru, Schiavone, and Mioduchowski (1999) and Ru (1999) have generalized the solutions (7.47) and (7.62) to allow for an arbitrary isotropic conducting or elastic medium surrounding the inclusion. For conductivity (or, equivalently, antiplane elasticity) they show that the field inside the core remains uniform even though the field outside the inclusion is generally not uniform. For planar elasticity they show that a solution exists where the field inside the core is uniform and hydrostatic.

7.10. Expressions for the depolarization factors†

The articles of Stoner (1945) and Osborn (1945) [see also the book of Kellogg (1953)] provide useful summaries of results concerning the depolarization factors d_1, d_2, and d_3 given by (7.53). They provide a way of characterizing the shape of an ellipsoid and can be evaluated explicitly when the ellipsoid is a spheroid with $\ell_2 = \ell_3$ (Maxwell 1873).

For prolate spheroids (with $\ell_1 \geq \ell_2 = \ell_3$) the expressions for the depolarization factors d_1 and $d_2 = d_3$ reduce to

$$d_1 = 1 - d_2/2 = \frac{1-\epsilon^2}{\epsilon^2}\left\{\frac{1}{2\epsilon}\ln\left(\frac{1+\epsilon}{1-\epsilon}\right) - 1\right\}, \quad \text{where } \epsilon = \sqrt{1 - (\ell_2/\ell_1)^2}, \tag{7.65}$$

while for oblate spheroids (with $\ell_1 \leq \ell_2 = \ell_3$) they reduce to

$$d_1 = 1 - d_2/2 = \frac{1}{\epsilon^2}\left\{1 - \frac{\sqrt{1-\epsilon^2}}{\epsilon}\sin^{-1}\epsilon\right\}, \quad \text{where } \epsilon = \sqrt{1 - (\ell_1/\ell_2)^2}, \tag{7.66}$$

where in both cases the quantity ϵ is called the eccentricity of the spheroid.

They can also be evaluated explicitly when the ellipsoid is an elliptical cylinder. In the limit as ℓ_3 approaches ∞, with ℓ_1 and ℓ_2 being held fixed, we have

$$d_1 = \ell_2/(\ell_1 + \ell_2), \quad d_2 = \ell_1/(\ell_1 + \ell_2), \quad d_3 = 0. \tag{7.67}$$

By substituting these expressions into (7.55) one finds after some algebraic manipulation that assemblages of confocal coated elliptical cylinders have a tensor

$$\boldsymbol{M} = \frac{1}{\ell_{c1}\ell_{e1} + \ell_{c2}\ell_{e2}}\begin{pmatrix} \ell_{c1}\ell_{e1} & 0 & 0 \\ 0 & \ell_{c2}\ell_{e2} & 0 \\ 0 & 0 & 0 \end{pmatrix}.$$

For ellipsoids of arbitrary shape the depolarization factors can be reexpressed in terms of Legendre's elliptic integrals of the first and second kind:

$$\begin{aligned}F(k,\phi) &= \int_0^\phi \frac{d\psi}{\sqrt{1 - k^2\sin^2\psi}} = \int_0^x \frac{dz}{\sqrt{(1-z^2)(1-k^2z^2)}}, \\ E(k,\phi) &= \int_0^\phi d\psi\sqrt{1 - k^2\sin^2\psi} = \int_0^x \frac{dz\sqrt{(1-k^2z^2)}}{\sqrt{(1-z^2)}},\end{aligned}$$

where $x = \sin\phi$ and $z = \sin\psi$. To accomplish this, let us suppose that the axes have been labeled so that $\ell_1 \geq \ell_2 \geq \ell_3$. Then introducing the variable $z = \sqrt{(\ell_1^2 - \ell_3^2)/(\ell_1^2 + y)}$, the formula (7.53) for the depolarization factors becomes

$$d_j = \frac{\ell_1\ell_2\ell_3}{(\ell_1^2 - \ell_3^2)^{3/2}} \int_0^x \frac{z^2 dz}{[1 - z^2(\ell_1^2 - \ell_j^2)/(\ell_1^2 - \ell_3^2)]\sqrt{(1-z^2)(1-k^2z^2)}},$$

where

$$k^2 = (\ell_1^2 - \ell_2^2)/(\ell_1^2 - \ell_3^2), \quad x^2 = 1 - \ell_3^2/\ell_1^2.$$

The expression for d_1 in terms of elliptic integrals is then obtained by using the identity

$$\frac{z^2}{\sqrt{(1-z^2)(1-k^2z^2)}} = \frac{1}{k^2}\left\{\frac{1}{\sqrt{(1-z^2)(1-k^2z^2)}} - \frac{\sqrt{(1-k^2z^2)}}{\sqrt{(1-z^2)}}\right\}, \tag{7.68}$$

while for d_2 and d_3 an integration by parts is required, using respectively the relations

$$\frac{d}{dz}\left\{\frac{z\sqrt{(1-z^2)}}{\sqrt{(1-k^2z^2)}}\right\} = \frac{\sqrt{(1-z^2)}}{\sqrt{(1-k^2z^2)}} - \frac{(1-k^2)z^2}{\sqrt{(1-z^2)(1-k^2z^2)^3}},$$

$$\frac{d}{dz}\left\{\frac{z\sqrt{(1-k^2z^2)}}{\sqrt{(1-z^2)}}\right\} = \frac{\sqrt{(1-k^2z^2)}}{\sqrt{(1-z^2)}} + \frac{(1-k^2)z^2}{\sqrt{(1-z^2)^3(1-k^2z^2)}},$$

and for d_2 the additional identity

$$\frac{\sqrt{(1-z^2)}}{\sqrt{(1-k^2z^2)}} = \frac{1}{\sqrt{(1-z^2)(1-k^2z^2)}} - \frac{z^2}{\sqrt{(1-z^2)(1-k^2z^2)}}$$

in conjunction with (7.68). We thereby obtain the desired formulas

$$\begin{aligned}
d_1 &= \frac{\ell_1\ell_2\ell_3[F(k,\phi) - E(k,\phi)]}{(\ell_1^2 - \ell_2^2)\sqrt{(\ell_1^2 - \ell_3^2)}}, \\
d_2 &= \frac{\ell_1\ell_2\ell_3[E(k,\phi) - F(k,\phi)]}{(\ell_1^2 - \ell_2^2)\sqrt{(\ell_1^2 - \ell_3^2)}} + \frac{\ell_1\ell_2\ell_3 E(k,\phi)}{(\ell_2^2 - \ell_3^2)\sqrt{(\ell_1^2 - \ell_3^2)}} - \frac{\ell_3^2}{\ell_2^2 - \ell_3^2}, \\
d_3 &= \frac{-\ell_1\ell_2\ell_3 E(k,\phi)}{(\ell_2^2 - \ell_3^2)\sqrt{(\ell_1^2 - \ell_3^2)}} + \frac{\ell_2^2}{\ell_2^2 - \ell_3^2}
\end{aligned} \tag{7.69}$$

for the depolarization factors in terms of elliptic integrals, in which

$$k^2 = (\ell_1^2 - \ell_2^2)/(\ell_1^2 - \ell_3^2), \quad \sin^2\phi = x^2 = 1 - \ell_3^2/\ell_1^2.$$

From these formulas one can see that the depolarization factors always sum to unity,

$$d_1 + d_2 + d_3 = 1, \tag{7.70}$$

leading again to the result (7.61). Clearly the integral expressions imply that they are positive quantities. Conversely, one can always find an ellipsoid corresponding to every triplet (d_1, d_2, d_3) of positive numbers satisfying (7.70). Triplets with one zero depolarization factor correspond to elliptical cylinders. Triplets with two zero depolarization factors correspond to flat slabs.

7.11. Neutral coated inclusions

Mansfield (1953) found that certain reinforced holes, which he called neutral inclusions, could be cut out of a uniformly stressed plate without disturbing the stress surrounding the hole. In this sense a single Hashin coated sphere is an example of a neutral coated inclusion: One can insert it into an isotropic medium with conductivity $\sigma_0 = \sigma_*$ or with bulk modulus $\kappa_0 = \kappa_*$ without disturbing the uniform current or the hydrostatic pressure field outside the inclusion. Similarly, the coated confocal ellipsoidal inclusion is a neutral coated inclusion. If one has an isotropic elastic medium with bulk and shear moduli

$$\kappa_0 = \kappa_2 + \frac{f_1}{1/(\kappa_1 - \kappa_2) + f_2/(\kappa_2 + 4\mu_2/3)}, \quad \mu_0 = \mu_2,$$

chosen so that $\boldsymbol{\tau}_0 = \boldsymbol{\mathcal{C}}_0\boldsymbol{\epsilon}_0$, where $\boldsymbol{\epsilon}_0$ and $\boldsymbol{\tau}_0$ are given by (7.63) and (7.64), then when the strain field in this medium is uniform and equal to $\boldsymbol{\epsilon}_0$ one can insert the coated confocal ellipsoidal inclusion into this medium without disturbing the surrounding uniform strain and stress fields $\boldsymbol{\epsilon}_0$ and $\boldsymbol{\tau}_0$. Here f_1 and f_2 are the volume fractions of the two phases within the coated inclusion.

In the same way that assemblages can be built from coated spheres or coated ellipsoids, so too can assemblages be built from neutral coated inclusions, and the fact that they are neutral allows us to determine some of the effective moduli of the assemblages. [When the coated inclusions are not neutral, it is still possible to bound the moduli of the associated assemblages (Bornert, Stolz, and Zaoui 1996).] Neutral coated inclusions are easiest to find when the inclusion coating is thin with large or small moduli of the coating to compensate for its thinness. The coating is called the interphase region and can be treated as a single interface with new jump conditions on the fields across the interface. This single interface is called an imperfect interface.

If the interphase consists of poorly conducting material between two closely separated smooth boundaries, then it can be replaced by a single interface, across which the normal component $\boldsymbol{n} \cdot \boldsymbol{j}$ of the current is continuous but the electrical potential ϕ has a jump $[\phi]$ proportional to $\boldsymbol{n} \cdot \boldsymbol{j}$ [for a proof see, for example, Sanchez-Palencia (1970) or Miloh and Benveniste (1999)]. For an interphase region of thickness $\epsilon\gamma(\boldsymbol{x})$ and conductivity $\sigma(\boldsymbol{x}, \epsilon)$ parametrized by ϵ one has

$$\beta[\phi] = \boldsymbol{n} \cdot \boldsymbol{j}, \tag{7.71}$$

in the limit $\epsilon \to 0$, where the nonnegative parameter

$$\beta(\boldsymbol{x}) = \lim_{\epsilon \to 0} \sigma(\boldsymbol{x}, \epsilon)/[\epsilon\gamma(\boldsymbol{x})]$$

measures the transverse conductance of the interface. Here $\sigma(\boldsymbol{x}, \epsilon)$ is assumed to approach zero linearly in ϵ. For thermal conductivity the resistance of the imperfect interface is known as the Kapitza resistance (Kapitza 1965).

For example, if we consider a Hashin coated sphere with thickness $r_e - r_c = \epsilon$ and coating conductivity $\sigma_2 = \epsilon\beta$, then (7.4) and (7.5) imply that in the limit $\epsilon \to 0$

$$\begin{aligned} a_1 &= -3b_2\sigma_2/[r_c^3(\sigma_1 - \sigma_2)] \to -3b_2\epsilon\beta/(r_c^3\sigma_1), \\ a_* &= -b_2[1 - r_c^3/r_e^3 - 3\sigma_2/(\sigma_1 - \sigma_2)]/r_c^3 \to -3b_2\epsilon[1/r_c + \beta/\sigma_1]/r_c^3. \end{aligned}$$

Thus in this limit we have the relation

$$a_* = a_1[1 + \sigma_1/(\beta r_c)].$$

At the imperfect interface boundary $r = r_c$ the jump in the potential is

$$[\phi] = \phi_* - \phi_1 = (a_* - a_1) r_c \cos\theta = \sigma_1 a_1 \cos\theta/\beta,$$

while the normal component of the current at the interface from (7.2) is

$$\boldsymbol{n} \cdot \boldsymbol{j} = \boldsymbol{v}_r \cdot \boldsymbol{j}_1 = \sigma_1 a_1 \cos\theta.$$

Thus, as expected, the boundary condition (7.71) is satisfied at the imperfect interface.

The neutral spherical inclusions of Torquato and Rintoul (1995), Lipton and Vernescu (1995, 1996), and Lipton (1997a, 1997b) with an imperfect interface correspond to the Hashin coated spheres with a thin coating having large or small moduli. [See also Bigoni, Serkov, Valentini, and Movchan (1998), who show that dilute concentrations of certain circular inclusions with imperfect interfaces do not influence the effective bulk and shear moduli to first order in the volume fraction.] Lipton and Talbot (1999) extend these results to nonlinear spherical inclusions with an imperfect interface in a nonlinear matrix.

Most interesting are the two-dimensional neutral elastic inclusions of Ru (1998) and the two-dimensional and three-dimensional neutral conducting inclusions of Benveniste and Miloh (1999) with an imperfect interface. They show that a wide variety of inclusion shapes are possible if one is free to vary the interphase properties (or, equivalently, the thickness of the interphase region) around the boundary of the inclusion. Let us suppose that the interphase is isotropic and poorly conducting, so that $\boldsymbol{j} \cdot \boldsymbol{n}$ is continuous across the imperfect interface and the jump $[\phi]$ in the potential is given by (7.71). The inclusion is taken to have constant isotropic conductivity σ_1 in its interior. Since $\boldsymbol{j}(\boldsymbol{x})$, by assumption, takes a constant value $\boldsymbol{j}_0$ outside the inclusion, the potential $\phi_1(\boldsymbol{x})$ inside the inclusion satisfies the Neuman boundary condition

$$\sigma_1 \boldsymbol{n} \cdot \nabla\phi_1 = \boldsymbol{n} \cdot \boldsymbol{j}(\boldsymbol{x}) = \boldsymbol{n} \cdot \boldsymbol{j}_0$$

at the inclusion boundary. Since $\phi_1(\boldsymbol{x})$ is harmonic, the solution to the Neuman problem is simply

$$\phi_1(\boldsymbol{x}) = (\boldsymbol{j}_0 \cdot \boldsymbol{x})/\sigma_1 + c,$$

where the constant c remains to be determined. The associated current $\boldsymbol{j}(\boldsymbol{x})$ is constant, taking the value $\boldsymbol{j}_0$ everywhere. By assumption the electric field $\boldsymbol{e}(\boldsymbol{x})$ also takes a constant value $\boldsymbol{e}_0$ outside the inclusion, where $\boldsymbol{e}_0$ and $\boldsymbol{j}_0$ are not necessarily parallel if the exterior medium is anisotropic. Therefore the potential $\phi_*(\boldsymbol{x})$ outside the inclusion is simply

$$\phi_* = \boldsymbol{e}_0 \cdot \boldsymbol{x} + c',$$

where c' is constant. Since we are free to add a constant to the potential, and since we are free to shift the origin of our spatial coordinates by a vector proportional to $\boldsymbol{j}_0$, we can set $c = c' = 0$ without any loss of generality.

At the imperfect interface the boundary condition (7.71) then implies that

$$\beta(\phi_* - \phi_1) = -\beta \boldsymbol{p}_0 \cdot \boldsymbol{x}/\sigma_1 = \boldsymbol{n} \cdot \boldsymbol{j}_0, \quad \text{where } \boldsymbol{p}_0 = \boldsymbol{j}_0 - \sigma_1 \boldsymbol{e}_0.$$

This has the solution

$$\beta = -\frac{\sigma_1 \boldsymbol{n} \cdot \boldsymbol{j}_0}{\boldsymbol{p}_0 \cdot \boldsymbol{x}},$$

which will be nonnegative provided $\boldsymbol{n} \cdot \boldsymbol{j}_0$ and $\boldsymbol{p}_0 \cdot \boldsymbol{x}$ always take opposite signs around the boundary of the neutral inclusion. Without loss of generality, by rotating the coordinate

system if necessary, we can assume $\boldsymbol{j}_0$ points along the direction of the positive x_1-axis. Then the boundary of the interface must be such that

$$n_1(\boldsymbol{p}_0 \cdot \boldsymbol{x}) \leq 0, \tag{7.72}$$

that is, such that n_1 is positive in the half-space $\boldsymbol{p}_0 \cdot \boldsymbol{x} < 0$ and negative in the half-space $\boldsymbol{p}_0 \cdot \boldsymbol{x} > 0$ for all points $\boldsymbol{x}$ along the interface. (By considering a point $\boldsymbol{x} = \lambda \boldsymbol{j}_0$ on the interface where $\lambda > 0$ and $n_1 > 0$, we see that a necessary condition for this to be possible is that $\boldsymbol{p}_0 \cdot \boldsymbol{j}_0 < 0$.) The criterion (7.72) for neutrality is a slight generalization of the one found by Benveniste and Miloh (1999), who assumed that the medium outside the inclusion was isotropic, that is, $\boldsymbol{p}_0$ was parallel to $\boldsymbol{j}_0$. Figure 7.6(a) shows an example of an inclusion that satisfies the condition (7.72) and which therefore can be made neutral for an appropriate choice of $\beta(\boldsymbol{x})$, while figure 7.6(b) shows an example of an inclusion that violates this condition (no matter where we place the origin) and which therefore can never be made neutral for any choice of $\beta(\boldsymbol{x}) \geq 0$. If the inclusion is convex and two-dimensional, the condition can always be satisfied by finding the two points on the boundary where n_1 changes sign, choosing the origin on the line joining these two points, and taking $\boldsymbol{p}_0$ perpendicular to this line and such that $\boldsymbol{p}_0 \cdot \boldsymbol{j}_0 < 0$. An assemblage of these neutral inclusions must have conductivity tensor $\boldsymbol{\sigma}_*$ such that $\boldsymbol{j}_0 = \boldsymbol{\sigma}_* \boldsymbol{e}_0$.

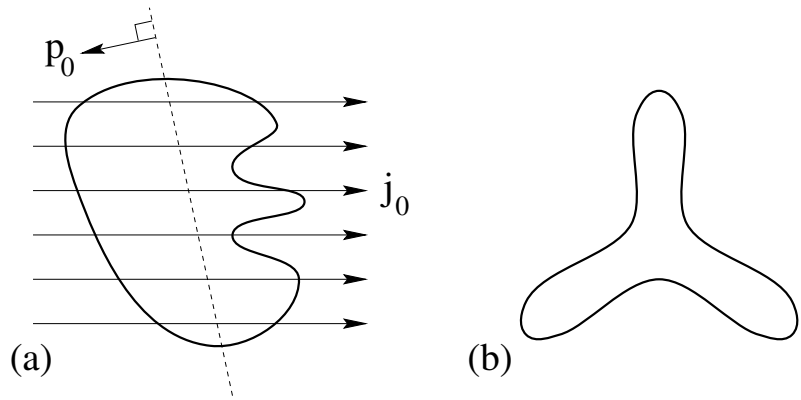

Figure 7.6. The inclusion shown in (a), containing an isotropic material with conductivity σ_1, is neutral for an appropriate choice of the interface resistance. The current $\boldsymbol{j}_0$ is constant everywhere, and the electric field takes the constant value $\boldsymbol{e}_0 = (\boldsymbol{j}_0 - \boldsymbol{p}_0)/\sigma_1$ outside the inclusion. The component n_1 of the interface normal $\boldsymbol{n}$ is positive to the right of the dashed line and negative to the left of it. The inclusion shown in (b) cannot be made neutral for any choice of the interface resistance.

In two dimensions, one can find neutral conducting coated inclusions with perfect interfaces that are not coated cylinders or coated elliptical cylinders (Milton and Serkov 2001). Let us suppose that we are given a homogeneous two-dimensional medium in which there is a uniform electric field $\boldsymbol{e}_0 = (e_1, e_2)$ and a uniform current field $\boldsymbol{j}_0 = (j_1, j_2)$, not necessarily parallel to $\boldsymbol{e}$. We want to insert into this medium a coated inclusion without disturbing the surrounding field. The following analysis applies to the case where the core of the inclusion is insulating, that is, the core has zero conductivity $\sigma_1 = 0$. (Using duality the analysis can easily be extended to the case where the core has infinite conductivity.) We assume that the coating is isotropic and its conductivity can then be taken to be $\sigma_2 = 1$, without loss of generality.

Since the fields $\boldsymbol{e}(\boldsymbol{x})$ and $\boldsymbol{j}(\boldsymbol{x})$ are, respectively, curl free and divergence free, there exist continuous potentials $\phi(\boldsymbol{x})$ and $\psi(\boldsymbol{x})$ such that $\boldsymbol{e} = \nabla\phi$ and $\boldsymbol{j} = \boldsymbol{R}_\perp\nabla\psi$. Also, because $\sigma_2 = 1$, the constitutive relation $\boldsymbol{j}(\boldsymbol{x}) = \boldsymbol{\sigma}(\boldsymbol{x})\boldsymbol{e}(\boldsymbol{x})$ within the coating phase reduces to the Cauchy-Riemann equation $\boldsymbol{R}_\perp\nabla\psi = \nabla\phi$, which implies that $w = \phi + i\psi$ is an analytic function of $z = x_1 + ix_2$ inside the coating. Since no current flows into the core, $\nabla\psi$ must be perpendicular to the core surface at that boundary, that is, ψ must be constant around the boundary of the core, and without loss of generality we can take that constant to be zero. In other words, w satisfies the boundary condition

$$w - \overline{w} = 0 \tag{7.73}$$

at the core boundary, where the bar denotes complex conjugation. In order to generate the constant fields $\boldsymbol{e}_0$ and $\boldsymbol{j}_0$ outside the inclusion the potentials there must take the form

$$\phi = e_1x_1 + e_2x_2 + \phi_0, \quad \psi = -j_2x_1 + j_1x_2 + \psi_0,$$

where ϕ_0 and ψ_0 are constants. Since we are free to shift the origin of our spatial coordinates x_1 and x_2, we can assume that $\phi_0 = \psi_0 = 0$. Finally, since the potentials ϕ and ψ are continuous, they must take these values at the outer boundary of the inclusion, that is, the potential w satisfies the boundary condition

$$w = gz + h\overline{z}, \tag{7.74}$$

on the outer boundary of the inclusion, in which

$$g = (\overline{e}_0 + \overline{j}_0)/2, \quad h = (e_0 - j_0)/2, \quad \text{where } e_0 = e_1 + ie_2, \quad j_0 = j_1 + ij_2.$$

In any conducting medium with bounded positive-definite conductivity tensor the electrical energy dissipation $\boldsymbol{e}_0 \cdot \boldsymbol{j}_0$ is strictly positive, which implies the constraint that $e_0\overline{j}_0 + j_0\overline{e}_0 > 0$ or, equivalently, that

$$|g| > |h|. \tag{7.75}$$

The task is to find a coated inclusion such that in the coating there exists an analytic function $w(z)$ satisfying the boundary conditions (7.73) and (7.74). This task is simplified if we conformally map the region in the z-plane occupied by the coating to an annulus with outer radius 1 and inner radius $r < 1$ located in a complex plane, which we label as the p-plane, parameterized by the complex variable p. A one-to-one conformal mapping from a doubly connected region to a annulus always exists [see, for example, Ahlfors (1966)]. The functions $z(p)$ and $w(p)$ can be expanded in Laurent series:

$$z(p) = \sum_{j=-\infty}^{\infty} a_n z^n, \quad w(p) = \sum_{j=-\infty}^{\infty} b_n z^n.$$

The boundary conditions (7.73) and (7.74), which must hold, respectively, for $p = re^{i\theta}$ and for $p = e^{i\theta}$ for all θ, are satisfied if and only if for all n

$$b_n r^n - \overline{b}_{-n} r^{-n} = 0, \quad b_n = ga_n + h\overline{a}_{-n}. \tag{7.76}$$

Substituting the second relation into the first gives

$$\overline{a}_{-n} = -q_n a_n, \quad \text{where } q_n = \frac{\overline{h} - r^{2n}g}{\overline{g} - r^{2n}h}, \tag{7.77}$$

and the condition (7.75) ensures that the denominator $\overline{g} + r^{2n}h$ is nonzero. A necessary condition for this equation with $n = 0$ to have a nonzero solution for a_0 is that $|q_0| = 1$. By setting $q_0 = e^{i\alpha}$ we see that this can occur if and only if $|h| = |g|$, which is excluded by (7.75). Therefore we take $a_0 = 0$ and regard the coefficients a_n with $n > 0$ as parameterizing all possible neutral inclusions. The formula (7.77) then gives the coefficients a_n with $n < 0$ and (7.76) gives the field coefficients b_n.

In this way one finds the inner and outer boundaries of the neutral inclusion, through the trajectories traced by $z(re^{i\theta})$ and $z(e^{i\theta})$ as θ is varied, and the potential $w(z)$ is given implicitly through the series expansions for $w(p)$ and $z(p)$. Figure 7.7 shows two examples of these neutral inclusions. Of course some restrictions on the choice of coefficients a_n with $n > 0$ are needed to ensure that the series expansions converge and that the mapping from the annulus to the coating region of the inclusion is one-to-one. These inclusions are neutral for the given applied field $\boldsymbol{e}_0$. An assemblage of these neutral coated inclusions must have conductivity tensor $\boldsymbol{\sigma}_*$ such that $\boldsymbol{j}_0 = \boldsymbol{\sigma}_*\boldsymbol{e}_0$. If one wants a coated inclusion (with insulating core and isotropic coating surrounded by a possibly anisotropic homogeneous matrix) to be neutral for two independent applied fields, then one can prove that the inclusion is necessarily a coated circle or coated confocal ellipse (Milton and Serkov 2001).

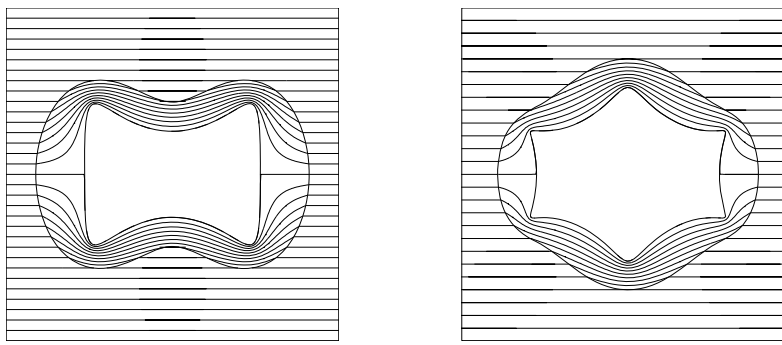

Figure 7.7. Examples of two neutral coated conducting inclusions with perfect interfaces and an insulating core, showing the lines of current flow. The only nonzero coefficients of the conformal map are chosen to be a_1, a_{-1}, a_m, and a_{-m}, where $m = 3$ in (a) and $m = 5$ in (b).

At present the problem of finding all neutral inclusions with perfect interfaces having finitely conducting isotropic materials as core and coating is still open. One would expect that coated circles or coated ellipses are not the only such neutral inclusions. However, coated circles and coated confocal ellipses are the only two-dimensional neutral inclusions where the electric and current fields in the core are uniform. To see this, assume that the electric and current fields and current fields in the core are uniform. Then the potential w must satisfy the boundary condition

$$w = g_0 z + h_0 \overline{z} \tag{7.78}$$

at the core boundary for appropriate values of the complex constants g_0 and h_0, corresponding to the values of the fields inside the core. Again one maps the region occupied by the coating to the annulus. The boundary conditions (7.78) and (7.74), which must hold respectively for $p = re^{i\theta}$ and for $p = e^{i\theta}$ for all θ, are satisfied if and only if for all n

$$b_n = g_0 a_n + h_0 r^{-2n}\overline{a}_{-n}, \quad b_n = g a_n + h\overline{a}_{-n}.$$

By eliminating b_n and by also considering the associated equation obtained by taking complex conjugates and replacing n with $-n$, one obtains the pair of equations

$$(g - g_0)a_n + (h - r^{-2n}h_0)\overline{a}_{-n} = 0, \quad (\overline{h} - r^{2n}\overline{h}_0)a_n + (\overline{g} - \overline{g}_0)\overline{a}_{-n} = 0.$$

These have a nontrivial solution if and only if the determinant vanishes:

$$(g - g_0)(\overline{g} - \overline{g}_0) = (h - r^{-2n}h_0)(\overline{h} - r^{2n}\overline{h}_0) = |h|^2 + |h_0|^2 - r^{-2n}h_0\overline{h} - r^{2n}\overline{h}_0 h.$$

This equation can be satisfied for at most two values of n because when multiplied by $a = r^{2n}$ it is a quadratic function of a that can have at most two solutions for a. If $n = m$ is one solution, then $n = -m$ is the other solution. The coefficients a_n must then be zero except for $n = m$ and $n = -m$. Furthermore, we must have $m = 1$ to ensure that the mapping from the annulus to the coating region of the inclusion has a possibility of being one-to-one. It is then easy to check that the associated mapping $z = a_1 p + a_{-1}/p$ maps the annulus to the coating of a coated confocal ellipsoid.

References

Ahlfors, L. V. 1966. *Complex Analysis: An Introduction to the Theory of Analytic Functions of One Complex Variable* (Second ed.), pp. 243–253. Tokyo: McGraw-Hill Kogakusha. {*137, 139*}

Avellaneda, M. 1991. Enhanced diffusivity and intercell transition layers in 2-D models of passive advection. *Journal of Mathematical Physics* 32(11):3209–3212. {*124, 139*}

Avellaneda, M., A. V. Cherkaev, K. A. Lurie, and G. W. Milton 1988. On the effective conductivity of polycrystals and a three-dimensional phase-interchange inequality. *Journal of Applied Physics* 63(10):4989–5003. {*120, 139, 439, 441, 450, 452, 512, 525, 538, 550, 555, 564*}

Benveniste, Y. and T. Miloh 1999. Neutral inhomogeneities in conduction phenomena. *Journal of the Mechanics and Physics of Solids* 47(9):1873–1892. {*135, 136, 139*}

Bergman, D. J. 1982. Rigorous bounds for the complex dielectric constant of a two-component composite. *Annals of Physics* 138(1):78–114. {*129, 139, 569, 597*}

Bigoni, D., S. K. Serkov, M. Valentini, and A. B. Movchan 1998. Asymptotic models of dilute composites with imperfectly bonded inclusions. *International Journal of Solids and Structures* 35(24):3239–3258. {*135, 139*}

Bornert, M., C. Stolz, and A. Zaoui 1996. Morphologically representative pattern-based bounding in elasticity. *Journal of the Mechanics and Physics of Solids* 44(3):307–331. {*134, 139, 458, 491*}

Grabovsky, Y. and R. V. Kohn 1995. Microstructures minimizing the energy of a two phase elastic composite in two space dimensions. I. The confocal ellipse construction. *Journal of the Mechanics and Physics of Solids* 43(6):933–947. {*130, 139, 467, 492*}

Hashin, Z. 1962. The elastic moduli of heterogeneous materials. *Journal of Applied Mechanics* 29:143–150. {*113, 116, 139*}

Hashin, Z. 1985. Large isotropic elastic deformation of composites and porous media. *International Journal of Solids and Structures* 21:711–720. {*117, 139*}

Hashin, Z. and S. Shtrikman 1962. A variational approach to the theory of the effective magnetic permeability of multiphase materials. *Journal of Applied Physics* 33:3125–3131. {*113, 116, 140, 271, 279, 287, 347, 350, 353, 457, 458, 460, 493, 574, 586, 598*}

Kapitza, P. L. 1965. The study of heat transfer in helium II. In D. ter Haar (ed.), *Collected Papers of P. L. Kapitza*, pp. 581–624. New York: Pergamon. {*134, 140*}

Kellogg, O. D. 1953. *Foundations of Potential Theory*, pp. 184–196. Berlin / Heidelberg / London / etc.: Springer-Verlag. {*124, 132, 140*}

Kerner, E. H. 1956. The elastic and thermo-elastic properties of composite media. *Proceedings of the Physical Society, London, B* 69:808–813. {*117, 140, 204, 216*}

Lipton, R. 1997a. Reciprocal relations, bounds, and size effects for composites with highly conducting interface. *SIAM Journal on Applied Mathematics* 57(2):347–363. {*135, 140*}

Lipton, R. 1997b. Variational methods, bounds, and size effects for composites with highly conducting interface. *Journal of the Mechanics and Physics of Solids* 45(3):361–384. {*135, 140*}

Lipton, R. and D. R. S. Talbot 1999. The effect of the interface on the dc transport properties of non-linear composite materials. *Journal of Applied Physics* 86(3):1480–1487. {*135, 140*}

Lipton, R. and B. Vernescu 1995. Variational methods, size effects and extremal microgeometries for elastic composites with imperfect interface. *Mathematical Models and Methods in Applied Sciences* 5(8):1139–1173. {*135, 140*}

Lipton, R. and B. Vernescu 1996. Composites with imperfect interface. *Proceedings of the Royal Society of London. Series A, Mathematical and Physical Sciences* 452(1945): 329–358. {*135, 140*}

Lurie, K. A. and A. V. Cherkaev 1985. The problem of formation of an optimal isotropic multicomponent composite. *Journal of Optimization Theory and Applications* 46:571–589. {*118, 140, 460, 494*}

Mansfield, E. H. 1953. Neutral holes in plane sheet- reinforced holes which are elastically equivalent to the uncut sheet. *Quarterly Journal of Mechanics and Applied Mathematics* VI:370–378. {*134, 140*}

Maxwell, J. C. 1873. *A Treatise on Electricity and Magnetism*. Oxford, United Kingdom: Clarendon Press. Articles 437 and 438 (pp. 62–67). {*132, 140, 252, 268*}

Milgrom, M. 1989. A layered-shell model of isotropic composites and exact expressions for the effective properties. *Journal of Applied Physics* 66:3429–3436. {*118, 140*}

Miloh, T. and Y. Benveniste 1999. On the effective conductivity of composites with ellipsoidal inhomogeneities and highly conducting interfaces. *Proceedings of the Royal Society of London. Series A, Mathematical and Physical Sciences* 455(1987):2687–2706. {*134, 140*}

Milton, G. W. 1980. Bounds on the complex dielectric constant of a composite material. *Applied Physics Letters* 37(3):300–302. {*124, 140, 452, 454, 478, 494, 569, 570, 577, 588, 599*}

Milton, G. W. 1981a. Bounds on the complex permittivity of a two-component composite material. *Journal of Applied Physics* 52(8):5286–5293. {*118, 120, 124, 125, 129, 140, 370, 394, 569, 588, 589, 592, 599*}

Milton, G. W. 1981b. Concerning bounds on the transport and mechanical properties of multicomponent composite materials. *Applied Physics* A26:125–130. {*118, 141, 459, 460, 471, 494*}

Milton, G. W. and S. K. Serkov 2001. Neutral coated inclusions in conductivity and anti-plane elasticity. *Proceedings of the Royal Society of London. Series A, Mathematical and Physical Sciences* 457(2012):1973–1997. {*136, 138, 141*}

Nesi, V. 1991. Multiphase interchange inequalities. *Journal of Mathematical Physics* 32 (8):2263–2275. {*120, 141*}

Nesi, V. 1996. Quasiconformal mappings as a tool to study certain two-dimensional G-closure problems. *Archive for Rational Mechanics and Analysis* 134(1):17–51. {*124, 141, 152, 156, 480, 481, 495, 646, 669*}

Osborn, J. A. 1945. Demagnetizing factors of the general ellipsoid. *Physical Review* 67 (11/12):351–357. {*132, 141*}

Perrins, W. T., D. R. McKenzie, and R. C. McPhedran 1979. Transport properties of regular arrays of cylinders. *Proceedings of the Royal Society of London. Series A, Mathematical and Physical Sciences* 369(1737):207–225. {*39, 45, 116, 141*}

Ru, C.-Q. 1998. Interface design of neutral elastic inclusions. *International Journal of Solids and Structures* 35(7–8):559–572. {*135, 141*}

Ru, C.-Q. 1999. Three-phase elliptical inclusions with internal uniform hydrostatic stresses. *Journal of the Mechanics and Physics of Solids* 47(2):259–273. {*132, 141*}

Ru, C.-Q., P. Schiavone, and A. Mioduchowski 1999. Uniformity of the stresses within a three-phase elliptical inclusion in anti-plane shear. *Journal of Elasticity* 52:121–128. {*132, 141*}

Sanchez-Palencia, E. 1970. Comportement limité d'un problème de transmission à travers une plaque faiblement conductrice. (French) [Limiting behavior of a transmission problem through a weakly conducting layer]. *Comptes rendus de l'Académie des sciences, Paris* A 270:1026–1028. {*134, 141*}

Schulgasser, K. 1976. On a phase interchange relationship for composite materials. *Journal of Mathematical Physics* 17:378–381. {*120, 141*}

Schulgasser, K. 1977. Concerning the effective transverse conductivity of a two-dimensional, two-phase, material. *International Journal of Heat and Mass Transfer* 20:1226–1230. {*118, 141*}

Schulgasser, K. 1983. Sphere assemblage model for polycrystals and symmetric materials. *Journal of Applied Physics* 54:1380–1382. {*119, 121, 122, 141*}

Stoner, E. C. 1945. The demagnetizing factors for ellipsoids. *Philosophical Magazine* 36: 803–820. {*132, 141*}

Tartar, L. 1985. Estimations fines des coefficients homogénéisés. (French) [Fine estimations of homogenized coefficients]. In P. Krée (ed.), *Ennio de Giorgi Colloquium: Papers Presented at a Colloquium Held at the H. Poincaré Institute in November 1983*, pp. 168–187. London: Pitman Publishing Ltd. ISBN 0-273-08680-4. {*129, 141, 165, 167, 174, 183, 462, 496, 499, 503, 506, 508, 527, 529, 552, 683, 698*}

Torquato, S. and M. D. Rintoul 1995. Effect of the interface on the properties of composite media. *Physical Review Letters* 75(22):4067–4070. {*135, 142*}

Zhikov, V. V. 1991. Estimates for the homogenized matrix and the homogenized tensor. *Uspekhi Matematicheskikh Nauk = Russian Mathematical Surveys* 46:49–109. English translation in *Russ. Math. Surv.* 46(3):65–136 (1991). {*120, 142, 164, 183, 280, 289, 462, 466, 471–473, 497*}

8

Tricks for generating other exactly solvable microgeometries

This section presents a sampling of general techniques for using solutions of the conductivity or elasticity equations in a given microgeometry to generate associated solutions in related microgeometries. In addition to the methods discussed here, it should be mentioned that conformal transformations are useful for finding exact solutions for the fields, in particular, two-dimensional geometries: See Berdichevskii (1985), who found the exact solution for the fields in a regular checkerboard geometry; Obnosov (1996, 1999), who obtained the explicit solution for rectangular and triangular checkerboards, as well as for certain rectangular arrays of rectangles at a volume fraction of $1/4$; the many papers of Vigdergauz referred to in section 23.9 on page 481, who found various periodic microstructures where the field was constant within one phase; and Reuben, Smith, and Radchik (1995).

8.1. Modifying the material moduli so the field is not disturbed

Consider the formula (7.13) for the effective bulk modulus κ_* of the coated sphere assemblage. It does not depend on the shear modulus μ_1 of the core material. The physical reason for this is quite clear: Under an externally applied hydrostatic loading the displacement field (7.11) in the core of each coated sphere is a pure dilation with no shear component, and so the effective bulk modulus is not influenced by the shear modulus of phase 1. This is an example of a more general principle, which says that if we modify the material moduli in any way that leaves the field undisturbed, then the response of the composite to that average field will remain unchanged. Applied to elasticity, the principle says that if periodic stress fields $\boldsymbol{\tau}(\boldsymbol{x})$ and strain fields $\boldsymbol{\epsilon}(\boldsymbol{x})$ are found that solve the elasticity equations

$$\boldsymbol{\tau}(\boldsymbol{x}) = \boldsymbol{\mathcal{C}}(\boldsymbol{x})\boldsymbol{\epsilon}(\boldsymbol{x}), \quad \nabla \cdot \boldsymbol{\tau}(\boldsymbol{x}) = 0, \quad \boldsymbol{\epsilon}(\boldsymbol{x}) = [\nabla \boldsymbol{u}(\boldsymbol{x}) + (\nabla \boldsymbol{u}(\boldsymbol{x}))^T]/2,$$

in a medium with a periodic elasticity tensor $\boldsymbol{\mathcal{C}}(\boldsymbol{x})$, then these same fields solve the elasticity equations

$$\boldsymbol{\tau}(\boldsymbol{x}) = \boldsymbol{\mathcal{C}}'(\boldsymbol{x})\boldsymbol{\epsilon}(\boldsymbol{x}), \quad \nabla \cdot \boldsymbol{\tau}(\boldsymbol{x}) = 0, \quad \boldsymbol{\epsilon}(\boldsymbol{x}) = [\nabla \boldsymbol{u}(\boldsymbol{x}) + (\nabla \boldsymbol{u}(\boldsymbol{x}))^T]/2$$

in a new material with elasticity tensor

$$\boldsymbol{\mathcal{C}}'(\boldsymbol{x}) = \boldsymbol{\mathcal{C}}(\boldsymbol{x}) + \boldsymbol{\mathcal{A}}(\boldsymbol{x})$$

for any choice of the tensor field $\boldsymbol{\mathcal{A}}(\boldsymbol{x})$ such that

$$\boldsymbol{\mathcal{A}}(\boldsymbol{x})\boldsymbol{\epsilon}(\boldsymbol{x}) = 0. \tag{8.1}$$

In addition, since the effective tensors govern the relation between the average fields, we deduce that the effective elasticity tensor $\mathcal{C}'_*$ of the new material satisfies

$$\mathcal{C}'_*\langle\epsilon\rangle = \mathcal{C}_*\langle\epsilon\rangle, \tag{8.2}$$

where $\langle\epsilon\rangle$ denotes the average over space of the known field $\epsilon(x)$.

In the coated sphere geometry we may, for example, take

$$\mathcal{A}(x) = 2(\mu'_1 - \mu_1)\chi_1(x)\left[\mathcal{I} - \frac{1}{3}I \otimes I\right]. \tag{8.3}$$

Then (8.1) is satisfied because the strain generated by the displacement field (7.8) is proportional to I in phase 1 and (8.3) implies that

$$\mathcal{A}(x)I = 0.$$

It follows from (8.2) that the effective bulk modulus κ_* does not change when the shear modulus of phase 1 is shifted from μ_1 to μ'_1.

In the special case where $\mathcal{C}(x)$ is independent of x, the elasticity equations are satisfied with a constant strain field $\epsilon(x) = V$. The uniform field relation implied by (8.2), that $\mathcal{C}'_*V = \mathcal{C}_*V$, also follows from the uniform field argument discussed in section 5.1 on page 75, because $W = \mathcal{C}'(x)V$ is independent of x. Conversely, any uniform field relation can be regarded as a corollary of the fact that we are free to modify the material so that the field is not disturbed.

8.2. Assemblages of coated spheres and coated ellipsoids with anisotropic cores

Naturally we can apply these same arguments to the conductivity problem. In particular, consider the assemblage of coated spheres each consisting of a core of conductivity $\sigma_1 I$ surrounded by a shell of conductivity $\sigma_2 I$. Since the field inside the core is uniform and aligned with the applied field, there will be no change to the effective conductivity in the direction of the applied field e_0 if the conductivity tensor of the core is modified from $\sigma_1 I$ to

$$\sigma_1 = \sigma_1 I + A, \quad \text{provided } Ae_0 = 0. \tag{8.4}$$

In other words, we can consider coated sphere geometries where the core is anisotropic with the same orientation in each coated sphere. Let σ_1 denote the conductivity tensor of the core phase, and let $\sigma_2 = \sigma_2 I$ denote the conductivity of the matrix phase. Then, when the applied field e_0 is an eigenvector of σ_1 with eigenvalue σ_1, (8.4) implies that the effective tensor σ_* of this coated sphere geometry satisfies

$$\sigma_* e_0 = \sigma_* e_0,$$

where the eigenvalue σ_* is given by (7.6). Since this same argument applies to all three choices of the eigenvector e_0, we deduce that the effective tensor σ_* is given implicitly by the formula

$$f_1\sigma_2(\sigma_2 I - \sigma_*)^{-1} = \sigma_2(\sigma_2 I - \sigma_1)^{-1} - f_2 I/3.$$

Additional care is required to apply the above arguments to an assemblage of coated ellipsoids when the eigenvectors of the conductivity tensor σ_1 of the core phase are not aligned

with the axes of the ellipse. However, the basic idea remains the same: A solution of the conductivity equations in an ellipsoid assemblage with isotropic core conductivity $\sigma_1 \boldsymbol{I}$ is also a solution of the conductivity equations in an assemblage with anisotropic core conductivity $\boldsymbol{\sigma}_1$, provided that the uniform field inside the core of the ellipsoids is an eigenvector of $\boldsymbol{\sigma}_1$ with eigenvalue σ_1.

Since the field inside the core phase is obviously important in this problem, it is useful to introduce the polarization field

$$\boldsymbol{p}(\boldsymbol{x}) = (\boldsymbol{\sigma}(\boldsymbol{x}) - \sigma_2 \boldsymbol{I})\boldsymbol{e}(\boldsymbol{x}) = \boldsymbol{j}(\boldsymbol{x}) - \sigma_2 \boldsymbol{e}(\boldsymbol{x}), \tag{8.5}$$

which takes the values

$$\begin{aligned} \boldsymbol{p}(\boldsymbol{x}) &= (\boldsymbol{\sigma}_1 - \sigma_2 \boldsymbol{I})\boldsymbol{e}(\boldsymbol{x}) \quad \text{in the ellipsoid cores,} \\ &= 0 \qquad \text{in the ellipsoid coating.} \end{aligned}$$

By averaging both sides of (8.5) we see that

$$\langle \boldsymbol{p}(\boldsymbol{x}) \rangle = (\boldsymbol{\sigma}_* - \sigma_2 \boldsymbol{I}) \langle \boldsymbol{e}(\boldsymbol{x}) \rangle.$$

One often selects the average field $\langle \boldsymbol{e} \rangle$ and then measures the average polarization $\langle \boldsymbol{p} \rangle$. However, one could equally well select $\langle \boldsymbol{p} \rangle$ and measure the average field

$$\langle \boldsymbol{e} \rangle = (\boldsymbol{\sigma}_* - \sigma_2 \boldsymbol{I})^{-1} \langle \boldsymbol{p} \rangle.$$

Let us choose the average polarization aligned with an eigenvector of $\boldsymbol{\sigma}_1$,

$$\boldsymbol{\sigma}_1 \langle \boldsymbol{p} \rangle = \sigma_1 \langle \boldsymbol{p} \rangle, \tag{8.6}$$

where here σ_1 represents the associated eigenvalue. As the field inside the ellipsoidal core is uniform, it follows that when the average polarization field is chosen so that (8.6) is satisfied then the solution to the field equations remains unperturbed when we change the moduli inside the core from $\sigma_1 \boldsymbol{I}$ to $\boldsymbol{\sigma}_1$. Accordingly, the average field $\langle \boldsymbol{e} \rangle$ does not change, implying that $\boldsymbol{\sigma}_*$ satisfies

$$(\boldsymbol{\sigma}_* - \sigma_2 \boldsymbol{I})^{-1} \langle \boldsymbol{p} \rangle = [(\sigma_1 - \sigma_2)^{-1} \boldsymbol{I} + f_2 \boldsymbol{M}/\sigma_2] \langle \boldsymbol{p} \rangle / f_1, \tag{8.7}$$

where $\boldsymbol{M}$ is given by (7.55). Thus the action of $(\boldsymbol{\sigma}_* - \sigma_2 \boldsymbol{I})^{-1}$ on any eigenvector of $\boldsymbol{\sigma}_1$ is given by (8.7), where σ_1 is the associated eigenvalue. By considering all eigenvectors of $\boldsymbol{\sigma}_1$ we see that $(\boldsymbol{\sigma}_* - \sigma_2 \boldsymbol{I})^{-1}$ and hence $\boldsymbol{\sigma}_*$ are completely determined by (8.7). In fact there is a simple expression for $\boldsymbol{\sigma}_*$,

$$f_1 (\boldsymbol{\sigma}_* - \sigma_2 \boldsymbol{I})^{-1} = (\boldsymbol{\sigma}_1 - \sigma_2 \boldsymbol{I})^{-1} + f_2 \boldsymbol{M}/\sigma_2, \tag{8.8}$$

which is easy to verify by noting that $(\boldsymbol{\sigma}_* - \sigma_2 \boldsymbol{I})^{-1}$ given by (8.8) satisfies (8.7).

8.3. Making an affine coordinate transformation

Let us consider how the conductivity equations

$$\boldsymbol{j}(\boldsymbol{x}) = \boldsymbol{\sigma}(\boldsymbol{x})\boldsymbol{e}(\boldsymbol{x}), \quad \nabla \cdot \boldsymbol{j}(\boldsymbol{x}) = 0, \quad \boldsymbol{e}(\boldsymbol{x}) = \nabla \phi(\boldsymbol{x}),$$

transform under an affine change of coordinates from $\boldsymbol{x}$ to

$$\boldsymbol{x}' = \boldsymbol{A}\boldsymbol{x},$$

where the transformation matrix $\boldsymbol{A}$ does not depend on $\boldsymbol{x}$. Using the chain rule of differentiation, we have

$$\begin{aligned}\frac{\partial \phi}{\partial x_i} &= \frac{\partial x'_k}{\partial x_i}\frac{\partial \phi}{\partial x'_k} = A_{ki}\frac{\partial \phi}{\partial x'_k},\\ \frac{\partial j_i}{\partial x_i} &= \frac{\partial x'_k}{\partial x_i}\frac{\partial j_i}{\partial x'_k} = A_{ki}\frac{\partial j_i}{\partial x'_k},\end{aligned} \tag{8.9}$$

where sums over repeated indices are implied. Thus we have

$$\nabla\phi(\boldsymbol{x}) = \boldsymbol{A}^T\nabla'\phi(\boldsymbol{x}), \quad \nabla\cdot\boldsymbol{j} = \nabla'\cdot(\boldsymbol{A}\boldsymbol{j}),$$

in which ∇' is the differential operator

$$\nabla' = \left(\frac{\partial}{\partial x'_1}, \frac{\partial}{\partial x'_2}, \frac{\partial}{\partial x'_3}\right).$$

Consequently the fields

$$\boldsymbol{j}'(\boldsymbol{x}') \equiv \boldsymbol{A}\boldsymbol{j}(\boldsymbol{x}), \quad \boldsymbol{e}'(\boldsymbol{x}') \equiv (\boldsymbol{A}^T)^{-1}\boldsymbol{e}(\boldsymbol{x}), \quad \phi'(\boldsymbol{x}') \equiv \phi(\boldsymbol{x}), \quad \text{where } \boldsymbol{x} = \boldsymbol{A}^{-1}\boldsymbol{x}', \tag{8.10}$$

satisfy the conductivity equations

$$\boldsymbol{j}'(\boldsymbol{x}') = \boldsymbol{\sigma}'(\boldsymbol{x}')\boldsymbol{e}'(\boldsymbol{x}'), \quad \nabla'\cdot\boldsymbol{j}'(\boldsymbol{x}') = 0, \quad \boldsymbol{e}'(\boldsymbol{x}') = \nabla'\phi'(\boldsymbol{x}')$$

in a medium with conductivity tensor

$$\boldsymbol{\sigma}'(\boldsymbol{x}') = \boldsymbol{A}\boldsymbol{\sigma}(\boldsymbol{x})\boldsymbol{A}^T. \tag{8.11}$$

Also by averaging the fields in (8.10) we see that

$$\langle\boldsymbol{j}'\rangle' = \boldsymbol{\sigma}'_*\langle\boldsymbol{e}'\rangle',$$

where

$$\boldsymbol{\sigma}'_* = \boldsymbol{A}\boldsymbol{\sigma}_*\boldsymbol{A}^T \tag{8.12}$$

is the effective tensor of the new medium and the angular brackets $\langle\cdot\rangle'$ denote an average over $\boldsymbol{x}'$. In other words, if a material with conductivity tensor $\boldsymbol{\sigma}(\boldsymbol{x})$ has effective tensor $\boldsymbol{\sigma}_*$, then a material with conductivity tensor $\boldsymbol{\sigma}'(\boldsymbol{x}')$ given by (8.11) will have effective conductivity tensor $\boldsymbol{\sigma}'_*$ given by (8.12).

For example, consider a two-phase medium with conductivity tensor

$$\boldsymbol{\sigma}(\boldsymbol{x}) = \chi_1(\boldsymbol{x})\boldsymbol{\sigma}_1 + \chi_2(\boldsymbol{x})\boldsymbol{\sigma}_2,$$

where $\chi_1(\boldsymbol{x}) = 1 - \chi_2(\boldsymbol{x})$ is the usual characteristic functions representing the microstructure of phase 1. By taking

$$\boldsymbol{A} = (\boldsymbol{\sigma}_2)^{-1/2},$$

we transform to a conductivity problem with conductivity tensor

$$\boldsymbol{\sigma}'(\boldsymbol{x}') = \chi_1(\boldsymbol{x})\boldsymbol{\sigma}'_1 + \chi_2(\boldsymbol{x})\boldsymbol{I}, \quad \text{where } \boldsymbol{x} = \boldsymbol{\sigma}_2^{1/2}\boldsymbol{x}',$$

which is isotropic in phase 2, and takes the value

$$\boldsymbol{\sigma}_1' = (\boldsymbol{\sigma}_2)^{-1/2}\boldsymbol{\sigma}_1(\boldsymbol{\sigma}_2)^{-1/2}$$

in phase 1. Thus in a two-phase composite (with each phase having a constant orientation) we can always transform to an equivalent conductivity problem where one of the phases has an isotropic conductivity tensor. Conversely, if the conductivity equations have an exact solution for a two-phase composite with an isotropically conducting phase 2, then we can use these affine transformations to generate a family of associated microstructures where the conductivity equations have an exact solution but phase 2 is anisotropic.

Following, for example, Olver (1988); Milgrom and Shtrikman (1992); and Alphutova, Movchan, and Nazarov (1991) we can also apply affine transformations to the elasticity equations. Introducing the new displacement field,

$$\boldsymbol{u}'(\boldsymbol{x}') = (\boldsymbol{A}^{-1})^T\boldsymbol{u}(\boldsymbol{x}), \quad \text{where } \boldsymbol{x}' = \boldsymbol{A}\boldsymbol{x},$$

the associated strain field

$$\boldsymbol{\epsilon}'(\boldsymbol{x}') = [\nabla'\boldsymbol{u}'(\boldsymbol{x}') + (\nabla'\boldsymbol{u}'(\boldsymbol{x}'))^T] = (\boldsymbol{A}^{-1})^T\boldsymbol{\epsilon}(\boldsymbol{x})\boldsymbol{A}^{-1},$$

and the new stress field

$$\boldsymbol{\tau}'(\boldsymbol{x}') = \boldsymbol{A}\boldsymbol{\tau}(\boldsymbol{x})\boldsymbol{A}^T,$$

we see that these fields solve the elasticity equations

$$\boldsymbol{\tau}' = \boldsymbol{\mathcal{C}}'\boldsymbol{\epsilon}', \quad \nabla'\cdot\boldsymbol{\tau} = 0, \quad \boldsymbol{\epsilon}' = [\nabla'\boldsymbol{u}' + (\nabla'\boldsymbol{u}')^T],$$

in a medium with elasticity tensor

$$\{\boldsymbol{\mathcal{C}}'(\boldsymbol{x}')\}_{ijk\ell} = \{\boldsymbol{A}\}_{im}\{\boldsymbol{A}\}_{jn}\{\boldsymbol{A}\}_{ko}\{\boldsymbol{A}\}_{\ell p}\{\boldsymbol{\mathcal{C}}(\boldsymbol{x})\}_{mnop}. \tag{8.13}$$

Also by averaging the fields we see that

$$\langle\boldsymbol{\tau}'\rangle' = \boldsymbol{\mathcal{C}}_*'\langle\boldsymbol{\epsilon}'\rangle',$$

where

$$\{\boldsymbol{\mathcal{C}}_*'\}_{ijk\ell} = \{\boldsymbol{A}\}_{im}\{\boldsymbol{A}\}_{jn}\{\boldsymbol{A}\}_{ko}\{\boldsymbol{A}\}_{\ell p}\{\boldsymbol{\mathcal{C}}_*\}_{mnop}. \tag{8.14}$$

Therefore, if a material with elasticity tensor $\boldsymbol{\mathcal{C}}(\boldsymbol{x})$ has effective tensor $\boldsymbol{\mathcal{C}}_*$, then a material with elasticity tensor $\boldsymbol{\mathcal{C}}'(\boldsymbol{x}')$ given by (8.13) will have effective elasticity tensor $\boldsymbol{\mathcal{C}}_*'$ given by (8.14). In a two-phase composite it is generally impossible to transform to an equivalent problem where one of the phases is elastically isotropic. Milgrom and Shtrikman (1992) note that this is possible if and only if the elasticity tensor of one of the phases can be expressed in the form

$$\{\boldsymbol{\mathcal{C}}\}_{ijk\ell} = \mu(\{\boldsymbol{D}\}_{ik}\{\boldsymbol{D}\}_{j\ell} + \{\boldsymbol{D}\}_{i\ell}\{\boldsymbol{D}\}_{jk}) + \lambda\{\boldsymbol{D}\}_{ij}\{\boldsymbol{D}\}_{k\ell}$$

for some choice of constants μ, λ and some choice of positive-definite symmetric matrix $\boldsymbol{D}$. To transform such a tensor to an isotropic tensor one takes $\boldsymbol{A} = \boldsymbol{D}^{-1/2}$. In two dimensions Olver (1988) and Alphutova, Movchan, and Nazarov (1991) have shown that one can transform an arbitrary positive-definite elasticity tensor to one with orthotropic symmetry [see also Milton and Movchan (1995)].

8.4. The conductivity of an assemblage of coated ellipsoids with an anisotropic core and coating

Suppose that we want an exact solution for the conductivity equations in an assemblage of coated ellipsoids where the core and coating have symmetric positive-definite conductivity tensors $\boldsymbol{\sigma}_1'$ and $\boldsymbol{\sigma}_2'$. Then starting from an assemblage of confocal coated ellipsoids each with an isotropic coating of conductivity $\boldsymbol{\sigma}_2 = \boldsymbol{I}$ surrounding an anisotropic core of conductivity $\boldsymbol{\sigma}_1$ given by

$$\boldsymbol{\sigma}_1 = (\boldsymbol{\sigma}_2')^{-1/2}\boldsymbol{\sigma}_1'(\boldsymbol{\sigma}_2')^{-1/2},$$

we can set

$$\boldsymbol{A} = (\boldsymbol{\sigma}_2')^{1/2}$$

and transform to an assemblage of coated ellipsoids with a coating of conductivity $\boldsymbol{\sigma}_2'$ surrounding a core of conductivity $\boldsymbol{\sigma}_1'$. In this process the effective conductivity of the assemblage is transformed from $\boldsymbol{\sigma}_*$ to

$$\boldsymbol{\sigma}_*' = (\boldsymbol{\sigma}_2')^{1/2}\boldsymbol{\sigma}_*(\boldsymbol{\sigma}_2')^{1/2}.$$

So from the formula (8.8) for $\boldsymbol{\sigma}_*$ we see that $\boldsymbol{\sigma}_*'$ satisfies

$$f_1(\boldsymbol{\sigma}_*' - \boldsymbol{\sigma}_2')^{-1} = (\boldsymbol{\sigma}_1' - \boldsymbol{\sigma}_2')^{-1} + f_2(\boldsymbol{\sigma}_2')^{-1/2}\boldsymbol{M}(\boldsymbol{\sigma}_2')^{-1/2}, \tag{8.15}$$

where $\boldsymbol{M}$ is given by (7.55) and depends only on the geometry of the original prototype confocal coated ellipsoid. The core and exterior surfaces of this confocal coated ellipsoid are described by the equations

$$\boldsymbol{x}\cdot(\boldsymbol{L}_c)^{-1}\boldsymbol{x} = 1, \qquad \boldsymbol{x}\cdot(\boldsymbol{L}_e)^{-1}\boldsymbol{x} = 1,$$

where the matrices $\boldsymbol{L}_c$ and $\boldsymbol{L}_e$ depend on the semi-axis lengths of the ellipsoid in the following way:

$$\boldsymbol{L}_c = \begin{pmatrix} \ell_{c1}^2 & 0 & 0 \\ 0 & \ell_{c2}^2 & 0 \\ 0 & 0 & \ell_{c3}^2 \end{pmatrix}, \qquad \boldsymbol{L}_e = \begin{pmatrix} \ell_{e1}^2 & 0 & 0 \\ 0 & \ell_{e2}^2 & 0 \\ 0 & 0 & \ell_{e3}^2 \end{pmatrix}. \tag{8.16}$$

These transform to the surfaces

$$\boldsymbol{x}'\cdot(\boldsymbol{L}_c')^{-1}\boldsymbol{x}' = 1, \qquad \boldsymbol{x}'\cdot(\boldsymbol{L}_e')^{-1}\boldsymbol{x}' = 1,$$

describing the core and exterior surfaces of the ellipsoid in the x' coordinates, where

$$\boldsymbol{L}_c' = \boldsymbol{A}\boldsymbol{L}_c\boldsymbol{A} = (\boldsymbol{\sigma}_2')^{1/2}\boldsymbol{L}_c(\boldsymbol{\sigma}_2')^{1/2}, \qquad \boldsymbol{L}_e' = \boldsymbol{A}\boldsymbol{L}_e\boldsymbol{A} = (\boldsymbol{\sigma}_2')^{1/2}\boldsymbol{L}_e(\boldsymbol{\sigma}_2')^{1/2}. \tag{8.17}$$

From (7.56) and (8.16) we see that

$$\boldsymbol{L}_e = \boldsymbol{L}_c + \alpha\boldsymbol{I},$$

which implies that the matrices $\boldsymbol{L}_c'$ and $\boldsymbol{L}_e'$ satisfy

$$\boldsymbol{L}_e' = \boldsymbol{L}_c' + \alpha\boldsymbol{\sigma}_2'. \tag{8.18}$$

In other words, an assemblage of coated ellipsoids in which both the core material and coating are anisotropic, with conductivity tensors $\boldsymbol{\sigma}_1'$ and $\boldsymbol{\sigma}_2'$, has an exact solution for its effective conductivity tensor $\boldsymbol{\sigma}_*'$ [given by (8.15)] provided the matrices $\boldsymbol{L}_c'$ and $\boldsymbol{L}_e'$ describing

the core and exterior surfaces of the prototype ellipsoid satisfy (8.18) for some positive choice of α. Every other coated ellipsoid in the assemblage must be similar to the prototype aside from a scale factor and must have the same orientation. The core and exterior surfaces of the coated ellipsoid are not in general confocal (except when $\boldsymbol{\sigma}_2'$ is isotropic) and need not have the same principal axes (see figure 8.1). The geometry of the prototype coated ellipsoid is completely determined from (8.18) if we specify the conductivity tensor $\boldsymbol{\sigma}_2'$, the orientation and semi-axis lengths of the elliptical core (which determine $\boldsymbol{L}_c'$), and the volume fraction f_1 occupied by the core (which determines α). The tensor $\boldsymbol{M}$ entering the expression (8.15) for the effective tensor $\boldsymbol{\sigma}_*'$ is obtained from the formula (7.55), in which the lengths ℓ_{cj} and ℓ_{ej}, $j = 1, 2, 3$ (that determine the depolarization tensors $\boldsymbol{D}_c$ and $\boldsymbol{D}_e$) are obtained from the tensors $\boldsymbol{L}_c$ and $\boldsymbol{L}_e$ given implicitly by (8.17).

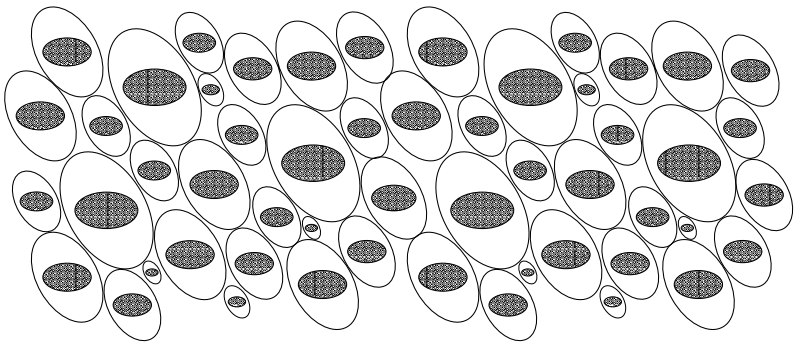

Figure 8.1. The stretched confocal coated ellipsoid assemblage. In each ellipsoid phase 1 occupies the cross-hatched core, while phase 2 occupies the coating. The symmetric conductivity tensors $\boldsymbol{\sigma}_1'$ and $\boldsymbol{\sigma}_2'$ of the phases and the eccentricity and orientation of the ellipsoid cores can be independently and arbitrarily chosen. When the coated ellipsoids fill all space, (8.15) provides an exact formula for the effective conductivity tensor.

The assemblage can of course be regarded as a suspension of ellipsoids embedded in a matrix of the coating material. With this interpretation, (8.15) gives an exact formula for the effective conductivity tensor of a special configuration of anisotropically conducting ellipsoidal inclusions of phase 1 embedded in an anisotropically conducting matrix of phase 2, where the tensor $\boldsymbol{M}$ entering this formula just depends on the volume fraction f_1, and on the orientation and shape of the elliptical inclusions. The ellipsoidal inclusions (which all have the same orientation and shape) need to have a variety of sizes ranging to the infinitesimal and need to be positioned so that the composite can be regarded as an assemblage of coated ellipsoids satisfying (8.18)

8.5. Making a curvilinear coordinate transformation†

Instead of making an affine transformation, let us make a general curvilinear coordinate transformation from $\boldsymbol{x}$ to a new set of coordinates,

$$\boldsymbol{x}'(\boldsymbol{x}) = \boldsymbol{B}\boldsymbol{x} + \boldsymbol{v}(\boldsymbol{x}), \tag{8.19}$$

where $\boldsymbol{B}$ is a fixed matrix and $\boldsymbol{v}(\boldsymbol{x})$ is a periodic function of $\boldsymbol{x}$ with the same periodicity as the composite such that the matrix $\boldsymbol{A} = (\nabla \boldsymbol{x}')^T$ with elements

$$A_{ki} = \frac{\partial x'_k}{\partial x_i} = B_{ki} + \frac{\partial v_k}{\partial x_i} \tag{8.20}$$

is nonsingular for all $\boldsymbol{x}$. (This ensures that the transformation is one-to-one.) The equations (8.9) still hold, but $\nabla \cdot \boldsymbol{j}$ can no longer be identified with $\nabla' \cdot (\boldsymbol{A}\boldsymbol{j})$ because $\boldsymbol{A}$ depends on $\boldsymbol{x}'$. Instead we use the identity

$$\frac{\partial}{\partial x'_k}\left(a^{-1}\frac{\partial x'_k}{\partial x_i}\right) = 0, \quad \text{where } a = \det \boldsymbol{A}, \tag{8.21}$$

which results because $a^{-1}\boldsymbol{A}^T$ is the matrix of cofactors of $\boldsymbol{A}^{-1}$. Specifically, in a three-dimensional medium we have

$$a^{-1}\frac{\partial x'_k}{\partial x_i} = \epsilon_{k\ell m}\epsilon_{irs}\frac{\partial x_r}{\partial x'_\ell}\frac{\partial x_s}{\partial x'_m},$$

in which ϵ_{ijk} is the completely antisymmetric Levi-Civita tensor with elements

$$\begin{aligned}\epsilon_{ijk} &= 1 \text{ if } i, j, k \text{ are an even permutation of } 1, 2, 3,\\ &= -1 \text{ if } i, j, k \text{ are an odd permutation of } 1, 2, 3,\\ &= 0 \text{ otherwise.}\end{aligned}$$

It then follows that

$$\frac{\partial}{\partial x'_k}\left(a^{-1}\frac{\partial x'_k}{\partial x_i}\right) = \epsilon_{k\ell m}\epsilon_{irs}\left(\frac{\partial^2 x_r}{\partial x'_k \partial x'_\ell}\frac{\partial x_s}{\partial x'_m} + \frac{\partial^2 x_s}{\partial x'_k \partial x'_m}\frac{\partial x_r}{\partial x'_\ell}\right) = 0,$$

which establishes (8.21). This now allows us to write

$$A_{ki}\frac{\partial j_i}{\partial x'_k} = a\frac{\partial}{\partial x'_k}\left(A_{ki}\, j_i/a\right),$$

and consequently (8.9) implies that

$$\nabla\phi = \boldsymbol{A}^T\nabla'\phi, \quad \nabla \cdot \boldsymbol{j} = a\nabla' \cdot (\boldsymbol{A}\boldsymbol{j}/a).$$

So the fields

$$\boldsymbol{j}' \equiv \boldsymbol{A}\boldsymbol{j}/a, \quad \boldsymbol{e}' \equiv (\boldsymbol{A}^T)^{-1}\boldsymbol{e}, \quad \phi' \equiv \phi,$$

when expressed as functions of $\boldsymbol{x}'$ satisfy the conductivity equations

$$\boldsymbol{j}' = \boldsymbol{\sigma}'\boldsymbol{e}', \quad \nabla' \cdot \boldsymbol{j}' = 0, \quad \boldsymbol{e}' = \nabla'\phi'$$

in a medium with conductivity tensor

$$\boldsymbol{\sigma}' = \boldsymbol{A}\boldsymbol{\sigma}\boldsymbol{A}^T/\det \boldsymbol{A}. \tag{8.22}$$

In this medium the average over $\boldsymbol{x}'$ of the k-th component the current field $\boldsymbol{j}'$ is

$$\langle j'_k\rangle' = \langle a j'_k\rangle/\det \boldsymbol{B} = \langle(\nabla x'_k) \cdot \boldsymbol{j}\rangle/\det \boldsymbol{B} = \langle\nabla x'_k\rangle \cdot \langle\boldsymbol{j}\rangle/\det \boldsymbol{B} = B_{ki}\langle j_i\rangle/\det \boldsymbol{B}.$$

The potential $\phi = \phi'$ is the sum of a part $\langle \boldsymbol{e} \rangle \cdot \boldsymbol{x}$ linear in $\boldsymbol{x}$ and a part periodic in $\boldsymbol{x}$. By making the substitution (8.19) we see that it can be re-expressed as the sum of a part $\langle \boldsymbol{e} \rangle \cdot \boldsymbol{B}^{-1}\boldsymbol{x}'$ linear in $\boldsymbol{x}'$ and a part periodic in $\boldsymbol{x}'$. Since the coefficient of the linear part can be identified with the average over $\boldsymbol{x}'$ of the electric field $\boldsymbol{e}'$, we conclude that

$$\langle \boldsymbol{e}' \rangle' = (\boldsymbol{B}^T)^{-1} \langle \boldsymbol{e} \rangle.$$

From these expressions for the average fields, it follows that $\langle \boldsymbol{j}' \rangle' = \boldsymbol{\sigma}'_* \langle \boldsymbol{e}' \rangle'$, where

$$\boldsymbol{\sigma}'_* = \boldsymbol{B}\boldsymbol{\sigma}_*\boldsymbol{B}^T / \det \boldsymbol{B} \tag{8.23}$$

is the effective tensor of the new medium. Moreover we see from (8.20) that $\boldsymbol{B} = \langle \boldsymbol{A} \rangle$, in which the average is over $\boldsymbol{x}$.

These coordinate transformations provide equivalences between a large family of conductivity problems. If the original medium has a locally isotropic conductivity tensor $\boldsymbol{\sigma}(\boldsymbol{x}) = \sigma(\boldsymbol{x})\boldsymbol{I}$, then the new medium will not be locally isotropic since this would require the transformation to be conformal, and there are no nontrivial periodic conformal mappings that do not have singularities.

As a simple example of these transformations, consider a two-dimensional homogeneous conducting medium with conductivity tensor $\boldsymbol{\sigma}(\boldsymbol{x}) = \boldsymbol{I}$ and take new coordinates

$$(x'_1, x'_2) = (x_1 + h(x_1), x_2 + h(x_2)),$$

where $h(y)$ is the periodic function

$$\begin{aligned} h(y) &= y/2 && \text{for } 0 \le y \le 1, \\ &= 1 - y/2 && \text{for } 1 \le y \le 2, \\ &= h(y-2) && \text{for all } y. \end{aligned}$$

Then $\boldsymbol{B} = \boldsymbol{I}$ and $\boldsymbol{A}(\boldsymbol{x})$ is periodic taking the four values

$$\begin{pmatrix} 3/2 & 0 \\ 0 & 3/2 \end{pmatrix}, \quad \begin{pmatrix} 3/2 & 0 \\ 0 & 1/2 \end{pmatrix}, \quad \begin{pmatrix} 1/2 & 0 \\ 0 & 3/3 \end{pmatrix}, \quad \begin{pmatrix} 1/2 & 0 \\ 0 & 1/2 \end{pmatrix}.$$

The associated conductivity field $\boldsymbol{\sigma}'(\boldsymbol{x}')$ is periodic and within the unit cell of periodicity $0 \le x'_1 \le 2, 0 \le x'_2 \le 2$ takes the four values

$$\begin{pmatrix} 1 & 0 \\ 0 & 1 \end{pmatrix}, \quad \begin{pmatrix} 3 & 0 \\ 0 & 1/3 \end{pmatrix}, \quad \begin{pmatrix} 1/3 & 0 \\ 0 & 3 \end{pmatrix}, \quad \begin{pmatrix} 1 & 0 \\ 0 & 1 \end{pmatrix}$$

in respectively the square $0 \le x'_1 \le 3/2$, $0 \le x'_2 \le 3/2$; the rectangle $0 \le x'_1 \le 3/2$, $3/2 \le x'_2 \le 2$; the rectangle $3/2 \le x'_1 \le 2$, $0 \le x'_2 \le 3/2$; and the square $3/2 \le x'_1 \le 2$, $3/2 \le x'_2 \le 2$. According to (8.23), the effective conductivity of this new medium is $\boldsymbol{\sigma}'_* = \boldsymbol{I}$. For this particular example the same result can be deduced from symmetry and duality: By symmetry $\boldsymbol{\sigma}'_*$ must be proportional to the identity tensor, and by duality (see section 3.3 on page 50) $\det \boldsymbol{\sigma}_* = 1$ because $\det \boldsymbol{\sigma}'(\boldsymbol{x}') = 1$ for all $\boldsymbol{x}'$. Other choices of the transformation also yield composites having $\det \boldsymbol{\sigma}_* = 1$ since (8.22) implies that $\det \boldsymbol{\sigma}'(\boldsymbol{x}') = 1$ when $\boldsymbol{\sigma}(\boldsymbol{x}) = \boldsymbol{I}$ for all $\boldsymbol{x}$.

8.6. Quasiconformal mappings

In the example of the previous section we saw how the conductivity problem in a certain two-dimensional anisotropic medium is equivalent to a trivial conductivity problem in a homogeneous medium. What is more surprising is the result of Astala and Nesi (2001) that (subject to minor technical assumptions) the conductivity problem in any two-dimensional anisotropic medium can be transformed to an equivalent problem in a locally isotropic conducting medium. Only a brief outline of the proof will be given here; for more details the reader is referred to the original paper, and the related papers of Nesi (1996, 1998). In those papers the transformation was used to obtain optimal bounds on the effective conductivity of a two-dimensional composite containing an isotropic phase mixed in fixed proportion with a polycrystalline phase (see section 23.8 on page 480).

Suppose that we are given a problem with a real, symmetric matrix-valued periodic conductivity tensor field $\boldsymbol{\sigma}(\boldsymbol{x})$ having eigenvalues $\lambda_2(\boldsymbol{x}) \geq \lambda_1(\boldsymbol{x}) > 0$ and with

$$K = \sup_{\boldsymbol{x}} \sqrt{\lambda_2(\boldsymbol{x})/\lambda_1(\boldsymbol{x})} \geq 1$$

being finite. An associated conductivity tensor field

$$\boldsymbol{\sigma}^{\mathcal{Q}}(\boldsymbol{x}) = \boldsymbol{\sigma}(\boldsymbol{x})/\sqrt{\det \boldsymbol{\sigma}(\boldsymbol{x})} \tag{8.24}$$

is introduced, which has unit determinant. From a pair of potentials $\phi^{\mathcal{Q}}(\boldsymbol{x})$ and $\psi^{\mathcal{Q}}(\boldsymbol{x})$ that solve the affiliated conductivity problem

$$\boldsymbol{R}_{\perp} \nabla \psi^{\mathcal{Q}} = \boldsymbol{\sigma}^{\mathcal{Q}} \nabla \phi^{\mathcal{Q}} \tag{8.25}$$

(and which are such that $\nabla \phi^{\mathcal{Q}}$ and $\nabla \psi^{\mathcal{Q}}$ are periodic and nonzero) we construct the mapping $\boldsymbol{x}'(\boldsymbol{x}) = (\phi^{\mathcal{Q}}(\boldsymbol{x}), \psi^{\mathcal{Q}}(\boldsymbol{x}))$.

It turns out that this mapping is one-to-one and continuous and that its inverse is also one-to-one and continuous, that is, it is a homeomorphism. Moreover, it is a K-quasiconformal mapping. To show the latter, following Alessandrini and Nesi (2000), one observes that (8.25) and the fact that $\det \boldsymbol{\sigma}^{\mathcal{Q}}(\boldsymbol{x}) = 1$ imply that

$$\boldsymbol{\sigma}^{\mathcal{Q}} \nabla \psi^{\mathcal{Q}} = -\boldsymbol{R}_{\perp} \nabla \phi^{\mathcal{Q}}.$$

This can be combined with (8.25) to form the single equation

$$\boldsymbol{\sigma}^{\mathcal{Q}} \boldsymbol{A}^T = \boldsymbol{R}_{\perp} \boldsymbol{A}^T \boldsymbol{R}_{\perp}^T = \boldsymbol{A}^{-1} \det \boldsymbol{A}, \quad \text{where } \boldsymbol{A}(\boldsymbol{x}) = [\nabla \boldsymbol{x}'(\boldsymbol{x})]^T, \tag{8.26}$$

in which the second identity is true for any 2×2 matrix $\boldsymbol{A}$. (This identity was also used in section 3.1 on page 47.) Equivalently we have

$$[\boldsymbol{A}(\boldsymbol{x})]^T \boldsymbol{A}(\boldsymbol{x}) = [\boldsymbol{\sigma}^{\mathcal{Q}}(\boldsymbol{x})]^{-1} \det \boldsymbol{A}(\boldsymbol{x}). \tag{8.27}$$

By definition, K-quasiconformal mappings are two-dimensional homeomorphisms such that

$$\nabla \boldsymbol{x}'(\boldsymbol{x}) [\nabla \boldsymbol{x}'(\boldsymbol{x})]^T = \boldsymbol{G}(\boldsymbol{x}) \det \nabla \boldsymbol{x}'(\boldsymbol{x})$$

for some real positive-definite symmetric matrix $\boldsymbol{G}(\boldsymbol{x})$ with unit determinant having its eigenvalues not greater than K for all $\boldsymbol{x}$. (The appearance of the transpose on the first term rather than the second term is a matter of notation. We have chosen to define $\nabla \boldsymbol{x}'$ as the matrix

having $\nabla x_1'$ and $\nabla x_2'$ as columns rather than as rows, so that $\boldsymbol{\sigma}^Q \nabla \boldsymbol{x}'(\boldsymbol{x})$ is the matrix $\boldsymbol{\sigma}^Q$ times the matrix $\nabla \boldsymbol{x}'(\boldsymbol{x})$.) Since $[\boldsymbol{\sigma}^Q(\boldsymbol{x})]^{-1}$ has a unit determinant and the largest eigenvalue $\sqrt{\lambda_2(\boldsymbol{x})/\lambda_1(\boldsymbol{x})} \leq K$, we see that the mapping is K-quasiconformal. Quasiconformal mappings have been studied extensively; for an introduction see Lehto and Virtanen (1973). The geometrical interpretation of K is roughly speaking the following. Away from singularities, infinitesimal circles are mapped to infinitesimal ellipses and K gives the maximum value of their eccentricity (the ratio of the longest axis to the shortest axis).

Now substituting (8.24) and (8.26) into (8.22) gives

$$\boldsymbol{\sigma}' = \frac{\boldsymbol{A}\boldsymbol{\sigma}\boldsymbol{A}^T}{\det \boldsymbol{A}} = \sqrt{\det \boldsymbol{\sigma}}\,\frac{\boldsymbol{A}\boldsymbol{\sigma}^Q\boldsymbol{A}^T}{\det \boldsymbol{A}} = \sqrt{\det \boldsymbol{\sigma}}\,\boldsymbol{I}. \tag{8.28}$$

Thus we have mapped to a problem where the conductivity tensor is locally isotropic. To obtain the relation between $\boldsymbol{\sigma}_*'$ and $\boldsymbol{\sigma}_*$ from (8.23) we need to determine $\boldsymbol{B} = \langle \boldsymbol{A} \rangle$, where the average is over $\boldsymbol{x}$. Associated with $\boldsymbol{\sigma}^Q(\boldsymbol{x})$ is an effective conductivity tensor $\boldsymbol{\sigma}_*^Q(\boldsymbol{x})$ that by definition governs the relation

$$\boldsymbol{R}_\perp \langle \nabla \psi^Q \rangle = \boldsymbol{\sigma}_*^Q \langle \nabla \phi^Q \rangle$$

between the average gradients. By manipulating this equation in the same way that (8.27) was obtained from (8.25) we find that

$$\boldsymbol{B}^T\boldsymbol{B} = (\boldsymbol{\sigma}_*^Q)^{-1} \det \boldsymbol{B}, \quad \text{where} \quad \boldsymbol{B} = [\langle \nabla \boldsymbol{x}'(\boldsymbol{x}) \rangle]^T = \langle \boldsymbol{A} \rangle.$$

This implies that

$$\boldsymbol{B} = \boldsymbol{R}^Q (\boldsymbol{\sigma}_*^Q)^{-1/2} \sqrt{\det \boldsymbol{B}}$$

for some choice of rotation matrix $\boldsymbol{R}^Q$ satisfying $(\boldsymbol{R}^Q)^T\boldsymbol{R}^Q = \boldsymbol{I}$. Thus the effective tensor $\boldsymbol{\sigma}_*^Q$ determines the overall distortion of the unit cell of periodicity. Substituting this back into (8.23) gives

$$\boldsymbol{\sigma}_*' = \boldsymbol{R}^Q (\boldsymbol{\sigma}_*^Q)^{-1/2} \boldsymbol{\sigma}_* (\boldsymbol{\sigma}_*^Q)^{-1/2} (\boldsymbol{R}^Q)^T. \tag{8.29}$$

Since $\det \boldsymbol{\sigma}^Q(\boldsymbol{x}) = 1$ for all $\boldsymbol{x}$, we have $\det \boldsymbol{\sigma}_*^Q = 1$. One immediate consequence of this, which follows from the fact that $\det \boldsymbol{\sigma}_*^Q = 1$ (because $\det \boldsymbol{\sigma}^Q(\boldsymbol{x}) = 1$ for all $\boldsymbol{x}$), is that $\det \boldsymbol{\sigma}_* = \det \boldsymbol{\sigma}_*'$.

Thus, aside from a rotation, the problem of determining $\boldsymbol{\sigma}_*$ has been broken into two: the problem of determining the effective conductivity tensor $\boldsymbol{\sigma}_*^Q$ of an anisotropic medium with local conductivity tensor having unit determinant, and the problem of determining the effective conductivity tensor $\boldsymbol{\sigma}_*'$ of a locally isotropic medium. Of course to solve the second problem we need to know the microgeometry, which requires determining the mapping $\boldsymbol{x}'(\boldsymbol{x})$, that is, obtaining a pair of potentials $\phi^Q(\boldsymbol{x})$ and $\psi^Q(\boldsymbol{x})$ that solve (8.25).

8.7. Generating microgeometries from fields

There is one other approach to finding conductivity tensor fields $\boldsymbol{\sigma}(\boldsymbol{x})$ for which a formula for the effective conductivity tensor $\boldsymbol{\sigma}_*$ can be easily obtained. The idea dates back to a paper of Marino and Spagnolo (1969). Here, in the context of three-dimensional conductivity, we begin with a generalization due to Dufour, Fabre, and Mossino (1996). The key step is to note that the fields

$$\boldsymbol{e}(\boldsymbol{x}) = \begin{pmatrix} c_1 a_1(x_1) \\ c_2 a_2(x_2) \\ c_3 a_3(x_3) \end{pmatrix} \qquad \boldsymbol{j}(\boldsymbol{x}) = \begin{pmatrix} c_1 b_1(x_2, x_3) \\ c_2 b_2(x_1, x_3) \\ c_3 b_3(x_1, x_2) \end{pmatrix}$$

are respectively curl free and divergence free for all choices of the constants c_1, c_2, and c_3 and for all choices of the functions $a_i(z)$ and $b_i(y, z)$, $i = 1, 2, 3$, which we take to be periodic and positive-valued. The constitutive law will be clearly satisfied if we choose our conductivity tensor to be

$$\boldsymbol{\sigma}(\boldsymbol{x}) = \begin{pmatrix} b_1(x_2, x_3)/a_1(x_1) & 0 & 0 \\ 0 & b_2(x_1, x_3)/a_2(x_2) & 0 \\ 0 & 0 & b_3(x_1, x_2)/a_3(x_3) \end{pmatrix}. \tag{8.30}$$

Then by taking averages of the fields it is clear that this medium will have the effective conductivity tensor

$$\boldsymbol{\sigma}_* = \begin{pmatrix} \langle b_1(x_2, x_3)\rangle/\langle a_1(x_1)\rangle & 0 & 0 \\ 0 & \langle b_2(x_1, x_3)\rangle/\langle a_2(x_2)\rangle & 0 \\ 0 & 0 & \langle b_3(x_1, x_2)\rangle/\langle a_3(x_3)\rangle \end{pmatrix}. \tag{8.31}$$

Of course an even wider range of exactly solvable microgeometries can be obtained by applying curvilinear coordinate transformations to these solutions.

In the particular case considered by Marino and Spagnolo, the locally isotropic conductivity tensor field $\boldsymbol{\sigma}(\boldsymbol{x}) = c_1(x_1)c_2(x_2)c_3(x_3)\boldsymbol{I}$ has effective conductivity

$$\boldsymbol{\sigma}_* = \begin{pmatrix} \langle c_2(x_2)c_3(x_3)\rangle/\langle 1/c_1(x_1)\rangle & 0 & 0 \\ 0 & \langle c_1(x_1)c_3(x_3)\rangle/\langle 1/c_2(x_2)\rangle & 0 \\ 0 & 0 & \langle c_1(x_1)c_2(x_2)\rangle/\langle 1/c_3(x_3)\rangle \end{pmatrix}.$$

The two-dimensional version of this result has an application to a periodic composite with a square unit cell, divided into four equal subsquares with conductivities labeled, in clockwise order, as σ_1, σ_2, σ_3, and σ_4. The effective conductivity tensor is diagonal, and when $\sigma_4 = \sigma_2\sigma_3/\sigma_1$ the result of Marino and Spagnolo implies that its eigenvalues are

$$\lambda_1^* = \frac{\sigma_2(\sigma_1 + \sigma_3)}{\sigma_1 + \sigma_2}, \quad \lambda_2^* = \frac{\sigma_3(\sigma_1 + \sigma_2)}{\sigma_1 + \sigma_3}.$$

For other values of σ_4 Mortola and Steffé (1985) obtained upper and lower bounds on λ_1^* and λ_2^*, and they conjectured that the exact values would be given by the square root of the product of their upper and lower bounds, resulting in the formulas

$$\begin{aligned} \lambda_1^* &= \sqrt{\frac{\sigma_1\sigma_2\sigma_3\sigma_4(1/\sigma_1 + 1/\sigma_2 + 1/\sigma_3 + 1/\sigma_4)(\sigma_1 + \sigma_4)(\sigma_2 + \sigma_3)}{(\sigma_1 + \sigma_2 + \sigma_3 + \sigma_4)(\sigma_1 + \sigma_2)(\sigma_3 + \sigma_4)}}, \\ \lambda_2^* &= \sqrt{\frac{\sigma_1\sigma_2\sigma_3\sigma_4(1/\sigma_1 + 1/\sigma_2 + 1/\sigma_3 + 1/\sigma_4)(\sigma_1 + \sigma_2)(\sigma_3 + \sigma_4)}{(\sigma_1 + \sigma_2 + \sigma_3 + \sigma_4)(\sigma_1 + \sigma_4)(\sigma_2 + \sigma_3)}}. \end{aligned} \tag{8.32}$$

Recently this conjecture was proved by Craster and Obnosov (2001), and Milton (2001). In the particular case when $\sigma_4 = \sigma_3 = \sigma_2$, the composite reduces to a square array of squares of conductivity σ_1 occupying a volume fraction $f_1 = 0.25$ in a matrix of conductivity σ_2. According to (8.32), the effective conductivity of this array is

$$\sigma_* = \sigma_2\sqrt{(\sigma_2 + 3\sigma_1)/(3\sigma_2 + \sigma_1)}. \tag{8.33}$$

Mortola and Steffé provided some numerical and analytical evidence in favor of this formula, and subsequently Obnosov (1999) proved that the effective conductivity is given exactly by

this expression. When $\sigma_1 = 100$ and $\sigma_2 = 1$, the formula gives $\sigma_* = 1.7094824061942$. Johan Helsing (private communication), using formulas (7) and (8) of Helsing (1998), has numerically calculated the result to be $\sigma_* = 1.7094824061(8)$ (digit within parenthesis not converged). So theory and numerical experiment certainly agree! For the square array of squares at other volume fractions, Kozlov and Vucans (1992) have obtained an implicit formula for σ_* when $\sigma_1 = 0$.

Other nonsymmetric forms of $\boldsymbol{\sigma}(\boldsymbol{x})$ yielding an exact result for $\boldsymbol{\sigma}_*$ were obtained by Dufour, Fabre, and Mossino (1996). More generally, following ideas of Tartar (1979) we might take periodic 3×3 matrix-valued fields $\boldsymbol{E}(\boldsymbol{x})$ and $\boldsymbol{J}(\boldsymbol{x})$ that are periodic and nonsingular and such that

$$\boldsymbol{E}(\boldsymbol{x}) = \nabla \boldsymbol{u}(\boldsymbol{x}), \qquad \nabla \cdot \boldsymbol{J}(\boldsymbol{x}) = 0,$$

for some choice of the vector potential $\boldsymbol{u}$, that is, the columns of $\boldsymbol{E}(\boldsymbol{x})$ are curl free and the columns of $\boldsymbol{J}(\boldsymbol{x})$ are divergence free. Then, for any choice of the vector $\boldsymbol{c}$, the conductivity equations are solved with

$$\boldsymbol{e}(\boldsymbol{x}) = \boldsymbol{E}(\boldsymbol{x})\boldsymbol{c}, \quad \boldsymbol{j}(\boldsymbol{x}) = \boldsymbol{J}(\boldsymbol{x})\boldsymbol{c}, \quad \boldsymbol{\sigma}(\boldsymbol{x}) = \boldsymbol{J}(\boldsymbol{x})[\boldsymbol{E}(\boldsymbol{x})]^{-1},$$

and consequently the effective tensor is

$$\boldsymbol{\sigma}_* = \langle \boldsymbol{J} \rangle \langle \boldsymbol{E} \rangle^{-1}.$$

This approach is an excellent way of generating exactly solvable microgeometries with conductivity tensor fields $\boldsymbol{\sigma}(\boldsymbol{x})$ that are not symmetric. However, it is hard to find matrix-valued fields $\boldsymbol{E}(\boldsymbol{x})$ and $\boldsymbol{J}(\boldsymbol{x})$ that result in symmetric tensor fields $\boldsymbol{\sigma}(\boldsymbol{x})$. These satisfy the additional constraint that $\boldsymbol{E}^T\boldsymbol{J} = \boldsymbol{J}^T\boldsymbol{E}$.

References

Alessandrini, G. and V. Nesi 2000. Univalence of σ-harmonic mappings and applications. Technical Report, Isaac Newton Institute for mathematical sciences. Preprint NI00006-SMM. {*152, 155*}

Alphutova, N. B., A. B. Movchan, and S. A. Nazarov 1991. On algebraic equivalence of planar problems in anisotropic and orthotropic elasticity. *Vestnik Leningradskogo Universiteta. Matematika, Mekhanika, Astronomiya* 3:64–68. {*147, 155*}

Astala, K. and V. Nesi 2001. Area distortion for periodic quasiconformal mappings. *Calculus of Variations and Partial Differential Equations*. Submitted. {*152, 155, 480, 491*}

Berdichevskii, V. L. 1985. Heat conduction of checkerboard structures. *Vestnik Moskovskogo Universiteta. Seriya I. Matematika, Mekhanika* 40(4):56–63. {*49, 57, 143, 155*}

Craster, R. V. and Y. V. Obnosov 2001. Four-phase checkerboard composites. *SIAM Journal on Applied Mathematics* 61(6):1839–1856. URL `http://epubs.siam.org/sam-bin/dbq/article/37182` {*154, 155*}

Dufour, R., S. Fabre, and J. Mossino 1996. H-convergence de matrices décomposables. (French) [H-convergence of decomposable matrices]. *Comptes Rendus des Séances de l'Académie des Sciences. Série I. Mathématique* 323(6):587–592. {*153, 155*}

Helsing, J. 1998. A high-order accurate algorithm for electrostatics of overlapping disks. *Journal of Statistical Physics* 90(5–6):1461–1473. {*39, 40, 43, 155, 156, 320, 337, 586, 598*}

Kozlov, S. and J. Vucans 1992. Explicit formula for effective thermoconductivity on the quadratic lattice structure. *Comptes Rendus des Séances de l'Académie des Sciences. Série I. Mathématique* 314(4):281–286. {*155, 156*}

Lehto, O. and K. I. Virtanen 1973. *Quasiconformal Mappings in the Plane* (Second ed.). Berlin / Heidelberg / London / etc.: Springer-Verlag. vii + 258 pp. ISBN 0-387-06093-6. {*153, 156*}

Marino, A. and S. Spagnolo 1969. Un tipo di approssimazione dell'operatore $\sum_{i,j=1}^{n} D_i(a_{ij}(x)D_j)$ con operatori $\sum_{j=1}^{n} D_j(\beta(x)D_j)$. (Italian). *Annali della Scuola Normale Superiore di Pisa* 23(3):657–673. {*153, 156*}

Milgrom, M. and S. Shtrikman 1992. The energy of inclusions in linear media exact shape-independent relations. *Journal of the Mechanics and Physics of Solids* 40(5):927–937. {*147, 156*}

Milton, G. W. 2001. Proof of a conjecture on the conductivity of checkerboards. *Journal of Mathematical Physics*. To appear. {*154, 156*}

Milton, G. W. and A. B. Movchan 1995. A correspondence between plane elasticity and the two-dimensional real and complex dielectric equations in anisotropic media. *Proceedings of the Royal Society of London. Series A, Mathematical and Physical Sciences* 450(1939):293–317. {*105, 111, 147, 156*}

Mortola, S. and S. Steffé 1985. A two-dimensional homogenization problem. (Italian). *Atti della Accademia Nazionale dei Lincei. Rendiconti. Classe di Scienze Fisiche, Matematiche e Naturali. Serie VIII* 78(3):77–82. {*154, 156*}

Nesi, V. 1996. Quasiconformal mappings as a tool to study certain two-dimensional G-closure problems. *Archive for Rational Mechanics and Analysis* 134(1):17–51. {*124, 141, 152, 156, 480, 481, 495, 646, 669*}

Nesi, V. 1998. Fine properties of solutions to conductivity equations with applications to composites. In K. Golden, G. R. Grimmett, R. D. James, G. W. Milton, and P. N. Sen (eds.), *Mathematics of Multiscale Materials*, pp. 179–208. Berlin / Heidelberg / London / etc.: Springer-Verlag. ISBN 0-387-98528-X. {*152, 156*}

Obnosov, Y. V. 1996. Exact solution of a boundary-value problem for a rectangular checkerboard field. *Proceedings of the Royal Society of London. Series A, Mathematical and Physical Sciences* 452(1954):2423–2442. {*143, 156, 207, 218*}

Obnosov, Y. V. 1999. Periodic heterogeneous structures: New explicit solutions and effective characteristics of refraction of an imposed field. *SIAM Journal on Applied Mathematics* 59(4):1267–1287. {*143, 154, 156*}

Olver, P. J. 1988. Canonical elastic moduli. *Journal of Elasticity* 19(3):189–212. {*147, 156*}

Reuben, A. J., G. B. Smith, and A. V. Radchik 1995. The polarisability of cylinder arrays in two dimensions. *Annals of Physics* 242(1):52–76. {*143, 156, 377, 394*}

Tartar, L. 1979. Estimation de coefficients homogénéisés. (French) [Estimation of homogenization coefficients]. In R. Glowinski and J.-L. Lions (eds.), *Computing Methods in*

Applied Sciences and Engineering: Third International Symposium, Versailles, France, December 5–9, 1977,, pp. 364–373. Berlin / Heidelberg / London / etc.: Springer-Verlag. English translation in *Topics in the Mathematical Modelling of Composite Materials*, pp. 9–20, ed. by A. Cherkaev and R. Kohn. ISBN 0-8176-3662-5. ISBN 0-387-09123-8. {*155, 156, 162, 183, 274, 289, 499, 503, 508, 509, 527, 529, 552*}

9

Laminate materials

9.1. The history of laminates and why they are important

The simplest conceivable composite is a stratified material, such as the one illustrated in figure 9.1 on the next page, where the material properties vary only in one direction, called the direction of lamination, represented by a unit vector $\boldsymbol{n}$. Of course lamination in direction $\boldsymbol{n}$ is equivalent to lamination in direction $-\boldsymbol{n}$. This chapter is devoted to obtaining formulas for the effective tensors of such laminates (called simple or rank-1 laminates), and also laminates of laminates (called multiple-rank laminates) where there is a large difference in the length scales of the successive laminations and the subsequent laminations are in different directions; see figure 9.2 on the following page. Laminates of laminates were introduced by Maxwell (1873), who provided a formula for the effective conductivity tensor of certain third-rank laminates, and later by Bruggeman (1930) for estimating the elastic moduli of polycrystalline aggregates. Beginning with the work of Schulgasser (1976), the effective tensors of appropriately designed multiple-rank laminates were found to attain many bounds on effective tensors. Numerous examples of such optimal laminate microstructures will be given in the latter part of this book. When one is trying to get some idea of the range of properties that composite materials can exhibit as the microstructure is varied, it is usually best to first examine the range of properties that multiple-rank laminate materials can exhibit. If in the course of exploring what is achievable in laminate microgeometries one finds desirable properties, then one can subsequently look for more realistic microgeometries exhibiting these properties. Backus (1962) found a general method for solving for the fields and effective tensors.

Some of the analysis presented in this chapter could be circumvented. It is included because it provides a useful stepping stone toward developments in subsequent chapters.

9.2. Elementary lamination formulas

The key to finding the effective tensors of laminate materials is to look for solutions to the field equations where the fields vary only in the lamination direction and to recognize that the differential constraints on these fields imply that certain components of the fields are constant or, equivalently, that certain projections of the fields are uniform fields. For example, consider the conductivity problem. We look for periodic fields $\boldsymbol{j}(\boldsymbol{x})$ and $\boldsymbol{e}(\boldsymbol{x})$ that solve the conductivity equations

$$\boldsymbol{j}(\boldsymbol{x}) = \boldsymbol{\sigma}(\boldsymbol{x})\boldsymbol{e}(\boldsymbol{x}), \qquad \nabla \cdot \boldsymbol{j} = 0, \qquad \nabla \times \boldsymbol{e} = 0,$$

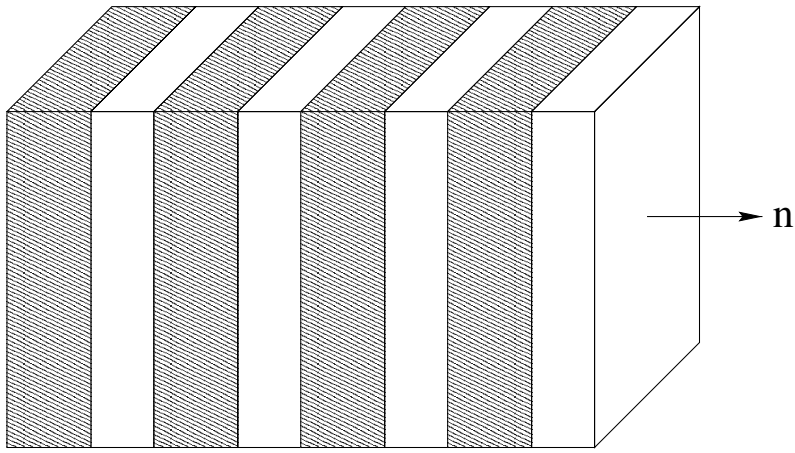

Figure 9.1. A three-dimensional, two-phase laminate that is laminated in direction $\boldsymbol{n}$. One phase occupies the shaded region while the other occupies the unshaded region.

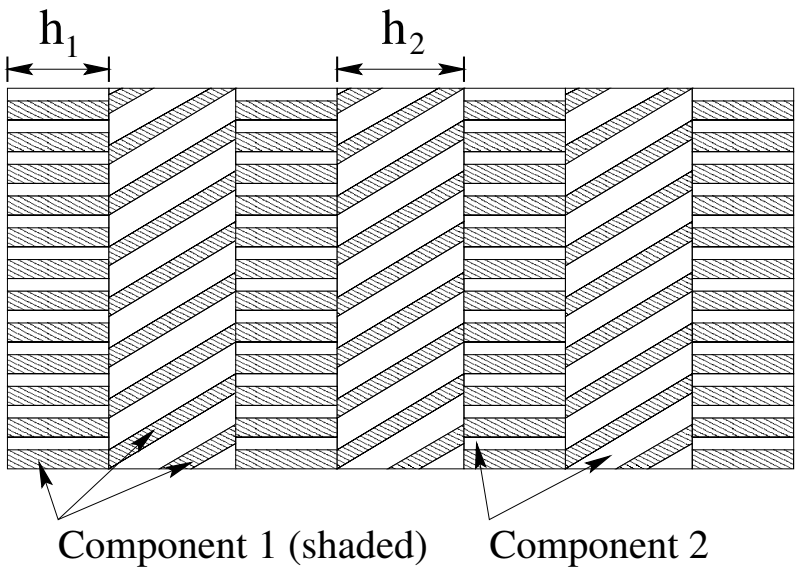

Figure 9.2. An example of a two-dimensional, two-phase, second-rank laminate. The widths h_1 and h_2 of the slabs should be much larger than the thicknesses of the layers within each slab.

where $\boldsymbol{\sigma}(\boldsymbol{x})$, $\boldsymbol{j}(\boldsymbol{x})$, and $\boldsymbol{e}(\boldsymbol{x})$ vary only in the direction of lamination, that is,

$$\boldsymbol{\sigma} = \boldsymbol{\sigma}(y), \quad \boldsymbol{j} = \boldsymbol{j}(y), \quad \boldsymbol{e} = \boldsymbol{e}(y), \quad \text{where } y = \boldsymbol{n} \cdot \boldsymbol{x}.$$

By resolving the differential operator ∇ into its components in the direction of lamination and orthogonal to the direction of lamination, we see that, for any function $f(y)$,

$$\nabla f(\boldsymbol{n} \cdot \boldsymbol{x}) = \boldsymbol{n} \frac{df(y)}{dy} = \frac{d}{dy}\Big[\boldsymbol{n} f(y)\Big].$$

In particular, the equation $\nabla \cdot \boldsymbol{j} = 0$ implies that

$$\frac{d}{dy}\Big[\boldsymbol{n} \cdot \boldsymbol{j}(y)\Big] = 0,$$

and so $\boldsymbol{n} \cdot \boldsymbol{j}(y)$ must be constant or, equivalently,

$$\boldsymbol{n} \cdot \boldsymbol{j} = \boldsymbol{n} \cdot \langle \boldsymbol{j} \rangle,$$

which just says that there are no variations in the component of the current field parallel to $\boldsymbol{n}$.

Also, since $\boldsymbol{e}(\boldsymbol{x})$ is curl free and periodic, we have

$$\boldsymbol{e} = \langle \boldsymbol{e} \rangle + \nabla \varphi(\boldsymbol{n} \cdot \boldsymbol{x}) = \langle \boldsymbol{e} \rangle + \boldsymbol{n} \frac{d\varphi(y)}{dy},$$

where $\varphi(y)$ is a periodic potential. This just says that the only variation in the electric field is in the component parallel to $\boldsymbol{n}$.

In summary, we have

$$\boldsymbol{e}(\boldsymbol{x}) - \langle \boldsymbol{e} \rangle \in \mathcal{E}_{\boldsymbol{n}}, \quad \boldsymbol{j}(\boldsymbol{x}) - \langle \boldsymbol{j} \rangle \in \mathcal{J}_{\boldsymbol{n}}, \quad \text{for all } \boldsymbol{x}, \tag{9.1}$$

in which

$$\mathcal{E}_{\boldsymbol{n}} = \{\alpha \boldsymbol{n} \mid \alpha \in \mathbb{R}\}, \quad \text{and} \quad \mathcal{J}_{\boldsymbol{n}} = \{\boldsymbol{a} \in \mathbb{R}^d \mid \boldsymbol{n} \cdot \boldsymbol{a} = 0\}$$

denote, respectively, the spaces comprised of vectors parallel and perpendicular to $\boldsymbol{n}$. Thus the fluctuating components of the fields appearing on the right- and left-hand sides of the constitutive equation take values in two mutually orthogonal spaces $\mathcal{E}_{\boldsymbol{n}}$ and $\mathcal{J}_{\boldsymbol{n}}$. We will see that this is true not just for conductivity, but also for a wide variety of physical problems. Introducing the matrices

$$\boldsymbol{\Gamma}_1^c(\boldsymbol{n}) = \boldsymbol{n} \otimes \boldsymbol{n}, \qquad \boldsymbol{\Gamma}_2^c(\boldsymbol{n}) = \boldsymbol{I} - \boldsymbol{n} \otimes \boldsymbol{n}, \tag{9.2}$$

representing projections onto the spaces $\mathcal{E}_{\boldsymbol{n}}$ and $\mathcal{J}_{\boldsymbol{n}}$, respectively, (9.1) implies that

$$\boldsymbol{\Gamma}_1(\boldsymbol{n})\boldsymbol{j} = \boldsymbol{\Gamma}_1(\boldsymbol{n})\langle \boldsymbol{j} \rangle, \quad \boldsymbol{\Gamma}_2(\boldsymbol{n})\boldsymbol{e} = \boldsymbol{\Gamma}_2(\boldsymbol{n})\langle \boldsymbol{e} \rangle, \tag{9.3}$$

where we have tentatively dropped the superscript c (which signifies that these are the expressions for $\boldsymbol{\Gamma}_1$ and $\boldsymbol{\Gamma}_2$ for the conductivity problem). At this point $\boldsymbol{\Gamma}_1(\boldsymbol{n})$ and $\boldsymbol{\Gamma}_2(\boldsymbol{n})$ should be equated with $\boldsymbol{\Gamma}_1^c(\boldsymbol{n})$ and $\boldsymbol{\Gamma}_2^c(\boldsymbol{n})$. Later in this chapter expressions for $\boldsymbol{\Gamma}_1$ and $\boldsymbol{\Gamma}_2$ will be given for elasticity, thermoelasticity, thermoelectricity, and piezoelectricity. Note that these matrices satisfy the expected properties

$$\boldsymbol{\Gamma}_i(\boldsymbol{n})\boldsymbol{\Gamma}_j(\boldsymbol{n}) = \delta_{ij}\boldsymbol{\Gamma}_i(\boldsymbol{n}), \quad \boldsymbol{\Gamma}_1(\boldsymbol{n}) + \boldsymbol{\Gamma}_2(\boldsymbol{n}) = \boldsymbol{I} \tag{9.4}$$

of projections onto mutually orthogonal spaces.

One elegant approach to obtaining a formula for the effective tensor is to rewrite the constitutive relation $\boldsymbol{j}(\boldsymbol{x}) = \boldsymbol{\sigma}(\boldsymbol{x})\boldsymbol{e}(\boldsymbol{x})$ in a form where the components of the fields that are constant appear on the right-hand side of the equation. Then, as we will see, the effective conductivity tensor can be found by just averaging both sides of this equation. This idea is due to Backus (1962): see also Tartar (1979).

For simplicity, let us suppose that we are in three dimensions and that the coordinates are chosen so that $\boldsymbol{n}$ is directed along the x_1-axis, that is, $\boldsymbol{n} = (1, 0, 0)$. [In geophysics it is more conventional to take $\boldsymbol{n} = (0, 0, 1)$ since one frequently considers materials that are layered in the vertical direction. Taking $\boldsymbol{n}$ directed along the x_1-axis is more convenient mathematically because then the selected index does not change when we consider two- rather than three-dimensional composites.] The components of the fields that are constant are j_1, e_2, and e_3. By rewriting the constitutive law so that these components are on the right-hand side we obtain the equivalent set of equations:

$$\begin{pmatrix} -e_1 \\ j_2 \\ j_3 \end{pmatrix} = \begin{pmatrix} -1/\sigma_{11} & \sigma_{12}/\sigma_{11} & \sigma_{13}/\sigma_{11} \\ \sigma_{12}/\sigma_{11} & \sigma_{22} - \sigma_{21}^2/\sigma_{11} & \sigma_{23} - \sigma_{21}\sigma_{13}/\sigma_{11} \\ \sigma_{13}/\sigma_{11} & \sigma_{23} - \sigma_{21}\sigma_{13}/\sigma_{11} & \sigma_{33} - \sigma_{31}^2/\sigma_{11} \end{pmatrix} \begin{pmatrix} j_1 \\ e_2 \\ e_3 \end{pmatrix}. \tag{9.5}$$

Similar algebraic manipulation of the effective constitutive law $\langle \boldsymbol{j} \rangle = \boldsymbol{\sigma}_* \langle \boldsymbol{e} \rangle$ yields

$$\begin{pmatrix} -\langle e_1 \rangle \\ \langle j_2 \rangle \\ \langle j_3 \rangle \end{pmatrix} = \begin{pmatrix} -1/\sigma_{11}^* & \sigma_{12}^*/\sigma_{11}^* & \sigma_{13}^*/\sigma_{11}^* \\ \sigma_{12}^*/\sigma_{11}^* & \sigma_{22}^* - (\sigma_{21}^*)^2/\sigma_{11}^* & \sigma_{23}^* - \sigma_{21}^*\sigma_{13}^*/\sigma_{11}^* \\ \sigma_{13}^*/\sigma_{11}^* & \sigma_{23}^* - \sigma_{21}^*\sigma_{13}^*/\sigma_{11}^* & \sigma_{33}^* - (\sigma_{31}^*)^2/\sigma_{11}^* \end{pmatrix} \begin{pmatrix} \langle j_1 \rangle \\ \langle e_2 \rangle \\ \langle e_3 \rangle \end{pmatrix}. \tag{9.6}$$

But since the field on the right-hand side of (9.5) is constant, we can average both sides of this equation and compare the result with (9.6). The resulting relations,

$$\begin{pmatrix} -1/\sigma_{11}^* & \sigma_{1j}^*/\sigma_{11}^* \\ \sigma_{i1}^*/\sigma_{11}^* & \sigma_{ij}^* - \sigma_{i1}^*\sigma_{1j}^*/\sigma_{11}^* \end{pmatrix} = \begin{pmatrix} -\langle 1/\sigma_{11} \rangle & \langle \sigma_{1j}/\sigma_{11} \rangle \\ \langle \sigma_{i1}/\sigma_{11} \rangle & \langle \sigma_{ij} - \sigma_{i1}\sigma_{1j}/\sigma_{11} \rangle \end{pmatrix},$$

which hold for all $i \neq 1$, $j \neq 1$, imply the following formulas of Tartar (1979) for the components of the effective conductivity tensor $\boldsymbol{\sigma}_*$:

$$\begin{aligned} \sigma_{11}^* &= \langle 1/\sigma_{11} \rangle^{-1}, \\ \sigma_{1j}^* &= \langle 1/\sigma_{11} \rangle^{-1} \langle \sigma_{1j}/\sigma_{11} \rangle, \\ \sigma_{ij}^* &= \langle \sigma_{ij} - \sigma_{i1}\sigma_{11}^{-1}\sigma_{1j} \rangle + \langle \sigma_{i1}/\sigma_{11} \rangle \langle 1/\sigma_{11} \rangle^{-1} \langle \sigma_{1j}/\sigma_{11} \rangle \end{aligned} \tag{9.7}$$

for all $i \neq 1$, $j \neq 1$.

In particular, if the off-diagonal elements of $\boldsymbol{\sigma}(\boldsymbol{x})$ are zero, we obtain the well-known result that the effective conductivity perpendicular to the layers is the harmonic mean of the conductivities in that direction, while the effective conductivity along any axis parallel to the layers is the arithmetic average of the conductivities in that direction; that is, when $\sigma_{ij} = 0$ for all $i \neq j$ we have

$$\sigma_{11}^* = 1/\langle 1/\sigma_{11} \rangle, \quad \sigma_{ii}^* = \langle \sigma_{ii} \rangle \quad \text{for all } i \neq 1, \quad \sigma_{ij}^* = 0 \quad \text{when } i \neq j.$$

This procedure of averaging the form of the constitutive law where the constant field components are on the right-hand side is easily generalized to elasticity, piezoelectricity, and other equations. For example, if we consider three-dimensional elasticity and choose coordinates so

that $\boldsymbol{n}$ is directed along the x_1-axis, that is, $\boldsymbol{n} = (1, 0, 0)$, then in the constitutive relation (2.6) the field components that are constant are τ_{11}, $\sqrt{2}\tau_{12}$, $\sqrt{2}\tau_{13}$, ϵ_{22}, ϵ_{33}, and $\sqrt{2}\epsilon_{23}$. Associated with this division of the field components is a separation of the elasticity matrix $\boldsymbol{\mathcal{C}}(x_1)$ into blocks comprised of the matrices

$$\boldsymbol{A}_{11} = \begin{pmatrix} C_{1111} & \sqrt{2}C_{1113} & \sqrt{2}C_{1112} \\ \sqrt{2}C_{1113} & 2C_{1313} & 2C_{1312} \\ \sqrt{2}C_{1112} & 2C_{1312} & 2C_{1212} \end{pmatrix},$$

$$\boldsymbol{A}_{12} = \begin{pmatrix} C_{1122} & C_{1133} & \sqrt{2}C_{1123} \\ \sqrt{2}C_{2213} & \sqrt{2}C_{3313} & 2C_{2313} \\ \sqrt{2}C_{2212} & \sqrt{2}C_{3312} & 2C_{2312} \end{pmatrix},$$

$$\boldsymbol{A}_{22} = \begin{pmatrix} C_{2222} & C_{2233} & \sqrt{2}C_{2223} \\ C_{2233} & C_{3333} & \sqrt{2}C_{3323} \\ \sqrt{2}C_{2223} & \sqrt{2}C_{3323} & 2C_{2323} \end{pmatrix},$$

together with $\boldsymbol{A}_{21} \equiv \boldsymbol{A}_{12}^T$. The associated blocks of the effective tensor $\boldsymbol{\mathcal{C}}_*$ (obtained by replacing the elasticity moduli with the effective elasticity moduli in the above definitions) are then given by the expressions

$$\begin{aligned} \boldsymbol{A}_{11}^* &= \langle \boldsymbol{A}_{11}^{-1} \rangle^{-1}, \\ \boldsymbol{A}_{12}^* &= \langle \boldsymbol{A}_{11}^{-1} \rangle^{-1} \langle \boldsymbol{A}_{11}^{-1} \boldsymbol{A}_{12} \rangle, \\ \boldsymbol{A}_{22}^* &= \langle \boldsymbol{A}_{22} - \boldsymbol{A}_{21}\boldsymbol{A}_{11}^{-1}\boldsymbol{A}_{12} \rangle + \langle \boldsymbol{A}_{21}\boldsymbol{A}_{11}^{-1} \rangle \langle \boldsymbol{A}_{11}^{-1} \rangle^{-1} \langle \boldsymbol{A}_{11}^{-1}\boldsymbol{A}_{12} \rangle \end{aligned} \tag{9.8}$$

of Backus (1962), which are similar in form to the conductivity relations (9.7).

In a locally isotropic laminate the blocks take the forms

$$\boldsymbol{A}_{11} = \begin{pmatrix} \lambda + 2\mu & 0 & 0 \\ 0 & 2\mu & 0 \\ 0 & 0 & 2\mu \end{pmatrix},$$

$$\boldsymbol{A}_{12} = \boldsymbol{A}_{21}^T = \begin{pmatrix} \lambda & \lambda & 0 \\ 0 & 0 & 0 \\ 0 & 0 & 0 \end{pmatrix},$$

$$\boldsymbol{A}_{22} = \begin{pmatrix} \lambda + 2\mu & \lambda & 0 \\ \lambda & \lambda + 2\mu & 0 \\ 0 & 0 & 2\mu \end{pmatrix},$$

and consequently (9.8) implies that the nonzero elements of the effective elasticity tensor $\boldsymbol{\mathcal{C}}_*$ are given by Backus's formulas,

$$\begin{aligned} C_{1111}^* &= \langle 1/(\lambda + 2\mu) \rangle^{-1}, \quad C_{1212}^* = C_{1313}^* = \langle 1/\mu \rangle^{-1}, \quad C_{2323}^* = \langle \mu \rangle \\ C_{1122}^* &= C_{1133}^* = \langle \lambda/(\lambda + 2\mu) \rangle \langle 1/(\lambda + 2\mu) \rangle^{-1}, \\ C_{2222}^* &= C_{3333}^* = \langle 4\mu(\lambda + \mu)\lambda/(\lambda + 2\mu) \rangle + \langle 1/(\lambda + 2\mu) \rangle^{-1} \langle \lambda/(\lambda + 2\mu) \rangle^2, \\ C_{2233}^* &= \langle 2\mu\lambda/(\lambda + 2\mu) \rangle + \langle 1/(\lambda + 2\mu) \rangle^{-1} \langle \lambda/(\lambda + 2\mu) \rangle^2. \end{aligned} \tag{9.9}$$

For a laminate of two isotropic materials, these latter formulas reduce to those of Postma (1955).

Avellaneda and Olson (1993) have used a similar approach to evaluate the moduli of a laminated piezoelectric composite [see also Gibiansky and Torquato (1999), who calculate the moduli of higher rank piezoelectric laminates]. Berryman (1998) has given formulas that are analogous to those of Backus for the effective moduli of laminar poroelastic media.

9.3. Lamination formulas when the direction of lamination is arbitrary

The method described in the previous sections, although straightforward and simple in many cases, becomes rather algebraically messy for three-dimensional composites when $\boldsymbol{n}$ is not directed along the coordinate axes. Here we follow another approach, which leads to a concise but equivalent formula for the effective tensor $\boldsymbol{\sigma}_*$ (Milton 1990; Zhikov 1991). The idea is to solve the conductivity equations for the polarization field

$$\boldsymbol{p}(\boldsymbol{x}) = (\boldsymbol{\sigma}(\boldsymbol{x}) - \sigma_0\boldsymbol{I})\boldsymbol{e}(\boldsymbol{x}) = \boldsymbol{j}(\boldsymbol{x}) - \sigma_0\boldsymbol{e}(\boldsymbol{x}), \tag{9.10}$$

where the reference constant σ_0 can be freely chosen. From (9.10) we can express the electric field $\boldsymbol{e}(\boldsymbol{x})$ and its average $\langle\boldsymbol{e}\rangle$ in terms of the polarization field $\boldsymbol{p}(\boldsymbol{x})$ and its average $\langle\boldsymbol{p}\rangle$:

$$\sigma_0\boldsymbol{e}(\boldsymbol{x}) = -\boldsymbol{S}(\boldsymbol{x})\boldsymbol{p}(\boldsymbol{x}), \quad \sigma_0\langle\boldsymbol{e}\rangle = -\boldsymbol{S}_*\langle\boldsymbol{p}\rangle,$$

where, for convenience, we have introduced the tensors

$$\boldsymbol{S}(\boldsymbol{x}) = \sigma_0(\sigma_0\boldsymbol{I} - \boldsymbol{\sigma}(\boldsymbol{x}))^{-1}, \quad \boldsymbol{S}_* = \sigma_0(\sigma_0\boldsymbol{I} - \boldsymbol{\sigma}_*)^{-1}, \tag{9.11}$$

which will be important in later analyses. Applying $\boldsymbol{\Gamma}_1(\boldsymbol{n}) = \boldsymbol{I} - \boldsymbol{\Gamma}_2(\boldsymbol{n})$ to both sides of (9.10) gives

$$\boldsymbol{\Gamma}_1(\boldsymbol{n})\boldsymbol{p}(\boldsymbol{x}) = -\sigma_0\boldsymbol{e}(\boldsymbol{x}) + \sigma_0\langle\boldsymbol{e}\rangle + \boldsymbol{\Gamma}_1(\boldsymbol{n})\langle\boldsymbol{j} - \sigma_0\boldsymbol{e}\rangle = \boldsymbol{S}(\boldsymbol{x})\boldsymbol{p}(\boldsymbol{x}) + \boldsymbol{v}, \tag{9.12}$$

where $\boldsymbol{v}$ is the uniform field

$$\boldsymbol{v} = \sigma_0\langle\boldsymbol{e}\rangle + \boldsymbol{\Gamma}_1(\boldsymbol{n})\langle\boldsymbol{p}\rangle = -[\boldsymbol{S}_* - \boldsymbol{\Gamma}_1(\boldsymbol{n})]\langle\boldsymbol{p}\rangle. \tag{9.13}$$

Equation (9.12) is easily solved for the polarization field, giving

$$\boldsymbol{p}(\boldsymbol{x}) = -[\boldsymbol{S}(\boldsymbol{x}) - \boldsymbol{\Gamma}_1(\boldsymbol{n})]^{-1}\boldsymbol{v}, \tag{9.14}$$

and by averaging this equation and noting the relation (9.13) we deduce that

$$\langle\boldsymbol{p}\rangle = -[\boldsymbol{S}_* - \boldsymbol{\Gamma}_1(\boldsymbol{n})]^{-1}\boldsymbol{v} = -\langle[\boldsymbol{S}(\boldsymbol{x}) - \boldsymbol{\Gamma}_1(\boldsymbol{n})]^{-1}\rangle\boldsymbol{v}; \tag{9.15}$$

since this holds for all applied fields or, equivalently, for all choices of $\boldsymbol{v}$, (9.15) implies the general lamination formula

$$[\boldsymbol{S}_* - \boldsymbol{\Gamma}_1(\boldsymbol{n})]^{-1} = \langle[\boldsymbol{S}(\boldsymbol{x}) - \boldsymbol{\Gamma}_1(\boldsymbol{n})]^{-1}\rangle, \tag{9.16}$$

which gives the effective tensor $\boldsymbol{\sigma}_*$ through equations (9.2) and (9.11). An alternative formula for the effective conductivity of an n-phase laminate, laminated in a single direction, has been given by Tartar (2000).

The lamination formula (9.16) is written in this form rather than directly in terms of $\boldsymbol{\sigma}_*$ and $\boldsymbol{\sigma}(\boldsymbol{x})$ to emphasize the simplicity of the formula when expressed in terms of $\boldsymbol{S}_*$ and $\boldsymbol{S}(\boldsymbol{x})$. This is not just cosmetic. If one wanted to calculate the effective tensor $\boldsymbol{\sigma}_*$ of multiple-rank laminates (i.e., laminates of laminates), then it is more convenient to work with the tensors $\boldsymbol{S}_*$ obtained at each stage of the lamination process and only compute $\boldsymbol{\sigma}_*$ at the end of the calculation.

When the composite is three-dimensional and the coordinates are chosen so $\boldsymbol{n}$ is directed along the x_1-axis, that is, $\boldsymbol{n} = (1, 0, 0)$, then the matrix $\boldsymbol{\Gamma}_1(\boldsymbol{n})$ entering this formula is simply

$$\boldsymbol{\Gamma}_1 = \begin{pmatrix} 1 & 0 & 0 \\ 0 & 0 & 0 \\ 0 & 0 & 0 \end{pmatrix}.$$

Upon substituting this into (9.16) one recovers the formulas (9.7) for the components of the effective conductivity tensor.

If the laminate is almost homogeneous, say, close to a tensor $\boldsymbol{S}_1$, then to the second order in $\delta\boldsymbol{S} = \boldsymbol{S}(\boldsymbol{x}) - \boldsymbol{S}_1$ we have

$$\begin{aligned}[\boldsymbol{S}_* - \boldsymbol{\Gamma}_1(\boldsymbol{n})]^{-1} = {} & [\boldsymbol{S}_1 - \boldsymbol{\Gamma}_1(\boldsymbol{n})]^{-1} - [\boldsymbol{S}_1 - \boldsymbol{\Gamma}_1(\boldsymbol{n})]^{-1}\langle\delta\boldsymbol{S}\rangle[\boldsymbol{S}_1 - \boldsymbol{\Gamma}_1(\boldsymbol{n})]^{-1} \\ & + [\boldsymbol{S}_1 - \boldsymbol{\Gamma}_1(\boldsymbol{n})]^{-1}\langle\delta\boldsymbol{S}[\boldsymbol{S}_1 - \boldsymbol{\Gamma}_1(\boldsymbol{n})]^{-1}\delta\boldsymbol{S}\rangle[\boldsymbol{S}_1 - \boldsymbol{\Gamma}_1(\boldsymbol{n})]^{-1} + \cdots,\end{aligned}$$

implying, to the second order in $\delta\boldsymbol{S}$, that

$$\boldsymbol{S}_* = \langle\boldsymbol{S}(\boldsymbol{x})\rangle + \langle\delta\boldsymbol{S}\rangle[\boldsymbol{S}_1 - \boldsymbol{\Gamma}_1(\boldsymbol{n})]^{-1}\langle\delta\boldsymbol{S}\rangle - \langle\delta\boldsymbol{S}[\boldsymbol{S}_1 - \boldsymbol{\Gamma}_1(\boldsymbol{n})]^{-1}\delta\boldsymbol{S}\rangle + \cdots. \tag{9.17}$$

9.4. Tartar's lamination formula for two-phase simple and coated laminates

Tartar (1985) found an elegant formula for the conductivity tensor of two-phase simple laminates and of an important class of two-phase, multiple-rank laminates, which we call coated laminates. Let us consider a two-phase laminate material with conductivity tensor

$$\boldsymbol{\sigma}(\boldsymbol{x}) = \chi_1(y)\boldsymbol{\sigma}_1 + \chi_2(y)\boldsymbol{\sigma}_2, \quad \text{where } y = \boldsymbol{n}\cdot\boldsymbol{x},$$

in which $\chi_1(y) = 1 - \chi_2(y)$ is a characteristic function that is periodic in y. From (9.16) we have

$$[\boldsymbol{S}_* - \boldsymbol{\Gamma}_1(\boldsymbol{n})]^{-1} = f_1[\boldsymbol{S}_1 - \boldsymbol{\Gamma}_1(\boldsymbol{n})]^{-1} + f_2[\boldsymbol{S}_2 - \boldsymbol{\Gamma}_1(\boldsymbol{n})]^{-1}, \tag{9.18}$$

where f_1 and $f_2 = 1 - f_1$ are the volume fractions of the two phases in the laminate. For simplicity, let us suppose that phase 2 is isotropic, that is, $\boldsymbol{\sigma}_2 = \sigma_2\boldsymbol{I}$. Later we will see that it is easy to generalize all of the formulas to the case where $\boldsymbol{\sigma}_2$ is anisotropic. Since we are free to choose the reference constant σ_0, let us take the limit as σ_0 tends to σ_2. Then $\boldsymbol{S}_2$ tends to infinity and the second term in (9.18) vanishes. By taking the inverse of both sides of (9.18) we obtain the formula

$$f_1\sigma_2(\sigma_2\boldsymbol{I} - \boldsymbol{\sigma}_*)^{-1} = \sigma_2(\sigma_2\boldsymbol{I} - \boldsymbol{\sigma}_1)^{-1} - f_2\boldsymbol{\Gamma}_1(\boldsymbol{n}) \tag{9.19}$$

of Tartar (1985) for the effective tensor $\boldsymbol{\sigma}_*$.

Following Maxwell (1873) and Tartar (1985), let us now consider the class of coated laminates. A third-rank laminate of this type is illustrated in figure 9.3 on the next page. They are obtained by a process of sequential lamination and, as Braidy and Pouilloux observed [see Tartar (1985)], the formula for their effective conductivity tensor happens to coincide with the formula for the effective conductivity tensor of the coated ellipsoid assemblages. We start with phase 1 having conductivity $\boldsymbol{\sigma}_*^0 = \boldsymbol{\sigma}_1$, which is called the core phase, and we first layer in direction $\boldsymbol{n}_1$ with phase 2, called the coating phase, to form a simple laminate with conductivity $\boldsymbol{\sigma}_*^{(1)}$. Then we slice this laminate on a much larger length scale in a different direction $\boldsymbol{n}_2$ and layer it again with phase 2 to form a rank-2 laminate with conductivity

tensor $\boldsymbol{\sigma}_*^{(2)}$. (The rank of a laminate refers to the minimum number of widely separated length scales needed in its construction.) This process is continued until we obtain a rank-m coated laminate having conductivity $\boldsymbol{\sigma}_* = \boldsymbol{\sigma}_*^{(m)}$: At the j-th stage the rank-$(j-1)$ laminate is sliced in direction $\boldsymbol{n}_j$ on a length scale much larger than the existing microstructure and layered with phase 2 to form a rank-j laminate of conductivity $\boldsymbol{\sigma}_*^{(j)}$. These coated laminates have also been called "matrix laminates" and "sequentially laminated microstructures." I have adopted the name coated laminate because it is simple and emphasizes the similarity with coated ellipsoid and coated sphere assemblages.

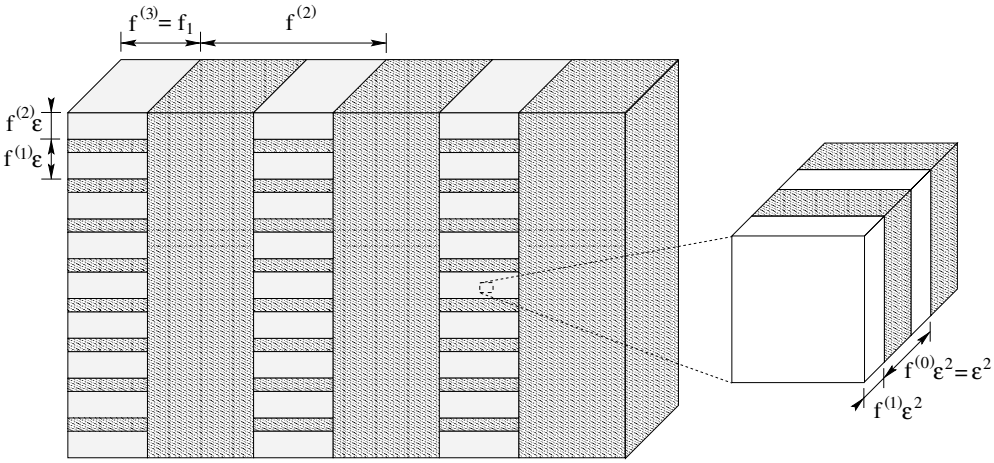

Figure 9.3. The third-rank coated laminate introduced by Maxwell (1873). Here the coating phase, phase 2, occupies the shaded region while the core phase, phase 1, occupies the unshaded region. The parameter $f^{(j)}$, for $j = 0, 1, 2, 3$, with $f^{(0)} = 1$ and $f^{(3)} = f_1$ represents the volume fraction of phase 1 in the rank-j laminate obtained in the construction process. In the limit $\epsilon \to 0$, the conductivity of this laminate is given by (9.20). By choosing $f^{(1)} = (2 + f_1)/3$ and $f^{(2)} = (1 + 2f_1)/3$ one obtains a coated laminate with the same conductivity as the Hashin-Shtrikman coated sphere assemblage.

Now let $f^{(j)}$ denote the proportion of phase 1 in the rank-j laminate, which monotonically decreases with increasing j because we are always adding phase 2. To form the rank-j laminate we need to layer the rank-$(j-1)$ laminate with phase 2 in proportions p_j and $1-p_j$, where $p_j = f^{(j)}/f^{(j-1)}$. Because of the wide separation of length scales we can calculate $\boldsymbol{\sigma}_*^{(j)}$ by treating the rank-$(j-1)$ laminate as a homogeneous material with conductivity $\boldsymbol{\sigma}_*^{(j-1)}$. Then the lamination formula (9.19) implies that

$$f^{(j)}\sigma_2(\sigma_2\boldsymbol{I} - \boldsymbol{\sigma}_*^{(j)})^{-1} = f^{(j-1)}\sigma_2(\sigma_2\boldsymbol{I} - \boldsymbol{\sigma}_*^{(j-1)})^{-1} - (f^{(j-1)} - f^{(j)})\boldsymbol{\Gamma}_1(\boldsymbol{n}_j).$$

Recalling that $f^0 = 1$, it follows by induction that

$$f_1\sigma_2(\sigma_2\boldsymbol{I} - \boldsymbol{\sigma}_*)^{-1} = \sigma_2(\sigma_2\boldsymbol{I} - \boldsymbol{\sigma}_1)^{-1} - f_2\boldsymbol{M}, \tag{9.20}$$

where $f_1 = 1 - f_2 = f^m$ is the volume fraction occupied by phase 1 in the final composite and

$$\boldsymbol{M} = \sum_{j=1}^{m} c_j\boldsymbol{\Gamma}_1(\boldsymbol{n}_j),$$

in which the constants

$$c_j = \frac{f^{(j-1)} - f^{(j)}}{1 - f_1} \tag{9.21}$$

satisfy

$$\sum_{j=1}^{m} c_j = 1, \quad c_j \geq 0 \text{ for all } j. \tag{9.22}$$

When phase 1 is isotropic, that is, $\boldsymbol{\sigma}_1 = \sigma_1 \boldsymbol{I}$, and there are three mutually orthogonal directions of lamination, as in figure 9.3 on the facing page, Tartar's formula (9.20) reduces to the equations for the principal conductivities given by Maxwell (1873) [see also Lurie and Cherkaev (1986)].

Conversely, for any choice of constants c_j satisfying (9.22) and for any choice of volume fraction $f_1 = f^m \in (0, 1)$, one can find a set of intermediate volume fractions $f^{(j)}$ given via

$$f^{(j)} = f_1 + (1 - f_1) \sum_{k=j+1}^{m} c_k, \quad j = 1, 2, \ldots, m-1, \quad f^m = f_1,$$

such that (9.21) is satisfied. Consequently one can construct a coated laminate of rank-m with intermediate volume fractions $f^{(j)}$ that reproduce this given set constants c_j and total volume fraction f_1 (Tartar 1985). In other words, as the geometry varies over all rank-m coated laminates with fixed core volume fraction f_1, the set of constants $(c_1, c_2, \ldots, c_m)$ ranges over all m-tuplets satisfying (9.22).

A comparison of Tartar's formula (9.20) with the formula (8.8) for the conductivity of the coated ellipsoid assemblage with an anisotropic core and isotropic coating shows that they coincide, and in both cases the matrix $\boldsymbol{M}$ is positive-semidefinite and satisfies $\mathrm{Tr}\boldsymbol{M} = 1$. This is not just coincidental, but as we will see later it is a consequence of the fact that the field inside the core phase is uniform in both microgeometries.

Moreover, as Tartar (1985) and Lurie and Cherkaev (1986) observed, given any matrix $\boldsymbol{M} \geq 0$ with $\mathrm{Tr}\boldsymbol{M} = 1$ one can find a rank-d laminate, where d is the spatial dimension, such that its effective tensor is given by (9.19). The lamination directions $\boldsymbol{n}_1, \boldsymbol{n}_2, \ldots, \boldsymbol{n}_d$ can be taken as the eigenvectors of $\boldsymbol{M}$ and $c_1, c_2, \ldots, c_d$ can be taken as the eigenvalues of $\boldsymbol{M}$. Thus we have a complete characterization of the set of all possible effective conductivity tensors of these coated laminates.

If the coated laminate is almost homogeneous (and $\boldsymbol{\sigma}_2$ is not necessarily isotropic), then we can keep σ_0 a free parameter. By repeatedly applying (9.17) one finds to the second order in $(\boldsymbol{S}_1 - \boldsymbol{S}_2)$ that in the coated laminate $\boldsymbol{S}_* = \sigma_0(\sigma_0 \boldsymbol{I} - \boldsymbol{\sigma}_*)^{-1}$ is given by

$$\boldsymbol{S}_* = f_1 \boldsymbol{S}_1 + f_2 \boldsymbol{S}_2 - f_1 f_2 (\boldsymbol{S}_2 - \boldsymbol{S}_1) \boldsymbol{N} (\boldsymbol{S}_2 - \boldsymbol{S}_1) + \cdots, \tag{9.23}$$

where

$$\boldsymbol{N} = \sum_{j=1}^{m} c_j [\boldsymbol{S}_1 - \boldsymbol{\Gamma}_1(\boldsymbol{n}_j)]^{-1}, \tag{9.24}$$

in which the weights c_j are given by (9.21).

9.5. Lamination formulas for elasticity, thermoelasticity, thermoelectricity, and piezoelectricity

All of the preceding analysis generalizes quite easily to the elastic, thermoelastic, thermoelectric, or piezoelectric problems. For example, consider the elasticity equations in a simple

rank-1 laminate,

$$\boldsymbol{\tau}(\boldsymbol{x}) = \boldsymbol{\mathcal{C}}(\boldsymbol{x})\boldsymbol{\epsilon}(\boldsymbol{x}), \quad \nabla \cdot \boldsymbol{\tau} = 0, \quad \boldsymbol{\epsilon} = [\nabla \boldsymbol{u} + (\nabla \boldsymbol{u})^T]/2, \tag{9.25}$$

where the elasticity tensor $\boldsymbol{\mathcal{C}}(\boldsymbol{x})$, the stress field $\boldsymbol{\tau}(\boldsymbol{x})$ and the strain field $\boldsymbol{\tau}(\boldsymbol{x})$ have only oscillations in the direction of lamination,

$$\boldsymbol{\mathcal{C}} = \boldsymbol{\mathcal{C}}(y), \quad \boldsymbol{\tau} = \boldsymbol{\tau}(y), \quad \boldsymbol{\epsilon} = \boldsymbol{\epsilon}(y), \quad \text{where } y = \boldsymbol{n} \cdot \boldsymbol{x}. \tag{9.26}$$

To simplify the analysis let us choose our coordinates so that $\boldsymbol{n}$ is directed along the x_1-axis. Then (9.26) and the differential restrictions (9.25) imply that the stress and strain fields have the forms

$$\boldsymbol{\tau} = \begin{pmatrix} \tau_{11} & \tau_{12} & \tau_{13} \\ \tau_{12} & \tau_{22}(y) & \tau_{23}(y) \\ \tau_{13} & \tau_{23}(y) & \tau_{33}(y) \end{pmatrix}, \qquad \boldsymbol{\epsilon} = \begin{pmatrix} \epsilon_{11}(y) & \epsilon_{12}(y) & \epsilon_{13}(y) \\ \epsilon_{12}(y) & \epsilon_{22} & \epsilon_{23} \\ \epsilon_{13}(y) & \epsilon_{23} & \epsilon_{33} \end{pmatrix}, \tag{9.27}$$

where those elements that are not written with an explicit y dependence are in fact constant. So if we define $\boldsymbol{\Gamma}_1(\boldsymbol{n})$ and $\boldsymbol{\Gamma}_2(\boldsymbol{n})$ by their action on an arbitrary symmetric second-order tensor $\boldsymbol{A}$ through the equations

$$\boldsymbol{\Gamma}_1(\boldsymbol{n})\boldsymbol{A} = \begin{pmatrix} a_{11} & a_{12} & a_{13} \\ a_{12} & 0 & 0 \\ a_{13} & 0 & 0 \end{pmatrix}, \qquad \boldsymbol{\Gamma}_2(\boldsymbol{n})\boldsymbol{A} = \begin{pmatrix} 0 & 0 & 0 \\ 0 & a_{22} & a_{23} \\ 0 & a_{23} & a_{33} \end{pmatrix}, \tag{9.28}$$

where the a_{ij} are the matrix elements of $\boldsymbol{A}$, then it is easy to see that $\boldsymbol{\Gamma}_1(\boldsymbol{n})$ and $\boldsymbol{\Gamma}_2(\boldsymbol{n})$ are projections onto mutually orthogonal subspaces [namely, those subspaces spanned by all matrices of the form of the right-hand side of the respective equation in (9.28)] and so satisfy the properties (9.4). Also (9.27) implies

$$\boldsymbol{\Gamma}_1(\boldsymbol{n})\boldsymbol{\tau} = \boldsymbol{\Gamma}_1(\boldsymbol{n})\langle\boldsymbol{\tau}\rangle, \quad \boldsymbol{\Gamma}_2(\boldsymbol{n})\boldsymbol{\epsilon} = \boldsymbol{\Gamma}_2(\boldsymbol{n})\langle\boldsymbol{\epsilon}\rangle,$$

and therefore all of the preceding analysis carries through directly to the elasticity problem.

In particular, the general lamination formula

$$[\boldsymbol{S}_* - \boldsymbol{\Gamma}_1(\boldsymbol{n})]^{-1} = \langle[\boldsymbol{S}(\boldsymbol{x}) - \boldsymbol{\Gamma}_1(\boldsymbol{n})]^{-1}\rangle$$

applies with

$$\boldsymbol{S}_* = \sigma_0(\sigma_0\boldsymbol{\mathcal{I}} - \boldsymbol{\mathcal{C}}_*)^{-1}, \quad \boldsymbol{S}(\boldsymbol{x}) = \sigma_0(\sigma_0\boldsymbol{\mathcal{I}} - \boldsymbol{\mathcal{C}}(\boldsymbol{x}))^{-1},$$

where $\boldsymbol{\mathcal{I}}$ is the fourth-order identity tensor. This gives an explicit formula for the effective elastic tensor $\boldsymbol{\mathcal{C}}_*$ of the laminate for any choice of the reference constant σ_0.

More generally, if $\boldsymbol{n}$ is not directed along the x_1-axis, then $\boldsymbol{\Gamma}_1(\boldsymbol{n})$ and $\boldsymbol{\Gamma}_2(\boldsymbol{n})$ can be defined through their action on a second-order tensor $\boldsymbol{A}$ by the equations

$$\boldsymbol{\Gamma}_1(\boldsymbol{n})\boldsymbol{A} = (\boldsymbol{A}\boldsymbol{n}) \otimes \boldsymbol{n} + \boldsymbol{n} \otimes (\boldsymbol{A}\boldsymbol{n}) - (\boldsymbol{n} \cdot \boldsymbol{A}\boldsymbol{n})\boldsymbol{n} \otimes \boldsymbol{n}, \qquad \boldsymbol{\Gamma}_2(\boldsymbol{n})\boldsymbol{A} = \boldsymbol{A} - \boldsymbol{\Gamma}_1(\boldsymbol{n})\boldsymbol{A}, \tag{9.29}$$

and it is easy to check that $\boldsymbol{\Gamma}_1(\boldsymbol{n})$ defined in this way projects onto the subspace of symmetric second-order tensors

$$\mathcal{E}_{\boldsymbol{n}} = \{\boldsymbol{B} = \boldsymbol{n} \otimes \boldsymbol{b} + \boldsymbol{b} \otimes \boldsymbol{n} \mid \boldsymbol{b} \in \mathbb{R}^d\},$$

while $\boldsymbol{\Gamma}_2(\boldsymbol{n})$ projects onto the subspace

$$\mathcal{J}_{\boldsymbol{n}} = \{\boldsymbol{B} \mid \boldsymbol{n} \cdot \boldsymbol{B} = 0\}.$$

Since $\boldsymbol{\Gamma}_1(\boldsymbol{n})$ and $\boldsymbol{\Gamma}_2(\boldsymbol{n})$ are linear transformations on second-order tensors, they can be represented by fourth-order tensors. Indeed from (9.29) it can be seen that the elements of these tensors in Cartesian coordinates are

$$\begin{aligned}
\{\boldsymbol{\Gamma}_1^e(\boldsymbol{n})\}_{ij\ell m} &= \tfrac{1}{2}\Big(n_i\delta_{j\ell}n_m + n_i\delta_{jm}n_\ell + n_j\delta_{i\ell}n_m + n_j\delta_{im}n_\ell\Big) - n_i n_j n_\ell n_m, \\
\{\boldsymbol{\Gamma}_2^e(\boldsymbol{n})\}_{ij\ell m} &= \tfrac{1}{2}\Big(\delta_{i\ell}\delta_{jm} + \delta_{im}\delta_{j\ell}\Big) - \{\boldsymbol{\Gamma}_1^e(\boldsymbol{n})\}_{ij\ell m},
\end{aligned} \tag{9.30}$$

where the superscript e signifies that these are the expressions for the elasticity problem.

For a two-phase coated laminate with a core of phase 1 with elasticity tensor $\boldsymbol{\mathcal{C}}_1$ coated by phase 2 with the rather special elasticity tensor $\boldsymbol{\mathcal{C}}_2 = \sigma_0\boldsymbol{\mathcal{I}}$, in which $\boldsymbol{\mathcal{I}}$ is the fourth-order identity tensor, we have by direct analogy with (9.20) the formula

$$f_1\sigma_2(\sigma_2\boldsymbol{\mathcal{I}} - \boldsymbol{\mathcal{C}}_*)^{-1} = \sigma_2(\sigma_2\boldsymbol{\mathcal{I}} - \boldsymbol{\mathcal{C}}_1)^{-1} - f_2\sum_{j=1}^{m} c_j\boldsymbol{\Gamma}_1(\boldsymbol{n}_j)$$

for the effective elasticity tensor $\boldsymbol{\mathcal{C}}_*$ in which the constants c_j are given by (9.21) in terms of the intermediate volume fractions $f^{(j)}$. The restriction that $\boldsymbol{\mathcal{C}}_2 = \sigma_0\boldsymbol{\mathcal{I}}$ is quite unnatural in the elasticity problem since it is stronger than the assumption of isotropy of phase 2. In fact we will see in the next section that this restriction is not needed.

For thermoelasticity, poroelasticity, thermoelectricity, or piezoelectricity, the constitutive law and effective constitutive law take the generic forms

$$\boldsymbol{J}(\boldsymbol{x}) = \boldsymbol{L}(\boldsymbol{x})\boldsymbol{E}(\boldsymbol{x}), \qquad \langle\boldsymbol{J}\rangle = \boldsymbol{L}_*\langle\boldsymbol{E}\rangle. \tag{9.31}$$

For thermoelasticity (or, equivalently, poroelasticity) the fields

$$\boldsymbol{J}(\boldsymbol{x}) = \begin{pmatrix} \boldsymbol{\epsilon}(\boldsymbol{x}) \\ \varsigma(\boldsymbol{x}) \end{pmatrix}, \qquad \boldsymbol{E}(\boldsymbol{x}) = \begin{pmatrix} \boldsymbol{\tau}(\boldsymbol{x}) \\ \theta \end{pmatrix}$$

satisfy the differential constraints

$$\nabla\cdot\boldsymbol{\tau} = 0, \quad \boldsymbol{\epsilon} = [\nabla\boldsymbol{u} + (\nabla\boldsymbol{u})^T]/2, \quad \theta = \text{constant}.$$

Consequently, when these fields only depend on $\boldsymbol{n}\cdot\boldsymbol{x}$ the differential constraints imply

$$\boldsymbol{E} - \langle\boldsymbol{E}\rangle \in \mathcal{E}_{\boldsymbol{n}}, \quad \boldsymbol{J} - \langle\boldsymbol{J}\rangle \in \mathcal{J}_{\boldsymbol{n}}, \tag{9.32}$$

in which $\mathcal{E}_{\boldsymbol{n}}$ and $\mathcal{J}_{\boldsymbol{n}}$ are the orthogonal subspaces

$$\begin{aligned}
\mathcal{E}_{\boldsymbol{n}} &= \{\begin{pmatrix} \boldsymbol{B} \\ 0 \end{pmatrix} \mid \boldsymbol{n}\cdot\boldsymbol{B} = 0\}, \\
\mathcal{J}_{\boldsymbol{n}} &= \{\begin{pmatrix} \boldsymbol{n}\otimes\boldsymbol{b} + \boldsymbol{b}\otimes\boldsymbol{n} \\ \alpha \end{pmatrix} \mid \boldsymbol{b}\in\mathbb{R}^d,\ \alpha\in\mathbb{R}\}.
\end{aligned}$$

Equivalently, the fields $\boldsymbol{J} = \boldsymbol{J}(\boldsymbol{n}\cdot\boldsymbol{x})$ and $\boldsymbol{E} = \boldsymbol{E}(\boldsymbol{n}\cdot\boldsymbol{x})$ satisfy

$$\boldsymbol{\Gamma}_1(\boldsymbol{n})\boldsymbol{J} = \boldsymbol{\Gamma}_1(\boldsymbol{n})\langle\boldsymbol{J}\rangle, \quad \boldsymbol{\Gamma}_2(\boldsymbol{n})\boldsymbol{E} = \boldsymbol{\Gamma}_2(\boldsymbol{n})\langle\boldsymbol{E}\rangle, \tag{9.33}$$

in which $\boldsymbol{\Gamma}_1$ and $\boldsymbol{\Gamma}_2$ are the projections onto $\mathcal{E}_{\boldsymbol{n}}$ and $\mathcal{J}_{\boldsymbol{n}}$, respectively:

$$\boldsymbol{\Gamma}_1(\boldsymbol{n}) = \begin{pmatrix} \boldsymbol{\Gamma}_2^e(\boldsymbol{n}) & 0 \\ 0 & 0 \end{pmatrix}, \quad \boldsymbol{\Gamma}_2(\boldsymbol{n}) = \begin{pmatrix} \boldsymbol{\Gamma}_1^e(\boldsymbol{n}) & 0 \\ 0 & 1 \end{pmatrix}.$$

Here $\boldsymbol{\Gamma}_1^e(\boldsymbol{n})$ and $\boldsymbol{\Gamma}_2^e(\boldsymbol{n})$ are the Γ-operators for elasticity given by (9.30).

For thermoelectricity or similar coupled problems where two divergence free fields are coupled with two curl free fields the constitutive relation and effective constitutive relation take the forms of (9.31) with fields

$$\boldsymbol{J}(\boldsymbol{x}) = \begin{pmatrix} \boldsymbol{j}_1 \\ \boldsymbol{j}_2 \end{pmatrix}, \quad \boldsymbol{E}(\boldsymbol{x}) = \begin{pmatrix} \boldsymbol{e}_1 \\ \boldsymbol{e}_2 \end{pmatrix}, \quad \text{where } \nabla \cdot \boldsymbol{j}_i = 0, \ \nabla \times \boldsymbol{e}_i = 0, \ i = 1, 2,$$

and when these fields only depend on $\boldsymbol{n} \cdot \boldsymbol{x}$, (9.32) and (9.33) hold with

$$\begin{aligned} \mathcal{E}_{\boldsymbol{n}} &= \{ \begin{pmatrix} \alpha \boldsymbol{n} \\ \beta \boldsymbol{n} \end{pmatrix} \mid \alpha, \beta \in \mathbb{R} \}, \\ \mathcal{J}_{\boldsymbol{n}} &= \{ \begin{pmatrix} \boldsymbol{a} \\ \boldsymbol{b} \end{pmatrix} \mid \boldsymbol{a}, \boldsymbol{b} \in \mathbb{R}^d, \ \boldsymbol{n} \cdot \boldsymbol{a} = \boldsymbol{n} \cdot \boldsymbol{b} = 0 \}, \end{aligned}$$

and

$$\boldsymbol{\Gamma}_1(\boldsymbol{n}) = \boldsymbol{I} - \boldsymbol{\Gamma}_2(\boldsymbol{n}) = \begin{pmatrix} \boldsymbol{\Gamma}_1^c(\boldsymbol{n}) & 0 \\ 0 & \boldsymbol{\Gamma}_1^c(\boldsymbol{n}) \end{pmatrix}, \quad \text{where } \boldsymbol{\Gamma}_1^c(\boldsymbol{n}) = \boldsymbol{n} \otimes \boldsymbol{n}.$$

Again, $\boldsymbol{\Gamma}_1(\boldsymbol{n})$ and $\boldsymbol{\Gamma}_2(\boldsymbol{n})$ represent the projections onto the subspaces $\mathcal{E}_{\boldsymbol{n}}$ and $\mathcal{J}_{\boldsymbol{n}}$, respectively. These formulas have an obvious generalization to the case where more than two divergence free and curl free fields are coupled.

For piezoelectricity the constitutive relation and effective constitutive relation take the forms of (9.31) with fields

$$\boldsymbol{J}(\boldsymbol{x}) = \begin{pmatrix} \boldsymbol{\epsilon} \\ \boldsymbol{d} \end{pmatrix}, \quad \boldsymbol{E}(\boldsymbol{x}) = \begin{pmatrix} \boldsymbol{\tau} \\ \boldsymbol{e} \end{pmatrix}, \quad \text{where} \quad \begin{matrix} \boldsymbol{\epsilon} = [\nabla \boldsymbol{u} + (\nabla \boldsymbol{u})^T]/2, & \nabla \cdot \boldsymbol{\tau} = 0, \\ \nabla \cdot \boldsymbol{d} = 0, & \nabla \times \boldsymbol{e} = 0, \end{matrix}$$

and when these fields only depend on $\boldsymbol{n} \cdot \boldsymbol{x}$, (9.32) and (9.33) hold with

$$\begin{aligned} \mathcal{E}_{\boldsymbol{n}} &= \{ \begin{pmatrix} \boldsymbol{B} \\ \alpha \boldsymbol{n} \end{pmatrix} \mid \boldsymbol{n} \cdot \boldsymbol{B} = 0, \ \alpha \in \mathbb{R} \}, \\ \mathcal{J}_{\boldsymbol{n}} &= \{ \begin{pmatrix} \boldsymbol{n} \otimes \boldsymbol{b} + \boldsymbol{b} \otimes \boldsymbol{n} \\ \boldsymbol{a} \end{pmatrix} \mid \boldsymbol{a}, \boldsymbol{b} \in \mathbb{R}^d, \ \boldsymbol{n} \cdot \boldsymbol{a} = 0 \}, \end{aligned}$$

and

$$\boldsymbol{\Gamma}_1(\boldsymbol{n}) = \boldsymbol{I} - \boldsymbol{\Gamma}_2(\boldsymbol{n}) = \begin{pmatrix} \boldsymbol{\Gamma}_2^e(\boldsymbol{n}) & 0 \\ 0 & \boldsymbol{\Gamma}_1^c(\boldsymbol{n}) \end{pmatrix},$$

where $\boldsymbol{\Gamma}_2^e(\boldsymbol{n})$ and $\boldsymbol{\Gamma}_1^c(\boldsymbol{n})$ are given by (9.30) and (9.2).

In summary it is clear that equations (9.31) and (9.33) apply to conductivity, thermoelasticity, poroelasticity, thermoelectricity, and piezoelectricity with an appropriate choice of the projections $\boldsymbol{\Gamma}_1(\boldsymbol{n})$ and $\boldsymbol{\Gamma}_2(\boldsymbol{n})$. Since the derivation of the lamination formulas only uses these equations, it follows that the effective tensor $\boldsymbol{L}_*$ of a simple laminate in all of these problems is given by

$$[\boldsymbol{S}_* - \boldsymbol{\Gamma}_1(\boldsymbol{n})]^{-1} = \langle [\boldsymbol{S}(\boldsymbol{x}) - \boldsymbol{\Gamma}_1(\boldsymbol{n})]^{-1} \rangle, \tag{9.34}$$

with

$$\boldsymbol{S}_* = \sigma_0(\sigma_0\boldsymbol{I} - \boldsymbol{L}_*)^{-1}, \quad \boldsymbol{S}(\boldsymbol{x}) = \sigma_0(\sigma_0\boldsymbol{I} - \boldsymbol{L}(\boldsymbol{x}))^{-1}. \tag{9.35}$$

Similarly, the effective tensor $\boldsymbol{L}_*$ of a coated laminate with a core of phase 1 with tensor $\boldsymbol{L}_1$ and coating of phase 2 with the special tensor $\boldsymbol{L}_2 = \sigma_2\boldsymbol{I}$ is given by

$$f_1\sigma_2(\sigma_2\boldsymbol{I} - \boldsymbol{L}_*)^{-1} = \sigma_2(\sigma_2\boldsymbol{I} - \boldsymbol{L}_1)^{-1} - f_2\sum_{j=1}^{m} c_j\boldsymbol{\Gamma}_1(\boldsymbol{n}_j), \tag{9.36}$$

where the constants c_j are given by (9.21) in terms of the intermediate volume fractions $f^{(j)}$.

9.6. The lamination formula for a coated laminate with anisotropic coating and anisotropic core

The lamination formula (9.36) for the effective conductivity, elastic, thermoelastic, thermoelectric, or piezoelectric tensor of a coated laminate is applicable only when the coating of phase 2 has tensor $\boldsymbol{L}_2$ proportional to the identity tensor. A more general formula that is valid for arbitrary choices of the tensor $\boldsymbol{L}_2$ is obtained if we recast the simple lamination formula (9.34) in another equivalent form. This is done by introducing a possibly anisotropic reference tensor $\boldsymbol{L}_0$ and considering the equation satisfied by the polarization field

$$\boldsymbol{P}(\boldsymbol{x}) = \boldsymbol{J}(\boldsymbol{x}) - \boldsymbol{L}_0\boldsymbol{E}(\boldsymbol{x}) = (\boldsymbol{L}(\boldsymbol{x}) - \boldsymbol{L}_0)\boldsymbol{E}(\boldsymbol{x}). \tag{9.37}$$

From (9.33) we have

$$\boldsymbol{\Gamma}_1(\boldsymbol{n})(\langle\boldsymbol{E}\rangle - \boldsymbol{E}(\boldsymbol{x})) = \langle\boldsymbol{E}\rangle - \boldsymbol{E}(\boldsymbol{x}),$$

$$\boldsymbol{\Gamma}_1(\boldsymbol{n})[\boldsymbol{P}(\boldsymbol{x}) - \langle\boldsymbol{P}\rangle - \boldsymbol{L}_0(\langle\boldsymbol{E}\rangle - \boldsymbol{E}(\boldsymbol{x}))] = \boldsymbol{\Gamma}_1(\boldsymbol{n})[\boldsymbol{J}(\boldsymbol{x}) - \langle\boldsymbol{J}\rangle] = 0. \tag{9.38}$$

Now let us define a new matrix $\boldsymbol{\Gamma}(\boldsymbol{n})$ defined through its action on a tensor $\boldsymbol{A}$: We say that

$$\boldsymbol{B} = \boldsymbol{\Gamma}(\boldsymbol{n})\boldsymbol{A} \quad \text{if and only if} \quad \boldsymbol{\Gamma}_1(\boldsymbol{n})\boldsymbol{B} = \boldsymbol{B} \ \text{ and } \ \boldsymbol{\Gamma}_1(\boldsymbol{n})(\boldsymbol{A} - \boldsymbol{L}_0\boldsymbol{B}) = 0, \tag{9.39}$$

which gives a linear set of equations that can be solved for $\boldsymbol{B}$. Using standard manipulations of linear algebra it is clear that $\boldsymbol{\Gamma}(\boldsymbol{n})$ is in fact given by the formula

$$\boldsymbol{\Gamma}(\boldsymbol{n}) = \boldsymbol{\Gamma}_1(\boldsymbol{n})[\boldsymbol{\Gamma}_1(\boldsymbol{n})\boldsymbol{L}_0\boldsymbol{\Gamma}_1(\boldsymbol{n})]^{-1}\boldsymbol{\Gamma}_1(\boldsymbol{n}), \tag{9.40}$$

in which the inverse is to be taken on the subspace $\mathcal{E}_{\boldsymbol{n}}$ onto which $\boldsymbol{\Gamma}_1(\boldsymbol{n})$ projects. [Note that we can identify $\boldsymbol{\Gamma}(\boldsymbol{n})$ with $\boldsymbol{\Gamma}_1(\boldsymbol{n})$ when $\boldsymbol{L}_0 = \boldsymbol{I}$.] With this definition of $\boldsymbol{\Gamma}(\boldsymbol{n})$, (9.38) and (9.37) imply that

$$\boldsymbol{\Gamma}(\boldsymbol{n})(\boldsymbol{P}(\boldsymbol{x}) - \langle\boldsymbol{P}\rangle) = \langle\boldsymbol{E}\rangle - \boldsymbol{E}(\boldsymbol{x}) = \langle\boldsymbol{E}\rangle - (\boldsymbol{L}(\boldsymbol{x}) - \boldsymbol{L}_0)^{-1}\boldsymbol{P}(\boldsymbol{x}).$$

Solving this linear equation for $\boldsymbol{P}(\boldsymbol{x})$ and averaging gives

$$\langle\boldsymbol{P}\rangle = \langle[(\boldsymbol{L}(\boldsymbol{x}) - \boldsymbol{L}_0)^{-1} + \boldsymbol{\Gamma}(\boldsymbol{n})]^{-1}\rangle\boldsymbol{V}, \tag{9.41}$$

where $\boldsymbol{V}$ is the constant field

$$\boldsymbol{V} = \langle\boldsymbol{E}\rangle + \boldsymbol{\Gamma}(\boldsymbol{n})\langle\boldsymbol{P}\rangle. \tag{9.42}$$

Also from (9.37) and the definition (9.31) of the effective tensor $\boldsymbol{L}_*$ we see that

$$\langle \boldsymbol{P} \rangle = (\boldsymbol{L}_* - \boldsymbol{L}_0)\langle \boldsymbol{E} \rangle,$$

which in conjunction with (9.42) implies that

$$\langle \boldsymbol{P} \rangle = [(\boldsymbol{L}_* - \boldsymbol{L}_0)^{-1} + \boldsymbol{\Gamma}(\boldsymbol{n})]^{-1}\boldsymbol{V}. \tag{9.43}$$

Since (9.41) and (9.43) hold for all choices of the constant field $\boldsymbol{V}$, we deduce that the effective tensor $\boldsymbol{L}_*$ of a simple laminate must be given by the lamination formula

$$[(\boldsymbol{L}_* - \boldsymbol{L}_0)^{-1} + \boldsymbol{\Gamma}(\boldsymbol{n})]^{-1} = \langle [(\boldsymbol{L}(\boldsymbol{x}) - \boldsymbol{L}_0)^{-1} + \boldsymbol{\Gamma}(\boldsymbol{n})]^{-1} \rangle. \tag{9.44}$$

This formula holds for any choice of the reference tensor $\boldsymbol{L}_0$ and in particular reduces to the lamination formula (9.34) when $\boldsymbol{L}_0 = \sigma_0 \boldsymbol{I}$. In a two-phase simple laminate we can let $\boldsymbol{L}_0$ approach the tensor $\boldsymbol{L}_2$ of phase 2, and in this limit the lamination formula (9.44) reduces to

$$f_1(\boldsymbol{L}_* - \boldsymbol{L}_2)^{-1} = (\boldsymbol{L}_1 - \boldsymbol{L}_2)^{-1} + f_2\boldsymbol{\Gamma}(\boldsymbol{n}), \tag{9.45}$$

which leads to the expression

$$f_1(\boldsymbol{L}_* - \boldsymbol{L}_2)^{-1} = (\boldsymbol{L}_1 - \boldsymbol{L}_2)^{-1} + f_2 \sum_{j=1}^{m} c_j \boldsymbol{\Gamma}(\boldsymbol{n}_j) \tag{9.46}$$

for the effective tensor of a coated laminate with a core of phase 1 with tensor $\boldsymbol{L}_1$ coated with phase 2 with tensor $\boldsymbol{L}_2$, where the constants c_j are given by (9.21) in terms of the intermediate volume fractions $f^{(j)}$ and $\boldsymbol{\Gamma}(\boldsymbol{n})$ is given by (9.40). (Phase 2 is assumed to have a fixed orientation relative to the spatial coordinates at each stage of lamination.)

9.7. Reference transformations

There is another simple way to derive the lamination formula (9.44), and by extension (9.46), when the tensor $\boldsymbol{L}_0$ of the reference medium is symmetric and self-adjoint. This is accomplished by transforming to a problem where the fields satisfy different differential restrictions and the material constants are $(\boldsymbol{L}_0)^{-1/2}\boldsymbol{L}(\boldsymbol{x})(\boldsymbol{L}_0)^{-1/2}$ and then applying the lamination formula given by (9.34) and (9.35). This alternative approach provides a good opportunity to introduce the idea of these transformations, which are called reference transformations

The basic idea (Milton and Kohn 1988) is to rewrite the constitutive law and effective constitutive law

$$\boldsymbol{J}(\boldsymbol{x}) = \boldsymbol{L}(\boldsymbol{x})\boldsymbol{E}(\boldsymbol{x}), \qquad \langle \boldsymbol{J} \rangle = \boldsymbol{L}_*\langle \boldsymbol{E} \rangle \tag{9.47}$$

in the form

$$\boldsymbol{J}'(\boldsymbol{x}) = \boldsymbol{L}'(\boldsymbol{x})\boldsymbol{E}'(\boldsymbol{x}), \qquad \langle \boldsymbol{J}' \rangle = \boldsymbol{L}'_*\langle \boldsymbol{E}' \rangle,$$

where

$$\boldsymbol{L}'(\boldsymbol{x}) = (\boldsymbol{L}_0)^{-1/2}\boldsymbol{L}(\boldsymbol{x})(\boldsymbol{L}_0)^{-1/2}, \qquad \boldsymbol{L}'_* = (\boldsymbol{L}_0)^{-1/2}\boldsymbol{L}_*(\boldsymbol{L}_0)^{-1/2}, \tag{9.48}$$

and

$$\boldsymbol{J}'(\boldsymbol{x}) = (\boldsymbol{L}_0)^{-1/2}\boldsymbol{J}(\boldsymbol{x}), \qquad \boldsymbol{E}'(\boldsymbol{x}) = \boldsymbol{L}_0^{1/2}\boldsymbol{E}(\boldsymbol{x}). \tag{9.49}$$

Clearly these fields $\boldsymbol{J}'(\boldsymbol{x})$ and $\boldsymbol{E}'(\boldsymbol{x})$ satisfy a new set of differential constraints.

Now consider a simple rank-1 laminate where $\boldsymbol{L}(\boldsymbol{x})$ and hence $\boldsymbol{L}'(\boldsymbol{x})$ depend only on $\boldsymbol{n}\cdot\boldsymbol{x}$. The conditions (9.47) satisfied by $\boldsymbol{J}$ and $\boldsymbol{E}$ imply that

$$\boldsymbol{J}(\boldsymbol{x})-\langle\boldsymbol{J}\rangle\in\mathcal{J}_{\boldsymbol{n}},\quad \boldsymbol{E}(\boldsymbol{x})-\langle\boldsymbol{E}\rangle\in\mathcal{E}_{\boldsymbol{n}},\tag{9.50}$$

where $\mathcal{J}_{\boldsymbol{n}}$ and $\mathcal{E}_{\boldsymbol{n}}$ are the mutually orthogonal subspaces onto which $\boldsymbol{\Gamma}_2(\boldsymbol{n})$ and $\boldsymbol{\Gamma}_1(\boldsymbol{n})$ project. It then follows directly from the definitions (9.49) of $\boldsymbol{J}'(\boldsymbol{x})$ and $\boldsymbol{E}'(\boldsymbol{x})$ that

$$\boldsymbol{J}'(\boldsymbol{x})-\langle\boldsymbol{J}'\rangle\in\mathcal{J}'_{\boldsymbol{n}}=(\boldsymbol{L}_0)^{-1/2}\mathcal{J}_{\boldsymbol{n}},\quad \boldsymbol{E}'(\boldsymbol{x})-\langle\boldsymbol{E}'\rangle\in\mathcal{E}'_{\boldsymbol{n}}=\boldsymbol{L}_0^{1/2}\mathcal{E}_{\boldsymbol{n}},\tag{9.51}$$

in which $\mathcal{J}'_{\boldsymbol{n}}$ is obtained by multiplying each element of $\mathcal{J}_{\boldsymbol{n}}$ by $(\boldsymbol{L}_0)^{-1/2}$ and $\mathcal{E}'_{\boldsymbol{n}}$ is obtained by multiplying each element of $\mathcal{E}_{\boldsymbol{n}}$ by $(\boldsymbol{L}_0)^{1/2}$. These new subspaces $\mathcal{J}'_{\boldsymbol{n}}$ and $\mathcal{E}'_{\boldsymbol{n}}$ are clearly orthogonal because $\mathcal{J}_{\boldsymbol{n}}$ and $\mathcal{E}_{\boldsymbol{n}}$ are orthogonal; the inner product of $(\boldsymbol{L}_0)^{-1/2}\boldsymbol{J}$ with $(\boldsymbol{L}_0)^{1/2}\boldsymbol{E}$ is the same as the inner product of $\boldsymbol{J}$ with $\boldsymbol{E}$ because the factors of $(\boldsymbol{L}_0)^{-1/2}$ and $(\boldsymbol{L}_0)^{1/2}$ cancel. Therefore the projections $\boldsymbol{\Gamma}'_2(\boldsymbol{n})$ and $\boldsymbol{\Gamma}'_1(\boldsymbol{n})$ onto these subspaces satisfy

$$\boldsymbol{\Gamma}'_i(\boldsymbol{n})\boldsymbol{\Gamma}'_j(\boldsymbol{n})=\delta_{ij}\boldsymbol{\Gamma}'_i(\boldsymbol{n}),\quad \boldsymbol{\Gamma}'_1(\boldsymbol{n})+\boldsymbol{\Gamma}'_2(\boldsymbol{n})=\boldsymbol{I},$$

and (9.51) implies that

$$\boldsymbol{\Gamma}'_1(\boldsymbol{n})\boldsymbol{J}'=\boldsymbol{\Gamma}'_1(\boldsymbol{n})\langle\boldsymbol{J}'\rangle,\quad \boldsymbol{\Gamma}'_2(\boldsymbol{n})\boldsymbol{E}=\boldsymbol{\Gamma}'_2(\boldsymbol{n})\langle\boldsymbol{E}'\rangle.$$

Since (9.50) and (9.51) are the only ingredients needed to derive the lamination formula, we immediately deduce from (9.34) and (9.35) that the effective tensor $\boldsymbol{L}'_*$ satisfies

$$[(\boldsymbol{L}'_*-\boldsymbol{I})^{-1}+\boldsymbol{\Gamma}'_1(\boldsymbol{n})]^{-1}=\langle[(\boldsymbol{L}'(\boldsymbol{x})-\boldsymbol{I})^{-1}+\boldsymbol{\Gamma}'_1(\boldsymbol{n})]^{-1}\rangle,\tag{9.52}$$

where we have chosen to take $\sigma_0=1$. Furthermore, as $\mathcal{E}'_{\boldsymbol{n}}$ is the range of the operator $\boldsymbol{L}_2^{1/2}\boldsymbol{\Gamma}_1(\boldsymbol{n})$, it follows from a standard result in linear algebra that the projection $\boldsymbol{\Gamma}'_1(\boldsymbol{n})$ onto $\mathcal{E}'_{\boldsymbol{n}}$ is given by the formula

$$\boldsymbol{\Gamma}'_1(\boldsymbol{n})=\boldsymbol{L}_2^{1/2}\boldsymbol{\Gamma}_1(\boldsymbol{n})[\boldsymbol{\Gamma}_1(\boldsymbol{n})\boldsymbol{L}_2\boldsymbol{\Gamma}_1(\boldsymbol{n})]^{-1}\boldsymbol{\Gamma}_1(\boldsymbol{n})\boldsymbol{L}_2^{1/2},\tag{9.53}$$

in which the inverse is to be taken on the subspace $\mathcal{E}_{\boldsymbol{n}}$. Substituting (9.48) and (9.53) into (9.52) gives

$$[(\boldsymbol{L}_*-\boldsymbol{L}_0)^{-1}+\boldsymbol{\Gamma}(\boldsymbol{n})]^{-1}=\langle[(\boldsymbol{L}(\boldsymbol{x})-\boldsymbol{L}_0)^{-1}+\boldsymbol{\Gamma}(\boldsymbol{n})]^{-1}\rangle,$$

in agreement with (9.44).

In a two-phase laminate we can again take $\boldsymbol{L}_0$=$\boldsymbol{L}_2$ and thereby obtain (9.45), which leads directly to the formula (9.46) for the effective tensor $\boldsymbol{L}_*$ of a coated laminate. In other words, the seemingly restrictive original assumption that the coating phase had a tensor proportional to $\boldsymbol{I}$ is in fact only a mild assumption since we can use a reference transformation of the equations so that the tensor $\boldsymbol{L}_2$ of the coating phase transforms to a tensor $\boldsymbol{L}'_2=\boldsymbol{I}$, provided that $\boldsymbol{L}_2$ is self-adjoint and positive-definite.

9.8. Explicit formulas for the conductivity and elasticity tensors of a coated laminate

For conductivity (9.46) with $\boldsymbol{\Gamma}(\boldsymbol{n})$ given by (9.2) and (9.40) reduces to the lamination formula

$$f_1(\boldsymbol{\sigma}_2-\boldsymbol{\sigma}_*)^{-1}=(\boldsymbol{\sigma}_2-\boldsymbol{\sigma}_1)^{-1}-f_2\sum_{j=1}^{m}c_j\frac{\boldsymbol{n}_j\otimes\boldsymbol{n}_j}{\boldsymbol{n}_j\cdot\boldsymbol{\sigma}_2\boldsymbol{n}_j}\tag{9.54}$$

of Tartar (1985), which can be rewritten in the equivalent form

$$f_1(\boldsymbol{\sigma}_2 - \boldsymbol{\sigma}_*)^{-1} = (\boldsymbol{\sigma}_2 - \boldsymbol{\sigma}_1)^{-1} - f_2(\boldsymbol{\sigma}_2)^{-1/2}\boldsymbol{M}(\boldsymbol{\sigma}_2)^{-1/2},$$

where

$$\boldsymbol{M} = \sum_{j=1}^{m} c_j \frac{\boldsymbol{m}_j \otimes \boldsymbol{m}_j}{\boldsymbol{m}_j \cdot \boldsymbol{m}_j} \quad \text{with } \boldsymbol{m}_j = (\boldsymbol{\sigma}_2)^{1/2}\boldsymbol{n}_j.$$

So the conductivity formula of a coated laminate again turns out to have exactly the same form as the conductivity formula (8.15) of the coated ellipsoids with an anisotropic core and an anisotropic coating, and in both cases the matrix $\boldsymbol{M}$ is positive-semidefinite and satisfies $\mathrm{Tr}\boldsymbol{M} = 1$.

For elasticity the lamination formula, due to Francfort and Murat (1986) and Gibiansky and Cherkaev (1987), is

$$f_1(\boldsymbol{\mathcal{C}}_2 - \boldsymbol{\mathcal{C}}_*)^{-1} = (\boldsymbol{\mathcal{C}}_2 - \boldsymbol{\mathcal{C}}_1)^{-1} - f_2 \sum_{j=1}^{m} c_j \boldsymbol{\Gamma}(\boldsymbol{n}_j), \tag{9.55}$$

where to obtain an explicit expression for the matrix $\boldsymbol{B}$ that results from the action of $\boldsymbol{\Gamma}(\boldsymbol{n})$ on a symmetric matrix $\boldsymbol{A}$ we need to solve the equations (9.39). For elasticity we have that $\boldsymbol{\Gamma}_1(\boldsymbol{n})\boldsymbol{B} = \boldsymbol{B}$ if and only if there exists a vector $\boldsymbol{b}$ such that

$$\boldsymbol{B} = \boldsymbol{n} \otimes \boldsymbol{b} + \boldsymbol{b} \otimes \boldsymbol{n}. \tag{9.56}$$

We also have that $\boldsymbol{\Gamma}_1(\boldsymbol{n})(\boldsymbol{A} - \boldsymbol{\mathcal{C}}_2\boldsymbol{B}) = 0$ if and only if

$$\boldsymbol{n} \cdot (\boldsymbol{A} - \boldsymbol{\mathcal{C}}_2\boldsymbol{B}) = 0. \tag{9.57}$$

Substituting (9.56) into (9.57) and solving for the vector $\boldsymbol{b}$ gives

$$\boldsymbol{b} = \boldsymbol{\mathcal{C}}(\boldsymbol{n})^{-1}\boldsymbol{A}\boldsymbol{n}/2,$$

in which $\boldsymbol{\mathcal{C}}(\boldsymbol{n})^{-1}$ is the inverse of the acoustic tensor, which is the 3×3 matrix $\boldsymbol{\mathcal{C}}(\boldsymbol{n}) = \boldsymbol{n}\cdot\boldsymbol{\mathcal{C}}_2\boldsymbol{n}$ with elements

$$\{\boldsymbol{\mathcal{C}}(\boldsymbol{n})\}_{ij} = \sum_{p,q} n_p C^{(2)}_{pijq} n_q,$$

where the $C^{(2)}_{pijq}$ are the tensor elements of $\boldsymbol{\mathcal{C}}_2$. The acoustic tensor gets its name from its role in the equations governing the propagation of acoustic waves (see section 11.3 on page 230). By inserting this back in (9.56) we obtain an expression for the matrix $\boldsymbol{B} = \boldsymbol{\Gamma}\boldsymbol{A}$, which in turn implies that the fourth-order tensor $\boldsymbol{\Gamma}(\boldsymbol{n})$ has matrix elements

$$\{\boldsymbol{\Gamma}(\boldsymbol{n})\}_{ij\ell m} = \frac{1}{4}\Big(n_i\{\boldsymbol{\mathcal{C}}(\boldsymbol{n})^{-1}\}_{j\ell}n_m + n_i\{\boldsymbol{\mathcal{C}}(\boldsymbol{n})^{-1}\}_{jm}n_\ell + n_j\{\boldsymbol{\mathcal{C}}(\boldsymbol{n})^{-1}\}_{i\ell}n_m + n_j\{\boldsymbol{\mathcal{C}}(\boldsymbol{n})^{-1}\}_{im}n_\ell\Big). \tag{9.58}$$

In particular, when phase 2 is isotropic, we have

$$\{\boldsymbol{\Gamma}(\boldsymbol{n})\}_{ij\ell m} = \frac{n_i n_j n_\ell n_m}{\lambda_2 + 2\mu_2} + \frac{1}{4\mu_2}\Big(n_i\delta_{j\ell}n_m + n_i\delta_{jm}n_\ell + n_j\delta_{i\ell}n_m + n_j\delta_{im}n_\ell - 4n_i n_j n_\ell n_m\Big). \tag{9.59}$$

These equations (9.58) and (9.59) give the correct formulas for $\boldsymbol{\Gamma}(\boldsymbol{n})$ in d-dimensional elasticity. The tensor $\boldsymbol{\Gamma}(\boldsymbol{n})$ can also be obtained directly from the formula (9.40), but we chose not to do so because it involves more work.

In two dimensions the formula (9.55) is best expressed in terms of the compliance tensors $\boldsymbol{\mathcal{S}}_i = \boldsymbol{\mathcal{C}}_i^{-1}$, $i = 1, 2, *$ or, equivalently, in terms of the tensors entering the plate equations. To do this, one repeats the analysis but with the role $\boldsymbol{\Gamma}_1(\boldsymbol{n})$ replaced by $\boldsymbol{\Gamma}_2(\boldsymbol{n})$. We have that $\boldsymbol{\Gamma}_2(\boldsymbol{n})\boldsymbol{B} = \boldsymbol{B}$ if and only if there exists a constant β such that

$$\boldsymbol{B} = \beta \boldsymbol{t} \otimes \boldsymbol{t}, \tag{9.60}$$

where $\boldsymbol{t} = \boldsymbol{R}_\perp \boldsymbol{n}$ is the vector perpendicular to $\boldsymbol{n}$. We also have that $\boldsymbol{\Gamma}_2(\boldsymbol{n})(\boldsymbol{A} - \boldsymbol{\mathcal{S}}_2\boldsymbol{B}) = 0$, if and only if

$$\boldsymbol{t} \cdot (\boldsymbol{A} - \boldsymbol{\mathcal{S}}_2\boldsymbol{B})\boldsymbol{t} = 0. \tag{9.61}$$

By substituting (9.60) into (9.61) and solving for β we see that

$$\boldsymbol{B} = (1/4\kappa_2 + 1/4\mu_2)(\boldsymbol{t} \cdot \boldsymbol{A}\boldsymbol{t})\boldsymbol{t} \otimes \boldsymbol{t},$$

where we have assumed that phase 2 is isotropic. Using this one obtains the lamination formula

$$f_1(\boldsymbol{\mathcal{S}}_2 - \boldsymbol{\mathcal{S}}_*)^{-1} = (\boldsymbol{\mathcal{S}}_2 - \boldsymbol{\mathcal{S}}_1)^{-1} - f_2(1/4\kappa_2 + 1/4\mu_2)\boldsymbol{\mathcal{M}} \tag{9.62}$$

of Gibiansky and Cherkaev (1987) [see their equations (2.37) and (2.38)], where

$$\{\boldsymbol{\mathcal{M}}\}_{hik\ell} = \sum_{j=1}^{m} c_j \{\boldsymbol{t}_j\}_h \{\boldsymbol{t}_j\}_i \{\boldsymbol{t}_j\}_k \{\boldsymbol{t}_j\}_\ell \tag{9.63}$$

and $\boldsymbol{t}_j = \boldsymbol{R}_\perp \boldsymbol{n}_j$ is the vector perpendicular to $\boldsymbol{n}_j$. An earlier paper of Lurie, Cherkaev, and Fedorov (1982) contains an alternative, but not as concise, formula.

Clearly $\boldsymbol{\mathcal{M}}$ is positive-semidefinite, satisfying

$$\{\boldsymbol{\mathcal{M}}\}_{iijj} = 1, \quad \{\boldsymbol{\mathcal{M}}\}_{ijij} = 1.$$

Conversely, given any positive-semidefinite tensor $\boldsymbol{\mathcal{M}}$ satisfying these conditions, one can find a positive set of weights c_j summing to 1 such that (9.63) holds (Avellaneda and Milton 1989). This gives a complete characterization of the set of all possible effective compliance tensors of two-dimensional coated laminates. As yet there is no similar algebraic characterization in three dimensions. However, considerable progress has been made by Francfort, Murat, and Tartar (1995), who show that the set of all possible effective compliance tensors of three-dimensional coated laminates is generated by laminates of rank 6 or less. Also, Lipton (1991, 1994) has given complete algebraic characterizations of the set of all effective compliance tensors that have transverse or orthotropic symmetry. The reason that such characterizations are important is that, when $\boldsymbol{\mathcal{C}}_1 - \boldsymbol{\mathcal{C}}_2$ is a positive- or negative-definite tensor, Avellaneda (1987) has shown that coated laminates are the stiffest or most compliant composites amongst all composites with the two phases occupying given volume fractions f_1 and $f_2 = 1 - f_1$ (see sections 23.3 on page 462 and 23.4 on page 465).

9.9. Ordinary differential laminates†

Doubly and multicoated laminates can be built in a similar way to the way in which doubly and multicoated sphere assemblages were built. One uses the coated laminate as the core

phase in another coated laminate to obtain a doubly coated laminate, and so forth. Repeated substitutions of (9.20) then generate a continued fraction expansion for the effective conductivity tensor $\boldsymbol{\sigma}_*$ of such laminates.

Also, laminates with continuously varying coating conductivity can be built in a similar way to the way in which sphere assemblages with continuously varying radially conductivity are built. Starting from a core material with possibly anisotropic conductivity $\boldsymbol{\sigma}_0$, suppose that we have already used a differential process to arrive at a continuously coated laminate with effective conductivity tensor $\boldsymbol{\sigma}_*(t)$ parametrized by $t = -\log f_0$, in which f_0 is the volume fraction occupied by the core material at that stage. Now suppose that we layer this material in a fixed direction $\boldsymbol{n}_1(t)$ with an infinitesimal proportion $\epsilon c_1(t)$ of a material that has conductivity λ_n parallel to $\boldsymbol{n}_1(t)$ and a conductivity λ_t perpendicular to $\boldsymbol{n}_1(t)$. This increases t by $\epsilon c_1(t)$ and, to first order in ϵ, (9.54) implies that

$$\begin{aligned}\boldsymbol{\sigma}_*(t+\epsilon c_1(t)) - \boldsymbol{\sigma}_*(t)\\ \approx \epsilon c_1(t)[\boldsymbol{\sigma}_2 - \boldsymbol{\sigma}_*(t) - (\boldsymbol{\sigma}_*(t) - \boldsymbol{\sigma}_2)\boldsymbol{n}_1(t)\otimes\boldsymbol{n}_1(t)(\boldsymbol{\sigma}_*(t) - \boldsymbol{\sigma}_2)/\lambda_n],\end{aligned}$$

where

$$\boldsymbol{\sigma}_2 = \lambda_t \boldsymbol{I} + (\lambda_n - \lambda_t)\boldsymbol{n}_1(t)\otimes\boldsymbol{n}_1(t)$$

is the conductivity tensor of the material that we have added. Next we repeat this process, changing the direction of lamination to successively $\boldsymbol{n}_2(t)$,$\boldsymbol{n}_3(t)$, ...,$\boldsymbol{n}_m(t)$ and adding proportions $\epsilon c_2(t)$,$\epsilon c_3(t)$, ...,$\epsilon c_m(t)$ with

$$\sum_{i=1}^{m} c_i(t) = 1.$$

Then to the first order in ϵ we have

$$\boldsymbol{\sigma}_*(t+\epsilon) - \boldsymbol{\sigma}_*(t) = \epsilon[\lambda_t \boldsymbol{I} - \boldsymbol{\sigma}_* - (\lambda_t - \lambda_n)\boldsymbol{M} - (\boldsymbol{\sigma}_* - \lambda_n \boldsymbol{I})\boldsymbol{M}(\boldsymbol{\sigma}_* - \lambda_n \boldsymbol{I})/\lambda_n], \quad (9.64)$$

where

$$\boldsymbol{M} = \boldsymbol{M}(t) = \sum_{i=1}^{n} c_i(t)\boldsymbol{n}_i \otimes \boldsymbol{n}_i. \quad (9.65)$$

The whole procedure is then repeated, laminating the material in the different directions in cyclical order, until the desired volume fraction is reached. In the limit $\epsilon \to 0$ (9.64) reduces to the Ricatti equation

$$\begin{aligned}\frac{d\boldsymbol{\sigma}_*}{dt} &= \lambda_t \boldsymbol{I} - \boldsymbol{\sigma}_* - (\lambda_t - \lambda_n)\boldsymbol{M} - (\boldsymbol{\sigma}_* - \lambda_n \boldsymbol{I})\boldsymbol{M}(\boldsymbol{\sigma}_* - \lambda_n \boldsymbol{I})/\lambda_n\\ &= \lambda_t \boldsymbol{I} - \boldsymbol{\sigma}_* + \boldsymbol{\sigma}_*\boldsymbol{M} + \boldsymbol{M}\boldsymbol{\sigma}_* - \lambda_t \boldsymbol{M} - \boldsymbol{\sigma}_*\boldsymbol{M}\boldsymbol{\sigma}_*/\lambda_n, \quad (9.66)\end{aligned}$$

governing the evolution of the effective tensor of the continuously coated laminate. In general we are free to choose any trajectory $\boldsymbol{M}(t)$ in the space of symmetric matrices with

$$\boldsymbol{M}(t) \geq 0, \quad \operatorname{Tr} \boldsymbol{M}(t) = 1.$$

To ensure that (9.65) holds, we can take $m = 3$ and set $\boldsymbol{n}_1(t)$, $\boldsymbol{n}_2(t)$, and $\boldsymbol{n}_3(t)$ equal to the normalized eigenvectors of $\boldsymbol{M}(t)$ and set $c_1(t)$, $c_2(t)$, and $c_3(t)$ equal to the eigenvalues of $\boldsymbol{M}(t)$. Associated with this trajectory $\boldsymbol{M}(t)$ will be an effective conductivity tensor $\boldsymbol{\sigma}_*(t)$ obtained by integrating (9.66) with the initial condition $\boldsymbol{\sigma}_* = \boldsymbol{\sigma}_0$ when $t = 0$. Of course, if

one takes $\lambda_t = \lambda_n = \sigma_2$ and $m = 1$ and chooses $\boldsymbol{M}(t) = \boldsymbol{n} \otimes \boldsymbol{n}$ to be independent of t, then, after integration, one recovers the lamination formula (9.19) of Tartar. It is interesting that this is the way in which Tartar first obtained this formula [or more precisely the formula (9.54): see Tartar (2000)].

If we orient our Cartesian axes so that the basis vectors are eigenvectors of $\boldsymbol{\sigma}_0$, and if we take $m = 3$ and $\boldsymbol{n}_1(t)$, $\boldsymbol{n}_2(t)$, and $\boldsymbol{n}_3(t)$ as the basis vectors aligned with the x_1-, x_2-, and x_3-axes, then (9.66) implies that the effective conductivity $\lambda_1^*(t)$ in the x_1 direction evolves according to the differential equation

$$\frac{d\lambda_1^*}{dt} = \lambda_t(t) - \lambda_1^* + \{2\lambda_1^* - \lambda_t(t) - [\lambda_1^*(t)]^2/\lambda_n(t)\}c_1(t),$$

where we have allowed the normal and tangential conductivities $\lambda_n(t)$ and $\lambda_t(t)$ to depend on t. This is exactly the same as the Ricatti equation (7.45) of the ellipsoid assemblage once we choose $c_1(t) = k_1(t)$. The example is indicative of how laminate microstructures can mimic the effective conductivity tensors of a wide variety of different microgeometries.

The construction scheme can obviously be generalized. For example, instead of laminating the material with conductivity tensor $\boldsymbol{\sigma}_*(t)$ at each stage with a homogeneous material, one could laminate it at each stage with a multiple-rank laminate of many different phases. We will call materials obtained through such construction processes ordinary differential laminates. They are a subclass of a family materials, which we call ordinary differential microstructures, that are associated with the generalized differential scheme for estimating the properties of a composite. This scheme will be discussed in section 10.7 on page 201.

9.10. Partial differential laminates†

Multiple-rank laminates are represented by a discrete tree structure as illustrated in figure 9.4 on the next page. Partial differential laminates, like ordinary differential laminates, are a continuum generalization. Often ordinary differential laminates are optimal composites in the sense that they attain bounds on effective tensors. The motivation for introducing partial differential laminates is the expectation (not yet realized) that they too may form an important class of optimal composites. Let us begin with a relatively simple example. Suppose that we are given a trajectory $\boldsymbol{L}(y)$ of initial materials, parameterized by a parameter y. For simplicity let us suppose that $\boldsymbol{L}(y)$ is twice differentiable and that the trajectory forms a continuous loop in tensor space, so that $\boldsymbol{L}(y)$ is periodic in y. We want to construct a two-parameter family $\boldsymbol{L}_*(y, t)$ of effective tensors of partial differential laminates with $\boldsymbol{L}_*(y, 0) = \boldsymbol{L}(y)$. Here t is a continuous parameter generalizing the integer-valued rank r of a multiple-rank laminate. In the same way that the structure of a finite-rank laminate is determined by the directions of lamination and volume fractions assigned to each node in the tree structure, so too is the structure of the partial differential laminate (in our example) determined by a unit vector valued field $\boldsymbol{n}(y, t)$ and by a scalar field $f(y, t)$ taking values between 0 and 1. Rather than working with $\boldsymbol{L}(y)$ and $\boldsymbol{L}_*(y, t)$ it is convenient to introduce the tensors

$$\boldsymbol{S}(y) = \sigma_0[\sigma_0\boldsymbol{I} - \boldsymbol{L}(y)]^{-1}, \quad \boldsymbol{S}_*(y, t) = \sigma_0[\sigma_0\boldsymbol{I} - \boldsymbol{L}_*(y, t)]^{-1},$$

where σ_0 is a fixed constant.

Let us introduce the discrete values of the parameters,

$$y_i = i\epsilon, \quad t_j = j\delta,$$

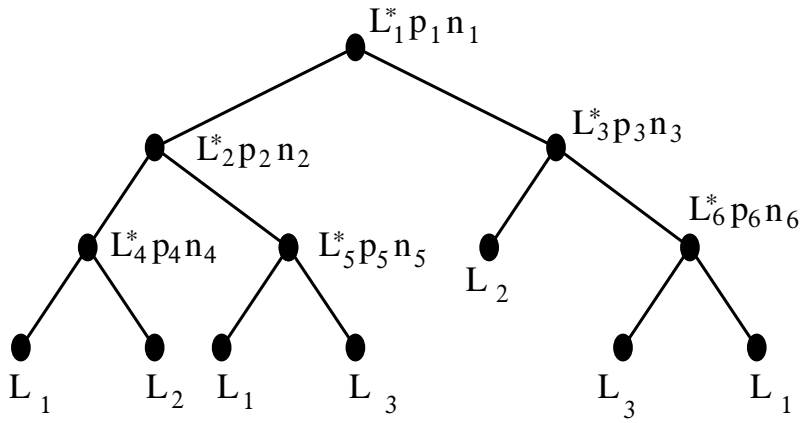

Figure 9.4. Any finite-rank laminate is represented by a tree structure. The tensors $\boldsymbol{L}_1$, $\boldsymbol{L}_2$, and $\boldsymbol{L}_3$ of the constituent phases are at terminating nodes of the tree. Every other node has an effective tensor $\boldsymbol{L}_j^*$, volume fraction p_j, and direction of lamination $\boldsymbol{n}_j$ associated with it. The parameters p_j and $\boldsymbol{n}_j$ determine the structure of the laminate. For example, the material with effective tensor $\boldsymbol{L}_2^*$ is obtained by laminating in direction $\boldsymbol{n}_2$ the materials with tensors $\boldsymbol{L}_4^*$ and $\boldsymbol{L}_5^*$ in proportions p_2 and $1 - p_2$. At the final stage of lamination one obtains the laminate with effective tensor $\boldsymbol{L}_1^*$.

indexed by the integers i and $j \geq 0$, where ϵ and δ are infinitesimal. Associated with $\boldsymbol{S}_*(y_i, t_1)$ is a simple laminate of three materials with tensors $\boldsymbol{S}(y_{i-1})$, $\boldsymbol{S}(y_i)$, and $\boldsymbol{S}(y_{i+1})$ laminated in direction $\boldsymbol{n}$ in proportions $f/2$, $1 - f$, and $f/2$, where $\boldsymbol{n} = \boldsymbol{n}(y_i, t_1)$ and $f = f(y_i, t_1)$. More generally, for $j \geq 1$, associated with $\boldsymbol{S}_*(y_i, t_{j+1})$ is a rank-$(j+1)$ laminate obtained by taking the three rank-j laminates associated with $\boldsymbol{S}_*(y_{i-1}, t_j)$, $\boldsymbol{S}_*(y_i, t_j)$, and $\boldsymbol{S}_*(y_{i+1}, t_j)$ and laminating these three materials together in direction $\boldsymbol{n}$ in proportions $f/2$, $1 - f$, and $f/2$, where $\boldsymbol{n} = \boldsymbol{n}(y_i, t_j)$ and $f = f(y_i, t_j)$. It is important to take equal proportions of $\boldsymbol{S}_*(y_{i-1}, t_j)$ and $\boldsymbol{S}_*(y_{i+1}, t_j)$ to obtain a sensible equation in the continuum limit. From the lamination formula (9.16) we have

$$[\boldsymbol{S}_*(y_i, t_{j+1}) - \boldsymbol{\Gamma}_1(\boldsymbol{n})]^{-1} = (f/2)[\boldsymbol{S}_*(y_{i-1}, t_j) - \boldsymbol{\Gamma}_1(\boldsymbol{n})]^{-1} + (1-f)[\boldsymbol{S}_*(y_i, t_j) - \boldsymbol{\Gamma}_1(\boldsymbol{n})]^{-1} + (f/2)[\boldsymbol{S}_*(y_{i+1}, t_j) - \boldsymbol{\Gamma}_1(\boldsymbol{n})]^{-1}. \quad (9.67)$$

This algorithm serves to define $\boldsymbol{S}_*(y_i, t_k)$ for all i and $k \geq 0$. Strictly speaking, we should write $\boldsymbol{S}_*(y_i, t_k, \epsilon, \delta)$ instead of $\boldsymbol{S}_*(y_i, t_k)$ to emphasize the dependence on ϵ and δ. As ϵ and δ approach zero in an appropriate way, we expect to find that at those points where it is defined $\boldsymbol{S}_*(y, t, \epsilon, \delta)$ approaches $\boldsymbol{S}_*(y, t)$, where $\boldsymbol{S}_*(y, t)$ depends smoothly on y and t. Then to the second order in ϵ and to the first order in δ,

$$\boldsymbol{S}_*(y_{i-1}, t_j) \approx \boldsymbol{S}_* - \epsilon \frac{\partial \boldsymbol{S}_*}{\partial y} + \frac{\epsilon^2}{2} \frac{\partial^2 \boldsymbol{S}_*}{\partial y^2}, \qquad \boldsymbol{S}_*(y_i, t_{j+1}) \approx \boldsymbol{S}_* + \delta \frac{\partial \boldsymbol{S}_*}{\partial t},$$
$$\boldsymbol{S}_*(y_{i+1}, t_j) \approx \boldsymbol{S}_* + \epsilon \frac{\partial \boldsymbol{S}_*}{\partial y} + \frac{\epsilon^2}{2} \frac{\partial^2 \boldsymbol{S}_*}{\partial y^2},$$

where the right-hand sides of these formulas are to be evaluated at the point (y_i, t_j). Substi-

tuting them into (9.67) and expanding both sides we see that to the leading order

$$\delta\frac{\partial \boldsymbol{S}_*}{\partial t} \approx (\epsilon^2/2) f\left\{\frac{\partial^2 \boldsymbol{S}_*}{\partial y^2} - 2\frac{\partial \boldsymbol{S}_*}{\partial y}[\boldsymbol{S}_* - \boldsymbol{\Gamma}_1(\boldsymbol{n})]^{-1}\frac{\partial \boldsymbol{S}_*}{\partial y}\right\}.$$

Taking $\delta = \epsilon^2/2$ is an appropriate scaling, and then in the limit $\epsilon \to 0$ we obtain the partial differential equation

$$\frac{\partial \boldsymbol{S}_*}{\partial t} = f\left\{\frac{\partial^2 \boldsymbol{S}_*}{\partial y^2} - 2\frac{\partial \boldsymbol{S}_*}{\partial y}[\boldsymbol{S}_* - \boldsymbol{\Gamma}_1(\boldsymbol{n})]^{-1}\frac{\partial \boldsymbol{S}_*}{\partial y}\right\}, \tag{9.68}$$

which, given $\boldsymbol{n}(y,t)$ and $f(y,t)$ and the initial condition $\boldsymbol{S}_*(y,0) = \boldsymbol{S}(y)$, can be solved for $\boldsymbol{S}_*(y,t)$. We have found the effective tensor for an ensemble of composites parameterized by y and $t > 0$.

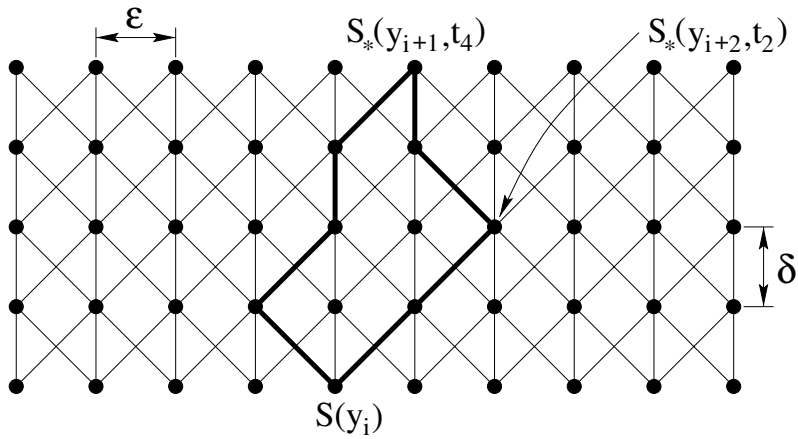

Figure 9.5. A lattice of laminates which is a discrete approximation to a partial differential laminate. The tensors $\boldsymbol{S}(y_i)$ of the constituent phases are at the nodes at the bottom of the lattice. Every other node represents a laminate, obtained by laminating together the three adjacent materials on the row below it. To signify this, lines have been drawn which connect the node to these three materials. Shown in bold are two paths in the lattice linking $\boldsymbol{S}_*(y_{i+1}, t_4)$ to $\boldsymbol{S}(y_i)$.

Figure 9.5 shows the lattice structure associated with the discrete approximation to the partial differential laminate. In the fourth-rank laminate associated with $\boldsymbol{S}_*(y_{i+1}, t_4)$ the phase with tensor $\boldsymbol{S}(y_i)$ has been used many times, and consequently the field in this phase takes a distribution of values, indexed by each path in the lattice linking $\boldsymbol{S}_*(y_{i+1}, t_4)$ to $\boldsymbol{S}(y_i)$ along which t always decreases. Two such paths are marked by bold lines in the figure. Similarly, the fourth-rank laminate associated with $\boldsymbol{S}_*(y_{i+2}, t_2)$ has been used twice in the laminate associated with $\boldsymbol{S}_*(y_{i+1}, t_4)$ [once for each of the two allowable paths joining $\boldsymbol{S}_*(y_{i+1}, t_4)$ to $\boldsymbol{S}_*(y_{i+2}, t_2)$]. Rather than keeping track of the whole distribution of field values, it is simpler to keep track of the average polarization field $\boldsymbol{P}_0(y_i, t_j)$ in the region occupied by the rank-j laminate associated with $\boldsymbol{S}_*(y_i, t_j)$. This laminate is used in the construction of the three rank-$(j+1)$ laminates associated with $\boldsymbol{S}_*(y_{i-1}, t_{j+1})$, $\boldsymbol{S}_*(y_i, t_{j+1})$, and $\boldsymbol{S}_*(y_{i+1}, t_{j+1})$. Again, strictly speaking, we should write $\boldsymbol{P}_0(y_i, t_j, \epsilon, \delta)$ instead of $\boldsymbol{P}_0(y_i, t_j)$ to emphasize

the dependence on ϵ and δ. As ϵ and $\delta = \epsilon^2/2$ approach zero and the applied field is scaled in an appropriate way, we expect to find that at those points where it is defined $\boldsymbol{P}_0(y,t,\epsilon,\delta)$ approaches $\boldsymbol{P}_0(y,t)$, where $\boldsymbol{P}_0(y,t)$ depends smoothly on y and t. From equations (9.14) and (9.15) it follows that

$$\begin{aligned}\boldsymbol{P}_0(y_i,t_j) = {} & (f_{i-1}/2)[\boldsymbol{S}_* - \boldsymbol{\Gamma}_1(\boldsymbol{n}_{i-1})]^{-1}[\boldsymbol{S}_{i-1} - \boldsymbol{\Gamma}_1(\boldsymbol{n}_{i-1})]\boldsymbol{P}_{i-1} \\ & +(1-f_i)[\boldsymbol{S}_* - \boldsymbol{\Gamma}_1(\boldsymbol{n}_i)]^{-1}[\boldsymbol{S}_i - \boldsymbol{\Gamma}_1(\boldsymbol{n}_i)]\boldsymbol{P}_i \\ & +(f_{i+1}/2)[\boldsymbol{S}_* - \boldsymbol{\Gamma}_1(\boldsymbol{n}_{i+1})]^{-1}[\boldsymbol{S}_{i+1} - \boldsymbol{\Gamma}_1(\boldsymbol{n}_{i+1})]\boldsymbol{P}_{i+1},\end{aligned}$$

where we have introduced the abbreviated notation $f_i = f(y_i,t_j)$, $\boldsymbol{n}_i = \boldsymbol{n}(y_i,t_j)$, $\boldsymbol{S}_* = \boldsymbol{S}_*(y_i,t_j)$, $\boldsymbol{S}_i = \boldsymbol{S}_*(y_i,t_{j+1})$, and $\boldsymbol{P}_i = \boldsymbol{P}_0(y_i,t_{j+1})$. In the limit as ϵ and $\delta = \epsilon^2/2$ tend to zero, one can show (after some algebraic manipulation) that this reduces to the parabolic differential equation

$$-\frac{\partial \boldsymbol{P}_0}{\partial t} = \frac{\partial^2}{\partial y^2}(f\boldsymbol{P}_0) + 2\frac{\partial}{\partial y}\left\{ f[\boldsymbol{S}_* - \boldsymbol{\Gamma}_1(\boldsymbol{n})]^{-1}\frac{\partial \boldsymbol{S}_*}{\partial y}\boldsymbol{P}_0 \right\}. \tag{9.69}$$

Since the right-hand side is the derivative with respect to y of a function that tends to zero as $y \to \infty$, it follows that

$$\frac{d\langle \boldsymbol{P}\rangle}{dt} \equiv \int_{-\infty}^{\infty} \frac{\partial \boldsymbol{P}_0}{\partial t} dy = 0.$$

Thus $\langle \boldsymbol{P}\rangle$ is constant for all t, as expected. The equation (9.69) is to be solved backwards in t with the boundary condition

$$\boldsymbol{P}_0(y,t_*) = \delta(y-y_*)\langle \boldsymbol{P}\rangle$$

representing an average polarization field $\langle \boldsymbol{P}\rangle$ applied to the differential laminate associated with $\boldsymbol{S}_*(y_*,t_*)$. Then $\boldsymbol{P}_0(y,0)dy$ represents the average polarization field within the region occupied by the phases associated with $\boldsymbol{S}(z)$, with z falling between y and $y+dy$.

One can also determine the relative volume fractions occupied by the phases. Let $\theta(y_i,t_j)$ denote a quantity that is proportional to the relative volume fraction occupied by the rank-j laminate associated with $\boldsymbol{S}_*(y_i,t_j)$. Taking the limit $\delta = \epsilon^2/2 \to 0$ in the relation

$$\theta(y_i,t_j) = (f_{i-1}/2)\theta(y_{i-1},t_{j+1}) + (1-f_i)\theta(y_i,t_{j+1}) + (f_{i+1}/2)\theta(y_{i+1},t_{j+1})$$

yields the parabolic differential equation

$$-\frac{\partial \theta}{\partial t} = \frac{\partial^2}{\partial y^2}(f\theta),$$

which is to be solved backwards in t with the boundary condition $\theta(y,t_*) = \delta(y-y_*)$. Then $\theta(y,0)dy$ represents the volume fractions occupied by the phases associated with $\boldsymbol{S}(z)$, with z falling between y and $y+dy$, in the differential laminate associated with $\boldsymbol{S}_*(y_*,t_*)$. The average of $\theta(y,t)$ with respect to y remains independent of t, as expected.

Again this construction can be generalized in many ways. For example, instead of combining the materials with tensors $\boldsymbol{S}_*(y_{i-1},t_j)$, $\boldsymbol{S}_*(y_i,t_j)$, and $\boldsymbol{S}_*(y_{i+1},t_j)$ in a simple laminate to obtain $\boldsymbol{S}_*(y_i,t_{j+1})$, one could combine them in a multiple-rank structure in proportions $f/2$, $1-f$, and $f/2$. One only needs a formula for $\boldsymbol{S}_*(y_i,t_{j+1})$ that is accurate to the second order in the differences $\boldsymbol{S}_*(y_{i-1},t_j) - \boldsymbol{S}_*(y_i,t_j)$ and $\boldsymbol{S}_*(y_{i+1},t_j) - \boldsymbol{S}_*(y_i,t_j)$ to obtain the

governing partial differential equation. Alternatively, instead of combining the materials in a multiple-rank laminate structure, one could combine them together in any microstructure, and in this way generate partial differential microstructures that are not necessarily partial differential laminates.

Another generalization is to assume that we are given another family of materials with tensors $\boldsymbol{S}_0(y,t)$ that depend continuously on y and t. Then, for example, we could take the material associated with $\boldsymbol{S}_0(y_i,t_j)$ and the three rank-j laminates associated with $\boldsymbol{S}_*(y_{i-1},t_j)$, $\boldsymbol{S}_*(y_i,t_j)$, and $\boldsymbol{S}_*(y_{i+1},t_j)$ and laminate these four materials together in direction $\boldsymbol{n}$ in proportions $q\delta$, $(1-q\delta)f/2$, $(1-q\delta)(1-f)$, and $(1-q\delta)f/2$ to obtain the rank-$(j+1)$ laminate associated with $\boldsymbol{S}_*(y_i,t_{j+1})$, where $\boldsymbol{n}=\boldsymbol{n}(y_i,t_j)$, $q=q(y_i,t_j)$, and $f=f(y_i,t_j)$. [The continuous functions $\boldsymbol{n}(y,t)$, $q(y,t)\ge 0$, and $f(y,t)$ are assumed to be given.] In the limit $\delta=\epsilon^2/2\to 0$ we obtain the partial differential equation

$$\frac{\partial \boldsymbol{S}_*}{\partial t} = q\left\{\boldsymbol{S}_* - \boldsymbol{\Gamma}_1(\boldsymbol{n}) - [\boldsymbol{S}_* - \boldsymbol{\Gamma}_1(\boldsymbol{n})][\boldsymbol{S}_0 - \boldsymbol{\Gamma}_1(\boldsymbol{n})]^{-1}[\boldsymbol{S}_* - \boldsymbol{\Gamma}_1(\boldsymbol{n})]\right\}$$
$$+f\left\{\frac{\partial^2 \boldsymbol{S}_*}{\partial y^2} - 2\frac{\partial \boldsymbol{S}_*}{\partial y}[\boldsymbol{S}_* - \boldsymbol{\Gamma}_1(\boldsymbol{n})]^{-1}\frac{\partial \boldsymbol{S}_*}{\partial y}\right\}.$$

An alternative generalization is to suppose that we are given a k-dimensional manifold of tensors $\boldsymbol{S}(\boldsymbol{y})$, parameterized by $\boldsymbol{y}=(y_1,y_2,\dots,y_k)$ and which is periodic in $\boldsymbol{y}$. To obtain $\boldsymbol{S}_*(\boldsymbol{y},t_{j+1})$ one could first take a material with tensor $\boldsymbol{S}_*(\boldsymbol{y},t_j)$ as the core phase in a coated laminate, and for $i=1,2,\dots,\ell$ coat it first with an infinitesimal volume fraction $fp_i/2$ of the material with tensor $\boldsymbol{S}_*(\boldsymbol{y}-\epsilon\boldsymbol{m}_i,t_j)$ and second with an identical coat of the material with tensor $\boldsymbol{S}_*(\boldsymbol{y}+\epsilon\boldsymbol{m}_i,t_j)$. Here the $\boldsymbol{m}_i=\boldsymbol{m}_i(\boldsymbol{y},t)$ are a set of ℓ unit vectors and the constants $p_i=p_i(\boldsymbol{y},t)$ are positive and bounded but do not necessarily sum to unity. By repeatedly applying the formula (9.23) we see that to the leading order

$$\delta\frac{\partial \boldsymbol{S}_*}{\partial t} \approx (f\epsilon^2/2)\sum_{i=1}^{n} p_i[\Delta_{\boldsymbol{y}}\boldsymbol{S}_* - 2(\boldsymbol{m}_i\cdot\nabla_{\boldsymbol{y}}\boldsymbol{S}_*)\boldsymbol{N}_i(\boldsymbol{m}_i\cdot\nabla_{\boldsymbol{y}}\boldsymbol{S}_*)],$$

where

$$\boldsymbol{N}_i=\boldsymbol{N}_i(t)=\int_{|\boldsymbol{n}|=1}[\boldsymbol{S}_*-\boldsymbol{\Gamma}_1(\boldsymbol{n})]^{-1}d\mu_{i,t}(\boldsymbol{n}),\quad \int_{|\boldsymbol{n}|=1}d\mu_{i,t}(\boldsymbol{n})=1,$$

in which the positive measure $d\mu_{i,t}(\boldsymbol{n})$ characterizes the way in which each infinitesimal coating was added. [This is merely the continuum analog of (9.24).] Here, $\Delta_{\boldsymbol{y}}=\nabla_{\boldsymbol{y}}\cdot\nabla_{\boldsymbol{y}}$ and $\nabla_{\boldsymbol{y}}$ are the Laplacian and gradient with respect to $\boldsymbol{y}$. By taking $f=2\epsilon$ and $\delta=\epsilon^3$ and taking the limit $\epsilon\to 0$ we obtain the governing partial differential equation

$$\frac{\partial \boldsymbol{S}_*}{\partial t} = \sum_{i=1}^{n} p_i[\Delta_{\boldsymbol{y}}\boldsymbol{S}_* - 2(\boldsymbol{m}_i\cdot\nabla_{\boldsymbol{y}}\boldsymbol{S}_*)\boldsymbol{N}_i(\boldsymbol{m}_i\cdot\nabla_{\boldsymbol{y}}\boldsymbol{S}_*)],$$

which is to be solved for $\boldsymbol{S}_*(\boldsymbol{y},t)$ given $p_i(\boldsymbol{y},t)$, $\boldsymbol{m}_i(\boldsymbol{y},t)$, the positive measures $d\mu_{i,t}(\boldsymbol{n})$, and the initial condition that $\boldsymbol{S}_*(\boldsymbol{y},0)=\boldsymbol{S}(\boldsymbol{y})$.

References

Avellaneda, M. 1987. Optimal bounds and microgeometries for elastic two-phase composites. *SIAM Journal on Applied Mathematics* 47(6):1216–1228. {*175, 181, 292, 294, 309, 463–465, 468, 471, 473, 491*}

Avellaneda, M. and G. W. Milton 1989. Bounds on the effective elasticity tensor of composites based on two point correlations. In D. Hui and T. Kozic (eds.), *Composite Material Technology*, pp. 89–93. Houston, Texas: American Society of Mechanical Engineers, Petroleum Division. {*175, 182*}

Avellaneda, M. and T. Olson 1993, January. Effective medium theories and effective electromechanical coupling factors for piezoelectric composites. *Journal of Intelligent Material Systems and Structures* 4(1):82–88. {*97, 110, 163, 182*}

Backus, G. E. 1962. Long-wave elastic anisotropy produced by horizontal layering. *Journal of Geophysical Research* 67(11):4427–4440. {*159, 162, 163, 182*}

Berryman, J. G. 1998. Transversely isotropic poroelasticity arising from thin isotropic layers. In K. M. Golden, G. R. Grimmett, R. D. James, G. W. Milton, and P. N. Sen (eds.), *Mathematics of Multiscale Materials*, pp. 37–50. Berlin / Heidelberg / London / etc.: Springer-Verlag. ISBN 0-387-98528-X. {*163, 182*}

Bruggeman, D. A. G. 1930. Elastizitätskonstanten von kristallaggregaten. (German) [Elastic constants of crystal aggregates]. Ph.D. thesis, Universiteit Utrecht, Utrecht, The Netherlands. See pp. 19–38. Published by Boekdrukkerij Van J. B. Wolters Uitgevers-Maatschappij, Groningen, Den Haag, The Netherlands,. {*159, 182*}

Francfort, G. A. and F. Murat 1986. Homogenization and optimal bounds in linear elasticity. *Archive for Rational Mechanics and Analysis* 94(4):307–334. {*174, 182, 471, 492, 501, 504, 525*}

Francfort, G. A., F. Murat, and L. Tartar 1995. Fourth order moments of non-negative measures on S^2 and applications. *Archive for Rational Mechanics and Analysis* 131(4): 305–333. {*175, 182*}

Gibiansky, L. V. and A. V. Cherkaev 1987. Microstructures of composites of extremal rigidity and exact bounds on the associated energy density. Technical Report 1115, Ioffe Physicotechnical Institute, Leningrad, USSR. 1–52 pp. English translation in *Topics in the Mathematical Modelling of Composite Materials*, pp. 273–317, ed. by A. Cherkaev and R. Kohn. ISBN 0-8176-3662-5. {*174, 175, 182, 468, 492*}

Gibiansky, L. V. and S. Torquato 1999. Matrix laminate composites: Realizable approximations for the effective moduli of piezoelectric dispersions. *Journal of Materials Research* 14(1):49–63. {*163, 182*}

Lipton, R. 1991. On the behavior of elastic composites with transverse isotropic symmetry. *Journal of the Mechanics and Physics of Solids* 39(5):663–681. {*175, 182, 473, 494*}

Lipton, R. 1994. Optimal bounds on effective elastic tensors for orthotropic composites. *Proceedings of the Royal Society of London. Series A, Mathematical and Physical Sciences* 444(1921):399–410. {*175, 182, 473, 494*}

Lurie, K. A. and A. V. Cherkaev 1986. Exact estimates of the conductivity of a binary mixture of isotropic materials. *Proceedings of the Royal Society of Edinburgh. Section A, Mathematical and Physical Sciences* 104(1–2):21–38. {*167, 182, 347, 353, 462, 494, 508, 521, 526*}

Lurie, K. A., A. V. Cherkaev, and A. V. Fedorov 1982. Regularization of optimal design problems for bars and plates, part II. *Journal of Optimization Theory and Applications* 37(4):523–543. {*175, 182, 431, 432, 435*}

Maxwell, J. C. 1873. *A Treatise on Electricity and Magnetism*, pp. 371–372. Oxford, United Kingdom: Clarendon Press. Article 322. {*159, 165–167, 183*}

Milton, G. W. 1990. On characterizing the set of possible effective tensors of composites: The variational method and the translation method. *Communications on Pure and Applied Mathematics (New York)* 43(1):63–125. {*164, 183, 248, 265, 268, 277, 287, 451, 454, 473, 494, 499, 505, 512, 513, 518, 526, 532, 551*}

Milton, G. W. and R. V. Kohn 1988. Variational bounds on the effective moduli of anisotropic composites. *Journal of the Mechanics and Physics of Solids* 36(6):597–629. {*172, 183, 280, 287, 462, 466, 469, 471, 474, 495*}

Postma, G. W. 1955. Wave propagation in a stratified medium. *Geophysics* 20(4):780–806. {*163, 183*}

Schulgasser, K. 1976. Relationship between single-crystal and polycrystal electrical conductivity. *Journal of Applied Physics* 47(5):1880–1886. {*159, 183*}

Tartar, L. 1979. Estimation de coefficients homogénéisés. (French) [Estimation of homogenization coefficients]. In R. Glowinski and J.-L. Lions (eds.), *Computing Methods in Applied Sciences and Engineering: Third International Symposium, Versailles, France, December 5–9, 1977,*, pp. 364–373. Berlin / Heidelberg / London / etc.: Springer-Verlag. English translation in *Topics in the Mathematical Modelling of Composite Materials*, pp. 9–20, ed. by A. Cherkaev and R. Kohn. ISBN 0-8176-3662-5. ISBN 0-387-09123-8. {*155, 156, 162, 183, 274, 289, 499, 503, 508, 509, 527, 529, 552*}

Tartar, L. 1985. Estimations fines des coefficients homogénéisés. (French) [Fine estimations of homogenized coefficients]. In P. Krée (ed.), *Ennio de Giorgi Colloquium: Papers Presented at a Colloquium Held at the H. Poincaré Institute in November 1983*, pp. 168–187. London: Pitman Publishing Ltd. ISBN 0-273-08680-4. {*129, 141, 165, 167, 174, 183, 462, 496, 499, 503, 506, 508, 527, 529, 552, 683, 698*}

Tartar, L. 2000. An introduction to the homogenization method in optimal design. In A. Cellina and A. Ornelas (eds.), *Optimal shape design. Lectures given at the Joint C.I.M./C.I.M.E. Summer School Held in Tróia, June 1–6, 1998*, pp. 47–156. Berlin / Heidelberg / London / etc.: Springer-Verlag. ISBN 3-540-67971-5. {*164, 177, 183, 426, 436*}

Zhikov, V. V. 1991. Estimates for the homogenized matrix and the homogenized tensor. *Uspekhi Matematicheskikh Nauk = Russian Mathematical Surveys* 46:49–109. English translation in *Russ. Math. Surv.* 46(3):65–136 (1991). {*120, 142, 164, 183, 280, 289, 462, 466, 471–473, 497*}

10

Approximations and asymptotic formulas

Countless approximations for estimating effective moduli have been introduced; some are semi-empirical, some are based on ad-hoc assumptions, and some have a reasonable theoretical basis. Here we will only review those well-known approximations that have a reasonable theoretical foundation, and which have withstood the test of time; see also the reviews of Van Beek (1967), Landauer (1978), Willis (1981), Markov (2000), and Buryachenko (2001). In addition, we discuss various asymptotic formulas that are applicable in high-contrast media.

10.1. Polarizability of a dielectric inclusion

Many approximations for the effective moduli of composites are based on the solution for dilute suspensions. For simplicity, let us suppose that we are interested in approximating the effective dielectric constant and require the solution for a dilute suspension of inclusions embedded in an isotropic matrix of dielectric constant $\varepsilon_0 \boldsymbol{I}$. Since the grains are well-separated from each other, the field acting on each inclusion will be approximately uniform. To a good approximation we can solve for the field in the neighborhood of any such inclusion by treating it as if it was embedded in an infinite homogeneous medium of dielectric constant ε_0 and subject to a uniform applied field at infinity. The analysis of this problem is the focus of the this section.

Consider an isolated, possibly inhomogeneous, inclusion that is embedded in an isotropic matrix of dielectric constant ε_0 and subject to a uniform applied electric field $\boldsymbol{a}$ at infinity. The dielectric tensor field is assumed to be isotropic, of the form $\varepsilon(\boldsymbol{x})\boldsymbol{I}$, where the local dielectric constant $\varepsilon(\boldsymbol{x})$ takes the value ε_0 outside the inclusion. The electric potential φ outside any sphere containing the inclusion has an expansion in spherical harmonics (Jackson 1975), the leading terms of which are

$$\varphi(\boldsymbol{x}) = \boldsymbol{a} \cdot \boldsymbol{x} - \boldsymbol{b} \cdot \boldsymbol{x}/(4\pi\varepsilon_0 r^3) + \cdots \tag{10.1}$$

and the associated electric field $\boldsymbol{e} = \nabla\varphi$ is

$$\boldsymbol{e} = \nabla\varphi = \boldsymbol{a} - \boldsymbol{b}/(4\pi\varepsilon_0 r^3) + 3\boldsymbol{x}(\boldsymbol{b} \cdot \boldsymbol{x})/(4\pi\varepsilon_0 r^5) + \cdots. \tag{10.2}$$

So we see that at large distances the dominant correction to the uniform field comes from terms involving the vector $\boldsymbol{b}$; this vector is known as the induced dipole moment. The factor of $4\pi\varepsilon_0$ has been introduced into the above expansions so that $\boldsymbol{b}$ has a physical interpretation when inclusion is in free space and ε_0 represents the dielectric constant (or, more precisely, the electrical permittivity) of free space. As we will see shortly, $\boldsymbol{b}$ can then be identified with the first moment of the induced charge density.

Since the equations for the fields are linear, there must be a linear relation between the induced dipole moment $\boldsymbol{b}$ and the applied field $\boldsymbol{a}$. This linear relation,

$$\boldsymbol{b} = \boldsymbol{\alpha}\boldsymbol{a},$$

defines the polarizability tensor $\boldsymbol{\alpha}$ of the inclusion. This tensor has also been called the Pólya-Szegő matrix; see Pólya and Szegő (1951) and Movchan and Movchan (1995).

For a fixed applied field $\boldsymbol{a}$ the vector $\boldsymbol{b}$ is determined by the integral of the polarization field,

$$\boldsymbol{p}(\boldsymbol{x}) = (\varepsilon(\boldsymbol{x}) - \varepsilon_0)\boldsymbol{e}(\boldsymbol{x}) = \boldsymbol{d}(\boldsymbol{x}) - \varepsilon_0\boldsymbol{e}(\boldsymbol{x}),$$

over the volume of the inclusion. To see this, consider a ball Ω of very large radius containing the inclusion. Since the polarization field is zero outside the inclusion, we can equate the integral of the polarization field over the inclusion with the integral of the polarization field over the ball Ω. Since the displacement field $\boldsymbol{d}(\boldsymbol{x})$ has zero divergence, and since $\boldsymbol{e}(\boldsymbol{x})$ is the gradient of the electrical potential $\varphi(\boldsymbol{x})$, it follows that for any vector $\boldsymbol{m}$

$$\begin{aligned}\int_\Omega \boldsymbol{m}\cdot\boldsymbol{p}(\boldsymbol{x}) &= \int_\Omega \boldsymbol{d}(\boldsymbol{x})\cdot\nabla(\boldsymbol{m}\cdot\boldsymbol{x}) - \varepsilon_0\boldsymbol{m}\cdot\int_\Omega \nabla\varphi(\boldsymbol{x})\\ &= \int_{\partial\Omega}(\boldsymbol{m}\cdot\boldsymbol{x})\boldsymbol{d}(\boldsymbol{x})\cdot\boldsymbol{n} - \varepsilon_0\varphi(\boldsymbol{x})\boldsymbol{m}\cdot\boldsymbol{n}\\ &= \varepsilon_0\boldsymbol{m}\cdot\int_{\partial\Omega}\boldsymbol{x}(\nabla\varphi(\boldsymbol{x})\cdot\boldsymbol{n}) - \varphi(\boldsymbol{x})\boldsymbol{n},\end{aligned}$$

where $\boldsymbol{n}$ is the outward normal to the surface $\partial\Omega$ of the ball Ω. When the radius r of the ball Ω is sufficiently large we can use the asymptotic formulas (10.1) and (10.2) to estimate these integrals,

$$\begin{aligned}\int_{\partial\Omega}\boldsymbol{x}(\nabla\varphi(\boldsymbol{x})\cdot\boldsymbol{n}) &\approx \int_{\partial\Omega}\boldsymbol{x}[(\boldsymbol{a}\cdot\boldsymbol{x})/r + 2(\boldsymbol{b}\cdot\boldsymbol{x})/(4\pi\varepsilon_0 r^4)] = \frac{4}{3}\pi r^3\boldsymbol{a} + \frac{2}{3\varepsilon_0}\boldsymbol{b},\\ \int_{\partial\Omega}\varphi(\boldsymbol{x})\boldsymbol{n} &\approx \int_{\partial\Omega}\boldsymbol{x}[(\boldsymbol{a}\cdot\boldsymbol{x})/r - (\boldsymbol{b}\cdot\boldsymbol{x})/(4\pi\varepsilon_0 r^4)] = \frac{4}{3}\pi r^3\boldsymbol{a} - \frac{1}{3\varepsilon_0}\boldsymbol{b},\end{aligned}$$

with these approximations becoming increasingly accurate as the radius r of the ball Ω approaches infinity. By subtracting these expressions and taking the limit as r approaches infinity we see that

$$\int_\Omega \boldsymbol{p}(\boldsymbol{x}) = \boldsymbol{b}. \tag{10.3}$$

As an example, suppose that the inclusion is a sphere of dielectric constant σ_1 and radius r_1. The solution for the electrical potential is

$$\begin{aligned}\varphi(\boldsymbol{x}) &= \boldsymbol{a}\cdot\boldsymbol{x} - \frac{r_1^3(\varepsilon_1-\varepsilon_0)}{r^3(\varepsilon_1+2\varepsilon_0)}\boldsymbol{a}\cdot\boldsymbol{x} \quad \text{in the matrix ,}\\ &= \frac{3\varepsilon_0}{\varepsilon_1+2\varepsilon_0}\boldsymbol{a}\cdot\boldsymbol{x} \qquad \text{in the sphere,}\end{aligned}$$

and it follows that

$$\boldsymbol{b} = \frac{4\pi r_1^3\varepsilon_0(\varepsilon_1-\varepsilon_0)\boldsymbol{a}}{\varepsilon_1+2\varepsilon_0}. \tag{10.4}$$

The associated polarization field is

$$\begin{aligned} \boldsymbol{p}(\boldsymbol{x}) = (\varepsilon(\boldsymbol{x}) - \varepsilon_0)\nabla\varphi(\boldsymbol{x}) &= 0 \qquad \text{in the matrix ,} \\ &= \frac{3\varepsilon_0(\varepsilon_1 - \varepsilon_0)\boldsymbol{a}}{\varepsilon_1 + 2\varepsilon_0} \quad \text{in the sphere,} \end{aligned} \tag{10.5}$$

and since this is constant within the sphere and zero outside, its integral over any ball Ω containing the sphere is simply

$$\int_\Omega \boldsymbol{p}(\boldsymbol{x}) = \frac{4\pi r_1^3 \varepsilon_0(\varepsilon_1 - \varepsilon_0)\boldsymbol{a}}{\varepsilon_1 + 2\varepsilon_0}.$$

In view of the formula (10.4) for $\boldsymbol{b}$ we see that the relation (10.3) is satisfied.

Also note from (10.4) that the polarizability tensor of the sphere is

$$\boldsymbol{\alpha} = \frac{4\pi r_1^3 \varepsilon_0(\varepsilon_1 - \varepsilon_0)\boldsymbol{I}}{\varepsilon_1 + 2\varepsilon_0}. \tag{10.6}$$

When the inclusion is an ellipse with its axes aligned with the coordinate axes the polarizability tensor $\boldsymbol{\alpha}$ is diagonal with diagonal elements

$$\alpha_i = \frac{V\varepsilon_0(\varepsilon_1 - \varepsilon_0)}{\varepsilon_0 + (\varepsilon_1 - \varepsilon_0)d_i}, \quad i = 1, 2, 3,$$

in which V is the volume of the ellipse and the d_i are the depolarizing (or demagnetizing) factors given by (7.65) and (7.66) for prolate and oblate spheroids, by (7.67) for elliptical cylinders, and by (7.69) for ellipsoids of arbitrary eccentricity. In section 12.5 on page 252 we will see how the polarizability tensor of an ellipsoidal inclusion can be computed for elasticity, thermoelasticity, piezoelectricity, or related problems, even when the inclusion or surrounding matrix material is anisotropic.

For a sphere containing an anisotropic crystal with dielectric tensor $\boldsymbol{\varepsilon}_1$ embedded in an isotropic matrix with dielectric constant ε_0, the formula for the polarizability tensor is especially simple:

$$\boldsymbol{\alpha} = 4\pi r_1^3 \varepsilon_0(\boldsymbol{\varepsilon}_1 - \varepsilon_0\boldsymbol{I})(\boldsymbol{\varepsilon}_1 + 2\varepsilon_0\boldsymbol{I})^{-1}. \tag{10.7}$$

This formula can be easily deduced from (10.6) by applying the arguments of section 8.2 on page 144. A collection of such spheres with uniformly distributed random orientations will have an average polarizability tensor

$$\langle\boldsymbol{\alpha}\rangle = 4\pi r_1^3 \varepsilon_0 \boldsymbol{I} \sum_{i=1}^{3} \frac{\lambda_i - \varepsilon_0}{3(\lambda_i + 2\varepsilon_0)}. \tag{10.8}$$

in which λ_1, λ_2, and λ_3 are the eigenvalues of $\boldsymbol{\varepsilon}_1$. To show this we consider six spheres, each in one of the six different orientations such that the principal axes of the anisotropic material are aligned with the coordinate axes. From (10.7) it follows that the average polarizability of these six spheres is given by the above expression. Since this is proportional to $\boldsymbol{I}$, it remains unchanged if we average over orientations.

When the inclusion is not ellipsoidal the polarizability tensor generally has to be computed numerically. For pairs of spheres or pairs of circles (in two dimensions) expressions for the polarizability tensor have been given by Peterson and Hermans (1969); Jeffrey (1973);

Love (1975); McPhedran and Perrins (1981); Djordjević, Hetherington, and Thorpe (1996); and Choy, Alexopoulos, and Thorpe (1998), among others. [See also Honein, Honein, and Herrmann (1990), who solve the problem of two circles in an arbitrary external field.] For the two-dimensional problem of a polygonal or arbitrary shaped hole or inclusion in a plate, Hetherington and Thorpe (1992); Thorpe (1992); Jasiuk, Chen, and Thorpe (1994); Kachanov, Tsukrov, and Shafiro (1994); and Movchan and Serkov (1997) show how the electric and elastic polarizability tensors can be easily computed. Greengard and Moura (1994) show how the fast multipole method provides an especially fast way of computing the fields and accompanying polarizability tensors, even when numerous inclusions of arbitrary shape are present. Lipton (1993) obtains bounds on electric and elastic polarizability tensors.

Returning to the general case and using integration by parts, (10.3) can be rewritten in the form

$$\boldsymbol{b} = -\int_\Omega \boldsymbol{x}\nabla\cdot\boldsymbol{p}(\boldsymbol{x}) = \varepsilon_0\int_\Omega \boldsymbol{x}\nabla\cdot\boldsymbol{e}(\boldsymbol{x}) = \int_\Omega \boldsymbol{x}\rho(\boldsymbol{x}),$$

where $\rho(\boldsymbol{x}) = \varepsilon_0\nabla\cdot\boldsymbol{e}(\boldsymbol{x})$ corresponds to the physical charge density when ε_0 is chosen as the dielectric constant (more precisely the electrical permittivity) of free space. This charge density, called the polarization or induced charge density, is confined to the boundary of the inclusion when the dielectric constant $\varepsilon(\boldsymbol{x})$ is constant within the inclusion. Thus, in this case, the dipole moment $\boldsymbol{b}$ has the physical interpretation of being the first moment of the induced charge density, which accounts for its name.

10.2. Dielectric constant of a dilute suspension of inclusions to the first order in the volume fraction

Let us return to the problem of estimating the effective dielectric constant tensor of a dilute suspension of identical inclusions embedded in an isotropic matrix of dielectric constant ε_0. We suppose that there are N inclusions per unit volume, each occupying a volume V and having polarizability $\boldsymbol{\alpha}$. It is assumed that the inclusions are well-separated from each other. Then to a first approximation the coefficient $\boldsymbol{a}$ in the expansion of the field around any given inclusion can be equated to the average field $\langle\boldsymbol{e}\rangle$. The average polarization field per unit volume is

$$\langle\boldsymbol{p}\rangle = N\boldsymbol{b} = f\boldsymbol{\alpha}\boldsymbol{a}/V \approx f\boldsymbol{\alpha}\langle\boldsymbol{e}\rangle/V,$$

in which $f = NV \ll 1$ is the volume fraction occupied by the inclusions. We also have

$$\langle\boldsymbol{p}\rangle = \langle\boldsymbol{d}\rangle - \varepsilon_0\langle\boldsymbol{e}\rangle = (\boldsymbol{\varepsilon}_* - \varepsilon_0\boldsymbol{I})\langle\boldsymbol{e}\rangle. \tag{10.9}$$

Equating these two expressions gives an approximation formula for the effective dielectric tensor,

$$\boldsymbol{\varepsilon}_* \approx \varepsilon_0\boldsymbol{I} + f\boldsymbol{\alpha}/V. \tag{10.10}$$

In particular, if the inclusions are spheres of radius r_1 and volume $V = 4\pi r_1^3/3$, then from the expression (10.6) for the polarizability we obtain the approximation formula

$$\boldsymbol{\varepsilon}_* \approx \varepsilon_0\boldsymbol{I} + \frac{3f\varepsilon_0(\varepsilon_1 - \varepsilon_0)\boldsymbol{I}}{\varepsilon_1 + 2\varepsilon_0} \tag{10.11}$$

for the effective dielectric tensor of a dilute suspension of spheres. For this approximation to be valid it is important that the spheres be well-separated. If, for example, the spheres

remained clustered in pairs as the volume fraction f approaches zero, then the average polarizability of these sphere pairs would enter the approximation formula for the effective tensor.

If we uniformly shrink each inclusion by a constant scale factor while keeping the center of each inclusion fixed and plot the effective tensor as a function of the volume fraction f, then the approximations (10.10) and (10.11) hold to the first order in the volume fraction f.

10.3. Dielectric constant of a suspension of well-separated spheres to the second order in the volume fraction

The approximation (10.11) is only correct to the first order in the volume fraction f. To improve this estimate we need to improve on our estimate for the factor $\boldsymbol{a}$ in the expansion of the field $\boldsymbol{e}(\boldsymbol{x})$ around each inclusion. This factor is called the local field. Evaluating the local field requires special care, because of the long range nature of the dipolar field. Often it is assumed that the local field acting on each inclusion is the same for all inclusions, but this is an oversimplification that is not generally valid.

Let us assume that the suspension is periodic and that the period cell Ω contains a large number n of well-separated spheres, which are not necessarily all of the same radius. Within the period cell we define the characteristic functions

$$\begin{aligned} \chi_i(\boldsymbol{x}) &= 1 \text{ when } \boldsymbol{x} \text{ is in sphere } i, \\ &= 0 \text{ elsewhere,} \end{aligned} \tag{10.12}$$

for $i = 1, 2, \ldots n$. We extend the definition of these characteristic functions outside of Ω using periodicity. The arguments in the previous two sections show that to a first approximation the polarization field inside each inclusion is constant and given by the formula

$$\boldsymbol{p}(\boldsymbol{x}) = \sum_{i=1}^{n} \frac{3\varepsilon_0(\varepsilon_1 - \varepsilon_0)\chi_i(\boldsymbol{x})\langle \boldsymbol{e} \rangle}{\varepsilon_1 + 2\varepsilon_0}. \tag{10.13}$$

The polarization charge density $\rho(\boldsymbol{x}) = \nabla \cdot \boldsymbol{p}(\boldsymbol{x})$ associated with this polarization field perturbs the electric field $\boldsymbol{e}(\boldsymbol{x})$ in the unit cell. The perturbing field $\boldsymbol{e}'(\boldsymbol{x}) = \boldsymbol{e}(\boldsymbol{x}) - \langle \boldsymbol{e} \rangle$, having zero average value, must be the gradient of a periodic potential $\phi'(\boldsymbol{x})$, that is, $\boldsymbol{e}'(\boldsymbol{x}) = \nabla\phi'(\boldsymbol{x})$. Since $\nabla \cdot \boldsymbol{p}(\boldsymbol{x}) = -\varepsilon_0 \nabla \cdot \boldsymbol{e}(\boldsymbol{x})$, it follows that this potential satisfies Poisson's equation,

$$\nabla^2 \phi'(\boldsymbol{x}) = -\rho(\boldsymbol{x})/\varepsilon_0.$$

By solving this equation in Fourier space one sees that the Fourier components $\hat{\boldsymbol{e}}'(\boldsymbol{k})$ and $\hat{\boldsymbol{p}}(\boldsymbol{k})$ of the fields $\boldsymbol{e}'(\boldsymbol{x})$ and $\boldsymbol{p}(\boldsymbol{x})$ are related through the formula

$$\hat{\boldsymbol{e}}'(\boldsymbol{k}) = -\boldsymbol{\Gamma}(\boldsymbol{k})\hat{\boldsymbol{p}}(\boldsymbol{k}), \tag{10.14}$$

where

$$\begin{aligned} \boldsymbol{\Gamma}(\boldsymbol{k}) &= \boldsymbol{k} \otimes \boldsymbol{k}/(\varepsilon_0 k^2) \text{ when } \boldsymbol{k} \neq 0, \\ &= 0 \qquad \text{when } \boldsymbol{k} = 0, \end{aligned} \tag{10.15}$$

in which $k = |\boldsymbol{k}|$. Since the relation between the fields $\boldsymbol{e}'$ and $\boldsymbol{p}$ is linear, let us write

$$\boldsymbol{e}' = -\boldsymbol{\Gamma}\boldsymbol{p}. \tag{10.16}$$

This serves to define the operator $\boldsymbol{\Gamma}$ whose action in real space is nonlocal and whose action in Fourier space is given by (10.14) and (10.15). The operator $-\boldsymbol{\Gamma}$ gives the perturbing electric field $\boldsymbol{e}'$ generated by a periodic polarization field $\boldsymbol{p}$.

Associated with sphere i in the unit cell is a local field $\boldsymbol{a}_i$. Its value is essentially the average field $\langle \boldsymbol{e} \rangle$ plus the perturbing electric field due to polarization charges on the surrounding spheres, not including the contribution due to the i-th sphere in the unit cell under consideration. In view of the relations (10.13) and (10.16), $\boldsymbol{a}_i$ is to a good approximation the value of the field

$$\boldsymbol{e}^{(i)} = \langle \boldsymbol{e} \rangle - \frac{3\varepsilon_0(\varepsilon_1 - \varepsilon_0)}{\varepsilon_1 + 2\varepsilon_0} \sum_{\substack{j=1 \\ j \neq i}}^{n} \boldsymbol{\Gamma} \chi_j \langle \boldsymbol{e} \rangle,$$

evaluated at the center of sphere i. This approximation is accurate only when the unit cell is very large, that is, when $n \gg 1$. When n is small one has to account for the perturbing electric field due to the copies of the i-th sphere in the surrounding unit cells. Since the spheres are well-separated, the field $\boldsymbol{e}^{(i)}$ will be approximately constant in the vicinity of sphere i and its value at the center of sphere i can be replaced by the average over sphere i. Thus we have

$$\boldsymbol{a}_i \approx \langle \boldsymbol{e} \rangle - \frac{3\varepsilon_0(\varepsilon_1 - \varepsilon_0)}{\varepsilon_1 + 2\varepsilon_0} \sum_{\substack{j=1 \\ j \neq i}}^{n} \langle \chi_i \boldsymbol{\Gamma} \chi_j \langle \boldsymbol{e} \rangle \rangle / f_i,$$

where

$$f_i = \langle \chi_i \rangle$$

is the volume fraction occupied by sphere i in the unit cell. We rewrite this as

$$\boldsymbol{a}_i \approx \langle \boldsymbol{e} \rangle - \frac{3\varepsilon_0(\varepsilon_1 - \varepsilon_0)}{\varepsilon_1 + 2\varepsilon_0} \boldsymbol{\Lambda}_i \langle \boldsymbol{e} \rangle / f_i,$$

where for any vector $\boldsymbol{v}$ the relation

$$\boldsymbol{\Lambda}_i \boldsymbol{v} = \sum_{\substack{j=1 \\ j \neq i}}^{n} \langle \chi_i \boldsymbol{\Gamma} \chi_j \boldsymbol{v} \rangle$$

defines the action of the matrix $\boldsymbol{\Lambda}_i$ on $\boldsymbol{v}$.

This improved estimate for the local field $\boldsymbol{a}_i$ gives an improved estimate for the polarization field,

$$\begin{aligned} \boldsymbol{p}(\boldsymbol{x}) &\approx \sum_{i=1}^{n} \frac{3\varepsilon_0(\varepsilon_1 - \varepsilon_0)\chi_i(\boldsymbol{x})\boldsymbol{a}_i}{\varepsilon_1 + 2\varepsilon_0} \\ &\approx \frac{3\varepsilon_0(\varepsilon_1 - \varepsilon_0)}{\varepsilon_1 + 2\varepsilon_0} \sum_{i=1}^{n} \chi_i(\boldsymbol{x}) \langle \boldsymbol{e} \rangle - \left[\frac{3\varepsilon_0(\varepsilon_1 - \varepsilon_0)}{\varepsilon_1 + 2\varepsilon_0} \right]^2 \sum_{i=1}^{n} \chi_i(\boldsymbol{x}) \boldsymbol{\Lambda}_i \langle \boldsymbol{e} \rangle / f_i, \end{aligned}$$

which should be accurate to the first order in the volume fraction. From the average value of this field we obtain, via (10.9), an improved estimate for the effective dielectric tensor:

$$\boldsymbol{\varepsilon}_* \approx \varepsilon_0 \boldsymbol{I} + \frac{3f\varepsilon_0(\varepsilon_1 - \varepsilon_0)\boldsymbol{I}}{\varepsilon_1 + 2\varepsilon_0} - \left[\frac{3\varepsilon_0(\varepsilon_1 - \varepsilon_0)}{\varepsilon_1 + 2\varepsilon_0} \right]^2 \sum_{i=1}^{n} \boldsymbol{\Lambda}_i. \tag{10.17}$$

If the spheres are distributed isotropically, then $\boldsymbol{\varepsilon}_*$ and hence $\sum_{i=1}^n \boldsymbol{\Lambda}_i$ are proportional to the identity tensor and we have

$$\sum_{i=1}^{n} \boldsymbol{\Lambda}_i = \boldsymbol{I} \sum_{i=1}^{n} \mathrm{Tr}[\boldsymbol{\Lambda}_i]/3. \tag{10.18}$$

The trace of the matrix $\boldsymbol{\Lambda}_i$ is easily evaluated in Fourier space:

$$\begin{aligned}
\mathrm{Tr}[\boldsymbol{\Lambda}_i] &= \sum_{\substack{j=1\\ j\neq i}}^{n} \sum_{\boldsymbol{k}\neq 0} \hat{\chi}_i(\boldsymbol{k})\, \mathrm{Tr}[\boldsymbol{\Gamma}(\boldsymbol{k})] \hat{\chi}_j(\boldsymbol{k}) = \sum_{\substack{j=1\\ j\neq i}}^{n} \sum_{\boldsymbol{k}\neq 0} \hat{\chi}_i(\boldsymbol{k}) \hat{\chi}_j(\boldsymbol{k})/\varepsilon_0 \\
&= \sum_{\substack{j=1\\ j\neq i}}^{n} \langle (\chi_i - f_i)(\chi_j - f_j)\rangle/\varepsilon_0 \\
&= \sum_{\substack{j=1\\ j\neq i}}^{n} -f_i f_j/\varepsilon_0 = -f_i(f - f_i)/\varepsilon_0 \approx -f_i f/\varepsilon_0,
\end{aligned} \tag{10.19}$$

where the final approximation becomes increasingly accurate as the number n of spheres in the unit cell tends to infinity, that is, as f_i/f approaches zero, where f is the total volume fraction occupied by all spheres within the unit cell. Substituting this back into (10.17) gives the desired expression for the effective dielectric constant of a dilute isotropic suspension of spheres:

$$\varepsilon_* \approx \varepsilon_0 + 3f\varepsilon_0 \left[\frac{(\varepsilon_1 - \varepsilon_0)}{\varepsilon_1 + 2\varepsilon_0}\right] + 3f^2\varepsilon_0 \left[\frac{(\varepsilon_1 - \varepsilon_0)}{\varepsilon_1 + 2\varepsilon_0}\right]^2. \tag{10.20}$$

It should be emphasized that this formula is only valid (to the second order in f) for suspensions of well-separated spheres. Unfortunately, many dilute suspensions are not well-separated. For example, we do not obtain a well-separated distribution if we shake a suspension of spheres in a fluid until it is well-mixed. In general, to evaluate the f^2 coefficient we need to know the pair correlation function $P(\boldsymbol{x}|0)$ giving the probability density of finding a sphere centered at $\boldsymbol{x}$, given that there is sphere centered at the origin, and we need to know the expression for the polarizability of such sphere pairs. Jeffrey (1973) [see also Finkel'berg (1963)] gives an explicit formula for this f^2 coefficient in terms of $P(\boldsymbol{x}|0)$, which Choy, Alexopoulos, and Thorpe (1998) have generalized to d-dimensional composites. For elasticity Willis and Acton (1976) give an approximate expression for the f^2 coefficient of the effective bulk and shear moduli in terms of $P(\boldsymbol{x}|0)$, based on an approximation for the elastic polarization tensor of sphere pairs. The exact expression was subsequently derived by Chen and Acrivos (1978). In well-separated distributions $P(\boldsymbol{x}|0)$ is approximately zero for $|\boldsymbol{x}|$ less than distances of the order of $r_1 f^{-1/3}$, where r_1 is the sphere radius. By contrast, in well-stirred distributions $P(\boldsymbol{x}|0)$ is often taken to be zero for $|\boldsymbol{x}| \leq 2r_1$ and constant for $|\boldsymbol{x}| > 2r_1$; that is, the spheres are forbidden to overlap, but otherwise their positions are uncorrelated. This choice of $P(\boldsymbol{x}|0)$ is appealing because of its simplicity, but Markov and Willis (1998) have shown that it violates rigorous bounds when $f > 1/8$.

When the spheres are well-separated but not isotropically distributed, the formula (10.20) is *not applicable*. There is no universal formula for the effective dielectric tensor that does not include higher order statistical information, or assumptions about these statistics. For anisotropic distributions the statistics characterizing the sphere configuration become evident at the second order in the volume fraction.

To see this, consider two dilute suspensions of well-separated, isotropically distributed spheres. According to the above formula these suspensions have effective conductivities

$$\begin{aligned}\varepsilon_*^{(1)} &\approx \varepsilon_0 + 3f^{(1)}\varepsilon_0\left[\frac{\varepsilon_1-\varepsilon_0}{\varepsilon_1+2\varepsilon_0}\right] + 3(f^{(1)})^2\varepsilon_0\left[\frac{\varepsilon_1-\varepsilon_0}{\varepsilon_1+2\varepsilon_0}\right]^2,\\ \varepsilon_*^{(2)} &\approx \varepsilon_0 + 3f^{(2)}\varepsilon_0\left[\frac{\varepsilon_1-\varepsilon_0}{\varepsilon_1+2\varepsilon_0}\right] + 3(f^{(2)})^2\varepsilon_0\left[\frac{\varepsilon_1-\varepsilon_0}{\varepsilon_1+2\varepsilon_0}\right]^2,\end{aligned} \tag{10.21}$$

where $f^{(1)} \ll 1$ and $f^{(2)} \ll 1$ are the volume fractions occupied by the spheres in the two suspensions. Note that the difference $\varepsilon_*^{(1)} - \varepsilon_*^{(2)}$ is small and proportional to $f^{(1)} - f^{(2)}$ to the leading order. Now let us take these two suspensions as the phases in some larger anisotropic macrostructure. For simplicity, let us laminate the two suspensions together, choosing the layer separation to be significantly larger than the sphere separation in each suspension. The effective dielectric tensor $\boldsymbol{\varepsilon}_*$ of this mixture will be a function of $\varepsilon_*^{(1)}$, $\varepsilon_*^{(2)}$, and the geometry of the macrostructure. By replacing $\boldsymbol{\sigma}_1$, σ_2, and $\boldsymbol{\sigma}_*$ with $\varepsilon_*^{(1)}\boldsymbol{I}$, $\varepsilon_*^{(2)}$, and $\boldsymbol{\varepsilon}_*$ in the lamination formula (9.19) and expanding to the second order in the difference $\varepsilon_*^{(1)} - \varepsilon_*^{(2)}$ we see that

$$\boldsymbol{\varepsilon}_* \approx (f_1\varepsilon_*^{(1)} + f_2\varepsilon_*^{(2)})\boldsymbol{I} - f_1 f_2(\varepsilon_*^{(1)} - \varepsilon_*^{(2)})^2\boldsymbol{A}/\varepsilon_*^{(2)}, \tag{10.22}$$

where f_1 and $f_2 = 1 - f_1$ are the volume fractions of the two suspensions in the laminate and $\boldsymbol{A}$ is the matrix

$$\boldsymbol{A} = \boldsymbol{\Gamma}_1(\boldsymbol{n}) = \boldsymbol{n} \otimes \boldsymbol{n},$$

which depends on the direction of lamination $\boldsymbol{n}$.

By substituting the expressions (10.21) for $\varepsilon_*^{(1)}$ and $\varepsilon_*^{(2)}$ into (10.22) we see that the overall effective tensor takes the value

$$\begin{aligned}\boldsymbol{\varepsilon}_* \approx\ & \varepsilon_0\boldsymbol{I} + 3[f_1 f^{(1)} + f_2 f^{(2)}]\boldsymbol{I}\varepsilon_0\left[\frac{\varepsilon_1-\varepsilon_0}{\varepsilon_1+2\varepsilon_0}\right]\\ &+3[(f_1(f^{(1)})^2 + f_2(f^{(2)})^2)\boldsymbol{I} - 3f_1 f_2(f^{(1)} - f^{(2)})^2\boldsymbol{A}]\varepsilon_0\left[\frac{\varepsilon_1-\varepsilon_0}{\varepsilon_1+2\varepsilon_0}\right]^2\end{aligned} \tag{10.23}$$

to the second order in the volume fractions $f^{(1)}$ and $f^{(2)}$. In particular, if we choose

$$f_1 = f_2 = 1/2, \quad f^{(1)} = 3f/2, \quad f^{(2)} = f/2,$$

so that the overall volume fraction $f_1 f^{(1)} + f_2 f^{(2)}$ of the spheres in the laminate macrostructure equals f, then it is clear that the overall effective tensor $\boldsymbol{\varepsilon}_*$ depends on the matrix $\boldsymbol{A}$ to the second order in f. If we had considered a different macrostructure, other than a laminate, then the formulas (10.22) and (10.23) would hold with a different value for $\boldsymbol{A}$. We will see in section 15.5 on page 323 [equations (15.24) and (15.25)] that $\boldsymbol{A}$ depends on the reduced two-point correlation function characterizing the macrostructure.

10.4. The Maxwell approximation formula

The Maxwell formula has a long and colorful history. Faraday in 1837 had proposed a model for dielectric materials, consisting of metallic globules separated by insulating material. Mossotti analyzed this model in two papers, published in 1847 and 1850, basing his analysis

on earlier work by Poisson in 1826 on a closely related problem for magnetic media. The publication of Mossotti's 1850 paper was delayed because after it was submitted in 1846 Mossotti fought at the head of a battalion of students and was taken prisoner by Austrians in 1848. The duties of professors were quite different in those days! The actual approximation formula for the effective dielectric constant of conducting spheres in a dielectric medium appears to have been first published by Clausius in 1879. Independently, Lorenz in 1869 and, around the same time, Lorentz (there seems to be some question as to whether it was 1868 or 1870) obtained the approximation formula as it relates to the frequency-dependent effective refractive index of a suspension of polarizable molecules. Maxwell in 1873 obtained the approximation formula as it relates to the effective conductivity of a dilute suspension of conducting spheres in a conducting matrix. Rayleigh in 1892 provided some rigorous justification of the formula as a first approximation to the conductivity of a cubic array of spheres. Maxwell-Garnett in 1904 obtained the approximation formula as it relates to the optical properties of suspensions of metallic spheres.

Due to its origins in these different contexts the approximation sometimes goes by the name of the Clausius-Mossotti formula, the Lorenz-Lorentz formula, or the Maxwell-Garnett formula. Gillispie (1971), Landauer (1978), and Scaife (1989) give excellent accounts of the history with extensive references.

Many derivations of the Maxwell formula assume that the local field takes the same value for each spherical inclusion. This is reasonable for cubic arrays of spheres, but for more random (still well-separated) distributions it is tantamount to assuming that the field produced by a distribution of dipoles is uniform, and this is clearly false. The following derivation avoids this assumption.

To calculate the local field in the preceding section we assumed that the polarization field, to a first approximation, is given by the formula (10.13). Instead we could have made the weaker initial assumption that the polarization field is constant inside each sphere:

$$\boldsymbol{p}(\boldsymbol{x}) \approx \sum_{i=1}^{n} \chi_i(\boldsymbol{x})\boldsymbol{v}, \tag{10.24}$$

where the value of the vector $\boldsymbol{v}$ remains to be estimated. The estimate for the local field then becomes

$$\boldsymbol{a}_i \approx \langle \boldsymbol{e} \rangle - \boldsymbol{\Lambda}_i \boldsymbol{v}/f_i, \tag{10.25}$$

and this leads to an improved estimate of the polarization field:

$$\boldsymbol{p}(\boldsymbol{x}) \approx \frac{3\varepsilon_0(\varepsilon_1 - \varepsilon_0)}{\varepsilon_1 + 2\varepsilon_0} \sum_{i=1}^{n} \chi_i(\boldsymbol{x})(\langle \boldsymbol{e} \rangle - \boldsymbol{\Lambda}_i \boldsymbol{v}/f_i). \tag{10.26}$$

Ideally one should find an improved estimate for the local field based on this improved estimate for the polarization field and iterate this procedure until successive estimates for polarization field become close [we are prevented from actually doing this because of the difficulty in evaluating the local field associated with the polarization field (10.26)]. One would expect the convergence of this scheme to be accelerated if the vector $\boldsymbol{v}$ was chosen so that the initial estimate (10.24) and subsequent estimate (10.26) for the polarization field were somehow close. At least it would be desirable if the average values of these fields are close, since it is the average value of the polarization field that determines the effective dielectric tensor. Let us therefore choose $\boldsymbol{v}$ so that both estimates for the polarization field have the

same average value $\langle \boldsymbol{p} \rangle$. If we take

$$\boldsymbol{v} = 3\varepsilon_0(\varepsilon_1 - \varepsilon_0)[(\varepsilon_1 + 2\varepsilon_0)\boldsymbol{I} + 3\varepsilon_0(\varepsilon_1 - \varepsilon_0)\sum_{i=1}^{n} \boldsymbol{\Lambda}_i/f]^{-1}\langle \boldsymbol{e} \rangle,$$

then both estimates for $\langle \boldsymbol{p} \rangle$ equal $f\boldsymbol{v}$, and equating this with $(\boldsymbol{\varepsilon}_* - \varepsilon_0\boldsymbol{I})\langle \boldsymbol{e} \rangle$ gives the approximation formula

$$\boldsymbol{\varepsilon}_* = \varepsilon_0\boldsymbol{I} + 3f\varepsilon_0(\varepsilon_1 - \varepsilon_0)[(\varepsilon_1 + 2\varepsilon_0)\boldsymbol{I} + 3\varepsilon_0(\varepsilon_1 - \varepsilon_0)\sum_{i=1}^{n} \boldsymbol{\Lambda}_i/f]^{-1}$$

for the effective dielectric tensor.

When the spheres are distributed isotropically, $\boldsymbol{\varepsilon}_* = \varepsilon_*\boldsymbol{I}$ and we may use (10.18) and (10.19). Making these substitutions gives the Maxwell formula for the effective dielectric constant:

$$\varepsilon_* \approx \varepsilon_0 + \frac{3f\varepsilon_0(\varepsilon_1 - \varepsilon_0)}{\varepsilon_1 + 2\varepsilon_0 - f(\varepsilon_1 - \varepsilon_0)} = \varepsilon_0 + \frac{3f\varepsilon_0(\varepsilon_1 - \varepsilon_0)}{3\varepsilon_0 + (1 - f)(\varepsilon_1 - \varepsilon_0)}. \tag{10.27}$$

Notice that this coincides with the formula (7.7) for the effective dielectric constant of the Hashin-Shtrikman coated spheres geometry, which accounts for why the approximation (for two-phase composites) makes sense even at large volume fractions. Experimentally (10.20) is found to work well for many suspensions. For example, Fricke and Morse (1925) consider the analogous formula for conductivity and apply it to estimate the conductivity of cream consisting of suspensions of (nonconducting) butter fat in (conducting) skim milk. They verify that the approximation works extremely well for volume fractions of cream up to 62% and suggest that this as a method for determining the butter fat content in milk and cream. Presumably the fat globules remained fairly well-separated, even though the mixture was stirred. However, it is unwise to put too much faith in the approximation since it is not even correct to the second order in f when the spheres are well-mixed, as discussed in the previous section.

The approximation formula is easily extended to nonspherical inclusions, provided that their centers are well-separated and distributed isotropically, and provided that each inclusion has the same polarizability per unit inclusion volume. Let us consider a periodic suspension with a period cell Ω containing a large number n of well-separated inclusions. These inclusions occupy volumes $V_1, V_2, \ldots, V_N$ and have polarizabilities $\boldsymbol{\alpha}_1, \boldsymbol{\alpha}_2, \ldots, \boldsymbol{\alpha}_n$ with $\boldsymbol{\alpha}_i = V_i\boldsymbol{\alpha}_0$ for all i for some constant tensor $\boldsymbol{\alpha}_0$. Associated with inclusion i is a dipole moment $\boldsymbol{b}_i$. To estimate the local field we assume that the dipole moments are aligned and proportional to the volume of the associated inclusion,

$$\boldsymbol{b}_i = V_i\boldsymbol{v}, \tag{10.28}$$

in which the vector $\boldsymbol{v}$ remains to be determined. This assumption certainly holds in the very dilute limit, provided that there is no clustering.

The dipole moment $\boldsymbol{b}_i$ is exactly the same as the dipole moment produced by a sphere of volume V_i centered on the inclusion with a constant polarization $\boldsymbol{v}$ inside the sphere. We call this sphere "sphere i," and we let χ_i given by (10.12) denote the characteristic function associated with these spheres. Since the spheres and the inclusions have the same set of dipole moments (and since higher order terms in the expansion of the field around each inclusion die off rapidly), the local field $\boldsymbol{a}_i$ acting on the inclusion i will be well-approximated by (10.25). This leads to the improved estimate,

$$\boldsymbol{b}_i = \boldsymbol{\alpha}_i\boldsymbol{a}_i = V_i\boldsymbol{\alpha}_0\boldsymbol{a}_i = V_i\boldsymbol{\alpha}_0\langle \boldsymbol{e} \rangle - V_\Omega\boldsymbol{\alpha}_0\boldsymbol{\Lambda}_i\boldsymbol{v}, \tag{10.29}$$

for the dipole moment of the field around inclusion i, in which V_Ω is the volume of the period cell. From these dipole moments we can calculate the average of the polarization field:

$$\langle \boldsymbol{p} \rangle = (\boldsymbol{\varepsilon}_* - \varepsilon_0 \boldsymbol{I})\langle \boldsymbol{e} \rangle = \sum_{i=1}^{n} \boldsymbol{b}_i / V_\Omega.$$

The vector $\boldsymbol{v}$ is determined by equating the values for the average polarization obtained using the expressions (10.28) and (10.29) for the dipole moments. This value of $\boldsymbol{v}$,

$$\boldsymbol{v} = [1 + \boldsymbol{\alpha}_0 \sum_{i=1}^{n} \boldsymbol{\Lambda}_i / f]^{-1} \boldsymbol{\alpha}_0 \langle \boldsymbol{e} \rangle,$$

in which f is the volume fraction occupied by the inclusions, gives $\langle \boldsymbol{p} \rangle = f\boldsymbol{v}$, which leads to the estimate

$$\boldsymbol{\varepsilon}_* \approx \varepsilon_0 \boldsymbol{I} + f[\boldsymbol{I} + \boldsymbol{\alpha}_0 \sum_{i=1}^{n} \boldsymbol{\Lambda}_i / f]^{-1} \boldsymbol{\alpha}_0$$

for the effective dielectric tensor.

If the centers of the inclusions are distributed isotropically, then $\sum_{i=1}^{n} \boldsymbol{\Lambda}_i \approx -f^2 \boldsymbol{I}/(3\varepsilon_0)$ and we obtain the approximation formula

$$\boldsymbol{\varepsilon}_* \approx \varepsilon_0 \boldsymbol{I} + f[\boldsymbol{I} - f\boldsymbol{\alpha}_0/3\varepsilon_0]^{-1} \boldsymbol{\alpha}_0$$

for the effective dielectric tensor of a dilute suspension of nonspherical inclusions. This is often written in the equivalent form

$$(\boldsymbol{\varepsilon}_* - \varepsilon_0 \boldsymbol{I})(\boldsymbol{\varepsilon}_* + 2\varepsilon_0 \boldsymbol{I})^{-1} \approx f\boldsymbol{\alpha}_0/3\varepsilon_0,$$

which for spherical inclusions reduces to the formula

$$\frac{\varepsilon_* - \varepsilon_0}{\varepsilon_* + 2\varepsilon_0} \approx \frac{f(\varepsilon_1 - \varepsilon_0)}{\varepsilon_1 + 2\varepsilon_0}, \tag{10.30}$$

in agreement with (10.27).

10.5. The effective medium approximation for the dielectric constant of an aggregate with spherical grains

Another widely used estimate is the effective medium approximation formula introduced by Bruggeman (1935). (It has also been called the coherent potential approximation, because of its similarity to the coherent potential approximation in solid state physics for estimating the properties of random alloys.)

Consider an aggregate comprised of grains that fill all space. Each grain either has dielectric constant ε_1 or dielectric constant ε_2 and is approximately spherical in shape. The phase-1 grains with dielectric constant ε_1 occupy a volume fraction f_1, while the phase-2 grains occupy a volume fraction $f_2 = 1 - f_1$. To obtain the effective medium approximation for the effective dielectric constant ε_* of this assemblage we pick out a representative sample of grains occupying a small volume fraction ϵ in the assemblage. The grains in the representative sample are chosen to be well-separated from each other and are chosen so that the sample contains the same proportion of phase 1 and phase 2 as in the aggregate.

The essence of the effective medium approximation is the "self-consistency" assumption that the effective dielectric constant of the aggregate remains equal to ε_* to the first order in ϵ when we replace the medium surrounding the representative grains by a homogeneous effective medium with dielectric constant ε_*. After making this replacement we can treat the representative grains as a dilute suspension of spherical inclusions embedded in a matrix of dielectric constant ε_*. To the first order in ϵ the effective dielectric constant of this suspension is

$$\varepsilon_* + \epsilon f_1 \frac{3\varepsilon_*(\varepsilon_1 - \varepsilon_*)}{\varepsilon_1 + 2\varepsilon_*} + \epsilon f_2 \frac{3\varepsilon_*(\varepsilon_2 - \varepsilon_*)}{\varepsilon_2 + 2\varepsilon_*},$$

and by the "self-consistency" assumption this should equal ε_*, giving rise to the equation

$$f_1 \frac{\varepsilon_1 - \varepsilon_*}{\varepsilon_1 + 2\varepsilon_*} + f_2 \frac{\varepsilon_2 - \varepsilon_*}{\varepsilon_2 + 2\varepsilon_*} = 0, \tag{10.31}$$

which has the solution

$$\varepsilon_* = \tfrac{1}{4}\big[\gamma + (\gamma^2 + 8\varepsilon_1\varepsilon_2)^{1/2}\big] \text{ with } \gamma = (3f_1 - 1)\varepsilon_1 + (3f_2 - 1)\varepsilon_2.$$

This solution represents the effective medium approximation for ε_*.

There is of course an analogous formula,

$$\sigma_* = \tfrac{1}{4}\big[\gamma + (\gamma^2 + 8\sigma_1\sigma_2)^{1/2}\big] \text{ with } \gamma = (3f_1 - 1)\sigma_1 + (3f_2 - 1)\sigma_2, \tag{10.32}$$

for the effective conductivity σ_* of a granular aggregate of spherical grains with conductivities σ_1 and σ_2, in proportions f_1 and f_2. The solution has an interesting behavior in the limit as σ_2 approaches zero. In this limit we have

$$\begin{aligned} \sigma_* &= (3f_1 - 1)\sigma_1/2 \text{ when } f_1 \geq 1/3, \\ &= 0 \text{ when } f_1 \leq 1/3. \end{aligned}$$

So we see that there is a critical volume fraction, namely, $f_1 = 1/3$, below which the effective conductivity is predicted to be zero and above which the effective conductivity is strictly positive. In actual granular aggregates such a conductivity threshold does occur and coincides with the percolation threshold f_c. It is the volume fraction of phase 1 above which the grains of phase 1 form a connected path through the aggregate and below which the grains of phase 1 lie in isolated clusters. The existence of the conductivity threshold in the effective medium scheme is one reason why the approximation and its generalizations have been favored by experimentalists, although the percolation threshold in an actual granular aggregate may be quite different from $1/3$.

A rigorous basis for Bruggeman's effective medium approximation was provided by the result that it is a realizable model (Milton 1984, 1985a). The realizability holds in the strong sense that the microgeometry realizing the approximation is independent of the values of ε_1 and ε_2 (or σ_1 and σ_2) and has the correct morphology, consisting of an assemblage of spheres of the two phases packed together to fill all space. Roughly speaking, there exists an aggregate of spheres, with a distribution of sphere sizes so wide that spheres of comparable size are well-separated, that has an effective dielectric constant arbitrarily close to the estimate of the effective medium approximation. Basically this is a hierarchical material with large well-separated spheres of the two phases, surrounded by a sea of much smaller well-separated spheres of the two phases which in turn are surrounded by a sea of still smaller well-separated spheres of the two phases, and so on, ad-infinitum; see figure 10.1. Even though there is only

a small volume fraction of spheres of any given size, the spheres of all sizes combine to essentially fill all space. The realizability explains why the effective medium approximation is always found to be compatible with known bounds and exact relations. Avellaneda (1987) extended this result, proving the realizability of the generalized effective medium approximation for the effective properties (including the elastic properties) of possibly anisotropic aggregates of arbitrarily shaped grains, each containing one or more possibly anisotropic phases.

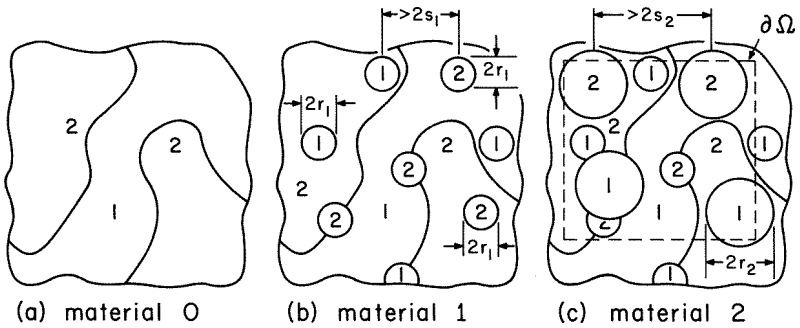

Figure 10.1. The first few stages in the construction of a material that has an effective dielectric constant arbitrarily close to the estimate of the effective medium approximation. Material 0 is chosen arbitrarily, otherwise material $j = 1, 2, \ldots$, consists of equisized spheres, called j-spheres, embedded in material $j - 1$. The sphere radii, r_j, asymptotically increase faster than exponentially with j. The spatial distribution of the j-spheres must satisfy a mild homogeneity condition, and the minimum spacing $2s_j$ between the j-spheres is such that the ratio r_j/s_j diverges. Also, the volume fraction of material 0 remaining in material j must tend to zero as $j \to \infty$. On the basis of these and some further ancillary conditions the effective dielectric constant of material j (defined in terms of the electrostatic energy stored in a sufficiently large test cube Ω) converges to the effective medium estimate as $j \to \infty$. Reprinted with permission from Milton (1985a). Copyright 1985, Springer-Verlag.

The approximation always requires that the effective moduli be chosen so that the average polarizability of the grains in the effective medium vanishes. For an isotropic polycrystalline material containing spherical grains of crystal in random orientations, the expression (10.8) for the average polarizability of the grains leads to the effective medium approximation

$$\frac{\lambda_1 - \varepsilon_*}{\lambda_1 + 2\varepsilon_*} + \frac{\lambda_2 - \varepsilon_*}{\lambda_2 + 2\varepsilon_*} + \frac{\lambda_3 - \varepsilon_*}{\lambda_3 + 2\varepsilon_*} = 0 \tag{10.33}$$

for the effective dielectric constant ε_* of the crystal, in which λ_1, λ_2, and λ_3 are the eigenvalues of the dielectric tensor of the constituent crystal. This formula of Helsing and Helte (1991) corrects an earlier result of Bolotin and Moskalenko (1967). For a uniaxial crystal in which $\lambda_3 = \lambda_2$ the formula reduces to the one given by Stroud (1975):

$$\varepsilon_* = \tfrac{1}{4}\big[\lambda_2 + (\lambda_2^2 + 8\lambda_1\lambda_2)^{1/2}\big]. \tag{10.34}$$

The effective medium approximation is easily extended to resistor networks where the resistances are randomly (and independently) assigned one of two values (Kirkpatrick 1973) and to spring networks where the spring constants are randomly (and independently) assigned one of two values (Feng, Thorpe, and Garboczi 1985; Garboczi and Thorpe 1985; Schwartz,

Feng, Thorpe, and Sen 1985). In the context of such networks the approximation works surprisingly well, in general agreeing with numerical simulations except very close to the conductivity threshold when the ratio of the resistances is large, or very close to the rigidity threshold when the ratio of the spring constants is large.

10.6. Average field approximations†

The effective medium approximation is not the only approximation based on an assumption of "self-consistency." Average field approximations use self-consistency arguments to estimate the average field within inclusions. Often average field approximations are confused with the effective medium approximation discussed in the previous section because they give the same formula when the phases are isotropic and the grains are spherical or aligned ellipsoids. However, it is important to recognize that they are different approximations based on different assumptions. The average field approximations were introduced by Polder and Van Santen (1946). They are essentially mean-field theories and have been frequently applied to estimate the elastic properties of composites. In this context they are known as the "self-consistent estimates."

As in the previous section, let us consider a granular aggregate comprised of nearly spherical grains that either have dielectric constant ε_1 or dielectric constant ε_2. Let

$$\langle \boldsymbol{e} \rangle_1 = \langle \chi_1 \boldsymbol{e} \rangle / f_1 \quad \text{and} \quad \langle \boldsymbol{e} \rangle_2 = \langle \chi_2 \boldsymbol{e} \rangle / f_2$$

denote the partial averages of the electric field, averaged over phases 1 and 2, respectively. Clearly the total average electric field is itself an average of these two partial averages, weighted in proportion to the volume fractions of the phases:

$$\langle \boldsymbol{e} \rangle = f_1 \langle \boldsymbol{e} \rangle_1 + f_2 \langle \boldsymbol{e} \rangle_2. \tag{10.35}$$

To estimate $\langle \boldsymbol{e} \rangle_1$ and $\langle \boldsymbol{e} \rangle_2$ we make a self-consistent approximation. We assume that these partial averages are the same as the partial averages of the electric fields in the chosen representative grains when the surrounding medium is replaced by a homogeneous medium of dielectric constant ε_* and the average field $\langle \boldsymbol{e} \rangle$ is held fixed. From the solution (10.5) for the polarization field inside a spherical grain in a uniform applied field $\boldsymbol{a} = \langle \boldsymbol{e} \rangle$ embedded in a matrix of dielectric constant $\varepsilon_0 = \varepsilon_*$ we obtain the estimates

$$\langle \boldsymbol{e} \rangle_1 \approx \frac{3\varepsilon_* \langle \boldsymbol{e} \rangle}{\varepsilon_1 + 2\varepsilon_*}, \qquad \langle \boldsymbol{e} \rangle_2 \approx \frac{3\varepsilon_* \langle \boldsymbol{e} \rangle}{\varepsilon_2 + 2\varepsilon_*}.$$

Substitution of these estimates in (10.35) yields the identity

$$1 = \frac{3 f_1 \varepsilon_*}{\varepsilon_1 + 2\varepsilon_*} + \frac{3 f_2 \varepsilon_*}{\varepsilon_2 + 2\varepsilon_*}, \tag{10.36}$$

which may be solved for ε_*. By subtracting $1 = f_1 + f_2$ from both sides this formula reduces to (10.31). In other words, when the grains are spherical the effective medium approximation and average electric field approximation yield identical formulas for the effective dielectric constant.

Alternatively one can define partial averages of the displacement field,

$$\langle \boldsymbol{d} \rangle_1 = \langle \chi_1 \boldsymbol{d} \rangle / f_1 \quad \text{and} \quad \langle \boldsymbol{d} \rangle_2 = \langle \chi_2 \boldsymbol{d} \rangle / f_2,$$

and base an approximation on the identity

$$\langle \boldsymbol{d} \rangle = f_1 \langle \boldsymbol{d} \rangle_1 + f_2 \langle \boldsymbol{d} \rangle_2,$$

estimating $\langle \boldsymbol{d} \rangle_1$ and $\langle \boldsymbol{d} \rangle_2$ by assuming that these partial averages are the same as the partial averages of the displacement fields in the chosen representative grains when the surrounding medium is replaced by a homogeneous medium of dielectric constant ε_* and the average displacement field $\langle \boldsymbol{d} \rangle$ is held fixed. For spherical grains this yields the approximation formula

$$1 = \frac{3f_1\varepsilon_1}{\varepsilon_1 + 2\varepsilon_*} + \frac{3f_2\varepsilon_2}{\varepsilon_2 + 2\varepsilon_*}, \tag{10.37}$$

which is again equivalent to the effective medium approximation (10.31) for ε_*, as can be seen by subtracting $1 = f_1 + f_2$ from both sides.

More generally, one can base an approximation on the partial averages of the polarization field $\boldsymbol{p}(\boldsymbol{x}) = \boldsymbol{d}(\boldsymbol{x}) - \varepsilon_0 \boldsymbol{e}(\boldsymbol{x})$, assuming that these partial averages are the same as the partial averages of the polarization fields in the chosen representative grains when the surrounding medium is replaced by a homogeneous medium of dielectric constant ε_* and the average polarization field $\langle \boldsymbol{p} \rangle$ is held fixed. In particular, by taking $\varepsilon_0 = \varepsilon_2$, one avoids having to estimate the average field within phase 2 because the polarization field vanishes there. One has

$$\langle \boldsymbol{p} \rangle = f_1 \langle \boldsymbol{p} \rangle_1, \quad \text{where } \langle \boldsymbol{p} \rangle_1 = \langle \chi_1 \boldsymbol{p} \rangle / f_1.$$

For spherical grains of phase 1 this yields the formula

$$\varepsilon_* - \varepsilon_2 = \frac{3f_1(\varepsilon_1 - \varepsilon_2)\varepsilon_*}{\varepsilon_1 + 2\varepsilon_*}, \tag{10.38}$$

which again coincides with the effective medium approximation (10.31), being a linear combination of the equations (10.36) and (10.37). Because this approach does not require an estimate of the average field within phase 2, it has been argued that it applies to suspensions of grains of phase 1 embedded in a matrix of phase 2. Of course the grains in the suspension must be in contact when $f_1 > 1/3$ to account for the fact that $\varepsilon_* \to \infty$ as $\varepsilon_1 \to \infty$.

Some caution must be used when applying average field approximations, since they are not necessarily realizable. Consider, for example, the average polarization approximation applied to a three-phase composite comprised of cubic grains of dielectric constant ε_1 (with random orientations) and spherical grains of dielectric constant ε_2 embedded in a matrix of dielectric constant ε_3. The approximation yields the formula

$$\varepsilon_* - \varepsilon_3 = \frac{f_1 \alpha(\varepsilon_*)(\varepsilon_1 - \varepsilon_3)}{\varepsilon_1 - \varepsilon_*} + \frac{3f_2(\varepsilon_2 - \varepsilon_3)\varepsilon_*}{\varepsilon_2 + 2\varepsilon_*}, \tag{10.39}$$

in which f_1 and f_2 are the volume fractions of phases 1 and 2 and $\alpha(\varepsilon_*)\boldsymbol{I}$ is the polarizability tensor of a cube of unit volume of dielectric constant ε_1 embedded in a matrix of dielectric constant $\varepsilon_0 = \varepsilon_*$. According to this approximation the dependence of ε_* on ε_3 does not disappear in the limit when $f_3 \to 0$. In other words, this approximation predicts that the matrix has a significant influence on the effective dielectric constant, even when it occupies an infinitesimally small volume fraction.

Contrary to what Kerner (1956b) and Walpole (1969) have argued, one can rigorously prove that this is impossible when the matrix has a fixed finite, nonzero dielectric constant.

Suppose that we are given constants $\beta > \alpha > 0$ and two composites having dielectric tensor fields $\varepsilon(\boldsymbol{x})\boldsymbol{I}$ and $\varepsilon'(\boldsymbol{x})\boldsymbol{I}$ satisfying

$$\beta > \varepsilon(\boldsymbol{x}) > \alpha, \quad \beta > \varepsilon'(\boldsymbol{x}) > \alpha, \quad \text{for all } \boldsymbol{x},$$

and which (for simplicity) are such that the effective dielectric tensors are isotropic, having values $\varepsilon_*\boldsymbol{I}$ and $\varepsilon'_*\boldsymbol{I}$. It has been established by Zhikov and Kozlov [see Zhikov, Kozlov, and Oleinik (1994)] that

$$|\varepsilon'_* - \varepsilon_*| \le k_0\langle|\varepsilon' - \varepsilon|^p\rangle^{1/p}, \tag{10.40}$$

where the constants $k_0 > 0$ and $p > 0$ depend only on α and β. The proof of this result relies on a theorem of Meyers (1963) on the higher integrability of the gradient of solutions of elliptic systems of partial differential equations. Now consider any isotropic three-phase medium and let

$$\begin{aligned}\varepsilon(\boldsymbol{x}) &= \varepsilon'(\boldsymbol{x}) = \varepsilon_i \ \text{ in phase } i = 1, 2,\\ \varepsilon(\boldsymbol{x}) &= \varepsilon_3, \quad \varepsilon'(\boldsymbol{x}) = \varepsilon'_3 \ \text{ in phase } 3.\end{aligned}$$

Then the bound (10.40) reduces to

$$|\varepsilon'_* - \varepsilon_*| \le k_0 f_3^{1/p}|\varepsilon'_3 - \varepsilon_3|,$$

and implies that ε'_* must approach ε_* as $f_3 \to 0$. Thus the average polarization approximation (10.39) is inappropriate when the volume fraction of the matrix is small because it violates this bound. More generally this example serves to warn of the danger of blindly applying average field approximations.

Willis (1981) has shown that the three average field approximations give three different predictions for the effective properties when the grains are not spherical (or aligned ellipsoids). One can regard the average electric field, average displacement field, and effective medium approximation as corresponding to the average polarization approximation in the limit in which ε_0 approaches infinity, approaches 0, and equals ε_*, respectively. When the composite is a granular aggregate, rather than a suspension, there are no apparent physical reasons for favoring a particular choice of ε_0. However, from a mathematical perspective the choice $\varepsilon_0 = \varepsilon_*$ is favored because the effective medium approximation is realizable in the sense that it is the limiting value of the effective dielectric constant of a sequence of actual granular microstructures. The effective medium approximation will never be found to violate constraints applicable to formulas for the effective dielectric constant of arbitrary microstructures, whereas the preceding example shows that other average field approximations may indeed violate these constraints.

Clearly the assumptions of the average field approximations must be violated in some way in the microgeometries that attain the effective medium approximations when the inclusions are not spheres or aligned ellipsoids. A close examination shows that the largest inclusions in these microgeometries have a field acting on them that can be identified with the average applied field, but smaller inclusions have a field acting on them that is influenced by the proximity of larger inclusions, but which on average is *smaller* in magnitude than the average applied field. This is why the average field approximation is not valid for these microgeometries. Additional reasons for favoring the effective medium approximation over average field approximations have been given by Noh, Song, and Sievers (1991).

10.7. The differential scheme for the effective conductivity of a suspension of spheres

Bruggeman (1935) also introduced another popular approximation formula that is now widely known as the differential scheme. (It has also been called Bruggeman's unsymmetrical effective medium theory or the iterated dilute limit approximation.)

Suppose that we want an approximation formula for the effective conductivity $\sigma_*(f_0)$ of a suspension of spheres of conductivity σ_1 in a matrix of conductivity σ_0, where the matrix occupies a volume fraction f_0. The idea of the differential scheme is as follows. If the volume fraction of the matrix is decreased from f_0 to $f_0 - \delta$ by carving out of the composite a volume fraction δ/f_0 of large spherical cavities [thereby removing a volume fraction δ of the matrix and a volume fraction $\delta(1 - f_0)/f_0$ of the existing spheres] and inserting large solid spheres of conductivity σ_1 into these cavities, then the medium surrounding these new inclusions can be treated as a homogeneous medium with conductivity $\sigma_*(f_0)$, provided that the cavities were placed well apart from each other and provided that their radius was chosen to be sufficiently large compared with the scale of inhomogeneities present in the original composite. To calculate the effective conductivity $\sigma_*(f_0 - \delta)$ of the new suspension we can treat it as a dilute suspension of large spheres of conductivity σ_1, occupying a volume fraction δ/f_0 in a matrix of conductivity $\sigma_*(f_0)$. It follows from (10.11) that to the first order in δ,

$$\sigma_*(f_0 - \delta) \approx \sigma_*(f_0) + \frac{3\sigma_*(f_0)(\sigma_1 - \sigma_*(f_0))\delta}{(\sigma_1 + 2\sigma_*(f_0))f_0}. \tag{10.41}$$

At the next stage we increase the volume from $f_1 - \delta$ to $f_1 - 2\delta$ by inserting even larger spheres of conductivity σ_1. By iterating this procedure, starting from a homogeneous medium with conductivity σ_0 containing no spherical inclusions, that is, with $f_0 = 1$, we build up a material with any desired volume fraction of spheres of conductivity σ_1 for which the effective conductivity can be estimated by repeated use of (10.41). Taking the limit where δ is infinitesimally small, this relation reduces to a first-order differential equation

$$\frac{d\sigma_*}{df_0} = -\frac{3\sigma_*(\sigma_1 - \sigma_*)}{(\sigma_1 + 2\sigma_*)f_0}$$

for the effective conductivity $\sigma_*(f_0)$ with the condition

$$\sigma_*(1) = \sigma_0.$$

Integrating gives the equation

$$\left(\frac{\sigma_1 - \sigma_*}{\sigma_1 - \sigma_0}\right)\left(\frac{\sigma_0}{\sigma_*}\right)^{1/3} = f_0, \tag{10.42}$$

which may be solved numerically for σ_* for given values of σ_1, σ_0, and f_0. The solution represents the differential approximation for the effective conductivity of a suspension of spheres. The arguments underlying its derivation suggests that the approximation best applies to a suspension containing spheres with a very wide distribution of sizes. Ideally, the size distribution should be so wide that any two spheres of comparable size are well-separated from each other.

When the spheres have zero conductivity, $\sigma_1 = 0$, the approximation (10.42) gives the estimate

$$\sigma_* = \sigma_0 f_0^{3/2}.$$

Sen, Scala, and Cohen (1981) have compared this estimate with experimental measurements of the effective conductivity of a porous medium of electrically insulating fused glass beads immersed in a conducting brine solution. The agreement is remarkably good; see figure 10.2. The significance of this result, however, is not clear since the approximation was designed to apply to suspensions of spherical grains in a matrix, as described above, rather than to porous materials. For real brine-filled rocks, the relation between the effective conductivity, σ_*, and the conductivity σ_0 of the brine is found empirically to be well-approximated by the formula

$$\sigma_* = \sigma_0 f_0^m,$$

where the exponent m depends on the particular rock being studied. This is known as Archie's law. Archie (1942) found that clean, unconsolidated sandstones are characterized by an exponent $m \approx 1.3$, which is quite close to the value $m = 1.5$ predicted by the differential scheme.

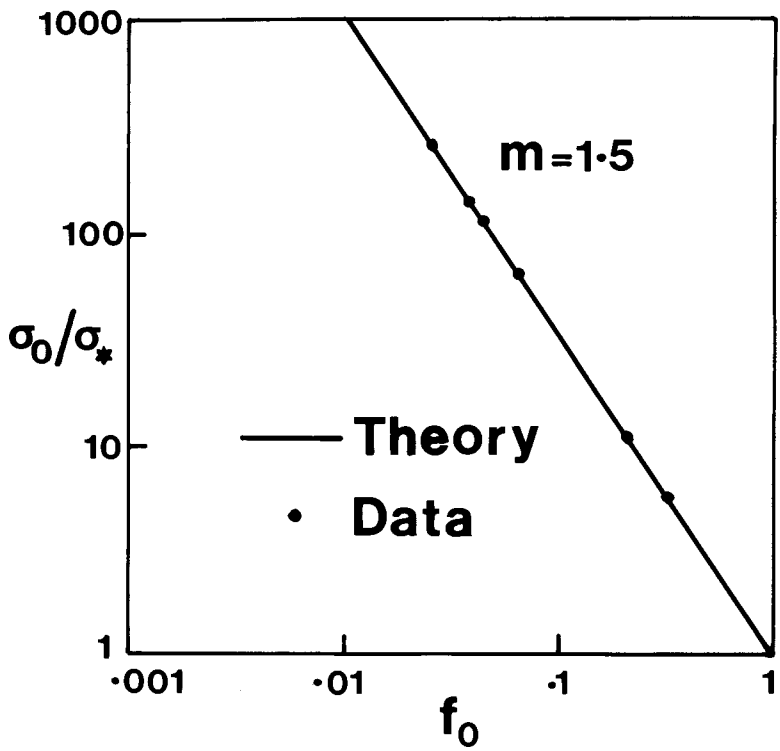

Figure 10.2. Effective conductivity of a fluid-filled porous medium of fused glass beads as a function of the volume fraction f_0 occupied by the conducting fluid, showing the $\sigma_* = \sigma_0 f_0^{3/2}$ behavior. The bead size ranges from 210 to 250 microns. After Sen, Scala, and Cohen (1981).

Bruggeman's differential scheme is also realizable (Milton 1985b). Roughly speaking, there exists a suspension of spheres in a matrix, with a distribution of sphere sizes so wide that spheres of comparable size are well-separated, which has an effective dielectric constant arbitrarily close to the estimate of the differential scheme. Norris, Callegari, and Sheng (1985)

recognized that the differential scheme can easily be generalized to allow for suspensions containing inclusions with a variety of shapes and compositions that possibly depend on the level in the hierarchy. Avellaneda (1987) proved the realizability of this generalized differential scheme for the effective properties (including the elastic properties) of possibly anisotropic suspensions of arbitrarily shaped inclusions, each containing one or more possibly anisotropic phases embedded in a possibly anisotropic matrix. We call such materials ordinary differential microstructures. They are a generalization of the ordinary differential laminates discussed in section 9.9 on page 175.

10.8. The effective medium approximation as the attractor of a differential scheme

Instead of filling the spherical cavities with spheres of phase 1 at each stage of the differential process, we could of course fill some cavities with spheres of phase 1 and some cavities with spheres of phase 2. Let us suppose that a fixed proportion p_1 of the cavities are filled with phase 1 and a fixed proportion $p_2 = 1 - p_1$ are filled with phase 2, so that the two phases occupy volume fractions $f_1 = p_1(1 - f_0)$ and $f_2 = p_2(1 - f_0)$ in the resulting composite, in which f_0 is the volume fraction occupied by the matrix. The resulting differential equation describing the evolution of the effective conductivity σ_* as a function of the variable

$$t = -\log f_0, \tag{10.43}$$

which ranges between zero and infinity, now takes the form

$$\frac{d\sigma_*}{dt} = g(\sigma_*), \quad \text{where } g(\sigma_*) = p_1 \frac{3\sigma_*(\sigma_1 - \sigma_*)}{(\sigma_1 + 2\sigma_*)} + p_2 \frac{3\sigma_*(\sigma_2 - \sigma_*)}{(\sigma_2 + 2\sigma_*)}. \tag{10.44}$$

This equation defines a flow on the real line. There are stationary points of this flow where $d\sigma_*/dt = 0$, namely, the trivial point $\sigma_* = 0$ and the point $\sigma_* = \sigma_*^0$, where σ_*^0 is the value of the effective conductivity given by the effective medium approximation (10.32) with $f_1 = p_1$ and $f_2 = p_2$. Since the derivative

$$\left.\frac{dg(\sigma_*)}{d\sigma_*}\right|_{\sigma_* = \sigma_*^0} = -p_1 \frac{9\sigma_1\sigma_*^0}{(\sigma_1 + 2\sigma_*^0)^2} - p_2 \frac{9\sigma_2\sigma_*^0}{(\sigma_2 + 2\sigma_*^0)^2}$$

is negative, it follows that $g(\sigma_*)$ must be positive when σ_* is slightly less than σ_*^0. Hence $g(\sigma_*)$ must be positive for all σ_* between zero and σ_*^0 because $\sigma_* = 0$ is the only other nonnegative root of the equation $g(\sigma_*) = 0$. Similarly, $g(\sigma_*)$ must be negative for all σ_* between σ_*^0 and infinity. This implies that

$$\begin{aligned} \frac{d\sigma_*}{dt} &\geq 0 \text{ when } 0 \leq \sigma_* \leq \sigma_*^0, \\ &\leq 0 \text{ when } \sigma_*^0 \geq \sigma_*^0. \end{aligned}$$

In other words, the flow is always towards the point σ_*^0. As t approaches infinity, σ_* must approach σ_*^0, that is,

$$\lim_{t \to \infty} \sigma_*(t) = \sigma_*^0.$$

Thus the effective medium approximation corresponds to this differential scheme in the limit in which the volume fraction f_0 of the matrix tends to zero. Norris (1985) realized the

effective medium approximation is a fixed point of the differential scheme and argued that it should always be the attractor, not only for the effective conductivity properties but also for the effective elastic properties. One needs to show that the effective properties predicted by the differential scheme are independent of the properties of the matrix in the limit as $f_0 \to 0$. A rigorous proof of this, for the generalized differential scheme, was given by Avellaneda (1987) based on results of Meyers (1963).

10.9. Approximation formulas for effective elastic moduli

The effective medium, average field, and differential approximation schemes can also be applied to estimate the effective elastic moduli of composite materials. Let us suppose that the composite is an elastically isotropic granular aggregate, comprised of grains of phase 1 with bulk modulus κ_1 and shear modulus μ_1 occupying a volume fraction f_1 mixed with grains of phase 2 with bulk modulus κ_2 and shear modulus μ_2 occupying the remaining volume fraction $f_2 = 1 - f_1$. If one treats the grains as spherical, then the effective medium approximation and the average field approximations yield exactly the same formulas for the effective elastic moduli of the aggregate. The estimates for the effective bulk modulus κ_* and effective shear modulus μ_* are taken to the unique nonnegative solutions of the coupled equations

$$f_1 \frac{\kappa_1 - \kappa_*}{\kappa_1 + 4\mu_*/3} + f_2 \frac{\kappa_2 - \kappa_*}{\kappa_2 + 4\mu_*/3} = 0,$$
$$f_1 \frac{\mu_1 - \mu_*}{\mu_1 + F_*} + f_2 \frac{\mu_2 - \mu_*}{\mu_2 + F_*} = 0, \quad F_* = \frac{\mu_*(9\kappa_* + 8\mu_*)}{6(\kappa_* + 2\mu_*)}. \tag{10.45}$$

Kerner (1956a) first derived these approximation formulas for both κ_* and μ_*, essentially using an average polarization field approximation. He took the moduli κ_0 and μ_0 of the reference medium equal to κ_* and μ_*. Thus his treatment is equivalent to an effective medium approximation. However, his approach is confusing since along the way he derives another approximation formula using arguments that are difficult to justify. Budiansky (1965) and Hill (1965) provided cleaner derivations using average field approximations.

The predicted value of μ_* has an interesting behavior when phase 2 is a fluid, with $\mu_2 = 0$ and $\kappa_2 \neq 0$, and phase 1 is a solid with finite nonzero moduli. When $f_1 \leq 2/5$ one finds that

$$\kappa_* = 1/(f_1/\kappa_1 + f_2/\kappa_2), \quad \mu_* = 0,$$

which is consistent with the exact results for the bulk and shear moduli of a suspension of particles of phase 1 in a fluid of phase 2. When f_1 is greater than 2/5, but sufficiently close to 2/5 so that we can assume that $\mu_* << \kappa_*$ and hence that $F_* \approx 3\mu_*/2$, one finds that

$$\kappa_* \approx 1/(f_1/\kappa_1 + f_2/\kappa_2), \quad \mu_* \approx (5f_1 - 2)\mu_1/3.$$

Thus the volume fraction $f_1 = 2/5$ is predicted to be the fluidity threshold, that is, the transition point between fluid- and solid-like behavior for the composite.

The predicted behavior is quite different when phase 2 is vacuous, with zero moduli. Suppose that we let κ_2 and μ_2 both approach zero while keeping the ratio κ_2/μ_2 fixed. In this limit we find that

$$\kappa_* = 0, \quad \mu_* = 0 \quad \text{for} \quad f_1 \leq 1/2,$$

while when f_1 is greater than 1/2, but still close to 1/2, we find that

$$\kappa_* \approx \frac{8(2f_1 - 1)}{5/\mu_1 + 4/3\kappa_1}, \quad \mu_* \approx \frac{6(2f_1 - 1)}{5/\mu_1 + 4/3\kappa_1}.$$

So as f_1 approaches $1/2$ the ratio κ_*/μ_* approaches the constant value $4/3$. Thus the volume fraction $f_1 = 1/2$ is predicted to be the rigidity threshold.

It is rather striking that when f_1 is between $2/5$ and $1/2$ the predicted value of the effective shear modulus becomes nonzero when the void region occupied by phase 2 is filled with a fluid with zero shear modulus. We would not expect such an unusual effect in any ordinary microgeometry. Indeed, the microgeometry corresponding to the effective medium approximation (when all of the moduli are finite and nonzero) is far from ordinary, having its microstructure on an infinite range of length scales. This warns of the danger of blindly applying the predictions of the effective medium approximations to ordinary microgeometries when there is a large ratio between the moduli of the phases. Except in special microstructures the conductivity, fluidity, and rigidity thresholds should be coincident. They should all equal the geometric percolation threshold f_c marking the volume fraction where phase 1 begins to have a connected component spanning the composite.

Korringa, Brown, Thompson, and Runge (1979) and Berryman (1980) have extended the effective medium approximation to obtain estimates of the effective bulk modulus and effective shear modulus of elastically isotropic aggregates of randomly oriented spheroidal grains of two or more isotropic phases. Wu (1966) and Walpole (1969) extended the average field approximation (10.38) to an elastically isotropic suspension of randomly oriented spheroidal inclusions of one or more isotropic phases embedded in an isotropic matrix. Because the spheroids are not aligned, the results of the average field approximation differ from those of the effective medium approximation, and in particular have an unphysical dependence on the moduli of the matrix when grains of more than one phase are present and the volume fraction occupied by the matrix goes to zero.

Van der Poel (1958); Smith (1974; 1975), correcting an error in Van der Poel's analysis; and Christensen and Lo (1979) have used an effective medium approximation to estimate the effective shear modulus of a coated sphere assemblage, or more generally, the effective shear modulus of a suspension of well-separated spheres in a matrix. Following Mackenzie (1950), who used a similar idea applied to a solid containing a dilute concentration of spherical holes, they consider a coated sphere in an effective medium and adjust the moduli of the effective medium so that the leading coefficient in the far-field expansion vanishes or, equivalently, so that the insertion of the coated sphere into the effective medium does not change the overall elastic energy. The estimate for the bulk modulus agrees with the exact expression. The estimate for the shear modulus is the solution of a quadratic equation. Since the coefficients of this quadratic are given by quite lengthy expressions, we do not provide them here, but instead refer the interested reader to the paper of Christensen (1990), which corrects some errors in the earlier paper of Christensen and Lo. This approximation generally gives reasonable estimates for the effective shear modulus for a suspension of spheres when the spheres are well-separated.

Incidentally, the realizability of the effective medium approximation provides a strong argument to suggest that the effective shear modulus of the Hashin-Shtrikman sphere assemblage depends on the way in which the coated spheres are arranged to fill all space. One realizable value of the effective shear modulus is the value μ_*, provided by the above approximation. However, the calculation, and the resulting value of the effective shear modulus, would surely change if one were to consider a pair of coated spheres at fixed separation in an effective medium and then average the leading coefficient in the far-field expansion over all orientations of the pair, requiring that the shear modulus of the effective medium be chosen so that this average vanishes. This would provide another realizable value of the effective shear modulus. One expects this value to be different because the "shear polarizability" of a

pair of coated spheres is not the same as the sum of the shear polarizabilities of the individual coated spheres taken separately. Even when the effective medium has shear modulus μ_* the field in the surrounding matrix is nonuniform and there will be interaction between the coated spheres.

An alternative estimate for the elastic moduli of a suspension of spheres is provided by the differential scheme. It gives estimates for the effective bulk and shear moduli $\kappa_*(f_0)$ and $\mu_*(f_0)$ of a suspension of spheres with bulk and shear moduli κ_1 and μ_1 in a matrix with moduli κ_0 and μ_0, where the matrix occupies a volume fraction f_0. These estimates of Roscoe (1973) [see also McLaughlin (1977)] are found by integrating

$$\frac{d\kappa_*}{df_0} = -\frac{(\kappa_* + 4\mu_*/3)(\kappa_1 - \kappa_*)}{(\kappa_1 + 4\mu_*/3)f_0},$$
$$\frac{d\mu_*}{df_0} = -\frac{(\mu_* + F_*)(\mu_1 - \mu_*)}{(\mu_1 + F_*)f_0}, \quad \text{where } F_* = \frac{\mu_*(9\kappa_* + 8\mu_*)}{6(\kappa_* + 2\mu_*)},$$

with $\kappa_* = \kappa_0$ and $\mu_* = \mu_0$ at $f_0 = 1$. (When f_0 approaches zero κ_* approaches κ_1, and μ_* approaches μ_1, so the right-hand sides of the above equations remain finite.) This approximation should give reasonable estimates when there is a wide distribution of sphere sizes in the suspension and the spheres are not well-separated.

When the spheres are voids, with $\kappa_1 = \mu_1 = 0$, the integration can be done explicitly. Norris (1985) finds that

$$\kappa_* = \frac{4\mu_0}{3R}\left(\frac{R-1}{4\mu_0/3\kappa_0 - 1}\right)^{5/3}, \quad \mu_* = \mu_0\left(\frac{R-1}{4\mu_0/3\kappa_0 - 1}\right)^{5/3},$$

where R is the root of the equation

$$\left(\frac{R-1}{4\mu_0/3\kappa_0 - 1}\right)^5\left(\frac{4\mu_0/3\kappa_0 + 1}{R+1}\right) = f_0^6.$$

Clearly R approaches 1 as f_0 approaches 0, and consequently the moduli vanish in the limit as $f_0 \to 0$ while the ratio κ_*/μ_* approaches $4/3$, that is, the same value it approaches at the transition point in the effective medium approximation.

If the inclusions are randomly oriented plates (or thin spherical shells) rather than spheres, the differential equations become

$$\frac{d\kappa_*}{df_0} = -\frac{(\kappa_* + 4\mu_1/3)(\kappa_1 - \kappa_*)}{(\kappa_1 + 4\mu_1/3)f_0},$$
$$\frac{d\mu_*}{df_0} = -\frac{(\mu_* + F_1)(\mu_1 - \mu_*)}{(\mu_1 + F_1)f_0}, \quad \text{where } F_1 = \frac{\mu_1(9\kappa_1 + 8\mu_1)}{6(\kappa_1 + 2\mu_1)},$$

with $\kappa_* = \kappa_0$ and $\mu_* = \mu_0$ at $f_0 = 1$. Upon integration (using separation of variables) these yield the formulas

$$\kappa_* = \kappa_1 + \frac{f_0}{1/(\kappa_0 - \kappa_1) + (1 - f_0)/(\kappa_1 + 4\mu_1/3)},$$
$$\mu_* = \mu_1 + \frac{f_0}{1/(\mu_0 - \mu_1) + (1 - f_0)/(\mu_1 + F_1)}$$

for the effective bulk and shear moduli. As Roscoe (1973) recognized [see also Norris (1985) and Milton (1986)] these formulas coincide with the Hashin-Shtrikman (1963) bounds on the

effective bulk and shear moduli of a two-phase composite with $(\kappa_1 - \kappa_0)(\mu_1 - \mu_0) \geq 0$, as discussed in section 23.5 on page 468. Roscoe also argued that one could utilize this result to prove the Hashin-Shtrikman bounds. However, there is an error in his analysis (where he assumed a particular value of an integration constant) and the correct statement is that one can use the Hashin-Shtrikman bounds for dilute composites to obtain them for nondilute composites (Milton and Nesi 1999).

10.10. Asymptotic approximation formulas

Sometimes one can obtain good estimates for the effective conductivity of a mixture of two isotropic phases with conductivities σ_1 and σ_2 in the asymptotic limit where $\sigma_1 \gg \sigma_2$. For example, a three-dimensional checkerboard (i.e., a face-centered cubic array of touching cubes of phase 1 surrounded by phase 2) has effective conductivity

$$\sigma_* \approx 2\sqrt{\sigma_1\sigma_2} \text{ when } \sigma_1 \gg \sigma_2, \tag{10.46}$$

as shown by Keller (1987). To see this, consider the checkerboard array of square prisms of the two phases with $\sigma_1 \gg \sigma_2$, with the average current flowing perpendicular to one prism face. In this situation the electrical potential is essentially constant within each prism of phase 1, except near the edges, and the current in phase 2 is negligibly small, except near the edges where two prisms of phase 1 meet. Thus the regions near the edges of the prisms form the main impedance to current within the material. We could even associate a resistance with each edge between the prisms. For the three-dimensional checkerboard there would be twice the number of these edges through which the current could flow. Thus it would have twice the conductivity of the checkerboard array of square prisms in the asymptotic limit. Hence (10.46) follows from the duality result (3.11) that the transverse effective conductivity of the checkerboard array of square prisms is exactly $\sqrt{\sigma_1\sigma_2}$. Keller also extended this asymptotic analysis to two-dimensional checkerboard patterns of rectangles or parallelepipeds [thereby providing a simple derivation of earlier results of Gautesen (1988) for the rectangular checkerboard] and to three-dimensional checkerboard patterns of rectangular blocks or parallelepipeds. Obnosov (1996) provided the exact solution for the fields in rectangular checkerboards.

Kozlov (1989) and Berlyand and Golden (1994) applied variational principles to rigorously justify the asymptotic behavior of the conductivity of periodic and random checkerboard arrays. [See Torquato, Kim, and Cule (1999) for numerical simulations of the conductivity of random checkerboards.] Curiously, as anticipated by Sheng and Kohn (1982), the random checkerboard array has two conductivity thresholds. It consists of a square lattice of touching squares where the squares are randomly chosen to have conductivity σ_1 with probability f, with the remaining squares having conductivity σ_2. As the volume fraction f of phase 1 is increased one encounters a critical volume fraction, $f_c^L \approx 0.41$ (the site percolation threshold), at which corner connected paths of phase 1 first span the composite. Then one encounters a second critical volume fraction, $f_c^U = 1 - f_c^L$, at which edge connected paths of phase 1 first span the composite, that is, when corner connected paths of phase 2 cease to span the composite. When $\sigma_1 \gg \sigma_2$, the effective conductivity σ_* is asymptotically proportional to σ_2, $\sqrt{\sigma_1\sigma_2}$ and σ_1, respectively, in the three regimes $0 \leq f < f_c^L$, $f_c^L < f < f_c^U$, and $f_c^U < f \leq 1$. Golden and Kozlov (1999) show that there is a generalization of this model which has infinitely many conductivity thresholds.

Berlyand and Kozlov (1992) have analyzed the effective elastic moduli of two-dimensional checkerboards when one phase is considerably stiffer than the other. Interestingly they found that the effective Poisson's ratio is close to zero when the material is stretched in the

direction of a diagonal of the checkerboard, even when both phases have Poisson's ratios equal to, say, 1/3. The physical explanation is quite simple: Most of the deformation occurs near the corners, and this deformation does not have much influence on the width of the material. See figure 10.3.

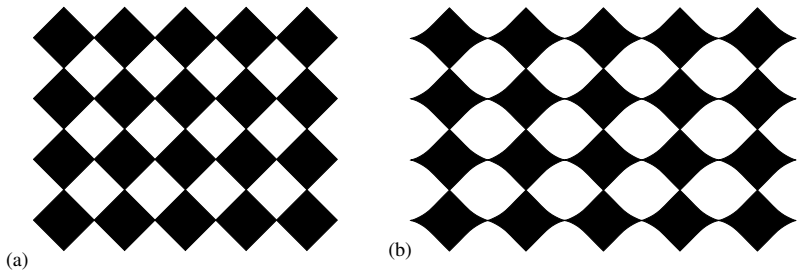

Figure 10.3. A checkerboard composed of a very stiff material occupying the black squares and a very compliant material occupying the white squares, as shown in (a), when stretched in the direction of a checkerboard diagonal, as in (b), has little change to its overall width and thus has an effective Poisson's ratio close to zero. After Berlyand and Kozlov (1992).

Another microstructure that can be analyzed asymptotically is a cubic array of spheres of phase 1, having infinite conductivity, that are close to touching and surrounded by phase 2, having finite conductivity σ_2. (The analogous dielectric problem is of an array of conducting spheres surrounded by a dielectric medium). The electrical potential is constant within each sphere and the current in phase 2 is negligibly small, except near where the spheres touch. Following Keller (1963), we consider two adjacent spheres, at, say, potentials $\phi = -V_g/2$ and $\phi = +V_g/2$, where V_g is the voltage across the gap. We center the origin midway between the spheres and use cylindrical coordinates (x_1, ρ), where the x_1-axis is along the line joining the sphere centers and ρ measures the distance to this line. Near the gap the surfaces of the spheres can be approximated by the parabolas

$$x_1 = \pm(h/2 + \rho^2/2r_0),$$

where r_0 is the sphere radius and h is the width of the gap between the spheres. To a first approximation the potential $\phi(x_1, \rho)$ in the gap should be just a linear function of x_1; since it takes the values $\phi = -V_g/2$ and $\phi = +V_g/2$ on the sphere surfaces, we have

$$\phi(x_1, \rho) \approx V_g x_1/[h + \rho^2/r_0],$$

and the associated current $\boldsymbol{j} = \sigma_2 \nabla\phi$ will have a component

$$j_1(0, \rho) \approx \sigma_2 V_g/[h + \rho^2/r_0]$$

flowing normal to the mid-plane between the cylinders. Thus the total current flowing between the spheres is

$$\begin{aligned} I_g \approx 2\pi\sigma_2 \int_0^{\rho_c} j_1(0, \rho)\rho d\rho \;&\approx\; 2\pi\sigma_2 V_g \int_0^{\rho_c} \frac{\rho d\rho}{h + \rho^2/r_0} \\ &\approx\; -\pi\sigma_2 V_g r_0 \log(h) \approx \pi\sigma_2 V_g r_0 \log(r_0/h), \end{aligned}$$

where ρ_c is a cutoff radius beyond which the preceding approximations are poor. This estimate has neglected the contributions from the region $\rho > \rho_c$ and also the contributions from terms

like $\log(r_0)$ and $\log(h + r_c^2/r_0)$, which remain finite as $h \to 0$. Thus the gap behaves like a resistor with resistance

$$R_g = V_g/I_g \approx \frac{1}{\pi\sigma_2 r_0 \log(r_0/h)}.$$

In the array of spheres the unit cell of periodicity is a cube of side length $2r_0 + h$. To ensure that V_g is the voltage across the gap, we set the average electric field $\langle \boldsymbol{e} \rangle$ along the x_1-axis with magnitude $V_g/(2r_0 + h)$. The average current $\langle \boldsymbol{j} \rangle$ is then also directed along the x_1-axis and has magnitude $I_g/(2r_0 + h)^2$, where $(2r_0 + h)^2$ is the area of the cube face of the unit cell of periodicity. Thus the effective conductivity is

$$\sigma_* = I_g/[(2r_0 + h)V_g] \approx \sigma_2(\pi/2)\log(r_0/h).$$

Batchelor and O'Brien (1977) show how this analysis can be extended to arbitrarily shaped inclusions with smooth boundaries that are close to contact. The x_1-axis is placed where it is perpendicular to both surfaces. Then the distance g separating the surfaces can be approximated by the quadratic

$$g = h + x_2^2/a + x_3^2/b$$

for an appropriate choice of the x_2- and x_3-axes (perpendicular to the x_1-axis), where a and b depend on the curvatures of the surfaces. They show that the gap behaves like a resistor with gap resistance

$$R_g \approx \frac{1}{\pi\sigma_2 (ab)^{1/2} \log[(ab)^{1/2}/h]}. \tag{10.47}$$

Thus, as illustrated figure 10.4, any assemblage of almost touching, smoothly shaped, perfectly conducting inclusions can be replaced by an equivalent resistor network. A rigorous basis for this approximation, for a two-dimensional assemblage of perfectly conducting disks in a matrix, was given by Berlyand and Kolpakov (2001).

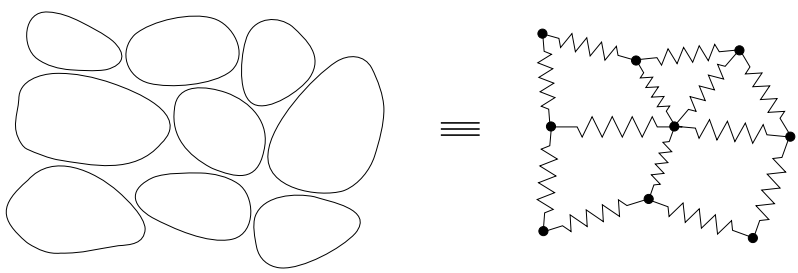

Figure 10.4. An assemblage of almost touching, perfectly conducting, inclusions embedded in a matrix of finite conductivity can be replaced by an equivalent resistor network. Each gap between neighboring inclusions is replaced by a resistance given by (10.47), and the electrical potentials at the nodes in the network correspond to the potentials in each inclusion. Of course, the assemblage should fill all space and the equivalent resistor network should have infinite extent.

Batchelor and O'Brien also consider touching spheres with finite conductivity and for large values of σ_1/σ_2 find that a current

$$I_g = V_g/R_g, \quad \text{where } R_g \approx \frac{1}{2\pi\sigma_2 r_0 \log(\sigma_1/\sigma_2)}$$

flows between them, in which V_g is now the voltage drop between the sphere centers. This leads to the estimate

$$\sigma_* \approx 1/(2r_0 R_g) \approx \pi\sigma_2 \log(\sigma_1/\sigma_2), \quad \text{when } \sigma_1 \gg \sigma_2,$$

for the effective conductivity of a touching cubic array of spheres.

In two dimensions, Keller (1963) finds that a pair of almost touching, perfectly conducting circular disks at potentials $-V_g/2$ and $V_g/2$ have a total current

$$I_g \approx \pi\sigma_2 V_g \sqrt{r_0/h}$$

flowing across the gap [see also Flaherty and Keller (1973) for the equivalent result in antiplane elasticity]. O'Brien (1977) finds that for finitely conducting touching disks

$$I_g \approx \frac{\pi\sigma_1 V_g}{2\log(\sigma_1/\sigma_2)} \quad \text{when } \sigma_1 \gg \sigma_2.$$

McPhedran, Poladian, and Milton (1988) consider finitely conducting disks separated by a small gap and find an expression for the current I_g that is uniformly valid throughout the whole asymptotic region:

$$I_g \approx \frac{\pi V_g (c-1)}{2s\log(c) + 1 - 2s[\gamma + \psi(1+s)]},$$

where ψ is the psi or digamma function and $\gamma \approx 0.57722$ is Euler's constant (Davis 1972), while

$$c = \frac{2r_0 + h}{\sqrt{h(4r_0 + h)}} \approx \sqrt{r_0/h}, \quad s = \frac{\log[(\sigma_1/\sigma_2 - 1)/(\sigma_1/\sigma_2 + 1)]}{\log[(c-1)/(c+1)]} \approx c\sigma_2/\sigma_1.$$

Thus c is a parameter that measures how close the circles are to touching (small values of h correspond to large values of c), while s is a parameter that measures the relative magnitudes of c and the conductivity ratio σ_1/σ_2. The above approximation is good for sufficiently high values of c and σ_1/σ_2 for all values of s (including $s = 0$ and $s = \infty$). It is derived by using the method of images and approximating the discrete distribution of image charges by a continuous distribution. McPhedran, Poladian, and Milton (1988) and Helsing (1994) find good agreement with numerical simulations of the conductivity of square arrays of disks in the asymptotic regime. The approach has been extended by McPhedran and Movchan (1994) to two-dimensional elasticity. They use it to estimate the stiffness of the junction between pairs of almost rigid, circular disks separated by a small gap. The case of completely rigid, nearly touching, circular disks was treated by Davis, Hass, Chen, and Thorpe (1994), and the case of completely rigid, nearly touching, spheres was treated by Nunan and Keller (1984). Accurate numerical methods for treating almost touching conducting inclusions in two-dimensional microstructures have been developed by Helsing (1996), Cheng and Greengard (1997), and Cheng and Greengard (1998).

Another class of media that can be treated using asymptotic analysis was introduced by Kozlov (1989). The conductivity tensor is assumed to be locally isotropic with $\boldsymbol{\sigma}(\boldsymbol{x}) = \sigma(\boldsymbol{x})\boldsymbol{I}$, where $\sigma(\boldsymbol{x})$ takes the form

$$\sigma(\boldsymbol{x}) = \sigma_0 e^{S(\boldsymbol{x})/\epsilon},$$

where $S(\boldsymbol{x})$ is some smooth periodic function of $\boldsymbol{x}$. When ϵ is very small the regions near where $S(\boldsymbol{x})$ has its maximum have comparatively high conductivity. The path of least resistance connecting two neighboring regions of high conductivity passes through a saddle point of the function $S(\boldsymbol{x})$. It is the region near this saddle point which forms the main bottleneck to current flow between the highly conducting regions. Kozlov shows through rigorous analysis that in the limit $\epsilon \to 0$ one can model conduction in the composite by a discrete resistor network. For example, in two-dimensional conductivity a saddle at the point $\boldsymbol{x} = \boldsymbol{x}^s$ can be replaced by a resistor with resistance

$$R_s \approx [1/\sigma(\boldsymbol{x}^s)]\sqrt{k^+/k^-},$$

where k^+ and $-k^-$ are the eigenvalues of the matrix $\boldsymbol{M}$, appearing in the approximate expression

$$S(\boldsymbol{x}) \approx S(\boldsymbol{x}^s) + (\boldsymbol{x} - \boldsymbol{x}^s) \cdot \boldsymbol{M}(\boldsymbol{x} - \boldsymbol{x}^s)/2,$$

for $S(\boldsymbol{x})$ near the saddle point.

Kozlov's work and the subsequent work of Golden and Kozlov (1999) gave a rigorous foundation for the critical path analysis of Ambegaokar, Halperin, and Langer (1971). They proposed that conduction in a medium with a very broad range of local conductivities σ is dominated by a critical conductivity σ_c that is the smallest conductivity such that the set $\{\sigma \mid \sigma > \sigma_c\}$ forms a connected path that spans the material. Borcea and Papanicolaou (1998) extended Kozlov's analysis to the complex conductivity of certain high-contrast materials and proved that they can be modeled (in the quasistatic limit: see section 11.1 on page 222) as suitable networks of resistors and capacitors.

Quantum effects can lead to additional corrections to these asymptotic formulas. This is most evident in a granular medium consisting of metal grains surrounded by a dielectric. If the grains are separated, then classical theory predicts that the effective conductivity will be zero. However, if there is a connected path of short gaps between adjacent grains, then electrons will tunnel through these gaps. This hopping of electrons from grain to grain is known as hopping conductivity. Once one allows for it, the predicted effective conductivity is nonzero and in excellent agreement with experiment (Sheng, Abeles, and Arie 1973; Sheng 1978).

10.11. Critical exponents and universality

In the previous section we saw how conduction in a high-contrast medium is sometimes equivalent to conduction in a resistor network. In random resistor networks conduction in the vicinity of the percolation threshold is characterized by some remarkable features. For example, consider the bond percolation problem where adjacent points, called sites, on a cubic (or square) lattice are connected by bonds (aligned with the coordinate axes) chosen randomly to have conductance σ_1, with probability f, or conductance σ_2, with probability $1 - f$. When σ_1 is nonzero and finite and $\sigma_2 = 0$, there is a threshold concentration f_c, the percolation threshold, such that for $f < f_c$ no conduction occurs, while for $f > f_c$ there is a connected cluster of bonds of conductance σ_1 having infinite extent. Thus the effective conductivity σ_* of the lattice is zero for $f < f_c$ and nonzero for $f > f_c$. In the vicinity of f_c one has

$$\sigma_* \sim \sigma_1(f - f_c)^t \text{ for } f > f_c,$$

where the symbol $\sim$ means asymptotically proportional to, as $f \to f_c$.

The striking discovery [see the review of Kirkpatrick (1973)] was that the critical exponent t (unlike f_c) apparently had a universal value [approximately 2.0 in three dimensions and

1.3 in two dimensions; see, for example, Normand and Herrmann (1995) and Frank and Lobb (1988) and references therein] independent of the underlying lattice (e.g., square and triangular lattices had the same value of t) and independent of the presence of short-range correlations between the conductances of the resistors in the lattice. The value of t was found to be the same (within numerical error) for the site percolation problem where sites (and those bonds connected to them) are removed at random from a complete lattice of bonds having conductance σ_1.

This universality of t has its explanation in renormalization group theory, which has its origins in quantum field theory and in the theory of second-order phase transitions in statistical physics. Unfortunately, a detailed explanation of this theory is beyond the scope of this book. The interested reader is urged to read, for example, the introductory book of Creswick, Farach, and Poole, Jr. (1998) and the many references cited in the historical review of Fisher (1998). There are still many open questions regarding the application of this theory to the conductivity of random resistor networks. Although calculations based on approximate (real space) renormalization group transformations give reasonable estimates of t, the existence of an exact renormalization group transformation is still uncertain. Such a transformation would provide a partial homogenization ("coarse graining") of the system; only fluctuations on the smallest length scales are averaged, and then the system is spatially rescaled so that the remaining fluctuations have oscillations down to the same length scale as were originally present. Repeated applications of the transformation effectively average over fluctuations on successively larger length scales in the original system. The hypothesis is that there exists an unstable fixed point of this transformation (in some appropriate space) with only a few unstable directions. Then one can show that the eigenvalues characterizing the linearization of the transformation at this fixed point determine the critical exponents. Specifically, only those eigenvalues with modulus greater than 1 (corresponding to the unstable directions) are relevant. After suitably many applications of the renormalization group transformation, different systems near percolation are mapped to the vicinity of the same fixed point, which explains the universality of the exponents.

Besides the exponent t there are other universal critical exponents that describe how the effective conductivity varies in the neighborhood of the critical point where $f = f_c$ and $\sigma_2/\sigma_1 = 0$. These other critical exponents are observed by approaching the critical point in different ways. When $\sigma_1 = \infty$ and σ_2 is nonzero and finite, the effective conductivity diverges as the conductivity threshold is approached from below, as

$$\sigma_* \sim \sigma_2 (f_c - f)^{-s} \quad \text{for} \quad f < f_c,$$

which defines the exponent s. When both σ_1 and σ_2 are nonzero and finite, and σ_2/σ_1 approaches zero, one has

$$\sigma_* \sim \sigma_1^{1-u} \sigma_2^u \quad \text{for} \quad f = f_c,$$

which defines the exponent u. These three exponents are not all independent. Due to the homogeneity property of the function $\sigma_*(\sigma_1, \sigma_2)$ one has the relation (Straley 1977)

$$u = t/(s + t).$$

In two dimensions the duality transformation discussed in section 3.1 on page 47, adapted to the discrete case of a resistor network (Straley 1977), provides the exact result that for bond percolation $\sigma_* = \sqrt{\sigma_1 \sigma_2}$ when $f = f_c = 1/2$. Thus in two dimensions the exponent u equals $1/2$, and consequently $s = t$.

Because of universality the hope was that the same exponent t would characterize conduction in two-phase random media in the vicinity of the percolation threshold, with phase 1 occupying a volume fraction f having conductivity σ_1, and phase 2 being void. In their experiment on conduction and percolation Last and Thouless (1971) measured the effective conductivity of conducting paper with holes randomly punched into it. As the holes were centered at lattice points on a square grid, this was essentially a site percolation problem and they would have observed the same value of $t \approx 1.3$ had they measured it. However, the hope was dashed when Feng, Halperin, and Sen (1987) showed that different exponents occur in "Swiss cheese models" where uniformly sized circular or spherical holes are randomly centered anywhere in the material. Due to the variation in the "neck" widths between holes, this corresponds to a discrete resistor network with the resistors having a distribution of conductances ranging to zero. The nature of this distribution places the problem in a different universality class with different exponents. Thus the exponents can depend on the microstructure of the random composite.

There are also many investigations of the critical exponents associated with elastic networks [see, for example, Feng and Sen (1984); Bergman (1985); Schwartz, Feng, Thorpe, and Sen (1985); Zabolitzky, Bergman, and Stauffer (1986) and references therein]. Of particular note is the result of Bergman (1985) that the effective Poisson's ratio takes a universal value at the percolation threshold.

References

Ambegaokar, V., B. I. Halperin, and J. S. Langer 1971. Hopping conductivity in disordered systems. *Physical Review B (Solid State)* 4(8):2612–2620. {*211, 213*}

Archie, G. E. 1942. The electrical resistivity log as an aid in determining some reservoir characteristics. *Transactions of the American Institute of Mining, Metallurgical, and Petroleum Engineers (AIME)* 146:54–62. {*202, 213*}

Avellaneda, M. 1987. Iterated homogenization, differential effective medium theory, and applications. *Communications on Pure and Applied Mathematics (New York)* 40(5): 527–554. {*197, 203, 204, 213*}

Batchelor, G. K. and R. W. O'Brien 1977. Thermal or electrical conduction through a granular material. *Proceedings of the Royal Society of London. Series A, Mathematical and Physical Sciences* 355:313–333. {*209, 213*}

Bergman, D. J. 1985. Elastic moduli near percolation: Universal ratio and critical exponent. *Physical Review B (Solid State)* 31(3):1696–1698. {*213*}

Berlyand, L. and K. Golden 1994. Exact result for the effective conductivity of a continuum percolation model. *Physical Review B (Solid State)* 50(4):2114–2117. {*207, 213*}

Berlyand, L. and A. Kolpakov 2001. Network approximation in the limit of small interparticle distance of the effective properties of a high-contrast random dispersed composite. *Archive for Rational Mechanics and Analysis*. To appear. URL `http://dx.doi.org/10.1007/s002050100142` {*209, 213*}

Berlyand, L. and S. M. Kozlov 1992. Asymptotics of the homogenized moduli for the elastic chess-board composite. *Archive for Rational Mechanics and Analysis* 118(2): 95–112. {*207, 208, 213*}

Berryman, J. G. 1980. Long-wavelength propagation in composite elastic media, II. Ellipsoidal inclusions. *Journal of the Acoustical Society of America* 68:1820–1831. {*205, 213*}

Bolotin, V. V. and V. N. Moskalenko 1967. The macroscopic coefficients of thermal conductivity and diffusion in microinhomogeneous solids. *Zhurnal Prikladnoi Mekhaniki i Tekhnicheskoi Fiziki* 8(6):7–13. English translation in *J. Appl. Mech. Tech. Phys.* 8:3–6 (1967). {*197, 214*}

Borcea, L. and G. Papanicolaou 1998. Network approximation for transport properties of high contrast materials. *SIAM Journal on Applied Mathematics* 58(2):501–539. {*211, 214*}

Bruggeman, D. A. G. 1935. Berechnung verschiedener physikalischer Konstanten von heterogen Substanzen. I Dielektrizitätskonstanten und Leitfähigkeiten der Mischkörper aus isotropen Substanzen. (German) [Calculation of various physical constants in heterogeneous substances. I. Dielectric constants and conductivity of composites from isotropic substances]. *Annals of Physics* 24:636–679. {*195, 201, 214*}

Budiansky, B. 1965. On the elastic moduli of some heterogeneous materials. *Journal of the Mechanics and Physics of Solids* 13:223–227. {*204, 214*}

Buryachenko, V. A. 2001. Multiparticle effective field and related methods in micromechanics of composite materials. *Applied Mechanics Reviews* 54(1):1–47. {*185, 214*}

Chen, H.-S. and A. Acrivos 1978. The effective elastic moduli of composite materials containing spherical inclusions at non-dilute concentrations. *International Journal of Solids and Structures* 14(5):349–364. {*191, 214*}

Cheng, H. and L. Greengard 1997. On the numerical evaluation of electrostatic fields in dense random dispersions of cylinders. *Journal of Computational Physics* 136(2):629–639. {*40, 41, 210, 214*}

Cheng, H. and L. Greengard 1998. A method of images for the evaluation of electrostatic fields in systems of closely spaced conducting cylinders. *SIAM Journal on Applied Mathematics* 58(1):122–141. {*40, 41, 210, 214*}

Choy, T. C., A. Alexopoulos, and M. F. Thorpe 1998. Dielectric function for a material containing hyperspherical inclusions to $O(c^2)$: I. Multipole expansions and II. Method of images. *Proceedings of the Royal Society of London. Series A, Mathematical and Physical Sciences* 454(1975):1973–1992, 1993–2013. {*188, 191, 214*}

Christensen, R. M. 1990. A critical evaluation for a class of micromechanics models. *Journal of the Mechanics and Physics of Solids* 38(3):379–404. {*205, 214*}

Christensen, R. M. and K. H. Lo 1979. Solutions for effective shear properties in three phase sphere and cylinder models. *Journal of the Mechanics and Physics of Solids* 27: 315–330. {*205, 214*}

Creswick, R. J., H. A. Farach, and C. P. Poole, Jr. 1998. *Introduction to Renormalization Group Methods in Physics*. New York / London / Sydney, Australia: John Wiley and Sons. xiv + 409 pp. ISBN 0-471-60013-X. {*212, 214*}

Davis, L. C., K. C. Hass, J. Chen, and M. F. Thorpe 1994. Elastic moduli of composites with with random rigid inclusions. *Applied Mechanics Reviews* 47(1):S5–S9. {*210, 214*}

Davis, P. J. 1972. Gamma function and related functions. In M. Abramowitz and I. A. Stegun (eds.), *Handbook of Mathematical Functions with Formulas, Graphs, and Mathematical Tables*, pp. 253–293. Washington, D.C.: U.S. Government Printing Office. {*210, 215*}

Djordjević, B. R., J. H. Hetherington, and M. F. Thorpe 1996. Spectral function for a conducting sheet containing circular inclusions. *Physical Review B (Solid State)* 53 (22):14862–14871. {*188, 215*}

Feng, S., B. I. Halperin, and P. N. Sen 1987. Transport properties of continuum systems near the percolation threshold. *Physical Review B (Solid State)* 35(1):197–214. {*213, 215*}

Feng, S. and P. N. Sen 1984. Percolation on elastic networks: New exponent and threshold. *Physical Review Letters* 52(3):216–219. {*213, 215*}

Feng, S., M. F. Thorpe, and E. J. Garboczi 1985. Effective-medium theory of percolation on central-force elastic networks. *Physical Review B (Solid State)* 31:276–280. {*197, 215*}

Finkel'berg, V. M. 1963. The virial expansion in the problem of the electrostatic polarization of a many-body system. *Doklady Akademii Nauk SSSR* 152:320–323. English translation in *Sov. Phys. Dokl.* 8:907–909 (1964). {*191, 215*}

Fisher, M. E. 1998. Renormalization group theory: Its basis and formulation in statistical physics. *Reviews of Modern Physics* 70(2):653–681. {*212, 215*}

Flaherty, J. E. and J. B. Keller 1973. Elastic behavior of composite media. *Communications on Pure and Applied Mathematics (New York)* 26:565–580. {*49, 57, 210, 215*}

Frank, D. J. and C. J. Lobb 1988. Highly efficient algorithm for percolative transport studies in two dimensions. *Physical Review B (Solid State)* 37(1):302–307. {*40, 42, 212, 215*}

Fricke, H. and S. Morse 1925. An experimental study of the electrical conductivity of disperse systems. I. Cream. *Physical Review* 25:361–367. {*194, 215*}

Garboczi, E. J. and M. F. Thorpe 1985. Effective-medium theory of percolation on central-force elastic networks. II. Further results. *Physical Review B (Solid State)* 31(11):7276–7281. {*197, 215*}

Gautesen, A. K. 1988. The effective conductivity of a composite material with a periodic rectangular geometry. *SIAM Journal on Applied Mathematics* 48(2):393–404. {*207, 215*}

Gillispie, C. C. (ed.) 1971. *Dictionary of Scientific Biography*. New York: Charles Scribners's Sons. ISBN 0-684-16967-3 (vol. 9–10). {*193, 215*}

Golden, K. and S. M. Kozlov 1999. Critical path analysis of transport in highly disordered random media. In V. Berdichevsky, V. V. Zhikov, and G. Papanicolaou (eds.), *Homogenization*, pp. 21–34. Singapore / Philadelphia / River Edge, New Jersey: World Scientific Publishing Co. ISBN 981-02-3096-6. {*207, 211, 215*}

Greengard, L. and M. Moura 1994. On the numerical evaluation of electrostatic fields in composite materials. *Acta Numerica* 3:379–410. Cambridge, United Kingdom: Cambridge University Press. {*39, 42, 188, 215*}

Hashin, Z. and S. Shtrikman 1963. A variational approach to the theory of the elastic behavior of multiphase materials. *Journal of the Mechanics and Physics of Solids* 11: 127–140. {*206, 216, 271, 287, 457, 470, 471, 473, 493*}

Helsing, J. 1994. Fast and accurate calculations of structural parameters for suspensions. *Proceedings of the Royal Society of London. Series A, Mathematical and Physical Sciences* 445:127–140. {*39, 42, 210, 216, 571, 598*}

Helsing, J. 1996. Thin bridges in isotropic electrostatics. *Journal of Computational Physics* 127(1):142–151. {*40, 43, 210, 216*}

Helsing, J. and A. Helte 1991. Effective conductivity of aggregates of anisotropic grains. *Journal of Applied Physics* 69(6):3583–3588. {*197, 216*}

Hetherington, J. H. and M. F. Thorpe 1992, September 8. The conductivity of a sheet containing inclusions with sharp corners. *Proceedings of the Royal Society of London. Series A, Mathematical and Physical Sciences* 438(1904):591–604. {*188, 216, 378, 393*}

Hill, R. 1965. A self-consistent mechanics of composite materials. *Journal of the Mechanics and Physics of Solids* 13:213–222. {*204, 216*}

Honein, E., T. Honein, and G. Herrmann 1990. On two circular inclusions in harmonic problems. *Quarterly of Applied Mathematics* 50(3):479–499. {*188, 216*}

Jackson, J. D. 1975. *Classical Electrodynamics* (Second ed.), pp. 136–143. New York / London / Sydney, Australia: John Wiley and Sons. ISBN 0-471-43132-X. {*185, 216*}

Jasiuk, I., J. Chen, and M. F. Thorpe 1994. Elastic moduli of two-dimensional materials with polygonal and elliptical holes. *Applied Mechanics Reviews* 47(1):S18–S28. {*188, 216*}

Jeffrey, D. J. 1973. Conduction through a random suspension of spheres. *Proceedings of the Royal Society of London. Series A, Mathematical and Physical Sciences* 335:355–367. {*187, 191, 216*}

Kachanov, M., I. Tsukrov, and B. Shafiro 1994. Effective moduli of solids with cavities of various shapes. *Applied Mechanics Reviews* 47(1):S151–S174. {*188, 216*}

Keller, J. B. 1963. Conductivity of a medium containing a dense array of perfectly conducting spheres or cylinders or nonconducting cylinders. *Journal of Applied Physics* 34(4):991–993. {*47, 58, 208, 210, 216*}

Keller, J. B. 1987. Effective conductivity of periodic composites composed of two very unequal conductors. *Journal of Mathematical Physics* 28(10):2516–2520. {*207, 216*}

Kerner, E. H. 1956a. The elastic and thermo-elastic properties of composite media. *Proceedings of the Physical Society, London, B* 69:808–813. {*117, 140, 204, 216*}

Kerner, E. H. 1956b. The electrical conductivity of composite media. *Proceedings of the Physical Society, London, B* 69:802–807. {*199, 216*}

Kirkpatrick, S. 1973. Percolation and conduction. *Reviews of Modern Physics* 45:574–588. {*197, 211, 216*}

Korringa, J., R. J. S. Brown, D. D. Thompson, and R. J. Runge 1979. Self-consistent embedding and the ellipsoidal model for porous rocks. *Journal of Geophysical Research* 84:5591–5598. {*205, 216*}

Kozlov, S. M. 1989. Geometric aspects of averaging. *Uspekhi Matematicheskikh Nauk = Russian Mathematical Surveys* 44(2):79–120. English translation in *Russ. Math. Surv.* 44(2):91–144 (1989). {*207, 210, 217*}

Landauer, R. 1978. Electrical conductivity in inhomogeneous media. In J. C. Garland and D. B. Tanner (eds.), *Electrical Transport and Optical Properties of Inhomogeneous Media*, pp. 2–43. Woodbury, New York: American Institute of Physics. ISBN 0-88318-139-8. {*2, 16, 185, 193, 217*}

Last, B. J. and D. J. Thouless 1971. Percolation theory and electrical conductivity. *Physical Review Letters* 27(25):1719–1721. {*213, 217*}

Lipton, R. 1993. Inequalities for electric and elastic polarization tensors with applications to random composites. *Journal of the Mechanics and Physics of Solids* 41(5):809–833. {*188, 217*}

Love, J. D. 1975. Dielectric sphere-sphere and sphere-plane problems in electrostatics. *Quarterly Journal of Mechanics and Applied Mathematics* 28:449–471. {*188, 217*}

Mackenzie, J. K. 1950. The elastic constants of a solid containing spherical holes. *Proceedings of the Physical Society, London, B* 63:2–11. {*205, 217*}

Markov, K. Z. 2000. Elementary micromechanics of heterogeneous media. In K. Markov and L. Preziosi (eds.), *Heterogeneous Media: Micromechanics Modeling Methods and Simulations*, Modeling and Simulation in Science, Engineering and Technology, pp. 1–162. Basel, Switzerland: Birkhäuser Verlag. ISBN 0-8176-4083-5. {*xxv, xxvii, 2, 16, 185, 217, 346, 353*}

Markov, K. Z. and J. R. Willis 1998. On the two-point correlation function for dispersions of nonoverlapping spheres. *Mathematical Models and Methods in Applied Sciences* 8 (2):359–377. {*191, 217*}

McLaughlin, R. 1977. A study of the differential scheme for composite materials. *International Journal of Engineering Science* 15:237–244. {*206, 217*}

McPhedran, R. C. and A. B. Movchan 1994. The Rayleigh multipole method for linear elasticity. *Journal of the Mechanics and Physics of Solids* 42(5):711–727. {*39, 44, 210, 217*}

McPhedran, R. C. and W. T. Perrins 1981. Electrostatic and optical resonances of cylinder pairs. *Applied Physics* 24:311–318. {*188, 217, 239, 244, 306, 311*}

McPhedran, R. C., L. Poladian, and G. W. Milton 1988. Asymptotic studies of closely spaced, highly conducting cylinders. *Proceedings of the Royal Society of London. Series A, Mathematical and Physical Sciences* 415:185–196. {*210, 217*}

Meyers, N. G. 1963. An L^p-estimate for the gradient of solutions of second order elliptic divergence form equations. *Annali della Scuola Normale Superiore di Pisa. Serie III* 17(3):189–206. {*200, 204, 217*}

Milton, G. W. 1984. Correlation of the electromagnetic and elastic properties of composites and microgeometries corresponding with effective medium theory. In D. L. Johnson and P. N. Sen (eds.), *Physics and Chemistry of Porous Media: Papers from a Symposium Held at Schlumberger-Doll Research, Oct. 24–25, 1983*, pp. 66–77. Woodbury, New York: American Institute of Physics. ISBN 0-88318-306-4. {*196, 217, 522, 526*}

Milton, G. W. 1985b. Some exotic models in statistical physics. I. The coherent potential approximation is a realizable effective medium scheme. II. Anomalous first-order transitions. Ph.D. thesis, Cornell University, Ithaca, New York. x + 164 pp. {*202, 218*}

Milton, G. W. 1985a. The coherent potential approximation is a realizable effective medium scheme. *Communications in Mathematical Physics* 99(4):463–500. {*196, 197, 218*}

Milton, G. W. 1986. Modeling the properties of composites by laminates. In J. L. Ericksen, D. Kinderlehrer, R. Kohn, and J.-L. Lions (eds.), *Homogenization and Effective Moduli of Materials and Media*, pp. 150–174. Berlin / Heidelberg / London / etc.: Springer-Verlag. ISBN 0-387-96306-5. {*206, 218, 384, 394, 463, 471, 472, 494, 578, 599, 603, 617*}

Milton, G. W. and V. Nesi 1999. Optimal G-closure bounds via stability under lamination. *Archive for Rational Mechanics and Analysis* 150(3):191–207. {*207, 218, 480, 495, 646, 669*}

Movchan, A. B. and N. V. Movchan 1995. *Mathematical Modelling of Solids with Nonregular Boundaries*. Boca Raton, Florida: CRC Press. xiv + 325 pp. ISBN 0-8493-8338-2. {*186, 218*}

Movchan, A. B. and S. K. Serkov 1997. The Pólya-Szegő matrices in asymptotic models of dilute composites. *European Journal of Applied Mathematics* 8(6):595–621. {*69, 72, 188, 218*}

Noh, T. W., P. H. Song, and A. J. Sievers 1991. Self-consistency conditions for the effective medium approximation in composite materials. *Physical Review B (Solid State)* 44(11): 5459–5464. {*200, 218*}

Normand, J.-M. and H. J. Herrmann 1995. Precise determination of the conductivity exponent of 3D percolation using "Percola". *International Journal of Modern Physics C* 6 (6):813–818. {*212, 218*}

Norris, A. 1985. A differential scheme for the effective moduli of composites. *Mechanics of Materials: An International Journal* 4:1–16. {*203, 206, 218, 471, 495*}

Norris, A., A. J. Callegari, and P. Sheng 1985. A generalized differential effective medium theory. *Journal of the Mechanics and Physics of Solids* 33:525–543. {*202, 218*}

Nunan, K. C. and J. B. Keller 1984. Effective elasticity tensor of a periodic composite. *Journal of the Mechanics and Physics of Solids* 32(4):259–280. {*39, 45, 210, 218*}

Obnosov, Y. V. 1996. Exact solution of a boundary-value problem for a rectangular checkerboard field. *Proceedings of the Royal Society of London. Series A, Mathematical and Physical Sciences* 452(1954):2423–2442. {*143, 156, 207, 218*}

O'Brien, R. W. 1977. Properties of suspensions of interacting particles. Ph.D. thesis, University of Cambridge, Cambridge, United Kingdom. {*210, 218*}

Peterson, J. M. and J. J. Hermans 1969. The dielectric constants of nonconducting suspensions. *Journal of Composite Materials* 3:338–354. {*187, 218*}

Polder, D. and J. H. Van Santen 1946. The effective permeability of mixtures of solids. *Physica* XII:257–271. {*198, 218*}

Pólya, G. and G. Szegő 1951. *Isoperimetric Inequalities in Mathematical Physics*. Princeton, New Jersey: Princeton University Press. xvi + 279 pp. {*186, 218*}

Roscoe, R. 1973. Isotropic composites with elastic or viscoelastic phases: General bounds for the moduli and solutions for special geometries. *Rheologica acta* 12:404–411. {*206, 219, 471, 496, 646, 669*}

Scaife, B. K. P. 1989. *Principles of Dielectrics*. Oxford, United Kingdom: Oxford University Press. xxxii + 384 pp. ISBN 0-19-851380-1. {*19, 46, 193, 219*}

Schwartz, L. M., S. Feng, M. F. Thorpe, and P. N. Sen 1985. Behavior of depleted elastic networks: Comparison of effective-medium and numerical calculations. *Physical Review B (Solid State)* 32(7):4607–4617. {*197, 213, 219*}

Sen, P., C. Scala, and M. H. Cohen 1981. A self-similar model for sedimentary rocks with application to the dielectric constant of fused glass beads. *Geophysics* 46:781–795. {*202, 219*}

Sheng, P. 1978. Low-field and high-field hopping conductivity in granular metal films. In J. C. Garland and D. B. Tanner (eds.), *Electrical Transport and Optical Properties of Inhomogeneous Media*, pp. 143–152. Woodbury, New York: American Institute of Physics. ISBN 0-88318-139-8. {*211, 219*}

Sheng, P., B. Abeles, and Y. Arie 1973. Hopping conductivity in granular metals. *Physical Review Letters* 31(1):44–47. {*211, 219*}

Sheng, P. and R. V. Kohn 1982. Geometric effects in continuous-media percolation. *Physical Review B (Solid State)* 26(3):1331–1335. {*207, 219*}

Smith, J. C. 1974. Correction and extension of van der Poel's method for calculating the shear modulus of a particulate composite. *Journal of Research of the National Bureau of Standards* 78A:355–361. {*205, 219*}

Smith, J. C. 1975. Simplification of van der Poel's formula for the shear modulus of a particulate composite. *Journal of Research of the National Bureau of Standards* 79A: 419–423. {*205, 219*}

Straley, J. P. 1977. Critical exponents for the conductivity of random resistor lattices. *Physical Review B (Solid State)* 15(12):5733–5737. {*212, 219*}

Stroud, D. 1975. Generalized effective-medium approach to the conductivity of an inhomogeneous material. *Physical Review B (Solid State)* 12(8):3368–3373. {*197, 219*}

Thorpe, M. F. 1992, April 8. The conductivity of a sheet containing a few polygonal holes and/or superconducting inclusions. *Proceedings of the Royal Society of London. Series A, Mathematical and Physical Sciences* 437:221–227. {*188, 219*}

Torquato, S., I. C. Kim, and D. Cule 1999. Effective conductivity, dielectric constant, and diffusion coefficient of digitized composite media via first-passage-time equations. *Journal of Applied Physics* 85(3):1560–1571. {*40, 46, 207, 219, 586, 600*}

Van Beek, L. K. H. 1967. Dielectric behaviour of heterogeneous systems. *Progress in Dielectrics* 7:69–114. {*185, 219*}

Van der Poel, C. 1958. On the rheology of concentrated dispersions. *Rheologica acta* 1 (2–3):198–205. {*205, 219*}

Walpole, L. J. 1969. On the overall elastic moduli of composite materials. *Journal of the Mechanics and Physics of Solids* 17:235–251. {*199, 205, 219, 474, 496*}

Willis, J. R. 1981. Variational and related methods for the overall properties of composites. *Advances in Applied Mechanics* 21:1–78. {*xxv, xxviii, 185, 200, 220, 252, 255, 269, 291, 312*}

Willis, J. R. and J. R. Acton 1976. The overall elastic moduli of a dilute suspension of spheres. *Quarterly Journal of Mechanics and Applied Mathematics* 29:163–177. {*191, 220, 252, 270*}

Wu, T. T. 1966. The effect of inclusion shape on elastic moduli of a two-phase material. *International Journal of Solids and Structures* 2:1–8. {*205, 220*}

Zabolitzky, J. G., D. J. Bergman, and D. Stauffer 1986. Precision calculation of elasticity for percolation. *Journal of Statistical Physics* 44(1/2):211–223. {*213, 220*}

Zhikov, V. V., S. M. Kozlov, and O. A. Oleinik 1994. *Homogenization of Differential Operators and Integral Functionals*. Berlin / Heidelberg / London / etc.: Springer-Verlag. xi + 570 pp. ISBN 3-540-54809-2 (Berlin), 0-387-54809-2 (New York). {*xxv, xxviii, 8, 11, 13, 18, 47, 58, 200, 220*}

11

Wave propagation in the quasistatic limit

Until now we have assumed the fields to be independent of time t. In this section we will see that our analysis can easily be extended to treat fields that oscillate with time, provided that the wavelengths and attenuation lengths associated with the fields are much larger than the microstructure. This limit, where the size of the microstructure goes to zero, is called the quasistatic limit. Our analysis will be restricted to periodic composites. In contrast to the previous sections, where the assumption of periodicity was made purely for convenience, the analysis of the present section does not extend directly to random composites. In particular, the phenomena of localization (which only pertains to random composites) is not treated in the ensuing analysis. Nevertheless, the results given here can usually be applied as an approximation to wave propagation in random composites, especially if the effects of localization are small.

Our objective is to show that the equations of electromagnetic wave propagation and elastic wave propagation in the quasistatic limit reduce to the usual equations of conductivity and elasticity, but with complex fields and complex tensors. In the course of this analysis we will make whatever assumptions are necessary, avoiding mathematical technicalities. Rather than providing a rigorous proof, we merely aim to give an understanding of how wave propagation in the quasistatic limit reduces to a set of equations with complex-valued fields and complex-valued moduli. For a more complete analysis the reader is referred to the books of Bensoussan, Lions, and Papanicolaou (1978) and Sanchez-Palencia (1980) and to the paper of Conca and Vanninathan (1997). See also the paper of Avellaneda, Berlyand, and Clouet (2000), who make a careful study of corrections to the quasistatic approximation for a wave incident on a slab cut from a laminate, with the layers oriented at some angle to the slab boundary. In addition see the papers of Allaire and Conca (1995a, 1995b, 1996, 1998), who study Bloch wave homogenization in media with moduli having variations on both microscopic and macroscopic length scales and make no assumptions about the size of the wavelengths relative to the microstructure.

Following Cherkaev and Gibiansky (1994) we will then show how these quasistatic equations can be transformed into a set of real equations with a symmetric positive-definite tensor entering the constitutive law. Subsequently we will see that in two dimensions complex electrical permittivity problems can be mapped to equivalent thermoelectric problems. Finally we will discuss the phenomena of resonance in composites.

11.1. Electromagnetic wave propagation in the quasistatic limit

Let us examine electromagnetic wave propagation in a sequence of three-dimensional periodic composite materials with successively smaller and smaller microstructures. We let the index η label the materials in the sequence. This index can be viewed as representing the size of the unit cell of periodicity. The index η will also be used to label the fields associated with each material in the sequence.

The relevant fields are the electric field $\boldsymbol{e}_\eta$, the electric displacement field $\boldsymbol{d}_\eta$, the magnetic field intensity $\boldsymbol{h}_\eta$, and the magnetic induction field $\boldsymbol{b}_\eta$. In the absence of any free unbound charges, these satisfy Maxwell's equations,

$$\begin{aligned} \nabla \cdot \boldsymbol{d}_\eta = 0, \qquad \nabla \cdot \boldsymbol{b}_\eta = 0, \\ \nabla \times \boldsymbol{e}_\eta + \frac{\partial \boldsymbol{b}_\eta}{\partial t} = 0, \qquad \nabla \times \boldsymbol{h}_\eta - \frac{\partial \boldsymbol{d}_\eta}{\partial t} = 0. \end{aligned} \tag{11.1}$$

The field $\boldsymbol{d}_\eta(\boldsymbol{x}, t)$, roughly speaking, measures the average displacement of the bound electrical charges from their equilibrium positions. Therefore its time derivative is associated with the motion of charges, that is, with the electrical current

$$\boldsymbol{j}_\eta = \frac{\partial \boldsymbol{d}_\eta}{\partial t}. \tag{11.2}$$

In a linear medium the constitutive relation between $\boldsymbol{d}_\eta$ and $\boldsymbol{e}_\eta$ is nonlocal in time and takes the form of an integral relation,

$$\boldsymbol{d}_\eta(\boldsymbol{x}, t) = \int_{-\infty}^{+\infty} d\boldsymbol{\nu}_\eta(\boldsymbol{x}, \tau)\boldsymbol{e}_\eta(\boldsymbol{x}, t - \tau), \tag{11.3}$$

where $d\boldsymbol{\nu}_\eta(\boldsymbol{x}, \tau)$ is a real symmetric, matrix-valued measure. This integral relation implies that the electric displacement field $\boldsymbol{d}_\eta$ depends on the value of the electric field not only at the present time, but also on its values at previous times. This makes good physical sense: The electric displacement field does not respond immediately to changes in the applied electric field because the electrical charges take some time to change their velocity due to their inertia. Of course the relation (11.3) must be compatible with the principle of causality, which says that $\boldsymbol{d}_\eta$ cannot be influenced by the values that $\boldsymbol{e}_\eta$ takes at times in the future. This imposes the constraint

$$d\boldsymbol{\nu}_\eta(\boldsymbol{x}, \tau) = 0, \qquad \text{for } \tau < 0.$$

Strictly speaking, the constitutive relation (11.3) is only an approximation to a more general constitutive relation that allows the dependence of $\boldsymbol{d}_\eta$ on $\boldsymbol{e}_\eta$ to be nonlocal both in time and in space. The use of (11.3) rather than the more general constitutive relation is justified provided that the spatial variation of $\boldsymbol{e}_\eta$ is large compared with the atomic scale.

Similarly, the relation between the induction field $\boldsymbol{b}_\eta$ and the magnetic field intensity $\boldsymbol{h}_\eta$ is governed by an integral relation,

$$\boldsymbol{b}_\eta(\boldsymbol{x}, t) = \int_{-\infty}^{+\infty} d\boldsymbol{\rho}_\eta(\boldsymbol{x}, \tau)\boldsymbol{h}_\eta(\boldsymbol{x}, t - \tau), \tag{11.4}$$

where the real symmetric, matrix-valued measure $d\boldsymbol{\rho}_\eta(\boldsymbol{x}, \tau)$ satisfies the constraint

$$d\boldsymbol{\rho}_\eta(\boldsymbol{x}, \tau) = 0, \qquad \text{for } \tau < 0,$$

implied by causality. Since the materials are periodic, the measures $d\boldsymbol{\nu}_\eta(\boldsymbol{x},\tau)$ and $d\boldsymbol{\rho}_\eta(\boldsymbol{x},\tau)$ are likewise periodic functions of $\boldsymbol{x}$. In accordance with the usual treatment of periodic homogenization, let us assume that each material in the sequence is similar, apart from a scale factor set by the parameter η; that is, let us assume that the dependence on η takes the simple form

$$d\boldsymbol{\nu}_\eta(\boldsymbol{x},\tau) = d\boldsymbol{\nu}(\boldsymbol{x}/\eta,\tau), \quad d\boldsymbol{\rho}_\eta(\boldsymbol{x},\tau) = d\boldsymbol{\rho}(\boldsymbol{x}/\eta,\tau), \tag{11.5}$$

where $d\boldsymbol{\nu}(\boldsymbol{y},\tau)$ and $d\boldsymbol{\rho}(\boldsymbol{y},\tau)$ are real matrix-valued measures that are periodic functions of $\boldsymbol{y}$. The periodicity in $\boldsymbol{y}$ implies that there exists a set of primitive lattice vectors $\boldsymbol{w}_i$, $i = 1, 2, \ldots, d$, such that

$$d\boldsymbol{\nu}(\boldsymbol{y}+\boldsymbol{w}_i,\tau) = d\boldsymbol{\nu}(\boldsymbol{y},\tau), \quad d\boldsymbol{\rho}(\boldsymbol{y}+\boldsymbol{w}_i,\tau) = d\boldsymbol{\rho}(\boldsymbol{y},\tau), \qquad \text{for all } \boldsymbol{y} \text{ and } i.$$

Let us now examine solutions of the field equations that correspond to Bloch waves of wavevector $\boldsymbol{k}$ and frequency ω, where the wavevector $\boldsymbol{k}$ is possibly complex. These are solutions of the forms

$$\begin{aligned}
\boldsymbol{e}_\eta(\boldsymbol{x},t) &= \mathrm{Re}[e^{i(\boldsymbol{k}\cdot\boldsymbol{x}-\omega t)}\hat{\boldsymbol{e}}_\eta(\boldsymbol{x})], \quad \boldsymbol{d}_\eta(\boldsymbol{x},t) = \mathrm{Re}[e^{i(\boldsymbol{k}\cdot\boldsymbol{x}-\omega t)}\hat{\boldsymbol{d}}_\eta(\boldsymbol{x})],\\
\boldsymbol{j}_\eta(\boldsymbol{x},t) &= \mathrm{Re}[e^{i(\boldsymbol{k}\cdot\boldsymbol{x}-\omega t)}\hat{\boldsymbol{j}}_\eta(\boldsymbol{x})],\\
\boldsymbol{h}_\eta(\boldsymbol{x},t) &= \mathrm{Re}[e^{i(\boldsymbol{k}\cdot\boldsymbol{x}-\omega t)}\hat{\boldsymbol{h}}_\eta(\boldsymbol{x})], \quad \boldsymbol{b}_\eta(\boldsymbol{x},t) = \mathrm{Re}[e^{i(\boldsymbol{k}\cdot\boldsymbol{x}-\omega t)}\hat{\boldsymbol{b}}_\eta(\boldsymbol{x})],
\end{aligned} \tag{11.6}$$

where $\mathrm{Re}(z)$ and $\mathrm{Im}(z)$ denote the real and imaginary parts of a complex quantity z, and where the complex-valued vector fields $\hat{\boldsymbol{e}}_\eta(\boldsymbol{x})$, $\hat{\boldsymbol{d}}_\eta(\boldsymbol{x})$, $\hat{\boldsymbol{h}}_\eta(\boldsymbol{x})$, and $\hat{\boldsymbol{b}}_\eta(\boldsymbol{x})$ have the same periodicity as the material constants,

$$\begin{aligned}
\hat{\boldsymbol{e}}_\eta(\boldsymbol{x}+\eta\boldsymbol{w}_i) &= \hat{\boldsymbol{e}}_\eta(\boldsymbol{x}), \quad \hat{\boldsymbol{d}}_\eta(\boldsymbol{x}+\eta\boldsymbol{w}_i) = \hat{\boldsymbol{d}}_\eta(\boldsymbol{x}), \quad \hat{\boldsymbol{j}}_\eta(\boldsymbol{x}+\eta\boldsymbol{w}_i) = \hat{\boldsymbol{j}}_\eta(\boldsymbol{x})\\
\hat{\boldsymbol{h}}_\eta(\boldsymbol{x}+\eta\boldsymbol{w}_i) &= \hat{\boldsymbol{h}}_\eta(\boldsymbol{x}), \quad \hat{\boldsymbol{b}}_\eta(\boldsymbol{x}+\eta\boldsymbol{w}_i) = \hat{\boldsymbol{b}}_\eta(\boldsymbol{x}).
\end{aligned}$$

Of course, the relation (11.2) implies that

$$\hat{\boldsymbol{j}}_\eta(\boldsymbol{x}) = -i\omega\hat{\boldsymbol{d}}_\eta(\boldsymbol{x}). \tag{11.7}$$

Crudely speaking, the Bloch wave solutions are periodic functions that have been modulated by solutions of the wave equation in a homogeneous material. The existence of such solutions is guaranteed by Bloch's theorem, which in the one-dimensional setting is known as Floquet's theorem. All other sufficiently regular solutions of the electromagnetic wave equations in a composite can be expressed as a linear combination of the Bloch wave solutions [see the original paper of Bloch (1928), the mathematical proofs of Gelfand (1950), Odeh and Keller (1964), and Wilcox (1978), and the books of Ashcroft and Mermin (1976) and Reed and Simon (1978)].

By substituting the expressions (11.6) into the field equations (11.1) we see that the complex fields satisfy

$$\begin{aligned}
\nabla\cdot[e^{i\boldsymbol{k}\cdot\boldsymbol{x}}\hat{\boldsymbol{d}}_\eta] = 0, \qquad & \nabla\cdot[e^{i\boldsymbol{k}\cdot\boldsymbol{x}}\hat{\boldsymbol{b}}_\eta] = 0,\\
\nabla\times[e^{i\boldsymbol{k}\cdot\boldsymbol{x}}\hat{\boldsymbol{e}}_\eta] - i\omega e^{i\boldsymbol{k}\cdot\boldsymbol{x}}\hat{\boldsymbol{b}}_\eta = 0, \quad & \nabla\times[e^{i\boldsymbol{k}\cdot\boldsymbol{x}}\hat{\boldsymbol{h}}_\eta] + i\omega e^{i\boldsymbol{k}\cdot\boldsymbol{x}}\hat{\boldsymbol{d}}_\eta = 0.
\end{aligned} \tag{11.8}$$

Furthermore, the constitutive relations (11.3) and (11.4) imply that

$$\hat{\boldsymbol{d}}_\eta(\boldsymbol{x}) = \boldsymbol{\varepsilon}_\eta(\boldsymbol{x},\omega)\hat{\boldsymbol{e}}_\eta(\boldsymbol{x}), \quad \hat{\boldsymbol{b}}_\eta(\boldsymbol{x}) = \boldsymbol{\mu}_\eta(\boldsymbol{x},\omega)\hat{\boldsymbol{h}}_\eta(\boldsymbol{x}), \tag{11.9}$$

where the tensors

$$\boldsymbol{\varepsilon}_\eta(\boldsymbol{x},\omega)=\int_{-\infty}^{\infty}e^{i\omega\tau}\,d\boldsymbol{\nu}_\eta(\boldsymbol{x},\tau),\qquad \boldsymbol{\mu}_\eta(\boldsymbol{x},\omega)=\int_{-\infty}^{\infty}e^{i\omega\tau}\,d\boldsymbol{\rho}_\eta(\boldsymbol{x},\tau) \tag{11.10}$$

are called the complex electrical permittivity tensor and complex magnetic permeability tensor of the medium, respectively. By dividing the complex electrical permittivity tensor by the electrical permittivity of free space one obtains the complex dielectric tensor of the medium. We will assume that our dimensions have been chosen so that the permittivity of free space is 1. Then there is no distinction between the permittivity tensor and the dielectric tensor, and we use the same symbol to denote both. From (11.7) one also has

$$\hat{\boldsymbol{j}}_\eta(\boldsymbol{x})=\boldsymbol{\sigma}_\eta(\boldsymbol{x},\omega)\hat{\boldsymbol{e}}_\eta(\boldsymbol{x}),\quad \text{where}\quad \boldsymbol{\sigma}_\eta(\boldsymbol{x},\omega)=-i\omega\boldsymbol{\varepsilon}_\eta(\boldsymbol{x},\omega), \tag{11.11}$$

which serves to define the complex conductivity tensor $\boldsymbol{\sigma}_\eta(\boldsymbol{x},\omega)$.

Within a homogeneous isotropic phase one has $\boldsymbol{\varepsilon}_\eta(\boldsymbol{x},\omega)=\varepsilon(\omega)\boldsymbol{I}$, where the complex dielectric constant $\varepsilon(\omega)$ depends on the material being studied. A typical model for the dependence of $\varepsilon(\omega)$ on frequency for ionic crystals and metals is the single oscillator model [see, for example, equation (7.129) in Jackson (1975)]:

$$\varepsilon(\omega)\approx\varepsilon_\infty+\frac{A}{\omega_r^2-\omega^2-i\omega\gamma}, \tag{11.12}$$

where A is determined by the oscillator strength, ω_r is the resonant frequency, γ is the damping constant, and ε_∞ is the high-frequency dielectric constant (at frequencies high compared with ω_r but low compared with other resonances that may be present at frequencies beyond the validity of the model; these other resonances influence the value of the constant ε_∞).

In a metal one has $\omega_r=0$ and the approximation reduces to the Drude model,

$$\varepsilon(\omega)\approx\varepsilon_\infty+\frac{i\sigma_0}{\omega(1-i\omega\tau)},$$

where $\sigma_0=A/\gamma$ is the electrical conductivity at $\omega=0$, ε_∞ represents the contribution to the dielectric constant from bound electrons, and $\tau=1/\gamma$ is a characteristic relaxation time. At very low frequencies the Drude model simplifies to $\varepsilon(\omega)\approx\varepsilon_\infty+i\sigma_0/\omega$.

In ionic crystals one can usually neglect γ for frequencies not close to ω_r and the approximation reduces to

$$\varepsilon(\omega)\approx\varepsilon_\infty+\frac{\varepsilon_0-\varepsilon_\infty}{1-\omega^2/\omega_r^2},$$

where ε_0 is the low-frequency dielectric constant (Ashcroft and Mermin 1976). These approximations break down at sufficiently high frequencies. For many substances, such as water, the single oscillator approximation is too crude: The dependence of $\varepsilon(\omega)$ on ω is quite complicated, with a rich spectrum of resonances.

According to (11.5), the dependence on η of the complex electrical permittivity tensor and complex magnetic permeability tensor takes the simple form

$$\boldsymbol{\varepsilon}_\eta(\boldsymbol{x},\omega)=\boldsymbol{\varepsilon}(\boldsymbol{x}/\eta,\omega),\quad \boldsymbol{\mu}_\eta(\boldsymbol{x},\omega)=\boldsymbol{\mu}(\boldsymbol{x}/\eta,\omega),$$

where

$$\boldsymbol{\varepsilon}(\boldsymbol{y},\omega)=\int_{-\infty}^{\infty}e^{i\omega\tau}\,d\boldsymbol{\nu}(\boldsymbol{y},\tau),\qquad \boldsymbol{\mu}(\boldsymbol{y},\omega)=\int_{-\infty}^{\infty}e^{i\omega\tau}\,d\boldsymbol{\rho}(\boldsymbol{y},\tau). \tag{11.13}$$

As the measures $d\boldsymbol{\nu}(\boldsymbol{y},\tau)$ and $d\boldsymbol{\rho}(\boldsymbol{y},\tau)$ vanish when $\tau < 0$, these integrals converge when $\mathrm{Im}(\omega) > 0$. Moreover, because $e^{i\omega\tau}$ is an analytic function of ω, it follows that for any value of $\boldsymbol{x}$ both $\boldsymbol{\varepsilon}_\eta(\boldsymbol{x},\omega)$ and $\boldsymbol{\mu}_\eta(\boldsymbol{x},\omega)$ are analytic functions of ω in the upper half ω-plane. Also, since the measures $d\boldsymbol{\nu}_\eta(\boldsymbol{x},\tau)$ and $d\boldsymbol{\rho}_\eta(\boldsymbol{x},\tau)$ are symmetric and real, (11.10) implies that the complex tensors satisfy

$$\begin{aligned} \boldsymbol{\varepsilon}_\eta(\boldsymbol{x},\omega)^T &= \boldsymbol{\varepsilon}_\eta(\boldsymbol{x},\omega), \qquad & \boldsymbol{\mu}_\eta(\boldsymbol{x},\omega)^T &= \boldsymbol{\mu}_\eta(\boldsymbol{x},\omega), \\ \boldsymbol{\varepsilon}_\eta(\boldsymbol{x},-\omega) &= \overline{\boldsymbol{\varepsilon}_\eta(\boldsymbol{x},\omega)}, & \boldsymbol{\mu}_\eta(\boldsymbol{x},-\omega) &= \overline{\boldsymbol{\mu}_\eta(\boldsymbol{x},\omega)}, \end{aligned} \tag{11.14}$$

where $\overline{z}$ denotes the complex conjugate of z.

The complex electrical permittivity tensor and complex magnetic permeability tensor satisfy an additional important physical restriction. Specifically, when the frequency ω is real and positive, their imaginary parts must be positive-semidefinite tensors, that is,

$$\boldsymbol{\varepsilon}''_\eta(\boldsymbol{x},\omega) \geq 0, \quad \boldsymbol{\mu}''_\eta(\boldsymbol{x},\omega) \geq 0 \quad \text{for all } \boldsymbol{x} \text{ and all real } \omega > 0, \tag{11.15}$$

in which $\boldsymbol{\varepsilon}''_\eta(\boldsymbol{x},\omega)$ and $\boldsymbol{\mu}''_\eta(\boldsymbol{x},\omega)$ denote the imaginary parts of the permittivity and permeability tensors,

$$\boldsymbol{\varepsilon}_\eta(\boldsymbol{x},\omega) = \boldsymbol{\varepsilon}'_\eta(\boldsymbol{x},\omega) + i\boldsymbol{\varepsilon}''_\eta(\boldsymbol{x},\omega), \quad \boldsymbol{\mu}_\eta(\boldsymbol{x},\omega) = \boldsymbol{\mu}'_\eta(\boldsymbol{x},\omega) + i\boldsymbol{\mu}''_\eta(\boldsymbol{x},\omega),$$

while $\boldsymbol{\varepsilon}'_\eta(\boldsymbol{x},\omega)$ and $\boldsymbol{\mu}'_\eta(\boldsymbol{x},\omega)$ denote their real parts. To see why these constraints arise we need to examine the average power dissipation, averaged over a cycle of oscillation.

At each point $\boldsymbol{x}$ the average electrical power dissipated into heat is

$$W(\boldsymbol{x}) = \frac{\omega}{2\pi}\int_0^{2\pi/\omega}\left[\boldsymbol{e}_\eta(\boldsymbol{x},t)\cdot\frac{\partial \boldsymbol{d}_\eta(\boldsymbol{x},t)}{\partial t} + \boldsymbol{h}_\eta(\boldsymbol{x},t)\cdot\frac{\partial \boldsymbol{b}_\eta(\boldsymbol{x},t)}{\partial t}\right]dt.$$

By substituting the expressions (11.6) into this formula and integrating the result over time we find that

$$\begin{aligned} W(\boldsymbol{x}) &= \frac{\omega}{2}e^{-2\,\mathrm{Im}(\boldsymbol{k}\cdot\boldsymbol{x})}[\mathrm{Re}(\hat{\boldsymbol{e}}_\eta)\cdot\mathrm{Im}(\hat{\boldsymbol{d}}_\eta) \;-\; \mathrm{Im}(\hat{\boldsymbol{e}}_\eta)\cdot\mathrm{Re}(\hat{\boldsymbol{d}}_\eta) \\ &\qquad + \mathrm{Re}(\hat{\boldsymbol{h}}_\eta)\cdot\mathrm{Im}(\hat{\boldsymbol{b}}_\eta) \;-\; \mathrm{Im}(\hat{\boldsymbol{h}}_\eta)\cdot\mathrm{Re}(\hat{\boldsymbol{b}}_\eta)] \\ &= \frac{\omega}{2}e^{-2\,\mathrm{Im}(\boldsymbol{k}\cdot\boldsymbol{x})}[\mathrm{Re}(\hat{\boldsymbol{e}}_\eta)\cdot\boldsymbol{\varepsilon}''_\eta\,\mathrm{Re}(\hat{\boldsymbol{e}}_\eta) \;+\; \mathrm{Im}(\hat{\boldsymbol{e}}_\eta)\cdot\boldsymbol{\varepsilon}''_\eta\,\mathrm{Im}(\hat{\boldsymbol{e}}_\eta) \\ &\qquad + \mathrm{Re}(\hat{\boldsymbol{h}}_\eta)\cdot\boldsymbol{\mu}''_\eta\,\mathrm{Re}(\hat{\boldsymbol{h}}_\eta) \;+\; \mathrm{Im}(\hat{\boldsymbol{h}}_\eta)\cdot\boldsymbol{\mu}''_\eta\,\mathrm{Im}(\hat{\boldsymbol{h}}_\eta)], \end{aligned} \tag{11.16}$$

where the last relation is obtained by using the fact, implied by (11.14), that $\boldsymbol{\varepsilon}'_\eta$ and $\boldsymbol{\mu}'_\eta$ are self-adjoint tensors. According to the second law of thermodynamics, the net power dissipation in the composite must necessarily be a nonnegative quantity. By examining (11.16) it is clear that the conditions (11.13) are necessary and sufficient to ensure the nonnegativity of $W(\boldsymbol{x})$ for all fields $\hat{\boldsymbol{e}}_\eta(\boldsymbol{x})$ and $\hat{\boldsymbol{h}}_\eta(\boldsymbol{x})$. When the frequency ω is real and negative, the relations (11.14) imply that $\boldsymbol{\varepsilon}''_\eta(\boldsymbol{x},\omega)$ and $\boldsymbol{\mu}''_\eta(\boldsymbol{x},\omega)$ are negative-semidefinite tensors. It then follows from (11.11) that the complex conductivity tensor $\boldsymbol{\sigma}_\eta(\boldsymbol{x},\omega)$ has a positive-semidefinite real part for all real ω.

At any given value of η and any fixed wavevector $\boldsymbol{k}$ the set of equations (11.8) and (11.9) will not have a solution unless ω takes one of a discrete set of values, that is, $\omega = \omega^j_\eta(\boldsymbol{k})$,

where the superscript $j = 1, 2 \ldots$ indexes each of the possible solution branches. The relation between ω and $\boldsymbol{k}$ is known as a dispersion relation. Let us examine what these Bloch wave solutions reduce to in the limit where the wavelength $\lambda = 2\pi/|\operatorname{Re}(\boldsymbol{k})|$ and attenuation length $\delta = 1/|\operatorname{Im}(\boldsymbol{k})|$ are much larger than the size of the unit cell of periodicity, that is, in the limit where $2\pi/|\boldsymbol{k}| \gg |\eta \boldsymbol{w}_i|$ for all i. This limit is called the quasistatic limit. To this end let us consider what equations the fields satisfy in the limit as $\eta \to 0$. Following the standard multiple-scale analysis, let us assume that the periodic complex fields have a perturbation expansion of the form

$$\begin{aligned}
\hat{\boldsymbol{e}}_\eta(\boldsymbol{x}) &= \hat{\boldsymbol{e}}_0(\boldsymbol{y}) + \eta\hat{\boldsymbol{e}}_1(\boldsymbol{y}) + \eta^2\hat{\boldsymbol{e}}_2(\boldsymbol{y}) + \cdots, \\
\hat{\boldsymbol{d}}_\eta(\boldsymbol{x}) &= \hat{\boldsymbol{d}}_0(\boldsymbol{y}) + \eta\hat{\boldsymbol{d}}_1(\boldsymbol{y}) + \eta^2\hat{\boldsymbol{d}}_2(\boldsymbol{y}) + \cdots, \\
\hat{\boldsymbol{h}}_\eta(\boldsymbol{x}) &= \hat{\boldsymbol{h}}_0(\boldsymbol{y}) + \eta\hat{\boldsymbol{h}}_1(\boldsymbol{y}) + \eta^2\hat{\boldsymbol{h}}_2(\boldsymbol{y}) + \cdots, \\
\hat{\boldsymbol{b}}_\eta(\boldsymbol{x}) &= \hat{\boldsymbol{b}}_0(\boldsymbol{y}) + \eta\hat{\boldsymbol{b}}_1(\boldsymbol{y}) + \eta^2\hat{\boldsymbol{b}}_2(\boldsymbol{y}) + \cdots,
\end{aligned} \tag{11.17}$$

where $\boldsymbol{y} = \boldsymbol{x}/\eta$, and $\hat{\boldsymbol{e}}_i(\boldsymbol{y})$, $\hat{\boldsymbol{d}}_i(\boldsymbol{y})$, $\hat{\boldsymbol{h}}_i(\boldsymbol{y})$, and $\hat{\boldsymbol{b}}_i(\boldsymbol{y})$, for $i = 0, 1, 2 \ldots$, are periodic functions of $\boldsymbol{y}$. Also let us assume that the dependence of $\omega = \omega_\eta^j(\boldsymbol{k})$ on η and $\boldsymbol{k}$ has an expansion of the form

$$\omega = \omega_\eta^j(\boldsymbol{k}) = \omega_0^j(\boldsymbol{k}) + \eta\omega_1^j(\boldsymbol{k}) + \eta^2\omega_2^j(\boldsymbol{k}) + \cdots. \tag{11.18}$$

Substituting these expansions into the field equations (11.8) and collecting terms of order η^{-1} gives the relations

$$\begin{aligned}
\nabla_y \cdot \hat{\boldsymbol{d}}_0(\boldsymbol{y}) = 0, \qquad \nabla_y \cdot \hat{\boldsymbol{b}}_0(\boldsymbol{y}) = 0, \\
\nabla_y \times \hat{\boldsymbol{e}}_0(\boldsymbol{y}) = 0, \qquad \nabla_y \times \hat{\boldsymbol{h}}_0(\boldsymbol{y}) = 0,
\end{aligned} \tag{11.19}$$

where ∇_y denotes the gradient with respect to the $\boldsymbol{y}$ variable. Continuing one step further and collecting terms of order η^0 gives the set of equations

$$\begin{aligned}
i\boldsymbol{k} \cdot \hat{\boldsymbol{d}}_0(\boldsymbol{y}) + \nabla_y \cdot \hat{\boldsymbol{d}}_1(\boldsymbol{y}) &= 0, \\
i\boldsymbol{k} \cdot \hat{\boldsymbol{b}}_0(\boldsymbol{y}) + \nabla_y \cdot \hat{\boldsymbol{b}}_1(\boldsymbol{y}) &= 0, \\
i\boldsymbol{k} \times \hat{\boldsymbol{e}}_0(\boldsymbol{y}) + \nabla_y \times \hat{\boldsymbol{e}}_1(\boldsymbol{y}) - i\omega_0^j\hat{\boldsymbol{b}}_0(\boldsymbol{y}) &= 0, \\
i\boldsymbol{k} \times \hat{\boldsymbol{h}}_0(\boldsymbol{y}) + \nabla_y \times \hat{\boldsymbol{h}}_1(\boldsymbol{y}) + i\omega_0^j\hat{\boldsymbol{d}}_0(\boldsymbol{y}) &= 0.
\end{aligned} \tag{11.20}$$

Since $\hat{\boldsymbol{d}}_1(\boldsymbol{y})$, $\hat{\boldsymbol{b}}_1(\boldsymbol{y})$, $\hat{\boldsymbol{e}}_1(\boldsymbol{y})$, and $\hat{\boldsymbol{h}}_1(\boldsymbol{y})$ are periodic functions of $\boldsymbol{y}$, it follows that

$$\begin{aligned}
\langle \nabla_y \cdot \hat{\boldsymbol{d}}_1 \rangle = 0, \qquad \langle \nabla_y \cdot \hat{\boldsymbol{b}}_1 \rangle = 0, \\
\langle \nabla_y \times \hat{\boldsymbol{e}}_1 \rangle = 0, \qquad \langle \nabla_y \times \hat{\boldsymbol{h}}_1 \rangle = 0.
\end{aligned}$$

So in order for the equations (11.20) to have a solution we necessarily must have

$$\boldsymbol{k} \cdot \langle \hat{\boldsymbol{d}}_0 \rangle = 0, \qquad \boldsymbol{k} \cdot \langle \hat{\boldsymbol{b}}_0 \rangle = 0, \tag{11.21}$$

$$\boldsymbol{k} \times \langle \hat{\boldsymbol{e}}_0 \rangle - \omega_0^j \langle \hat{\boldsymbol{b}}_0 \rangle = 0, \qquad \boldsymbol{k} \times \langle \hat{\boldsymbol{h}}_0 \rangle + \omega_0^j \langle \hat{\boldsymbol{d}}_0 \rangle = 0. \tag{11.22}$$

Amongst these equations we need only consider the latter pair as (11.21) is a direct consequence of (11.22). Finally, it is clear that substitution of the expansions (11.17) and (11.18) in the constitutive equations (11.9) leads to the relations

$$\hat{\boldsymbol{d}}_0(\boldsymbol{y}) = \boldsymbol{\varepsilon}(\boldsymbol{y}, \omega_0^j)\hat{\boldsymbol{e}}_0(\boldsymbol{y}), \qquad \hat{\boldsymbol{b}}_0(\boldsymbol{y}) = \boldsymbol{\mu}(\boldsymbol{y}, \omega_0^j)\hat{\boldsymbol{h}}_0(\boldsymbol{y}). \tag{11.23}$$

Notice that the field equations (11.19) *together with the constitutive equations* (11.23) *are exactly the same as the usual equations for conductivity in a composite medium, with the roles of* $\boldsymbol{j}(\boldsymbol{x})$, $\boldsymbol{e}(\boldsymbol{x})$, *and* $\boldsymbol{\sigma}(\boldsymbol{x})$ *replaced by* $\hat{\boldsymbol{d}}_0(\boldsymbol{y})$, $\hat{\boldsymbol{e}}_0(\boldsymbol{y})$, *and* $\boldsymbol{\varepsilon}(\boldsymbol{y}, \omega_0^j)$ *or alternatively replaced by* $\hat{\boldsymbol{b}}_0(\boldsymbol{y})$, $\hat{\boldsymbol{h}}_0(\boldsymbol{y})$, *and* $\boldsymbol{\mu}(\boldsymbol{y}, \omega_0^j)$. The only difference is that now the fields and material constants take complex values. So it is quite clear that solutions of the usual conductivity equations generalized to complex fields and complex conductivities have important applications to electromagnetic wave propagation in composite materials. In other words, the Bloch wave solutions reduce to solutions of the complex conductivity equations in the quasistatic limit. Associated with the complex dielectric tensor field $\boldsymbol{\varepsilon}(\boldsymbol{y}, \omega_0^j)$ will be a complex effective dielectric tensor $\boldsymbol{\varepsilon}_*(\omega_0^j)$, and associated with the complex magnetic permeability tensor field $\boldsymbol{\mu}(\boldsymbol{y}, \omega_0^j)$ will be a complex effective magnetic permeability tensor $\boldsymbol{\mu}_*(\omega_0^j)$. These are defined through the usual relations between the average fields,

$$\langle \hat{\boldsymbol{d}}_0 \rangle = \boldsymbol{\varepsilon}_*(\omega_0^j)\langle \hat{\boldsymbol{e}}_0 \rangle, \quad \langle \hat{\boldsymbol{b}}_0 \rangle = \boldsymbol{\mu}_*(\omega_0^j)\langle \hat{\boldsymbol{h}}_0 \rangle. \tag{11.24}$$

By substituting these relations back into (11.22) we see that

$$\boldsymbol{k} \times \langle \hat{\boldsymbol{e}}_0 \rangle - \omega_0^j \boldsymbol{\mu}_*(\omega_0^j)\langle \hat{\boldsymbol{h}}_0 \rangle = 0, \quad \boldsymbol{k} \times \langle \hat{\boldsymbol{h}}_0 \rangle + \omega_0^j \boldsymbol{\varepsilon}_*(\omega_0^j)\langle \hat{\boldsymbol{e}}_0 \rangle = 0,$$

and by eliminating $\langle \hat{\boldsymbol{h}}_0 \rangle$ we arrive at the equation

$$\boldsymbol{A}_*(\boldsymbol{k}, \omega_0^j)\langle \hat{\boldsymbol{e}}_0 \rangle = (\omega_0^j)^2 \langle \hat{\boldsymbol{e}}_0 \rangle, \tag{11.25}$$

where $\boldsymbol{A}_*(\boldsymbol{k}, \omega_0^j)$ is that matrix whose action on a given vector $\boldsymbol{v}$ is given by

$$\boldsymbol{A}_*(\boldsymbol{k}, \omega_0^j)\boldsymbol{v} = -[\boldsymbol{\varepsilon}_*(\omega_0^j)]^{-1}\{\boldsymbol{k} \times \{[\boldsymbol{\mu}_*(\omega_0^j)]^{-1}(\boldsymbol{k} \times \boldsymbol{v})\}\}. \tag{11.26}$$

From this equation we can determine the dispersion relation $\omega_0^j(\boldsymbol{k})$ and the possible values of $\langle \hat{\boldsymbol{e}}_0 \rangle$, and hence $\langle \hat{\boldsymbol{h}}_0 \rangle$, associated with each Bloch wave mode. In practice, for a given value of $\boldsymbol{k}$ it is necessary to plot the eigenvalues of $\boldsymbol{A}_*(\boldsymbol{k}, \omega_0^j)$ as a function of ω_0^j to find those frequencies ω_0^j where the eigenvalues take the value $(\omega_0^j)^2$. Notice that $\boldsymbol{A}_*(\boldsymbol{k}, \omega_0^j)$ has one trivial eigenvector, $\boldsymbol{v} = \boldsymbol{k}$, with a zero eigenvalue. So it is necessary to examine only the two remaining eigenvalues to see if either one equals $(\omega_0^j)^2$.

When either $\boldsymbol{\varepsilon}_*(\omega_0^j)$ or $\boldsymbol{\mu}_*(\omega_0^j)$ has a strictly positive-definite imaginary part, the dissipation of electromagnetic energy in the composite is necessarily positive [see equation (11.16)]. Consequently, any wave propagating into the material will be damped, that is, the attenuation length $\delta = 1/|\operatorname{Im}(\boldsymbol{k})|$ will be finite. In other words, if ω_0^j is real, then $\boldsymbol{k}$ will necessarily be complex. So to find solutions such that ω_0^j is real we would need to examine the eigenvalues of the matrix $\boldsymbol{A}_*(\boldsymbol{k}, \omega_0^j)$ for complex wavevectors $\boldsymbol{k}$.

In summary, in order to correspond to a Bloch solution of wavevector $\boldsymbol{k}$ and frequency ω_0^j the average field $\langle \hat{\boldsymbol{e}}_0 \rangle$ must be an eigenvector of the matrix $\boldsymbol{A}_*(\boldsymbol{k}, \omega_0^j)$, and $(\omega_0^j)^2$ must be the associated eigenvalue. More general quasistatic solutions of the Maxwell equations can be obtained by taking linear superpositions of these Bloch wave solutions.

As an example, let us consider electromagnetic wave propagation in a composite that is isotropic. In an isotropic composite medium the effective tensors take the forms

$$\boldsymbol{\varepsilon}_*(\omega_0^j) = \varepsilon_*(\omega_0^j)\boldsymbol{I}, \quad \boldsymbol{\mu}_*(\omega_0^j) = \mu_*(\omega_0^j)\boldsymbol{I}.$$

Let us further assume, for simplicity, that the moduli $\varepsilon_*(\omega_0^j)$ and $\mu_*(\omega_0^j)$ are real. Physically this implies that there is no dissipation of electromagnetic energy into heat, at least in the frequency range under consideration. With these assumptions the expression (11.26) reduces to

$$\boldsymbol{A}_*(\boldsymbol{k}, \omega_0^j)\boldsymbol{v} = [(\boldsymbol{k}\cdot\boldsymbol{k})\boldsymbol{v} - (\boldsymbol{k}\cdot\boldsymbol{v})\boldsymbol{k}]/[\varepsilon_*(\omega_0^j)\mu_*(\omega_0^j)].$$

So if we exclude the trivial solution with $\omega_0^j = 0$, (11.25) implies that

$$\boldsymbol{k}\cdot\langle\hat{\boldsymbol{e}}_0\rangle = 0, \quad (\omega_0^j)^2 = (\boldsymbol{k}\cdot\boldsymbol{k})/[\varepsilon_*(\omega_0^j)\mu_*(\omega_0^j)]. \tag{11.27}$$

If we assume that $\boldsymbol{k} = (2\pi/\lambda + i/\delta)\boldsymbol{n}$, where the wavelength λ and attenuation length δ are real and $\boldsymbol{n}$ is a real unit vector, then this latter relation implies that

$$2\pi/\lambda + i/\delta = \omega_0^j\sqrt{\varepsilon_*(\omega_0^j)\mu_*(\omega_0^j)}.$$

In other words, for a wave of a given frequency ω_0^j the complex dielectric constant $\varepsilon_*(\omega_0^j)$ and the complex magnetic permeability $\mu_*(\omega_0^j)$ determine the wavelength and attenuation length of the associated electromagnetic radiation in the quasistatic limit.

11.2. Electromagnetic signals can propagate faster in a composite than in the constituent phases

We saw in section 5.11 on page 88 that sound can propagate slower in a bubbly fluid than it propagates in either the fluid or in the air. Here we will see that for electromagnetic waves the opposite phenomena can occur: The speed at which a signal propagates in a two-phase composite can be faster than it propagates in either of the two phases (Sølna and Milton 2000, 2001). We assume that the composite is such that $\varepsilon_*(\omega_0^j)$ and $\mu_*(\omega_0^j)$ are both real and positive. Observe that the modulating factor $u(\boldsymbol{x}, t) = e^{i(\boldsymbol{k}\cdot\boldsymbol{x}-\omega t)}$ associated with the Bloch solution (11.6) is a plane wave solution to the scalar wave equation

$$\frac{\partial^2 u}{\partial t^2} = c_p^2\Delta u,$$

with a wave velocity

$$c_p = \omega/|\boldsymbol{k}|.$$

This in conjunction with (11.27) suggests that we can interpret $1/\sqrt{\varepsilon_*(\omega_0^j)\mu_*(\omega_0^j)}$ as the speed that electromagnetic waves of frequency ω_0^j propagate in an isotropic composite material. However, some caution must be exercised. We need to distinguish this velocity c_p, called the phase velocity, from the group velocity c_g, which determines the speed at which a wave packet can propagate. It is the group velocity that generally reflects the speed at which information can be propagated, and hence it is the group velocity that is the more physically meaningful quantity. A localized wave packet is a superposition of waves with a range of frequencies. A more detailed analysis, such as that given in section 7.8 of Jackson (1975), for example, shows that a wave packet comprised of waves with a distribution of frequencies sharply peaked around ω_0^j propagates at the group velocity

$$c_g = \left[\frac{d|\boldsymbol{k}|}{d\omega_0^j}\right]^{-1} = \left\{\frac{d}{d\omega_0^j}\left[\omega_0^j\sqrt{\varepsilon_*(\omega_0^j)\mu_*(\omega_0^j)}\right]\right\}^{-1}. \tag{11.28}$$

This is not the same as the phase velocity because of the dependence of $\varepsilon_*(\omega_0^j)$ and $\mu_*(\omega_0^j)$ on the frequency ω_0^j. The point to emphasize in this discussion is that the dispersion relation $\omega_0^j(\boldsymbol{k})$ is determined once we know the dependence of the effective parameters $\varepsilon_*(\omega_0^j)$ and $\mu_*(\omega_0^j)$ on frequency. Then from the dispersion relation we can compute the wavelength, phase velocity, and group velocity of waves of a given frequency ω_0^j.

To simplify notation, let us drop the superscript and subscript from ω_0^j. Also let us assume that the magnetic permeability $\boldsymbol{\mu}(\boldsymbol{y}, \omega)$ is independent of $\boldsymbol{y}$ and ω, taking a constant isotropic value $\mu \boldsymbol{I}$. The associated effective magnetic permeability will then be $\mu \boldsymbol{I}$ and (11.28) implies that

$$\frac{1}{c_g \sqrt{\mu}} = \sqrt{\varepsilon_*(\omega)} + \frac{\omega}{2\sqrt{\varepsilon_*(\omega)}} \frac{d\varepsilon_*(\omega)}{d\omega}. \tag{11.29}$$

Thus the group velocity depends on both the effective electrical permittivity and on its variation with frequency. The idea is that by combining a material with high permittivity but slow frequency variation with a material with low permittivity but high frequency variation one might obtain a composite that has comparatively low permittivity and comparatively slow frequency variation, having a faster group velocity than either phase.

We take two phases having the same frequency-independent magnetic permeability μ but different electrical permittivities,

$$\varepsilon_1 = 1/\Delta, \quad \varepsilon_2(\omega) = 1 + \frac{\sqrt{\Delta}}{1 - \omega^2},$$

where Δ is a sufficiently small fixed parameter. Thus phase 1 has a high frequency-independent dielectric constant $1/\Delta$ and the group velocity within phase 1 is $c_{g1} = \sqrt{\Delta/\mu}$. [Strictly speaking, we should modify $\varepsilon_1(\omega)$ at very high frequencies so that it approaches 1 as $\omega \to \infty$, but this is a minor technicality.] The functional form of $\varepsilon_2(\omega)$ is the standard Lorentzian model given by (11.12) with $\varepsilon_\infty = 1$ and $\gamma = 0$, that is, with no damping. Thus phase 2 has a dielectric constant that is close to 1 except in the near vicinity of the sharp resonance at $\omega^2 = 1$. We consider what happens near this resonance, in particular at the frequency $\omega = 1 - \sqrt{\Delta}$. At this frequency, in the limit when Δ is very small, we have

$$\varepsilon_2 \approx 1.5, \quad \frac{d\varepsilon_2}{d\omega} = \frac{2\omega\sqrt{\Delta}}{(1 - \omega^2)^2} \approx \frac{1}{2\sqrt{\Delta}},$$

and thus the group velocity within phase 2 is $c_{g2} \approx \sqrt{24\Delta/\mu}$.

Now consider an electromagnetic signal propagating through a laminate of these two phases, with phase 1 occupying a small volume fraction that we take to be $f_1 = \sqrt{\Delta}$. The direction of propagation is chosen to be normal to the layers. The electric field is then parallel to the layer boundaries and the effective dielectric constant in this direction is the arithmetic average

$$\varepsilon_* = f_1 \varepsilon_1 + (1 - f_1)\varepsilon_2 = 1/\sqrt{\Delta} + (1 - \sqrt{\Delta}) + \frac{(1 - \sqrt{\Delta})\sqrt{\Delta}}{1 - \omega^2}.$$

Therefore at the frequency $\omega = 1 - \sqrt{\Delta}$, in the limit when Δ is very small, we have

$$\varepsilon_* \approx \frac{1}{\sqrt{\Delta}}, \quad \frac{d\varepsilon_*}{d\omega} \approx \frac{1}{2\sqrt{\Delta}}.$$

Thus the group velocity within the composite is $c_g \approx 4\Delta^{1/4}/(5\sqrt{\mu})$, and when Δ is small this is much larger than the group velocities c_{g1} and c_{g2} in the two phases.

Bounds have been derived on the group velocity in isotropic and anisotropic two-phase composites and these bounds show that laminates, among all anisotropic composites, achieve the largest and smallest possible group velocities (Sølna and Milton 2001). To obtain a small, rather than a large, group velocity one can use the same phases but with phase 1 laminated with a small volume fraction of phase 2 and with the signal propagating parallel to the layer interfaces, polarized so that the electric field is normal to the layers. In this way one can achieve a group velocity c_g in the laminate that is much less than the group velocities c_{g1} and c_{g2} in the two phases.

11.3. Elastic wave propagation in the quasistatic limit

A similar analysis can be applied to the propagation of elastic waves in periodic composite materials in the quasistatic limit. Let us consider a sequence of periodic composites with successively smaller microstructures. Again we let the index η label each composite in this sequence. In the absence of body forces, the divergence of the stress field $\nabla \cdot \boldsymbol{\tau}_\eta(\boldsymbol{x}, t)$ determines the force acting on each element of the body and governs the resultant acceleration of that element through the equation of momentum conservation,

$$\varrho_\eta(\boldsymbol{x}) \frac{\partial^2 \boldsymbol{u}_\eta(\boldsymbol{x}, t)}{\partial t^2} = \nabla \cdot \boldsymbol{\tau}_\eta(\boldsymbol{x}, t), \tag{11.30}$$

in which $\varrho_\eta(\boldsymbol{x})$ represents the mass density of the body at the point $\boldsymbol{x}$ and $\boldsymbol{u}_\eta(\boldsymbol{x}, t)$ represents the displacement of the body at that point, which we are assuming is infinitesimal, in accordance with the standard theory of linearized elasticity. In linear viscoelastic media it is assumed that the stress field $\boldsymbol{\tau}_\eta(\boldsymbol{x}, t)$ depends on the strain field

$$\boldsymbol{\epsilon}_\eta(\boldsymbol{x}, t) = [\nabla \boldsymbol{u}_\eta(\boldsymbol{x}, t) + (\nabla \boldsymbol{u}_\eta(\boldsymbol{x}, t))^T]/2 \tag{11.31}$$

through the integral relation

$$\boldsymbol{\tau}(\boldsymbol{x}, t) = \int_{-\infty}^{+\infty} d\boldsymbol{\mathcal{K}}_\eta(\boldsymbol{x}, \tau) \boldsymbol{\epsilon}_\eta(\boldsymbol{x}, t - \tau), \tag{11.32}$$

in which $d\boldsymbol{\mathcal{K}}_\eta(\boldsymbol{x}, \tau)$ is a real fourth-order tensor valued measure with Cartesian elements $dK_\eta(\boldsymbol{x}, \tau)_{ijkl}$ satisfying the usual symmetries

$$dK_\eta(\boldsymbol{x}, \tau)_{ijkl} = dK_\eta(\boldsymbol{x}, \tau)_{ijlk} = dK_\eta(\boldsymbol{x}, \tau)_{klij} \tag{11.33}$$

of elasticity tensors, and satisfying the constraint

$$d\boldsymbol{\mathcal{K}}_\eta(\boldsymbol{x}, \tau) = 0 \text{ for } \tau < 0,$$

which is implied by causality.

This nonlocal time dependence of stress on strain or, equivalently, the nonlocal time dependence of strain on stress is most evident if we release a stretched piece of rubber. The rubber does not relax to its original length immediately, but instead takes some time to contract. Other materials also exhibit this property, but the relaxation time is usually much shorter or much longer and less noticeable. The books of Lakes (1999) and Christensen (1971) provide good introductions to the theory of viscoelasticity.

We again assume that each composite material in the sequence is similar, apart from a scale factor set by the parameter η. Specifically we assume that the dependence of $d\mathcal{K}_\eta(\boldsymbol{x}, \tau)$ on η has the simple form

$$d\mathcal{K}_\eta(\boldsymbol{x}, \tau) = d\mathcal{K}(\boldsymbol{x}/\eta, \tau), \tag{11.34}$$

where $d\mathcal{K}(\boldsymbol{y}, \tau)$ is a real fourth-order tensor valued measure that is periodic in $\boldsymbol{y} = \boldsymbol{x}/\eta$. We also assume that the mass density $\varrho_\eta(\boldsymbol{x})$ has a similar dependence on η,

$$\varrho_\eta(\boldsymbol{x}) = \varrho(\boldsymbol{x}/\eta).$$

The solutions of these elastodynamic equations that correspond to Bloch waves of wavevector $\boldsymbol{k}$ and frequency ω take the forms,

$$\begin{aligned}
\boldsymbol{\tau}_\eta(\boldsymbol{x}, t) &= \mathrm{Re}[e^{i(\boldsymbol{k}\cdot\boldsymbol{x}-\omega t)}\hat{\boldsymbol{\tau}}_\eta(\boldsymbol{x})],\\
\boldsymbol{u}_\eta(\boldsymbol{x}, t) &= \mathrm{Re}[e^{i(\boldsymbol{k}\cdot\boldsymbol{x}-\omega t)}\hat{\boldsymbol{u}}_\eta(\boldsymbol{x})],\\
\boldsymbol{\epsilon}_\eta(\boldsymbol{x}, t) &= \mathrm{Re}[e^{i(\boldsymbol{k}\cdot\boldsymbol{x}-\omega t)}\hat{\boldsymbol{\epsilon}}_\eta(\boldsymbol{x})],
\end{aligned} \tag{11.35}$$

where the fields $\hat{\boldsymbol{\tau}}_\eta(\boldsymbol{x})$, $\hat{\boldsymbol{u}}_\eta(\boldsymbol{x})$, and $\hat{\boldsymbol{\epsilon}}_\eta(\boldsymbol{x})$ have the same periodicity as the material constants and satisfy the equations

$$\begin{aligned}
0 &= \nabla\cdot(e^{i\boldsymbol{k}\cdot\boldsymbol{x}}\hat{\boldsymbol{\tau}}_\eta) + \omega^2\varrho_\eta e^{i\boldsymbol{k}\cdot\boldsymbol{x}}\hat{\boldsymbol{u}}_\eta,\\
e^{i\boldsymbol{k}\cdot\boldsymbol{x}}\hat{\boldsymbol{\epsilon}}_\eta &= \{\nabla(e^{i\boldsymbol{k}\cdot\boldsymbol{x}}\hat{\boldsymbol{u}}_\eta) + [\nabla(e^{i\boldsymbol{k}\cdot\boldsymbol{x}}\hat{\boldsymbol{u}}_\eta)]^T\}/2,\\
\hat{\boldsymbol{\tau}}_\eta(\boldsymbol{x}) &= \boldsymbol{\mathcal{C}}_\eta(\boldsymbol{x}, \omega)\hat{\boldsymbol{\epsilon}}_\eta(\boldsymbol{x}),
\end{aligned} \tag{11.36}$$

which are implied by (11.30), (11.31), and (11.32), in which

$$\boldsymbol{\mathcal{C}}_\eta(\boldsymbol{x}, \omega) = \int_{-\infty}^{\infty} e^{i\omega\tau}\, d\mathcal{K}_\eta(\boldsymbol{x}, \tau).$$

This tensor is called the complex elasticity tensor, and (11.34) implies that its dependence on η is given by

$$\boldsymbol{\mathcal{C}}_\eta(\boldsymbol{x}, \omega) = \boldsymbol{\mathcal{C}}(\boldsymbol{x}/\eta, \omega),$$

in which $\boldsymbol{\mathcal{C}}(\boldsymbol{y}, \omega)$ is the periodic fourth-order tensor field

$$\boldsymbol{\mathcal{C}}(\boldsymbol{y}, \omega) = \int_{-\infty}^{\infty} e^{-i\omega\tau}\, d\mathcal{K}(\boldsymbol{y}, \tau).$$

Since the measures $dK_\eta(\boldsymbol{x}, \tau)$ are real, satisfying the symmetry properties (11.33), it follows that the complex elasticity tensors satisfy

$$\boldsymbol{\mathcal{C}}_\eta(\boldsymbol{x}, \omega)_{ijkl} = \boldsymbol{\mathcal{C}}_\eta(\boldsymbol{x}, \tau)_{ijlk} = \boldsymbol{\mathcal{C}}_\eta(\boldsymbol{x}, \tau)_{klij}, \qquad \boldsymbol{\mathcal{C}}_\eta(\boldsymbol{x}, -\omega) = \overline{\boldsymbol{\mathcal{C}}_\eta(\boldsymbol{x}, \omega)}. \tag{11.37}$$

In addition, physical considerations imply that when the frequency ω is real and positive the complex elasticity tensor must have a negative-semidefinite imaginary part,

$$\boldsymbol{\mathcal{C}}''_\eta(\boldsymbol{x}, \omega) \le 0 \quad \text{for all } \boldsymbol{x} \text{ and all real } \omega > 0, \tag{11.38}$$

where $\boldsymbol{\mathcal{C}}''_\eta(\boldsymbol{x}, \omega)$ denotes the imaginary part of the elasticity tensor

$$\boldsymbol{\mathcal{C}}_\eta(\boldsymbol{x}, \omega) = \boldsymbol{\mathcal{C}}'_\eta(\boldsymbol{x}, \omega) + i\boldsymbol{\mathcal{C}}''_\eta(\boldsymbol{x}, \omega),$$

while $\mathcal{C}'_\eta(\boldsymbol{x},\omega)$ denotes its real part. Indeed, in one cycle of oscillation, the elastic forces do an average amount of mechanical work,

$$W(\boldsymbol{x}) = \frac{\omega}{2\pi}\int_0^{2\pi/\omega}\left[\boldsymbol{\tau}_\eta(\boldsymbol{x},t)\cdot\frac{\partial\boldsymbol{\epsilon}_\eta(\boldsymbol{x},t)}{\partial t}\right]dt. \tag{11.39}$$

Since the body is in the same state at the end of a cycle as it was in at the beginning of the cycle, this mechanical work must be dissipated into heat. It follows from the second law of thermodynamics that this heat dissipation $W(\boldsymbol{x})$ must always be a positive quantity. By substituting (11.35) into (11.39) and using the symmetry properties (11.37) we see that

$$\begin{aligned} W(\boldsymbol{x}) &= \frac{\omega}{2}e^{-2\,\mathrm{Im}(\boldsymbol{k}\cdot\boldsymbol{x})}\left[\mathrm{Re}(\hat{\boldsymbol{\tau}}_\eta)\cdot\mathrm{Im}(\hat{\boldsymbol{\epsilon}}_\eta) - \mathrm{Im}(\hat{\boldsymbol{\tau}}_\eta)\cdot\mathrm{Re}(\hat{\boldsymbol{\epsilon}}_\eta)\right] \\ &= -\frac{\omega}{2}e^{-2\,\mathrm{Im}(\boldsymbol{k}\cdot\boldsymbol{x})}\left[\mathrm{Re}(\hat{\boldsymbol{\epsilon}}_\eta)\cdot\boldsymbol{\mathcal{C}}''_\eta\,\mathrm{Re}(\hat{\boldsymbol{\epsilon}}_\eta) + \mathrm{Im}(\hat{\boldsymbol{\epsilon}}_\eta)\cdot\boldsymbol{\mathcal{C}}''_\eta\,\mathrm{Im}(\hat{\boldsymbol{\epsilon}}_\eta)\right]. \end{aligned}$$

From this expression it is clear that the condition (11.38) is necessary and sufficient to ensure the nonnegativity of $W(\boldsymbol{x})$ for all fields $\hat{\boldsymbol{\epsilon}}_\eta(\boldsymbol{x})$.

The Bloch wave equations have a solution provided that the frequency ω takes one of a discrete set of values, $\omega_\eta^j(\boldsymbol{k})$, $j = 1, 2, \ldots$. Following the same approach as before, we assume that the fields have a perturbation expansion in powers of η,

$$\begin{aligned} \hat{\boldsymbol{\tau}}_\eta(\boldsymbol{x}) &= \hat{\boldsymbol{\tau}}_0(\boldsymbol{y}) + \eta\hat{\boldsymbol{\tau}}_1(\boldsymbol{y}) + \cdots, \\ \hat{\boldsymbol{u}}_\eta(\boldsymbol{x}) &= \hat{\boldsymbol{u}}_0(\boldsymbol{y}) + \eta\hat{\boldsymbol{u}}_1(\boldsymbol{y}) + \cdots, \\ \hat{\boldsymbol{\epsilon}}_\eta(\boldsymbol{x}) &= \hat{\boldsymbol{\epsilon}}_0(\boldsymbol{y}) + \eta\hat{\boldsymbol{\epsilon}}_1(\boldsymbol{y}) + \cdots, \end{aligned}$$

in which $\boldsymbol{y} = \boldsymbol{x}/\eta$, and $\hat{\boldsymbol{\tau}}_i(\boldsymbol{y})$, $\hat{\boldsymbol{u}}_i(\boldsymbol{y})$, and $\hat{\boldsymbol{\epsilon}}_i(\boldsymbol{y})$, for $i = 0, 1, 2, \ldots$, are periodic functions of $\boldsymbol{y}$. We also assume that the dependence of the frequency $\omega = \omega_\eta^j(\boldsymbol{k})$ on η has an expansion

$$\omega = \omega_\eta(\boldsymbol{k}) = \omega_\eta^j(\boldsymbol{k}) = \omega_0^j(\boldsymbol{k}) + \eta\omega_1^j(\boldsymbol{k}) + \cdots.$$

Substitution of these expansions back in the field equations (11.36) and collecting terms of order η^{-1} and of order η^0 yields the equations

$$\nabla_y\hat{\boldsymbol{u}}_0(\boldsymbol{y}) = 0, \tag{11.40}$$

$$\nabla_y\cdot\hat{\boldsymbol{\tau}}_0(\boldsymbol{y}) = 0, \tag{11.41}$$

$$\hat{\boldsymbol{\epsilon}}_0(\boldsymbol{y}) = \{i\boldsymbol{k}\otimes\hat{\boldsymbol{u}}_0 + \nabla_y\hat{\boldsymbol{u}}_1(\boldsymbol{y}) + [i\boldsymbol{k}\otimes\hat{\boldsymbol{u}}_0 + \nabla_y\hat{\boldsymbol{u}}_1(\boldsymbol{y})]^T\}/2, \tag{11.42}$$

$$\hat{\boldsymbol{\tau}}_0(\boldsymbol{y}) = \boldsymbol{\mathcal{C}}(\boldsymbol{y},\omega_0^j)\hat{\boldsymbol{\epsilon}}_0(\boldsymbol{y}), \tag{11.43}$$

$$i\boldsymbol{k}\cdot\hat{\boldsymbol{\tau}}_0(\boldsymbol{y}) + \nabla_y\cdot\hat{\boldsymbol{\tau}}_1(\boldsymbol{y}) + (\omega_0^j)^2\varrho(\boldsymbol{y})\hat{\boldsymbol{u}}_0 = 0. \tag{11.44}$$

The first equation (11.40) implies that $\hat{\boldsymbol{u}}_0(\boldsymbol{y})$ is a linear function of $\boldsymbol{y}$ and, since $\hat{\boldsymbol{u}}_0(\boldsymbol{y})$ is periodic in $\boldsymbol{y}$, it forces

$$\hat{\boldsymbol{u}}_0(\boldsymbol{y}) = \hat{\boldsymbol{u}}_0 = \text{ a constant.} \tag{11.45}$$

For this reason the dependence on $\boldsymbol{y}$ of $\hat{\boldsymbol{u}}_0(\boldsymbol{y})$ has been deleted from the subsequent equations (11.41)–(11.44).

Next note that by using (11.45) we can rewrite (11.42) in the form

$$\hat{\boldsymbol{\epsilon}}_0(\boldsymbol{y}) = \{\nabla_y\underline{\hat{\boldsymbol{u}}}(\boldsymbol{y}) + [\nabla_y\underline{\hat{\boldsymbol{u}}}(\boldsymbol{y})]^T\}/2, \tag{11.46}$$

with

$$\underline{\hat{\boldsymbol{u}}}(\boldsymbol{y}) = i(\boldsymbol{k}\cdot\boldsymbol{y})\hat{\boldsymbol{u}}_0 + \hat{\boldsymbol{u}}_1(\boldsymbol{y}).$$

Clearly (11.41), (11.43), and (11.46) are exactly the same as the usual static equations of elasticity in a composite material, except that now the fields and elastic tensor are complex. The complex effective elasticity tensor $\boldsymbol{\mathcal{C}}_*(\omega_0^j)$, by definition, links the volume averaged fields $\langle\hat{\boldsymbol{\tau}}_0\rangle$ and $\langle\hat{\boldsymbol{\epsilon}}_0\rangle$ through the equation

$$\langle\hat{\boldsymbol{\tau}}_0\rangle = \boldsymbol{\mathcal{C}}_*(\omega_0^j)\langle\hat{\boldsymbol{\epsilon}}_0\rangle. \tag{11.47}$$

By taking averages of (11.42) and (11.44) over the volume of the unit cell of periodicity we obtain the additional relations

$$\langle\hat{\boldsymbol{\epsilon}}_0\rangle = (i\boldsymbol{k}\otimes\hat{\boldsymbol{u}}_0 + i\hat{\boldsymbol{u}}_0\otimes\boldsymbol{k})/2, \qquad i\boldsymbol{k}\cdot\langle\hat{\boldsymbol{\tau}}_0\rangle + (\omega_0^j)^2\langle\varrho\rangle\hat{\boldsymbol{u}}_0 = 0. \tag{11.48}$$

In contrast to the static equations of elasticity, where no restriction is imposed on the average strain field, we see that in the Bloch elastodynamic solutions the field $\langle\hat{\boldsymbol{\epsilon}}_0\rangle$ is necessarily a rank-1 or a rank-2 tensor. Furthermore, by combining (11.47) with (11.48) we obtain

$$\boldsymbol{A}_*(\boldsymbol{k},\omega_0^j)\hat{\boldsymbol{u}}_0 = (\omega_0^j)^2\hat{\boldsymbol{u}}_0,$$

where $\boldsymbol{A}_*(\boldsymbol{k},\omega_0^j)$ is the matrix whose action on a vector $\boldsymbol{v}$ is given by

$$\boldsymbol{A}_*(\boldsymbol{k},\omega_0^j)\boldsymbol{v} = \{\boldsymbol{k}\cdot[\boldsymbol{\mathcal{C}}_*(\omega_0^j)\boldsymbol{k}\otimes\boldsymbol{v}]\}/\langle\varrho\rangle.$$

This equation gives us the dispersion relation $\omega_0^j(\boldsymbol{k})$, found by computing the eigenvalues of the matrix $\boldsymbol{A}_*(\boldsymbol{k},\omega_0^j)$ as a function of frequency ω_0^j and locating those frequencies where an eigenvalue takes the value $(\omega_0^j)^2$. The associated eigenvector gives the value of $\hat{\boldsymbol{u}}_0$ associated with that Bloch wave mode. Notice that $\langle\varrho\rangle\boldsymbol{A}_*(\boldsymbol{k},\omega_0^j)$ depends only on $\boldsymbol{k}\cdot\boldsymbol{\mathcal{C}}_*(\omega_0^j)\boldsymbol{k}$, that is, on the effective acoustic tensor.

11.4. The correspondence principle and the attenuation of sound in a bubbly fluid

We have seen that in the quasistatic limit the Bloch solutions of electrodynamics and elastodynamics satisfy equations directly analogous to the usual conductivity or elasticity equations but with complex fields and complex tensors. In this context the effective tensors play an important role since they determine the dispersion relation $\omega_0^j(\boldsymbol{k})$ and hence the phase and group velocities. In chapter 18 on page 369 we will prove that in an n component composite the dependence of the effective tensor on the local component tensors is analytic. This means that if we have a formula for the effective tensor as a function of the component tensors, valid when the component tensors are real, then by analytic continuation we can use the same formula when the component tensors take complex values. This is called the correspondence principle [see, for example, Hashin (1965) and Christensen (1979)]. It implies, for instance, that the complex permittivity $\varepsilon_*(\omega_0^j)$ of a checkerboard structure is $\sqrt{\varepsilon_1(\omega_0^j)\varepsilon_2(\omega_0^j)}$ when the two component phases have complex permittivities $\varepsilon_1(\omega_0^j)$ and $\varepsilon_2(\omega_0^j)$.

As another example, consider an assemblage of coated spheres of phase 1 in a matrix of phase 2. When the bulk and shear moduli of the two phases are real it has an effective bulk modulus κ_* that is given by (7.13). By the correspondence principle this formula should

also be valid when the moduli are complex. In particular, suppose that phase 1 is gas while phase 2 is water, so that the assemblage is a bubbly fluid. Then the water can be treated as incompressible and in the limit $\kappa_2 \to \infty$ (7.13) reduces to

$$\kappa_* \approx \frac{\kappa_1 + 4f_2\mu_2/3}{f_1}. \tag{11.49}$$

To a good approximation the complex bulk modulus κ_1 of the air is independent of frequency. Now consider a plane shear wave propagating into water at a real frequency ω and being spatially attenuated with a complex wavevector $\boldsymbol{k}$. The associated strain and stress fields are given by

$$\boldsymbol{\epsilon}(t) = \mathrm{Re}[e^{i\boldsymbol{k}\cdot\boldsymbol{x}-\omega t}\hat{\boldsymbol{\epsilon}}], \quad \boldsymbol{\tau}(t) = \eta_\mu \frac{d\boldsymbol{\epsilon}(t)}{dt} = \mathrm{Re}[-i\omega\eta_\mu e^{i\boldsymbol{k}\cdot\boldsymbol{x}-\omega t}\hat{\boldsymbol{\epsilon}}],$$

where $\hat{\boldsymbol{\epsilon}}$ is a constant trace free matrix and η_μ is the shear viscosity of the water, which we assume to be frequency-independent (which is reasonable at sufficiently low frequencies). We deduce from this relation that water has a complex shear modulus $\mu_2 = -i\omega\eta_\mu$. Substituting this into (11.49) gives

$$\kappa_* \approx \kappa_1/f_1 - i\eta_\kappa^*\omega, \quad \text{where } \eta_\kappa^* \approx 4f_2\eta_\mu/(3f_1).$$

In particular, when the volume fraction occupied by the gas is small, the bulk viscosity η_κ^* of the bubbly fluid approaches $4\eta_\mu/(3f_1)$, which is the result of Taylor (1954). Thus the shear viscosity of the water has been converted to the bulk viscosity of the bubbly fluid. This explains why sound is so strongly damped in bubbly fluids, as was mentioned in section 1.2 on page 2. Of course in a real bubbly fluid the bubbles are unlikely to have a very wide distribution of sizes, and therefore the coated sphere assemblage is not realistic. Nevertheless, formula (11.49) should be a reasonable approximation for κ_*, provided that the volume fraction is not too large and not too small. At large volume fractions the bubbles interact through the fields surrounding them, they oscillate nonradially, there are pressure gradients inside the bubbles, and there is a drift between the bubbles and the water (Caflisch, Miksis, Papanicolaou, and Ting 1985b). At very small volume fractions the compressibility of the water and nonlinear effects come into play and the formula has to be modified (Taylor 1954; Van Wijngaarden 1968, 1972; Caflisch, Miksis, Papanicolaou, and Ting 1985a).

11.5. Transformation to real equations

Despite the obvious advantages for keeping the equations in complex form, where the correspondence principle can be directly applied, there are important reasons for desiring to transform the equations to an alternative form where the tensor that enters the constitutive law is real, symmetric, and positive-definite. Such a transformation of the equations was found by Cherkaev and Gibiansky (1994). They used it to develop variational principles for the complex effective tensor, which as we will see in sections 22.6 on page 450 and 23.7 on page 476 are useful for deriving bounds.

Consider, for example, the equations

$$\boldsymbol{d}(\boldsymbol{x}) = \boldsymbol{\varepsilon}(\boldsymbol{x})\boldsymbol{e}(\boldsymbol{x}), \quad \nabla\cdot\boldsymbol{d} = 0, \quad \nabla\times\boldsymbol{e} = 0, \tag{11.50}$$

which determine the effective complex permittivity tensor $\boldsymbol{\varepsilon}_*$ through the relation between the average fields

$$\langle\boldsymbol{d}\rangle = \boldsymbol{\varepsilon}_*\langle\boldsymbol{e}\rangle. \tag{11.51}$$

These are the same as equations (11.19), (11.23), and (11.24), except that to avoid cumbersome notation we have dropped the hat and subscript 0 from the fields, replaced $\boldsymbol{y}$ by $\boldsymbol{x}$, and suppressed the dependence of $\boldsymbol{\varepsilon}(\boldsymbol{x})$ and ε_* on the frequency ω.

Let us replace the constraint (11.15) by the slightly more stringent assumption that $\boldsymbol{\varepsilon}''(\boldsymbol{x})$ is bounded and coercive for all $\boldsymbol{x}$, that is, there exist constants α and β such that

$$\alpha \boldsymbol{I} > \boldsymbol{\varepsilon}''(\boldsymbol{x}) > \beta \boldsymbol{I} > 0, \quad \text{for all } \boldsymbol{x}. \tag{11.52}$$

This assumption is not as restrictive as it may seem. If the fields $\boldsymbol{d}(\boldsymbol{x})$ and $\boldsymbol{e}(\boldsymbol{x})$ solve the above set of equations with a permittivity tensor $\boldsymbol{\varepsilon}(\boldsymbol{x})$, then for any constant λ the fields $\lambda \boldsymbol{d}(\boldsymbol{x})$ and $\boldsymbol{e}(\boldsymbol{x})$ will solve the same set of equations when $\boldsymbol{\varepsilon}(\boldsymbol{x})$ is replaced by the permittivity tensor field $\lambda \boldsymbol{\varepsilon}(\boldsymbol{x})$. It follows, by taking $\lambda = e^{i\theta}$, that we are free to shift the phase of the tensor field $\boldsymbol{\varepsilon}(\boldsymbol{x})$. In other words, (11.52) can be replaced by the less restrictive assumption that there exists an angle θ and constants α and β such that

$$\alpha \boldsymbol{I} > \operatorname{Im}[e^{i\theta} \boldsymbol{\varepsilon}(\boldsymbol{x})] > \beta \boldsymbol{I} > 0, \quad \text{for all } \boldsymbol{x}.$$

For example, by this trick one can consider materials where $\boldsymbol{\varepsilon}(\boldsymbol{x})$ is real within one or more phases.

Taking the real and imaginary parts of the equations (11.50) gives

$$\begin{pmatrix} \operatorname{Re}(\boldsymbol{d}) \\ \operatorname{Im}(\boldsymbol{d}) \end{pmatrix} = \begin{pmatrix} -\varepsilon'' & \varepsilon' \\ \varepsilon' & \varepsilon'' \end{pmatrix} \begin{pmatrix} \operatorname{Im}(\boldsymbol{e}) \\ \operatorname{Re}(\boldsymbol{e}) \end{pmatrix}, \quad \begin{array}{ll} \nabla \cdot \operatorname{Re}(\boldsymbol{d}) = 0, & \nabla \times \operatorname{Re}(\boldsymbol{e}) = 0, \\ \nabla \cdot \operatorname{Im}(\boldsymbol{d}) = 0, & \nabla \times \operatorname{Im}(\boldsymbol{e}) = 0. \end{array} \tag{11.53}$$

Written in this form the constitutive relation incorporates a tensor that is symmetric but not positive-definite. Indeed, in view of (11.52), the associated quadratic form

$$f(\operatorname{Im}(\boldsymbol{e}), \operatorname{Re}(\boldsymbol{e})) = \begin{pmatrix} \operatorname{Im}(\boldsymbol{e}) \\ \operatorname{Re}(\boldsymbol{e}) \end{pmatrix} \cdot \begin{pmatrix} -\varepsilon'' & \varepsilon' \\ \varepsilon' & \varepsilon'' \end{pmatrix} \begin{pmatrix} \operatorname{Im}(\boldsymbol{e}) \\ \operatorname{Re}(\boldsymbol{e}) \end{pmatrix} \tag{11.54}$$

takes negative values when $\operatorname{Im}(\boldsymbol{e}) \neq 0$ and $\operatorname{Re}(\boldsymbol{e}) = 0$, and takes positive values when $\operatorname{Im}(\boldsymbol{e}) = 0$ and $\operatorname{Re}(\boldsymbol{e}) \neq 0$. Nevertheless, $f(\operatorname{Im}(\boldsymbol{e}), \operatorname{Re}(\boldsymbol{e}))$ is closely related to a quantity that is strictly positive. To see this notice from (11.54) and (11.53) that

$$f(\operatorname{Im}(\boldsymbol{e}), \operatorname{Re}(\boldsymbol{e})) = \begin{pmatrix} \operatorname{Im}(\boldsymbol{e}) \\ \operatorname{Re}(\boldsymbol{e}) \end{pmatrix} \cdot \begin{pmatrix} \operatorname{Re}(\boldsymbol{d}) \\ \operatorname{Im}(\boldsymbol{d}) \end{pmatrix} = \operatorname{Im}(\boldsymbol{e}) \cdot \operatorname{Re}(\boldsymbol{d}) + \operatorname{Re}(\boldsymbol{e}) \cdot \operatorname{Im}(\boldsymbol{d}). \tag{11.55}$$

Although this quantity is not positive, (11.16) and (11.52) imply that

$$-\operatorname{Re}(\boldsymbol{d}) \cdot \operatorname{Im}(\boldsymbol{e}) + \operatorname{Re}(\boldsymbol{e}) \cdot \operatorname{Im}(\boldsymbol{d}) = \operatorname{Re}(\boldsymbol{e}) \cdot \boldsymbol{\varepsilon}'' \operatorname{Re}(\boldsymbol{e}) + \operatorname{Im}(\boldsymbol{e}) \cdot \boldsymbol{\varepsilon}'' \operatorname{Im}(\boldsymbol{e}) \geq 0. \tag{11.56}$$

A comparison of (11.55) and (11.56) suggests that we might try rewriting the constitutive law in the form

$$\begin{pmatrix} \operatorname{Im}(\boldsymbol{e}) \\ \operatorname{Im}(\boldsymbol{d}) \end{pmatrix} = \boldsymbol{\mathcal{L}} \begin{pmatrix} -\operatorname{Re}(\boldsymbol{d}) \\ \operatorname{Re}(\boldsymbol{e}) \end{pmatrix}, \tag{11.57}$$

where the role of $\operatorname{Im}(\boldsymbol{e})$ is replaced by that of its dual field, $-\operatorname{Re}(\boldsymbol{d})$, and the role of $\operatorname{Re}(\boldsymbol{d})$ is replaced by that of the dual field $\operatorname{Im}(\boldsymbol{e})$. [This is a natural transformation to make because the quadratic form associated with $\boldsymbol{\mathcal{L}}$ is a partial Legendre transform of the saddle-shaped quadratic function $f(\operatorname{Im}(\boldsymbol{e}), \operatorname{Re}(\boldsymbol{e}))$ and it is well-known that such partial Legendre

transforms convert saddle-shaped functions into convex functions; see, for example, Callen (1960).] It remains to find the tensor $\boldsymbol{\mathcal{L}}$. The constitutive law in (11.53) implies that

$$\begin{aligned}\operatorname{Im}(\boldsymbol{e}) &= -[\boldsymbol{\varepsilon}'']^{-1}\operatorname{Re}(\boldsymbol{d}) + [\boldsymbol{\varepsilon}'']^{-1}\boldsymbol{\varepsilon}'\operatorname{Re}(\boldsymbol{e}),\\ \operatorname{Im}(\boldsymbol{d}) &= \boldsymbol{\varepsilon}'\operatorname{Im}(\boldsymbol{e}) + \boldsymbol{\varepsilon}''\operatorname{Re}(\boldsymbol{e}) = -\boldsymbol{\varepsilon}'[\boldsymbol{\varepsilon}'']^{-1}\operatorname{Re}(\boldsymbol{d}) + \boldsymbol{\varepsilon}'[\boldsymbol{\varepsilon}'']^{-1}\boldsymbol{\varepsilon}'\operatorname{Re}(\boldsymbol{e}) + \boldsymbol{\varepsilon}''\operatorname{Re}(\boldsymbol{e}),\end{aligned}$$

from which it follows that

$$\boldsymbol{\mathcal{L}} = \begin{pmatrix} [\boldsymbol{\varepsilon}'']^{-1} & [\boldsymbol{\varepsilon}'']^{-1}\boldsymbol{\varepsilon}' \\ \boldsymbol{\varepsilon}'[\boldsymbol{\varepsilon}'']^{-1} & \boldsymbol{\varepsilon}'' + \boldsymbol{\varepsilon}'[\boldsymbol{\varepsilon}'']^{-1}\boldsymbol{\varepsilon}' \end{pmatrix}. \tag{11.58}$$

This matrix $\boldsymbol{\mathcal{L}}$ is clearly symmetric. It is also positive-definite because the associated quadratic form

$$\begin{aligned}\begin{pmatrix} -\operatorname{Re}(\boldsymbol{d}) \\ \operatorname{Re}(\boldsymbol{e}) \end{pmatrix} \cdot \boldsymbol{\mathcal{L}} \begin{pmatrix} -\operatorname{Re}(\boldsymbol{d}) \\ \operatorname{Re}(\boldsymbol{e}) \end{pmatrix} &= \begin{pmatrix} -\operatorname{Re}(\boldsymbol{d}) \\ \operatorname{Re}(\boldsymbol{e}) \end{pmatrix} \cdot \begin{pmatrix} \operatorname{Im}(\boldsymbol{e}) \\ \operatorname{Im}(\boldsymbol{d}) \end{pmatrix}\\ &= -\operatorname{Re}(\boldsymbol{d}) \cdot \operatorname{Im}(\boldsymbol{e}) + \operatorname{Re}(\boldsymbol{e}) \cdot \operatorname{Im}(\boldsymbol{d}),\end{aligned}$$

is nonnegative by virtue of the result (11.56), and zero only when $\operatorname{Re}(\boldsymbol{e}) = \operatorname{Im}(\boldsymbol{e}) = 0$, that is, when $-\operatorname{Re}(\boldsymbol{d}) = \operatorname{Re}(\boldsymbol{e}) = 0$. Alternatively, necessary and sufficient conditions for a symmetric matrix

$$\boldsymbol{L} = \begin{pmatrix} \boldsymbol{A} & \boldsymbol{B} \\ \boldsymbol{B}^T & \boldsymbol{D} \end{pmatrix} \tag{11.59}$$

to be positive-definite are that the submatrix $\boldsymbol{A}$ be positive-definite, and that the Schur complement

$$\boldsymbol{S} = \boldsymbol{D} - \boldsymbol{B}^T\boldsymbol{A}^{-1}\boldsymbol{B} \tag{11.60}$$

be positive-definite. In the case of the matrix $\boldsymbol{\mathcal{L}}$ given by (11.58), the submatrix $\boldsymbol{A} = [\boldsymbol{\varepsilon}'']^{-1}$ is clearly positive-definite and the Schur complement

$$\boldsymbol{S} = \boldsymbol{\varepsilon}'' + \boldsymbol{\varepsilon}'[\boldsymbol{\varepsilon}'']^{-1}\boldsymbol{\varepsilon}' - \boldsymbol{\varepsilon}'[\boldsymbol{\varepsilon}'']^{-1}[\boldsymbol{\varepsilon}''][\boldsymbol{\varepsilon}'']^{-1}\boldsymbol{\varepsilon}' = \boldsymbol{\varepsilon}'' \tag{11.61}$$

is also positive-definite.

We can apply the same transformation to the effective constitutive law (11.51) to obtain the relation

$$\begin{pmatrix} \langle \operatorname{Im}(\boldsymbol{e}) \rangle \\ \langle \operatorname{Im}(\boldsymbol{d}) \rangle \end{pmatrix} = \boldsymbol{\mathcal{L}}_* \begin{pmatrix} -\langle \operatorname{Re}(\boldsymbol{d}) \rangle \\ \langle \operatorname{Re}(\boldsymbol{e}) \rangle \end{pmatrix}, \tag{11.62}$$

where

$$\boldsymbol{\mathcal{L}}_* = \begin{pmatrix} [\boldsymbol{\varepsilon}_*'']^{-1} & [\boldsymbol{\varepsilon}_*'']^{-1}\boldsymbol{\varepsilon}_*' \\ \boldsymbol{\varepsilon}_*'[\boldsymbol{\varepsilon}_*'']^{-1} & \boldsymbol{\varepsilon}_*'' + \boldsymbol{\varepsilon}_*'[\boldsymbol{\varepsilon}_*'']^{-1}\boldsymbol{\varepsilon}_*' \end{pmatrix}. \tag{11.63}$$

Since the fields appearing on the left- and right-hand sides of (11.62) are the averages of the fields appearing on the left- and right-hand sides of (11.57), we see that $\boldsymbol{\mathcal{L}}_*$ is in fact the effective tensor associated with the constitutive law (11.57) in which the fields satisfy the differential constraints

$$\begin{aligned} \nabla \times \operatorname{Im}(\boldsymbol{e}) &= 0, & \nabla \cdot \operatorname{Re}(\boldsymbol{d}) &= 0,\\ \nabla \cdot \operatorname{Im}(\boldsymbol{d}) &= 0, & \nabla \times \operatorname{Re}(\boldsymbol{e}) &= 0. \end{aligned} \tag{11.64}$$

In other words, one can calculate the effective tensor $\boldsymbol{\varepsilon}_*$ by working with the transformed equations (11.57) and (11.64) to compute $\boldsymbol{\mathcal{L}}_*$, and then use the relation (11.63) to recover $\boldsymbol{\varepsilon}_*$.

Following Cherkaev and Gibiansky (1994), we can also apply this same transformation to the complex elasticity equations,

$$\boldsymbol{\tau}(\boldsymbol{x}) = \boldsymbol{\mathcal{C}}(\boldsymbol{x})\boldsymbol{\epsilon}(\boldsymbol{x}), \quad \nabla \cdot \boldsymbol{\tau} = 0, \quad \boldsymbol{\epsilon} = [\nabla \boldsymbol{u} + (\nabla \boldsymbol{u})^T]/2$$

and the complex effective equation

$$\langle \boldsymbol{\tau} \rangle = \boldsymbol{\mathcal{C}}_* \langle \boldsymbol{\epsilon} \rangle.$$

The constitutive equation and the effective constitutive equation become

$$\begin{pmatrix} \mathrm{Im}(\boldsymbol{\epsilon}) \\ \mathrm{Im}(\boldsymbol{\tau}) \end{pmatrix} = \boldsymbol{\mathcal{L}} \begin{pmatrix} -\mathrm{Re}(\boldsymbol{\tau}) \\ \mathrm{Re}(\boldsymbol{\epsilon}) \end{pmatrix}, \quad \begin{pmatrix} \langle \mathrm{Im}(\boldsymbol{\epsilon}) \rangle \\ \langle \mathrm{Im}(\boldsymbol{\tau}) \rangle \end{pmatrix} = \boldsymbol{\mathcal{L}}_* \begin{pmatrix} -\langle \mathrm{Re}(\boldsymbol{\tau}) \rangle \\ \langle \mathrm{Re}(\boldsymbol{\epsilon}) \rangle \end{pmatrix},$$

where $\boldsymbol{\mathcal{L}}$ and $\boldsymbol{\mathcal{L}}_*$ are the tensors

$$\boldsymbol{\mathcal{L}} = \begin{pmatrix} [\boldsymbol{\mathcal{C}}'']^{-1} & [\boldsymbol{\mathcal{C}}'']^{-1}\boldsymbol{\mathcal{C}}' \\ \boldsymbol{\mathcal{C}}'[\boldsymbol{\mathcal{C}}'']^{-1} & \boldsymbol{\mathcal{C}}'' + \boldsymbol{\mathcal{C}}'[\boldsymbol{\mathcal{C}}'']^{-1}\boldsymbol{\mathcal{C}}' \end{pmatrix},$$

$$\boldsymbol{\mathcal{L}}_* = \begin{pmatrix} [\boldsymbol{\mathcal{C}}''_*]^{-1} & [\boldsymbol{\mathcal{C}}''_*]^{-1}\boldsymbol{\mathcal{C}}'_* \\ \boldsymbol{\mathcal{C}}'_*[\boldsymbol{\mathcal{C}}''_*]^{-1} & \boldsymbol{\mathcal{C}}''_* + \boldsymbol{\mathcal{C}}'_*[\boldsymbol{\mathcal{C}}''_*]^{-1}\boldsymbol{\mathcal{C}}'_* \end{pmatrix}.$$

and the fields have components that satisfy the differential constraints,

$$\begin{aligned} \mathrm{Im}(\boldsymbol{\epsilon}) = \{\nabla \mathrm{Im}(\boldsymbol{u}) + [\nabla \mathrm{Im}(\boldsymbol{u})]^T\}/2, \qquad & \nabla \cdot \mathrm{Re}(\boldsymbol{\tau}) = 0, \\ \nabla \cdot \mathrm{Im}(\boldsymbol{\tau}) = 0, \qquad & \mathrm{Re}(\boldsymbol{\epsilon}) = \{\nabla \mathrm{Re}(\boldsymbol{u}) + [\nabla \mathrm{Re}(\boldsymbol{u})]^T\}/2. \end{aligned}$$

Once again the tensor $\boldsymbol{\mathcal{L}}$ is symmetric and will be positive- or negative-definite according to whether $\mathrm{Im}[\boldsymbol{\mathcal{C}}(\boldsymbol{x})]$ is positive- or negative-definite.

11.6. Correspondence with thermoelectricity in two dimensions

The equations (11.53) describing complex electrical permittivity are clearly directly analogous to the equations of thermoelectricity:

$$\begin{pmatrix} \boldsymbol{j}_1 \\ \boldsymbol{j}_2 \end{pmatrix} = \boldsymbol{\mathcal{L}}' \begin{pmatrix} \boldsymbol{e}_1 \\ \boldsymbol{e}_2 \end{pmatrix}, \quad \text{where} \quad \begin{matrix} \nabla \cdot \boldsymbol{j}_1 = 0, & \nabla \times \boldsymbol{e}_1 = 0, \\ \nabla \cdot \boldsymbol{j}_2 = 0, & \nabla \times \boldsymbol{e}_2 = 0. \end{matrix}$$

This can be seen by making the identifications

$$\boldsymbol{j}_1 = \mathrm{Re}(\boldsymbol{d}), \quad \boldsymbol{j}_2 = \mathrm{Im}(\boldsymbol{d}), \quad \boldsymbol{e}_1 = \mathrm{Im}(\boldsymbol{e}), \quad \boldsymbol{e}_2 = \mathrm{Re}(\boldsymbol{e})$$

between the fields, and the identification

$$\boldsymbol{\mathcal{L}}' = \begin{pmatrix} -\varepsilon'' & \varepsilon' \\ \varepsilon' & \varepsilon'' \end{pmatrix} \tag{11.65}$$

between the tensors entering the constitutive law. From a physical viewpoint this correspondence is not so interesting, because the tensor $\boldsymbol{\mathcal{L}}$ given by (11.65) is not positive-definite when ε'' is positive-definite. In other words, it cannot correspond to a thermoelectric tensor of a real material.

In two dimensions there is a direct correspondence with a thermoelectric problem, in which the tensor entering the constitutive law is in fact self-adjoint and positive-definite. In the

reformulated equations (11.57) the tensor $\boldsymbol{\mathcal{L}}$ entering the constitutive law is positive-definite and self-adjoint, but the fields on the left-hand side of the constitutive law are not divergence free and the fields on right-hand side are not curl free. In two dimensions this can be corrected by rewriting the constitutive law in the form

$$\boldsymbol{\mathcal{Q}}\begin{pmatrix}\operatorname{Im}(\boldsymbol{e})\\ \operatorname{Im}(\boldsymbol{d})\end{pmatrix} = \boldsymbol{\mathcal{Q}}\boldsymbol{\mathcal{L}}\boldsymbol{\mathcal{Q}}^T\boldsymbol{\mathcal{Q}}\begin{pmatrix}-\operatorname{Re}(\boldsymbol{d})\\ \operatorname{Re}(\boldsymbol{e})\end{pmatrix},$$

where $\boldsymbol{\mathcal{Q}}$ is the unitary matrix

$$\boldsymbol{\mathcal{Q}} = \begin{pmatrix}\boldsymbol{R}_\perp & 0\\ 0 & \boldsymbol{I}\end{pmatrix} \quad \text{in which} \quad \boldsymbol{R}_\perp = \begin{pmatrix}0 & 1\\ -1 & 0\end{pmatrix}.$$

In other words, the constitutive law now takes the form

$$\begin{pmatrix}\boldsymbol{R}_\perp \operatorname{Im}(\boldsymbol{e})\\ \operatorname{Im}(\boldsymbol{d})\end{pmatrix} = \boldsymbol{\mathcal{L}}'\begin{pmatrix}-\boldsymbol{R}_\perp \operatorname{Re}(\boldsymbol{d})\\ \operatorname{Re}(\boldsymbol{e})\end{pmatrix},$$

where the tensor

$$\boldsymbol{\mathcal{L}}'(\boldsymbol{x}) = \boldsymbol{\mathcal{Q}}\boldsymbol{\mathcal{L}}(\boldsymbol{x})\boldsymbol{\mathcal{Q}}^T = \begin{pmatrix}\boldsymbol{R}_\perp[\varepsilon'']^{-1}\boldsymbol{R}_\perp^T & \boldsymbol{R}_\perp[\varepsilon'']^{-1}\varepsilon'\\ \varepsilon'[\varepsilon'']^{-1}\boldsymbol{R}_\perp^T & \varepsilon'' + \varepsilon'[\varepsilon'']^{-1}\varepsilon'\end{pmatrix}$$

entering this constitutive law is clearly positive-definite and self-adjoint when the tensor $\varepsilon''(\boldsymbol{x})$ is positive-definite. Furthermore, since $\boldsymbol{R}_\perp$ converts curl free fields to divergence free fields, and vice versa (see section 3.1 on page 47), it follows that the fields

$$\boldsymbol{j}_1 = \boldsymbol{R}_\perp \operatorname{Im}(\boldsymbol{e}), \quad \boldsymbol{j}_2 = \operatorname{Im}(\boldsymbol{d}), \quad \boldsymbol{e}_1 = -\boldsymbol{R}_\perp \operatorname{Re}(\boldsymbol{d}), \quad \boldsymbol{e}_2 = \operatorname{Re}(\boldsymbol{e})$$

entering this new constitutive relation satisfy the differential constraints

$$\nabla \cdot \boldsymbol{j}_1 = 0, \quad \nabla \cdot \boldsymbol{j}_2 = 0, \quad \nabla \times \boldsymbol{e}_1 = 0, \quad \nabla \times \boldsymbol{e}_2 = 0.$$

So we see that the equations take exactly the same form as those of thermoelectricity, with a positive-definite tensor entering the constitutive law. The converse is not however true: Not all thermoelectric problems correspond to complex electrical permittivity problems. If the composite is locally isotropic, that is, $\varepsilon(\boldsymbol{x}) = \varepsilon(\boldsymbol{x})\boldsymbol{I}$, then the associated tensor $\boldsymbol{\mathcal{L}}'(\boldsymbol{x})$ is unusual in that the off-diagonal blocks are proportional to $\boldsymbol{R}_\perp$.

11.7. Resonance and localized resonance in composites†

At a fixed frequency the complex dielectric constant ε of an isotropic material has a positive imaginary part, but the real part can take either positive or negative values. Now consider the effective dielectric constant

$$\varepsilon_* = \varepsilon_2 + \frac{3f_1\varepsilon_2(\varepsilon_1 - \varepsilon_2)}{3\varepsilon_2 + f_2(\varepsilon_1 - \varepsilon_2)}$$

of the Hashin-Shtrikman sphere assemblage. Suppose for simplicity that ε_2 is fixed, real, and positive, and that $\varepsilon_1 = -(3 - f_2)\varepsilon_2/f_2 + i\delta$. Then as $\delta \to 0$ the value of the denominator in the above expression for ε_* approaches zero and consequently the effective dielectric constant blows up to infinity. Thus even a very small applied electric field $\boldsymbol{e}_0 = \langle \boldsymbol{e} \rangle$ can induce an

enormous average electric displacement field $\boldsymbol{d}_0 = \langle \boldsymbol{d} \rangle = \varepsilon_* \boldsymbol{e}_0$ when δ is sufficiently small. For a fixed applied field $\boldsymbol{e}_0$, the local fields $\boldsymbol{e}(\boldsymbol{x})$ and $\boldsymbol{d}(\boldsymbol{x})$ blow up almost everywhere in the material as $\delta \to 0$. The integral of the squares of these fields over any ball Θ approaches infinity. This is the phenomena of resonance, which in the Hashin-Shtrikman sphere assemblage occurs as the ratio $\varepsilon_1/\varepsilon_2$ approaches the value $-(3 - f_2)\varepsilon_2$. The resonance accounts for the beautiful ruby red color of glass containing a suspension of minute spherical gold particles (Maxwell Garnett 1904). Blue light is absorbed because at those frequencies $\varepsilon_1/\varepsilon_2$ approaches the value $-(3 - f_2)\varepsilon_2$.

As was discussed in section 10.4 on page 192, the Hashin-Shtrikman formula coincides with the Maxwell (i.e., the Clausius-Mossotti) approximation for the effective dielectric constant of a dilute suspension of spheres. In a random dilute dispersion of spheres there are local fluctuations in the volume fraction, and accordingly one expects to see a broadening of the resonance. Such broadening is seen experimentally, for example, by Gittleman and Abeles (1976). The spectral broadening has been investigated theoretically by Felderhof and Jones (1985, 1986a, 1986b) and Hinsen and Felderhof (1992), among others.

More generally, depending on the microstructure, resonance can occur at other negative real values of $\varepsilon_1/\varepsilon_2$. These values occur at the poles of $\varepsilon_*/\varepsilon_2$ when expressed as a function of $\varepsilon_1/\varepsilon_2$. For example, for a regular cubic array of spheres or square array of cylinders with fixed volume fraction, resonance occurs at an infinite number of ratios $\varepsilon_1/\varepsilon_2$ because this function has an infinite number of poles accumulating at an essential singularity at $\varepsilon_1/\varepsilon_2 = -1$ (Bergman 1979; McPhedran and McKenzie 1980). At the poles a solution to the field equations can still be obtained if one prescribes the average electric displacement field $\boldsymbol{d}_0$ rather than the average electric field $\boldsymbol{e}_0$. McPhedran and Perrins (1981) show that similar sorts of resonances also occur in the polarizability of cylinder pairs.

The fields $\boldsymbol{e}(\boldsymbol{x})$ and $\boldsymbol{d}(\boldsymbol{x})$ can lose their square integrability in other ways. For example, consider the Schulgasser assemblage, discussed in section 7.5 on page 121, where each sphere has dielectric constant λ_1 in the radial direction and dielectric constant λ_2 in the tangential direction. Suppose that the constant α, which is the solution of the quadratic $\alpha^2\lambda_1 + \alpha\lambda_1 - 2\lambda_2 = 0$, approaches the imaginary axis. This occurs when λ_2/λ_1 approaches some real value less than $-1/8$. Let us set $\alpha = \delta + i\gamma$ and see what happens as $\delta \to 0$. Inside the prototype sphere the electric field is

$$\begin{aligned}\boldsymbol{e}(\boldsymbol{x}) &= r^{\alpha-1}(\alpha \boldsymbol{v}_r \cos\theta - \boldsymbol{v}_\theta \sin\theta) \\ &= r^{\delta-1}[\cos(\gamma \log r) + i \sin(\gamma \log r)][(\delta + i\gamma)\boldsymbol{v}_r \cos\theta - \boldsymbol{v}_\theta \sin\theta].\end{aligned}$$

Thus as $\delta \to 0$ the integral of the square of the electric field over a ball Θ blows up if the ball contains the sphere center, but it remains finite if the ball does not contain the sphere center. In this example σ_*/λ_1, when expressed as a function of λ_2/λ_1,

$$\sigma_*/\lambda_1 = [-1 + \sqrt{1 + 8\lambda_2/\lambda_1}]/2,$$

has a branch cut along the negative real axis for $\lambda_2/\lambda_1 < -1/8$

There is another, more surprising, phenomena (Nicorovici, McPhedran, and Milton 1993, 1994). To illustrate it let us consider the two-dimensional problem of a coated circular inclusion centered at the origin, consisting of a circular core of phase 1 with dielectric constant ϵ_1 and radius r_i surrounded by a annular shell of phase 2 with dielectric constant ϵ_2 and exterior radius r_e, embedded in a material that we assume has dielectric constant ϵ_3 at least within a radius r_m of the cylinder center. In the exterior shell and core regions the complex electrical

potential ϕ is an analytic function of $z = x + iy$ and takes values

$$\phi_3(z) = A_0 + \sum_{\ell=1}^{\infty} A_\ell z^\ell + B_\ell z^{-\ell} \quad \text{for } r_e < |z| < r_m,$$
$$\phi_2(z) = C_0 + \sum_{\ell=1}^{\infty} C_\ell z^\ell + D_\ell z^{-\ell} \quad \text{for } r_c < |z| < r_e,$$
$$\phi_1(z) = E_0 + \sum_{\ell=1}^{\infty} E_\ell z^\ell \quad \text{for } |z| < r_c.$$

It is convenient to introduce the parameters

$$\eta_e = \frac{\epsilon_3 - \epsilon_2}{\epsilon_3 + \epsilon_2}, \quad \eta_c = \frac{\epsilon_2 - \epsilon_1}{\epsilon_2 + \epsilon_1},$$

in terms of which the relations between the coefficients A_ℓ, B_ℓ, C_ℓ, D_ℓ, and E_ℓ implied by the continuity of potential and the continuity of the normal component of the electrical displacement across $|z| = r_c$ and $|z| = r_e$ take the forms

$$B_\ell = [\eta_e + \eta_c(r_c/r_e)^{2\ell}] r_e^{2\ell} A_\ell/\Delta,$$
$$C_\ell = (1 + \eta_e) A_\ell/\Delta,$$
$$D_\ell = \eta_c(1 + \eta_e) r_c^{2\ell} A_\ell/\Delta,$$
$$E_\ell = (1 + \eta_c)(1 + \eta_e) A_\ell/\Delta,$$

where

$$\Delta = 1 + \eta_c \eta_e (r_c/r_e)^{2\ell}.$$

In the limit as the ratio ϵ_2/ϵ_3 approaches -1, that is, as η_e approaches infinity, the relation between B_ℓ and A_ℓ reduces to

$$B_\ell = \frac{\epsilon_3 - \epsilon_1}{\epsilon_3 + \epsilon_1} a^{2\ell} A_\ell, \quad \text{where } a = r_e^2/r_c.$$

This is exactly the same relation as would be attained for a single homogeneous circular inclusion of dielectric constant ϵ_1 and radius $a = r_e^2/r_c$ embedded in a matrix of dielectric constant ϵ_3. In this limit, and assuming that $r_m > a$, the response of the coated circular inclusion with exterior radius r_e approaches the response of the homogeneous circular inclusion of radius a. The coated inclusion and the solid inclusion are equivalent inclusions. The radius of this equivalent single inclusion will be much larger than the radius of the coated inclusion when the ratio r_e/r_c is large. By taking $\epsilon_3 = \epsilon_1$ we see that the coated inclusion can be inserted into a homogeneous body with dielectric constant ϵ_1 without disturbing the surrounding nonuniform field. This is an example of a neutral inclusion (see section 7.11 on page 134) that is neutral (in the quasistatic limit) to any applied field, not just to uniform fields.

One can apply this equivalence (in the general case, with $\epsilon_3 \neq \epsilon_1$) to bodies containing many such coated circular inclusions. In particular, consider a composite consisting of these coated inclusions placed on a square lattice, with lattice spacing slightly larger than $2r_e^2/r_c$, and embedded in a matrix of dielectric constant ϵ_3. It will have an effective dielectric constant ϵ_* that approaches the effective dielectric constant ϵ_*' of a square lattice of *nearly touching* homogeneous circular inclusions of dielectric constant ϵ_1 embedded in a matrix of dielectric

constant ϵ_3 as the ratio ϵ_2/ϵ_3 approaches -1. This striking result has been verified numerically (Nicorovici, McPhedran, and Milton 1993). In this square lattice, let us consider the field around the homogeneous circular inclusion centered at the origin. The potential $\varrho_3'(z)$ outside the inclusion will have some analytic extension inside the inclusion. Let $r_s < a$ denote the radius at which singularities in this analytically extended field first appear. The Laurent series

$$\phi_3'(z) = A_0' + \sum_{\ell=1}^{\infty} A_\ell' z^\ell + B_\ell' z^{-\ell}$$

for the potential $\varrho_3'(z)$ will have an inner radius of convergence equal to r_s. It may happen that r_s is greater than r_e. Then the potential $\phi_3(z)$ will converge to $\phi_3'(z)$ for $|z| > r_s$. Based on the solution for the Green's function, that is, the solution when a single pole is placed outside the coated circular inclusion (Nicorovici, McPhedran, and Milton 1994), we conjecture that the gradient of the potential $\phi(z)$ blows up to infinity within an entire region contained in and touching the boundary of the domain $|z| < r_s$ or, equivalently, that the integral of the square of the electric field over a ball Θ within the unit cell blows up if and only if the ball intersects this region. This blowing up of the field within an entire region, and the convergence of the field outside the region, is what I call localized resonance.

Let us return to the square lattice of nearly touching homogeneous circular inclusions of dielectric constant ϵ_1 in a matrix of dielectric constant $\epsilon_3 = 1$. When ϵ_1 is very large and positive, the effective dielectric constant can be determined from an analysis of the fields in the vicinity of where the cylinders almost touch (see section 10.10 on page 207 and references therein). This makes good physical sense when one thinks of the equivalent conductivity problem of highly conducting cylinders separated by small gaps: The potential will be almost constant within each cylinder and the electrical current in the matrix will be concentrated in the gaps. Now, as illustrated in figure 11.1, consider the (almost) equivalent problem of the

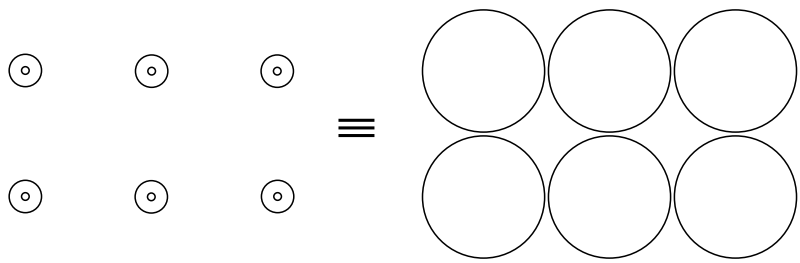

Figure 11.1. A periodic lattice of coated cylinders, with the core, coating, and surrounding matrix having dielectric constants ϵ_1, ϵ_2, and ϵ_3 has, in the limit $\epsilon_2/\epsilon_3 \to -1$, the same transverse effective dielectric constant as a lattice of solid cylinders of dielectric constant ϵ_1 embedded in a matrix of dielectric constant ϵ_3. As $\epsilon_2/\epsilon_3 \to -1$ the fields outside the coated cylinders develop enormous short wavelength oscillations near the inclusions, but converge to smooth fields in the regions away from the inclusions. These smooth fields match the fields between the cylinders in the lattice of solid cylinders.

coated circular inclusions in a square array, with lattice spacing slightly larger than $2r_e^2/r_c$. By analogy, one sees that when ϵ_1 is very large the effective dielectric constant is dominated by the behavior of the fields in the vicinity of where the locally resonant regions almost touch. The physical reason for this remains unclear.

Further work on equivalent responses has been done. Levy (1995) recognized that a coated cylinder comprised of a nonlinear core surrounded by a linear shell and matrix materials, with dielectric constants ϵ_2 and $\epsilon_3 = -\epsilon_2$, has the same response to a *uniform* applied field as a solid cylinder of radius r_e^2/r_c filled with a different nonlinear material. In other words, both have the same nonlinear polarizability. Liu and Li (1996) observed that coated spheres and solid spheres can have the same response to uniform applied fields.

References

Allaire, G. and C. Conca 1995a. Analyse asymptotique spectrale de l'équation des ondes. Complétude du spectre de Bloch. (French) [Asymptotic spectral analysis of the wave equation. Completeness of the Bloch spectrum]. *Comptes Rendus des Séances de l'Académie des Sciences. Série I. Mathématique* 321(5):557–562. {*221, 242*}

Allaire, G. and C. Conca 1995b. Analyse asymptotique spectrale de l'équation des ondes. Homogénéisation par ondes de Bloch. (French) [Asymptotic spectral analysis of the wave equation. Homogenization by Bloch waves]. *Comptes Rendus des Séances de l'Académie des Sciences. Série I. Mathématique* 321(3):293–298. {*221, 242*}

Allaire, G. and C. Conca 1996. Bloch-wave homogenization for a spectral problem in fluid-solid structures. *Archive for Rational Mechanics and Analysis* 135(3):197–257. {*221, 242*}

Allaire, G. and C. Conca 1998. Bloch wave homogenization and spectral asymptotic analysis. *Journal de Mathématiques Pures et Appliquées* 77(2):153–208. {*221, 242*}

Ashcroft, N. W. and N. D. Mermin 1976. *Solid State Physics*. Philadelphia: Saunders College. xxi + 826 pp. ISBN 0-03-083993-9 (College edition), 0-03-049346-3 (International edition). {*28, 40, 223, 224, 242*}

Avellaneda, M., L. Berlyand, and J.-F. Clouet 2000. Frequency dependent acoustics of composites with interfaces. *SIAM Journal on Applied Mathematics* 60(6):2143–2181. {*221, 242*}

Bensoussan, A., J.-L. Lions, and G. Papanicolaou 1978. *Asymptotic Analysis for Periodic Structures*. Amsterdam: North-Holland Publishing Co. xxiv + 700 pp. ISBN 0-444-85172-0. {*8, 10, 11, 14, 221, 242*}

Bergman, D. J. 1979. The dielectric constant of a simple cubic array of identical spheres. *Journal of Physics C: Solid State Physics* 12:4947–4960. {*39, 40, 239, 242, 377, 380, 392*}

Bloch, F. 1928. Über die Quantenmechanik der Electronen in Kristallgittern. (German) [On the quantum mechanics of electrons in crystal lattices]. *Zeitschrift für Physik* 52: 555–600. {*223, 242*}

Caflisch, R. E., M. J. Miksis, G. Papanicolaou, and L. Ting 1985a. Effective equation for wave propagation in bubbly liquids. *Journal of Fluid Mechanics* 153:259–273. {*234, 242*}

Caflisch, R. E., M. J. Miksis, G. Papanicolaou, and L. Ting 1985b. Wave propagation in bubbly liquids at finite volume fraction. *Journal of Fluid Mechanics* 160:1–14. {*234, 242*}

Callen, H. B. 1960. *Thermodynamics: An Introduction to the Physical Theories of Equilibrium Thermostatics and Irreversible Thermodynamics*, pp. 361–364. New York / London / Sydney, Australia: John Wiley and Sons. {*236, 242*}

Cherkaev, A. V. and L. V. Gibiansky 1994. Variational principles for complex conductivity, viscoelasticity, and similar problems in media with complex moduli. *Journal of Mathematical Physics* 35(1):127–145. {*221, 234, 237, 243, 264, 267, 271, 276, 277, 286, 639, 641*}

Christensen, R. M. 1971. *Theory of Viscoelasticity; an Introduction*. New York: Academic Press. xi + 245 pp. ISBN 0-12-174250-4. {*230, 243*}

Christensen, R. M. 1979. *Mechanics of Composite Materials*. New York: Wiley-Interscience. xiv + 348 pp. ISBN 0-471-05167-5. {*xxiv, xxvi, 233, 243*}

Conca, C. and M. Vanninathan 1997. Homogenization of periodic structures via Bloch decomposition. *SIAM Journal on Applied Mathematics* 57(6):1639–1659. {*221, 243*}

Felderhof, B. U. and R. B. Jones 1985. Spectral broadening in suspensions of metallic spheres. *Zeitschrift für Physik. B, Condensed Matter* 62:43–50. {*239, 243*}

Felderhof, B. U. and R. B. Jones 1986a. Effective dielectric constant of dilute polydisperse suspensions of spheres. *Zeitschrift für Physik. B, Condensed Matter* 62:225–230. {*239, 243*}

Felderhof, B. U. and R. B. Jones 1986b. Multipolar corrections to the Clausius-Mossotti formula for the effective dielectric constant of a polydisperse suspension of spheres. *Zeitschrift für Physik. B, Condensed Matter* 62:231–237. {*239, 243*}

Gelfand, I. M. 1950. Expansion in series of eigenfunctions of an equation with periodic coefficients. *Doklady Akademii Nauk SSSR* 73:1117–1120. {*223, 243*}

Gittleman, J. I. and B. Abeles 1976. Comparison of the effective medium and the Maxwell-Garnett predictions for the dielectric constants of granular metals. *Physical Review B (Solid State)* 15:3273–3275. {*239, 243*}

Hashin, Z. 1965. Viscoelastic behavior of heterogeneous media. *Journal of Applied Mechanics* 32:630–636. {*233, 243*}

Hinsen, K. and B. U. Felderhof 1992, November 15. Dielectric constant of a suspension of uniform spheres. *Physical Review B (Solid State)* 46(20):12955–12963. {*239, 243, 377, 393*}

Jackson, J. D. 1975. *Classical Electrodynamics* (Second ed.). New York / London / Sydney, Australia: John Wiley and Sons. xxii + 848 pp. ISBN 0-471-43132-X. {*224, 228, 243, 592, 598*}

Lakes, R. 1999. *Viscoelastic Solids*. Mechanical Engineering Series Notes. Boca Raton, Florida: CRC Press. 476 pp. ISBN 0-8493-9658-1. {*230, 243*}

Levy, O. 1995. Nonlinear properties of partially resonant composites. *Journal of Applied Physics* 77(4):1696–1700. {*242, 243*}

Liu, X.-Y. and Z.-Y. Li 1996. Nonlinear dielectric response of partially resonant composites. *Physics Letters A* 223(6):475–480. {*242, 243*}

Maxwell Garnett, J. C. 1904. Colours in metal glasses and in metallic films. *Philosophical Transactions of the Royal Society of London* 203:385–420. {*3, 16, 239, 243*}

McPhedran, R. C. and D. R. McKenzie 1980. Electrostatic and optical resonances of arrays of cylinders. *Applied Physics* 23:223–235. {*239, 244, 377, 381, 394*}

McPhedran, R. C. and W. T. Perrins 1981. Electrostatic and optical resonances of cylinder pairs. *Applied Physics* 24:311–318. {*188, 217, 239, 244, 306, 311*}

Nicorovici, N. A., R. C. McPhedran, and G. W. Milton 1993. Transport properties of a three-phase composite material: The square array of coated cylinders. *Proceedings of the Royal Society of London. Series A, Mathematical and Physical Sciences* 442:599–620. {*239, 241, 244, 390, 394*}

Nicorovici, N. A., R. C. McPhedran, and G. W. Milton 1994. Optical and dielectric properties of partially resonant composites. *Physical Review B (Solid State)* 49(12):8479–8482. {*239, 241, 244*}

Odeh, F. and J. B. Keller 1964. Partial differential equations with periodic coefficients and Bloch waves in crystals. *Journal of Mathematical Physics* 5:1499–1504. {*223, 244*}

Reed, M. and B. Simon 1978. *Analysis of Operators*, pp. 279–315. New York: Academic Press. ISBN 0-12-585004-2. {*223, 244*}

Sanchez-Palencia, E. 1980. *Non-Homogeneous Media and Vibration Theory*. Berlin / Heidelberg / London / etc.: Springer-Verlag. ix + 398 pp. ISBN 0-540-10000-8. {*xxiii, xxvii, 8, 17, 221, 244*}

Sølna, K. and G. W. Milton 2000. Bounds for the group velocity of electromagnetic signals in two phase materials. *Physica. B, Condensed Matter* 279(1–3):9–12. {*228, 244*}

Sølna, K. and G. W. Milton 2001. Can mixing materials make electromagnetic signals travel faster? *SIAM Journal on Applied Mathematics*. To Appear. {*228, 230, 244*}

Taylor, G. I. 1954. The two coefficients of viscosity for an incompressible fluid containing air bubbles. *Proceedings of the Royal Society of London. Series A, Mathematical and Physical Sciences* 226:34–39. {*3, 18, 234, 244*}

Van Wijngaarden, L. 1968. On equations of motion for mixtures of liquid and gas bubbles. *Journal of Fluid Mechanics* 33:465–474. {*234, 244*}

Van Wijngaarden, L. 1972. One-dimensional flow of liquids containing small gas bubbles. *Annual Review of Fluid Mechanics* 4:369–394. {*234, 244*}

Wilcox, C. H. 1978. Theory of Bloch waves. *Journal d'analyse mathématique* 33:146–167. {*223, 244*}

12

Reformulating the problem of finding effective tensors

So far we have been treating conductivity, elasticity, thermoelectricity, piezoelectricity, thermoelasticity, and poroelasticity separately from each other. Yet it is evident that certain formulas, such the formula (9.44) for the effective tensor of a laminate material, take much the same form irrespective of what problem we are considering. This suggests that we can avoid duplicating proofs by treating the different problems under the one umbrella. Then if we come across a new problem that also fits under this umbrella, the results that we have derived immediately extend to it. Of course, the disadvantage is that one has to represent the fields and tensors by some sort of generic notation, and it requires some interpretation to express the results in familiar terms that are applicable to the specific problem of interest. This dilemma is nothing new. We already used the electrical conductivity equations as a generic example for the equations of thermal conduction, diffusion, magnetic permeability, and dielectric behavior, and one has to make appropriate substitutions to reexpress results in the language of the problem of direct interest. In what follows, we are just carrying this generic representation one step further.

12.1. Resolving a periodic field into its three component fields: The Γ-operators

In the problems studied so far the constitutive law takes the form

$$\boldsymbol{J}(\boldsymbol{x}) = \boldsymbol{L}(\boldsymbol{x})\boldsymbol{E}(\boldsymbol{x}), \tag{12.1}$$

with appropriate definitions of the fields $\boldsymbol{J}(\boldsymbol{x})$, $\boldsymbol{E}(\boldsymbol{x})$, and the tensor $\boldsymbol{L}(\boldsymbol{x})$. Let us define $\mathcal{T}$ as the m-dimensional space in which the fields $\boldsymbol{J}(\boldsymbol{x})$ and $\boldsymbol{E}(\boldsymbol{x})$ take their values. For conductivity this space consists of all d-dimensional vectors, while for elasticity it is the $d(d+1)/2$-dimensional space of symmetric d-dimensional second-order tensors. We assume that there is a natural scalar product $\boldsymbol{A} \cdot \boldsymbol{B}$ between any two elements $\boldsymbol{A}$ and $\boldsymbol{B}$ of $\mathcal{T}$, which is a real-valued bilinear form such that $\boldsymbol{A} \cdot \boldsymbol{B} = \boldsymbol{B} \cdot \boldsymbol{A}$ and $\boldsymbol{A} \cdot \boldsymbol{A} > 0$ for all $\boldsymbol{A} \neq 0$. For example, the scalar products $\boldsymbol{A} \cdot \boldsymbol{B} = \boldsymbol{A}^T\boldsymbol{B}$ and $\boldsymbol{A} \cdot \boldsymbol{B} = \mathrm{Tr}(\boldsymbol{A}\boldsymbol{B})$ are convenient choices for conductivity and elasticity, respectively. In the applications of interest $\mathcal{T}$ will be a tensor space, which means that for every d-dimensional rotation $\boldsymbol{R}$ there exists an associated linear operator $\boldsymbol{Q} = \boldsymbol{Q}(\boldsymbol{R})$ acting on $\mathcal{T}$ such that $(\boldsymbol{Q}\boldsymbol{A}) \cdot (\boldsymbol{Q}\boldsymbol{B}) = \boldsymbol{A} \cdot \boldsymbol{B}$ for any two elements $\boldsymbol{A}$ and $\boldsymbol{B}$ of $\mathcal{T}$ (i.e., such that $\boldsymbol{Q}^T\boldsymbol{Q} = \boldsymbol{I}$). For conductivity we have $\boldsymbol{Q}\boldsymbol{A} = \boldsymbol{R}\boldsymbol{A}$, while for elasticity we have $\boldsymbol{Q}\boldsymbol{A} = \boldsymbol{R}\boldsymbol{A}\boldsymbol{R}^T$.

In each example we considered there exists, for every unit vector $\boldsymbol{k} \in \mathbb{R}^d$, a pair of

orthogonal subspaces $\mathcal{E}_{\boldsymbol{k}}$ and $\mathcal{J}_{\boldsymbol{k}}$ spanning $\mathcal{T}$,

$$\mathcal{E}_{\boldsymbol{k}} \oplus \mathcal{J}_{\boldsymbol{k}} = \mathcal{T}, \tag{12.2}$$

such that the relations

$$\boldsymbol{J}(\boldsymbol{x}) - \langle \boldsymbol{J} \rangle \in \mathcal{J}_{\boldsymbol{k}}, \quad \boldsymbol{E}(\boldsymbol{x}) - \langle \boldsymbol{E} \rangle \in \mathcal{E}_{\boldsymbol{k}}, \quad \text{for all } \boldsymbol{x}, \tag{12.3}$$

hold for all periodic fields $\boldsymbol{J}(\boldsymbol{x})$ and $\boldsymbol{E}(\boldsymbol{x})$ that are compatible with the appropriate differential constraints, and which oscillate only in the direction $\boldsymbol{k}$, so that $\boldsymbol{J}(\boldsymbol{x}) = \boldsymbol{J}(\boldsymbol{k} \cdot \boldsymbol{x})$ and $\boldsymbol{E}(\boldsymbol{x}) = \boldsymbol{E}(\boldsymbol{k} \cdot \boldsymbol{x})$. In the general setting the orthogonality of $\mathcal{E}_{\boldsymbol{k}}$ and $\mathcal{J}_{\boldsymbol{k}}$ means that $\boldsymbol{A} \cdot \boldsymbol{B} = 0$ for all $\boldsymbol{A} \in \mathcal{E}_{\boldsymbol{k}}$ and all $\boldsymbol{B} \in \mathcal{J}_{\boldsymbol{k}}$.

Clearly any function of $\boldsymbol{k} \cdot \boldsymbol{x}$ is also a function of $-\boldsymbol{k} \cdot \boldsymbol{x}$ and this implies that

$$\mathcal{J}_{-\boldsymbol{k}} = \mathcal{J}_{\boldsymbol{k}}, \quad \mathcal{E}_{-\boldsymbol{k}} = \mathcal{E}_{\boldsymbol{k}}. \tag{12.4}$$

When $\boldsymbol{k}$ is not a unit vector, but $\boldsymbol{k} \neq 0$, it seems natural to define $\mathcal{E}_{\boldsymbol{k}}$ and $\mathcal{J}_{\boldsymbol{k}}$ so that (12.3) remains valid for all fields $\boldsymbol{J}(\boldsymbol{x})$ and $\boldsymbol{E}(\boldsymbol{x})$ that satisfy the appropriate differential constraints and which are functions of $\boldsymbol{k} \cdot \boldsymbol{x}$. This is ensured if we set

$$\mathcal{J}_{\boldsymbol{k}} = \mathcal{J}_{\boldsymbol{k}/|\boldsymbol{k}|}, \quad \mathcal{E}_{\boldsymbol{k}} = \mathcal{E}_{\boldsymbol{k}/|\boldsymbol{k}|}, \qquad \text{for all } \boldsymbol{k} \neq 0. \tag{12.5}$$

These spaces have an important significance even when the fields $\boldsymbol{J}(\boldsymbol{x})$ and $\boldsymbol{E}(\boldsymbol{x})$ have oscillations in more than one direction. To see this, let us first define the complex extension of $\mathcal{T}$ to consist of those tensors $\boldsymbol{A} = \boldsymbol{A}_1 + i\boldsymbol{A}_2$, where $\boldsymbol{A}_1 \in \mathcal{T}$ and $\boldsymbol{A}_2 \in \mathcal{T}$. We call $\boldsymbol{A}_1$ the real part of $\boldsymbol{A}$ and $\boldsymbol{A}_2$ the imaginary part of $\boldsymbol{A}$. On the complex extension the scalar product of $\boldsymbol{A}$ with any other tensor $\boldsymbol{B} = \boldsymbol{B}_1 + i\boldsymbol{B}_2$ is taken to be

$$\begin{aligned} \boldsymbol{A} \cdot \boldsymbol{B} &= (\boldsymbol{A}_1 + i\boldsymbol{A}_2) \cdot (\boldsymbol{B}_1 + i\boldsymbol{B}_2) \\ &= \boldsymbol{A}_1 \cdot \boldsymbol{B}_1 - \boldsymbol{A}_2 \cdot \boldsymbol{B}_2 + i(\boldsymbol{A}_1 \cdot \boldsymbol{B}_2 + \boldsymbol{A}_2 \cdot \boldsymbol{B}_1). \end{aligned}$$

The complex extension of $\mathcal{J}_{\boldsymbol{k}}$, or $\mathcal{E}_{\boldsymbol{k}}$, is defined to be the subspace consisting of all tensors whose real and imaginary parts lie in $\mathcal{J}_{\boldsymbol{k}}$, or $\mathcal{E}_{\boldsymbol{k}}$. By an abuse of notation we denote a space and its complex extension by the same symbol. Now notice that the Fourier expansions of the fields $\boldsymbol{J}(\boldsymbol{x})$ and $\boldsymbol{E}(\boldsymbol{x})$,

$$\boldsymbol{J}(\boldsymbol{x}) = \sum_{\boldsymbol{k}} e^{i\boldsymbol{k}\cdot\boldsymbol{x}} \widehat{\boldsymbol{J}}(\boldsymbol{k}), \quad \boldsymbol{E}(\boldsymbol{x}) = \sum_{\boldsymbol{k}} e^{i\boldsymbol{k}\cdot\boldsymbol{x}} \widehat{\boldsymbol{E}}(\boldsymbol{k}), \quad \text{where } \widehat{\boldsymbol{J}}(0) = \langle \boldsymbol{J} \rangle, \ \widehat{\boldsymbol{E}}(0) = \langle \boldsymbol{E} \rangle,$$

effectively decompose them into a sum of (possibly complex-valued) fields, each with oscillations only in one direction. Furthermore, since the differential constraints are local in Fourier space, each of these component fields must also satisfy the same differential constraints as $\boldsymbol{J}(\boldsymbol{x})$ and $\boldsymbol{E}(\boldsymbol{x})$. So clearly (12.3) implies that the Fourier components of $\boldsymbol{J}$ and $\boldsymbol{E}$ lie respectively in the complex extensions of the spaces $\mathcal{J}_{\boldsymbol{k}}$ and $\mathcal{E}_{\boldsymbol{k}}$ for each nonzero wavevector $\boldsymbol{k}$:

$$\widehat{\boldsymbol{J}}(\boldsymbol{k}) \in \mathcal{J}_{\boldsymbol{k}}, \quad \widehat{\boldsymbol{E}}(\boldsymbol{k}) \in \mathcal{E}_{\boldsymbol{k}} \ \text{ for all } \boldsymbol{k} \neq 0. \tag{12.6}$$

We view this as defining the differential constraints on the fields $\boldsymbol{J}(\boldsymbol{x})$ and $\boldsymbol{E}(\boldsymbol{x})$. The constraints on the subspaces $\mathcal{J}_{\boldsymbol{k}}$ and $\mathcal{E}_{\boldsymbol{k}}$ are that they are orthogonal, span $\mathcal{T}$, satisfy (12.4) and (12.5), and have dimensions, say, $m - \ell$ and ℓ, that are independent of $\boldsymbol{k}$.

A useful corollary follows from (12.6). It implies that the scalar product of $\boldsymbol{J}(\boldsymbol{x})$ with $\boldsymbol{E}(\boldsymbol{x})$ can be integrated over the unit cell Ω of periodicity and equated with the scalar product of $\langle \boldsymbol{J} \rangle$ with $\langle \boldsymbol{E} \rangle$. Indeed, by applying Plancherel's theorem, we have

$$\frac{1}{|\Omega|} \int_\Omega \boldsymbol{J}(\boldsymbol{x}) \cdot \boldsymbol{E}(\boldsymbol{x}) = \langle \boldsymbol{J} \rangle \cdot \langle \boldsymbol{E} \rangle + \sum_{\boldsymbol{k} \neq 0} \widehat{\boldsymbol{J}}(-\boldsymbol{k}) \cdot \widehat{\boldsymbol{E}}(\boldsymbol{k}) = \langle \boldsymbol{J} \rangle \cdot \langle \boldsymbol{E} \rangle, \tag{12.7}$$

where we have used the fact that the scalar product of $\widehat{\boldsymbol{J}}(-\boldsymbol{k})$ with $\widehat{\boldsymbol{E}}(\boldsymbol{k})$ vanishes because the real and imaginary parts of these fields lie in the orthogonal subspaces $\mathcal{J}_{\boldsymbol{k}}$ and $\mathcal{E}_{\boldsymbol{k}}$. In physical terms, half this scalar product usually represents the energy density, or power dissipation rate, and (12.7) expresses the fact that the average energy, or average power dissipation rate, can also be expressed as the scalar product between the average fields. For linear elasticity, this result was proved independently by Hill (1963) and Hashin (1964), not just for composites, but for any inhomogeneous body subject to either uniform tractions at the boundary or affine displacement boundary conditions [see also the average virtual work theorems of Hashin (1972) for elasticity and for conductivity].

Moreover, the decomposition (12.2) implies that there is a natural splitting of any square integrable periodic field $\boldsymbol{P}$ into three component fields:

$$\boldsymbol{P} = \boldsymbol{P}_0 + \boldsymbol{P}_1 + \boldsymbol{P}_2, \tag{12.8}$$

where $\boldsymbol{P}_0$ is a constant field, $\boldsymbol{P}_1$ is a field with zero mean over the unit cell satisfying the same differential constraints as the field $\boldsymbol{E}$, and $\boldsymbol{P}_2$ is a field with zero mean over the unit cell satisfying the same differential constraints as the field $\boldsymbol{J}$. This is evident if we expand $\boldsymbol{P}(\boldsymbol{x})$ in a Fourier series,

$$\boldsymbol{P}(\boldsymbol{x}) = \sum_{\boldsymbol{k}} e^{i\boldsymbol{k}\cdot\boldsymbol{x}} \widehat{\boldsymbol{P}}(\boldsymbol{k}),$$

and set

$$\begin{aligned} \boldsymbol{P}_0 &= \boldsymbol{\Gamma}_0 \boldsymbol{P} \equiv \langle \boldsymbol{P} \rangle = \widehat{\boldsymbol{P}}(0), \\ \boldsymbol{P}_1(\boldsymbol{x}) &= \boldsymbol{\Gamma}_1 \boldsymbol{P} \equiv \sum_{\boldsymbol{k} \neq 0} e^{i\boldsymbol{k}\cdot\boldsymbol{x}} \boldsymbol{\Gamma}_1(\boldsymbol{k}) \widehat{\boldsymbol{P}}(\boldsymbol{k}), \\ \boldsymbol{P}_2(\boldsymbol{x}) &= \boldsymbol{\Gamma}_2 \boldsymbol{P} \equiv \sum_{\boldsymbol{k} \neq 0} e^{i\boldsymbol{k}\cdot\boldsymbol{x}} \boldsymbol{\Gamma}_2(\boldsymbol{k}) \widehat{\boldsymbol{P}}(\boldsymbol{k}), \end{aligned} \tag{12.9}$$

in which $\boldsymbol{\Gamma}_1(\boldsymbol{k})$ and $\boldsymbol{\Gamma}_2(\boldsymbol{k})$ denote the projections onto the spaces $\mathcal{E}_{\boldsymbol{k}}$ and $\mathcal{J}_{\boldsymbol{k}}$. In the various problems considered in sections 9.2 on page 159 and 9.5 on page 167, expressions for $\boldsymbol{\Gamma}_1(\boldsymbol{k})$ and $\boldsymbol{\Gamma}_2(\boldsymbol{k})$ have been obtained for $\boldsymbol{k}$ a unit vector. These expressions can be extended to arbitrary $\boldsymbol{k} \neq 0$ using the relations

$$\boldsymbol{\Gamma}_1(\boldsymbol{k}) = \boldsymbol{\Gamma}_1(\boldsymbol{k}/|\boldsymbol{k}|), \quad \boldsymbol{\Gamma}_2(\boldsymbol{k}) = \boldsymbol{\Gamma}_2(\boldsymbol{k}/|\boldsymbol{k}|),$$

which are implied by (12.5). For example, for conductivity we have

$$\boldsymbol{\Gamma}_1(\boldsymbol{k}) = \frac{\boldsymbol{k} \otimes \boldsymbol{k}}{|\boldsymbol{k}|^2}, \quad \boldsymbol{\Gamma}_2(\boldsymbol{k}) = \boldsymbol{I} - \frac{\boldsymbol{k} \otimes \boldsymbol{k}}{|\boldsymbol{k}|^2}.$$

The equations (12.9) serve to define the Γ operators $\boldsymbol{\Gamma}_0$, $\boldsymbol{\Gamma}_1$, and $\boldsymbol{\Gamma}_2$ that, when applied to $\boldsymbol{P}(\boldsymbol{x})$, produce the fields $\boldsymbol{P}_0$, $\boldsymbol{P}_1(\boldsymbol{x})$, and $\boldsymbol{P}_2(\boldsymbol{x})$. For the conductivity problem the components $\boldsymbol{P}_0$, $\boldsymbol{P}_1(\boldsymbol{x})$, and $\boldsymbol{P}_2(\boldsymbol{x})$ can be identified with the constant component, the curl free

mean zero component, and the divergence free mean zero component of the vector field $\boldsymbol{P}(\boldsymbol{x})$. Thus the field decomposition (12.8) is simply a generalization of the Helmholtz decomposition of a vector field into its constant, curl free, and divergence free parts.

The three field components are mutually orthogonal in the sense that

$$\begin{aligned}\langle \boldsymbol{P}_0 \cdot \boldsymbol{P}_1\rangle &= 0, \qquad\qquad \langle \boldsymbol{P}_0 \cdot \boldsymbol{P}_2\rangle = 0,\\ \langle \boldsymbol{P}_1 \cdot \boldsymbol{P}_2\rangle &= \sum_{\boldsymbol{k}\neq 0}[\boldsymbol{\Gamma}_1(-\boldsymbol{k})\widehat{\boldsymbol{P}}(-\boldsymbol{k})]\cdot[\boldsymbol{\Gamma}_2(\boldsymbol{k})\widehat{\boldsymbol{P}}(\boldsymbol{k})]\\ &= \sum_{\boldsymbol{k}\neq 0}[\widehat{\boldsymbol{P}}(-\boldsymbol{k})]\cdot[\boldsymbol{\Gamma}_1(\boldsymbol{k})\boldsymbol{\Gamma}_2(\boldsymbol{k})\widehat{\boldsymbol{P}}(\boldsymbol{k})] = 0,\end{aligned}$$

where we have used the fact that $\boldsymbol{\Gamma}_1(-\boldsymbol{k}) = \boldsymbol{\Gamma}_1(\boldsymbol{k})$ and $\boldsymbol{\Gamma}_1(\boldsymbol{k})\boldsymbol{\Gamma}_2(\boldsymbol{k}) = 0$. In other words, $\boldsymbol{\Gamma}_0$, $\boldsymbol{\Gamma}_1$, and $\boldsymbol{\Gamma}_2$ are projections satisfying

$$\boldsymbol{\Gamma}_i\boldsymbol{\Gamma}_j = \delta_{ij}\boldsymbol{\Gamma}_i, \quad \boldsymbol{\Gamma}_0 + \boldsymbol{\Gamma}_1 + \boldsymbol{\Gamma}_2 = \boldsymbol{I}.$$

They project, respectively, onto the space $\mathcal{U}$ of uniform fields, onto the space $\mathcal{E}$ of square integrable fields with zero mean over the unit cell satisfying the same differential constraints as the field $\boldsymbol{E}$, and onto the space $\mathcal{J}$ of square integrable fields with zero mean over the unit cell satisfying the same differential constraints as the field $\boldsymbol{J}$. In summary, the differential constraints provide a natural decomposition of the Hilbert space $\mathcal{H}$ of square integrable fields into three orthogonal subspaces of fields,

$$\mathcal{H} = \mathcal{U} \oplus \mathcal{E} \oplus \mathcal{J}, \tag{12.10}$$

and the operators $\boldsymbol{\Gamma}_0$, $\boldsymbol{\Gamma}_1$, and $\boldsymbol{\Gamma}_2$ represent the projections onto these subspaces.

In this Hilbert space the inner product between any two (possibly complex-valued) fields $\boldsymbol{P}'(\boldsymbol{x})$ and $\boldsymbol{P}(\boldsymbol{x})$ is taken to be the usual one,

$$(\boldsymbol{P}, \boldsymbol{P}') = \langle \overline{\boldsymbol{P}} \cdot \boldsymbol{P}'\rangle, \tag{12.11}$$

and the norm of a field $\boldsymbol{P}(\boldsymbol{x})$ is

$$|\boldsymbol{P}| = (\boldsymbol{P}, \boldsymbol{P})^{1/2} = \langle \overline{\boldsymbol{P}} \cdot \boldsymbol{P}\rangle^{1/2},$$

in which the bar denotes complex conjugation. This setting (Milton 1987, 1990) involving three mutually orthogonal subspaces $\mathcal{U}$, $\mathcal{E}$, and $\mathcal{J}$ is one of many possible Hilbert space settings for the problem; other settings have been introduced by Fokin (1982); Kohler and Papanicolaou (1982); Papanicolaou and Varadhan (1982); Golden and Papanicolaou (1983); Kantor and Bergman (1984); and Dell'Antonio, Figari, and Orlandi (1986). As we will see in section 12.7 on page 260, it provides a framework for defining effective tensors in a more general context.

12.2. A wider class of partial differential equations with associated effective tensors†

We have talked about treating different problems under one umbrella but have not given any indication as to what other problems come under this umbrella; we need to define an appropriate class of equations for which effective tensors can be defined. We will not refer to this

general class of equations elsewhere in the book, so this section can be safely skipped by those not interested in getting a more precise idea of what class of equations we are considering.

Let us consider a generalized problem where $\boldsymbol{J}(\boldsymbol{x})$ is a tensor field that in some representation has m components $J_s(\boldsymbol{x})$, $s = 1, 2, \ldots, m$ that satisfy a set of ℓ homogeneous h-th–order linear partial differential equations,

$$\sum_{s=1}^{m} \sum_{a_1,\ldots,a_h=1}^{d} \frac{\partial}{\partial x_{a_1}} \frac{\partial}{\partial x_{a_2}} \ldots \frac{\partial}{\partial x_{a_h}} A_{qs}^{a_1 \ldots a_h} J_s(\boldsymbol{x}) = 0 \quad \text{for } q = 1, 2, \ldots, \ell, \tag{12.12}$$

in a space of dimension d with real-valued constant coefficients $A_{qs}^{a_1 \ldots a_h}$. The tensor field $\boldsymbol{E}(\boldsymbol{x})$ in the same representation has m components $E_r(\boldsymbol{x})$, $r = 1, 2, \ldots, m$ and with the subtraction of a constant field $\boldsymbol{E}_0$ it derives from a (possibly nonunique) periodic potential $\boldsymbol{U}(\boldsymbol{x})$, with ℓ components $U_1(\boldsymbol{x}), \ldots, U_\ell(\boldsymbol{x})$, through the equations

$$E_r(\boldsymbol{x}) = \{\boldsymbol{E}_0\}_r + \sum_{q=1}^{\ell} \sum_{a_1,\ldots,a_h=1}^{d} A_{qr}^{a_1 \ldots a_h} \frac{\partial}{\partial x_{a_1}} \frac{\partial}{\partial x_{a_2}} \ldots \frac{\partial}{\partial x_{a_h}} U_q(\boldsymbol{x}) \quad \text{for } r = 1, 2, \ldots, m. \tag{12.13}$$

The tensor $\boldsymbol{L}(\boldsymbol{x})$ linking the fields via the constitutive law is then represented by a periodic $m \times m$ matrix-valued field of material constants. Since the order of differentiation in (12.12) and (12.13) does not matter, we may as well assume that the coefficients $A_{qs}^{a_1 \ldots a_h}$ are symmetric with respect to the interchange of any of the indices $a_1, a_2, \ldots, a_h$. In many problems of physical interest the constant field $\boldsymbol{E}_0 = \langle \boldsymbol{E} \rangle$ can be absorbed into the potential $\boldsymbol{U}(\boldsymbol{x})$. [An exception is the thermoelasticity equations (2.24), where the temperature increase θ cannot be absorbed into the potential.] Without going into the technical details, the constant field can be absorbed into the potential if and only if the $d^h \ell \times m$ matrix with coefficients $A_{qr}^{a_1 \ldots a_h}$ has rank m.

At first sight this formulation appears to be much more general than necessary, since in most physical equations the fields satisfy first-order differential constraints, corresponding to $h = 1$. However, it is sometimes advantageous to rewrite the equations in conjugate form, where the field $\boldsymbol{J}(\boldsymbol{x})$ derives from a potential, and these conjugate equations may be of higher order. For example, the conjugate equations of two-dimensional elasticity are of order $h = 2$ [see equation (2.12)].

A convenient way to represent the set of coefficients $A_{qs}^{a_1 \ldots a_h}$ is through the $\ell \times m$ matrix $\boldsymbol{A}(\boldsymbol{k})$ with elements

$$A_{qs}(\boldsymbol{k}) = \sum_{a_1,\ldots,a_h=1}^{d} k_{a_1} k_{a_2} \ldots k_{a_h} A_{qs}^{a_1 \ldots a_h} \tag{12.14}$$

that are homogeneous polynomials of degree h in the variables $k_1, k_2, \ldots k_d$. There is clearly a one-to-one correspondence between such matrices and sets of coefficients $A_{qs}^{a_1 \ldots a_h}$ that are symmetric with respect to the interchange of any of the indices $a_1, a_2, \ldots, a_h$.

The differential constraints can be rewritten symbolically in the more compact form,

$$\nabla^h \cdot \boldsymbol{A}\boldsymbol{J} = 0, \qquad \boldsymbol{E} = \boldsymbol{E}_0 + \boldsymbol{A}^T \nabla^h \boldsymbol{U}, \tag{12.15}$$

where ∇^h is the h-th–order tensorial differential operator with elements

$$(\nabla^h)_{a_1 a_2 \ldots a_h} = \frac{\partial}{\partial x_{a_1}} \frac{\partial}{\partial x_{a_2}} \ldots \frac{\partial}{\partial x_{a_h}}, \tag{12.16}$$

and the dot in (12.15) denotes a full contraction of the spatial indices $a_1, a_2, \ldots, a_h$ of ∇^h with the associated spatial indices of the tensor $\boldsymbol{AJ}$.

With these differential constraints on the fields it is easy to check that $\mathcal{J}_{\boldsymbol{k}}$ and $\mathcal{E}_{\boldsymbol{k}}$ can be identified with the nullspace and range of $\boldsymbol{A}(\boldsymbol{k})$:

$$\begin{aligned} \mathcal{J}_{\boldsymbol{k}} &= \{\boldsymbol{J} \in \mathbb{R}^m \mid \boldsymbol{A}(\boldsymbol{k})\boldsymbol{J} = 0\}, \\ \mathcal{E}_{\boldsymbol{k}} &= \{\boldsymbol{E} \in \mathbb{R}^m \mid \boldsymbol{E} = \boldsymbol{A}^T(\boldsymbol{k})\boldsymbol{U} \text{ for some } \boldsymbol{U} \in \mathbb{R}^\ell\}. \end{aligned} \tag{12.17}$$

Then (12.6) holds and furthermore $\mathcal{J}_{\boldsymbol{k}}$ and $\mathcal{E}_{\boldsymbol{k}}$ are mutually orthogonal and span $\mathbb{R}^m$:

$$\mathcal{J}_{\boldsymbol{k}} \oplus \mathcal{E}_{\boldsymbol{k}} = \mathbb{R}^m. \tag{12.18}$$

We need to assume that the rank of $\boldsymbol{A}(\boldsymbol{k})$ does not change with $\boldsymbol{k}$ for all $\boldsymbol{k} \neq 0$. Otherwise, the dimensionality of the spaces $\mathcal{J}_{\boldsymbol{k}}$ and $\mathcal{E}_{\boldsymbol{k}}$ would change discontinuously with $\boldsymbol{k}$ and then the effective tensor of a simple laminate would also change discontinuously with $\boldsymbol{n}$. For example, the choice of coefficients corresponding to the matrix

$$\boldsymbol{A}(\boldsymbol{k}) = \begin{pmatrix} k_1 & k_2 & k_1 \\ k_2 & k_1 & k_2 \end{pmatrix} \tag{12.19}$$

is excluded since the rank changes from 2 to 1 at $k_1 = k_2$. This assumption of constancy of the rank was introduced by Murat (1978, 1981) in a related context.

If we make the additional simplifying assumption that $\boldsymbol{A}(\boldsymbol{k})\boldsymbol{A}^T(\boldsymbol{k})$ is nonsingular for all $\boldsymbol{k} \neq 0$, then the projection onto $\mathcal{E}_{\boldsymbol{n}}$, which is the range of the matrix $\boldsymbol{A}^T(\boldsymbol{n})$, is given by the formula

$$\boldsymbol{\Gamma}_1(\boldsymbol{n}) = \boldsymbol{A}^T(\boldsymbol{n})[\boldsymbol{A}(\boldsymbol{n})\boldsymbol{A}^T(\boldsymbol{n})]^{-1}\boldsymbol{A}(\boldsymbol{n}), \tag{12.20}$$

as is well known from linear algebra. The associated tensor $\boldsymbol{\Gamma}(\boldsymbol{n})$ defined by (9.40) is

$$\boldsymbol{\Gamma}(\boldsymbol{n}) = \boldsymbol{A}^T(\boldsymbol{n})[\boldsymbol{A}(\boldsymbol{n})\boldsymbol{L}_0\boldsymbol{A}^T(\boldsymbol{n})]^{-1}\boldsymbol{A}(\boldsymbol{n}). \tag{12.21}$$

The effective tensor $\boldsymbol{L}_*$ for this generalized problem is defined through the linear relation

$$\langle \boldsymbol{J} \rangle = \boldsymbol{L}_* \langle \boldsymbol{E} \rangle \tag{12.22}$$

between any periodic fields $\boldsymbol{J}(\boldsymbol{x})$ and $\boldsymbol{E}(\boldsymbol{x})$ that solve (12.1), (12.12), and (12.13). Of course this definition is meaningful only if the equations have a unique solution for $\langle \boldsymbol{J} \rangle$ given $\langle \boldsymbol{E} \rangle$. We will prove in section 14.6 on page 298 that the equations do have unique periodic solutions $\boldsymbol{J}(\boldsymbol{x})$ and $\boldsymbol{E}(\boldsymbol{x})$ for any choice of $\langle \boldsymbol{E} \rangle$ provided that $\boldsymbol{L}(\boldsymbol{x})$ satisfies the appropriate constraints.

12.3. A related Γ-operator

The operator $\boldsymbol{\Gamma}_1$ has the natural interpretation as the projection onto the subspaces $\mathcal{E}$ of square integrable fields with zero mean satisfying the same differential constraints as the field $\boldsymbol{E}$. Given a reference medium $\boldsymbol{L}_0$ one can introduce a closely related nonlocal operator $\boldsymbol{\Gamma}$ defined through its action: We say that

$$\boldsymbol{E}' = \boldsymbol{\Gamma}\boldsymbol{P} \text{ if and only if } \boldsymbol{E}' \in \mathcal{E} \text{ and } \boldsymbol{P} - \boldsymbol{L}_0\boldsymbol{E}' \in \mathcal{U} \oplus \mathcal{J}. \tag{12.23}$$

From this definition it is clear that $\boldsymbol{\Gamma}$ can be identified with $\boldsymbol{\Gamma}_1/\sigma_0$ when $\boldsymbol{L}_0 = \sigma_0\boldsymbol{I}$. Even when $\boldsymbol{L}_0 \neq \sigma_0\boldsymbol{I}$ there is still a simple expression for the action of $\boldsymbol{\Gamma}$ in Fourier space. According to (12.23), the Fourier components $\widehat{\boldsymbol{E}}'(\boldsymbol{k})$ and $\widehat{\boldsymbol{P}}(\boldsymbol{k})$ of $\boldsymbol{E}'(\boldsymbol{x})$ and $\boldsymbol{P}(\boldsymbol{x})$ satisfy

$$\boldsymbol{\Gamma}_1(\boldsymbol{k})\widehat{\boldsymbol{E}}'(\boldsymbol{k}) = \widehat{\boldsymbol{E}}'(\boldsymbol{k}) \text{ and } \boldsymbol{\Gamma}_1(\boldsymbol{k})(\widehat{\boldsymbol{P}}(\boldsymbol{k}) - \boldsymbol{L}_0\widehat{\boldsymbol{E}}'(\boldsymbol{k})) = 0 \text{ for all } \boldsymbol{k} \neq 0,$$

and (9.39) and (9.40) imply that

$$\boldsymbol{E}'(\boldsymbol{x}) = \sum_{\boldsymbol{k}\neq 0} e^{i\boldsymbol{k}\cdot\boldsymbol{x}}\widehat{\boldsymbol{E}}'(\boldsymbol{k}) = \sum_{\boldsymbol{k}\neq 0} e^{i\boldsymbol{k}\cdot\boldsymbol{x}}\boldsymbol{\Gamma}(\boldsymbol{k})\widehat{\boldsymbol{P}}(\boldsymbol{k}), \tag{12.24}$$

where, as in (9.40),

$$\boldsymbol{\Gamma}(\boldsymbol{k}) = \boldsymbol{\Gamma}_1(\boldsymbol{k})[\boldsymbol{\Gamma}_1(\boldsymbol{k})\boldsymbol{L}_0\boldsymbol{\Gamma}_1(\boldsymbol{k})]^{-1}\boldsymbol{\Gamma}_1(\boldsymbol{k}),$$

and the inverse is to be taken on the space $\mathcal{E}_{\boldsymbol{k}}$.

It follows that the operator $\boldsymbol{\Gamma}$ satisfies

$$\boldsymbol{\Gamma}\boldsymbol{L}_0\boldsymbol{\Gamma} = \boldsymbol{\Gamma}, \tag{12.25}$$

as observed by Dederichs and Zeller (1972) and Kröner (1972). Also, since $\boldsymbol{L}_0^{1/2}\boldsymbol{\Gamma}(\boldsymbol{k})\boldsymbol{L}_0^{1/2}$ is a projection onto the space $\boldsymbol{L}_0^{1/2}\mathcal{E}_{\boldsymbol{k}}$, its trace is precisely the dimensionality of this space, which is the same as the dimensionality ℓ of the space $\mathcal{E}_{\boldsymbol{k}}$. So we see that

$$\mathrm{Tr}[\boldsymbol{L}_0\boldsymbol{\Gamma}(\boldsymbol{k})] = \ell \ \text{ for all } \boldsymbol{k} \neq 0,$$

and this implies that the operator $\mathrm{Tr}(\boldsymbol{L}_0\boldsymbol{\Gamma})$ has a very simple action on periodic scalar fields $p(\boldsymbol{x})$:

$$\mathrm{Tr}(\boldsymbol{L}_0\boldsymbol{\Gamma})p = \sum_{\boldsymbol{k}\neq 0} e^{i\boldsymbol{k}\cdot\boldsymbol{x}}\,\mathrm{Tr}[\boldsymbol{L}_0\boldsymbol{\Gamma}(\boldsymbol{k})]\widehat{p}(\boldsymbol{k}) = \ell(p - \langle p\rangle), \tag{12.26}$$

in which the $\widehat{p}(\boldsymbol{k})$ are the Fourier components of $p(\boldsymbol{x})$.

12.4. The equation satisfied by the polarization field

The operator $\boldsymbol{\Gamma}$ is particularly useful for finding the equation solved by the polarization field

$$\boldsymbol{P}(\boldsymbol{x}) = (\boldsymbol{L} - \boldsymbol{L}_0)\boldsymbol{E}(\boldsymbol{x}) = \boldsymbol{J}(\boldsymbol{x}) - \boldsymbol{L}_0\boldsymbol{E}(\boldsymbol{x}). \tag{12.27}$$

From the definition of $\boldsymbol{\Gamma}$ we have

$$\boldsymbol{\Gamma}\boldsymbol{P} = \langle\boldsymbol{E}\rangle - \boldsymbol{E}, \tag{12.28}$$

implying that

$$[\boldsymbol{I} + (\boldsymbol{L} - \boldsymbol{L}_0)\boldsymbol{\Gamma}]\boldsymbol{P} = (\boldsymbol{L} - \boldsymbol{L}_0)\langle\boldsymbol{E}\rangle. \tag{12.29}$$

Alternatively this can be rewritten as an equation for $\boldsymbol{E}$,

$$[\boldsymbol{I} + \boldsymbol{\Gamma}(\boldsymbol{L} - \boldsymbol{L}_0)]\boldsymbol{E} = \langle\boldsymbol{E}\rangle,$$

which, as observed by Kröner (1977), has the same form as the Lippmann-Schwinger equation of quantum mechanical scattering theory.

In principle, the field $\boldsymbol{P}$ can be found by taking the inverse of the operator $[\boldsymbol{I}+(\boldsymbol{L}-\boldsymbol{L}_0)\boldsymbol{\Gamma}]$ and applying it to both sides of (12.29), giving

$$\boldsymbol{P} = [\boldsymbol{I} + (\boldsymbol{L} - \boldsymbol{L}_0)\boldsymbol{\Gamma}]^{-1}(\boldsymbol{L} - \boldsymbol{L}_0)\langle\boldsymbol{E}\rangle. \tag{12.30}$$

Once $\boldsymbol{P}$ is found, we can compute the action of $\boldsymbol{L}_*$ on $\langle\boldsymbol{E}\rangle$ from the relation

$$\langle\boldsymbol{P}\rangle = (\boldsymbol{L}_* - \boldsymbol{L}_0)\langle\boldsymbol{E}\rangle, \tag{12.31}$$

which is implied by (12.27).

Now a linear operator $\boldsymbol{A}$ that acts on any field taking values in $\mathcal{T}$ producing a field taking values in $\mathcal{T}$ has a natural extension to an operator, which we will also call $\boldsymbol{A}$, acting on any field $\boldsymbol{Q}(\boldsymbol{x})$ taking values in $\mathcal{T} \otimes \mathcal{T}$ and producing a field $\boldsymbol{R}(\boldsymbol{x})$ taking values in $\mathcal{T} \otimes \mathcal{T}$. Specifically we say that $\boldsymbol{R} = \boldsymbol{A}\boldsymbol{Q}$ if

$$\boldsymbol{R}\boldsymbol{E}_0 = \boldsymbol{A}(\boldsymbol{Q}\boldsymbol{E}_0) \text{ for all } \boldsymbol{E}_0 \in \mathcal{U}. \tag{12.32}$$

For example, if $\boldsymbol{A}$ acts locally in Fourier space, then

$$\boldsymbol{R}(\boldsymbol{x}) = \sum_{\boldsymbol{k}} e^{i\boldsymbol{k}\cdot\boldsymbol{x}} \boldsymbol{A}(\boldsymbol{k})\widehat{\boldsymbol{Q}}(\boldsymbol{k}),$$

where the $\widehat{\boldsymbol{Q}}(\boldsymbol{k})$ are the Fourier components of $\boldsymbol{Q}(\boldsymbol{x})$. When $\boldsymbol{A}(\boldsymbol{k})$ and $\widehat{\boldsymbol{Q}}(\boldsymbol{k})$ are represented by matrices, $\boldsymbol{A}(\boldsymbol{k})\widehat{\boldsymbol{Q}}(\boldsymbol{k})$ is represented as the product of these matrices. By combining (12.30) and (12.31) we see that

$$\boldsymbol{L}_* = \boldsymbol{L}_0 + \langle [\boldsymbol{I} + (\boldsymbol{L} - \boldsymbol{L}_0)\boldsymbol{\Gamma}]^{-1}(\boldsymbol{L} - \boldsymbol{L}_0)\rangle, \tag{12.33}$$

where the operator $\boldsymbol{A} = [\boldsymbol{I} + (\boldsymbol{L} - \boldsymbol{L}_0)\boldsymbol{\Gamma}]^{-1}$ (which is not local in Fourier space) acts on the field $\boldsymbol{L}(\boldsymbol{x}) - \boldsymbol{L}_0$ taking values in $\mathcal{T} \otimes \mathcal{T}$.

12.5. The effective tensor of dilute suspensions of aligned ellipsoids

To calculate the effective tensor of a dilute suspension of aligned ellipsoids we need to solve the problem of a single ellipsoid in a uniform external applied field. The solution to this problem has a long history. For an isotropic conducting (or dielectric or magnetic) ellipsoid in an isotropic matrix, Poisson (1826) recognized that the field inside the ellipsoid must be uniform. Explicit expressions for this field were obtained by Maxwell (1873). The problem of computing the elastic fields around an isotropic ellipsoid in an isotropic matrix was solved much later by Eshelby (1957). For an elastically anisotropic ellipsoid in an elastically anisotropic matrix, the solution follows from the paper of Khachaturyan (1966) [see also Khachaturyan (1983)]. Using Fourier analysis he effectively considers the thermoelastic problem (actually a phase transition problem) with a constant applied temperature difference and no applied external elastic field, and with the inclusion and matrix having the same elasticity tensor $\boldsymbol{\mathcal{C}}_0$ but different thermal expansion coefficients. Since the stress and strain fields within the ellipsoidal inclusion turn out to be constant, one can modify the elastic moduli of the ellipsoid so that the field is not disturbed (see section 8.1 on page 143), and this leads directly to the general solution associated with an elastically anisotropic ellipsoid in an elastically anisotropic matrix with a constant applied field.

Let us first obtain the solution to the field equations for a single spherical inclusion with tensor $\boldsymbol{L}_1$ centered at the origin and with radius r_c embedded in an infinite medium with tensor $\boldsymbol{L}_0$ such that the field $\boldsymbol{E}(\boldsymbol{x})$ approaches a constant field $\boldsymbol{E}_0$ as $\boldsymbol{x}$ approaches infinity. Willis (1976, 1981, 1982) has shown that a general solution to this problem can be obtained based on a plane-wave decomposition of the delta function and the associated solution for the infinite body Green's function for the potential. Here we take a different but related approach that avoids the need for introducing Green's functions.

With $\boldsymbol{L}_0$ as our reference medium the polarization field $\boldsymbol{P}(\boldsymbol{x}) = (\boldsymbol{L}(\boldsymbol{x}) - \boldsymbol{L}_0)\boldsymbol{E}(\boldsymbol{x})$ is clearly zero outside the inclusion. Guided by the solution to the conductivity problem one

might suspect that $\boldsymbol{P}(\boldsymbol{x})$ takes a constant value $\boldsymbol{P}_1$ inside the inclusion and is zero outside the inclusion. We decompose $\boldsymbol{P}(\boldsymbol{x})$ into its plane-wave expansion:

$$\boldsymbol{P}(\boldsymbol{x}) = \langle f(\boldsymbol{x}\cdot\boldsymbol{n})\boldsymbol{P}_1\rangle_{\boldsymbol{n}},$$

where the angular brackets $\langle\cdot\rangle_{\boldsymbol{n}}$ denote an average over the surface $|\boldsymbol{n}| = 1$ of the unit ball, that is,

$$\langle f(\boldsymbol{x}\cdot\boldsymbol{n})\boldsymbol{P}_1\rangle_{\boldsymbol{n}} = \frac{1}{4\pi}\int_{|\boldsymbol{n}|=1} f(\boldsymbol{x}\cdot\boldsymbol{n})\boldsymbol{P}_1,$$

in which 4π is the surface area of the unit ball. The function $f(y)$ appearing here is given by

$$f(y) = f(-y) = h(y) - r_c\delta(y - r_c) - r_c\delta(y + r_c),$$

in which $\delta(y - r_c)$ and $\delta(y + r_c)$ are Dirac delta functions centered at $y = r_c$ and at $y = -r_c$, and $h(y)$ is the characteristic function

$$\begin{aligned} h(y) &= 1 \quad \text{when } |y| < r_c, \\ &= 0 \quad \text{when } |y| \geq r_c. \end{aligned}$$

Although the plane waves have delta function singularities when $|\boldsymbol{x}\cdot\boldsymbol{n}| = r_c$, these singularities are washed out when the average over $\boldsymbol{n}$ is taken. Letting θ parameterize the angle between $\boldsymbol{n}$ and $\boldsymbol{x}$, the form of $f(y)$ guarantees that

$$\boldsymbol{P}(\boldsymbol{x}) = \langle f(\boldsymbol{x}\cdot\boldsymbol{n})\boldsymbol{P}_1\rangle_{\boldsymbol{n}} = \frac{\boldsymbol{P}_1}{2}\int_0^\pi f(|\boldsymbol{x}|\cos\theta)\sin\theta\, d\theta = \frac{\boldsymbol{P}_1}{2|\boldsymbol{x}|}\int_{-|\boldsymbol{x}|}^{|\boldsymbol{x}|} f(y)dy$$

takes the value $\boldsymbol{P}_1$ when $|\boldsymbol{x}| < r_c$ and is zero when $|\boldsymbol{x}| > r_c$, as desired.

From (12.24) (generalized to allow for Fourier transforms and not just Fourier series) and from the plane-wave expansion for $\boldsymbol{P}(\boldsymbol{x})$ we deduce that $\boldsymbol{E} = \boldsymbol{E}_0 - \boldsymbol{\Gamma}\boldsymbol{P}$ and $\boldsymbol{J} = \boldsymbol{P} + \boldsymbol{L}_0\boldsymbol{E}$ have the plane-wave expansions

$$\begin{aligned} \boldsymbol{E}(\boldsymbol{x}) &= \boldsymbol{E}_0 - \langle f(\boldsymbol{x}\cdot\boldsymbol{n})\boldsymbol{\Gamma}(\boldsymbol{n})\boldsymbol{P}_1\rangle_{\boldsymbol{n}}, \\ \boldsymbol{J}(\boldsymbol{x}) &= \boldsymbol{L}_0\boldsymbol{E}_0 + \langle f(\boldsymbol{x}\cdot\boldsymbol{n})(\boldsymbol{I} - \boldsymbol{L}_0\boldsymbol{\Gamma}(\boldsymbol{n}))\boldsymbol{P}_1\rangle_{\boldsymbol{n}}, \end{aligned} \tag{12.34}$$

which guarantee that they satisfy the required differential constraints. The constitutive law is automatically satisfied outside the sphere because $\boldsymbol{P}(\boldsymbol{x}) = 0$ there. Inside the sphere the fields $\boldsymbol{E}(\boldsymbol{x})$ and $\boldsymbol{J}(\boldsymbol{x})$ take constant values,

$$\boldsymbol{E}_1 = \boldsymbol{E}_0 - \boldsymbol{\gamma}\boldsymbol{P}_1 \text{ and } \boldsymbol{J}_1 = \boldsymbol{L}_0\boldsymbol{E}_0 + (\boldsymbol{I} - \boldsymbol{L}_0\boldsymbol{\gamma})\boldsymbol{P}_1,$$

where

$$\boldsymbol{\gamma} = \langle\boldsymbol{\Gamma}(\boldsymbol{n})\rangle_{\boldsymbol{n}} \tag{12.35}$$

is the average of $\boldsymbol{\Gamma}(\boldsymbol{n})$ over all directions of the unit vector $\boldsymbol{n}$. So the constitutive relation $\boldsymbol{J}_1 = \boldsymbol{L}_1\boldsymbol{E}_1$ will be satisfied provided that we choose

$$\boldsymbol{P}_1 = [(\boldsymbol{L}_1 - \boldsymbol{L}_0)^{-1} + \boldsymbol{\gamma}]^{-1}\boldsymbol{E}_0, \tag{12.36}$$

where we have assumed, for simplicity, that $\boldsymbol{L}_1 - \boldsymbol{L}_0$ is nonsingular.

The solution for $\boldsymbol{E}(\boldsymbol{x})$ has one property that follows from the fact that $\langle f(\boldsymbol{x}\cdot\boldsymbol{n})\rangle_{\boldsymbol{n}}$ is zero when $|\boldsymbol{x}| > r_c$. This implies that with $\boldsymbol{n}$ held fixed the average of $f(\boldsymbol{x}\cdot\boldsymbol{n})$ and hence of $\boldsymbol{E}(\boldsymbol{x}) - \boldsymbol{E}_0$ around the ball $|\boldsymbol{x}| = r > r_c$ must vanish:

$$\int_{|\boldsymbol{x}|=r} \boldsymbol{E}(\boldsymbol{x}) - \boldsymbol{E}_0 = 0 \quad \text{when } r > r_c. \tag{12.37}$$

Thus we have constructed fields $\boldsymbol{E}(\boldsymbol{x})$ and $\boldsymbol{J}(\boldsymbol{x})$ given by (12.34) that satisfy the required differential constraints and the constitutive relation both inside and outside the sphere. For an anisotropic elastic spherical inclusion in an anisotropic elastic matrix this is the solution of Kneer (1965). From the solution we conclude that the field inside the sphere is uniform when the applied field is uniform [see also Korringa, Lin, and Mills (1978), who provide a direct explanation of the uniformity of the field based on properties of the Green's function]. More generally, for an elastically isotropic ellipsoidal inclusion in an elastically isotropic matrix, Eshelby (1961) showed that the field in the ellipsoid is polynomial when the applied field is polynomial. Kunin and Sosnina (1971) extended this result to elastically anisotropic ellipsoidal inclusions in an elastically anisotropic matrix; see also Asaro and Barnett (1975) and Willis (1975).

Since $f(y)$ is zero when $y > 1$, only those plane-wave fields with $\boldsymbol{x}\cdot\boldsymbol{n} \le r_c$ contribute to $\boldsymbol{E}(\boldsymbol{x})$. When $\boldsymbol{x}$ is large this forces $\boldsymbol{n}$ to be almost perpendicular to $\boldsymbol{x}$, and to a good approximation we have

$$\boldsymbol{E}(\boldsymbol{x}) \approx \boldsymbol{E}_0 - (4\pi r_c^3/3)\boldsymbol{\Gamma}_\infty(\boldsymbol{x})\boldsymbol{P}_1 \quad \text{when } |\boldsymbol{x}| \gg r_c, \tag{12.38}$$

where

$$\boldsymbol{\Gamma}_\infty(\boldsymbol{x}) = \frac{-1}{4\pi|\boldsymbol{x}|^5}\langle \boldsymbol{x}\cdot\frac{d^2\boldsymbol{\Gamma}(\boldsymbol{n}/|\boldsymbol{n}|)}{d\boldsymbol{n}^2}\boldsymbol{x}\rangle_{\boldsymbol{n}\perp\boldsymbol{x}}, \tag{12.39}$$

in which the average is over all unit vectors $\boldsymbol{n}$ perpendicular to $\boldsymbol{x}$. Clearly $\boldsymbol{E}(\boldsymbol{x})$ approaches $\boldsymbol{E}_0$ as $\boldsymbol{x}$ approaches infinity.

As an example, consider a sphere of radius r_c with conductivity tensor $\sigma_1\boldsymbol{I}$ embedded in a matrix with conductivity tensor $\boldsymbol{L}_0 = \sigma_0\boldsymbol{I}$. The electric field $\boldsymbol{e}(\boldsymbol{x})$ can be found explicitly and is a combination of uniform and dipolar fields. It is given by the formula

$$\begin{aligned}\boldsymbol{e}(\boldsymbol{x}) &= \boldsymbol{P}_1/(\sigma_1-\sigma_0) \quad \text{when } |\boldsymbol{x}| < r_c,\\ &= [1/(\sigma_1-\sigma_0) + 1/3\sigma_0]\boldsymbol{P}_1 + r_c^3[3\boldsymbol{x}\otimes\boldsymbol{x} - |\boldsymbol{x}|^2\boldsymbol{I}]\boldsymbol{P}_1/3\sigma_0|\boldsymbol{x}|^5 \quad \text{when } |\boldsymbol{x}| \ge r_c,\end{aligned}$$

when expressed in terms of the constant polarization field $\boldsymbol{P}_1 = (\sigma_1-\sigma_0)\boldsymbol{e}$ inside the sphere. Now, since $\boldsymbol{\Gamma}(\boldsymbol{n}/|\boldsymbol{n}|) = \boldsymbol{n}\otimes\boldsymbol{n}/\sigma_0|\boldsymbol{n}|^2$, we have $\langle\boldsymbol{\Gamma}(\boldsymbol{n})\rangle_{\boldsymbol{n}} = \boldsymbol{I}/3\sigma_0$ and

$$\boldsymbol{x}\cdot\frac{d^2\boldsymbol{\Gamma}(\boldsymbol{n}/|\boldsymbol{n}|)}{d\boldsymbol{n}^2}\boldsymbol{x} = 2\boldsymbol{x}\otimes\boldsymbol{x}/\sigma_0 - 2\boldsymbol{n}\otimes\boldsymbol{n}|\boldsymbol{x}|^2/\sigma_0$$

for all unit vectors $\boldsymbol{n}$ perpendicular to $\boldsymbol{x}$. Averaging over $\boldsymbol{n}$ perpendicular to $\boldsymbol{x}$ gives

$$\boldsymbol{\Gamma}_\infty(\boldsymbol{x}) = \frac{|\boldsymbol{x}|^2\boldsymbol{I} - 3\boldsymbol{x}\otimes\boldsymbol{x}}{4\pi\sigma_0|\boldsymbol{x}|^5}.$$

Thus we see that

$$\boldsymbol{e}(\boldsymbol{x}) = [\boldsymbol{I}/(\sigma_1-\sigma_0) + \langle\boldsymbol{\Gamma}(\boldsymbol{n})\rangle_{\boldsymbol{n}}]\boldsymbol{P}_1 - (4\pi r_c^3/3)\boldsymbol{\Gamma}_\infty(\boldsymbol{x})\boldsymbol{P}_1 \quad \text{when } |\boldsymbol{x}| \ge r_c.$$

Hence for the conductivity problem relation (12.36) holds and (12.38) is satisfied as an equality for all $|\boldsymbol{x}| \geq r_c$.

If the inclusion is not a sphere but instead an ellipsoid with boundary $|\boldsymbol{B}\boldsymbol{x}| = 1$, then following Willis (1981, 1982) we make an affine transformation from $\boldsymbol{x}$ to $\boldsymbol{x}' = \boldsymbol{B}\boldsymbol{x}$ in order to transform the ellipsoid to the unit sphere. Any field that is constant in the plane $\boldsymbol{x} \cdot \boldsymbol{n} = k$ transforms to a field that is constant in the plane $\boldsymbol{x}' \cdot \boldsymbol{n}' = k$, where $\boldsymbol{n}' = (\boldsymbol{B}^{-1})^T \boldsymbol{n}$. Consequently the operator $\boldsymbol{\Gamma}(\boldsymbol{n})$ transforms to

$$\boldsymbol{\Gamma}'(\boldsymbol{n}') = \boldsymbol{\Gamma}(\boldsymbol{B}^T \boldsymbol{n}').$$

The solutions $\boldsymbol{E}'(\boldsymbol{x}')$ and $\boldsymbol{J}'(\boldsymbol{x}')$ for the fields associated with the spherical inclusion in the transformed problem give us the solutions

$$\boldsymbol{E}(\boldsymbol{x}) = \boldsymbol{E}'(\boldsymbol{B}\boldsymbol{x}), \qquad \boldsymbol{J}(\boldsymbol{x}) = \boldsymbol{J}'(\boldsymbol{B}\boldsymbol{x})$$

for the fields associated with the ellipsoidal inclusion. Inside the ellipse the fields are constant and the polarization field $\boldsymbol{P}(\boldsymbol{x}) = (\boldsymbol{L}_1 - \boldsymbol{L}_0)\boldsymbol{E}(\boldsymbol{x})$ takes the value

$$\boldsymbol{P}_1 = [(\boldsymbol{L}_1 - \boldsymbol{L}_0)^{-1} + \boldsymbol{\gamma}_B]^{-1} \boldsymbol{E}_0,$$

in which $\boldsymbol{E}_0$ is the value of $\boldsymbol{E}(\boldsymbol{x})$ as $\boldsymbol{x}$ approaches ∞ and

$$\boldsymbol{\gamma}_B = \langle \boldsymbol{\Gamma}'(\boldsymbol{n}') \rangle_{\boldsymbol{n}'} = \langle \boldsymbol{\Gamma}(\boldsymbol{B}^T \boldsymbol{n}') \rangle_{\boldsymbol{n}'}, \tag{12.40}$$

where the average is over the surface $|\boldsymbol{n}'| = 1$ of the unit ball.

For an isotropic matrix with conductivity $\sigma_0 \boldsymbol{I}$ containing an isotropic ellipsoidal conducting inclusion aligned with the coordinate axes it is well known that

$$\boldsymbol{\gamma}_B = \frac{\boldsymbol{D}}{\sigma_0} \equiv \frac{1}{\sigma_0} \begin{pmatrix} d_1 & 0 & 0 \\ 0 & d_2 & 0 \\ 0 & 0 & d_3 \end{pmatrix},$$

where $\boldsymbol{D}$ is the depolarization tensor and d_1, d_2, and d_3 are the depolarization factors of the ellipsoid given by (7.53) or (7.69). Explicit formulas for $\boldsymbol{\gamma}_B$ have been calculated by Eshelby (1957) for an elastically isotropic ellipsoidal inclusion in an elastically isotropic matrix; by Deeg (1980), Dunn and Taya (1993), and Wang (1992) for ellipsoidal inclusions in a piezoelectric matrix; and by Berryman (1997) for ellipsoidal inclusions in a poroelastic or thermoelastic matrix. Walpole (1991) considered the problem of a rigid ellipsoidal inclusion rotated in an elastic medium.

Now consider a composite comprised of a well-separated dilute suspension of these ellipsoids embedded in a matrix with tensor $\boldsymbol{L}_0$, and let $\boldsymbol{E}_0 = \langle \boldsymbol{E} \rangle$ denote the average field in the composite. As a first approximation, the field acting on each ellipsoid can be equated with $\boldsymbol{E}_0$ and the average of the polarization field in the composite can be equated with $f_1 \boldsymbol{P}_1$, where f_1 is the volume fraction occupied by the ellipsoids. Since the average polarization field can also be equated with $(\boldsymbol{L}_* - \boldsymbol{L}_0)\boldsymbol{E}_0$, we obtain from (12.36) the formula

$$\boldsymbol{L}_* \approx \boldsymbol{L}_0 + f_1[(\boldsymbol{L}_1 - \boldsymbol{L}_0)^{-1} + \langle \boldsymbol{\Gamma}(\boldsymbol{B}^T \boldsymbol{n}') \rangle_{\boldsymbol{n}'}]^{-1} \tag{12.41}$$

for the effective tensor $\boldsymbol{L}_*$, which is correct to the first order in the volume fraction. For comparison, a coated laminate with a core of phase 1 with tensor $\boldsymbol{L}_1$ coated by a material with tensor $\boldsymbol{L}_0$ has to the first order in the volume fraction f_1 an effective tensor $\boldsymbol{L}_*$ given by

$$\boldsymbol{L}_* \approx \boldsymbol{L}_0 + f_1[(\boldsymbol{L}_1 - \boldsymbol{L}_0)^{-1} + \sum_{j=1}^{m} c_j \boldsymbol{\Gamma}(\boldsymbol{n}_j)]^{-1}.$$

So we see that coated laminates can mimic the effective tensor of a dilute suspension of ellipsoids to the first order in the volume fraction.

Having obtained the effective tensor for a dilute suspension of ellipsoids one can immediately write the formula

$$\sum_{i=1}^{n} f_i[(\boldsymbol{L}_i - \boldsymbol{L}_*)^{-1} + \langle \boldsymbol{\Gamma}_*(\boldsymbol{B}_i^T \boldsymbol{n}')\rangle_{\boldsymbol{n}'}]^{-1} = 0$$

of Willis (1977), which when solved for $\boldsymbol{L}_*$ with

$$\boldsymbol{\Gamma}_*(\boldsymbol{n}) = \boldsymbol{\Gamma}_1(\boldsymbol{n})[\boldsymbol{\Gamma}_1(\boldsymbol{n})\boldsymbol{L}_*\boldsymbol{\Gamma}_1(\boldsymbol{n})]^{-1}\boldsymbol{\Gamma}_1(\boldsymbol{n})$$

gives the effective medium approximation for the effective tensor of an aggregate of ellipsoidal grains of n different phases with tensors $\boldsymbol{L}_1, \boldsymbol{L}_2, \ldots, \boldsymbol{L}_n$ mixed in proportions $f_1, f_2, \ldots, f_n$. The ellipsoidal grains of phase i are assumed to all have the same eccentricity and orientation with surfaces described by the equation $|\boldsymbol{B}_i(\boldsymbol{x} - \boldsymbol{x}_j)| = a_j$, where the center $\boldsymbol{x}_j$ and size parameter a_j vary from grain to grain, while the matrix $\boldsymbol{B}_i$ only varies from phase to phase. For aggregates of spherical grains this reduces to the formula

$$\sum_{i=1}^{n} f_i[(\boldsymbol{L}_i - \boldsymbol{L}_*)^{-1} + \langle \boldsymbol{\Gamma}_*(\boldsymbol{n})\rangle_{\boldsymbol{n}}]^{-1} = 0. \tag{12.42}$$

As an example, consider a dilute suspension of spherical grains of an isotropic material with bulk modulus κ_1 and shear modulus μ_1 embedded in an isotropic matrix with bulk modulus κ_0 and shear modulus μ_0. The fourth-order tensor $\langle \boldsymbol{\Gamma}(\boldsymbol{n})\rangle_{\boldsymbol{n}}$ is rotationally invariant with elements

$$\begin{aligned}\langle \Gamma_{ij\ell m}(\boldsymbol{n})\rangle_{\boldsymbol{n}} &= \frac{3\langle n_i n_j n_\ell n_m\rangle_{\boldsymbol{n}}}{3\kappa_0 + 4\mu_0} \\ &\quad + \frac{1}{4\mu_0}\langle n_i\delta_{j\ell}n_m + n_i\delta_{jm}n_\ell + n_j\delta_{i\ell}n_m + n_j\delta_{im}n_\ell - 4n_i n_j n_\ell n_m\rangle_{\boldsymbol{n}} \\ &= \alpha_1\delta_{ij}\delta_{\ell m}/3 + \alpha_2(\delta_{i\ell}\delta_{jm} + \delta_{im}\delta_{j\ell})/2,\end{aligned} \tag{12.43}$$

where the constants α_1 and α_2 can be determined by contracting indices in the above equation, giving

$$\alpha_1 = \frac{-(3\kappa_0 + \mu_0)}{5\mu_0(3\kappa_0 + 4\mu_0)}, \qquad \alpha_2 = \frac{3(\kappa_0 + 2\mu_0)}{5\mu_0(3\kappa_0 + 4\mu_0)}. \tag{12.44}$$

Consequently (12.41), with $\boldsymbol{B} = \boldsymbol{I}$, implies that to the first order in volume fraction the effective bulk and shear moduli are given by the formulas

$$\begin{aligned}\kappa_* &\approx \kappa_0 + \frac{f_1}{1/(\kappa_1 - \kappa_0) + 3(\alpha_1 + \alpha_2)} = \kappa_0 + \frac{f_1}{1/(\kappa_1 - \kappa_0) + 3/(3\kappa_0 + 4\mu_0)}, \\ \mu_* &\approx \mu_0 + \frac{f_1}{1/(\mu_1 - \mu_0) + 2\alpha_2} = \mu_0 + \frac{f_1}{1/(\mu_1 - \mu_0) + 6(\kappa_0 + 2\mu_0)/5\mu_0(3\kappa_0 + 4\mu_0)}\end{aligned}$$

of Bruggeman (1937) and Oldroyd (1956), respectively. [Oldroyd considered an elastic body containing a dilute concentration of spherical cavities filled with viscous fluid, but due to the correspondence principle (see section 11.4 on page 233) his result extends immediately to spherical elastic inclusions.] For ellipsoidal inclusions of an isotropic phase in an isotropic matrix the analogous approximation for the effective elasticity tensor was obtained by Eshelby (1957). The effective medium approximation (12.42) for elasticity with $\langle \boldsymbol{\Gamma}_*(\boldsymbol{n})\rangle_{\boldsymbol{n}}$ being given by (12.43), but with κ_0 and μ_0 being replaced by κ_* and μ_*, yields the formulas (10.45).

12.6. Expressions for the action of the Γ-operators in real space

The formula (12.24) for computing $\boldsymbol{E}' = \boldsymbol{\Gamma P}$ requires one to evaluate the Fourier components of $\boldsymbol{P}(\boldsymbol{x})$, apply $\boldsymbol{\Gamma}(\boldsymbol{k})$ to each Fourier component, and then sum the resulting Fourier series. Rather than doing these computations it is sometimes preferable to work directly in real space.

Clearly the value of the field $\boldsymbol{E}'$ at a point $\boldsymbol{x}$ depends on the value of $\boldsymbol{P}$, not just at the point $\boldsymbol{x}$ but also on its value at surrounding points $\boldsymbol{x}'$. In other words, $\boldsymbol{\Gamma}$ acts nonlocally in real space. Since $\boldsymbol{\Gamma}$ is a linear operator, we deduce that there must exist an tensor-valued integral kernel, $\boldsymbol{\Gamma}_\Omega(\boldsymbol{x}, \boldsymbol{x}')$, that is periodic both in $\boldsymbol{x}$ and in $\boldsymbol{x}'$ with unit cell Ω, and such that

$$\boldsymbol{E}'(\boldsymbol{x}) = \int_\Omega d\boldsymbol{x}' \boldsymbol{\Gamma}_\Omega(\boldsymbol{x}, \boldsymbol{x}') \boldsymbol{P}(\boldsymbol{x}'). \tag{12.45}$$

In fact, this integral kernel can depend only on the difference $\boldsymbol{y} = \boldsymbol{x} - \boldsymbol{x}'$, that is,

$$\boldsymbol{\Gamma}_\Omega(\boldsymbol{x}, \boldsymbol{x}') = \boldsymbol{\Gamma}_\Omega(\boldsymbol{y}), \quad \text{where } \boldsymbol{y} = \boldsymbol{x} - \boldsymbol{x}',$$

because the action of $\boldsymbol{\Gamma}$ on the shifted field $\boldsymbol{P}(\boldsymbol{x} + \boldsymbol{a})$ will produce a correspondingly shifted field $\boldsymbol{E}'(\boldsymbol{x}+\boldsymbol{a})$ for all choices of the shift $\boldsymbol{a}$. Special care is required to evaluate the integral in (12.45) due to the singular behavior of $\boldsymbol{\Gamma}_\Omega(\boldsymbol{x} - \boldsymbol{x}')$ near $\boldsymbol{x} = \boldsymbol{x}'$. As a result of this singularity the integral should be interpreted in the sense of generalized functions.

There is some freedom in the choice of our unit cell of periodicity, since a function that is periodic with a unit cell Ω will also be periodic in a unit cell $k\Omega$ with the same center as Ω obtained by multiplying all of the dimensions of Ω by some large odd integer k. Let us use this freedom to our advantage and replace Ω by $k\Omega$ in the above equations, keeping $\boldsymbol{x}$ inside Ω. Also, since $\boldsymbol{\Gamma}$ annihilates constant fields, let us replace $\boldsymbol{P}(\boldsymbol{x}')$ with $\widetilde{\boldsymbol{P}}(\boldsymbol{x}') = \boldsymbol{P}(\boldsymbol{x}') - \langle \boldsymbol{P} \rangle$. Then the contribution to $\boldsymbol{E}'(\boldsymbol{x})$ from unit cells outside $k\Omega$ will be negligible for large enough k. Finally, let us assume that $\boldsymbol{P}(\boldsymbol{x}')$ is smooth, or at least piecewise smooth.

To evaluate the action of $\boldsymbol{\Gamma}$ on $\widetilde{\boldsymbol{P}}(\boldsymbol{x}')$ we follow an argument that is similar to one used by Bruno, Reitich, and Leo (1996) to numerically evaluate the action of $\boldsymbol{\Gamma}$. We subdivide $k\Omega$ into small spherical regions ranging to the infinitesimally small and filling all of $k\Omega$. We choose the spherical regions sufficiently small so that $\boldsymbol{P}(\boldsymbol{x}')$ is essentially constant over each sphere and so that one sphere $\Theta(\epsilon)$ with radius ϵ is centered at $\boldsymbol{x}$ and is surrounded by spheres with radii much smaller than ϵ (see figure 12.1 on the following page). Since $\boldsymbol{\Gamma}$ is a linear operator, we can add the contributions from each sphere separately. When appropriately translated and rescaled, the field $-\boldsymbol{E}(\boldsymbol{x})$ in (12.34) with $\boldsymbol{E}_0 = 0$ gives the contribution from each sphere provided that $\boldsymbol{P}_1$ is set equal to the polarization field in that sphere. Since the spheres surrounding $\Theta(\epsilon)$ have radii much less than ϵ, we can use approximation (12.38) to evaluate their contribution. The sphere $\Theta(\epsilon)$ will give a contribution $\boldsymbol{\gamma}\widetilde{\boldsymbol{P}}(\boldsymbol{x})$.

In the limit as k goes to infinity and the sphere radii shrink to zero we find that (12.45) reduces to the formula

$$\boldsymbol{E}'(\boldsymbol{x}) = \boldsymbol{\gamma}\widetilde{\boldsymbol{P}}(\boldsymbol{x}) + \lim_{\epsilon \to 0} \int_{\mathbb{R}^d \setminus \Theta(\epsilon)} d\boldsymbol{y}\, \boldsymbol{\Gamma}_\infty(\boldsymbol{y}) \widetilde{\boldsymbol{P}}(\boldsymbol{x} - \boldsymbol{y}), \tag{12.46}$$

where

$$\widetilde{\boldsymbol{P}}(\boldsymbol{x}) = \boldsymbol{P}(\boldsymbol{x}) - \langle \boldsymbol{P} \rangle, \qquad \boldsymbol{y} = \boldsymbol{x} - \boldsymbol{x}', \qquad \boldsymbol{\gamma} = \langle \boldsymbol{\Gamma}(\boldsymbol{n}) \rangle \boldsymbol{n}.$$

Here the integral is now over all space excluding the sphere $\Theta(\epsilon)$ of radius ϵ centered at the origin $\boldsymbol{y} = 0$. The leading term $\boldsymbol{\gamma}\widetilde{\boldsymbol{P}}(\boldsymbol{x})$ represents the contribution from this sphere $\Theta(\epsilon)$.

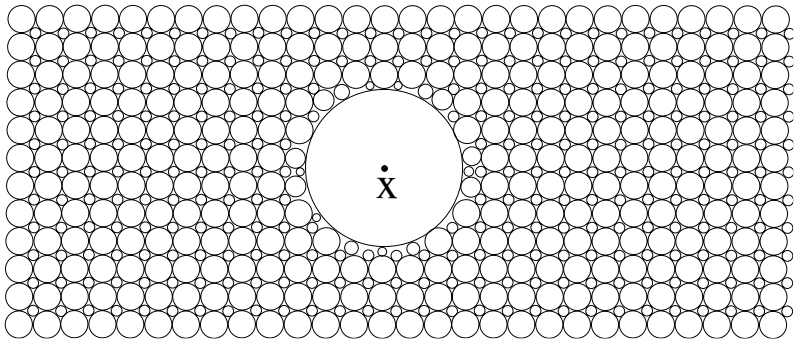

Figure 12.1. To calculate, at the point $\boldsymbol{x}$, the field $\boldsymbol{E}'$ resulting from the action of $\boldsymbol{\Gamma}$ on a smooth periodic field $\widetilde{\boldsymbol{P}}$ with zero average value, we partition the space into spheres that fill all space and then add the contributions from each sphere. The sphere centered at $\boldsymbol{x}$ has radius much smaller than the length scale of variation of $\widetilde{\boldsymbol{P}}$ and is surrounded by much smaller spheres. The partitioning is periodic, with periodicity much larger than the periodicity of $\widetilde{\boldsymbol{P}}$.

The tensor-valued integral kernel $\boldsymbol{\Gamma}_\infty(\boldsymbol{y})$ given by (12.39) satisfies the symmetry and scaling relations,

$$\boldsymbol{\Gamma}_\infty(-\boldsymbol{y}) = \boldsymbol{\Gamma}_\infty(\boldsymbol{y}), \quad \boldsymbol{\Gamma}_\infty(\boldsymbol{y}) = |\boldsymbol{y}|^{-d}\boldsymbol{\Gamma}_\infty(\boldsymbol{y}/|\boldsymbol{y}|), \tag{12.47}$$

and has the additional property that its average over the surface of the unit ball vanishes:

$$\int_{|\boldsymbol{\eta}|=1} \boldsymbol{\Gamma}_\infty(\boldsymbol{\eta}) = 0, \quad \text{where } \boldsymbol{\eta} = \boldsymbol{y}/|\boldsymbol{y}|. \tag{12.48}$$

This last property is a corollary of (12.37) and (12.38). These relations satisfied by $\boldsymbol{\Gamma}_\infty(\boldsymbol{y})$ turn out to have a natural significance: We will see shortly that they ensure that the action of $\boldsymbol{\Gamma}$ is scale and reflection invariant, in the sense that $\boldsymbol{\Gamma}$ applied to $\boldsymbol{P}(\boldsymbol{x}/\lambda)$ produces the field $\boldsymbol{E}'(\boldsymbol{x}/\lambda)$ for all choices of the constant $\lambda \neq 0$.

As an example, if we consider the problem of three-dimensional conductivity and take an isotropic reference medium of conductivity $\boldsymbol{L}_0 = \sigma_0 \boldsymbol{I}$, then we have

$$\boldsymbol{\gamma} = \frac{\boldsymbol{I}}{3\sigma_0}, \quad \boldsymbol{\Gamma}_\infty(\boldsymbol{y}) = \frac{|\boldsymbol{y}|^2\boldsymbol{I} - 3\boldsymbol{y}\otimes\boldsymbol{y}}{4\pi\sigma_0|\boldsymbol{y}|^5}, \tag{12.49}$$

and consequently the operator $\boldsymbol{\Gamma}$ acting on a polarization field $\boldsymbol{P}(\boldsymbol{x})$ produces an electric field

$$\boldsymbol{e}'(\boldsymbol{x}) = \frac{\widetilde{\boldsymbol{P}}(\boldsymbol{x})}{3\sigma_0} + \lim_{\epsilon\to 0}\int_{\mathbb{R}^d\setminus\Theta(\epsilon)} d\boldsymbol{y}\left[\frac{|\boldsymbol{y}|^2\boldsymbol{I} - 3\boldsymbol{y}\otimes\boldsymbol{y}}{4\pi\sigma_0|\boldsymbol{y}|^5}\right]\widetilde{\boldsymbol{P}}(\boldsymbol{x}-\boldsymbol{y}).$$

For three-dimensional elasticity with an isotropic reference medium with bulk modulus κ_0 and shear modulus μ_0, the fourth-order tensor $\boldsymbol{\gamma} = \langle\boldsymbol{\Gamma}(\boldsymbol{n})\rangle_{\boldsymbol{n}}$ is given by (12.43) and (12.44), and Willis (1987) and Torquato (1997) among others provide a formula for $\boldsymbol{\Gamma}_\infty(\boldsymbol{y})$.

In order for $\boldsymbol{\Gamma}$ to satisfy the trace constraint (12.26), the tensor $\boldsymbol{\gamma}$ and the integral kernel $\boldsymbol{\Gamma}_\infty(\boldsymbol{y})$ must have the additional property that

$$\mathrm{Tr}(\boldsymbol{L}_0\boldsymbol{\gamma}) = \ell, \quad \mathrm{Tr}[\boldsymbol{L}_0\boldsymbol{\Gamma}_\infty(\boldsymbol{y})] = 0 \ \text{ for all } \boldsymbol{y}.$$

In our conductivity example (12.49), the tensor $\boldsymbol{\gamma}$ and the integral kernel $\boldsymbol{\Gamma}_\infty(\boldsymbol{y})$ clearly have this property, with $\ell = 1$.

It is vitally important when evaluating the integral in (12.46) to exclude the infinitesimal ball $\Theta(\epsilon)$. Indeed the scaling behavior (12.47) of $\boldsymbol{\Gamma}_\infty(\boldsymbol{y})$ implies that this integral is conditionally convergent: If we had taken $\Theta(\epsilon)$ to be an infinitesimal ellipse or other shaped region, then the value of integral would change, and accordingly $\boldsymbol{\gamma}$ would also take a different value to compensate for this change. The only exception to this occurs at those points $\boldsymbol{x}$ where $\boldsymbol{P}(\boldsymbol{x}) = \langle \boldsymbol{P} \rangle$. At such points the scaling relation (12.47) implies that the integrand has an integrable singularity of order $|\boldsymbol{y}|^{d-1}$ at those points $\boldsymbol{x}$ where $\boldsymbol{P}(\boldsymbol{x}) = \langle \boldsymbol{P} \rangle$, assuming that $\boldsymbol{P}(\boldsymbol{x})$ has a Taylor series expansion around these points.

There is a simple way to avoid these problems of conditional convergence that necessitate writing (12.46) as a limit. In view of the property (12.48) of $\boldsymbol{\Gamma}_\infty(\boldsymbol{y})$ we can rewrite (12.46) as

$$\boldsymbol{E}'(\boldsymbol{x}) = \boldsymbol{\gamma}\widetilde{\boldsymbol{P}}(\boldsymbol{x}) + \int_{\mathbb{R}^d} d\boldsymbol{y}\boldsymbol{\Gamma}_\infty(\boldsymbol{y})[\boldsymbol{P}(\boldsymbol{x}-\boldsymbol{y}) - \boldsymbol{Q}(|\boldsymbol{y}|, \boldsymbol{x})],$$

in which $\boldsymbol{Q}(r, \boldsymbol{x})$ is any smooth normalizing function satisfying

$$\boldsymbol{Q}(0, \boldsymbol{x}) = \boldsymbol{P}(\boldsymbol{x}), \quad \lim_{r\to\infty} \boldsymbol{Q}(r, \boldsymbol{x}) = \langle \boldsymbol{P} \rangle.$$

Now the dependence on the matrix $\boldsymbol{\gamma}$ arises not because of conditional convergence, but rather because of the radially symmetric form of the normalizing function.

For example, a suitable choice of the normalizing function is

$$\boldsymbol{Q}(r, \boldsymbol{x}) = \langle \boldsymbol{P} \rangle + e^{-\alpha r^2}[\boldsymbol{P}(\boldsymbol{x}) - \langle \boldsymbol{P} \rangle],$$

where α is a positive constant. Thus, in a three-dimensional medium with conductivity tensor $\sigma_0 \boldsymbol{I}$ the operator $\boldsymbol{\Gamma}$ acting on a smooth polarization field $\boldsymbol{P}(\boldsymbol{x})$ produces an electric field

$$\boldsymbol{e}'(\boldsymbol{x}) = \frac{\widetilde{\boldsymbol{P}}(\boldsymbol{x})}{3\sigma_0} + \int_{\mathbb{R}^d} d\boldsymbol{y}\left[\frac{|\boldsymbol{y}|^2\boldsymbol{I} - 3\boldsymbol{y}\otimes\boldsymbol{y}}{4\pi\sigma_0|\boldsymbol{y}|^5}\right]\left[\widetilde{\boldsymbol{P}}(\boldsymbol{x}-\boldsymbol{y}) - e^{-\alpha|\boldsymbol{y}|^2}\widetilde{\boldsymbol{P}}(\boldsymbol{x})\right].$$

Of course there are many alternative choices for the normalizing function, and these will lead to other integral expressions.

Now that we have an absolutely convergent expression we can perform the integral over $r = |\boldsymbol{y}|$ before computing the integral over $\boldsymbol{\eta} = \boldsymbol{y}/|\boldsymbol{y}|$. This gives

$$\boldsymbol{E}'(\boldsymbol{x}) = \boldsymbol{\gamma}[\boldsymbol{P}(\boldsymbol{x}) - \langle \boldsymbol{P} \rangle] + \int_{|\boldsymbol{\eta}|=1} \boldsymbol{\Gamma}_\infty(\boldsymbol{\eta})\breve{\boldsymbol{P}}(\boldsymbol{\eta}, \boldsymbol{x}), \tag{12.50}$$

where $\breve{\boldsymbol{P}}(\boldsymbol{\eta}, \boldsymbol{x})$ is obtained by integrating, with an appropriate weighting factor, the normalized polarization field along rays issuing from the point $\boldsymbol{x}$:

$$\breve{\boldsymbol{P}}(\boldsymbol{\eta}, \boldsymbol{x}) = \boldsymbol{V}(\boldsymbol{x}) + \int_0^\infty dr\,\frac{\boldsymbol{P}(\boldsymbol{x}-r\boldsymbol{\eta}) - \boldsymbol{Q}(r, \boldsymbol{x})}{r}, \tag{12.51}$$

where we have added the field $\boldsymbol{V}(\boldsymbol{x})$ to compensate for the freedom in the choice in the normalizing function $\boldsymbol{Q}(r, \boldsymbol{x})$. The value of the field $\boldsymbol{V}(\boldsymbol{x})$ does not contribute to the integral in (12.50) because the integral of $\boldsymbol{\Gamma}_\infty(\boldsymbol{\eta})$ over the unit ball vanishes [c.f. (12.48)]. So if we choose $\boldsymbol{V}(\boldsymbol{x})$ so that

$$\int_{|\boldsymbol{\eta}|=1} \breve{\boldsymbol{P}}(\boldsymbol{\eta}, \boldsymbol{x}) = 0 \text{ for all } \boldsymbol{x},$$

then $\breve{\boldsymbol{P}}(\boldsymbol{\eta}, \boldsymbol{x})$ will be independent of the choice of the normalizing function $\boldsymbol{Q}(r, \boldsymbol{x})$.

We are now in a position to check that the action of $\boldsymbol{\Gamma}$ is scale invariant. Suppose that we replace the field $\boldsymbol{P}(\boldsymbol{x})$ by $\boldsymbol{P}(\boldsymbol{x}/\lambda)$. By changing variables and normalizing functions in the integration (12.51) it is evident that $\breve{\boldsymbol{P}}(\boldsymbol{\eta}, \boldsymbol{x})$ will be replaced by $\breve{\boldsymbol{P}}(\boldsymbol{\eta}, \boldsymbol{x}/\lambda)$ when λ is positive and by $\breve{\boldsymbol{P}}(-\boldsymbol{\eta}, \boldsymbol{x}/\lambda)$ when λ is negative. Accordingly, from (12.50) and from the symmetry property $\boldsymbol{\Gamma}_\infty(\boldsymbol{\eta}) = \boldsymbol{\Gamma}_\infty(-\boldsymbol{\eta})$ it follows that $\boldsymbol{\Gamma}$ applied to $\boldsymbol{P}(\boldsymbol{x}/\lambda)$ produces the field $\boldsymbol{E}'(\boldsymbol{x}/\lambda)$. So we see that the properties (12.47) and (12.48) of the integral kernel $\boldsymbol{\Gamma}_\infty(\boldsymbol{\eta})$ are connected with the scale and reflection invariance associated with the action of the operator $\boldsymbol{\Gamma}$.

12.7. A framework for defining effective tensors in a more general context

The differential constraints on the fields $\boldsymbol{E}$ and $\boldsymbol{J}$ are equivalent to the requirement that

$$\boldsymbol{J} \in \mathcal{U} \oplus \mathcal{J}, \quad \boldsymbol{E} \in \mathcal{U} \oplus \mathcal{E}, \tag{12.52}$$

and the constitutive relation implies that

$$\boldsymbol{J} = \boldsymbol{L}\boldsymbol{E}. \tag{12.53}$$

This reformulation suggests that we can generalize the notion of "effective tensors" in the following way. Suppose that we are given any three mutually orthogonal subspaces $\mathcal{U}$, $\mathcal{E}$, and $\mathcal{J}$ that span a Hilbert space $\mathcal{H}$ as in (12.10) and a linear operator $\boldsymbol{L}$ that acts in $\mathcal{H}$. Then for any elements $\boldsymbol{J}$ and $\boldsymbol{E}$ of $\mathcal{H}$ that satisfy (12.52) and (12.53) the effective operator $\boldsymbol{L}_*$ can be defined as the linear operator that acts in $\mathcal{U}$ and which governs the relation

$$\boldsymbol{J}_0 = \boldsymbol{L}_* \boldsymbol{E}_0$$

between the components

$$\boldsymbol{J}_0 = \boldsymbol{\Gamma}_0 \boldsymbol{J}, \quad \boldsymbol{E}_0 = \boldsymbol{\Gamma}_0 \boldsymbol{E}, \tag{12.54}$$

which represent the projections onto the subspace $\mathcal{U}$ of $\boldsymbol{J}$ and $\boldsymbol{E}$. In particular, $\mathcal{U}$, $\mathcal{E}$, and $\mathcal{J}$ could represent finite-dimensional orthogonal vector spaces, rather than infinite-dimensional spaces of fields. We will see that this is applicable to the study of electrical networks.

An illustrative example is when $\mathcal{H}$ is a three-dimensional vector space and $\mathcal{U}$, $\mathcal{E}$, and $\mathcal{J}$ are a triad of orthogonal one-dimensional subspaces. Let us choose a basis of three orthonormal vectors $\boldsymbol{v}_1$, $\boldsymbol{v}_2$, and $\boldsymbol{v}_3$ such that $\boldsymbol{v}_1 \in \mathcal{U}$, $\boldsymbol{v}_2 \in \mathcal{E}$, and $\boldsymbol{v}_3 \in \mathcal{J}$. This ensures that the operators $\boldsymbol{\Gamma}_0$, $\boldsymbol{\Gamma}_1$, and $\boldsymbol{\Gamma}_2$ have a particularly simple representation in this basis:

$$\boldsymbol{\Gamma}_0 = \begin{pmatrix} 1 & 0 & 0 \\ 0 & 0 & 0 \\ 0 & 0 & 0 \end{pmatrix}, \quad \boldsymbol{\Gamma}_1 = \begin{pmatrix} 0 & 0 & 0 \\ 0 & 1 & 0 \\ 0 & 0 & 0 \end{pmatrix}, \quad \boldsymbol{\Gamma}_2 = \begin{pmatrix} 0 & 0 & 0 \\ 0 & 0 & 0 \\ 0 & 0 & 1 \end{pmatrix}. \tag{12.55}$$

Now let us suppose that $\boldsymbol{L}$ is represented in this basis by a matrix

$$\boldsymbol{L} = \begin{pmatrix} a_{00} & a_{01} & a_{02} \\ a_{10} & a_{11} & a_{12} \\ a_{20} & a_{21} & a_{22} \end{pmatrix}. \tag{12.56}$$

The constraints (12.52) imply that $\boldsymbol{J}$ and $\boldsymbol{E}$ are represented by three-dimensional vectors,

$$\boldsymbol{J} = \begin{pmatrix} j_0 \\ 0 \\ j_2 \end{pmatrix}, \qquad \boldsymbol{E} = \begin{pmatrix} e_0 \\ e_1 \\ 0 \end{pmatrix},$$

and the constitutive relation (12.53) implies that

$$j_0 = a_{00}e_0 + a_{01}e_1, \quad 0 = a_{10}e_0 + a_{11}e_1, \quad j_2 = a_{20}e_0 + a_{21}e_1.$$

From these equations we see that the components j_0 and e_0 are related via

$$j_0 = (a_{00} - a_{01}a_{10}/a_{11})e_0,$$

and we conclude that the effective operator $\boldsymbol{L}_*$ in this trivial example is simply the scalar

$$\boldsymbol{L}_* = a_{00} - a_{01}a_{10}/a_{11}.$$

More generally, when $\mathcal{U}$, $\mathcal{E}$, and $\mathcal{J}$ have dimension greater than 1, but are still finite-dimensional, then we can choose an orthonormal basis of $\mathcal{H}$ in which the first set of basis vectors span $\mathcal{U}$, the next set of basis vectors span $\mathcal{E}$, and the remaining set of basis vectors span $\mathcal{J}$. Thus, generalizing (12.55), the projections onto these three subspaces are represented in this basis by three matrices with block structures

$$\boldsymbol{\Gamma}_0 = \begin{pmatrix} \boldsymbol{I} & 0 & 0 \\ 0 & 0 & 0 \\ 0 & 0 & 0 \end{pmatrix}, \quad \boldsymbol{\Gamma}_1 = \begin{pmatrix} 0 & 0 & 0 \\ 0 & \boldsymbol{I} & 0 \\ 0 & 0 & 0 \end{pmatrix}, \quad \boldsymbol{\Gamma}_2 = \begin{pmatrix} 0 & 0 & 0 \\ 0 & 0 & 0 \\ 0 & 0 & \boldsymbol{I} \end{pmatrix},$$

in which each of the three identity matrices appearing along the block diagonals may have a different dimension, according to the dimensionality of the subspaces $\mathcal{U}$, $\mathcal{E}$, and $\mathcal{J}$. The linear operator $\boldsymbol{L}$, as represented in this basis by the matrix with block structure

$$\boldsymbol{L} = \begin{pmatrix} \boldsymbol{L}_{00} & \boldsymbol{L}_{01} & \boldsymbol{L}_{02} \\ \boldsymbol{L}_{10} & \boldsymbol{L}_{11} & \boldsymbol{L}_{12} \\ \boldsymbol{L}_{20} & \boldsymbol{L}_{21} & \boldsymbol{L}_{22} \end{pmatrix},$$

has an associated effective operator

$$\boldsymbol{L}_* = \boldsymbol{L}_{00} - \boldsymbol{L}_{01}\boldsymbol{L}_{11}^{-1}\boldsymbol{L}_{10}. \tag{12.57}$$

The ensuing analysis will apply irrespective of whether the spaces $\mathcal{U}$, $\mathcal{E}$, and $\mathcal{J}$ have finite dimension or not. However, because our primary interest is in the effective moduli of composites, we will call the elements of the spaces of $\mathcal{H}$ fields rather than vectors, and we will call $\boldsymbol{L}_*$ an effective tensor rather than an effective operator.

12.8. Various solutions for the fields and effective tensor

Naturally we need to ensure that equations (12.52) through (12.54) actually define $\boldsymbol{L}_*$ in a unique way, without contradictions. When $\mathcal{E}$ and $\mathcal{J}$ have infinite dimension it is straightforward to show that the formula (12.57) for the effective tensor $\boldsymbol{L}_*$ generalizes to

$$\boldsymbol{L}_* = \boldsymbol{\Gamma}_0\boldsymbol{L}\boldsymbol{\Gamma}_0 - \boldsymbol{\Gamma}_0\boldsymbol{L}\boldsymbol{\Gamma}_1(\boldsymbol{\Gamma}_1\boldsymbol{L}\boldsymbol{\Gamma}_1)^{-1}\boldsymbol{\Gamma}_1\boldsymbol{L}\boldsymbol{\Gamma}_0, \tag{12.58}$$

where the inverse of $\boldsymbol{\Gamma}_1\boldsymbol{L}\boldsymbol{\Gamma}_1$ is to be taken on the subspace $\mathcal{E}$. When $\mathcal{E}$ is finite-dimensional this only entails inverting a matrix, which will be no problem for almost all choices of the linear map $\boldsymbol{L}$. However, when $\mathcal{E}$ is infinite-dimensional the existence of the inverse of the operator $\boldsymbol{\Gamma}_1\boldsymbol{L}\boldsymbol{\Gamma}_1$ on the subspace $\mathcal{E}$ is not so clear. A sufficient condition to ensure the existence

of an inverse is that the operator $\boldsymbol{L}$ be bounded and coercive on the subspace $\mathcal{E}$, that is, there exist positive constants α and β such that

$$\beta > \sup_{\substack{\boldsymbol{E}\in\mathcal{E}\\ |\boldsymbol{E}|=1}} |\boldsymbol{L}\boldsymbol{E}|, \qquad \text{and } (\boldsymbol{E}, \boldsymbol{L}\boldsymbol{E}) > \alpha|\boldsymbol{E}|^2 \text{ for all } \boldsymbol{E}\in\mathcal{E} \text{ with } \boldsymbol{E}\neq 0,$$

where $|\boldsymbol{P}| = (\boldsymbol{P}, \boldsymbol{P})^{1/2}$ is the norm of any field $\boldsymbol{P}$.

An even simpler formula for the effective tensor $\boldsymbol{L}_*$ results by applying the operator $\boldsymbol{\Gamma}_0 + \boldsymbol{\Gamma}_2$ (which projects on the space $\mathcal{U}\oplus\mathcal{J}$) to both sides of the constitutive law $\boldsymbol{E} = \boldsymbol{L}^{-1}\boldsymbol{J}$. Solving the resulting equation,

$$\boldsymbol{\Gamma}_0\boldsymbol{E} = (\boldsymbol{\Gamma}_0 + \boldsymbol{\Gamma}_2)\boldsymbol{L}^{-1}(\boldsymbol{\Gamma}_0 + \boldsymbol{\Gamma}_2)\boldsymbol{J},$$

for $\boldsymbol{J}$ gives

$$\boldsymbol{J} = [(\boldsymbol{\Gamma}_0 + \boldsymbol{\Gamma}_2)\boldsymbol{L}^{-1}(\boldsymbol{\Gamma}_0 + \boldsymbol{\Gamma}_2)]^{-1}\boldsymbol{\Gamma}_0\boldsymbol{E},$$

where the last inverse is to be taken on the subspace $\mathcal{U}\oplus\mathcal{J}$. By applying $\boldsymbol{\Gamma}_0$ to both sides of this equation we see that

$$\boldsymbol{L}_* = \boldsymbol{\Gamma}_0[(\boldsymbol{\Gamma}_0 + \boldsymbol{\Gamma}_2)\boldsymbol{L}^{-1}(\boldsymbol{\Gamma}_0 + \boldsymbol{\Gamma}_2)]^{-1}\boldsymbol{\Gamma}_0. \tag{12.59}$$

To obtain other formulas for the fields and effective tensor let us choose an operator $\boldsymbol{L}_0$ that commutes with $\boldsymbol{\Gamma}_0$. Then by direct analogy with (12.28) we have

$$\boldsymbol{\Gamma}(\boldsymbol{L}-\boldsymbol{L}_0)\boldsymbol{E} = \boldsymbol{E}_0 - \boldsymbol{E}, \quad \boldsymbol{\Gamma}_0(\boldsymbol{L}-\boldsymbol{L}_0)\boldsymbol{E} = (\boldsymbol{L}_* - \boldsymbol{L}_0)\boldsymbol{E}_0,$$

where the operator $\boldsymbol{\Gamma}$, defined by (12.23), is given by

$$\boldsymbol{\Gamma} = \boldsymbol{\Gamma}_1(\boldsymbol{\Gamma}_1\boldsymbol{L}_0\boldsymbol{\Gamma}_1)^{-1}\boldsymbol{\Gamma}_1,$$

in which the inverse is to be taken on the space $\mathcal{E}$. Solving these equations yields the formulas

$$\boldsymbol{E} = [\boldsymbol{I} + \boldsymbol{\Gamma}(\boldsymbol{L}-\boldsymbol{L}_0)]^{-1}\boldsymbol{E}_0, \quad \boldsymbol{L}_* = \boldsymbol{L}_0 - \boldsymbol{\Gamma}_0(\boldsymbol{L}-\boldsymbol{L}_0)[\boldsymbol{I} + \boldsymbol{\Gamma}(\boldsymbol{L}-\boldsymbol{L}_0)]^{-1}\boldsymbol{\Gamma}_0 \tag{12.60}$$

for the field and effective tensor. (The $\boldsymbol{L}_0$ appearing at the beginning of the second formula, $\boldsymbol{L}_* = \boldsymbol{L}_0 - \cdots$, should be interpreted as the restriction of $\boldsymbol{L}_0$ to the subspace $\mathcal{U}$, i.e., as $\boldsymbol{\Gamma}_0\boldsymbol{L}_0$.)

We will see in the next chapter that these formulas are very useful for developing series expansions for the fields and effective tensor. In the special case where $\boldsymbol{L}_0$ is proportional to the identity tensor, that is, $\boldsymbol{L}_0 = \sigma_0\boldsymbol{I}$, and $\boldsymbol{L}_0 - \boldsymbol{L}$ has an inverse, then (12.60) reduces to

$$\boldsymbol{L}_* = \sigma_0\boldsymbol{\Gamma}_0 - \sigma_0\boldsymbol{\Gamma}_0(\boldsymbol{S} - \boldsymbol{\Gamma}_1)^{-1}\boldsymbol{\Gamma}_0, \tag{12.61}$$

where

$$\boldsymbol{S} = \sigma_0(\sigma_0\boldsymbol{I} - \boldsymbol{L})^{-1}.$$

12.9. The duality principle

The equations

$$\boldsymbol{J}\in\mathcal{U}\oplus\mathcal{J}, \quad \boldsymbol{E}\in\mathcal{U}\oplus\mathcal{E}, \quad \boldsymbol{J} = \boldsymbol{L}\boldsymbol{E}, \quad \boldsymbol{\Gamma}_0\boldsymbol{J} = \boldsymbol{L}_*\boldsymbol{\Gamma}_0\boldsymbol{E} \tag{12.62}$$

can be rewritten in the forms

$$\boldsymbol{E} \in \mathcal{U} \oplus \mathcal{E}, \quad \boldsymbol{J} \in \mathcal{U} \oplus \mathcal{J}, \quad \boldsymbol{E} = \boldsymbol{L}^{-1}\boldsymbol{J}, \quad \boldsymbol{\Gamma}_0\boldsymbol{E} = \boldsymbol{L}_*^{-1}\boldsymbol{\Gamma}_0\boldsymbol{J}. \tag{12.63}$$

Now notice that equations (12.62) are identical to equations (12.63) once we make the replacements

$$\begin{gathered} \boldsymbol{J} \to \boldsymbol{E}, \qquad \boldsymbol{E} \to \boldsymbol{J}, \\ \mathcal{U} \to \mathcal{U}, \qquad \mathcal{J} \to \mathcal{E}, \qquad \mathcal{E} \to \mathcal{J}, \\ \boldsymbol{L} \to \boldsymbol{L}^{-1}, \qquad \boldsymbol{L}_* \to \boldsymbol{L}_*^{-1}. \end{gathered} \tag{12.64}$$

Therefore any general result pertaining to all sets of equations of the form (12.62) will remain true if we make the above replacements. The replacement corresponds to applying the original result to the second set of equations (12.63). Of course if the result involves the operators $\boldsymbol{\Gamma}_0$, $\boldsymbol{\Gamma}_1$, and $\boldsymbol{\Gamma}_2$, which project onto $\mathcal{U}$, $\mathcal{E}$, and $\mathcal{J}$, respectively, then we should also make the replacements

$$\boldsymbol{\Gamma}_0 \to \boldsymbol{\Gamma}_0, \qquad \boldsymbol{\Gamma}_1 \to \boldsymbol{\Gamma}_2, \qquad \boldsymbol{\Gamma}_2 \to \boldsymbol{\Gamma}_1. \tag{12.65}$$

If an arbitrary constant like σ_0 enters a formula, then we are free to either leave it unchanged, or to replace it everywhere by σ_0^{-1}. For example, this duality principle applied to the expression (12.61) gives an alternative formula:

$$\boldsymbol{L}_*^{-1} = \sigma_0^{-1}\boldsymbol{\Gamma}_0 - \sigma_0^{-1}\boldsymbol{\Gamma}_0(\boldsymbol{T} - \boldsymbol{\Gamma}_2)^{-1}\boldsymbol{\Gamma}_0 \tag{12.66}$$

for the effective tensor $\boldsymbol{L}_*$, in which

$$\boldsymbol{T} = \sigma_0^{-1}(\sigma_0^{-1}\boldsymbol{I} - \boldsymbol{L}^{-1})^{-1} = \boldsymbol{L}(\boldsymbol{L} - \sigma_0\boldsymbol{I})^{-1} = \boldsymbol{I} - \boldsymbol{S}.$$

The duality principle is useful because it provides a quick means of obtaining results like (12.66) without having to go through a detailed analysis. In any case, such an analysis would just be a repetition of the proof of the original result; the only change needed would be to make the above replacements (12.64) and (12.65) at each step in the argument.

12.10. The effective tensor of the adjoint equation

The adjoint $\boldsymbol{L}^\dagger$ of $\boldsymbol{L}$ is defined as the linear operator such that

$$(\boldsymbol{P}', \boldsymbol{L}\boldsymbol{P}) = (\boldsymbol{L}^\dagger\boldsymbol{P}', \boldsymbol{P}) \quad \text{for all } \boldsymbol{P}', \boldsymbol{P} \in \mathcal{H}.$$

If $\mathcal{H}$ is finite-dimensional, then $\boldsymbol{L}^\dagger$ is represented in an orthonormal basis as the transpose of the matrix representing $\boldsymbol{L}$, unless the matrix representing $\boldsymbol{L}$ happens to be complex, in which case we should take the Hermitian conjugate rather than the transpose to obtain $\boldsymbol{L}^\dagger$.

Our assumption that $\boldsymbol{L}$ has bounded norm and is coercive clearly implies that the adjoint operator $\boldsymbol{L}^\dagger$ has bounded norm and is coercive. So it makes sense to ask if the effective tensor $\boldsymbol{L}'_*$ of $\boldsymbol{L}^\dagger$ is related to the effective tensor $\boldsymbol{L}_*$ of $\boldsymbol{L}$. Given any two fields $\boldsymbol{E}_0$ and $\boldsymbol{E}'_0$ in $\mathcal{U}$, let $\boldsymbol{E}$ and $\boldsymbol{J}$ denote the solutions of the equations

$$\boldsymbol{J} = \boldsymbol{L}\boldsymbol{E}, \quad \boldsymbol{J} \in \mathcal{U} \oplus \mathcal{J}, \quad \boldsymbol{E} \in \mathcal{U} \oplus \mathcal{E}, \quad \boldsymbol{\Gamma}_0\boldsymbol{E} = \boldsymbol{E}_0,$$

and let $\boldsymbol{E}'$ and $\boldsymbol{J}'$ denote the solutions of the adjoint equations

$$\boldsymbol{J}' = \boldsymbol{L}^\dagger \boldsymbol{E}', \quad \boldsymbol{J}' \in \mathcal{U} \oplus \mathcal{J}, \quad \boldsymbol{E}' \in \mathcal{U} \oplus \mathcal{E}, \quad \boldsymbol{\Gamma}_0 \boldsymbol{E}' = \boldsymbol{E}_0'. \tag{12.67}$$

Also, from the definition of the effective tensors we have

$$\boldsymbol{J}_0 = \boldsymbol{\Gamma}_0 \boldsymbol{J} = \boldsymbol{L}_* \boldsymbol{E}_0, \quad \boldsymbol{J}_0' = \boldsymbol{\Gamma}_0 \boldsymbol{J}' = \boldsymbol{L}_*' \boldsymbol{E}_0'.$$

Now let us evaluate the inner product

$$(\boldsymbol{E}', \boldsymbol{L}\boldsymbol{E}) = (\boldsymbol{L}^\dagger \boldsymbol{E}', \boldsymbol{E}) \tag{12.68}$$

in two different ways and compare the answers. It follows directly from the orthogonality of the subspaces $\mathcal{U}$, $\mathcal{E}$, and $\mathcal{J}$ and from the above equations that

$$(\boldsymbol{E}', \boldsymbol{L}\boldsymbol{E}) = (\boldsymbol{E}', \boldsymbol{J}) = (\boldsymbol{E}_0', \boldsymbol{J}_0) = (\boldsymbol{E}_0', \boldsymbol{L}_* \boldsymbol{E}_0),$$

and similarly we have

$$(\boldsymbol{L}^\dagger \boldsymbol{E}', \boldsymbol{E}) = (\boldsymbol{J}', \boldsymbol{E}) = (\boldsymbol{J}_0', \boldsymbol{E}_0) = (\boldsymbol{L}_*' \boldsymbol{E}_0', \boldsymbol{E}_0).$$

So from (12.68) we deduce that

$$(\boldsymbol{E}_0', \boldsymbol{L}_* \boldsymbol{E}_0) = (\boldsymbol{L}_*' \boldsymbol{E}_0', \boldsymbol{E}_0) \ \text{ for all } \boldsymbol{E}_0', \boldsymbol{E}_0 \in \mathcal{U}.$$

In other words, we can identify $\boldsymbol{L}_*'$ with the adjoint of $\boldsymbol{L}_*$, that is,

$$\boldsymbol{L}_*' = \boldsymbol{L}_*^\dagger. \tag{12.69}$$

In particular, if $\boldsymbol{L}$ is self-adjoint, then we can equate $\boldsymbol{L}^\dagger$ with $\boldsymbol{L}$ and $\boldsymbol{L}_*'$ with $\boldsymbol{L}_*$, which in conjunction with (12.69) implies that $\boldsymbol{L}_*$ must also be self-adjoint.

One other important result follows from the identity

$$(\boldsymbol{E}_0, (\boldsymbol{L}_* + \boldsymbol{L}_*^\dagger)\boldsymbol{E}_0) = (\boldsymbol{E}_0, \boldsymbol{J}_0) + (\boldsymbol{J}_0, \boldsymbol{E}_0) = (\boldsymbol{E}, \boldsymbol{J}) + (\boldsymbol{J}, \boldsymbol{E}) = (\boldsymbol{E}, (\boldsymbol{L} + \boldsymbol{L}^\dagger)\boldsymbol{E}).$$

Defining

$$\boldsymbol{L}_S^* = (\boldsymbol{L}_* + \boldsymbol{L}_*^\dagger)/2, \quad \boldsymbol{L}_S = (\boldsymbol{L} + \boldsymbol{L}^\dagger)/2$$

as the self-adjoint parts of $\boldsymbol{L}_*$ and $\boldsymbol{L}$, we see that $\boldsymbol{L}_S^*$ is positive-definite on $\mathcal{U}$ whenever $\boldsymbol{L}_S$ is positive-definite on $\mathcal{H}$.

12.11. Magnetotransport and its equivalence to thermoelectricity in two dimensions

Although the adjoint equations (12.67) are of secondary interest in physical problems, they are of primary importance from the mathematical viewpoint because of the relation (12.69) linking the effective tensor of the adjoint equation with the effective tensor of the original equation. In other words, the adjoint equations should be considered in conjunction with the original set of equations.

This set of equations can easily be written in a self-adjoint form. The complex conductivity equations are non-self-adjoint equations, and Cherkaev and Gibiansky (1994) showed how

these could be recast in a self-adjoint form. It is a simple matter to generalize their approach to other non-self-adjoint equations [see Milton (1990) and Fannjiang and Papanicolaou (1994)].

As an example, consider the equations of conductivity in the presence of a magnetic field:

$$\boldsymbol{j}(\boldsymbol{x}) = \boldsymbol{\sigma}(\boldsymbol{x})\boldsymbol{e}(\boldsymbol{x}), \quad \nabla \cdot \boldsymbol{j}(\boldsymbol{x}) = 0, \quad \boldsymbol{e}(\boldsymbol{x}) = \nabla\phi(\boldsymbol{x}), \quad \langle \boldsymbol{j} \rangle = \boldsymbol{\sigma}_* \langle \boldsymbol{e} \rangle,$$

in which the conductivity field $\boldsymbol{\sigma}(\boldsymbol{x})$ and the effective tensor $\boldsymbol{\sigma}_*$ are real but not necessarily symmetric. They have symmetric and antisymmetric parts:

$$\boldsymbol{\sigma}_s(\boldsymbol{x}) = \boldsymbol{\sigma}(\boldsymbol{x}) + \boldsymbol{\sigma}^T(\boldsymbol{x}), \quad \boldsymbol{\sigma}_a(\boldsymbol{x}) = \boldsymbol{\sigma}(\boldsymbol{x}) - \boldsymbol{\sigma}^T(\boldsymbol{x}), \quad \boldsymbol{\sigma}_s^* = \boldsymbol{\sigma}_* + \boldsymbol{\sigma}_*^T, \quad \boldsymbol{\sigma}_a^* = \boldsymbol{\sigma}_* - \boldsymbol{\sigma}_*^T.$$

The equations for the adjoint problem are

$$\boldsymbol{j}'(\boldsymbol{x}) = \boldsymbol{\sigma}^T(\boldsymbol{x})\boldsymbol{e}'(\boldsymbol{x}), \quad \nabla \cdot \boldsymbol{j}'(\boldsymbol{x}) = 0, \quad \boldsymbol{e}'(\boldsymbol{x}) = \nabla\phi'(\boldsymbol{x}), \quad \langle \boldsymbol{j}' \rangle = \boldsymbol{\sigma}_*^T \langle \boldsymbol{e}' \rangle.$$

By adding and subtracting the constitutive equations $\boldsymbol{j} = \boldsymbol{\sigma}\boldsymbol{e}$ and $\boldsymbol{j}' = \boldsymbol{\sigma}^T\boldsymbol{e}'$ and letting

$$\boldsymbol{j}_s = (\boldsymbol{j} + \boldsymbol{j}')/2, \quad \boldsymbol{j}_a = (\boldsymbol{j} - \boldsymbol{j}')/2, \quad \boldsymbol{e}_s = (\boldsymbol{e} + \boldsymbol{e}')/2, \quad \boldsymbol{e}_a = (\boldsymbol{e} - \boldsymbol{e}')/2,$$

we obtain an equivalent set of equations

$$\begin{pmatrix} -\boldsymbol{j}_s \\ \boldsymbol{j}_a \end{pmatrix} = \begin{pmatrix} -\boldsymbol{\sigma}_s & -\boldsymbol{\sigma}_a \\ \boldsymbol{\sigma}_a & \boldsymbol{\sigma}_s \end{pmatrix} \begin{pmatrix} \boldsymbol{e}_s \\ \boldsymbol{e}_a \end{pmatrix}, \tag{12.70}$$

where now the tensor that relates the field on the left to the field on the right is self-adjoint. However, the tensor is not positive-definite. The quadratic form,

$$f(\boldsymbol{e}_s, \boldsymbol{e}_a) = (\boldsymbol{e}_s, -\boldsymbol{\sigma}_s\boldsymbol{e}_s) + (\boldsymbol{e}_s, -\boldsymbol{\sigma}_a\boldsymbol{e}_a) + (\boldsymbol{e}_a, \boldsymbol{\sigma}_a\boldsymbol{e}_s) + (\boldsymbol{e}_a, \boldsymbol{\sigma}_s\boldsymbol{e}_a),$$

associated with the matrix in (12.70) takes negative values when $\boldsymbol{e}_s \neq 0$ and $\boldsymbol{e}_a = 0$ and positive values when $\boldsymbol{e}_s = 0$ and $\boldsymbol{e}_a \neq 0$, that is, it represents a saddle-shaped function.

Following the approach taken in section 11.5 on page 234 we re-express the constitutive relation (12.70) and the constraints on the associated fields in the form

$$\begin{pmatrix} \boldsymbol{e}_s \\ \boldsymbol{j}_a \end{pmatrix} = \boldsymbol{\mathcal{L}} \begin{pmatrix} \boldsymbol{j}_s \\ \boldsymbol{e}_a \end{pmatrix}, \quad \begin{matrix} \nabla \times \boldsymbol{e}_s = 0, \\ \nabla \cdot \boldsymbol{j}_a = 0, \end{matrix} \quad \begin{matrix} \boldsymbol{j}_s = \nabla \times \boldsymbol{\psi}_s, \\ \boldsymbol{e}_a = \nabla\phi_a. \end{matrix} \tag{12.71}$$

A straightforward calculation shows that

$$\boldsymbol{\mathcal{L}} = \begin{pmatrix} \boldsymbol{\sigma}_s^{-1} & -\boldsymbol{\sigma}_s^{-1}\boldsymbol{\sigma}_a \\ \boldsymbol{\sigma}_a\boldsymbol{\sigma}_s^{-1} & \boldsymbol{\sigma}_s - \boldsymbol{\sigma}_a\boldsymbol{\sigma}_s^{-1}\boldsymbol{\sigma}_a \end{pmatrix}. \tag{12.72}$$

Evidently this matrix is symmetric because the transpose of $-\boldsymbol{\sigma}_s^{-1}\boldsymbol{\sigma}_a$ is $\boldsymbol{\sigma}_a\boldsymbol{\sigma}_s^{-1}$. Furthermore, it is positive-semidefinite when $\boldsymbol{\sigma}_s$ is positive-semidefinite because the associated quadratic form,

$$\begin{aligned} \begin{pmatrix} \boldsymbol{j}_s \\ \boldsymbol{e}_a \end{pmatrix} \cdot \boldsymbol{\mathcal{L}} \begin{pmatrix} \boldsymbol{j}_s \\ \boldsymbol{e}_a \end{pmatrix} &= \begin{pmatrix} \boldsymbol{j}_s \\ \boldsymbol{e}_a \end{pmatrix} \cdot \begin{pmatrix} \boldsymbol{e}_s \\ \boldsymbol{j}_a \end{pmatrix} \\ &= (\boldsymbol{j}_s, \boldsymbol{e}_s) + (\boldsymbol{e}_a, \boldsymbol{j}_a) \\ &= (\boldsymbol{\sigma}_s\boldsymbol{e}_s + \boldsymbol{\sigma}_a\boldsymbol{e}_a, \boldsymbol{e}_s) + (\boldsymbol{e}_a, \boldsymbol{\sigma}_a\boldsymbol{e}_s + \boldsymbol{\sigma}_s\boldsymbol{e}_a) \\ &= (\boldsymbol{e}_s, \boldsymbol{\sigma}_s\boldsymbol{e}_s) + (\boldsymbol{e}_a, \boldsymbol{\sigma}_s\boldsymbol{e}_a) \geq 0, \end{aligned}$$

is positive when $\boldsymbol{\sigma}_s$ is positive-definite and $\boldsymbol{e}_a$ and $\boldsymbol{e}_s$ are not both zero.

Of course we can perform the same sort of algebraic manipulations on the effective constitutive equations $\langle \boldsymbol{j} \rangle = \boldsymbol{\sigma}_* \langle \boldsymbol{e} \rangle$ and $\langle \boldsymbol{j}' \rangle = \boldsymbol{\sigma}_*^T \langle \boldsymbol{e}' \rangle$, and thereby obtain the transformed equations

$$\begin{pmatrix} \langle \boldsymbol{e}_s \rangle \\ \langle \boldsymbol{j}_a \rangle \end{pmatrix} = \boldsymbol{\mathcal{L}}_* \begin{pmatrix} \langle \boldsymbol{j}_s \rangle \\ \langle \boldsymbol{e}_a \rangle \end{pmatrix}, \quad \text{where } \boldsymbol{\mathcal{L}}_* = \begin{pmatrix} (\boldsymbol{\sigma}_s^*)^{-1} & -(\boldsymbol{\sigma}_s^*)^{-1}\boldsymbol{\sigma}_a^* \\ \boldsymbol{\sigma}_a^*(\boldsymbol{\sigma}_s^*)^{-1} & \boldsymbol{\sigma}_s^* - \boldsymbol{\sigma}_a^*(\boldsymbol{\sigma}_s^*)^{-1}\boldsymbol{\sigma}_a^* \end{pmatrix}. \tag{12.73}$$

Thus $\boldsymbol{\sigma}_s^*$ and $\boldsymbol{\sigma}_a^*$ can be determined from the symmetric effective tensor $\boldsymbol{\mathcal{L}}_*$ associated with the system of equations (12.71). Of course this analysis extends to other non-self-adjoint problems. In summary, there is no loss of generality in restricting one's attention to self-adjoint problems. A problem with a non-self-adjoint $\boldsymbol{L}$, with $\boldsymbol{L}_s = (\boldsymbol{L}+\boldsymbol{L}^\dagger)/2$ being positive-definite, can be embedded in a larger problem with a self-adjoint, positive-definite tensor $\boldsymbol{\mathcal{L}}$ entering the constitutive law.

In two dimensions there is direct correspondence between these equations of conductivity and those of a thermoelectric problem with a real self-adjoint, positive-definite tensor entering the constitutive law. This is made evident by rewriting the constitutive law in the form

$$\begin{pmatrix} \boldsymbol{j}_1 \\ \boldsymbol{j}_2 \end{pmatrix} = \boldsymbol{\mathcal{L}}' \begin{pmatrix} \boldsymbol{e}_1 \\ \boldsymbol{e}_2 \end{pmatrix},$$

with tensor

$$\boldsymbol{\mathcal{L}}'(\boldsymbol{x}) = \begin{pmatrix} \boldsymbol{R}_\perp \boldsymbol{\sigma}_s^{-1} \boldsymbol{R}_\perp^T & -\boldsymbol{R}_\perp \boldsymbol{\sigma}_s^{-1} \boldsymbol{\sigma}_a \\ \boldsymbol{\sigma}_a \boldsymbol{\sigma}_s^{-1} \boldsymbol{R}_\perp^T & \boldsymbol{\sigma}_s - \boldsymbol{\sigma}_a \boldsymbol{\sigma}_s^{-1} \boldsymbol{\sigma}_a \end{pmatrix},$$

which is self-adjoint and positive-definite when $\boldsymbol{\sigma}_s(\boldsymbol{x})$ is positive-definite for all $\boldsymbol{x}$, and with the fields

$$\boldsymbol{j}_1 = \boldsymbol{R}_\perp \boldsymbol{e}_s, \quad \boldsymbol{j}_2 = \boldsymbol{j}_a, \quad \boldsymbol{e}_1 = \boldsymbol{R}_\perp \boldsymbol{j}_s, \quad \boldsymbol{e}_2 = \boldsymbol{e}_a$$

satisfying the differential constraints

$$\nabla \cdot \boldsymbol{j}_1 = 0, \ \ \nabla \cdot \boldsymbol{j}_2 = 0, \ \ \nabla \times \boldsymbol{e}_1 = 0, \ \ \nabla \times \boldsymbol{e}_2 = 0,$$

which are appropriate to thermoelectricity. From the associated effective thermoelectric tensor $\boldsymbol{\mathcal{L}}_*'$ we can recover the effective conductivity tensor through the relation

$$\boldsymbol{\mathcal{L}}_*' = \begin{pmatrix} \boldsymbol{R}_\perp (\boldsymbol{\sigma}_s^*)^{-1} \boldsymbol{R}_\perp^T & -\boldsymbol{R}_\perp (\boldsymbol{\sigma}_s^*)^{-1} \boldsymbol{\sigma}_a^* \\ \boldsymbol{\sigma}_a^* (\boldsymbol{\sigma}_s^*)^{-1} \boldsymbol{R}_\perp^T & \boldsymbol{\sigma}_s^* - \boldsymbol{\sigma}_a^* (\boldsymbol{\sigma}_s^*)^{-1} \boldsymbol{\sigma}_a^* \end{pmatrix},$$

which is implied by (12.73).

When the two-dimensional material is locally isotropic, $\boldsymbol{\sigma}(\boldsymbol{x})$ takes the form

$$\boldsymbol{\sigma}(\boldsymbol{x}) = [\boldsymbol{\rho}(\boldsymbol{x})]^{-1} = [\varrho \boldsymbol{I} + \mu \boldsymbol{R}_\perp]^{-1} = \frac{\varrho \boldsymbol{I} - \mu \boldsymbol{R}_\perp}{\varrho^2 + \mu^2},$$

where $\varrho = \varrho(\boldsymbol{x})$ and $\mu = \mu(\boldsymbol{x})$ depend on $\boldsymbol{x}$. The formula for $\boldsymbol{\mathcal{L}}'(\boldsymbol{x})$ then simplifies to

$$\boldsymbol{\mathcal{L}}' = \begin{pmatrix} (\varrho + \mu^2/\varrho)\boldsymbol{I} & -(\mu/\varrho)\boldsymbol{I} \\ -(\mu/\varrho)\boldsymbol{I} & (1/\varrho)\boldsymbol{I} \end{pmatrix},$$

and represents the thermoelectric tensor of a locally isotropic material.

References

Asaro, R. J. and D. M. Barnett 1975. The non-uniform transformation strain problem for an anisotropic ellipsoidal inclusion. *Journal of the Mechanics and Physics of Solids* 23: 77–83. {*254, 267*}

Berryman, J. G. 1997. Generalization of Eshelby's formula for a single ellipsoidal elastic inclusion to poroelasticity and thermoelasticity. *Physical Review Letters* 79(6):1142–1145. {*255, 267*}

Bruggeman, D. A. G. 1937. Berechnung verschiedener physikalischer Konstanten von heterogenen Substanzen. III. Die Elastische Konstanten der Quasiisotropen Mischkörper aus isotropen Substanzen. (German) [Calculation of various physical constants in heterogeneous substances. III. The elastic constants of quasi-isotropic composites from isotropic substances]. *Annals of Physics* 29:160–178. {*256, 267*}

Bruno, O. P., F. Reitich, and P. H. Leo 1996. The overall elastic energy of polycrystalline martensitic solids. *Journal of the Mechanics and Physics of Solids* 44:1051–1101. {*257, 267*}

Cherkaev, A. V. and L. V. Gibiansky 1994. Variational principles for complex conductivity, viscoelasticity, and similar problems in media with complex moduli. *Journal of Mathematical Physics* 35(1):127–145. {*221, 234, 237, 243, 264, 267, 271, 276, 277, 286, 639, 641*}

Dederichs, P. H. and R. Zeller 1972. Elastische Konstanten von Vielkristallen. (German) [Elastic constants of polycrystals)]. Bericht der Kernforschungsanlage (KFA) Jülich 877, Institut für Festkörperforschang Jülich, Jülich, Germany. {*251, 267*}

Deeg, W. F. 1980. The analysis of dislocation, crack, and inclusion problems in piezoelectric solids. Ph.D. Thesis, Stanford University, Stanford, California. {*255, 267*}

Dell'Antonio, G. F., R. Figari, and E. Orlandi 1986. An approach through orthogonal projections to the study of inhomogeneous or random media with linear response. *Annales de l'Institut Henri Poincaré. Section B, Probabilités et statistiques* 44:1–28. {*248, 267, 371, 373, 393*}

Dunn, M. L. and M. Taya 1993. An analysis of piezoelectric composite materials containing ellipsoidal inhomogeneities. *Proceedings of the Royal Society of London. Series A, Mathematical and Physical Sciences* 443:265–287. {*255, 267*}

Eshelby, J. D. 1957. The determination of the elastic field of an ellipsoidal inclusion and related problems. *Proceedings of the Royal Society of London* 241:376–396. {*252, 255, 256, 267*}

Eshelby, J. D. 1961. Elastic inclusions and inhomogeneities. In I. N. Sneddon and R. Hill (eds.), *Progress in Solid Mechanics*, pp. 87–140. Amsterdam: North-Holland Publishing Co. {*254, 267*}

Fannjiang, A. and G. Papanicolaou 1994. Convection enhanced diffusion for periodic flows. *SIAM Journal on Applied Mathematics* 54(2):333–408. {*22, 42, 265, 267, 277, 278, 287*}

Fokin, A. G. 1982. Iteration method in the theory of nonhomogeneous dielectrics. *Physica Status Solidi. B, Basic Research* 111:281–288. {*248, 267, 298, 310*}

Golden, K. and G. Papanicolaou 1983. Bounds for effective parameters of heterogeneous media by analytic continuation. *Communications in Mathematical Physics* 90(4):473–491. {*11, 12, 15, 248, 268, 370, 376, 393, 571, 598, 603, 617*}

Hashin, Z. 1964. Theory of mechanical behavior of heterogeneous media. *Applied Mechanics Reviews* 17(1):1–9. {*247, 268, 272, 287*}

Hashin, Z. 1972. Theory of fiber reinforced materials. NASA contractor report CR-1974, NASA, Washington, D.C. xv + 690 pp. {*xxiv, xxvii, 247, 268, 272, 287*}

Hill, R. 1963. Elastic properties of reinforced solids: Some theoretical principles. *Journal of the Mechanics and Physics of Solids* 11:357–372. {*77, 90, 247, 268, 272, 287, 471, 473, 493*}

Kantor, Y. and D. J. Bergman 1984. Improved rigorous bounds on the effective elastic moduli of a composite material. *Journal of the Mechanics and Physics of Solids* 32: 41–62. {*248, 268, 569, 598, 603, 617*}

Khachaturyan, A. G. 1966. Some questions concerning the theory of phase transitions in solids. *Fizika Tverdogo Tela.* 8:2709–2717. English translation in *Soviet Phys. Solid State.* 8:2163–2168 (1967). {*252, 268, 295, 311, 474, 493, 672, 696*}

Khachaturyan, A. G. 1983. *Theory of Structural Transformations in Solids*, pp. 226–241. New York / London / Sydney, Australia: John Wiley and Sons. ISBN 0-471-07873-5. {*252, 268*}

Kneer, G. 1965. Calculation of elastic moduli of polycrystalline aggregates with texture. *Physica Status Solidi* 9:825–838. {*254, 268*}

Kohler, W. and G. Papanicolaou 1982. Bounds for the effective conductivity of random media. In R. Burridge, S. Childress, and G. Papanicolaou (eds.), *Macroscopic Properties of Disordered Media: Proceedings of a Conference Held at the Courant Institute, June 1–3, 1981*, pp. 111–130. Berlin / Heidelberg / London / etc.: Springer-Verlag. ISBN 0-8224-8461-7, 0-273-08461-5. {*248, 268*}

Korringa, J., I.-H. Lin, and R. L. Mills 1978. General theorems about homogeneous ellipsoidal inclusions. *American Journal of Physics* 46:517–521. {*254, 268*}

Kröner, E. 1972. *Statistical Continuum Mechanics: Course Held at the Department of General Mechanics, Udine, October, 1971*, pp. 109–120. Berlin / Heidelberg / London / etc.: Springer-Verlag. {*251, 268*}

Kröner, E. 1977. Bounds for the effective elastic moduli of disordered materials. *Journal of the Mechanics and Physics of Solids* 25:137–155. {*251, 268, 282, 287, 291, 311, 458, 493, 553, 566*}

Kunin, I. A. and E. G. Sosnina 1971. Ellipsoidal inhomogeneity in an elastic medium. *Doklady Akademii Nauk SSSR* 199:571–574. {*254, 268*}

Maxwell, J. C. 1873. *A Treatise on Electricity and Magnetism*. Oxford, United Kingdom: Clarendon Press. Articles 437 and 438 (pp. 62–67). {*132, 140, 252, 268*}

Milton, G. W. 1987. Multicomponent composites, electrical networks and new types of continued fraction. I. *Communications in Mathematical Physics* 111(2):281–327. {*248, 268, 397, 412, 619, 641*}

Milton, G. W. 1990. On characterizing the set of possible effective tensors of composites: The variational method and the translation method. *Communications on Pure and Applied Mathematics (New York)* 43(1):63–125. {*164, 183, 248, 265, 268, 277, 287, 451, 454, 473, 494, 499, 505, 512, 513, 518, 526, 532, 551*}

Murat, F. 1978. Compacité par compensation. *Annali Scuola Normale Superiore-Pisa, Classe di Scienze, Serie IV.* 5(3):489–507. {*59, 72, 250, 269, 275, 276, 287*}

Murat, F. 1981. Compacité par compensation: Condition nécessaire et suffisante de continuité faible sous une hypothèse de rang constant. (French) [Compensated compactness: Necessary and sufficient conditions for weak continuity under a constant-rank hypothesis]. *Annali Scuola Normale Superiore-Pisa, Classe di Scienze, Serie IV* 8(1):69–102. {*250, 269, 275, 288*}

Oldroyd, J. G. 1956. The effect of small viscous inclusions on the mechanical properties of an elastic solid. In R. Grammel (ed.), *Deformation and Flow of Solids: Colloquium, Madrid, September 26–30, 1955. Berlin, Springer, 1956*, pp. 304–313. Berlin / Heidelberg / London / etc.: Springer-Verlag. {*256, 269*}

Papanicolaou, G. and S. Varadhan 1982. Boundary value problems with rapidly oscillating random coefficients. *Colloquia Mathematica Societatis János Bolyai* 27:835–873. {*11, 12, 17, 248, 269*}

Poisson, S. D. 1826. Second mémoire sur la théorie de magnétisme. *Mémoires de l'Académie royale des Sciences de l'Institut de France* 5:488–533. {*252, 269*}

Torquato, S. 1997. Effective stiffness tensor of composite media. I. Exact series expansions. *Journal of the Mechanics and Physics of Solids* 45(9):1421–1448. {*258, 269, 305, 312, 461, 496*}

Walpole, L. J. 1991. A rotated rigid ellipsoidal inclusion in an elastic medium. *Proceedings of the Royal Society of London. Series A, Mathematical and Physical Sciences* 433 (1887):179–207. {*255, 269*}

Wang, B. 1992. Three-dimensional analysis of an ellipsoidal inclusion in a piezoelectric material. *International Journal of Solids and Structures* 29:293–308. {*255, 269*}

Willis, J. R. 1975. The interaction of gas bubbles in an anisotropic elastic solid. *Journal of the Mechanics and Physics of Solids* 23:129–138. {*254, 269*}

Willis, J. R. 1977. Bounds and self-consistent estimates for the overall properties of anisotropic composites. *Journal of the Mechanics and Physics of Solids* 25:185–202. {*256, 269, 327, 340, 347, 353, 464, 497*}

Willis, J. R. 1981. Variational and related methods for the overall properties of composites. *Advances in Applied Mechanics* 21:1–78. {*xxv, xxviii, 185, 200, 220, 252, 255, 269, 291, 312*}

Willis, J. R. 1982. Elasticity theory of composites. In H. G. Hopkins and M. J. Sewell (eds.), *Mechanics of Solids*, pp. 653–686. New York: Pergamon. ISBN 0-08-025443-8. {*252, 255, 269*}

Willis, J. R. 1987. Randomly inhomogeneous media. In E. Sanchez-Palencia and A. Zaoui (eds.), *Part V of Homogenization Techniques for Composite Media Proceedings, 1985, Udine, Italy*, pp. 279–336. Berlin / Heidelberg / London / etc.: Springer-Verlag. {*258, 269*}

Willis, J. R. and J. R. Acton 1976. The overall elastic moduli of a dilute suspension of spheres. *Quarterly Journal of Mechanics and Applied Mathematics* 29:163–177. {*191, 220, 252, 270*}

13

Variational principles and inequalities

Variational principles have long been known in the context of both conductivity type problems and elasticity problems. Their application to composites was initiated by Hill (1952), who used them to show that the Voigt (1889, 1910) and Reuss (1929) estimates of the elastic moduli of polycrystals were in fact bounds. A new type of variational principle was discovered by Hashin and Shtrikman (1962a, 1962b, 1963), which become famous because it lead to optimal bounds on the conductivity, bulk, and shear moduli of isotropic composites of two isotropic phases. Hill (1963b) gave rigorous proof of their variational principles, showing how they could be derived from the classical variational principles. Subsequently, Hashin (1967) generalized the variational principles to inhomogeneous elastic bodies (not just composites) subject to body forces and mixed boundary conditions. Cherkaev and Gibiansky (1994) extended all of these variational principles to media with complex moduli. Talbot and Willis (1985) extended the Hashin and Shtrikman variational principles to nonlinear media. Other variational inequalities[1] for nonlinear media, based on comparisons with linear inhomogeneous media, were obtained by Ponte Castañeda (1991). In a development that falls outside the range of this book, Smyshlyaev and Fleck (1994, 1996) extended the Hashin and Shtrikman variational principles to elastic composites, where the elastic energy depends not only on the strain, but also on the strain gradient.

13.1. Classical variational principles and inequalities

We have seen how to manipulate equations into a form where the tensor entering the constitutive law is self-adjoint and positive-definite. The main motivation for doing this is that it leads to a variational expression for the effective tensor through energy minimization principles. The following derivation of these energy minimization principles is nonstandard but parallels the subsequent derivation of the Hashin-Shtrikman variational principles.

Let us suppose that $\boldsymbol{L}$ is self-adjoint and positive-definite. Then the effective tensor $\boldsymbol{L}_*$ will also be self-adjoint and is determined once we know the values that the quadratic form

$$W(\boldsymbol{E}_0) = \tfrac{1}{2}\boldsymbol{E}_0 \cdot \boldsymbol{L}_* \boldsymbol{E}_0 \tag{13.1}$$

takes as $\boldsymbol{E}_0$ varies over all fields in $\mathcal{U}$. Physically, this quadratic form usually represents either the average field energy stored in the composite, or the rate at which average field energy is

[1] In this book we use the term variational inequality to mean an expression that provides a bound when evaluated for any choice of admissible trial field. If the bound becomes an equality for some choice of trial field, the variational inequality can be rewritten as a variational principle.

dissipated into heat. For example, for elasticity $\frac{1}{2}\boldsymbol{\epsilon}_0 \cdot \boldsymbol{\mathcal{C}}_*\boldsymbol{\epsilon}_0$ represents the average elastic energy per unit volume; for dielectrics $\frac{1}{2}\boldsymbol{e}_0 \cdot \boldsymbol{\varepsilon}_*\boldsymbol{e}_0$ represents the average electrical energy per unit volume; while for conductors $\frac{1}{2}\boldsymbol{e}_0 \cdot \boldsymbol{\sigma}_*\boldsymbol{e}_0$ represents the average dissipation of electrical energy into heat per unit volume. The identification of the quadratic form with the average energy or average energy dissipation is a corollary of (12.7) and was proved by Hill (1963a) and Hashin (1964, 1972).

Now any variational principle should reduce to an inequality involving a trial field that becomes an equality when the trial field equals the actual field. This suggests that variational principles might stem naturally from quadratic forms involving the difference between the actual field and the trial field. Of course this quadratic form should also incorporate the tensor $\boldsymbol{L}$, which we know to be self-adjoint and positive-semidefinite. These considerations indicate that a variational principle might arise from an analysis of the quadratic form

$$\langle (\boldsymbol{E} - \underline{\boldsymbol{E}}) \cdot \boldsymbol{L}(\boldsymbol{E} - \underline{\boldsymbol{E}}) \rangle \geq 0, \tag{13.2}$$

where $\boldsymbol{E}$ is the actual solution of the usual equations

$$\boldsymbol{E} \in \mathcal{U} \oplus \mathcal{E}, \quad \langle \boldsymbol{E} \rangle = \boldsymbol{E}_0, \quad \boldsymbol{J} = \boldsymbol{L}\boldsymbol{E} \in \mathcal{U} \oplus \mathcal{J}, \tag{13.3}$$

and $\underline{\boldsymbol{E}}$ is a trial field. We have not yet imposed any constraints on the trial field $\underline{\boldsymbol{E}}$; these will be introduced as needed.

By expanding (13.2) and using (13.3) and the self-adjointness of $\boldsymbol{L}$, we obtain

$$2\langle \underline{\boldsymbol{E}} \cdot \boldsymbol{J} \rangle - \langle \boldsymbol{E} \cdot \boldsymbol{J} \rangle \leq \langle \underline{\boldsymbol{E}} \cdot \boldsymbol{L}\underline{\boldsymbol{E}} \rangle. \tag{13.4}$$

We would like the left-hand side of this equation not to depend on the explicit form of the fields $\boldsymbol{E}$ and $\boldsymbol{J}$ (since these fields might be unknown) but rather to depend on their average values. This is ensured if we require that the trial field $\underline{\boldsymbol{E}}$ is in the subspace $\mathcal{U} \oplus \mathcal{E}$, that is,

$$\underline{\boldsymbol{E}} \in \mathcal{U} \oplus \mathcal{E}.$$

Then the orthogonality of the subspaces $\mathcal{E}$ and $\mathcal{U} \oplus \mathcal{J}$ implies that

$$\langle \boldsymbol{E} \cdot \boldsymbol{J} \rangle = \boldsymbol{E}_0 \cdot \boldsymbol{J}_0, \quad \langle \underline{\boldsymbol{E}} \cdot \boldsymbol{J} \rangle = \underline{\boldsymbol{E}}_0 \cdot \boldsymbol{J}_0, \tag{13.5}$$

in which

$$\boldsymbol{J}_0 = \langle \boldsymbol{J} \rangle = \boldsymbol{L}_*\boldsymbol{E}_0 \quad \text{and} \quad \underline{\boldsymbol{E}}_0 = \langle \underline{\boldsymbol{E}} \rangle. \tag{13.6}$$

Substitution of (13.5) and (13.6) back into (13.4) gives the inequality

$$(2\underline{\boldsymbol{E}}_0 - \boldsymbol{E}_0) \cdot \boldsymbol{L}_*\boldsymbol{E}_0 \leq \langle \underline{\boldsymbol{E}} \cdot \boldsymbol{L}\underline{\boldsymbol{E}} \rangle. \tag{13.7}$$

This inequality holds for all choices of $\boldsymbol{E}_0$ and for all choices of $\underline{\boldsymbol{E}} \in \mathcal{U} \oplus \mathcal{E}$. As such it is useful for bounding $\boldsymbol{L}_*\boldsymbol{E}_0$ for a given $\boldsymbol{E}_0$ when the average value of the trial field is not aligned with $\boldsymbol{E}_0$, that is, when $\langle \underline{\boldsymbol{E}} \rangle$ is not proportional to $\boldsymbol{E}_0$.

If our interest is in bounding the effective tensor $\boldsymbol{L}_*$, then for a given choice of trial field $\underline{\boldsymbol{E}}$ we should choose $\boldsymbol{E}_0$ to maximize the quadratic form on the left-hand side of (13.7). This choice of $\boldsymbol{E}_0$, namely, $\boldsymbol{E}_0 = \underline{\boldsymbol{E}}_0$, generates the inequality

$$\boldsymbol{E}_0 \cdot \boldsymbol{L}_*\boldsymbol{E}_0 \leq \langle \underline{\boldsymbol{E}} \cdot \boldsymbol{L}\underline{\boldsymbol{E}} \rangle, \quad \text{where } \boldsymbol{E}_0 = \langle \underline{\boldsymbol{E}} \rangle. \tag{13.8}$$

For a given choice of trial field $\underline{\boldsymbol{E}}$ this provides a linear constraint on the matrix elements of $\boldsymbol{L}_*$. Furthermore, since

$$\langle \underline{\boldsymbol{E}} \cdot \boldsymbol{L} \underline{\boldsymbol{E}} \rangle - \boldsymbol{E}_0 \cdot \boldsymbol{L}_* \boldsymbol{E}_0 = \langle (\boldsymbol{E} - \underline{\boldsymbol{E}}) \cdot \boldsymbol{L} (\boldsymbol{E} - \underline{\boldsymbol{E}}) \rangle, \tag{13.9}$$

it follows that the difference between the energy computed with a trial field and the actual energy is a quadratic function of the difference between the trial field and the actual field. Therefore a reasonable approximation of the field should typically produce a very good estimate of the energy.

Notice that because $\boldsymbol{L}$ is positive-definite, equality in (13.2), and hence equality in (13.8), is achieved if and only if $\underline{\boldsymbol{E}} = \boldsymbol{E}$, that is, if and only if the trial field equals the actual field. It follows that we can rewrite (13.8) as a variational principle,

$$\boldsymbol{E}_0 \cdot \boldsymbol{L}_* \boldsymbol{E}_0 = \min_{\substack{\underline{\boldsymbol{E}} \in \mathcal{U} \oplus \mathcal{E} \\ \langle \underline{\boldsymbol{E}} \rangle = \boldsymbol{E}_0}} \langle \underline{\boldsymbol{E}} \cdot \boldsymbol{L} \underline{\boldsymbol{E}} \rangle, \tag{13.10}$$

or, equivalently,

$$W_*(\boldsymbol{E}_0) = \min_{\substack{\underline{\boldsymbol{E}} \in \mathcal{U} \oplus \mathcal{E} \\ \langle \underline{\boldsymbol{E}} \rangle = \boldsymbol{E}_0}} \langle W(\boldsymbol{x}, \underline{\boldsymbol{E}}(\boldsymbol{x})) \rangle, \tag{13.11}$$

where $W(\boldsymbol{x}, \boldsymbol{A}) = \boldsymbol{A} \cdot \boldsymbol{L}(\boldsymbol{x}) \boldsymbol{A}/2$ gives the energy density (or energy dissipation density) at the point $\boldsymbol{x}$ when the field there takes the value $\boldsymbol{A}$. This variational principle is usually called the classical energy minimization principle; it says that the energy is minimized when the trial field $\underline{\boldsymbol{E}}$ equals the actual field $\boldsymbol{E}$.

By applying the duality principle, we also have the complementary energy minimization principle,

$$\boldsymbol{J}_0 \cdot \boldsymbol{L}_*^{-1} \boldsymbol{J}_0 = \min_{\substack{\underline{\boldsymbol{J}} \in \mathcal{U} \oplus \mathcal{J} \\ \langle \underline{\boldsymbol{J}} \rangle = \boldsymbol{J}_0}} \langle \underline{\boldsymbol{J}} \cdot \boldsymbol{L}^{-1} \underline{\boldsymbol{J}} \rangle. \tag{13.12}$$

These variational principles can be applied to obtain bounds on the effective tensor $\boldsymbol{L}_*$. For example, the simplest choice of trial fields, namely, $\underline{\boldsymbol{E}} = \boldsymbol{E}_0$ and $\underline{\boldsymbol{J}} = \boldsymbol{J}_0$, gives the elementary bounds

$$\boldsymbol{E}_0 \cdot \boldsymbol{L}_* \boldsymbol{E}_0 \le \langle \boldsymbol{E}_0 \cdot \boldsymbol{L} \boldsymbol{E}_0 \rangle, \qquad \boldsymbol{J}_0 \cdot \boldsymbol{L}_*^{-1} \boldsymbol{J}_0 \le \langle \boldsymbol{J}_0 \cdot \boldsymbol{L}^{-1} \boldsymbol{J}_0 \rangle.$$

In particular, as applied to a composite material, since these relations hold for all constant fields $\boldsymbol{E}_0$ and $\boldsymbol{J}_0$, they imply the arithmetic and harmonic mean bounds

$$\langle \boldsymbol{L}^{-1} \rangle^{-1} \le \boldsymbol{L}_* \le \langle \boldsymbol{L} \rangle \tag{13.13}$$

of Hill (1952). We will examine the question of bounds in more detail later.

In the above derivation we assumed that the operator $\boldsymbol{L}$ is self-adjoint and positive-semidefinite. In fact this is a much stronger assumption than is actually needed. Indeed, since $\boldsymbol{E} - \underline{\boldsymbol{E}} \in \mathcal{E}$, the inequality (13.2) and hence the variational principle (13.10) holds, provided that

$$\boldsymbol{\Gamma}_1 \boldsymbol{L} \boldsymbol{\Gamma}_1 \ge 0,$$

that is, provided that $\boldsymbol{L}$ is positive-semidefinite on the subspace $\mathcal{E}$. For example, the matrix $\boldsymbol{L}$ given by (12.56) satisfies this condition when $a_{11} \ge 0$. Similarly, the dual variational principle

(13.12) holds provided that $\boldsymbol{L}^{-1}$ is positive-semidefinite on the subspace $\mathcal{J}$, that is, provided that

$$\boldsymbol{\Gamma}_2\boldsymbol{L}^{-1}\boldsymbol{\Gamma}_2 \geq 0.$$

Of course, for these statements to have meaning we need to show that the effective tensor $\boldsymbol{L}_*$ exists when $\boldsymbol{L}$ is positive-semidefinite on $\mathcal{E}$, and when $\boldsymbol{L}^{-1}$ is positive-semidefinite on $\mathcal{J}$. One approach is to take (13.10) or (13.12) as the definition of $\boldsymbol{L}_*$. Alternatively, $\boldsymbol{L}_*$ can be defined through formula (12.58) or its dual, or, as will be seen in section 14.8 on page 301, $\boldsymbol{L}_*$ can be defined through convergent series expansions.

13.2. Monotonicity of the effective tensor

The variational principles imply that in composite material $\boldsymbol{L}_*$ is a monotonic function of $\boldsymbol{L}(\boldsymbol{x})$ in the sense that

$$\boldsymbol{L}'_* \geq \boldsymbol{L}_* \quad \text{when} \quad \boldsymbol{L}'(\boldsymbol{x}) \geq \boldsymbol{L}(\boldsymbol{x}) > 0 \ \text{ for all } \boldsymbol{x},$$

where both $\boldsymbol{L}'(\boldsymbol{x})$ and $\boldsymbol{L}(\boldsymbol{x})$ are self-adjoint and positive-definite tensor fields while $\boldsymbol{L}'_*$ and $\boldsymbol{L}_*$ are their associated effective tensors. This is easy to establish [as shown, for example, by Tartar (1979b)]. Since $\boldsymbol{L}'(\boldsymbol{x}) \geq \boldsymbol{L}(\boldsymbol{x})$ for all $\boldsymbol{x}$, it follows that

$$\langle \underline{\boldsymbol{E}} \cdot \boldsymbol{L}'\underline{\boldsymbol{E}} \rangle \geq \langle \underline{\boldsymbol{E}} \cdot \boldsymbol{L}\underline{\boldsymbol{E}} \rangle$$

for every field $\underline{\boldsymbol{E}} \in \mathcal{H}$ and in particular for every field $\underline{\boldsymbol{E}} \in \mathcal{U} \oplus \mathcal{E}$. Consequently we have

$$\boldsymbol{E}_0 \cdot \boldsymbol{L}'_*\boldsymbol{E}_0 = \min_{\substack{\underline{\boldsymbol{E}} \in \mathcal{U} \oplus \mathcal{E} \\ \langle \underline{\boldsymbol{E}} \rangle = \boldsymbol{E}_0}} \langle \underline{\boldsymbol{E}} \cdot \boldsymbol{L}'\underline{\boldsymbol{E}} \rangle \geq \min_{\substack{\underline{\boldsymbol{E}} \in \mathcal{U} \oplus \mathcal{E} \\ \langle \underline{\boldsymbol{E}} \rangle = \boldsymbol{E}_0}} \langle \underline{\boldsymbol{E}} \cdot \boldsymbol{L}\underline{\boldsymbol{E}} \rangle = \boldsymbol{E}_0 \cdot \boldsymbol{L}_*\boldsymbol{E}_0,$$

which establishes that $\boldsymbol{L}'_* \geq \boldsymbol{L}_*$. This makes good physical sense. For example, in a conducting locally isotropic material one expects the overall effective conductivity σ_* to increase when the local conductivity $\sigma(\boldsymbol{x})$ is increased.

13.3. Null Lagrangians

Suppose that we have a scalar-valued function $Q(\boldsymbol{A})$, independent of $\boldsymbol{x}$, such that

$$\langle Q(\boldsymbol{E}) \rangle = Q(\langle \boldsymbol{E} \rangle) \ \text{ for all } \boldsymbol{E} \in \mathcal{U} \oplus \mathcal{E}. \tag{13.14}$$

Now consider a composite material with energy density (or energy dissipation density)

$$W'(\boldsymbol{x}, \boldsymbol{A}) = W(\boldsymbol{x}, \boldsymbol{A}) - cQ(\boldsymbol{A}),$$

in which c is a fixed constant. From the variational principle (13.11) it has an associated average energy density,

$$\begin{aligned} W'_*(\boldsymbol{E}_0) &= \min_{\substack{\underline{\boldsymbol{E}} \in \mathcal{U} \oplus \mathcal{E} \\ \langle \underline{\boldsymbol{E}} \rangle = \boldsymbol{E}_0}} \langle W'(\boldsymbol{x}, \underline{\boldsymbol{E}}(\boldsymbol{x})) \rangle \\ &= \min_{\substack{\underline{\boldsymbol{E}} \in \mathcal{U} \oplus \mathcal{E} \\ \langle \underline{\boldsymbol{E}} \rangle = \boldsymbol{E}_0}} \langle W(\boldsymbol{x}, \underline{\boldsymbol{E}}(\boldsymbol{x})) \rangle - c\langle Q(\underline{\boldsymbol{E}}(\boldsymbol{x})) \rangle \\ &= W_*(\boldsymbol{E}_0) - cQ(\boldsymbol{E}_0). \end{aligned}$$

In other words, when the local energy density function is shifted by cQ, the average energy density function is also shifted by cQ. In particular, if the functions are quadratic, then

$$W(\boldsymbol{x}, \boldsymbol{A}) = \boldsymbol{A} \cdot \boldsymbol{L}(\boldsymbol{x})\boldsymbol{A}/2, \quad W_*(\boldsymbol{E}_0) = \boldsymbol{E}_0 \cdot \boldsymbol{L}_*\boldsymbol{E}_0/2, \quad Q(\boldsymbol{A}) = \boldsymbol{A} \cdot \boldsymbol{T}\boldsymbol{A}/2$$
$$W'(\boldsymbol{x}, \boldsymbol{A}) = \boldsymbol{A} \cdot \boldsymbol{L}'(\boldsymbol{x})\boldsymbol{A}/2, \quad W'_*(\boldsymbol{E}_0) = \boldsymbol{E}_0 \cdot \boldsymbol{L}'_*\boldsymbol{E}_0/2,$$

where $\boldsymbol{T}$ is a real-valued symmetric tensor. We see that a medium with tensor $\boldsymbol{L}'(\boldsymbol{x}) = \boldsymbol{L}(\boldsymbol{x}) - c\boldsymbol{T}$ will have effective tensor $\boldsymbol{L}'_* = \boldsymbol{L}_* - c\boldsymbol{T}$; that is, if we translate $\boldsymbol{L}(\boldsymbol{x})$ by a multiple of $\boldsymbol{T}$, then the effective tensor will be translated in exactly the same way.

Functions satisfying (13.14) are called null Lagrangians or, equivalently, weakly continuous functions. More precisely, a function Q is weakly continuous if for any sequence of fields $\boldsymbol{E}_\epsilon(\boldsymbol{x})$ satisfying the required differential constraints and having a weak limit $\boldsymbol{E}_0(\boldsymbol{x})$, one has that $Q(\boldsymbol{E}_\epsilon(\boldsymbol{x}))$ converges weakly to $Q(\boldsymbol{E}_0(\boldsymbol{x}))$. Necessary and essentially sufficient algebraic conditions to determine whether a (quadratic or nonquadratic) function is a null Lagrangian have been given by Murat (1978, 1981, 1987) [see also Pedregal (1989)]. In the important case where the fields are constrained to be gradients of an ℓ-component potential $\boldsymbol{u}$, that is, $\boldsymbol{E}(\boldsymbol{x}) = \nabla\boldsymbol{u}(\boldsymbol{x})$, $Q(\boldsymbol{E})$ is a null Lagrangian if and only if it is a linear combination of the subdeterminants (minors) of any order p ($1 \geq p \geq \min\{d, \ell\}$) of the $d \times \ell$ matrix $\boldsymbol{E}$. Such functions can be expressed as the divergence of a vector field, which explains why they are null Lagrangians. For references see Ball, Currie, and Olver (1981), who also show that when $\boldsymbol{E}(\boldsymbol{x}) = \nabla^k\boldsymbol{u}(\boldsymbol{x})$ there are no new null Lagrangians $Q(\boldsymbol{E})$ beyond those obtained by applying the result for $k = 1$ to the $d\ell^{k-1}$-component potential $\boldsymbol{U}(\boldsymbol{x}) = \nabla^{k-1}\boldsymbol{u}(\boldsymbol{x})$.

When Q is quadratic, the necessary and sufficient conditions can be determined quite simply through an argument that lies at the heart of the compensated compactness method (Murat 1978, 1981, 1987; Tartar 1979a). By expanding $\boldsymbol{E}(\boldsymbol{x})$ in a Fourier series

$$\boldsymbol{E}(\boldsymbol{x}) = \langle \boldsymbol{E} \rangle + \sum_{\boldsymbol{k} \neq 0} e^{i\boldsymbol{k}\cdot\boldsymbol{x}} \widehat{\boldsymbol{E}}(\boldsymbol{k}),$$

we see that (13.14) holds if and only if the expression

$$\begin{aligned} \langle \boldsymbol{E} \cdot \boldsymbol{T}\boldsymbol{E} \rangle - \langle \boldsymbol{E} \rangle \cdot \boldsymbol{T} \langle \boldsymbol{E} \rangle &= \sum_{\boldsymbol{k} \neq 0} \widehat{\boldsymbol{E}}(-\boldsymbol{k}) \cdot \boldsymbol{T}\widehat{\boldsymbol{E}}(\boldsymbol{k}) \\ &= \sum_{\boldsymbol{k} \neq 0} \mathrm{Re}[\widehat{\boldsymbol{E}}(\boldsymbol{k})] \cdot \boldsymbol{T}\,\mathrm{Re}[\widehat{\boldsymbol{E}}(\boldsymbol{k})] + \sum_{\boldsymbol{k} \neq 0} \mathrm{Im}[\widehat{\boldsymbol{E}}(\boldsymbol{k})] \cdot \boldsymbol{T}\,\mathrm{Im}[\widehat{\boldsymbol{E}}(\boldsymbol{k})] \end{aligned} \tag{13.15}$$

is zero where $\widehat{\boldsymbol{E}}(-\boldsymbol{k})$ is the complex conjugate of $\widehat{\boldsymbol{E}}(\boldsymbol{k})$ because $\boldsymbol{E}(\boldsymbol{x})$ is real. Also, the constraint that $\boldsymbol{E} \in \mathcal{U} \oplus \mathcal{E}$ is satisfied if and only if the real and imaginary parts of $\widehat{\boldsymbol{E}}(\boldsymbol{k})$ lie in the subspace $\mathcal{E}_{\boldsymbol{k}}$ for all $\boldsymbol{k} \neq 0$. Now we are free to choose $\boldsymbol{E}(\boldsymbol{x})$ so that only one Fourier component is nonzero and real, that is,

$$\begin{aligned} \widehat{\boldsymbol{E}}(\boldsymbol{k}) &= \boldsymbol{B}, \qquad \text{if } \boldsymbol{k} = \boldsymbol{m} \text{ or } \boldsymbol{k} = -\boldsymbol{m}, \\ &= 0, \qquad \text{otherwise.} \end{aligned} \tag{13.16}$$

Substituting this into (13.15) and relabeling $\boldsymbol{m}$ as $\boldsymbol{k}$ we see that a necessary condition for the quadratic form associated with $\boldsymbol{T}$ to be a null Lagrangian is that for all $\boldsymbol{k} \neq 0$,

$$\boldsymbol{B} \cdot \boldsymbol{T}\boldsymbol{B} = 0 \text{ for all real } \boldsymbol{B} \in \mathcal{E}_{\boldsymbol{k}}. \tag{13.17}$$

Conversely, if this condition holds, then for an arbitrary choice of field $\boldsymbol{E} \in \mathcal{U} \oplus \mathcal{E}$ each term in the sum (13.15) is zero and hence the quadratic function associated with $\boldsymbol{T}$ is a null Lagrangian. For simplicity we will just say that $\boldsymbol{T}$ is a null Lagrangian.

Since $\boldsymbol{T}$ is real-valued and symmetric, we deduce that (13.17) holds if and only if

$$\boldsymbol{T}\mathcal{E}_{\boldsymbol{k}} \subset \mathcal{J}_{\boldsymbol{k}} \text{ for all } \boldsymbol{k} \neq 0$$

or, equivalently, if and only if $\boldsymbol{T}\mathcal{E} \subset \mathcal{J}$. Thus $\boldsymbol{T}$, like the translations encountered in chapter 4 on page 59, maps fields on the right side of the constitutive equation to fields satisfying the same differential constraints as those fields on the left side of the constitutive equation. Conversely, if $\boldsymbol{T}$ has this property and is self-adjoint, then the quadratic form associated with $\boldsymbol{T}$ is a null Lagrangian.

When $\boldsymbol{T}$ is not self-adjoint, the orthogonality of the spaces $\mathcal{U}$, $\mathcal{E}$, and $\mathcal{J}$ implies that

$$\langle \boldsymbol{E}' \cdot \boldsymbol{T}\boldsymbol{E} \rangle = \langle \boldsymbol{E}' \rangle \cdot \boldsymbol{T} \langle \boldsymbol{E} \rangle \text{ for all } \boldsymbol{E}, \boldsymbol{E}' \in \mathcal{U} \oplus \mathcal{E}. \tag{13.18}$$

if and only if $\boldsymbol{T}\mathcal{E} \subset \mathcal{J}$, that is, if and only if $\boldsymbol{T}$ maps fields on the right side of the constitutive equation to fields satisfying the same differential constraints as those fields on the left side of the constitutive equation. By expanding the fields $\boldsymbol{E}(\boldsymbol{x})$ and $\boldsymbol{E}'(\boldsymbol{x})$ in Fourier series we see that the condition (13.18) holds if and only if for all $\boldsymbol{k} \neq 0$,

$$\boldsymbol{B}' \cdot \boldsymbol{T}\boldsymbol{B} = 0 \text{ for all real } \boldsymbol{B}', \boldsymbol{B} \in \mathcal{E}_{\boldsymbol{k}}. \tag{13.19}$$

Functions $\boldsymbol{E}' \cdot \boldsymbol{T}\boldsymbol{E}$ satisfying (13.18) are weakly continuous bilinear forms. For any two sequences of fields $\boldsymbol{E}_\epsilon(\boldsymbol{x})$ and $\boldsymbol{E}'_\epsilon(\boldsymbol{x})$ satisfying the required differential constraints and having weak limits $\boldsymbol{E}_0(\boldsymbol{x})$ and $\boldsymbol{E}'_0(\boldsymbol{x})$, one has that $\boldsymbol{E}'_\epsilon(\boldsymbol{x})\boldsymbol{T}\boldsymbol{E}_\epsilon(\boldsymbol{x})$ converges weakly to $\boldsymbol{E}'_0(\boldsymbol{x})\boldsymbol{T}\boldsymbol{E}_0(\boldsymbol{x})$. For fields satisfying first-order differential constraints, the condition (13.19) is equivalent to the one given by Murat (1978), theorem 3, which he found was necessary and sufficient to ensure weak continuity of the bilinear form; see also Tartar (1979a).

13.4. Variational principles for problems with a complex or other non-self-adjoint tensor

If the tensor $\boldsymbol{L}(\boldsymbol{x})$ is complex, but with a positive-definite imaginary part, we have seen in section 11.5 on page 234 how to transform the equations to an equivalent set of equations where the associated tensor $\boldsymbol{\mathcal{L}}(\boldsymbol{x})$ is real and positive-definite. By applying the classical variational principles to $\boldsymbol{\mathcal{L}}(\boldsymbol{x})$ one obtains variational principles for the complex effective tensor $\boldsymbol{L}_* = \boldsymbol{L}'_* + i\boldsymbol{L}''_*$. For example, in the context of the dielectric problem we obtain the variational principle of Cherkaev and Gibiansky (1994)

$$\begin{aligned}
&\begin{pmatrix} -\boldsymbol{d}'_0 \\ \boldsymbol{e}'_0 \end{pmatrix} \cdot \begin{pmatrix} [\boldsymbol{\varepsilon}''_*]^{-1} & [\boldsymbol{\varepsilon}''_*]^{-1}\boldsymbol{\varepsilon}'_* \\ \boldsymbol{\varepsilon}'_*[\boldsymbol{\varepsilon}''_*]^{-1} & \boldsymbol{\varepsilon}''_* + \boldsymbol{\varepsilon}'_*[\boldsymbol{\varepsilon}''_*]^{-1}\boldsymbol{\varepsilon}'_* \end{pmatrix} \begin{pmatrix} -\boldsymbol{d}'_0 \\ \boldsymbol{e}'_0 \end{pmatrix} \\
&\quad = \min_{\substack{\underline{\boldsymbol{d}}'(\boldsymbol{x}) \\ \nabla \cdot \underline{\boldsymbol{d}}' = 0 \\ \langle \underline{\boldsymbol{d}}' \rangle = \boldsymbol{d}'_0}} \min_{\substack{\underline{\boldsymbol{e}}'(\boldsymbol{x}) \\ \nabla \times \underline{\boldsymbol{e}}' = 0 \\ \langle \underline{\boldsymbol{e}}' \rangle = \boldsymbol{e}'_0}} \left\langle \begin{pmatrix} -\underline{\boldsymbol{d}}' \\ \underline{\boldsymbol{e}}' \end{pmatrix} \cdot \begin{pmatrix} [\boldsymbol{\varepsilon}'']^{-1} & [\boldsymbol{\varepsilon}'']^{-1}\boldsymbol{\varepsilon}' \\ \boldsymbol{\varepsilon}'[\boldsymbol{\varepsilon}'']^{-1} & \boldsymbol{\varepsilon}'' + \boldsymbol{\varepsilon}'[\boldsymbol{\varepsilon}'']^{-1}\boldsymbol{\varepsilon}' \end{pmatrix} \begin{pmatrix} -\underline{\boldsymbol{d}}' \\ \underline{\boldsymbol{e}}' \end{pmatrix} \right\rangle,
\end{aligned} \tag{13.20}$$

with equality when $\underline{\boldsymbol{d}}'(\boldsymbol{x})$ equals the real part of the electric displacement field $\boldsymbol{d}(\boldsymbol{x})$ and the real part of the electric field $\boldsymbol{e}(\boldsymbol{x})$. Thus one applies these variational principles by substituting

estimates of the real parts of the electric displacement field and electric field into this formula. There is also the complementary variational principle,

$$\begin{pmatrix} \boldsymbol{e}_0'' \\ \boldsymbol{d}_0'' \end{pmatrix} \cdot \begin{pmatrix} \varepsilon_*'' + \varepsilon_*'[\varepsilon_*'']^{-1}\varepsilon_*' & -\varepsilon_*'[\varepsilon_*'']^{-1} \\ -[\varepsilon_*'']^{-1}\varepsilon_*' & [\varepsilon_*'']^{-1} \end{pmatrix} \begin{pmatrix} \boldsymbol{e}_0'' \\ \boldsymbol{d}_0'' \end{pmatrix}$$
$$= \min_{\underline{\boldsymbol{e}}''(\boldsymbol{x})} \min_{\underline{\boldsymbol{d}}''(\boldsymbol{x})} \left\langle \begin{pmatrix} \underline{\boldsymbol{e}}'' \\ \underline{\boldsymbol{d}}'' \end{pmatrix} \cdot \begin{pmatrix} \varepsilon'' + \varepsilon'[\varepsilon'']^{-1}\varepsilon' & -\varepsilon'[\varepsilon'']^{-1} \\ -[\varepsilon'']^{-1}\varepsilon' & [\varepsilon'']^{-1} \end{pmatrix} \begin{pmatrix} \underline{\boldsymbol{e}}'' \\ \underline{\boldsymbol{d}}'' \end{pmatrix} \right\rangle,$$
$$\nabla \times \underline{\boldsymbol{e}}'' = 0 \quad \nabla \cdot \underline{\boldsymbol{d}}'' = 0$$
$$\langle \underline{\boldsymbol{e}}'' \rangle = \boldsymbol{e}_0'' \quad \langle \underline{\boldsymbol{d}}'' \rangle = \boldsymbol{d}_0''$$

but this turns out to be equivalent to the original variational principle (13.20), as can be seen by making the substitutions $\boldsymbol{e}_0'' \to \boldsymbol{e}_0'$, $\boldsymbol{d}_0'' \to \boldsymbol{d}_0'$, $\underline{\boldsymbol{e}}'' \to \underline{\boldsymbol{e}}'$, $\underline{\boldsymbol{d}}'' \to \underline{\boldsymbol{d}}'$ and comparing the quadratic forms.

I first learned of these variational principles from Cherkaev and Gibiansky during a trip to Russia in 1986, although it was not until eight years later that their work was published (Cherkaev and Gibiansky 1994). Their variational principles are easily extended to other non-self-adjoint problems when the tensor $\boldsymbol{L}(\boldsymbol{x})$ is real but not symmetric, having a positive-definite symmetric part [see Milton (1990) and also Fannjiang and Papanicolaou (1994) and Norris (1997)]. In the context of conduction in a magnetic field one obtains from (12.71), (12.72), and (12.73) the variational principle

$$\begin{pmatrix} \boldsymbol{j}_{s0} \\ \boldsymbol{e}_{s0} \end{pmatrix} \cdot \begin{pmatrix} (\boldsymbol{\sigma}_s^*)^{-1} & -(\boldsymbol{\sigma}_s^*)^{-1}\boldsymbol{\sigma}_a^* \\ \boldsymbol{\sigma}_a^*(\boldsymbol{\sigma}_s^*)^{-1} & \boldsymbol{\sigma}_s^* - \boldsymbol{\sigma}_a^*(\boldsymbol{\sigma}_s^*)^{-1}\boldsymbol{\sigma}_a^* \end{pmatrix} \begin{pmatrix} \boldsymbol{j}_{s0} \\ \boldsymbol{e}_{s0} \end{pmatrix}$$
$$= \min_{\underline{\boldsymbol{j}}_s(\boldsymbol{x})} \min_{\underline{\boldsymbol{e}}_s(\boldsymbol{x})} \left\langle \begin{pmatrix} \underline{\boldsymbol{j}}_s \\ \underline{\boldsymbol{e}}_s \end{pmatrix} \cdot \begin{pmatrix} \boldsymbol{\sigma}_s^{-1} & -\boldsymbol{\sigma}_s^{-1}\boldsymbol{\sigma}_a \\ \boldsymbol{\sigma}_a\boldsymbol{\sigma}_s^{-1} & \boldsymbol{\sigma}_s - \boldsymbol{\sigma}_a\boldsymbol{\sigma}_s^{-1}\boldsymbol{\sigma}_a \end{pmatrix} \begin{pmatrix} \underline{\boldsymbol{j}}_s \\ \underline{\boldsymbol{e}}_s \end{pmatrix} \right\rangle,$$
$$\nabla \cdot \underline{\boldsymbol{j}}_s = 0 \quad \nabla \times \underline{\boldsymbol{e}}_s = 0$$
$$\langle \underline{\boldsymbol{j}}_s \rangle = \boldsymbol{j}_{s0} \quad \langle \underline{\boldsymbol{e}}_s \rangle = \boldsymbol{e}_{s0}$$

with equality when $\underline{\boldsymbol{j}}_s = (\boldsymbol{j} + \boldsymbol{j}')/2$ and $\underline{\boldsymbol{e}}_s = (\boldsymbol{e} + \boldsymbol{e}')/2$, where $\boldsymbol{j}$ and $\boldsymbol{e}$ are solutions of the conductivity equations, while $\boldsymbol{j}'$ and $\boldsymbol{e}'$ are solutions of the adjoint conductivity equations.

Besides these "energy minimization" principles, we also mention that there are saddle-point variational principles,

$$\begin{pmatrix} \boldsymbol{e}_0'' \\ \boldsymbol{e}_0' \end{pmatrix} \cdot \begin{pmatrix} -\varepsilon'' & \varepsilon' \\ \varepsilon' & \varepsilon'' \end{pmatrix} \begin{pmatrix} \boldsymbol{e}_0'' \\ \boldsymbol{e}_0' \end{pmatrix}$$
$$= \max_{\underline{\boldsymbol{e}}''(\boldsymbol{x})} \min_{\underline{\boldsymbol{e}}'(\boldsymbol{x})} \left\langle \begin{pmatrix} \underline{\boldsymbol{e}}'' \\ \underline{\boldsymbol{e}}' \end{pmatrix} \cdot \begin{pmatrix} -\varepsilon'' & \varepsilon' \\ \varepsilon' & \varepsilon'' \end{pmatrix} \begin{pmatrix} \underline{\boldsymbol{e}}'' \\ \underline{\boldsymbol{e}}' \end{pmatrix} \right\rangle,$$
$$\nabla \times \underline{\boldsymbol{e}}'' = 0 \quad \nabla \times \underline{\boldsymbol{e}}' = 0$$
$$\langle \underline{\boldsymbol{e}}' \rangle = \boldsymbol{e}_0' \quad \langle \underline{\boldsymbol{e}}'' \rangle = \boldsymbol{e}_0''$$

and

$$\begin{pmatrix} \boldsymbol{e}_{s0} \\ \boldsymbol{e}_{a0} \end{pmatrix} \cdot \begin{pmatrix} -\boldsymbol{\sigma}_s^* & -\boldsymbol{\sigma}_a^* \\ \boldsymbol{\sigma}_a^* & \boldsymbol{\sigma}_s^* \end{pmatrix} \begin{pmatrix} \boldsymbol{e}_{s0} \\ \boldsymbol{e}_{a0} \end{pmatrix}$$
$$= \max_{\underline{\boldsymbol{e}}_s(\boldsymbol{x})} \min_{\underline{\boldsymbol{e}}_a(\boldsymbol{x})} \left\langle \begin{pmatrix} \underline{\boldsymbol{e}}_s \\ \underline{\boldsymbol{e}}_a \end{pmatrix} \cdot \begin{pmatrix} -\boldsymbol{\sigma}_s & -\boldsymbol{\sigma}_a \\ \boldsymbol{\sigma}_a & \boldsymbol{\sigma}_s \end{pmatrix} \begin{pmatrix} \underline{\boldsymbol{e}}_s \\ \underline{\boldsymbol{e}}_a \end{pmatrix} \right\rangle,$$
$$\nabla \times \underline{\boldsymbol{e}}_s = 0 \quad \nabla \times \underline{\boldsymbol{e}}_a = 0$$
$$\langle \underline{\boldsymbol{e}}_s \rangle = \boldsymbol{e}_{s0} \quad \langle \underline{\boldsymbol{e}}_a \rangle = \boldsymbol{e}_{a0}$$

which follow from the equations (11.53) and (12.70). These saddle-point variational principles have proven useful in asymptotic analysis (Fannjiang and Papanicolaou 1994). It should also be mentioned that Borcea (1999) has obtained a saddle-point variational principle for the quasistatic electromagnetic problem, which does not assume that the electric field is curl free. Variational principles for a wide class of non-self-adjoint equations can be formulated in terms of the equations and their adjoints [see, for example, Finlayson (1972)], although these are not usually minimum principles.

13.5. Hashin-Shtrikman variational principles and inequalities

To obtain a variational inequality based on a choice of trial polarization field $\underline{\boldsymbol{P}} \in \mathcal{H}$, let us look at the equations satisfied by the polarization field $\boldsymbol{P}(\boldsymbol{x})$ and its average $\boldsymbol{P}_0 = \langle \boldsymbol{P} \rangle$:

$$[(\boldsymbol{L} - \boldsymbol{L}_0)^{-1} + \boldsymbol{\Gamma}]\boldsymbol{P} = \boldsymbol{E}_0, \quad \boldsymbol{P}_0 = (\boldsymbol{L}_* - \boldsymbol{L}_0)\boldsymbol{E}_0, \tag{13.21}$$

which were derived in section 12.4 on page 251. Since (13.21) only involves the operator $(\boldsymbol{L} - \boldsymbol{L}_0)^{-1} + \boldsymbol{\Gamma}$, any variational principle for the polarization field must naturally involve this operator. The operators $(\boldsymbol{L} - \boldsymbol{L}_0)^{-1}$ and $\boldsymbol{\Gamma}$ will both be positive-semidefinite when the reference tensor $\boldsymbol{L}_0$ is such that

$$\boldsymbol{L} > \boldsymbol{L}_0, \quad \boldsymbol{\Gamma}_1 \boldsymbol{L}_0 \boldsymbol{\Gamma}_1 \geq 0. \tag{13.22}$$

Hence $(\boldsymbol{L} - \boldsymbol{L}_0)^{-1} + \boldsymbol{\Gamma}$ will surely be positive-definite when these constraints are satisfied.

Of course, we would want any variational inequality involving the polarization field to reduce to an equality when the trial polarization field $\underline{\boldsymbol{P}}$ equals the true polarization field $\boldsymbol{P}$. This suggests that a variational principle might arise from the inequality

$$\langle (\boldsymbol{P} - \underline{\boldsymbol{P}}) \cdot [(\boldsymbol{L} - \boldsymbol{L}_0)^{-1} + \boldsymbol{\Gamma}](\boldsymbol{P} - \underline{\boldsymbol{P}}) \rangle \geq 0, \tag{13.23}$$

implied by the positive-definiteness of the operator $[(\boldsymbol{L} - \boldsymbol{L}_0)^{-1} + \boldsymbol{\Gamma}]$ when (13.22) holds. By expanding this inequality and using (13.21) we see that

$$2\langle \boldsymbol{E}_0 \cdot \underline{\boldsymbol{P}} \rangle - \boldsymbol{E}_0 \cdot (\boldsymbol{L}_* - \boldsymbol{L}_0)\boldsymbol{E}_0 = 2\langle \boldsymbol{E}_0 \cdot \underline{\boldsymbol{P}} \rangle - \langle \boldsymbol{E}_0 \cdot \boldsymbol{P} \rangle \leq \langle \underline{\boldsymbol{P}} \cdot [(\boldsymbol{L} - \boldsymbol{L}_0)^{-1} + \boldsymbol{\Gamma}]\underline{\boldsymbol{P}} \rangle, \tag{13.24}$$

which gives the Hashin-Shtrikman variational inequality,

$$\boldsymbol{E}_0 \cdot \boldsymbol{L}_* \boldsymbol{E}_0 \geq \boldsymbol{E}_0 \cdot \boldsymbol{L}_0 \boldsymbol{E}_0 + 2\langle \boldsymbol{E}_0 \cdot \underline{\boldsymbol{P}} \rangle - \langle \underline{\boldsymbol{P}} \cdot [(\boldsymbol{L} - \boldsymbol{L}_0)^{-1} + \boldsymbol{\Gamma}]\underline{\boldsymbol{P}} \rangle, \tag{13.25}$$

which holds for all choices of applied field $\boldsymbol{E}_0 \in \mathcal{U}$ and all choices of trial polarization field $\underline{\boldsymbol{P}} \in \mathcal{H}$.

Another variational inequality arises when $\boldsymbol{L}$ is positive-definite and the reference tensor is chosen with moduli

$$\boldsymbol{L}_0 > \boldsymbol{L} > 0.$$

Since $\boldsymbol{L}_0^{1/2} \boldsymbol{\Gamma} \boldsymbol{L}_0^{1/2}$ is a projection, we have

$$\boldsymbol{L}_0^{1/2} \boldsymbol{\Gamma} \boldsymbol{L}_0^{1/2} \leq \boldsymbol{I}, \qquad \text{implying that } \boldsymbol{\Gamma} - \boldsymbol{L}_0^{-1} \leq 0. \tag{13.26}$$

Also, by taking the inverse of both sides of the inequality $\boldsymbol{L}_0 > \boldsymbol{L}_0 - \boldsymbol{L}$ (which is allowed because each side is positive-definite), we have

$$(\boldsymbol{L} - \boldsymbol{L}_0)^{-1} + \boldsymbol{L}_0^{-1} < 0. \tag{13.27}$$

Adding (13.26) and (13.27) allows us to conclude that $(\boldsymbol{L} - \boldsymbol{L}_0)^{-1} + \boldsymbol{\Gamma}$ is negative-definite when $\boldsymbol{L}_0 > \boldsymbol{L} > 0$. As a consequence, equations (13.23)–(13.25) hold, but with the sign of the inequalities reversed. In particular, the Hashin-Shtrikman variational inequality takes the form

$$\boldsymbol{E}_0 \cdot \boldsymbol{L}_* \boldsymbol{E}_0 \leq \boldsymbol{E}_0 \cdot \boldsymbol{L}_0 \boldsymbol{E}_0 + 2\langle \boldsymbol{E}_0 \cdot \underline{\boldsymbol{P}} \rangle + \langle \underline{\boldsymbol{P}} \cdot [(\boldsymbol{L}_0 - \boldsymbol{L})^{-1} - \boldsymbol{\Gamma}] \underline{\boldsymbol{P}} \rangle. \tag{13.28}$$

Hashin and Shtrikman (1962b) derived these variational principles in the context of magnetic permeability or, equivalently, electrical conductivity. Their variational principles quickly became famous because they led to optimal bounds on the effective conductivity, bulk, and shear modulus of isotropic composites of two isotropic phases mixed in fixed proportions (see chapter 23 on page 457). Brown played an influential role in the development of the variational principles; see Brown (1965) for some interesting historical remarks.

If we are interested in bounding the energy $W = \boldsymbol{E}_0 \cdot \boldsymbol{L}_* \boldsymbol{E}_0/2$ for a particular value of $\boldsymbol{E}_0$, then it is preferable to work with the variational inequalities (13.25) and (13.28) since they provide a direct bound on W. But if our interest is in bounding the effective tensor $\boldsymbol{L}_*$, then for a given trial polarization field it is best to choose $\boldsymbol{E}_0$ to optimize the bounds. [This is directly analogous to way in which the standard classical variational principle (13.8) was obtained from (13.7).] Since the inequality (13.24) holds for all choices of $\boldsymbol{E}_0$, we may as well choose $\boldsymbol{E}_0$ to minimize the left-hand side, that is, to make the inequality as sharp as possible. With this optimal choice of $\boldsymbol{E}_0$, namely,

$$\boldsymbol{E}_0 = (\boldsymbol{L}_* - \boldsymbol{L}_0)^{-1} \langle \underline{\boldsymbol{P}} \rangle, \tag{13.29}$$

the inequality reduces to

$$\boldsymbol{P}_0 \cdot (\boldsymbol{L}_* - \boldsymbol{L}_0)^{-1} \boldsymbol{P}_0 \leq \langle \underline{\boldsymbol{P}} \cdot [\boldsymbol{\Gamma} + (\boldsymbol{L} - \boldsymbol{L}_0)^{-1}] \underline{\boldsymbol{P}} \rangle, \quad \text{with } \boldsymbol{P}_0 = \langle \underline{\boldsymbol{P}} \rangle, \tag{13.30}$$

and holds for all choices of trial polarization field $\boldsymbol{P} \in \mathcal{H}$. This will surely provide a bound that is at least as good as the bound provided by (13.25). Specifically, for a given choice of $\boldsymbol{E}_0$ and $\underline{\boldsymbol{P}}$ the inequality (13.25) provides a linear constraint on the matrix elements of $\boldsymbol{L}_*$: In a multidimensional space where the matrix elements are the axes, the inequality (13.25) constrains $\boldsymbol{L}_*$ to lie on one side of a hyperplane. For a different choice of $\boldsymbol{E}_0$ one obtains a different plane. As $\boldsymbol{E}_0$ is varied, with $\underline{\boldsymbol{P}}$ held fixed, the effective tensor $\boldsymbol{L}_*$ must lie within the region enveloped by the collection of all such hyperplanes. This region is precisely what one would obtain by directly applying the variational inequality (13.30).

Since equality holds when $\underline{\boldsymbol{P}} = \boldsymbol{P}$, the variational inequality (13.30) can be rewritten as a variational principle:

$$\begin{aligned} \boldsymbol{P}_0 \cdot (\boldsymbol{L}_* - \boldsymbol{L}_0)^{-1} \boldsymbol{P}_0 = \quad & \min_{\substack{\underline{\boldsymbol{P}} \in \mathcal{H} \\ \langle \underline{\boldsymbol{P}} \rangle = \boldsymbol{P}_0}} \langle \underline{\boldsymbol{P}} \cdot [\boldsymbol{\Gamma} + (\boldsymbol{L} - \boldsymbol{L}_0)^{-1}] \underline{\boldsymbol{P}} \rangle, \\ & \text{when } \boldsymbol{L} > \boldsymbol{L}_0, \quad \boldsymbol{\Gamma}_1 \boldsymbol{L}_0 \boldsymbol{\Gamma}_1 \geq 0. \end{aligned} \tag{13.31}$$

Similarly, (13.28) yields the variational principle

$$\begin{aligned} \boldsymbol{P}_0 \cdot (\boldsymbol{L}_0 - \boldsymbol{L}_*)^{-1} \boldsymbol{P}_0 = \quad & \min_{\substack{\underline{\boldsymbol{P}} \in \mathcal{H} \\ \langle \underline{\boldsymbol{P}} \rangle = \boldsymbol{P}_0}} \langle \underline{\boldsymbol{P}} \cdot [(\boldsymbol{L}_0 - \boldsymbol{L})^{-1} - \boldsymbol{\Gamma}] \underline{\boldsymbol{P}} \rangle, \\ & \text{when } \boldsymbol{L}_0 > \boldsymbol{L} > 0. \end{aligned} \tag{13.32}$$

These simplified forms of the Hashin-Shtrikman variational principles were derived independently by Milton and Kohn (1988) and Zhikov (1991a). By applying the duality principle we obtain the complementary pair of variational inequalities,

$$\begin{aligned} \boldsymbol{P}_0 \cdot (\boldsymbol{L}_*^{-1} - \boldsymbol{L}_0^{-1})^{-1} \boldsymbol{P}_0 = \quad & \min_{\substack{\underline{\boldsymbol{P}} \in \mathcal{H} \\ \langle \underline{\boldsymbol{P}} \rangle = \boldsymbol{P}_0}} \langle \underline{\boldsymbol{P}} \cdot [\boldsymbol{\Delta} + (\boldsymbol{L}^{-1} - \boldsymbol{L}_0^{-1})^{-1}] \, \underline{\boldsymbol{P}} \rangle, \\ & \text{when } \boldsymbol{L}^{-1} > \boldsymbol{L}_0^{-1}, \ \boldsymbol{\Gamma}_1 \boldsymbol{L}_0^{-1} \boldsymbol{\Gamma}_1 \geq 0 \end{aligned} \tag{13.33}$$

and

$$\begin{aligned} \boldsymbol{P}_0 \cdot (\boldsymbol{L}_0^{-1} - \boldsymbol{L}_*^{-1})^{-1} \boldsymbol{P}_0 = \quad & \min_{\substack{\underline{\boldsymbol{P}} \in \mathcal{H} \\ \langle \underline{\boldsymbol{P}} \rangle = \boldsymbol{P}_0}} \langle \underline{\boldsymbol{P}} \cdot [(\boldsymbol{L}_0^{-1} - \boldsymbol{L}^{-1})^{-1} - \boldsymbol{\Delta}] \, \underline{\boldsymbol{P}} \rangle, \\ & \text{when } \boldsymbol{L}_0^{-1} > \boldsymbol{L}^{-1} > 0, \end{aligned} \tag{13.34}$$

where

$$\boldsymbol{\Delta} = \boldsymbol{\Gamma}_2 (\boldsymbol{\Gamma}_2 \boldsymbol{L}_0^{-1} \boldsymbol{\Gamma}_2)^{-1} \boldsymbol{\Gamma}_2.$$

It appears that there are four different variational principles. However, when $\boldsymbol{L}_0$ is positive-definite (13.31) and (13.34) are essentially the same, as are (13.32) and (13.33). To see this equivalence let us suppose without loss of generality (by making a reference transformation if necessary) that $\boldsymbol{L}_0 = \sigma_0 \boldsymbol{I}$. Then the pair of variational principles (13.31) and (13.34) takes the form

$$\boldsymbol{P}_0 \cdot \boldsymbol{S}_* \boldsymbol{P}_0 = \max_{\substack{\underline{\boldsymbol{P}} \in \mathcal{H} \\ \langle \underline{\boldsymbol{P}} \rangle = \boldsymbol{P}_0}} \langle \underline{\boldsymbol{P}} \cdot (\boldsymbol{S} - \boldsymbol{\Gamma}_1) \underline{\boldsymbol{P}} \rangle, \quad \text{when } \boldsymbol{L} > \boldsymbol{I} > 0,$$

and

$$\boldsymbol{P}_0 \cdot \boldsymbol{T}_* \boldsymbol{P}_0 = \min_{\substack{\underline{\boldsymbol{P}} \in \mathcal{H} \\ \langle \underline{\boldsymbol{P}} \rangle = \boldsymbol{P}_0}} \langle \underline{\boldsymbol{P}} \cdot (\boldsymbol{T} - \boldsymbol{\Gamma}_2) \underline{\boldsymbol{P}} \rangle, \quad \text{when } \boldsymbol{L} > \boldsymbol{I} > 0,$$

where

$$\begin{aligned} \boldsymbol{S} &= \sigma_0 (\sigma_0 \boldsymbol{I} - \boldsymbol{L})^{-1}, \quad \boldsymbol{T} = \sigma_0 (\sigma_0 \boldsymbol{I} - \boldsymbol{L}^{-1})^{-1}, \\ \boldsymbol{S}_* &= \sigma_0 (\sigma_0 \boldsymbol{I} - \boldsymbol{L}_*)^{-1}, \quad \boldsymbol{T}_* = \sigma_0 (\sigma_0 \boldsymbol{I} - \boldsymbol{L}_*^{-1})^{-1}. \end{aligned} \tag{13.35}$$

The equivalence of these pair of variational principles is easily seen to be a consequence of the relations

$$\boldsymbol{S} + \boldsymbol{T} = \boldsymbol{I}, \quad \boldsymbol{S}_* + \boldsymbol{T}_* = \boldsymbol{I}, \quad \boldsymbol{\Gamma}_0 + \boldsymbol{\Gamma}_1 + \boldsymbol{\Gamma}_2 = \boldsymbol{I},$$

satisfied by the various operators. The equivalence of the pair of variational principles (13.32) and (13.33) follows by similar analysis.

When $\boldsymbol{L}_0$ is not positive-definite the validity of the variational principles (13.32) and (13.34) is uncertain. Instead one should use the variational principles (13.31) and (13.33).

13.6. Relation between the Hashin-Shtrikman and classical variational inequalities†

Hill (1963b) found that there is a close relation between the Hashin-Shtrikman and classical variational inequalities when the reference tensor $\boldsymbol{L}_0$ is positive-definite. Let us rewrite the classical variational principle in the form

$$\boldsymbol{E}_0 \cdot \boldsymbol{L}_* \boldsymbol{E}_0 \le \langle \underline{\boldsymbol{E}} \cdot \boldsymbol{L}_0 \underline{\boldsymbol{E}} \rangle + \langle \underline{\boldsymbol{E}} \cdot \delta \boldsymbol{L} \underline{\boldsymbol{E}} \rangle, \quad \text{where } \delta \boldsymbol{L} = \boldsymbol{L} - \boldsymbol{L}_0.$$

Now, given any field $\underline{\boldsymbol{P}}$, we are free to make the substitution

$$\langle \underline{\boldsymbol{E}} \cdot \delta \boldsymbol{L} \underline{\boldsymbol{E}} \rangle = \langle (\underline{\boldsymbol{P}} - \delta \boldsymbol{L} \underline{\boldsymbol{E}}) \cdot (\delta \boldsymbol{L})^{-1} (\underline{\boldsymbol{P}} - \delta \boldsymbol{L} \underline{\boldsymbol{E}}) \rangle + 2 \langle \underline{\boldsymbol{E}} \cdot \underline{\boldsymbol{P}} \rangle - \langle \underline{\boldsymbol{P}} \cdot (\delta \boldsymbol{L})^{-1} \underline{\boldsymbol{P}} \rangle,$$

to yield an equivalent form of the classical variational inequality that is easier to compare with the Hashin-Shtrikman inequality, namely,

$$\boldsymbol{E}_0 \cdot \boldsymbol{L}_* \boldsymbol{E}_0 \le \langle \underline{\boldsymbol{E}} \cdot \boldsymbol{L}_0 \underline{\boldsymbol{E}} \rangle + 2 \langle \underline{\boldsymbol{E}} \cdot \underline{\boldsymbol{P}} \rangle - \langle \underline{\boldsymbol{P}} \cdot (\delta \boldsymbol{L})^{-1} \underline{\boldsymbol{P}} \rangle + \langle (\underline{\boldsymbol{P}} - \delta \boldsymbol{L} \underline{\boldsymbol{E}}) \cdot (\delta \boldsymbol{L})^{-1} (\underline{\boldsymbol{P}} - \delta \boldsymbol{L} \underline{\boldsymbol{E}}) \rangle. \tag{13.36}$$

Suppose that we are given a trial polarization field $\underline{\boldsymbol{P}}$ and that $\boldsymbol{L}_0 > \boldsymbol{L}$. Substituting the trial field

$$\underline{\boldsymbol{E}} = \boldsymbol{E}_0 - \boldsymbol{\Gamma} \underline{\boldsymbol{P}} \tag{13.37}$$

into the classical variational inequality (13.36), using the fact that $\boldsymbol{\Gamma} \boldsymbol{L}_0 \boldsymbol{E}_0 = 0$, and recalling from (12.25) that $\boldsymbol{\Gamma} \boldsymbol{L}_0 \boldsymbol{\Gamma} = \boldsymbol{\Gamma}$ generates the bound

$$\begin{aligned} \boldsymbol{E}_0 \cdot \boldsymbol{L}_* \boldsymbol{E}_0 \le \boldsymbol{E}_0 \cdot \boldsymbol{L}_0 \boldsymbol{E}_0 + 2 \langle \boldsymbol{E}_0 \cdot \underline{\boldsymbol{P}} \rangle - \langle \underline{\boldsymbol{P}} \cdot [(\delta \boldsymbol{L})^{-1} + \boldsymbol{\Gamma}] \underline{\boldsymbol{P}} \rangle \\ + \langle (\underline{\boldsymbol{P}} - \delta \boldsymbol{L} \underline{\boldsymbol{E}}) \cdot (\delta \boldsymbol{L})^{-1} (\underline{\boldsymbol{P}} - \delta \boldsymbol{L} \underline{\boldsymbol{E}}) \rangle. \end{aligned} \tag{13.38}$$

This is almost the same bound as would be obtained from the Hashin-Shtrikman variational inequality (13.28). The only difference is the appearance in (13.38) of the last term, which is surely negative or zero because $\delta \boldsymbol{L}$ is negative-definite when $\boldsymbol{L}_0 > \boldsymbol{L}$. In other words, the classical variational inequality is guaranteed to produce a better bound than the Hashin-Shtrikman variational inequality when the trial field $\underline{\boldsymbol{E}}$ is given by (13.37). Of course the last term in (13.38) might be more difficult to evaluate than the remaining terms, and for this reason it may be preferable to use the Hashin-Shtrikman variational inequality.

Conversely, suppose that a trial field $\underline{\boldsymbol{E}} \in \mathcal{U} \oplus \mathcal{E}$ has been given, with $\langle \underline{\boldsymbol{E}} \rangle = \boldsymbol{E}_0$, and that we take a trial polarization field

$$\underline{\boldsymbol{P}} = \delta \boldsymbol{L} \underline{\boldsymbol{E}}. \tag{13.39}$$

Substitution of this in (13.36) gives

$$\boldsymbol{E}_0 \cdot \boldsymbol{L}_* \boldsymbol{E}_0 \le \langle \underline{\boldsymbol{E}} \cdot \boldsymbol{L}_0 \underline{\boldsymbol{E}} \rangle + 2 \langle \underline{\boldsymbol{E}} \cdot \underline{\boldsymbol{P}} \rangle - \langle \underline{\boldsymbol{P}} \cdot (\delta \boldsymbol{L})^{-1} \underline{\boldsymbol{P}} \rangle.$$

To make a comparison with the Hashin-Shtrikman inequality we re-express this result in the form

$$\begin{aligned} \boldsymbol{E}_0 \cdot \boldsymbol{L}_* \boldsymbol{E}_0 \le \boldsymbol{E}_0 \cdot \boldsymbol{L}_0 \boldsymbol{E}_0 + 2 \langle \boldsymbol{E}_0 \cdot \underline{\boldsymbol{P}} \rangle - \langle \underline{\boldsymbol{P}} \cdot [(\delta \boldsymbol{L})^{-1} + \boldsymbol{\Gamma}] \underline{\boldsymbol{P}} \rangle \\ + \langle (\underline{\boldsymbol{E}} - \boldsymbol{E}_0 + \boldsymbol{\Gamma} \underline{\boldsymbol{P}}) \cdot \boldsymbol{L}_0 (\underline{\boldsymbol{E}} - \boldsymbol{E}_0 + \boldsymbol{\Gamma} \underline{\boldsymbol{P}}) \rangle. \end{aligned}$$

Again, this is almost the same bound as would be obtained from the Hashin-Shtrikman variational inequality (13.28), except for the appearance of the last term, which is surely nonnegative when $\boldsymbol{L}_0$ is positive-definite. Therefore the Hashin-Shtrikman inequality will produce a

better bound than the classical variational inequality when we take a trial polarization field of the form (13.39).

This suggests that, given a field $\boldsymbol{E}_0 \in \mathcal{U}$, we could consider a sequence of associated trial fields,

$$\underline{\boldsymbol{E}}^{(k)} = \sum_{j=0}^{k} (-\boldsymbol{\Gamma}\delta\boldsymbol{L})^j \boldsymbol{E}_0, \qquad \underline{\boldsymbol{P}}^{(k)} = \sum_{j=0}^{k} \delta\boldsymbol{L}(-\boldsymbol{\Gamma}\delta\boldsymbol{L})^{j-1} \boldsymbol{E}_0.$$

Since these are related via

$$\underline{\boldsymbol{E}}^{(k+1)} = \boldsymbol{E}_0 - \boldsymbol{\Gamma}\underline{\boldsymbol{P}}^{(k)}, \qquad \underline{\boldsymbol{P}}^{(k)} = \delta\boldsymbol{L}\underline{\boldsymbol{E}}^{(k)},$$

they will produce a sequence of successively better upper bounds on the energy $W = \boldsymbol{E}_0 \cdot \boldsymbol{L}_*\boldsymbol{E}_0/2$, with the Hashin-Shtrikman bounds interlaced between the classical bounds (Kröner 1977). In the next chapter we will see that these fields converge to the actual fields in the composite when $\boldsymbol{L}_0$ is appropriately chosen. In a similar fashion, by using the duality principle, one can obtain a sequence of successively better lower bounds on the energy, with the Hashin-Shtrikman bounds interlaced between the classical bounds.

In the case when $\boldsymbol{L}_0$ is not positive-definite, the relation between the Hashin-Shtrikman and classical variational inequalities has not yet been explored.

13.7. Variational inequalities for nonlinear media

The classical energy minimization principle (13.10) has a natural extension to nonlinear media,

$$W_*(\boldsymbol{E}_0) = \inf_{\substack{\underline{\boldsymbol{E}} \in \mathcal{U} \oplus \mathcal{E} \\ \langle \underline{\boldsymbol{E}} \rangle = \boldsymbol{E}_0}} \langle W(\boldsymbol{x}, \underline{\boldsymbol{E}}(\boldsymbol{x})) \rangle, \tag{13.40}$$

where the potential $W(\boldsymbol{x}, \boldsymbol{A})$ gives the energy density at the point $\boldsymbol{x}$ when the field there takes the value $\boldsymbol{A}$. For example, in a two-phase nonlinear composite this potential takes the form

$$W(\boldsymbol{x}, \boldsymbol{A}) = \chi_1(\boldsymbol{x})W_1(\boldsymbol{A}) + \chi_2(\boldsymbol{x})W_2(\boldsymbol{A}),$$

where $\chi_1(\boldsymbol{x})$ and $\chi_2(\boldsymbol{x}) = 1 - \chi_1(\boldsymbol{x})$ are the characteristic functions associated with the phases, while $W_1(\boldsymbol{A})$ and $W_2(\boldsymbol{A})$ are the energy functions of the phases, which are not necessarily quadratic functions of $\boldsymbol{A}$. The definition of the subspace $\mathcal{E}$ has to be modified if the functions $W_1(\boldsymbol{A})$ and $W_2(\boldsymbol{A})$ do not have quadratic growth as $|\boldsymbol{A}| \to \infty$. If these functions both grow as $|\boldsymbol{A}|^p$, then $\mathcal{E}$ should be taken as the space consisting of all functions $\boldsymbol{E}'(\boldsymbol{x})$ satisfying the appropriate differential constraints, and which are such that $\langle \boldsymbol{E}' \rangle = 0$ and $|\boldsymbol{E}'(\boldsymbol{x})|^p$ is integrable. Otherwise, $\langle W(\boldsymbol{x}, \underline{\boldsymbol{E}}(\boldsymbol{x})) \rangle$ will not necessarily be finite when $\underline{\boldsymbol{E}} = \boldsymbol{E}_0 + \boldsymbol{E}'$. If the functions $W_1(\boldsymbol{A})$ and $W_2(\boldsymbol{A})$ have different power law growths, then, by considering the example of a checkerboard microstructure, Zhikov (1991b) has shown that the function $W_*(\boldsymbol{E}_0)$ can depend on the choice made for $\mathcal{E}$. To avoid getting lost in the details, we will not explicitly mention these technicalities again. However, the reader should keep in mind that they exist.

Depending on the form of $W(\boldsymbol{x}, \boldsymbol{A})$ the infimum in (13.40) might not be achieved by any field $\underline{\boldsymbol{E}} \in \mathcal{U} \oplus \mathcal{E}$. Instead there might be a minimizing sequence that achieves the infimum. However, if the infimum is achieved by some smooth field $\underline{\boldsymbol{E}}(\boldsymbol{x}) = \boldsymbol{E}(\boldsymbol{x})$, then the Euler-Lagrange equation implies that

$$\boldsymbol{J}(\boldsymbol{x}) = \left. \frac{\partial W(\boldsymbol{x}, \boldsymbol{A})}{\partial \boldsymbol{A}} \right|_{\boldsymbol{A} = \boldsymbol{E}(\boldsymbol{x})} \tag{13.41}$$

lies in the subspace $\mathcal{U} \oplus \mathcal{J}$. The minimizing field $\boldsymbol{E}(\boldsymbol{x})$ may represent, for instance, the strain field $\boldsymbol{\epsilon}(\boldsymbol{x})$ in a nonlinear elasticity problem (assuming that the displacements are still small, so the problem is geometrically linear) or it may represent the electric field $\boldsymbol{e}(\boldsymbol{x})$ in a nonlinear dielectric problem. Of course for this variational problem to have any relevance the physics of the problem must be such that the field $\boldsymbol{E}(\boldsymbol{x})$ adjusts itself to minimize the average energy. Then the effective energy function $W_*(\boldsymbol{E}_0)$ represents the average energy density in the composite when the applied field is $\boldsymbol{E}_0$. In a nonlinear media the variational principle (13.40) (rather than the associated nonlinear constitutive equation) is often taken as the starting point upon which all subsequent analysis is based. We will see that variational inequalities analogous to the dual classical variational inequality and the Hashin-Shtrikman variational inequality can be derived from this starting point.

The key idea is to realize that in a nonlinear setting Legendre transforms play the role that inverses of matrices play in the linear setting. Consider, for example, the Legendre transform $W^\circ(\boldsymbol{x}, \boldsymbol{B})$ of $W(\boldsymbol{x}, \boldsymbol{A})$ as defined by the equation,

$$W^\circ(\boldsymbol{x}, \boldsymbol{B}) = \sup_{\boldsymbol{A}}[\boldsymbol{A} \cdot \boldsymbol{B} - W(\boldsymbol{x}, \boldsymbol{A})],$$

where the circle superscript is used to denote a Legendre transform. If $W(\boldsymbol{x}, \boldsymbol{A}) = \boldsymbol{A} \cdot \boldsymbol{L}(\boldsymbol{x})\boldsymbol{A}/2$ and $\boldsymbol{L}(\boldsymbol{x}) > 0$, then it is easy to show that $W^\circ(\boldsymbol{x}, \boldsymbol{B}) = \boldsymbol{B} \cdot \boldsymbol{L}(\boldsymbol{x})^{-1}\boldsymbol{B}/2$. It follows directly from the definition of the Legendre transform that

$$W^\circ(\boldsymbol{x}, \boldsymbol{B}) \geq \boldsymbol{A} \cdot \boldsymbol{B} - W(\boldsymbol{x}, \boldsymbol{A}) \quad \text{for all } \boldsymbol{A} \text{ and } \boldsymbol{B}. \tag{13.42}$$

In particular we have

$$W(\boldsymbol{x}, \underline{\boldsymbol{E}}(\boldsymbol{x})) \geq \underline{\boldsymbol{E}}(\boldsymbol{x}) \cdot \underline{\boldsymbol{J}}(\boldsymbol{x}) - W^\circ(\boldsymbol{x}, \underline{\boldsymbol{J}}(\boldsymbol{x})), \tag{13.43}$$

where $\underline{\boldsymbol{E}}(\boldsymbol{x})$ and $\underline{\boldsymbol{J}}(\boldsymbol{x})$ are arbitrary periodic trial fields. Substituting this into the classical variational principle (13.40) gives

$$W_*(\boldsymbol{E}_0) \geq -\langle W^\circ(\boldsymbol{x}, \underline{\boldsymbol{J}})\rangle + \inf_{\substack{\underline{\boldsymbol{E}} \in \mathcal{U} \oplus \mathcal{E} \\ \langle \underline{\boldsymbol{E}} \rangle = \boldsymbol{E}_0}} \langle \underline{\boldsymbol{E}} \cdot \underline{\boldsymbol{J}} \rangle. \tag{13.44}$$

If we choose $\underline{\boldsymbol{J}} \in \mathcal{U} \oplus \mathcal{J}$, then we obtain the inequality

$$\boldsymbol{E}_0 \cdot \boldsymbol{J}_0 - W_*(\boldsymbol{E}_0) \leq \langle W^\circ(\boldsymbol{x}, \underline{\boldsymbol{J}})\rangle, \tag{13.45}$$

where $\boldsymbol{J}_0 = \langle \underline{\boldsymbol{J}} \rangle$. Since this holds for all $\boldsymbol{E}_0$, we can take the maximum over $\boldsymbol{E}_0$ of the left-hand side and thereby obtain the complementary classical variational inequality

$$W_*^\circ(\boldsymbol{J}_0) = \sup_{\boldsymbol{E}_0}[\boldsymbol{E}_0 \cdot \boldsymbol{J}_0 - W_*(\boldsymbol{E}_0)] \leq \langle W^\circ(\boldsymbol{x}, \underline{\boldsymbol{J}})\rangle, \tag{13.46}$$

which holds for all $\underline{\boldsymbol{J}} \in \mathcal{U} \oplus \mathcal{J}$ with $\langle \underline{\boldsymbol{J}} \rangle = \boldsymbol{J}_0$.

Although it is not always physically justified, it is often mathematically convenient to assume that $W(\boldsymbol{x}, \boldsymbol{A})$ is a strictly convex function of $\boldsymbol{A}$ for each value of $\boldsymbol{x}$ and grows sufficiently rapidly as $|\boldsymbol{A}| \to \infty$ to guarantee that $W^\circ(\boldsymbol{x}, \boldsymbol{B})$ is finite for all $\boldsymbol{B}$. This latter condition requires that $W(\boldsymbol{x}, \boldsymbol{A})/|\boldsymbol{A}| \to \infty$ as $|\boldsymbol{A}| \to \infty$. Then the infimum in (13.40) will be achieved and equality holds in (13.42) when

$$\boldsymbol{B} = \frac{\partial W(\boldsymbol{x}, \boldsymbol{A})}{\partial \boldsymbol{A}}.$$

Therefore, if we take $\underline{\boldsymbol{E}} = \boldsymbol{E}$ and $\underline{\boldsymbol{J}} = \boldsymbol{J}$, where $\boldsymbol{J}(\boldsymbol{x})$ is given by (13.41), we have equality in (13.43), (13.44), and (13.45). In other words, for this fixed value of $\boldsymbol{J}_0 = \langle \boldsymbol{J} \rangle$, there is no other choice of $\boldsymbol{E}_0$ having a greater left-hand side of (13.45) because it would violate the inequality. It follows (Suquet 1987; Willis 1989) that

$$W_*^\circ(\boldsymbol{J}_0) = \boldsymbol{E}_0 \cdot \boldsymbol{J}_0 - W_*(\boldsymbol{E}_0), \tag{13.47}$$

when $\boldsymbol{J}_0 = \langle \boldsymbol{J} \rangle$, $\boldsymbol{E}_0 = \langle \boldsymbol{E} \rangle$.

Let us next establish that $\boldsymbol{E}_0$ can be chosen so that $\boldsymbol{J}_0$ takes any desired value. To do this we need to show that $W_*(\boldsymbol{E}_0)$ is a strictly convex function of $\boldsymbol{E}_0$. This property (Ponte Castañeda and Willis 1988) can be seen from the relations,

$$\begin{aligned}
&W_*(p\boldsymbol{E}_0' + (1-p)\boldsymbol{E}_0'') \\
&\quad = \inf_{\substack{\underline{\boldsymbol{E}}' \in \mathcal{U} \oplus \mathcal{E},\ \underline{\boldsymbol{E}}'' \in \mathcal{U} \oplus \mathcal{E} \\ p\langle \underline{\boldsymbol{E}}' \rangle + (1-p)\langle \underline{\boldsymbol{E}}'' \rangle \\ \qquad = p\boldsymbol{E}_0' + (1-p)\boldsymbol{E}_0''}} \langle W(\boldsymbol{x}, p\underline{\boldsymbol{E}}'(\boldsymbol{x}) + (1-p)\underline{\boldsymbol{E}}''(\boldsymbol{x})) \rangle \\
&\quad < \inf_{\substack{\underline{\boldsymbol{E}}' \in \mathcal{U} \oplus \mathcal{E} \\ \langle \underline{\boldsymbol{E}}' \rangle = \boldsymbol{E}_0'}} \ \inf_{\substack{\underline{\boldsymbol{E}}'' \in \mathcal{U} \oplus \mathcal{E} \\ \langle \underline{\boldsymbol{E}}'' \rangle = \boldsymbol{E}_0''}} p\langle W(\boldsymbol{x}, \underline{\boldsymbol{E}}'(\boldsymbol{x})) \rangle + (1-p)\langle W(\boldsymbol{x}, \underline{\boldsymbol{E}}''(\boldsymbol{x})) \rangle \\
&\quad < pW_*(\boldsymbol{E}_0') + (1-p)W_*(\boldsymbol{E}_0''),
\end{aligned}$$

which hold for any $\boldsymbol{E}_0' \neq \boldsymbol{E}_0''$ and for any p between 0 and 1, where the inequality arises because of the convexity of W and because the infimum is taken over a smaller set of fields. Now let us consider other values of $\boldsymbol{J}_0$ that are not necessarily equal to $\langle \boldsymbol{J} \rangle$. Given any $\boldsymbol{J}_0$, the inequality (13.46) with $\underline{\boldsymbol{J}} = \boldsymbol{J}_0$ implies that $W_*^\circ(\boldsymbol{J}_0)$ is finite. Therefore there exists an $\boldsymbol{E}_0$ [namely, the value that achieves the supremum in (13.46)] such that equality in (13.47) holds, and for this value of $\boldsymbol{E}_0$ the convexity of $W_*(\boldsymbol{E}_0)$ implies that the equality holds only for one value of $\boldsymbol{J}_0$, namely,

$$\boldsymbol{J}_0 = \frac{\partial W_*(\boldsymbol{E}_0)}{\partial \boldsymbol{E}_0}, \tag{13.48}$$

which therefore must be identified with the given $\boldsymbol{J}_0$. Associated with $\boldsymbol{E}_0$ is the minimizing field $\boldsymbol{E}(\boldsymbol{x})$ and the field $\boldsymbol{J}(\boldsymbol{x})$ given by (13.41). From the uniqueness of $\boldsymbol{J}_0$ in (13.47) it follows that $\langle \boldsymbol{J} \rangle = \boldsymbol{J}_0$.

Therefore for any choice of $\boldsymbol{J}_0$ we can find a field $\boldsymbol{J}(\boldsymbol{x})$ with $\langle \boldsymbol{J} \rangle = \boldsymbol{J}_0$ that achieves equality in (13.46). We conclude that $W_*^\circ(\boldsymbol{J}_0)$ is given by the complementary energy minimization principle,

$$W_*^\circ(\boldsymbol{J}_0) = \inf_{\substack{\underline{\boldsymbol{J}} \in \mathcal{U} \oplus \mathcal{J} \\ \langle \underline{\boldsymbol{J}} \rangle = \boldsymbol{J}_0}} \langle W^\circ(\boldsymbol{x}, \underline{\boldsymbol{J}}(\boldsymbol{x})) \rangle, \tag{13.49}$$

as shown by Willis (1989) [see also Toland and Willis (1989) for the precise technical restrictions]. Thus there is a complete symmetry between the original variational problem and the complementary variational problem. The variational principles (13.40) and (13.49) can be used to obtain rigorous bounds on the potentials $W_*(\boldsymbol{E}_0)$ and $W_*^\circ(\boldsymbol{J}_0)$, as was recognized by Bishop and Hill (1951a, 1951b) and Drucker (1966).

The derivation of nonlinear variational inequalities analogous to those of Hashin and Shtrikman follows a similar route. It also parallels Hill's derivation of the Hashin-Shtrikman

variational inequalities from the classical variational inequalities discussed in the previous section. Here we follow Talbot and Willis (1992), who generalize earlier treatments of Talbot and Willis (1985) and Ponte Castañeda (1991). We begin by choosing a reference energy function $W_0(\boldsymbol{x}, \boldsymbol{A})$, possibly dependent on $\boldsymbol{x}$, that in the linear case can be identified with $\boldsymbol{A} \cdot \boldsymbol{L}_0(\boldsymbol{x})\boldsymbol{A}/2$. Then the classical variational principal is rewritten in the form

$$W_*(\boldsymbol{E}_0) = \inf_{\substack{\underline{\boldsymbol{E}} \in \mathcal{U} \oplus \mathcal{E} \\ \langle \underline{\boldsymbol{E}} \rangle = \boldsymbol{E}_0}} \langle W(\boldsymbol{x}, \underline{\boldsymbol{E}}(\boldsymbol{x})) - W_0(\boldsymbol{x}, \underline{\boldsymbol{E}}(\boldsymbol{x})) \rangle + \langle W_0(\boldsymbol{x}, \underline{\boldsymbol{E}}(\boldsymbol{x})) \rangle. \tag{13.50}$$

Next the Legendre transform of $W - W_0$ is introduced,

$$(W - W_0)^\circ(\boldsymbol{x}, \boldsymbol{B}) = \sup_{\boldsymbol{A}} \boldsymbol{A} \cdot \boldsymbol{B} - [W(\boldsymbol{x}, \boldsymbol{A}) - W_0(\boldsymbol{x}, \boldsymbol{A})],$$

the definition of which implies that

$$W(\boldsymbol{x}, \underline{\boldsymbol{E}}(\boldsymbol{x})) - W_0(\boldsymbol{x}, \underline{\boldsymbol{E}}(\boldsymbol{x})) \geq \underline{\boldsymbol{E}}(\boldsymbol{x}) \cdot \underline{\boldsymbol{P}}(\boldsymbol{x}) - (W - W_0)^\circ(\boldsymbol{x}, \underline{\boldsymbol{P}}(\boldsymbol{x})), \tag{13.51}$$

for all $\boldsymbol{x}$ and for all fields $\underline{\boldsymbol{E}}(\boldsymbol{x})$ and $\underline{\boldsymbol{P}}(\boldsymbol{x})$. The function $W_0(\boldsymbol{x}, \boldsymbol{A})$ should be chosen so that $(W - W_0)^\circ(\boldsymbol{x}, \boldsymbol{B})$ is finite for all $\boldsymbol{x}$ and $\boldsymbol{B}$, which requires that

$$[W(\boldsymbol{x}, \boldsymbol{A}) - W_0(\boldsymbol{x}, \boldsymbol{A})]/|\boldsymbol{A}| \to \infty \text{ as } |\boldsymbol{A}| \to \infty. \tag{13.52}$$

Substituting the inequality into (13.50) gives the variational inequality

$$W_*(\boldsymbol{E}_0) \geq -\langle (W - W_0)^\circ(\boldsymbol{x}, \underline{\boldsymbol{P}}(\boldsymbol{x})) \rangle + \inf_{\substack{\underline{\boldsymbol{E}} \in \mathcal{U} \oplus \mathcal{E} \\ \langle \underline{\boldsymbol{E}} \rangle = \boldsymbol{E}_0}} \langle W_0(\boldsymbol{x}, \underline{\boldsymbol{E}}(\boldsymbol{x})) + \underline{\boldsymbol{E}}(\boldsymbol{x}) \cdot \underline{\boldsymbol{P}}(\boldsymbol{x}) \rangle. \tag{13.53}$$

This is the generalization of the Hashin-Shtrikman variational inequality (13.25). The difficulty in its application is in the evaluation of the term involving the infimum over $\underline{\boldsymbol{E}}$. If we choose $W_0(\boldsymbol{x}, \boldsymbol{A}) = \boldsymbol{A} \cdot \boldsymbol{L}_0\boldsymbol{A}/2$ and $\boldsymbol{L}_0$ does not depend on $\boldsymbol{x}$, then the infimum over $\underline{\boldsymbol{E}}$ can be evaluated explicitly, giving the variational inequality

$$W_*(\boldsymbol{E}_0) \geq \boldsymbol{E}_0 \cdot \boldsymbol{L}_0\boldsymbol{E}_0/2 + \boldsymbol{E}_0 \cdot \langle \underline{\boldsymbol{P}} \rangle - \langle (W - W_0)^\circ(\boldsymbol{x}, \underline{\boldsymbol{P}}) + \underline{\boldsymbol{P}}\boldsymbol{\Gamma}\underline{\boldsymbol{P}} \rangle$$

of Talbot and Willis (1985). The condition (13.52) will be satisfied for some choice of $\boldsymbol{L}_0 > 0$ provided that $W(\boldsymbol{x}, \boldsymbol{A})$ grows at least as fast as quadratically as $|\boldsymbol{A}| \to \infty$.

Another approach is to keep the reference medium inhomogeneous and to set $\underline{\boldsymbol{P}}(\boldsymbol{x}) = 0$. Then the variational inequality (13.53) implies the bound

$$W_*(\boldsymbol{E}_0) \geq W_0^*(\boldsymbol{E}_0) + \langle \inf_{\boldsymbol{A}} [W(\boldsymbol{x}, \boldsymbol{A}) - W_0(\boldsymbol{x}, \boldsymbol{A})] \rangle$$

of Ponte Castañeda (1991), in which $W_0^*(\boldsymbol{E}_0)$ is the effective potential associated with the reference energy function $W_0(\boldsymbol{x}, \boldsymbol{A})$. For linear reference media we have

$$W_0(\boldsymbol{x}, \boldsymbol{A}) = \boldsymbol{A} \cdot \boldsymbol{L}_0(\boldsymbol{x})\boldsymbol{A}/2, \quad W_0^*(\boldsymbol{E}_0) = \boldsymbol{E}_0 \cdot \boldsymbol{L}_0^*\boldsymbol{E}_0/2,$$

where $\boldsymbol{L}_0^*$ is the effective tensor associated with $\boldsymbol{L}_0(\boldsymbol{x})$. Therefore any lower bound on the effective tensor of a linear comparison composite can provide us with a lower bound on the effective potential of a nonlinear composite.

Alternatively we can introduce the function

$$(W_0 - W)^\circ(\boldsymbol{x}, \boldsymbol{B}) = \sup_{\boldsymbol{A}}\{\boldsymbol{A} \cdot \boldsymbol{B} - [W_0(\boldsymbol{x}, \boldsymbol{A}) - W(\boldsymbol{x}, \boldsymbol{A})]\},$$

the definition of which implies that

$$W(\boldsymbol{x}, \underline{\boldsymbol{E}}(\boldsymbol{x})) - W_0(\boldsymbol{x}, \underline{\boldsymbol{E}}(\boldsymbol{x})) \le (W_0 - W)^\circ(\boldsymbol{x}, -\underline{\boldsymbol{P}}(\boldsymbol{x})) + \underline{\boldsymbol{E}}(\boldsymbol{x}) \cdot \underline{\boldsymbol{P}}(\boldsymbol{x})$$

for all $\boldsymbol{x}$ and for all fields $\underline{\boldsymbol{E}}(\boldsymbol{x})$ and $\underline{\boldsymbol{P}}(\boldsymbol{x})$. Substituting this inequality into the classical variational principle gives a second variational inequality,

$$W_*(\boldsymbol{E}_0) \le \langle (W_0 - W)^\circ(\boldsymbol{x}, -\underline{\boldsymbol{P}})\rangle + \inf_{\substack{\underline{\boldsymbol{E}} \in \mathcal{U} \oplus \mathcal{E} \\ \boldsymbol{\Gamma}_0 \underline{\boldsymbol{E}} = \boldsymbol{E}_0}} \langle W_0(\boldsymbol{x}, \underline{\boldsymbol{E}}(\boldsymbol{x})) + \underline{\boldsymbol{E}} \cdot \underline{\boldsymbol{P}}\rangle. \tag{13.54}$$

This is the generalization of the Hashin-Shtrikman variational inequality (13.28). If we choose $W_0(\boldsymbol{x}, \boldsymbol{A}) = \boldsymbol{A} \cdot \boldsymbol{L}_0\boldsymbol{A}/2$, we obtain the Talbot-Willis variational inequality,

$$W_*(\boldsymbol{E}_0) \le \boldsymbol{E}_0 \cdot \boldsymbol{L}_0\boldsymbol{E}_0/2 + \boldsymbol{E}_0 \cdot \langle \underline{\boldsymbol{P}}\rangle + \langle (W_0 - W)^\circ(\boldsymbol{x}, -\underline{\boldsymbol{P}}) - \underline{\boldsymbol{P}}\boldsymbol{\Gamma}\underline{\boldsymbol{P}}\rangle.$$

For this to be useful $(W_0 - W)^\circ$ must be finite, that is, $W(\boldsymbol{x}, \boldsymbol{A})$ must not grow faster than quadratically as $|\boldsymbol{A}| \to \infty$. Taking an inhomogeneous reference medium and setting $\underline{\boldsymbol{P}} = 0$ gives the other bound

$$W_*(\boldsymbol{E}_0) \le W_0^*(\boldsymbol{E}_0) + \langle \sup_{\boldsymbol{A}}[W(\boldsymbol{x}, \boldsymbol{A}) - W_0(\boldsymbol{x}, \boldsymbol{A})]\rangle$$

of Ponte Castañeda (1991). By taking $W_0(\boldsymbol{x}, \boldsymbol{A})$ to be quadratic we now see that any upper bound on the effective tensor of a linear comparison composite can provide us with an upper bound on the effective potential of a nonlinear composite.

We will not discuss the application of these nonlinear variational inequalities to specific bounding problems for nonlinear composites. Instead the interested reader is referred to the recent review of Ponte Castañeda and Suquet (1998) and references therein.

References

Ball, J. M., J. C. Currie, and P. J. Olver 1981. Null Lagrangians, weak continuity, and variational problems of arbitrary order. *Journal of Functional Analysis* 41(2):135–174. {*275, 286*}

Bishop, J. F. W. and R. Hill 1951a. A theoretical derivation of the plastic properties of a polycrystalline face-center metal. *Philosophical Magazine* 42:1298–1307. {*284, 286*}

Bishop, J. F. W. and R. Hill 1951b. A theory of the plastic distortion of a polycrystalline aggregate under combined stresses. *Philosophical Magazine* 42:414–427. {*284, 286*}

Borcea, L. 1999. Asymptotic analysis of quasistatic transport in high contrast conductive media. *SIAM Journal on Applied Mathematics* 59(2):597–635. {*278, 286*}

Brown, W. F. 1965. Dielectric constants, permeabilities, and conductivities of random media. *Transactions of the Society of Rheology* 9:357–380. {*279, 286, 329, 336*}

Cherkaev, A. V. and L. V. Gibiansky 1994. Variational principles for complex conductivity, viscoelasticity, and similar problems in media with complex moduli. *Journal of Mathematical Physics* 35(1):127–145. {*221, 234, 237, 243, 264, 267, 271, 276, 277, 286, 639, 641*}

Drucker, D. C. 1966. The continuum theory of plasticity on the macroscale and the microscale. *Journal of Materials* 1:873–910. {*284, 287*}

Fannjiang, A. and G. Papanicolaou 1994. Convection enhanced diffusion for periodic flows. *SIAM Journal on Applied Mathematics* 54(2):333–408. {*22, 42, 265, 267, 277, 278, 287*}

Finlayson, B. A. 1972. *The Method of Weighted Residuals and Variational Principles, with Application in Fluid Mechanics, Heat and Mass Transfer*, pp. 307–312. New York: Academic Press. ISBN 0-12-257050-2. {*278, 287*}

Hashin, Z. 1964. Theory of mechanical behavior of heterogeneous media. *Applied Mechanics Reviews* 17(1):1–9. {*247, 268, 272, 287*}

Hashin, Z. 1967. Variational principles of elasticity in terms of the polarization tensor. *International Journal of Engineering Science* 5:213–223. {*271, 287*}

Hashin, Z. 1972. Theory of fiber reinforced materials. NASA contractor report CR-1974, NASA, Washington, D.C. xv + 690 pp. {*xxiv, xxvii, 247, 268, 272, 287*}

Hashin, Z. and S. Shtrikman 1962b. A variational approach to the theory of the effective magnetic permeability of multiphase materials. *Journal of Applied Physics* 33:3125–3131. {*113, 116, 140, 271, 279, 287, 347, 350, 353, 457, 458, 460, 493, 574, 586, 598*}

Hashin, Z. and S. Shtrikman 1962a. On some variational principles in anisotropic and nonhomogeneous elasticity. *Journal of the Mechanics and Physics of Solids* 10:335–342. {*271, 287*}

Hashin, Z. and S. Shtrikman 1963. A variational approach to the theory of the elastic behavior of multiphase materials. *Journal of the Mechanics and Physics of Solids* 11: 127–140. {*206, 216, 271, 287, 457, 470, 471, 473, 493*}

Hill, R. 1952. The elastic behavior of a crystalline aggregate. *Proceedings of the Physical Society, London, A* 65:349–354. {*75, 77, 90, 271, 273, 287, 442, 453*}

Hill, R. 1963a. Elastic properties of reinforced solids: Some theoretical principles. *Journal of the Mechanics and Physics of Solids* 11:357–372. {*77, 90, 247, 268, 272, 287, 471, 473, 493*}

Hill, R. 1963b. New derivations of some elastic extremum principles. In *Progress in Applied Mathematics: The Prager Anniversary Volume*, pp. 99–106. New York: Macmillan Publishing Company. {*271, 281, 287*}

Kröner, E. 1977. Bounds for the effective elastic moduli of disordered materials. *Journal of the Mechanics and Physics of Solids* 25:137–155. {*251, 268, 282, 287, 291, 311, 458, 493, 553, 566*}

Milton, G. W. 1990. On characterizing the set of possible effective tensors of composites: The variational method and the translation method. *Communications on Pure and Applied Mathematics (New York)* 43(1):63–125. {*164, 183, 248, 265, 268, 277, 287, 451, 454, 473, 494, 499, 505, 512, 513, 518, 526, 532, 551*}

Milton, G. W. and R. V. Kohn 1988. Variational bounds on the effective moduli of anisotropic composites. *Journal of the Mechanics and Physics of Solids* 36(6):597–629. {*172, 183, 280, 287, 462, 466, 469, 471, 474, 495*}

Murat, F. 1978. Compacité par compensation. *Annali Scuola Normale Superiore-Pisa, Classe di Scienze, Serie IV.* 5(3):489–507. {*59, 72, 250, 269, 275, 276, 287*}

Murat, F. 1981. Compacité par compensation: Condition nécessaire et suffisante de continuité faible sous une hypothèse de rang constant. (French) [Compensated compactness: Necessary and sufficient conditions for weak continuity under a constant-rank hypothesis]. *Annali Scuola Normale Superiore-Pisa, Classe di Scienze, Serie IV* 8(1):69–102. {*250, 269, 275, 288*}

Murat, F. 1987. A survey on compensated compactness. In L. Cesari (ed.), *Contributions to Modern Calculus of Variations*, pp. 145–183. Harlow, Essex, United Kingdom: Longman Scientific and Technical. ISBN 0-470-20378-1 (Wiley), 0-582-99458-6. {*275, 288, 529, 551, 676, 697*}

Norris, J. R. 1997. Long time behavior of heat flow: Global estimates and exact asymptotics. *Archive for Rational Mechanics and Analysis* 140:161–195. {*277, 288*}

Pedregal, P. 1989. Weak continuity and weak lower semicontinuity for some compensation operators. *Proceedings of the Royal Society of Edinburgh. Section A, Mathematical and Physical Sciences* 113(3–4):267–279. {*275, 288*}

Ponte Castañeda, P. 1991. The effective mechanical properties of non-linear isotropic composites. *Journal of the Mechanics and Physics of Solids* 39(1):45–71. {*271, 285, 286, 288*}

Ponte Castañeda, P. and P. Suquet 1998. Nonlinear composites. *Advances in Applied Mechanics* 34:171–302. {*286, 288*}

Ponte Castañeda, P. and J. R. Willis 1988. On the overall properties of nonlinearly viscous composites. *Proceedings of the Royal Society of London. Series A, Mathematical and Physical Sciences* 416(1850):217–244. {*284, 288*}

Reuss, A. 1929. Berechnung der Fließgrenze von Mischkristallen auf Grund der Plastizitätsbedingung für Einkristalle. (German) [Calculation of the yield point of mixed crystals from plasticity conditions for single crystals]. *Zeitschrift für Angewandte Mathematik und Mechanik* 9:49–58. {*271, 288, 442, 454*}

Smyshlyaev, V. P. and N. A. Fleck 1994. Bounds and estimates for linear composites with strain gradient effects. *Journal of the Mechanics and Physics of Solids* 42(12):1851–1882. {*271, 288*}

Smyshlyaev, V. P. and N. A. Fleck 1996. The role of strain gradients in the grain size effect for polycrystals. *Journal of the Mechanics and Physics of Solids* 44(4):465–495. {*271, 288*}

Suquet, P. 1987. Elements of homogenization for inelastic solid mechanics. In E. Sanchez-Palencia and A. Zaoui (eds.), *Homogenization Techniques for Composite Media: Lectures Delivered at the CISM International Center for Mechanical Sciences, Udine, Italy, July 1–5, 1985*, pp. 193–278. Berlin / Heidelberg / London / etc.: Springer-Verlag. ISBN 0-387-17616-0. {*284, 288*}

Talbot, D. R. S. and J. R. Willis 1985. Variational principles for inhomogeneous nonlinear media. *IMA Journal of Applied Mathematics* 35(1):39–54. {*271, 285, 288*}

Talbot, D. R. S. and J. R. Willis 1992. Some simple explicit bounds for the overall behavior of non-linear composites. *International Journal of Solids and Structures* 29(14–15): 1981–1987. {*285, 288*}

Tartar, L. 1979a. Compensated compactness and applications to partial differential equations. In R. J. Knops (ed.), *Nonlinear Analysis and Mechanics, Heriot-Watt Symposium, Volume IV*, pp. 136–212. London: Pitman Publishing Ltd. ISBN 0-8224-8461-7, 0-273-08461-5. {*59, 72, 275, 276, 288, 503, 527, 529, 552, 676, 677, 684, 698*}

Tartar, L. 1979b. Estimation de coefficients homogénéisés. (French) [Estimation of homogenization coefficients]. In R. Glowinski and J.-L. Lions (eds.), *Computing Methods in Applied Sciences and Engineering: Third International Symposium, Versailles, France, December 5–9, 1977,*, pp. 364–373. Berlin / Heidelberg / London / etc.: Springer-Verlag. English translation in *Topics in the Mathematical Modelling of Composite Materials*, pp. 9–20, ed. by A. Cherkaev and R. Kohn. ISBN 0-8176-3662-5. ISBN 0-387-09123-8. {*155, 156, 162, 183, 274, 289, 499, 503, 508, 509, 527, 529, 552*}

Toland, J. F. and J. R. Willis 1989. Duality for families of natural variational principles in nonlinear electrostatics. *SIAM Journal on Mathematical Analysis* 20(6):1283–1292. {*284, 289*}

Voigt, W. 1889. Über die Beziehung zwischen den beiden Elastizitätskonstanten isotroper Körper. (German) [On the relation between the two elasticity constants of isotropic bodies]. *Wiedemanns Annalen der Physik und Chemie (Leipzig)* 38:573–587. {*271, 289, 442, 455*}

Voigt, W. 1910. *Lehrbuch der Krystallphysik*. Stuttgart, Germany / Leipzig, Germany: Teubner. xxiv + 964 pp. {*271, 289, 442, 455*}

Willis, J. R. 1989. The structure of overall constitutive relations for a class of nonlinear composites. *IMA Journal of Applied Mathematics* 43(3):231–242. {*284, 289*}

Zhikov, V. V. 1991a. Estimates for the homogenized matrix and the homogenized tensor. *Uspekhi Matematicheskikh Nauk = Russian Mathematical Surveys* 46:49–109. English translation in *Russ. Math. Surv.* 46(3):65–136 (1991). {*120, 142, 164, 183, 280, 289, 462, 466, 471–473, 497*}

Zhikov, V. V. 1991b. Lavrentiev effect and the averaging of nonlinear variational problems. *Differentsial'nye Uravneniya* 27(1):42–50. English translation in *Differential Equations* 27(1):32–39 (1991). {*282, 289*}

14

Series expansions for the fields and effective tensors

Here we derive series expansions, which when truncated form good approximations for the fields and effective tensors in a nearly homogeneous material. Such series expansions, and related perturbation solutions, were derived by Brown (1955), Beran and Molyneux (1963), Beran (1968), Fokin and Shermergor (1969), Beran and McCoy (1970), Dederichs and Zeller (1973), Hori (1973), Zeller and Dederichs (1973), Gubernatis and Krumhansl (1975), Kröner (1977), and Willis (1981), among others.

14.1. Expanding the formulas for the effective tensors and fields in power series

Let us assume that the tensor $\boldsymbol{L}$ is close to a reference tensor $\boldsymbol{L}_0$. In section 12.8 on page 261 we obtained expressions for the field $\boldsymbol{E}$ and effective tensor $\boldsymbol{L}_*$, which we rewrite here as

$$\boldsymbol{E} = [\boldsymbol{I} + \boldsymbol{\Gamma}\delta\boldsymbol{L}]^{-1}\boldsymbol{E}_0, \quad \boldsymbol{L}_* = \boldsymbol{L}_0 + \boldsymbol{\Gamma}_0\delta\boldsymbol{L}[\boldsymbol{I} + \boldsymbol{\Gamma}\delta\boldsymbol{L}]^{-1}\boldsymbol{\Gamma}_0, \quad \text{where} \quad \delta\boldsymbol{L} = \boldsymbol{L} - \boldsymbol{L}_0,$$

and the action of the projection $\boldsymbol{\Gamma}_0$ is just to take average values. Now when the operator $\boldsymbol{\Gamma}\delta\boldsymbol{L}$ is small we can expand $[\boldsymbol{I} + \boldsymbol{\Gamma}\delta\boldsymbol{L}]^{-1}$ in powers of $\boldsymbol{\Gamma}\delta\boldsymbol{L}$ and obtain the following series expansions for the fields and effective tensor:

$$\begin{aligned} \boldsymbol{E} &= \sum_{j=0}^{\infty}(-\boldsymbol{\Gamma}\delta\boldsymbol{L})^j\boldsymbol{E}_0, \quad \boldsymbol{J} = \boldsymbol{L}\boldsymbol{E} = \sum_{j=0}^{\infty}\boldsymbol{L}(-\boldsymbol{\Gamma}\delta\boldsymbol{L})^j\boldsymbol{E}_0, \\ \boldsymbol{L}_* &= \boldsymbol{L}_0 + \sum_{j=0}^{\infty}\boldsymbol{\Gamma}_0\delta\boldsymbol{L}(-\boldsymbol{\Gamma}\delta\boldsymbol{L})^j\boldsymbol{\Gamma}_0. \end{aligned} \tag{14.1}$$

These fields $\boldsymbol{E}$ and $\boldsymbol{J}$ satisfy $\boldsymbol{\Gamma}_2\boldsymbol{E} = 0$ and $\boldsymbol{\Gamma}_1\boldsymbol{J} = 0$, as demanded by the requirement that $\boldsymbol{E} \in \mathcal{U} \oplus \mathcal{E}$ and $\boldsymbol{J} \in \mathcal{U} \oplus \mathcal{J}$. In these formulas $\delta\boldsymbol{L}$ is to be regarded as an operator that, when applied to a field $\boldsymbol{P}(\boldsymbol{x})$, produces the field $\boldsymbol{Q}(\boldsymbol{x}) = (\boldsymbol{L}(\boldsymbol{x}) - \boldsymbol{L}_0)\boldsymbol{P}(\boldsymbol{x})$. Thus $(-\boldsymbol{\Gamma}\delta\boldsymbol{L})^j$ should not be interpreted as $-\boldsymbol{\Gamma}$ acting on the field $\delta\boldsymbol{L}(\boldsymbol{x})$ raised to the j-th power. Rather, it should be interpreted as the operator $-\boldsymbol{\Gamma}\delta\boldsymbol{L}$ applied j times.

The series expansion for $\boldsymbol{L}_*$ can be rewritten in the equivalent form

$$\boldsymbol{L}_* = \boldsymbol{L}_0 + \sum_{j=0}^{\infty}\langle(-\delta\boldsymbol{L}\boldsymbol{\Gamma})^j\delta\boldsymbol{L}\rangle,$$

where the operator $(-\delta \boldsymbol{L}\boldsymbol{\Gamma})^j$ acts on the field $\delta \boldsymbol{L}(\boldsymbol{x})$, taking values in $\mathcal{T} \otimes \mathcal{T}$ according to the extension prescribed by (12.32). The first few terms in this expansion form a good approximation to the effective tensor $\boldsymbol{L}_*$ when $\boldsymbol{L}$ is close to $\boldsymbol{L}_0$. To the third order in perturbation we see that

$$\boldsymbol{L}_* = \langle \boldsymbol{L} \rangle - \langle \delta \boldsymbol{L}\boldsymbol{\Gamma}\delta \boldsymbol{L} \rangle + \langle \delta \boldsymbol{L}\boldsymbol{\Gamma}\delta \boldsymbol{L}\boldsymbol{\Gamma}\delta \boldsymbol{L} \rangle - \cdots. \tag{14.2}$$

So to the first order the effective tensor $\boldsymbol{L}_*$ can be equated with the average of $\boldsymbol{L}(\boldsymbol{x})$.

When $\boldsymbol{L}$ is the tensor field

$$\boldsymbol{L}(\boldsymbol{x}) = \chi_1(\boldsymbol{x})\boldsymbol{L}_1 + \chi_2(\boldsymbol{x})\boldsymbol{L}_2 = \chi_1(\boldsymbol{x})(\boldsymbol{L}_1 - \boldsymbol{L}_2) + \boldsymbol{L}_2, \tag{14.3}$$

associated with a two-phase composite, and the reference tensor $\boldsymbol{L}_0$ is set equal to $\boldsymbol{L}_2$, this expansion reduces to

$$\begin{aligned} \boldsymbol{L}_* = {} & f_1\boldsymbol{L}_1 + f_2\boldsymbol{L}_2 - \langle (\boldsymbol{L}_1 - \boldsymbol{L}_2)\chi_1\boldsymbol{\Gamma}(\boldsymbol{L}_1 - \boldsymbol{L}_2)\chi_1 \rangle \\ & + \langle (\boldsymbol{L}_1 - \boldsymbol{L}_2)\chi_1\boldsymbol{\Gamma}(\boldsymbol{L}_1 - \boldsymbol{L}_2)\chi_1\boldsymbol{\Gamma}(\boldsymbol{L}_1 - \boldsymbol{L}_2)\chi_1 \rangle - \cdots, \end{aligned} \tag{14.4}$$

and the associated expansion for the field $\boldsymbol{E}(\boldsymbol{x})$ is

$$\boldsymbol{E}(\boldsymbol{x}) = \boldsymbol{E}_0 - \boldsymbol{\Gamma}(\boldsymbol{L}_1 - \boldsymbol{L}_2)\chi_1\boldsymbol{E}_0 + \boldsymbol{\Gamma}(\boldsymbol{L}_1 - \boldsymbol{L}_2)\chi_1\boldsymbol{\Gamma}(\boldsymbol{L}_1 - \boldsymbol{L}_2)\chi_1\boldsymbol{E}_0 - \cdots. \tag{14.5}$$

14.2. The series expansion in a composite to second order

Let us consider a composite material with a real symmetric tensor field $\boldsymbol{L}(\boldsymbol{x})$ and examine the second-order term in the expansion (14.2). This is easily evaluated in Fourier space. By expressing the field $\boldsymbol{L}(\boldsymbol{x})$ as a Fourier series,

$$\boldsymbol{L} = \sum_{\boldsymbol{k}} e^{i\boldsymbol{k}\cdot\boldsymbol{x}}\widehat{\boldsymbol{L}}(\boldsymbol{k}),$$

recalling that $\boldsymbol{\Gamma}$ acts locally in Fourier space, and applying Plancherel's theorem, we see that

$$\langle (\boldsymbol{L}_0 - \boldsymbol{L})\boldsymbol{\Gamma}(\boldsymbol{L}_0 - \boldsymbol{L}) \rangle = \sum_{\boldsymbol{k}\neq 0} \widehat{\boldsymbol{L}}(-\boldsymbol{k})\boldsymbol{\Gamma}(\boldsymbol{k})\widehat{\boldsymbol{L}}(\boldsymbol{k}).$$

Avellaneda (1987) and, in a more general setting, Tartar (1989, 1990) independently recognized that because $\boldsymbol{\Gamma}(\boldsymbol{k})$ depends only on $\boldsymbol{\xi} = \boldsymbol{k}/|\boldsymbol{k}|$, this sum can be broken into a sum over rays in Fourier space and a sum along each ray. To the second order in perturbation we have that

$$\{\boldsymbol{L}_*\}_{ij} = \{\langle \boldsymbol{L} \rangle\}_{ij} - \sum_{\substack{\boldsymbol{\xi} \\ |\boldsymbol{\xi}|=1}} \{\boldsymbol{H}(\boldsymbol{\xi})\}_{ik\ell j}\{\boldsymbol{\Gamma}(\boldsymbol{\xi})\}_{k\ell} + \cdots, \tag{14.6}$$

in which sums over repeated indices are implied and the tensor $\boldsymbol{H}(\boldsymbol{\xi})$ has matrix elements

$$\{\boldsymbol{H}(\boldsymbol{\xi})\}_{ikj\ell} = \sum_{\substack{\boldsymbol{k}\neq 0 \\ \boldsymbol{k}/|\boldsymbol{k}|=\boldsymbol{\xi}}} \{\widehat{\boldsymbol{L}}(-\boldsymbol{k})\}_{ik}\{\widehat{\boldsymbol{L}}(\boldsymbol{k})\}_{j\ell} = \sum_{\substack{\boldsymbol{k}\neq 0 \\ \boldsymbol{k}/|\boldsymbol{k}|=\boldsymbol{\xi}}} \overline{\{\widehat{\boldsymbol{L}}(\boldsymbol{k})\}_{ik}}\{\widehat{\boldsymbol{L}}(\boldsymbol{k})\}_{j\ell}, \tag{14.7}$$

where we have assumed that $\boldsymbol{L}(\boldsymbol{x})$ is real to allow us to equate $\widehat{\boldsymbol{L}}(-\boldsymbol{k})$ with $\overline{\widehat{\boldsymbol{L}}(\boldsymbol{k})}$, the complex conjugate of $\widehat{\boldsymbol{L}}(\boldsymbol{k})$. In this equation the sum extends over all points in Fourier space such that

the vector $\boldsymbol{k}$ is parallel and pointing in the same direction as the unit vector $\boldsymbol{\xi}$, whereas in (14.6) the sum is over those unit vectors $\boldsymbol{\xi}$ that are aligned with some vector $\boldsymbol{k}$ in the reciprocal lattice in Fourier space.

Following Tartar (1989) we call $\boldsymbol{H}(\boldsymbol{\xi})$ the H-measure associated with $\boldsymbol{L}(\boldsymbol{x})$. Tartar defines H-measures more generally, using them to give a partial characterization of oscillations associated with subsequences of tensor fields $\boldsymbol{L}_\epsilon(\boldsymbol{x})$ in the limit as $\epsilon \to 0$. In this more general setting the H-measure $\boldsymbol{H}(\boldsymbol{x}, \boldsymbol{\xi})$ depends on both $\boldsymbol{x}$ and $\boldsymbol{\xi}$, and for small ϵ it roughly characterizes the degree to which $\boldsymbol{L}_\epsilon(\boldsymbol{x})$ oscillates in the direction $\boldsymbol{\xi}$ in the vicinity of a point $\boldsymbol{x}$. More precisely, because it is a measure, it is associated with integrals over a small volume in space centered at the point $\boldsymbol{x}$ and over a small cone in Fourier space with its axis aligned with the vector $\boldsymbol{\xi}$. The interested reader is referred to the paper of Tartar (1990) for a complete definition and also to the work of Gérard (1989, 1994), who independently introduced H-measures under the name of microlocal defect measures. It suffices to say that if $\boldsymbol{L}(\boldsymbol{x})$ is periodic and $\boldsymbol{L}_\epsilon(\boldsymbol{x}) = \boldsymbol{L}(\boldsymbol{x}/\epsilon)$, then the more general definition of an H-measure coincides with the simpler one given here [see also Kohn (1991)].

Our assumption that the moduli $\boldsymbol{L}(\boldsymbol{x})$ are real and symmetric implies that the H-measure $\boldsymbol{H}(\boldsymbol{\xi})$ has the symmetry properties,

$$\begin{aligned} \{\boldsymbol{H}(\boldsymbol{\xi})\}_{ikj\ell} &= \{\boldsymbol{H}(\boldsymbol{\xi})\}_{kij\ell} = \{\boldsymbol{H}(\boldsymbol{\xi})\}_{ik\ell j}, \\ \{\boldsymbol{H}(\boldsymbol{\xi})\}_{ikj\ell} &= \overline{\{\boldsymbol{H}(\boldsymbol{\xi})\}_{j\ell ik}} = \{\boldsymbol{H}(-\boldsymbol{\xi})\}_{j\ell ik} \end{aligned}$$

and is positive-semidefinite for all $\boldsymbol{\xi}$ in the sense that

$$\overline{A_{ik}}\{\boldsymbol{H}(\boldsymbol{\xi})\}_{ikj\ell}A_{j\ell} \geq 0 \qquad \text{for all } \boldsymbol{\xi},$$

in which sums over repeated indices are implied and the A_{ik} denote elements of an arbitrary $m \times m$ complex matrix $\boldsymbol{A}$. This latter property can be seen by substituting (14.7) into the above expression.

Now consider a two-phase composite. Then the tensor $\boldsymbol{L} = \boldsymbol{L}(\boldsymbol{x})$ takes the form (14.3) and consequently $\boldsymbol{H}(\boldsymbol{\xi})$ has elements

$$\{\boldsymbol{H}(\boldsymbol{\xi})\}_{ikj\ell} = f_1 f_2 c(\boldsymbol{\xi})\{\boldsymbol{L}_1 - \boldsymbol{L}_2\}_{ik}\{\boldsymbol{L}_1 - \boldsymbol{L}_2\}_{\ell j}, \tag{14.8}$$

where

$$c(\boldsymbol{\xi}) = \frac{1}{f_1 f_2} \sum_{\substack{\boldsymbol{k}\neq 0 \\ \boldsymbol{k}/|\boldsymbol{k}|=\boldsymbol{\xi}}} \widehat{\chi}_1^*(\boldsymbol{k})\widehat{\chi}_1(\boldsymbol{k})$$

and $\widehat{\chi}_1(\boldsymbol{k})$ is the Fourier component of $\chi(\boldsymbol{x})$. The factor of $f_1 f_2$ has been introduced into the definition of $c(\boldsymbol{\xi})$, so that the sum of $c(\boldsymbol{\xi})$ over $\boldsymbol{\xi}$ is unity:

$$\sum_{\substack{\boldsymbol{\xi} \\ |\boldsymbol{\xi}|=1}} c(\boldsymbol{\xi}) = \frac{1}{f_1 f_2} \sum_{\boldsymbol{k}\neq 0} \widehat{\chi}_1^*(\boldsymbol{k})\widehat{\chi}_1(\boldsymbol{k}) = \frac{1}{f_1 f_2}\Big\langle (\chi_1 - \langle\chi_1\rangle)(\chi_1 - \langle\chi_1\rangle)\Big\rangle = 1.$$

Also, from this definition it is evident that the constants $c(\boldsymbol{\xi})$ are real and

$$c(\boldsymbol{\xi}) \geq 0 \qquad \text{for all } \boldsymbol{\xi}.$$

So by substituting (14.8) back into (14.6) we obtain an expression,

$$\boldsymbol{L}_* = \langle \boldsymbol{L} \rangle - f_1 f_2 (\boldsymbol{L}_1 - \boldsymbol{L}_2) \Big[\sum_{\substack{\boldsymbol{\xi} \\ |\boldsymbol{\xi}|=1}} c(\boldsymbol{\xi}) \boldsymbol{\Gamma}(\boldsymbol{\xi}) \Big] (\boldsymbol{L}_1 - \boldsymbol{L}_2) + \cdots, \tag{14.9}$$

for the effective tensor that is correct to the second order in the difference $\boldsymbol{L}_1 - \boldsymbol{L}_2$. The geometry of the composite enters through the set of positive weights $c(\boldsymbol{\xi})$.

Remarkably, as Avellaneda (1987) and Tartar (1989, 1990) observed [see also Lipton (1992)] no matter what the geometry of the composite happens to be, there exists a coated laminate that has exactly the same expansion of its effective tensor to the second order. Indeed, by expanding formula (9.46) for the effective tensor of a sequential coated laminate to the second order in $\boldsymbol{L}_1 - \boldsymbol{L}_2$, we see that

$$\boldsymbol{L}_* = \langle \boldsymbol{L} \rangle - f_1 f_2 (\boldsymbol{L}_1 - \boldsymbol{L}_2) \Big[\sum_{j=1}^{m} c_j \boldsymbol{\Gamma}(\boldsymbol{n}_j) \Big] (\boldsymbol{L}_1 - \boldsymbol{L}_2) + \cdots. \tag{14.10}$$

So if we take the limit $m \to \infty$, let the lamination directions $\boldsymbol{n}_j$ range over every vector $\boldsymbol{\xi}$ that is aligned with some vector $\boldsymbol{k}$ in the reciprocal lattice, and choose lamination constants $c_j = c(\boldsymbol{\xi})$, then (14.10) coincides with (14.9). In other words, sequential laminates can mimic the functional dependence of the effective tensor $\boldsymbol{L}_*$ on $\boldsymbol{L}_1$ and $\boldsymbol{L}_2$ to the second order in $\boldsymbol{L}_1 - \boldsymbol{L}_2$. Following Avellaneda (1987) we will see later in section 23.3 on page 462 that this has applications to bounding the effective tensor of two-phase composites.

If the two-phase composite is geometrically isotropic, in the sense that one cannot statistically distinguish $\chi_1(\boldsymbol{x})$ from $\chi_1(\boldsymbol{R}\boldsymbol{x})$ for any given rotation matrix $\boldsymbol{R}$, then the weights $c(\boldsymbol{\xi})$ are distributed evenly over the surface of the sphere $|\boldsymbol{\xi}| = 1$ and the series expansion (14.9) reduces to

$$\boldsymbol{L}_* = \langle \boldsymbol{L} \rangle - f_1 f_2 (\boldsymbol{L}_1 - \boldsymbol{L}_2) \boldsymbol{\gamma} (\boldsymbol{L}_1 - \boldsymbol{L}_2) + \cdots, \quad \text{where } \boldsymbol{\gamma} = \langle \boldsymbol{\Gamma}(\boldsymbol{n}) \rangle_{\boldsymbol{n}}. \tag{14.11}$$

Strictly speaking, geometric isotropy applies only to random composites since for periodic composites $c(\boldsymbol{\xi})$ is nonzero only when $\boldsymbol{\xi}$ is aligned with some vector $\boldsymbol{k}$ in the reciprocal lattice. We will discuss series expansions for two-phase geometrically isotropic materials in more detail in section 15.6 on page 327. For a geometrically isotropic three-dimensional composite of two isotropic phases with conductivities $\sigma_1 \boldsymbol{I}$ and $\sigma_2 \boldsymbol{I}$ and effective conductivity $\sigma_* \boldsymbol{I}$ we have $\boldsymbol{\gamma} = \boldsymbol{I}/3\sigma_2$ and the above expansion implies that

$$\sigma_* = f_1 \sigma_1 + f_2 \sigma_2 - f_1 f_2 (\sigma_1 - \sigma_2)^2 / 3\sigma_2 + \cdots. \tag{14.12}$$

14.3. Thermoelastic composites for which the third and higher order terms in the expansion vanish

For certain classes of thermoelastic composites an exact expression for the effective tensor can be obtained once we know its expansion to the second order. The equations of thermoelasticity take the form

$$\begin{pmatrix} \boldsymbol{\epsilon}(\boldsymbol{x}) \\ \varsigma(\boldsymbol{x}) \end{pmatrix} = \boldsymbol{L}(\boldsymbol{x}) \begin{pmatrix} \boldsymbol{\tau}(\boldsymbol{x}) \\ \theta \end{pmatrix}, \quad \text{with} \quad \nabla \cdot \boldsymbol{\tau} = 0, \quad \boldsymbol{\epsilon} = [\nabla \boldsymbol{u} + (\nabla \boldsymbol{u})^T]/2,$$

where $\boldsymbol{L}(\boldsymbol{x})$ is the thermoelastic tensor. We confine our attention to those thermoelastic composites where

$$\boldsymbol{L}(\boldsymbol{x}) = \begin{pmatrix} \boldsymbol{\mathcal{S}} & \boldsymbol{\alpha}(\boldsymbol{x}) \\ \boldsymbol{\alpha}(\boldsymbol{x}) & c(\boldsymbol{x})/T_0 \end{pmatrix},$$

that is, for which the compliance tensor $\boldsymbol{\mathcal{S}}$ is independent of $\boldsymbol{x}$. A natural choice for the reference tensor is then

$$\boldsymbol{L}_0 = \begin{pmatrix} \boldsymbol{\mathcal{S}} & 0 \\ 0 & c_0/T_0 \end{pmatrix},$$

where c_0 is a positive constant. The associated operator $\boldsymbol{\Gamma}$ is

$$\boldsymbol{\Gamma} = \begin{pmatrix} \boldsymbol{\Gamma}_2^e[\boldsymbol{\Gamma}_2^e\boldsymbol{\mathcal{S}}\boldsymbol{\Gamma}_2^e]^{-1}\boldsymbol{\Gamma}_2^e & 0 \\ 0 & 0 \end{pmatrix}, \tag{14.13}$$

in which $\boldsymbol{\Gamma}_2^e$ is the projection onto the space of divergence free stress fields with zero average value. [The Fourier components $\boldsymbol{\Gamma}_2^e(\boldsymbol{k})$ of $\boldsymbol{\Gamma}_2^e$ are given by (9.30).] By directly computing the product

$$\boldsymbol{\Gamma}\delta\boldsymbol{L} = \begin{pmatrix} 0 & \boldsymbol{\Gamma}_2^e[\boldsymbol{\Gamma}_2^e\boldsymbol{\mathcal{S}}\boldsymbol{\Gamma}_2^e]^{-1}\boldsymbol{\Gamma}_2^e\boldsymbol{\alpha}(\boldsymbol{x}) \\ 0 & 0 \end{pmatrix}$$

and squaring it, we see that $(\boldsymbol{\Gamma}\delta\boldsymbol{L})^2 = 0$. This implies that

$$(\boldsymbol{\Gamma}\delta\boldsymbol{L})^n = 0 \quad \text{for all } n \geq 2.$$

Thus all terms beyond second order vanish in the expansions (14.1) and in particular we obtain an exact expression for the effective tensor

$$\boldsymbol{L}_* = \langle \boldsymbol{L} \rangle - \begin{pmatrix} 0 & 0 \\ 0 & \langle \boldsymbol{\alpha}(\boldsymbol{x}) \cdot \boldsymbol{\Gamma}_2^e[\boldsymbol{\Gamma}_2^e\boldsymbol{\mathcal{S}}\boldsymbol{\Gamma}_2^e]^{-1}\boldsymbol{\Gamma}_2^e\boldsymbol{\alpha}(\boldsymbol{x})\rangle \end{pmatrix} \tag{14.14}$$

once we know the second-order term $\langle \boldsymbol{\alpha}(\boldsymbol{x}) \cdot \boldsymbol{\Gamma}_2^e[\boldsymbol{\Gamma}_2^e\boldsymbol{\mathcal{S}}\boldsymbol{\Gamma}_2^e]^{-1}\boldsymbol{\Gamma}_2^e\boldsymbol{\alpha}(\boldsymbol{x})\rangle$. For two-phase composites we have a complete characterization through H-measures of what second-order terms are possible and therefore a complete characterization of what effective tensors $\boldsymbol{L}_*$ are possible. This explains why Khachaturyan (1966, 1983) found that two-phase simple laminates minimize the thermoelastic energy or, equivalently, the energy under phase transformations, which like the temperature field θ cause additional stresses and strains within the composite. [See Kohn (1991) for a complete discussion and other pertinent references.] For three-phase composites Kohn (1991) and Firoozye and Kohn (1993) give a partial characterization of possible H-measures. Smyshlyaev and Willis (1999) use this to identify three-phase, multiple-rank laminate microstructures minimizing the thermoelastic energy in some cases.

14.4. A large class of exactly solvable materials with complex moduli†

There is a large class of materials with complex-valued tensors $\boldsymbol{L}(\boldsymbol{x})$ for which all but the first term in the series expansion vanishes and an exact expression for the effective tensor $\boldsymbol{L}_*$ is easily obtained. To see this suppose that there exists (a possibly complex) matrix $\boldsymbol{L}_0$ and a vector $\boldsymbol{n} \neq 0$ such that the Fourier components $\widehat{\delta\boldsymbol{L}}(\boldsymbol{k})$ of the field $\delta\boldsymbol{L}(\boldsymbol{x}) = \boldsymbol{L}(\boldsymbol{x}) - \boldsymbol{L}_0$ satisfy

$$\widehat{\delta\boldsymbol{L}}(\boldsymbol{k}) = 0 \text{ whenever } \boldsymbol{k} \cdot \boldsymbol{n} \leq 0. \tag{14.15}$$

Under this assumption the associated field $\delta\boldsymbol{L}(\boldsymbol{x})$, if nonzero, is necessarily complex-valued.

Now consider the various terms in the series expansion (14.2). The first term, $\langle \boldsymbol{L} \rangle$, can be equated with $\boldsymbol{L}_0$ because $\widehat{\delta \boldsymbol{L}}(\boldsymbol{k}) = 0$ when $\boldsymbol{k} = 0$. The second term,

$$\langle \delta \boldsymbol{L} \boldsymbol{\Gamma} \delta \boldsymbol{L} \rangle = \sum_{\boldsymbol{k} \neq 0} \widehat{\delta \boldsymbol{L}}(-\boldsymbol{k}) \boldsymbol{\Gamma}(\boldsymbol{k}) \widehat{\delta \boldsymbol{L}}(\boldsymbol{k}),$$

is zero because if $\widehat{\delta \boldsymbol{L}}(\boldsymbol{k})$ is nonzero, that is, $\boldsymbol{k} \cdot \boldsymbol{n} > 0$, then $\widehat{\delta \boldsymbol{L}}(-\boldsymbol{k})$ is necessarily zero. The third term,

$$\langle \delta \boldsymbol{L} \boldsymbol{\Gamma} \delta \boldsymbol{L} \boldsymbol{\Gamma} \delta \boldsymbol{L} \rangle = \sum_{\boldsymbol{k} \neq 0} \sum_{\boldsymbol{m} \neq 0} \widehat{\delta \boldsymbol{L}}(-\boldsymbol{m}) \boldsymbol{\Gamma}(\boldsymbol{m}) \widehat{\delta \boldsymbol{L}}(\boldsymbol{m} - \boldsymbol{k}) \boldsymbol{\Gamma}(\boldsymbol{k}) \widehat{\delta \boldsymbol{L}}(\boldsymbol{k}), \tag{14.16}$$

is also zero, because otherwise if $\widehat{\delta \boldsymbol{L}}(-\boldsymbol{m})$, $\widehat{\delta \boldsymbol{L}}(\boldsymbol{m}-\boldsymbol{k})$, $\widehat{\delta \boldsymbol{L}}(\boldsymbol{k})$ were all nonzero, then $-\boldsymbol{m} \cdot \boldsymbol{n}$, $(\boldsymbol{m} - \boldsymbol{k}) \cdot \boldsymbol{n}$, and $\boldsymbol{k} \cdot \boldsymbol{n}$ would all be strictly positive, which is impossible because their sum is zero. By a similar argument, all successive terms in the series expansion are zero too. Therefore we have an exact formula for the effective tensor:

$$\boldsymbol{L}_* = \boldsymbol{L}_0.$$

Despite this very simple expression the fields in the material are nontrivial. In particular, the Fourier components $\widehat{\boldsymbol{P}}(\boldsymbol{k})$ of the polarization field $\boldsymbol{P}(\boldsymbol{x}) = (\boldsymbol{L}(\boldsymbol{x}) - \boldsymbol{L}_0)\boldsymbol{E}(\boldsymbol{x})$ are necessarily zero only when $\boldsymbol{k} \cdot \boldsymbol{n} \leq 0$.

As an example, consider a three-dimensional, locally isotropic composite where the complex dielectric constant takes the form

$$\varepsilon(\boldsymbol{x}) = \varepsilon(x_1, x_2, x_3) = \varepsilon_0 + f(x_1, x_2, x_3),$$

where ε_0 is a complex number. The function $f(x_1, x_2, x_3)$ is required to be periodic with, say, the unit cube C as a unit cell, implying that

$$f(x_1, x_2, x_3) = f(x_1 + 1, x_2, x_3) = f(x_1, x_2 + 1, x_3) = f(x_1, x_2, x_3 + 1)$$

for all x_1, x_2, and x_3. In addition, let us assume that for each fixed real x_1 and x_2, $f(x_1, x_2, x_3)$ is a bounded analytic function of x_3 in the upper half plane $\mathrm{Im}(x_3) > 0$ with

$$\int_0^1 dx_3 f(x_1, x_2, x_3) = 0, \tag{14.17}$$

where the integral is over one period along the real axis. For instance, we could take

$$\varepsilon(\boldsymbol{x}) = \varepsilon_0 + h(x_1, x_2)[\cos(2\pi c x_3) + i \sin(2\pi c x_3)],$$

where c is an integer and $h(x_1, x_2)$ is a real- or complex-valued periodic function of x_1 and x_2, not necessarily analytic in these variables. Associated with $\varepsilon(\boldsymbol{x})$ is the dielectric tensor field $\boldsymbol{\varepsilon}(\boldsymbol{x}) = \varepsilon(\boldsymbol{x})\boldsymbol{I}$. Taking $\boldsymbol{L}_0 = \varepsilon_0 \boldsymbol{I}$, the Fourier components $\widehat{\delta \boldsymbol{L}}(\boldsymbol{k})$ satisfy the required condition (14.15) with $\boldsymbol{n} = (0, 0, 1)$ because when $k_3 \leq 0$ we have

$$\int_C d\boldsymbol{x} e^{-i\boldsymbol{k}\cdot\boldsymbol{x}} \delta \boldsymbol{L}(\boldsymbol{x}) = \int_0^1 dx_1 \int_0^1 dx_2 e^{-i(k_1 x_1 + k_2 x_2)} \left[\int_0^1 dx_3 e^{-ik_3 x_3} f(x_1, x_2, x_3) \right] \boldsymbol{I} = 0,$$

where the expression in the square brackets vanishes for $k_3 = 0$ by our assumption (14.17) and vanishes for $k_3 < 0$ because we can equate it with a contour interval in the upper half x_3-plane, around the rectangle enclosed by the real axis, the lines $\mathrm{Re}(x_3) = 0$, $\mathrm{Re}(x_3) = 1$, and the line $\mathrm{Im}(x_3) = t$ in the limit as $t \to \infty$. We conclude that the composite has $\varepsilon_0 \boldsymbol{I}$ as its effective dielectric tensor.

Of course we can easily generalize this example to obtain exactly solvable, locally anisotropic tensor fields $\boldsymbol{\varepsilon}(\boldsymbol{x})$ that have special analytic properties along each line parallel to the x_3-axis. By making a subsequent curvilinear coordinate transformation, as described in section 8.5 on page 149, we obtain an even wider class of exactly solvable materials with $\boldsymbol{\varepsilon}(\boldsymbol{x})$ having special analytic properties along each curve amongst a certain family of curves. In two dimensions we can then generate an associated family of exactly solvable thermoelectric materials by applying the transformation discussed in section 11.6 on page 237.

14.5. Reducing the dimensionality of the problem†

If instead of requiring that the Fourier components $\widehat{\delta \boldsymbol{L}}(\boldsymbol{k})$ vanish whenever $\boldsymbol{k} \cdot \boldsymbol{n} \leq 0$ we impose the weaker constraint that

$$\widehat{\boldsymbol{L}}(\boldsymbol{k}) = 0 \text{ whenever } \boldsymbol{k} \cdot \boldsymbol{n} < 0,$$

then the problem of calculating the effective tensor $\boldsymbol{L}_*$ can be reduced from a three-dimensional problem to an equivalent two-dimensional problem, or from a two-dimensional problem to an equivalent one-dimensional problem (which can be exactly solved).

Indeed, if the above condition is satisfied, then, for example, the only nonzero contributions to the third-order term (14.16) come from those $\boldsymbol{m}$ and $\boldsymbol{k}$ such that $\widehat{\delta \boldsymbol{L}}(-\boldsymbol{m})$, $\widehat{\delta \boldsymbol{L}}(\boldsymbol{m}-\boldsymbol{k})$, and $\widehat{\delta \boldsymbol{L}}(\boldsymbol{k})$ are nonzero. By assumption this forces $-\boldsymbol{m}\cdot\boldsymbol{n}$, $(\boldsymbol{m}-\boldsymbol{k})\cdot\boldsymbol{n}$, and $\boldsymbol{k}\cdot\boldsymbol{n}$ to be nonnegative. Since the sum is zero, each term must be zero, that is, $\boldsymbol{k}\cdot\boldsymbol{n} = \boldsymbol{m}\cdot\boldsymbol{n} = 0$. By such considerations we see that every term in the series expansion remains unchanged if we replace $\widehat{\delta \boldsymbol{L}}(\boldsymbol{k})$ with

$$\begin{aligned} \widehat{\underline{\delta \boldsymbol{L}}}(\boldsymbol{k}) &= \widehat{\delta \boldsymbol{L}}(\boldsymbol{k}) \quad \text{when } \boldsymbol{k}\cdot\boldsymbol{n} = 0, \\ &= 0 \qquad\quad \text{otherwise.} \end{aligned}$$

Suppose that the coordinates have been chosen so that $\boldsymbol{n} = (0, 0, 1)$. Then the effective tensor $\boldsymbol{L}_*$ remains unchanged if we replace $\boldsymbol{L}(\boldsymbol{x})$ by

$$\underline{\boldsymbol{L}}(\boldsymbol{x}) = \underline{\boldsymbol{L}}(x_1, x_2) = \langle \boldsymbol{L}(x_1, x_2, x_3) \rangle_{x_3},$$

where the angular brackets $\langle\ \rangle_{x_3}$ denote an average over x_3, keeping x_1 and x_2 fixed. Since $\underline{\boldsymbol{L}}(\boldsymbol{x})$ does not depend on x_3, we have effectively reduced the problem of calculating $\boldsymbol{L}_*$ to the problem of calculating the effective tensor of an associated two-dimensional problem. If we had started with a two-dimensional problem, then we would have effectively reduced it to a one-dimensional problem.

For example, it follows that the formulas (9.7) for the components of the effective conductivity tensor $\boldsymbol{\sigma}_*$ of a laminate also apply to materials for which $\boldsymbol{\sigma}(x_1, x_2, x_3)$ is a bounded analytic function of x_2 and x_3 in the upper half-planes $\mathrm{Im}(x_2) > 0$ and $\mathrm{Im}(x_3) > 0$. Alternatively, for the formulas to apply, $\boldsymbol{\sigma}(x_1, x_2, x_3)$ could be bounded and analytic in the lower half-planes $\mathrm{Im}(x_2) < 0$ and $\mathrm{Im}(x_3) < 0$, or it could be bounded and analytic in the upper

half-plane $\mathrm{Im}(x_2) > 0$ and the lower half-plane $\mathrm{Im}(x_3) < 0$. In particular, we could take

$$\boldsymbol{\sigma}(x_1, x_2, x_3) = \\ \boldsymbol{s}(\boldsymbol{x}_1)[a_2 + \cos(2\pi c_2 x_2) + i\sin(2\pi c_2 x_2)][a_3 + \cos(2\pi c_3 x_3) + i\sin(2\pi c_2 x_3)],$$

where $\boldsymbol{s}(\boldsymbol{x}_1)$ is a complex matrix-valued function, and a_2 and a_3 are complex numbers while c_2 and c_3 are (positive or negative) real numbers. To ensure that the medium is physically realistic (and to ensure that the series expansions for the fields converge) the function $\boldsymbol{s}$ and the parameters a_1 and a_2 should be chosen so that the real part of $\boldsymbol{\sigma}(\boldsymbol{x})$ is positive-definite for all $\boldsymbol{x}$. [More precisely, we require that there exist positive constants α and β such that $\beta \boldsymbol{I} \geq \mathrm{Re}[\boldsymbol{\sigma}(\boldsymbol{x})] \geq \alpha \boldsymbol{I}$ for all $\boldsymbol{x}$.]

We remark in passing that a related simplification extends to nonlinear equations when the coefficients vanish in half of Fourier space. For example, Caflisch (1993) has obtained a reduction in dimensionality for complex-valued solutions of the three-dimensional incompressible Euler equations.

14.6. Convergence of the expansions and the existence and uniqueness of the fields and effective tensors

The convergence of the expansions (14.1) for the fields and effective tensors was investigated for a dielectric composite material by Fokin (1982) [see also Fokin (1996)], and for an elastic composite material by Bruno (1991b) and Michel, Moulinec, and Suquet (2001). The subject of convergence is an important issue, because if the expansions for the fields converge, then the limiting fields provide us with a solution to the equations

$$\boldsymbol{J} = \boldsymbol{L}\boldsymbol{E}, \quad \boldsymbol{J} \in \mathcal{U} \oplus \mathcal{J}, \quad \boldsymbol{E} \in \mathcal{U} \oplus \mathcal{E}.$$

In other words, this constitutes a constructive proof of the existence of fields $\boldsymbol{E}$ and $\boldsymbol{J}$ that solve these equations. To establish convergence we need to make some assumptions about the linear map $\boldsymbol{L}$. To simplify the mathematics let us begin by assuming (by making a reference transformation if necessary) that the reference tensor $\boldsymbol{L}_0$ is proportional to the identity tensor, that is, $\boldsymbol{L}_0 = \sigma_0 \boldsymbol{I}$, and that $\boldsymbol{L}$ is self-adjoint with

$$\beta \boldsymbol{I} \geq \boldsymbol{L} \geq \alpha \boldsymbol{I} \tag{14.18}$$

for some choice of positive constants β and α. In other words, we assume the ellipticity condition that the eigenvalues of $\boldsymbol{L}$ lie between α and β.

The question of convergence of the series expansion for the field $\boldsymbol{E}$ is clearly equivalent to the question of whether the sequence of fields $\boldsymbol{E}^1, \boldsymbol{E}^2, \ldots$ defined via

$$\boldsymbol{E}^m = \sum_{j=0}^{m} (-\boldsymbol{\Gamma}\delta\boldsymbol{L})^j \boldsymbol{V} = \sum_{j=0}^{m} [\boldsymbol{\Gamma}_1(\boldsymbol{I} - \boldsymbol{L}/\sigma_0)]^j \boldsymbol{V} \tag{14.19}$$

converges when we set $\boldsymbol{V} = \boldsymbol{E}_0$. We shall prove convergence of this series for any choice of $\boldsymbol{V} \in \mathcal{H}$ under the assumption that $\sigma_0 > \beta/2$. Recall that in section 12.1 on page 245 we defined

$$|\boldsymbol{P}| = (\boldsymbol{P}, \boldsymbol{P})^{1/2} = \langle \overline{\boldsymbol{P}} \cdot \boldsymbol{P} \rangle^{1/2}$$

as the norm of any (possibly complex-valued) field $\boldsymbol{P} \in \mathcal{H}$. Here $(\boldsymbol{P}', \boldsymbol{P})$, given by (12.11), denotes the inner product of any two fields $\boldsymbol{P}'$ and $\boldsymbol{P}$ in $\mathcal{H}$. Now let us define

$$\|\boldsymbol{A}\| = \sup_{\substack{\boldsymbol{P} \in \mathcal{H} \\ |\boldsymbol{P}| = 1}} |\boldsymbol{A}\boldsymbol{P}| \tag{14.20}$$

as the norm of any linear operator $\boldsymbol{A}$ acting on fields in $\mathcal{H}$. When $\boldsymbol{A}$ is self-adjoint the norm is just the supremum of the absolute values of the eigenvalues of $\boldsymbol{A}$. Hence the constraint (14.18) implies that

$$\|\boldsymbol{I} - \boldsymbol{L}/\sigma_0\| \le \gamma \quad \text{with} \quad \gamma = \max\{|\beta/\sigma_0 - 1|, |\alpha/\sigma_0 - 1|\}, \tag{14.21}$$

which is strictly less than 1 when $\sigma_0 > \beta/2$. In particular we have

$$\gamma = (\beta/\alpha - 1)/(\beta/\alpha + 1) \quad \text{when} \quad \sigma_0 = (\alpha + \beta)/2.$$

This is the value of σ_0 that minimizes γ.

From the definition (14.20) it is evident that the norm $\|\boldsymbol{A}\boldsymbol{B}\|$ of two linear maps $\boldsymbol{A}$ and $\boldsymbol{B}$ is at most equal to the product $\|\boldsymbol{A}\|\|\boldsymbol{B}\|$ of the norms of the individual maps. Since $\boldsymbol{\Gamma}_1$ is a projection, its norm is simply $\|\boldsymbol{\Gamma}_1\| = 1$, and so it follows that for all m,

$$\|[\boldsymbol{\Gamma}_1(\boldsymbol{I} - \boldsymbol{L}/\sigma_0)]^m\| < \gamma^m, \tag{14.22}$$

which in turn implies that

$$|\boldsymbol{E}^m - \boldsymbol{E}^{m-1}| = |[\boldsymbol{\Gamma}_1(\boldsymbol{I} - \boldsymbol{L}/\sigma_0)]^m \boldsymbol{V}| < \gamma^m |\boldsymbol{V}|.$$

Since $\gamma < 1$, we deduce that the sequence $\boldsymbol{E}^m$, $m = 1, 2, 3, \ldots$ is a Cauchy sequence that necessarily converges because a Hilbert space by definition is complete. The limit $\boldsymbol{E}$ satisfies

$$[\boldsymbol{I} + \boldsymbol{\Gamma}_1(\boldsymbol{L}/\sigma_0 - \boldsymbol{I})]\boldsymbol{E} = \boldsymbol{V}.$$

To prove uniqueness of this solution $\boldsymbol{E}$ when $\sigma_0 > \beta/2$, we examine the homogeneous equation

$$[\boldsymbol{I} + \boldsymbol{\Gamma}_1(\boldsymbol{L}/\sigma_0 - \boldsymbol{I})]\boldsymbol{E}' = 0.$$

From (14.21) and recalling that $|\boldsymbol{\Gamma}_1| = 1$ we have

$$|\boldsymbol{E}'| = |\boldsymbol{\Gamma}_1(\boldsymbol{I} - \boldsymbol{L}/\sigma_0)\boldsymbol{E}'| \le \gamma |\boldsymbol{E}'|,$$

and because $\gamma < 1$ it follows that $\boldsymbol{E}' = 0$. Since there are no nontrivial solutions to the homogeneous equation, we conclude that the solution $\boldsymbol{E}$ of the inhomogeneous equation is unique. This establishes that the inverse operator $(\boldsymbol{I} + \boldsymbol{\Gamma}_1(\boldsymbol{L}/\sigma_0 - \boldsymbol{I}))^{-1}$ exists.

The above analysis shows that the field $\boldsymbol{E}$ can be computed as the limit as $m \to \infty$ of the sequence of fields $\boldsymbol{E}^m$ defined by (14.19) when we set $\boldsymbol{V} = \boldsymbol{E}_0$. Moreover, using (14.22) we can obtain an estimate of the error incurred by replacing $\boldsymbol{L}_*$ by the approximant

$$\boldsymbol{L}_*^{(m)} = \sigma_0 \boldsymbol{\Gamma}_0 + \sum_{j=0}^{m} \boldsymbol{\Gamma}_0(\boldsymbol{L} - \sigma_0 \boldsymbol{I})[\boldsymbol{\Gamma}_1(\boldsymbol{I} - \boldsymbol{L}/\sigma_0)]^j \boldsymbol{\Gamma}_0, \tag{14.23}$$

obtained by truncating the series expansion (14.1) for $\boldsymbol{L}_*$ at some finite number of terms m. Using the fact that the norm of any two linear maps $\boldsymbol{A}$ and $\boldsymbol{B}$ satisfies the triangle inequality $\|\boldsymbol{A}+\boldsymbol{B}\| \le \|\boldsymbol{A}\| + \|\boldsymbol{B}\|$, we have the following bound on the error:

$$\begin{aligned}\|\boldsymbol{L}_* - \boldsymbol{L}_*^{(m)}\| &< \sigma_0 \sum_{j=m+1}^{\infty} \|\boldsymbol{\Gamma}_0(\boldsymbol{I} - \boldsymbol{L}/\sigma_0)[\boldsymbol{\Gamma}_1(\boldsymbol{I} - \boldsymbol{L}/\sigma_0)]^j \boldsymbol{\Gamma}_0\| \\ &< \sigma_0 \sum_{j=m+1}^{\infty} \gamma^{j+1} = \frac{\sigma_0 \gamma^{m+2}}{1-\gamma}, \end{aligned} \tag{14.24}$$

where $\gamma = (\beta/\alpha - 1)/(\beta/\alpha + 1)$ when $\sigma_0 = (\alpha+\beta)/2$. This error clearly tends to zero as m tends to infinity. Setting $\sigma_0 = (\alpha+\beta)/2$ and considering the worst case scenario, which occurs when the ratio β/α is very large, we see that M iterations where

$$M \approx \frac{-\beta/\alpha}{2} \log(4\epsilon\alpha/\beta)$$

are sufficient (and likely more than necessary) to ensure that $\|\boldsymbol{L}_* - \boldsymbol{L}_*^{(M)}\| \le \epsilon\beta$, where ϵ is a measure of the desired tolerance. For example, this shows that 74,000 iterations will certainly achieve a $\epsilon = 0.1\%$ tolerance when $\beta/\alpha = 10,000$. Less extreme ratios of β/α achieve much faster convergence.

14.7. Convergence when $\boldsymbol{L}$ is not self-adjoint†

If the map $\boldsymbol{L}$ is not self-adjoint but has a finite norm, that is, there exists a constant β such that

$$\beta > \|\boldsymbol{L}\|, \tag{14.25}$$

and in addition is coercive, that is, there exists a positive constant $\alpha > 0$ such that

$$(\boldsymbol{P}, \boldsymbol{L}\boldsymbol{P}) > \alpha |\boldsymbol{P}|^2 \quad \text{for all } \boldsymbol{P} \in \mathcal{H} \text{ with } \boldsymbol{P} \neq 0, \tag{14.26}$$

then the series still converges for sufficiently large values of σ_0. As in the previous analysis, it suffices to establish that the norm of $(\boldsymbol{I} - \boldsymbol{L}/\sigma_0)$ is strictly less than 1.

Given any field $\boldsymbol{Q}$ let us set

$$\boldsymbol{Q}' = (\boldsymbol{I} - \boldsymbol{L}/\sigma_0)\boldsymbol{Q}.$$

Then we have

$$\boldsymbol{L}\boldsymbol{Q} = \sigma_0(\boldsymbol{Q} - \boldsymbol{Q}'),$$

and (14.26) with $\boldsymbol{P} = \boldsymbol{Q}$ implies that

$$\sigma_0 \Big[|\boldsymbol{Q}|^2 - (\boldsymbol{Q}, \boldsymbol{Q}') \Big] > \alpha |\boldsymbol{Q}|^2, \tag{14.27}$$

while (14.25) implies that

$$\beta^2 |\boldsymbol{Q}|^2 > \sigma_0^2 |(\boldsymbol{Q} - \boldsymbol{Q}')|^2$$

or, equivalently, that

$$2(\boldsymbol{Q}, \boldsymbol{Q}') > \Big[1 - (\beta^2/\sigma_0^2) \Big] |\boldsymbol{Q}|^2 + |\boldsymbol{Q}'|^2. \tag{14.28}$$

By substituting (14.28) into (14.27) we see that

$$(\sigma_0 + \beta^2/\sigma_0 - 2\alpha)|\boldsymbol{Q}|^2 > \sigma_0|\boldsymbol{Q}'|^2,$$

implying that when σ_0 is positive

$$|\boldsymbol{I} - \boldsymbol{L}/\sigma_0| \le \gamma \equiv \Big[1 + \frac{\beta^2}{\sigma_0^2} - \frac{2\alpha}{\sigma_0}\Big]^{1/2}, \tag{14.29}$$

which is strictly less than 1 when $\sigma_0 > \beta^2/2\alpha$. In particular,

$$\gamma = \sqrt{1 - \alpha^2/\beta^2} \ \text{ when } \ \sigma_0 = \beta^2/\alpha, \tag{14.30}$$

which is the value that minimizes γ. For given values of α and β, this bound on $|\boldsymbol{I} - \boldsymbol{L}/\sigma_0|$ is not as tight as the bound when $\boldsymbol{L}$ is self-adjoint, but nevertheless is sufficiently restrictive to guarantee convergence of the series. The bound

$$\|\boldsymbol{L}_* - \boldsymbol{L}_*^{(m)}\| < \frac{\sigma_0\gamma^{m+2}}{1-\gamma}$$

implied by (14.24) still holds, where now γ is given by (14.29).

14.8. Extending the domain of convergence†

The expansions (14.1) typically have a larger domain of convergence than indicated by the preceding analysis. Clearly a sufficient condition for convergence is that the operator $\boldsymbol{\Gamma}(\boldsymbol{L}_0 - \boldsymbol{L})$ has norm less than 1. Let us take a reference tensor of the form

$$\boldsymbol{L}_0 = \sigma_0\boldsymbol{I} + \boldsymbol{L}_0',$$

where the tensor $\boldsymbol{L}_0'$ is assumed to be bounded and self-adjoint but need not be positive-definite. The preceding analysis suggests that we should choose a large positive value of σ_0 to ensure that the domain of convergence is as large as possible. Expanding the operator $\boldsymbol{\Gamma}$ in powers of $1/\sigma_0$ gives the series expansion

$$\boldsymbol{\Gamma} = \boldsymbol{\Gamma}_1(\boldsymbol{\Gamma}_1\boldsymbol{L}_0\boldsymbol{\Gamma}_1)^{-1}\boldsymbol{\Gamma}_1 = \sum_{j=0}^{\infty}(-1)^j\boldsymbol{\Gamma}_1(\boldsymbol{L}_0'\boldsymbol{\Gamma}_1)^j/\sigma_0^{j+1},$$

which certainly converges for $\sigma_0 > \|\boldsymbol{L}_0'\|$. When σ_0 is sufficiently large it suffices to keep the first few terms in this expansion, and we obtain the following estimate for the norm of the operator $\boldsymbol{\Gamma}(\boldsymbol{L}_0 - \boldsymbol{L})$:

$$\|\boldsymbol{\Gamma}(\boldsymbol{L}_0 - \boldsymbol{L})\| \approx \|\boldsymbol{\Gamma}_1[\boldsymbol{I} + (\boldsymbol{L}_0' - \boldsymbol{\Gamma}_1\boldsymbol{L}_0'\boldsymbol{\Gamma}_1 - \boldsymbol{L})/\sigma_0]\| \le \|\boldsymbol{I} + (\boldsymbol{L}_0' - \boldsymbol{\Gamma}_1\boldsymbol{L}_0'\boldsymbol{\Gamma}_1 - \boldsymbol{L})/\sigma_0\|. \tag{14.31}$$

Also, the definition (14.20) of the norm implies that

$$\|\boldsymbol{I} + (\boldsymbol{L}_0' - \boldsymbol{\Gamma}_1\boldsymbol{L}_0'\boldsymbol{\Gamma}_1 - \boldsymbol{L})/\sigma_0\| \approx 1 - 2\max_{\substack{\boldsymbol{P}\in\mathcal{H}\\ |\boldsymbol{P}|=1}}(\boldsymbol{P}, (\boldsymbol{L}_S - \boldsymbol{L}_0' + \boldsymbol{\Gamma}_1\boldsymbol{L}_0'\boldsymbol{\Gamma}_1)\boldsymbol{P})/\sigma_0, \tag{14.32}$$

where $\boldsymbol{L}_S = (\boldsymbol{L} + \boldsymbol{L}^\dagger)/2$ is the self-adjoint part of the operator $\boldsymbol{L}$. The approximations in (14.31) and (14.32) become increasingly accurate as σ_0 tends to infinity. They are made

merely for mathematical expediency and can be turned into rigorous inequalities by estimating the norm of the remainder of the series expansion and adding a term proportional to $1/\sigma_0^2$ to the right-hand sides of (14.31) and (14.32).

By combining (14.31) and (14.32) we see that the series expansion converges for sufficiently large values of σ_0 provided that the operator $\boldsymbol{L}_S - \boldsymbol{L}_0' + \boldsymbol{\Gamma}_1\boldsymbol{L}_0'\boldsymbol{\Gamma}_1$ is coercive, that is, provided that there exists a constant $\alpha' > 0$ such that

$$\boldsymbol{L}_S - \boldsymbol{L}_0' + \boldsymbol{\Gamma}_1\boldsymbol{L}_0'\boldsymbol{\Gamma}_1 > \alpha'\boldsymbol{I}. \tag{14.33}$$

This condition can only be satisfied when the operator $\boldsymbol{L}$ is positive-definite on the subspace $\mathcal{E}$, that is, when there exists a constant $\alpha' > 0$ such that

$$\boldsymbol{\Gamma}_1\boldsymbol{L}_S\boldsymbol{\Gamma}_1 \geq \alpha'\boldsymbol{\Gamma}_1,$$

as can be seen by projecting the inequality on the subspace $\mathcal{E}$, in effect multiplying (14.33) on the left and right by $\boldsymbol{\Gamma}_1$. Conversely, if there exists a constant tensor $\boldsymbol{L}_0'$ that is positive-semidefinite on the subspace $\mathcal{E}$, and a positive constant α' such that

$$\boldsymbol{\Gamma}_1\boldsymbol{L}_0'\boldsymbol{\Gamma}_1 \geq 0, \quad \boldsymbol{L}_S > \boldsymbol{L}_0' + \alpha'\boldsymbol{I},$$

then (14.33) is surely satisfied, and the series expansion will converge for that choice of $\boldsymbol{L}_0'$ when σ_0 is sufficiently large. Such tensors $\boldsymbol{L}_0'$ will be called quasiconvex.

14.9. A series with a faster convergence rate

There are many other useful series expansions for the effective tensor. Here we will consider a series expansion that has a much faster rate of convergence than (14.1).

Let us return to the formula (12.29) for the polarization field $\boldsymbol{P}$ and rewrite it in the form

$$\begin{aligned}\boldsymbol{P} &= [\boldsymbol{I} + (\boldsymbol{L} - \boldsymbol{L}_0)\boldsymbol{\Gamma}]^{-1}(\boldsymbol{L} - \boldsymbol{L}_0)\boldsymbol{E}_0 \\ &= [\boldsymbol{I} + (\boldsymbol{L} - \boldsymbol{L}_0)\boldsymbol{M} + (\boldsymbol{L} - \boldsymbol{L}_0)(\boldsymbol{\Gamma} - \boldsymbol{M})]^{-1}(\boldsymbol{L} - \boldsymbol{L}_0)\boldsymbol{E}_0 \\ &= (\boldsymbol{I} - \boldsymbol{K}\boldsymbol{\Upsilon})^{-1}\boldsymbol{K}\boldsymbol{E}_0,\end{aligned}$$

where

$$\boldsymbol{K} = [\boldsymbol{I} + (\boldsymbol{L} - \boldsymbol{L}_0)\boldsymbol{M}]^{-1}(\boldsymbol{L} - \boldsymbol{L}_0), \quad \boldsymbol{\Upsilon} = \boldsymbol{M} - \boldsymbol{\Gamma}$$

and $\boldsymbol{M}$ is an arbitrary tensor that remains to be chosen. Expanding $(\boldsymbol{I} - \boldsymbol{K}\boldsymbol{\Upsilon})^{-1}$ in powers of $\boldsymbol{K}\boldsymbol{\Upsilon}$ then gives the series expansions

$$\boldsymbol{P} = \sum_{j=0}^{\infty} \boldsymbol{K}(\boldsymbol{\Upsilon}\boldsymbol{K})^j\boldsymbol{E}_0, \quad \boldsymbol{L}_* = \boldsymbol{L}_0 + \sum_{j=0}^{\infty} \boldsymbol{\Gamma}_0\boldsymbol{K}(\boldsymbol{\Upsilon}\boldsymbol{K})^j\boldsymbol{\Gamma}_0, \tag{14.34}$$

for the polarization and effective tensor. The convergence of these series is enhanced when $\boldsymbol{M}$ is chosen to make the norm of $\boldsymbol{\Upsilon}$ small. Since $0 \leq \boldsymbol{\Gamma} \leq \boldsymbol{L}_0^{-1}$, one natural choice is $\boldsymbol{M} = \boldsymbol{L}_0^{-1}/2$, which gives

$$\boldsymbol{K} = 2\boldsymbol{L}_0(\boldsymbol{L} + \boldsymbol{L}_0)^{-1}(\boldsymbol{L} - \boldsymbol{L}_0), \quad \boldsymbol{\Upsilon} = (\boldsymbol{I} - 2\boldsymbol{\Gamma}\boldsymbol{L}_0)\boldsymbol{L}_0^{-1}/2.$$

The convergence rate of the expansions can then be estimated from the norm of the operator

$$\boldsymbol{\Upsilon}\boldsymbol{K} = (\boldsymbol{I} - 2\boldsymbol{\Gamma}\boldsymbol{L}_0)(\boldsymbol{L} + \boldsymbol{L}_0)^{-1}(\boldsymbol{L} - \boldsymbol{L}_0).$$

Let us again assume that the operator $\boldsymbol{L}$ is self-adjoint, satisfying the bounds (14.18). The series converge for any positive-definite choice of $\boldsymbol{L}_0$, but to simplify the analysis let us suppose that $\boldsymbol{L}_0 = \sigma_0 \boldsymbol{I}$, where σ_0 is a positive constant. (By making a reference transformation we can easily extend this proof to allow for any positive-definite choice of $\boldsymbol{L}_0$.) Then we have

$$\|(\boldsymbol{L} + \boldsymbol{L}_0)^{-1}(\boldsymbol{L} - \boldsymbol{L}_0)\| = \|(\boldsymbol{L} + \sigma_0 \boldsymbol{I})^{-1}(\boldsymbol{L} - \sigma_0 \boldsymbol{I})\| < \gamma',$$

where

$$\gamma' = \max\{|(\beta - \sigma_0)/(\beta + \sigma_0)|, |(\alpha - \sigma_0)/(\alpha + \sigma_0)|\}$$

is surely less than 1. In particular it follows that

$$\gamma' = (\sqrt{\beta/\alpha} - 1)/(\sqrt{\beta/\alpha} + 1) \qquad \text{when } \sigma_0 = \sqrt{\alpha\beta}, \tag{14.35}$$

which is the value of σ_0 that minimizes γ'. The operator $\boldsymbol{\Gamma}_1$, being a projection, has eigenvalues of 0 and 1. Therefore $\boldsymbol{I} - 2\boldsymbol{\Gamma}\boldsymbol{L}_0 = \boldsymbol{I} - 2\boldsymbol{\Gamma}_1$ has eigenvalues of -1 and 1, and consequently has norm 1. We conclude that $\boldsymbol{\Upsilon}\boldsymbol{K}$ has norm less than γ'.

The approximant

$$\boldsymbol{L}_*^{\prime\,(m)} = \sigma_0 \boldsymbol{I} + \sigma_0 \sum_{j=0}^{m} \boldsymbol{\Gamma}_0 \boldsymbol{K} (\boldsymbol{\Upsilon}\boldsymbol{K})^j \boldsymbol{\Gamma}_0, \tag{14.36}$$

obtained by truncating the series expansion for $\boldsymbol{L}_*$ at $m+1$ terms, differs from the exact value of $\boldsymbol{L}_*$ by at most

$$\|\boldsymbol{L}_* - \boldsymbol{L}_*^{\prime\,(m)}\| < \frac{2\sigma_0 (\gamma')^{m+1}}{1 - \gamma'}. \tag{14.37}$$

A comparison of expression (14.30) for the optimal value of γ with the expression (14.35) for the optimal value of γ' suggests that the series expansion (14.23) with $\beta/\alpha = r$ will have a comparable rate of convergence as the series expansion (14.36) with $\beta/\alpha = r^2$. This indicates that if a numerical calculation of the series (14.23) converges satisfactorily for a contrast ratio β/α of, say, 100, then the series (14.36) should converge satisfactorily for a contrast ratio β/α of about 10,000. Of course this is by no means certain, as the estimates given here are bounds on the convergence rate, not calculations of the actual rate of convergence. Moreover, the expansion (14.36) converges for any choice of $\sigma_0 < 0$, irrespective of the values that β and α take, so long as $\beta > \alpha > 0$. By contrast, for a given value of $\sigma_0 > 0$, the expansion (14.23) is not generally guaranteed to converge when $\beta > 2\sigma_0$.

Setting $\sigma_0 = \sqrt{\alpha\beta}$ and considering the worst case scenario, where the ratio β/α is very large, we see that M iterations with

$$M \approx \frac{-\sqrt{\beta/\alpha}}{2} \log(\epsilon)$$

are sufficient (and likely more than necessary) to ensure that $\|\boldsymbol{L}_* - \boldsymbol{L}_*^{\prime\,(M)}\| \leq \epsilon\beta$. For example, this shows that 346 iterations will certainly achieve a $\epsilon = 0.1\%$ tolerance when $\beta/\alpha = 10,000$. This is considerably less than the 74,000 iterations that guarantee convergence to same level of tolerance using the standard series expansion.

A series expansion of this type for conducting composites of n isotropic phases was first suggested by Milton and Golden (1990). However, they did not investigate the rate of convergence; this was done by Eyre and Milton (1999) and Michel, Moulinec, and Suquet (2001). For isotropic composites of two isotropic phases with conductivities σ_1 and σ_2 there is an

approach of Bruno and Reitich (1994) that yields the same expansion for the effective tensor. Without loss of generality let us suppose that $\sigma_2 = 1$. As we will see in section 18.3 on page 375, the effective conductivity σ_* considered as a function $\sigma_*(\sigma_1)$ of σ_1 with the geometry held fixed is analytic in the cut complex plane. Its singularities can lie anywhere along the negative real σ_1-axis. The function $\sigma_*(\sigma_1)/\sqrt{\sigma_1}$ is also analytic in this cut complex plane and is introduced to make the connection with the expansion (14.34). Now it would be desirable to have a series expansion that converges in this entire domain of analyticity as such an expansion should converge faster than a series expansion with a smaller domain of convergence. Since a series expansions in powers of z converges only within a circle in the z-plane, we introduce the transformation

$$z = \frac{\sqrt{\sigma_1} - 1}{\sqrt{\sigma_1} + 1},$$

which maps the cut complex σ_1-plane to the unit circle in the z-plane. From the series expansion for $\sigma_*/\sqrt{\sigma_1}$ in powers of z we obtain the expansion

$$\sigma_*(\sigma_1)/\sqrt{\sigma_1} = 1 + \sum_{k=1}^{\infty} a_k \frac{(\sqrt{\sigma_1} - 1)^k}{(\sqrt{\sigma_1} + 1)^k}, \tag{14.38}$$

which will converge in the entire cut complex plane and have an especially fast rate of convergence.

Now let us compare this expansion with the expansion (14.34). When σ_1 is fixed, real, and positive we can take α and β as the minimum and maximum of σ_1 and $\sigma_2 = 1$ and set $\sigma_0 = \sqrt{\alpha\beta} = \sqrt{\sigma_1}$. With $\boldsymbol{L}_0 = \sigma_0 \boldsymbol{I}$ and $\boldsymbol{M} = \boldsymbol{I}/2\sigma_0$ we have

$$\boldsymbol{K} = (2\chi_1 - 1)\frac{2\sqrt{\sigma_1}(\sqrt{\sigma_1} - 1)}{\sqrt{\sigma_1} + 1}, \quad \boldsymbol{\Upsilon K} = (\boldsymbol{I} - 2\boldsymbol{\Gamma}_1)(2\chi_1 - 1)\frac{\sqrt{\sigma_1} - 1}{\sqrt{\sigma_1} + 1}.$$

Making these substitutions we see that the expansions (14.34) and (14.38) are equivalent with

$$2\langle(2\chi_1 - 1)[(\boldsymbol{I} - 2\boldsymbol{\Gamma}_1)(2\chi_1 - 1)]^j\rangle = a_{j+1}\boldsymbol{I}.$$

Moreover we see that with this choice of σ_0 the expansion (14.34) converges for complex and not only real values of σ_1 and σ_2. Convergence is assured unless σ_1/σ_2 is zero, infinite, or real and negative.

14.10. A related series that converges quickly

The formula (14.34) gives an expansion for $\boldsymbol{L}_*$ in powers of $\boldsymbol{K}$. We will see in section 17.3 on page 359 that for establishing microstructure-independent relations and links between effective tensors it proves useful to consider the expansion of

$$\boldsymbol{K}_* = [\boldsymbol{I} + (\boldsymbol{L}_* - \boldsymbol{L}_0)\boldsymbol{M}]^{-1}(\boldsymbol{L}_* - \boldsymbol{L}_0)$$

in powers of $\boldsymbol{K}$. To derive this expansion we return to the formula (12.29) satisfied by the polarization field $\boldsymbol{P}(\boldsymbol{x})$ and express it as

$$[\boldsymbol{I} + (\boldsymbol{L} - \boldsymbol{L}_0)\boldsymbol{M} - (\boldsymbol{L} - \boldsymbol{L}_0)\boldsymbol{A}]\boldsymbol{P} = (\boldsymbol{L} - \boldsymbol{L}_0)\boldsymbol{V}, \tag{14.39}$$

where $\boldsymbol{M}$ is an arbitrary tensor,

$$\boldsymbol{V} = \langle \boldsymbol{E}\rangle + \boldsymbol{M}\langle \boldsymbol{P}\rangle,$$

and $\boldsymbol{A}$ is the nonlocal operator defined by

$$\boldsymbol{AP} = \boldsymbol{M}(\boldsymbol{P} - \langle \boldsymbol{P} \rangle) - \boldsymbol{\Gamma P}.$$

Equivalently, we have

$$\boldsymbol{A} = \boldsymbol{M}(\boldsymbol{I} - \boldsymbol{\Gamma}_0) - \boldsymbol{\Gamma} = \boldsymbol{\Upsilon}(\boldsymbol{I} - \boldsymbol{\Gamma}_0).$$

The action of $\boldsymbol{A}$ is local in Fourier space. The field $\boldsymbol{AP}$ has Fourier components $\boldsymbol{A}(\boldsymbol{k})\widehat{\boldsymbol{P}}(\boldsymbol{k})$ where

$$\begin{aligned} \boldsymbol{A}(\boldsymbol{k}) &= \boldsymbol{M} - \boldsymbol{\Gamma}(\boldsymbol{k}) \quad \text{for } \boldsymbol{k} \neq 0, \\ &= 0 \qquad\qquad\quad \text{for } \boldsymbol{k} = 0. \end{aligned} \tag{14.40}$$

Multiplying both sides of (14.39) on the left by $[\boldsymbol{I} + (\boldsymbol{L} - \boldsymbol{L}_0)\boldsymbol{M}]^{-1}$ gives a simple equation for the polarization field:

$$[\boldsymbol{I} - \boldsymbol{KA}]\boldsymbol{P} = \boldsymbol{KV}. \tag{14.41}$$

By considering the average fields we obtain the relation

$$(\boldsymbol{L}_* - \boldsymbol{L}_0)\boldsymbol{V} = \langle \boldsymbol{P} \rangle + (\boldsymbol{L}_* - \boldsymbol{L}_0)\boldsymbol{M}\langle \boldsymbol{P} \rangle,$$

which can be expressed as

$$\langle \boldsymbol{P} \rangle = \boldsymbol{K}_* \boldsymbol{V}. \tag{14.42}$$

Combining this with (14.41) gives the formula (Grabovsky, Milton, and Sage 2000)

$$\boldsymbol{K}_* = \langle [\boldsymbol{I} - \boldsymbol{KA}]^{-1} \boldsymbol{K} \rangle, \tag{14.43}$$

where the operator $[\boldsymbol{I} - \boldsymbol{KA}]^{-1}$ acts on the field $\boldsymbol{K}(\boldsymbol{x})$, taking values in $\mathcal{T} \otimes \mathcal{T}$ according to the extension prescribed by (12.32). Expanding $[\boldsymbol{I} - \boldsymbol{KA}]^{-1}$ in powers of $\boldsymbol{KA}$ gives the expansion

$$\boldsymbol{K}_* = \sum_{j=0}^{\infty} \langle (\boldsymbol{KA})^j \boldsymbol{K} \rangle. \tag{14.44}$$

Now since $\boldsymbol{A} = \boldsymbol{\Upsilon}(\boldsymbol{I} - \boldsymbol{\Gamma}_0)$ and $\boldsymbol{I} - \boldsymbol{\Gamma}_0$ is a projection with norm 1, the norm of $\boldsymbol{A}$ will at most be equal to the norm of $\boldsymbol{\Upsilon}$. Therefore one can expect this series expansion to converge as fast as the series expansion (14.34). For a two-phase composite the expansion reduces to

$$\boldsymbol{K}_* = f_1 \boldsymbol{K}_1 + f_2 \boldsymbol{K}_2 + \sum_{j=0}^{\infty} \langle [\chi_1 (\boldsymbol{K}_1 - \boldsymbol{K}_2)\boldsymbol{A}]^j \chi_1 (\boldsymbol{K}_1 - \boldsymbol{K}_2) \rangle,$$

where

$$\boldsymbol{K}_1 = [\boldsymbol{I} + (\boldsymbol{L}_1 - \boldsymbol{L}_0)\boldsymbol{M}]^{-1}(\boldsymbol{L}_1 - \boldsymbol{L}_0), \quad \boldsymbol{K}_2 = [\boldsymbol{I} + (\boldsymbol{L}_2 - \boldsymbol{L}_0)\boldsymbol{M}]^{-1}(\boldsymbol{L}_2 - \boldsymbol{L}_0).$$

A somewhat similar expansion was derived by Torquato (1997a, 1997b, 1998), who takes $\boldsymbol{L}_0 = \boldsymbol{L}_2$ and $\boldsymbol{M} = \boldsymbol{\gamma}$, where $\boldsymbol{\gamma}$ is given by (12.35). His expansion is for $\boldsymbol{K}_*^{-1}$ rather than $\boldsymbol{K}_*$. If for simplicity we consider an isotropic composite of two isotropic phases with conductivities σ_1 and σ_2, we have $\boldsymbol{L}_1 = \sigma_1 \boldsymbol{I}$, $\boldsymbol{L}_2 = \sigma_2 \boldsymbol{I}$, and $\boldsymbol{M} = \boldsymbol{I}/3\sigma_2$ and his expansion takes the form

$$\frac{\sigma_* + 2\sigma_2}{\sigma_* - \sigma_2} = \frac{1}{f_1 z} + \sum_{j=0}^{\infty} a_j z^j, \quad \text{where } z = \frac{\sigma_1 - \sigma_2}{\sigma_1 + 2\sigma_2}. \tag{14.45}$$

This expansion has the appealing property that the first term gives the Maxwell (i.e., the Clausius-Mossotti) approximation formula (10.27) and so succeeding terms can be regarded as corrections to this approximation formula. By keeping a few more terms in the expansion Torquato obtains good estimates of the moduli for some suspensions of spheres. Unfortunately this expansion will often not converge when σ_1 and σ_2 are real, positive, and $\sigma_1 > 4\sigma_2$. With $\sigma_2 = 1$ the possible singularities of the function on the left of (14.45) are at $\sigma_1 = 1$ and at negative real values of σ_1, that is, at $z = 0$ or at real values of z outside the interval $(-1/2, 1)$. If R denotes the distance from the origin to the nearest singularity in the z-plane, excluding the singularity at $z = 0$, the series will not converge when $|z| > R > 1/2$. If the composite is a suspension of spheres, the precise value of R will depend on the sphere configuration but will be close to $1/2$ if there are spheres that come close to touching other spheres [see McPhedran and Perrins (1981) and Bruno (1991a).]

It should be remarked that one has to be careful taking truncated series expansions as approximation formulas for effective tensors. For example, for an isotropic conducting composite of two isotropic conducting phases, the approximate to the function $\sigma_*(\sigma_1, \sigma_2)$ that one obtains from truncated series expansions is generally not compatible with the known analytic properties of effective conductivity functions discussed in section 18.3 on page 375. In particular, such approximations typically predict that σ_* can have a negative real part when σ_1 and σ_2 are appropriately chosen with positive real parts, that is, the composite would turn heat into electrical energy when both phases dissipate electrical energy into heat. In other words, for a given truncated series expansion one can find values of σ_1 and σ_2 for which the predicted value of σ_* is not just a bad approximation but is physically impossible. Truncated series expansions give reasonable approximations when σ_1/σ_2 is restricted to a limited domain in the complex plane. As more and more terms are added to the truncated series expansion this domain approaches the domain of convergence of the series expansion.

14.11. Numerical computation of the fields and effective tensor using series expansions

Moulinec and Suquet (1994, 1998) recognized that the series expansions provide a convenient iterative procedure for numerically computing the fields and effective tensor. Consider the approximants

$$\boldsymbol{E}^m = \sum_{j=0}^{m} (-\boldsymbol{\Gamma}\delta\boldsymbol{L})^j \boldsymbol{E}_0 \tag{14.46}$$

for the field $\boldsymbol{E}$. These satisfy

$$\boldsymbol{E}^{m+1} = \boldsymbol{E}_0 - \boldsymbol{\Gamma}\delta\boldsymbol{L}\boldsymbol{E}^m = \boldsymbol{E}^m - \boldsymbol{\Gamma}\boldsymbol{L}\boldsymbol{E}^m, \tag{14.47}$$

where the last relation follows from the identity $\boldsymbol{\Gamma}\boldsymbol{L}_0\boldsymbol{E}^m = \boldsymbol{E}^m - \boldsymbol{E}_0$, which holds because $\boldsymbol{E}^m - \boldsymbol{E}_0$ lies in the space $\mathcal{E}$. Associated with each field $\boldsymbol{E}^m$ is the approximate

$$\boldsymbol{J}^m = \boldsymbol{L}_0\boldsymbol{E}_0 + (\boldsymbol{I} - \boldsymbol{L}_0\boldsymbol{\Gamma})(\boldsymbol{L} - \boldsymbol{L}_0)\boldsymbol{E}^m = \boldsymbol{L}\boldsymbol{E}^m + \boldsymbol{L}_0(\boldsymbol{E}^{m+1} - \boldsymbol{E}^m)$$

to the field $\boldsymbol{J}$. This approximant to $\boldsymbol{J}$ necessarily lies in the space $\mathcal{U} \oplus \mathcal{J}$ because $\boldsymbol{\Gamma}_1(\boldsymbol{I} - \boldsymbol{L}_0\boldsymbol{\Gamma}) = 0$. As the fields converge the last term in the above expression for $\boldsymbol{J}^m$ becomes negligible and we have $\boldsymbol{J}^m \approx \boldsymbol{L}\boldsymbol{E}^{m+1}$, that is, the constitutive relation is nearly satisfied by the approximate fields.

Now the action of $\boldsymbol{L}$ on $\boldsymbol{E}^m$ is easy to compute in real space. The field $\boldsymbol{L}\boldsymbol{E}^m$ can then be transformed to Fourier space, where the action of $\boldsymbol{\Gamma}$ on it is easily computed. After transformation back to real space the resulting field $\boldsymbol{\Gamma}\boldsymbol{L}\boldsymbol{E}^m$ can be added to $\boldsymbol{E}^m$ to obtain $\boldsymbol{E}^{m+1}$. By discretizing the fields, using fast Fourier transforms, and iterating the procedure one obtains a workable scheme for calculating the field $\boldsymbol{E}$. At each stage it is necessary to keep track of only the current and the most recent iterates of the field, such as $\boldsymbol{\Gamma}\boldsymbol{L}\boldsymbol{E}^m$ and $\boldsymbol{E}^m$. After the iteration has stopped, at say $m = M$, one has an approximant $\boldsymbol{E}^M$ for the field $\boldsymbol{E}$. Associated with this approximant $\boldsymbol{E}^M \in \mathcal{E}$ to $\boldsymbol{E}$ is the approximant $\boldsymbol{J}^M \in \mathcal{J}$ to $\boldsymbol{J}$. When the reference medium $\boldsymbol{L}_0$ is set equal to $(\alpha + \beta)\boldsymbol{I}/2$ an analysis similar to that in the previous section [see (14.24)] shows that $|\boldsymbol{E} - \boldsymbol{E}^M|$ is at most of the order of γ^M [see (14.24)] with $\gamma = (\beta/\alpha - 1)/(\beta/\alpha + 1)$.

One can then calculate selected elements of the effective tensor either from the constitutive relation

$$\langle \boldsymbol{L}\boldsymbol{E}^M \rangle \approx \boldsymbol{L}_* \langle \boldsymbol{E}^M \rangle,$$

in which $\langle \boldsymbol{E}^M \rangle$ can be identified with $\boldsymbol{E}_0$, or (assuming that $\boldsymbol{L}$ and $\boldsymbol{L}_0$ are self-adjoint) from the expression

$$\langle \boldsymbol{E}^M \cdot \rangle \boldsymbol{L}_* \langle \boldsymbol{E}^M \rangle \approx \langle \boldsymbol{E}^M \cdot \boldsymbol{L}\boldsymbol{E}^M \rangle$$

for the energy. Using the constitutive relation yields (for each choice of $\boldsymbol{E}_0$) many elements of $\boldsymbol{L}_*$, each accurate to at least the order of γ^M. Using the energy approximation yields a single element of $\boldsymbol{L}_*$ that is accurate to at least the order of γ^{2M} [see (13.9)]. If one needs to determine only a single element of $\boldsymbol{L}_*$, such as the effective shear modulus of an elastically isotropic composite, then it is best to work with the energy approximation. However, if two or more elements of $\boldsymbol{L}_*$ are needed, then it is probably best to use the constitutive relation and to double the number of iterations to achieve the same order of accuracy as would be obtained using the energy approximation.

Faster convergence can be expected if one works with the approximants

$$\boldsymbol{P}^m = \sum_{j=0}^{m} \boldsymbol{K}(\boldsymbol{\Upsilon}\boldsymbol{K})^j \boldsymbol{E}_0$$

to the polarization field, which are based on the series expansion (14.34). These satisfy the recursion relations

$$\boldsymbol{P}^{m+1} = \boldsymbol{K}\boldsymbol{E}_0 + \boldsymbol{K}\boldsymbol{\Upsilon}\boldsymbol{P}^m.$$

The action of $\boldsymbol{\Upsilon}$ on the field $\boldsymbol{P}^m$ is easy to compute in Fourier space whereas the action of $\boldsymbol{K}$ on $\boldsymbol{\Upsilon}\boldsymbol{P}^m$ is easy to compute in real space. Therefore the same procedure of swapping between real space and Fourier space using fast Fourier transforms can be used to numerically compute a high-accuracy approximation to the true polarization field. Associated with the approximant $\boldsymbol{P}^m$ for the polarization field is the approximant

$$\begin{aligned} \boldsymbol{E}^m &= \boldsymbol{E}_0 - \boldsymbol{\Gamma}\boldsymbol{P}^m = \boldsymbol{K}^{-1}\boldsymbol{P}^{m+1} - \boldsymbol{M}\boldsymbol{P}^m \\ &= (\boldsymbol{L} - \boldsymbol{L}_0)^{-1}\boldsymbol{P}^{m+1} + \boldsymbol{M}(\boldsymbol{P}^{m+1} - \boldsymbol{P}^m) \end{aligned}$$

for the field $\boldsymbol{E}$. This approximant lies in $\mathcal{U} \oplus \mathcal{E}$. As the approximants to the polarization field converge, the last term in the above expression becomes negligible and we have $(\boldsymbol{L} - \boldsymbol{L}_0)\boldsymbol{E}^m \approx \boldsymbol{P}^{m+1} \approx \boldsymbol{P}^m$. Also associated with $\boldsymbol{P}^m$ is the approximant

$$\boldsymbol{J}^m = \boldsymbol{L}_0\boldsymbol{E}_0 + (\boldsymbol{I} - \boldsymbol{L}_0\boldsymbol{\Gamma})\boldsymbol{P}^m = \boldsymbol{P}^m + \boldsymbol{L}_0\boldsymbol{E}^m$$

for the field $\boldsymbol{J}$. This approximant lies in $\mathcal{U} \oplus \mathcal{J}$. The relation $\boldsymbol{P}^m \approx (\boldsymbol{L} - \boldsymbol{L}_0)\boldsymbol{E}^m$, which holds as the approximants to the polarization field converge, implies that $\boldsymbol{J}^m \approx \boldsymbol{L}\boldsymbol{E}^m$. Thus the constitutive law will be nearly satisfied by these approximate fields when m is large.

When the reference medium $\boldsymbol{L}_0$ is set equal to $\sqrt{\alpha\beta}\boldsymbol{I}$ an analysis similar to that in the previous section [see (14.24)] shows that $|\boldsymbol{E} - \boldsymbol{E}^M|$ is at most of the order of $(\gamma')^M$ [see (14.37)] with $\gamma' = (\sqrt{\beta/\alpha} - 1)/(\sqrt{\beta/\alpha} + 1)$. Eyre and Milton (1999) as a test example applied this scheme to calculating the transverse conductivity of a square array of cylinders and verified that it converged substantially faster than the iterative scheme based on (14.46). Even faster convergence rates were obtained by first solving the equations on a coarse grid and then successively refining the grid. Michel, Moulinec, and Suquet (2001) found a similar acceleration of convergence for two-dimensional elasticity computations.

One advantage of these approaches to computing the fields and effective tensors is that they are easily generalized to nonlinear materials (Moulinec and Suquet 1998). For example, consider an n-phase composite where the constitutive relation takes the form

$$\boldsymbol{J}(\boldsymbol{x}) = \boldsymbol{F}_i(\boldsymbol{E}(\boldsymbol{x})) \text{ when } \boldsymbol{x} \text{ is in phase } i = 1, 2, \ldots, n.$$

We rewrite this as $\boldsymbol{J} = \boldsymbol{F}(\boldsymbol{E})$, that is, the field $\boldsymbol{J}$ is some nonlinear function of the field $\boldsymbol{E}$. Now the recursion relation (14.47) clearly has a natural generalization to nonlinear composites:

$$\boldsymbol{E}^{m+1} = \boldsymbol{E}^m - \boldsymbol{\Gamma}\boldsymbol{F}(\boldsymbol{E}^m). \tag{14.48}$$

To get some idea of when this iteration scheme will converge let us suppose that $\boldsymbol{L}_0 = \sigma_0\boldsymbol{I}$. This implies that $\boldsymbol{\Gamma} = \boldsymbol{\Gamma}_1/\sigma_0$, and from (14.48) we have

$$\begin{aligned}\boldsymbol{E}^{m+2} - \boldsymbol{E}^{m+1} &= \boldsymbol{E}^{m+1} - \boldsymbol{E}^m - \boldsymbol{\Gamma}_1[\boldsymbol{F}(\boldsymbol{E}^{m+1}) - \boldsymbol{F}(\boldsymbol{E}^m)]/\sigma_0 \\ &= \boldsymbol{\Gamma}_1\{[\boldsymbol{E}^{m+1} - \boldsymbol{E}^m] - [\boldsymbol{F}(\boldsymbol{E}^{m+1}) - \boldsymbol{F}(\boldsymbol{E}^m)]/\sigma_0\}.\end{aligned}$$

Since $\boldsymbol{\Gamma}_1$ is a projection operator, it follows that

$$\begin{aligned}|\boldsymbol{E}^{m+2} - \boldsymbol{E}^{m+1}|^2 &\le |\boldsymbol{E}^{m+1} - \boldsymbol{E}^m - [\boldsymbol{F}(\boldsymbol{E}^{m+1}) - \boldsymbol{F}(\boldsymbol{E}^m)]/\sigma_0|^2 \\ &\le |\boldsymbol{E}^{m+1} - \boldsymbol{E}^m|^2 - 2(\boldsymbol{E}^{m+1} - \boldsymbol{E}^m, \boldsymbol{F}(\boldsymbol{E}^{m+1}) - \boldsymbol{F}(\boldsymbol{E}^m))/\sigma_0 \\ &\quad + |\boldsymbol{F}(\boldsymbol{E}^{m+1}) - \boldsymbol{F}(\boldsymbol{E}^m)|^2/\sigma_0^2.\end{aligned}$$

To bound the terms appearing here, let us assume that there exist positive constants α and β such that

$$(\boldsymbol{P} - \boldsymbol{P}', \boldsymbol{F}(\boldsymbol{P}) - \boldsymbol{F}(\boldsymbol{P}')) \ge \alpha|\boldsymbol{P} - \boldsymbol{P}'|^2, \quad |\boldsymbol{F}(\boldsymbol{P}) - \boldsymbol{F}(\boldsymbol{P}')| \le \beta|\boldsymbol{P} - \boldsymbol{P}'|, \tag{14.49}$$

for any fields $\boldsymbol{P}$ and $\boldsymbol{P}'$ in $\mathcal{H}$. [When the material is linear, i.e., $\boldsymbol{F}(\boldsymbol{P}) = \boldsymbol{L}\boldsymbol{P}$, these conditions reduce to the conditions (14.25) and (14.26).] Then we have the inequality

$$|\boldsymbol{E}^{m+2} - \boldsymbol{E}^{m+1}|^2 \le (1 - 2\alpha/\sigma_0 + \beta^2/\sigma_0^2)|\boldsymbol{E}^{m+1} - \boldsymbol{E}^m|^2.$$

When σ_0 is chosen sufficiently large, so that

$$|1 - 2\alpha/\sigma_0 + \beta/\sigma_0^2| < 1,$$

this inequality guarantees that the sequence of fields $\boldsymbol{E}^m(\boldsymbol{x})$ is Cauchy and hence convergent.

In our n-phase composite, the condition (14.49) will be satisfied if and only if the functions $\boldsymbol{F}_i$ are such that

$$(\boldsymbol{A}-\boldsymbol{A}')\cdot[\boldsymbol{F}_i(\boldsymbol{A})-\boldsymbol{F}_i(\boldsymbol{A}')]\geq\alpha|\boldsymbol{A}-\boldsymbol{A}'|^2,\quad|\boldsymbol{F}_i(\boldsymbol{A})-\boldsymbol{F}_i(\boldsymbol{A}')|\leq\beta|\boldsymbol{A}-\boldsymbol{A}'|,\tag{14.50}$$

for all choices of the tensors $\boldsymbol{A}$ and $\boldsymbol{A}'$. The first condition holds only when $\boldsymbol{F}_i(\boldsymbol{A})$ is a monotone function of $\boldsymbol{A}$. The second condition holds only when $\boldsymbol{F}_i(\boldsymbol{A})$ does not grow faster than linearly with $\boldsymbol{A}$. To get some more insight into the first condition, suppose that the function $\boldsymbol{F}_i(\boldsymbol{A})$ derives from an energy, that is,

$$\boldsymbol{F}_i(\boldsymbol{A})=\frac{\partial W_i(\boldsymbol{A})}{\partial\boldsymbol{A}},$$

for some choice of the function $W_i(\boldsymbol{A})$. Let us consider the line of matrices $\boldsymbol{A}'(\lambda)=\boldsymbol{A}-\lambda\boldsymbol{B}$ parameterized by λ, where without loss of generality we can assume that $|\boldsymbol{B}|=1$, by rescaling λ if necessary. Then, defining $W_i(\lambda)=W_i(\boldsymbol{A}'(\lambda))$, the first condition becomes

$$\lambda\left[\frac{dW_i(\lambda)}{d\lambda}-\frac{dW_i(\lambda)}{d\lambda}\bigg|_{\lambda=0}\right]\geq\alpha\lambda^2,\tag{14.51}$$

which in the limit $\lambda\to 0$ implies that

$$\frac{d^2W_i(\lambda)}{d\lambda^2}\geq\alpha,\tag{14.52}$$

at $\lambda=0$. In other words, the function $W_i(\boldsymbol{A})$ must have some minimum positive curvature at the point $\boldsymbol{A}$ in the direction $\boldsymbol{B}$. Since $\boldsymbol{A}$ and $\boldsymbol{B}$, with $|\boldsymbol{B}|=1$, are arbitrary, we conclude that $W_i(\boldsymbol{A})$ must be a convex function of $\boldsymbol{A}$ with some minimum curvature. Conversely, if (14.52) holds for all λ (and all $\boldsymbol{A}$ and $\boldsymbol{B}$), then by integrating it we deduce that (14.51) holds, and hence that the first condition in (14.50) must also hold. Of course, if the conditions in (14.50) are not satisfied, then the iteration scheme might still converge, as shown in the linear case in section 14.8 on page 301.

These iteration schemes generally fail to converge when the material contains voids or rigid inclusions. To overcome this difficulty Michel, Moulinec, and Suquet (2000, 2001) have introduced an iteration method based on augmented Lagrangians that works rather well even when voids or rigid inclusions are present.

References

Avellaneda, M. 1987. Optimal bounds and microgeometries for elastic two-phase composites. *SIAM Journal on Applied Mathematics* 47(6):1216–1228. {*175, 181, 292, 294, 309, 463–465, 468, 471, 473, 491*}

Beran, M. J. 1968. *Statistical Continuum Theories*. New York: Interscience Publishers. xv + 424 pp. ISBN 0-470-06861-2. {*xxv, xxvi, 11, 15, 291, 309, 489, 491*}

Beran, M. J. and J. J. McCoy 1970. Mean field variations in a statistical sample of heterogeneous linear elastic solids. *International Journal of Solids and Structures* 6:1035–1054. {*291, 309*}

Beran, M. J. and J. Molyneux 1963. Statistical properties of the electric field in a medium with small random variations in permittivity. *Nuovo Cimento* 30:1406–1422. {*291, 309*}

Brown, W. F. 1955. Solid mixture permittivities. *Journal of Chemical Physics* 23:1514–1517. {*291, 310, 313, 336*}

Bruno, O. P. 1991b. Taylor expansions and bounds for the effective conductivity and the effective elastic moduli of multicomponent composites and polycrystals. *Asymptotic Analysis* 4(4):339–365. {*298, 310, 372, 392*}

Bruno, O. P. 1991a. The effective conductivity of strongly heterogeneous composites. *Proceedings of the Royal Society of London. Series A, Mathematical and Physical Sciences* 433(1888):353–381. {*306, 310, 373, 392, 569, 597*}

Bruno, O. P. and F. Reitich 1994. Approximation of analytic functions: A method of enhanced convergence. *Mathematics of Computation* 63(207):195–213. {*304, 310*}

Caflisch, R. E. 1993. Singularity formation for complex solutions of the 3D incompressible Euler equations. *Physica. D, Nonlinear Phenomena* 67(1–3):1–18. {*298, 310*}

Dederichs, P. H. and R. Zeller 1973. Variational treatment of the elastic constants of disordered materials. *Zeitschrift für Physik* 259:103–116. {*291, 310, 553, 565*}

Eyre, D. J. and G. W. Milton 1999. A fast numerical scheme for computing the response of composites using grid refinement. *The European Physical Journal. Applied Physics* 6(1):41–47. {*40, 42, 303, 308, 310*}

Firoozye, N. B. and R. V. Kohn 1993. Geometric parameters and the relaxation of multiwell energies. In D. Kinderlehrer, R. D. James, M. Luskin, and J. L. Ericksen (eds.), *Microstructure and Phase Transition*, pp. 85–109. Berlin / Heidelberg / London / etc.: Springer-Verlag. ISBN 0-387-94112-6 (New York), 3-540-94112-6 (Berlin). {*295, 310*}

Fokin, A. G. 1982. Iteration method in the theory of nonhomogeneous dielectrics. *Physica Status Solidi. B, Basic Research* 111:281–288. {*248, 267, 298, 310*}

Fokin, A. G. 1996. Macroscopic conductivity of random inhomogeneous media. calculational methods. *Uspekhi Fizicheskikh Nauk* 166:1069–1093. English translation in *Physics-Uspekhi* 39:1009–1032 (1996). {*298, 310*}

Fokin, A. G. and T. D. Shermergor 1969. Calculation of effective elastic moduli of composite materials with multiphase interactions taken into account. *Journal of Applied Mechanics and Technical Physics* 10:48–54. {*291, 310*}

Gérard, P. 1989. Compacité par compensation et régularité 2-microlocale. (French) [Compensated compactness and 2-microlocal regularity]. *Séminaire sur les Équations aux Dérivées Partielles, 1988–1989, École Polytechnique, Centre de Mathematiques* 6:1–18. {*293, 310*}

Gérard, P. 1994. Microlocal analysis of compactness. In *Nonlinear Partial Differential Equations and Their Applications. Collège de France Seminar, Volume XII (Paris, 1991–1993)*, pp. 75–86. Harlow, Essex, United Kingdom: Longman Scientific and Technical. ISBN 0-582-23801-3. {*293, 310*}

Grabovsky, Y., G. W. Milton, and D. S. Sage 2000. Exact relations for effective tensors of composites: Necessary conditions and sufficient conditions. *Communications on Pure and Applied Mathematics (New York)* 53(3):300–353. {*305, 310, 355, 360, 363, 365–367*}

Gubernatis, J. E. and J. A. Krumhansl 1975. Macroscopic engineering properties of polycrystalline materials: Elastic properties. *Journal of Applied Physics* 46:1875–1883. {*291, 311*}

Hori, M. 1973. Statistical theory of effective electrical, thermal, and magnetic properties of random heterogeneous materials. I. Perturbation expansions for the effective permittivity of cell materials. *Journal of Mathematical Physics* 14(4):514–523. {*291, 311, 331, 337*}

Khachaturyan, A. G. 1966. Some questions concerning the theory of phase transitions in solids. *Fizika Tverdogo Tela.* 8:2709–2717. English translation in *Soviet Phys. Solid State.* 8:2163–2168 (1967). {*252, 268, 295, 311, 474, 493, 672, 696*}

Khachaturyan, A. G. 1983. *Theory of Structural Transformations in Solids*. New York / London / Sydney, Australia: John Wiley and Sons. xiii + 574 pp. ISBN 0-471-07873-5. {*295, 311, 672, 696*}

Kohn, R. V. 1991. The relaxation of a double-well energy. *Continuum Mechanics and Thermodynamics* 3(3):193–236. {*293, 295, 311, 672, 677, 696*}

Kröner, E. 1977. Bounds for the effective elastic moduli of disordered materials. *Journal of the Mechanics and Physics of Solids* 25:137–155. {*251, 268, 282, 287, 291, 311, 458, 493, 553, 566*}

Lipton, R. 1992. Bounds and perturbation series for incompressible elastic composites with transverse isotropic symmetry. *Journal of Elasticity* 27(3):193–225. {*294, 311, 472, 473, 494*}

McPhedran, R. C. and W. T. Perrins 1981. Electrostatic and optical resonances of cylinder pairs. *Applied Physics* 24:311–318. {*188, 217, 239, 244, 306, 311*}

Michel, J. C., H. Moulinec, and P. Suquet 2000. A computational method based on augmented Lagrangians and fast Fourier transforms for composites with high contrast. *Computer Modeling in Engineering and Sciences* 1(2):79–88. {*40, 44, 309, 311*}

Michel, J. C., H. Moulinec, and P. Suquet 2001. A computational scheme for linear and nonlinear composites with arbitrary phase contrast. *International Journal Numerical Methods in Engineering* 52(1–2):139–160. {*40, 45, 298, 303, 308, 309, 311*}

Milton, G. W. and K. Golden 1990. Representations for the conductivity functions of multicomponent composites. *Communications on Pure and Applied Mathematics (New York)* 43(5):647–671. {*303, 311, 387, 389, 390, 394, 451, 454, 638, 641*}

Moulinec, H. and P. Suquet 1994. A fast numerical method for computing the linear and non-linear properties of composites. *Comptes Rendus des Séances de l'Académie des Sciences. Série II* 318:1417–1423. {*40, 45, 306, 311*}

Moulinec, H. and P. Suquet 1998. A numerical method for computing the overall response of non-linear composites with complex microstructure. *Computer Methods in Applied Mechanics and Engineering* 157(1–2):69–94. {*40, 45, 306, 308, 311*}

Smyshlyaev, V. P. and J. R. Willis 1999. On the relaxation of a three-well energy. *Proceedings of the Royal Society of London. Series A, Mathematical and Physical Sciences* 455 (1983):779–814. {*295, 311, 515, 527*}

Tartar, L. 1989. H-measures and small amplitude homogenization. In R. V. Kohn and G. W. Milton (eds.), *Proceedings of the SIAM Workshop on Random Media and Composites,*

Leesburg, Virginia, December 7–10, 1988, pp. 89–99. Philadelphia: SIAM Press. ISBN 0-89871-246-7. {*292–294, 311*}

Tartar, L. 1990. H-measures, a new approach for studying homogenization, oscillations and concentration effects in partial differential equations. *Proceedings of the Royal Society of Edinburgh. Section A, Mathematical and Physical Sciences* 115(3–4):193–230. {*292–294, 312*}

Torquato, S. 1997a. Effective stiffness tensor of composite media. I. Exact series expansions. *Journal of the Mechanics and Physics of Solids* 45(9):1421–1448. {*258, 269, 305, 312, 461, 496*}

Torquato, S. 1997b. Exact expression for the effective elastic tensor of disordered composites. *Physical Review Letters* 79(4):681–684. {*305, 312*}

Torquato, S. 1998. Effective stiffness tensor of composite media: II. Applications to isotropic dispersions. *Journal of the Mechanics and Physics of Solids* 46(8):1411–1440. {*305, 312, 333, 339*}

Willis, J. R. 1981. Variational and related methods for the overall properties of composites. *Advances in Applied Mechanics* 21:1–78. {*xxv, xxviii, 185, 200, 220, 252, 255, 269, 291, 312*}

Zeller, R. and P. H. Dederichs 1973. Elastic constants of polycrystals. *Physica Status Solidi. B, Basic Research* 55:831–842. {*291, 312*}

15

Correlation functions and how they enter series expansions†

What information about the composite material is needed to compute the effective tensor? Since the series expansion converges to the effective tensor, this is clearly equivalent to the question of what geometrical information is relevant to determining the successive terms in the series expansion (14.2). Brown (1955) found that the terms in the series expansion of the effective conductivity depend on the correlation functions characterizing the composite microgeometry.

15.1. Expressing the third-order term of the series expansion in terms of correlation functions

To see how the terms in the series expansion (14.2) depend on correlation functions let us look at a particular term, say the third-order term,

$$\delta \boldsymbol{L}_*^{(3)} \equiv \langle (\boldsymbol{L} - \boldsymbol{L}_0)\boldsymbol{\Gamma}(\boldsymbol{L} - \boldsymbol{L}_0)\boldsymbol{\Gamma}(\boldsymbol{L} - \boldsymbol{L}_0)\rangle.$$

We could of course examine the second-order term, but then the generalization of the ensuing analysis to higher order terms in the expansion would be less transparent.

We assume that a basis for $\mathcal{T}$ has been chosen so that $\delta \boldsymbol{L}_*^{(3)}$, $\boldsymbol{L}$, and $\boldsymbol{L}_0$ are represented by $m \times m$ matrices. From formula (12.45), which expresses the action of the operator $\boldsymbol{\Gamma}$ in terms of the integral kernel $\boldsymbol{\Gamma}_\Omega(\boldsymbol{x}, \boldsymbol{x}')$, it follows that

$$\{\delta \boldsymbol{L}_*^{(3)}\}_{a_1 b_3} = \frac{1}{|\Omega|} \int_\Omega d\boldsymbol{x}_3 \int_\Omega d\boldsymbol{x}_2 \int_\Omega d\boldsymbol{x}_1 \{\delta \boldsymbol{L}(\boldsymbol{x}_1)\}_{a_1 b_1} \{\boldsymbol{\Gamma}_\Omega(\boldsymbol{x}_1, \boldsymbol{x}_2)\}_{b_1 a_2} \{\delta \boldsymbol{L}(\boldsymbol{x}_2)\}_{a_2 b_2} \{\boldsymbol{\Gamma}_\Omega(\boldsymbol{x}_2, \boldsymbol{x}_3)\}_{b_2 a_3} \{\delta \boldsymbol{L}(\boldsymbol{x}_3)\}_{a_3 b_3}, \tag{15.1}$$

where

$$\delta \boldsymbol{L}(\boldsymbol{x}) = \boldsymbol{L}(\boldsymbol{x}) - \boldsymbol{L}_0$$

is assumed to be smooth or piecewise smooth and where, following the Einstein summation convention, sums over repeated indices are implied. Special care must be taken when evaluating these integrals because $\boldsymbol{\Gamma}_\Omega(\boldsymbol{y})$ has a singularity of order $|\boldsymbol{y}|^{-d}$ at $\boldsymbol{y} = 0$ (and similar singularities at points periodically displaced from the point $\boldsymbol{y} = 0$). Accordingly, the integrals should be treated in the manner discussed in section 12.6 on page 257. Bypassing this technical question, let us make the change of variables from $\boldsymbol{x}_1$, $\boldsymbol{x}_2$, and $\boldsymbol{x}_3$ to $\boldsymbol{y}_1 = \boldsymbol{x}_1 - \boldsymbol{x}_2$, $\boldsymbol{y}_2 = \boldsymbol{x}_2 - \boldsymbol{x}_3$, and $\boldsymbol{x}_3$. Due to the periodicity we can integrate $\boldsymbol{y}_1$ over the region Ω rather

than over the region $\Omega - \boldsymbol{x}_3 - \boldsymbol{y}_2$, and we can integrate $\boldsymbol{y}_2$ over Ω rather than over $\Omega - \boldsymbol{x}_3$. Performing the integral over $\boldsymbol{x}_3$ first and noticing that relation (15.1) holds for all choices of the field $\boldsymbol{E}_0$ leads to

$$\{\delta \boldsymbol{L}_*^{(3)}\}_{a_1 b_3} = \int_\Omega d\boldsymbol{y}_2 \int_\Omega d\boldsymbol{y}_1 \{\boldsymbol{F}_3(\boldsymbol{y}_1 + \boldsymbol{y}_2, \boldsymbol{y}_2)\}_{a_1 b_1 a_2 b_2 a_3 b_3} \{\boldsymbol{\Gamma}_\Omega(\boldsymbol{y}_1)\}_{b_1 a_2} \{\boldsymbol{\Gamma}_\Omega(\boldsymbol{y}_2)\}_{b_2 a_3}, \tag{15.2}$$

in which $\boldsymbol{F}_3(\boldsymbol{z}_1, \boldsymbol{z}_2)$ is a tensor with six indices with elements

$$\{\boldsymbol{F}_3(\boldsymbol{z}_1, \boldsymbol{z}_2)\}_{a_1 b_1 a_2 b_2 a_3 b_3} = \frac{1}{|\Omega|} \int_\Omega d\boldsymbol{x} \{\delta \boldsymbol{L}(\boldsymbol{z}_1 + \boldsymbol{x})\}_{a_1 b_1} \{\delta \boldsymbol{L}(\boldsymbol{z}_2 + \boldsymbol{x})\}_{a_2 b_2} \{\delta \boldsymbol{L}(\boldsymbol{x})\}_{a_3 b_3}.$$

This object is called a three-point correlation function because it involves an average over $\boldsymbol{x}$ of a quantity that depends on the value of material moduli $\boldsymbol{L}$ at the three points $\boldsymbol{z}_1 + \boldsymbol{x}$, $\boldsymbol{z}_2 + \boldsymbol{x}$, and $\boldsymbol{x}$. It is a periodic function of $\boldsymbol{z}_1$ and $\boldsymbol{z}_2$ because $\boldsymbol{L}(\boldsymbol{x})$ is a periodic function of $\boldsymbol{x}$.

This result can clearly be generalized to other terms in the series expansion. The expansion of the effective tensor to the p-th order in perturbation can be computed once we know the appropriate p-point correlation function. Specifically, we need to know the p-point correlation function $\boldsymbol{F}_p(\boldsymbol{z}_1, \boldsymbol{z}_2, \ldots, \boldsymbol{z}_{p-1})$ defined as the tensor with elements

$$\{\boldsymbol{F}_p(\boldsymbol{z}_1, \boldsymbol{z}_2, \ldots, \boldsymbol{z}_{p-1})\}_{a_1 b_1 a_2 b_2 \ldots a_p b_p} =$$
$$\frac{1}{|\Omega|} \int_\Omega d\boldsymbol{x} \{\delta \boldsymbol{L}(\boldsymbol{z}_1 + \boldsymbol{x})\}_{a_1 b_1} \{\delta \boldsymbol{L}(\boldsymbol{z}_2 + \boldsymbol{x})\}_{a_2 b_2} \cdots \{\delta \boldsymbol{L}(\boldsymbol{z}_{p-1} + \boldsymbol{x})\}_{a_{p-1} b_{p-1}} \{\delta \boldsymbol{L}(\boldsymbol{x})\}_{a_p b_p}.$$

Such correlation functions provide a partial description of the composite geometry.

The terms in the series expansion can also be expressed in terms of the integral kernel $\boldsymbol{\Gamma}_\infty(\boldsymbol{y})$ of the free-space Γ-operator. The key is to rewrite (15.2) in a form where $\boldsymbol{\Gamma}_\Omega(\boldsymbol{y}_1)$ and $\boldsymbol{\Gamma}_\Omega(\boldsymbol{y}_2)$ are integrated against a function that has zero average value over $\boldsymbol{y}_1$ and over $\boldsymbol{y}_2$. Notice that we can subtract from $\boldsymbol{F}_3(\boldsymbol{y}_1 + \boldsymbol{y}_2, \boldsymbol{y}_2)$ any function that is independent of $\boldsymbol{y}_1$, or any function that is independent of $\boldsymbol{y}_2$, without altering the value of the integral. This is permitted because $\boldsymbol{\Gamma}$ acting on any constant field gives zero. In particular we can subtract from $\boldsymbol{F}_3(\boldsymbol{y}_1 + \boldsymbol{y}_2, \boldsymbol{y}_2)$ its average over $\boldsymbol{y}_1$ and then subtract the average over $\boldsymbol{y}_2$ of the resultant expression. In other words, we can replace $\boldsymbol{F}_3(\boldsymbol{y}_1 + \boldsymbol{y}_2, \boldsymbol{y}_2)$ by the function

$$\begin{aligned} \boldsymbol{F}'_3(\boldsymbol{y}_1 + \boldsymbol{y}_2, \boldsymbol{y}_2) = \boldsymbol{F}_3(\boldsymbol{y}_1 + \boldsymbol{y}_2, \boldsymbol{y}_2) &- \frac{1}{|\Omega|} \int_\Omega d\boldsymbol{y}_1 \boldsymbol{F}_3(\boldsymbol{y}_1 + \boldsymbol{y}_2, \boldsymbol{y}_2) \\ &- \frac{1}{|\Omega|} \int_\Omega d\boldsymbol{y}_2 \boldsymbol{F}_3(\boldsymbol{y}_1 + \boldsymbol{y}_2, \boldsymbol{y}_2) + \frac{1}{|\Omega|^2} \int_\Omega d\boldsymbol{y}_2 \int_\Omega d\boldsymbol{y}_1 \boldsymbol{F}_3(\boldsymbol{y}_1 + \boldsymbol{y}_2, \boldsymbol{y}_2), \end{aligned} \tag{15.3}$$

which has the property that

$$\frac{1}{|\Omega|} \int_\Omega d\boldsymbol{y}_1 \boldsymbol{F}'_3(\boldsymbol{y}_1 + \boldsymbol{y}_2, \boldsymbol{y}_2) = 0, \qquad \frac{1}{|\Omega|} \int_\Omega d\boldsymbol{y}_2 \boldsymbol{F}'_3(\boldsymbol{y}_1 + \boldsymbol{y}_2, \boldsymbol{y}_2) = 0.$$

A similar operation can be performed on higher order correlation functions. Once this substitution is made, these integral kernels can be replaced by $\boldsymbol{\Gamma}_\infty(\boldsymbol{y}_1)$ and $\boldsymbol{\Gamma}_\infty(\boldsymbol{y}_2)$ while the regions of integration can be extended to all space, that is,

$$\{\delta \boldsymbol{L}_*^{(3)}\}_{a_1b_3} = \int_{\mathbb{R}^d} d\boldsymbol{y}_2 \int_{\mathbb{R}^d} d\boldsymbol{y}_1 \{\boldsymbol{F}'_3(\boldsymbol{y}_1 + \boldsymbol{y}_2, \boldsymbol{y}_2)\}_{a_1b_1a_2b_2a_3b_3} \{\boldsymbol{\Gamma}_\infty(\boldsymbol{y}_1)\}_{b_1a_2} \{\boldsymbol{\Gamma}_\infty(\boldsymbol{y}_2)\}_{b_2a_3}. \tag{15.4}$$

Some care still must be taken in evaluating these integrals because $\boldsymbol{\Gamma}_\infty(\boldsymbol{y})$ has a singularity of order $|\boldsymbol{y}|^{-d}$ at $\boldsymbol{y} = 0$.

15.2. The terms in the series expansion for random media

These formulas can be extended to random media that are statistically homogeneous with no long-range correlations. Rather than going through a detailed mathematical derivation, let us dispense with rigor and apply a simple argument that yields the result directly from the preceding formulas. The absence of long-range correlations in the random composite implies that if a set of p points can be divided into a first cluster of p' points and a second cluster of $p - p'$ points that is separated from the first cluster by a distance that is much larger than the microstructure, then the p-point correlation function is approximately a product of the p'-point correlation function for the first cluster and the $(p - p')$-point correlation function for the second cluster.

In particular, consider the three-point correlation function in the random composite, defined by

$$\{\boldsymbol{F}_3(\boldsymbol{z}_1, \boldsymbol{z}_2)\}_{a_1b_1a_2b_2a_3b_3} = \lim_{\lambda\to\infty} \frac{1}{\lambda^d|\Omega|} \int_{\lambda\Omega} d\boldsymbol{x} \{\delta \boldsymbol{L}(\boldsymbol{z}_1 + \boldsymbol{x})\}_{a_1b_1} \{\delta \boldsymbol{L}(\boldsymbol{z}_2 + \boldsymbol{x})\}_{a_2b_2} \{\delta \boldsymbol{L}(\boldsymbol{x})\}_{a_3b_3}, \tag{15.5}$$

in which $\lambda\Omega$ is a cube of side length λ centered at the origin (rather than a unit cell of periodicity). The absence of long-range correlations implies that

$$\begin{aligned}
&\{\boldsymbol{F}_3(\boldsymbol{z}_1, \boldsymbol{z}_2)\}_{a_1b_1a_2b_2a_3b_3} \\
&\quad \approx \{\boldsymbol{F}_1\}_{a_1b_1} \{\boldsymbol{F}_2(\boldsymbol{z}_2)\}_{a_2b_2a_3b_3} && \text{when } |\boldsymbol{z}_1| \text{ and } |\boldsymbol{z}_1 - \boldsymbol{z}_2| \gg \text{microstructure}, \\
&\quad \approx \{\boldsymbol{F}_1\}_{a_2b_2} \{\boldsymbol{F}_2(\boldsymbol{z}_1)\}_{a_1b_1a_3b_3} && \text{when } |\boldsymbol{z}_2| \text{ and } |\boldsymbol{z}_1 - \boldsymbol{z}_2| \gg \text{microstructure}, \\
&\quad \approx \{\boldsymbol{F}_1\}_{a_3b_3} \{\boldsymbol{F}_2(\boldsymbol{z}_1 - \boldsymbol{z}_2)\}_{a_1b_1a_2b_2} && \text{when } |\boldsymbol{z}_1| \text{ and } |\boldsymbol{z}_2| \gg \text{microstructure}, \\
&\quad \approx \{\boldsymbol{F}_1\}_{a_1b_1} \{\boldsymbol{F}_1\}_{a_2b_2} \{\boldsymbol{F}_1\}_{a_3b_3} && \text{when } |\boldsymbol{z}_1|,\ |\boldsymbol{z}_2|, \text{ and } |\boldsymbol{z}_1 - \boldsymbol{z}_2| \gg \text{microstructure},
\end{aligned} \tag{15.6}$$

in which $\boldsymbol{F}_1$ and $\boldsymbol{F}_2(\boldsymbol{z})$ are the one-point and two-point correlation functions in the random composite:

$$\begin{aligned}
\{\boldsymbol{F}_1\}_{ab} &= \lim_{\lambda\to\infty} \frac{1}{\lambda^d|\Omega|} \int_{\lambda\Omega} d\boldsymbol{x} \{\delta \boldsymbol{L}(\boldsymbol{x})\}_{ab}, \\
\{\boldsymbol{F}_2(\boldsymbol{z})\}_{a_1b_1a_2b_2} &= \lim_{\lambda\to\infty} \frac{1}{\lambda^d|\Omega|} \int_{\lambda\Omega} d\boldsymbol{x} \{\delta \boldsymbol{L}(\boldsymbol{z} + \boldsymbol{x})\}_{a_1b_1} \{\delta \boldsymbol{L}(\boldsymbol{x})\}_{a_2b_2}.
\end{aligned} \tag{15.7}$$

These correlation functions are of course no longer periodic in $\boldsymbol{z}_1$ and $\boldsymbol{z}_2$. The next step is to recognize that the effective tensor of a random composite is perturbed only slightly when the random composite is replaced by a periodic composite obtained by periodically extending a sufficiently large cubic sample. The dimensions of this cubic sample must of course be

much larger than the size of the microstructure of the random composite. Now consider, for example, the third-order term in the series expansion for this periodic material. Since the size of the period cell is much larger than the microstructure, the dominant contributions to the integrals in (15.3) come from points where we can use the approximations (15.6) to simplify the integrands.

For example, we have that

$$\begin{aligned}\frac{1}{|\Omega|}\int_\Omega d\boldsymbol{y}_1\{\boldsymbol{F}_3(\boldsymbol{y}_1+\boldsymbol{y}_2,\boldsymbol{y}_2)\}_{a_1b_1a_2b_2a_3b_3} &\approx \frac{1}{|\Omega|}\int_\Omega d\boldsymbol{y}_1\{\boldsymbol{F}_1\}_{a_1b_1}\{\boldsymbol{F}_2(\boldsymbol{y}_2)\}_{a_2b_2a_3b_3}\\ &\approx \{\boldsymbol{F}_1\}_{a_1b_1}\{\boldsymbol{F}_2(\boldsymbol{y}_2)\}_{a_2b_2a_3b_3},\end{aligned}$$

with this approximation becoming increasingly accurate as the size of the cubic sample is increased, where $\boldsymbol{F}_3(\boldsymbol{z}_1,\boldsymbol{z}_2)$, $\boldsymbol{F}_2(\boldsymbol{z})$, and $\boldsymbol{F}_1$ are the correlation functions of the periodic material. When $\boldsymbol{z}_1$, $\boldsymbol{z}_2$, and $\boldsymbol{z}$ all lie within the unit cell, these are approximately the same as the correlation functions in the random composite. Consequently, for $\boldsymbol{z}_1$ and $\boldsymbol{z}_2$ within the unit cell, the correlation function $\boldsymbol{F}'(\boldsymbol{z}_1,\boldsymbol{z}_2)$ of the periodic material will be negligible whenever $|\boldsymbol{z}_1|$ or $|\boldsymbol{z}_2|$ is much larger than the microstructure. In other words, the correlation function differs significantly from zero only when both $\boldsymbol{z}_1$ and $\boldsymbol{z}_2$ lie within a relatively small region of the unit cell (and in those regions periodically displaced from this region). This region becomes increasingly more localized in comparison with the size of the unit cell when we take successively larger cubic samples of the random composite. Since the tensor field $\boldsymbol{L}(\boldsymbol{x})$ is bounded for all $\boldsymbol{x}$, the correlation function is also bounded and it follows that the contribution to the integral (15.4) comes almost entirely from points $\boldsymbol{z}_1$ and $\boldsymbol{z}_2$ within the unit cell, and in fact comes predominantly from points $\boldsymbol{z}_1$ and $\boldsymbol{z}_2$ close to the origin.

Hence the integral (15.4) is perturbed only slightly if we make the second step of replacing the correlation function in the periodic composite by the associated correlation function in the original random composite, namely,

$$\begin{aligned}\{\boldsymbol{F}'_3(\boldsymbol{y}_1+\boldsymbol{y}_2,\boldsymbol{y}_2)\}_{a_1b_1a_2b_2a_3b_3} &= \{\boldsymbol{F}_3(\boldsymbol{y}_1+\boldsymbol{y}_2,\boldsymbol{y}_2)\}_{a_1b_1a_2b_2a_3b_3}\\ &\quad -\{\boldsymbol{F}_1\}_{a_1b_1}\{\boldsymbol{F}_2(\boldsymbol{y}_2)\}_{a_2b_2a_3b_3}-\{\boldsymbol{F}_2(\boldsymbol{y}_1)\}_{a_1b_1a_2b_2}\{\boldsymbol{F}_1\}_{a_3b_3}+\{\boldsymbol{F}_1\}_{a_1b_1}\{\boldsymbol{F}_1\}_{a_2b_2}\{\boldsymbol{F}_1\}_{a_3b_3},\end{aligned} \tag{15.8}$$

in which $\boldsymbol{F}_3(\boldsymbol{z}_1,\boldsymbol{z}_2)$, $\boldsymbol{F}_2(\boldsymbol{z})$, and $\boldsymbol{F}_1$ are now the correlation functions in the random composite, as defined by (15.5) and (15.7). The error incurred in each step in this argument becomes negligible in the limit in which the size of the cubic sample tends to infinity. It follows that the final expression for $\delta\boldsymbol{L}^{(3)}_*$, given by substituting (15.8) into (15.4), provides an exact formula for the third-order term in the series expansion in the random composite. This formula simplifies if we choose a reference tensor $\boldsymbol{L}_0=\langle\boldsymbol{L}\rangle$. Then $\boldsymbol{F}_1=0$ and as a consequence $\boldsymbol{F}'_3(\boldsymbol{z}_1,\boldsymbol{z}_2)$ can be identified with $\boldsymbol{F}_3(\boldsymbol{z}_1,\boldsymbol{z}_2)$.

In a two-phase random composite there are many natural choices for the reference tensor $\boldsymbol{L}_0$, such as $\boldsymbol{L}_0=\boldsymbol{L}_1$, $\boldsymbol{L}_0=\boldsymbol{L}_2$, $\boldsymbol{L}_0=\langle\boldsymbol{L}\rangle$, and $\boldsymbol{L}_0=(\boldsymbol{L}_1+\boldsymbol{L}_2)/2$. To simplify the series expansion let us make the choice $\boldsymbol{L}_0=\boldsymbol{L}_2$. Then we have

$$\delta\boldsymbol{L}(\boldsymbol{x})=\chi_1(\boldsymbol{x})(\boldsymbol{L}_1-\boldsymbol{L}_2),$$

which when substituted in (15.5) and (15.7) gives correlation functions

$$\{\boldsymbol{F}_3(\boldsymbol{z}_1,\boldsymbol{z}_2)\}_{a_1b_1a_2b_2a_3b_3}=f_{111}(\boldsymbol{z}_1,\boldsymbol{z}_2)\{\boldsymbol{L}_1-\boldsymbol{L}_2\}_{a_1b_1}\{\boldsymbol{L}_1-\boldsymbol{L}_2\}_{a_2b_2}\{\boldsymbol{L}_1-\boldsymbol{L}_2\}_{a_3b_3},$$

$$\{\boldsymbol{F}_2(\boldsymbol{z})\}_{a_1b_1a_2b_2} = f_{11}(\boldsymbol{z})\{\boldsymbol{L}_1 - \boldsymbol{L}_2\}_{a_1b_1}\{\boldsymbol{L}_1 - \boldsymbol{L}_2\}_{a_2b_2},$$

$$\{\boldsymbol{F}_1\}_{ab} = f_1\{\boldsymbol{L}_1 - \boldsymbol{L}_2\}_{ab}, \tag{15.9}$$

where f_1, $f_{11}(\boldsymbol{z})$, and $f_{111}(\boldsymbol{z}_1, \boldsymbol{z}_2)$ are the scalar-valued correlation functions

$$\begin{aligned} f_1 &= \lim_{\lambda\to\infty} \frac{1}{\lambda^d|\Omega|}\int_{\lambda\Omega} d\boldsymbol{x}\ \chi_1(\boldsymbol{x}), \\ f_{11}(\boldsymbol{z}) &= \lim_{\lambda\to\infty} \frac{1}{\lambda^d|\Omega|}\int_{\lambda\Omega} d\boldsymbol{x}\ \chi_1(\boldsymbol{z}+\boldsymbol{x})\chi_1(\boldsymbol{x}), \\ f_{111}(\boldsymbol{z}_1, \boldsymbol{z}_2) &= \lim_{\lambda\to\infty} \frac{1}{\lambda^d|\Omega|}\int_{\lambda\Omega} d\boldsymbol{x}\ \chi_1(\boldsymbol{z}_1+\boldsymbol{x})\chi_1(\boldsymbol{z}_2+\boldsymbol{x})\chi_1(\boldsymbol{x}), \end{aligned} \tag{15.10}$$

associated with the characteristic function $\chi_1(\boldsymbol{x})$. By changing the variable of integration from $\boldsymbol{x}$ to $\boldsymbol{x}' = \boldsymbol{z} + \boldsymbol{x}$ in the definition of $f_{11}(\boldsymbol{z})$ and from $\boldsymbol{x}$ to $\boldsymbol{x}' = \boldsymbol{z}_1 + \boldsymbol{x}$ or $\boldsymbol{x}' = \boldsymbol{z}_2 + \boldsymbol{x}$ in the definition of $f_{111}(\boldsymbol{z}_1, \boldsymbol{z}_2)$, one sees that these correlation functions have the symmetry properties

$$\begin{aligned} f_{11}(\boldsymbol{z}) &= f_{11}(-\boldsymbol{z}), \\ f_{111}(\boldsymbol{z}_1, \boldsymbol{z}_2) &= f_{111}(\boldsymbol{z}_2, \boldsymbol{z}_1) = f_{111}(\boldsymbol{z}_2 - \boldsymbol{z}_1, -\boldsymbol{z}_1) = f_{111}(\boldsymbol{z}_1 - \boldsymbol{z}_2, -\boldsymbol{z}_2). \end{aligned} \tag{15.11}$$

The correlation functions have a simple geometrical interpretation that is evident from their definitions (15.10). The one-point correlation function f_1 is simply the probability that a point lands in phase 1 when it is dropped randomly in the composite: It is the volume fraction of phase 1. The two-point correlation function $f_{11}(\boldsymbol{z})$ is the probability that a rod, with endpoints at the origin and at $\boldsymbol{z}$, lands with both endpoints in phase 1 when it is translated and dropped at a random position in the composite. Similarly, the three-point correlation function $f_{111}(\boldsymbol{z}_1, \boldsymbol{z}_2)$ is the probability that a triangle with vertices at the origin and at the points $\boldsymbol{z}_1$ and $\boldsymbol{z}_2$ lands with all three vertices in phase 1 when it is translated and dropped randomly in the composite. Thus the value of the correlation function for triangles or rods lying within a given plane can be determined by taking a cross section of the composite geometry in that plane and randomly dropping rods or triangles in it to see what proportion land with all their vertices in phase 1. In other words, the one-point, two-point, and three-point correlation functions can be determined from cross-sectional photographs. If the geometry of the composite is statistically isotropic, so that the cross-sectional statistics are independent of the orientation and positioning of the cross section, then it suffices to take a single cross-sectional photograph. By this means Berryman (1988) has developed image processing techniques to determine the one-point, two-point and three-point correlation functions from photographs of the composite microstructure.

For dilute suspensions of spheres Weissberg and Prager (1962) obtained approximate expressions for these correlation functions. For nondilute suspensions of spheres Torquato and Stell (1982) have derived a formula giving the n-point correlation function in terms of the correlation functions characterizing the distribution of sphere centers. For suspensions of possibly nonspherical inclusions of phase 1 in a matrix of phase 2, a triangle with all vertices in phase 1 may have all vertices lying within a single inclusion, or two vertices in one inclusion and the third in a second inclusion, or three vertices in three different inclusions. Accordingly, as Gillette and McCoy (1986) show [see also McPhedran and Milton (1981)],

there is a decomposition of $f_{111}(\boldsymbol{z}_1, \boldsymbol{z}_2)$ [and similarly $f_{11}(\boldsymbol{z})$] into correlation functions depending on these different possibilities. The single inclusion probabilities that all points lie within a specific inclusion given that a particular point lies within that inclusion can be expressed in terms of certain areas of intersection for the two-dimensional problem and volumes of intersection for the three-dimensional problem (Gillette and McCoy 1986, 1987). For polycrystalline materials the evaluation of the three-point correlations requires one to know the crystal orientation at each point in the cross-sectional photograph. Adams, Wright, and Kunze (1993) have developed an experimental technique for accurately obtaining maps of the cross-sectional crystal orientation. See also Etinghof and Adams (1993), who show how polycrystalline correlation functions can be represented concisely using symmetry considerations and group theory.

The four-point correlation function cannot be determined from a single cross-sectional photograph, since four points typically do not lie within a plane. For this reason, the experimental measurement of four-point correlation functions is difficult, and this usually prohibits the evaluation of the terms in the series expansion beyond the third order in real three-dimensional composites.

By substituting the formulas (15.9) back into (15.8) we see that

$$\begin{aligned}\{\boldsymbol{F}_3'(\boldsymbol{y}_1 + \boldsymbol{y}_2, \boldsymbol{y}_2)\}_{a_1b_1a_2b_2a_3b_3} = &\Big[f_{111}(\boldsymbol{y}_1 + \boldsymbol{y}_2, \boldsymbol{y}_2) - f_1\Big(f_{11}(\boldsymbol{y}_1) + f_{11}(\boldsymbol{y}_2)\Big) + f_1^3\Big] \\ &\times\{\boldsymbol{L}_1 - \boldsymbol{L}_2\}_{a_1b_1}\{\boldsymbol{L}_1 - \boldsymbol{L}_2\}_{a_2b_2}\{\boldsymbol{L}_1 - \boldsymbol{L}_2\}_{a_3b_3},\end{aligned} \tag{15.12}$$

which when inserted into (15.4) gives an expression for the third-order term in the series expansion in terms of integrals that involve the correlation functions f_1, $f_{11}(\boldsymbol{z})$, and $f_{111}(\boldsymbol{z}_1, \boldsymbol{z}_2)$. The usual care is required when evaluating these integrals because of the singularity of $\boldsymbol{\Gamma}_\infty(\boldsymbol{y})$ at $\boldsymbol{y} = 0$. This singularity must be treated in the manner discussed in section 12.6 on page 257. There are no convergence problems at large values of $\boldsymbol{y}_1$ and $\boldsymbol{y}_2$ since the absence of long-range correlations ensures that $\boldsymbol{F}_3'(\boldsymbol{y}_1 + \boldsymbol{y}_2, \boldsymbol{y}_2)$ approaches zero when either $|\boldsymbol{y}_1| \to \infty$ or $|\boldsymbol{y}_2| \to \infty$.

We can also introduce correlation functions f_2, $f_{22}(\boldsymbol{z})$, and $f_{222}(\boldsymbol{z}_1, \boldsymbol{z}_2)$ associated with the characteristic function $\chi_2(\boldsymbol{x}) = 1 - \chi_1(\boldsymbol{x})$. These are easily expressed in terms of the correlation functions f_1, $f_{11}(\boldsymbol{z})$, and $f_{111}(\boldsymbol{z}_1, \boldsymbol{z}_2)$. Indeed, by replacing $\chi_1(\boldsymbol{x})$ by $1 - \chi_1(\boldsymbol{x})$ in (15.10) and expanding the expressions we see that

$$\begin{aligned} f_2 &= 1 - f_1, \qquad f_{22}(\boldsymbol{z}) = 1 - 2f_1 + f_{11}(\boldsymbol{z}), \\ f_{222}(\boldsymbol{z}_1, \boldsymbol{z}_2) &= 1 - 3f_1 + f_{11}(\boldsymbol{z}_1) + f_{11}(\boldsymbol{z}_2) + f_{11}(\boldsymbol{z}_1 - \boldsymbol{z}_2) - f_{111}(\boldsymbol{z}_1, \boldsymbol{z}_2).\end{aligned}$$

There are also mixed correlation functions, such as the correlation function

$$f_{12}(\boldsymbol{z}) = \lim_{\lambda\to\infty} \frac{1}{\lambda^d|\Omega|}\int_{\lambda\Omega} d\boldsymbol{x}\ \chi_1(\boldsymbol{z} + \boldsymbol{x})\chi_2(\boldsymbol{x}) = f_1 - f_{11}(\boldsymbol{z}),$$

giving the probability that a rod with endpoints at the origin and at $\boldsymbol{z}$ lands with these endpoints in phase 2 and phase 1, respectively, when it is translated and dropped at a random position in the composite. When the rod is sufficiently short, relative to the microstructure, the only way that this can happen is if the rod straddles the interface between the two phases. The probability of this happening, averaged over all orientations of the rod, should be proportional to the specific surface area A of the interface. (The specific area is the internal surface area per

unit volume.) The precise result, derived by Debye, Anderson, Jr., and Brumberger (1957) for isotropic composites and generalized to anisotropic composites by Berryman (1987), is that

$$A = \lim_{r\to 0} \frac{4\langle f_{12}(r\boldsymbol{n})\rangle_{\boldsymbol{n}}}{r} = \lim_{r\to 0} -4\frac{d\langle f_{11}(r\boldsymbol{n})\rangle_{\boldsymbol{n}}}{dr},$$

where the averages $\langle\cdot\rangle_{\boldsymbol{n}}$ are over all orientations of the unit vector $\boldsymbol{n}$.

15.3. Correlation functions for penetrable spheres

To give some insight into the nature of these correlation functions, let us look at a specific example, for which the correlation functions take a particularly simple form. In a footnote, Weissberg (1963) attributes this model to W. F. Brown. The composite is constructed as follows. First we take a large cubic region and successively drop seed points into it in a random fashion, so that each successive seed point is equally likely to land anywhere in the cubic region, irrespective of where the previous points are positioned. This is continued until the desired density of points is reached. Taking the limit in which the size of the cubic region goes to infinity gives us a distribution of seed points known as a Poisson-point distribution. Then spheres of, say, uniform radius r are inscribed around each of these seed points and phase 2 is taken to be the union of these spherical regions, while phase 1 is taken to be the remaining region. Thus phase 1 consists of all points that are at least a distance r away from the seed points.

Let us suppose that λ represents the average density of seed points per unit volume, and let us ask the question: Given a region V with volume $|V|$, what is the probability $P(V)$ that V does not contain any seed points? To answer this, let us enlarge the region V to $V \cup \delta V$ by adding a region δV with infinitesimal volume $|\delta V|$ such that $V \cap \delta V = 0$. Since the probability that the region V is devoid of points is independent of whether the region δV contains any points or not, it follows that

$$P(V \cup \delta V) = P(V)P(\delta V) = P(V)(1 - \lambda|\delta V|).$$

By integrating this equation, and noting that $P(V) = 0$ when $|V| = 0$, we deduce that

$$P(V) = e^{-\lambda|V|}.$$

Now let us consider any correlation function, say the three-point correlation function $f_{111}(\boldsymbol{z}_1, \boldsymbol{z}_2)$. It is the probability that the origin and the points $\boldsymbol{z}_1$ and $\boldsymbol{z}_2$ all lie in phase 1 when a triangle with vertices at these points is thrown randomly into the composite. In the context of the model it is the probability that the region $V_r(\boldsymbol{z}_1, \boldsymbol{z}_2)$, consisting of the union of three spheres of radius r centered, respectively, at the origin and at the points $\boldsymbol{z}_1$ and $\boldsymbol{z}_2$, does not contain any seed points. In other words, the three-point correlation function is

$$f_{111}(\boldsymbol{z}_1, \boldsymbol{z}_2) = P(V_r(\boldsymbol{z}_1, \boldsymbol{z}_2)) = e^{-\lambda|V_r(\boldsymbol{z}_1,\boldsymbol{z}_2)|}.$$

Weissberg and Prager (1962) give a formula for the total volume $|V_r(\boldsymbol{z}_1, \boldsymbol{z}_2)|$ occupied by three, possibly overlapping, spheres of radius r. More generally, the p-point correlation function $f_{11\ldots1}(\boldsymbol{z}_1, \boldsymbol{z}_2, \ldots \boldsymbol{z}_{p-1})$ is related in a similar fashion to the volume occupied by the union of p spheres of radius r centered at the points $0, \boldsymbol{z}_1, \boldsymbol{z}_2, \ldots \boldsymbol{z}_{p-1}$. Helte (1994) has derived an explicit formula for the volume occupied by the union of four spheres, and thereby

obtains the four-point correlation function. Specializing to the one-point correlation function, we obtain a formula for λ in terms of the volume fraction f_1:

$$\lambda = -\frac{\log(f_1)}{|V_r|},$$

where V_r is the volume occupied by a single sphere of radius r, which is of course $4\pi r^3/3$ when $d = 3$ and πr^2 when $d = 2$.

The penetrable sphere model can be generalized in various ways. The simplest generalization is to stretch the geometry by making an affine transformation. In this way one obtains a penetrable ellipse model where all of the ellipses are aligned. Alternatively, one can take the original Poisson distribution of seed points and place an inclusion at each seed point. This inclusion might be a sphere, ellipse, cylinder, plate, or some other shaped object such as a cube. The inclusion shape, size, orientation, and position relative to the seed point are selected randomly from a probability distribution that is uncorrelated with the position of the surrounding seed points and uncorrelated with the shapes, sizes, orientations, and positions of the surrounding inclusions. Phase 1 is then taken to be the region that is not occupied by any inclusion, while phase 2 consists of those points that lie in at least one inclusion. The calculation of the p-point correlation function then requires one to compute the total volume occupied by p possibly intersecting inclusions. For the two-dimensional penetrable disk model, Helsing (1998) has obtained accurate numerical results for the effective conductivity.

15.4. Correlation functions for cell materials

Another class of composites for which the correlation functions take a special form was introduced independently by Frisch (1965), Matheron (1968), and Miller (1969b), in varying degrees of generality. Miller called them "symmetric cell materials" and also introduced another class of materials, which he called "asymmetric cell materials." The existence of asymmetric cell materials was questioned by Brown (1974) and explored further by Hori (1975). Since their relevance is unclear, we will not discuss them. Accordingly we will refer to symmetric cell materials as simply cell materials.

A two-phase cell material is constructed as follows. The first step is to divide space into an infinite number of cells in a statistically homogeneous fashion. For example, one could divide space into a stack of irregularly spaced layers, or into a network of tubes, or into a periodic array of boxes. One can even divide space into a space-filling assemblage of spherical cells, with radii ranging to the infinitesimally small. The cells do not have to be finite in extent, nor of the same shape or topology. Each cell could even be a cluster of disconnected regions. But the division into cells does have to made in a statistically homogeneous fashion. The probability of finding a cell of a particular shape and size in a sufficiently large test region cannot depend on where that test region is positioned.

The second and key step is to randomly assign each cell as phase 1 or phase 2 in a way that is uncorrelated both with the shape of the cell and with the phases assigned to the surrounding cells. In other words, we could go around to each cell and flip a "loaded" coin that gives heads with probability f_1 and tails with probability $f_2 = 1 - f_1$: If the coin lands heads, then we assign the cell as phase 1; and if it lands tails, we assign it as phase 2. Ultimately this gives a two-phase cell material where phase 1 occupies a volume fraction f_1.

Now consider, for example, the three-point correlation function. Suppose that we take a triangle with vertices at the origin, $\boldsymbol{z}_1$ and $\boldsymbol{z}_2$, and place it a random position in the cell material. Now if $g_3(\boldsymbol{z}_1, \boldsymbol{z}_2)$ denotes the probability that all three vertices lie in the same cell,

then $f_1 g_3(\boldsymbol{z}_1, \boldsymbol{z}_2)$ is the probability that all three vertices lie in the same cell and that the cell is phase 1. Similarly, if $g_{1,2}(\boldsymbol{z}_1, \boldsymbol{z}_2)$ denotes the probability that any two of the three vertices lie in the same cell, while the remaining vertex lies in a different cell, then $f_1^2 g_{1,2}(\boldsymbol{z}_1, \boldsymbol{z}_2)$ is the probability that this holds and that both cells are phase 1. Finally, if $g_{1,1,1}(\boldsymbol{z}_1, \boldsymbol{z}_2)$ denotes the probability that the vertices lie in three different cells, then $f_1^3 g_{1,1,1}(\boldsymbol{z}_1, \boldsymbol{z}_2)$ is the probability that this holds and that all three cells are phase 1. Since one of these three possibilities necessarily occurs, it follows that

$$g_3(\boldsymbol{z}_1, \boldsymbol{z}_2) + g_{1,2}(\boldsymbol{z}_1, \boldsymbol{z}_2) + g_{1,1,1}(\boldsymbol{z}_1, \boldsymbol{z}_2) = 1,$$

and that

$$f_{111}(\boldsymbol{z}_1, \boldsymbol{z}_2) = f_1 g_3(\boldsymbol{z}_1, \boldsymbol{z}_2) + f_1^2 g_{1,2}(\boldsymbol{z}_1, \boldsymbol{z}_2) + f_1^3 g_{1,1,1}(\boldsymbol{z}_1, \boldsymbol{z}_2).$$

Since each of the three probabilities $g_3(\boldsymbol{z}_1, \boldsymbol{z}_2)$, $g_{1,2}(\boldsymbol{z}_1, \boldsymbol{z}_2)$, and $g_{1,1,1}(\boldsymbol{z}_1, \boldsymbol{z}_2)$ do not depend on f_1, we conclude that $f_{111}(\boldsymbol{z}_1, \boldsymbol{z}_2)$ has a polynomial dependence on f_1 of degree 3. More generally, it is evident from this reasoning that the p-point correlation function $f_{11\ldots1}(\boldsymbol{z}_1, \boldsymbol{z}_2, \ldots, \boldsymbol{z}_{p-1})$ has a polynomial dependence on f_1 of degree p with no constant term. Provided that the reference tensor $\boldsymbol{L}_0$ is chosen independent of f_1, we conclude that the p-th–order term in the series expansion has a polynomial dependence on f_1 of degree p. In light of this, it is natural to take $\boldsymbol{L}_0 = (\boldsymbol{L}_1 + \boldsymbol{L}_2)/2$ as a reference tensor, since this tensor does not depend on f_1 and remains unchanged when $\boldsymbol{L}_1$ and $\boldsymbol{L}_2$ are swapped, reflecting the symmetry between the two phases in the cell material. Then the p-th–order term in the series expansion for $\boldsymbol{L}_* - \langle \boldsymbol{L} \rangle$ has a polynomial dependence on f_1 of degree p. Furthermore, this polynomial can have no constant term because $\boldsymbol{L}_* - \langle \boldsymbol{L} \rangle$ is zero to all orders in $\delta \boldsymbol{L}$ when $f_1 = 0$. Consequently, the polynomial can be factored into f_1 times a polynomial of degree $p - 1$.

There is one other important consideration: Since both phases are treated on an equal basis (aside from the assigning of different probabilities f_1 and f_2 for a cell to be of phase 1 or phase 2) it follows that the effective tensor $\boldsymbol{L}_*$ should remain unchanged if the tensors $\boldsymbol{L}_1$ and $\boldsymbol{L}_2$ are interchanged and at the same time the volume fractions f_1 and f_2 are swapped. Consequently, with the choice $\boldsymbol{L}_0 = (\boldsymbol{L}_1 + \boldsymbol{L}_2)/2$ of reference tensor the p-th–order term in the perturbation expansion must be an even polynomial function of $f_1 - f_2$ when p is even (since this term is an even function of $\boldsymbol{L}_1 - \boldsymbol{L}_2$) and it must be an odd polynomial function of $f_1 - f_2$ when p is odd (since then the term is an odd function of $\boldsymbol{L}_1 - \boldsymbol{L}_2$). Moreover, because f_1 is a factor of these polynomials, it follows that f_2 must likewise be a factor. So each polynomial must be divisible by $f_1 f_2 = [1 - (f_1 - f_2)^2]/4$. These considerations imply that the effective tensor to, say, the fifth order in perturbation has an expansion of the form

$$\begin{aligned}
\{\boldsymbol{L}_*\}_{ab} \;=\; & \{f_1 \boldsymbol{L}_1 + f_2 \boldsymbol{L}_2\}_{ab} + f_1 f_2 A_{b_1 a_2} \ell_{ab_1} \ell_{a_2 b} + f_1 f_2 (f_1 - f_2) B_{b_1 a_2 b_2 a_3} \ell_{ab_1} \ell_{a_2 b_2} \ell_{a_3 b} \\
& + f_1 f_2 [C_{b_1 a_2 b_2 a_3 b_3 a_4} + (f_1 - f_2)^2 C'_{b_1 a_2 b_2 a_3 b_3 a_4}] \ell_{ab_1} \ell_{a_2 b_2} \ell_{a_3 b_3} \ell_{a_4 b} \\
& + f_1 f_2 (f_1 - f_2) [D_{b_1 a_2 b_2 a_3 b_3 a_4 b_4 a_5} + (f_1 - f_2)^2 D'_{b_1 a_2 b_2 a_3 b_3 a_4 b_4 a_5}] \ell_{ab_1} \ell_{a_2 b_2} \ell_{a_3 b_3} \ell_{a_4 b_4} \ell_{a_5 b} \\
& + \cdots,
\end{aligned} \tag{15.13}$$

in which the ℓ_{ij} denote the matrix elements $\ell_{ij} = \{\boldsymbol{L}_1 - \boldsymbol{L}_2\}_{ij}$ and the tensors $\boldsymbol{A}$, $\boldsymbol{B}$, $\boldsymbol{C}$, $\boldsymbol{C}'$, $\boldsymbol{D}$, and $\boldsymbol{D}'$ depend only on the reference tensor $\boldsymbol{L}_0 = (\boldsymbol{L}_1 + \boldsymbol{L}_2)/2$ and on the geometrical configuration of the cells.

Since the terms in the series expansion have such a simple dependence on f_1, we can determine the coefficients $\boldsymbol{A}$, $\boldsymbol{B}$, $\boldsymbol{C} + \boldsymbol{C}'$, and $\boldsymbol{D} + \boldsymbol{D}'$ once we know the effective tensor $\boldsymbol{L}_*$

to the first order in the volume fraction f_1. Since these combinations of parameters depend only on the polarizability of individual cells, and thus on the cell shape, they are called cell shape parameters or simply shape factors. We can determine the remaining coefficients in the fifth-order expansion once we know the effective tensor to the second order in the volume fraction. These remaining parameters typically depend on both the cell shape and on how they are packed together.

For a macroscopically isotropic cell material of two isotropic phases with conductivities $\sigma_1\boldsymbol{I}$ and $\sigma_2\boldsymbol{I}$ and effective conductivity $\sigma_*\boldsymbol{I}$ the above expansion reduces to

$$\begin{aligned}\sigma_* = {} & f_1\sigma_1 + f_2\sigma_2 + f_1f_2a\delta_\sigma^2/\overline{\sigma} + f_1f_2(f_1-f_2)b\delta_\sigma^3/\overline{\sigma}^2 \\ & + f_1f_2[c + (f_1-f_2)^2c']\delta_\sigma^4/\overline{\sigma}^3 + f_1f_2(f_1-f_2)[d + (f_1-f_2)^2d']\delta_\sigma^5/\overline{\sigma}^4 + \cdots,\end{aligned}$$

where $\delta_\sigma = \sigma_1 - \sigma_2$ and $\overline{\sigma} = (\sigma_1+\sigma_2)/2$. The six parameters a, b, c, c', d, and d' depend only on the geometrical configuration of the cells. From the second-order series expansion (14.12) we see that $a = -1/3$. Thus only five parameters depend on the cell configuration. An equivalent fifth-order expansion in terms of five parameters was obtained by Elsayed (1974). For two-dimensional cell materials (which have $a = -1/2$) the analogous fifth-order expansion in terms of five parameters was derived by Elsayed and McCoy (1973); see also Milton (1982), where it is shown that Keller's relation (3.6) implies that c and c' can be expressed in terms of b. A similar result for random resistor networks was obtained by Bruno and Golden (1990), who moreover proved that σ_* is an analytic function of $f_1 = 1 - f_2$ in a suitable domain containing the interval [0, 1].

The general polynomial dependence of the coefficients on the volume fraction was established by Bruno (1990) by regarding them as infinitely interchangeable materials. Instead of considering correlation functions Bruno realized that a two-phase cell material with conductivities σ_1 and σ_2 and $f_1 = p/q$ being rational could be regarded as a q-phase cell material with each phase occupying a volume fraction $1/q$ and with p of the phases having conductivity σ_1 and the remaining $q - p$ phases having conductivity σ_2. The effective conductivity of the q-phase cell material is symmetric with respect to the interchange of any pair of the q-phases. Bruno shows that this interchangeability, in the limit $q \to \infty$, implies the polynomial dependence of the coefficients on the volume fraction. Using this Bruno and Golden (1990) proved that for fixed positive real σ_1 and σ_2 the effective conductivity is an analytic function of f_1 in a suitable domain containing the interval [0, 1]. Avellaneda and Bruno (1990) extended the interchangeability argument to cell polycrystals, that is, cell materials where each cell is filled by a crystallite whose orientation is independent of the cell shape and the orientation of neighboring crystallites.

The concept of a cell material can easily be extended to encompass multiphase composites that are possibly polycrystalline. The tensor field $\boldsymbol{L}(\boldsymbol{x})$ is taken to be constant within each cell, with a value $\boldsymbol{M}$ in each cell that is selected from some probability distribution. Specifically, let us suppose that there exists a positive measure $\mu(\boldsymbol{M})$ on the space of tensors such that

$$P(\Theta) = \int_\Theta d\mu(\boldsymbol{M}) \tag{15.14}$$

gives the probability that the tensor $\boldsymbol{M}$ assigned to given cell takes a value in the set Θ. The definition of a cell material requires that this probability be uncorrelated with the cell shape and with the moduli assigned to surrounding cells. To compute the correlation functions it is convenient to consider a configuration of points in a given position relative to the cell geometry and to ensemble average over the possible moduli that these cells can take. The

result of this ensemble average depends only on the grouping of the points relative to the cells, that is, on which sets of points occupy the same cell. Next the configuration of points is translated to a new position and the same ensemble average is performed. Finally, a volume average is performed over all of these translates.

The analysis is simplest when we choose a reference medium

$$\boldsymbol{L}_0 = \langle \boldsymbol{L} \rangle = \int d\mu(\boldsymbol{M}) \boldsymbol{M}.$$

Then, for example, the ensemble average of $\{\delta \boldsymbol{L}(\boldsymbol{x}_1)\}_{a_1 b_1} \{\delta \boldsymbol{L}(\boldsymbol{x}_2)\}_{a_2 b_2} \{\delta \boldsymbol{L}(\boldsymbol{x}_3)\}_{a_3 b_3}$ will be zero unless all three points $\boldsymbol{x}_1$, $\boldsymbol{x}_2$, and $\boldsymbol{x}_3$ lie within the same cell. This reasoning shows that the effective tensor to the third order in perturbation depends on the distribution $\mu(\boldsymbol{M})$, on the probability $g_2(\boldsymbol{y})$ that a rod with endpoints at the origin and at $\boldsymbol{y}$ lands with both endpoints in a single cell when translated to a random position in the composite, and on the probability $g_3(\boldsymbol{z}_1, \boldsymbol{z}_2)$ that a triangle with vertices at the origin and at $\boldsymbol{z}_1$ and at $\boldsymbol{z}_2$ lands with all vertices in a single cell.

Specifically, to the third order, we have

$$\begin{aligned} \{\boldsymbol{L}_*\}_{ab} = \{\langle \boldsymbol{L} \rangle\}_{ab} - \left[\int_{\mathbb{R}^d} d\boldsymbol{y}\, g_2(\boldsymbol{y}) \{\boldsymbol{\Gamma}_\infty(\boldsymbol{y})\}_{b_1 a_2} \right] \{\boldsymbol{W}_2\}_{a b_1 a_2 b} \\ + \left[\int_{\mathbb{R}^d} d\boldsymbol{y}_2 \int_{\mathbb{R}^d} d\boldsymbol{y}_1\, g_3(\boldsymbol{y}_1 + \boldsymbol{y}_2, \boldsymbol{y}_2) \{\boldsymbol{\Gamma}_\infty(\boldsymbol{y}_1)\}_{b_1 a_2} \{\boldsymbol{\Gamma}_\infty(\boldsymbol{y}_2)\}_{b_2 a_3} \right] \{\boldsymbol{W}_3\}_{a b_1 a_2 b_2 a_3 b} + \cdots, \end{aligned} \tag{15.15}$$

in which $\boldsymbol{W}_2$ and $\boldsymbol{W}_3$ are tensors representing the second and third moments of the distribution when it is centered at $\boldsymbol{L}_0$:

$$\begin{aligned} \{\boldsymbol{W}_2\}_{a_1 b_1 a_2 b_2} &= \int d\mu(\boldsymbol{M})\, \{\boldsymbol{M} - \boldsymbol{L}_0\}_{a_1 b_1} \{\boldsymbol{M} - \boldsymbol{L}_0\}_{a_2 b_2} \\ &= \int d\mu(\boldsymbol{M}' + \boldsymbol{L}_0)\, M'_{a_1 b_1} M'_{a_2 b_2}, \\ \{\boldsymbol{W}_3\}_{a_1 b_1 a_2 b_2 a_3 b_3} &= \int d\mu(\boldsymbol{M})\, \{\boldsymbol{M} - \boldsymbol{L}_0\}_{a_1 b_1} \{\boldsymbol{M} - \boldsymbol{L}_0\}_{a_2 b_2} \{\boldsymbol{M} - \boldsymbol{L}_0\}_{a_3 b_3} \\ &= \int d\mu(\boldsymbol{M}' + \boldsymbol{L}_0)\, M'_{a_1 b_1} M'_{a_2 b_2} M'_{a_3 b_3}, \end{aligned} \tag{15.16}$$

in which the M'_{ij} are the matrix elements of $\boldsymbol{M}' = \boldsymbol{M} - \boldsymbol{L}_0$.

To calculate $g_2(\boldsymbol{y})$ [or $g_3(\boldsymbol{z}_1, \boldsymbol{z}_2)$] it is helpful to first determine the probability that both endpoints of the rod [all vertices of the triangle] all lie within a specific cell given that a particular endpoint [vertex] lies within that cell. Gillette and McCoy (1986, 1987) show how these probabilities can be calculated in terms of certain areas of intersection for the two-dimensional problem and volumes of intersection for the three-dimensional problem. By averaging these probabilities over all cells one obtains $g_2(\boldsymbol{y})$ and $g_3(\boldsymbol{z}_1, \boldsymbol{z}_2)$.

15.5. Reduced correlation functions

A quick examination of (15.1) shows that we can compute the third-order term in the series expansion once we know the function

$$\{\boldsymbol{G}(\boldsymbol{x}_1, \boldsymbol{x}_2, \boldsymbol{x}_3)\}_{a_1 b_1 a_2 b_2 a_3 b_3} = \{\delta \boldsymbol{L}(\boldsymbol{x}_1)\}_{a_1 b_1} \{\delta \boldsymbol{L}(\boldsymbol{x}_2)\}_{a_2 b_2} \{\delta \boldsymbol{L}(\boldsymbol{x}_3)\}_{a_3 b_3}.$$

This function contains a tremendous amount of information, not all of which is relevant to the determination of the third-order term. Indeed, we saw that the third-order term depends only on the three-point correlation function $\boldsymbol{F}'(\boldsymbol{z}_1, \boldsymbol{z}_2)$. This reduction from a function of three variables to a function of two variables of information is possible because the periodic Green's function $\boldsymbol{\Gamma}_\Omega(\boldsymbol{x}, \boldsymbol{x}') = \boldsymbol{\Gamma}_\Omega(\boldsymbol{x} - \boldsymbol{x}')$ remains invariant under translation, that is, it remains unchanged if we shift $\boldsymbol{x}$ and $\boldsymbol{x}'$ to $\boldsymbol{x}+\boldsymbol{a}$ and $\boldsymbol{x}'+\boldsymbol{a}$. A further reduction of information can be achieved by using another invariance property, namely, the invariance of $|\boldsymbol{y}|^d \boldsymbol{\Gamma}_\infty(\boldsymbol{y})$, under a change of scale from $\boldsymbol{y}$ to $\lambda \boldsymbol{y}$. This reduction can be made without specifying the problem under consideration, that is, without specifying $\boldsymbol{\Gamma}_\infty(\boldsymbol{y})$. The scale invariance reflects the fact that the effective tensor remains unchanged if we rescale the geometry of our composite material. Consequently, it makes sense to introduce a set of correlation functions that also remain invariant when we rescale the geometry. Although simply stated, this task requires some care.

Let us examine expression (15.4) for the third-order term in the series expansion. Rewriting it in a form that removes the conditional convergence gives

$$
\begin{aligned}
\{\delta \boldsymbol{L}_*^{(3)}\}_{a_1 b_3} &= \{\boldsymbol{F}'_3(0,0)\}_{a_1 b_1 a_2 b_2 a_3 b_3} \gamma_{b_1 a_2} \gamma_{b_2 a_3} \\
&+ \int_{\mathbb{R}^d} d\boldsymbol{y}_1 \{\boldsymbol{F}'_3(\boldsymbol{y}_1, 0) - \boldsymbol{Q}(|\boldsymbol{y}_1|)\}_{a_1 b_1 a_2 b_2 a_3 b_3} \{\boldsymbol{\Gamma}_\infty(\boldsymbol{y}_1)\}_{b_1 a_2} \gamma_{b_2 a_3} \\
&+ \int_{\mathbb{R}^d} d\boldsymbol{y}_2 \{\boldsymbol{F}'_3(\boldsymbol{y}_2, \boldsymbol{y}_2) - \boldsymbol{Q}'(|\boldsymbol{y}_2|)\}_{a_1 b_1 a_2 b_2 a_3 b_3} \{\boldsymbol{\Gamma}_\infty(\boldsymbol{y}_2)\}_{b_2 a_3} \gamma_{b_1 a_2} \\
&+ \int_{\mathbb{R}^d} d\boldsymbol{y}_2 \int_{\boldsymbol{R}^d} d\boldsymbol{y}_1 \{\boldsymbol{F}'_3(\boldsymbol{y}_1 + \boldsymbol{y}_2, \boldsymbol{y}_2) - \boldsymbol{Q}(|\boldsymbol{y}_1|, \boldsymbol{y}_2) - \boldsymbol{Q}'(|\boldsymbol{y}_2|, \boldsymbol{y}_1)\}_{a_1 b_1 a_2 b_2 a_3 b_3} \\
&\qquad \times \{\boldsymbol{\Gamma}_\infty(\boldsymbol{y}_1)\}_{b_1 a_2} \{\boldsymbol{\Gamma}_\infty(\boldsymbol{y}_2)\}_{b_2 a_3},
\end{aligned}
\tag{15.17}
$$

in which the γ_{ij} denote the matrix elements of the tensor $\boldsymbol{\gamma}$ defined by (12.35) and $\boldsymbol{Q}(r)$, $\boldsymbol{Q}'(r)$, $\boldsymbol{Q}(r, \boldsymbol{y})$, and $\boldsymbol{Q}'(r, \boldsymbol{y})$ are normalizing functions chosen so that the above integrals are absolutely convergent: This requires that they approach zero when either r or $|\boldsymbol{y}|$ goes to infinity and that they satisfy

$$
\begin{aligned}
\boldsymbol{Q}(0) = \boldsymbol{Q}'(0) &= \boldsymbol{F}'_3(0,0), \\
\boldsymbol{Q}(0, \boldsymbol{y}_2) + \boldsymbol{Q}'(|\boldsymbol{y}_2|, 0) &= \boldsymbol{F}'_3(\boldsymbol{y}_2, \boldsymbol{y}_2), \\
\boldsymbol{Q}(|\boldsymbol{y}_1|, 0) + \boldsymbol{Q}'(0, \boldsymbol{y}_1) &= \boldsymbol{F}'_3(\boldsymbol{y}_1, 0).
\end{aligned}
$$

For example, we could take

$$
\begin{aligned}
\boldsymbol{Q}(r) = \boldsymbol{Q}'(r) &= e^{-\alpha r^2} \boldsymbol{F}'_3(0,0), \\
\boldsymbol{Q}(|\boldsymbol{y}_1|, \boldsymbol{y}_2) + \boldsymbol{Q}'(|\boldsymbol{y}_2|, \boldsymbol{y}_1) &= e^{-\alpha |\boldsymbol{y}_1|^2} \boldsymbol{F}'_3(\boldsymbol{y}_2, \boldsymbol{y}_2) + e^{-\alpha |\boldsymbol{y}_2|^2} \boldsymbol{F}'_3(\boldsymbol{y}_1, 0) \\
&\quad - e^{-\alpha (|\boldsymbol{y}_1|^2 + |\boldsymbol{y}_2|^2)} \boldsymbol{F}'_3(0,0),
\end{aligned}
$$

where α is any positive constant.

An inspection of (15.17) shows that the third-order term in the series expansion depends on a function $\breve{\boldsymbol{F}}_3(\boldsymbol{w}_1, \boldsymbol{w}_2)$ defined as follows: Its arguments $\boldsymbol{w}_1$ and $\boldsymbol{w}_2$ can be either zero or a unit vector, and accordingly its components are given by

$$
\breve{\boldsymbol{F}}_3(0,0) = \boldsymbol{F}'_3(0,0),
$$

$$
\begin{aligned}
\breve{\boldsymbol{F}}_3(\boldsymbol{\eta}_1, 0) &= \boldsymbol{V} + \int_0^\infty dr \frac{\boldsymbol{F}'_3(r\boldsymbol{\eta}_1, 0) - \boldsymbol{Q}(r)}{r}, \\
\breve{\boldsymbol{F}}_3(0, \boldsymbol{\eta}_2) &= \boldsymbol{V}' + \int_0^\infty dr \frac{\boldsymbol{F}'_3(r\boldsymbol{\eta}_2, r\boldsymbol{\eta}_2) - \boldsymbol{Q}'(r)}{r}, \\
\breve{\boldsymbol{F}}_3(\boldsymbol{\eta}_1, \boldsymbol{\eta}_2) &= \boldsymbol{V}(\boldsymbol{\eta}_2) + \boldsymbol{V}'(\boldsymbol{\eta}_1) \\
&\quad + \int_0^\infty dr_2 \int_0^\infty dr_1 \frac{\boldsymbol{F}'_3(r_1\boldsymbol{\eta}_1 + r_2\boldsymbol{\eta}_2, r_2\boldsymbol{\eta}_2) - \boldsymbol{Q}(r_1, r_2\boldsymbol{\eta}_2) - \boldsymbol{Q}'(r_2, r_1\boldsymbol{\eta}_1)}{r_1 r_2},
\end{aligned}
$$

where $\boldsymbol{\eta}_1$ and $\boldsymbol{\eta}_2$ are unit vectors and $\boldsymbol{V}$, $\boldsymbol{V}'$, $\boldsymbol{V}(\boldsymbol{\eta})$, and $\boldsymbol{V}'(\boldsymbol{\eta})$ are compensating terms chosen so that

$$
\begin{aligned}
\int_{|\boldsymbol{\eta}_1|=1} \breve{\boldsymbol{F}}_3(\boldsymbol{\eta}_1, 0) &= 0, \qquad & \int_{|\boldsymbol{\eta}_2|=1} \breve{\boldsymbol{F}}_3(0, \boldsymbol{\eta}_2) &= 0, \\
\int_{|\boldsymbol{\eta}_2|=1} \breve{\boldsymbol{F}}_3(\boldsymbol{\eta}_1, \boldsymbol{\eta}_2) &= 0, \qquad & \int_{|\boldsymbol{\eta}_1|=1} \breve{\boldsymbol{F}}_3(\boldsymbol{\eta}_1, \boldsymbol{\eta}_2) &= 0,
\end{aligned}
$$

to ensure that $\breve{\boldsymbol{F}}_3(\boldsymbol{w}_1, \boldsymbol{w}_2)$ does not depend on the choice of normalizing functions. We call this function a third-order reduced correlation function. In terms of it, the expression for the third-order term in the series expansion becomes

$$
\begin{aligned}
\{\delta \boldsymbol{L}_*^{(3)}\}_{a_1 b_3} &= \{\breve{\boldsymbol{F}}_3(0,0)\}_{a_1 b_1 a_2 b_2 a_3 b_3} \gamma_{b_1 a_2} \gamma_{b_2 a_3} \\
&\quad + \int_{|\boldsymbol{\eta}_1|=1} \{\breve{\boldsymbol{F}}_3(\boldsymbol{\eta}_1, 0)\}_{a_1 b_1 a_2 b_2 a_3 b_3} \{\boldsymbol{\Gamma}_\infty(\boldsymbol{\eta}_1)\}_{b_1 a_2} \gamma_{b_2 a_3} \\
&\quad + \int_{|\boldsymbol{\eta}_2|=1} \{\breve{\boldsymbol{F}}_3(0, \boldsymbol{\eta}_2)\}_{a_1 b_1 a_2 b_2 a_3 b_3} \{\boldsymbol{\Gamma}_\infty(\boldsymbol{\eta}_2)\}_{b_2 a_3} \gamma_{b_1 a_2} \\
&\quad + \int_{|\boldsymbol{\eta}_2|=1} \int_{|\boldsymbol{\eta}_1|=1} \{\breve{\boldsymbol{F}}_3(\boldsymbol{\eta}_1, \boldsymbol{\eta}_2)\}_{a_1 b_1 a_2 b_2 a_3 b_3} \{\boldsymbol{\Gamma}_\infty(\boldsymbol{\eta}_1)\}_{b_1 a_2} \{\boldsymbol{\Gamma}_\infty(\boldsymbol{\eta}_2)\}_{b_2 a_3}.
\end{aligned}
\tag{15.18}
$$

Higher order terms in the series expansion involve higher order reduced correlation functions, which can be defined in a similar manner. For example, the fourth-order reduced correlation function is obtained from the four-point correlation function $\boldsymbol{F}'(\boldsymbol{y}_1 + \boldsymbol{y}_2 + \boldsymbol{y}_3, \boldsymbol{y}_2 + \boldsymbol{y}_3, \boldsymbol{y}_3)$ by setting a (possibly empty) subset of the three variables $\{\boldsymbol{y}_1, \boldsymbol{y}_2, \boldsymbol{y}_3\}$ to zero, and letting the other variables range along rays issuing from the origin. The correlation function is integrated along these rays (with the appropriate weighting factor). Normalizing functions are introduced so that the integrals converge, and compensating terms are added to ensure that the resulting reduced correlation function is independent of the choice made for these normalizing functions.

In a two-phase composite we can introduce second- and third-order reduced correlation functions associated with the composite geometry:

$$
\begin{aligned}
\breve{f}_{11}(\boldsymbol{\eta}) &= v + \int_0^\infty dr \frac{f_{11}(r\boldsymbol{\eta}) - q(r)}{r}, \\
\breve{f}_{111}(\boldsymbol{\eta}_1, \boldsymbol{\eta}_2) &= v(\boldsymbol{\eta}_2) + v'(\boldsymbol{\eta}_1) \\
&\quad + \int_0^\infty dr_2 \int_0^\infty dr_1 \frac{f_{111}(r_1\boldsymbol{\eta}_1 + r_2\boldsymbol{\eta}_2, r_2\boldsymbol{\eta}_2) - q(r_1, r_2\boldsymbol{\eta}_2) - q'(r_2, r_1\boldsymbol{\eta}_1)}{r_1 r_2},
\end{aligned}
$$

$$= v(\boldsymbol{\eta}_2) + v'(\boldsymbol{\eta}_1) + \int_0^\infty dr_2 \int_0^\infty dr_1 \frac{f_{111}(r_1\boldsymbol{\eta}_1, -r_2\boldsymbol{\eta}_2) - q(r_1, r_2\boldsymbol{\eta}_2) - q'(r_2, r_1\boldsymbol{\eta}_1)}{r_1 r_2}, \tag{15.19}$$

where (15.11) has been used to simplify the last equation and $q(r)$, $q(r, \boldsymbol{y})$, and $q'(r, \boldsymbol{y})$ are scalar-valued normalizing functions chosen so that the above integrals are absolutely convergent, while v, $v(\boldsymbol{\eta})$, and $v'(\boldsymbol{\eta})$ are compensating terms chosen so that

$$\int_{|\boldsymbol{\eta}|=1} \breve{f}_{11}(\boldsymbol{\eta}) = 0, \quad \int_{|\boldsymbol{\eta}_2|=1} \breve{f}_{111}(\boldsymbol{\eta}_1, \boldsymbol{\eta}_2) = 0, \quad \int_{|\boldsymbol{\eta}_1|=1} \breve{f}_{111}(\boldsymbol{\eta}_1, \boldsymbol{\eta}_2) = 0. \tag{15.20}$$

Thus the third-order reduced correlation function involves weighted averages of the three-point correlation function f_{111} over all triangles with two sides having a given orientation. Similarly the n-th–order reduced correlation function involves weighted averages of the n-point correlation function over all configurations of points such that the $n-1$ lines joining successive points have given orientations.

The matrix-valued reduced correlation $\breve{\boldsymbol{F}}_3(\boldsymbol{w}_1, \boldsymbol{w}_2)$ can easily be expressed in terms of these scalar reduced correlation functions. For instance, if we take a reference tensor $\boldsymbol{L}_0 = \boldsymbol{L}_2$, then (15.12) implies that

$$\begin{aligned}
\{\breve{\boldsymbol{F}}_3(0,0)\}_{a_1b_1a_2b_2a_3b_3} &= f_1 f_2^2 \{\boldsymbol{L}_1 - \boldsymbol{L}_2\}_{a_1b_1}\{\boldsymbol{L}_1 - \boldsymbol{L}_2\}_{a_2b_2}\{\boldsymbol{L}_1 - \boldsymbol{L}_2\}_{a_3b_3},\\
\{\breve{\boldsymbol{F}}_3(\boldsymbol{\eta}_1,0)\}_{a_1b_1a_2b_2a_3b_3} &= f_2 \breve{f}_{11}(\boldsymbol{\eta}_1)\{\boldsymbol{L}_1 - \boldsymbol{L}_2\}_{a_1b_1}\{\boldsymbol{L}_1 - \boldsymbol{L}_2\}_{a_2b_2}\{\boldsymbol{L}_1 - \boldsymbol{L}_2\}_{a_3b_3},\\
\{\breve{\boldsymbol{F}}_3(0,\boldsymbol{\eta}_2)\}_{a_1b_1a_2b_2a_3b_3} &= f_2 \breve{f}_{11}(\boldsymbol{\eta}_2)\{\boldsymbol{L}_1 - \boldsymbol{L}_2\}_{a_1b_1}\{\boldsymbol{L}_1 - \boldsymbol{L}_2\}_{a_2b_2}\{\boldsymbol{L}_1 - \boldsymbol{L}_2\}_{a_3b_3},\\
\{\breve{\boldsymbol{F}}_3(\boldsymbol{\eta}_1,\boldsymbol{\eta}_2)\}_{a_1b_1a_2b_2a_3b_3} &= \breve{f}_{111}(\boldsymbol{\eta}_1,\boldsymbol{\eta}_2)\{\boldsymbol{L}_1 - \boldsymbol{L}_2\}_{a_1b_1}\{\boldsymbol{L}_1 - \boldsymbol{L}_2\}_{a_2b_2}\{\boldsymbol{L}_1 - \boldsymbol{L}_2\}_{a_3b_3},
\end{aligned}$$

which when substituted in (15.18) give

$$\begin{aligned}
\delta\boldsymbol{L}_*^{(3)} &= f_1 f_2^2 (\boldsymbol{L}_1 - \boldsymbol{L}_2)\boldsymbol{\gamma}(\boldsymbol{L}_1 - \boldsymbol{L}_2)\boldsymbol{\gamma}(\boldsymbol{L}_1 - \boldsymbol{L}_2)\\
&\quad + \int_{|\boldsymbol{\eta}_1|=1} f_2 \breve{f}_{11}(\boldsymbol{\eta}_1)(\boldsymbol{L}_1 - \boldsymbol{L}_2)\boldsymbol{\Gamma}_\infty(\boldsymbol{\eta}_1)(\boldsymbol{L}_1 - \boldsymbol{L}_2)\boldsymbol{\gamma}(\boldsymbol{L}_1 - \boldsymbol{L}_2)\\
&\quad + \int_{|\boldsymbol{\eta}_2|=1} f_2 \breve{f}_{11}(\boldsymbol{\eta}_2)(\boldsymbol{L}_1 - \boldsymbol{L}_2)\boldsymbol{\gamma}(\boldsymbol{L}_1 - \boldsymbol{L}_2)\boldsymbol{\Gamma}_\infty(\boldsymbol{\eta}_2)(\boldsymbol{L}_1 - \boldsymbol{L}_2)\\
&\quad + \int_{|\boldsymbol{\eta}_2|=1}\int_{|\boldsymbol{\eta}_1|=1} \breve{f}_{111}(\boldsymbol{\eta}_1,\boldsymbol{\eta}_2)(\boldsymbol{L}_1 - \boldsymbol{L}_2)\boldsymbol{\Gamma}_\infty(\boldsymbol{\eta}_1)(\boldsymbol{L}_1 - \boldsymbol{L}_2)\boldsymbol{\Gamma}_\infty(\boldsymbol{\eta}_2)(\boldsymbol{L}_1 - \boldsymbol{L}_2).
\end{aligned} \tag{15.21}$$

Similarly, the second-order term in the series expansion (14.2) is

$$\begin{aligned}
\delta\boldsymbol{L}_*^{(2)} &= -\langle(\boldsymbol{L} - \boldsymbol{L}_2)\boldsymbol{\Gamma}(\boldsymbol{L} - \boldsymbol{L}_2)\rangle = -\langle(\boldsymbol{L}_1 - \boldsymbol{L}_2)\chi_1\boldsymbol{\Gamma}\chi_1(\boldsymbol{L}_1 - \boldsymbol{L}_2)\rangle\\
&= -f_1 f_2 (\boldsymbol{L}_1 - \boldsymbol{L}_2)\boldsymbol{\gamma}(\boldsymbol{L}_1 - \boldsymbol{L}_2) - \int_{|\boldsymbol{\eta}|=1} \breve{f}_{11}(\boldsymbol{\eta})(\boldsymbol{L}_1 - \boldsymbol{L}_2)\boldsymbol{\Gamma}_\infty(\boldsymbol{\eta})(\boldsymbol{L}_1 - \boldsymbol{L}_2).
\end{aligned} \tag{15.22}$$

In particular, if we consider a two-phase conducting composite where both phases are isotropic, that is, where $\boldsymbol{L}_1 = \sigma_1\boldsymbol{I}$ and $\boldsymbol{L}_2 = \sigma_2\boldsymbol{I}$, then from (12.49) it follows that

$$\boldsymbol{\gamma} = \frac{\boldsymbol{I}}{3\sigma_2}, \quad \boldsymbol{\Gamma}_\infty(\boldsymbol{\eta}) = \frac{\boldsymbol{I} - 3\boldsymbol{\eta}\otimes\boldsymbol{\eta}}{4\pi\sigma_2}. \tag{15.23}$$

Consequently the series expansion of $\boldsymbol{\sigma}_*$ to the second order in $\sigma_1 - \sigma_2$ is

$$\boldsymbol{\sigma}_* = (f_1\sigma_1 + f_2\sigma_2)\boldsymbol{I} - f_1 f_2(\sigma_1 - \sigma_2)^2 \boldsymbol{A}/\sigma_2, \tag{15.24}$$

where

$$\boldsymbol{A} = \tfrac{1}{3}\boldsymbol{I} + \frac{1}{4\pi f_1 f_2}\int_{|\boldsymbol{\eta}|=1} \check{f}_{11}(\boldsymbol{I} - 3\boldsymbol{\eta}\otimes\boldsymbol{\eta}). \tag{15.25}$$

The averaging of suitably normalized correlation functions along rays in real space to obtain reduced correlation functions is somewhat analogous to the averaging along rays in Fourier space used to obtain the H-measures $\boldsymbol{H}(\boldsymbol{\xi})$ in (14.7). However, there is a difference because a ray in Fourier space corresponds to a set of parallel planes in real space. We preferred to work in real space, rather than in Fourier space, in the hope that it may ultimately provide some physical intuition regarding the reduced correlation functions. The disadvantage is that one needs to introduce the normalizing functions and the associated compensating terms. Another approach is to compute the action of the operators $\boldsymbol{\Gamma}$ on the correlation function by using Radon transforms. For example, using this second approach it follows from the work of Willis (1977) that in three-dimensional random composites the second-order term in the series expansion is

$$\delta\boldsymbol{L}_*^{(2)} = \frac{1}{8\pi^2}\int_{|\boldsymbol{\xi}|=1} \boldsymbol{\Gamma}(\boldsymbol{\xi})\frac{\partial^2 \check{f}_{11}(\boldsymbol{\xi}, p)}{\partial p^2}\bigg|_{p=0},$$

in which $\check{f}_{11}(\boldsymbol{\xi}, p)$ is the Radon transform of the two-point correlation function $f_{11}(\boldsymbol{y})$.

15.6. Expansions for two-phase random composites with geometric isotropy

In periodic composites isotropy often refers to the invariance of an effective tensor under rotation. For instance, a periodic composite with cubic symmetry has a rotationally invariant conductivity tensor, but it does not necessarily have a rotationally invariant elasticity tensor. In random composites isotropy usually refers to a stronger rotational invariance, namely, the invariance of all correlation functions when the material is rotated. In such a material any effective property remains unchanged when the material is rotated. One can also say that the composite is reflection invariant about a plane when all correlation functions remain unchanged when the microstructure is reflected about that plane. Of course reflection invariance about one plane coupled with geometric isotropy is enough to ensure reflection invariance about an arbitrary plane.

In multiphase composites and cell materials we can also speak about a less restrictive form of rotational (or reflection) invariance, namely, the invariance under rotation (or reflection) of all correlation functions associated with the geometry represented by the characteristic functions (Willis 1977). The tensors assigned to the phases need not be isotropic, and as a consequence the effective tensor is not necessarily rotationally (or reflection) invariant. Nevertheless, as we will see, the terms in the series expansion take an especially simple form. We will call such materials geometrically isotropic. Willis (1977) has shown that such simplifications also occur if one makes the weaker assumption that the composite is geometrically isotropic after an appropriate affine transformation. We will suppose that this affine transformation has been made, so we are left considering geometrically isotropic materials.

For example, let us consider two-phase materials. Then geometric isotropy and reflection invariance imply that $f_{11}(\boldsymbol{y})$ depends only on $|\boldsymbol{y}|$ and that $f_{111}(\boldsymbol{y}_1 + \boldsymbol{y}_2, \boldsymbol{y}_2)$ depends only

on the reflection and rotational invariants $|\boldsymbol{y}_1|$, $|\boldsymbol{y}_2|$, and $\boldsymbol{y}_1 \cdot \boldsymbol{y}_2$. Moreover the second-order reduced correlation function $\breve{f}_{11}(\boldsymbol{\eta})$ must be constant, and in fact zero by virtue of (15.20), while the third-order reduced correlation function $\breve{f}_{111}(\boldsymbol{\eta}_1, \boldsymbol{\eta}_2)$ can depend only on $\boldsymbol{\eta}_1 \cdot \boldsymbol{\eta}_2$, that is,

$$\breve{f}_{11}(\boldsymbol{\eta}) = 0, \quad \breve{f}_{111}(\boldsymbol{\eta}_1, \boldsymbol{\eta}_2) = \breve{f}_{111}(u), \quad \text{where } u = -\boldsymbol{\eta}_1 \cdot \boldsymbol{\eta}_2. \tag{15.26}$$

To find an expression for $\breve{f}_{111}(u)$ we first notice that

$$f_{111}(r_1\boldsymbol{\eta}_1, -r_2\boldsymbol{\eta}_2) = f_{111}(r_1, r_2, \theta),$$

in which $f_{111}(r_1, r_2, \theta)$ is the probability that a triangle with sides r_1, r_2 and included angle $\theta = \cos^{-1} u$ lands with all vertices in phase 1. Substituting this into (15.19) and choosing $q'(r_2, r_1\boldsymbol{\eta}_1) = 0$ and $q(r_1, r_2\boldsymbol{\eta}_2) = q(r_1, r_2)$ to be independent of $\boldsymbol{\eta}_2$ gives

$$\breve{f}_{111}(u) = \breve{f}_{111}(\cos\theta) = v + \int_0^\infty dr_2 \int_0^\infty dr_1 \frac{f_{111}(r_1, r_2, \theta) - q(r_1, r_2)}{r_1 r_2}, \tag{15.27}$$

where $q(r_1, r_2)$ is chosen so that the integral is absolutely convergent and the compensating constant v is chosen so that

$$\int_{|\boldsymbol{\eta}_2|=1} \breve{f}_{111}(\boldsymbol{\eta}_1, \boldsymbol{\eta}_2) = \int_{|\boldsymbol{\eta}_1|=1} \breve{f}_{111}(\boldsymbol{\eta}_1, \boldsymbol{\eta}_2) = 2\pi \int_{-1}^{1} du\, \breve{f}_{111}(u) = 0.$$

This single scalar-valued function $\breve{f}_{111}(u)$ contains all of the information needed to compute the effective tensor to the third order in perturbation, irrespective of whether we happen to be studying the conductivity, elasticity, thermoelastic, or piezoelectric problem, and irrespective of whether the phases and reference media happen to be anisotropic or not. As an example, consider the problem of conductivity in a three-dimensional, geometrically isotropic, two-phase composite. For simplicity, let us suppose that the conductivity tensor $\boldsymbol{\sigma}_2$ of phase 2 is isotropic, and let us choose $\boldsymbol{\sigma}_2 = \sigma_2 \boldsymbol{I}$ as a reference tensor so that $\boldsymbol{\gamma}$ and $\boldsymbol{\Gamma}_\infty(\boldsymbol{\eta})$ are given by (15.23). Also, the particular form that any rotationally invariant fourth-order tensor must take implies that

$$\int_{|\boldsymbol{\eta}_2|=1} \int_{|\boldsymbol{\eta}_1|=1} \breve{f}_{111}(-\boldsymbol{\eta}_1 \cdot \boldsymbol{\eta}_2)\{\boldsymbol{\Gamma}_\infty(\boldsymbol{\eta}_1)\}_{ij}\{\boldsymbol{\Gamma}_\infty(\boldsymbol{\eta}_2)\}_{k\ell} = \alpha_1 \delta_{ij}\delta_{k\ell} + \alpha_2 \delta_{ik}\delta_{j\ell} + \alpha_3 \delta_{i\ell}\delta_{jk}, \tag{15.28}$$

where the constants α_1, α_2, and α_3 can be determined by contracting indices in the above equation. This gives

$$\begin{aligned}
\alpha_2 = \alpha_3 = -3\alpha_1/2 &= \frac{1}{10} \int_{|\boldsymbol{\eta}_2|=1} \int_{|\boldsymbol{\eta}_1|=1} \breve{f}_{111}(-\boldsymbol{\eta}_1 \cdot \boldsymbol{\eta}_2)\{\boldsymbol{\Gamma}_\infty(\boldsymbol{\eta}_1)\}_{ij}\{\boldsymbol{\Gamma}_\infty(\boldsymbol{\eta}_2)\}_{ij} \\
&= \frac{3}{160\pi^2\sigma_2^2} \int_{|\boldsymbol{\eta}_2|=1} \int_{|\boldsymbol{\eta}_1|=1} \breve{f}_{111}(-\boldsymbol{\eta}_1 \cdot \boldsymbol{\eta}_2)[3(\boldsymbol{\eta}_1 \cdot \boldsymbol{\eta}_2)^2 - 1] \\
&= \frac{3}{10\sigma_2^2} \int_{-1}^{+1} du\, \breve{f}_{111}(u) P_2(u),
\end{aligned} \tag{15.29}$$

in which $P_2(u)$ is the second Legendre polynomial: $P_2(u) = (3u^2 - 1)/2$.

Higher order terms in the series expansion can be evaluated in a similar fashion, using the fact that (in Cartesian coordinates) any rotationally invariant tensor is represented as a

linear combination of products of Kronecker delta functions. By substituting (15.28) back into (15.21) and recalling that $\boldsymbol{\gamma} = \boldsymbol{I}/(3\sigma_2)$, we deduce that the expansion of the effective conductivity tensor to the third order in perturbation is

$$\begin{aligned}\boldsymbol{\sigma}_* = f_1\boldsymbol{\sigma}_1 + f_2\boldsymbol{\sigma}_2 - f_1f_2(\boldsymbol{\sigma}_1-\boldsymbol{\sigma}_2)^2/3\sigma_2 + f_1f_2^2(\boldsymbol{\sigma}_1-\boldsymbol{\sigma}_2)^3/9\sigma_2^2 \\ +f_1f_2\zeta_1[(\boldsymbol{\sigma}_1-\boldsymbol{\sigma}_2)^3 + 3(\boldsymbol{\sigma}_1-\boldsymbol{\sigma}_2)^2\,\mathrm{Tr}(\boldsymbol{\sigma}_1-\boldsymbol{\sigma}_2)]/45\sigma_2^2 + \cdots,\end{aligned} \tag{15.30}$$

in which ζ_1 is the geometric parameter

$$\zeta_1 = \frac{9}{2f_1f_2}\int_{-1}^{+1} du\, \breve{f}_{111}(u)P_2(u), \quad \text{where } P_2(u) = (3u^2-1)/2. \tag{15.31}$$

The prefactor of $9/(2f_1f_2)$ is introduced into this definition so that the constant ζ_1 satisfies relations similar to those satisfied by the volume fraction f_1, namely,

$$0 \le \zeta_1 \le 1 \text{ and } \zeta_1+\zeta_2 = 1, \quad \text{where } \zeta_2 = \frac{9}{2f_1f_2}\int_{-1}^{+1} du\, \breve{f}_{222}(u)P_2(u), \tag{15.32}$$

and $\breve{f}_{222}(u)$ is the third-order reduced correlation function associated with phase 2. The identity $\zeta_1+\zeta_2 = 1$ can be established by various means. One way is to suppose that both phases have isotropic conductivity tensors $\boldsymbol{\sigma}_1 = \sigma_1\boldsymbol{I}$ and $\boldsymbol{\sigma}_2 = \sigma_2\boldsymbol{I}$. Then the effective tensor is also isotropic, that is, $\boldsymbol{\sigma}_* = \sigma_*\boldsymbol{I}$, and from (15.30) the effective conductivity σ_* has the third-order expansion (Brown 1965)

$$\begin{aligned}\sigma_* &= f_1\sigma_1 + f_2\sigma_2 - f_1f_2(\sigma_1-\sigma_2)^2/3\sigma_2 + f_1f_2(f_2+2\zeta_1)(\sigma_1-\sigma_2)^3/9\sigma_2^2 + \cdots \\ &= \langle\sigma\rangle - \frac{f_1f_2\delta_\sigma^2}{3\langle\sigma\rangle} + \frac{f_1f_2[(f_2-f_1)\delta_\sigma + 2(\zeta_1-f_1)\delta_\sigma]\delta_\sigma^2}{9\langle\sigma\rangle^2} + \cdots.\end{aligned} \tag{15.33}$$

A comparison of this expansion with the equivalent expansion obtained by swapping the indices 1 and 2 in the second expression in (15.33) shows that $\zeta_1 - f_1 = f_2 - \zeta_2$, that is, $\zeta_1+\zeta_2 = 1$.

To prove that ζ_1 is nonnegative, let us introduce the vector-valued field

$$\boldsymbol{g}(\boldsymbol{x}) = \int d\boldsymbol{y}\boldsymbol{\Gamma}_\infty(\boldsymbol{y})[\chi_1(\boldsymbol{x}-\boldsymbol{y}) - q(|\boldsymbol{y}|,\boldsymbol{x})]\boldsymbol{u}, \tag{15.34}$$

in which $\boldsymbol{u}$ is a constant vector and $q(r,\boldsymbol{x})$ is a normalizing function satisfying

$$q(0,\boldsymbol{x}) = \chi_1(\boldsymbol{x}), \quad \lim_{r\to\infty} q(r,\boldsymbol{x}) = f_1,$$

to ensure that the integral in (15.34) converges. Since the scalar field $\boldsymbol{g}(\boldsymbol{x})\cdot\chi_1(\boldsymbol{x})\boldsymbol{g}(\boldsymbol{x})$ takes only nonnegative values for all $\boldsymbol{x}$ and $\boldsymbol{\Gamma}_\infty(\boldsymbol{y}) = \boldsymbol{\Gamma}_\infty(-\boldsymbol{y})$, it follows that

$$\begin{aligned}0 \le \langle\boldsymbol{g}\cdot\chi_1\boldsymbol{g}\rangle &= \int_{|\boldsymbol{\eta}|=1}\int_{|\boldsymbol{\eta}'|=1} \breve{f}_{111}(\boldsymbol{\eta},\boldsymbol{\eta}')\boldsymbol{u}\cdot\boldsymbol{\Gamma}_\infty(\boldsymbol{\eta})\boldsymbol{\Gamma}_\infty(\boldsymbol{\eta}')\boldsymbol{u} \\ &= (\alpha_1+\alpha_2+3\alpha_3)|\boldsymbol{u}|^2 = f_1f_2\zeta_1|\boldsymbol{u}|^2/9\sigma_2^2,\end{aligned}$$

and this clearly implies that ζ_1 must be nonnegative. By interchanging the roles of the phases we deduce that $\zeta_2 = 1-\zeta_1$ must also be nonnegative.

Now suppose that we are given a fixed value of the volume fraction f_1. A comparison of (15.33) with the series expansion for the effective conductivity tensor of the Hashin-Shtrikman coated sphere geometry shows that for the given volume fraction f_1 this geometry attains the maximum possible value of ζ_1, namely, $\zeta_1 = 1$, when the spheres have a core of phase 2 and a coating of phase 1, and achieves the minimum possible value of ζ_1, namely, $\zeta_1 = 0$, when the spheres have a core of phase 1 and a coating of phase 2. By continuity it follows that assemblages of doubly coated spheres achieve all values of ζ_1 in the interval between 0 and 1, at the given volume fraction f_1. In other words, every parameter pair (f_1, ζ_1) in the square defined by the inequalities $0 < f_1 < 1$ and $0 \le \zeta_1 \le 1$ corresponds to a geometry; there can be no further restrictions on the possible values of these parameter pairs.

A similar analysis can be applied to the effective elasticity tensor of a three-dimensional, geometrically isotropic, two-phase material. When the two phases have isotropic elasticity tensors, with bulk moduli κ_1 and κ_2, and shear moduli μ_1 and μ_2, then the effective elasticity tensor is also isotropic. With a choice of reference tensor $\mathcal{C}_0 = \langle \mathcal{C} \rangle$ the effective bulk modulus κ_* and the effective shear modulus μ_* to the third order in perturbation are given (Milton 1982) by the formulas

$$\begin{aligned} \kappa_* &= \langle \kappa \rangle - \frac{3f_1f_2\delta_\kappa^2}{\langle 3\kappa + 4\mu \rangle} + \frac{3f_1f_2[3(f_2 - f_1)\delta_\kappa + 4(\zeta_1 - f_1)\delta_\mu]\delta_\kappa^2}{\langle 3\kappa + 4\mu \rangle^2} + \cdots, \\ \mu_* &= \langle \mu \rangle - \frac{6f_1f_2\langle \kappa + 2\mu \rangle \delta_\mu^2}{5\langle \mu \rangle \langle 3\kappa + 4\mu \rangle} + \frac{6f_1f_2\gamma\delta_\mu^2}{25\langle \mu \rangle^2 \langle 3\kappa + 4\mu \rangle^2} + \cdots, \end{aligned} \tag{15.35}$$

in which $\delta_\kappa = \kappa_1 - \kappa_2$, $\delta_\mu = \mu_1 - \mu_2$,

$$\begin{aligned} \gamma = {} & [5\langle \mu \rangle \langle 2\kappa + 3\mu \rangle (\zeta_1 - f_1) + 6\langle \kappa + 2\mu \rangle^2 (f_2 - f_1) + \langle 3\kappa + \mu \rangle^2 (\eta_1 - f_1)]\delta_\mu \\ & + 10\langle \mu \rangle^2 (\zeta_1 - f_1)\delta_\kappa, \end{aligned}$$

and

$$\eta_1 = \frac{5\zeta_1}{21} + \frac{150}{7f_1f_2} \int_{-1}^{+1} du\, \breve{f}_{111}(u) P_4(u), \quad \text{where } P_4(u) = (35u^4 - 30u^2 + 3)/8. \tag{15.36}$$

Here $P_4(u)$ is the fourth-order Legendre polynomial.

So we see that to the third order in perturbation the expansion for the effective bulk modulus involves exactly the same geometric parameter ζ_1 that appears in the expansion for the effective conductivity. In other words, one could compute the series expansion for the bulk modulus to the third order in perturbation if one knew the series expansion for the effective conductivity. The expansion for the shear modulus involves only one additional geometric parameter, namely, the constant η_1, which satisfies

$$\eta_1 \ge 5\zeta_1/21, \quad \eta_2 \ge 5\zeta_2/21, \quad \eta_1 + \eta_2 = 1,$$

in which

$$\eta_2 = \frac{5\zeta_2}{21} + \frac{150}{7f_1f_2} \int_{-1}^{+1} du\, \breve{f}_{222}(u) P_4(u)$$

is defined in the same way as η_1 except that the roles of the two phases are interchanged. In view of these inequalities it would seem natural to introduce the parameter

$$\xi_1 = \frac{21}{16}(\eta_1 - \frac{5}{21}\zeta_1) = \frac{225}{8f_1f_2} \int_{-1}^{+1} du\, \breve{f}_{111}(u) P_4(u), \quad \text{which satisfies } 0 \le \xi_1 \le 1,$$

and to take (f_1, ζ_1, ξ_1), rather than (f_1, ζ_1, η_1), as the triplet of geometric parameters that describe the effective bulk and shear moduli to the third order in perturbation. However, we choose not to do this because the existing bounds are usually expressed in terms of f_1, ζ_1, and η_1, and there are many tabulations of ζ_1 and η_1 for various microstructures. Also, it is still not known what region in three-dimensional space the triplet (f_1, ζ_1, η_1) covers as the geometry varies over all geometrically isotropic configurations, so it may be premature to decide what parameter is most natural.

For three-dimensional cell materials the expansions (15.33) and (15.35) are implicit in the results of Miller (1969a, 1969b) and Silnutzer (1972). Their expansions involve two cell shape parameters G and E, dependent on the cell shape, in terms of which

$$\begin{aligned} \zeta_1 &= f_1 + (f_2 - f_1)\zeta_1^0, \quad \text{where } \zeta_1^0 = (9G - 1)/2, \\ \eta_1 &= f_1 + (f_2 - f_1)\eta_1^0, \quad \text{where } \eta_1^0 = 4(5E - 1) - 5(9G - 1) \end{aligned} \tag{15.37}$$

(see Milton 1982). The parameters ζ_1^0 and η_1^0 take values between 0 and 1, depending on the cell shape. Miller and Silnutzer find that for spherical cells $G = 1/9$, $E = 1/5$; for platelike cells $G = 1/3$, $E = 1$; and for needlelike cells $G = 1/6$, $E = 3/8$. Thus for spherical cells $\zeta_1^0 = \eta_1^0 = 0$, for platelike cells $\zeta_1^0 = \eta_1^0 = 1$, and for needlelike cells $\zeta_1^0 = 1/4$ and $\eta_1^0 = 1/6$. Expressions for ζ_1^0 and η_1^0 for spheroidal cells with arbitrary eccentricity have been given by Hori (1973) and McPhedran and Milton (1981). Helsing (1994b) calculates G for cubic cells.

The three-dimensional parameter ζ_1 has been computed by McPhedran and Milton (1981) for simple cubic, body-centered cubic, and face-centered cubic arrays of spheres [see also Miller and Torquato (1990)], and by Helsing (1993) for face-centered cubic lattices of cubes. Both parameters ζ_1 and η_1 have been computed by Torquato and Stell (1985); Torquato, Stell, and Beasley (1985); and Berryman (1985) for the penetrable sphere model, that is, for randomly dispersed, penetrable, uniformly sized spheres; by Stell and Rikvold (1987) for randomly dispersed, penetrable, nonuniformly sized (polydispersed) spheres; by Torquato and Lado (1986) and Sen, Lado, and Torquato (1987) using a superposition approximation for the three-particle distribution function; by Sangani and Yao (1988a) for periodic arrays containing 16 randomly dispersed spheres in the unit cell; and by Miller and Torquato (1990) using Monte Carlo simulations for randomly dispersed, impenetrable, uniformly sized spheres; by Thovert, Kim, Torquato, and Acrivos (1990) for randomly dispersed, impenetrable, nonuniformly sized (polydispersed) spheres; and by Roberts and Teubner (1995) and Roberts and Knackstedt (1996a, 1996b) for media defined by the level cut, or level cuts, of a Gaussian random field. Many of these results for ζ_1 and η_1 are summarized in the review article of Torquato (1991). Helsing (1995) shows how ζ_1 and η_1 can be computed from cross-sectional photographs for an arbitrary microgeometry in an efficient manner using interface integral techniques and the fast multipole method.

The expansions (15.35) are useful when the differences $\delta_\kappa = \kappa_1 - \kappa_2$ and $\delta_\mu = \mu_1 - \mu_2$ are both small. Phan-Thien and Milton (1983) obtained an alternative series expansion, which is superior in the sense that it only requires δ_μ to be small. To the first order in δ_μ the effective bulk modulus has the expansion

$$\kappa_* = \langle\kappa\rangle - \frac{3f_1f_2\delta_\kappa^2}{3(f_1\kappa_2 + f_2\kappa_1) + 4\langle\mu\rangle} + \frac{12f_1f_2(\zeta_1 - f_1)\delta_\kappa^2\delta_\mu}{[3(f_1\kappa_2 + f_2\kappa_1) + 4\langle\mu\rangle]^2} + \cdots, \tag{15.38}$$

and to the second order in δ_μ the expansion of the effective shear modulus is

$$\mu_* = \langle\mu\rangle - \frac{6f_1f_2\{\langle\kappa + 2\mu\rangle[3(f_1\kappa_2 + f_2\kappa_1) + 4\langle\mu\rangle] - 3f_1f_2\delta_\kappa^2 - 2\langle\mu\rangle(\zeta_1 - f_1)\delta_\kappa\}\delta_\mu^2}{5\langle\mu\rangle(3\kappa_1 + 4\langle\mu\rangle)(3\kappa_2 + 4\langle\mu\rangle)} + \cdots. \tag{15.39}$$

These expansions are valid even when the bulk moduli of the two phases are not close to each other. When the shear moduli of both phases are equal, that is, when $\delta_\mu = 0$, the formula (15.38) for κ_* coincides with that given by Hill's formula (5.19).

By eliminating the parameter ζ_1 from (15.38) and (15.39) we see that there is a linear microstructure-independent relation

$$\frac{5(\langle\mu\rangle - \mu_*)(3\kappa_1 + 4\langle\mu\rangle)(3\kappa_2 + 4\langle\mu\rangle)\langle\mu\rangle}{3f_1f_2\delta_\mu} - \frac{(\langle\kappa\rangle - \kappa_*)[3(f_1\kappa_2 + f_2\kappa_1) + 4\langle\mu\rangle]^2\langle\mu\rangle}{3f_1f_2\delta_\kappa}$$
$$\approx [3(f_1\kappa_2 + f_2\kappa_1) + 4\langle\mu\rangle](2\langle\kappa + 2\mu\rangle\delta_\mu - \langle\mu\rangle\delta_\kappa) - 6f_1f_2\delta_\kappa^2\delta_\mu,$$

between κ_* and μ_* that holds in the limit when δ_μ is small, to the first order in δ_μ.

The expansions (Schulgasser 1976; Milton 1982) analogous to (15.33) and (15.35) for the effective conductivity σ_*, the effective bulk modulus κ_*, and the effective shear modulus μ_* of a two-dimensional composite are

$$\begin{aligned}
\sigma_* &= \langle\sigma\rangle - \frac{f_1f_2\delta_\sigma^2}{2\langle\sigma\rangle} + \frac{f_1f_2[(f_2 - f_1)\delta_\sigma + (\zeta_1 - f_1)\delta_\sigma]\delta_\sigma^2}{4\langle\sigma\rangle^2} + \cdots,\\
\kappa_* &= \langle\kappa\rangle - \frac{f_1f_2\delta_\kappa^2}{\langle\kappa + \mu\rangle} + \frac{f_1f_2[(f_2 - f_1)\delta_\kappa + (\zeta_1 - f_1)\delta_\mu]\delta_\kappa^2}{\langle\kappa + \mu\rangle^2} + \cdots,\\
\mu_* &= \langle\mu\rangle - \frac{f_1f_2\langle\kappa + 2\mu\rangle\delta_\mu^2}{2\langle\mu\rangle\langle\kappa + \mu\rangle} + \frac{f_1f_2\gamma\delta_\mu^2}{4\langle\mu\rangle^2\langle\kappa + \mu\rangle^2} + \cdots,
\end{aligned} \tag{15.40}$$

in which $\sigma_\kappa = \sigma_1 - \sigma_2$, $\delta_\kappa = \kappa_1 - \kappa_2$, $\delta_\mu = \mu_1 - \mu_2$,

$$\gamma = [\langle\kappa + 2\mu\rangle^2(f_2 - f_1) + \langle\kappa\rangle^2(\eta_1 - f_1)]\delta_\mu + 2\langle\mu\rangle^2(\zeta_1 - f_1)\delta_\kappa,$$

and

$$\begin{aligned}
\zeta_1 &= \frac{4}{\pi f_1f_2}\int_0^\pi d\theta\, \breve{f}_{111}(\cos^{-1}\theta)\cos(2\theta),\\
\eta_1 &= \frac{16}{\pi f_1f_2}\int_0^\pi d\theta\, \breve{f}_{111}(\cos^{-1}\theta)\cos(4\theta).
\end{aligned} \tag{15.41}$$

For two-dimensional cell materials these expansions are implicit in the results of Silnutzer (1972). His expansions involved two cell shape parameters G' and H dependent on the cell shape in terms of which

$$\begin{aligned}
\zeta_1 &= f_1 + (f_2 - f_1)\zeta_1^0, \quad \text{where } \zeta_1^0 = (4G' - 1),\\
\eta_1 &= f_1 + (f_2 - f_1)\eta_1^0, \quad \text{where } \eta_1^0 = (8H - 3) - 4(4G' - 1)
\end{aligned}$$

(see Milton 1982).

It follows from the work of Beran and Silnutzer (1971) and Silnutzer (1972) that for circular cells $\zeta_1^0 = \eta_1^0 = 0$, while for flat cells $\zeta_1^0 = \eta_1^0 = 1$. Expressions for G' for elliptical cells with arbitrary eccentricity have been given by Hori and Yonezawa (1975). Milton (1982) gives G' for square cells and Le Coënt and Jeulin (1996) give G' for rectangular cells. Le Coënt and Jeulin also give G' for a dead-leaves cell material obtained by taking rectangular leaves, randomly assigned to be phase 1 or phase 2, with probabilities f_1 and $f_2 = 1 - f_1$, and randomly positioning them one at a time on a plate replacing whatever

material is beneath them until all of the original plate is covered by such leaves. The cells in this cell material have a variety of shapes and some are not even connected. The model obtains its name from the similarity with the process where dead leaves fall on a forest floor during autumn, where of course the leaves are irregularly shaped. Suquet and Moulinec (1999) give numerical results for the effective shear modulus of two-dimensional cell materials with a honeycomb cell structure.

The two-dimensional parameter ζ_1 (also called ζ_1') has been computed by McPhedran and Milton (1981) for square and hexagonal arrays of disks, and for incomplete arrays where a certain proportion of disks in the complete array are randomly removed and replaced by the matrix. Helsing (1994a) showed how η_1 can be expressed as an integral over the interfaces and evaluated it for a hexagonal array of disks. Both parameters ζ_1 and η_1 (also called ζ_1' and η_1') have been computed by Torquato and Beasley (1986a, 1986b) and Joslin and Stell (1986a) for randomly dispersed, penetrable, uniformly sized disks [see also Babos and Chassapis (1990)]; by Joslin and Stell (1986b) for randomly dispersed, penetrable, nonuniformly sized (polydispersed) disks; by Torquato and Lado (1988, 1992), by Sangani and Yao (1988b), and, with high accuracy (for ζ_1), by Greengard and Helsing (1995), for randomly dispersed impenetrable uniformly sized disks; by Miller and Torquato (1991) for the penetrable disk model, that is, for randomly dispersed, impenetrable, nonuniformly sized (polydispersed) disks; and by Christiansson and Helsing (1995) for hexagonal arrays of concentric circular shell structures. Le Coënt and Jeulin (1996) give ζ_1 for randomly dispersed, penetrable squares, rectangles, and random polygons.

Torquato (1998) has generalized the third-order series expansions for the effective moduli σ_*, κ_*, and μ_* and the definitions of ζ_1 and η_1 to d-dimensional, two-phase composites. He also showed how knowledge of these parameters can lead to reasonable approximation formulas for the effective moduli.

15.7. Series expansions for cell materials with geometric isotropy

In a cell material with geometric isotropy all correlation functions associated with the cell geometry are isotropic. In particular, this implies that the two-point correlation function $g_2(\boldsymbol{y})$ depends only on $|\boldsymbol{y}|$ and implies that the three-point correlation function $g_3(\boldsymbol{y}_1 + \boldsymbol{y}_2, \boldsymbol{y}_2)$ depends only on $|\boldsymbol{y}_1|$, $|\boldsymbol{y}_2|$, and $\boldsymbol{y}_1 \cdot \boldsymbol{y}_2$. Consequently, to the third order in perturbation the effective tensor $\boldsymbol{L}_*$ depends only on the third-order reduced correlation function

$$\breve{g}_3(\boldsymbol{\eta}_1, \boldsymbol{\eta}_2) = v(\boldsymbol{\eta}_2) + v'(\boldsymbol{\eta}_1) + \int_0^\infty dr_2 \int_0^\infty dr_1 \frac{g_3(r_1\boldsymbol{\eta}_1 + r_2\boldsymbol{\eta}_2, r_2\boldsymbol{\eta}_2) - q(r_1, r_2\boldsymbol{\eta}_2) - q'(r_2, r_1\boldsymbol{\eta}_1)}{r_1 r_2},$$

which in turn depends only on the rotational invariant $u = -\boldsymbol{\eta}_1 \cdot \boldsymbol{\eta}_2$. Here $q(r, \boldsymbol{y})$ and $q'(r, \boldsymbol{y})$ are scalar-valued normalizing functions chosen so that the above integrals are absolutely convergent, while $v(\boldsymbol{\eta})$ and $v'(\boldsymbol{\eta})$ are compensating terms chosen so that

$$\int_{|\boldsymbol{\eta}_2|=1} \breve{g}_3(\boldsymbol{\eta}_1, \boldsymbol{\eta}_2) = 0, \qquad \int_{|\boldsymbol{\eta}_1|=1} \breve{g}_3(\boldsymbol{\eta}_1, \boldsymbol{\eta}_2) = 0.$$

Specifically, when we choose a reference tensor $\boldsymbol{L}_0 = \langle \boldsymbol{L} \rangle$ it follows from (15.15) that the matrix elements of the effective tensor have the expansion

$$\{\boldsymbol{L}_*\}_{ab} = \{\langle \boldsymbol{L}\rangle\}_{ab} - \gamma_{b_1a_2}\{\boldsymbol{W}_2\}_{ab_1a_2b} + \gamma_{b_1a_2}\gamma_{b_2a_3}\{\boldsymbol{W}_3\}_{ab_1a_2b_2a_3b} + \Big[\int_{|\boldsymbol{\eta}_2|=1}\int_{|\boldsymbol{\eta}_1|=1} \breve{g}_3(\boldsymbol{\eta}_1,\boldsymbol{\eta}_2)\{\boldsymbol{\Gamma}_\infty(\boldsymbol{\eta}_1)\}_{b_1a_2}\{\boldsymbol{\Gamma}_\infty(\boldsymbol{\eta}_2)\}_{b_2a_3}\Big]\{\boldsymbol{W}_3\}_{ab_1a_2b_2a_3b} + \cdots, \tag{15.42}$$

in which $\boldsymbol{W}_2$ and $\boldsymbol{W}_3$ are the tensors defined by (15.16) and the γ_{ij} are the matrix elements of the tensor $\boldsymbol{\gamma}$ defined by (12.35).

For simplicity let us consider the three-dimensional conductivity problem. The cells are assigned conductivity tensors $\boldsymbol{\sigma}$ chosen from a probability measure $\boldsymbol{\mu}(\boldsymbol{\sigma})$. For simplicity we suppose that this distribution is concentrated on symmetric matrices and such that the average value of the conductivity is an isotropic tensor, that is,

$$\int d\mu(\boldsymbol{\sigma})\boldsymbol{\sigma} = \langle\boldsymbol{\sigma}\rangle = \sigma_0\boldsymbol{I}, \quad \text{where } \sigma_0 = \langle \mathrm{Tr}(\boldsymbol{\sigma})\rangle/3.$$

With a choice of reference tensor $\boldsymbol{\sigma}_0 = \sigma_0\boldsymbol{I}$ the rotational invariance implies that

$$\int_{|\boldsymbol{\eta}_2|=1}\int_{|\boldsymbol{\eta}_1|=1} \breve{g}_3(\boldsymbol{\eta}_1\cdot\boldsymbol{\eta}_2)\{\boldsymbol{\Gamma}_\infty(\boldsymbol{\eta}_1)\}_{b_1a_2}\{\boldsymbol{\Gamma}_\infty(\boldsymbol{\eta}_2)\}_{b_2a_3} = \frac{\zeta_1^0}{15\sigma_0^2}\Big[\delta_{b_1b_2}\delta_{a_2a_3} + \delta_{b_1a_3}\delta_{a_2b_2} - \frac{2}{3}\delta_{b_1a_2}\delta_{b_2a_3}\Big], \tag{15.43}$$

where

$$\zeta_1^0 = (9G-1)/2 = \frac{9}{2}\int_{-1}^{+1} du\ \breve{g}_3(u)P_2(u) \tag{15.44}$$

and G is the cell shape parameter of Miller (1969a, 1969b). By substituting (15.43) back into (15.42) and recalling that $\boldsymbol{\gamma} = \boldsymbol{I}/3\sigma_0$, we see that the effective conductivity tensor has the expansion

$$\boldsymbol{\sigma}_* = \langle\boldsymbol{\sigma}\rangle - \frac{1}{3\sigma_0}\int d\mu(\boldsymbol{\sigma})(\boldsymbol{\sigma}-\langle\boldsymbol{\sigma}\rangle)^2 + \frac{(5+\zeta_1^0)}{45\sigma_0^2}\int d\mu(\boldsymbol{\sigma})(\boldsymbol{\sigma}-\langle\boldsymbol{\sigma}\rangle)^3 + \frac{\zeta_1^0}{15\sigma_0^2}\int d\mu(\boldsymbol{\sigma})(\boldsymbol{\sigma}-\langle\boldsymbol{\sigma}\rangle)^2\,\mathrm{Tr}(\boldsymbol{\sigma}-\langle\boldsymbol{\sigma}\rangle) + \cdots. \tag{15.45}$$

For example, suppose that the measure is concentrated on two isotropic conductivity tensors $\boldsymbol{\sigma}_1 = \sigma_1\boldsymbol{I}$ and $\boldsymbol{\sigma}_2 = \sigma_2\boldsymbol{I}$ with weights f_1 and $f_2 = 1-f_1$. Then the effective conductivity tensor $\boldsymbol{\sigma}_*$ is also isotropic, that is, $\boldsymbol{\sigma}_* = \sigma_*\boldsymbol{I}$, and

$$\begin{aligned}\int d\mu(\boldsymbol{\sigma})(\boldsymbol{\sigma}-\langle\boldsymbol{\sigma}\rangle)^2 &= f_1(\sigma_1 - f_1\sigma_1 - f_2\sigma_2)^2\boldsymbol{I} + f_2(\sigma_2 - f_1\sigma_1 - f_2\sigma_2)^2\boldsymbol{I}\\ &= f_1f_2(\sigma_1-\sigma_2)^2\boldsymbol{I},\end{aligned}$$

and similarly,

$$\int d\mu(\boldsymbol{\sigma})(\boldsymbol{\sigma}-\langle\boldsymbol{\sigma}\rangle)^3 = f_1f_2(f_2-f_1)(\sigma_1-\sigma_2)^3\boldsymbol{I},$$

$$\int d\mu(\boldsymbol{\sigma})(\boldsymbol{\sigma}-\langle\boldsymbol{\sigma}\rangle)^2\,\mathrm{Tr}(\boldsymbol{\sigma}-\langle\boldsymbol{\sigma}\rangle) = 3f_1f_2(f_2-f_1)(\sigma_1-\sigma_2)^3\boldsymbol{I},$$

in which f_1 and $f_2 = 1 - f_1$ are the respective probabilities for finding phase 1 or phase 2 in a given cell. Consequently, (15.45) implies that the effective conductivity has the expansion

$$\sigma_* = f_1\sigma_1 + f_2\sigma_2 - \frac{f_1 f_2 \delta_\sigma^2}{3\langle\sigma\rangle} + \frac{f_1 f_2 (f_2 - f_1)(1 + 2\zeta_1^0)\delta_\sigma^3}{9\langle\sigma\rangle^2} + \cdots,$$

in which $\delta_\sigma = (\sigma_1 - \sigma_2)$. This is in agreement with (15.33), with $\zeta_1 = f_1 + (f_2 - f_1)\zeta_1^0$ as in (15.37).

As another example, suppose that the material is a cell polycrystal, that is, each cell is occupied by a crystal with conductivity tensor having eigenvalues λ_1, λ_2, and λ_3, with the crystal orientation varying randomly from cell to cell. The measure $\boldsymbol{\mu}(\boldsymbol{\sigma})$ is uniformly distributed on the set of symmetric matrices having these eigenvalues, and we have

$$\begin{aligned}
\langle\boldsymbol{\sigma}\rangle &= \sigma_0 \boldsymbol{I}, \quad \text{where } \sigma_0 = (\lambda_1 + \lambda_2 + \lambda_3)/3, \\
\int d\mu(\boldsymbol{\sigma})(\boldsymbol{\sigma} - \langle\boldsymbol{\sigma}\rangle)^2 &= \frac{\boldsymbol{I}}{3}\int d\mu(\boldsymbol{\sigma})\,\mathrm{Tr}[(\boldsymbol{\sigma} - \langle\boldsymbol{\sigma}\rangle)^2] \\
&= 2(\lambda_1^2 + \lambda_2^2 + \lambda_3^2 - \lambda_1\lambda_2 - \lambda_1\lambda_3 - \lambda_2\lambda_3)\boldsymbol{I}/9, \\
\int d\mu(\boldsymbol{\sigma})(\boldsymbol{\sigma} - \langle\boldsymbol{\sigma}\rangle)^3 &= \frac{\boldsymbol{I}}{3}\int d\mu(\boldsymbol{\sigma})\,\mathrm{Tr}[(\boldsymbol{\sigma} - \langle\boldsymbol{\sigma}\rangle)^3] \\
&= [2(\lambda_1^3 + \lambda_3^2 + \lambda_3^3) - 3\lambda_1^2(\lambda_2 + \lambda_3) - 3\lambda_2^2(\lambda_1 + \lambda_3) - 3\lambda_3^2(\lambda_1 + \lambda_2) + 12\lambda_1\lambda_2\lambda_3]\boldsymbol{I}/27, \\
\int d\mu(\boldsymbol{\sigma})(\boldsymbol{\sigma} - \langle\boldsymbol{\sigma}\rangle)^2\,\mathrm{Tr}(\boldsymbol{\sigma} - \langle\boldsymbol{\sigma}\rangle) &= 0.
\end{aligned}$$

The third-order expansion for the effective conductivity σ_* of the polycrystal is obtained by substituting these expressions back into (15.45), giving

$$\begin{aligned}
\sigma_* \approx\ & (\lambda_1 + \lambda_2 + \lambda_3)/3 - \frac{2(\lambda_1^2 + \lambda_2^2 + \lambda_3^2 - \lambda_1\lambda_2 - \lambda_1\lambda_3 - \lambda_2\lambda_3)}{9(\lambda_1 + \lambda_2 + \lambda_3)} \\
&+ \frac{(5 + \zeta_1^0)[2(\lambda_1^3 + \lambda_3^2 + \lambda_3^3) - 3\lambda_1^2(\lambda_2 + \lambda_3) - 3\lambda_2^2(\lambda_1 + \lambda_3) - 3\lambda_3^2(\lambda_1 + \lambda_2) + 12\lambda_1\lambda_2\lambda_3]}{135(\lambda_1 + \lambda_2 + \lambda_3)^2}.
\end{aligned} \tag{15.46}$$

This is the expansion obtained by Willemse and Caspers (1979); see also Avellaneda and Bruno (1990), who give an alternative derivation.

References

Adams, B. L., S. I. Wright, and K. Kunze 1993. Orientation imaging: The emergence of a new microscopy. *Metallurgical Transactions. A, Physical Metallurgy and Materials Science* 24:819–831. {*318, 335*}

Avellaneda, M. and O. P. Bruno 1990. Effective conductivity and average polarizability of random polycrystals. *Journal of Mathematical Physics* 31(8):2047–2056. {*322, 335*}

Babos, G. and D. Chassapis 1990. The calculation of the effective values of physical properties for random composites with circular inclusions. *The Journal of Physics and Chemistry of Solids* 51(3):209–215. {*333, 335*}

Beran, M. J. and N. R. Silnutzer 1971. Effective electrical, thermal, and magnetic properties of fiber reinforced materials. *Journal of Composite Materials* 5:246–249. {*332, 336, 553, 564*}

Berryman, J. G. 1985. Variational bounds on elastic constants for the penetrable sphere model. *Journal of Physics D: Applied Physics* 18:585–597. {*331, 336*}

Berryman, J. G. 1987. Relationship between specific surface area and spatial correlation functions for anisotropic porous media. *Journal of Mathematical Physics* 28(1):244–245. {*319, 336*}

Berryman, J. G. 1988. Interpolating and integrating three-point correlation functions on a lattice. *Journal of Computational Physics* 75:86–102. {*317, 336*}

Brown, W. F. 1955. Solid mixture permittivities. *Journal of Chemical Physics* 23:1514–1517. {*291, 310, 313, 336*}

Brown, W. F. 1965. Dielectric constants, permeabilities, and conductivities of random media. *Transactions of the Society of Rheology* 9:357–380. {*279, 286, 329, 336*}

Brown, W. F. 1974. Properties of two-phase "cell materials". *Journal of Mathematical Physics* 15:1516–1524. {*320, 336*}

Bruno, O. P. 1990. The effective conductivity of an infinitely interchangeable mixture. *Communications on Pure and Applied Mathematics (New York)* 43(6):769–807. {*322, 336*}

Bruno, O. P. and K. Golden 1990. Interchangeability and bounds on the effective conductivity of the square lattice. *Journal of Statistical Physics* 61(1–2):365–386. {*322, 336, 379, 392*}

Christiansson, H. and J. Helsing 1995. A numerical study of the ζ_2 and η_2 structural parameters for a class of fiber-reinforced composites. *Journal of Applied Physics* 77(9): 4734–4738. {*333, 336*}

Debye, P., H. R. Anderson, Jr., and H. Brumberger 1957. Scattering by an inhomogeneous solid. II. The correlation function and its application. *Journal of Applied Physics* 28(6): 679–683. {*319, 336*}

Elsayed, M. A. 1974. Bounds for the effective thermal, electrical, and magnetic properties of heterogeneous materials using high order statistical information. *Journal of Mathematical Physics* 15(11):2001–2015. {*322, 336, 553, 565*}

Elsayed, M. A. and J. J. McCoy 1973. Effect of fiber positioning on the effective physical properties of composite materials. *Journal of Composite Materials* 7:466–480. {*322, 336, 553, 565*}

Etinghof, P. and B. L. Adams 1993. Representations of polycrystalline microstructure by n-point correlation tensors. *Textures and Microstructures* 21:17–37. {*318, 336*}

Frisch, H. L. 1965. Statistics of random media. *Transactions of the Society of Rheology* 9: 293–312. {*320, 336*}

Gillette, G. J. and J. J. McCoy 1986. Statistical moments for random two-phase suspensions: A computational framework. *Journal of Chemical Physics* 85(6):3505–3514. {*317, 318, 323, 336*}

Gillette, G. J. and J. J. McCoy 1987. The calculation of single inclusion probability functions. *Journal of Chemical Physics* 86(2):1010–1019. {*318, 323, 336*}

Greengard, L. and J. Helsing 1995. A numerical study of the ζ_2 parameter for random suspensions of disks. *Journal of Applied Physics* 77(5):2015–2019. {*333, 337*}

Helsing, J. 1993. Bounds to the conductivity of some two-component composites. *Journal of Applied Physics* 73(3):1240–1245. {*331, 337*}

Helsing, J. 1994a. Bounds on the shear modulus of composites by interface integral methods. *Journal of the Mechanics and Physics of Solids* 42(7):1123–1138. {*333, 337*}

Helsing, J. 1994b. Third-order bounds on the conductivity of a random stacking of cubes. *Journal of Mathematical Physics* 35(4):1688–1692. {*331, 337*}

Helsing, J. 1995. Estimating effective properties of composites from cross-sectional photographs. *Journal of Computational Physics* 117(2):281–288. {*331, 337*}

Helsing, J. 1998. A high-order accurate algorithm for electrostatics of overlapping disks. *Journal of Statistical Physics* 90(5–6):1461–1473. {*39, 40, 43, 155, 156, 320, 337, 586, 598*}

Helte, A. 1994. Fourth-order bounds on the effective conductivity for a system of fully penetrable spheres. *Proceedings of the Royal Society of London. Series A, Mathematical and Physical Sciences* 445:247–256. {*319, 337, 554, 566*}

Hori, M. 1973. Statistical theory of effective electrical, thermal, and magnetic properties of random heterogeneous materials. I. Perturbation expansions for the effective permittivity of cell materials. *Journal of Mathematical Physics* 14(4):514–523. {*291, 311, 331, 337*}

Hori, M. 1975. Statistical theory of effective electrical, thermal, and magnetic properties of random heterogeneous materials. VI. Comment on the notion of a cell material. *Journal of Mathematical Physics* 16(9):1772–1775. See erratum: *J. Math. Phys.* 17:598. {*320, 337*}

Hori, M. and F. Yonezawa 1975. Statistical theory of effective electrical, thermal, and magnetic properties of random heterogeneous materials. V. One- and two-dimensional systems. *Journal of Mathematical Physics* 16(2):365–377. {*332, 337*}

Joslin, C. G. and G. Stell 1986a. Bounds on the properties of fiber-reinforced composites. *Journal of Applied Physics* 60:1607–1610. {*333, 337*}

Joslin, C. G. and G. Stell 1986b. Effective properties of fiber-reinforced composites: Effects of polydispersivity in fiber diameter. *Journal of Applied Physics* 60:1611–1613. {*333, 337*}

Le Coënt, A. and D. Jeulin 1996. Bounds of effective physical properties for random polygon composites. *Comptes Rendus des Séances de l'Académie des Sciences. Série II b. Mécanique des Solides et des Structures* 323:299–306. {*332, 333, 337*}

Matheron, G. 1968. Composition des perméabilitiés en milieu poreux hétérogène: Critique de la règle de pondération géométrique. (French) [Composition of permeabilities in heterogeneous porous media: Critique of the rule of geometric balance]. *Revue de l'Institut français du pétrole et annales des combustibles liquides* 23:201–218. {*320, 337*}

McPhedran, R. C. and G. W. Milton 1981. Bounds and exact theories for the transport properties of inhomogeneous media. *Applied Physics A* 26:207–220. {*39, 44, 317, 331, 333, 337, 571, 575–577, 583, 599*}

Miller, C. A. and S. Torquato 1990. Effective conductivity of hard-sphere dispersions. *Journal of Applied Physics* 68(11):5486–5493. {*331, 338*}

Miller, C. A. and S. Torquato 1991. Improved bounds on elastic and transport properties of fiber-reinforced composites: Effect of polydispersivity in fiber radius. *Journal of Applied Physics* 69:1948–1955. {*333, 338*}

Miller, M. N. 1969a. Bounds for effective bulk modulus of heterogeneous materials. *Journal of Mathematical Physics* 10(11):2005–2013. See erratum: *J. Math. Phys.* 12:1057. {*331, 334, 338, 553, 566*}

Miller, M. N. 1969b. Bounds for effective electrical, thermal, and magnetic properties of heterogeneous materials. *Journal of Mathematical Physics* 10(11):1988–2004. {*320, 331, 334, 338, 553, 566*}

Milton, G. W. 1982. Bounds on the elastic and transport properties of two-component composites. *Journal of the Mechanics and Physics of Solids* 30(3):177–191. {*322, 330–332, 338, 553, 558, 566, 586, 599*}

Phan-Thien, N. and G. W. Milton 1983. New third-order bounds on the effective moduli of N-phase composites. *Quarterly of Applied Mathematics* 41:59–74. {*331, 338*}

Roberts, A. P. and M. A. Knackstedt 1996a. Structure-property correlations in model composite materials. *Physical Review E (Statistical Physics, Plasmas, Fluids, and Related Interdisciplinary Topics)* 54:2313–2328. {*331, 338, 555, 567*}

Roberts, A. P. and M. A. Knackstedt 1996b. Transport and elastic properties of fractal media. *Physica A* 233(3–4):848–858. {*331, 338*}

Roberts, A. P. and M. Teubner 1995. Transport properties of heterogeneous materials derived from Gaussian random fields: Bounds and simulation. *Physical Review E (Statistical Physics, Plasmas, Fluids, and Related Interdisciplinary Topics)* 51(5):4141–4154. {*331, 338, 555, 567*}

Sangani, A. S. and C. Yao 1988a. Bulk thermal conductivity of composites with spherical inclusions. *Journal of Applied Physics* 63(5):1334–1341. {*39, 46, 331, 338, 571, 575, 600*}

Sangani, A. S. and C. Yao 1988b. Transport processes in random arrays of cylinders. I Thermal conduction. *Physics of Fluids* 31(9):2426–2434. {*39, 46, 333, 338, 571, 575, 600*}

Schulgasser, K. 1976. On the conductivity of fiber reinforced materials. *Journal of Mathematical Physics* 17(3):382–387. {*332, 338, 553, 567*}

Sen, A. K., F. Lado, and S. Torquato 1987. Bulk properties of composite media. II. Evaluation of bounds on the shear modulus of suspensions of impenetrable spheres. *Journal of Applied Physics* 62(10):4135–4141. {*331, 338, 557, 567*}

Silnutzer, N. R. 1972. Effective constants of statistically homogeneous materials. Ph.D. thesis, University of Pennsylvania, Philadelphia. xvi + 267 pp. {*331, 332, 338, 553, 558, 567*}

Stell, G. and P. A. Rikvold 1987. Polydispersivity in fluids and composites: Some theoretical results. *Chemical Engineering Communications* 51:233–260. {*331, 338*}

Suquet, P. and H. Moulinec 1999. Numerical simulation of the effective elastic properties of a class of cell materials. In K. M. Golden, G. R. Grimmett, R. D. James, G. W. Milton, and P. N. Sen (eds.), *Mathematics of Multiscale Materials*, pp. 271–280. Berlin / Heidelberg / London / etc.: Springer-Verlag. ISBN 0-387-98528-X. {*333, 338*}

Thovert, J. F., I. C. Kim, S. Torquato, and A. Acrivos 1990. Bounds on the effective properties of polydispersed suspensions of spheres: An evaluation of two relevant morphological parameters. *Journal of Applied Physics* 67(10):6088–6098. {*331, 339*}

Torquato, S. 1991. Random heterogeneous media: Microstructure and improved bounds on effective properties. *ASME Applied Mechanics Reviews* 44(2):37–76. {*xxv, xxviii, 331, 339, 425, 436, 553, 567*}

Torquato, S. 1998. Effective stiffness tensor of composite media: II. Applications to isotropic dispersions. *Journal of the Mechanics and Physics of Solids* 46(8):1411–1440. {*305, 312, 333, 339*}

Torquato, S. and J. D. Beasley 1986a. Effective properties of fiber-reinforced materials. I. Bounds on the thermal conductivity of dispersions of fully penetrable cylinders. *International Journal of Engineering Science* 24(3):415–434. {*333, 339, 586, 600*}

Torquato, S. and J. D. Beasley 1986b. Effective properties of fiber-reinforced materials. II. Bounds on the effective elastic moduli of dispersions of fully penetrable cylinders. *International Journal of Engineering Science* 24(3):435–447. {*333, 339*}

Torquato, S. and F. Lado 1986. Effective properties of two-phase disordered composite media: II. Evaluation of bounds on the conductivity and bulk modulus of dispersions of impenetrable spheres. *Physical Review B (Solid State)* 33(9):6428–6435. {*331, 339, 557, 567*}

Torquato, S. and F. Lado 1988. Bounds on the conductivity of a random array of cylinders. *Proceedings of the Royal Society of London. Series A, Mathematical and Physical Sciences* 417:59–80. {*333, 339, 586, 601*}

Torquato, S. and F. Lado 1992. Improved bounds on the effective elastic moduli of random arrays of cylinders. *Journal of Applied Mechanics* 59(1):1–6. {*333, 339*}

Torquato, S. and G. Stell 1982. Microstructure of two-phase random media. I. The n-point probability functions. *Journal of Chemical Physics* 77(4):2071–2077. {*317, 339*}

Torquato, S. and G. Stell 1985. Bounds on the effective thermal conductivity of a dispersion of fully penetrable spheres. *Letters in Applied and Engineering Sciences: An International Journal* 23(3):375–383. {*331, 339, 553, 568*}

Torquato, S., G. Stell, and J. D. Beasley 1985. Third-order bounds on the effective bulk and shear modulus of a dispersion of fully penetrable spheres. *Letters in Applied and Engineering Sciences: An International Journal* 23(3):385–392. {*331, 339*}

Weissberg, H. L. 1963. Effective diffusion coefficients in porous media. *Journal of Applied Physics* 34:2636–2639. {*319, 339*}

Weissberg, H. L. and S. Prager 1962. Viscous flow through porous media. II Approximate three-point correlation function. *Physics of Fluids* 5(11):1390–1392. {*317, 319, 339*}

Willemse, M. W. M. and W. J. Caspers 1979. Electrical conductivity of polycrystalline materials. *Journal of Mathematical Physics* 20(8):1824–1831. {*335, 339, 490, 497*}

Willis, J. R. 1977. Bounds and self-consistent estimates for the overall properties of anisotropic composites. *Journal of the Mechanics and Physics of Solids* 25:185–202. {*256, 269, 327, 340, 347, 353, 464, 497*}

16

Other perturbation solutions

16.1. Effect of a small variation in the material moduli

Whenever one has a solution for the fields and effective tensor for a given set of material constants, it is natural to examine how the effective tensor is changed when the material constants are perturbed. Here we consider the question of how the effective tensor $\boldsymbol{L}_*$ is perturbed in response to a small variation in the tensor field $\boldsymbol{L}$. Specifically, let us suppose that this tensor field depends smoothly on a continuous parameter η, that is, $\boldsymbol{L} = \boldsymbol{L}_\eta$, but that the unit cell of periodicity remains fixed independent of η. We first consider the case where the tensor field $\boldsymbol{L}(\boldsymbol{x})$ is symmetric. This implies that the tensor $\boldsymbol{L}_*$ is symmetric, and so to calculate the derivative $d\boldsymbol{L}_*/d\eta$ of the effective tensor $\boldsymbol{L}_*$ it suffices to consider the derivative of the energy,

$$\frac{d}{d\eta}\boldsymbol{E}_0 \cdot \boldsymbol{L}_*\boldsymbol{E}_0 = \frac{d}{d\eta}\langle \boldsymbol{E}_\eta \cdot \boldsymbol{L}_\eta \boldsymbol{E}_\eta\rangle = \langle \boldsymbol{E}_\eta \cdot \frac{d\boldsymbol{L}_\eta}{d\eta}\boldsymbol{E}_\eta\rangle + 2\langle \frac{d\boldsymbol{E}_\eta}{d\eta} \cdot \boldsymbol{L}_\eta \boldsymbol{E}_\eta\rangle, \tag{16.1}$$

for all constant fields $\boldsymbol{E}_0$, where $\boldsymbol{E}_\eta(\boldsymbol{x})$ solves the field equations

$$\boldsymbol{E}_\eta \in \mathcal{U} \oplus \mathcal{E}, \quad \langle \boldsymbol{E}_\eta\rangle = \boldsymbol{E}_0, \quad \boldsymbol{J}_\eta = \boldsymbol{L}_\eta\boldsymbol{E}_\eta \in \mathcal{U} \oplus \mathcal{J} \text{ for all } \eta. \tag{16.2}$$

Since $\boldsymbol{E}_\eta$ remains in $\mathcal{U} \oplus \mathcal{E}$ for all η, and since its component $\boldsymbol{E}_0$ in the space $\mathcal{U}$ remains fixed independent of η, it follows that

$$\frac{d\boldsymbol{E}_\eta}{d\eta} \in \mathcal{E} \text{ for all } \eta,$$

which in turn implies, because of the orthogonality of the subspaces $\mathcal{E}$ and $\mathcal{U} \oplus \mathcal{J}$, that the last term in expression (16.1) vanishes. Hence the derivative of the energy with respect to η is

$$\frac{d}{d\eta}\boldsymbol{E}_0 \cdot \boldsymbol{L}_*\boldsymbol{E}_0 = \boldsymbol{E}_0 \cdot \frac{d\boldsymbol{L}_*}{d\eta}\boldsymbol{E}_0 = \langle \boldsymbol{E}_\eta \cdot \frac{d\boldsymbol{L}_\eta}{d\eta}\boldsymbol{E}_\eta\rangle, \tag{16.3}$$

which is the expression obtained by Bergman (1978). At any fixed value of η it depends only on the field $\boldsymbol{E}_\eta$ at that value of η, and on the derivative of the moduli $\boldsymbol{L}_\eta$ with respect to η. In other words, if we have a field $\boldsymbol{E}(\boldsymbol{x})$ solving the field equations and vary the material moduli by a small amount $\delta\boldsymbol{L}(\boldsymbol{x})$, while maintaining the value of the applied field $\langle \boldsymbol{E}\rangle$, the energy changes by an amount

$$\langle \boldsymbol{E}\rangle \cdot \delta\boldsymbol{L}_*\langle \boldsymbol{E}\rangle \approx \langle \boldsymbol{E} \cdot (\delta\boldsymbol{L})\boldsymbol{E}\rangle, \tag{16.4}$$

in which $\delta \boldsymbol{L}_*$ is the associated change in the effective tensor $\boldsymbol{L}_*$. By using (16.4) to estimate the change in the energy for a sufficient number of average fields $\langle \boldsymbol{E} \rangle$, we obtain an expression for $\delta \boldsymbol{L}_*$ that is correct to the first order in the variations $\delta \boldsymbol{L}(\boldsymbol{x})$.

If the tensor field $\boldsymbol{L}(\boldsymbol{x})$ is not symmetric, then we consider the derivative of the bilinear form

$$\begin{aligned} \frac{d}{d\eta}\boldsymbol{E}_0' \cdot \boldsymbol{L}_* \boldsymbol{E}_0 &= \frac{d}{d\eta}\langle \boldsymbol{E}_\eta' \cdot \boldsymbol{L}_\eta \boldsymbol{E}_\eta \rangle \\ &= \langle \boldsymbol{E}_\eta' \cdot \frac{d\boldsymbol{L}_\eta}{d\eta}\boldsymbol{E}_\eta \rangle + \langle \frac{d\boldsymbol{E}_\eta'}{d\eta} \cdot \boldsymbol{L}_\eta \boldsymbol{E}_\eta \rangle + \langle (\boldsymbol{L}_\eta^T \boldsymbol{E}_\eta') \cdot \frac{d\boldsymbol{E}_\eta}{d\eta} \rangle, \end{aligned} \tag{16.5}$$

for pairs of constant fields $\boldsymbol{E}_0$ and $\boldsymbol{E}_0'$, where $\boldsymbol{E}_\eta(\boldsymbol{x})$ solves (16.2) while $\boldsymbol{E}_\eta'(\boldsymbol{x})$ solves the adjoint problem

$$\boldsymbol{E}_\eta' \in \mathcal{U} \oplus \mathcal{E}, \quad \langle \boldsymbol{E}_\eta' \rangle = \boldsymbol{E}_0', \quad \boldsymbol{J}_\eta' = \boldsymbol{L}_\eta^T \boldsymbol{E}_\eta' \in \mathcal{U} \oplus \mathcal{J} \text{ for all } \eta.$$

Since $d\boldsymbol{E}_\eta/d\eta$ and $d\boldsymbol{E}_\eta'/d\eta$ both lie in the space $\mathcal{E}$, it follows that the last two terms in (16.5) are zero and we have

$$\frac{d}{d\eta}\boldsymbol{E}_0' \cdot \boldsymbol{L}_* \boldsymbol{E}_0 = \boldsymbol{E}_0' \cdot \frac{d\boldsymbol{L}_*}{d\eta}\boldsymbol{E}_0 = \langle \boldsymbol{E}_\eta' \cdot \frac{d\boldsymbol{L}_\eta}{d\eta}\boldsymbol{E}_\eta \rangle. \tag{16.6}$$

In other words, if we have a field $\boldsymbol{E}(\boldsymbol{x})$ solving the field equations and a field $\boldsymbol{E}'(\boldsymbol{x})$ solving the adjoint equations and vary the material moduli by a small amount $\delta \boldsymbol{L}(\boldsymbol{x})$, while maintaining the values of $\langle \boldsymbol{E} \rangle$ and $\langle \boldsymbol{E}' \rangle$, the associated bilinear form changes by an amount

$$\langle \boldsymbol{E}' \rangle \cdot \delta \boldsymbol{L}_* \langle \boldsymbol{E} \rangle \approx \langle \boldsymbol{E}' \cdot (\delta \boldsymbol{L}) \boldsymbol{E} \rangle. \tag{16.7}$$

By using (16.4) to estimate the change in the bilinear form for a sufficient number of average fields $\langle \boldsymbol{E} \rangle$ and $\langle \boldsymbol{E}' \rangle$, we obtain an expression for $\delta \boldsymbol{L}_*$ that is correct to the first order in the variations $\delta \boldsymbol{L}(\boldsymbol{x})$.

16.2. Application to weakly coupled equations of thermoelectricity or piezoelectricity

The preceding analysis has immediate application to weakly coupled problems since when the coupling is weak it can be treated as a perturbation to an uncoupled problem. For example, let us consider the coupled problem,

$$\boldsymbol{J}_\eta = \boldsymbol{\mathcal{L}}_\eta \boldsymbol{E}_\eta, \quad \text{with} \quad \boldsymbol{J}_\eta = \begin{pmatrix} \boldsymbol{j}_1^\eta \\ \boldsymbol{j}_2^\eta \end{pmatrix}, \quad \boldsymbol{E}_\eta = \begin{pmatrix} \boldsymbol{e}_1^\eta \\ \boldsymbol{e}_2^\eta \end{pmatrix}, \quad \text{and} \quad \boldsymbol{\mathcal{L}}_\eta = \begin{pmatrix} \boldsymbol{L}_{11} & \eta \boldsymbol{L}_{12} \\ \eta \boldsymbol{L}_{12}^T & \boldsymbol{L}_{22} \end{pmatrix},$$

where the matrix $\boldsymbol{\mathcal{L}}_\eta(\boldsymbol{x})$, and hence the matrices $\boldsymbol{L}_{11}(\boldsymbol{x})$ and $\boldsymbol{L}_{22}(\boldsymbol{x})$, are symmetric and the fields satisfy the differential restrictions,

$$\nabla \cdot \boldsymbol{j}_1^\eta = 0, \quad \nabla \cdot \boldsymbol{j}_2^\eta = 0, \quad \nabla \times \boldsymbol{e}_1^\eta = 0, \quad \nabla \times \boldsymbol{e}_2^\eta = 0.$$

The constitutive relation between the average fields,

$$\langle \boldsymbol{J}_\eta \rangle = \boldsymbol{\mathcal{L}}_*^\eta \langle \boldsymbol{E}_\eta \rangle,$$

then defines the effective tensor $\boldsymbol{\mathcal{L}}^{\eta}_{*}$. These equations could, for example, represent the equations of thermoelectricity.

When the coupling constant η is zero, these reduce to an uncoupled set of equations,

$$\begin{aligned} \boldsymbol{j}_1^0(\boldsymbol{x}) &= \boldsymbol{L}_{11}\boldsymbol{e}_1^0, \quad \nabla \cdot \boldsymbol{j}_1^0 = 0, \quad \nabla \times \boldsymbol{e}_1^0 = 0, \\ \boldsymbol{j}_2^0(\boldsymbol{x}) &= \boldsymbol{L}_{22}\boldsymbol{e}_2^0, \quad \nabla \cdot \boldsymbol{j}_2^0 = 0, \quad \nabla \times \boldsymbol{e}_2^0 = 0, \end{aligned}$$

and the effective tensor becomes block diagonal,

$$\boldsymbol{\mathcal{L}}^0_{*} = \begin{pmatrix} \boldsymbol{L}^*_{11} & 0 \\ 0 & \boldsymbol{L}^*_{22} \end{pmatrix},$$

with matrices $\boldsymbol{L}^*_{11}$ and $\boldsymbol{L}^*_{22}$ along the diagonal that correspond to the effective tensors of the uncoupled equations,

$$\langle \boldsymbol{j}_1^0 \rangle = \boldsymbol{L}^*_{11}\langle \boldsymbol{e}_1^0 \rangle, \quad \langle \boldsymbol{j}_2^0 \rangle = \boldsymbol{L}^*_{22}\langle \boldsymbol{e}_2^0 \rangle.$$

When the coupling constant η is small but nonzero, we can treat the coupling as a perturbation to the uncoupled problem and (16.4) gives an approximation to the energy

$$\begin{pmatrix} \langle \boldsymbol{e}_1^0 \rangle \\ \langle \boldsymbol{e}_2^0 \rangle \end{pmatrix} \cdot \boldsymbol{\mathcal{L}}^{\eta}_{*} \begin{pmatrix} \langle \boldsymbol{e}_1^0 \rangle \\ \langle \boldsymbol{e}_2^0 \rangle \end{pmatrix} \approx \langle \boldsymbol{e}_1^0 \rangle \cdot \boldsymbol{L}^*_{11}\langle \boldsymbol{e}_1^0 \rangle + \langle \boldsymbol{e}_2^0 \rangle \cdot \boldsymbol{L}^*_{22}\langle \boldsymbol{e}_2^0 \rangle + 2\eta \langle \boldsymbol{e}_1^0 \cdot \boldsymbol{L}_{12}\boldsymbol{e}_2^0 \rangle, \tag{16.8}$$

which is correct to the first order in η. Since it is usually simpler to solve the uncoupled problem, (16.8) provides a useful formula for estimating the effective tensor $\boldsymbol{\mathcal{L}}^{\eta}_{*}$ when the coupling is small, as is frequently the case.

A similar analysis can of course be applied to the piezoelectric equations

$$\begin{pmatrix} \boldsymbol{\epsilon}^{\eta} \\ \boldsymbol{d}^{\eta} \end{pmatrix} = \boldsymbol{\mathcal{L}}_{\eta} \begin{pmatrix} \boldsymbol{\tau}^{\eta} \\ \boldsymbol{e}^{\eta} \end{pmatrix}, \quad \text{in which} \quad \boldsymbol{\mathcal{L}}_{\eta} = \begin{pmatrix} \boldsymbol{\mathcal{S}} & \eta\boldsymbol{\mathcal{D}} \\ \eta\boldsymbol{\mathcal{D}}^T & \boldsymbol{\varepsilon} \end{pmatrix},$$

where the strain field $\boldsymbol{\epsilon}^{\eta}(\boldsymbol{x})$, the stress field $\boldsymbol{\tau}^{\eta}(\boldsymbol{x})$, the electric displacement field $\boldsymbol{d}^{\eta}(\boldsymbol{x})$, and the electric field $\boldsymbol{e}^{\eta}$ satisfy the usual differential constraints. When $\eta = 0$ these reduce to a set of uncoupled equations

$$\boldsymbol{\epsilon}^0 = \boldsymbol{\mathcal{S}}\boldsymbol{\tau}^0, \qquad \boldsymbol{d}^0 = \boldsymbol{\varepsilon}\boldsymbol{e}^0,$$

and the relation between the average fields

$$\langle \boldsymbol{\epsilon}^0 \rangle = \boldsymbol{\mathcal{S}}^0_{*}\langle \boldsymbol{\tau}^0 \rangle, \quad \langle \boldsymbol{d}^0 \rangle = \boldsymbol{\varepsilon}^0_{*}\langle \boldsymbol{e}^0 \rangle$$

is governed by an effective compliance tensor $\boldsymbol{\mathcal{S}}^0_{*}$ and effective dielectric tensor $\boldsymbol{\varepsilon}^0_{*}$. When the coupling η is small, the energy associated with the effective tensor $\boldsymbol{\mathcal{L}}^{\eta}_{*}$ is approximately

$$\begin{pmatrix} \langle \boldsymbol{\tau}^0 \rangle \\ \langle \boldsymbol{e}^0 \rangle \end{pmatrix} \cdot \boldsymbol{\mathcal{L}}^{\eta}_{*} \begin{pmatrix} \langle \boldsymbol{\tau}^0 \rangle \\ \langle \boldsymbol{e}^0 \rangle \end{pmatrix} \approx \langle \boldsymbol{\tau}^0 \rangle \cdot \boldsymbol{\mathcal{S}}^0_{*}\langle \boldsymbol{\tau}^0 \rangle + \langle \boldsymbol{e}^0 \rangle \cdot \boldsymbol{\varepsilon}^0_{*}\langle \boldsymbol{e}^0 \rangle + 2\eta \langle \boldsymbol{\tau}^0 \cdot \boldsymbol{\mathcal{D}}\boldsymbol{e}^0 \rangle.$$

In other words, we can compute the effective tensor $\boldsymbol{\mathcal{L}}^{\eta}_{*}$ to the first order in η if we know the stress and electric fields that solve the uncoupled elasticity and dielectric equations.

16.3. Application to computing the effective Hall coefficient

Let us consider, for simplicity, an isotropic composite comprised of isotropic conducting phases subject to a magnetic field $\boldsymbol{h}$ directed parallel to the x_3-axis, that is, with $h_1 = h_2 = 0$. To the first order in h_3 the local resistivity tensor and effective resistivity tensor are given by

$$\boldsymbol{\rho}(\boldsymbol{x}) = \begin{pmatrix} \alpha(\boldsymbol{x}) & -R(\boldsymbol{x})h_3 & 0 \\ R(\boldsymbol{x})h_3 & \alpha(\boldsymbol{x}) & 0 \\ 0 & 0 & \alpha(\boldsymbol{x}) \end{pmatrix}, \quad \boldsymbol{\rho}_* = \begin{pmatrix} \alpha_* & -R_*h_3 & 0 \\ R_*h_3 & \alpha_* & 0 \\ 0 & 0 & \alpha_* \end{pmatrix},$$

where $\boldsymbol{R}(\boldsymbol{x})$ and R_* are local and effective Hall coefficients. Treating this as a perturbation of the problem with no magnetic field present, that is, with $h_3 = 0$, we have

$$\delta\boldsymbol{\rho}(\boldsymbol{x}) = \begin{pmatrix} 0 & -R(\boldsymbol{x})h_3 & 0 \\ R(\boldsymbol{x})h_3 & 0 & 0 \\ 0 & 0 & 0 \end{pmatrix}, \quad \delta\boldsymbol{\rho}_* = \begin{pmatrix} 0 & -R_*h_3 & 0 \\ R_*h_3 & 0 & 0 \\ 0 & 0 & 0 \end{pmatrix}.$$

We now let $\boldsymbol{j}'(\boldsymbol{x})$ and $\boldsymbol{j}(\boldsymbol{x})$ be the current fields that have the prescribed average values

$$\langle \boldsymbol{j} \rangle = \begin{pmatrix} 1 \\ 0 \\ 0 \end{pmatrix}, \quad \langle \boldsymbol{j}' \rangle = \begin{pmatrix} 0 \\ 1 \\ 0 \end{pmatrix}$$

and which solve the conductivity equations

$$\begin{aligned} \boldsymbol{e}(\boldsymbol{x}) &= \alpha(\boldsymbol{x})\boldsymbol{j}(\boldsymbol{x}), \quad \nabla \cdot \boldsymbol{j} = 0, \quad \nabla \times \boldsymbol{e} = 0, \\ \boldsymbol{e}'(\boldsymbol{x}) &= \alpha(\boldsymbol{x})\boldsymbol{j}'(\boldsymbol{x}), \quad \nabla \cdot \boldsymbol{j}' = 0, \quad \nabla \times \boldsymbol{e}' = 0, \end{aligned}$$

with no magnetic field present. From the relation

$$\langle \boldsymbol{j}' \rangle \cdot \delta\boldsymbol{\rho}_* \langle \boldsymbol{j} \rangle \approx \langle \boldsymbol{j}' \cdot (\delta\boldsymbol{\rho})\boldsymbol{j} \rangle,$$

which is implied by (16.7), and which holds as an equality to the first order in h_3, we obtain the result of Bergman (1983) that

$$R_* = \langle [j_1(\boldsymbol{x})j_2'(\boldsymbol{x}) - j_1'(\boldsymbol{x})j_2(\boldsymbol{x})]R(\boldsymbol{x}) \rangle.$$

Thus the effective Hall coefficient R_* can be obtained from the local Hall coefficient $R(\boldsymbol{x})$ and a knowledge of the two current fields $\boldsymbol{j}(\boldsymbol{x})$ and $\boldsymbol{j}'(\boldsymbol{x})$ that solve the conductivity equations *in the absence of a magnetic field*.

16.4. The variance of the electric field in a two-phase conducting composite

Bobeth and Diener (1986) and Axell (1992) [see also Beran (1980)] recognized that (16.4) is useful for determining the variances of the fields in two-phase composites. To illustrate this let us consider a two-phase composite with a locally isotropic conductivity tensor. Then the conductivity equations take the forms

$$\boldsymbol{j} = \boldsymbol{\sigma}\boldsymbol{e}, \quad \nabla \cdot \boldsymbol{j} = 0, \quad \nabla \times \boldsymbol{e} = 0, \quad \boldsymbol{\sigma}(\boldsymbol{x}) = \chi_1\sigma_1\boldsymbol{I} + \chi_2\sigma_2\boldsymbol{I},$$

in which χ_1 and χ_2 are the characteristic functions of the two phases. To compute the variance of the field $\boldsymbol{e}$ we need to first compute its average value in each of the phases.

By resolving the fields $\boldsymbol{e}$ and $\boldsymbol{j}$ into their components in each phase,

$$\begin{aligned} \boldsymbol{e} &= \boldsymbol{e}_1 + \boldsymbol{e}_2, && \text{where} \quad \boldsymbol{e}_1 = \chi_1 \boldsymbol{e}, \quad \boldsymbol{e}_2 = \chi_2 \boldsymbol{e}, \\ \boldsymbol{j} &= \boldsymbol{j}_1 + \boldsymbol{j}_2 = \sigma_1 \boldsymbol{e}_1 + \sigma_2 \boldsymbol{e}_2, && \text{where} \quad \boldsymbol{j}_1 = \chi_1 \boldsymbol{j}, \quad \boldsymbol{j}_2 = \chi_2 \boldsymbol{j}, \end{aligned}$$

and using the relation $\boldsymbol{\sigma}_* \langle \boldsymbol{e} \rangle = \langle \boldsymbol{j} \rangle$ we see that

$$\boldsymbol{\sigma}_* \langle \boldsymbol{e} \rangle = \sigma_1 \langle \boldsymbol{e}_1 \rangle + \sigma_2 \langle \boldsymbol{e}_2 \rangle = (\sigma_1 - \sigma_2) \langle \boldsymbol{e}_1 \rangle + \sigma_2 \langle \boldsymbol{e} \rangle = \sigma_1 \langle \boldsymbol{e} \rangle + (\sigma_2 - \sigma_1) \langle \boldsymbol{e}_2 \rangle.$$

This gives us the expressions

$$\langle \boldsymbol{e}_1 \rangle = (\sigma_1 - \sigma_2)^{-1} (\boldsymbol{\sigma}_* - \sigma_2 \boldsymbol{I}) \langle \boldsymbol{e} \rangle, \quad \langle \boldsymbol{e}_2 \rangle = (\sigma_2 - \sigma_1)^{-1} (\boldsymbol{\sigma}_* - \sigma_1 \boldsymbol{I}) \langle \boldsymbol{e} \rangle$$

for the average values of the field components $\boldsymbol{e}_1$ and $\boldsymbol{e}_2$.

The next step is to determine the average of the square of the fields in each phase, which is where the relation (16.4) is helpful. To see the connection let us perturb the conductivities σ_1 and σ_2 of the components by small amounts $\delta\sigma_1$ and $\delta\sigma_2$ while leaving the geometrical configuration of the phases fixed (i.e., while leaving the characteristic function χ_1 unchanged). Then, to the first order in these variations, (16.4) implies that the resultant change $\delta\boldsymbol{\sigma}_*$ in the effective conductivity tensor $\boldsymbol{\sigma}_*$ is given by

$$\langle \boldsymbol{e} \rangle \cdot \delta\boldsymbol{\sigma}_* \langle \boldsymbol{e} \rangle \approx \delta\sigma_1 \langle \boldsymbol{e} \cdot \chi_1 \boldsymbol{e} \rangle + \delta\sigma_2 \langle \boldsymbol{e} \cdot \chi_2 \boldsymbol{e} \rangle = \delta\sigma_1 \Big\langle |\boldsymbol{e}_1|^2 \Big\rangle + \delta\sigma_2 \Big\langle |\boldsymbol{e}_2|^2 \Big\rangle. \tag{16.9}$$

In other words, if the effective conductivity tensor $\boldsymbol{\sigma}_* = \boldsymbol{\sigma}_*(\sigma_1, \sigma_2)$ is known as a function of σ_1 and σ_2, then (16.9) gives us formulas

$$\Big\langle |\boldsymbol{e}_1|^2 \Big\rangle = \langle \boldsymbol{e} \rangle \cdot \frac{\partial \boldsymbol{\sigma}_*}{\partial \sigma_1} \langle \boldsymbol{e} \rangle, \quad \Big\langle |\boldsymbol{e}_2|^2 \Big\rangle = \langle \boldsymbol{e} \rangle \cdot \frac{\partial \boldsymbol{\sigma}_*}{\partial \sigma_2} \langle \boldsymbol{e} \rangle \tag{16.10}$$

for the averages of the square of the field components $\boldsymbol{e}_1$ and $\boldsymbol{e}_2$. The derivatives that enter these formulas are not independent. Indeed, by differentiating the homogeneity relation [see equation (1.6)]

$$\boldsymbol{\sigma}_*(\lambda\sigma_1, \lambda\sigma_2) = \lambda \boldsymbol{\sigma}_*(\sigma_1, \sigma_2),$$

with respect to λ, and then setting $\lambda = 1$, we see that

$$\sigma_1 \frac{\partial \boldsymbol{\sigma}_*}{\partial \sigma_1} + \sigma_2 \frac{\partial \boldsymbol{\sigma}_*}{\partial \sigma_2} = \boldsymbol{\sigma}_*.$$

Now, from the expressions (16.10) it follows that the total field $\boldsymbol{e}$ has average variance

$$V = \Big\langle \Big| \boldsymbol{e} - \langle \boldsymbol{e} \rangle \Big|^2 \Big\rangle = \Big\langle |\boldsymbol{e}_1|^2 + |\boldsymbol{e}_2|^2 \Big\rangle - \langle \boldsymbol{e} \rangle^2 = \langle \boldsymbol{e} \rangle \cdot \Big[\frac{\partial \boldsymbol{\sigma}_*}{\partial \sigma_1} + \frac{\partial \boldsymbol{\sigma}_*}{\partial \sigma_2} - \boldsymbol{I} \Big] \langle \boldsymbol{e} \rangle.$$

Next, by using (16.10) in conjunction with the expression for the average field $\langle \boldsymbol{e}_1 \rangle$, we find that the electric field in phase 1 has an average variance over phase 1 of

$$V_1 = \frac{1}{f_1} \Big\langle \Big| \boldsymbol{e}_1 - \frac{\chi_1}{f_1} \langle \boldsymbol{e}_1 \rangle \Big|^2 \Big\rangle = \frac{1}{f_1} \langle \boldsymbol{e} \rangle \cdot \Big[\frac{\partial \boldsymbol{\sigma}_*}{\partial \sigma_1} - \frac{(\boldsymbol{\sigma}_* - \sigma_2 \boldsymbol{I})^2}{f_1 (\sigma_1 - \sigma_2)^2} \Big] \langle \boldsymbol{e} \rangle, \tag{16.11}$$

where the factors of $1/f_1$, where $f_1 = \langle \chi_1 \rangle$ denotes the volume fraction of phase 1, have been introduced to allow for the fact that the angular brackets represent an average over the entire composite, rather than an average over phase 1.

Similarly, the electric field in phase 2 has an average variance over phase 2 of

$$V_2 = \frac{1}{f_2}\left\langle \left| \boldsymbol{e}_2 - \frac{\chi_2}{f_2}\langle \boldsymbol{e}_2\rangle \right|^2 \right\rangle = \frac{1}{f_2}\langle \boldsymbol{e}\rangle \cdot \Big[\frac{\partial \boldsymbol{\sigma}_*}{\partial \sigma_2} - \frac{(\boldsymbol{\sigma}_* - \sigma_1 \boldsymbol{I})^2}{f_2(\sigma_2 - \sigma_1)^2}\Big]\langle \boldsymbol{e}\rangle,$$

in which $f_2 = 1 - f_1$ is the volume fraction occupied by phase 2. So if the conductivity function $\boldsymbol{\sigma}_*(\sigma_1, \sigma_2)$ and the average electric field $\langle \boldsymbol{e}\rangle$ are known, then we can determine the variance of the electric field in each of the phases and in the composite. Using this result Axell (1992) derived bounds on the field variance. An alternative approach has been taken by Lipton (2000, 2001), who uses a Stieltjes integral representation formula to bound the covariance tensor. Higher order moments of the field distributions, and the field distributions themselves, have been numerically computed by Cheng and Torquato (1997) for two-dimensional random dispersions of disk-shaped, needle-shaped, and square-shaped inclusions.

16.5. Bounds on the conductivity tensor of a composite of two isotropic phases

The expression for the average variance of the electric field over phase 1 leads to well-known bounds on the effective tensor $\boldsymbol{\sigma}_*$, as shown by Matheron (1993) [see also Markov (2000)]. Let us suppose that the conductivities of the two phases have been labeled so that $\sigma_1 > \sigma_2$. We treat σ_2 as being fixed and consider $\boldsymbol{\sigma}_*$ as a function $\boldsymbol{\sigma}_*(\sigma_1)$ of σ_1 for $\sigma_1 > \sigma_2$. Since the average variance over phase 1 is necessarily always positive, it follows from (16.11) that

$$\frac{\partial \boldsymbol{\sigma}_*}{\partial \sigma_1} \geq \frac{(\boldsymbol{\sigma}_* - \sigma_2 \boldsymbol{I})^2}{f_1(\sigma_1 - \sigma_2)^2}. \tag{16.12}$$

(Such an inequality between matrices means that the left-hand side minus the right-hand side is a positive-definite matrix.) This implies that

$$f_1 \frac{\partial (\boldsymbol{\sigma}_* - \sigma_2 \boldsymbol{I})^{-1}}{\partial \sigma_1} = -f_1 (\boldsymbol{\sigma}_* - \sigma_2 \boldsymbol{I})^{-1} \frac{\partial \boldsymbol{\sigma}_*}{\partial \sigma_1} (\boldsymbol{\sigma}_* - \sigma_2 \boldsymbol{I})^{-1} \leq \frac{-\boldsymbol{I}}{(\sigma_1 - \sigma_2)^2}.$$

Integrating this inequality with respect to σ_1 from $\sigma_1 = \sigma_2 + \delta$, where δ is infinitesimal and positive, to $\sigma_1 = \sigma_1'$ gives

$$f_1(\boldsymbol{\sigma}_*(\sigma_1') - \sigma_2 \boldsymbol{I})^{-1} - f_1(\boldsymbol{\sigma}_*(\sigma_2 + \delta) - \sigma_2 \boldsymbol{I})^{-1} \leq (\sigma_1' - \sigma_2)^{-1} \boldsymbol{I} - \delta^{-1} \boldsymbol{I}.$$

Now when δ is infinitesimal we have

$$\boldsymbol{\sigma}_*(\sigma_2 + \delta) = \sigma_2 \boldsymbol{I} + f_1 \delta \boldsymbol{I} - f_1 f_2 \delta^2 \boldsymbol{M}/\sigma_2 + \mathcal{O}(\delta^3).$$

By substituting this back into the inequality and taking the limit $\delta \to 0$ we obtain the bound

$$f_1(\boldsymbol{\sigma}_* - \sigma_2 \boldsymbol{I})^{-1} \leq (\sigma_1 - \sigma_2)^{-1} \boldsymbol{I} + f_2 \boldsymbol{M}/\sigma_2, \tag{16.13}$$

where the prime on σ_1' has been dropped.

This is a lower bound on the effective conductivity tensor $\boldsymbol{\sigma}_*$ that depends on the two-point correlation function through the matrix $\boldsymbol{M}$. Notice that the conductivity tensor of the coated ellipsoid assemblage, given by (7.54), and the conductivity tensor of the sequentially layered laminate, given by (9.20), are such that they achieve the bound. This is no surprise. Since the field in phase 1 is constant in both of these geometries for all values of σ_1 and σ_2,

it follows that the average variance over phase 1 must vanish, implying that equality holds in (16.12).

If the two-point correlation function is unknown, then we can still obtain a useful bound by utilizing the fact that $\mathrm{Tr}(\boldsymbol{M}) = 1$. Taking the trace of (16.13) yields the inequality

$$f_1 \,\mathrm{Tr}[(\boldsymbol{\sigma}_* - \sigma_2\boldsymbol{I})^{-1}] \le d(\sigma_1 - \sigma_2)^{-1} + f_2/\sigma_2, \tag{16.14}$$

where d denotes the dimensionality of the composite.

A similar analysis based on the positivity of the average variance over phase 2 gives an upper bound on the effective conductivity tensor $\boldsymbol{\sigma}_*$,

$$f_2(\sigma_1\boldsymbol{I} - \boldsymbol{\sigma}_*)^{-1} \le (\sigma_1 - \sigma_2)^{-1}\boldsymbol{I} - f_1\boldsymbol{M}/\sigma_1, \tag{16.15}$$

and by taking the trace of this we obtain a bound,

$$f_2 \,\mathrm{Tr}[(\sigma_1\boldsymbol{I} - \boldsymbol{\sigma}_*)^{-1}] \le d(\sigma_1 - \sigma_2)^{-1} - f_1/\sigma_1, \tag{16.16}$$

that is independent of the two-point correlation function. The bounds (16.13) and (16.15) (generalized to multiphase composites) were first derived by Willis (1977). At the time, the problem of obtaining correlation function independent bounds was not considered. The correlation function independent bounds (16.14) and (16.16) were derived independently by Murat and Tartar (1985) and Lurie and Cherkaev (1986) using the translation method (see section 24.6 on page 506). When the composite is isotropic, that is, $\boldsymbol{\sigma}_* = \sigma_*\boldsymbol{I}$, these bounds reduce to the well-known Hashin-Shtrikman (1962) bounds

$$\sigma_1 + \frac{df_2\sigma_1}{d\sigma_1 + f_1(\sigma_2 - \sigma_1)} \ge \sigma_* \ge \sigma_2 + \frac{df_1\sigma_2}{d\sigma_2 + f_2(\sigma_1 - \sigma_2)}, \tag{16.17}$$

which will be discussed again in section 23.1 on page 457.

16.6. The change in the effective tensor due to a shift in the phase boundary†

We have answered the question of how the effective tensor $\boldsymbol{L}_*$ changes when the there is a small perturbation that shifts the moduli $\boldsymbol{L}(\boldsymbol{x})$ by a small amount at each point $\boldsymbol{x}$. Here we analyze a different type of small perturbation, namely, a slight shift in the position of a phase boundary, or any interface that marks a discontinuity in the tensor field $\boldsymbol{L}(\boldsymbol{x})$. As the interface is shifted there is a finite jump in the moduli $\boldsymbol{L}(\boldsymbol{x})$ at points $\boldsymbol{x}$ in the vicinity of the interface, and the previous perturbation analysis is no longer applicable.

Specifically, let us suppose that this interface depends on a continuous parameter η, that is, $\Gamma = \Gamma_\eta$. Let us assume, for simplicity, that as η is increased the tensor field $\boldsymbol{L} = \boldsymbol{L}_\eta(\boldsymbol{x})$ changes only at any given point $\boldsymbol{x}$ when the interface Γ_η passes through that point. To simplify the analysis let us further assume that the fields $\boldsymbol{E} = \boldsymbol{E}_\eta$ and $\boldsymbol{J} = \boldsymbol{J}_\eta$ are matrix-valued fields satisfying the differential constraints,

$$\nabla \cdot \boldsymbol{J}_\eta = 0, \quad \boldsymbol{E} = \nabla \boldsymbol{u}_\eta, \quad \langle \boldsymbol{E} \rangle = \boldsymbol{E}_0,$$

for some vector (or scalar) potential $\boldsymbol{u}_\eta$, where $\boldsymbol{E}_0$ is chosen to be independent of η. At the interface Γ_η the appropriate continuity conditions are

$$\boldsymbol{u}_\eta \text{ and } \boldsymbol{n} \cdot \boldsymbol{J}_\eta \text{ are continuous across } \Gamma_\eta, \tag{16.18}$$

where $\boldsymbol{n}(\boldsymbol{x})$ is the normal to the interface. It is convenient to suppose that the interface Γ_η has two sides and to label the fields adjacent to one side of the interface by a plus superscript and to label the fields adjacent to the other side by a minus superscript. With this notation the interface condition (16.18) can be rewritten as,

$$\boldsymbol{u}_\eta^+(\boldsymbol{x}) = \boldsymbol{u}_\eta^-(\boldsymbol{x}), \quad \boldsymbol{n}\cdot\boldsymbol{J}_\eta^+(\boldsymbol{x}) = \boldsymbol{n}\cdot\boldsymbol{J}_\eta^-(\boldsymbol{x}), \quad \text{for all } \boldsymbol{x}\in\Gamma_\eta, \tag{16.19}$$

where $\boldsymbol{n}$ is taken to be directed outward from the $+$ side of the interface, pointing toward the $-$ side.

Let us also introduce, for all points $\boldsymbol{x}$ along the interface Γ_η, the scalar quantity $\gamma_\eta(\boldsymbol{x})$ representing the speed at which the interface Γ_η moves in the direction of the outward normal $\boldsymbol{n}$ as η is increased. In other words, if η is increased to $\eta+\epsilon$, then the set of points

$$\Gamma'_{\eta,\epsilon} = \{\boldsymbol{x}' \mid \boldsymbol{x}' = \boldsymbol{x} + \epsilon\gamma_\eta(\boldsymbol{x})\boldsymbol{n},\ \boldsymbol{x}\in\Gamma_\eta\} \tag{16.20}$$

represents a first-order approximation to the interface $\Gamma_{\eta+\epsilon}$ in the limit $\epsilon\to 0$; see figure 16.1.

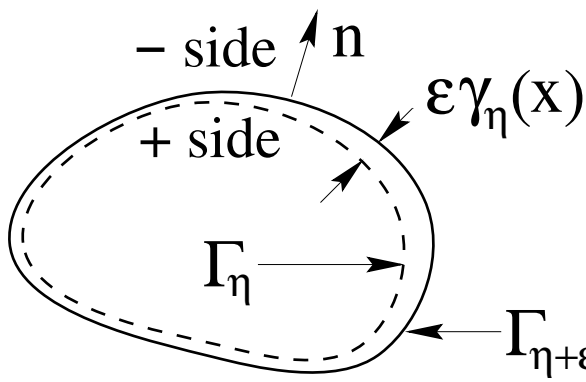

Figure 16.1. Perturbation of an interface separating two phases or marking a discontinuity in the tensor field $\boldsymbol{L}(\boldsymbol{x})$. When ϵ is small $\epsilon|\gamma_\eta(\boldsymbol{x})|$ is a first approximation to the distance between the interfaces Γ_η and $\Gamma_{\eta+\epsilon}$.

The key step is to recognize that the derivative of the energy with respect to η is

$$\begin{aligned}\frac{d}{d\eta}\langle \boldsymbol{E}_0\cdot\boldsymbol{L}_*\boldsymbol{E}_0\rangle &= \frac{d}{d\eta}\langle \boldsymbol{E}_\eta\cdot\boldsymbol{L}_\eta\boldsymbol{E}_\eta\rangle \\ &= \frac{2}{|\Omega|}\int_{\Omega\setminus\Gamma_\eta}\frac{d\boldsymbol{E}_\eta}{d\eta}\cdot\boldsymbol{L}_\eta\boldsymbol{E}_\eta + \frac{1}{|\Omega|}\int_{\Gamma_\eta}\gamma_\eta[\boldsymbol{E}_\eta^+\cdot\boldsymbol{L}^+\boldsymbol{E}_\eta^+ - \boldsymbol{E}_\eta^-\cdot\boldsymbol{L}^-\boldsymbol{E}_\eta^-].\end{aligned} \tag{16.21}$$

The origin of the terms in this expression requires some explanation. The first integral is over the unit cell Ω, excluding the interface Γ_η, and represents the change in the energy due to variations $d\boldsymbol{E}_\eta/d\eta$ in the field, treating the interface as if it remained fixed. The second integral represents the change in the energy due to movement of the interface, treating the field $\boldsymbol{E}_\eta(\boldsymbol{x})$ as if it remained fixed outside the neighborhood of the interface and within the neighborhood of the interface was analytically extended to the new position of the interface so that the discontinuity in the field remains at the interface.

The first integral in (16.21) can be integrated by parts,

$$\begin{aligned}\int_{\Omega\setminus\Gamma_\eta} \frac{d\boldsymbol{E}_\eta}{d\eta}\cdot \boldsymbol{L}_\eta \boldsymbol{E}_\eta &= \int_{\Gamma_\eta} \frac{\partial \boldsymbol{u}_\eta^+}{\partial \eta}\cdot(\boldsymbol{n}\cdot\boldsymbol{J}_\eta^+) - \frac{\partial \boldsymbol{u}_\eta^-}{\partial \eta}\cdot(\boldsymbol{n}\cdot\boldsymbol{J}_\eta^-)\\ &= \int_{\Gamma_\eta} [\frac{\partial \boldsymbol{u}_\eta^+}{\partial \eta} - \frac{\partial \boldsymbol{u}_\eta^-}{\partial \eta}]\cdot(\boldsymbol{n}\cdot\boldsymbol{J}_\eta^+),\end{aligned} \tag{16.22}$$

in which we have used the continuity condition (16.19) on the field $\boldsymbol{J}$ to simplify the result. Here the partial derivatives $\partial \boldsymbol{u}_\eta^+/\partial\eta$ and $\partial \boldsymbol{u}_\eta^-/\partial\eta$ are partial derivatives of $\boldsymbol{u}_\eta^+(\boldsymbol{x})$ and $\boldsymbol{u}_\eta^-(\boldsymbol{x})$ with respect to η keeping $\boldsymbol{x}$ fixed. They should be evaluated at a point $\boldsymbol{x}$ slightly away from the interface, and then the limit should be taken as $\boldsymbol{x}$ approaches the interface Γ_η from, respectively, the plus and minus sides of the interface. Now notice that (16.20) and the continuity condition (16.19) on the potential imply that to the first order in ϵ,

$$\boldsymbol{u}_{\eta+\epsilon}^+(\boldsymbol{x}+\epsilon\gamma_\eta(\boldsymbol{x})\boldsymbol{n}) \approx \boldsymbol{u}_{\eta+\epsilon}^-(\boldsymbol{x}+\epsilon\gamma_\eta(\boldsymbol{x})\boldsymbol{n}).$$

By expanding this and equating the terms of order ϵ we see that

$$\frac{\partial \boldsymbol{u}_\eta^+}{\partial\eta} + \gamma_\eta \boldsymbol{n}\cdot\nabla \boldsymbol{u}_\eta^+ = \frac{\partial \boldsymbol{u}_\eta^+}{\partial\eta} + \gamma_\eta \boldsymbol{n}\cdot\nabla \boldsymbol{u}_\eta^-,$$

which in conjunction with (16.22) implies that

$$\begin{aligned}\int_{\Omega\setminus\Gamma_\eta} \frac{d\boldsymbol{E}_\eta}{d\eta}\cdot \boldsymbol{L}_\eta \boldsymbol{E}_\eta &= \int_{\Gamma_\eta} \gamma_\eta[\boldsymbol{n}\cdot(\nabla \boldsymbol{u}_\eta^- - \nabla \boldsymbol{u}_\eta^+)]\cdot(\boldsymbol{n}\cdot\boldsymbol{J}_\eta^+)\\ &= \int_{\Gamma_\eta} \gamma_\eta(\nabla \boldsymbol{u}_\eta^- - \nabla \boldsymbol{u}_\eta^+)\cdot(\boldsymbol{n}\otimes\boldsymbol{n})\cdot\boldsymbol{J}_\eta^+.\end{aligned} \tag{16.23}$$

Since the potential is continuous across the interface, it follows that the tangential derivative of the potential is also continuous across the interface. So if $\boldsymbol{w}_1(\boldsymbol{x})$, $\boldsymbol{w}_2(\boldsymbol{x})$,...,$\boldsymbol{w}_{d-1}(\boldsymbol{x})$ and $\boldsymbol{n}(\boldsymbol{x})$ form an orthonormal set of basis vectors at each point $\boldsymbol{x}$ on the interface, then we have

$$\boldsymbol{w}_i\cdot[\nabla \boldsymbol{u}_\eta^- - \nabla \boldsymbol{u}_\eta^+] = 0 \ \text{ for } i = 1, 2, \ldots, d-1.$$

This enables us to rewrite (16.23) as

$$\begin{aligned}\int_{\Omega\setminus\Gamma_\eta} \frac{d\boldsymbol{E}_\eta}{d\eta}\cdot \boldsymbol{L}_\eta \boldsymbol{E}_\eta &= \int_{\Gamma_\eta} \gamma_\eta(\nabla \boldsymbol{u}_\eta^- - \nabla \boldsymbol{u}_\eta^+)\cdot(\boldsymbol{n}\otimes\boldsymbol{n} + \sum_{i=1}^{d-1}\boldsymbol{w}_i\otimes\boldsymbol{w}_i)\cdot\boldsymbol{J}_\eta^+\\ &= \int_{\Gamma_\eta} \gamma_\eta[\nabla \boldsymbol{u}_\eta^- - \nabla \boldsymbol{u}_\eta^+]\cdot\boldsymbol{J}_\eta^+\\ &= \int_{\Gamma_\eta} \gamma_\eta[\boldsymbol{E}_\eta^- - \boldsymbol{E}_\eta^+]\cdot\boldsymbol{L}^+\boldsymbol{E}_\eta^+.\end{aligned} \tag{16.24}$$

Of course we could have equally well replaced $\boldsymbol{n}\cdot\boldsymbol{J}_\eta^+$ by $\boldsymbol{n}\cdot\boldsymbol{J}_\eta^-$ in the expression (16.22). This would have lead to the identity

$$\int_{\Omega\setminus\Gamma_\eta} \frac{d\boldsymbol{E}_\eta}{d\eta}\cdot \boldsymbol{L}_\eta \boldsymbol{E}_\eta = \int_{\Gamma_\eta} \gamma_\eta[\boldsymbol{E}_\eta^- - \boldsymbol{E}_\eta^+]\cdot\boldsymbol{L}^-\boldsymbol{E}_\eta^-. \tag{16.25}$$

By substituting (16.24) and (16.25) back into (16.21) we arrive at the result

$$\begin{aligned}\langle \boldsymbol{E}_0 \cdot \frac{d\boldsymbol{L}_*}{d\eta}\boldsymbol{E}_0\rangle &= \frac{1}{|\Omega|}\int_{\Gamma_\eta} \gamma_\eta[\boldsymbol{E}_\eta^- \cdot \boldsymbol{L}^+\boldsymbol{E}_\eta^+ - \boldsymbol{E}_\eta^+ \cdot \boldsymbol{L}^-\boldsymbol{E}_\eta^-] \\ &= \frac{1}{|\Omega|}\int_{\Gamma_\eta} \gamma_\eta[\boldsymbol{E}_\eta^+ \cdot (\boldsymbol{L}^+ - \boldsymbol{L}^-)\boldsymbol{E}_\eta^-] \\ &= \frac{1}{|\Omega|}\int_{\Gamma_\eta} \gamma_\eta[\boldsymbol{E}^- \cdot \boldsymbol{J}^+ - \boldsymbol{E}^+ \cdot \boldsymbol{J}^-]. \end{aligned} \tag{16.26}$$

In other words, the derivative of the energy depends only on the values that the fields $\boldsymbol{E}$ and $\boldsymbol{J}$ take along that interface. If we perturb the position of the interface by a distance $\epsilon\gamma(\boldsymbol{x})$ in the direction normal to the interface, keeping $\langle \boldsymbol{E}\rangle$ fixed, then (16.26) implies that the resultant change in the energy to the first order in ϵ will be

$$\langle \boldsymbol{E}\rangle \cdot (\delta \boldsymbol{L}_*)\langle \boldsymbol{E}\rangle \approx \frac{1}{|\Omega|}\int_{\Gamma_\eta} \epsilon\gamma(\boldsymbol{x})[\boldsymbol{E}^-(\boldsymbol{x}) \cdot \boldsymbol{J}^+(\boldsymbol{x}) - \boldsymbol{E}^+(\boldsymbol{x}) \cdot \boldsymbol{J}^-(\boldsymbol{x})], \tag{16.27}$$

where $\delta \boldsymbol{L}_*$ is the associated change in the effective tensor $\boldsymbol{L}_*$. Thus $\delta \boldsymbol{L}_*$ can be computed to the first order in ϵ by evaluating the change in energy (16.27) for sufficiently many average fields $\langle \boldsymbol{E}\rangle$.

As an example, consider what happens when we change the volume fraction in the Hashin-Shtrikman (1962) coated sphere geometry by increasing the core radius r_c in each coated sphere by an amount proportional to r_c, that is, by an amount $\delta r_c = \epsilon r_c$, while keeping the outer radius r_e fixed. The resultant change in the overall volume fraction of phase 1 will then be

$$\delta f_1 = \frac{3r_c^2 \delta r_c}{r_e^3} = 3\epsilon f_1.$$

Now from formulas (7.2) and (7.3) for the fields in the coated sphere geometry we see that the electric field at the interface between the core and coating takes values

$$\boldsymbol{e}_1 = a_1[\cos\theta\ \boldsymbol{v}_r - \sin\theta\ \boldsymbol{v}_\theta]$$

on the core side of the interface and values

$$\boldsymbol{e}_2 = \nabla\phi_2 = [a_2 - 2b_2/r_c^3]\cos\theta\ \boldsymbol{v}_r - [a_2 + b_2/r_c^3]\sin\theta\ \boldsymbol{v}_\theta$$

on the coating side of the interface, where $\boldsymbol{v}_r$ is the unit radial vector and $\boldsymbol{v}_\theta$ is the unit vector perpendicular to $\boldsymbol{v}_r$ in the plane containing $\boldsymbol{r}$ and $\langle \boldsymbol{e}\rangle$. Also, according to formulas (7.4) and (7.5), the constants entering these equations satisfy

$$a_1 = -\frac{3\sigma_2 b_2}{r_c^3(\sigma_1 - \sigma_2)}, \quad a_2 = -\frac{(\sigma_1 + 2\sigma_2)b_2}{r_c^3(\sigma_1 - \sigma_2)},$$

and b_2 is related to the magnitude of the average electric field through the equation

$$|\langle \boldsymbol{e}\rangle| = |a_*| = |a_2 + b_2/r_e^3| = \left|\frac{[3\sigma_2 + f_2(\sigma_1 - \sigma_2)]b_2}{(\sigma_1 - \sigma_2)r_c^3}\right|.$$

According to (16.27), the resultant change $\delta\sigma_*$ in the effective conductivity should be given, to the first order in ϵ, by the formula

$$\begin{aligned}\delta\sigma_* &\approx \frac{3}{4\pi r_e^3\langle \boldsymbol{e}\rangle^2}\int_0^\pi \delta r_c[\boldsymbol{e}_1\cdot(\sigma_1-\sigma_2)\boldsymbol{e}_2]2\pi r_c^2\sin\theta\, d\theta\\ &\approx \frac{3\epsilon f_1(\sigma_1-\sigma_2)}{2\langle \boldsymbol{e}\rangle^2}\int_0^\pi a_1(a_2-2b_2/r_c^3)\cos^2\theta\ \sin\theta\ + a_1(a_2+b_2/r_c^3)\sin^3\theta\, d\theta\\ &\approx \frac{3\epsilon f_1(\sigma_1-\sigma_2)a_1a_2}{\langle \boldsymbol{e}\rangle^2} = \frac{3\sigma_2(\sigma_1-\sigma_2)(\sigma_1+2\sigma_2)}{[3\sigma_2+f_2(\sigma_1-\sigma_2)]^2}\delta f_1.\end{aligned}$$

This implies that the derivative of σ_* with respect to f_1 must be

$$\frac{\partial\sigma_*}{\partial f_1} = \frac{3\sigma_2(\sigma_1-\sigma_2)(\sigma_1+2\sigma_2)}{[3\sigma_2+f_2(\sigma_1-\sigma_2)]^2},$$

which agrees with the result obtained by direct differentiation of the formula

$$\sigma_* = \sigma_2 + \frac{3f_1\sigma_2(\sigma_1-\sigma_2)}{3\sigma_2+f_2(\sigma_1-\sigma_2)}$$

for the effective conductivity as a function of f_1. Of course we can use (16.27) to treat quite general perturbations to the interface. For instance, in the coated sphere geometry one could analyze the first-order effect of nonspherical perturbations to the shape of the core in each coated inclusion.

If we are aiming to find multicomponent composites that, for a given applied field $\boldsymbol{E}_0 = \langle \boldsymbol{E}\rangle$, have maximum or minimum energy amongst all composites constructed from the same set of component materials, then (16.27) tells us that at each interface Γ the fields must satisfy the constraint

$$\boldsymbol{E}^-(\boldsymbol{x})\cdot\boldsymbol{J}^+(\boldsymbol{x}) = \boldsymbol{E}^+(\boldsymbol{x})\cdot\boldsymbol{J}^-(\boldsymbol{x}) \quad \text{for all } \boldsymbol{x}\in\Gamma. \tag{16.28}$$

This provides a necessary but not sufficient condition for optimality. It turns out that optimal microstructures frequently have structure on widely separated length scales. In that event condition (16.28) also applies to the interfaces separating two different types of microstructure, that is, to interfaces between composites constructed from the component materials. At such interfaces the fields $\boldsymbol{E}^-$, $\boldsymbol{E}^+$, $\boldsymbol{J}^-$, and $\boldsymbol{J}^+$ appearing in (16.28) should be taken to be local averages of the associated fields $\boldsymbol{E}$ and $\boldsymbol{J}$ on each side of the interface.

16.7. Perturbing the lamination directions in a multiple-rank laminate†

Suppose that we are searching amongst multiple-rank laminate materials for optimal laminates that for a given applied field $\boldsymbol{E}_0$ have maximum or minimum energy. The condition (16.28), applied at each level of lamination, is necessary for the energy of an optimal laminate to be stable under small variations in the relative widths of the laminae, that is, under small variations in the relative proportions of the materials laminated together at each level of lamination. Here we will derive conditions that are necessary for the energy of an optimal laminate to be stable under small variations in the directions of lamination.

To begin, consider a simple two-phase laminate, of phases with symmetric tensors $\boldsymbol{L}_1$ and $\boldsymbol{L}_2$, laminated in direction $\boldsymbol{n}$ in proportions f_1 and $f_2 = 1-f_1$, and subject to an applied field $\boldsymbol{E}_0$. From (9.45), the effective tensor $\boldsymbol{L}_*$ of such a laminate is given by the formula

$$\boldsymbol{L}_* = \boldsymbol{L}_2 + f_1[(\boldsymbol{L}_1-\boldsymbol{L}_2)^{-1} + f_2\boldsymbol{\Gamma}(\boldsymbol{n})]^{-1},$$

where

$$\boldsymbol{\Gamma}(\boldsymbol{n}) = \boldsymbol{\Gamma}_1(\boldsymbol{n})[\boldsymbol{\Gamma}_1(\boldsymbol{n})\boldsymbol{L}_2\boldsymbol{\Gamma}_1(\boldsymbol{n})]^{-1}\boldsymbol{\Gamma}_1(\boldsymbol{n}).$$

A necessary condition for the energy $\boldsymbol{E}_0 \cdot \boldsymbol{L}_*\boldsymbol{E}_0$ to be minimized, or maximized, with respect to variations in $\boldsymbol{n}$ (while $\boldsymbol{E}_0$, $\boldsymbol{L}_1$, $\boldsymbol{L}_2$, and the proportions f_1 and $f_2 = 1 - f_1$ are kept fixed) is that

$$\begin{aligned}
&\frac{\partial(\boldsymbol{E}_0 \cdot \boldsymbol{L}_*\boldsymbol{E}_0)}{\partial \boldsymbol{n}} \\
&\quad = -f_1 f_2 \boldsymbol{E}_0 \cdot [(\boldsymbol{L}_1 - \boldsymbol{L}_2)^{-1} + f_2\boldsymbol{\Gamma}(\boldsymbol{n})]^{-1}\frac{d\boldsymbol{\Gamma}(\boldsymbol{n}/|\boldsymbol{n}|)}{d\boldsymbol{n}}[(\boldsymbol{L}_1 - \boldsymbol{L}_2)^{-1} + f_2\boldsymbol{\Gamma}(\boldsymbol{n})]^{-1}\boldsymbol{E}_0 \\
&\quad = -(f_2/f_1)[(\boldsymbol{L}_* - \boldsymbol{L}_2)\boldsymbol{E}_0] \cdot \frac{d\boldsymbol{\Gamma}(\boldsymbol{n}/|\boldsymbol{n}|)}{d\boldsymbol{n}}[(\boldsymbol{L}_* - \boldsymbol{L}_2)\boldsymbol{E}_0] = 0. \qquad (16.29)
\end{aligned}$$

Let $\boldsymbol{E}_1$ and $\boldsymbol{E}_2$ denote the values that the field $\boldsymbol{E}(\boldsymbol{x})$ takes within phases 1 and 2. Then the field $\boldsymbol{J}(\boldsymbol{x})$ takes the value $\boldsymbol{L}_1\boldsymbol{E}_1$ in phase 1 and $\boldsymbol{L}_2\boldsymbol{E}_2$ in phase 2 and we have

$$\begin{aligned}
(\boldsymbol{L}_* - \boldsymbol{L}_2)\boldsymbol{E}_0 = \langle \boldsymbol{J} \rangle - \boldsymbol{L}_2\langle \boldsymbol{E} \rangle &= f_1\boldsymbol{L}_1\boldsymbol{E}_1 + f_2\boldsymbol{L}_2\boldsymbol{E}_2 - \boldsymbol{L}_2(f_1\boldsymbol{E}_1 + f_2\boldsymbol{E}_2) \\
&= f_1(\boldsymbol{L}_1 - \boldsymbol{L}_2)\boldsymbol{E}_1.
\end{aligned}$$

Hence (16.29) reduces to the condition

$$\boldsymbol{E}_1 \cdot (\boldsymbol{L}_1 - \boldsymbol{L}_2)\frac{d\boldsymbol{\Gamma}(\boldsymbol{n}/|\boldsymbol{n}|)}{d\boldsymbol{n}}(\boldsymbol{L}_1 - \boldsymbol{L}_2)\boldsymbol{E}_1 = 0. \qquad (16.30)$$

In a multiple-rank laminate subject to an applied field $\boldsymbol{E}_0$, the relation (16.4) implies that the condition (16.30) must necessarily hold at each level in the laminate if the energy is to be stable under small variations in the directions of lamination. At any given level in the multiple-rank laminate $\boldsymbol{L}_1$ and $\boldsymbol{L}_2$ should be identified with the effective tensors of the materials that are laminated together, and $\boldsymbol{E}_1$ should be identified with the average of the field $\boldsymbol{E}(\boldsymbol{x})$ taken over the material with effective tensor $\boldsymbol{L}_1$.

The conditions (16.28) and (16.30) provide equalities that must necessarily be satisfied at each level in a multiple-rank laminate if the structure is to minimize the overall energy. Cherkaev (2000) found that there are additional inequalities that the fields must necessarily satisfy. These arise when one considers how the energy changes when a portion of one phase is replaced by another phase or by a composite of several phases.

References

Axell, J. 1992, August 15. Bounds for field fluctuations in two-phase materials. *Journal of Applied Physics* 72(4):1217–1220. {*344, 346, 352*}

Beran, M. J. 1980. Field fluctuations in a two-phase random medium. *Journal of Mathematical Physics* 21:2583–2585. {*344, 352*}

Bergman, D. J. 1978. The dielectric constant of a composite material — A problem in classical physics. *Physics Reports* 43(9):377–407. {*341, 352, 370, 371, 376, 377, 379, 382, 387, 390, 392, 569, 581, 590, 597, 603, 617*}

Bergman, D. J. 1983. Self-duality and the low field Hall effect in 2D and 3D metal-insulator composites. In G. Deutscher, R. Zallen, and J. Adler (eds.), *Percolation Structures and Processes*, pp. 297–321. Jerusalem: Israel Physical Society. ISBN 0-85274-477-3. {*65, 70, 344, 352*}

Bobeth, M. and G. Diener 1986. Field fluctuations in multicomponent mixtures. *Journal of the Mechanics and Physics of Solids* 34:1–17. {*344, 353*}

Cheng, H. and S. Torquato 1997. Electric-field fluctuations in random dielectric composites. *Physical Review B (Solid State)* 56(13):8060–8068. {*346, 353*}

Cherkaev, A. V. 2000. *Variational Methods for Structural Optimization*. Berlin / Heidelberg / London / etc.: Springer-Verlag. xxvi + 545 pp. ISBN 0-387-98462-3. {*xxv, xxvi, 352, 353, 426, 434, 666, 668*}

Hashin, Z. and S. Shtrikman 1962. A variational approach to the theory of the effective magnetic permeability of multiphase materials. *Journal of Applied Physics* 33:3125–3131. {*113, 116, 140, 271, 279, 287, 347, 350, 353, 457, 458, 460, 493, 574, 586, 598*}

Lipton, R. 2000. Optimal bounds on electric field fluctuations for random composites. *Journal of Applied Physics* 88(7):4287–4293. {*346, 353, 370, 394*}

Lipton, R. 2001. Optimal bounds on field fluctuations for random composites - three dimensional problems. *Journal of Applied Physics* 89(2):1371–1376. {*346, 353*}

Lurie, K. A. and A. V. Cherkaev 1986. Exact estimates of the conductivity of a binary mixture of isotropic materials. *Proceedings of the Royal Society of Edinburgh. Section A, Mathematical and Physical Sciences* 104(1–2):21–38. {*167, 182, 347, 353, 462, 494, 508, 521, 526*}

Markov, K. Z. 2000. Elementary micromechanics of heterogeneous media. In K. Markov and L. Preziosi (eds.), *Heterogeneous Media: Micromechanics Modeling Methods and Simulations*, Modeling and Simulation in Science, Engineering and Technology, pp. 1–162. Basel, Switzerland: Birkhäuser Verlag. ISBN 0-8176-4083-5. {*xxv, xxvii, 2, 16, 185, 217, 346, 353*}

Matheron, G. 1993. Quelques inégalités pour la perméabilité effective d'un milieu poreux hétérogène. (French) [Some inequalities for the effective permeability of a heterogeneous porous medium]. *Cahiers de Géostatistique* 3:1–20. {*346, 353*}

Murat, F. and L. Tartar 1985. Calcul des variations et homogénísation. (French) [Calculus of variation and homogenization]. In *Les méthodes de l'homogénéisation: théorie et applications en physique*, pp. 319–369. Paris: Eyrolles. English translation in *Topics in the Mathematical Modelling of Composite Materials*, pp. 139–173, ed. by A. Cherkaev and R. Kohn, ISBN 0-8176-3662-5. {*12, 13, 17, 347, 353, 429, 431, 432, 435, 444, 454, 462, 495, 499, 503, 506, 508, 521, 527, 529, 551*}

Willis, J. R. 1977. Bounds and self-consistent estimates for the overall properties of anisotropic composites. *Journal of the Mechanics and Physics of Solids* 25:185–202. {*256, 269, 327, 340, 347, 353, 464, 497*}

17

The general theory of exact relations and links between effective tensors

So far we have been considering exact relations and links between effective tensors on a case-by-case basis. Grabovsky (1998) recognized that there should be some general theory of exact relations. Utilizing the fact that an exact relation must hold for laminate materials, he derived restrictive constraints on the form that an exact relation can take. This reduced the search for candidate exact relations to an algebraic question that was analyzed by Grabovsky and Sage (1998). Subsequently sufficient conditions were found for an exact relation to hold for all composite microgeometries, and not just laminates or multiple-rank laminates (Grabovsky and Milton 1998a; Grabovsky, Milton, and Sage 2000). A measure of the success of this approach is that it has produced complete lists of all (rotationally invariant) exact relations for three-dimensional thermoelectricity and for three-dimensional thermopiezoelectric composites that include all exact relations for elasticity, thermoelasticity, and piezoelectricity as particular cases (Grabovsky, Milton, and Sage 2000). At present the general theory of exact relations is still not finished. There is an apparent gap between the known necessary conditions and the known sufficient conditions for an exact relation to hold. In addition, the associated algebraic questions have only begun to be investigated.

17.1. Links between effective tensors as exact relations: The idea of embedding

Any exact microstructure-independent relation satisfied by an effective tensor $\boldsymbol{L}_*$ implies that $\boldsymbol{L}_*$ lies on smooth manifold $\mathcal{M}$ with an empty interior in tensor space. For example, we have seen that the effective conductivity tensor $\boldsymbol{\sigma}_*$ of a two-dimensional polycrystal formed from a single crystal with conductivity $\boldsymbol{\sigma}_0$ lies on the manifold $\det \boldsymbol{\sigma}_* = \det \boldsymbol{\sigma}_0$ (see section 3.3 on page 50). Besides this type of exact relation, there are also various links between effective tensors or effective moduli (which are also known as cross-property relations). For example, given a two-dimensional material with a (possibly nonsymmetric) conductivity tensor $\boldsymbol{\sigma}(\boldsymbol{x})$ and effective tensor $\boldsymbol{\sigma}_*$, we have seen that the dual material with conductivity tensor $\boldsymbol{\sigma}'(\boldsymbol{x}) = [\boldsymbol{\sigma}(\boldsymbol{x})]^T / \det \boldsymbol{\sigma}(\boldsymbol{x})$ has effective conductivity tensor $\boldsymbol{\sigma}'_* = [\boldsymbol{\sigma}_*]^T / \det \boldsymbol{\sigma}_*$ (see section 3.1 on page 47). This result can be regarded as an exact relation if we embed the problem in a coupled field setting. The idea of embedding was initially introduced as a tool for bounding effective tensors using the translation method. It will be discussed again in section 24.5 on page 505.

Consider the coupled field problem

$$\begin{pmatrix} \boldsymbol{j}(\boldsymbol{x}) \\ \boldsymbol{j}'(\boldsymbol{x}) \end{pmatrix} = \boldsymbol{\mathcal{L}}(\boldsymbol{x}) \begin{pmatrix} \boldsymbol{e}(\boldsymbol{x}) \\ \boldsymbol{e}'(\boldsymbol{x}) \end{pmatrix}, \quad \text{where} \quad \begin{matrix} \nabla \cdot \boldsymbol{j} = 0, & \nabla \times \boldsymbol{e} = 0, \\ \nabla \cdot \boldsymbol{j}' = 0, & \nabla \times \boldsymbol{e}' = 0. \end{matrix}$$

Define our manifold $\mathcal{M}$ as the set of tensors $\boldsymbol{\mathcal{L}}$ expressible in the form

$$\boldsymbol{\mathcal{L}} = \begin{pmatrix} \boldsymbol{\sigma} & 0 \\ 0 & [\boldsymbol{\sigma}]^T / \det \boldsymbol{\sigma} \end{pmatrix},$$

for some $\boldsymbol{\sigma}$ with a positive-definite symmetric part. In this setting, the duality result is equivalent to saying that $\boldsymbol{\mathcal{L}}_*$ lies in $\mathcal{M}$ whenever $\boldsymbol{\mathcal{L}}(\boldsymbol{x})$ lies in $\mathcal{M}$ for all $\boldsymbol{x}$, that is, the manifold $\mathcal{M}$ defines an exact relation.

We have seen in chapter 4 on page 59 that when a tensor field $\boldsymbol{L}(\boldsymbol{x})$ is translated by certain constant tensors $\boldsymbol{T}$ (with the property that $\boldsymbol{T}\mathcal{E} \subset \mathcal{J}$) the effective tensor $\boldsymbol{L}_*$ undergoes exactly the same translation. This result can also be regarded as an exact relation in a coupled field setting. Consider the coupled field problem

$$\begin{pmatrix} \boldsymbol{J}(\boldsymbol{x}) \\ \boldsymbol{J}'(\boldsymbol{x}) \end{pmatrix} = \boldsymbol{\mathcal{L}}(\boldsymbol{x}) \begin{pmatrix} \boldsymbol{E}(\boldsymbol{x}) \\ \boldsymbol{E}'(\boldsymbol{x}) \end{pmatrix}, \quad \text{where } \boldsymbol{E}, \boldsymbol{E}' \in \mathcal{U} \oplus \mathcal{E} \text{ and } \boldsymbol{J}, \boldsymbol{J}' \in \mathcal{U} \oplus \mathcal{J},$$

and let $\boldsymbol{\mathcal{L}}_*$ denote the associated effective tensor. Let $\boldsymbol{T}$ be fixed and define our manifold $\mathcal{M} = \mathcal{M}(\boldsymbol{T})$ as the set of positive-definite tensors $\boldsymbol{\mathcal{L}}$ expressible in the form

$$\boldsymbol{\mathcal{L}} = \begin{pmatrix} \boldsymbol{L} & 0 \\ 0 & \boldsymbol{L} + \boldsymbol{T} \end{pmatrix},$$

for some choice of $\boldsymbol{L}$. The statement that the effective tensor $\boldsymbol{L}_*$ is translated by $\boldsymbol{T}$ when $\boldsymbol{L}(\boldsymbol{x})$ is translated by $\boldsymbol{T}$ is equivalent to saying that this manifold $\mathcal{M}$ defines an exact relation.

Similarly, the covariance property (6.9) associated with coupled equations can be regarded as being equivalent to an exact relation in an extended coupled equation setting, with twice the number of fields. Given fixed, nonsingular matrices $\boldsymbol{\mathcal{V}}$ and $\boldsymbol{\mathcal{W}}$ of the form (6.5) we define our manifold $\mathcal{M} = \mathcal{M}(\boldsymbol{\mathcal{V}}, \boldsymbol{\mathcal{W}})$ to consist of positive-definite tensors expressible in the form

$$\begin{pmatrix} \boldsymbol{\mathcal{L}} & 0 \\ 0 & \boldsymbol{\mathcal{W}}\boldsymbol{\mathcal{L}}\boldsymbol{\mathcal{V}}^{-1} \end{pmatrix},$$

for some choice of $\boldsymbol{\mathcal{L}}$. Then the covariance property is equivalent to saying that $\mathcal{M}$ defines an exact relation.

Hill's formula,

$$(\lambda_* + 2\mu)^{-1} = \langle\, (\lambda + 2\mu)^{-1} \rangle \tag{17.1}$$

(see section 5.3 on page 77), for the effective Lame modulus λ_* of a locally isotropic composite with constant shear modulus can be reinterpreted as a link between effective moduli, and hence as an exact relation in a coupled field setting. Consider the equations of thermoelasticity in the absence of coupling,

$$\begin{pmatrix} \boldsymbol{\tau}(\boldsymbol{x}) \\ \theta \end{pmatrix} = \boldsymbol{L}(\boldsymbol{x}) \begin{pmatrix} \boldsymbol{\epsilon}(\boldsymbol{x}) \\ \varsigma(\boldsymbol{x}) \end{pmatrix}, \quad \text{where } \boldsymbol{L}(\boldsymbol{x}) = \begin{pmatrix} \boldsymbol{\mathcal{C}}(\boldsymbol{x}) & 0 \\ 0 & T_0/c(\boldsymbol{x}) \end{pmatrix},$$

in which θ is the (constant) change in temperature measured from the base temperature T_0, $\varsigma(\boldsymbol{x})$ is the entropy increase per unit volume over the entropy of the state where $\theta = 0$, and $c(\boldsymbol{x})$ is the specific heat. Since θ is constant, the associated effective specific heat is simply

$$c_* = \langle c \rangle.$$

So in a locally isotropic composite with constant shear modulus μ, Hill's result implies that if for some constant k,

$$c(\boldsymbol{x}) = T_0/k[\lambda(\boldsymbol{x}) + 2\mu], \quad \text{then } c_* = T_0/k[\lambda_* + 2\mu].$$

Thus the effective moduli c_*, λ_*, and $\mu_* = \mu$ are linked in this medium. Equivalently, an exact relation is defined by the one-dimensional manifold $\mathcal{M} = \mathcal{M}(\mu, k)$ consisting of thermoelastic tensors expressible in the form

$$\boldsymbol{L} = \begin{pmatrix} \lambda \boldsymbol{I} \otimes \boldsymbol{I} + 2\mu \boldsymbol{\mathcal{I}} & 0 \\ 0 & k(\lambda + 2\mu) \end{pmatrix},$$

for some choice of λ.

These examples show that an understanding of exact relations is also key to understanding the links between effective tensors.

17.2. Necessary conditions for an exact relation

Assume that we are looking for a manifold $\mathcal{M}$ that defines an exact relation. Let us make the simplifying assumption that the tensors in $\mathcal{M}$ are symmetric. Naturally this manifold must be stable under lamination; that is, if we take any two tensors $\boldsymbol{A}$ and $\boldsymbol{B}$ in the manifold $\mathcal{M}$ and laminate them together in proportions f and $1 - f$, then the effective tensor $\boldsymbol{A}_*$ must also lie in the manifold. This stability under lamination imposes rather stringent conditions on the nature of the manifold.

Let us take $\boldsymbol{L}_0$ to be a positive-definite tensor in the manifold and introduce the transformation

$$W_{\boldsymbol{n}}(\boldsymbol{L}) = [\boldsymbol{I} + (\boldsymbol{L} - \boldsymbol{L}_0)\boldsymbol{\Gamma}(\boldsymbol{n})]^{-1}(\boldsymbol{L} - \boldsymbol{L}_0) = \boldsymbol{K}, \tag{17.2}$$

and the associated inverse transformation

$$W_{\boldsymbol{n}}^{-1}(\boldsymbol{K}) = \boldsymbol{L}_0 + [\boldsymbol{I} - \boldsymbol{K}\boldsymbol{\Gamma}(\boldsymbol{n})]^{-1}\boldsymbol{K} = \boldsymbol{L}.$$

It then follows from formula (9.44) (adapted to the case where $\boldsymbol{L} - \boldsymbol{L}_0$ is possibly singular) that

$$W_{\boldsymbol{n}}(\boldsymbol{A}_*) = f W_{\boldsymbol{n}}(\boldsymbol{A}) + (1 - f) W_{\boldsymbol{n}}(\boldsymbol{B}).$$

So, as f is varied from 0 to 1, $W_{\boldsymbol{n}}(\boldsymbol{A}_*)$ varies along the straight line in tensor space joining $W_{\boldsymbol{n}}(\boldsymbol{A})$ with $W_{\boldsymbol{n}}(\boldsymbol{B})$. Therefore, stability under lamination implies that $W_{\boldsymbol{n}}(\mathcal{M})$ must be convex. Since it is has an empty interior, it follows that for a fixed value of $\boldsymbol{n}$, $W_{\boldsymbol{n}}(\mathcal{M})$ lies in a hyperplane $\mathcal{K}$. (Strictly speaking, we should label this hyperplane as $\mathcal{K}_{\boldsymbol{n}}$, but we will see shortly that $\mathcal{K}_{\boldsymbol{n}}$ does not vary with the choice of $\boldsymbol{n}$.) The hyperplane $\mathcal{K}$ must pass through the origin because $W_{\boldsymbol{n}}(\boldsymbol{L}_0) = 0$, that is, $\mathcal{K}$ is a subspace in the space of symmetric tensors. Moreover, $W_{\boldsymbol{m}}(W_{\boldsymbol{n}}^{-1}(\mathcal{K}))$ must also be a subspace for each choice of unit vector $\boldsymbol{m}$. Now, given some tensor $\boldsymbol{K} \in \mathcal{K}$ and expanding $W_{\boldsymbol{m}}(W_{\boldsymbol{n}}^{-1}(\epsilon \boldsymbol{K}))$ in powers of ϵ gives

$$\begin{aligned} W_{\boldsymbol{m}}(W_{\boldsymbol{n}}^{-1}(\epsilon \boldsymbol{K})) &= \epsilon \boldsymbol{K}\{\boldsymbol{I} - [\boldsymbol{\Gamma}(\boldsymbol{n}) - \boldsymbol{\Gamma}(\boldsymbol{m})]\epsilon \boldsymbol{K}\}^{-1} \\ &= \epsilon \boldsymbol{K} + \epsilon^2 \boldsymbol{K}\boldsymbol{A}(\boldsymbol{m})\boldsymbol{K} + \epsilon^3 \boldsymbol{K}\boldsymbol{A}(\boldsymbol{m})\boldsymbol{K}\boldsymbol{A}(\boldsymbol{m})\boldsymbol{K} \\ &\quad + \epsilon^4 \boldsymbol{K}\boldsymbol{A}(\boldsymbol{m})\boldsymbol{K}\boldsymbol{A}(\boldsymbol{m})\boldsymbol{K}\boldsymbol{A}(\boldsymbol{m})\boldsymbol{K} + \cdots, \end{aligned}$$

where $\boldsymbol{A}(\boldsymbol{m})$ is the symmetric matrix

$$\boldsymbol{A}(\boldsymbol{m}) = \boldsymbol{\Gamma}(\boldsymbol{n}) - \boldsymbol{\Gamma}(\boldsymbol{m}). \tag{17.3}$$

Since the linear term is $\epsilon \boldsymbol{K}$, the subspace $W_{\boldsymbol{m}}(W_{\boldsymbol{n}}^{-1}(\mathcal{K}))$ must in fact be $\mathcal{K}$ itself, that is, $\mathcal{K}$ does not depend on $\boldsymbol{n}$. From an examination of the quadratic term we then see that

$$\boldsymbol{K}\boldsymbol{A}(\boldsymbol{m})\boldsymbol{K} \in \mathcal{K} \text{ for all } \boldsymbol{m} \text{ and for all } \boldsymbol{K} \in \mathcal{K}. \tag{17.4}$$

Higher order terms in the expansion do not yield any additional constraints. Indeed, substitution of $\boldsymbol{K} = \boldsymbol{K}_1 + \boldsymbol{K}_2$ in (17.4), where $\boldsymbol{K}_1$ and $\boldsymbol{K}_2$ both lie in $\mathcal{K}$, yields the corollary,

$$\boldsymbol{K}_1\boldsymbol{A}(\boldsymbol{m})\boldsymbol{K}_2 + \boldsymbol{K}_2\boldsymbol{A}(\boldsymbol{m})\boldsymbol{K}_1 \in \mathcal{K} \text{ for all } \boldsymbol{K}_1, \boldsymbol{K}_2 \in \mathcal{K}. \tag{17.5}$$

Applying this with $\boldsymbol{K}_1 = \boldsymbol{K}$ and $\boldsymbol{K}_2 = \boldsymbol{K}\boldsymbol{A}(\boldsymbol{m})\boldsymbol{K}$ shows that the cubic term lies in the space $\mathcal{K}$. Similarly, all of the remaining higher order terms must also lie in $\mathcal{K}$ once (17.4) is satisfied. Therefore condition (17.4) suffices to ensure the stability under lamination of the set of all positive-definite symmetric tensors in $W_{\boldsymbol{n}}^{-1}(\mathcal{K})$.

For example, consider two-dimensional conductivity and take $\boldsymbol{L}_0 = \sigma_0\boldsymbol{I}$. Then $\boldsymbol{A}(\boldsymbol{m}) = (\boldsymbol{n}\otimes\boldsymbol{n} - \boldsymbol{m}\otimes\boldsymbol{m})/\sigma_0$ is a trace free 2×2 symmetric matrix. Now trace free 2×2 symmetric matrices have the property that the product of any three such matrices is also trace free and symmetric. So (17.4) will be satisfied when $\mathcal{K}$ is the space of trace free 2×2 symmetric matrices. Then $W_{\boldsymbol{n}}^{-1}(\mathcal{K})$ consists of 2×2 symmetric matrices $\boldsymbol{\sigma}_*$ such that $\mathrm{Tr}[(\sigma_0\boldsymbol{I}-\boldsymbol{\sigma}_*)^{-1}] = 1/\sigma_0$. Equivalently, it consists of matrices $\boldsymbol{\sigma}_*$ such that $\det\boldsymbol{\sigma}_* = \sigma_0^2$. Thus the manifold $\mathcal{M}$ of two-dimensional conductivity tensors with constant determinant is stable under lamination.

This suggests a way of narrowing the search for candidate exact relations. Namely, one should look for tensors $\boldsymbol{L}_0$ and tensor subspaces $\mathcal{K}$ such that the algebraic constraint (17.4) is satisfied. Then any multiple-rank laminate constructed from materials with tensors in $W_{\boldsymbol{n}}^{-1}(\mathcal{K})$ will necessarily have an effective tensor in $W_{\boldsymbol{n}}^{-1}(\mathcal{K})$. One important class of exact relations is those in which the manifold $\mathcal{M}$ is rotationally invariant, that is, such that when a tensor $\boldsymbol{L}_*$ lies in $\mathcal{M}$, so too does the rotation of the tensor $\boldsymbol{L}_*$. When $\boldsymbol{L}_0$ is chosen to be isotropic, that is, rotationally invariant, the subspace $\mathcal{K}$ containing $W_{\boldsymbol{n}}(\mathcal{M})$ must be also rotationally invariant, because it is independent of $\boldsymbol{n}$. Therefore in the search for rotationally invariant exact relations one can restrict attention to rotationally invariant subspaces $\mathcal{K}$ satisfying (17.4). The fact that rotationally invariant subspaces of tensors have been completely characterized makes the systematic search for such subspaces $\mathcal{K}$ numerically feasible.

One of the many nontrivial candidate exact relations found in this way by Grabovsky and Sage (1998) is for three-dimensional elasticity. The manifold $\mathcal{M} = \mathcal{M}(\mu_0)$ consists of all positive-definite elasticity tensors $\boldsymbol{\mathcal{C}}$ expressible in the form

$$\boldsymbol{\mathcal{C}} = 2\mu_0\boldsymbol{T} + \boldsymbol{A}\otimes\boldsymbol{A}, \tag{17.6}$$

for some choice of symmetric second-order tensor $\boldsymbol{A}$, where $\boldsymbol{T}$ is the fourth-order isotropic tensor with elements

$$T_{ijk\ell} = (\delta_{ij}\delta_{k\ell} + \delta_{ij}\delta_{k\ell})/2 - \delta_{ij}\delta_{k\ell}.$$

The elasticity tensor $\boldsymbol{\mathcal{C}}$ will be positive-definite if and only μ_0 is positive and $\boldsymbol{A}$ is chosen so that

$$[\mathrm{Tr}(\boldsymbol{A})]^2 - 2\,\mathrm{Tr}(\boldsymbol{A}^2) \geq 4\mu_0 \geq 0. \tag{17.7}$$

In section 17.4 on page 361 we will establish that this manifold $\mathcal{M}$ does in fact define an exact relation valid for all composites and not just laminates. The condition (17.7) is important because the relation does not extend to arbitrary positive-semidefinite matrices $\boldsymbol{\mathcal{C}}$ of the form (17.6). As noticed by Leonid Gibiansky (private communication), laminating two

rank-1 elasticity tensors with tensors $\mathcal{C}_1 = \boldsymbol{n}_1\boldsymbol{n}_1\boldsymbol{n}_1\boldsymbol{n}_1$ and $\mathcal{C}_2 = \boldsymbol{n}_2\boldsymbol{n}_2\boldsymbol{n}_2\boldsymbol{n}_2$ in proportions f_1 and $f_2 = 1 - f_1$ in direction $\boldsymbol{n}_3$, where $\boldsymbol{n}_1$, $\boldsymbol{n}_2$, and $\boldsymbol{n}_3$ are three mutually orthogonal vectors, produces an effective elasticity tensor $\mathcal{C}_* = f_1\mathcal{C}_1 + f_2\mathcal{C}_2$ that is rank 2, and therefore not of the form (17.6).

For two-dimensional elasticity the stability under homogenization of the manifold $\mathcal{M}$ was established by Grabovsky and Milton (1998b) using elliptic partial differential theory. Gibiansky (1998) subsequently found a much simpler proof using quasiconvexity.

17.3. Sufficient conditions for an exact relation

Naturally we would like to ensure that the set of all positive-definite tensors in $W_{\boldsymbol{n}}^{-1}(\mathcal{K})$ is stable under homogenization and not just lamination, that is, to ensure that any composite with $\boldsymbol{L}(\boldsymbol{x}) \in W_{\boldsymbol{n}}^{-1}(\mathcal{K})$ always has an effective tensor $\boldsymbol{L}_* \in W_{\boldsymbol{n}}^{-1}(\mathcal{K})$. Here we will prove that it is sufficient that there exist a larger space $\overline{\mathcal{K}}$ such that

$$\boldsymbol{K}_1\boldsymbol{A}(\boldsymbol{m})\boldsymbol{K}_2 \in \overline{\mathcal{K}} \quad \text{for all } \boldsymbol{m} \text{ and for all } \boldsymbol{K}_1, \boldsymbol{K}_2 \in \overline{\mathcal{K}}, \tag{17.8}$$

and such that $\mathcal{K}$ equals the subspace of all symmetric matrices in $\overline{\mathcal{K}}$. This condition is sufficient to guarantee the stability under homogenization of not just the set of positive-definite tensors in $W_{\boldsymbol{n}}^{-1}(\mathcal{K})$, but also of the larger set of tensors in $W_{\boldsymbol{n}}^{-1}(\overline{\mathcal{K}})$ that have positive-definite symmetric parts.

To establish this consider the series expansion (14.44), which we rewrite here as

$$\boldsymbol{K}_* = \sum_{j=0}^{\infty} \langle \boldsymbol{Q}_j \rangle, \tag{17.9}$$

where the fields $\boldsymbol{Q}_i(\boldsymbol{x})$ are given by the recursion relations

$$\boldsymbol{Q}_0 = \boldsymbol{K}, \quad \boldsymbol{Q}_{j+1} = \boldsymbol{K}\boldsymbol{A}\boldsymbol{Q}_j, \quad \text{where } \boldsymbol{A} = \boldsymbol{M}(\boldsymbol{I} - \boldsymbol{\Gamma}_0) - \boldsymbol{\Gamma}, \tag{17.10}$$

in which

$$\begin{aligned} \boldsymbol{K}(\boldsymbol{x}) &= [\boldsymbol{I} + (\boldsymbol{L}(\boldsymbol{x}) - \boldsymbol{L}_0)\boldsymbol{M}]^{-1}(\boldsymbol{L}(\boldsymbol{x}) - \boldsymbol{L}_0), \\ \boldsymbol{K}_* &= [\boldsymbol{I} + (\boldsymbol{L}_* - \boldsymbol{L}_0)\boldsymbol{M}]^{-1}(\boldsymbol{L}_* - \boldsymbol{L}_0), \end{aligned}$$

and $\boldsymbol{M}$ is now not necessarily equal to $\boldsymbol{\Gamma}(\boldsymbol{n})$, although we will see shortly that there are good reasons for taking $\boldsymbol{M} = \boldsymbol{\Gamma}(\boldsymbol{n})$. Our objective is to prove by induction that all of the fields $\boldsymbol{Q}_i(\boldsymbol{x})$ take values in the space $\overline{\mathcal{K}}$ when $\boldsymbol{Q}_0(\boldsymbol{x}) = \boldsymbol{K}(\boldsymbol{x})$ takes values in the space $\overline{\mathcal{K}}$ and condition (17.8) is satisfied with

$$\boldsymbol{A}(\boldsymbol{m}) = \boldsymbol{M} - \boldsymbol{\Gamma}(\boldsymbol{m}). \tag{17.11}$$

Let us assume that for some j the field $\boldsymbol{Q}_j(\boldsymbol{x})$ takes values in $\overline{\mathcal{K}}$. This is certainly true when $j = 0$. The real and imaginary parts of the Fourier coefficients $\widehat{\boldsymbol{Q}}_j(\boldsymbol{k})$ of $\boldsymbol{Q}_j(\boldsymbol{x})$ naturally will also take values in $\overline{\mathcal{K}}$. Then, since $\boldsymbol{Q}_{j+1} = \boldsymbol{K}\boldsymbol{A}\boldsymbol{Q}_j$, we have

$$\boldsymbol{Q}_{j+1}(\boldsymbol{x}) = \sum_{\boldsymbol{k}\neq 0} e^{i\boldsymbol{k}\cdot\boldsymbol{x}}\boldsymbol{K}(\boldsymbol{x})\boldsymbol{A}(\boldsymbol{k})\widehat{\boldsymbol{Q}}_j(\boldsymbol{k}), \tag{17.12}$$

where $\boldsymbol{A}(\boldsymbol{m})$ is given by (17.11). Applying (17.8) with $\boldsymbol{K}_1 = \boldsymbol{K}(\boldsymbol{x}) \in \overline{\mathcal{K}}$ and with $\boldsymbol{K}_2$ equal to the real and imaginary parts of $\widehat{\boldsymbol{Q}}_j(\boldsymbol{k})$, we conclude that $\boldsymbol{Q}_{j+1}(\boldsymbol{x})$, being real, takes values in $\overline{\mathcal{K}}$. By induction it follows that all of the fields $\boldsymbol{Q}_i(\boldsymbol{x})$ take values in $\overline{\mathcal{K}}$. Provided that the series expansion converges, this implies that $\boldsymbol{K}_*$ lies in $\overline{\mathcal{K}}$.

Now define $W_{\boldsymbol{M}}$ as the fractional linear matrix transformation

$$W_{\boldsymbol{M}}(\boldsymbol{L}) = [\boldsymbol{I} + (\boldsymbol{L} - \boldsymbol{L}_0)\boldsymbol{M}]^{-1}(\boldsymbol{L} - \boldsymbol{L}_0), \tag{17.13}$$

$W_{\boldsymbol{M}}^{-1}$ as the associated inverse transformation

$$W_{\boldsymbol{M}}^{-1}(\boldsymbol{K}) = \boldsymbol{L}_0 + [\boldsymbol{I} - \boldsymbol{K}\boldsymbol{M}]^{-1}\boldsymbol{K},$$

and $\mathcal{M}$ as the manifold consisting of tensors in $W_{\boldsymbol{M}}^{-1}(\overline{\mathcal{K}})$ with positive-definite symmetric parts. We have established that the effective tensor $\boldsymbol{L}_*$ necessarily lies in $\mathcal{M}$ when $\boldsymbol{L}(\boldsymbol{x})$ takes values in $\mathcal{M}$, provided that at least $\boldsymbol{K}(\boldsymbol{x}) = W_{\boldsymbol{M}}(\boldsymbol{L}(\boldsymbol{x}))$ is small enough (for all $\boldsymbol{x}$) that the series expansion converges.

By differentiating the constraint (17.8) with respect to $\boldsymbol{m}$ we see that it implies that

$$\boldsymbol{K}_1 \frac{d\boldsymbol{\Gamma}(\boldsymbol{m})}{d\boldsymbol{m}} \boldsymbol{K}_2 \in \overline{\mathcal{K}} \quad \text{for all } \boldsymbol{m} \text{ and for all } \boldsymbol{K}_1, \boldsymbol{K}_2 \in \overline{\mathcal{K}}. \tag{17.14}$$

Conversely, if this condition holds, and in addition (17.8) is satisfied for any one value of $\boldsymbol{m}$, say $\boldsymbol{m} = \boldsymbol{n}$, where $\boldsymbol{n}$ is a fixed unit vector, that is,

$$\boldsymbol{K}_1[\boldsymbol{M} - \boldsymbol{\Gamma}(\boldsymbol{n})]\boldsymbol{K}_2 \in \overline{\mathcal{K}} \quad \text{and for all } \boldsymbol{K}_1, \boldsymbol{K}_2 \in \overline{\mathcal{K}}, \tag{17.15}$$

then by integrating (17.14) we see that the condition (17.8) will be satisfied for all values of $\boldsymbol{m}$. Clearly this second condition is automatically satisfied if we take $\boldsymbol{M} = \boldsymbol{\Gamma}(\boldsymbol{n})$. Other choices of $\boldsymbol{M}$ satisfying (17.15) all lead to the same exact relation. To establish this it suffices to show that $W_{\boldsymbol{M}}^{-1}(\overline{\mathcal{K}}) = W_{\boldsymbol{n}}^{-1}(\overline{\mathcal{K}})$, in which $W_{\boldsymbol{n}}$ is the transformation defined by (17.2), that is, $W_{\boldsymbol{n}} = W_{\boldsymbol{\Gamma}(\boldsymbol{n})}$. We omit the proof that $W_{\boldsymbol{M}}(W_{\boldsymbol{n}}^{-1}(\overline{\mathcal{K}}))$ equals $\overline{\mathcal{K}}$ since it proceeds in the same way as the proof given in the previous section that $W_{\boldsymbol{m}}(W_{\boldsymbol{n}}^{-1}(\mathcal{K}))$ equals $\mathcal{K}$ when (17.4) is satisfied: At each step it is only necessary to replace $\boldsymbol{\Gamma}(\boldsymbol{m})$ with $\boldsymbol{M}$ and $\mathcal{K}$ with $\overline{\mathcal{K}}$.

Even if the perturbation expansion does not converge, analytic continuation arguments imply that the exact relation still holds provided $\boldsymbol{L}(\boldsymbol{x})$ is bounded and coercive. Briefly, we can consider a one-parameter family of composite materials with $\boldsymbol{K}(\boldsymbol{x})$ replaced by $\boldsymbol{K}_\lambda(\boldsymbol{x}) = \lambda\boldsymbol{K}(\boldsymbol{x})$. The one-parameter family of associated tensors $\boldsymbol{K}_*$, which we denote as $\boldsymbol{K}_{\lambda *}$, defines a matrix-valued function of λ that will be analytic for λ between zero and 1. (One can check that $\boldsymbol{K}_{\lambda *}$ is bounded when the associated effective tensor $\boldsymbol{L}_{\lambda *}$ is bounded and coercive.) So if we take any matrix $\boldsymbol{K}_\perp$ orthogonal to $\overline{\mathcal{K}}$, then the function $f(\lambda) = \mathrm{Tr}(\boldsymbol{K}_\perp^T \boldsymbol{K}_{\lambda *})$ is also an analytic function of λ for λ between zero and 1. For small values of λ, say $|\lambda| < \lambda^+$, the perturbation expansion converges and the exact relation holds. Therefore we have $f(\lambda) = 0$ for $|\lambda| < \lambda^+$. Analytic continuation then implies that $f(\lambda) = 0$ for all λ between zero and 1, and in particular for $\lambda = 1$. Since this holds for any $\boldsymbol{K}_\perp$ orthogonal to $\overline{\mathcal{K}}$, the exact relation must hold when $\lambda = 1$; see also Grabovsky, Milton, and Sage (2000).

This suggests the following way of generating exact relations. First find a subspace $\overline{\mathcal{K}}$ satisfying (17.14), and second pick a tensor $\boldsymbol{M}$ such that (17.15) holds. It certainly suffices to take $\boldsymbol{M} = \boldsymbol{\Gamma}(\boldsymbol{n})$, but other choices of $\boldsymbol{M}$ are also possible. Once this is done the set of tensors

in $W_{\boldsymbol{M}}^{-1}(\overline{\mathcal{K}})$ that have positive-definite symmetric parts will be stable under homogenization. Since $\boldsymbol{L}_*$ is symmetric when $\boldsymbol{L}(\boldsymbol{x})$ is symmetric for all $\boldsymbol{x}$, we have the corollary that the set of symmetric positive-definite tensors in $W_{\boldsymbol{M}}^{-1}(\overline{\mathcal{K}})$ is also stable under homogenization. For example, given any vector $\boldsymbol{v}$, the space $\overline{\mathcal{K}}$ consisting of all matrices $\boldsymbol{K}$ such that $\boldsymbol{K}\boldsymbol{v} = 0$ satisfies (17.14) and (17.15) holds with $\boldsymbol{M} = 0$. The associated manifold $\mathcal{M}$ consists of all tensors $\boldsymbol{L}_* = \boldsymbol{L}_0 + \boldsymbol{K}$ such that $\boldsymbol{L}_*\boldsymbol{v} = \boldsymbol{L}_0\boldsymbol{v}$. Thus we easily recover the class of exact relations established in section 5.1 on page 75 using the uniform field argument.

17.4. An exact formula for the shear modulus of certain three-dimensional polycrystals

To illustrate the power of this method of generating exact relations, let us consider three-dimensional elasticity and prove that the manifold $\mathcal{M}$ consisting of all positive-definite tensors expressible in the form (17.6) for some choice of $\boldsymbol{A}$ defines an exact relation (Grabovsky and Milton 1998a). We take $\boldsymbol{L}_0$ to be an arbitrary isotropic elasticity tensor with bulk modulus κ_0 and shear modulus μ_0. The associated tensor $\boldsymbol{\Gamma}(\boldsymbol{n})$, given by (9.59) with μ_2 replaced by μ_0 and λ_2 replaced by $\kappa_0 - 2\mu_0/3$, has the property that $\mathrm{Tr}[\boldsymbol{\Gamma}(\boldsymbol{n})\boldsymbol{I}]$ is independent of $\boldsymbol{n}$, implying that

$$\mathrm{Tr}\{[\boldsymbol{\Gamma}(\boldsymbol{n}) - \boldsymbol{\Gamma}(\boldsymbol{m})]\boldsymbol{I}\} = 0 \text{ for all } \boldsymbol{n} \text{ and } \boldsymbol{m}, \tag{17.16}$$

in which $\boldsymbol{I}$ is the second-order identity tensor upon which the fourth-order tensor $\boldsymbol{\Gamma}(\boldsymbol{n}) - \boldsymbol{\Gamma}(\boldsymbol{m})$ acts. Now consider the subspace $\overline{\mathcal{K}}$ consisting of all fourth-order tensors $\boldsymbol{K}$ expressible in the form

$$\boldsymbol{K} = \boldsymbol{I} \otimes \boldsymbol{B} + \boldsymbol{B}' \otimes \boldsymbol{I},$$

for some choice of symmetric second-order tensors $\boldsymbol{B}$ and $\boldsymbol{B}'$. Given symmetric second-order tensors $\boldsymbol{B}_1$, $\boldsymbol{B}'_1$, $\boldsymbol{B}_2$, and $\boldsymbol{B}'_2$, (17.16) implies that

$$[\boldsymbol{I} \otimes \boldsymbol{B}_1 + \boldsymbol{B}'_1 \otimes \boldsymbol{I}]\boldsymbol{A}(\boldsymbol{m})[\boldsymbol{I} \otimes \boldsymbol{B}_2 + \boldsymbol{B}'_2 \otimes \boldsymbol{I}] = \boldsymbol{I} \otimes \boldsymbol{B}_3 + \boldsymbol{B}'_3 \otimes \boldsymbol{I},$$

with

$$\boldsymbol{B}_3 = [\mathrm{Tr}(\boldsymbol{A}(\boldsymbol{m})\boldsymbol{B}_1)]\boldsymbol{B}_2 + [\mathrm{Tr}(\boldsymbol{B}_1^{\mathrm{T}}\boldsymbol{A}(\boldsymbol{m})\boldsymbol{B}'_2)]\boldsymbol{I}, \quad \boldsymbol{B}'_3 = [\mathrm{Tr}(\boldsymbol{A}(\boldsymbol{m})\boldsymbol{B}'_2)]\boldsymbol{B}'_1.$$

Therefore the subspace $\overline{\mathcal{K}}$ satisfies the desired property (17.8). The subspace $\mathcal{K}$ of symmetric fourth-order tensors within $\overline{\mathcal{K}}$ is six-dimensional and is comprised of tensors of the form $\boldsymbol{K} = \boldsymbol{I} \otimes \boldsymbol{B} + \boldsymbol{B} \otimes \boldsymbol{I}$, where $\boldsymbol{B}$ is a symmetric second-order tensor. Since the relation (17.16) also holds when we replace $\boldsymbol{\Gamma}(\boldsymbol{m})$ with $\boldsymbol{M} = \boldsymbol{I} \otimes \boldsymbol{I}/3(3\kappa_0 + 4\mu_0)$, we have that $W_{\boldsymbol{n}}^{-1}(\mathcal{K}) = W_{\boldsymbol{M}}^{-1}(\mathcal{K})$. This provides an easier way of calculating the manifold $\mathcal{M}$ because the latter transformation is simpler. Explicit calculation shows that

$$\begin{aligned} W_{\boldsymbol{M}}^{-1}&(\boldsymbol{I} \otimes \boldsymbol{B} + \boldsymbol{B} \otimes \boldsymbol{I}) \\ &= \boldsymbol{L}_0 + \{\boldsymbol{\mathcal{I}} - [(\mathrm{Tr}\,\boldsymbol{B})\boldsymbol{I} + 3\boldsymbol{B}] \otimes \boldsymbol{I}/3(3\kappa_0 + 4\mu_0)\}^{-1}(\boldsymbol{I} \otimes \boldsymbol{B} + \boldsymbol{B} \otimes \boldsymbol{I}) \\ &= 2\mu_0(\boldsymbol{\mathcal{I}} - \boldsymbol{I} \otimes \boldsymbol{I}) + \frac{[(3\kappa_0 + 4\mu_0 - \mathrm{Tr}\,\boldsymbol{B})\boldsymbol{I} + 3\boldsymbol{B}] \otimes [(3\kappa_0 + 4\mu_0 - \mathrm{Tr}\,\boldsymbol{B})\boldsymbol{I} + 3\boldsymbol{B}]}{3(3\kappa_0 + 4\mu_0 - 2\,\mathrm{Tr}\,\boldsymbol{B})}, \end{aligned}$$

in which $\boldsymbol{\mathcal{I}}$ is the fourth-order identity tensor. A necessary condition for this to be positive-definite is that $3\kappa_0 + 4\mu_0 - 2\,\mathrm{Tr}\,\boldsymbol{B}$ be positive. The associated manifold $\mathcal{M}$, which consists of all positive-definite elasticity tensors $\boldsymbol{\mathcal{C}}$ expressible in the form (17.6) for some choice of

$$\boldsymbol{A} = [(3\kappa_0 + 4\mu_0 - \mathrm{Tr}\,\boldsymbol{B})\boldsymbol{I} + 3\boldsymbol{B}]/\sqrt{3(3\kappa_0 + 4\mu_0 - 2\,\mathrm{Tr}\,\boldsymbol{B})},$$

is therefore stable under homogenization.

As an example, consider a three-dimensional elastic polycrystal where the elasticity tensor takes the form

$$\mathcal{C}(\boldsymbol{x}) = \boldsymbol{R}(\boldsymbol{x})\boldsymbol{R}(\boldsymbol{x})\mathcal{C}_0\boldsymbol{R}^T(\boldsymbol{x})\boldsymbol{R}^T(\boldsymbol{x}),$$

where $\boldsymbol{R}(\boldsymbol{x})$ is a rotation matrix, giving the orientation of the crystal at each point $\boldsymbol{x}$, and $\mathcal{C}_0$ is the elasticity tensor of a single crystal that we assume has the form

$$\mathcal{C}_0 = 2\mu_0\boldsymbol{T} + \boldsymbol{A}_0 \otimes \boldsymbol{A}_0, \quad \text{where } [\mathrm{Tr}(\boldsymbol{A}_0)]^2 - 2\,\mathrm{Tr}(\boldsymbol{A}_0^2) \geq 4\mu_0 \geq 0.$$

The elasticity tensor field $\mathcal{C}(\boldsymbol{x})$ is of the required form (17.6) with $\boldsymbol{A}(\boldsymbol{x}) = \boldsymbol{R}(\boldsymbol{x})\boldsymbol{A}_0\boldsymbol{R}^T(\boldsymbol{x})$ and therefore the effective tensor $\mathcal{C}_*$ of the polycrystal must lie on the manifold $\mathcal{M}$. In particular, if $\mathcal{C}_*$ is isotropic, then its shear modulus is μ_0, independent of the polycrystal microgeometry. A similar result also holds for two-dimensional polycrystals (Avellaneda, Cherkaev, Gibiansky, Milton, and Rudelson 1996).

17.5. More exact relations for coupled equations†

Consider a coupled field problem where there are m divergence free fields $\boldsymbol{j}_1(\boldsymbol{x})$, $\boldsymbol{j}_2(\boldsymbol{x})$, …, $\boldsymbol{j}_m(\boldsymbol{x})$ and m curl free fields $\boldsymbol{e}_1(\boldsymbol{x})$, $\boldsymbol{e}_2(\boldsymbol{x})$, …, $\boldsymbol{e}_m(\boldsymbol{x})$ that are linked through the constitutive relation

$$j_{i\alpha}(\boldsymbol{x}) = \sum_{j=1}^{d}\sum_{\beta=1}^{m} L_{i\alpha j\beta}(\boldsymbol{x})e_{j\beta}(\boldsymbol{x}),$$

where α and β are field indices while i and j are space indices. Let us first look for exact relations such that the manifold $\mathcal{M}$ contains the identity tensor $\mathcal{I}$. With $\mathcal{L}_0 = \mathcal{I}$ as a reference tensor the associated tensor $\boldsymbol{A}(\boldsymbol{m}) = \boldsymbol{\Gamma}(\boldsymbol{n}) - \boldsymbol{\Gamma}(\boldsymbol{m})$ has elements

$$A_{i\alpha j\beta} = \delta_{\alpha\beta}(n_i n_j - m_i m_j).$$

Now take an r-dimensional subspace $\mathcal{R}$ of $m \times m$ matrices and an s-dimensional subspace $\mathcal{S}$ of $d \times d$ matrices, and consider the rs-dimensional subspace $\overline{\mathcal{K}}$ spanned by all tensors $\boldsymbol{K}$ that are tensor products of matrices $\boldsymbol{R} \in \mathcal{R}$ and matrices $\boldsymbol{S} \in \mathcal{S}$, that is, which have elements

$$K_{i\alpha j\beta} = R_{\alpha\beta}S_{ij}.$$

Given a tensor $\boldsymbol{K}_1$ that is the tensor product of $\boldsymbol{R}_1 \in \mathcal{R}$ and $\boldsymbol{S}_1 \in \mathcal{S}$, and a tensor $\boldsymbol{K}_2$ that is the tensor product of $\boldsymbol{R}_2$ and $\boldsymbol{S}_2 \in \mathcal{S}$, the product $\boldsymbol{K}_1\boldsymbol{A}(\boldsymbol{m})\boldsymbol{K}_2$ will certainly be in $\overline{\mathcal{K}}$ provided that

$$\boldsymbol{R}_1\boldsymbol{R}_2 \in \mathcal{R} \text{ and } \boldsymbol{S}_1(\boldsymbol{n}\otimes\boldsymbol{n} - \boldsymbol{m}\otimes\boldsymbol{m})\boldsymbol{S}_2 \in \mathcal{S}. \tag{17.17}$$

Moreover, if (17.17) holds for all $\boldsymbol{R}_1, \boldsymbol{R}_2 \in \mathcal{R}$, all $\boldsymbol{S}_1, \boldsymbol{S}_2 \in \mathcal{S}$, and all unit vectors $\boldsymbol{n}$ and $\boldsymbol{m}$, then $\overline{\mathcal{K}}$ defines an exact relation because it is spanned matrices of the same form as $\boldsymbol{K}_1$ and $\boldsymbol{K}_2$. This observation allows us to generate countless exact relations (Grabovsky and Milton 1998a). The condition on $\mathcal{R}$ just says that it is closed under multiplication, that is, it is an algebra. The condition on $\mathcal{S}$ will be automatically satisfied if we take $\mathcal{S}$ to be the space of all $d \times d$ matrices. Then (17.15) will be satisfied with $\boldsymbol{M}$=0, and the manifold $\mathcal{M}$ consists of all matrices of the form $\mathcal{L}_* = \mathcal{I} + \boldsymbol{K}$, where $\boldsymbol{K} \in \overline{\mathcal{K}}$. Given fixed, nonsingular matrices $\boldsymbol{V}$ and $\boldsymbol{W}$ of the form (6.5) the covariance property implies that the manifold $\mathcal{M}'$ consisting of all matrices that are of the form $\mathcal{L}_* = \mathcal{W}(\mathcal{I} + \boldsymbol{K})\mathcal{V}^{-1}$, where $\boldsymbol{K} \in \overline{\mathcal{K}}$, is also an exact relation.

For example, in the case $m = 2$, by taking $\mathcal{R}$ to consist of all 2×2 matrices of the form

$$\boldsymbol{R} = \begin{pmatrix} a & b \\ -b & a \end{pmatrix},$$

which is clearly closed under multiplication, we see [using the representation of equation (6.2)] that if the tensor $\boldsymbol{\mathcal{L}}(\boldsymbol{x})$ takes the form

$$\boldsymbol{\mathcal{L}}(\boldsymbol{x}) = \begin{pmatrix} \boldsymbol{A}(\boldsymbol{x}) & \boldsymbol{B}(\boldsymbol{x}) \\ -\boldsymbol{B}(\boldsymbol{x}) & \boldsymbol{A}(\boldsymbol{x}) \end{pmatrix},$$

with $\boldsymbol{A}(\boldsymbol{x})$ being positive-definite for all $\boldsymbol{x}$, then the effective tensor $\boldsymbol{\mathcal{L}}_*$ should take a similar form:

$$\boldsymbol{\mathcal{L}}_* = \begin{pmatrix} \boldsymbol{A}_* & \boldsymbol{B}_* \\ -\boldsymbol{B}_* & \boldsymbol{A}_* \end{pmatrix}.$$

This can be verified by rewriting the constitutive law in the equivalent form of a complex equation

$$\boldsymbol{j}_1(\boldsymbol{x}) + i\boldsymbol{j}_2(\boldsymbol{x}) = (\boldsymbol{A}(\boldsymbol{x}) + i\boldsymbol{B}(\boldsymbol{x}))(\boldsymbol{e}_1(\boldsymbol{x}) + i\boldsymbol{e}_2(\boldsymbol{x})),$$

which will have an associated complex effective tensor $\boldsymbol{A}_* + i\boldsymbol{B}_*$. In two dimensions we can alternatively take $\mathcal{S}$ to be the space of trace free symmetric matrices.

The general question of which subspaces $\mathcal{R}$ are closed under multiplication is a difficult algebraic question, whose general solution is not known. Therefore the general task of characterizing which tensor subspaces $\mathcal{K}$ satisfy the condition (17.4) or which subspaces $\overline{\mathcal{K}}$ satisfy the condition (17.8) is at least as difficult and unlikely to be completely solved in the near future.

17.6. Exact relations with limited statistical information

So far we have been considering exact relations that are microstructure-independent. There are also exact relations that involve limited statistical information about the composite geometry, such as Hill's formula (17.1), which for multiphase composites involves only the moduli and volume fractions of the phases. To see how this type of exact relation can arise consider the condition (17.8) for an exact microstructure-dependent relation to hold. It can be rewritten in the equivalent form

$$\overline{\mathcal{K}}\mathcal{A}\overline{\mathcal{K}} \subset \overline{\mathcal{K}},$$

in which $\mathcal{A}$ is the tensor subspace spanned by the tensors $\boldsymbol{A}(\boldsymbol{m})$ as $\boldsymbol{m}$ varies over all unit vectors, and $\overline{\mathcal{K}}\mathcal{A}\overline{\mathcal{K}}$ is the product of $\overline{\mathcal{K}}$ with $\mathcal{A}\overline{\mathcal{K}}$ while $\mathcal{A}\overline{\mathcal{K}}$ is the product of $\mathcal{A}$ with $\overline{\mathcal{K}}$, where the product $\mathcal{BC}$ of two tensor subspaces $\mathcal{B}$ and $\mathcal{C}$ is defined as the space spanned by all possible products $\boldsymbol{BC}$ of tensors $\boldsymbol{B} \in \mathcal{B}$ and tensors $\boldsymbol{C} \in \mathcal{C}$. Thus $\overline{\mathcal{K}}\mathcal{A}\overline{\mathcal{K}}$ is spanned by tensors of the form $\boldsymbol{K}_1\boldsymbol{A}(\boldsymbol{m})\boldsymbol{K}_2$, where $\boldsymbol{K}_1, \boldsymbol{K}_2 \in \overline{\mathcal{K}}$ and $\boldsymbol{m}$ is a unit vector.

Now, following Grabovsky, Milton, and Sage (2000), suppose that $\overline{\mathcal{K}}$ is such that $\overline{\mathcal{K}}\mathcal{A}\overline{\mathcal{K}}$ is contained within but does not equal $\overline{\mathcal{K}}$. Then there exists a nonempty subspace $\mathcal{S}_1$ that is the orthogonal complement of $\overline{\mathcal{K}}\mathcal{A}\overline{\mathcal{K}}$ in the subspace $\overline{\mathcal{K}}$, that is,

$$\overline{\mathcal{K}} = \overline{\mathcal{K}}\mathcal{A}\overline{\mathcal{K}} \oplus \mathcal{S}_1. \tag{17.18}$$

If $\boldsymbol{\Lambda}_1$ denotes the projection onto $\mathcal{S}_1$, we have

$$\boldsymbol{\Lambda}_1[\boldsymbol{K}_1\boldsymbol{A}(\boldsymbol{m})\boldsymbol{K}_2] = 0$$

for all $\boldsymbol{K}_1, \boldsymbol{K}_2 \in \overline{\mathcal{K}}$ and all unit vectors $\boldsymbol{m}$. Since the field $\boldsymbol{Q}_j(\boldsymbol{x})$ given by the recursion relations (17.10) takes values in $\overline{\mathcal{K}}$ for all $j \geq 0$, the projection $\boldsymbol{\Lambda}_1$ will annihilate the field $\boldsymbol{Q}_{j+1} = \boldsymbol{K}\boldsymbol{A}\boldsymbol{Q}_j$ for all $j \geq 0$, that is,

$$\boldsymbol{\Lambda}_1 \boldsymbol{Q}_{j+1} = 0 \quad \text{for all } j \geq 0.$$

It follows from the series expansion (17.9) that

$$\boldsymbol{\Lambda}_1 \boldsymbol{K}_* = \boldsymbol{\Lambda}_1 \langle \boldsymbol{K} \rangle. \tag{17.19}$$

This is an exact relation that involves only the one-point statistics of the medium.

For example, consider three-dimensional elasticity and take $\boldsymbol{L}_0 = \boldsymbol{\mathcal{C}}_0$ to be an isotropic elasticity tensor with Lame modulus λ_0 and shear modulus μ_0. If $\overline{\mathcal{K}}$ is the one-dimensional space comprised of all fourth-order tensors $\boldsymbol{K}$ that are multiples of $\boldsymbol{I} \otimes \boldsymbol{I}$, then (17.16) implies that $\overline{\mathcal{K}}\mathcal{A}\overline{\mathcal{K}} = 0$. Thus (17.18) is satisfied with $\mathcal{S}_1 = \overline{\mathcal{K}}$ and (17.19) implies that

$$\boldsymbol{K}_* = \langle \boldsymbol{K} \rangle. \tag{17.20}$$

The associated manifold $\mathcal{M}$ consists of all positive-definite isotropic elasticity tensors

$$\boldsymbol{\mathcal{C}} = 2\mu_0 \boldsymbol{\mathcal{I}} + \lambda \boldsymbol{I} \otimes \boldsymbol{I},$$

with fixed shear modulus μ_0 but variable Lame modulus λ. Using (9.59) we have

$$\boldsymbol{\mathcal{C}} - \boldsymbol{\mathcal{C}}_0 = (\lambda - \lambda_0)\boldsymbol{I} \otimes \boldsymbol{I}, \quad (\boldsymbol{\mathcal{C}} - \boldsymbol{\mathcal{C}}_0)\boldsymbol{\Gamma}(\boldsymbol{n}) = [(\lambda - \lambda_0)/(\lambda_0 + 2\mu_0)]\boldsymbol{I} \otimes (\boldsymbol{n} \otimes \boldsymbol{n}),$$

giving

$$\begin{aligned} \boldsymbol{K} &= [\boldsymbol{\mathcal{I}} + (\boldsymbol{\mathcal{C}} - \boldsymbol{\mathcal{C}}_0)\boldsymbol{\Gamma}(\boldsymbol{n})]^{-1}(\boldsymbol{\mathcal{C}} - \boldsymbol{\mathcal{C}}_0) \\ &= \{\boldsymbol{\mathcal{I}} - [(\lambda - \lambda_0)/(\lambda + 2\mu_0)]\boldsymbol{I} \otimes (\boldsymbol{n} \otimes \boldsymbol{n})\}(\lambda - \lambda_0)\boldsymbol{I} \otimes \boldsymbol{I} \\ &= (\lambda_0 + 2\mu_0)[1 - (\lambda_0 + 2\mu_0)/(\lambda + 2\mu_0)]\boldsymbol{I} \otimes \boldsymbol{I}. \end{aligned}$$

By substituting this expression into (17.20) we recover Hill's formula (17.1) for the effective Lame modulus λ_*.

An exact relation that involves only the two-point statistics of the medium is obtained if there exists a nonempty subspace $\mathcal{S}_2$ that is the orthogonal complement of $\overline{\mathcal{K}}\mathcal{A}\overline{\mathcal{K}}\mathcal{A}\overline{\mathcal{K}}$ in the subspace $\overline{\mathcal{K}}$, that is,

$$\overline{\mathcal{K}} = \overline{\mathcal{K}}\mathcal{A}\overline{\mathcal{K}}\mathcal{A}\overline{\mathcal{K}} \oplus \mathcal{S}_2.$$

If $\boldsymbol{\Lambda}_2$ denotes the projection onto $\mathcal{S}_2$, it is easy to see that

$$\boldsymbol{\Lambda}_2 \boldsymbol{K}_* = \boldsymbol{\Lambda}_2 \langle \boldsymbol{K} \rangle + \boldsymbol{\Lambda}_2 \langle \boldsymbol{K}\boldsymbol{A}\boldsymbol{K} \rangle, \tag{17.21}$$

which is the desired exact relation incorporating the two-point statistics of the medium. An example of an exact relation of this type for thermoelasticity is given in section 14.3 on page 294. The subspace $\overline{\mathcal{K}}$ consists of all tensors that can be expressed in the form

$$\boldsymbol{K} = \begin{pmatrix} 0 & \boldsymbol{b} \\ \boldsymbol{b} & d \end{pmatrix},$$

for some choice of second-order tensor $\boldsymbol{b}$ and constant d. From the formula (14.13) for $\boldsymbol{\Gamma}$ we see that $\overline{\mathcal{K}}\mathcal{A}\overline{\mathcal{K}}\mathcal{A}\overline{\mathcal{K}} = 0$, so (17.21) implies that

$$\boldsymbol{K}_* = \langle \boldsymbol{K} \rangle + \langle \boldsymbol{K}\boldsymbol{A}\boldsymbol{K} \rangle,$$

which is equivalent to (14.14).

17.7. Additional necessary conditions for an exact relation†

In section 17.2 on page 357 we saw that a necessary condition for $\mathcal{M}$ to be stable under homogenization is that $W_{\boldsymbol{n}}(\mathcal{M})$ lie in a subspace $\mathcal{K}$ such that (17.5) holds. Let us now use series expansions to look for additional conditions that are necessary to ensure stability under homogenization. Given $\boldsymbol{L}(\boldsymbol{x})$ taking values in $\mathcal{M}$, let $\boldsymbol{K} = \boldsymbol{K}(\boldsymbol{x}) = W_{\boldsymbol{n}}(\boldsymbol{L}(\boldsymbol{x}))$ be the associated tensor field taking values in $\mathcal{K}$. Stability under homogenization requires $\boldsymbol{K}_* = W_{\boldsymbol{n}}(\boldsymbol{L}_*)$ to also lie in $\mathcal{K}$. Recall the series expansion (14.44) for $\boldsymbol{K}_*$,

$$\boldsymbol{K}_* = \langle \boldsymbol{K} \rangle + \langle \boldsymbol{K}\boldsymbol{A}\boldsymbol{K} \rangle + \langle \boldsymbol{K}\boldsymbol{A}\boldsymbol{K}\boldsymbol{A}\boldsymbol{K} \rangle + \langle \boldsymbol{K}\boldsymbol{A}\boldsymbol{K}\boldsymbol{A}\boldsymbol{K}\boldsymbol{A}\boldsymbol{K} \rangle + \cdots . \tag{17.22}$$

The first-order term $\langle \boldsymbol{K} \rangle$ clearly lies in $\mathcal{K}$ because $\boldsymbol{K}(\boldsymbol{x})$ takes values in $\boldsymbol{K}$. Using the fact that $\boldsymbol{A}(\boldsymbol{k}) = \boldsymbol{A}(-\boldsymbol{k})$, the second-order term

$$\begin{aligned} \langle \boldsymbol{K}\boldsymbol{A}\boldsymbol{K} \rangle &= \sum_{\boldsymbol{k} \neq 0} \widehat{\boldsymbol{K}}(-\boldsymbol{k}) \boldsymbol{A}(\boldsymbol{k}) \widehat{\boldsymbol{K}}(\boldsymbol{k}) \\ &= \tfrac{1}{2} \sum_{\boldsymbol{k} \neq 0} [\widehat{\boldsymbol{K}}(-\boldsymbol{k}) \boldsymbol{A}(\boldsymbol{k}) \widehat{\boldsymbol{K}}(\boldsymbol{k}) + \widehat{\boldsymbol{K}}(\boldsymbol{k}) \boldsymbol{A}(\boldsymbol{k}) \widehat{\boldsymbol{K}}(-\boldsymbol{k})] \end{aligned} \tag{17.23}$$

also lies in $\mathcal{K}$ because the real and imaginary parts of the Fourier components $\widehat{\boldsymbol{K}}(\boldsymbol{k})$ take values in $\mathcal{K}$ and $\mathcal{K}$ satisfies the condition (17.5).

Now let us examine the third-order term:

$$\langle \boldsymbol{K}\boldsymbol{A}\boldsymbol{K}\boldsymbol{A}\boldsymbol{K} \rangle = \sum_{\boldsymbol{k} \neq 0} \sum_{\boldsymbol{m} \neq 0} \widehat{\boldsymbol{K}}(-\boldsymbol{m}) \boldsymbol{A}(\boldsymbol{m}) \widehat{\boldsymbol{K}}(\boldsymbol{m} - \boldsymbol{k}) \boldsymbol{A}(\boldsymbol{k}) \widehat{\boldsymbol{K}}(\boldsymbol{k}). \tag{17.24}$$

For the manifold $\mathcal{M}$ to be stable under homogenization we require that this be in $\mathcal{K}$ for all choices of $\boldsymbol{K}(\boldsymbol{x})$ taking values in $\mathcal{K}$. Naturally there should be an analytic extension of the exact relation which implies that $\boldsymbol{K}_*$ has real and imaginary parts lying in $\mathcal{K}$ when $\boldsymbol{K}(\boldsymbol{x})$ has real and imaginary parts lying in $\mathcal{K}$. In other words, the third-order term should lie in $\mathcal{K}$ for any choice of Fourier components $\widehat{\boldsymbol{K}}(\boldsymbol{k})$ with real and imaginary parts taking values in $\mathcal{K}$. In particular, let us take three vectors $\boldsymbol{q}_1$, $\boldsymbol{q}_2$, and $\boldsymbol{q}_3$ in Fourier space such that $\boldsymbol{q}_1 + \boldsymbol{q}_2 + \boldsymbol{q}_3 = 0$ and set

$$\begin{aligned} \widehat{\boldsymbol{K}}(\boldsymbol{k}) &= \boldsymbol{K}_j \quad \text{when } \boldsymbol{k} = \boldsymbol{q}_j \text{ for } j = 1, 2, 3, \\ &= 0 \qquad \text{otherwise,} \end{aligned}$$

where $\boldsymbol{K}_1$, $\boldsymbol{K}_2$, and $\boldsymbol{K}_3$ are matrices in $\mathcal{K}$. Then the requirement that the third-order term lie in $\mathcal{K}$ implies that

$$\begin{aligned} &\boldsymbol{K}_1 \boldsymbol{A}(\boldsymbol{q}_1) \boldsymbol{K}_2 \boldsymbol{A}(\boldsymbol{q}_3) \boldsymbol{K}_3 + \boldsymbol{K}_3 \boldsymbol{A}(\boldsymbol{q}_3) \boldsymbol{K}_2 \boldsymbol{A}(\boldsymbol{q}_1) \boldsymbol{K}_1 \\ + \; &\boldsymbol{K}_2 \boldsymbol{A}(\boldsymbol{q}_2) \boldsymbol{K}_3 \boldsymbol{A}(\boldsymbol{q}_1) \boldsymbol{K}_1 + \boldsymbol{K}_1 \boldsymbol{A}(\boldsymbol{q}_1) \boldsymbol{K}_3 \boldsymbol{A}(\boldsymbol{q}_2) \boldsymbol{K}_2 \\ + \; &\boldsymbol{K}_3 \boldsymbol{A}(\boldsymbol{q}_3) \boldsymbol{K}_1 \boldsymbol{A}(\boldsymbol{q}_2) \boldsymbol{K}_1 + \boldsymbol{K}_2 \boldsymbol{A}(\boldsymbol{q}_2) \boldsymbol{K}_1 \boldsymbol{A}(\boldsymbol{q}_3) \boldsymbol{K}_3 \in \mathcal{K}. \end{aligned} \tag{17.25}$$

This condition, which must hold for any vectors $\boldsymbol{q}_1$, $\boldsymbol{q}_2$, $\boldsymbol{q}_3$ such that $\boldsymbol{q}_1 + \boldsymbol{q}_2 + \boldsymbol{q}_3 = 0$ and any $\boldsymbol{K}_1, \boldsymbol{K}_2, \boldsymbol{K}_3 \in \mathcal{K}$, is necessary for stability under homogenization. It does not appear to be a consequence of the conditions for the stability under lamination, although it remains an open question as to whether there exists a subspace $\mathcal{K}$ satisfying (17.5) but not satisfying the above constraint. Other additional conditions can be obtained by considering higher order terms in the expansion (Grabovsky, Milton, and Sage 2000).

To ensure that all terms in the expansion lie in $\mathcal{K}$ it suffices that any chain of the form $\boldsymbol{K}_1\boldsymbol{A}(\boldsymbol{q}_1)\boldsymbol{K}_2\boldsymbol{A}(\boldsymbol{q}_2)\boldsymbol{K}_3\boldsymbol{A}(\boldsymbol{q}_3)\ldots\boldsymbol{K}_{j-1}\boldsymbol{A}(\boldsymbol{q}_{j-1})\boldsymbol{K}_j$, which we will call a j-chain, satisfy the "j-chain property": The symmetrized j-chain

$$\begin{aligned}&\boldsymbol{K}_1\boldsymbol{A}(\boldsymbol{q}_1)\boldsymbol{K}_2\boldsymbol{A}(\boldsymbol{q}_2)\boldsymbol{K}_3\boldsymbol{A}(\boldsymbol{q}_3)\ldots\boldsymbol{K}_{j-1}\boldsymbol{A}(\boldsymbol{q}_{j-1})\boldsymbol{K}_j\\&\quad+\boldsymbol{K}_j\boldsymbol{A}(\boldsymbol{q}_{j-1})\boldsymbol{K}_{j-1}\ldots\boldsymbol{A}(\boldsymbol{q}_3)\boldsymbol{K}_3\boldsymbol{A}(\boldsymbol{q}_2)\boldsymbol{K}_2\boldsymbol{A}(\boldsymbol{q}_1)\boldsymbol{K}_1\end{aligned}$$

lies in $\mathcal{K}$ for all $\boldsymbol{K}_i$, $i = 1, 2, 3, \ldots, j$ in $\mathcal{K}$, and for all vectors $\boldsymbol{q}_i$, $i = 1, 2, 3, \ldots, j-1$. The two-chain property is implied by the stability under lamination. If in addition the three-chain and four-chain properties are satisfied, then the j-chain property is satisfied for all j.

To see this, we rewrite the two-chain property as

$$\boldsymbol{K}_1\boldsymbol{A}(\boldsymbol{m})\boldsymbol{K}_2 = -\boldsymbol{K}_2\boldsymbol{A}(\boldsymbol{m})\boldsymbol{K}_1 + \boldsymbol{K}', \tag{17.26}$$

for some $\boldsymbol{K}' \in \mathcal{K}$. This identity allows us to successively swap the positions of adjacent $\boldsymbol{K}$ in any j-chain, leaving $(j-1)$-chains as the remainder. With the three-chain property it implies that

$$\boldsymbol{K}_1\boldsymbol{A}(\boldsymbol{q}_1)\boldsymbol{K}_2\boldsymbol{A}(\boldsymbol{q}_2)\boldsymbol{K}_3 = \boldsymbol{K}_1\boldsymbol{A}(\boldsymbol{q}_2)\boldsymbol{K}_2\boldsymbol{A}(\boldsymbol{q}_1)\boldsymbol{K}_3 + \boldsymbol{K}'' + \text{a sum of two-chains},$$

for some $\boldsymbol{K}'' \in \mathcal{K}$. This allows us to successively swap the positions of adjacent $\boldsymbol{A}$ in any j-chain, leaving $(j-1)$-chains and $(j-2)$-chains as the remainder. By first reversing the order of the $\boldsymbol{A}$ and then reversing the order of the $\boldsymbol{K}$ we see that

$$\begin{aligned}&\boldsymbol{K}_1\boldsymbol{A}(\boldsymbol{q}_1)\boldsymbol{K}_2\boldsymbol{A}(\boldsymbol{q}_2)\boldsymbol{K}_3\boldsymbol{A}(\boldsymbol{q}_3)\ldots\boldsymbol{K}_{j-1}\boldsymbol{A}(\boldsymbol{q}_{j-1})\boldsymbol{K}_j\\&\quad+(-1)^{j(j-1)/2}\boldsymbol{K}_j\boldsymbol{A}(\boldsymbol{q}_{j-1})\boldsymbol{K}_{j-1}\ldots\boldsymbol{A}(\boldsymbol{q}_3)\boldsymbol{K}_3\boldsymbol{A}(\boldsymbol{q}_2)\boldsymbol{K}_2\boldsymbol{A}(\boldsymbol{q}_1)\boldsymbol{K}_1\\&\quad+\text{ a sum of }(j-1)\text{-chains and }(j-2)\text{-chains},\end{aligned}$$

in which $j(j-1)/2$ is the number of swaps of adjacent $\boldsymbol{K}$ needed to achieve this reordering. If the sign of $(-1)^{j(j-1)/2}$ is positive (as it is when $j = 4$), then we apply the four-chain property once, replacing the chain header

$$\boldsymbol{K}_1\boldsymbol{A}(\boldsymbol{q}_1)\boldsymbol{K}_2\boldsymbol{A}(\boldsymbol{q}_2)\boldsymbol{K}_3\boldsymbol{A}(\boldsymbol{q}_3)\boldsymbol{K}_4 \text{ with } -\boldsymbol{K}_4\boldsymbol{A}(\boldsymbol{q}_3)\boldsymbol{K}_3\boldsymbol{A}(\boldsymbol{q}_2)\boldsymbol{K}_2\boldsymbol{A}(\boldsymbol{q}_1)\boldsymbol{K}_1 + \boldsymbol{K}',$$

where $\boldsymbol{K}' \in \mathcal{K}$ before swapping the $\boldsymbol{A}$ and $\boldsymbol{K}$ to obtain minus the reversed order chain plus shorter chains. This allows us to identify the symmetrized j-chain with a sum of symmetrized $(j-1)$-chains, $(j-2)$-chains, and $(j-3)$-chains. By induction the j-chain property is then satisfied for all j.

Now let $\overline{\mathcal{K}}$ be the subspace spanned by j-chains of all lengths, $j = 1, 2, 3, \ldots$. Clearly we have

$$\overline{\boldsymbol{K}}_1\boldsymbol{A}(\boldsymbol{m})\overline{\boldsymbol{K}}_2 \in \overline{\mathcal{K}} \quad \text{for all } \boldsymbol{m} \text{ and for all } \overline{\boldsymbol{K}}_1, \overline{\boldsymbol{K}}_2 \in \overline{\mathcal{K}}, \tag{17.27}$$

and the j-chain property holds if and only if we can equate $\mathcal{K}$ with the subspace $\overline{\mathcal{K}}_S$ consisting of all symmetric matrices in $\overline{\mathcal{K}}$. Conversely, if we are given a subspace $\overline{\mathcal{K}}$ satisfying (17.27), and we set $\mathcal{K}$ equal to $\overline{\mathcal{K}}_S$, then the elements of $\mathcal{K}$ necessarily satisfy the j-chain property for all positive integers j. Thus the task of finding subspaces $\mathcal{K}$ satisfying the two-chain, three-chain, and four-chain properties is equivalent to the task of finding subspaces $\overline{\mathcal{K}}$ satisfying (17.27). Moreover, the two-chain, three-chain, and four-chain properties can be rephrased as conditions on certain subspaces generated from $\mathcal{A}$ and $\mathcal{K}$. The interested reader is referred to theorem 3.6 of Grabovsky, Milton, and Sage (2000) for more details. These conditions provide a practical way of determining whether or not a candidate exact relation, which is stable under lamination, is also stable under homogenization.

References

Avellaneda, M., A. V. Cherkaev, L. V. Gibiansky, G. W. Milton, and M. Rudelson 1996. A complete characterization of the possible bulk and shear moduli of planar polycrystals. *Journal of the Mechanics and Physics of Solids* 44(7):1179–1218. {*362, 367, 502, 525, 537, 550*}

Gibiansky, L. V. 1998. Effective moduli of plane polycrystals with a rank-one local compliance tensor. *Proceedings of the Royal Society of Edinburgh. Section A, Mathematical and Physical Sciences* 128(6):1325–1354. {*359, 367*}

Grabovsky, Y. 1998. Exact relations for effective tensors of polycrystals. I: Necessary conditions. *Archive for Rational Mechanics and Analysis* 143(4):309–329. {*355, 367*}

Grabovsky, Y. and G. W. Milton 1998a. Exact relations for composites: Towards a complete solution. *Documenta Mathematica, Journal der Deutschen Mathematiker-Vereinigung* Extra Volume ICM III:623–632. {*355, 361, 362, 367*}

Grabovsky, Y. and G. W. Milton 1998b. Rank one plus a null-Lagrangian is an inherited property of two-dimensional compliance tensors under homogenization. *Proceedings of the Royal Society of Edinburgh* 128A(2):283–299. {*359, 367*}

Grabovsky, Y., G. W. Milton, and D. S. Sage 2000. Exact relations for effective tensors of composites: Necessary conditions and sufficient conditions. *Communications on Pure and Applied Mathematics (New York)* 53(3):300–353. {*305, 310, 355, 360, 363, 365–367*}

Grabovsky, Y. and D. S. Sage 1998. Exact relations for effective tensors of polycrystals. II: Applications to elasticity and piezoelectricity. *Archive for Rational Mechanics and Analysis* 143(4):331–356. {*355, 358, 367*}

18

Analytic properties

18.1. Analyticity of the effective dielectric constant of two-phase media

Consider an isotropic composite of two isotropic phases. When the microgeometry is fixed it has a complex effective dielectric constant $\varepsilon_*(\varepsilon_1, \varepsilon_2)$, which is a function of the complex dielectric constants ε_1 and ε_2 of the phases that depend on the frequency ω of the applied field. As a prelude to the proof given in the next section, we will now present a strong argument that shows why $\varepsilon_*(\varepsilon_1, \varepsilon_2)$ should have some rather special analytic properties. The argument is based on the premise that analyticity properties of the dielectric constant as a function of the frequency ω should extend to composite materials.

The properties of the function $\varepsilon_1(\omega)$ [or $\varepsilon_2(\omega)$] are well-known and are discussed, for example, by Jackson (1975); see also section 11.1 on page 222. The function $\varepsilon_1(\omega)$ is analytic in the upper half ω-plane, $\mathrm{Im}(\omega) > 0$. When $\mathrm{Re}(\omega) = 0$ the function takes real values of $\varepsilon_1(\omega) \geq 1$, which decrease and approach 1 as $|\omega| \to \infty$. Positive imaginary values of $\varepsilon_1(\omega)$ occur when ω has a positive real part and negative imaginary values of $\varepsilon_1(\omega)$ when ω has a negative real part. As ω ranges over the upper half-plane $\varepsilon_1(\omega)$ can in principle range anywhere in the cut complex plane, where the cut extends along the real axis from $-\infty$ to 1. The actual range depends on the material being studied.

Let us assume that $\varepsilon_1(\omega)$ is given by the single oscillator model (11.12) with $\gamma = 0$ and $\varepsilon_\infty = 1$, that is,

$$\varepsilon(\omega) = 1 + \frac{A}{\omega_r^2 - \omega^2},$$

in which A and ω_r are real and positive. Given any point a in the complex plane we can choose ω to be complex and given by

$$\omega = \sqrt{\omega_r^2 - A/(a-1)}$$

to ensure that $\varepsilon(\omega) = a$. The value of ω will be in the upper half-plane and unique unless a is real and less than 1 or greater than $1 + A/\omega_r^2$. In other words, $\varepsilon_1(\omega)$ is a one-to-one mapping from the upper half complex plane onto a cut complex plane with the cut extending from $-\infty$ to 1 and from $1 + A/\omega_r^2$ to ∞. Let us assume that $\varepsilon_2(\omega)$ is frequency independent and real (except at very high frequencies, where it must tend to 1).

In order for these analyticity properties to automatically extend to the function

$$\varepsilon_*(\omega) = \varepsilon_*(\varepsilon_1(\omega), \varepsilon_2),$$

one sees that $\varepsilon_*(\varepsilon_1, \varepsilon_2)$ should be an analytic function of ε_1, except possibly when ε_1 is real and less than or equal to 1 or greater than or equal to $1 + A/\omega_r^2$. Any nonanalyticity at other

values of ε_1 would propagate into nonanalyticity of $\varepsilon_*(\omega)$ at the corresponding values of ω in the upper half-plane. Of course ω_r could be arbitrarily small, and so it should be analytic for any real value of ε_1 greater than 1. Since this is true for any real value of $\varepsilon_2 \geq 1$, and since the homogeneity of the function [see (1.6)] implies that

$$\varepsilon_*(\varepsilon_1/\varepsilon_2, 1) = \varepsilon_*(\varepsilon_1, \varepsilon_2)/\varepsilon_2,$$

for all values of ε_2, we deduce that $\varepsilon_*(z, 1)$ should be analytic in the cut complex z-plane where the cut extends along the negative real z-axis. Additionally, one knows that $\varepsilon_1(\omega)$ ranges over the entire upper half-plane as ω ranges over the quadrant $\mathrm{Re}(\omega) > 0$, $\mathrm{Im}(\omega) > 0$. In order for $\varepsilon_*(\omega)$ to have positive imaginary values in this quadrant we see that the function $\varepsilon_*(z, 1)$ must have a positive imaginary part whenever z has a positive imaginary part.

For resistor networks the study of the analytic properties of the total resistance as a function of the resistances of the component resistors dates back at least to the work of Foster (1924a, 1924b); see Storer (1957) for a summary of his work, and also Baker, Jr. (1975) and Straley (1979). For composites Bergman (1978a, 1978b) pioneered the investigation of analyticity and obtained a representation formula for the function $\varepsilon_*(z, 1)$ that is similar to representations proposed by Fuchs (1978) and Lysne (1983), which were based on models that were valid for dilute suspensions. In 1979, while studying periodic two-phase composites, I independently realized that $\varepsilon_*(z, 1)$ should be analytic in the cut complex z-plane. David McKenzie pointed me to Bergman's work, which I found contained some erroneous assumptions (Milton 1979). Bergman assumed that the function should be a rational function of z when the geometry is periodic (a checkerboard geometry is a counterexample) and assumed that if there is not a solution for the fields when the average electric field $\langle \boldsymbol{e} \rangle$ is prescribed, then there is a solution when the average displacement field $\langle \boldsymbol{d} \rangle$ is prescribed (sometimes neither problem has a solution, such as for a periodic array of cylinders of dielectric constant -1 surrounded by a matrix of conductivity 1). To avoid these difficulties and still justify the analyticity of $\varepsilon_*(z, 1)$ one could approximate the composite by a large impedance network (Milton 1981a). Subsequently, Golden and Papanicolaou (1983) gave a proof of the analytic properties of $\varepsilon_*(z, 1)$, thereby providing a rigorous basis for the integral representation of the function. Moreover, they extended the representation to the matrix-valued function $\boldsymbol{\varepsilon}_*(z, 1)$, giving the effective dielectric tensor of anisotropic composites of the two isotropic phases.

Integral representations were derived by Kantor and Bergman (1982) for the effective elasticity tensor and by Avellaneda and Majda (1989, 1991) for the effective diffusivity in convection-enhanced diffusion. Barrera and Fuchs (1995) derived an integral representation for the frequency-dependent effective dielectric constant, which was valid at all wavelengths, not just in the quasistatic limit. Lipton (2000, 2001) has obtained integral representation formulas for the L^2-norm and covariance tensor of the field. Golden (1995, 1997) has used integral representations to draw parallels between conduction in two-phase composites and phase transitions in statistical mechanics.

18.2. Analyticity of the effective tensor for problems involving many eigenvalues

In many problems of interest the tensor $\boldsymbol{L}$ takes the form

$$\boldsymbol{L} = \sum_{i=1}^{n} \lambda_i \boldsymbol{\Lambda}_i, \tag{18.1}$$

where the λ_i, for $i = 1, 2, \ldots, n$, represent its possibly complex eigenvalues and the $\boldsymbol{\Lambda}_i$ represent projections onto the associated eigenspaces $\mathcal{P}_i$, which we assume to be mutually orthogonal and to span $\mathcal{H}$:

$$\mathcal{H} = \mathcal{U} \oplus \mathcal{E} \oplus \mathcal{J} = \mathcal{P}_1 \oplus \mathcal{P}_2 \oplus \ldots \oplus \mathcal{P}_n.$$

One example, considered by Bergman (1978b), is the conductivity (or dielectric) tensor of an n-component composite with isotropic phases that takes the form

$$\boldsymbol{\sigma}(\boldsymbol{x}) = \sum_{i=1}^{n} \sigma_i \chi_i(\boldsymbol{x}) \boldsymbol{I}, \tag{18.2}$$

where $\chi_i \boldsymbol{I}$ projects onto the space of fields $\mathcal{P}_i$ that are nonzero only inside phase i.

A second example, considered by Milton (1981b) and Dell'Antonio, Figari, and Orlandi (1986), is the conductivity (or dielectric) tensor of a three-dimensional polycrystal, which takes the form

$$\boldsymbol{\sigma}(\boldsymbol{x}) = \boldsymbol{R}(\boldsymbol{x})\boldsymbol{\sigma}_0\boldsymbol{R}^T(\boldsymbol{x}) = \lambda_1\boldsymbol{\Lambda}_1(\boldsymbol{x}) + \lambda_2\boldsymbol{\Lambda}_2(\boldsymbol{x}) + \lambda_3\boldsymbol{\Lambda}_3(\boldsymbol{x}), \tag{18.3}$$

where the λ_i denote the eigenvalues of the conductivity tensor $\boldsymbol{\sigma}_0$ of the pure crystal and

$$\boldsymbol{\Lambda}_i(\boldsymbol{x}) = \boldsymbol{R}(\boldsymbol{x})\boldsymbol{v}_i \otimes \boldsymbol{v}_i\boldsymbol{R}^T(\boldsymbol{x}),$$

projects onto those fields that are aligned with the associated crystal eigenvector. Here $\boldsymbol{v}_1$, $\boldsymbol{v}_2$, and $\boldsymbol{v}_3$ denote the eigenvectors of

$$\boldsymbol{\sigma}_0 = \sum_{i=1}^{3} \lambda_i \boldsymbol{v}_i \otimes \boldsymbol{v}_i.$$

We assume that these eigenvectors are real and mutually orthogonal.

A third example, considered by Kantor and Bergman (1982) and Dell'Antonio, Figari, and Orlandi (1986), is the compliance tensor of a d-dimensional composite comprised of two isotropic phases, which takes the form

$$\boldsymbol{\mathcal{S}}(\boldsymbol{x}) = \frac{1}{d\kappa_1}\boldsymbol{\Lambda}_h\chi_1(\boldsymbol{x}) + \frac{1}{2\mu_1}\boldsymbol{\Lambda}_s\chi_1(\boldsymbol{x}) + \frac{1}{d\kappa_2}\boldsymbol{\Lambda}_h\chi_2(\boldsymbol{x}) + \frac{1}{2\mu_2}\boldsymbol{\Lambda}_s\chi_2(\boldsymbol{x}), \tag{18.4}$$

where κ_1, κ_2 and μ_1, μ_2 are the bulk and shear moduli of the phases, while $\boldsymbol{\Lambda}_h$ and $\boldsymbol{\Lambda}_s = \boldsymbol{I} - \boldsymbol{\Lambda}_h$ are fourth-order tensors, with components

$$\{\boldsymbol{\Lambda}_h\}_{ijk\ell} = \frac{1}{d}\delta_{ij}\delta_{k\ell}, \quad \{\boldsymbol{\Lambda}_s\}_{ijk\ell} = \frac{1}{2}\Big[\delta_{ik}\delta_{j\ell} + \delta_{i\ell}\delta_{jk}\Big] - \frac{1}{d}\delta_{ij}\delta_{k\ell}$$

that project respectively onto the two orthogonal spaces of hydrostatic fields and shear fields, that is, matrix-valued fields that are respectively everywhere proportional to the second-order identity tensor $\boldsymbol{I}$ and everywhere trace free. These operators commute with $\chi_1(\boldsymbol{x})$ and $\chi_2(\boldsymbol{x})$, implying, for example, that $\boldsymbol{\Lambda}_h\chi_1$ projects onto those fields that are proportional to the second-order identity within phase 1 and zero in phase 2. Of course, the tensor $\boldsymbol{L}$ can always be represented in the form (18.1) when $\boldsymbol{L}$ is self-adjoint and the Hilbert space $\mathcal{H}$ is finite-dimensional.

The eigenvalues λ_i might depend on some parameter of the system, while the eigenspaces $\mathcal{P}_i$ remain independent of this parameter. For example, in the case of wave propagation in

the quasistatic limit, the complex dielectric constants, or complex bulk and shear moduli, depend on the frequency ω of the incident wave, while the characteristic functions $\chi_i(\boldsymbol{x})$ do not. These moduli may also depend on the temperature, whereas the characteristic functions may be relatively insensitive to temperature changes, assuming that the effect of thermal expansion can be neglected. This provides a physical motivation for studying the dependence of $\boldsymbol{L}_*$ on the eigenvalues $\lambda_1, \lambda_2, \ldots, \lambda_n$ when the projections $\boldsymbol{\Lambda}_1, \boldsymbol{\Lambda}_2, \ldots \boldsymbol{\Lambda}_n$, and hence the spaces $\mathcal{P}_1, \mathcal{P}_2, \ldots \mathcal{P}_n$, are held fixed. In the context of the conductivity problem (18.2) or the elasticity problem (18.4) this amounts to studying the dependence of the effective conductivity tensor $\boldsymbol{\sigma}_*$ or the effective compliance tensor $\boldsymbol{\mathcal{S}}_*$ on the conductivities, or on the bulk and shear moduli of the phases, while the geometric configuration of the phases is held fixed. In the context of the polycrystal problem (18.3) it amounts to studying how the effective conductivity tensor depends on the principal conductivities λ_1, λ_2, and λ_3 of the pure crystal while keeping the crystal orientation in the polycrystal fixed. In general, in the abstract setting of section 12.7 on page 260, the function $\boldsymbol{L}_*(\lambda_1, \lambda_2, \ldots \lambda_3)$ is determined by the orientation of the n-spaces $\mathcal{P}_1, \mathcal{P}_2, \ldots, \mathcal{P}_n$ with respect to the three spaces $\mathcal{U}$, $\mathcal{E}$, and $\mathcal{J}$.

Let us establish that $\boldsymbol{L}_*(\lambda_1, \lambda_2, \ldots \lambda_n)$ is an analytic function whenever the variables $\lambda_1, \lambda_2, \ldots \lambda_n$ all have positive real parts. Here we follow a simple argument of Bruno (1991b) [see also Bruno and Leo (1992)], which is based on considering the analyticity of each term in the series expansion (14.2) for the effective tensor $\boldsymbol{L}_*$. If the reference tensor $\boldsymbol{L}_0$ is taken to be constant, it is clear that each term in the expansion is an analytic function, and in fact a polynomial function, of the variables $\lambda_1, \lambda_2, \ldots \lambda_n$. For example, with $\boldsymbol{L}_0 = \sigma_0 \boldsymbol{I}$, the expansion to the second order is the following polynomial of degree 2 in these variables:

$$\begin{aligned}\boldsymbol{L}_* = \sigma_0 \boldsymbol{\Gamma}_0 \; - \; & \sum_{i=1}^{n} (1 - \lambda_i/\sigma_0) \boldsymbol{\Gamma}_0 \boldsymbol{\Lambda}_i \boldsymbol{\Gamma}_0 \\ & - \; \sigma_0 \sum_{i,\,j=1}^{n} (1 - \lambda_i/\sigma_0)(1 - \lambda_j/\sigma_0) \boldsymbol{\Gamma}_0 \boldsymbol{\Lambda}_i \boldsymbol{\Gamma}_1 \boldsymbol{\Lambda}_j \boldsymbol{\Gamma}_0 - \cdots .\end{aligned}$$

In subsection 14.6 on page 298 we proved that the expansion converges, for a sufficiently large choice of σ_0, whenever the tensor $\boldsymbol{L}$ is bounded and coercive, which in the current context is whenever the variables λ_i all lie in the right half-plane H_0 of the complex plane, that is, whenever

$$\lambda_1, \lambda_2, \ldots, \lambda_n \in H_0, \quad \text{where } H_0 = \{\lambda \in \mathbb{C} \mid \operatorname{Re}(\lambda) > 0\}.$$

We can rewrite this as

$$\boldsymbol{\lambda} = (\lambda_1, \lambda_2, \ldots \lambda_n) \in H_0^n.$$

Moreover, it is easy to see from the bounds (14.29) that the convergence is uniform on any compact subset of H_0^n. Since a sequence of analytic functions that converge uniformly on any compact subset of a domain is analytic in that domain [see theorem 10.28 of Rudin (1987)] it immediately follows that $\boldsymbol{L}_*$ is an analytic function of the eigenvalues $\lambda_1, \lambda_2, \ldots \lambda_n$ for all $\boldsymbol{\lambda} \in H_0^n$, in the sense that each matrix element of $\boldsymbol{L}_*$ is an analytic function of $\boldsymbol{\lambda}$ for all $\boldsymbol{\lambda} \in H_0^n$.

In fact the function $\boldsymbol{L}_*(\lambda_1, \ldots \lambda_n)$ has a wider domain of analyticity. The linearity of the equations implies that the function satisfies

The homogeneity property:

$$\boldsymbol{L}_*(\lambda_1, \lambda_2, \ldots \lambda_n) = \frac{1}{c} \boldsymbol{L}_*(c\lambda_1, c\lambda_2, \ldots c\lambda_n),$$

for all choices of the constants $c \neq 0$ and in particular for $c = e^{i\theta}$. Therefore analyticity in the domain H_0^n implies analyticity in the domain H_θ^n, where H_θ is obtained by a clockwise rotation of the half-plane H_0 through the angle θ:

$$H_\theta = \{\lambda \in \mathbb{C} \mid \operatorname{Re}(e^{i\theta}\lambda) > 0\}.$$

Consequently, as noticed by Dell'Antonio, Figari, and Orlandi (1986), the function must be analytic at least for

$$\boldsymbol{\lambda} \in \bigcup_\theta H_\theta^n. \tag{18.5}$$

Sometimes this domain of analyticity can be enlarged even further without making any assumptions about the composite geometry. For example, suppose that there exists a translation $\boldsymbol{T}$ of the form

$$\boldsymbol{T} = \sum_{i=1}^{n} \tau_i \boldsymbol{\Lambda}_i,$$

such that whenever $\boldsymbol{L}$ is translated by a multiple of $\boldsymbol{T}$ the effective tensor undergoes the same translation, that is,

$$(\boldsymbol{L} - c\boldsymbol{T})_* = \boldsymbol{L}_* - c\boldsymbol{T} \text{ for all } c.$$

From this property we deduce that $\boldsymbol{L}_*(\lambda_1, \ldots \lambda_n)$ is analytic at least for those $\boldsymbol{\lambda}$ for which there exists a constant c such that

$$\boldsymbol{\lambda} - c\boldsymbol{\tau} \in \bigcup_\theta H_\theta^n, \quad \text{where } \boldsymbol{\tau} = (\tau_1, \tau_2, \ldots \tau_n).$$

For example, when the compliance tensor of a two-dimensional, two-phase composite is shifted by the translation

$$\boldsymbol{\mathcal{R}}_\perp = \boldsymbol{\Lambda}_h \chi_1(\boldsymbol{x}) - \boldsymbol{\Lambda}_s \chi_1(\boldsymbol{x}) + \boldsymbol{\Lambda}_h \chi_2(\boldsymbol{x}) - \boldsymbol{\Lambda}_s \chi_2(\boldsymbol{x}),$$

the effective compliance tensor $\boldsymbol{\mathcal{S}}_*$ is shifted by the same translation. (c.f. section 4.5 on page 66). It follows that $\boldsymbol{\mathcal{S}}_*$ is an analytic function of the bulk and shear compliances $1/\kappa_1$, $1/\kappa_2$, $1/\mu_1$, and $1/\mu_2$ whenever there exists a straight line in the complex plane such that $1/\kappa_1$ and $1/\kappa_2$ lie on one side of this line while $-1/\mu_1$ and $-1/\mu_2$ lie on the other side. Using the translation $\boldsymbol{\mathcal{R}}_\perp$ we can translate these four points so the line separating them goes through the origin; after this translation the points $1/\kappa_1$, $1/\kappa_2$, $1/\mu_1$, and $1/\mu_2$ all lie in the same half-plane H_θ.

More generally, the function $\boldsymbol{L}_*(\lambda_1, \ldots \lambda_n)$ will be analytic in any domain where it has a uniformly convergent series expansion with analytic terms. This domain of convergence will be especially large in the case of the series expansion discussed in section 14.8 on page 301.

Further enlargements of the domain of analyticity can be made if we have some information about the composite microgeometry. Bruno (1991a) has shown that for composites consisting of isotropic inclusions of conductivity σ_1 embedded in a matrix of unit conductivity $\sigma_2 = 1$ the function $\sigma_*(\sigma_1)$ is analytic for $|\sigma_1| \leq 1/A$ and for $|\sigma_1| \geq B$, where the constants A and B depend on the inclusion shape and on how well the inclusions are separated. Bruno and Leo (1992) extended these results to elasticity.

When all of the eigenvalues λ_i lie in the right half-plane H_0, the self-adjoint component of $\boldsymbol{L}$ is positive-definite, that is, the real part of $\boldsymbol{L}$ is positive-definite. It follows from section 12.10 on page 263 that the self-adjoint component of the effective tensor $\boldsymbol{L}_*$ must be

positive-definite, that is, the real part of $\boldsymbol{L}_*$ must be positive-definite. In other words, the function satisfies

The Herglotz property:

$$\mathrm{Im}(\boldsymbol{L}_*) > 0 \text{ when } \mathrm{Im}(\lambda_i) > 0 \text{ for } i = 1, 2, \ldots, n,$$

which, when combined with the homogeneity property, implies that

$$\mathrm{Re}(e^{i\theta}\boldsymbol{L}_*) > 0 \text{ when } \boldsymbol{\lambda} \in H^n_\theta. \tag{18.6}$$

Some elementary bounds on the symmetric complex effective tensor $\boldsymbol{L}_*$ follow from these equations. For example, consider the region

$$W_{\theta,\theta'} = H_\theta \cap H_{\theta'},$$

which represents a wedge in the complex plane. From (18.6) we have

The wedge bounds: For all real $\boldsymbol{E}_0$,

$$\boldsymbol{E}_0 \cdot \boldsymbol{L}_*\boldsymbol{E}_0 \in W_{\theta,\theta'} \text{ whenever } \lambda_i \in W_{\theta,\theta'} \text{ for } i = 1, 2, \ldots, n. \tag{18.7}$$

In particular, by taking $\theta = -\theta' = \pi/2 - \epsilon$ and considering the limit $\epsilon \to 0$, this implies that the symmetric tensor $\boldsymbol{L}_*$ must be real and positive-definite when all of the eigenvalues λ_i lie along the positive real axis. So the identity

$$\boldsymbol{L}_*(\lambda_1, \lambda_2, \ldots \lambda_n) = \overline{\boldsymbol{L}_*(\overline{\lambda}_1, \overline{\lambda}_2, \ldots \overline{\lambda}_n)} \tag{18.8}$$

(where the bar denotes complex conjugation) holds whenever all of the λ_i lie along the positive real axis, and by analytic continuation holds throughout the domain of analyticity defined by (18.5). In fact the relation (18.8) follows directly from (18.1) on recalling from section 12.10 on page 263 that if $\boldsymbol{L}$ is replaced by its adjoint tensor, then the effective tensor $\boldsymbol{L}_*$ gets replaced by its adjoint, that is, its Hermitian conjugate, which is its complex conjugate because $\boldsymbol{L}_*$ is symmetric. But we see that this is also a consequence of the homogeneity and Herglotz properties.

There is one other property of the function $\boldsymbol{L}_*(\lambda_1, \ldots \lambda_n)$ that follows immediately from the fact that $\boldsymbol{L}_* = \boldsymbol{I}$ when $\boldsymbol{L} = \boldsymbol{I}$. It is

The normalization property:

$$\boldsymbol{L}_*(1, 1, \ldots, 1) = \boldsymbol{I}. \tag{18.9}$$

These analytic properties can be generalized to a broader class of composite problems, namely, those n-phase composites for which the tensor field $\boldsymbol{L}$ takes the form

$$\boldsymbol{L}(\boldsymbol{x}) = \boldsymbol{Q}(\boldsymbol{R}(\boldsymbol{x}))\left[\sum_{i=1}^{n} \chi_i(\boldsymbol{x})\boldsymbol{L}_i\right][\boldsymbol{Q}(\boldsymbol{R}(\boldsymbol{x}))]^T, \tag{18.10}$$

in which $\boldsymbol{Q}(\boldsymbol{R})$ is the orthogonal matrix (satisfying $\boldsymbol{Q}\boldsymbol{Q}^T = \boldsymbol{I}$) associated with a rotation $\boldsymbol{R}$ acting on elements in the tensor space, $\boldsymbol{R}(\boldsymbol{x})$ is a field of rotation matrices giving the local orientation of each phase, and $\chi_i(\boldsymbol{x})$ represents the characteristic function that is 1 in

phase i and zero elsewhere. For example, $\boldsymbol{L}(\boldsymbol{x})$ could represent the moduli in an n-phase polycrystalline material. In that case the matrices $\boldsymbol{L}_1, \ldots, \boldsymbol{L}_n$ represent the moduli of the pure crystalline phases, while $\boldsymbol{R}(\boldsymbol{x})$ represents the field of rotation matrices required to account for the different crystal orientations throughout space.

Now, what are the properties of the function $\boldsymbol{L}_*(\boldsymbol{L}_1, \boldsymbol{L}_2, \ldots \boldsymbol{L}_n)$ when the geometry of the composite, as represented by the fields $\boldsymbol{R}(\boldsymbol{x})$ and $\chi_i(\boldsymbol{x})$, is held fixed? Let us define $\boldsymbol{H}_0$ to be the set of $m \times m$ matrices that are bounded with a positive-definite self-adjoint part:

$$\boldsymbol{H}_0 = \{\boldsymbol{M} \mid \boldsymbol{M} + \boldsymbol{M}^\dagger > 0\},$$

where the dagger superscript denotes the Hermitian conjugate, that is, the transpose of the complex conjugate of the matrix. The series expansion for the effective tensor $\boldsymbol{L}_*$ is uniformly convergent whenever all of the matrices $\boldsymbol{L}_1,\ldots,\boldsymbol{L}_n$ all lie in any compact subset of the domain $\boldsymbol{H}_0$. Consequently, when these matrices all lie in this domain $\boldsymbol{L}_*(\boldsymbol{L}_1, \boldsymbol{L}_2, \ldots \boldsymbol{L}_n)$ is an analytic function of them, in the sense that it is an analytic function of all elements of the matrices $\boldsymbol{L}_1, \boldsymbol{L}_2, \ldots \boldsymbol{L}_n$. The homogeneity, Herglotz, and normalization properties generalize in the obvious fashion:

$$\boldsymbol{L}_*(\boldsymbol{L}_1, \boldsymbol{L}_2, \ldots \boldsymbol{L}_n) = \frac{1}{c}\boldsymbol{L}_*(c\boldsymbol{L}_1, c\boldsymbol{L}_2 \ldots c\boldsymbol{L}_n),$$

$$\boldsymbol{L}_* + \boldsymbol{L}_*^\dagger > 0 \qquad \text{when } \boldsymbol{L}_i + \boldsymbol{L}_i^\dagger > 0, \qquad \text{for } i = 1, 2 \ldots n,$$

$$\boldsymbol{L}_*(\boldsymbol{I}, \boldsymbol{I}, \ldots, \boldsymbol{I}) = \boldsymbol{I}.$$

18.3. Integral representations for the effective tensor for problems involving two eigenvalues

Let us focus on the simplest case, where the tensor $\boldsymbol{L}$ takes the form (18.1) and only two eigenvalues are present, that is, $n = 2$. For example, $\boldsymbol{L}$ could represent the conductivity tensor of a two-phase composite, with isotropic components, or it could represent the conductivity tensor of a three-dimensional polycrystal constructed from a single uniaxial crystal. By taking $c = 1/\lambda_2$ we see that the homogeneity property implies

$$\boldsymbol{L}_*(\lambda_1, \lambda_2) = \lambda_2 \boldsymbol{L}_*(\lambda_1/\lambda_2, 1).$$

So without any loss of generality we can set $\lambda_2 = 1$ and study the analytic properties of

$$\boldsymbol{L}_*(\lambda) = \boldsymbol{L}_*(\lambda, 1)$$

as a function of the single variable $\lambda = \lambda_1/\lambda_2$. From (18.5) we see that the function is analytic whenever the points λ_1 and λ_2 lie in the same half-plane H_θ, that is, whenever λ lies anywhere in the complex plane, except along the negative real axis. For example, if λ represents the conductivity of the white squares in a checkerboard, while the black squares have unit conductivity, then the effective conductivity $\boldsymbol{\sigma}_* = \sqrt{\lambda}\boldsymbol{I}$ of the checkerboard has a branch cut along the entire negative real axis and is analytic everywhere else in the complex plane.

The wedge bounds (18.7) imply that

$$\begin{aligned}
&\mathrm{Im}(\boldsymbol{L}_*) = 0, \ \ \mathrm{Re}(\boldsymbol{L}_*) > 0, \ \ \text{when } \mathrm{Im}(\lambda) = 0, \ \ \mathrm{Re}(\lambda) > 0, \\
&\mathrm{Im}(\boldsymbol{L}_*) > 0, \qquad\qquad\quad \text{when } \mathrm{Im}(\lambda) > 0, \\
&\mathrm{Im}(\boldsymbol{L}_*) < 0, \qquad\qquad\quad \text{when } \mathrm{Im}(\lambda) < 0.
\end{aligned} \tag{18.11}$$

Furthermore, (18.8) implies that the function $\boldsymbol{L}_*(\lambda)$ is real symmetric:

$$\boldsymbol{L}_*(\overline{\lambda}) = \overline{\boldsymbol{L}_*(\lambda)}, \tag{18.12}$$

where the bar denotes the complex conjugation.

It is convenient, following Bergman (1978b) and Golden and Papanicolaou (1983), to introduce a new variable,

$$s = \frac{\lambda_2}{\lambda_2 - \lambda_1} = \frac{1}{1-\lambda}, \tag{18.13}$$

and a new matrix-valued function,

$$\boldsymbol{F}(s) = \boldsymbol{I} - \boldsymbol{L}_*(\lambda) = \boldsymbol{I} - \boldsymbol{L}_*(1 - 1/s),$$

and obtain an integral representation for the function $\boldsymbol{F}(s)$. This is convenient because the normalization property (18.9) together with the analyticity at the point $\boldsymbol{\lambda} = (1, 1)$ implies that $\boldsymbol{F}(s)$ approaches zero as s tends to infinity. One should remember that $\boldsymbol{F}(s)$ is introduced, not because it has any special physical interpretation, but just because it is a mathematically convenient parameterization of the function $\boldsymbol{L}_*(\lambda, 1)$. The fractional linear transformation (18.13) maps the upper and lower halves of the complex λ-plane to the upper and lower halves of the complex s-plane, and maps the negative real axis, including the points zero and infinity, to the interval $[0, 1]$. So from (18.11) and (18.12) we see that $\boldsymbol{F}(s)$ is real symmetric and has a negative-definite imaginary part when s lies in the upper half of the complex plane.

The Cauchy integral formula can be applied separately to each matrix element of $\boldsymbol{F}(s)$ or, equivalently, it can be applied to the entire matrix-valued function. Suppose that we are given a point $s \notin [0, 1]$. Then we take a contour Γ comprised of two simply connected contours Γ^+ and Γ^-. The contour Γ^+ is a circle in the complex plane with a very large radius, while Γ^- loops tightly around, say, the interval $[-a, 1 + a]$ on the real axis, remaining close to the real axis. The constant $a > 0$ is chosen so that Γ^- does not enclose the point s. Let w be a complex variable on the contour Γ. Then, recalling that $\boldsymbol{F}(w)$ approaches zero as w tends to infinity, and that $\boldsymbol{F}(w)$ is real symmetric, the Cauchy integral formula,

$$\boldsymbol{F}(s) = \frac{1}{2\pi i} \int_\Gamma dw \frac{\boldsymbol{F}(w)}{w - s},$$

reduces to

$$\begin{aligned} \boldsymbol{F}(s) &= \lim_{\substack{\epsilon \to 0 \\ \epsilon > 0}} \frac{1}{2\pi i} \int_{-a}^{1+a} dy \frac{\boldsymbol{F}(y + i\epsilon) - \boldsymbol{F}(y - i\epsilon)}{y - s} \\ &= \lim_{\substack{\epsilon \to 0 \\ \epsilon > 0}} \frac{1}{\pi} \int_0^1 dy \frac{\operatorname{Im}(\boldsymbol{F}(y + i\epsilon))}{y - s}. \end{aligned}$$

This can be rewritten as the integral representation of Golden and Papanicolaou (1983)

$$\boldsymbol{F}(s) = \int_0^1 \frac{d\boldsymbol{\mu}(y)}{s - y}, \tag{18.14}$$

in which the integral of any smooth scalar test function $g(y)$ with respect to this measure $\boldsymbol{\mu}(y)$ is given by

$$\int_0^1 g(y) d\boldsymbol{\mu}(y) = -\lim_{\substack{\epsilon \to 0 \\ \epsilon > 0}} \frac{1}{\pi} \int_0^1 g(y) \operatorname{Im}(\boldsymbol{F}(y + i\epsilon))\, dy, \tag{18.15}$$

which serves to define the matrix-valued measure $\boldsymbol{\mu}(y)$. It is a positive measure in the sense that (18.15) is a positive-semidefinite matrix for all nonnegative test functions $g(y)$, due to the fact that $\boldsymbol{F}(y + i\epsilon)$ has a negative-definite imaginary part when $\epsilon > 0$. The beauty of the integral representation (18.14) is that it separates the dependence of $\boldsymbol{F}$ on the material moduli (through the variable s) from the dependence of $\boldsymbol{F}$ on the geometry [through the measure $\boldsymbol{\mu}(y)$]. Moreover, the dependence of $\boldsymbol{F}(s)$ on $\boldsymbol{\mu}(y)$ is linear.

For example, when $\boldsymbol{L}_*(\lambda)$, and hence $\boldsymbol{F}(s)$, are rational functions the measure is concentrated at the poles $s_1, s_2, \ldots, s_m$ of the rational function $\boldsymbol{F}(s)$ and (18.14) reduces to the form proposed by Bergman (1978b),

$$\boldsymbol{F}(s) = \sum_{\alpha=1}^{m} \frac{\boldsymbol{B}_\alpha}{s - s_\alpha}, \tag{18.16}$$

in which the poles s_α lie in the interval $[0, 1)$ and the residues $\boldsymbol{B}_\alpha$ are positive-semidefinite matrices, that is,

$$0 \le s_1 \le s_2 \le \ldots \le s_m < 1, \quad \text{and } \boldsymbol{B}_\alpha \ge 0 \text{ for all } \alpha.$$

In particular we see from (7.54) that for conduction in a coated ellipsoid assemblage, with core conductivity $\sigma_1 = \lambda$ and coating conductivity $\sigma_2 = 1$, the function $\boldsymbol{F}(s)$ has three poles with residues that are rank-1 matrices:

$$\boldsymbol{F}(s) = \boldsymbol{I} - \boldsymbol{\sigma}_* = \sum_{i=1}^{3} \frac{f_1 \boldsymbol{m}_i \otimes \boldsymbol{m}_i}{s - f_2 m_i},$$

in which the $\boldsymbol{m}_i$ and m_i are the eigenvectors and eigenvalues of the matrix $\boldsymbol{M}$ defined by (7.55) satisfying $\operatorname{Tr} \boldsymbol{M} = m_1 + m_2 + m_3 = 1$.

The poles s_α and residues $\boldsymbol{B}_\alpha$ were numerically computed by Bergman (1979) for a simple cubic array of spheres and by McPhedran and McKenzie (1980) for a square array of circular cylinders. Their work indicated that $\boldsymbol{F}(s)$ had an infinite number of poles accumulating at the point $s = 1/2$, corresponding to a conductivity ratio $\sigma_1/\sigma_2 = -1$. Liu and Wu (1997) estimated the position of those poles with dominant residues for body-centered and face-centered arrays of spheres. Reuben, Smith, and Radchik (1995) used conformal transformations to find exact closed-form expressions for the poles and residues for certain lattices of noncircular cylinders. Hinsen and Felderhof (1992) estimated the measure $d\boldsymbol{\mu}(y)$ for random suspensions of spheres by extrapolating the information contained in the series expansion for $\boldsymbol{F}(s)$ in powers of $1/s$. Thorpe, Djordjević, and Hetherington (1994) obtained approximations for the measure $d\boldsymbol{\mu}(y)$ for two-dimensional composites containing a dilute concentration of polygonal or elliptic inclusions. Ma, Zhang, Tam, and Sheng (2000) developed a Fourier-based computational scheme for calculating the measure, which they applied to two- and three-dimensional checkerboards, and to random suspensions of spheres. Day and Thorpe (1996) calculated the measure for random resistor networks. In a major achievement Day, Thorpe, Grant, and Sievers (2000) and Day, Grant, Sievers, and Thorpe (2000) have calculated the measure for KCl-diamond composites and RbCl-KCl composites from real reflectance data at different temperatures, using an algorithm developed by Day and Thorpe (1999). These provide the first examples of real composites for which the measure has been determined.

When the microstructure is periodic and the interface between the phases is a smooth surface with radii of curvature that are bounded above, Bergman (1985) has shown that the singularities of $\boldsymbol{F}(s)$ are all poles, apart from a possible essential singularity at $s = 1/2$,

corresponding to an accumulation point of poles. When the interface has sharp corners the following ingenious argument of Hetherington and Thorpe (1992) strongly suggests that it is the angles at the corners that determine the position of the branch cuts of $\boldsymbol{F}(s)$.

Suppose that the composite is composed of two dielectric materials with permittivities ε_1 and ε_2 such that $s = \varepsilon_2/(\varepsilon_2 - \varepsilon_1)$ is close to the branch cut. Then both phases are very low loss materials (i.e., ε_1 and ε_2 have very small imaginary parts) while the composite is quite lossy (i.e., $\boldsymbol{\varepsilon}_*$ has a significant imaginary part). The only way that this can occur is if the field is enormous (i.e., only barely square integrable) in a region of the composite, so that the electrical power dissipation given by (11.16) is significant in that region. The likely place for enormous fields to occur is near a corner or edge, and an asymptotic analysis can determine whether or not the field in this region can become close to being not square integrable. Then, when s is close to the branch cut, essentially all of the power dissipation occurs within a region of infinitesimal volume surrounding these corners and edges. For instance, consider a two-dimensional composite and suppose that the interface has a corner with an included angle of 2ψ radians. Suppose that the coordinate system has been chosen so that the corner is at the origin, with the interface meeting the real axis at angles of ψ and $-psi$. Also suppose that the phases have been labeled so phase 1 is immediately to the right of the origin and phase 2 is immediately to the left of the origin. Then in polar coordinates the electrical potential near the corner will be

$$\begin{aligned}\phi(r,\theta) &= a_1 r^\alpha \cos\alpha\theta + b_1 r^\alpha \sin\alpha\theta \ \text{ in phase 1,}\\ &= a_2 r^\alpha \cos\alpha(\pi-\theta) + b_2 r^\alpha \sin\alpha(\pi-\theta) \ \text{ in phase 2.}\end{aligned}$$

Continuity of the potential and the normal component of the electric displacement field across the interface leads to the constraints

$$\begin{aligned} a_1\cos\alpha\psi &= a_2\cos\alpha(\pi-\theta), & b_1\sin\alpha\psi &= b_2\sin\alpha(\pi-\theta)\\ -\varepsilon_1 a_1\sin\alpha\psi &= \varepsilon_2 a_2\sin\alpha(\pi-\theta), & \varepsilon_1 b_1\cos\alpha\psi &= -\varepsilon_2 b_2\cos\alpha(\pi-\theta).\end{aligned}$$

These have a nontrivial solution if and only if

$$\tan\alpha(\pi-\psi)/\tan\alpha\psi = -\varepsilon_1/\varepsilon_2 \tag{18.17}$$

or

$$\tan\alpha(\pi-\psi)/\tan\alpha\psi = -\varepsilon_2/\varepsilon_1. \tag{18.18}$$

Now the field will become close to being not square integrable if and only if the exponent α approaches the imaginary axis. But from (18.17) and (18.18) we see that values of α ranging along the imaginary axis correspond to values of $\varepsilon_1/\varepsilon_2$ ranging along the interval between $-(\pi-\psi)/\psi$ and -1 or ranging along the interval between -1 and $-\psi/(\pi-\psi)$, respectively. Consequently, one expects $\boldsymbol{F}(s)$ to have a branch cut along the interval $s \in [\psi/\pi, 1-\psi/\pi]$. Hetherington and Thorpe (1992) provided numerical evidence supporting this claim for dilute composites of polygonal inclusions. When the corner is a right angle, that is, when $\psi = \pi/4$, one expects the branch cut to lie between $s = 1/4$ and $s = 3/4$, corresponding to ratios of $\varepsilon_1/\varepsilon_2$ between $-1/3$ and -3. For example, the formula (8.33) for the effective conductivity of a square array of squares aligned with the unit cell and occupying a volume fraction of $1/4$ has a branch cut precisely along this interval. It is interesting to consider what must happen in an square array of squares aligned at 45° to the unit cell. When the squares touch it becomes a checkerboard, with $\boldsymbol{F}(s) = \boldsymbol{I} - \boldsymbol{I}\sqrt{1-1/s}$ having a branch cut when $s \in [0, 1]$. Otherwise

there is a branch cut when $s \in [1/4, 3/4]$. Clearly, when the squares almost touch the function $\boldsymbol{F}(s)$ must have an enormous number of isolated singularities in the intervals $s \in (0, 1/4)$ and $s \in (3/4, 1)$ in order to approximate the function $\boldsymbol{I} - \boldsymbol{I}\sqrt{1 - 1/s}$.

There is another obvious constraint on the measure. Since $\boldsymbol{L}_*(\lambda)$ is real and positive-definite along the positive real λ-axis, and in particular as $\lambda \to 0$ or, equivalently, as $s \to 1$, it follows that

$$\boldsymbol{F}(1) = \int_0^1 \frac{d\boldsymbol{\mu}(y)}{1 - y} \leq \boldsymbol{I}.$$

In the case of rational functions this reduces to the constraint

$$\boldsymbol{F}(1) = \sum_{\alpha=1}^{m} \frac{\boldsymbol{B}_\alpha}{1 - s_\alpha} \leq \boldsymbol{I}.$$

The moments of the measure $\boldsymbol{\mu}(y)$ can be related to the series expansion coefficients in a nearly homogeneous medium. Indeed, when λ is close to 1 or, equivalently, when s is large, the denominator in (18.14) can be expanded in powers of $1/s$ to give

$$\boldsymbol{F}(s) = \sum_{j=0}^{\infty} \frac{\boldsymbol{A}_j}{s^{j+1}}, \quad \text{where } \boldsymbol{A}_j = \int_0^1 y^j \, d\boldsymbol{\mu}(y),$$

which we can rewrite as

$$\boldsymbol{L}_*(\lambda_1, \lambda_2) = \lambda_2 \boldsymbol{I} - \sum_{j=0}^{\infty} \frac{(\lambda_2 - \lambda_1)^{j+1} \boldsymbol{A}_j}{\lambda_2^j}.$$

Thus knowledge of the leading terms in the series, such as $\boldsymbol{A}_0$ and $\boldsymbol{A}_1$, provides constraints on the moments of the measure. These constraints are known as sum rules; see Bergman (1978b) and Stroud (1979). For example, for two-phase conductivity with $\lambda_1 = \sigma_1$ and $\lambda_2 = \sigma_2$ we have $\boldsymbol{A}_0 = f_1 \boldsymbol{I}$ and $\operatorname{Tr} \boldsymbol{A}_1 = f_1 f_2$, which provides the two sum rules

$$\int_0^1 d\boldsymbol{\mu}(y) = f_1 \boldsymbol{I}, \quad \operatorname{Tr} \int_0^1 y \, d\boldsymbol{\mu}(y) = f_1 f_2.$$

For rational functions these reduce to the constraints

$$\sum_{\alpha=1}^{m} \boldsymbol{B}_\alpha = f_1 \boldsymbol{I}, \quad \operatorname{Tr} \sum_{\alpha=1}^{m} s_\alpha \boldsymbol{B}_\alpha = f_1 f_2.$$

For two-dimensional isotropic composites of two isotropic phases, Keller's relation (3.6) implies that all of the even-order moments can be expressed in terms of the lower odd-order moments [see sections 27.7 on page 585 and also Milton (1981b) and Bruno and Golden (1990)]. For phase interchange invariant composites of two isotropic phases, all of the odd-order moments can be expressed in terms of the lower even-order moments (see section 27.8 on page 588).

There is a close connection between the integral representation formula (18.14) and integral representations for Stieltjes functions. Introducing the variable w and function $\boldsymbol{G}(w)$ defined by

$$w = \lambda - 1 = -1/s, \quad \boldsymbol{G}(w) = [\boldsymbol{L}_*(1 + w) - \boldsymbol{I}]/w = -\boldsymbol{F}(-1/w)/w,$$

we see directly from (18.14) that $\boldsymbol{G}(w)$ has the integral representation

$$\boldsymbol{G}(w) = \int_0^1 \frac{d\boldsymbol{\mu}(y)}{1 + yw}.$$

Aside from the fact that $\boldsymbol{\mu}(y)$ is a positive-semidefinite matrix-valued measure, rather than a positive scalar-valued measure, this is the usual representation for a Stieltjes function of w with a radius of convergence of at least 1. So it is not surprising that various bounds on the effective tensor function $\boldsymbol{L}(\lambda)$ correspond to bounds on Stieltjes functions. This will be explored in chapter 27 on page 569.

As Bergman (1979) observed, the measure $\boldsymbol{\mu}(y)$ also has a direct interpretation in terms of the spectral measure associated with the operator $\boldsymbol{\Lambda}_1\boldsymbol{\Gamma}_1\boldsymbol{\Lambda}_1$. This operator is clearly self-adjoint, positive-semidefinite, and has norm less than 1. For simplicity let us assume that it has a discrete spectrum:

$$\boldsymbol{\Lambda}_1\boldsymbol{\Gamma}_1\boldsymbol{\Lambda}_1 = \sum_{\alpha=1}^{m'} \varphi_\alpha \boldsymbol{\Phi}_\alpha, \tag{18.19}$$

where

$$0 \le \varphi_1 \le \varphi_2 \le \ldots \le \varphi_{m'} \le 1 \text{ and } \sum_{\alpha=1}^{m} \boldsymbol{\Phi}_\alpha = \boldsymbol{\Lambda}_1, \quad \boldsymbol{\Phi}_\alpha\boldsymbol{\Phi}_\beta = \delta_{\alpha\beta}\boldsymbol{\Phi}_\alpha,$$

in which the φ_α are its eigenvalues and the $\boldsymbol{\Phi}_\alpha$ are projections onto the associated (possibly infinite-dimensional) eigenspaces that span $\mathcal{P}_1$. The formula (12.61) for the effective tensor $\boldsymbol{L}_*$ with $\sigma_0 = \lambda_2 = 1$ implies that

$$\boldsymbol{L}_* = \boldsymbol{I} - \boldsymbol{\Gamma}_0\boldsymbol{\Lambda}_1(s\boldsymbol{I} - \boldsymbol{\Lambda}_1\boldsymbol{\Gamma}_1\boldsymbol{\Lambda}_1)^{-1}\boldsymbol{\Lambda}_1\boldsymbol{\Gamma}_0,$$

where the inverse is to be taken on the subspace $\mathcal{P}_1$. Substitution of (18.19) into this formula gives the result that we are after:

$$\boldsymbol{F}(s) = \sum_{\alpha=1}^{m} \frac{\boldsymbol{\Gamma}_0\boldsymbol{\Phi}_\alpha\boldsymbol{\Gamma}_0}{s - \varphi_\alpha}. \tag{18.20}$$

This provides an alternative justification of the representation formula (18.16), and by extension provides an alternative justification of (18.14). Moreover, by comparing the two formulas (18.16) and (18.20) we see that the eigenvalues φ_α can be identified with the poles s_α and that the orientation of the associated eigenspaces with respect to the space $\mathcal{U}$ determines the residues through the equation

$$\boldsymbol{B}_\alpha = \boldsymbol{\Gamma}_0\boldsymbol{\Phi}_\alpha\boldsymbol{\Gamma}_0.$$

Notice that if $\varphi_\alpha = 1$ for some α, then $\boldsymbol{\Phi}_\alpha$ projects onto a subspace of $\mathcal{E}$, implying that the associated residue $\boldsymbol{B}_\alpha$ is zero. In other words, the sum in (18.20) can be restricted to those α such that $\varphi_\alpha \neq 1$.

The fields in the eigenspaces of $\boldsymbol{\Lambda}_1\boldsymbol{\Gamma}_1\boldsymbol{\Lambda}_1$ are associated with resonant solutions. Let $\boldsymbol{P}_\alpha$ be an eigenfield corresponding to the eigenvalue φ_α, that is,

$$\boldsymbol{\Lambda}_1\boldsymbol{\Gamma}_1\boldsymbol{P}_\alpha = \varphi_\alpha\boldsymbol{P}_\alpha. \tag{18.21}$$

Then the associated fields

$$\boldsymbol{E} = -\boldsymbol{\Gamma}_1\boldsymbol{P}, \quad \boldsymbol{J} = (\boldsymbol{I} - \boldsymbol{\Gamma}_1)\boldsymbol{P}$$

solve the equations

$$\boldsymbol{J} = \boldsymbol{L}\boldsymbol{E}, \quad \boldsymbol{L} = \lambda\boldsymbol{\Lambda}_1 + \boldsymbol{\Lambda}_2, \quad \boldsymbol{E} \in \mathcal{E}, \quad \boldsymbol{J} \in \mathcal{U} \oplus \mathcal{J}, \tag{18.22}$$

with

$$\lambda = 1 - 1/\varphi_\alpha.$$

The field $\boldsymbol{E}$ solving (18.22) is called a resonant solution since the equations are solved with $\boldsymbol{\Gamma}_0\boldsymbol{E} = 0$, that is, with no applied field (see section 11.7 on page 238). Conversely, given a resonant solution $\boldsymbol{E}$, the field $\boldsymbol{P}_\alpha = (\lambda - 1)\boldsymbol{\Gamma}_1\boldsymbol{E}$ satisfies (18.21) with $\varphi_\alpha = 1/(1-\lambda)$. It is only for certain values of λ that resonant solutions exist, and each such value (having $\boldsymbol{\Gamma}_0\boldsymbol{J} \neq 0$) corresponds to a pole of the function $\boldsymbol{F}(s)$ at $s = \varphi_\alpha = 1/(1-\lambda)$. McPhedran and McKenzie (1980) have pictures of some of the electrostatic resonant solutions for a square array of circular cylinders.

18.4. The correspondence between energy functions and microgeometries

Let us now focus on the effective conductivity function $\boldsymbol{\sigma}_*(\sigma_1, \sigma_2)$ of a two-component composite comprised of two isotropic components with conductivities σ_1 and σ_2. We choose to discuss the conductivity problem rather than the dielectric problem [which involves the same analytic function, i.e., $\boldsymbol{\sigma}_*(\sigma_1, \sigma_2) = \boldsymbol{\varepsilon}_*(\sigma_1, \sigma_2)$] merely because the inverse of $\boldsymbol{\sigma}_*$ has a name, namely, the resistivity tensor, and because electrical currents are easier to think about than displacement fields. We have seen that for every composite geometry, as represented by $\chi_1(\boldsymbol{x})$, there corresponds a positive-semidefinite measure $\boldsymbol{\mu}(y)$ that characterizes the conductivity function. But this leaves open the converse question: What measures correspond to geometries? Ideally one would like a complete list of all constraints satisfied by the measure, and a class of representative microgeometries that generate every measure compatible with these constraints.

First let us address a simpler problem, namely, let us look for a class of representative geometries associated with the function

$$\sigma_e(\sigma_1, \sigma_2) = \boldsymbol{e}_0 \cdot \boldsymbol{\sigma}_*(\sigma_1, \sigma_2)\boldsymbol{e}_0, \quad \text{where } \boldsymbol{e}_0 \cdot \boldsymbol{e}_0 = 1,$$

in which we take the applied electric field $\boldsymbol{e}_0$ to be fixed, real, and of unit magnitude, while the component conductivities σ_1 and σ_2 are allowed to vary in the complex plane. For real values of σ_1 and σ_2, we can think of $\sigma_e/2$ as representing the energy dissipation in the composite when it is subject to the applied field $\boldsymbol{e}_0$. For complex values of σ_1 and σ_2, we can think of σ_e as representing a diagonal element of the effective conductivity tensor $\boldsymbol{\sigma}_*$ in a basis where $\boldsymbol{e}_0$ is chosen as one of the basis vectors.

The analytic properties of the effective conductivity function imply that $\sigma_e(\lambda) = \sigma_e(\lambda, 1)$ is an analytic function of λ, except possibly on the negative real axis; is real symmetric; and maps the positive real axis onto itself, the upper plane onto itself, and the lower half-plane onto itself. To simplify the analysis let us work in the $(1/\lambda)$-plane, and suppose that σ_e is a rational function of $1/\lambda$. This latter assumption can be made without loss of generality because it amounts to replacing the infinite-dimensional Hilbert space $\mathcal{H}$ by a finite-dimensional approximant. Then by applying the Cauchy integral formula in the $(1/\lambda)$-plane, we see that the function has the representation

$$\sigma_e(\lambda) = a_0\lambda + a_{m+1} + \sum_{\alpha=1}^{m} \frac{b_\alpha}{c_\alpha + 1/\lambda}, \tag{18.23}$$

where the constants a_0 and a_{m+1}, residues b_α, and poles c_α are all real, and in addition satisfy the constraints

$$a_0 \geq 0, \quad b_\alpha > 0 \text{ for all } \alpha, \qquad c_m > c_{m-1} > \ldots > c_2 > c_1 > 0,$$
$$a_{m+1} = \sigma_e(0) \geq 0, \qquad a_0 + a_{m+1} + \sum_{\alpha=1}^{m} \frac{b_\alpha}{c_\alpha + 1} = \sigma_e(1) = 1.$$

Notice that because all of the residues b_α are positive and a_0 is nonnegative, $\sigma_e(\lambda)$ for real values of λ is a real-valued monotonic increasing function of λ except at the poles. Therefore, as Bergman (1978b) observed, a zero must lie between every pair of poles, that is, the zeros and poles of $\sigma_e(\lambda)$ alternate along the negative real λ-axis with a zero nearest or at the origin and with a pole nearest or at infinity.

The representation (18.23) together with the homogeneity property of the conductivity function yields a formula for the function $\sigma_e(\sigma_1, \sigma_2)$ that we choose to write in the form

$$\sigma_e(\sigma_1, \sigma_2) = \sum_{\alpha=0}^{m+1} \frac{a_\alpha}{q_\alpha/\sigma_1 + (1 - q_\alpha)/\sigma_2}, \tag{18.24}$$

where the constants a_0 and a_{m+1} remain unchanged while

$$q_0 = 1, \quad q_{m+1} = 0, \quad q_\alpha = \frac{1}{1 + c_\alpha}, \quad a_\alpha = \frac{b_\alpha}{1 + c_\alpha}, \quad \alpha = 1, 2, \ldots, m.$$

These parameters generally depend on the direction of the applied field $\boldsymbol{e}_0$. They satisfy the constraints

$$1 = q_0 > q_1 > q_2 \ldots > q_m > q_{m+1} = 0, \quad a_\alpha \geq 0 \text{ for all } \alpha, \quad \sum_{\alpha=0}^{m+1} a_\alpha = 1. \tag{18.25}$$

Now consider the rank-2 laminate material illustrated in figure 18.1 on the facing page for $m = 3$, which is constructed by the following two-step procedure. The first step is to make a total of $m + 2$ simple rank-1 laminates: Laminate α for $\alpha = 0, 1, 2, \ldots, m + 1$ is comprised of phase 1 laminated with phase 2, in proportions q_α and $1 - q_\alpha$, respectively. The laminates are oriented so that the applied field $\boldsymbol{e}_0$ is in the direction of lamination. Hence their effective conductivity $\sigma_e^{(\alpha)}$ in this direction is the harmonic mean:

$$\sigma_e^{(\alpha)} = [q_\alpha/\sigma_1 + (1 - q_\alpha)/\sigma_2]^{-1}.$$

The second step is to layer together these simple laminates (on a much larger length scale) in proportions $a_0, a_1, \ldots, a_m$ with the direction $\boldsymbol{n}$ of lamination taken perpendicular to $\boldsymbol{e}_0$, (i.e., with $\boldsymbol{e}_0$ in the plane of slicing). Then the energy function is just an arithmetic average:

$$\sigma_e(\sigma_1, \sigma_2) = \sum_{\alpha=0}^{m+1} a_\alpha \sigma_*^{(\alpha)} = \sum_{\alpha=0}^{m+1} \frac{a_\alpha}{q_\alpha/\sigma_1 + (1 - q_\alpha)/\sigma_2}. \tag{18.26}$$

The agreement between (18.26) and (18.24) shows that these rank-2 laminates form a representative class of microstructures: They can simulate, to an arbitrarily high degree of approximation, the energy function of any composite geometry (Milton 1981b).

A similar analysis can be applied to the dual function

$$\rho_j(\rho_1, \rho_2) = \boldsymbol{j}_0 \cdot [\boldsymbol{\sigma}_*(1/\rho_1, 1/\rho_2)]^{-1} \boldsymbol{j}_0, \quad \text{where } \boldsymbol{j}_0 \cdot \boldsymbol{j}_0 = 1,$$

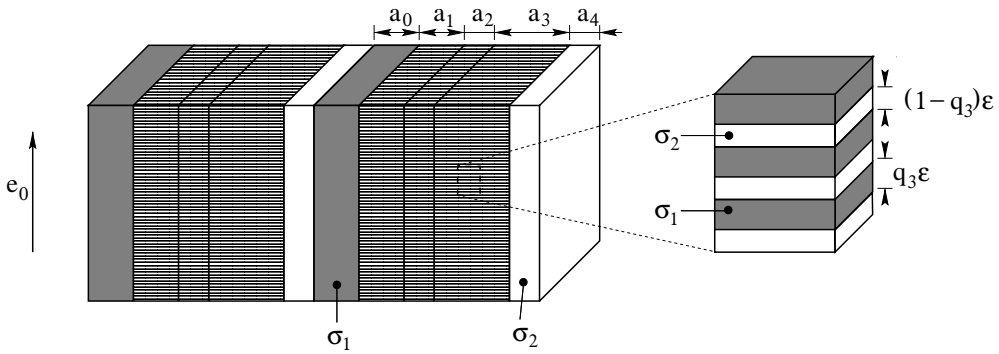

Figure 18.1. A laminate microgeometry that when periodically extended has, in the limit as $\epsilon \to 0$, the conductivity function $\sigma_e(\sigma_1, \sigma_2)$ given by (18.26) with $m = 3$. The applied field $\boldsymbol{e}_0$ is assumed to be parallel to the outermost layers. By considering the limit as $m \to \infty$, one can use such second-rank laminates to mimic the conductivity function of any microstructure.

in which the applied current field $\boldsymbol{j}_0$ is now taken to be real, of unit magnitude, and held fixed independent of the resistivities $\rho_1 = 1/\sigma_1$ and $\rho_2 = 1/\sigma_2$. For real values of ρ_1 and ρ_2, we can again think of $\rho_j/2$ as representing the energy dissipation in the composite when it is subject to an applied current field $\boldsymbol{j}_0$. For complex values of σ_1 and σ_2, we can think of ρ_j as representing a diagonal element of the effective resistivity tensor $\boldsymbol{\sigma}_*^{-1}$ in a basis where $\boldsymbol{j}_0$ is chosen as one of the basis vectors. Supposing that the dual function is rational, we find that it has a representation

$$\rho_j(\rho_1, \rho_2) = \sum_{\alpha=0}^{m+1} \frac{a_\alpha}{q_\alpha/\rho_1 + (1 - q_\alpha)/\rho_2},$$

where the constants a_α and q_α that appear here depend on the direction of $\boldsymbol{j}_0$ and are not necessarily the same as those in (18.24), but nevertheless satisfy the same constraints (18.25). The same family of second-rank laminate geometries generates all possible rational dual functions. However, now the applied current field $\boldsymbol{j}_0$ needs to be aligned parallel to the final direction of lamination $\boldsymbol{n}$.

18.5. The correspondence between effective conductivity functions and microgeometries in two dimensions†

The class of second-rank laminate geometries is not sufficiently diverse to generate all effective conductivity functions. Indeed, in these geometries the axes of principal conductivity remain fixed and independent of σ_1 and σ_2, whereas in many microstructures the axes of principal conductivity rotate as σ_1 and σ_2 are varied; see figure 18.2 on the next page. One class of microgeometry that exhibits this rotation is the class of multicoated laminate geometries. These are constructed in stages. The first stage is to manufacture a coated laminate, taking, say, phase 1 with conductivity tensor

$$\boldsymbol{\sigma}_*^0 = \sigma_1 \boldsymbol{I} \tag{18.27}$$

as core and phase 2 as coating. At the second stage this composite, with effective conductivity tensor $\boldsymbol{\sigma}_*^{(1)}$, is taken as the core phase in another coated laminate, now with phase 1 as the

coating. This gives a doubly coated laminate with conductivity tensor $\boldsymbol{\sigma}_*^{(2)}$. One continues this process, alternately taking phase 2 or phase 1 as coating, until one obtains a multicoated laminate with, say, ℓ-coatings, and effective conductivity tensor $\boldsymbol{\sigma}_*^{(\ell)}$.

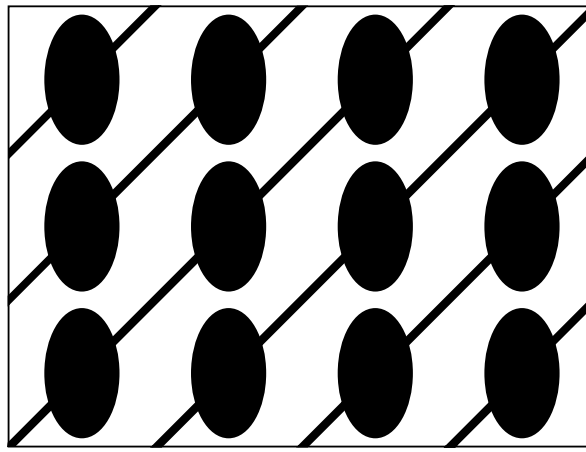

Figure 18.2. A microgeometry for which the eigenvectors of $\boldsymbol{\sigma}_*(\sigma_1, \sigma_2)$ rotate as the ratio σ_1/σ_2 is varied. When this ratio is close to 1 the eigenvectors of $\boldsymbol{\sigma}_*(\sigma_1, \sigma_2)$ almost align with the axes of the ellipsoids. The filamentary threads of component 1 have little influence on the effective conductivity. As this ratio is increased, the threads carry more current and thereby cause the eigenvectors to rotate. After Milton (1986a).

The formula (9.20) for the effective conductivity of a coated laminate can be applied at each stage in this construction to compute $\boldsymbol{\sigma}_*^{(\ell)}$. For integer values of j, from $j = 0$ up to the largest integer less than or equal to $(\ell+1)/2$, one has

$$\begin{aligned}(1 - p_{2j+1})\sigma_2\Big[\sigma_2\boldsymbol{I} - \boldsymbol{\sigma}_*^{(2j+1)}\Big]^{-1} &= \sigma_2\Big[\sigma_2\boldsymbol{I} - \boldsymbol{\sigma}_*^{(2j)}\Big]^{-1} - p_{2j+1}\boldsymbol{M}_{2j+1},\\ (1 - p_{2j+2})\sigma_1\Big[\sigma_1\boldsymbol{I} - \boldsymbol{\sigma}_*^{(2j+2)}\Big]^{-1} &= \sigma_1\Big[\sigma_1\boldsymbol{I} - \boldsymbol{\sigma}_*^{(2j+1)}\Big]^{-1} - p_{2j+2}\boldsymbol{M}_{2j+1},\end{aligned} \tag{18.28}$$

in which p_i represents the volume fraction of coating material added at the i-th stage and $\boldsymbol{M}_i$ is a positive-semidefinite tensor satisfying $\mathrm{Tr}(\boldsymbol{M}_i) = 1$ that is determined by the directions of layering and by the amounts layered in these directions at the i-th stage in the construction process. As these directions and amounts are varied, $\boldsymbol{M}_i$ ranges over the set of all positive-semidefinite matrices satisfying $\mathrm{Tr}(\boldsymbol{M}_i) = 1$ (see section 9.4 on page 165). By eliminating the tensors $\boldsymbol{\sigma}_*^{(i)}$ for $i = 0$ up to $i = \ell$–1 from the set of equations (18.28) one obtains a formula for the effective conductivity function $\boldsymbol{\sigma}_*^{(\ell)}(\sigma_1, \sigma_2)$ as a continued fraction incorporating the constants $p_1, p_2, \ldots, p_\ell$ and the matrices $\boldsymbol{M}_1, \boldsymbol{M}_2, \ldots, \boldsymbol{M}_\ell$. The eigenvectors of $\boldsymbol{\sigma}_*^{(\ell)}$ rotate as σ_1 and σ_2 are varied unless the matrices $\boldsymbol{M}_1, \boldsymbol{M}_2, \ldots, \boldsymbol{M}_\ell$ happen to be simultaneously diagonal in some basis.

Now, is this family of multicoated laminates sufficiently diverse to encompass all possible effective conductivity functions? In two dimensions the answer is yes, it is! (Milton 1986b). Specifically, there is a complete correspondence between the continued fractions generated

from (18.27) and (18.28) and the set of all rational functions $\boldsymbol{\sigma}_*(\sigma_1, \sigma_2)$ satisfying homogeneity,

$$\boldsymbol{\sigma}_*(c\sigma_1, c\sigma_2) = c\boldsymbol{\sigma}_*(\sigma_1, \sigma_2), \tag{18.29}$$

the Herglotz property,

$$\text{Re}\,(\boldsymbol{\sigma}_*) > 0 \text{ when } \text{Re}\,(\sigma_1) > 0 \text{ and } \text{Re}\,(\sigma_2) > 0, \tag{18.30}$$

normalization,

$$\boldsymbol{\sigma}_*(1, 1) = \boldsymbol{I},$$

and the phase interchange identity,

$$\boldsymbol{\sigma}_*(\sigma_2, \sigma_1)\boldsymbol{R}_\perp\boldsymbol{\sigma}_*(\sigma_1, \sigma_2)\boldsymbol{R}_\perp^T = \sigma_1\sigma_2\boldsymbol{I}, \tag{18.31}$$

which is implied by (3.9).

To understand the key idea behind the ensuing analysis, suppose that we were given a rational function $\boldsymbol{\sigma}_*(\sigma_1, \sigma_2)$ and wanted to find an associated multicoated laminate with $\boldsymbol{\sigma}_*(\sigma_1, \sigma_2)$ as its effective tensor for all values of σ_1 and σ_2. Assuming that phase 2 was the last coating in the construction of the laminate, we should get an indication of how much of this component was layered and in what directions by setting $\sigma_1 = 0$ (or $\sigma_2 = \infty$). For example, if $\boldsymbol{\sigma}_*(\sigma_1, 0)$ has only one nonzero eigenvalue, then at the last stage phase 2 must have been layered with the layers parallel to the direction of the associated eigenvector. By subtracting from $\boldsymbol{\sigma}_*(\sigma_1, \sigma_2)$ the contribution of this layering (in effect removing the last layering) one would expect to get a rational function $\boldsymbol{\sigma}_*(\sigma_1, \sigma_2)$ of reduced degree, still satisfying (18.29), (18.30), and (18.31). By repeating this procedure, alternately setting σ_2 or σ_1 to zero, we would eventually obtain information about the entire sequence of layerings from which a laminate with conductivity function $\boldsymbol{\sigma}_*(\sigma_1, \sigma_2)$ could be constructed.

The proof of the correspondence proceeds by induction. The first step is to define the degree of rationality of a conductivity function in a way that is independent of the labeling of the phases. To this end we define the degree g to be the number of poles of the function $\boldsymbol{\sigma}_*(\lambda, 1)$ weighted in proportion to the rank of the associated residue, which is either a rank-1 or rank-2 matrix. Any pole at $\lambda = \infty$ is to be excluded from this count.

Let us suppose that there exists some value of g such that any rational conductivity function of degree g or less satisfying (18.29)–(18.31) corresponds to the conductivity function of some multicoated laminate with at most g coatings. This is certainly true for $g = 0$ since the only rational functions of degree 0 satisfying these constraints are $\boldsymbol{\sigma}_*(\sigma_1, \sigma_2) = \sigma_1$ and $\boldsymbol{\sigma}_*(\sigma_1, \sigma_2) = \sigma_2$, which correspond respectively to pure phase 1 or pure phase 2. Now consider any rational function $\boldsymbol{\sigma}_*(\sigma_1, \sigma_2)$ of degree $g + 1$ that satisfies these constraints. When $\sigma_2 = 0$ and $\sigma_1 = 1$, (18.31) implies that either $\boldsymbol{\sigma}_*(0, 1)$ or $\boldsymbol{\sigma}_*(1, 0)$ is a singular matrix. (It may happen that both matrices are singular.) Let us assume that $\boldsymbol{\sigma}_*(1, 0)$ is singular; when it is not singular, $\boldsymbol{\sigma}_*(0, 1)$ is singular and we need to swap the roles of the two phases in the subsequent analysis.

Now examine the rational function

$$\boldsymbol{S}_*(s) = [\boldsymbol{F}(s)]^{-1} = [\boldsymbol{I} - \boldsymbol{\sigma}_*(1 - 1/s, 1)]^{-1}.$$

The restrictions (18.29) – (18.31) imply that $\boldsymbol{S}_*(s)$ satisfies

$$\begin{aligned}
&\boldsymbol{S}_*(s) + \boldsymbol{R}\boldsymbol{S}_*(1 - s)\boldsymbol{R}^T = \boldsymbol{I}, \qquad && \boldsymbol{S}_*(\overline{s}) = \overline{\boldsymbol{S}_*(s)},\\
&\boldsymbol{S}_*(s) \geq \boldsymbol{I} \quad \text{for all real } s \geq 1, \qquad && \boldsymbol{S}_*(s) \leq 0 \quad \text{for all real } s \leq 0,\\
&\text{Im}\ \boldsymbol{S}_*(s) > 0 \quad \text{whenever Im } s > 0,
\end{aligned} \tag{18.32}$$

and conversely any rational function $\boldsymbol{S}(s)$ satisfying these constraints produces a function

$$\boldsymbol{\sigma}_*(\sigma_1, \sigma_2) = \sigma_2 \boldsymbol{I} - \sigma_2[\boldsymbol{S}_*(\sigma_2/(\sigma_2 - \sigma_1))]^{-1} \tag{18.33}$$

satisfying (18.29)–(18.31). The constraints imply that $\boldsymbol{S}_*(s)$ has a pole at $s = \infty$ and all other poles in the open interval (0, 1). The residues associated with these poles are negative-semidefinite matrices, and this implies that elsewhere on the real s-axis $\boldsymbol{S}_*(s)$ is a monotonic increasing function of s, in the sense that its derivative with respect to s is a positive-semidefinite matrix. In particular, it follows that the eigenvalues of $\boldsymbol{S}_*(s)$ are monotonic increasing functions of s except at the poles.

The degree g now refers to the total number of points s in the *open interval* (0, 1), where $\boldsymbol{S}_*(s)$ has an eigenvalue equal to unity. Those points s where $\boldsymbol{S}_*(s) = \boldsymbol{I}$ count double. From (18.32) we see that $\boldsymbol{S}_*(0)$ is negative-semidefinite. It is certainly nonzero because otherwise [using the fact that $\boldsymbol{S}(s)$ is rational] we could expand $\boldsymbol{S}_*(s)$ in a Taylor series about $s = 0$ and (18.33) would imply that $\boldsymbol{\sigma}_*(1, 0)$ is nonsingular, in contradiction with our assumption. This allows us to introduce the symmetric real matrix

$$\boldsymbol{M} = \boldsymbol{S}_*(0)/\mathrm{Tr}[\boldsymbol{S}_*(0)], \quad \text{which satisfies } \mathrm{Tr}(\boldsymbol{M}) = 1, \ \ \boldsymbol{M} \geq 0.$$

The form of the relations (18.28) suggests that we should introduce the function

$$\boldsymbol{S}'_*(s) = (1 - p)\boldsymbol{S}_*(s) + p\boldsymbol{M} \tag{18.34}$$

and study its analytic properties as a function of s for p in the interval

$$0 \leq p \leq p^+ \equiv -\mathrm{Tr}[\boldsymbol{S}_*(0)]/\{1 - \mathrm{Tr}[\boldsymbol{S}_*(0)]\}.$$

This constant p^+ is positive and less than unity because $\boldsymbol{S}_*(0)$ is negative-semidefinite. It is easy to check that this function $\boldsymbol{S}'_*(s)$ satisfies the required constraints (18.32) for any choice of p in this interval. Moreover, the fact that for real values of s the eigenvalues of $\boldsymbol{S}_*(s)$ are monotonic increasing functions of s, except at the poles, implies that the degree g remains constant as p remains in the interval $(0, p^+)$. As p approaches p^+ the matrix $\boldsymbol{S}'_*(0)$ approaches zero, and due to the phase interchange relationship it follows that $\boldsymbol{S}'_*(1)$ approaches the identity matrix. In other words, if we consider those points $s \in (0, 1)$ where $\boldsymbol{S}_*(s)$ has unit eigenvalue, then at least one of those points approaches $s = 1$ as p approaches p^+. Consequently, in the limit $p = p^+$, the degree of the rational function is reduced. Specifically it is reduced by the rank of the matrix $\boldsymbol{S}_*(0)$. By hypothesis there exists a multicoated laminate corresponding to this rational function, and from (18.34) we see that by constructing a sequential coated laminate with this composite as core and phase 2 as coating, in proportions $1 - p^+$ and p^+, we obtain a multicoated laminate corresponding to the given function $\boldsymbol{\sigma}_*(\sigma_1, \sigma_2)$. In this last stage of lamination the matrix $\boldsymbol{S}_*(0)$ determines the directions of laminations and amounts of phase 2 to be laminated in each direction.

This correspondence does not hold in three dimensions. The class of multicoated laminates is not sufficiently diverse to mimic the behavior of the conductivity function of an arbitrary three-dimensional, two-phase composite. Indeed there exist many three-dimensional composites such that $\boldsymbol{\sigma}(1, 0)$ and $\boldsymbol{\sigma}(0, 1)$ are both nonsingular matrices. For example, this occurs if phase 1 is the connected solid phase in an isotropic porous medium and phase 2 is the connected fluid phase occupying the pore space. By contrast, in any multicoated laminate of finite rank, at least one of the matrices $\boldsymbol{\sigma}(1, 0)$ or $\boldsymbol{\sigma}(0, 1)$ must be singular. For example, if at the last stage in the construction of a multicoated laminate phase 2 was laminated in

direction $\boldsymbol{n}$, then $\boldsymbol{\sigma}(1, 0)$ will have $\boldsymbol{n}$ as a null vector because the current cannot flow across a nonconducting layer.

A related correspondence holds for two-dimensional conducting polycrystals. In a two-dimensional polycrystal the local conductivity tensor takes the form

$$\boldsymbol{\sigma}(\boldsymbol{x}) = \boldsymbol{R}(\boldsymbol{x})\boldsymbol{\sigma}_0\boldsymbol{R}^T(\boldsymbol{x}),$$

where the rotation field $\boldsymbol{R}(\boldsymbol{x})$ [satisfying $\boldsymbol{R}(\boldsymbol{x})\boldsymbol{R}^T(\boldsymbol{x}) = \boldsymbol{I}$] gives the orientation of the crystal at the point $\boldsymbol{x}$. One can consider the effective conductivity tensor $\boldsymbol{\sigma}_*$ as a function $\boldsymbol{\sigma}_*(\boldsymbol{\sigma}_0)$ of the conductivity tensor $\boldsymbol{\sigma}_0$ of the underlying crystal. Clark and Milton (1994) have shown that a certain family of coated laminates is sufficiently diverse to encompass all possible conductivity functions $\boldsymbol{\sigma}_*(\boldsymbol{\sigma}_0)$. This is accomplished in a new way, by making a correspondence between fields in the Hilbert space associated with the given polycrystal and fields in the Hilbert space associated with an appropriate coated laminate.

18.6. Integral representations for problems involving more than two eigenvalues: The trajectory method

For two-component composites the integral representation (18.14) provides a formula for $\boldsymbol{L}_*$ in terms of a positive measure $\boldsymbol{\mu}$ that derives from the values that $\mathrm{Im}[\boldsymbol{L}_*(\lambda_1, \lambda_2)]$ takes as λ_1 and λ_2 approach the real axis. For problems involving more than two eigenvalues, such as conduction in a multicomponent composite or elasticity in a two-component composite, one can similarly obtain an integral representation for $\boldsymbol{L}_*$ in terms of a positive measure $\boldsymbol{\mu}$ that derives from the values that $\mathrm{Im}[\boldsymbol{L}_*]$ takes as $\lambda_1, \lambda_2, \ldots, \lambda_n$ approach the real axis. Such an integral representation was first obtained by Golden and Papanicolaou (1985). Other integral representations, which treated the phases symmetrically, were subsequently obtained (Dell'Antonio and Nesi 1988; Milton and Golden 1990). Here we show that an integral representation can be obtained simply by reducing the problem to one involving functions of a single complex variable. This approach is known as the trajectory method. It is similar to one taken by Bergman (1978b), who did not view it as a representation for the multivariable function $\boldsymbol{L}_*(\lambda_1, \lambda_2, \ldots, \lambda_n)$, but rather regarded it only as a representation for $\boldsymbol{L}_*$ along a certain trajectory $(\lambda_1(s), \lambda_2(s), \ldots, \lambda_n(s))$ parameterized by a variable s. To obtain the representation formula for the multivariable function it is necessary to introduce a suitable family of trajectories that are sufficiently general so as to pass through any given point $(\lambda_1, \lambda_2, \ldots, \lambda_n)$.

Let us derive an integral formula for $\boldsymbol{L}_*$ at a given point $(\lambda_1, \lambda_2, \ldots, \lambda_n)$. For simplicity (by making a rotation in the complex plane if necessary) let us assume that

$$\mathrm{Im}(\lambda_j) > 0 \ \text{ for } j = 1, 2, \ldots, n.$$

Our objective is to express $\boldsymbol{L}_*(\lambda_1, \lambda_2, \ldots, \lambda_n)$ in terms of a measure that derives from the values that $\mathrm{Im}[\boldsymbol{L}_*(\lambda_1', \lambda_2', \ldots, \lambda_n')]$ takes as $\lambda_1', \lambda_2', \ldots, \lambda_n'$ approach the real axis. To do this we consider a trajectory

$$(\lambda_1'(s), \lambda_2'(s), \ldots, \lambda_n'(s)), \quad \text{where } \lambda_j'(s) = 1 - 1/(a_j + sb_j), \tag{18.35}$$

parameterized by the complex variable s. (Strictly speaking, this is a two-dimensional sheet parameterized by the real and imaginary parts of s, but we call it a trajectory to conform with the terminology used by Bergman.) The constants a_j and b_j are real and chosen so that the

trajectory passes through the given point $(\lambda_1, \lambda_2, \ldots, \lambda_n)$ for one particular value of s, say, $s = i$, that is, so that $(\lambda_1'(i), \lambda_2'(i), \ldots, \lambda_n'(i)) = (\lambda_1, \lambda_2, \ldots, \lambda_n)$. This is ensured with

$$a_j = \mathrm{Re}[1/(1-\lambda_j)], \quad b_j = \mathrm{Im}[1/(1-\lambda_j)] > 0.$$

The positivity of the constants b_j (guaranteed by our assumption of the positivity of $\mathrm{Im}[\lambda_j]$) ensures that

$$\mathrm{Im}[\lambda_j'(s)] > 0 \text{ when } \mathrm{Im}[s] > 0, \quad \text{and } \mathrm{Im}[\lambda_j'(s)] < 0 \text{ when } \mathrm{Im}[s] < 0. \tag{18.36}$$

It follows from this that the function

$$\begin{aligned} \boldsymbol{F}(s) &= \boldsymbol{I} - \boldsymbol{L}_*(\lambda_1'(s), \lambda_2'(s), \ldots, \lambda_n'(s)) \\ &= \boldsymbol{I} - \boldsymbol{L}_*(1 - 1/(a_1 + sb_1), 1 - 1/(a_2 + sb_2), \ldots, 1 - 1/(a_n + sb_n)) \end{aligned}$$

is real symmetric and has a negative-definite imaginary part when s lies in the upper half of the complex plane. Since $\boldsymbol{F}(s)$ approaches zero as s tends to infinity, we deduce that $\boldsymbol{F}(s)$ has the integral representation

$$\boldsymbol{F}(s) = \int_{-\infty}^{\infty} \frac{d\boldsymbol{\mu}(y)}{s - y},$$

in which the integral of any smooth scalar test function $g(y)$ with respect to this measure $\boldsymbol{\mu}(y)$ is given by

$$\begin{aligned} \int_{-\infty}^{\infty} d\boldsymbol{\mu}(y) g(y) &= -\lim_{\substack{\epsilon \to 0 \\ \epsilon > 0}} \frac{1}{\pi} \int_{-\infty}^{\infty} dy \ \mathrm{Im}[\boldsymbol{F}(y + i\epsilon)] g(y) \\ &= \lim_{\substack{\epsilon \to 0 \\ \epsilon > 0}} \frac{1}{\pi} \int_{-\infty}^{\infty} dy \ \mathrm{Im}[\boldsymbol{L}_*(\lambda_1'(y + i\epsilon), \lambda_2'(y + i\epsilon), \ldots, \lambda_n'(y + i\epsilon))], \end{aligned}$$

which serves to define the positive-semidefinite matrix-valued measure $\boldsymbol{\mu}(y)$. By setting $s = i$ in the integral representation for $\boldsymbol{F}(s)$ we obtain

$$\boldsymbol{L}_*(\lambda_1, \lambda_2, \ldots, \lambda_n) = \boldsymbol{I} - \int_{-\infty}^{\infty} \frac{d\boldsymbol{\mu}(y)}{i - y}. \tag{18.37}$$

These are the desired formulas for $\boldsymbol{L}_*(\lambda_1, \lambda_2, \ldots, \lambda_n)$ in terms of a measure $\boldsymbol{\mu}$ that derives from the values that $\mathrm{Im}[\boldsymbol{L}_*(\lambda_1', \lambda_2', \ldots, \lambda_n')]$ takes as $\lambda_1', \lambda_2', \ldots, \lambda_n'$ approach the real axis. Notice that the dependence of $\boldsymbol{L}_*$ on the complex variables $\lambda_1, \lambda_2, \ldots, \lambda_n$ is hidden in the dependence of the measure on these variables.

The measure $\boldsymbol{\mu}(y)$ certainly vanishes for $y \le y_-$ and for $y \ge y_+$, where

$$y_- \equiv \min\{-a_1/b_1, \ldots, -a_n/b_n\}, \quad \text{and } y_+ \equiv \max\{(1 - a_1)/b_1, \ldots, (1 - a_n)/b_n\},$$

since for y satisfying either one of these inequalities the parameters $\lambda_1'(y), \ldots, \lambda_n'(y)$ are all positive and the imaginary part of $\boldsymbol{L}_*(\lambda_1'(y + i\epsilon), \lambda_2'(y + i\epsilon), \ldots, \lambda_n'(y + i\epsilon))$ approaches zero as ϵ approaches zero. Consequently, the integral in the representation formula (18.37) can be restricted to the range between y_- and y_+:

$$\boldsymbol{L}_*(\lambda_1, \lambda_2, \ldots, \lambda_n) = \boldsymbol{I} - \int_{y_-}^{y_+} \frac{d\boldsymbol{\mu}(y)}{i - y}.$$

18.7. The lack of uniqueness in the choice of integral kernel: Constraints on the measure†

We could have chosen trajectories other than (18.35). It is only required that they pass through the given point and satisfy (18.36). These choices would have led to alternative integral representations. To shed further light on this lack of uniqueness in the integral representation it is helpful to introduce the variables

$$z_j = (i - \lambda_j)/(i + \lambda_j),$$

which take values in the unit disk when the λ_j take values in the upper half-plane. Consequently $(z_1, z_2, \ldots, x_n)$ is said to take values in the polydisk. We now consider $\boldsymbol{L}_*$ as a function of the z_j, that is, $\boldsymbol{L}_* = \boldsymbol{L}_*(z_1, z_2, \ldots, z_n)$. The integral representation (18.37) shows that $\boldsymbol{L}_*$ at a given point depends linearly on the values that $\mathrm{Im}[\boldsymbol{L}_*]$ takes as $\lambda_1', \lambda_2', \ldots, \lambda_n'$ approach the real axis. Therefore the integral representation (18.37) could be rewritten in the equivalent form of a polydisk representation formula,

$$\boldsymbol{L}_*(z_1, z_2, \ldots, z_n) = \int_{T^n} \boldsymbol{K}(z_1, z_2, \ldots, z_n, \theta_1, \theta_2, \ldots, \theta_n) d\boldsymbol{\mu}'(\theta_1, \theta_2, \ldots, \theta_n), \qquad (18.38)$$

incorporating an integral kernel $\boldsymbol{K}(z_1, z_2, \ldots, z_n, \theta_1, \theta_2, \ldots, \theta_n)$ and a positive measure $\boldsymbol{\mu}'$ that derives from the values that $\mathrm{Im}(\boldsymbol{L}_*)$ takes as $z_1, z_2, \ldots, z_n$ approach the edge of the unit disk, that is, as z_j approaches $e^{i\theta_j}$ for $j = 1, 2, \ldots, n$. The integral in (18.38) is over the n-dimensional torus T^n, which is parameterized by the angular variables $\theta_1, \theta_2, \ldots, \theta_n$ with $0 \le \theta_j < 2\pi$ for all j. The measure $\boldsymbol{\mu}'$ is defined through the integral of any smooth scalar test function $g(\theta_1, \theta_2, \ldots, \theta_n)$ with respect to it. We define

$$\int_{T^n} g(\theta_1, \theta_2, \ldots, \theta_n) d\boldsymbol{\mu}'(\theta_1, \theta_2, \ldots, \theta_n) = \lim_{\substack{r \to 1 \\ r<1}} \int_{T^n} g(\theta_1, \theta_2, \ldots, \theta_n)\, \mathrm{Im}[\boldsymbol{L}_*(re^{i\theta_1}, re^{i\theta_2}, \ldots, re^{i\theta_n})] d\theta_1 d\theta_2 \ldots d\theta_n. \qquad (18.39)$$

One advantage of rewriting the integral representation (18.37) in the polydisk form (18.38) is that it separates the dependence of $\boldsymbol{L}_*$ on the complex variables $\lambda_1, \lambda_2, \ldots, \lambda_n$ from the dependence of $\boldsymbol{L}_*$ on the characteristic functions; the integral kernel $\boldsymbol{K}$ depends on the complex variables but not on the characteristic functions, whereas the measure $\boldsymbol{\mu}'$ (unlike the measure $\boldsymbol{\mu}$) depends on the characteristic functions but not on the complex variables. Interpreted in this way, we see that the trajectory method has been wrongly criticized for failing to make the separation between the dependence on the material properties and the dependence on the geometry.

With some additional effort one could derive an explicit formula for the integral kernel $\boldsymbol{K}(z_1, z_2, \ldots, z_n, \theta_1, \theta_2, \ldots, \theta_n)$. Even without this explicit formula at hand it is clear that the support of the integral kernel is singular. For fixed values of $z_1, z_2, \ldots, z_n$ it is nonzero only along a trajectory on the torus T^n. This trajectory corresponds to the trajectory traced by (18.35) as s varies along the real axis. Other integral representations have been derived that involve kernels with nonsingular support, such as the Szégo kernel. One such representation formula is the one given by Milton and Golden (1990)

$$\boldsymbol{L}_*(z_1, z_2, \ldots, z_n) = \int_{T^n} \left[-1 + 2 \prod_{k=1}^{n} (1 - z_k e^{-i\theta_k})^{-1} \right] d\boldsymbol{\mu}'(\theta_1, \theta_2, \ldots, \theta_n),$$

which derives from a polydisk representation formula of Korányi and Pukánszky (1963). The nonuniqueness in the choice of integral kernel stems from certain Fourier constraints on the measure $\boldsymbol{\mu}'$. These arise (Rudin 1969) because the series expansion for $\boldsymbol{L}_*$ in powers of the variables z_j,

$$\boldsymbol{L}_*(z_1, z_2, \ldots, z_n) = \sum_{a_1,a_2,\ldots,a_n} c_{a_1,a_2,\ldots,a_n} z_1^{a_1} z_2^{a_2} \ldots z_n^{a_n},$$

incorporates only positive powers. [Negative powers are not allowed because the function $\boldsymbol{L}_*(z_1, z_2, \ldots, z_n)$ is nonsingular at the origin.] By substituting the test function

$$g(\theta_1, \theta_2, \ldots, \theta_n) = e^{i(k_1\theta_1 + k_2\theta_2 + \cdots + k_n\theta_n)}$$

into (18.39) and noting that

$$\begin{aligned}\operatorname{Im}[\boldsymbol{L}_*(re^{i\theta_1}, re^{i\theta_2}, \ldots, re^{i\theta_n})] \\ = \sum_{a_1,a_2,\ldots,a_n} c_{a_1,a_2,\ldots,a_n} r^{a_1+a_2+\cdots+a_n} [e^{i(a_1\theta_1+a_2\theta_2+\cdots+a_n\theta_n)} - e^{-i(a_1\theta_1+a_2\theta_2+\cdots+a_n\theta_n)}]/2,\end{aligned}$$

we see that

$$\int_{T^n} e^{i(k_1\theta_1+k_2\theta_2+\cdots+k_n\theta_n)} d\boldsymbol{\mu}'(\theta_1, \theta_2, \ldots, \theta_n) = 0$$
$$\text{unless } \boldsymbol{k} = (k_1, k_2, \ldots, k_n) \in \mathbb{Z}_+^n \cup \mathbb{Z}_-^n,$$

where $\mathbb{Z}_+ = \{0, 1, 2, \ldots\}$ and $\mathbb{Z}_- = -\mathbb{Z}_+$. In other words, the Fourier coefficients of the measure are zero whenever the k_j have mixed signs.

Due to these Fourier constraints we are free to replace the integral kernel $\boldsymbol{K}(\boldsymbol{z}, \boldsymbol{\theta})$ with the integral kernel

$$\boldsymbol{K}'(\boldsymbol{z}, \boldsymbol{\theta}) = \boldsymbol{K}(\boldsymbol{z}, \boldsymbol{\theta}) + \sum_{\boldsymbol{k} \notin \mathbb{Z}_+^n \cup \mathbb{Z}_-^n} f(\boldsymbol{k}, \boldsymbol{z}) e^{i\boldsymbol{k}\cdot\boldsymbol{\theta}},$$

in which $\boldsymbol{z} = (z_1, \ldots, z_n)$, $\boldsymbol{\theta} = (\theta_1, \ldots, \theta_n)$, $\boldsymbol{k} = (k_1, \ldots, k_n)$, and f is an arbitrary function of $\boldsymbol{k}$ and $\boldsymbol{z}$.

There are other linear constraints on the measure $\boldsymbol{\mu}'$. Due to the fact that $\boldsymbol{L}_*$ is a homogeneous function of $\lambda_1, \lambda_2, \ldots, \lambda_n$, the measure in the vicinity of the point $(\theta_1, \ldots, \theta_n)$ must be related to the measure in the vicinity of $(2\tan^{-1}\{c\tan(\theta_1/2)\}, \ldots, 2\tan^{-1}\{c\tan(\theta_n/2)\})$ for all values of c (Milton and Golden 1990). Taking the derivative of this relation with respect to c and (without loss of generality) setting $c = 1$ gives the constraint

$$\sum_{k=1}^{n} \sin\theta_k \frac{\partial \boldsymbol{\mu}'}{\partial \theta_k} = \boldsymbol{\mu}'$$

of Sawicz (1995). These constraints permit an even wider choice of integral kernel.

When $\boldsymbol{L}_*(\lambda_1, \lambda_2, \ldots, \lambda_n)$ is rational, or at least has no branch cuts, then the measure $\boldsymbol{\mu}'$ will be concentrated along the pole lines of the function $\boldsymbol{L}_*(\lambda_1, \lambda_2, \ldots, \lambda_n)$ (Bergman 1978b). For a square array of dielectric coated cylinders, with one phase being the core material, a second phase being the coating, and a third phase being the surrounding matrix material, Nicorovici, McPhedran, and Milton (1993) have computed these pole lines for the effective dielectric function $\varepsilon_*(\varepsilon_1, \varepsilon_2, \varepsilon_3)$. They also computed the zero lines, which provide enough information for one to obtain the measure $\boldsymbol{\mu}'$. [From the poles and zeros of ε_* along a trajectory $(\varepsilon_1(s), \varepsilon_2(s), \varepsilon_3(s))$ one can recover the residues at the poles and thereby obtain the measure by considering a family of such trajectories.]

18.8. Integral representations for a broader class of composite problems†

When the tensor field $\boldsymbol{L}(\boldsymbol{x})$ has the form (18.10) we can still obtain integral representations using the trajectory method. Generalizing (18.35) we consider a trajectory

$$(\boldsymbol{L}_1'(s), \boldsymbol{L}_2'(s), \ldots, \boldsymbol{L}_n'(s)), \quad \text{where } \boldsymbol{L}_j'(s) = \boldsymbol{I} - (\boldsymbol{A}_j + s\boldsymbol{B}_j)^{-1}$$

passing through the space of n-tuples of matrices parameterized by the complex variable s, in which the tensors $\boldsymbol{A}_j$ and $\boldsymbol{B}_j$ are chosen so that the trajectory passes through a chosen point $(\boldsymbol{L}_1, \boldsymbol{L}_2, \ldots, \boldsymbol{L}_n)$ in this space at one particular value of s, say, $s = i$. This is ensured with

$$\boldsymbol{A}_j = \mathrm{Re}[(\boldsymbol{I} - \boldsymbol{L}_j)^{-1}], \quad \boldsymbol{B}_j = \mathrm{Im}[(\boldsymbol{I} - \boldsymbol{L}_j)^{-1}].$$

We assume that the imaginary part of each tensor $\boldsymbol{L}_j$ is positive-definite, by making a rotation in the complex plane if necessary. Then each tensor $\boldsymbol{B}_j$ is positive-definite and it follows that the function

$$\begin{aligned}\boldsymbol{F}(s) &= \boldsymbol{I} - \boldsymbol{L}_*(\boldsymbol{L}_1'(s), \boldsymbol{L}_2'(s), \ldots, \boldsymbol{L}_n'(s)) \\ &= \boldsymbol{I} - \boldsymbol{L}_*(\boldsymbol{I} - (\boldsymbol{A}_1 + s\boldsymbol{B}_1)^{-1}, \boldsymbol{I} - (\boldsymbol{A}_2 + s\boldsymbol{B}_2)^{-1}, \ldots, \boldsymbol{I} - (\boldsymbol{A}_n + s\boldsymbol{B}_n)^{-1})\end{aligned}$$

is real symmetric and has a negative-definite imaginary part when s lies in the upper half of the complex plane. Since $\boldsymbol{F}(s)$ approaches zero as s tends to infinity, we deduce that $\boldsymbol{F}(s)$ has the integral representation

$$\boldsymbol{F}(s) = \int_{-\infty}^{\infty} \frac{d\boldsymbol{\mu}(y)}{s - y},$$

in which the integral of any smooth scalar test function $g(y)$ with respect to this measure $\boldsymbol{\mu}(y)$ is given by

$$\begin{aligned}\int_{-\infty}^{\infty} g(y) d\boldsymbol{\mu}(y) &= -\lim_{\substack{\epsilon \to 0 \\ \epsilon > 0}} \frac{1}{\pi} \int_{-\infty}^{\infty} g(y)\, \mathrm{Im}[\boldsymbol{F}(y + i\epsilon)]\, dy \\ &= \lim_{\substack{\epsilon \to 0 \\ \epsilon > 0}} \frac{1}{\pi} \int_{-\infty}^{\infty} g(y)\, \mathrm{Im}[\boldsymbol{L}_*(\boldsymbol{L}_1'(y + i\epsilon), \boldsymbol{L}_2'(y + i\epsilon), \ldots, \boldsymbol{L}_n'(y + i\epsilon))]\, dy,\end{aligned}$$

which serves to define the matrix-valued measure $\boldsymbol{\mu}(y)$. By setting $s = i$ in the integral representation for $F(s)$ we obtain

$$\boldsymbol{L}_*(\boldsymbol{L}_1, \boldsymbol{L}_2, \ldots, \boldsymbol{L}_n) = \boldsymbol{I} - \int_{-\infty}^{\infty} \frac{d\boldsymbol{\mu}(y)}{i - y}.$$

This is the desired formula for $\boldsymbol{L}_*(\boldsymbol{L}_1, \boldsymbol{L}_2, \ldots, \boldsymbol{L}_n)$ in terms of a measure $\boldsymbol{\mu}$ that derives from the values that $\mathrm{Im}[\boldsymbol{L}_*(\boldsymbol{L}_1', \boldsymbol{L}_2', \ldots, \boldsymbol{L}_n')]$ takes as the imaginary part of each of the tensors $\boldsymbol{L}_1', \boldsymbol{L}_2', \ldots, \boldsymbol{L}_n'$ approaches zero. In other words, we can recover the entire function $\boldsymbol{L}_*(\boldsymbol{L}_1, \boldsymbol{L}_2, \ldots, \boldsymbol{L}_n)$ from the values that its imaginary part takes when $\boldsymbol{L}_1, \boldsymbol{L}_2, \ldots, \boldsymbol{L}_n$ are nearly real.

References

Avellaneda, M. and A. J. Majda 1989. Stieltjes integral representation and effective diffusivity bounds for turbulent transport. *Physical Review Letters* 62:753–755. {*370, 391*}

Avellaneda, M. and A. J. Majda 1991. An integral representation and bounds on the effective diffusivity in passive advection by laminar and turbulent flows. *Communications in Mathematical Physics* 138(2):339–391. {*370, 392*}

Baker, Jr., G. A. 1975. *Essentials of Padé Approximants*, pp. 288–291. New York: Academic Press. ISBN 0-12-074855-X. {*370, 392, 571, 578, 596*}

Barrera, R. G. and R. Fuchs 1995. Theory of electron energy loss in a random system of spheres. *Physical Review B (Solid State)* 52(5):3256–3273. {*370, 392*}

Bergman, D. J. 1978a. Analytical properties of the complex effective dielectric constant of a composite medium with applications to the derivation of rigorous bounds and to percolation problems. In J. C. Garland and D. B. Tanner (eds.), *Electrical Transport and Optical Properties of Inhomogeneous Media*, pp. 46–61. Woodbury, New York: American Institute of Physics. ISBN 0-88318-139-8. {*370, 392*}

Bergman, D. J. 1978b. The dielectric constant of a composite material — A problem in classical physics. *Physics Reports* 43(9):377–407. {*341, 352, 370, 371, 376, 377, 379, 382, 387, 390, 392, 569, 581, 590, 597, 603, 617*}

Bergman, D. J. 1979. The dielectric constant of a simple cubic array of identical spheres. *Journal of Physics C: Solid State Physics* 12:4947–4960. {*39, 40, 239, 242, 377, 380, 392*}

Bergman, D. J. 1985. Bulk physical properties of composite media. In *Les méthodes de l'homogénéisation: théorie et applications en physique*, pp. 1–128. Paris: Eyrolles. {*377, 392*}

Bruno, O. P. 1991b. Taylor expansions and bounds for the effective conductivity and the effective elastic moduli of multicomponent composites and polycrystals. *Asymptotic Analysis* 4(4):339–365. {*298, 310, 372, 392*}

Bruno, O. P. 1991a. The effective conductivity of strongly heterogeneous composites. *Proceedings of the Royal Society of London. Series A, Mathematical and Physical Sciences* 433(1888):353–381. {*306, 310, 373, 392, 569, 597*}

Bruno, O. P. and K. Golden 1990. Interchangeability and bounds on the effective conductivity of the square lattice. *Journal of Statistical Physics* 61(1–2):365–386. {*322, 336, 379, 392*}

Bruno, O. P. and P. H. Leo 1992. On the stiffness of materials containing a disordered array of microscopic holes or hard inclusions. *Archive for Rational Mechanics and Analysis* 121(4):303–338. {*372, 373, 392, 569, 597*}

Clark, K. E. and G. W. Milton 1994. Modeling the effective conductivity function of an arbitrary two-dimensional polycrystal using sequential laminates. *Proceedings of the Royal Society of Edinburgh* 124A(4):757–783. {*387, 392*}

Day, A. R., A. R. Grant, A. J. Sievers, and M. F. Thorpe 2000. Spectral function of composites from reflectivity measurements. *Physical Review Letters* 84(9):1978–1981. {*377, 392*}

Day, A. R. and M. F. Thorpe 1996, June 10. The spectral function of random resistor networks. *Journal of Physics: Condensed Matter* 8(24):4389–4409. {*377, 392*}

Day, A. R. and M. F. Thorpe 1999, March 29. The spectral function of composites: The inverse problem. *Journal of Physics: Condensed Matter* 11(12):2551–2568. {*377, 392*}

Day, A. R., M. F. Thorpe, A. R. Grant, and A. J. Sievers 2000. The spectral function of a composite from reflectance data. *Physica. B, Condensed Matter* 279(1–3):17–20. {*377, 393*}

Dell'Antonio, G. F., R. Figari, and E. Orlandi 1986. An approach through orthogonal projections to the study of inhomogeneous or random media with linear response. *Annales de l'Institut Henri Poincaré. Section B, Probabilités et statistiques* 44:1–28. {*248, 267, 371, 373, 393*}

Dell'Antonio, G. F. and V. Nesi 1988. A general representation for the effective dielectric constant of a composite. *Journal of Mathematical Physics* 29(12):2688–2694. {*387, 393*}

Foster, R. M. 1924a. A reactance theorem. *The Bell System Technical Journal* 3:259–267. {*370, 393*}

Foster, R. M. 1924b. Theorems regarding the driving-point impedance of two-mesh circuits. *The Bell System Technical Journal* 3:651–685. {*370, 393*}

Fuchs, R. 1978. Optical properties of small-particle composites. In J. C. Garland and D. B. Tanner (eds.), *Electrical Transport and Optical Properties of Inhomogeneous Media*, pp. 276–281. Woodbury, New York: American Institute of Physics. ISBN 0-88318-139-8. {*370, 393*}

Golden, K. 1995. Statistical mechanics of conducting phase transitions. *Journal of Mathematical Physics* 36(10):5627–5642. {*370, 393*}

Golden, K. 1997. Critical behavior of transport in lattice and continuum percolation models. *Physical Review Letters* 78(20):3935–3938. {*370, 393*}

Golden, K. and G. Papanicolaou 1983. Bounds for effective parameters of heterogeneous media by analytic continuation. *Communications in Mathematical Physics* 90(4):473–491. {*11, 12, 15, 248, 268, 370, 376, 393, 571, 598, 603, 617*}

Golden, K. and G. Papanicolaou 1985. Bounds for effective parameters of multicomponent media by analytic continuation. *Journal of Statistical Physics* 40(5–6):655–667. {*387, 393, 451, 453, 638, 639, 641*}

Hetherington, J. H. and M. F. Thorpe 1992, September 8. The conductivity of a sheet containing inclusions with sharp corners. *Proceedings of the Royal Society of London. Series A, Mathematical and Physical Sciences* 438(1904):591–604. {*188, 216, 378, 393*}

Hinsen, K. and B. U. Felderhof 1992, November 15. Dielectric constant of a suspension of uniform spheres. *Physical Review B (Solid State)* 46(20):12955–12963. {*239, 243, 377, 393*}

Jackson, J. D. 1975. *Classical Electrodynamics* (Second ed.), pp. 299–303. New York / London / Sydney, Australia: John Wiley and Sons. ISBN 0-471-43132-X. {*369, 393*}

Kantor, Y. and D. J. Bergman 1982. Elastostatic resonances- a new approach to the calculation of the effective elastic constants of composites. *Journal of the Mechanics and Physics of Solids* 30:355–376. {*39, 43, 370, 371, 393*}

Korányi, A. and L. Pukánszky 1963. Holmorphic functions with positive real part on polycylinders. *American Mathematical Society Translations* 108:449–456. {*390, 393*}

Lipton, R. 2000. Optimal bounds on electric field fluctuations for random composites. *Journal of Applied Physics* 88(7):4287–4293. {*346, 353, 370, 394*}

Lipton, R. 2001. Optimal inequalities for gradients of solutions of elliptic equations occurring in two-phase heat conductors. *SIAM Journal on Mathematical Analysis* 32(5): 1081–1093. {*370, 394*}

Liu, C. and H. Wu 1997. Computation of the effective dielectric constant of two-component, three-dimensional mixtures using a simple pole expansion method. *Journal of Applied Physics* 82(1):345–350. {*40, 44, 377, 394*}

Lysne, P. C. 1983. A model for the high-frequency electrical response of wet rocks. *Geophysics* 48:775–786. {*370, 394*}

Ma, H., B. Zhang, W. Y. Tam, and P. Sheng 2000. Dielectric-constant evaluation from microstructures. *Physical Review B (Solid State)* 61(2):962–966. {*40, 44, 377, 394*}

McPhedran, R. C. and D. R. McKenzie 1980. Electrostatic and optical resonances of arrays of cylinders. *Applied Physics* 23:223–235. {*239, 244, 377, 381, 394*}

Milton, G. W. 1979. Theoretical studies of the transport properties of inhomogeneous media. Unpublished report TP/79/1, University of Sydney, Sydney, Australia. 1–65 pp. Unpublished report. (Available on request from the author). {*370, 394, 569, 577, 599*}

Milton, G. W. 1981a. Bounds on the complex permittivity of a two-component composite material. *Journal of Applied Physics* 52(8):5286–5293. {*118, 120, 124, 125, 129, 140, 370, 394, 569, 588, 589, 592, 599*}

Milton, G. W. 1981b. Bounds on the transport and optical properties of a two-component composite material. *Journal of Applied Physics* 52(8):5294–5304. {*371, 379, 382, 394, 553, 566, 569, 574, 581, 583, 586, 587, 592, 599, 610, 617*}

Milton, G. W. 1986b. A proof that laminates generate all possible effective conductivity functions of two-dimensional, two-phase media. In G. Papanicolaou (ed.), *Advances in Multiphase Flow and Related Problems: Proceedings of the Workshop on Cross Disciplinary Research in Multiphase Flow, Leesburg, Virginia, June 2–4, 1986*, pp. 136–146. Philadelphia: SIAM Press. ISBN 0-89871-212-2. {*384, 394*}

Milton, G. W. 1986a. Modeling the properties of composites by laminates. In J. L. Ericksen, D. Kinderlehrer, R. Kohn, and J.-L. Lions (eds.), *Homogenization and Effective Moduli of Materials and Media*, pp. 150–174. Berlin / Heidelberg / London / etc.: Springer-Verlag. ISBN 0-387-96306-5. {*206, 218, 384, 394, 463, 471, 472, 494, 578, 599, 603, 617*}

Milton, G. W. and K. Golden 1990. Representations for the conductivity functions of multicomponent composites. *Communications on Pure and Applied Mathematics (New York)* 43(5):647–671. {*303, 311, 387, 389, 390, 394, 451, 454, 638, 641*}

Nicorovici, N. A., R. C. McPhedran, and G. W. Milton 1993. Transport properties of a three-phase composite material: The square array of coated cylinders. *Proceedings of the Royal Society of London. Series A, Mathematical and Physical Sciences* 442:599–620. {*239, 241, 244, 390, 394*}

Reuben, A. J., G. B. Smith, and A. V. Radchik 1995. The polarisability of cylinder arrays in two dimensions. *Annals of Physics* 242(1):52–76. {*143, 156, 377, 394*}

Rudin, W. 1969. *Function Theory in Polydiscs*. New York: W. A. Benjamin, Inc. vii + 188 pp. {*390, 394*}

Rudin, W. 1987. *Real and Complex Analysis*. New York: McGraw-Hill. xiv + 416 pp. ISBN 0-07-054234-1. {*372, 395*}

Sawicz, R. 1995. Homogeneity in integral representations for effective properties of composite materials. *Journal of Mathematical Physics* 36(12):6737–6745. {*390, 395*}

Storer, J. E. 1957. *Passive Network Synthesis*, pp. 15–37. New York: McGraw-Hill. {*370, 395*}

Straley, J. P. 1979. Analytic properties of the specific macroscopic conductivity of a composite medium. *Journal of Physics C: Solid State Physics* 12:2143–2150. {*370, 395*}

Stroud, D. 1979. Percolation effects and sum rules in the optical properties of composites. *Physical Review B (Solid State)* 19:1783–1791. {*379, 395*}

Thorpe, M. F., B. R. Djordjević, and J. H. Hetherington 1994. Spectral functions for two-dimensional random conductors. *Physica A* 207(1–3):65–78. {*377, 395*}

19

Y-tensors

Affiliated with the effective tensor $\boldsymbol{L}_*$ in multicomponent composites is another tensor $\boldsymbol{Y}_*$, which is called the Y-tensor. Whereas the effective tensor $\boldsymbol{L}_*$ gives us information about the relation between the average fields in a composite, the tensor $\boldsymbol{Y}_*$ tells us about the average values of the fields in each phase.

The realization that Y-tensors are natural objects to introduce came gradually. It was recognized (Milton 1981) that many bounds on effective moduli of two-phase composites could be reduced to a common form. Motivated by the form of these bounds Berryman (1982) introduced a set of y-parameters, which were fractional linear transformations of the effective conductivity, bulk, and shear moduli. The bounds took an especially simple form when expressed in terms of these parameters. Interestingly, he found that his y-parameters were also helpful in simplifying the form of the self-consistent equations satisfied by the effective medium approximations for the effective moduli. The conductivity y-parameter and effective conductivity were found to have essentially the same analytic properties as functions of the component conductivities σ_1 and σ_2 (Milton and Golden 1985). A tensor related to the Y-tensor made its appearance in continued fraction expansions of the effective tensor [see equation (11.27) in Milton (1987), where $\hat{N}^{(1)}\Omega^{(1)}\hat{N}^{(1)}$ should be identified with $\boldsymbol{Y}_*$]. Subsequently a variational formulation for the Y-tensor was found and the definition of $\boldsymbol{Y}_*$ was extended to multiphase materials (Milton 1991). Independent of these developments Cherkaev and Gibiansky (1992) found that the translation bounds for two-phase composites could be simplified if expressed in terms of the Y-tensor.

19.1. The *Y*-tensor in two-phase composites

In two-phase composites the tensor $\boldsymbol{Y}_*$ can be defined (Gibiansky and Milton 1993) as that tensor that governs the linear relation

$$\Big\langle \chi_1(\boldsymbol{J} - \langle \boldsymbol{J}\rangle)\Big\rangle = -\boldsymbol{Y}_*\Big\langle \chi_1(\boldsymbol{E} - \langle \boldsymbol{E}\rangle)\Big\rangle \tag{19.1}$$

between the average values within phase 1 of the fields $\boldsymbol{J}(\boldsymbol{x}) - \langle \boldsymbol{J}\rangle$ and $\boldsymbol{E}(\boldsymbol{x}) - \langle \boldsymbol{E}\rangle$ representing the fluctuating parts of the fields $\boldsymbol{J}(\boldsymbol{x})$ and $\boldsymbol{E}(\boldsymbol{x})$. By replacing $\chi_1(\boldsymbol{x})$ with $1 - \chi_2(\boldsymbol{x})$ in (19.1) we see that $\boldsymbol{Y}_*$ also governs the linear relation

$$\Big\langle \chi_2(\boldsymbol{J} - \langle \boldsymbol{J}\rangle)\Big\rangle = -\boldsymbol{Y}_*\Big\langle \chi_2(\boldsymbol{E} - \langle \boldsymbol{E}\rangle)\Big\rangle$$

between the average values within phase 2 of the fields $\boldsymbol{J}(\boldsymbol{x}) - \langle \boldsymbol{J}\rangle$ and $\boldsymbol{E}(\boldsymbol{x}) - \langle \boldsymbol{E}\rangle$. So there is appealing symmetry in the definition of $\boldsymbol{Y}_*$.

In two-phase composites $\boldsymbol{L}_*$ can be expressed in terms of the effective tensor $\boldsymbol{Y}_*$ through the formula

$$\boldsymbol{L}_* = f_1\boldsymbol{L}_1 + f_2\boldsymbol{L}_2 - f_1f_2(\boldsymbol{L}_1 - \boldsymbol{L}_2)[f_2\boldsymbol{L}_1 + f_1\boldsymbol{L}_2 + \boldsymbol{Y}_*]^{-1}(\boldsymbol{L}_1 - \boldsymbol{L}_2). \tag{19.2}$$

The proof of this is a little indirect but straightforward. We observe that

$$\begin{aligned}\boldsymbol{L}_*\langle\boldsymbol{E}\rangle &= \langle\boldsymbol{L}\boldsymbol{E}\rangle = \langle\boldsymbol{L}\rangle\langle\boldsymbol{E}\rangle + \Big\langle\boldsymbol{L}(\boldsymbol{E} - \langle\boldsymbol{E}\rangle)\Big\rangle \\ &= (f_1\boldsymbol{L}_1 + f_2\boldsymbol{L}_2)\langle\boldsymbol{E}\rangle + (\boldsymbol{L}_1 - \boldsymbol{L}_2)\Big\langle\chi_1(\boldsymbol{E} - \langle\boldsymbol{E}\rangle)\Big\rangle,\end{aligned}$$

and that

$$\begin{aligned}&[f_2\boldsymbol{L}_1 + f_1\boldsymbol{L}_2 + \boldsymbol{Y}_*]\Big\langle\chi_1(\boldsymbol{E} - \langle\boldsymbol{E}\rangle)\Big\rangle \\ &\quad= f_2\boldsymbol{L}_1\langle\chi_1\boldsymbol{E}\rangle - f_1\boldsymbol{L}_2\langle\chi_2\boldsymbol{E}\rangle - f_1f_2(\boldsymbol{L}_1 - \boldsymbol{L}_2)\langle\boldsymbol{E}\rangle - \Big\langle\chi_1(\boldsymbol{J} - \langle\boldsymbol{J}\rangle)\Big\rangle \\ &\quad= -f_1f_2(\boldsymbol{L}_1 - \boldsymbol{L}_2)\langle\boldsymbol{E}\rangle.\end{aligned}$$

Combining these formulas gives (19.2), assuming that $f_2\boldsymbol{L}_1 + f_1\boldsymbol{L}_2 + \boldsymbol{Y}_*$ is nonsingular. We will see in the next section that $\boldsymbol{Y}_*$ is positive-semidefinite when $\boldsymbol{L}_1$ and $\boldsymbol{L}_2$ are positive-definite, which justifies this assumption. Due to the appearance of the factors of $(\boldsymbol{L}_1 - \boldsymbol{L}_2)$ in (19.2), any term that enters the series expansion of $\boldsymbol{Y}_*$ in powers of $\boldsymbol{L}_1 - \boldsymbol{L}_2$ at order j will first enter the series expansion of $\boldsymbol{L}_*$ at order $j + 2$.

Assuming that $\boldsymbol{L}_1 - \boldsymbol{L}_2$ and $f_1\boldsymbol{L}_1 + f_2\boldsymbol{L}_2 - \boldsymbol{L}_*$ are nonsingular, the relation (19.2) can be inverted, giving a formula for $\boldsymbol{Y}_*$ in terms of $\boldsymbol{L}_*$:

$$\begin{aligned}\boldsymbol{Y}_* &= Y(\boldsymbol{L}_*, \boldsymbol{L}_1, \boldsymbol{L}_2) \\ &= -f_2\boldsymbol{L}_1 - f_1\boldsymbol{L}_2 + f_1f_2(\boldsymbol{L}_1 - \boldsymbol{L}_2)(f_1\boldsymbol{L}_1 + f_2\boldsymbol{L}_2 - \boldsymbol{L}_*)^{-1}(\boldsymbol{L}_1 - \boldsymbol{L}_2).\end{aligned} \tag{19.3}$$

This defines the Y-transformation $Y(\boldsymbol{L}_*, \boldsymbol{L}_1, \boldsymbol{L}_2)$ of $\boldsymbol{L}_*$. For example, if we consider the conductivity of a three-dimensional isotropic composite of two isotropic phases, with conductivity tensors $\boldsymbol{L}_1 = \sigma_1\boldsymbol{I}$ and $\boldsymbol{L}_2 = \sigma_1\boldsymbol{I}$, and substitute the series expansion (15.33) for the effective conductivity tensor $\boldsymbol{L}_* = \sigma_*\boldsymbol{I}$ into (19.3), we see that the tensor $\boldsymbol{Y}_*$, to the first order in the difference $\sigma_1 - \sigma_2$, has an expansion

$$\boldsymbol{Y}_* = 2(\zeta_1\sigma_1 + \zeta_2\sigma_2)\boldsymbol{I} + \cdots,$$

in which ζ_1 and $\zeta_2 = 1 - \zeta_1$ are the geometric parameters given by (15.31) and (15.32), which depend on the three-point correlation functions. These geometric parameters, which enter the series expansion for σ_* at the third order, enter the series expansion for $\boldsymbol{Y}_*$ at the first order. In other words, the effect of the Y-transformation is to shift information contained at order k in the series expansion of $\boldsymbol{L}_*(\boldsymbol{L}_1, \boldsymbol{L}_2)$ in powers of $\boldsymbol{L}_1 - \boldsymbol{L}_2$ to information contained at order $k - 2$ in the transformed function. By rewriting (19.1) in the form

$$\Big\langle\chi_1(\boldsymbol{E} - \langle\boldsymbol{E}\rangle)\Big\rangle = -\boldsymbol{Y}_*^{-1}\Big\langle\chi_1(\boldsymbol{J} - \langle\boldsymbol{J}\rangle)\Big\rangle,$$

and applying the duality principle it is immediately evident that

$$\begin{aligned}\boldsymbol{Y}_*^{-1} &= Y(\boldsymbol{L}_*^{-1}, \boldsymbol{L}_1^{-1}, \boldsymbol{L}_2^{-1}) \\ &= -f_2\boldsymbol{L}_1^{-1} - f_1\boldsymbol{L}_2^{-1} + f_1f_2(\boldsymbol{L}_1^{-1} - \boldsymbol{L}_2^{-1})(f_1\boldsymbol{L}_1^{-1} + f_2\boldsymbol{L}_2^{-1} - \boldsymbol{L}_*^{-1})^{-1}(\boldsymbol{L}_1^{-1} - \boldsymbol{L}_2^{-1})\end{aligned}$$

or, equivalently, that

$$\boldsymbol{L}_*^{-1} = f_1\boldsymbol{L}_1^{-1} + f_2\boldsymbol{L}_2^{-1} - f_1f_2(\boldsymbol{L}_1^{-1} - \boldsymbol{L}_2^{-1})[f_2\boldsymbol{L}_1^{-1} + f_1\boldsymbol{L}_2^{-1} + \boldsymbol{Y}_*^{-1}]^{-1}(\boldsymbol{L}_1^{-1} - \boldsymbol{L}_2^{-1}). \tag{19.4}$$

In other words, the Y-transformation has the property that

$$Y(\boldsymbol{L}_*^{-1}, \boldsymbol{L}_1^{-1}, \boldsymbol{L}_2^{-1}) = [Y(\boldsymbol{L}_*, \boldsymbol{L}_1, \boldsymbol{L}_2)]^{-1}. \tag{19.5}$$

It is also clear from the definition (19.3) that the Y-transformation satisfies

$$Y(\boldsymbol{L}_* - \boldsymbol{L}_0, \boldsymbol{L}_1 - \boldsymbol{L}_0, \boldsymbol{L}_2 - \boldsymbol{L}_0) = Y(\boldsymbol{L}_*, \boldsymbol{L}_1, \boldsymbol{L}_2) + \boldsymbol{L}_0, \tag{19.6}$$

for any choice of the tensor $\boldsymbol{L}_0$. The scalar variant of (19.5) was used to obtain the simplified bounds given in Milton (1981). Berryman (1982) subsequently used this relation to recast the bounds in an equivalent form. This property of the Y-transformation was also noticed by Cherkaev and Gibiansky (1992). Additionally they observed that

$$Y(\boldsymbol{L}_1, \boldsymbol{L}_1, \boldsymbol{L}_2) = -\boldsymbol{L}_1, \quad Y(\boldsymbol{L}_2, \boldsymbol{L}_1, \boldsymbol{L}_2) = -\boldsymbol{L}_2.$$

The one-to-one correspondence between effective tensors $\boldsymbol{L}_*$ and tensors $\boldsymbol{Y}_*$ in two-phase composites implies that the problem of finding bounds on $\boldsymbol{L}_*$ is equivalent to the problem of finding bounds on $\boldsymbol{Y}_*$. Moreover, as we will see in sections 23.6 on page 474, 24.10 on page 516, 24.11 on page 518, 24.14 on page 522, 26.2 on page 554, and 26.3 on page 557, the bounds on $\boldsymbol{Y}_*$ can be considerably simpler than the corresponding bounds on $\boldsymbol{L}_*$. For example, in an isotropic conducting composite one has $\boldsymbol{Y}_* = y_\sigma \boldsymbol{I}$, and the Hashin-Shtrikman bounds (16.17) on the effective conductivity σ_* reduce to the elementary bounds

$$(d-1)\sigma_1 \geq y_\sigma \geq (d-1)\sigma_2$$

on the y-parameter y_σ. Moreover, we will see in section 28.3 on page 610 that the Y-transformation preserves many of the analytic properties of the effective tensor discussed in chapter 18 on page 369.

19.2. The Y-tensor in multiphase composites

In multiphase composites the Y-tensor $\boldsymbol{Y}_*$ has a natural interpretation as a nonlocal linear operator that when applied to a field that is constant in each phase, but having overall zero average value, produces another field of the same type. While the effective tensor $\boldsymbol{L}_*$ governs the relation between average fields, the tensor $\boldsymbol{Y}_*$ governs the relations between the averages of the fields over the individual phases. The definition of $\boldsymbol{Y}_*$ is a bit more abstract than for two-phase composites, but we will see that there is a correspondence between the definitions when only two phases are present. We also will see that there is a natural variational principle for $\boldsymbol{Y}_*$.

Let us start with the variational expression for the effective tensor in an n-phase composite:

$$\langle \boldsymbol{E}_0 \cdot \boldsymbol{L}_*\boldsymbol{E}_0\rangle = \min_{\substack{\underline{\boldsymbol{E}} \in \mathcal{U} \oplus \mathcal{E} \\ \langle \underline{\boldsymbol{E}} \rangle = \boldsymbol{E}_0}} \langle \underline{\boldsymbol{E}} \cdot \boldsymbol{L}\underline{\boldsymbol{E}}\rangle,$$

where

$$\boldsymbol{L} = \sum_{i=1}^{n} \chi_i \boldsymbol{L}_i.$$

Now any field, such as the trial field $\underline{\boldsymbol{E}}$, has a natural decomposition as the sum of three orthogonal fields:

$$\underline{\boldsymbol{E}} = \boldsymbol{E}_0 + \underline{\boldsymbol{E}}_1 + \underline{\boldsymbol{E}}_2,$$

comprised of a constant field

$$\boldsymbol{E}_0 = \boldsymbol{\Gamma}_0 \underline{\boldsymbol{E}} \equiv \langle \underline{\boldsymbol{E}} \rangle,$$

a field

$$\underline{\boldsymbol{E}}_1(\boldsymbol{x}) = \boldsymbol{\Pi}_1 \underline{\boldsymbol{E}} \equiv \sum_{i=1}^{n} \frac{1}{f_i} \langle \chi_i (\underline{\boldsymbol{E}} - \langle \underline{\boldsymbol{E}} \rangle) \rangle \chi_i(\boldsymbol{x}) \quad \text{satisfying } \langle \underline{\boldsymbol{E}}_1 \rangle = 0, \tag{19.7}$$

which is constant in each phase with overall average value zero, and a field

$$\underline{\boldsymbol{E}}_2 = \boldsymbol{\Pi}_2 \underline{\boldsymbol{E}} \equiv \underline{\boldsymbol{E}} - \sum_{i=1}^{n} \frac{1}{f_i} \langle \chi_i \underline{\boldsymbol{E}} \rangle \chi_i(\boldsymbol{x}) \quad \text{satisfying } \langle \chi_j \underline{\boldsymbol{E}}_2 \rangle = 0 \text{ for } j = 1, 2, \ldots, n,$$

which has average value zero within each phase. The above formulas serve to define the projections $\boldsymbol{\Pi}_1$ and $\boldsymbol{\Pi}_2$, which when applied to $\underline{\boldsymbol{E}}$ give the component fields $\underline{\boldsymbol{E}}_1$ and $\underline{\boldsymbol{E}}_2$. Not only are these three component fields mutually orthogonal, but more significantly the field $\boldsymbol{L}(\boldsymbol{E}_0 + \underline{\boldsymbol{E}}_1)$ is constant within each phase and hence orthogonal to $\underline{\boldsymbol{E}}_2$. Due to this latter orthogonality the quadratic form associated with the trial field $\underline{\boldsymbol{E}}$ splits into the sum of two quadratic terms,

$$\langle \underline{\boldsymbol{E}} \cdot \boldsymbol{L} \underline{\boldsymbol{E}} \rangle = \langle (\boldsymbol{E}_0 + \underline{\boldsymbol{E}}_1) \cdot \boldsymbol{L}(\boldsymbol{E}_0 + \underline{\boldsymbol{E}}_1) \rangle + \langle \underline{\boldsymbol{E}}_2 \cdot \boldsymbol{L} \underline{\boldsymbol{E}}_2 \rangle,$$

and as a direct consequence the variational principle for $\boldsymbol{L}_*$ splits into two separate variational problems, namely, the computation of the function

$$f(\boldsymbol{E}_1) = \min_{\substack{\underline{\boldsymbol{E}}_2 \\ \boldsymbol{E}_1 + \underline{\boldsymbol{E}}_2 \in \mathcal{E} \\ \langle \chi_i \underline{\boldsymbol{E}}_2 \rangle = 0}} \langle \underline{\boldsymbol{E}}_2 \cdot \boldsymbol{L} \underline{\boldsymbol{E}}_2 \rangle, \tag{19.8}$$

for all fields $\boldsymbol{E}_1$ that are constant in each phase with $\langle \boldsymbol{E}_1 \rangle = 0$ (and in particular for $\boldsymbol{E}_1 = \underline{\boldsymbol{E}}_1$) and the subsequent evaluation of

$$\langle \boldsymbol{E}_0 \cdot \boldsymbol{L}_* \boldsymbol{E}_0 \rangle = \min_{\underline{\boldsymbol{E}}_1 \in \mathcal{V}} \langle (\boldsymbol{E}_0 + \underline{\boldsymbol{E}}_1) \cdot \boldsymbol{L}(\boldsymbol{E}_0 + \underline{\boldsymbol{E}}_1) \rangle + f(\underline{\boldsymbol{E}}_1), \tag{19.9}$$

in which $\mathcal{V}$ is the space fields, which are constant in each phase with average value zero. We will refer to the fields in $\mathcal{V}$ as piecewise constant average value zero fields (piecewise constant will be taken to mean that the fields are constant throughout each phase).

By variation of the trial field $\underline{\boldsymbol{E}}_2$ by an amount $\delta \underline{\boldsymbol{E}}_2$ it can be seen that the minimum in (19.8) is achieved when the identity

$$\langle \delta \underline{\boldsymbol{E}}_2 \cdot \boldsymbol{L} \underline{\boldsymbol{E}}_2 \rangle = 0$$

holds for all fields $\delta\underline{\boldsymbol{E}}_2$ with

$$\delta\underline{\boldsymbol{E}}_2 \in \mathcal{E}, \quad \langle \chi_i \delta\underline{\boldsymbol{E}}_2 \rangle = 0 \quad \text{for } i = 1, 2, \ldots n.$$

In other words, the minimum in (19.8) is achieved by a field $\underline{\boldsymbol{E}}_2 = \boldsymbol{E}_2$ enjoying the special property that there exists a piecewise constant field $\boldsymbol{J}_1$ with $\langle \boldsymbol{J}_1 \rangle = 0$ and a field $\boldsymbol{J}_2$ with average value zero in each phase, that is, with $\langle \chi_i \boldsymbol{J}_2 \rangle = 0$ for $i = 1, 2, \ldots, n$, such that

$$\boldsymbol{J}_2 = \boldsymbol{L}\boldsymbol{E}_2, \quad \boldsymbol{J}_1 + \boldsymbol{J}_2 \in \mathcal{J}, \quad \boldsymbol{E}_1 + \boldsymbol{E}_2 \in \mathcal{E}. \tag{19.10}$$

Since these are linear equations, we might expect that there exists some linear operator $\boldsymbol{Y}_*$ that maps piecewise constant average value zero fields to piecewise constant average value zero fields, such that

$$\boldsymbol{J}_1 = -\boldsymbol{Y}_* \boldsymbol{E}_1, \tag{19.11}$$

where the minus sign is introduced to ensure that the quadratic form associated with $\boldsymbol{Y}_*$ is nonnegative when $\boldsymbol{L}$ is positive-definite. Indeed the orthogonality of $\mathcal{J}$ and $\mathcal{E}$ implies that

$$0 = \langle (\boldsymbol{E}_1 + \boldsymbol{E}_2) \cdot (\boldsymbol{J}_1 + \boldsymbol{J}_2) \rangle = \langle \boldsymbol{E}_1 \cdot \boldsymbol{J}_1 \rangle + \langle \boldsymbol{E}_2 \cdot \boldsymbol{J}_2 \rangle = \langle \boldsymbol{E}_2 \cdot \boldsymbol{L}\boldsymbol{E}_2 \rangle - \langle \boldsymbol{E}_1 \cdot \boldsymbol{Y}_* \boldsymbol{E}_1 \rangle; \tag{19.12}$$

and since $\langle \boldsymbol{E}_2 \cdot \boldsymbol{L}\boldsymbol{E}_2 \rangle$ is nonnegative when $\boldsymbol{L}$ is positive-definite, it follows that $\langle \boldsymbol{E}_1 \cdot \boldsymbol{Y}_* \boldsymbol{E}_1 \rangle$ must likewise be nonnegative for all choices of $\boldsymbol{E}_1$. The equations (19.10) and (19.11) define the Y-tensor $\boldsymbol{Y}_*$. We will therefore call the problem of finding fields $\boldsymbol{E}_1$, $\boldsymbol{E}_2$, $\boldsymbol{J}_1$, and $\boldsymbol{J}_2$ that solve (19.10) the Y-tensor problem. Following an argument similar to that used in section 12.10 on page 263, to establish the self-adjointness of $\boldsymbol{L}_*$ when $\boldsymbol{L}$ is self-adjoint, it is a simple matter to check that the self-adjointness of $\boldsymbol{L}$ implies the self-adjointness of $\boldsymbol{Y}_*$.

From (19.8) and (19.12) we see that the function $f(\boldsymbol{E}_1)$ is simply the quadratic form associated with $\boldsymbol{Y}_*$:

$$f(\boldsymbol{E}_1) = \langle \boldsymbol{E}_1 \cdot \boldsymbol{Y}_* \boldsymbol{E}_1 \rangle. \tag{19.13}$$

This in conjunction with (19.8) provides the variational principle for $\boldsymbol{Y}_*$.

The subsequent evaluation of (19.9) requires a minimization over a finite-dimensional space, namely, the space $\mathcal{V}$ of all piecewise constant average value zero fields. By variation of the trial field $\underline{\boldsymbol{E}}_1$ it can be seen that the minimum in (19.9) is achieved by a field $\underline{\boldsymbol{E}}_1 = \boldsymbol{E}_1 \in \mathcal{V}$ enjoying the special property that there exists a constant field $\boldsymbol{J}_0$ such that

$$\boldsymbol{J}_0 = \boldsymbol{L}(\boldsymbol{E}_0 + \boldsymbol{E}_1) + \boldsymbol{Y}_* \boldsymbol{E}_1. \tag{19.14}$$

By combining this with (19.10) and (19.11) we see that

$$\boldsymbol{L}(\boldsymbol{E}_0 + \boldsymbol{E}_1 + \boldsymbol{E}_2) = \boldsymbol{J}_0 - \boldsymbol{Y}_* \boldsymbol{E}_1 + \boldsymbol{J}_2 = \boldsymbol{J}_0 + \boldsymbol{J}_1 + \boldsymbol{J}_2.$$

In other words, the fields

$$\boldsymbol{J} = \boldsymbol{J}_0 + \boldsymbol{J}_1 + \boldsymbol{J}_2 \in \mathcal{U} \oplus \mathcal{J}, \quad \boldsymbol{E} = \boldsymbol{E}_0 + \boldsymbol{E}_1 + \boldsymbol{E}_2 \in \mathcal{U} \oplus \mathcal{E} \tag{19.15}$$

can be identified with the solutions to the original equations, and in particular $\boldsymbol{J}_0$ can be identified with the average value of $\boldsymbol{J}$. To solve (19.14) we project the equation onto the space $\mathcal{V}$ of piecewise constant average value zero fields, producing the relation

$$[\boldsymbol{\Pi}_1 \boldsymbol{L} \boldsymbol{\Pi}_1 + \boldsymbol{Y}_*] \boldsymbol{E}_1 = -\boldsymbol{\Pi}_1 \boldsymbol{L} \boldsymbol{E}_0,$$

where $\boldsymbol{\Pi}_1$ defined by (19.7) denotes the projection onto $\mathcal{V}$, and $\boldsymbol{\Pi}_1\boldsymbol{J}_0 = 0$ because $\mathcal{V}$ is orthogonal to the space $\mathcal{U}$ of constant fields. This has the solution

$$\boldsymbol{E}_1 = -[\boldsymbol{\Pi}_1\boldsymbol{L}\boldsymbol{\Pi}_1 + \boldsymbol{Y}_*]^{-1}\boldsymbol{\Pi}_1\boldsymbol{L}\boldsymbol{E}_0, \tag{19.16}$$

where the inverse is to be taken on the subspace $\mathcal{V}$. An additional relation is obtained by multiplying (19.14) by the projection $\boldsymbol{\Gamma}_0$ onto the space of constant fields, giving

$$\boldsymbol{J}_0 = \langle \boldsymbol{L} \rangle \boldsymbol{E}_0 + \boldsymbol{\Gamma}_0\boldsymbol{L}\boldsymbol{E}_1.$$

Substitution of (19.16) into this gives us an expression for $\boldsymbol{J}_0$ in terms $\boldsymbol{E}_0$ and hence a formula for the effective tensor $\boldsymbol{L}_*$ in terms of the Y-tensor:

$$\boldsymbol{L}_* = \langle \boldsymbol{L} \rangle - \boldsymbol{\Gamma}_0\boldsymbol{L}\boldsymbol{\Pi}_1[\boldsymbol{\Pi}_1\boldsymbol{L}\boldsymbol{\Pi}_1 + \boldsymbol{Y}_*]^{-1}\boldsymbol{\Pi}_1\boldsymbol{L}\boldsymbol{\Gamma}_0. \tag{19.17}$$

Also notice that (19.16) gives us a formula for the average value of the field $\boldsymbol{E}$ within each phase in terms of the Y-tensor:

$$\langle \chi_i \boldsymbol{E} \rangle = \langle \chi_i(\boldsymbol{E}_0 + \boldsymbol{E}_1) \rangle = f_i \boldsymbol{E}_0 - \boldsymbol{\Gamma}_0\chi_i[\boldsymbol{\Pi}_1\boldsymbol{L}\boldsymbol{\Pi}_1 + \boldsymbol{Y}_*]^{-1}\boldsymbol{\Pi}_1\boldsymbol{L}\boldsymbol{E}_0.$$

In general the relation (19.17) cannot be inverted to recover $\boldsymbol{Y}_*$ from $\boldsymbol{L}_*$ because $\boldsymbol{Y}_*$ is represented by a higher dimensional matrix. In an n-phase composite the tensor $\boldsymbol{L}_*$ is represented by an $m \times m$ matrix while the tensor $\boldsymbol{Y}_*$ is represented by $(n-1)m \times (n-1)m$ matrix because the space $\mathcal{V}$ of piecewise constant average value zero fields has dimension $(n-1)m$. The one exception is a two-phase composite, where both $\boldsymbol{L}_*$ and $\boldsymbol{Y}_*$ are represented by $m \times m$ matrices. In two-phase composites there is a natural correspondence between constant fields and piecewise constant fields with zero average value. Given a constant field $\boldsymbol{v} \in \mathcal{U}$, the associated field $\boldsymbol{V} \in \mathcal{V}$ is

$$\boldsymbol{V}(\boldsymbol{x}) = \frac{1}{\sqrt{f_1 f_2}}(f_2\chi_1(\boldsymbol{x}) - f_1\chi_2(\boldsymbol{x}))\boldsymbol{v} = \frac{1}{\sqrt{f_1 f_2}}(\chi_1(\boldsymbol{x}) - f_1)\boldsymbol{v}, \tag{19.18}$$

where the prefactor of $1/\sqrt{f_1 f_2}$ ensures that the inner product between two fields in $\mathcal{V}$ is the same as the inner product between their associated fields in $\mathcal{U}$.

Due to this correspondence between fields in $\mathcal{V}$ and fields in $\mathcal{U}$ (which implies a one-to-one correspondence between basis fields) any operator that maps $\mathcal{V}$ to $\mathcal{V}$, or which maps $\mathcal{V}$ to $\mathcal{U}$, or which maps $\mathcal{U}$ to $\mathcal{V}$ can be represented by an associated tensor that maps $\mathcal{U}$ to $\mathcal{U}$. By an abuse of notation, let us label the operator $\boldsymbol{Y}_*$ and its associated tensor by the same symbol. If an operator $\boldsymbol{A}$ maps $\mathcal{V}$ to $\mathcal{V}$, its action on $\boldsymbol{V}$ given by (19.18) produces the field

$$\boldsymbol{A}\boldsymbol{V} = \frac{1}{\sqrt{f_1 f_2}}(\chi_1(\boldsymbol{x}) - f_1)\boldsymbol{A}\boldsymbol{v},$$

where the associated tensor $\boldsymbol{A}$ appearing on the right of this equation maps $\mathcal{U}$ to $\mathcal{U}$ and represents the operator $\boldsymbol{A}$. If an operator $\boldsymbol{B}$ maps $\mathcal{V}$ to $\mathcal{U}$, its action on $\boldsymbol{V}$ produces the field $\boldsymbol{B}\boldsymbol{V} = \boldsymbol{B}\boldsymbol{v}$, where the associated tensor $\boldsymbol{B}$ on the right-hand side maps $\mathcal{U}$ to $\mathcal{U}$ and represents the operator $\boldsymbol{B}$. From the action of $\boldsymbol{L}$ on $\boldsymbol{V}$,

$$\begin{aligned}\boldsymbol{L}\boldsymbol{V} &= \frac{1}{\sqrt{f_1 f_2}}(f_2\boldsymbol{L}_1\chi_1(\boldsymbol{x}) - f_1\boldsymbol{L}_2\chi_2(\boldsymbol{x}))\boldsymbol{v} \\ &= \sqrt{f_1 f_2}(\boldsymbol{L}_1 - \boldsymbol{L}_2)\boldsymbol{v} + \frac{1}{\sqrt{f_1 f_2}}(\chi_1(\boldsymbol{x}) - f_1)[(f_2\boldsymbol{L}_1 + f_1\boldsymbol{L}_2)\boldsymbol{v}],\end{aligned}$$

we see that

$$\begin{aligned}\boldsymbol{\Gamma}_0\boldsymbol{L}\boldsymbol{V} &= \boldsymbol{\Gamma}_0\boldsymbol{L}\boldsymbol{\Pi}_1\boldsymbol{V} = \sqrt{f_1 f_2}(\boldsymbol{L}_1 - \boldsymbol{L}_2)\boldsymbol{v},\\ \boldsymbol{\Pi}_1\boldsymbol{L}\boldsymbol{V} &= \boldsymbol{\Pi}_1\boldsymbol{L}\boldsymbol{\Pi}_1\boldsymbol{V} = \frac{1}{\sqrt{f_1 f_2}}(\chi_1(\boldsymbol{x}) - f_1)[(f_2\boldsymbol{L}_1 + f_1\boldsymbol{L}_2)\boldsymbol{v}],\end{aligned}$$

which implies that $\sqrt{f_1 f_2}(\boldsymbol{L}_1 - \boldsymbol{L}_2)$ and $f_2\boldsymbol{L}_1 + f_1\boldsymbol{L}_2$ are the tensors associated with $\boldsymbol{\Gamma}_0\boldsymbol{L}\boldsymbol{\Pi}_1$ and $\boldsymbol{\Pi}_1\boldsymbol{L}\boldsymbol{\Pi}_1$, respectively. Also from the action of $\boldsymbol{L}$ on the constant field $\boldsymbol{v}$,

$$\begin{aligned}\boldsymbol{L}\boldsymbol{v} &= (\chi_1(\boldsymbol{x})\boldsymbol{L}_1 + \chi_2(\boldsymbol{x})\boldsymbol{L}_2)\boldsymbol{v}\\ &= (f_1\boldsymbol{L}_1 + f_2\boldsymbol{L}_2)\boldsymbol{v} + \frac{1}{\sqrt{f_1 f_2}}(\chi_1(\boldsymbol{x}) - f_1)[\sqrt{f_1 f_2}(\boldsymbol{L}_1 - \boldsymbol{L}_2)\boldsymbol{v}],\end{aligned}$$

which implies that

$$\boldsymbol{\Pi}_1\boldsymbol{L}\boldsymbol{v} = \boldsymbol{\Pi}_1\boldsymbol{L}\boldsymbol{\Gamma}_0\boldsymbol{v} = \frac{1}{\sqrt{f_1 f_2}}(\chi_1(\boldsymbol{x}) - f_1)[\sqrt{f_1 f_2}(\boldsymbol{L}_1 - \boldsymbol{L}_2)\boldsymbol{v}],$$

we see that $\sqrt{f_1 f_2}(\boldsymbol{L}_1 - \boldsymbol{L}_2)$ is the tensor associated with $\boldsymbol{\Pi}_1\boldsymbol{L}\boldsymbol{\Gamma}_0$. Since the relation (19.17) remains true if we replace each operator by its associated tensor, it follows that $\boldsymbol{L}_*$ and the associated tensor $\boldsymbol{Y}_*$ are linked through the relation

$$\boldsymbol{L}_* = f_1\boldsymbol{L}_1 + f_2\boldsymbol{L}_2 - f_1 f_2(\boldsymbol{L}_1 - \boldsymbol{L}_2)[f_2\boldsymbol{L}_1 + f_1\boldsymbol{L}_2 + \boldsymbol{Y}_*]^{-1}(\boldsymbol{L}_1 - \boldsymbol{L}_2). \tag{19.19}$$

in agreement with (19.2). Thus, for two-phase composites, we have established a correspondence between the definition of $\boldsymbol{Y}_*$ as an operator and the definition of $\boldsymbol{Y}_*$ given in the previous section.

19.3. A formula for the effective thermoelastic tensor in terms of the elasticity Y-tensor

In section 5.6 on page 82 we considered a composite of two anisotropic phases and (following Rosen and Hashin) derived explicit formulas for the effective tensor $\boldsymbol{\alpha}_*$ of thermal expansion, and the effective specific heat c_* at constant pressure, in terms of the effective compliance tensor $\boldsymbol{\mathcal{S}}_*$ and the volume fractions and thermoelastic moduli of the two phases. In multicomponent composites, there is no universal formula relating $\boldsymbol{\alpha}_*$ and c_* to $\boldsymbol{\mathcal{S}}_*$, but instead there is a formula giving $\boldsymbol{\alpha}_*$, c_*, and $\boldsymbol{\mathcal{S}}_*$ in terms of the tensor $\boldsymbol{Y}_*$ associated with the elasticity problem. To obtain this relation we start with the thermoelastic classical variational principle:

$$\begin{pmatrix}\boldsymbol{\tau}_0\\ \theta\end{pmatrix}\cdot\boldsymbol{\mathcal{L}}_*\begin{pmatrix}\boldsymbol{\tau}_0\\ \theta\end{pmatrix} = \min_{\substack{\underline{\boldsymbol{\tau}}(\boldsymbol{x})\\ \langle\underline{\boldsymbol{\tau}}\rangle = \boldsymbol{\tau}_0\\ \nabla\cdot\underline{\boldsymbol{\tau}} = 0}} \left\langle\begin{pmatrix}\underline{\boldsymbol{\tau}}\\ \theta\end{pmatrix}\cdot\boldsymbol{\mathcal{L}}\begin{pmatrix}\underline{\boldsymbol{\tau}}\\ \theta\end{pmatrix}\right\rangle,$$

in which

$$\begin{aligned}\boldsymbol{\mathcal{L}}_* &= \begin{pmatrix}\boldsymbol{\mathcal{S}}_* & \boldsymbol{\alpha}_*\\ \boldsymbol{\alpha}_* & c_*/T_0\end{pmatrix},\\ \boldsymbol{\mathcal{L}}(\boldsymbol{x}) &= \begin{pmatrix}\boldsymbol{\mathcal{S}}(\boldsymbol{x}) & \boldsymbol{\alpha}(\boldsymbol{x})\\ \boldsymbol{\alpha}(\boldsymbol{x}) & c(\boldsymbol{x})/T_0\end{pmatrix} = \sum_{i=1}^{n}\chi_i(\boldsymbol{x})\begin{pmatrix}\boldsymbol{\mathcal{S}}_i & \boldsymbol{\alpha}_i\\ \boldsymbol{\alpha}_i & c_i/T_0\end{pmatrix}.\end{aligned}$$

No minimization over temperature fields is needed in this variational principle because the differential constraints imply that θ is constant. By expanding the quadratic forms, we see that

$$\boldsymbol{\tau}_0 \cdot \boldsymbol{\mathcal{S}}_* \boldsymbol{\tau}_0 + 2\theta \boldsymbol{\alpha}_* \boldsymbol{\tau}_0 + \theta^2 c_*/T_0 = \min_{\substack{\underline{\boldsymbol{\tau}}(\boldsymbol{x}) \\ \langle \underline{\boldsymbol{\tau}} \rangle = \boldsymbol{\tau}_0 \\ \nabla \cdot \underline{\boldsymbol{\tau}} = 0}} \langle \underline{\boldsymbol{\tau}} \cdot \boldsymbol{\mathcal{S}} \underline{\boldsymbol{\tau}} \rangle + 2\theta \langle \boldsymbol{\alpha} \underline{\boldsymbol{\tau}} \rangle + \theta^2 \langle c \rangle / T_0.$$

As before, the next step is to express the trial field $\underline{\boldsymbol{\tau}}$ as a sum

$$\underline{\boldsymbol{\tau}} = \boldsymbol{\tau}_0 + \underline{\boldsymbol{\tau}}_1 + \underline{\boldsymbol{\tau}}_2$$

of a constant field $\boldsymbol{\tau}_0$, a field $\underline{\boldsymbol{\tau}}_1$ that is constant in each phase with $\langle \underline{\boldsymbol{\tau}}_1 \rangle = 0$, and a field $\underline{\boldsymbol{\tau}}_2$ satisfying $\langle \chi_i \underline{\boldsymbol{\tau}}_2 \rangle = 0$ for $i = 1, 2, \ldots, n$. Upon substitution, we see that the variational principle splits into the computation of the quadratic form associated with the $\boldsymbol{Y}_*$ tensor,

$$\langle \boldsymbol{\tau}_1 \cdot \boldsymbol{Y}_* \boldsymbol{\tau}_1 \rangle = \min_{\substack{\underline{\boldsymbol{\tau}}_2 \\ \nabla \cdot (\boldsymbol{\tau}_1 + \underline{\boldsymbol{\tau}}_2) = 0 \\ \langle \chi_i \underline{\boldsymbol{\tau}}_2 \rangle = 0}} \langle \underline{\boldsymbol{\tau}}_2 \cdot \boldsymbol{\mathcal{S}} \underline{\boldsymbol{\tau}}_2 \rangle, \tag{19.20}$$

for all fields $\boldsymbol{\tau}_1 \in \mathcal{V}$, where $\mathcal{V}$ is comprised of all symmetric tensor fields that are constant in each phase with $\langle \boldsymbol{\tau}_1 \rangle = 0$, and the subsequent determination of

$$\begin{aligned} \boldsymbol{\tau}_0 \cdot \boldsymbol{\mathcal{S}}_* \boldsymbol{\tau}_0 \; + \; & 2\theta \boldsymbol{\alpha}_* \boldsymbol{\tau}_0 + \theta^2 c_*/T_0 = 2\theta \langle \boldsymbol{\alpha} \boldsymbol{\tau}_0 \rangle + \theta^2 \langle c \rangle / T_0 \\ & + \min_{\underline{\boldsymbol{\tau}}_1 \in \mathcal{V}} \Big[\langle (\boldsymbol{\tau}_0 + \underline{\boldsymbol{\tau}}_1) \cdot \boldsymbol{\mathcal{S}} (\boldsymbol{\tau}_0 + \underline{\boldsymbol{\tau}}_1) \rangle + \langle \underline{\boldsymbol{\tau}}_1 \cdot \boldsymbol{Y}_* \underline{\boldsymbol{\tau}}_0 \rangle + 2\theta \langle \boldsymbol{\alpha} \cdot \underline{\boldsymbol{\tau}}_1 \rangle \Big]. \end{aligned}$$

The minimum in (19.20) is attained when $\underline{\boldsymbol{\tau}}_1 = \boldsymbol{\tau}_1$, where $\boldsymbol{\tau}_1$ has the special property that there exists a constant field $\boldsymbol{\epsilon}_0$ such that

$$\boldsymbol{\epsilon}_0 = \boldsymbol{\mathcal{S}} (\boldsymbol{\tau}_0 + \boldsymbol{\tau}_1) + \boldsymbol{Y}_* \boldsymbol{\tau}_1 + \theta \boldsymbol{\alpha}. \tag{19.21}$$

In the same way that the field $\boldsymbol{J}_0$ appearing in (19.14) was identified with $\langle \boldsymbol{J} \rangle$, so too can the field $\boldsymbol{\epsilon}_0$ appearing here be identified with the average strain $\langle \boldsymbol{\epsilon}_0 \rangle$. By projecting (19.21) onto the spaces $\mathcal{V}$ we see that the minimizer of (19.20) is

$$\boldsymbol{\tau}_1 = -(\boldsymbol{\Pi}_1 \boldsymbol{\mathcal{S}} \boldsymbol{\Pi}_1 + \boldsymbol{Y}_*)^{-1} \boldsymbol{\Pi}_1 (\boldsymbol{\mathcal{S}} \boldsymbol{\tau}_0 + \theta \boldsymbol{\alpha}), \tag{19.22}$$

where the inverse is to be taken on the subspace $\mathcal{V}$. Having determined $\boldsymbol{\tau}_1$, we next substitute the expression for it into the formula

$$\boldsymbol{\epsilon}_0 = \langle \boldsymbol{\mathcal{S}} \rangle \boldsymbol{\tau}_0 + \boldsymbol{\Gamma}_0 \boldsymbol{\mathcal{S}} \boldsymbol{\tau}_1 + \theta \langle \boldsymbol{\alpha} \rangle,$$

obtained by projecting (19.21) onto the space $\mathcal{U}$. A comparison of the resultant expression with the effective constitutive relation allows us to make the identifications

$$\begin{aligned} \boldsymbol{\mathcal{S}}_* &= \langle \boldsymbol{\mathcal{S}} \rangle - \boldsymbol{\Gamma}_0 \boldsymbol{\mathcal{S}} \boldsymbol{\Pi}_1 (\boldsymbol{\Pi}_1 \boldsymbol{\mathcal{S}} \boldsymbol{\Pi}_1 + \boldsymbol{Y}_*)^{-1} \boldsymbol{\Pi}_1 \boldsymbol{\mathcal{S}} \boldsymbol{\Gamma}_0, \\ \boldsymbol{\alpha}_* &= \langle \boldsymbol{\alpha} \rangle - \langle \boldsymbol{\mathcal{S}} \boldsymbol{\Pi}_1 (\boldsymbol{\Pi}_1 \boldsymbol{\mathcal{S}} \boldsymbol{\Pi}_1 + \boldsymbol{Y}_*)^{-1} \boldsymbol{\Pi}_1 \boldsymbol{\alpha} \rangle, \\ c_* &= \langle c \rangle - T_0 \langle \boldsymbol{\alpha} \cdot \boldsymbol{\Pi}_1 (\boldsymbol{\Pi}_1 \boldsymbol{\mathcal{S}} \boldsymbol{\Pi}_1 + \boldsymbol{Y}_*)^{-1} \boldsymbol{\Pi}_1 \boldsymbol{\alpha} \rangle. \end{aligned} \tag{19.23}$$

So knowledge of the Y-tensor enables us to compute the effective compliance tensor $\boldsymbol{\mathcal{S}}_*$, the effective thermal expansion tensor $\boldsymbol{\alpha}_*$, and the effective specific heat c_* at constant stress as a function of the specific heats c_i and thermal expansion tensors $\boldsymbol{\alpha}_i$ of the phases.

Knowing $\boldsymbol{Y}_*$ we can also determine the average values of the stress within each phase. We see from (19.22) that the average stress $\langle \chi_s(\boldsymbol{\tau}_0 + \boldsymbol{\tau}_1)\rangle/f_s$ within phase s depends linearly on $\boldsymbol{\tau}_0$ and the thermal expansion tensors $\boldsymbol{\alpha}_r$, $r = 1, 2, \ldots, n$ of each phase. Following Dvorak and Benveniste (1992), let us write this relation as

$$\langle \chi_s \boldsymbol{\tau}(\boldsymbol{x})\rangle/f_s = \langle \chi_s(\boldsymbol{\tau}_0 + \boldsymbol{\tau}_1)\rangle/f_s = \boldsymbol{B}_s\boldsymbol{\tau}_0 + \sum_{r=1}^{n} \boldsymbol{F}_{sr}\boldsymbol{\lambda}_r, \quad \text{where } \boldsymbol{\lambda}_r = -\theta\boldsymbol{\mathcal{C}}_r\boldsymbol{\alpha}_r. \tag{19.24}$$

Here $\boldsymbol{\lambda}_r$ is called the eigenstress of phase r. It enters the constitutive relation, implied by (2.24), between the stress and strain in phase r:

$$\boldsymbol{\tau}(\boldsymbol{x}) = \boldsymbol{\mathcal{C}}_r(\boldsymbol{\epsilon}(\boldsymbol{x}) - \theta\boldsymbol{\alpha}_r) = \boldsymbol{\mathcal{C}}_r\boldsymbol{\epsilon}(\boldsymbol{x}) + \boldsymbol{\lambda}_r \text{ when } \boldsymbol{x} \text{ is in phase } r,$$

where $\boldsymbol{\mathcal{C}}_r = \boldsymbol{\mathcal{S}}_r^{-1}$ is the elasticity tensor of phase r. Eigenstresses can be caused not only by thermal expansion but also, for example, by phase transformations. (They should not be confused with eigenvectors of the compliance tensor.) The tensor $\boldsymbol{B}_s$ is called the mechanical stress concentration factor tensor of phase s. The tensors $\boldsymbol{F}_{ss}$ and $\boldsymbol{F}_{sr}$ are called the self-induced and transmitted eigenstress concentration factor tensors. Now (19.22) and (19.24) imply that

$$\begin{aligned} \boldsymbol{B}_s &= \boldsymbol{I} - \langle \chi_s \boldsymbol{\Pi}_1(\boldsymbol{\Pi}_1\boldsymbol{\mathcal{S}}\boldsymbol{\Pi}_1 + \boldsymbol{Y}_*)^{-1}\boldsymbol{\Pi}_1\boldsymbol{\mathcal{S}}\rangle/f_s, \\ \boldsymbol{F}_{sr} &= \langle \chi_s \boldsymbol{\Pi}_1(\boldsymbol{\Pi}_1\boldsymbol{\mathcal{S}}\boldsymbol{\Pi}_1 + \boldsymbol{Y}_*)^{-1}\boldsymbol{\Pi}_1\chi_r\rangle\boldsymbol{\mathcal{S}}_r/f_s. \end{aligned} \tag{19.25}$$

These formulas are unwieldy, but from them we can see that the concentration factor tensors satisfy the relations

$$\begin{aligned} \sum_{r=1}^{n} \boldsymbol{F}_{sr} &= \boldsymbol{I} - \boldsymbol{B}_s, \\ f_s\boldsymbol{F}_{sr}\boldsymbol{\mathcal{C}}_r &= \langle \chi_s \boldsymbol{\Pi}_1(\boldsymbol{\Pi}_1\boldsymbol{\mathcal{S}}\boldsymbol{\Pi}_1 + \boldsymbol{Y}_*)^{-1}\boldsymbol{\Pi}_1\chi_r\rangle = f_r\boldsymbol{\mathcal{C}}_s\boldsymbol{F}_{rs}^T, \\ \sum_{r=1}^{n} \boldsymbol{F}_{sr}\boldsymbol{\mathcal{C}}_r &= \langle \chi_s \boldsymbol{\Pi}_1(\boldsymbol{\Pi}_1\boldsymbol{\mathcal{S}}\boldsymbol{\Pi}_1 + \boldsymbol{Y}_*)^{-1}\boldsymbol{\Pi}_1\boldsymbol{I}\rangle/f_s = 0 \end{aligned} \tag{19.26}$$

of Dvorak and Benveniste (1992), where the last relation holds because $\boldsymbol{\Pi}_1$ annihilates any field that is constant.

Conversely, if the concentration factor tensors are known, we can easily compute the field $\boldsymbol{\tau}_1$ as a function of the values of the thermal expansion tensors $\boldsymbol{\alpha}_i$, for $i = 1, 2 \ldots n$, with $\boldsymbol{\mathcal{S}}$, $\boldsymbol{\tau}_0$, and θ held fixed. Then the linear relation (19.22) between $\boldsymbol{\tau}_1$ and $\boldsymbol{\alpha}$ allows us to obtain the operator $(\boldsymbol{\Pi}_1\boldsymbol{\mathcal{S}}\boldsymbol{\Pi}_1 + \boldsymbol{Y}_*)^{-1}$ and thereby determine $\boldsymbol{Y}_*$. Thus the Y-tensor and the concentration factor tensors carry exactly the same information. From a physical perspective, we should really think of the Y-tensor as being determined from the linear relation between the average values of the stress (or strain) fields within each phase and the thermal expansion tensors of the phases.

19.4. The Hilbert space setting for the Y-tensor problem†

In our two-phase composite we can define the following spaces of fields:

- $\mathcal{K}$, the Hilbert space of all square integrable periodic fields with mean value zero;
- $\mathcal{E}$ and $\mathcal{J}$, the usual spaces associated with the differential equations of interest;
- $\mathcal{V}$, the space comprised of all fields that are constant in each phase and with zero average value,
$$\mathcal{V} = \{\boldsymbol{P} \in \mathcal{K} \mid \boldsymbol{P}(\boldsymbol{x}) = \sum_{i=1}^{n} \boldsymbol{v}_i \chi_i(\boldsymbol{x}), \quad \boldsymbol{v}_i \in \mathcal{T}, \quad \sum_{i=1}^{n} f_i \boldsymbol{v}_i = 0\};$$
- $\mathcal{H}^{(1)}$, the space comprised of all fields that have zero average value in each phase,
$$\mathcal{H}^{(1)} = \{\boldsymbol{P} \in \mathcal{K} \mid \langle \chi_i \boldsymbol{P} \rangle = 0 \text{ for all } i\}.$$

With the inner product of fields in $\mathcal{K}$ being the usual one, given by (12.11), the pair of subspaces $\mathcal{V}$ and $\mathcal{H}^{(1)}$, like the pair subspaces $\mathcal{E}$ and $\mathcal{J}$, are clearly orthogonal and span $\mathcal{K}$. This suggests that we can define Y-tensors in a more general abstract setting, without reference to composite materials. This abstract setting will be useful in chapter 29 on page 619, where we will see that hierarchies of embedded subspace collections generalize the notion of continued fraction expansions of analytic functions.

Suppose that $\mathcal{K}$ represents a vector or Hilbert space that is split into the sum of two orthogonal spaces in two different ways,

$$\mathcal{K} = \mathcal{E} \oplus \mathcal{J} = \mathcal{V} \oplus \mathcal{H}^{(1)},$$

in which the subspace $\mathcal{V}$ is assumed to be finite-dimensional. Let $\boldsymbol{L}$ represent a linear operator that maps $\mathcal{H}^{(1)}$ to itself. Given any vectors or fields $\boldsymbol{J}'$ and $\boldsymbol{E}'$ that solve the equations

$$\boldsymbol{E}' \in \mathcal{E}, \quad \boldsymbol{J}' \in \mathcal{J}, \quad \boldsymbol{J}_2 = \boldsymbol{L}\boldsymbol{E}_2, \quad \text{where } \boldsymbol{J}_2 = \boldsymbol{\Pi}_2 \boldsymbol{J}', \quad \boldsymbol{E}_2 = \boldsymbol{\Pi}_2 \boldsymbol{E}', \tag{19.27}$$

in which $\boldsymbol{\Pi}_2$ denotes the projection onto $\mathcal{H}^{(1)}$, the tensor $\boldsymbol{Y}_*$, by definition, governs the linear relation

$$\boldsymbol{J}_1 = -\boldsymbol{Y}_* \boldsymbol{E}_1, \quad \text{where } \boldsymbol{J}_1 = \boldsymbol{\Pi}_1 \boldsymbol{J}' \text{ and } \boldsymbol{E}_1 = \boldsymbol{\Pi}_1 \boldsymbol{E}', \tag{19.28}$$

in which $\boldsymbol{\Pi}_1$ denotes the projection onto $\mathcal{V}$.

To obtain a formula for $\boldsymbol{Y}_*$ in this general setting notice that (19.27) and (19.28) imply that

$$0 = \boldsymbol{\Gamma}_2 \boldsymbol{E}' = \boldsymbol{\Gamma}_2 \boldsymbol{E}_1 + \boldsymbol{\Gamma}_2 \boldsymbol{E}_2 = \boldsymbol{\Gamma}_2 \boldsymbol{E}_1 + \boldsymbol{\Gamma}_2 \boldsymbol{L}^{-1} \boldsymbol{\Pi}_2 \boldsymbol{\Gamma}_2 \boldsymbol{J}',$$

where the inverse of $\boldsymbol{L}$ is to be taken on the subspace $\mathcal{H}^{(1)}$. Solving for $\boldsymbol{J}'$ gives

$$\boldsymbol{J}' = -(\boldsymbol{\Gamma}_2 \boldsymbol{L}^{-1} \boldsymbol{\Pi}_2 \boldsymbol{\Gamma}_2)^{-1} \boldsymbol{\Gamma}_2 \boldsymbol{E}_1,$$

where the inverse is to be taken on the subspace $\mathcal{J}$. Then by applying $\boldsymbol{\Pi}_1$ to both sides of this equation and equating $\boldsymbol{\Pi}_1 \boldsymbol{J}' = \boldsymbol{J}_1$ with $-\boldsymbol{Y}_* \boldsymbol{E}_1$ we obtain the desired formula

$$\boldsymbol{Y}_* = \boldsymbol{\Pi}_1 \boldsymbol{\Gamma}_2 (\boldsymbol{\Gamma}_2 \boldsymbol{L}^{-1} \boldsymbol{\Pi}_2 \boldsymbol{\Gamma}_2)^{-1} \boldsymbol{\Gamma}_2 \boldsymbol{\Pi}_1 \tag{19.29}$$

for $\boldsymbol{Y}_*$.

From the structure of the equations (19.27) and (19.28) it is clear there is a duality principle: Any general result pertaining to all equations of this form must remain valid once we make the replacements

$$\begin{aligned}&\boldsymbol{E}' \to \boldsymbol{J}', \quad \boldsymbol{J}' \to \boldsymbol{E}',\\ &\mathcal{E} \to \mathcal{J}, \quad \mathcal{E} \to \mathcal{J}, \quad \mathcal{V} \to \mathcal{V}, \quad \mathcal{H}^{(1)} \to \mathcal{H}^{(1)},\\ &\boldsymbol{L} \to \boldsymbol{L}^{-1}, \quad \boldsymbol{Y}_* \to \boldsymbol{Y}_*^{-1};\end{aligned} \tag{19.30}$$

and if the relation involves the projections $\boldsymbol{\Gamma}_1$ and $\boldsymbol{\Gamma}_2$ onto the subspaces $\mathcal{E}$ and $\mathcal{J}$, then in accordance with (19.30) we should also make the replacements

$$\boldsymbol{\Gamma}_1 \to \boldsymbol{\Gamma}_2, \quad \boldsymbol{\Gamma}_2 \to \boldsymbol{\Gamma}_1.$$

For technical reasons, to ensure that $\boldsymbol{Y}_*$ is bounded and strictly positive-definite, we will assume that there exist positive constants α and β such that

$$\beta \boldsymbol{I} \geq \boldsymbol{L} \geq \alpha \boldsymbol{I} \ \text{ on } \mathcal{H}^{(1)}, \tag{19.31}$$

and that there exists another pair of positive constants $\gamma_1 < 1$ and $\gamma_2 < 1$ such that

$$|\boldsymbol{\Pi}_2 \boldsymbol{E}| \geq \gamma_1 |\boldsymbol{E}|, \quad |\boldsymbol{\Pi}_2 \boldsymbol{J}| \geq \gamma_2 |\boldsymbol{J}| \quad \text{for all } \boldsymbol{E} \in \mathcal{E} \text{ and } \boldsymbol{J} \in \mathcal{J}. \tag{19.32}$$

In particular, since $|\boldsymbol{\Pi}_2 \boldsymbol{E}| = 0$ for any $\boldsymbol{E} \in \mathcal{E} \cap \mathcal{V}$ and $|\boldsymbol{\Pi}_2 \boldsymbol{J}| = 0$ for any $\boldsymbol{J} \in \mathcal{J} \cap \mathcal{V}$, it is clear that this assumption ensures that the space $\mathcal{V}$ has no field in common with either $\mathcal{E}$ or $\mathcal{J}$:

$$\mathcal{E} \cap \mathcal{V} = 0, \quad \mathcal{J} \cap \mathcal{V} = 0. \tag{19.33}$$

Taking $\boldsymbol{E}$ to be the field $\boldsymbol{E}' = \boldsymbol{E}_1 + \boldsymbol{E}_2$ that solves the equations (19.27), we see the constraint (19.32) implies that

$$|\boldsymbol{E}_2|^2 \geq \gamma_1^2 |\boldsymbol{E}_1 + \boldsymbol{E}_2|^2 = \gamma_1^2 |\boldsymbol{E}_1|^2 + \gamma_1^2 |\boldsymbol{E}_2|^2.$$

Combining this with the identity (19.12) and the constraint (19.31) on $\boldsymbol{L}$ gives a sequence of inequalities:

$$(\boldsymbol{E}_1, \boldsymbol{Y}_* \boldsymbol{E}_1) = (\boldsymbol{E}_2, \boldsymbol{L} \boldsymbol{E}_2) \geq \alpha |\boldsymbol{E}_2|^2 \geq \frac{\alpha \gamma_1^2}{1 - \gamma_1^2} |\boldsymbol{E}_1|^2,$$

which provides an elementary lower bound on the Y-tensor:

$$\boldsymbol{Y}_* \geq \frac{\alpha \gamma_1^2}{1 - \gamma_1^2} \boldsymbol{I}.$$

So we see that our assumptions (19.31) and (19.32) do indeed guarantee that $\boldsymbol{Y}_*$ will be strictly positive-definite. By applying the duality principle we obtain a corresponding bound on the inverse tensor:

$$\boldsymbol{Y}_*^{-1} \geq \frac{\gamma_2^2}{\beta(1 - \gamma_2^2)} \boldsymbol{I}.$$

In certain composite materials both (19.33) and the conditions (19.32) can be violated. For example, if we consider conduction in a laminate of two phases laminated in direction $\boldsymbol{n}$, the piecewise constant average value zero fields,

$$\boldsymbol{e}(\boldsymbol{x}) = [f_2 \chi_1(\boldsymbol{x}) - f_1 \chi_2(\boldsymbol{x})] \boldsymbol{n}, \qquad \boldsymbol{j}(\boldsymbol{x}) = [f_2 \chi_1(\boldsymbol{x}) - f_1 \chi_2(\boldsymbol{x})] \boldsymbol{v} \ \text{ with } \boldsymbol{n} \cdot \boldsymbol{v} = 0,$$

are curl free and divergence free, respectively, and therefore lie in $\mathcal{E} \cap \mathcal{V}$ and $\mathcal{J} \cap \mathcal{V}$, respectively. Accordingly the tensor $\boldsymbol{Y}_*$ has a combination of infinite and zero eigenvalues: Its associated tensor $\boldsymbol{Y}_*$, which maps $\mathcal{U}$ to $\mathcal{U}$, has inverse

$$\boldsymbol{Y}_*^{-1} = \infty(\boldsymbol{n} \otimes \boldsymbol{n}).$$

Such extreme values of $\boldsymbol{Y}_*$ are exceptional, and a perturbation of the composite geometry will most likely produce a tensor $\boldsymbol{Y}_*$ that is bounded and strictly positive-definite. In other words, if the assumption (19.32) is not valid, then we can probably make a small perturbation to the composite geometry with little change to the effective tensor $\boldsymbol{L}_*$, to obtain a composite for which the assumption is valid. The assumption is made merely for convenience, to avoid mathematical technicalities.

19.5. The Y-tensor polarization problem†

We can recast the equations (19.27) in terms of polarization fields and thereby find another formula for the tensor $\boldsymbol{Y}_*$. To this end we take a reference operator $\boldsymbol{L}_0$ that is self-adjoint and commutes with $\boldsymbol{\Pi}_2$, and we define the polarization field

$$\boldsymbol{P}' = \boldsymbol{J}' - \boldsymbol{L}_0\boldsymbol{E}', \tag{19.34}$$

in which $\boldsymbol{J}'$ and $\boldsymbol{E}'$ solve (19.27). Applying the usual operator

$$\boldsymbol{\Gamma} = \boldsymbol{\Gamma}_1[\boldsymbol{\Gamma}_1\boldsymbol{L}_0\boldsymbol{\Gamma}_1]^{-1}\boldsymbol{\Gamma}_1$$

to $\boldsymbol{P}'$ gives

$$\boldsymbol{\Gamma}\boldsymbol{P}' = -\boldsymbol{E}' = -\boldsymbol{E}_1 - \boldsymbol{E}_2. \tag{19.35}$$

To obtain an expression for $\boldsymbol{E}_2$ in terms of $\boldsymbol{P}'$ we apply $\boldsymbol{\Pi}_2$ to both sides of (19.34). This gives

$$\boldsymbol{\Pi}_2\boldsymbol{P}' = \boldsymbol{J}_2 - \boldsymbol{L}_0\boldsymbol{E}_2 = (\boldsymbol{L} - \boldsymbol{L}_0)\boldsymbol{E}_2.$$

By combining these results we see that $\boldsymbol{P}'$ satisfies

$$[\boldsymbol{\Gamma} + (\boldsymbol{L} - \boldsymbol{L}_0)^{-1}\boldsymbol{\Pi}_2]\boldsymbol{P}' = -\boldsymbol{E}_1. \tag{19.36}$$

The operator $\boldsymbol{\Gamma} + (\boldsymbol{L} - \boldsymbol{L}_0)^{-1}\boldsymbol{\Pi}_2$ is self-adjoint because $\boldsymbol{\Pi}_2$ commutes with both $\boldsymbol{L}_0$ and $\boldsymbol{L}$. Assuming that its inverse exists, the solution for $\boldsymbol{P}'$ is

$$\boldsymbol{P}' = -[\boldsymbol{\Gamma} + (\boldsymbol{L} - \boldsymbol{L}_0)^{-1}\boldsymbol{\Pi}_2]^{-1}\boldsymbol{E}_1.$$

By applying $\boldsymbol{\Pi}_1 = \boldsymbol{I} - \boldsymbol{\Pi}_2$ to both sides we find that

$$\boldsymbol{J}_1 - \boldsymbol{L}_0\boldsymbol{E}_1 = -(\boldsymbol{Y}_* + \boldsymbol{L}_0)\boldsymbol{E}_1 = -\boldsymbol{\Pi}_1[\boldsymbol{\Gamma} + (\boldsymbol{L} - \boldsymbol{L}_0)^{-1}\boldsymbol{\Pi}_2]^{-1}\boldsymbol{E}_1.$$

Since this holds for all fields $\boldsymbol{E}_1 \in \mathcal{V}$, we deduce that the tensor $\boldsymbol{Y}_*$ is given by the formula

$$\boldsymbol{Y}_* = -\boldsymbol{L}_0\boldsymbol{\Pi}_1 + \boldsymbol{\Pi}_1[\boldsymbol{\Gamma} + (\boldsymbol{L} - \boldsymbol{L}_0)^{-1}\boldsymbol{\Pi}_2]^{-1}\boldsymbol{\Pi}_1. \tag{19.37}$$

One technical point remains. We need to check that the inverse of $\boldsymbol{\Gamma} + (\boldsymbol{L} - \boldsymbol{L}_0)^{-1}\boldsymbol{\Pi}_2$ exists, at least for some choice of $\boldsymbol{L}_0$. Let us suppose that $\boldsymbol{L}_0$ is such that there exist positive constants δ_1, δ_2, and ϵ such that

$$\boldsymbol{\Gamma}_1\boldsymbol{L}_0\boldsymbol{\Gamma}_1 \geq \delta_1\boldsymbol{\Gamma}_1, \quad \boldsymbol{\Pi}_2/\epsilon \geq (\boldsymbol{L} - \boldsymbol{L}_0)\boldsymbol{\Pi}_2 \geq \delta_2\boldsymbol{\Pi}_2.$$

Then $\boldsymbol{\Gamma}$ and $(\boldsymbol{L}-\boldsymbol{L}_0)^{-1}$ are both bounded positive-semidefinite operators satisfying

$$\boldsymbol{\Gamma}_1/\delta_1 \geq \boldsymbol{\Gamma} \geq \boldsymbol{\Gamma}_1/\beta, \quad \boldsymbol{\Pi}_2/\delta_2 \geq (\boldsymbol{L}-\boldsymbol{L}_0)^{-1}\boldsymbol{\Pi}_2 \geq \epsilon\boldsymbol{\Pi}_2, \tag{19.38}$$

where β is the positive constant entering (19.31). It follows immediately that $\boldsymbol{\Gamma} + (\boldsymbol{L} - \boldsymbol{L}_0)^{-1}\boldsymbol{\Pi}_2$ is a bounded positive-semidefinite operator. The existence of an inverse will be assured if we can prove that this operator is coercive.

Since the bounds (19.38) imply the inequality

$$\boldsymbol{\Gamma} + (\boldsymbol{L}-\boldsymbol{L}_0)^{-1}\boldsymbol{\Pi}_2 \geq \boldsymbol{\Gamma}_1/\beta + \epsilon\boldsymbol{\Pi}_2,$$

it suffices to prove the coercivity of $\boldsymbol{\Gamma}_1 + k\boldsymbol{\Pi}_2$ for at least one value of $k > 0$, that is, we need to establish that there exists a positive constant γ such that

$$(\boldsymbol{P}, (\boldsymbol{\Gamma}_1 + k\boldsymbol{\Pi}_2)\boldsymbol{P}) \geq \gamma|\boldsymbol{P}|^2 \text{ for all } \boldsymbol{P} \in \mathcal{K}.$$

It then follows that

$$\begin{aligned}(\boldsymbol{P}, (\boldsymbol{\Gamma}_1/\beta + \epsilon\boldsymbol{\Pi}_2)\boldsymbol{P}) &\geq (\boldsymbol{P}, \min\{1/\beta, \epsilon/k\}(\boldsymbol{\Gamma}_1 + k\boldsymbol{\Pi}_2)\boldsymbol{P}) \\ &\geq \min\{1/\beta, \epsilon/k\}\gamma|\boldsymbol{P}|^2 \text{ for all } \boldsymbol{P} \in \mathcal{K}.\end{aligned}$$

It is convenient to take $k = 1/2$. By decomposing $\boldsymbol{P}$ into a sum $\boldsymbol{P} = \boldsymbol{E} + \boldsymbol{J}$ of its two orthogonal component fields $\boldsymbol{E} \in \mathcal{E}$ and $\boldsymbol{J} \in \mathcal{J}$, and using (19.32) to bound the norm of $\boldsymbol{\Pi}_2\boldsymbol{J}$ (in which $1 > \gamma_2 > 0$), we see that

$$\begin{aligned}(\boldsymbol{P}, (\boldsymbol{\Gamma}_1 + \boldsymbol{\Pi}_2/2)\boldsymbol{P}) &\geq (\boldsymbol{E}, \boldsymbol{E}) + (\boldsymbol{E}, \boldsymbol{\Pi}_2\boldsymbol{J}) + |\boldsymbol{\Pi}_2\boldsymbol{J}|^2/2 \\ &\geq |\boldsymbol{E}|^2 - \gamma_2|\boldsymbol{E}|\,|\boldsymbol{J}| + \gamma_2^2|\boldsymbol{J}|^2/2 \\ &\geq |\boldsymbol{E}|^2/4 + \gamma_2^2|\boldsymbol{J}|^2/6 + (3|\boldsymbol{E}|/2 - \gamma_2|\boldsymbol{J}|)^2/3 \\ &\geq \gamma_2^2(|\boldsymbol{E}|^2 + |\boldsymbol{J}|^2)/6 = \gamma_2^2|\boldsymbol{P}|/6.\end{aligned}$$

This establishes the coercivity of $\boldsymbol{\Gamma} + (\boldsymbol{L}-\boldsymbol{L}_0)^{-1}\boldsymbol{\Pi}_2$ and thereby establishes the existence of its inverse.

19.6. Variational inequalities and principles for Y-tensors†

One of the appealing features of the Y-tensor is that the classical and Hashin-Shtrikman variational principles have extensions that apply to $\boldsymbol{Y}_*$. In the Hilbert space context, the variational principle for the Y-tensor implied by (19.8) and (19.13) takes the form

$$(\boldsymbol{E}_1, \boldsymbol{Y}_*\boldsymbol{E}_1) = \min_{\substack{\underline{\boldsymbol{E}}_2 \in \mathcal{H}^{(1)} \\ \boldsymbol{E}_1 + \underline{\boldsymbol{E}}_2 \in \mathcal{E}}} (\underline{\boldsymbol{E}}_2, \boldsymbol{L}\underline{\boldsymbol{E}}_2),$$

and holds provided that $\boldsymbol{L}$ is bounded and positive-definite on $\mathcal{E} \cap \mathcal{H}^{(1)}$. It can be regarded as a consequence of the positivity of the quadratic form

$$(\boldsymbol{E}_2 - \underline{\boldsymbol{E}}_2, \boldsymbol{L}(\boldsymbol{E}_2 - \underline{\boldsymbol{E}}_2)) \geq 0, \tag{19.39}$$

where $\boldsymbol{E}_2$ solves the equations (20.7), (20.8), and (20.9) and $\underline{\boldsymbol{E}}_2$ is any field satisfying

$$\underline{\boldsymbol{E}}_2 \in \mathcal{H}^{(1)}, \quad \boldsymbol{E}_1 + \underline{\boldsymbol{E}}_2 \in \mathcal{E}. \tag{19.40}$$

These constraints ensure that $\boldsymbol{E}_2 - \underline{\boldsymbol{E}}_2 \in \mathcal{E} \cap \mathcal{H}^{(1)}$. By expanding (19.39), and using the identity (19.12), we arrive at the variational inequality

$$(\boldsymbol{E}_1, \boldsymbol{Y}_* \boldsymbol{E}_1) \le (\underline{\boldsymbol{E}}_2, \boldsymbol{L}\underline{\boldsymbol{E}}_2), \tag{19.41}$$

which implies the variational principle, by virtue of the fact that equality holds in (19.40) and hence in (19.41) when $\underline{\boldsymbol{E}}_2 = \boldsymbol{E}_2$.

Similarly we have the complementary variational principle,

$$(\boldsymbol{J}_1, \boldsymbol{Y}_*^{-1}\boldsymbol{J}_1) = \min_{\substack{\underline{\boldsymbol{J}}_2 \in \mathcal{H}^{(1)} \\ \boldsymbol{J}_1 + \underline{\boldsymbol{J}}_2 \in \mathcal{J}}} (\underline{\boldsymbol{J}}_2, \boldsymbol{L}^{-1}\underline{\boldsymbol{J}}_2),$$

which is valid provided that $\boldsymbol{L}^{-1}$ is bounded and positive-definite on $\mathcal{J} \cap \mathcal{H}^{(1)}$.

To obtain variational principles analogous to the Hashin-Shtrikman ones, we take a reference operator $\boldsymbol{L}_0$ that is self-adjoint, positive-definite on $\mathcal{E}$, commutes with $\boldsymbol{\Pi}_2$, and satisfies the inequalities

$$\boldsymbol{L}_0 > 0 \ \text{ on } \mathcal{E} \ \text{ and with } \boldsymbol{L} > \boldsymbol{L}_0 \ \text{ on } \mathcal{H}^{(1)}. \tag{19.42}$$

The self-adjoint operator $\boldsymbol{\Gamma} + (\boldsymbol{L} - \boldsymbol{L}_0)^{-1}\boldsymbol{\Pi}_2$ is then positive-definite and by expanding the inequality

$$(\boldsymbol{P}' - \underline{\boldsymbol{P}}', [\boldsymbol{\Gamma} + (\boldsymbol{L} - \boldsymbol{L}_0)^{-1}\boldsymbol{\Pi}_2](\boldsymbol{P}' - \underline{\boldsymbol{P}}')) \ge 0,$$

where $\underline{\boldsymbol{P}}'$ is an arbitrary field in $\mathcal{K}$, making the substitution (19.36), and choosing $\boldsymbol{E}_1$ to make the inequality as sharp as possible, we arrive at the variational inequality

$$(\boldsymbol{P}_1, (\boldsymbol{Y}_* + \boldsymbol{L}_0)^{-1}\boldsymbol{P}_1) \le (\underline{\boldsymbol{P}}', \ [\boldsymbol{\Gamma} + (\boldsymbol{L} - \boldsymbol{L}_0)^{-1}\boldsymbol{\Pi}_2]\underline{\boldsymbol{P}}'), \quad \text{where } \boldsymbol{P}_1 = \boldsymbol{\Pi}_1\underline{\boldsymbol{P}}'.$$

Since equality holds when $\underline{\boldsymbol{P}}' = \boldsymbol{P}'$, we can rewrite this as a variational principle:

$$(\boldsymbol{P}_1, (\boldsymbol{Y}_* + \boldsymbol{L}_0)^{-1}\boldsymbol{P}_1) = \min_{\substack{\underline{\boldsymbol{P}}' \in \mathcal{K} \\ \boldsymbol{\Pi}_1\underline{\boldsymbol{P}}' = \boldsymbol{P}_1}} (\underline{\boldsymbol{P}}', [\boldsymbol{\Gamma} + (\boldsymbol{L} - \boldsymbol{L}_0)^{-1}\boldsymbol{\Pi}_2]\underline{\boldsymbol{P}}'), \tag{19.43}$$

and similarly we have the complementary variational principle:

$$(\boldsymbol{P}_1, (\boldsymbol{Y}_*^{-1} + \boldsymbol{L}_0^{-1})^{-1}\boldsymbol{P}_1) = \min_{\substack{\underline{\boldsymbol{P}}' \in \mathcal{K} \\ \boldsymbol{\Pi}_1\underline{\boldsymbol{P}}' = \boldsymbol{P}_1}} (\underline{\boldsymbol{P}}', \ [\boldsymbol{\Delta} + (\boldsymbol{L}^{-1} - \boldsymbol{L}_0^{-1})^{-1}\boldsymbol{\Pi}_2]\underline{\boldsymbol{P}}'), \tag{19.44}$$

where

$$\boldsymbol{\Delta} = \boldsymbol{\Gamma}_2[\boldsymbol{\Gamma}_2\boldsymbol{L}_0^{-1}\boldsymbol{\Gamma}_2]^{-1}\boldsymbol{\Gamma}_2.$$

This complementary variational principle is valid provided that $\boldsymbol{L}_0$ commutes with $\boldsymbol{\Pi}_2$ and satisfies the constraints

$$\boldsymbol{L}_0^{-1} > 0 \ \text{ on } \mathcal{J} \ \text{ and with } \boldsymbol{L}^{-1} > \boldsymbol{L}_0^{-1} \ \text{ on } \mathcal{H}^{(1)}. \tag{19.45}$$

The simplest choice of trial polarization field consistent with the constraint that $\boldsymbol{\Pi}_1\underline{\boldsymbol{P}}' = \boldsymbol{P}_1$ is of course $\underline{\boldsymbol{P}}' = \boldsymbol{P}_1$. Substitution of this field in (19.43) gives an elementary lower bound on $\boldsymbol{Y}_*$:

$$(\boldsymbol{Y}_* + \boldsymbol{L}_0)^{-1} \le \boldsymbol{\Pi}_1\boldsymbol{\Gamma}\boldsymbol{\Pi}_1 \ \text{ on } \mathcal{V}, \tag{19.46}$$

and substitution of the same trial field in (19.44) gives an elementary upper bound on $\boldsymbol{Y}_*$:

$$(\boldsymbol{Y}_*^{-1} + \boldsymbol{L}_0^{-1})^{-1} \leq \boldsymbol{\Pi}_1 \boldsymbol{\Delta} \boldsymbol{\Pi}_1 \quad \text{on } \mathcal{V}.$$

In a two-phase composite these elementary bounds still hold if we replace the operators $\boldsymbol{Y}_*$, $\boldsymbol{L}_0$, and $\boldsymbol{\Pi}_1 \boldsymbol{\Gamma} \boldsymbol{\Pi}_1$ acting in $\mathcal{V}$ by their associated tensors acting in $\mathcal{U}$. Assuming that $\boldsymbol{L}_0$ represents a constant tensor that acts locally, the action of $\boldsymbol{L}_0$ on the field $\boldsymbol{V}$ given in (19.18) is

$$\boldsymbol{L}_0 \boldsymbol{V} = \frac{1}{\sqrt{f_1 f_2}} (\chi_1(\boldsymbol{x}) - f_1) \boldsymbol{L}_0 \boldsymbol{v}.$$

In other words, the action of $\boldsymbol{L}_0$ on $\mathcal{U}$ is the same as that of the associated tensor representing the action of $\boldsymbol{L}_0$ on $\mathcal{V}$. Also, from the action of $\boldsymbol{\Pi}_1 \boldsymbol{\Gamma}$ on this field $\boldsymbol{V}$,

$$\begin{aligned} \boldsymbol{\Pi}_1 \boldsymbol{\Gamma} \boldsymbol{V}(\boldsymbol{x}) &= \frac{1}{f_1 f_2} (\chi_1(\boldsymbol{x}) - f_1) \langle \chi_1 \boldsymbol{\Gamma} \boldsymbol{V} \rangle \\ &= \frac{1}{\sqrt{f_1 f_2}} (\chi_1(\boldsymbol{x}) - f_1) [(\boldsymbol{\Gamma}_0 \chi_1 \boldsymbol{\Gamma} \chi_1)/(f_1 f_2)] \boldsymbol{v}, \end{aligned}$$

we deduce that $(\boldsymbol{\Gamma}_0 \chi_1 \boldsymbol{\Gamma} \chi_1 \boldsymbol{\Gamma}_0)/(f_1 f_2)$ is the associated tensor acting in $\mathcal{U}$ representing the action of the operator $\boldsymbol{\Pi}_1 \boldsymbol{\Gamma} \boldsymbol{\Pi}_1$ in $\mathcal{V}$. By replacing the operators in (19.46) with their associated tensors we see that the tensor associated with $\boldsymbol{Y}_*$ satisfies the lower bound

$$(\boldsymbol{Y}_* + \boldsymbol{L}_0)^{-1} \leq \frac{1}{f_1 f_2} \boldsymbol{\Gamma}_0 \chi_1 \boldsymbol{\Gamma} \chi_1 \boldsymbol{\Gamma}_0 \tag{19.47}$$

for all choices of $\boldsymbol{L}_0$ satisfying (19.42). The corresponding upper bound,

$$(\boldsymbol{Y}_*^{-1} + \boldsymbol{L}_0^{-1})^{-1} \leq \frac{1}{f_1 f_2} \boldsymbol{\Gamma}_0 \chi_1 \boldsymbol{\Delta} \chi_1 \boldsymbol{\Gamma}_0, \tag{19.48}$$

holds for all choices of $\boldsymbol{L}_0$ satisfying (19.45). We will see in section 23.7 on page 476 that these inequalities are useful for bounding the effective complex moduli (dielectric constant and bulk and shear moduli) of two-phase composites.

References

Berryman, J. G. 1982. Effective medium theory for elastic composites. In V. K. Varadan and V. V. Varadan (eds.), *Elastic Wave Scattering and Propagation: Based on Presentations made at a Special Session of the Midwestern Mechanics Conference Held at the University of Michigan, Ann Arbor, May 7–9, 1981*, pp. 111–129. Ann Arbor, Michigan: Ann Arbor Science. ISBN 0-250-40534-2. {*397, 399, 411, 556, 565*}

Cherkaev, A. V. and L. V. Gibiansky 1992. The exact coupled bounds for effective tensors of electrical and magnetic properties of two-component two-dimensional composites. *Proceedings of the Royal Society of Edinburgh. Section A, Mathematical and Physical Sciences* 122(1–2):93–125. {*397, 399, 411, 450, 453, 517, 522, 525, 614, 617*}

Dvorak, G. J. and Y. Benveniste 1992. On transformation strains and uniform fields in multiphase elastic media. *Proceedings of the Royal Society of London. Series A, Mathematical and Physical Sciences* 437:291–310. {*405, 411*}

Gibiansky, L. V. and G. W. Milton 1993. On the effective viscoelastic moduli of two-phase media. I. Rigorous bounds on the complex bulk modulus. *Proceedings of the Royal Society of London. Series A, Mathematical and Physical Sciences* 440(1908):163–188. {*397, 412, 475, 477–480, 492*}

Milton, G. W. 1981. Bounds on the electromagnetic, elastic, and other properties of two-component composites. *Physical Review Letters* 46(8):542–545. {*397, 399, 412, 474, 494, 553, 566, 577, 599*}

Milton, G. W. 1987. Multicomponent composites, electrical networks and new types of continued fraction. I. *Communications in Mathematical Physics* 111(2):281–327. {*248, 268, 397, 412, 619, 641*}

Milton, G. W. 1991. The field equation recursion method. In G. Dal Maso and G. F. Dell'Antonio (eds.), *Composite Media and Homogenization Theory: Proceedings of the Workshop on Composite Media and Homogenization Theory Held in Trieste, Italy, from January 15 to 26, 1990*, pp. 223–245. Basel, Switzerland: Birkhäuser Verlag. ISBN 0-8176-3511-4, 3-7643-3511-4. {*397, 412, 517, 526, 612, 613, 618, 619, 641*}

Milton, G. W. and K. Golden 1985. Thermal conduction in composites. In T. Ashworth and D. R. Smith (eds.), *Thermal Conductivity*, pp. 571–582. New York / London: Plenum Press. ISBN 0-306-41918-1. {*397, 412, 610, 618*}

20

Y-tensors and effective tensors in electrical circuits†

This section is largely based on notes that I prepared for a composite materials class given at the Courant Institute in 1989. The idea was to show that electrical circuits have a Y-tensor that has a direct physical significance. This allows one to develop some physical intuition regarding Y-tensors. We have seen that in an n-phase composite material the tensor $\boldsymbol{Y}_*$ has a physical interpretation that is somewhat abstract compared with the physical interpretation of the effective tensor $\boldsymbol{L}_*$. In electrical circuits, the situation is precisely the opposite: The effective tensor $\boldsymbol{Y}_*$ is of primary physical significance, while the interpretation of the associated effective tensor $\boldsymbol{\sigma}_*$ is less direct. We will see that in an electrical network $\boldsymbol{\sigma}_*$ gives the response of the network relative to the response when all of the conductances σ_i in the circuit are set equal to 1.

This section also provides a stepping stone toward understanding the field equation recursion method discussed in chapter 29 on page 619. A composite has an effective tensor $\boldsymbol{L}_*$ that is obtained from the associated Y-tensor $\boldsymbol{Y}_*$ via a fractional linear transformation. The tensor $\boldsymbol{Y}_*$ should have an associated effective tensor $\boldsymbol{L}_*^{(1)}$, obtained through a normalization transformation [of the type given in (20.31) at the end of this section] that in turn will have an associated Y-tensor $\boldsymbol{Y}_*^{(1)}$, and this will have an associated effective tensor $\boldsymbol{L}_*^{(2)}$, and so on, ad-infinitum. By combining everything together we generate a continued fraction expansion for $\boldsymbol{L}_*$ that is useful for obtaining bounds. These ideas will be developed in chapter 29 on page 619.

20.1. The incidence matrix and the fields of potential drops and currents

An electrical circuit is represented by a graph consisting of, say, m bonds linking together, say, ℓ nodes. The circuit geometry is most easily described by an $m \times \ell$ incidence matrix $\boldsymbol{M}$. For example, the Wheatstone bridge circuit illustrated in figure 20.1 on the next page has six bonds and four nodes and is represented [see, for example, Strang (1986)] by the 6×4 incidence matrix

$$\boldsymbol{M} = \begin{pmatrix} 1 & 0 & 0 & -1 \\ 1 & -1 & 0 & 0 \\ 1 & 0 & -1 & 0 \\ 0 & 1 & -1 & 0 \\ 0 & 1 & 0 & -1 \\ 0 & 0 & 1 & -1 \end{pmatrix}. \tag{20.1}$$

Each row in the incidence matrix represents a bond in the circuit, and each column in the incidence matrix represents a node in the circuit. To obtain the elements of the incidence matrix we first need to arbitrarily assign a direction to each bond, that is, an arrow to each bond. Then the elements of the matrix $\boldsymbol{M}$ are assigned the values

$$\begin{aligned} M_{ij} &= +1 \text{ if the arrow of bond } i \text{ points towards node } j, \\ &= -1 \text{ if the arrow of bond } i \text{ points away from node } j, \\ &= 0 \text{ if bond } i \text{ and node } j \text{ are not connected.} \end{aligned}$$

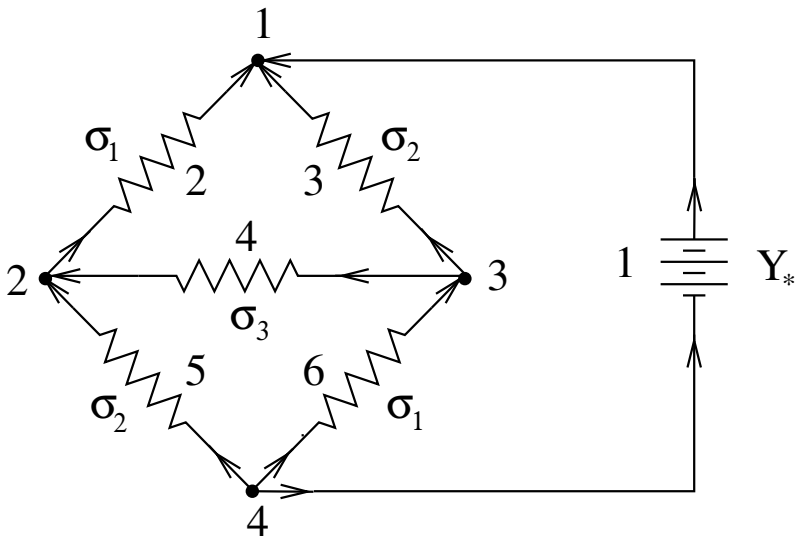

Figure 20.1. The Wheatstone bridge circuit referred to in the text. The numbering of the nodes, the numbering of the bonds, and the direction of each arrow can be assigned as desired. The choice made here produces the incidence matrix given in (20.1).

Electrical potentials in the network are represented by ℓ-dimensional vectors. The component φ_i of a potential $\boldsymbol{\varphi}$ represents the value of the electrical potential at node i. By contrast, each field in the circuit is represented by an m-dimensional vector. The component P_j of a field $\boldsymbol{P}$ represents the value of the field in bond j with the convention that P_j is positive if the field is directed in the direction of the arrow associated with bond j and negative if the field is in the opposite direction. These fields span an m-dimensional vector space $\mathcal{K}$. This space has a complex extension consisting of fields $\boldsymbol{P} = \boldsymbol{P}_1 + i\boldsymbol{P}_2$, where $\boldsymbol{P}_1$ and $\boldsymbol{P}_2$ lie in the space $\mathcal{K}$. Such complex-valued fields are needed to describe the response of the circuit when oscillating voltage or current sources are present and the circuit elements include capacitors or inductors [see, for example, Brophy (1983)]. By an abuse of notation we denote a space and its complex extension by the same symbol. The inner product between two fields $\boldsymbol{P},\ \boldsymbol{P}' \in \mathcal{K}$ is taken to be the standard one,

$$(\boldsymbol{P}, \boldsymbol{P}') = \sum_{j=1}^{m} \overline{P}_j P'_j,$$

where the bar denotes complex conjugation. This vector space $\mathcal{K}$ has a natural splitting,

$$\mathcal{K} = \mathcal{J} \oplus \mathcal{E},$$

into the two orthogonal subspaces:

- $\mathcal{J}$, the nullspace of the transposed incidence matrix $\boldsymbol{M}^T$;
- $\mathcal{E}$, the column space of $\boldsymbol{M}$, that is, the range of the matrix $\boldsymbol{M}$.

The orthogonality of these subspaces is an immediate consequence of the fact that they are the nullspace and row space of a matrix.

More importantly, these spaces have a natural physical interpretation. Associated with any potential $\boldsymbol{\varphi}$ is the field

$$\boldsymbol{E}' = -\boldsymbol{M}\boldsymbol{\varphi}.$$

The definition of the incidence matrix ensures that the matrix element E_j of $\boldsymbol{E}'$ represents the potential drop across the bond j. For example, in the Wheatstone bridge the vector $\boldsymbol{E}'$ takes the value

$$\boldsymbol{E}' = \begin{pmatrix} \varphi_4 - \varphi_1 \\ \varphi_2 - \varphi_1 \\ \varphi_3 - \varphi_1 \\ \varphi_3 - \varphi_2 \\ \varphi_4 - \varphi_2 \\ \varphi_4 - \varphi_3 \end{pmatrix}.$$

In other words, fields in the space $\mathcal{E}$ represent fields of potential drops.

Notice also that for any field $\boldsymbol{P}$ the element Q_i of the vector $\boldsymbol{Q} = \boldsymbol{M}^T\boldsymbol{P}$ represents the net component of the field $\boldsymbol{P}$ directed toward node i. Hence any field $\boldsymbol{J}'$ in the nullspace $\mathcal{J}$ of $\boldsymbol{M}^T$ satisfies the conservation law for electrical currents, namely, Kirchoff's law that the net flow of current out of or into any node is zero in an electrical circuit. In other words, fields in the space $\mathcal{J}$ represent fields of electrical current. For example, in the Wheatstone bridge the constraint that

$$\boldsymbol{M}^T\boldsymbol{J}' = \begin{pmatrix} J_1 + J_2 + J_3 \\ -J_2 + J_4 + J_5 \\ -J_3 - J_4 + J_6 \\ -J_1 - J_5 - J_6 \end{pmatrix} = 0$$

clearly implies that the net flux of current into or out of any node is zero.

20.2. The subdivision of bonds in an electrical circuit

The bonds in an electrical circuit can typically be subdivided into two groups, according to their electrical function. We will call one group the passive network: It consists of resistors, and dissipates electrical energy. We will call the remaining group, of say d bonds, the active network: It primarily consists of energy sources such as batteries, but may also include resistive elements. The active network adjusts itself until the power produced in the active network balances the power dissipated in the passive network. Associated with the division of bonds in these two groups is a splitting of the vector space $\mathcal{K}$ into two orthogonal subspaces

$$\mathcal{K} = \mathcal{V} \oplus \mathcal{H}^{(1)}, \tag{20.2}$$

where

• $\mathcal{V}$ is the d-dimensional space consisting of all fields $\boldsymbol{V}$ with elements V_j that are nonzero only when bond j is in the active network;

• $\mathcal{H}^{(1)}$ consists of all fields $\boldsymbol{P}$ with elements P_j that are nonzero only when bond j is in the passive network.

The projection operator $\boldsymbol{\Pi}_1$ onto the space $\mathcal{V}$ is therefore a diagonal matrix with elements

$$\begin{aligned} \{\Lambda_0\}_{jk} &= 1 \text{ if } j = k \text{ and bond } j \text{ is in the active network,} \\ &= 0 \text{ otherwise.} \end{aligned}$$

In the Wheatstone bridge circuit the active network is the battery, which is represented as bond 1. Consequently the space $\mathcal{V}$ is one-dimensional ($d = 1$) and the operator $\boldsymbol{\Pi}_1$ is given by

$$\boldsymbol{\Pi}_1 = \begin{pmatrix} 1 & 0 & 0 & 0 & 0 & 0 \\ 0 & 0 & 0 & 0 & 0 & 0 \\ 0 & 0 & 0 & 0 & 0 & 0 \\ 0 & 0 & 0 & 0 & 0 & 0 \\ 0 & 0 & 0 & 0 & 0 & 0 \\ 0 & 0 & 0 & 0 & 0 & 0 \end{pmatrix}.$$

Let us also introduce the diagonal matrix

$$\boldsymbol{\Pi}_2 = \boldsymbol{I} - \boldsymbol{\Pi}_1,$$

which projects onto the orthogonal subspace $\mathcal{H}^{(1)}$.

I like to think of the passive network as being confined within a black box, with the nodes that are attached to the active network being terminals on the surface of the box. The active network is outside the box and can be regarded as a tool for measuring the response of the passive network: The currents through each bond in the active network and the voltages across them give us some information about the passive network.

For simplicity we will assume that each connected part of the active network consists of a treelike graph with at most a single path connecting any pair of nodes. The absence of biconnected nodes implies that there are no loops in the active network around which current can flow. This is mathematically equivalent to requiring that the spaces $\mathcal{J}$ and $\mathcal{V}$ have no field in common,

$$\mathcal{J} \cap \mathcal{V} = 0. \tag{20.3}$$

Let us also assume for simplicity that all nodes in the active network are also connected to the passive network. This implies that if the potential drops are zero in the passive network, then they are also zero in the active network. This is mathematically equivalent to requiring that the spaces $\mathcal{E}$ and $\mathcal{V}$ have no field in common,

$$\mathcal{E} \cap \mathcal{V} = 0. \tag{20.4}$$

The bonds in the passive network are further subdivided into n groups representing the different components, $1, 2, \ldots, n$, in the passive network. The bonds within a given group have the same value of their electrical conductance. In other words, the space $\mathcal{H}^{(1)}$ is split into n orthogonal subspaces,

$$\mathcal{H}^{(1)} = \mathcal{P}_1^{(1)} \oplus \mathcal{P}_2^{(1)} \oplus \ldots \oplus \mathcal{P}_n^{(1)},$$

where $\mathcal{P}_i^{(1)}$ consists of all fields $\boldsymbol{P} \in \mathcal{K}$ with elements P_j that are nonzero only when bond j is in group i.

Clearly the projection operator $\boldsymbol{\chi}_i$ onto the space $\mathcal{P}_i^{(1)}$ is diagonal and has elements

$$\begin{aligned} \{\chi_i\}_{jk} &= 1 \text{ if } j = k \text{ and bond } j \text{ is in group } i, \\ &= 0 \text{ otherwise.} \end{aligned} \tag{20.5}$$

These projections satisfy

$$\boldsymbol{\chi}_i \boldsymbol{\chi}_j = \delta_{ij} \boldsymbol{\chi}_i, \quad \sum_{i=1}^{n} \boldsymbol{\chi}_i = \boldsymbol{\Pi}_2.$$

The total electrical conductance of the passive network is then represented by an operator $\boldsymbol{\sigma}$ that acts on the space $\mathcal{H}^{(1)}$ and takes the form

$$\boldsymbol{\sigma} = \sum_{i=1}^{n} \sigma_i \boldsymbol{\chi}_i. \tag{20.6}$$

In the passive part of the circuit the conductances σ_i are positive, which implies that the tensor $\boldsymbol{\sigma}$ is positive-definite on the space $\mathcal{H}^{(1)}$.

In the Wheatstone bridge of figure 20.1 on page 414, the operator $\boldsymbol{\sigma}$ takes the form

$$\boldsymbol{\sigma} = \begin{pmatrix} 0 & 0 & 0 & 0 & 0 & 0 \\ 0 & \sigma_1 & 0 & 0 & 0 & 0 \\ 0 & 0 & \sigma_2 & 0 & 0 & 0 \\ 0 & 0 & 0 & \sigma_3 & 0 & 0 \\ 0 & 0 & 0 & 0 & \sigma_2 & 0 \\ 0 & 0 & 0 & 0 & 0 & \sigma_1 \end{pmatrix},$$

20.3. The Y-tensor of the electrical circuit

Due to the splitting of the Hilbert space $\mathcal{K}$ into the two orthogonal spaces $\mathcal{V}$ and $\mathcal{H}^{(1)}$, it is clear that any field can be split into components in $\mathcal{V}$ and $\mathcal{H}^{(1)}$. In particular, for the actual current field $\boldsymbol{J}'$ and the actual field $\boldsymbol{E}'$ of potential drops in the network we have

$$\boldsymbol{J}' = \boldsymbol{J}_1 + \boldsymbol{J}_2 \in \mathcal{J}, \quad \boldsymbol{E}' = \boldsymbol{E}_1 + \boldsymbol{E}_2 \in \mathcal{E}, \tag{20.7}$$

where $\boldsymbol{J}_1$ and $\boldsymbol{E}_1$ are fields in the active network, while $\boldsymbol{J}_2$ and $\boldsymbol{E}_2$ are fields in the passive network, that is,

$$\boldsymbol{J}_1, \boldsymbol{E}_1 \in \mathcal{V} \quad \text{and} \quad \boldsymbol{J}_2, \boldsymbol{E}_2 \in \mathcal{H}^{(1)}. \tag{20.8}$$

Ohm's law implies that in each bond in the passive part of the network the current through the bond is equal to the conductance multiplied by the potential drop across that bond. In other words, Ohm's law implies that the current fields and potential drops existing within the passive part of the circuit are such that

$$\boldsymbol{J}_2 = \boldsymbol{\sigma} \boldsymbol{E}_2, \tag{20.9}$$

where $\boldsymbol{\sigma}$ is given by (20.6).

We will see that when the potential drops $\boldsymbol{E}_1 \in \mathcal{V}$ in the active network are specified, then there exists a unique solution for the fields $\boldsymbol{J}'$ and $\boldsymbol{E}'$ satisfying (20.7), (20.8), and (20.9) so

long as the assumption (20.3) is met. Furthermore, from the linearity of the equations it is clear that $\boldsymbol{J}_1$ must depend linearly on $\boldsymbol{E}_1$. This linear relation

$$\boldsymbol{J}_1 = -\boldsymbol{Y}_* \boldsymbol{E}_1, \tag{20.10}$$

defines the Y-tensor $\boldsymbol{Y}_*$. Strictly speaking, we should call $\boldsymbol{Y}_*$ an operator (represented by a matrix) rather than a tensor, but we choose not to do so because of the close connection with the Y-tensors introduced in the previous chapter.

The quadratic form associated with $\boldsymbol{Y}_*$,

$$W(\boldsymbol{E}_1) = (\boldsymbol{E}_1, \boldsymbol{Y}_* \boldsymbol{E}_1)/2 = -(\boldsymbol{E}_1, \boldsymbol{J}_1)/2 = (\boldsymbol{E}_2, \boldsymbol{J}_2)/2 = (\boldsymbol{E}_2, \boldsymbol{\sigma} \boldsymbol{E}_2)/2, \tag{20.11}$$

gives the electrical power that must be produced in the active network to maintain the potential drops $\boldsymbol{E}_1$. In the context of electrical networks, (20.11) is a restatement of the physical fact that the production of electrical power in the active network balances the dissipation of electrical power in the passive network.

The tensor $\boldsymbol{Y}_*$ can be computed from the formula

$$\boldsymbol{Y}_* = -\sigma_0 \boldsymbol{\Pi}_1 - \sigma_0 \boldsymbol{\Pi}_1 (\boldsymbol{S}' - \boldsymbol{\Gamma}_1)^{-1} \boldsymbol{\Pi}_1, \quad \text{where } \boldsymbol{S}' = \sigma_0 \boldsymbol{\Pi}_2 (\sigma_0 \boldsymbol{I} - \boldsymbol{L})^{-1}, \tag{20.12}$$

which is implied by (19.37) with $\boldsymbol{L}_0 = \sigma_0 \boldsymbol{I}$, once we identify

$$\boldsymbol{\Gamma}_1 = \boldsymbol{M} (\boldsymbol{M}^T \boldsymbol{M})^{-1} \boldsymbol{M}^T$$

with the projection operator onto the space $\mathcal{E}$ and recognize that $\boldsymbol{S}'$ is simply the diagonal matrix

$$\boldsymbol{S}' = \sum_{i=1}^{n} s_i \boldsymbol{\chi}_i, \quad \text{where } s_i = \sigma_0/(\sigma_0 - \sigma_i).$$

In practice there are easier ways of obtaining the fields of potential drops and currents that may be used to compute the tensor $\boldsymbol{Y}_*$ without introducing polarization fields. For example, one could solve directly for the potential φ, fixing the potential at one node to be zero to ensure uniqueness of the solution (This assumes that the circuit forms a connected graph; if it does not, then it is necessary to set the potential to zero at one node in each connected component of the graph.) The solution involving polarization fields is interesting, however, because it highlights the close similarity between solving these network equations and solving the conductivity problem in a composite.

20.4. The effective tensor of the passive network

The close similarity between the formula (12.61) for the effective tensor $\boldsymbol{L}_*$ and the formula (20.12) for the tensor $\boldsymbol{Y}_*$ suggests that there may be some deeper correspondence between the two problems. However it is also clear that there are some differences. In particular, the tensor $\boldsymbol{Y}_*$ does not take any special value when $\boldsymbol{\sigma} = \boldsymbol{I}$, whereas $\boldsymbol{\sigma}_*$ always takes the value $\boldsymbol{\sigma}_* = \boldsymbol{I}$ when $\boldsymbol{\sigma} = \boldsymbol{I}$.

There is an effective tensor $\boldsymbol{\sigma}_*$ naturally associated with the passive network. To define it let us introduce the spaces:

- $\mathcal{E}^{(1)} = \mathcal{E} \cap \mathcal{H}^{(1)}$, comprised of fields of potential drops that derive from potentials that take the value zero on the nodes associated with the active network;

- $\mathcal{J}^{(1)} = \mathcal{J} \cap \mathcal{H}^{(1)}$, comprised of those circulating currents that do not flow into the active network;
- $\mathcal{U}^{(1)}$, the orthogonal complement of $\mathcal{E}^{(1)} \oplus \mathcal{J}^{(1)}$ in the space $\mathcal{H}^{(1)}$.

The spaces $\mathcal{E}^{(1)}$ and $\mathcal{J}^{(1)}$ are clearly orthogonal, being subspaces of the orthogonal spaces $\mathcal{E}$ and $\mathcal{J}$. Also, $\mathcal{U}^{(1)}$ is clearly orthogonal to both $\mathcal{E}^{(1)}$ and $\mathcal{J}^{(1)}$. So we have

$$\mathcal{H}^{(1)} = \mathcal{U}^{(1)} \oplus \mathcal{E}^{(1)} \oplus \mathcal{J}^{(1)}. \tag{20.13}$$

Since $\boldsymbol{\sigma}$ acts in the space $\mathcal{H}^{(1)}$, we can define an effective tensor $\boldsymbol{\sigma}_*$ associated with the passive network through the solution of the equations

$$\boldsymbol{J} = \boldsymbol{\sigma}\boldsymbol{E} \text{ with } \boldsymbol{J} \in \mathcal{U}^{(1)} \oplus \mathcal{J}^{(1)}, \quad \boldsymbol{E} \in \mathcal{U}^{(1)} \oplus \mathcal{E}^{(1)}. \tag{20.14}$$

If $\boldsymbol{\Gamma}_0^{(1)}$ denotes the projection onto the vector space $\mathcal{U}^{(1)}$, then the linear relation

$$\boldsymbol{\Gamma}_0^{(1)}\boldsymbol{J} = \boldsymbol{\sigma}_*(\boldsymbol{\Gamma}_0^{(1)}\boldsymbol{E})$$

between the components of the fields $\boldsymbol{J}$ and $\boldsymbol{E}$ projected on the subspace $\mathcal{U}^{(1)}$ defines the effective tensor $\boldsymbol{\sigma}_*$.

20.5. The interpretation of the subspace $\mathcal{U}^{(1)}$

While the subspaces $\mathcal{E}^{(1)}$ and $\mathcal{J}^{(1)}$ have been given rather direct physical interpretations, the interpretation of $\mathcal{U}^{(1)}$ given above is somewhat abstract. Here we seek a more direct physical interpretation of $\mathcal{U}^{(1)}$ in terms of solutions to the conductivity equations in the circuit when $\boldsymbol{\sigma} = \boldsymbol{I}$, that is, when all of the conductances in the passive circuit are set equal to unity.

Let us first establish a rather basic feature of $\mathcal{U}^{(1)}$ – that it has dimension d. It is helpful to introduce the subspace

- $\mathcal{W}$, the orthogonal complement of $\mathcal{E}^{(1)} \oplus \mathcal{J}^{(1)}$ in the space $\mathcal{K}$.

The space $\mathcal{W}$ can be equivalently defined as the space spanned by $\boldsymbol{\Gamma}_1\mathcal{V}$ and $\boldsymbol{\Gamma}_2\mathcal{V}$, in which $\boldsymbol{\Gamma}_1$ and $\boldsymbol{\Gamma}_2$ are the projections onto the subspaces $\mathcal{E}$ and $\mathcal{J}$, respectively. To prove that

$$\mathcal{W} = (\boldsymbol{\Gamma}_1\mathcal{V}) \oplus (\boldsymbol{\Gamma}_2\mathcal{V}), \tag{20.15}$$

we notice that the relation

$$\mathcal{K} = \mathcal{W} \oplus \mathcal{E}^{(1)} \oplus \mathcal{J}^{(1)} \tag{20.16}$$

implies first that $\mathcal{W}$ contains $\mathcal{V}$, since $\mathcal{V}$ is orthogonal to both $\mathcal{E}^{(1)}$ and $\mathcal{J}^{(1)}$, and second that $\mathcal{W}$ is closed under the action of both $\boldsymbol{\Gamma}_1$ and $\boldsymbol{\Gamma}_2$, since $\mathcal{K}$, $\mathcal{E}^{(1)}$, and $\mathcal{J}^{(1)}$ are each closed under the action of these operators. It follows that

$$(\boldsymbol{\Gamma}_1\mathcal{V}) \oplus (\boldsymbol{\Gamma}_2\mathcal{V}) \subset \mathcal{W}.$$

Now suppose that these sets are not equal. Then there exists some field $\boldsymbol{P} \in \mathcal{W}$ that is orthogonal to $(\boldsymbol{\Gamma}_1\mathcal{V}) \oplus (\boldsymbol{\Gamma}_2\mathcal{V})$. Therefore, $\boldsymbol{\Gamma}_1\boldsymbol{P}$ is orthogonal to $(\boldsymbol{\Gamma}_1\mathcal{V}) \oplus (\boldsymbol{\Gamma}_2\mathcal{V})$, and in particular orthogonal to $\mathcal{V}$. Similarly, $\boldsymbol{\Gamma}_2\boldsymbol{P}$ is orthogonal to $\mathcal{V}$, and consequently we have

$$\boldsymbol{\Gamma}_1\boldsymbol{P} \in \mathcal{E}^{(1)}, \quad \boldsymbol{\Gamma}_2\boldsymbol{P} \in \mathcal{J}^{(1)}, \quad \text{implying that } \boldsymbol{P} \in \mathcal{E}^{(1)} \oplus \mathcal{J}^{(1)}.$$

But as $\mathcal{W}$ is orthogonal to $\mathcal{E}^{(1)} \oplus \mathcal{J}^{(1)}$, we conclude that $\boldsymbol{P}$ must be zero. This completes the proof of (20.15). From the definitions of the subspaces $\mathcal{J}^{(1)}$ and $\mathcal{E}^{(1)}$ it follows that

$$\mathcal{E} = (\boldsymbol{\Gamma}_1\mathcal{V}) \oplus \mathcal{E}^{(1)}, \quad \mathcal{J} = (\boldsymbol{\Gamma}_2\mathcal{V}) \oplus \mathcal{J}^{(1)}.$$

The assumptions (20.3) and (20.4) imply that $\mathcal{W}$ is a $2d$-dimensional space. Indeed if $\boldsymbol{v}_1, \boldsymbol{v}_2, \ldots, \boldsymbol{v}_d$ is a basis of $\mathcal{V}$, then the existence of any nontrivial linear relation

$$\sum_{i=1}^{d} c_i \boldsymbol{v}_i + \boldsymbol{\Gamma}_1 c_i' \boldsymbol{v}_i = 0$$

either implies the existence of a vector

$$\sum_{i=1}^{d} c_i \boldsymbol{v}_i \in \mathcal{V} \cap \mathcal{E},$$

or, in the event that this vector is zero, implies the existence of a vector

$$\sum_{i=1}^{d} c_i' \boldsymbol{v}_i \in \mathcal{V} \cap \mathcal{J}.$$

Both of these possibilities are excluded by our assumptions that $\mathcal{V} \cap \mathcal{E}$ and $\mathcal{V} \cap \mathcal{J}$ are empty sets.

From (20.2), (20.13), and (20.16) we see that

$$\mathcal{W} = \mathcal{V} \oplus \mathcal{U}^{(1)},$$

that is, $\mathcal{U}^{(1)}$ is the orthogonal complement of $\mathcal{V}$ in the subspace $\mathcal{W}$. Since $\mathcal{W}$ has dimension $2d$ and $\mathcal{V}$ has dimension d, it follows immediately that $\mathcal{U}^{(1)}$ has dimension d.

As a basis for the physical interpretation of $\mathcal{U}^{(1)}$, let us next establish that

$$\mathcal{U}^{(1)} = [\boldsymbol{\Pi}_2\mathcal{E}] \cap [\boldsymbol{\Pi}_2\mathcal{J}]. \tag{20.17}$$

As a first step toward proving this notice that the relations $\boldsymbol{\Pi}_2 = \boldsymbol{I} - \boldsymbol{\Pi}_1$ and $\boldsymbol{\Gamma}_2\mathcal{E} = 0$ imply that

$$\boldsymbol{\Gamma}_2[\boldsymbol{\Pi}_2\mathcal{E}] = \boldsymbol{\Gamma}_2[(\boldsymbol{I} - \boldsymbol{\Pi}_1)\mathcal{E}] = \boldsymbol{\Gamma}_2[\boldsymbol{\Pi}_1\mathcal{E}] \subset \boldsymbol{\Gamma}_2\mathcal{V} \subset \mathcal{W},$$

and by a similar argument we have $\boldsymbol{\Gamma}_1[\boldsymbol{\Pi}_2\mathcal{J}] \subset \mathcal{W}$. These equations imply that

$$\begin{aligned} [\boldsymbol{\Pi}_2\mathcal{E}] \cap [\boldsymbol{\Pi}_2\mathcal{J}] &= (\boldsymbol{\Gamma}_1 + \boldsymbol{\Gamma}_2)\{[\boldsymbol{\Pi}_2\mathcal{E}] \cap [\boldsymbol{\Pi}_2\mathcal{J}]\} \\ &\subset \boldsymbol{\Gamma}_1\{[\boldsymbol{\Pi}_2\mathcal{E}] \cap [\boldsymbol{\Pi}_2\mathcal{J}]\} \oplus \boldsymbol{\Gamma}_2\{[\boldsymbol{\Pi}_2\mathcal{E}] \cap [\boldsymbol{\Pi}_2\mathcal{J}]\} \\ &\subset \boldsymbol{\Gamma}_1[\boldsymbol{\Pi}_2\mathcal{J}] \oplus \boldsymbol{\Gamma}_2[\boldsymbol{\Pi}_2\mathcal{E}] \subset \mathcal{W}, \end{aligned} \tag{20.18}$$

where we have used the fact that $[\boldsymbol{\Pi}_2\mathcal{E}] \cap [\boldsymbol{\Pi}_2\mathcal{J}]$ is contained both in $\boldsymbol{\Pi}_2\mathcal{E}$ and in $\boldsymbol{\Pi}_2\mathcal{J}$. Also, because $\boldsymbol{\Pi}_2$ projects onto $\mathcal{H}^{(1)}$, it is obvious that (20.18) implies

$$[\boldsymbol{\Pi}_2\mathcal{E}] \cap [\boldsymbol{\Pi}_2\mathcal{J}] \subset \mathcal{W} \cap \mathcal{H}^{(1)} = \mathcal{U}^{(1)}. \tag{20.19}$$

Now, to prove the converse, notice that all fields $\boldsymbol{W} \in \mathcal{W}$ have the form

$$\boldsymbol{W} = \boldsymbol{V} + \boldsymbol{\Gamma}_1\boldsymbol{V}' \text{ with } \boldsymbol{V} \in \mathcal{V},\ \boldsymbol{V}' \in \mathcal{V},$$

as follows from the definition of $\mathcal{W}$ as the closure of $\mathcal{V}$ under the action of the projection $\mathbf{\Gamma}_1$. By applying $\mathbf{\Pi}_2$ to both sides of this identity we see that

$$\mathbf{\Pi}_2 \boldsymbol{W} = \mathbf{\Pi}_2 \mathbf{\Gamma}_1 \boldsymbol{V}',$$

from which we deduce that $\mathcal{U}^{(1)} \subset \mathbf{\Pi}_2 \mathcal{E}$. Similarly it follows that $\mathcal{U}^{(1)} \subset \mathbf{\Pi}_2 \mathcal{J}$, and we conclude that

$$\mathcal{U}^{(1)} \subset [\mathbf{\Pi}_2 \mathcal{E}] \cap [\mathbf{\Pi}_2 \mathcal{J}],$$

which in conjunction with (20.19) proves (20.17).

With this relation (20.17) established we can now identify the fields in $\mathcal{U}^{(1)}$ with solutions to the conductivity equations in the circuit with $\boldsymbol{\sigma} = \boldsymbol{I}$. To see this, notice that if $\boldsymbol{U} \in \mathcal{U}^{(1)}$, then (20.17) implies that

$$\boldsymbol{U} = \mathbf{\Pi}_2 \boldsymbol{E} = \mathbf{\Pi}_2 \boldsymbol{J} \text{ for some } \boldsymbol{E} \in \mathcal{E},\ \boldsymbol{J} \in \mathcal{J}.$$

So the equations (20.7), (20.8), and (20.9) are satisfied with

$$\boldsymbol{E}_2 = \mathbf{\Pi}_2 \boldsymbol{E},\ \ \boldsymbol{J}_2 = \mathbf{\Pi}_2 \boldsymbol{J},\ \text{ and } \boldsymbol{\sigma} = \boldsymbol{I}.$$

Conversely, it is clear that any solution to these equations can be identified with fields in the space $\mathcal{U}^{(1)}$.

20.6. The relation between the effective tensor and the Y-tensor in an electrical circuit

Now suppose that we have fields $\boldsymbol{E}' = \boldsymbol{E}_1 + \boldsymbol{E}_2 \in \mathcal{E}$ and $\boldsymbol{J} = \boldsymbol{J}_1 + \boldsymbol{J}_2 \in \mathcal{J}$ satisfying both (20.8) and Ohm's law (20.9). The component field $\boldsymbol{E}_2$ satisfies

$$\boldsymbol{E}_2 = \mathbf{\Pi}_2 \boldsymbol{E} \subset \mathbf{\Pi}_2 \mathcal{E} \subset \mathbf{\Pi}_2 (\mathcal{W} \oplus \mathcal{E}^{(1)}) = \mathcal{U} \oplus \mathcal{E}^{(1)}, \tag{20.20}$$

and similarly,

$$\boldsymbol{J}_2 \subset \mathcal{U} \oplus \mathcal{J}^{(1)}. \tag{20.21}$$

So we have constructed a solution $\boldsymbol{J} = \boldsymbol{J}_2$ and $\boldsymbol{E} = \boldsymbol{E}_2$ to the equations (20.14) from a solution to the equations (20.7), (20.8), and (20.9).

It remains to find a relation between the tensor $\boldsymbol{Y}_*$ and the effective tensor $\boldsymbol{\sigma}_*$. It turns out that this is strikingly similar to the problem of finding the tensor $\boldsymbol{Y}_*$ given $\boldsymbol{\sigma}$. To see this connection let us define

$$\boldsymbol{E}_0^{(1)} = \mathbf{\Gamma}_0^{(1)} \boldsymbol{E}_2 \in \mathcal{U}^{(1)},\quad \boldsymbol{J}_0^{(1)} = \mathbf{\Gamma}_0^{(1)} \boldsymbol{J}_2 \in \mathcal{U}^{(1)}.$$

According to the definition of the effective tensor $\boldsymbol{\sigma}_*$, these are related via

$$\boldsymbol{J}_0^{(1)} = \boldsymbol{\sigma}_* \boldsymbol{E}_0^{(1)}, \tag{20.22}$$

and from (20.20) and (20.21) it is clear that

$$\boldsymbol{E}_0^{(1)} - \boldsymbol{E}_2 \in \mathcal{E}^{(1)} \subset \mathcal{E},\quad \boldsymbol{J}_0^{(1)} - \boldsymbol{J}_2 \in \mathcal{J}^{(1)} \subset \mathcal{J}.$$

Consequently we have

$$\boldsymbol{E}_1 + \boldsymbol{E}_0^{(1)} = \boldsymbol{E}' + \boldsymbol{E}_0^{(1)} - \boldsymbol{E}_2 \in \mathcal{W} \cap \mathcal{E},\ \ \boldsymbol{J}_1 + \boldsymbol{J}_0^{(1)} = \boldsymbol{J}' + \boldsymbol{J}_0^{(1)} - \boldsymbol{J}_2 \in \mathcal{W} \cap \mathcal{J}. \tag{20.23}$$

So if we define the subspaces

$$\tilde{\mathcal{E}} = \mathcal{W} \cap \mathcal{E} = \mathbf{\Gamma}_1 \mathcal{W} = \mathbf{\Gamma}_1 \mathcal{V}, \quad \tilde{\mathcal{J}} = \mathcal{W} \cap \mathcal{J} = \mathbf{\Gamma}_2 \mathcal{W} = \mathbf{\Gamma}_2 \mathcal{V},$$

then (20.23) implies that

$$\boldsymbol{E}_1 + \boldsymbol{E}_0^{(1)} \in \tilde{\mathcal{E}}, \quad \boldsymbol{J}_1 + \boldsymbol{J}_0^{(1)} \in \tilde{\mathcal{J}}. \tag{20.24}$$

By comparing (20.9) with (20.22) and (20.7) with (20.24) we see that $\boldsymbol{Y}_*$ is the Y-tensor associated with the operator $\boldsymbol{\sigma}_*$ in the vector space

$$\mathcal{W} = \tilde{\mathcal{E}} \oplus \tilde{\mathcal{J}} = \mathcal{V} \oplus \mathcal{U}^{(1)}.$$

In other words, to find the tensor $\boldsymbol{Y}_*$ we can replace the passive network, represented by the tensor $\boldsymbol{\sigma}$ acting in the space $\mathcal{H}^{(1)}$, by an equivalent "network," represented by the effective tensor $\boldsymbol{\sigma}_*$ acting in the space $\mathcal{U}^{(1)}$.

Clearly (20.12) could now be applied to obtain an expression for $\boldsymbol{Y}_*$ in terms of $\boldsymbol{\sigma}_*$. However, there is another approach that yields a much simpler formula for $\boldsymbol{Y}_*$ in terms of $\boldsymbol{\sigma}_*$. The first observation to make is that given any vector $\boldsymbol{J}_2 \in \mathcal{U}^{(1)}$ there exists a unique associated vector $\boldsymbol{J}_1 \in \mathcal{V}$ such that $\boldsymbol{J}_1 + \boldsymbol{J}_2 \in \tilde{\mathcal{J}}$. Uniqueness follows since by assumption $\mathcal{J} \cap \mathcal{V} = 0$. Existence follows because the equation

$$\mathbf{\Gamma}_1 \boldsymbol{J}_1 = -\mathbf{\Gamma}_1 \boldsymbol{J}_2 \tag{20.25}$$

always has a solution for $\boldsymbol{J}_1 \in \mathcal{V}$ because $\mathbf{\Gamma}_1 \mathcal{V}$ spans all of $\tilde{\mathcal{E}}$. Since $\boldsymbol{J}_1$ must depend linearly on $\boldsymbol{J}_2$, we can write

$$\boldsymbol{J}_1 = \boldsymbol{K} \boldsymbol{J}_2, \tag{20.26}$$

where $\boldsymbol{K}$ is a nonsingular operator that maps $\mathcal{U}^{(1)}$ to $\mathcal{V}$. This operator $\boldsymbol{K}$ provides a correspondence between vectors in $\mathcal{U}^{(1)}$ and vectors in $\mathcal{V}$. To obtain an explicit expression for $\boldsymbol{K}$ we project (20.25) onto the space $\mathcal{V}$. This gives

$$\mathbf{\Pi}_1 \mathbf{\Gamma}_1 \mathbf{\Pi}_1 \boldsymbol{J}_1 = -\mathbf{\Pi}_1 \mathbf{\Gamma}_1 \mathbf{\Pi}_2 \boldsymbol{J}_2. \tag{20.27}$$

The operator $\mathbf{\Pi}_1 \mathbf{\Gamma}_1 \mathbf{\Pi}_1 = \mathbf{\Pi}_1 \mathbf{\Gamma}_1 \mathbf{\Gamma}_1 \mathbf{\Pi}_1$ is clearly positive-semidefinite. In fact, it is strictly positive-definite because $\mathbf{\Gamma}_1 \boldsymbol{J}_1$ is nonzero for all nonzero $\boldsymbol{J}_1 \in \mathcal{V}$, since otherwise $\mathcal{V}$ would share a common vector with $\mathcal{J}$, which is forbidden by our assumptions. Solving (20.27) for $\boldsymbol{J}_1$ and equating the result with (20.26) shows that

$$\boldsymbol{K} = -[\mathbf{\Pi}_1 \mathbf{\Gamma}_1 \mathbf{\Pi}_1]^{-1} \mathbf{\Pi}_1 \mathbf{\Gamma}_1 \mathbf{\Pi}_2, \tag{20.28}$$

where the inverse is to be taken on $\mathcal{V}$.

Similarly we have

$$\boldsymbol{E}_1 = \boldsymbol{K}' \boldsymbol{E}_2,$$

where

$$\boldsymbol{K}' = -[\mathbf{\Pi}_1 \mathbf{\Gamma}_2 \mathbf{\Pi}_1]^{-1} \mathbf{\Pi}_1 \mathbf{\Gamma}_2 \mathbf{\Pi}_2$$

is a nonsingular operator that also maps $\mathcal{U}^{(1)}$ to $\mathcal{V}$. Now notice that

$$\begin{aligned} \boldsymbol{K}' \boldsymbol{K}^T &= [\mathbf{\Pi}_1 \mathbf{\Gamma}_2 \mathbf{\Pi}_1]^{-1} \mathbf{\Pi}_1 \mathbf{\Gamma}_2 (\boldsymbol{I} - \mathbf{\Pi}_1) \mathbf{\Gamma}_1 \mathbf{\Pi}_1 [\mathbf{\Pi}_1 \mathbf{\Gamma}_1 \mathbf{\Pi}_1]^{-1} \\ &= -[\mathbf{\Pi}_1 \mathbf{\Gamma}_2 \mathbf{\Pi}_1]^{-1} \mathbf{\Pi}_1 \mathbf{\Gamma}_2 \mathbf{\Pi}_1 \mathbf{\Gamma}_1 \mathbf{\Pi}_1 [\mathbf{\Pi}_1 \mathbf{\Gamma}_1 \mathbf{\Pi}_1]^{-1} = -\boldsymbol{I}. \end{aligned}$$

In other words, $-\boldsymbol{K}^T$ is the inverse of $\boldsymbol{K}'$.

Now it follows directly from (20.22) that

$$\boldsymbol{J}_1 = \boldsymbol{K}\boldsymbol{J}_2 = \boldsymbol{K}\boldsymbol{\sigma}_*\boldsymbol{E}_2 = \boldsymbol{K}\boldsymbol{\sigma}_*(\boldsymbol{K}')^{-1}\boldsymbol{E}_1 = -\boldsymbol{K}\boldsymbol{\sigma}_*\boldsymbol{K}^T\boldsymbol{E}_1,$$

which according to the definition (20.10) of $\boldsymbol{Y}_*$ implies that

$$\boldsymbol{Y}_* = \boldsymbol{K}\boldsymbol{\sigma}_*\boldsymbol{K}^T. \tag{20.29}$$

This equation has separated the dependence of $\boldsymbol{Y}_*$ on $\boldsymbol{\sigma}_*$ from the dependence of $\boldsymbol{Y}_*$ on the orientation of the subspace $\tilde{\mathcal{E}}$ with respect to the subspace $\mathcal{V}$, which is embodied in the operator $\boldsymbol{K}$.

Now suppose that we have chosen an orthonormal basis in each of the d-dimensional subspaces $\mathcal{U}^{(1)}$ and $\mathcal{V}$. The operator $\boldsymbol{K}$, regarded as a map from $\mathcal{U}^{(1)}$ to $\mathcal{V}$, is then represented by a $d \times d$ matrix $\boldsymbol{K}$. Using the standard polar decomposition, this matrix can be factored into the form

$$\boldsymbol{K} = \boldsymbol{N}^{1/2}\boldsymbol{Q} \text{ with } \boldsymbol{N} = \boldsymbol{K}\boldsymbol{K}^T \text{ and } \boldsymbol{Q}\boldsymbol{Q}^T = \boldsymbol{I}, \;\; \boldsymbol{Q}^T\boldsymbol{Q} = \boldsymbol{I}. \tag{20.30}$$

Different choices of basis in the d-dimensional space $\mathcal{U}^{(1)}$ will result in different values of $\boldsymbol{Q}$. A natural basis to take is one where $\boldsymbol{Q} = \boldsymbol{I}$. Let us therefore suppose without loss of generality that the basis has been chosen so that $\boldsymbol{Q} = \boldsymbol{I}$. Then (20.29) and (20.30) imply that the $d \times d$ matrices representing $\boldsymbol{\sigma}_*$ and $\boldsymbol{Y}$ in this basis are linked by the equation

$$\boldsymbol{\sigma}_* = \boldsymbol{N}^{-1/2}\boldsymbol{Y}\boldsymbol{N}^{-1/2}.$$

Furthermore, since $\boldsymbol{\sigma}_*$ takes the value $\boldsymbol{I}$ on $\mathcal{U}_0$ when $\boldsymbol{\sigma} = \boldsymbol{\Pi}_2$, it follows that $\boldsymbol{N}$ can be identified with the value of $\boldsymbol{Y}$ when $\boldsymbol{\sigma} = \boldsymbol{\Pi}_2$. If we consider $\boldsymbol{\sigma}_*$ and $\boldsymbol{Y}$ as functions of the conductances $\sigma_1, \sigma_2, \ldots, \sigma_n$, then we have

$$\boldsymbol{\sigma}_*(\sigma_1, \sigma_2, \ldots, \sigma_n) = [\boldsymbol{Y}(1, 1, \ldots, 1)]^{-1/2}\boldsymbol{Y}(\sigma_1, \sigma_2, \ldots, \sigma_n)[\boldsymbol{Y}(1, 1, \ldots, 1)]^{-1/2}. \tag{20.31}$$

In other words, by a suitable normalization, determined by the normalization matrix

$$\boldsymbol{N} = \boldsymbol{Y}(1, 1, \ldots, 1),$$

which is chosen to ensure that $\boldsymbol{\sigma}_*(1, 1, \ldots, 1) = \boldsymbol{I}$, the tensor $\boldsymbol{Y}(\sigma_1, \sigma_2, \ldots, \sigma_n)$ is reduced through the formula (20.31) to the effective tensor $\boldsymbol{\sigma}_*(\sigma_1, \sigma_2, \ldots, \sigma_n)$ for all conductances $\sigma_1, \sigma_2, \ldots, \sigma_n$. Thus the effective tensor $\boldsymbol{\sigma}_*(\sigma_1, \sigma_2, \ldots, \sigma_n)$ measures the response of the network relative to its response when all of the conductances are set equal to 1.

References

Brophy, J. J. 1983. *Basic Electronics for Scientists* (Fourth ed.), Chapter AC-Circuit Analysis, pp. 71–96. New York: McGraw-Hill. ISBN 0-07-008133-6. {*414, 423*}

Strang, G. 1986. *Introduction to Applied Mathematics*, pp. 87–95. Wellesley, Massachusetts: Wellesley-Cambridge Press. ISBN 0-9614088-0-4. {*413, 423*}

21

Bounds on the properties of composites

21.1. Why are bounds useful?

Very efficient numerical algorithms are currently available for calculating the effective tensors of quite complicated two-dimensional microgeometries. The numerical evaluation of effective tensors for three-dimensional microgeometries is also progressing rapidly. In light of these advances one might ask: Why is there a need for developing bounds on effective tensors? One reason is that they often provide quick and simple estimates for the effective tensors.

Another reason for favoring bounds is that in most experimental situations we do not have a complete knowledge of the composite geometry. Even when an accurate determination of the three-dimensional composite microgeometry is possible, obtaining this information and numerically parameterizing it (which may involve the triangulation of boundaries between phases) can be a very time-consuming process. Cross-sectional photographs give only limited information. For example, in a two-phase microgeometry it can be difficult to judge whether a phase is connected if a cross-sectional photograph shows only islands of that phase surrounded by the second phase. In the three-dimensional microgeometry, does the first phase consist of connected wire-like filaments, or does it consist of isolated elongated inclusions? The answer could have a large influence on one's estimates for, say, the effective conductivity when both phases have widely different conductivities. The problem of reconstructing the three-dimensional microstructure from a cross-sectional photograph is the subject of active research; see Yeong and Torquato (1998) and references therein.

In a two-phase composite the only available information might be the volume fractions of the two phases, and the values of the tensors $\boldsymbol{L}_1$ and $\boldsymbol{L}_2$. Approximation schemes can be used to estimate the effective tensor from what we do know about the composite geometry, but to be assured that the approximation is a good one we need to have some estimate of the possible (or probable) error involved in making this approximation. Bounds on effective tensors provide such an estimate, and they serve as a benchmark to test approximation formulas: Clearly an approximation formula should be amended when it predicts values for $\boldsymbol{L}_*$ that lie outside the bounds. Moreover, the bounds themselves can often be regarded as useful approximations. For example, if a bound is derived by substituting a trial field into a variational principle, and if for some physical reason the trial field is expected to be close to the actual field in the given composite, then that bound should be close to the value of $\boldsymbol{L}_*$. In other words, $\boldsymbol{L}_*$ might be close to a particular bound even when the complete set of bounds allows a very wide range of tensor values [see, for example, Torquato (1991)].

Bounds are also important in problems of structural optimization, where one needs to characterize the set of possible macroscopic responses of a composite as $\boldsymbol{L}(\boldsymbol{x})$ varies over a

set of admissible tensor fields, and to identify fields $\boldsymbol{L}(\boldsymbol{x})$ that produce extremal responses. We will clarify the role of bounds in this context in section 21.3 on page 429. For a more comprehensive treatment, see the articles of Tartar (1975); Armand, Lurie, and Cherkaev (1984); Kohn and Strang (1986); Kohn (1992); Bendsøe (1997); Cherkaev (1999); Tartar (2000); the books of Bendsøe (1995); Kalamkarov and Kolpakov (1997); Cherkaev (2000); and Allaire (2001) and references therein.

21.2. What are bounds?

Bounds are inequalities correlating various physical and/or microstructural quantities. To give some idea as to what this means, let us consider the simple example of conduction in a two-dimensional polycrystal. The admissible conductivity fields $\boldsymbol{\sigma}(\boldsymbol{x})$ for this problem are fields of the form

$$\boldsymbol{\sigma}(\boldsymbol{x}) = \boldsymbol{R}(\boldsymbol{x}) \begin{pmatrix} \lambda_1 & 0 \\ 0 & \lambda_2 \end{pmatrix} \boldsymbol{R}^T(\boldsymbol{x}),$$

in which the eigenvalues λ_1 and λ_2 of the pure crystal are real and held fixed. No restrictions will be placed on the field of crystal orientations, that is, the field $\boldsymbol{R}(\boldsymbol{x})$ of rotation matrices is not subject to any constraints beyond periodicity. We already know from (3.12) and (13.13) that the effective tensor $\boldsymbol{\sigma}_*$ satisfies

$$\det(\boldsymbol{\sigma}_*) = \lambda_1\lambda_2, \quad \langle \boldsymbol{\sigma}^{-1} \rangle^{-1} \leq \boldsymbol{\sigma}_* \leq \langle \boldsymbol{\sigma} \rangle. \tag{21.1}$$

One useful quantity to bound is the rate of energy dissipation W, given by

$$2W = \langle \boldsymbol{e} \rangle \cdot \langle \boldsymbol{j} \rangle = \langle \boldsymbol{e} \rangle \cdot \boldsymbol{\sigma}_* \langle \boldsymbol{e} \rangle = \langle \boldsymbol{j} \rangle \cdot \boldsymbol{\sigma}_*^{-1} \langle \boldsymbol{j} \rangle, \tag{21.2}$$

when either the applied electric field $\langle \boldsymbol{e} \rangle$ or the applied current field $\langle \boldsymbol{j} \rangle$ is held fixed. Let us suppose that the eigenvalues of the pure crystal have been labeled so that $\lambda_1 \geq \lambda_2$. Then the arithmetic and harmonic mean bounds in (21.1) imply that

$$\lambda_2 \boldsymbol{I} \leq \boldsymbol{\sigma}_* \leq \lambda_1 \boldsymbol{I}, \quad \boldsymbol{I}/\lambda_1 \leq \boldsymbol{\sigma}_*^{-1} \leq \boldsymbol{I}/\lambda_2, \tag{21.3}$$

and this in conjunction with (21.2) gives us the desired bound on the energy dissipation in terms of $\langle \boldsymbol{e} \rangle$,

$$\lambda_2 |\langle \boldsymbol{e} \rangle|^2 \leq 2W \leq \lambda_1 |\langle \boldsymbol{e} \rangle|^2, \tag{21.4}$$

and the desired bound on the energy dissipation in terms of $\langle \boldsymbol{j} \rangle$,

$$|\langle \boldsymbol{j} \rangle|^2/\lambda_1 \leq 2W \leq |\langle \boldsymbol{j} \rangle|^2/\lambda_2. \tag{21.5}$$

These bounds are optimal in the sense that the upper and lower bounds in (21.4) and (21.5) are achieved for a fixed value of $\langle \boldsymbol{e} \rangle$ or $\langle \boldsymbol{j} \rangle$ when the polycrystal is pure crystal oriented so that the appropriate axis of principal conductivity is aligned with the field $\langle \boldsymbol{e} \rangle$ or $\langle \boldsymbol{j} \rangle$. Another way to visualize the bounds (21.4) is to regard them as constraining the possible values of the pair $(W, \langle \boldsymbol{e} \rangle)$ to a region in three-dimensional space with the two components of $\langle \boldsymbol{e} \rangle$ as the y_1- and y_2-axes and with W as the y_3-axis. Similarly, one can regard (21.5) as constraining the possible values of the pair $(W, \langle \boldsymbol{j} \rangle)$.

Another useful bound is on the possible values of the pairs $(\langle \boldsymbol{j} \rangle, \langle \boldsymbol{e} \rangle)$ or, equivalently, on the possible values of the average current field $\langle \boldsymbol{j} \rangle$ given an average electric field $\langle \boldsymbol{e} \rangle$. Such bounds tell us about what direction the average current can flow relative to the direction of the

applied electric field. Letting λ_1^* and λ_2^* denote the eigenvalues of the effective tensor, these average fields satisfy the relation

$$\langle \boldsymbol{j} \rangle = \boldsymbol{R}_* \begin{pmatrix} \lambda_1^* & 0 \\ 0 & \lambda_2^* \end{pmatrix} \boldsymbol{R}_*^T \langle \boldsymbol{e} \rangle,$$

which implies that

$$|\langle \boldsymbol{j} \rangle|^2 - (\lambda_1^* + \lambda_2^*)\langle \boldsymbol{e} \rangle \cdot \langle \boldsymbol{j} \rangle + \lambda_1^* \lambda_2^* |\langle \boldsymbol{e} \rangle|^2 = 0. \tag{21.6}$$

From (21.1) we see that $\lambda_1^* \lambda_2^* = \lambda_1 \lambda_2$ and, under this constraint, (21.3) implies that $\lambda_1^* + \lambda_2^*$ is at most equal to $\lambda_1 + \lambda_2$. Also, $\langle \boldsymbol{e} \rangle \cdot \langle \boldsymbol{j} \rangle = \langle \boldsymbol{e} \cdot \boldsymbol{\sigma} \boldsymbol{e} \rangle$ is clearly nonnegative. Therefore, we have the inequality

$$|\langle \boldsymbol{j} \rangle|^2 - (\lambda_1 + \lambda_2)\langle \boldsymbol{e} \rangle \cdot \langle \boldsymbol{j} \rangle + \lambda_1 \lambda_2 |\langle \boldsymbol{e} \rangle|^2 \leq 0, \tag{21.7}$$

which we can rewrite in the form

$$|\langle \boldsymbol{j} \rangle - (\lambda_1 + \lambda_2)\langle \boldsymbol{e} \rangle/2|^2 \leq (\lambda_1 - \lambda_2)^2 |\langle \boldsymbol{e} \rangle|^2/4. \tag{21.8}$$

In other words, as illustrated in figure 21.1, if the applied electric field $\langle \boldsymbol{e} \rangle$ is fixed, the vector representing the average current field $\langle \boldsymbol{j} \rangle$ has the property that its endpoint must lie within a circle centered at $(\lambda_1 + \lambda_2)\langle \boldsymbol{e} \rangle/2$ and with radius $(\lambda_1 - \lambda_2)|\langle \boldsymbol{e} \rangle|/2$, no matter what the microstructure of the polycrystal happens to be. In particular, this places constraints on the angle between the vectors $\langle \boldsymbol{j} \rangle$ and $\langle \boldsymbol{e} \rangle$. The bounds are optimal: If we take a pure crystal as our polycrystal, then (21.7) is satisfied as an equality, and as we vary the orientation of the crystal with respect to $\langle \boldsymbol{e} \rangle$ the endpoint of the vector $\langle \boldsymbol{j} \rangle$ traces around the circle. Points in the interior of the circle can be realized by suitably oriented simple laminates of the pure crystal and rotated crystal.

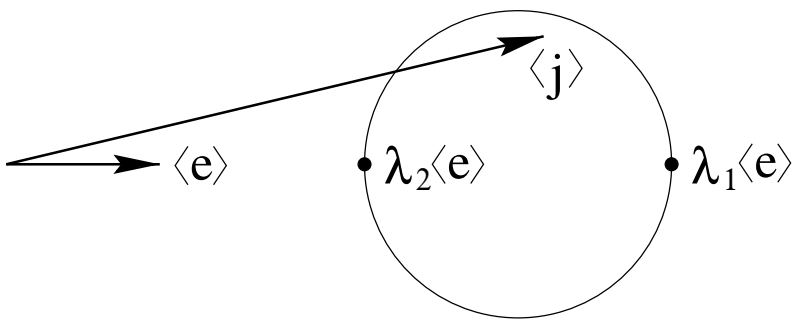

Figure 21.1. When the average electric field vector $\langle \boldsymbol{e} \rangle$ is prescribed, the average current field vector $\langle \boldsymbol{j} \rangle$ in a two-dimensional polycrystal can lie anywhere inside the circle. Here λ_1 and λ_2 are the principal conductivities of the pure crystal. Currents $\langle \boldsymbol{j} \rangle$ touching the boundary of the circle can be realized when the polycrystal is just the pure crystal, suitably oriented. Currents $\langle \boldsymbol{j} \rangle$ in the circle interior can be realized in a simple laminate of the pure crystal with a rotation of itself.

We can also consider bounds on the effective tensor $\boldsymbol{\sigma}_*$. Since we are free to rotate any polycrystal, it follows that if $\boldsymbol{\sigma}_*$ is the effective tensor of some polycrystal, then so too are

all rotations of $\boldsymbol{\sigma}_*$. In other words, it suffices to bound the possible eigenvalue pairs $(\lambda_1^*, \lambda_2^*)$. According to (21.1) and (21.3) these satisfy the constraints

$$\lambda_1^*\lambda_2^* = \lambda_1\lambda_2, \qquad \lambda_2 \le \lambda_1^* \le \lambda_1. \tag{21.9}$$

Again these bounds are optimal [as shown, for example, by Lurie and Cherkaev (1981, 1984)]. They provide a complete characterization of the set of possible effective tensors $\boldsymbol{\sigma}_*$. The relations (21.9) imply that the point $(\lambda_1^*, \lambda_2^*)$ lies on the arc of a hyperbola and the endpoints of this arc correspond to pure crystal. By considering a simple laminate of the pure crystal with a 90° rotation of itself, we can attain all points along the arc of the hyperbola.

In general one usually either considers an n-phase composite where the admissible fields take the form

$$\boldsymbol{L}(\boldsymbol{x}) = \sum_{i=1}^{n} \chi_i(\boldsymbol{x})\boldsymbol{L}_i,$$

or an n-phase polycrystal where the admissible fields take the form

$$\boldsymbol{L}(\boldsymbol{x}) = \boldsymbol{Q}(\boldsymbol{R}(\boldsymbol{x}))\Big[\sum_{i=1}^{n} \chi_i(\boldsymbol{x})\boldsymbol{L}_i\Big][\boldsymbol{Q}(\boldsymbol{R}(\boldsymbol{x}))]^T,$$

in which $\boldsymbol{Q}(\boldsymbol{R})$, satisfying $\boldsymbol{Q}(\boldsymbol{R})[\boldsymbol{Q}(\boldsymbol{R})]^T = \boldsymbol{I}$, is the orthogonal matrix representing the action of a rotation $\boldsymbol{R}$ on tensors in $\mathcal{T}$. The tensors $\boldsymbol{L}_1, \boldsymbol{L}_2, \ldots, \boldsymbol{L}_n$ are given, while the characteristic functions and field of rotation matrices $\boldsymbol{R}(\boldsymbol{x})$ are periodic but otherwise free to vary subject to the usual constraints:

$$\chi_i(\boldsymbol{x})\chi_j(\boldsymbol{x}) = \delta_{ij}\chi_i(\boldsymbol{x}), \quad \sum_{i=1}^{n} \chi_i(\boldsymbol{x}) = 1, \quad \boldsymbol{R}(\boldsymbol{x})[\boldsymbol{R}(\boldsymbol{x})]^T = \boldsymbol{I}.$$

The bounds themselves can be regarded as inequalities that correlate different quantities of interest in any given geometry. For instance, they may correlate a selection of one or more of the following quantities: the energy (or energy dissipation) W; the average field $\langle \boldsymbol{E} \rangle$; the average field $\langle \boldsymbol{J} \rangle$; the effective tensor $\boldsymbol{L}_*$; and the volume fractions $f_i = \langle \chi_i \rangle$, for $i = 1, 2, \ldots, n$ or other descriptors of the composite geometry such as a set of parameters depending on the reduced correlation functions. This list can be extended if we allow the tensors $\boldsymbol{L}_1, \boldsymbol{L}_2, \ldots, \boldsymbol{L}_n$ and the fields $\langle \boldsymbol{E} \rangle$ and $\langle \boldsymbol{J} \rangle$ to depend on some parameter ω that might take a selection of different values. For example, $\boldsymbol{L}_1, \boldsymbol{L}_2, \ldots, \boldsymbol{L}_n$ might represent the complex dielectric tensors or complex elasticity tensors, and ω might represent the frequency of oscillation of the fields. Then one might be interested in deriving bounds that correlate a selection of the quantities $W(\omega)$, $\langle \boldsymbol{E}(\omega) \rangle$, $\langle \boldsymbol{J}(\omega) \rangle$, $\boldsymbol{L}_*(\omega)$, and $\boldsymbol{f} = (f_1, f_2, \ldots, f_n)$ for several different values of ω. Alternatively, if $\boldsymbol{L}_1, \boldsymbol{L}_2, \ldots, \boldsymbol{L}_n$ are temperature-dependent, but the microstructure does not change with temperature, then ω might represent the temperature.

The quantities to be correlated can typically be represented by some k-tuplet $(a_1, a_2, \ldots a_k)$ where various subsets of the a_i represent the quantities to be correlated. For example, for conductivity in a three-dimensional, two-phase medium the subsets $\{a_1, a_2, a_3\}$ and $\{a_4, a_5, a_6\}$ could represent the components of the fields $\langle \boldsymbol{j} \rangle$ and $\langle \boldsymbol{e} \rangle$ while a_7 could represent the volume fraction f_1 of component 1. Alternatively, $\{a_1, a_2, a_3\}$ could represent the diagonal elements of the tensor $\boldsymbol{\sigma}_*$ while $\{a_4, a_5, a_6\}$ could represent the off-diagonal elements of the tensor, a_7 could represent the volume fraction, and a_8 could represent the parameter ζ_1 defined by (15.31).

The bounds can be visualized as defining a region in this k-dimensional space, within which the k-tuplet $(a_1^*, a_2^*, \ldots a_k^*)$ associated with any composite must lie. A set of bounds is said to be optimal when every point within this region corresponds to a k-tuplet associated with at least one microgeometry. In other words, optimal bounds give a complete characterization of the possible correlations that can occur in composite materials. Since the effective tensor $\boldsymbol{L}_*$ governs the relation between $\langle \boldsymbol{E} \rangle$ and $\langle \boldsymbol{J} \rangle$, and since these fields determine the energy $W = \langle \boldsymbol{E} \rangle \cdot \langle \boldsymbol{J} \rangle / 2$, it follows that optimal bounds on the effective tensor $\boldsymbol{L}_*$ imply optimal bounds on the set of $(\langle \boldsymbol{J} \rangle, \langle \boldsymbol{E} \rangle)$ pairs, which in turn imply optimal bounds on the set of $(W, \langle \boldsymbol{E} \rangle)$ pairs and $(W, \langle \boldsymbol{J} \rangle)$ pairs. However, the converse statements are not generally true. Optimal bounds on the set of $(W, \langle \boldsymbol{E} \rangle)$ or $(W, \langle \boldsymbol{J} \rangle)$ pairs do not usually contain enough information to determine optimal bounds on the set of $(\langle \boldsymbol{J} \rangle, \langle \boldsymbol{E} \rangle)$ pairs, although they certainly do provide some bounds. Similarly, optimal bounds on the set of $(\langle \boldsymbol{J} \rangle, \langle \boldsymbol{E} \rangle)$ pairs do not generally contain enough information to determine optimal bounds on the effective tensor $\boldsymbol{L}_*$.

Additional constraints, such as geometric isotropy, may sometimes be imposed on the fields of characteristic functions and rotation matrices. From an experimental viewpoint it might be useful to impose other restrictions. For instance, if it is known that a two-phase composite consists of spheres of equal radius dispersed in a matrix of the other phase, then it would be useful to incorporate this information into the bounds. It is difficult to do this unless the spheres have some minimum separation. Thus not all geometric information is easy to incorporate into bounds. Even in the two-dimensional case, for suspensions of aligned circular cylinders of equal radius with conductivity σ_1 in a matrix of conductivity $\sigma_2 < \sigma_1$, it is not known which configurations with transverse isotropy have the lowest and highest transverse effective conductivities for fixed-volume fractions of the phases. Some progress has been made by Berlyand and Mityushev (2001), who show that simple periodic arrays have the lowest conductivity amongst a certain class of random arrays. Probably the hexagonal array has the lowest conductivity amongst all configurations. The configuration with the highest conductivity might be the one obtained by first packing the cylinders together in a hexagonal array of touching cylinders, and then using this material as the coating and phase 2 as the core in a coated cylinder assemblage to achieve the desired volume fractions of the phases.

We will see in section 30.1 on page 643 that many bounding problems reduce to the G-closure problem, which is the problem of determining the set GU of values that $\boldsymbol{L}_*$ takes as $\boldsymbol{L}(\boldsymbol{x})$ ranges over all fields taking values in a given set U. Thus GU represents the set of all possible effective tensors built from composites with phases having tensors in the set U. Following Lurie and Cherkaev (1981), the set GU is called the G-closure of U. For example, in the case of two-dimensional conductivity where U consists of all symmetric conductivity tensors with eigenvalues λ_1 and λ_2, the set GU consists of all symmetric conductivity tensors with eigenvalues λ_1^* and λ_2^* satisfying (21.9). The set GU is closed in the sense that if we form composites from phases with tensors in the set GU, then the resulting effective tensor will still remain in the set GU, that is, $G(GU) = GU$. Basically, each such composite can be regarded as a "supercomposite" of phases, where the phases themselves are composites of materials having tensors in U (with their microstructure being much smaller than the microstructure of the supercomposite).

21.3. The role of bounds in structural optimization: A model problem

A classic model problem is the following one, analyzed by Murat and Tartar (1985); see also Tartar (1975, 1987). Suppose that heat is produced at a uniform rate h throughout a region,

which for simplicity we take to be a sphere Θ of unit radius, and suppose that the sphere is immersed in a fluid at a uniform temperature T_0. Inside the sphere there is a fixed volume p of good conductor, with thermal conductivity σ_1, and a remaining volume of poor conductor, with thermal conductivity $\sigma_2 < \sigma_1$. The question is: How should one configure the phases, while keeping p fixed, to minimize, say, the average temperature throughout the sphere? In mathematical terms one can consider a set $\mathcal{S}_p$ comprised of all temperature fields $T(\boldsymbol{x})$, each of which solves the equations

$$-\nabla \cdot [(\sigma_1 - \sigma_2)\chi(\boldsymbol{x}) + \sigma_2]\nabla T(\boldsymbol{x}) = h \ \text{ for } \boldsymbol{x} \in \Theta, \quad T(\boldsymbol{x}) = T_0 \ \text{ for } \boldsymbol{x} \in \partial\Theta,$$

for some choice of the characteristic function $\chi(\boldsymbol{x})$ satisfying

$$\langle \chi \rangle_\Theta = p,$$

in which the angular brackets denote averages over Θ. We can then ask which temperature field $T(\boldsymbol{x})$, and hence which characteristic function $\chi(\boldsymbol{x})$, is needed to achieve the infimum

$$T_* = \inf_{T \in \mathcal{S}_p} \langle T \rangle_\Theta. \tag{21.10}$$

The answer is that the infimum is never achieved, at least not in the classical sense. The physical explanation is quite simple, as illustrated in figure 21.2. The first idea would be to put the poor conductor in a spherical core and surround it by a shell of the good conductor. However, this is unstable. It is much better to take some of the material from the shell and reshape it into fingers of good conducting material that protrude into the poor conducting region to provide a conduit for the heat produced there. The improvement is enhanced if we break the large fingers into finer ones still pointing in the radial direction. By continuing in this way we obtain a sequence of characteristic functions with progressively finer and finer microstructures. Only in the limit of infinitely fine microstructures is the limit in (21.10) achieved.

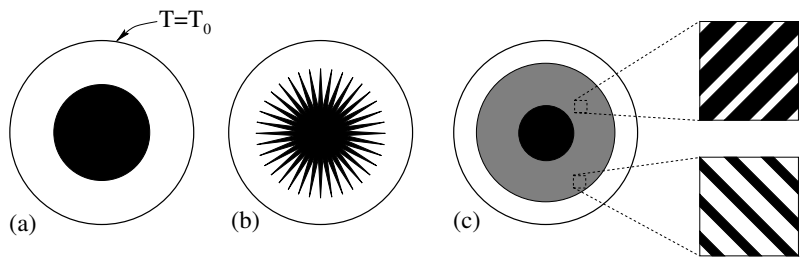

Figure 21.2. A model optimization problem. The black region is the poor heat conductor, while the white region is the good conductor. To minimize the overall temperature when heat is produced uniformly inside the sphere, a first guess is to put the good conductor outside of a spherical core of the poor conductor, as in (a). However, this is unstable and it is better to have fingers of the good conductor protruding into the poor conductor, as in (b). The best solution is to allow composites (in this case laminates) into the design, as in (c).

Such "chattering" sequences are typical of nonconvex optimization problems and have to be treated carefully. For example, if one seeks the optimal configuration by using the standard finite-element numerical approach, the result will be a configuration with a microstructure

on the same length scale as the finite elements, indicating that the finite-element approach is unreliable. One cure is to penalize such configurations by adding to the quantity to be minimized a small term proportional to the area of the interface between the phases, and then take the limit as the mesh size and the penalizing term approach zero in a suitable way. Since this is computationally inefficient, a better solution is to reformulate the original problem. The appearance of microstructure on a small length scale signifies that the optimal configuration involves composite materials. In other words, we should reformulate the original problem to reflect this, allowing not just phase 1 or phase 2, but all possible composites of the two phases. The reformulated problem is called the relaxed problem. The idea of introducing a relaxed formulation based on composite materials originated in various different settings in the work of Tartar (1975); Cheng and Olhoff (1981); Lurie, Cherkaev, and Fedorov (1982a, 1982b); Murat and Tartar (1985); and Kohn and Strang (1986).

To formulate the relaxed problem one can introduce the set $G_f U$ representing the set of all possible effective conductivity tensors associated with composites of phase 1 and phase 2, with phase 1 occupying the volume fraction f. Specifically, $\boldsymbol{\sigma}_*$ lies in the set $G_f U$ if and only if there exists a composite of phases 1 and 2 mixed in proportions f and $1-f$ that has $\boldsymbol{\sigma}_*$ as its effective tensor. To compute the set $G_f U$ (or, more generally, to compute any G-closure) it suffices to consider periodic composites; proofs of this are given by Raitums (2001) and Allaire (2001). (There are also references in the literature to a theorem of Kohn and Dal-Maso, but unfortunately their work was never published.) This set $G_f U$ is called the G-closure at a constant volume fraction of the set $U = \{\sigma_1 \boldsymbol{I},\ \sigma_2 \boldsymbol{I}\}$ representing the conductivity tensors of the initial component materials. In terms of the set $G_f U$, the admissible temperature fields $T(\boldsymbol{x})$ are those for which there exists a pair of fields $\boldsymbol{\sigma}_*(\boldsymbol{x})$ and $f(\boldsymbol{x})$, with $1 \geq f(\boldsymbol{x}) \geq 0$, such that

$$\begin{aligned} &\boldsymbol{\sigma}_*(\boldsymbol{x}) \in G_{f(\boldsymbol{x})} U, \quad \text{and} \quad -\nabla \cdot \boldsymbol{\sigma}_* \nabla T = h \ \text{ for all } \boldsymbol{x} \in \Theta, \\ &T(\boldsymbol{x}) = T_0 \ \text{ for } \boldsymbol{x} \in \partial\Theta, \qquad \langle f \rangle_\Theta = p. \end{aligned}$$

In fact, the set $G_f U$ contains more information than is needed to solve this problem. Since $\boldsymbol{\sigma}_*$ appears only in the combination $-\boldsymbol{\sigma}_* \nabla T$, all we need to know, for each value of a vector $\boldsymbol{e}_0$, is the set $G_f U \boldsymbol{e}_0$ comprised of all vectors $\boldsymbol{q}_0$ such that $\boldsymbol{q}_0 = \boldsymbol{\sigma}_* \boldsymbol{e}_0$ for some $\boldsymbol{\sigma}_* \in G_f U$ (Raĭtum 1978; Tartar 1995). Equivalently, $\boldsymbol{q}_0$ lies in $G_f U \boldsymbol{e}_0$ if and only if there exists a periodic composite of phases 1 and 2 mixed in proportions f and $1-f$, such that the average heat flux is $\boldsymbol{q}_0$ when no heat sources are present and the temperature gradient is periodic with average $-\boldsymbol{e}_0$. Thus knowledge of all possible (average flux, average temperature gradient, volume fraction) triplets associated with composites of phases 1 and 2 provides a characterization of $G_f U \boldsymbol{e}_0$ for all f and all $\boldsymbol{e}_0$, and vice versa. The set $G_f U \boldsymbol{e}_0$ can be regarded as a projection of the set $G_f U$.

Due to rotational invariance and linearity it follows that if $\boldsymbol{q}_0 \in G_f U \boldsymbol{e}_0$, then

$$\begin{aligned} &\boldsymbol{q}_0' \in G_f U \boldsymbol{e}_0' \ \text{ for } \ \boldsymbol{q}_0' = \lambda \boldsymbol{q}_0 \ \text{ and } \ \boldsymbol{e}_0' = \lambda \boldsymbol{e}_0, \\ &\boldsymbol{q}_0'' \in G_f U \boldsymbol{e}_0'' \ \text{ for } \ \boldsymbol{q}_0'' = \boldsymbol{R} \boldsymbol{q}_0 \ \text{ and } \ \boldsymbol{e}_0'' = \boldsymbol{R} \boldsymbol{e}_0, \end{aligned}$$

for all constants λ and all rotation matrices $\boldsymbol{R}$. Thus it suffices to determine the set $G_f U \boldsymbol{e}_0$ for one value of $\boldsymbol{e}_0$. Whether $\boldsymbol{q}_0$ lies in $G_f U \boldsymbol{e}_0$ is then governed by the values that the three invariants $\boldsymbol{q}_0 \cdot \boldsymbol{e}_0 / |\boldsymbol{e}_0|^2$, $|\boldsymbol{q}_0|^2 / |\boldsymbol{e}_0|^2$, and f take.

In terms of these sets $G_f U \boldsymbol{e}_0$, the admissible temperature fields are those for which there exists a heat flux $\boldsymbol{q}_0(\boldsymbol{x})$ and volume fraction distribution $f(\boldsymbol{x})$, with $1 \geq f(\boldsymbol{x}) \geq 0$, such that

$$\boldsymbol{q}_0(\boldsymbol{x}) \in G_{f(\boldsymbol{x})}U\boldsymbol{e}_0(\boldsymbol{x}), \quad \boldsymbol{e}_0 = -\nabla T \text{ and } \nabla \cdot \boldsymbol{q} = h, \quad \text{for all } \boldsymbol{x} \in \Theta,$$
$$T(\boldsymbol{x}) = T_0 \text{ for } \boldsymbol{x} \in \partial\Theta, \quad \langle f \rangle_\Theta = p.$$

In the relaxed formulation the problem can be solved analytically (Murat and Tartar 1985; Tartar 1987). As one might expect, the volume fraction distribution $f_1(\boldsymbol{x})$ and the minimizing temperature field $T(\boldsymbol{x})$ in the relaxed problem turn out to be radially symmetric, with

$$\begin{aligned} f_1(r) &= 0 && \text{for } 2\sigma_2 c \geq r \geq 0 \\ &= (r/2c - \sigma_2)/(\sigma_1 - \sigma_2) && \text{for } \min\{R, 2\sigma_1 c\} \geq r \geq 2\sigma_2 c \\ &= 1 && \text{for } R \geq r \geq \min\{R, 2\sigma_1 c\}, \end{aligned}$$

and

$$\begin{aligned} dT/dr &= -r/2\sigma_2 && \text{for } 2\sigma_2 c \geq r \geq 0 \\ &= -c && \text{for } \min\{R, 2\sigma_1 c\} \geq r \geq 2\sigma_2 c \\ &= -r/2\sigma_1 && \text{for } R \geq r \geq \min\{R, 2\sigma_1 c\}, \end{aligned}$$

where $r = |\boldsymbol{x}|$ and the positive constant c is determined by the constraint that $\langle f_1 \rangle_\Theta = p$. Thus the core of the sphere is filled with the poor conductor. This is surrounded by an annular zone where we have a layered mixture of both materials where the proportion f_1 of the good conductor is a linear function of r. This annular zone may extend out to the radius R when the total proportion p of the good conductor is small, that is, provided $R \leq 2\sigma_1 c$; otherwise, it is surrounded by a region filled with the good conductor. When the heat is not produced uniformly within the sphere, or when the sphere is replaced by a body with a different shape, an analytic solution is no longer generally possible and one must solve the relaxed problem numerically.

A related problem is the "heat lens" problem of Gibiansky, Lurie, and Cherkaev (1988), where the two phases in the body are distributed to maximize (or minimize) the heat flow through a "window" at the boundary of the object. The optimal design has regions occupied by the pure phases and regions occupied by layered mixtures of both phases, which serve to channel the heat toward (or away from) the window. Knowledge of the sets $G_f U\boldsymbol{e}_0$ allows one to solve this problem.

Another closely related optimization problem is to maximize the torsional rigidity of a bar made of two materials with given volume fractions. This has been considered by Lurie, Cherkaev, and Fedorov (1982a, 1982b); Goodman, Kohn, and Reyna (1986); and Kawohl, Stara, and Wittum (1991). There are regions in the cross section of the bar that are occupied by the pure phases and regions occupied by layered mixtures of both phases.

Composites also appear in elastic plate optimization problems (Cheng and Olhoff 1981; Lurie, Cherkaev, and Fedorov (1982a, 1982b); Gibiansky and Cherkaev 1984) and in two- and three-dimensional elasticity problems involving the minimization of the total elastic or compliance energy under single loading or multiple loading conditions (Diaz and Bendsøe 1992; Allaire and Kohn (1993a, 1993b); Allaire and Francfort 1993; Jog, Haber, and Bendsøe 1994; Cherkaev and Palais 1995; Allaire, Bonnetier, Francfort, and Jouve 1997; Cherkaev, Krog, and Küçük 1998). In general, the relaxed problem has to be solved numerically. Grabovsky (1996) gives examples where it can be solved analytically.

Often it is not possible to formulate the relaxed problem because we do not yet know the range of composite behavior, for example, we do not yet have a complete characterization of the appropriate set such as GU, $G_f U$ or $G_f U\boldsymbol{E}_0$. Also, not all composites are easy to

manufacture. Therefore, from an engineering perspective it makes sense to try to restrict the type of composite microstructure in a design. Such partial relaxations were considered by Rozvany, Olhoff, Cheng, and Taylor (1982); Rozvany, Ong, Szeto, Sandler, Olhoff, and Bendsøe (1987); Bendsøe and Kikuchi (1988, 1989); and Suzuki and Kikuchi (1991), among others.

References

Allaire, G. 2001. *Shape Optimization by the Homogenization Method*. Berlin / Heidelberg / London / etc.: Springer-Verlag. 464 pp. ISBN 0-387-95298-5. {*xxv, xxvi, 426, 431, 433*}

Allaire, G., E. Bonnetier, G. A. Francfort, and F. Jouve 1997. Shape optimization by the homogenization method. *Numerische Mathematik* 76(1):27–68. {*432, 433*}

Allaire, G. and G. A. Francfort 1993. A numerical algorithm for topology and shape optimization. In M. P. Bendsøe and C. A. M. Soares (eds.), *Proceedings of the NATO Advanced Research Workshop on Topology Design of Structures, Sesimbra, Portugal, June 20–June 26, 1992*, pp. 239–248. Norwell, Massachusetts / Dordrecht, The Netherlands: Kluwer Academic Publishers Group. ISBN 0-7923-2055-7. {*432, 433*}

Allaire, G. and R. V. Kohn 1993a. Optimal design for minimum weight and compliance in plane stress using extremal microstructures. *European Journal of Mechanics, A, Solids.* 12(6):839–878. {*432, 433*}

Allaire, G. and R. V. Kohn 1993b. Topology optimization and optimal shape design using homogenization. In M. P. Bendsøe and C. A. M. Soares (eds.), *Topology Design of Structures*, pp. 207–218. Norwell, Massachusetts / Dordrecht, The Netherlands: Kluwer Academic Publishers Group. ISBN 0-7923-2055-7. {*432, 433*}

Armand, J.-L., K. A. Lurie, and A. V. Cherkaev 1984. Optimal control theory and structural design. In E. Atrek, R. H. Gallagher, K. M. Ragsdell, and O. C. Zienkiewicz (eds.), *New Directions in Optimum Structural Design*, pp. 211–229. New York / London / Sydney, Australia: John Wiley and Sons. {*426, 433*}

Bendsøe, M. P. 1995. *Optimization of Structural Topology, Shape, and Material*. Berlin / Heidelberg / London / etc.: Springer-Verlag. xi + 271 pp. ISBN 3-540-59057-9 (Berlin), 0-387-59057-9 (New York). {*426, 433*}

Bendsøe, M. P. 1997. Structural optimization of and with advanced materials. In T. Tatsumi, E. Watanabe, and T. Kambe (eds.), *Theoretical and Applied Mechanics 1996: Proceedings of the XIXth International Congress of Theoretical and Applied Mechanics, Kyoto, Japan, 25–31 August 1996*, pp. 269–284. Amsterdam: Elsevier. ISBN 0-444-82446-4. {*426, 433*}

Bendsøe, M. P. and N. Kikuchi 1988. Generating optimal topologies in structural design using a homogenization method. *Computer Methods in Applied Mechanics and Engineering* 71(2):197–224. {*433*}

Bendsøe, M. P. and N. Kikuchi 1989. Optimal shape design as a material distribution problem. *Structural Optimization* 1:193–202. {*433*}

Berlyand, L. and V. Mityushev 2001. Generalized clausius-mossotti formula for random composite with circular fibers. *Journal of Statistical Physics* 102(1/2):115–145. {*429, 433*}

Cheng, K.-T. and N. Olhoff 1981. An investigation concerning optimal design of solid elastic plates. *International Journal of Solids and Structures* 17(3):305–323. {*431, 432, 434*}

Cherkaev, A. V. 1999. Variational approach to structural optimization. In C. T. Leondes (ed.), *Structural Dynamical Systems, Computational Techniques, and Optimization. Optimization Techniques*, pp. 199–236. Langhorne, Pennsylvania: Gordon and Breach. ISBN 90-5699-644-4. {*426, 434*}

Cherkaev, A. V. 2000. *Variational Methods for Structural Optimization*. Berlin / Heidelberg / London / etc.: Springer-Verlag. xxvi + 545 pp. ISBN 0-387-98462-3. {*xxv, xxvi, 352, 353, 426, 434, 666, 668*}

Cherkaev, A. V., L. A. Krog, and İ. Küçük 1998. Stable optimal design of two-dimensional elastic structures. *Control and Cybernetics* 27(2):265–282. {*432, 434, 468, 491*}

Cherkaev, A. V. and R. Palais 1995. Optimal design of three-dimensional elastic structures. In N. Olhoff and G. Rozvany (eds.), *Proceedings of the First World Congress of Structural and Multidisciplinary Optimization: 28 May–2 June 1995, Goslar, Germany: WCSMO-1*, pp. 201–206. New York: Pergamon. ISBN 0-08-042267-5. {*432, 434*}

Diaz, A. and M. P. Bendsøe 1992, March. Shape optimization of structures for multiple loading conditions using a homogenization method. *Structural Optimization* 4(1):17–22. {*432, 434*}

Gibiansky, L. V. and A. V. Cherkaev 1984. Design of composite plates of extremal rigidity. Technical Report 914, Ioffe Physicotechnical Institute, Leningrad, USSR. 1–60 pp. English translation in *Topics in the Mathematical Modelling of Composite Materials*, pp. 95–137, ed. by A. Cherkaev and R. Kohn. ISBN 0-8176-3662-5. {*432, 434, 466, 492, 501, 525, 529, 550*}

Gibiansky, L. V., K. A. Lurie, and A. V. Cherkaev 1988. Optimum focusing of a heat flux by a nonuniform heat-conducting medium (the "heat lens" problem). *Zhurnal tekhnicheskoi fiziki* 58:67–74. English translation in *Sov. Phys. Tech. Phys.* 33:38–42 (1988). {*432, 434, 444, 453*}

Goodman, J., R. V. Kohn, and L. Reyna 1986. Numerical study of a relaxed variational problem from optimal design. *Computer Methods in Applied Mechanics and Engineering* 57(1):107–127. {*432, 434*}

Grabovsky, Y. 1996. Explicit solution of an optimal design problem with non-affine displacement boundary conditions. *Proceedings of the Royal Society of London. Series A, Mathematical and Physical Sciences* 452(1947):909–918. {*432, 434*}

Jog, C. S., R. B. Haber, and M. P. Bendsøe 1994. Topology design with optimized, self-adaptive materials. *International Journal for Numerical Methods in Engineering* 37(8): 1323–1350. {*432, 434*}

Kalamkarov, A. L. and A. G. Kolpakov 1997. *Analysis, Design and Optimization of Composite Structures*. New York / London / Sydney, Australia: John Wiley and Sons. x + 356 pp. ISBN 0-471-97189-8. {*426, 434*}

Kawohl, B., J. Stara, and G. Wittum 1991. Analysis and numerical studies of a problem of shape design. *Archive for Rational Mechanics and Analysis* 114(4):349–363. {*432, 434*}

Kohn, R. V. 1992. Numerical structural optimization via a relaxed formulation. In M. C. Delfour and G. Sabidussi (eds.), *Shape Optimization and Free Boundaries: Proceedings of the NATO Advanced Study Institute and Séminaire de Mathématiques Supérieures on Shape Optimization and Free Boundaries, Montréal, Canada, June 25–July 13, 1990*, pp. 173–210. Norwell, Massachusetts / Dordrecht, The Netherlands: Kluwer Academic Publishers Group. ISBN 0-7923-1944-3. {*426, 435*}

Kohn, R. V. and G. Strang 1986. Optimum Design and Relaxation of Variational Problems, I, II, and III. *Communications on Pure and Applied Mathematics (New York)* 39:113–377. {*426, 431, 435, 680, 697*}

Lurie, K. A. and A. V. Cherkaev 1981. *G*-closure of a set of anisotropic conducting media in the case of two-dimensions. *Doklady Akademii Nauk SSSR* 259:328–331. English translation in *Soviet Phys. Dokl.* 26:657–659 (1981). {*428, 429, 435, 447, 453, 521, 526*}

Lurie, K. A. and A. V. Cherkaev 1984. *G*-closure of a set of anisotropically conducting media in the two-dimensional case. *Journal of Optimization Theory and Applications* 42(2):283–304. {*428, 435, 447, 454, 521, 526*}

Lurie, K. A., A. V. Cherkaev, and A. V. Fedorov 1982a. Regularization of optimal design problems for bars and plates, part I. *Journal of Optimization Theory and Applications* 37(4):499–522. {*431, 432, 435*}

Lurie, K. A., A. V. Cherkaev, and A. V. Fedorov 1982b. Regularization of optimal design problems for bars and plates, part II. *Journal of Optimization Theory and Applications* 37(4):523–543. {*175, 182, 431, 432, 435*}

Murat, F. and L. Tartar 1985. Calcul des variations et homogénéisation (French) [Calculus of variation and homogenization]. In *Les méthodes de l'homogénéisation: théorie et applications en physique*, pp. 319–369. Paris: Eyrolles. English translation in *Topics in the Mathematical Modelling of Composite Materials*, pp. 139–173, ed. by A. Cherkaev and R. Kohn, ISBN 0-8176-3662-5. {*12, 13, 17, 347, 353, 429, 431, 432, 435, 444, 454, 462, 495, 499, 503, 506, 508, 521, 527, 529, 551*}

Raĭtum, U. Ë. 1978. The extension of extremal problems connected with a linear elliptic equation. *Doklady Akademii Nauk SSSR* 243(2):281–283. English translation in *Soviet Math. Dokl.* 19(6):1342–1345 (1978). {*431, 435, 447, 454, 521, 527*}

Raitums, U. E. 2001. On the local representation of *G*-closure. *Archive for Rational Mechanics and Analysis* 158(3):213–234. {*431, 435*}

Rozvany, G., N. Olhoff, K. T. Cheng, and J. E. Taylor 1982. On the solid plate paradox in structural optimization. *Journal of Structural Mechanics* 10(1):1–32. {*433, 435*}

Rozvany, G., T. Ong, W. Szeto, R. Sandler, N. Olhoff, and M. P. Bendsøe 1987. Least weight design of perforated plates I, II. *International Journal of Solids and Structures* 23:521–536. {*433, 435*}

Suzuki, K. and N. Kikuchi 1991. Shape and layout optimization using the homogenization method. *Computer Methods in Applied Mechanics and Engineering* 93:291–318. {*433, 435*}

Tartar, L. 1975. Problèmes de contrôle des coefficients dans des équations aux dérivées partielles. In A. Bensoussan and J.-L. Lions (eds.), *Control Theory, Numerical Methods and Computer Systems Modelling (Proceedings IRIA 1974)*, pp. 420–426. Berlin /

Heidelberg / London / etc.: Springer-Verlag. English translation in *Topics in the Mathematical Modelling of Composite Materials*, pp. 1–8, ed. by A. Cherkaev and R. Kohn. ISBN 0-8176-3662-5. {*426, 429, 431, 435, 447, 454, 521, 527*}

Tartar, L. 1987. The appearance of oscillations in optimization problems. In R. J. Knops and A. A. Lacey (eds.), *Non-Classical Continuum Mechanics: Proceedings of the London Mathematical Society Symposium, Durham, July 1986*, pp. 129–150. Cambridge, United Kingdom: Cambridge University Press. ISBN 0-521-34935-4. {*429, 432, 436, 444, 455*}

Tartar, L. 1995. Remarks on the homogenization method in optimal design methods. In *Proceedings of the International Conference: Homogenization and Applications to Material Sciences: Held in Nice, June 6–10, 1995*, pp. 393–412. Tokyo: Gakkōtosho. ISBN 4-7625-0418-1. {*431, 436, 444, 445, 455*}

Tartar, L. 2000. An introduction to the homogenization method in optimal design. In A. Cellina and A. Ornelas (eds.), *Optimal shape design. Lectures given at the Joint C.I.M./C.I.M.E. Summer School Held in Tróia, June 1–6, 1998*, pp. 47–156. Berlin / Heidelberg / London / etc.: Springer-Verlag. ISBN 3-540-67971-5. {*164, 177, 183, 426, 436*}

Torquato, S. 1991. Random heterogeneous media: Microstructure and improved bounds on effective properties. *ASME Applied Mechanics Reviews* 44(2):37–76. {*xxv, xxviii, 331, 339, 425, 436, 553, 567*}

Yeong, C. L. Y. and S. Torquato 1998. Reconstructing random media. II. Three-dimensional media from two-dimensional cuts. *Physical Review E (Statistical Physics, Plasmas, Fluids, and Related Interdisciplinary Topics)* 58(1):224–233. {*425, 436*}

22

Classical variational principle bounds

In section 13.1 on page 271 we saw how the substitution of constant fields into the classical variational principles gave rise to the arithmetic and harmonic mean bounds,

$$\langle \boldsymbol{L}^{-1} \rangle^{-1} \leq \boldsymbol{L}_* \leq \langle \boldsymbol{L} \rangle,$$

on the effective tensor $\boldsymbol{L}_*$. These elementary bounds hold when $\boldsymbol{L}(\boldsymbol{x})$ is symmetric and positive-definite for all $\boldsymbol{x}$. Besides being easy to calculate, they are sometimes attained. For example, from the classical variational principle it follows that the upper bound is attained when the actual field $\boldsymbol{E}(\boldsymbol{x})$ coincides with the trial field, that is, when $\boldsymbol{E}(\boldsymbol{x}) = \boldsymbol{E}_0$. What is interesting is that this condition can sometimes be fulfilled in a variety of nontrivial microstructures. Briefly, $\boldsymbol{L}(\boldsymbol{x})$ must satisfy the differential constraint that $\boldsymbol{L}\boldsymbol{E}_0 \in \mathcal{U} \oplus \mathcal{J}$.

22.1. Multiphase conducting composites attaining energy bounds

Let us consider a multiphase composite comprised of n isotropic phases with real conductivities

$$\sigma_1 > \sigma_2 > \sigma_3 > \ldots \sigma_n.$$

The arithmetic and harmonic mean bounds on the effective conductivity tensor $\boldsymbol{\sigma}_*$ imply that for any given applied field $\boldsymbol{e}_0$ the energy $W = \boldsymbol{e}_0 \cdot \boldsymbol{\sigma}_* \boldsymbol{e}_0/2$ (representing the electrical power dissipation) satisfies the inequality

$$(\sum_{i=1}^{n} f_i/\sigma_i)^{-1} \boldsymbol{e}_0 \cdot \boldsymbol{e}_0/2 \leq W \leq (\sum_{i=1}^{n} f_i \sigma_i) \boldsymbol{e}_0 \cdot \boldsymbol{e}_0/2, \tag{22.1}$$

where the f_i, $i = 1, 2, \ldots, n$ are the volume fractions of the phases. Clearly the lower bound is attained (in two or three dimensions) when the composite is a laminate of the n-phases oriented so that the direction $\boldsymbol{n}$ of lamination is parallel to $\boldsymbol{e}_0$. The upper bound is attained when the microgeometry does not vary along lines parallel to $\boldsymbol{e}_0$. In particular, it is attained by laminate materials with $\boldsymbol{n}$ perpendicular to $\boldsymbol{e}_0$, and it is attained by microstructures consisting of cylinders of the first $n-1$ phases oriented with their cylinder axes directed parallel to $\boldsymbol{e}_0$ and embedded in the remaining phase.

Curiously, these are not the only microgeometries that attain the energy bounds when more than two phases are present. Cherkaev and Gibiansky (1993) found that there are many more. For example, consider two-dimensional, three-phase composites. Let us try to construct

a different type of microgeometry that attains the upper bound on the energy. First note that since σ_2 lies between σ_1 and σ_3, there exists a positive weight $p < 1$ such that

$$\sigma_2 = p\sigma_1 + (1-p)\sigma_3, \quad p = (\sigma_2 - \sigma_3)/(\sigma_1 - \sigma_3).$$

Accordingly, a laminate of materials 1 and 3 mixed in volume fractions p and $1-p$, oriented with its lamination direction parallel to the x_2-axis, has effective conductivity tensor

$$\begin{pmatrix} p\sigma_1 + (1-p)\sigma_3 & 0 \\ 0 & [p/\sigma_1 + (1-p)/\sigma_3]^{-1} \end{pmatrix} = \begin{pmatrix} \sigma_2 & 0 \\ 0 & \sigma_1\sigma_3/(\sigma_1 + \sigma_3 - \sigma_2) \end{pmatrix}.$$

If we next laminate this composite together with phase 2 in proportions q and $1-q$ with the lamination direction now parallel to the x_1-axis, the resulting mixture has conductivity tensor

$$\boldsymbol{\sigma}_* = \begin{pmatrix} \sigma_2 & 0 \\ 0 & q\sigma_1\sigma_3/(\sigma_1 + \sigma_3 - \sigma_2) + (1-q)\sigma_2 \end{pmatrix}.$$

Consequently, when $\boldsymbol{e}_0$ is aligned parallel to the x_1-axis the energy

$$W = \boldsymbol{e}_0 \cdot \boldsymbol{\sigma}_* \boldsymbol{e}_0/2 = \sigma_2 \boldsymbol{e}_0 \cdot \boldsymbol{e}_0/2 = [qp\sigma_1 + (1-q)\sigma_2 + q(1-p)\sigma_3]\boldsymbol{e}_0 \cdot \boldsymbol{e}_0/2$$

attains the upper bound in (22.1). Here qp, $1-q$, and $q(1-p)$ can be identified with the volume fractions of the three phases. The discontinuity in microstructure in the x_1 direction does not matter because the effective conductivity of the laminate of materials 1 and 3 in the direction x_1 has been matched with the conductivity of phase 2. Of course this material is rather special because the ratio $p/(1-p)$ of the volume fraction of phase 1 to the volume fraction of phase 3 takes the particular value

$$qp/q(1-p) = p/(1-p) = (\sigma_2 - \sigma_3)/(\sigma_1 - \sigma_2).$$

However, we are free to take this material and laminate it together with slices of the three phases, with this final lamination direction being parallel to the x_2-axis. The resulting material will again attain the upper energy bound, but will have no special relations amongst the volume fractions of the phases.

A similar procedure can be followed to obtain nontrivial microgeometries attaining the lower bound in (22.1). One first laminates phases 1 and 3 in the direction of the x_2-axis in proportions p' and $1-p'$, where p' is chosen so that $1/(p'/\sigma_1 + (1-p')/\sigma_3) = \sigma_2$. Then one laminates this composite with phase 2 in the direction of the x_1-axis, and finally one laminates the resulting material with phases 1, 2, and 3 in the direction of the x_2-axis. A simple calculation shows that the lower bound on the energy is attained when $\boldsymbol{e}_0$ is aligned parallel to the x_2-axis.

There are countless other microgeometries that also attain these bounds. For example, at the second step, instead of laminating σ_2 with the mixture of σ_1 and σ_3, one could combine these two materials in any configuration. Alternatively, one could combine two laminates, each laminated in direction x_1 and assembled from the three phases in proportions chosen so that the effective conductivity tensors of the two laminates have a common diagonal element.

As we will see in the next section, this idea of Schulgasser (1977), of combining laminates that have some common effective properties, allows one to construct three-dimensional isotropic polycrystals with maximal conductivity or with minimal or maximal bulk modulus.

22.2. Optimal bounds on the conductivity of isotropic polycrystals

In a three-dimensional polycrystal the local conductivity tensor field takes the form

$$\boldsymbol{\sigma}(\boldsymbol{x}) = \boldsymbol{R}(\boldsymbol{x})\boldsymbol{\sigma}_0\boldsymbol{R}^T(\boldsymbol{x}), \quad \text{where } \boldsymbol{\sigma}_0 = \begin{pmatrix} \lambda_1 & 0 & 0 \\ 0 & \lambda_2 & 0 \\ 0 & 0 & \lambda_3 \end{pmatrix},$$

and the arithmetic and harmonic mean bounds imply that

$$\boldsymbol{\sigma}_* \le \langle \boldsymbol{\sigma} \rangle, \quad \boldsymbol{\sigma}_*^{-1} \le \langle \boldsymbol{\sigma}^{-1} \rangle.$$

For simplicity, let us suppose that the conductivity tensor $\boldsymbol{\sigma}_*$ of the composite is isotropic, so that $\boldsymbol{\sigma}_* = \sigma_* \boldsymbol{I}$. Then by taking the trace of the above bounds we see that

$$\frac{3}{1/\lambda_1 + 1/\lambda_2 + 1/\lambda_3} \le \sigma_* \le \frac{\lambda_1 + \lambda_2 + \lambda_3}{3}. \tag{22.2}$$

The lower bound is not optimal. In section 24.8 on page 510 we will see how to derive a better bound. By contrast, the upper bound is the best that one can do without incorporating additional information about the composite geometry. Schulgasser (1977) found that the upper bound is achieved by a rank-3 laminate material. Here we show that a rank-2 laminate suffices (Avellaneda, Cherkaev, Lurie, and Milton 1988).

Schulgasser's key observation is that the effective conductivity tensor of a simple laminate of two crystals is sometimes just a linear average of the crystal conductivity tensors. Specifically, suppose that the crystals have conductivities

$$\boldsymbol{\sigma}_0 = \begin{pmatrix} \lambda_1 & 0 & 0 \\ 0 & \lambda_2 & 0 \\ 0 & 0 & \lambda_3 \end{pmatrix} \quad \text{and} \quad \boldsymbol{\sigma}_0' = \begin{pmatrix} \lambda_1' & 0 & 0 \\ 0 & \lambda_2' & 0 \\ 0 & 0 & \lambda_3' \end{pmatrix},$$

and that they are laminated in proportions f and $f' = 1 - f$ with the direction of lamination $\boldsymbol{n}$ parallel to the x_1-axis. In the special case when $\lambda_1' = \lambda_1$, the effective conductivity tensor of the laminate can be identified with the arithmetic average of the conductivity tensors of the crystals:

$$\begin{aligned} \boldsymbol{\sigma}_* &= \begin{pmatrix} 1/(f/\lambda_1 + f'/\lambda_1') & 0 & 0 \\ 0 & f\lambda_2 + f'\lambda_2' & 0 \\ 0 & 0 & f\lambda_3 + f'\lambda_3' \end{pmatrix} \\ &= \begin{pmatrix} \lambda_1 & 0 & 0 \\ 0 & f\lambda_2 + f'\lambda_2' & 0 \\ 0 & 0 & f\lambda_3 + f'\lambda_3' \end{pmatrix} = f\boldsymbol{\sigma}_0 + f'\boldsymbol{\sigma}_0'. \end{aligned}$$

The physical explanation is that the electric field $\boldsymbol{e}(\boldsymbol{x})$ is constant irrespective of the direction of the applied field $\boldsymbol{e}_0 = \langle \boldsymbol{e} \rangle$.

So by laminating the pure crystal with conductivity tensor $\boldsymbol{\sigma}_0 = \text{Diag}[\lambda_1,\ \lambda_2,\ \lambda_3]$ with a rotation of itself with conductivity tensor $\boldsymbol{\sigma}_0' = \text{Diag}[\lambda_1,\ \lambda_3,\ \lambda_2]$ we obtain a simple laminate with effective conductivity

$$\boldsymbol{\sigma}_1 = f\boldsymbol{\sigma}_0 + f'\boldsymbol{\sigma}_0' = \begin{pmatrix} \lambda_1 & 0 & 0 \\ 0 & f\lambda_2 + f'\lambda_3 & 0 \\ 0 & 0 & f\lambda_3 + f'\lambda_2 \end{pmatrix}.$$

The volume fraction $f = 1 - f'$ can be chosen so that the principal conductivity $f\lambda_3 + f'\lambda_2$ equals the desired arithmetic average $(\lambda_1 + \lambda_2 + \lambda_3)/3$. This value of f, namely,

$$f = \frac{\lambda_1 + \lambda_3 - 2\lambda_2}{3(\lambda_3 - \lambda_2)},$$

lies between 0 and 1, if we assume, without loss of generality, that the principal axes have been labeled so that $\lambda_3 \geq \lambda_1 \geq \lambda_2$. The laminate is less anisotropic than the original crystal, and the trace of its conductivity tensor is the same as in the original crystal. This simple laminate is then laminated in the x_3 direction with an equal proportion of a rotation of itself with conductivity tensor

$$\boldsymbol{\sigma}_1' = \begin{pmatrix} f\lambda_2 + f'\lambda_3 & 0 & 0 \\ 0 & \lambda_1 & 0 \\ 0 & 0 & f\lambda_3 + f'\lambda_2 \end{pmatrix}.$$

The resulting rank-2 laminate, illustrated in figure 22.1 on the next page, will have an isotropic effective conductivity tensor

$$\boldsymbol{\sigma}_* = (\boldsymbol{\sigma}_1 + \boldsymbol{\sigma}_1')/2 = (\lambda_1 + \lambda_2 + \lambda_3)\boldsymbol{I}/3.$$

In this construction the geometry of the composite is dependent on λ_1, λ_2, and λ_3. In other words, if we change the values of the principal conductivities, then the geometry must also be modified to maintain the isotropy of the effective tensor $\boldsymbol{\sigma}_*$. More significantly, the construction fails when λ_1, λ_2, and λ_3 are complex. At the cost of introducing another stage of lamination one can construct a laminate material that achieves the upper bound (22.2) for all combinations of λ_1, λ_2, and λ_3. To do this we follow Schulgasser (1977) and repeat the first stage of the above construction, now setting $f = 1/2$ to produce a rank-1 laminate with effective tensor

$$\boldsymbol{\sigma}_1 = \begin{pmatrix} \lambda_1 & 0 & 0 \\ 0 & (\lambda_2 + \lambda_3)/2 & 0 \\ 0 & 0 & (\lambda_2 + \lambda_3)/2 \end{pmatrix}.$$

We then take this laminate and a rotation of itself with conductivity tensor

$$\boldsymbol{\sigma}_1' = \begin{pmatrix} (\lambda_2 + \lambda_3)/2 & 0 & 0 \\ 0 & \lambda_1 & 0 \\ 0 & 0 & (\lambda_2 + \lambda_3)/2 \end{pmatrix}$$

and laminate them together in the x_3 direction in proportions $1/3$ and $2/3$ to obtain a rank-2 laminate with conductivity tensor

$$\boldsymbol{\sigma}_2 = (\boldsymbol{\sigma}_1 + 2\boldsymbol{\sigma}_1')/3 = \begin{pmatrix} (\lambda_1 + \lambda_2 + \lambda_3)/3 & 0 & 0 \\ 0 & (4\lambda_1 + \lambda_2 + \lambda_3)/6 & 0 \\ 0 & 0 & (\lambda_2 + \lambda_3)/2 \end{pmatrix}.$$

At the final stage we take this rank-2 laminate and a rotation of itself with conductivity tensor

$$\boldsymbol{\sigma}_2' = \begin{pmatrix} (\lambda_1 + \lambda_2 + \lambda_3)/3 & 0 & 0 \\ 0 & (\lambda_2 + \lambda_3)/2 & 0 \\ 0 & 0 & (4\lambda_1 + \lambda_2 + \lambda_3)/6 \end{pmatrix}$$

and we laminate them in equal proportions to obtain a material with effective conductivity tensor

$$\boldsymbol{\sigma}_* = (\boldsymbol{\sigma}_2 + \boldsymbol{\sigma}_2')/2 = (\lambda_1 + \lambda_2 + \lambda_3)\boldsymbol{I}/3.$$

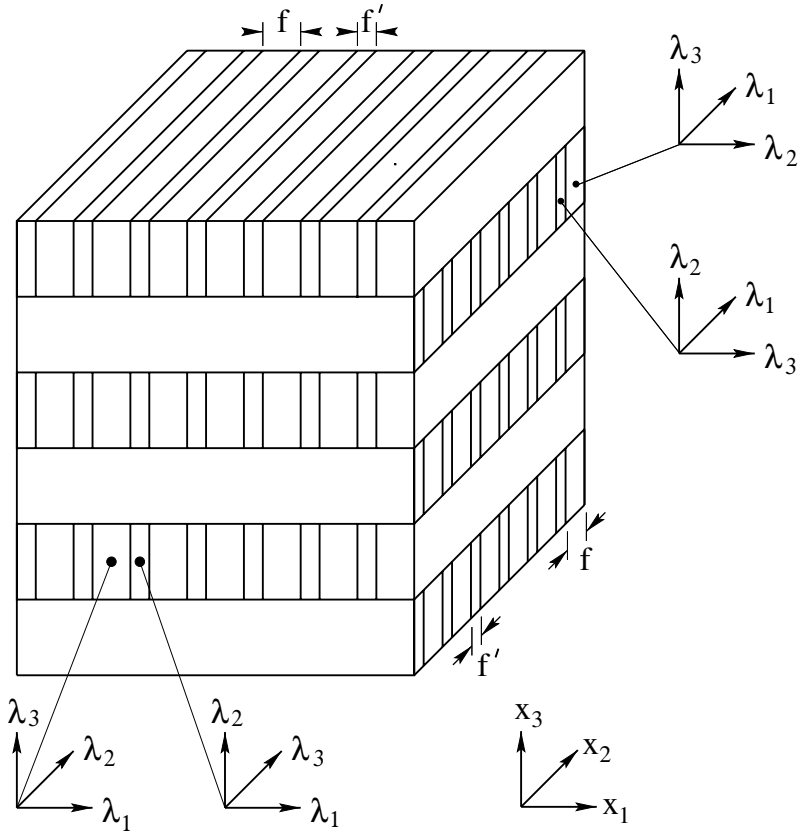

Figure 22.1. A second-rank laminate polycrystal that has the largest effective conductivity amongst all isotropic conducting polycrystals. The volume fractions f and $f' = 1 - f$ are chosen so that the conductivity in the x_3 direction is the arithmetic average $(\lambda_1 + \lambda_2 + \lambda_3)/3$. The conductivities in the other two directions are then also the arithmetic average. After Avellaneda, Cherkaev, Lurie, and Milton (1988).

22.3. Optimal bounds on the bulk modulus of isotropic polycrystals

Schulgasser's arguments can be extended to the effective bulk modulus of isotropic polycrystals (Avellaneda and Milton 1989; Rudelson 1989). The elasticity tensor $\boldsymbol{\mathcal{C}}(\boldsymbol{x})$ and compliance tensor $\boldsymbol{\mathcal{S}}(\boldsymbol{x}) = \boldsymbol{\mathcal{C}}^{-1}(\boldsymbol{x})$ of a polycrystal take the form

$$\boldsymbol{\mathcal{C}}(\boldsymbol{x}) = \boldsymbol{\mathcal{R}}(\boldsymbol{x})\boldsymbol{\mathcal{C}}_0[\boldsymbol{\mathcal{R}}(\boldsymbol{x})]^T, \quad \boldsymbol{\mathcal{S}}(\boldsymbol{x}) = \boldsymbol{\mathcal{R}}(\boldsymbol{x})\boldsymbol{\mathcal{S}}_0[\boldsymbol{\mathcal{R}}(\boldsymbol{x})]^T,$$

in which $\boldsymbol{\mathcal{C}}_0$ and $\boldsymbol{\mathcal{S}}_0 = \boldsymbol{\mathcal{C}}_0^{-1}$ are the elasticity tensor and compliance tensor of the pure crystal. The arithmetic and harmonic mean bounds now imply the inequalities

$$\langle \boldsymbol{\epsilon} \rangle \cdot \boldsymbol{\mathcal{C}}_* \langle \boldsymbol{\epsilon} \rangle \le \langle \boldsymbol{\epsilon} \rangle \cdot \langle \boldsymbol{\mathcal{C}} \rangle \langle \boldsymbol{\epsilon} \rangle, \quad \langle \boldsymbol{\tau} \rangle \cdot \boldsymbol{\mathcal{S}}_* \langle \boldsymbol{\tau} \rangle \le \langle \boldsymbol{\tau} \rangle \cdot \langle \boldsymbol{\mathcal{S}} \rangle \langle \boldsymbol{\tau} \rangle,$$

which hold for choices of the average strain field $\langle \boldsymbol{\epsilon} \rangle$ and average stress field $\langle \boldsymbol{\tau} \rangle$. In particular, by choosing $\langle \boldsymbol{\epsilon} \rangle = \boldsymbol{I}$ and $\langle \boldsymbol{\tau} \rangle = \boldsymbol{I}$, respectively, we obtain the Voigt-Reuss-Hill bounds on

the effective bulk modulus,

$$\kappa_R \le \kappa_* \le \kappa_V, \quad \text{where } \kappa_V = \{\mathcal{C}_0\}_{iijj}/9, \ \ \kappa_R = 1/\{\mathcal{S}_0\}_{iijj}.$$

These bounds are due to Hill (1952). Voigt (1889, 1910) and Reuss (1929) suggested that κ_V and κ_R might be reasonable approximations for the effective bulk modulus, which is why they are commonly referred to as the Voigt-Reuss bounds.

The key to proving that the Voigt-Hill bound is achievable is to realize that one can sometimes laminate together two crystals with elasticity tensors $\mathcal{C}_0$ and $\mathcal{C}'_0$ so that the effective elasticity tensor $\mathcal{C}_*$ is such that the second-order tensor $\mathcal{C}_*\boldsymbol{I}$ is just a linear average of the tensors $\mathcal{C}_0\boldsymbol{I}$ and $\mathcal{C}'_0\boldsymbol{I}$. Specifically, suppose that the crystals have been oriented so that these stress tensors are diagonal:

$$\mathcal{C}_0\boldsymbol{I} = \begin{pmatrix} \lambda_1 & 0 & 0 \\ 0 & \lambda_2 & 0 \\ 0 & 0 & \lambda_3 \end{pmatrix} \quad \text{and} \quad \mathcal{C}'_0\boldsymbol{I} = \begin{pmatrix} \lambda'_1 & 0 & 0 \\ 0 & \lambda'_2 & 0 \\ 0 & 0 & \lambda'_3 \end{pmatrix},$$

and that they have been laminated in proportions f and $f' = 1 - f$ with their direction of lamination $\boldsymbol{n}$ along the x_1-axis. Under the constraint that $\lambda'_1 = \lambda_1$, the elasticity equations have a solution with a uniform strain $\boldsymbol{e} = \boldsymbol{I}$ and stresses $\mathcal{C}_0\boldsymbol{I}$ and $\mathcal{C}'_0\boldsymbol{I}$ in each crystal phase. The constraint $\lambda'_1 = \lambda_1$ is needed to ensure the compatibility of the stresses across the interfaces between layers, that is, it is needed to ensure that $\boldsymbol{n} \cdot (\mathcal{C}_0\boldsymbol{I}) = \boldsymbol{n} \cdot (\mathcal{C}'_0\boldsymbol{I})$. From the definition of the effective elasticity tensor it follows that the average stress is

$$\mathcal{C}_*\boldsymbol{I} = f\mathcal{C}_0\boldsymbol{I} + f'\mathcal{C}'_0\boldsymbol{I}.$$

The above formulas and the constraint $\lambda'_1 = \lambda_1$ are exactly the same as we encountered in the conductivity problem, only now the role of the effective conductivity tensor $\boldsymbol{\sigma}_*$ is played by the tensor $\mathcal{C}_*\boldsymbol{I}$. So the same laminate constructions used in the conductivity problem also produce rank-2 and rank-3 laminates with effective elasticity tensors $\mathcal{C}_*$ such that $\mathcal{C}_*\boldsymbol{I} = 3\kappa_V\boldsymbol{I}$. The first step in the constructions is to laminate the crystal with a rotation of itself as shown in figure 22.2(a) and then subsequent steps proceed as before. At each stage of lamination it suffices to keep track of $\mathcal{C}_*\boldsymbol{I}$, rather than the full elasticity tensor $\mathcal{C}_*$. The resulting composites, with $\mathcal{C}_*\boldsymbol{I} = 3\kappa_V\boldsymbol{I}$, are not necessarily elastically isotropic, but we see from section 5.2 on page 76 that any elastically isotropic polycrystal produced from them necessarily has effective bulk modulus $\kappa_* = \kappa_V$.

In contrast to the conductivity problem, there exist laminate constructions that achieve the lower bound on the effective bulk modulus. The key to proving that the Reuss-Hill bound is achievable is to realize that one can sometimes laminate together two crystals with compliance tensors $\mathcal{S}_0$ and $\mathcal{S}'_0$ so that the effective compliance tensor $\mathcal{S}_*$ is such that the second-order tensor $\mathcal{S}_*\boldsymbol{I}$ is just a linear average of the tensors $\mathcal{S}_0\boldsymbol{I}$ and $\mathcal{S}'_0\boldsymbol{I}$.

We suppose that the crystals have been oriented so that these strain tensors take the form

$$\mathcal{S}_0\boldsymbol{I} = \begin{pmatrix} e_1\cos^2\theta + e_2\sin^2\theta & (e_1 - e_2)\cos\theta\sin\theta & 0 \\ (e_1 - e_2)\cos\theta\sin\theta & e_1\sin^2\theta + e_2\cos^2\theta & 0 \\ 0 & 0 & e_3 \end{pmatrix},$$

$$\mathcal{S}'_0\boldsymbol{I} = \begin{pmatrix} e'_1\cos^2\theta' + e'_2\sin^2\theta' & (e'_1 - e'_2)\cos\theta'\sin\theta' & 0 \\ (e'_1 - e'_2)\cos\theta'\sin\theta' & e'_1\sin^2\theta' + e'_2\cos^2\theta' & 0 \\ 0 & 0 & e'_3 \end{pmatrix},$$

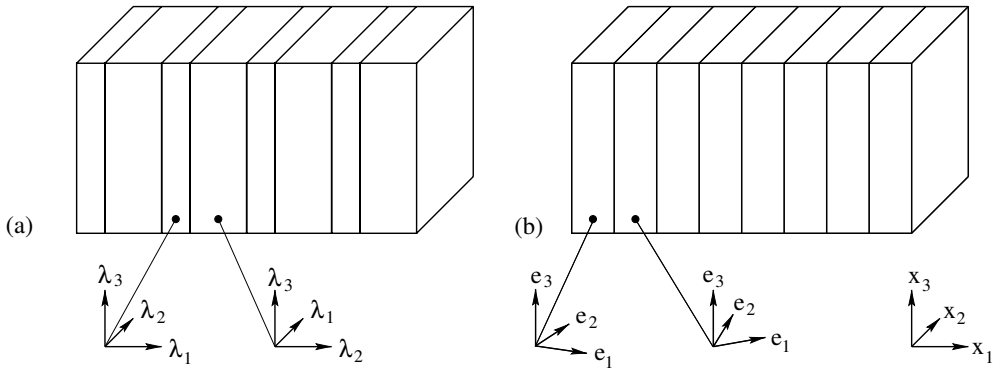

Figure 22.2. When one laminates a crystal with a rotation of itself, one can choose the crystal orientations so that either the strain field is constant and equal to $\boldsymbol{I}$, as in (a), or the stress field is constant and equal to $\boldsymbol{I}$, as in (b). The axes shown in (a) are the eigenvectors of the stress and λ_1, λ_2, and λ_3 are the corresponding eigenvalues. The axes shown in (b) are the eigenvectors of the strain and e_1, e_2, and e_3 are the corresponding eigenvalues. With the exception of the e_3-axis, these are not aligned with the coordinate axes.

in which $e_1,\ e_2,\ e_3$ and $e'_1,\ e'_2,\ e'_3$ are the eigenvalues of $\boldsymbol{\mathcal{S}}_0\boldsymbol{I}$ and $\boldsymbol{\mathcal{S}}'_0\boldsymbol{I}$ while the angles θ and θ' remain to be chosen. We laminate these crystals in proportions f and $f' = 1 - f$ with the direction of lamination $\boldsymbol{n}$ aligned with the x_1-axis. Under the constraints that

$$e_1 \sin^2\theta + e_2 \cos^2\theta = e'_1 \sin^2\theta' + e'_2 \cos^2\theta' \quad \text{and} \quad e_3 = e'_3, \tag{22.3}$$

there exists a solution to the elasticity equations in the laminate with a uniform stress field $\boldsymbol{\tau} = \boldsymbol{I}$ and strains $\boldsymbol{\mathcal{S}}_0\boldsymbol{I}$ and $\boldsymbol{\mathcal{S}}'_0\boldsymbol{I}$ in each phase. The conditions (22.3) are required to ensure that these strains are compatible, that is, to ensure that ϵ_{22}, ϵ_{23}, and ϵ_{33} are constant [see (9.27)]. It follows that the average strain is

$$\boldsymbol{\mathcal{S}}_*\boldsymbol{I} = f\boldsymbol{\mathcal{S}}_0\boldsymbol{I} + f'\boldsymbol{\mathcal{S}}'_0\boldsymbol{I}. \tag{22.4}$$

In particular, as illustrated in figure 22.2(b), when the second crystal is simply a rotation of the first with $e'_1 = e_1$, $e'_2 = e_2$, and $e'_3 = e_3$, we can set

$$\theta' = -\theta, \qquad f = f' = 1/2,$$

to ensure that (22.3) holds and (22.4) then implies that

$$\boldsymbol{\mathcal{S}}_*\boldsymbol{I} = \begin{pmatrix} pe_1 + p'e_2 & 0 & 0 \\ 0 & pe_2 + p'e_1 & 0 \\ 0 & 0 & e_3 \end{pmatrix}, \quad \text{with } p = 1 - p' = \cos^2\theta \in [0, 1].$$

So now the angle θ plays an analogous role to the volume fraction f in the conductivity problem. Aside from this difference, we can proceed as before and obtain rank-2 and rank-3 laminates with an effective compliance tensor $\boldsymbol{\mathcal{S}}_*$ such that $\boldsymbol{\mathcal{S}}_*\boldsymbol{I} = \boldsymbol{I}/(3\kappa_R)$. Again, although these laminates are not necessarily elastically isotropic, any elastically isotropic polycrystal produced from them necessarily has effective bulk modulus $\kappa_* = \kappa_R$.

For two-dimensional polycrystals, a similar argument (Avellaneda and Milton 1989; Rudelson 1989) shows that the lower Reuss-Hill bound

$$\kappa_* \geq 1/(S_{1111} + S_{2222} + 2S_{1122}) \tag{22.5}$$

on the effective bulk modulus is achieved. The translation method (see section 24.2 on page 500) gives the optimal upper bound, which improves on the upper Voigt-Hill bound.

22.4. The complete characterization of the set $G_f U e_0$ for n-phase composites and polycrystals

In section 21.3 on page 429 we saw that knowledge of the set $G_f U e_0$ allows one to solve a variety of optimization problems. Here we consider n-phase, three-dimensional polycrystals where the admissible conductivity tensor fields take the form

$$\boldsymbol{\sigma}(\boldsymbol{x}) = \sum_{i=1}^{n} \boldsymbol{R}(\boldsymbol{x})\chi_i(\boldsymbol{x})\boldsymbol{\sigma}_i \boldsymbol{R}^T(\boldsymbol{x}), \tag{22.6}$$

in which $\boldsymbol{\sigma}_i$ denotes the conductivity tensor of the i-th phase, which we assume to be real and symmetric so that it can be represented in the form

$$\boldsymbol{\sigma}_i = \begin{pmatrix} \lambda_1^{(i)} & 0 & 0 \\ 0 & \lambda_2^{(i)} & 0 \\ 0 & 0 & \lambda_3^{(i)} \end{pmatrix}, \qquad \text{with } \lambda_1^{(i)} \geq \lambda_2^{(i)} \geq \lambda_3^{(i)}. \tag{22.7}$$

No restrictions are placed on the geometric configuration of the phases nor on the crystal orientations, that is, there are no restrictions imposed on the characteristic functions $\chi_i(\boldsymbol{x})$ nor on the field of rotation matrices $\boldsymbol{R}(\boldsymbol{x})$.

We seek bounds on the triplet $(\langle \boldsymbol{j} \rangle, \langle \boldsymbol{e} \rangle, \boldsymbol{f})$, where $\boldsymbol{f} = (f_1, f_2, \ldots f_n)$ denotes an n-component vector representing the set of volume fractions of the phases. Equivalently, for each value of the vector $\boldsymbol{e}_0$ and for each vector $\boldsymbol{f}$ satisfying the obvious constraints

$$f_i = \langle \chi_i \rangle \geq 0 \ \text{ for all } i, \quad \sum_{i=1}^{n} f_i = 1, \tag{22.8}$$

we need to find the set $G_f U e_0$, which by definition is comprised of all values of $\langle \boldsymbol{j} \rangle$ when $\langle \boldsymbol{e} \rangle = \boldsymbol{e}_0$ and when the volume fractions of the phases equal $\boldsymbol{f}$. Here $G_f U$ is the G-closure at constant $\boldsymbol{f}$ of the set U containing the n tensors $\sigma_i, i = 1, 2, \ldots, n$ and all rotations of these tensors. This set $G_f U$ is comprised of all effective conductivity tensors $\boldsymbol{\sigma}_*$ associated with conductivity fields $\boldsymbol{\sigma}(\boldsymbol{x})$ of the form (22.6) when the volume fractions of the phases equal $\boldsymbol{f}$. With few exceptions (such as when only two isotropic phases are present) we do not have a complete characterization of $G_f U$. However, as we will now see, a complete characterization of the projection $G_f U e_0$ is available (Tartar 1995). In the special case of a conducting composite of two isotropic phases, this characterization was found by Raĭtum (1983) [see also Murat and Tartar (1985); Tartar (1987, 1994); and Gibiansky, Lurie, and Cherkaev (1988) for related results].

Each tensor $\boldsymbol{\sigma}_i$ satisfies the inequalities $\lambda_3^{(i)} \boldsymbol{I} \leq \boldsymbol{\sigma}_i \leq \lambda_1^{(i)} \boldsymbol{I}$. By combining these inequalities with the arithmetic and harmonic mean bounds on the effective tensor $\boldsymbol{\sigma}_*$ we see that for all three-dimensional vectors $\boldsymbol{v}$,

$$\lambda^- |\boldsymbol{v}|^2 \leq \boldsymbol{v} \cdot \boldsymbol{\sigma}_* \boldsymbol{v} \leq \lambda^+ |\boldsymbol{v}|^2, \quad \text{where } \lambda^- \equiv \Big[\sum_{i=1}^{n} f_i / \lambda_3^{(i)} \Big]^{-1}, \quad \lambda^+ \equiv \sum_{i=1}^{n} f_i \lambda_1^{(i)}. \tag{22.9}$$

Now suppose that $\langle \boldsymbol{j} \rangle$ and $\langle \boldsymbol{e} \rangle$ represent a pair of average current fields and average electric fields that can coexist in the polycrystal. Let $\mathcal{V}$ represent a two-dimensional subspace containing these two vectors, and let Λ denote the projection onto $\mathcal{V}$. The fields $\langle \boldsymbol{j} \rangle$ and $\langle \boldsymbol{e} \rangle$ satisfy

$$\langle \boldsymbol{j} \rangle = \Lambda \boldsymbol{\sigma}_* \Lambda \langle \boldsymbol{e} \rangle,$$

and by direct analogy with (21.6) and (21.8) this implies that

$$|\langle \boldsymbol{j} \rangle - (\nu_1 + \nu_2)\langle \boldsymbol{e} \rangle/2|^2 = (\nu_1 - \nu_2)^2 |\langle \boldsymbol{e} \rangle|^2/4, \tag{22.10}$$

where ν_1 and ν_2 represent the two nonzero eigenvalues of the matrix $\Lambda \boldsymbol{\sigma}_* \Lambda$. Since the inequality (22.9) holds for all $\boldsymbol{v}$ and in particular for $\boldsymbol{v} \in \mathcal{V}$, it follows that these eigenvalues must satisfy the constraints

$$\lambda^- \le \nu_1 \le \lambda^+, \quad \lambda^- \le \nu_2 \le \lambda^+. \tag{22.11}$$

The identity (22.10) constrains the endpoint of the vector $\langle \boldsymbol{j} \rangle$ to lie on the boundary of a sphere of radius $(\nu_1 - \nu_2)|\langle \boldsymbol{e} \rangle|/2$ centered at $(\nu_1 + \nu_2)\langle \boldsymbol{e} \rangle/2$. This sphere certainly lies inside the sphere of radius $(\lambda^+ - \lambda^-)|\langle \boldsymbol{e} \rangle|/2$ centered at $(\lambda^+ + \lambda^-)\langle \boldsymbol{e} \rangle/2$. In other words, (22.10) together (22.11) implies the bound

$$|\langle \boldsymbol{j} \rangle - (\lambda^+ + \lambda^-)\langle \boldsymbol{e} \rangle/2|^2 \le (\lambda^+ - \lambda^-)^2 |\langle \boldsymbol{e} \rangle|^2/4 \tag{22.12}$$

of Tartar (1995).

The bound (22.12) is illustrated in figure 22.3. In conjunction with the trivial bounds (22.8) on the volume fractions, it gives us constraints on the set of possible triplets $(\langle \boldsymbol{j} \rangle, \langle \boldsymbol{e} \rangle, \boldsymbol{f})$. In particular, when $\langle \boldsymbol{j} \rangle$ is parallel to $\langle \boldsymbol{e} \rangle$, the bound implies that $|\langle \boldsymbol{j} \rangle|$ is between $\lambda^- |\langle \boldsymbol{e} \rangle|$ and $\lambda^+ |\langle \boldsymbol{e} \rangle|$, as expected.

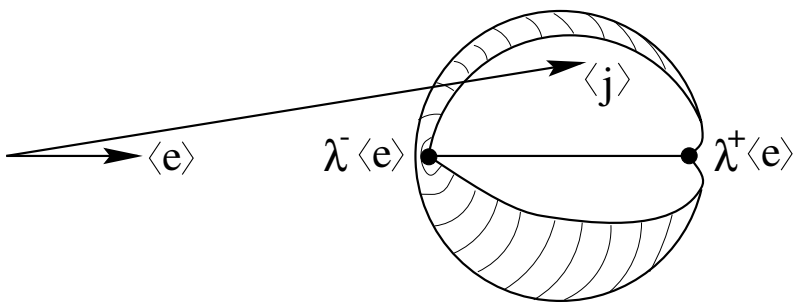

Figure 22.3. When the volume fractions of the phases and the average electric field vector $\langle \boldsymbol{e} \rangle$ are prescribed, the average current field vector $\langle \boldsymbol{j} \rangle$ in a multiphase composite or multiphase polycrystal can lie anywhere inside the sphere. Here λ^- and λ^+ are given by (22.9). Currents $\langle \boldsymbol{j} \rangle$ touching the boundary of the sphere can be realized when the composite (polycrystal) is just a simple laminate of the (suitably oriented) phases.

To show that these bounds are optimal we need to show that any triplet $(\langle \boldsymbol{j} \rangle, \langle \boldsymbol{e} \rangle, \boldsymbol{f})$ compatible with them is realized in some microgeometry. We start by supposing that the volume fractions $\boldsymbol{f}$ have been given. Also, without loss of generality, we can take $\langle \boldsymbol{e} \rangle$ as a unit vector and suppose that a coordinate system has been chosen so that $\langle \boldsymbol{e} \rangle$ lies along the x_1-axis while $\langle \boldsymbol{j} \rangle$ lies in the (x_1, x_3)-plane. We first construct a simple rank-1 laminate of the n crystalline

phases, with a direction of lamination $\boldsymbol{n}$ in the (x_1, x_3)-plane. Each phase is oriented so that the axes of lowest and highest conductivity also lie in the (x_1, x_3)-plane, with the axis of lowest conductivity aligned parallel to the direction of lamination $\boldsymbol{n}$. In other words, the local conductivity tensor $\boldsymbol{\sigma}(\boldsymbol{x})$ has $\boldsymbol{n}$ as an eigenvector and takes the form

$$\boldsymbol{\sigma}(\boldsymbol{x}) = \sum_{i=1}^{n} \chi_i(\boldsymbol{n}\cdot\boldsymbol{x}) \begin{pmatrix} \cos\theta & 0 & \sin\theta \\ 0 & 1 & 0 \\ -\sin\theta & 0 & \cos\theta \end{pmatrix} \begin{pmatrix} \lambda_1^{(i)} & 0 & 0 \\ 0 & \lambda_2^{(i)} & 0 \\ 0 & 0 & \lambda_3^{(i)} \end{pmatrix} \begin{pmatrix} \cos\theta & 0 & -\sin\theta \\ 0 & 1 & 0 \\ \sin\theta & 0 & \cos\theta \end{pmatrix},$$

in which $\boldsymbol{n} = (\sin\theta,\ 0,\ \cos\theta)^T$ and $\langle\chi_i\rangle = f_i$. This laminate has effective conductivity

$$\boldsymbol{\sigma}_* = \begin{pmatrix} \cos\theta & 0 & \sin\theta \\ 0 & 1 & 0 \\ -\sin\theta & 0 & \cos\theta \end{pmatrix} \begin{pmatrix} \lambda^+ & 0 & 0 \\ 0 & \lambda & 0 \\ 0 & 0 & \lambda^- \end{pmatrix} \begin{pmatrix} \cos\theta & 0 & -\sin\theta \\ 0 & 1 & 0 \\ \sin\theta & 0 & \cos\theta \end{pmatrix},$$

where

$$\lambda \equiv \sum_{i=1}^{n} f_i \lambda_2^{(i)},$$

and λ^- and λ^+ are defined by (22.9). This implies that

$$\langle\boldsymbol{j}\rangle = (\lambda^+\cos^2\theta + \lambda^-\sin^2\theta,\ 0,\ (\lambda^+ - \lambda^-)\sin\theta\cos\theta)^T \quad \text{when } \langle\boldsymbol{e}\rangle = (1,\ 0,\ 0)^T.$$

So as θ varies we see that $\langle\boldsymbol{j}\rangle$ ranges over all vectors in the (x_1, x_3)-plane satisfying

$$|\langle\boldsymbol{j}\rangle - (\lambda^+ + \lambda^-)\langle\boldsymbol{e}\rangle/2|^2 = (\lambda^+ - \lambda^-)^2|\langle\boldsymbol{e}\rangle|^2/4.$$

Equivalently, $\langle\boldsymbol{j}\rangle$ ranges over all vectors in the (x_1, x_3)-plane on the boundary of the region defined by (22.12). By laminating together two of these simple laminates we obtain average currents that correspond to any vector $\langle\boldsymbol{j}\rangle$ in the interior of the region defined by (22.12).

These optimal bounds allow one to solve many structural optimization problems of practical importance. In particular, if the objective of the optimization is to try to channel current into a particular region or, more generally, to optimize some functional of the locally averaged current field, the locally averaged electric field, and the locally averaged volume fractions, then it suffices to use these laminate geometries to construct an optimal solution.

It is interesting that the bounds on $(\langle\boldsymbol{j}\rangle, \langle\boldsymbol{e}\rangle, \boldsymbol{f})$ triplets were derived from the energy bounds (22.9) on $(W, \langle\boldsymbol{e}\rangle, \boldsymbol{f})$ triplets. In other words, the two sets of bounds contain exactly the same information, expressed in a different form. This is not true for the elasticity problem, and at present the characterization of possible (average stress, average strain) pairs is still an open problem, even for two-dimensional composites of two isotropic phases.

22.5. The G-closure in two dimensions of an arbitrary set of conducting materials

There are very few examples where we have a complete characterization of the set GU of effective tensors that can be produced by mixing together materials with tensors in a given set U. An exception is two-dimensional conductivity, where the classical variational principles in conjunction with the duality transformation [see section 3.1 on page 47] can be used to obtain a complete characterization of GU for an arbitrary rotationally invariant set U of positive-definite tensors, with eigenvalues bounded away from zero and infinity. [Another exception is

for three-dimensional conductivity when U consists of two isotropic tensors; see sections 23.2 on page 461 and 24.6 on page 506.] Here the rotational invariance of U means that we allow the constituent phases to have any orientation; that is, if $\boldsymbol{\sigma} \in U$, then $\boldsymbol{R\sigma R}^T \in U$ for all rotations $\boldsymbol{R}$ satisfying $\boldsymbol{RR}^T = \boldsymbol{I}$. Then GU will also be rotationally invariant since if $\boldsymbol{\sigma}_* \in GU$, we can rotate the entire composite and thereby deduce that $\boldsymbol{R\sigma}_*\boldsymbol{R}^T \in GU$. Thus whether a tensor $\boldsymbol{\sigma}$ lies in U or GU is determined solely by the eigenvalues λ_1 and λ_2 of $\boldsymbol{\sigma}$.

For mixtures of two isotropic materials Tartar (1975) presented without proof the characterization of GU. Working independently, Raĭtum (1978) [see also Lurie and Cherkaev (1981, 1984)] gave a proof of this characterization. For mixtures of two anisotropic materials, Lurie and Cherkaev (1981, 1984) provided a set of bounds on the G-closure. In the examples that they considered these bounds were sharp and completely characterized GU. They claimed to have completely solved the problem, but they failed to properly consider all cases. For some orderings of crystal moduli there was a flaw in their arguments, and one of their proposed bounds was violated. This was realized by Francfort and Murat (1987), who found the complete characterization of GU for two anisotropic materials for all moduli orderings. Francfort and Milton (1987) extended the characterization to an arbitrary number of materials, subject to a minor technical correction mentioned below.

It is convenient to let $\boldsymbol{\sigma}$ be represented by the two points $(\lambda_1\lambda_2, \lambda_1)$ and $(\lambda_1\lambda_2, \lambda_2)$, where the first coordinate represents the determinant of $\boldsymbol{\sigma}$ and the second coordinate represents an eigenvalue of $\boldsymbol{\sigma}$. We will call this the (d, λ) representation. In this representation U and GU are represented by sets that we still label as U and GU. Let T denote the "reflection transformation"

$$T(d, \lambda) = (d, d/\lambda),$$

corresponding to swapping eigenvalues. Clearly, both U and GU are invariant under this transformation, that is, $T(U) = U$ and $T(GU) = GU$. With these definitions in hand let us define V as that simply connected region with the same outer boundary as the set $U_C \cup T(U_C)$, where U_C denotes the convexification of the set U in the (d, λ) representation. We will see that $GU = V$, which provides the desired characterization of GU. Figure 22.4 on the next page shows the construction of GU for a three-phase mixture.

The key to establishing this result is lemma 2 of Francfort and Murat (1987). Since their complete proof was never published, I am grateful to Gilles Francfort (private communication) for providing the details. The first step is to establish that, if for some choice of constants $a > 0$, $b > 0$ and for all $\boldsymbol{x}$ we have

$$\boldsymbol{I} \geq a\boldsymbol{\sigma}(\boldsymbol{x}) + b\boldsymbol{\sigma}'(\boldsymbol{x}), \quad \text{where } \boldsymbol{\sigma}'(\boldsymbol{x}) = \boldsymbol{\sigma}(\boldsymbol{x})/\det[\boldsymbol{\sigma}(\boldsymbol{x})], \tag{22.13}$$

then the effective tensor $\boldsymbol{\sigma}_*$ satisfies a bound of the same form:

$$\boldsymbol{I} \geq a\boldsymbol{\sigma}_* + b\boldsymbol{\sigma}'_*, \quad \text{where } \boldsymbol{\sigma}'_* = \boldsymbol{\sigma}_*/\det[\boldsymbol{\sigma}_*]. \tag{22.14}$$

To see this, we first notice that from duality (see section 3.1 on page 47) $\boldsymbol{\sigma}'_*$ is the effective tensor associated with a medium with conductivity $\boldsymbol{\sigma}'(\boldsymbol{x})$. Therefore the arithmetic mean bounds imply that

$$\langle \boldsymbol{\sigma}(\boldsymbol{x}) \rangle \geq \boldsymbol{\sigma}_*, \quad \langle \boldsymbol{\sigma}'(\boldsymbol{x}) \rangle \geq \boldsymbol{\sigma}'_*. \tag{22.15}$$

Now it follows from (22.13) that for all vectors $\boldsymbol{e}_0$,

$$\boldsymbol{e}_0 \cdot \boldsymbol{e}_0 \geq a\boldsymbol{e}_0 \cdot \boldsymbol{\sigma}(\boldsymbol{x})\boldsymbol{e}_0 + b\boldsymbol{e}_0 \cdot \boldsymbol{\sigma}'(\boldsymbol{x})\boldsymbol{e}_0.$$

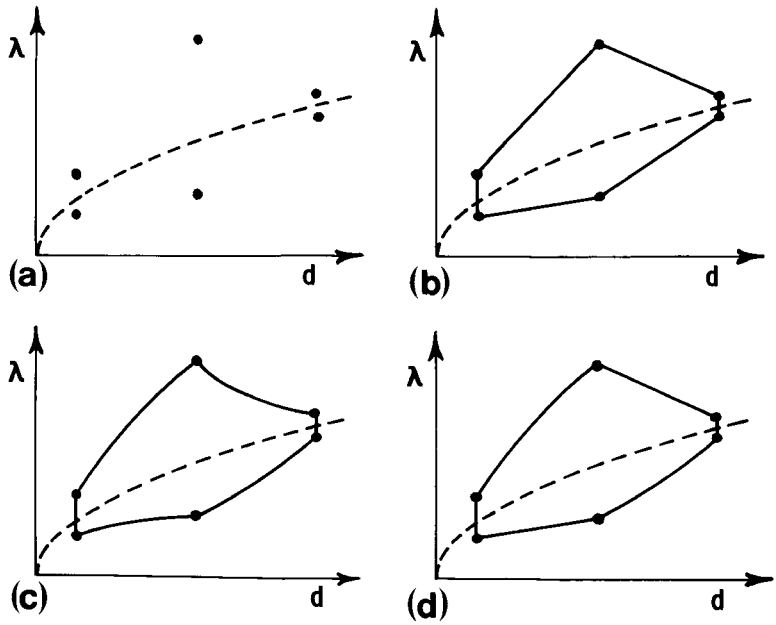

Figure 22.4. Geometrical construction of the set GU of all possible eigenvalue pairs (λ_1, λ_2) of the effective tensor of a three-phase, two-dimensional composite. First the eigenvalue pairs associated with the conductivity tensors of the phases are plotted in the (d, λ)-plane as in (a). Then the convex hull is taken as in (b), to give the set U_C. Its image under the reflection transformation is constructed as in (c), to give the set $T(U_C)$. Finally, the outer boundary of the union of the sets in (b) and (c) is plotted as in (d). Then the set GU, in the (d, λ)-plane, is the region enclosed by this curve. In each figure the dashed line is the line $\lambda = \sqrt{d}$, corresponding to isotropic materials with $\lambda_1 = \lambda_2$. After Francfort and Milton (1987).

By taking the average over $\boldsymbol{x}$ and making the substitutions (22.15) we obtain the desired bound (22.14). Expressed in the (d, λ) representation this result says that if the set U lies above a line ℓ with positive slope and positive intercept (described by the equation $\lambda = ad + b$), then the set GU also lies above this line. Since GU is invariant under T it must also lie below the curve $T(\ell)$.

The second step is to establish that, if for some choice of constants a, b, and c with $ab < 0$ and $c \geq 0$ we have, for all $\boldsymbol{x}$,

$$c\boldsymbol{I} \leq a\boldsymbol{\sigma}(\boldsymbol{x}) + b\boldsymbol{\sigma}'(\boldsymbol{x}), \quad \text{where } \boldsymbol{\sigma}'(\boldsymbol{x}) = \boldsymbol{\sigma}(\boldsymbol{x})/\det[\boldsymbol{\sigma}(\boldsymbol{x})], \tag{22.16}$$

then the effective tensor $\boldsymbol{\sigma}_*$ satisfies a bound of the same form:

$$c\boldsymbol{I} \leq a\boldsymbol{\sigma}_* + b\boldsymbol{\sigma}'_*, \quad \text{where } \boldsymbol{\sigma}'_* = \boldsymbol{\sigma}_*/\det[\boldsymbol{\sigma}_*]. \tag{22.17}$$

Due to the symmetry it suffices to consider the case where $a < 0$ and $b > 0$. Now, given an applied field $\boldsymbol{e}_0$, let $\boldsymbol{e}'(\boldsymbol{x})$ with $\langle \boldsymbol{e}' \rangle = \boldsymbol{e}_0$ be the electric field that solves the conductivity problem associated with $\boldsymbol{\sigma}'(\boldsymbol{x})$, that is, which is such that $\boldsymbol{\sigma}'(\boldsymbol{x})\boldsymbol{e}'(\boldsymbol{x})$ is divergence free. Then we have

$$\langle \boldsymbol{e}'(\boldsymbol{x}) \cdot \boldsymbol{\sigma}(\boldsymbol{x})\boldsymbol{e}'(\boldsymbol{x}) \rangle \geq \boldsymbol{e}_0 \cdot \boldsymbol{\sigma}_* \boldsymbol{e}_0, \quad \langle \boldsymbol{e}'(\boldsymbol{x}) \cdot \boldsymbol{\sigma}'(\boldsymbol{x})\boldsymbol{e}'(\boldsymbol{x}) \rangle = \boldsymbol{e}_0 \cdot \boldsymbol{\sigma}'_* \boldsymbol{e}_0, \tag{22.18}$$

where the first relation comes from the classical variational principle with $\boldsymbol{e}'(\boldsymbol{x})$ as a trial field. Now from (22.16) we have

$$c\boldsymbol{e}'(\boldsymbol{x})\cdot\boldsymbol{e}'(\boldsymbol{x}) \le a\boldsymbol{e}'(\boldsymbol{x})\cdot\boldsymbol{\sigma}(\boldsymbol{x})\boldsymbol{e}'(\boldsymbol{x}) + b\boldsymbol{e}'(\boldsymbol{x})\cdot\boldsymbol{\sigma}'(\boldsymbol{x})\boldsymbol{e}'(\boldsymbol{x}).$$

Taking the average over $\boldsymbol{x}$ and using the relations (22.18) and the inequality

$$\langle\boldsymbol{e}'(\boldsymbol{x})\cdot\boldsymbol{e}'(\boldsymbol{x})\rangle \ge \boldsymbol{e}_0\cdot\boldsymbol{e}_0,$$

which expresses the fact that the variance of the field $\boldsymbol{e}'(\boldsymbol{x})$ must be positive, gives the desired bound (22.17). Expressed in the (d,λ) representation this result, with $c=1$, says that if the set U lies below a line ℓ with either positive slope and negative intercept, or negative slope and positive intercept (described by the equation $\lambda = ad+b$), then the set GU also lies below this line. Since GU is invariant under T, it must also lie above the curve $T(\ell)$. The result with $c=0$ says that if the set U lies on one side of a vertical line, then the set GU also lies on the same side of that vertical line.

The set GU therefore lies inside the region of intersection of the narrowest vertical strip containing U and all sets bounded by ℓ and $T(\ell)$ as ℓ varies both over all lines with positive slope and positive intercept lying below U and over all lines with either positive slope and negative intercept, or negative slope and positive intercept, lying above U. Omitting the technical details, this region of intersection is the set V and the result implies that $GU\subset V$. [The results and proofs in the paper of Francfort and Milton (1987) have to be modified slightly because it was incorrectly assumed that $U_C\cup T(U_C)$ equals V. This is not always the case, as happens when U consists of two isotropic materials. Then U_C is a straight line and $T(U_C)$ is its reflection under T. Thus $U_C\cup T(U_C)$ has an empty interior while V does not.]

To prove the opposite inclusion $V\subset GU$, we first show that points on the boundary of V are associated with rank-1 laminates of two materials in U. Any point $\boldsymbol{p}_* = (d_*,\lambda_*)$ on the boundary of V, by the definition of V, must be either on the boundary of U_C or on the boundary of $T(U_C)$. If $\boldsymbol{p}_*\in\partial U_C$, then there exist two points $\boldsymbol{p}' = (d',\lambda')\in U$ and $\boldsymbol{p}'' = (d'',\lambda'')\in U$ such that $\boldsymbol{p}_*$ lies on the line joining these two points, namely,

$$\lambda = ad+b, \quad \text{where } a = \frac{\lambda'-\lambda''}{d'-d''},\ \ b = \frac{d'\lambda''-d''\lambda'}{d'-d''}. \tag{22.19}$$

Now we take two materials with conductivity tensors

$$\boldsymbol{\sigma}' = \begin{pmatrix}\lambda' & 0\\ 0 & d'/\lambda'\end{pmatrix} \equiv \begin{pmatrix}\lambda_1' & 0\\ 0 & \lambda_2'\end{pmatrix},\quad \boldsymbol{\sigma}'' = \begin{pmatrix}\lambda'' & 0\\ 0 & d''/\lambda''\end{pmatrix} \equiv \begin{pmatrix}\lambda_1'' & 0\\ 0 & \lambda_2''\end{pmatrix},$$

represented by the points $\boldsymbol{p}_a$, $T(\boldsymbol{p}_a)$, $\boldsymbol{p}_b$, and $T(\boldsymbol{p}_b)$ in the (d,λ) representation, and laminate them together in proportions f and $1-f$ with the lamination direction $\boldsymbol{n}$ being directed along the x_1-axis. The resulting effective tensor $\boldsymbol{\sigma}_*$ will have eigenvalues given by

$$1/\lambda_1^* = f/\lambda_1' + (1-f)/\lambda_1'',\ \ \lambda_2^* = f\lambda_2' + (1-f)\lambda_2'',$$

and as f is varied a linear relation between $1/\lambda_1^*$ and λ_2^* holds:

$$1 = a\lambda_2^* + b/\lambda_1^* \text{ or, equivalently, } \lambda_1^* = a\lambda_1^*\lambda_2^* + b,$$

where a and b are given by (22.19). Therefore the point $(\lambda_1^*\lambda_2^*,\lambda_1^*)$ representing the tensor $\boldsymbol{\sigma}_*$ lies on the line joining $\boldsymbol{p}'$ and $\boldsymbol{p}''$ in the (d,λ) representation. One chooses f so that this

point coincides with $\boldsymbol{p}_*$. If, alternatively, $\boldsymbol{p}_* \in \partial T(U_C)$, then $T(\boldsymbol{p}_*) \in U_C$ and by applying the previous arguments one obtains a laminate of two materials in U whose effective tensor in the (d, λ) representation is represented by the two points $T(\boldsymbol{p}_*)$ and $T[T(\boldsymbol{p}_*)] = \boldsymbol{p}_*$.

In summary, all points on the boundary of V are associated with simple rank-1 laminates of two materials in U. Given a point $\boldsymbol{q}_*$ inside V one looks for the points $\boldsymbol{p}_*$ and $T(\boldsymbol{p}_*)$ on the boundary of V that have the same value of d as $\boldsymbol{q}_*$. By laminating the laminate associated with $\boldsymbol{p}_*$ and $T(\boldsymbol{p}_*)$ with a 90° rotation of the same laminate, one obtains a rank-2 laminate whose effective tensor is represented by the points $\boldsymbol{q}_*$ and $T(\boldsymbol{q}_*)$. This shows that any polycrystalline composite formed from an arbitrary (possibly infinite) number of phases can be replaced by a rank-2 laminate formed from only two of the given phases without altering the effective conductivity.

It would be wonderful if a similar construction gave the G-closure for an arbitrary number of materials in three dimensions. Lurie and Cherkaev (1983) had claimed such a result, but there was an error in their arguments. Even for conducting polycrystalsformed from a single anisotropic material with uniaxial symmetry the complete G-closure is unknown, although some progress has been made (Avellaneda, Cherkaev, Lurie, and Milton 1988). The fact that infinite-rank laminates are sometimes needed in constructions suggests that the three-dimensional G-closure cannot be obtained through a finite number of convexification steps. It is not even known whether or not laminate microgeometries suffice to generate the entire G-closure.

22.6. Bounds on complex effective tensors†

Another example that illustrates the usefulness of the arithmetic mean bounds is their application to bounding the effective complex dielectric tensor $\varepsilon_* = \varepsilon'_* + i\varepsilon''_*$ of a three-dimensional composite material. After making the Cherkaev-Gibiansky transformation to the analogous problem (11.57) in which the tensor field $\boldsymbol{\mathcal{L}}(\boldsymbol{x})$ given by (11.58) that enters the constitutive relation is positive-semidefinite, the arithmetic mean bounds imply that $\boldsymbol{\mathcal{L}}_* \le \langle \boldsymbol{\mathcal{L}} \rangle$. Equivalently, the inequality

$$\begin{pmatrix} -\boldsymbol{d}_0 \\ \boldsymbol{e}_0 \end{pmatrix} \cdot \begin{pmatrix} [\varepsilon''_*]^{-1} & [\varepsilon''_*]^{-1}\varepsilon'_* \\ \varepsilon'_*[\varepsilon''_*]^{-1} & \varepsilon''_* + \varepsilon'_*[\varepsilon''_*]^{-1}\varepsilon'_* \end{pmatrix} \begin{pmatrix} -\boldsymbol{d}_0 \\ \boldsymbol{e}_0 \end{pmatrix} \le \begin{pmatrix} -\boldsymbol{d}_0 \\ \boldsymbol{e}_0 \end{pmatrix} \cdot \begin{pmatrix} \langle [\varepsilon'']^{-1} \rangle & \langle [\varepsilon'']^{-1}\varepsilon' \rangle \\ \langle \varepsilon'[\varepsilon'']^{-1} \rangle & \langle \varepsilon'' + \varepsilon'[\varepsilon'']^{-1}\varepsilon' \rangle \end{pmatrix} \begin{pmatrix} -\boldsymbol{d}_0 \\ \boldsymbol{e}_0 \end{pmatrix} \tag{22.20}$$

of Cherkaev and Gibiansky (1992) must hold for all choices of the fields $\boldsymbol{d}_0 = \langle \mathrm{Re}(\boldsymbol{d}) \rangle$ and $\boldsymbol{e}_0 = \langle \mathrm{Re}(\boldsymbol{e}) \rangle$. In particular, by setting

$$\boldsymbol{d}_0 = \varepsilon_0 \boldsymbol{e}_0,$$

where ε_0 is any real symmetric tensor, (22.20) reduces to

$$\varepsilon_0[\varepsilon''_*]^{-1} - \varepsilon_0[\varepsilon''_*]^{-1}\varepsilon'_* - \varepsilon'_*[\varepsilon''_*]^{-1}\varepsilon_0 + \varepsilon''_* + \varepsilon'_*[\varepsilon''_*]^{-1}\varepsilon'_* \le \Big\langle \varepsilon_0[\varepsilon'']^{-1} - \varepsilon_0[\varepsilon'']^{-1}\varepsilon' - \varepsilon'[\varepsilon'']^{-1}\varepsilon_0 + \varepsilon'' + \varepsilon'[\varepsilon'']^{-1}\varepsilon' \Big\rangle,$$

which can be rewritten as

$$\varepsilon''_* + (\varepsilon'_* - \varepsilon_0)[\varepsilon''_*]^{-1}(\varepsilon'_* - \varepsilon_0) \le \Big\langle \varepsilon'' + (\varepsilon' - \varepsilon_0)[\varepsilon'']^{-1}(\varepsilon' - \varepsilon_0) \Big\rangle. \tag{22.21}$$

A further simplification can be made once one notices that the terms appearing in this inequality can be identified with the inverses of the imaginary parts of the tensors $(\boldsymbol{\varepsilon}_* - \boldsymbol{\varepsilon}_0)^{-1}$ and $(\boldsymbol{\varepsilon}(\boldsymbol{x}) - \boldsymbol{\varepsilon}_0)^{-1}$:

$$\begin{aligned} \text{Im}[(\boldsymbol{\varepsilon}_* - \boldsymbol{\varepsilon}_0)^{-1}] &= -\{\boldsymbol{\varepsilon}_*'' + (\boldsymbol{\varepsilon}_*' - \boldsymbol{\varepsilon}_0)[\boldsymbol{\varepsilon}_*'']^{-1}(\boldsymbol{\varepsilon}_*' - \boldsymbol{\varepsilon}_0)\}^{-1}, \\ \text{Im}[(\boldsymbol{\varepsilon}(\boldsymbol{x}) - \boldsymbol{\varepsilon}_0)^{-1}] &= -\{\boldsymbol{\varepsilon}''(\boldsymbol{x}) + (\boldsymbol{\varepsilon}'(\boldsymbol{x}) - \boldsymbol{\varepsilon}_0)[\boldsymbol{\varepsilon}''(\boldsymbol{x})]^{-1}(\boldsymbol{\varepsilon}'(\boldsymbol{x}) - \boldsymbol{\varepsilon}_0)\}^{-1}, \end{aligned} \tag{22.22}$$

in which we have used the matrix identity,

$$\begin{aligned} (\boldsymbol{M}' + i\boldsymbol{M}'')^{-1} &= (\boldsymbol{M}' + i\boldsymbol{M}'')^{-1}(\boldsymbol{M}' - i\boldsymbol{M}'')(\boldsymbol{M}' - i\boldsymbol{M}'')^{-1} \\ &= \Big[(\boldsymbol{M}' - i\boldsymbol{M}'')(\boldsymbol{M}')^{-1}(\boldsymbol{M}' + i\boldsymbol{M}'')\Big]^{-1} - i\Big[(\boldsymbol{M}' - i\boldsymbol{M}'')(\boldsymbol{M}'')^{-1}(\boldsymbol{M}' + i\boldsymbol{M}'')\Big]^{-1} \\ &= \Big[\boldsymbol{M}' + \boldsymbol{M}''(\boldsymbol{M}')^{-1}\boldsymbol{M}''\Big] - i\Big[\boldsymbol{M}'' + \boldsymbol{M}'(\boldsymbol{M}'')^{-1}\boldsymbol{M}'\Big], \end{aligned}$$

to separate the inverse of a complex symmetric matrix $\boldsymbol{M}' + i\boldsymbol{M}''$ into its real and symmetric parts, without assuming that $\boldsymbol{M}'$ and $\boldsymbol{M}''$ commute. With the aid of (22.22) we see that (22.21) simplifies to the matrix inequality

$$\Big\{\text{Im}[(\boldsymbol{\varepsilon}_* - \boldsymbol{\varepsilon}_0)^{-1}]\Big\}^{-1} \geq \Big\langle\Big\{\text{Im}[(\boldsymbol{\varepsilon}(\boldsymbol{x}) - \boldsymbol{\varepsilon}_0)^{-1}]\Big\}^{-1}\Big\rangle. \tag{22.23}$$

This holds for all real symmetric tensors $\boldsymbol{\varepsilon}_0$ and for all symmetric complex fields $\boldsymbol{\varepsilon}(\boldsymbol{x})$ such that $\boldsymbol{\varepsilon}''(\boldsymbol{x}) = \text{Im}[\boldsymbol{\varepsilon}(\boldsymbol{x})]$ is positive-semidefinite (Milton 1990). Since we are free to make rotations in the complex plane, (22.23) implies the more general bounds

$$\Big\{\text{Im}[(e^{-i\theta}\boldsymbol{\varepsilon}_* - \boldsymbol{\varepsilon}_0)^{-1}]\Big\}^{-1} \geq \Big\langle\Big\{\text{Im}[(e^{-i\theta}\boldsymbol{\varepsilon}(\boldsymbol{x}) - \boldsymbol{\varepsilon}_0)^{-1}]\Big\}^{-1}\Big\rangle, \tag{22.24}$$

which must hold for all real symmetric tensors $\boldsymbol{\varepsilon}_0$ and for all angles $\theta \in [0, 2\pi]$ such that

$$\text{Im}[e^{-i\theta}\boldsymbol{\varepsilon}(\boldsymbol{x})] \geq 0 \ \text{ for all } \boldsymbol{x}.$$

For instance, suppose that the composite is isotropic, that is, $\boldsymbol{\varepsilon}(\boldsymbol{x}) = \varepsilon(\boldsymbol{x})\boldsymbol{I}$, and that the real and imaginary parts of $\boldsymbol{\varepsilon}_*$ commute. Then by taking an isotropic tensor $\boldsymbol{\varepsilon}_0 = \varepsilon_0\boldsymbol{I}$ (22.24) implies that any eigenvalue λ of $\boldsymbol{\varepsilon}_*$ satisfies the inequality

$$\frac{1}{\text{Im}[1/(e^{-i\theta}\lambda - \varepsilon_0)]} \geq \left\langle\frac{1}{\text{Im}[1/(e^{-i\theta}\varepsilon - \varepsilon_0)]}\right\rangle, \tag{22.25}$$

which for given values of θ and ε_0 confines λ to lie inside a circle in the complex plane. Consequently, as ε_0 and θ are varied, subject to the constraint that $\text{Im}[e^{-i\theta}\varepsilon(\boldsymbol{x})] \geq 0$, the eigenvalues of $\boldsymbol{\varepsilon}_*$ must lie inside the region of intersection of these circles. These bounds for multicomponent composites were first conjectured by Golden and Papanicolaou (1985) and Golden (1986) and were proved later (Bergman 1986; Milton 1987; Milton and Golden 1990).

In particular, consider a two-phase composite where the local complex dielectric constant takes the form

$$\varepsilon(\boldsymbol{x}) = \varepsilon_1\chi_1(\boldsymbol{x}) + \varepsilon_2\chi_2(\boldsymbol{x}),$$

and suppose that the phases have been labeled so that $\mathrm{Im}(\varepsilon_1/\varepsilon_2) \geq 0$. By first setting $\theta = \arg(\varepsilon_2)$ and $\varepsilon_0 = e^{-i\theta}\varepsilon_2$ and then setting $\theta = \pi + \arg(\varepsilon_1)$ and $\varepsilon_0 = e^{-i\theta}\varepsilon_1$, we obtain from (22.25) the pair of bounds (Bergman 1980; Milton 1980)

$$f_1 \,\mathrm{Im}[\varepsilon_2/(\lambda-\varepsilon_2)] \leq \mathrm{Im}[\varepsilon_2/(\varepsilon_1-\varepsilon_2)], \qquad f_2 \,\mathrm{Im}[\varepsilon_1/(\lambda-\varepsilon_1)] \geq \mathrm{Im}[\varepsilon_1/(\varepsilon_2-\varepsilon_1)], \quad (22.26)$$

each of which confines λ to a circle in the complex plane. These circles can also be defined geometrically by specifying three points through which each circle passes: The first circle passes through the three points $\lambda = \varepsilon_1$, $\lambda = f_1\varepsilon_1 + f_2\varepsilon_2$, and $\lambda = 1/(f_1/\varepsilon_1 + f_2/\varepsilon_2)$, while the second circle passes through the three points $\lambda = \varepsilon_2$, $\lambda = f_1\varepsilon_1 + f_2\varepsilon_2$, and $\lambda = 1/(f_1/\varepsilon_1 + f_2/\varepsilon_2)$. In other words, the bounds (22.26) constrain λ to lie within a lens-shaped region of the complex plane (represented by the region $\boldsymbol{\Omega}'$ in figure 27.1 on page 570).

In fact, this is an optimal set of bounds on the pairs (λ, f_1); for a fixed value of f_1 any point on the circular arcs that form the boundary of this lens-shaped region can be achieved by using either the assemblages of coated elliptical cylinders of figure 7.5 on page 125 or using the coated laminate geometries of figure 9.3 on page 166. By varying the eccentricity of the elliptical cylinders, or by varying the proportions laminated in each direction of lamination, we can move λ along the circular arc, achieving the two endpoints $\lambda = f_1\varepsilon_1 + f_2\varepsilon_2$ and $\lambda = 1/(f_1/\varepsilon_1 + f_2/\varepsilon_2)$ when the geometry reduces to a simple laminate of the two phases. By swapping the roles of the core and coating materials we can achieve any point on the other circular arc. Bounds on the complex dielectric constant of two-phase composites will be discussed in more detail in chapter 27 on page 569 (see also sections 23.7 on page 476 and 29.6 on page 638).

Analogous bounds apply to the complex effective elasticity tensor $\boldsymbol{\mathcal{C}}_* = \boldsymbol{\mathcal{C}}'_* + i\boldsymbol{\mathcal{C}}''_*$ of viscoelastic composite media. For every real, self-adjoint, fourth-order tensor $\boldsymbol{\mathcal{C}}_0$, and for every angle θ such that

$$\mathrm{Im}[e^{-i\theta}\boldsymbol{\mathcal{C}}(\boldsymbol{x})] \geq 0 \ \text{ for all } \boldsymbol{x},$$

we have the bounds

$$\Big\{\mathrm{Im}[(e^{-i\theta}\boldsymbol{\mathcal{C}}_* - \boldsymbol{\mathcal{C}}_0)^{-1}]\Big\}^{-1} \geq \Big\langle\Big\{\mathrm{Im}[(e^{-i\theta}\boldsymbol{\mathcal{C}}(\boldsymbol{x}) - \boldsymbol{\mathcal{C}}_0)^{-1}]\Big\}^{-1}\Big\rangle. \quad (22.27)$$

As an example, let us consider a two-phase composite where the complex elasticity tensor takes the form

$$\boldsymbol{\mathcal{C}}(\boldsymbol{x}) = \boldsymbol{\mathcal{C}}_1\chi_1(\boldsymbol{x}) + \boldsymbol{\mathcal{C}}_2\chi_2(\boldsymbol{x}) \ \text{ with } \boldsymbol{\mathcal{C}}_2 \text{ real and } \mathrm{Im}(\boldsymbol{\mathcal{C}}_1) \geq 0.$$

By taking $\theta = 0$ and $\boldsymbol{\mathcal{C}}_0 = \boldsymbol{\mathcal{C}}_2$, the bound (22.27) reduces to

$$f_1 \,\mathrm{Im}[(\boldsymbol{\mathcal{C}}_* - \boldsymbol{\mathcal{C}}_2)^{-1}] \leq \mathrm{Im}[(\boldsymbol{\mathcal{C}}_1 - \boldsymbol{\mathcal{C}}_2)^{-1}].$$

This is an attainable bound. From the lamination formula (9.55) we see that it is achieved whenever the composite is a coated laminate with phase 1 as core and phase 2 as coating.

References

Avellaneda, M., A. V. Cherkaev, K. A. Lurie, and G. W. Milton 1988. On the effective conductivity of polycrystals and a three-dimensional phase-interchange inequality. *Journal of Applied Physics* 63(10):4989–5003. {*120, 139, 439, 441, 450, 452, 512, 525, 538, 550, 555, 564*}

Avellaneda, M. and G. W. Milton 1989. Optimal bounds on the effective bulk modulus of polycrystals. *SIAM Journal on Applied Mathematics* 49(3):824–837. {*441, 444, 453, 501, 525, 536, 550*}

Bergman, D. J. 1980. Exactly solvable microscopic geometries and rigorous bounds for the complex dielectric constant of a two-component composite material. *Physical Review Letters* 44:1285–1287. {*452, 453, 478, 491, 569, 577, 588, 597*}

Bergman, D. J. 1986. The effective dielectric coefficient of a composite medium: Rigorous bounds from analytic properties. In J. L. Ericksen, D. Kinderlehrer, R. Kohn, and J.-L. Lions (eds.), *Homogenization and Effective Moduli of Materials and Media*, pp. 27–51. Berlin / Heidelberg / London / etc.: Springer-Verlag. ISBN 0-387-96306-5. {*451, 453, 571, 597, 603, 604, 617, 638, 641*}

Cherkaev, A. V. and L. V. Gibiansky 1992. The exact coupled bounds for effective tensors of electrical and magnetic properties of two-component two-dimensional composites. *Proceedings of the Royal Society of Edinburgh. Section A, Mathematical and Physical Sciences* 122(1–2):93–125. {*397, 399, 411, 450, 453, 517, 522, 525, 614, 617*}

Cherkaev, A. V. and L. V. Gibiansky 1993. Extremal structures of multiphase conducting composites. *International Journal of Solids and Structures* 33(18):2609–2623. {*437, 453*}

Francfort, G. A. and G. W. Milton 1987. Optimal bounds for conduction in two-dimensional, multiphase, polycrystalline media. *Journal of Statistical Physics* 46(1–2): 161–177. {*447–449, 453*}

Francfort, G. A. and F. Murat 1987. Optimal bounds for conduction in two-dimensional, two-phase, anisotropic media. In R. J. Knops and A. A. Lacey (eds.), *Non-Classical Continuum Mechanics: Proceedings of the London Mathematical Society Symposium, Durham, July 1986*, pp. 197–212. Cambridge, United Kingdom: Cambridge University Press. ISBN 0-521-34935-4. {*47, 57, 447, 453*}

Gibiansky, L. V., K. A. Lurie, and A. V. Cherkaev 1988. Optimum focusing of a heat flux by a nonuniform heat-conducting medium (the "heat lens" problem). *Zhurnal tekhnicheskoi fiziki* 58:67–74. English translation in *Sov. Phys. Tech. Phys.* 33:38–42 (1988). {*432, 434, 444, 453*}

Golden, K. 1986. Bounds on the complex permittivity of a multicomponent material. *Journal of the Mechanics and Physics of Solids* 34(4):333–358. {*451, 453, 638, 639, 641*}

Golden, K. and G. Papanicolaou 1985. Bounds for effective parameters of multicomponent media by analytic continuation. *Journal of Statistical Physics* 40(5–6):655–667. {*387, 393, 451, 453, 638, 639, 641*}

Hill, R. 1952. The elastic behavior of a crystalline aggregate. *Proceedings of the Physical Society, London, A* 65:349–354. {*75, 77, 90, 271, 273, 287, 442, 453*}

Lurie, K. A. and A. V. Cherkaev 1981. *G*-closure of a set of anisotropic conducting media in the case of two-dimensions. *Doklady Akademii Nauk SSSR* 259:328–331. English translation in *Soviet Phys. Dokl.* 26:657–659 (1981). {*428, 429, 435, 447, 453, 521, 526*}

Lurie, K. A. and A. V. Cherkaev 1983. Optimal structural design and relaxed controls. *Optimal Control Applications and Methods* 4:387–392. {*450, 453*}

Lurie, K. A. and A. V. Cherkaev 1984. G-closure of a set of anisotropically conducting media in the two-dimensional case. *Journal of Optimization Theory and Applications* 42(2):283–304. {*428, 435, 447, 454, 521, 526*}

Milton, G. W. 1980. Bounds on the complex dielectric constant of a composite material. *Applied Physics Letters* 37(3):300–302. {*124, 140, 452, 454, 478, 494, 569, 570, 577, 588, 599*}

Milton, G. W. 1987. Multicomponent composites, electrical networks and new types of continued fraction. II. *Communications in Mathematical Physics* 111(3):329–372. {*451, 454, 619, 638–641*}

Milton, G. W. 1990. On characterizing the set of possible effective tensors of composites: The variational method and the translation method. *Communications on Pure and Applied Mathematics (New York)* 43(1):63–125. {*164, 183, 248, 265, 268, 277, 287, 451, 454, 473, 494, 499, 505, 512, 513, 518, 526, 532, 551*}

Milton, G. W. and K. Golden 1990. Representations for the conductivity functions of multicomponent composites. *Communications on Pure and Applied Mathematics (New York)* 43(5):647–671. {*303, 311, 387, 389, 390, 394, 451, 454, 638, 641*}

Murat, F. and L. Tartar 1985. Calcul des variations et homogéńisation. (French) [Calculus of variation and homogenization]. In *Les méthodes de l'homogénéisation: théorie et applications en physique*, pp. 319–369. Paris: Eyrolles. English translation in *Topics in the Mathematical Modelling of Composite Materials*, pp. 139–173, ed. by A. Cherkaev and R. Kohn, ISBN 0-8176-3662-5. {*12, 13, 17, 347, 353, 429, 431, 432, 435, 444, 454, 462, 495, 499, 503, 506, 508, 521, 527, 529, 551*}

Raĭtum, U. Ë. 1978. The extension of extremal problems connected with a linear elliptic equation. *Doklady Akademii Nauk SSSR* 243(2):281–283. English translation in *Soviet Math. Dokl.* 19(6):1342–1345 (1978). {*431, 435, 447, 454, 521, 527*}

Raĭtum, U. Ë. 1983. Questions of the existence of a solution in problems of optimal control of leading coefficients of linear elliptic equations. *Differentsial'nye Uravneniya* 19(6):1040–1047. English translation in *Differential Equations* 19(6):775–783 (1983). {*444, 454*}

Reuss, A. 1929. Berechnung der Fließgrenze von Mischkristallen auf Grund der Plastizitätsbedingung für Einkristalle. (German) [Calculation of the yield point of mixed crystals from plasticity conditions for single crystals]. *Zeitschrift für Angewandte Mathematik und Mechanik* 9:49–58. {*271, 288, 442, 454*}

Rudelson, M. 1989. Phase transitions in solids. Master's Thesis, St. Petersburg Technical University, St. Petersburg, Russia, 1989. {*441, 444, 454, 501, 527*}

Schulgasser, K. 1977. Bounds on the conductivity of statistically isotropic polycrystals. *Journal of Physics C: Solid State Physics* 10:407–417. {*47, 51, 58, 438–440, 454, 589, 600*}

Tartar, L. 1975. Problèmes de contrôle des coefficients dans des équations aux dérivées partielles. In A. Bensoussan and J.-L. Lions (eds.), *Control Theory, Numerical Methods and Computer Systems Modelling (Proceedings IRIA 1974)*, pp. 420–426. Berlin / Heidelberg / London / etc.: Springer-Verlag. English translation in *Topics in the Mathematical Modelling of Composite Materials*, pp. 1–8, ed. by A. Cherkaev and R. Kohn. ISBN 0-8176-3662-5. {*426, 429, 431, 435, 447, 454, 521, 527*}

Tartar, L. 1987. The appearance of oscillations in optimization problems. In R. J. Knops and A. A. Lacey (eds.), *Non-Classical Continuum Mechanics: Proceedings of the London Mathematical Society Symposium, Durham, July 1986*, pp. 129–150. Cambridge, United Kingdom: Cambridge University Press. ISBN 0-521-34935-4. {*429, 432, 436, 444, 455*}

Tartar, L. 1994. Remarks on optimal design problems. In G. Bouchitté, G. Buttazzo, and P. Suquet (eds.), *Calculus of Variations, Homogenization and Continuum Mechanics: June 21–25, 1993, CIRM-Luminy, Marseille, France*, pp. 279–296. Singapore / Philadelphia / River Edge, New Jersey: World Scientific Publishing Co. ISBN 981-02-1783-8. {*444, 455*}

Tartar, L. 1995. Remarks on the homogenization method in optimal design methods. In *Proceedings of the International Conference: Homogenization and Applications to Material Sciences: Held in Nice, June 6–10, 1995*, pp. 393–412. Tokyo: Gakkōtosho. ISBN 4-7625-0418-1. {*431, 436, 444, 445, 455*}

Voigt, W. 1889. Über die Beziehung zwischen den beiden Elastizitätskonstanten isotroper Körper. (German) [On the relation between the two elasticity constants of isotropic bodies]. *Wiedemanns Annalen der Physik und Chemie (Leipzig)* 38:573–587. {*271, 289, 442, 455*}

Voigt, W. 1910. *Lehrbuch der Krystallphysik*. Stuttgart, Germany / Leipzig, Germany: Teubner. xxiv + 964 pp. {*271, 289, 442, 455*}

23

Bounds from the Hashin-Shtrikman variational inequalities

DeLoor (1956) studied experimental results for the effective dielectric constants of isotropic two-phase composites and compared them with various approximation formulas. He found that the results always fell between the Maxwell (i.e., the Clausius-Mossotti) approximation formula with one phase as inclusion and the Maxwell approximation formula with the other phase as inclusion. Hashin and Shtrikman (1962a), using their variational principles, proved that these approximation formulas were in fact upper and lower bounds on the effective dielectric constant, and were realizable by the Hashin coated sphere assemblages. Hashin and Shtrikman, in their original paper, also provided bounds for isotropic multiphase media. They subsequently extended their results to elasticity (Hashin and Shtrikman 1963b). The Hashin-Strikman bounds for conductivity and elasticity have since become the benchmarks against which most experimental results are compared.

23.1. Bounds on the effective conductivity of an isotropic composite of n isotropic phases

Consider a d-dimensional composite of n isotropic phases with conductivities

$$\sigma_1 > \sigma_2 > \sigma_3 > \ldots > \sigma_n.$$

If we choose an isotropic reference tensor $\boldsymbol{\sigma}_0 = \sigma_0 \boldsymbol{I}$, and assume that the conductivity tensor of the composite is also isotropic, that is, $\boldsymbol{\sigma}_* = \sigma_* \boldsymbol{I}$, then the Hashin-Shtrikman variational inequality (13.30) implies that

$$\langle \underline{\boldsymbol{P}} \rangle \cdot \langle \underline{\boldsymbol{P}} \rangle / (\sigma_* - \sigma_0) \leq \langle \underline{\boldsymbol{P}} \cdot (\boldsymbol{\sigma} - \sigma_0 \boldsymbol{I})^{-1} \underline{\boldsymbol{P}} \rangle + \langle \underline{\boldsymbol{P}} \cdot \boldsymbol{\Gamma}_1 \underline{\boldsymbol{P}} \rangle / \sigma_0.$$

This holds for any choice of trial polarization field $\underline{\boldsymbol{P}}$ and for any constant σ_0 with $\sigma_n > \sigma_0 > 0$ (which ensures that $\boldsymbol{\sigma} > \boldsymbol{\sigma}_0$ and that $\boldsymbol{\Gamma}_1 \boldsymbol{\sigma}_0 \boldsymbol{\Gamma}_1 \geq 0$). The simplest choice of polarization field is one that is constant in each phase and, say, parallel to a constant unit vector $\boldsymbol{v}_\ell$ aligned in the direction of the x_ℓ-axis for some choice of ℓ:

$$\underline{\boldsymbol{P}}(\boldsymbol{x}) = \sum_{i=1}^{n} \alpha_i \chi_i(\boldsymbol{x}) \boldsymbol{v}_\ell, \tag{23.1}$$

where the $\chi_i(\boldsymbol{x})$ are the characteristic functions representing the geometry of the phases and the amplitudes α_i remain to be determined.

There are many alternative choices of trial polarization fields, which lead to other bounds. For example, Bergman (1976) considers a two-phase medium and takes a trial polarization

field that is a linear superposition of this piecewise constant field and one associated with the exact solution when the phases have another pair of conductivities σ_1' and σ_2'. Formulas for the resulting cross-property bounds, correlating the two different effective conductivities, are given later in equations (27.16) and (27.20). Kröner (1977) and Milton and Phan-Thien (1982) take trial fields that are obtained from the series expansion for the polarization field in a nearly homogeneous medium and obtain correlation function dependent bounds. Bornert, Stolz, and Zaoui (1996) obtain bounds for assemblages of one or more types of coated inclusions by taking polarization fields that are the same in each inclusion having a similar type (after spatial translation and rescaling). They show that considerable simplifications result when, after an affine transformation, the outer boundaries of the inclusions are all spherical with an isotropic distribution of centers.

Substituting the trial polarization field (23.1) into the variational inequality gives

$$(\sum_{i=1}^{n}\alpha_i f_i)^2/(\sigma_*-\sigma_0) \le \sum_{i=1}^{n}\alpha_i^2 f_i/(\sigma_i-\sigma_0)+\sum_{i=1}^{n}\sum_{j=1}^{n}\alpha_i\alpha_j\sum_{\boldsymbol{k}\neq 0}\widehat{\chi}_i^*(\boldsymbol{k})\widehat{\chi}_j(\boldsymbol{k})k_\ell^2/(k^2\sigma_0), \quad (23.2)$$

where the last term involving $\boldsymbol{\Gamma}_1$ has been replaced by its equivalent expression in Fourier space (using Plancherel's theorem). This term looks difficult to evaluate, but since the inequality holds for each value of $\ell = 1, 2, \ldots, d$, we are free to sum over ℓ and use the identity

$$\sum_{\boldsymbol{k}\neq 0}\widehat{\chi}_i^*(\boldsymbol{k})\widehat{\chi}_j(\boldsymbol{k}) = \langle(\chi_i - \langle\chi_i\rangle)(\chi_j - \langle\chi_j\rangle)\rangle = \delta_{ij}f_i - f_i f_j, \quad (23.3)$$

which follows from Plancherel's theorem. We thereby obtain the bound

$$d(\sum_{i=1}^{n}\alpha_i f_i)^2/(\sigma_* - \sigma_0) \le d\sum_{i=1}^{n}\alpha_i^2 f_i/(\sigma_i - \sigma_0) + \sum_{i=1}^{n}\sum_{j=1}^{n}\alpha_i\alpha_j(\delta_{ij}f_i - f_i f_j)/\sigma_0,$$

which can be rewritten as

$$(\sum_{i=1}^{n}\alpha_i f_i)^2[d/(\sigma_* - \sigma_0) + 1/\sigma_0] \le \sum_{i=1}^{n}\alpha_i^2 f_i[d/(\sigma_i - \sigma_0) + 1/\sigma_0].$$

The amplitudes α_i are now varied to minimize the right-hand side of this inequality while keeping $\sum_{i=1}^{n}\alpha_i f_i$ fixed. By multiplying this latter constraint with a Lagrange multiplier -2λ and adding it to the right-hand side, we see that the minimum occurs when

$$\alpha_i = \lambda[d/(\sigma_i - \sigma_0) + 1/\sigma_0]^{-1}. \quad (23.4)$$

Making this substitution and letting σ_0 approach σ_n gives the Hashin-Shtrikman (1962a) bound:

$$\sigma_* \ge \sigma_{HS}^-, \quad (23.5)$$

where σ_{HS}^- is given implicitly by the formula

$$\frac{1}{d/(\sigma_{HS}^- - \sigma_n) + 1/\sigma_n} = \sum_{i=1}^{n-1}\frac{f_i}{d/(\sigma_i - \sigma_n) + 1/\sigma_n}.$$

For a two-phase, three-dimensional medium the bound reduces to

$$\sigma_* \ge \sigma_2 + \frac{3f_1\sigma_2(\sigma_1 - \sigma_2)}{3\sigma_2 + f_2(\sigma_1 - \sigma_2)} = f_1\sigma_1 + f_2\sigma_2 - \frac{f_1 f_2(\sigma_1 - \sigma_2)^2}{f_2\sigma_1 + f_1\sigma_2 + 2\sigma_2}. \quad (23.6)$$

Comparing the right-hand side with (7.7) we see that this bound is attained for an assemblage of coated spheres with phase 1 as the core and phase 2 as the coating. In fact, one can see directly from the attainability criterion that the coated sphere assemblage necessarily must attain the bound. Indeed, with $\sigma_0 = \sigma_2$ the polarization field in the coated sphere assemblage is of the form (23.1), being zero in phase 2 and constant in phase 1. Therefore, since the trial field matches the actual field, the Hashin-Shtrikman bound is attained.

The same reasoning can be applied (Milton 1981b) to show the optimality of the lower bound (23.5) for n-phase composites whenever

$$\sigma_{HS}^{-} \leq \sigma_{n-1}. \tag{23.7}$$

For three-phase mixtures the coated sphere assemblage that attains the bound is illustrated in figure 23.1. To see the basic idea, consider a homogeneous matrix material, with conductivity

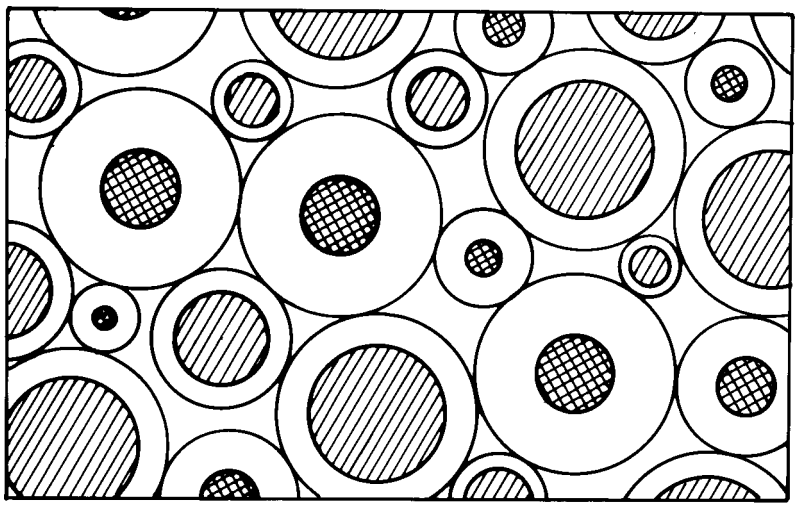

Figure 23.1. Cross section of the coated sphere assemblage that attains the Hashin-Shtrikman bounds for three-phase mixtures. The coated spheres should fill all space. Phase 1 occupies the cross-hatched region, phase 2 occupies the shaded region, and phase 3 occupies the remaining portion of the coated spheres. Reprinted with permission from Milton (1981b). Copyright 1981, Springer-Verlag.

σ_* chosen to lie between σ_{n-1} and σ_n, to which a uniform electric field $\boldsymbol{e}_0$ is applied. Coated spheres of $n-1$ different types are then inserted into the matrix, where type i has a core of phase i surrounded by a coating of phase n, with its relative thickness chosen so that the field in the matrix is not disturbed by the insertion. (The assumption that σ_* lies between σ_{n-1} and σ_n ensures that this can be done.) The field within each core will then be uniform and parallel to $\boldsymbol{e}_0$, and the overall effective conductivity will remain equal to σ_* as more and more coated spheres are added. Finally, when the coated spheres ultimately fill all space, the polarization field with $\sigma_0 = \sigma_n$ will be of the form (23.1) with $\alpha_n = 0$. Therefore, the attainability criterion implies that σ_* must in fact equal σ_{HS}^{-} for this microstructure. The flexibility that one has in the choice of σ_0 and in the choice of the proportions occupied by each type of coated sphere in the final mixture guarantees that one can achieve any desired combination of the volume

fractions $f_1, f_2, \ldots f_n$ compatible with the condition (23.7). Lurie and Cherkaev (1985) found that the bound was also attained by assemblages of multicoated spheres.

For two-dimensional, three-phase composites the condition (23.7) is satisfied if

$$f_3 \geq \frac{2(1-f_2)\sigma_3(\sigma_1-\sigma_2)}{(\sigma_2+\sigma_3)(\sigma_1-\sigma_3)}.$$

In a recent development Gibiansky and Sigmund (2000) found two-dimensional, three-phase microstructures that achieve the Hashin-Shtrikman lower bound under the less restrictive condition that

$$f_3 \geq \frac{2(\sqrt{f_2}-f_2)\sigma_3(\sigma_1-\sigma_2)}{(\sigma_2+\sigma_3)(\sigma_1-\sigma_3)}. \tag{23.8}$$

Moreover, when this condition was not satisfied, they found microstructures that have the lowest currently known conductivity.

From the other Hashin-Shtrikman variational principle (13.32) one obtains (by similar analysis) an upper bound on the effective conductivity

$$\sigma_* \leq \sigma_{HS}^+,$$

where σ_{HS}^+ is given implicitly by the formula

$$\frac{1}{d/(\sigma_1-\sigma_{HS}^+)-1/\sigma_1} = \sum_{i=2}^{n} \frac{f_i}{d/(\sigma_1-\sigma_i)-1/\sigma_1}.$$

Provided that

$$\sigma_{HS}^+ \geq \sigma_2, \tag{23.9}$$

this bound is attained by assemblages of coated spheres of $n-1$ different types, where type i has a core of phase $i+1$ and a coating of phase 1 (Milton 1981b) or, alternatively, by a multicoated sphere assemblage (Lurie and Cherkaev 1985). For two-dimensional, three-phase composites the condition (23.9) is satisfied if

$$f_1 \geq \frac{2(1-f_2)\sigma_1(\sigma_2-\sigma_3)}{(\sigma_1+\sigma_2)(\sigma_1-\sigma_3)}.$$

Gibiansky and Sigmund (2000) found another class of two-dimensional, three-phase microstructures that achieve the Hashin-Shtrikman upper bound under the less restrictive condition that

$$f_1 \geq \frac{2(\sqrt{f_2}-f_2)\sigma_1(\sigma_2-\sigma_3)}{(\sigma_1+\sigma_2)(\sigma_1-\sigma_3)}.$$

When this condition was not satisfied, they found microstructures that have the highest currently known conductivity.

For a two-phase, three-dimensional medium, with $\sigma_1 > \sigma_2$, the upper bound reduces to

$$\sigma_* \leq \sigma_1 - \frac{3f_2\sigma_1(\sigma_1-\sigma_2)}{3\sigma_1-f_1(\sigma_1-\sigma_2)} = f_1\sigma_1 + f_2\sigma_2 - \frac{f_1f_2(\sigma_1-\sigma_2)^2}{f_2\sigma_1+f_1\sigma_2+2\sigma_1}, \tag{23.10}$$

and is attained for an assemblage of coated spheres with phase 2 as the core and phase 1 as the coating (Hashin and Shtrikman 1962a).

There are two limits where the upper and lower Hashin-Shtrikman bounds coincide and therefore uniquely determine the effective conductivity σ_* of a d-dimensional isotropic composite: when $d = 1$ the effective conductivity is the harmonic average,

$$\sigma_* = \sigma_{HS}^- = \sigma_{HS}^+ = [\sum_{i=1}^n f_i/\sigma_i]^{-1},$$

as expected, while in the limit as $d \to \infty$ the effective conductivity is the arithmetic average,

$$\sigma_* = \sigma_{HS}^- = \sigma_{HS}^+ = \sum_{i=1}^n f_i \sigma_i,$$

as noted, for example, by Torquato (1997).

23.2. Optimal bounds on the effective conductivity of an anisotropic composite of two isotropic phases

The preceding analysis is easily generalized to anisotropic composites, for which the effective conductivity tensor $\boldsymbol{\sigma}_*$ is not necessarily proportional to the identity tensor. Instead of (23.2) we have

$$(\sum_{i=1}^n \alpha_i f_i)^2 \boldsymbol{v}_\ell \cdot (\boldsymbol{\sigma}_* - \sigma_0 \boldsymbol{I})^{-1} \boldsymbol{v}_\ell \le \sum_{i=1}^n \frac{\alpha_i^2 f_i}{\sigma_i - \sigma_0} + \sum_{i=1}^n \sum_{j=1}^n \alpha_i \alpha_j \sum_{\boldsymbol{k} \neq 0} \frac{\widehat{\chi}_i^*(\boldsymbol{k}) \widehat{\chi}_j(\boldsymbol{k}) k_\ell^2}{k^2 \sigma_0}.$$

Summing this over ℓ, making the substitutions (23.3) and (23.4), and letting σ_0 approach σ_n gives the lower bound

$$\{\mathrm{Tr}[(\boldsymbol{\sigma}_* - \sigma_n \boldsymbol{I})^{-1}] + 1/\sigma_n\}^{-1} \ge \sum_{i=1}^{n-1} f_i \{3/(\sigma_i - \sigma_n) + 1/\sigma_n\}^{-1}. \tag{23.11}$$

We also have the upper bound

$$\{\mathrm{Tr}[(\sigma_1 \boldsymbol{I} - \boldsymbol{\sigma}_*)^{-1}] - 1/\sigma_1\}^{-1} \ge \sum_{i=2}^{n} f_i \{3/(\sigma_1 - \sigma_i) - 1/\sigma_1\}^{-1}, \tag{23.12}$$

which follows analogously from the other Hashin-Shtrikman variational equality (13.32).

For a two-phase composite these bounds, after taking the inverses of both sides of the inequalities, reduce to

$$f_1 \sum_{i=1}^3 \frac{1}{\lambda_i^* - \sigma_2} \le \frac{3}{\sigma_1 - \sigma_2} + \frac{f_2}{\sigma_2}, \tag{23.13}$$

$$f_2 \sum_{i=1}^3 \frac{1}{\sigma_1 - \lambda_i^*} \le \frac{3}{\sigma_1 - \sigma_2} - \frac{f_1}{\sigma_1}, \tag{23.14}$$

where λ_1^*, λ_2^*, and λ_3^* are the eigenvalues of $\boldsymbol{\sigma}_*$. Also, the arithmetic and harmonic mean bounds imply that

$$f_1\sigma_1 + f_2\sigma_2 \ge \lambda_i^* \ge (f_1/\sigma_1 + f_2/\sigma_2)^{-1} \text{ for } i = 1, 2, 3. \tag{23.15}$$

These bounds were first derived by Murat and Tartar (1985) and by Lurie and Cherkaev (1986) using the translation method, which will described in the next chapter. As we see here, their derivation from the Hashin-Shtrikman variational principles is straightforward [see also Kohn and Milton (1986), Milton and Kohn (1988), and Zhikov (1988, 1991)].

The bounds can be pictured visually in a three-dimensional space where the axes represent λ_1^*, λ_2^*, and λ_3^*. The effective tensor $\boldsymbol{\sigma}_*$ is represented by one of at most six points in this space (each being associated with a different permutation of the eigenvalues), which we also label as $\boldsymbol{\sigma}_*$. The arithmetic and harmonic mean bounds confine this point $\boldsymbol{\sigma}_*$ to lie within a cube. The additional bounds (23.13) and (23.14) further confine $\boldsymbol{\sigma}_*$ to lie within a clam-shaped region that intersects three faces of the cube [which are those faces touching the vertex $(\sigma_a, \sigma_a, \sigma_a)$, where $\sigma_a = f_1\sigma_1 + f_2\sigma_2$].

The bounds taken together completely characterize the G-closure at a fixed volume fraction, that is, the set of all possible (conductivity tensor, volume fraction) pairs associated with composites of phase 1 and phase 2. Tartar (1985) and Lurie and Cherkaev (1986) show that any tensor $\boldsymbol{\sigma}_*$ that is compatible with the bounds is in fact the effective conductivity tensor of some composite obtained by mixing phases 1 and 2 in proportions f_1 and f_2. Points on the lower or upper surface of the clam are attained by assemblages of ellipsoids of phase 1 coated with phase 2 or ellipsoids of phase 2 coated with phase 1, respectively. The edges where the clam surfaces meet the cube faces are attained by assemblages of coated elliptical cylinders (which degenerate to simple laminate microstructures at the corners where these edges intersect). One then takes pairs of diagonal effective tensors $\boldsymbol{\sigma}_*'$ and $\boldsymbol{\sigma}_*''$ on the upper and lower clam surfaces (each corresponding to a coated ellipsoid assemblage) such that $\boldsymbol{\sigma}_*' - \boldsymbol{\sigma}_*''$ is rank 1 (i.e., such that they both lie along a line parallel to the λ_i^*-axis for some $i = 1, 2$ or 3). The effective tensor of any mixture of these two materials necessarily lies on the line joining $\boldsymbol{\sigma}_*'$ and $\boldsymbol{\sigma}_*''$ (see section 5.3 on page 77, where the analogous result is discussed for elasticity) and has the same volume fraction of phase 1. In this way one can reach any point allowed by the bounds. Of course coated laminates can replace the assemblages of coated ellipsoids since they have the same effective tensor; see section 7.8 on page 127. Conditions for the attainability of the multiphase bounds (23.11) and (23.12) have been given by Milton and Kohn (1988).

23.3. Bounds for two-phase, well-ordered materials

Now let us see how these variational principles apply to two-phase materials, without narrowing our attention to conductivity problems alone, or assuming isotropy of the phases or composite. For simplicity we assume that the tensor field $\boldsymbol{L}(\boldsymbol{x})$ takes the form

$$\boldsymbol{L}(\boldsymbol{x}) = \boldsymbol{L}_1\chi_1(\boldsymbol{x}) + \boldsymbol{L}_2\chi_2(\boldsymbol{x}), \quad \text{with } \boldsymbol{L}_1 > \boldsymbol{L}_2 > 0.$$

Tensors $\boldsymbol{L}_1$ and $\boldsymbol{L}_2$ satisfying this condition are called well-ordered. To generate a bound we need to choose a trial polarization field. The simplest choice is one that is constant in phase 1 and zero in phase 2:

$$\underline{\boldsymbol{P}}(\boldsymbol{x}) = \chi_1(\boldsymbol{x})\boldsymbol{v}. \tag{23.16}$$

Substituting this into the Hashin-Shtrikman variational inequality,

$$\langle \boldsymbol{P}_0 \cdot (\boldsymbol{L}_* - \boldsymbol{L}_0)^{-1}\boldsymbol{P}_0\rangle \le \langle \underline{\boldsymbol{P}} \cdot [(\boldsymbol{L} - \boldsymbol{L}_0)^{-1} + \boldsymbol{\Gamma}]\underline{\boldsymbol{P}}\rangle \quad \text{with } \boldsymbol{P}_0 = \langle \underline{\boldsymbol{P}}\rangle, \tag{23.17}$$

gives the bound

$$f_1^2\boldsymbol{v} \cdot (\boldsymbol{L}_* - \boldsymbol{L}_0)^{-1}\boldsymbol{v} \le f_1\boldsymbol{v} \cdot (\boldsymbol{L}_1 - \boldsymbol{L}_0)^{-1}\boldsymbol{v} + \langle \boldsymbol{v} \cdot \chi_1\boldsymbol{\Gamma}\chi_1\boldsymbol{v}\rangle, \tag{23.18}$$

which holds for all choices of $\boldsymbol{L}_0$ which are such that $\boldsymbol{L}_2 > \boldsymbol{L}_0$ and $\boldsymbol{\Gamma}_1\boldsymbol{L}_0\boldsymbol{\Gamma}_1 > 0$. In particular, by letting $\boldsymbol{L}_0$ approach $\boldsymbol{L}_2$ from below and noting that (23.18) holds for all choices of the vector $\boldsymbol{v}$, the bound reduces to

$$f_1(\boldsymbol{L}_* - \boldsymbol{L}_2)^{-1} \leq (\boldsymbol{L}_1 - \boldsymbol{L}_2)^{-1} + (1/f_1)\boldsymbol{\Gamma}_0\chi_1\boldsymbol{\Gamma}\chi_1\boldsymbol{\Gamma}_0, \tag{23.19}$$

where now, because phase 2 is the reference medium,

$$\boldsymbol{\Gamma} = \boldsymbol{\Gamma}_1(\boldsymbol{\Gamma}_1\boldsymbol{L}_2\boldsymbol{\Gamma}_1)^{-1}\boldsymbol{\Gamma}_1.$$

To evaluate the term $\boldsymbol{\Gamma}_0\chi_1\boldsymbol{\Gamma}\chi_1\boldsymbol{\Gamma}_0$ we apply Plancherel's theorem, in the same manner as was done in section 14.2 on page 292, and following Avellaneda (1987) we find that

$$\boldsymbol{\Gamma}_0\chi_1\boldsymbol{\Gamma}\chi_1\boldsymbol{\Gamma}_0 = f_1 f_2 \sum_{\substack{\boldsymbol{\xi} \\ |\boldsymbol{\xi}|=1}} c(\boldsymbol{\xi})\boldsymbol{\Gamma}(\boldsymbol{\xi}), \tag{23.20}$$

where the constants

$$c(\boldsymbol{\xi}) = \frac{1}{f_1 f_2} \sum_{\substack{\boldsymbol{k}\neq 0 \\ \boldsymbol{k}\parallel\boldsymbol{\xi}}} \widehat{\chi}_1^*(\boldsymbol{k})\widehat{\chi}_1(\boldsymbol{k}) = \frac{1}{f_1 f_2} \sum_{\substack{\boldsymbol{k}\neq 0 \\ \boldsymbol{k}\parallel\boldsymbol{\xi}}} \widehat{\chi}_2^*(\boldsymbol{k})\widehat{\chi}_2(\boldsymbol{k}) \tag{23.21}$$

satisfy

$$\sum_{\substack{\boldsymbol{\xi} \\ |\boldsymbol{\xi}|=1}} c(\boldsymbol{\xi}) = 1 \ \text{ and } \ c(\boldsymbol{\xi}) \geq 0 \ \text{ for all } \boldsymbol{\xi}, \tag{23.22}$$

as proved in section 14.2 on page 292. Since the harmonic mean bounds imply that $\boldsymbol{L}_* > \boldsymbol{L}_2$, we can now rewrite the bound (23.19) in the equivalent form

$$\boldsymbol{L}_* > \boldsymbol{L}_2 + f_1\Big[(\boldsymbol{L}_1 - \boldsymbol{L}_2)^{-1} + f_2 \sum_{\substack{\boldsymbol{\xi} \\ |\boldsymbol{\xi}|=1}} c(\boldsymbol{\xi})\boldsymbol{\Gamma}(\boldsymbol{\xi})\Big]^{-1}. \tag{23.23}$$

It follows directly from a simple argument [see, for example, Milton (1986)] that such bounds are necessarily attained whenever the composite is a coated laminate with a core of phase 1 and a coating of phase 2. In these geometries the attainability criterion is met. The field $\boldsymbol{E}(\boldsymbol{x})$ is constant in the core phase, and consequently the trial polarization field (23.16) matches the actual polarization field. What is more remarkable is what Avellaneda (1987) observed, namely, that the constants $c(\boldsymbol{\xi})$ of the coated laminate range over the entire set allowed by (23.22). Given an arbitrary composite there exists a sequential coated laminate that has the same volume fraction f_1 of phase 1 and which has the same set of constants $c(\boldsymbol{\xi})$ as the given composite. In other words, no matter what the geometry of the composite happens to be, there exists an associated coated laminate, with phase 1 as core and phase 2 as coating, having an effective tensor $\boldsymbol{L}_*^-$ such that

$$\boldsymbol{L}_* \geq \boldsymbol{L}_*^-, \tag{23.24}$$

which is just a restatement of the bound (23.23) once one realizes that the right-hand side of (23.23) with the substitution (23.20) matches the effective tensor of the associated coated laminate, as given by (9.46). (See also section 14.2 on page 292.)

By applying the duality principle to obtain a lower bound on $\boldsymbol{L}_*^{-1}$ we see that there exists another associated coated laminate, with phase 2 as core and phase 1 as coating, having an effective tensor $\boldsymbol{L}_*^+$ such that $\boldsymbol{L}_*^{-1} \geq (\boldsymbol{L}_*^+)^{-1}$ or, equivalently, such that

$$\boldsymbol{L}_*^+ \geq \boldsymbol{L}_*. \tag{23.25}$$

Again this coated laminate and the composite share the same volume fraction of phase 1, and they share the same set of constants $c(\boldsymbol{\xi})$. The bounds (23.24) and (23.25) are due to Avellaneda (1987).

In particular, if we are interested in bounds on the energy $W = \boldsymbol{E}_0 \cdot \boldsymbol{L}_* \boldsymbol{E}_0/2$, then (23.24) and the corresponding dual bound imply the bounds

$$W^+ \geq W \geq W^- \tag{23.26}$$

of Willis (1977), where

$$\begin{aligned} W^- &= W^-(\boldsymbol{E}_0, \{c\}, f_1) \\ &= \tfrac{1}{2}\Big\{\boldsymbol{E}_0 \cdot \boldsymbol{L}_2 \boldsymbol{E}_0 + f_1 \boldsymbol{E}_0 \cdot \Big[(\boldsymbol{L}_1 - \boldsymbol{L}_2)^{-1} + f_2 \sum_{\substack{\boldsymbol{\xi} \\ |\boldsymbol{\xi}|=1}} c(\boldsymbol{\xi}) \boldsymbol{\Gamma}(\boldsymbol{\xi})\Big]^{-1} \boldsymbol{E}_0\Big\}, \\ W^+ &= W^+(\boldsymbol{E}_0, \{c\}, f_1) \\ &= \tfrac{1}{2}\Big\{\boldsymbol{E}_0 \cdot \boldsymbol{L}_1 \boldsymbol{E}_0 + f_2 \boldsymbol{E}_0 \cdot \Big[(\boldsymbol{L}_2 - \boldsymbol{L}_1)^{-1} + f_1 \sum_{\substack{\boldsymbol{\xi} \\ |\boldsymbol{\xi}|=1}} c(\boldsymbol{\xi}) \boldsymbol{\Gamma}'(\boldsymbol{\xi})\Big]^{-1} \boldsymbol{E}_0\Big\}, \end{aligned}$$

in which $\{c\}$ represents the set of constants $c(\boldsymbol{\xi})$ defined by (23.21) and

$$\begin{aligned} \boldsymbol{\Gamma}(\boldsymbol{\xi}) &= \boldsymbol{\Gamma}_1(\boldsymbol{\xi})[\boldsymbol{\Gamma}_1(\boldsymbol{\xi}) \boldsymbol{L}_2 \boldsymbol{\Gamma}_1(\boldsymbol{\xi})]^{-1} \boldsymbol{\Gamma}_1(\boldsymbol{\xi}), \\ \boldsymbol{\Gamma}'(\boldsymbol{\xi}) &= \boldsymbol{\Gamma}_1(\boldsymbol{\xi})[\boldsymbol{\Gamma}_1(\boldsymbol{\xi}) \boldsymbol{L}_1 \boldsymbol{\Gamma}_1(\boldsymbol{\xi})]^{-1} \boldsymbol{\Gamma}_1(\boldsymbol{\xi}). \end{aligned}$$

The attainability of the bounds by coated laminates implies that these inequalities in conjunction with (23.22) completely characterize all possible $(W, \boldsymbol{E}_0, \{c\}, f_1)$ quadruplets. In other words, given any volume fraction $f_1 \in (0, 1)$, any set of constants $c(\boldsymbol{\xi})$ compatible with (23.22), an arbitrary applied field $\boldsymbol{E}_0 \in \mathcal{U}$, and any value of W compatible with (23.26), one can find a composite with f_1 as the volume fraction of phase 1, with characteristic function $\chi_1(\boldsymbol{x})$ such that the right-hand side of (23.21) matches the given values of $c(\boldsymbol{\xi})$ and with energy W for the given applied field $\boldsymbol{E}_0$. If the value of W coincides with one of the bounds (23.26), then it suffices to take a coated laminate as our composite; otherwise, we need to laminate together two such coated laminates.

In random composites these bounds can also be expressed in terms of the reduced second-order correlation functions. An analysis essentially the same as that involved in the calculation of the second-order term $\delta \boldsymbol{L}_*^{(2)}$ in the series expansion [see (15.22)] shows that

$$\boldsymbol{\Gamma}_0 \chi_1 \boldsymbol{\Gamma} \chi_1 \boldsymbol{\Gamma}_0 = f_1 f_2 \boldsymbol{\gamma} + \int_{|\boldsymbol{\eta}|=1} \breve{f}_{11}(\boldsymbol{\eta}) \boldsymbol{\Gamma}_\infty(\boldsymbol{\eta}), \tag{23.27}$$

where $\breve{f}_{11}(\boldsymbol{\eta})$ is the reduced second-order correlation function and $\boldsymbol{\gamma} = \langle \boldsymbol{\Gamma}(\boldsymbol{n}) \rangle_{\boldsymbol{n}}$, in which the average is over all unit vectors $\boldsymbol{n}$. Substituting this back into (23.19) gives the optimal

lower Willis bound

$$\boldsymbol{L}_* \geq \boldsymbol{L}_2 + f_1\Big[(\boldsymbol{L}_1 - \boldsymbol{L}_2)^{-1} + f_2\boldsymbol{\gamma} + \frac{1}{f_1}\int_{|\boldsymbol{\eta}|=1} \breve{f}_{11}(\boldsymbol{\eta})\boldsymbol{\Gamma}_\infty(\boldsymbol{\eta})\Big]^{-1},$$

and similarly we have the upper Willis bound

$$\boldsymbol{L}_* \leq \boldsymbol{L}_1 + f_2\Big[(\boldsymbol{L}_2 - \boldsymbol{L}_1)^{-1} + f_1\boldsymbol{\gamma}' + \frac{1}{f_2}\int_{|\boldsymbol{\eta}|=1} \breve{f}_{11}(\boldsymbol{\eta})\boldsymbol{\Gamma}'_\infty(\boldsymbol{\eta})\Big]^{-1},$$

where $\boldsymbol{\gamma}' = \langle \boldsymbol{\Gamma}'(\boldsymbol{n})\rangle_{\boldsymbol{n}}$. Kim and Torquato (1993) found that these bounds were consistent with numerical simulations of the conductivity of composites containing aligned spheroidal inclusions. When the composite is geometrically isotropic, then $\breve{f}_{11}(\boldsymbol{\eta}) = 0$ and the bounds reduce to

$$\boldsymbol{L}_1 + f_2\Big[(\boldsymbol{L}_2 - \boldsymbol{L}_1)^{-1} + f_1\boldsymbol{\gamma}'\Big]^{-1} \geq \boldsymbol{L}_* \geq \boldsymbol{L}_2 + f_1\Big[(\boldsymbol{L}_1 - \boldsymbol{L}_2)^{-1} + f_2\boldsymbol{\gamma}\Big]^{-1}.$$

23.4. Bounds on the energy that involve only the volume fractions

One often seeks bounds that incorporate only the volume fraction f_1 and tensors $\boldsymbol{L}_1$ and $\boldsymbol{L}_2$ but which do not depend on the set of constants $c(\boldsymbol{\xi})$ or, equivalently, which do not depend on the reduced correlation function $\breve{f}_{11}(\boldsymbol{\eta})$.

If we are interested in bounds on the energy $W = \boldsymbol{E}_0 \cdot \boldsymbol{L}_*\boldsymbol{E}_0/2$, then from (23.26) we obtain the bounds

$$\max_{\{c\}} W^+(\boldsymbol{E}_0, \{c\}, f_1) \geq W \geq \min_{\{c\}} W^-(\boldsymbol{E}_0, \{c\}, f_1) \tag{23.28}$$

of Avellaneda (1987), where the maximum and minimum are to be taken over all sets of constants $\{c\}$ satisfying (23.22). Moreover, the optimality of the bounds (23.26) and (23.22) implies the optimality of the bounds (23.28): They completely characterize the set of all possible $(W, \boldsymbol{E}_0, f_1)$ triplets. For the two-phase conductivity problem, with isotropic components with tensors $\sigma_1\boldsymbol{I}$ and $\sigma_2\boldsymbol{I}$, these bounds reduce to those obtained directly from the arithmetic and harmonic mean bounds,

$$(f_1\sigma_1 + f_2\sigma_2)|\boldsymbol{e}_0|^2 \geq \boldsymbol{e}_0 \cdot \boldsymbol{\sigma}_*\boldsymbol{e}_0 \geq (f_1/\sigma_1 + f_2/\sigma_2)^{-1}|\boldsymbol{e}_0|^2,$$

which is not surprising because these bounds are optimal.

For the elasticity problem, one does better with the bounds (23.28) as recognized by Kohn and Lipton (1988), who used this approach to obtain optimal bounds on the energy of mixtures of isotropic incompressible elastic materials. In two dimensions the formulas for the bounds have been explicitly calculated and depend on the eigenvalues ϵ_1 and ϵ_2 of the average strain tensor $\boldsymbol{\epsilon}_0$. Allowing for the phases to be compressible, but assuming that the bulk and shear moduli of the two phases are well-ordered with

$$\kappa_1 > \kappa_2 > 0 \text{ and } \mu_1 > \mu_2 > 0,$$

the formula for the lower bound on the energy is

$$\epsilon_0 \cdot \mathcal{C}_* \epsilon_0 \geq (\epsilon_1+\epsilon_2)^2/(f_1/\kappa_1 + f_2/\kappa_2) + (\epsilon_1-\epsilon_2)^2/(f_1/\mu_1 + f_2/\mu_2)$$
$$\text{if } (\kappa_1-\kappa_2)(f_1\mu_2+f_2\mu_1)|\epsilon_1+\epsilon_2| \leq (\mu_1-\mu_2)(f_1\kappa_2+f_2\kappa_1)|\epsilon_1-\epsilon_2|;$$

$$\epsilon_0 \cdot \mathcal{C}_* \epsilon_0 \geq (\epsilon_1+\epsilon_2)^2(f_1\kappa_1+f_2\kappa_2) + (\epsilon_1-\epsilon_2)^2(f_1\mu_1+f_2\mu_2) - f_1 f_2 \frac{[(\kappa_1-\kappa_2)|\epsilon_1+\epsilon_2| + (\mu_1-\mu_2)|\epsilon_1+\epsilon_2|]^2}{f_1(\mu_2+\kappa_2)+f_2(\mu_1+\kappa_1)}$$
$$\text{if } (\mu_2+f_1\kappa_2+f_2\kappa_1)|\epsilon_1-\epsilon_2| \geq f_2(\kappa_1-\kappa_2)|\epsilon_1+\epsilon_2|$$
$$\text{and } (\kappa_1-\kappa_2)(f_1\mu_2+f_2\mu_1)|\epsilon_1+\epsilon_2| \geq (\mu_1-\mu_2)(f_1\kappa_2+f_2\kappa_1)|\epsilon_1-\epsilon_2|;$$

$$\epsilon_0 \cdot \mathcal{C}_* \epsilon_0 \geq \mu_2(\epsilon_1-\epsilon_2)^2 + \frac{\kappa_1\kappa_2+\mu_2(f_1\kappa_1+f_2\kappa_2)}{\mu_2+f_1\kappa_2+f_2\kappa_1}(\epsilon_1+\epsilon_2)^2$$
$$\text{if } (\mu_2+f_1\kappa_2+f_2\kappa_1)|\epsilon_1-\epsilon_2| \leq f_2(\kappa_1-\kappa_2)|\epsilon_1+\epsilon_2|, \tag{23.29}$$

and the formula for the upper bound is

$$\epsilon_0 \cdot \mathcal{C}_* \epsilon_0 \leq (\epsilon_1+\epsilon_2)^2(f_1\kappa_1+f_2\kappa_2) + (\epsilon_1-\epsilon_2)^2(f_1\mu_1+f_2\mu_2) - f_1 f_2 \frac{[(\kappa_1-\kappa_2)|\epsilon_1+\epsilon_2| - (\mu_1-\mu_2)|\epsilon_1+\epsilon_2|]^2}{f_1(\mu_2+\kappa_2)+f_2(\mu_1+\kappa_1)}$$
$$\text{if } (\mu_1+f_1\kappa_2+f_2\kappa_1)|\epsilon_1-\epsilon_2| \geq f_1(\kappa_1-\kappa_2)|\epsilon_1+\epsilon_2|$$
$$\text{and } (\kappa_1+f_1\mu_2+f_2\mu_1)|\epsilon_1+\epsilon_2| \geq f_1(\mu_1-\mu_2)|\epsilon_1-\epsilon_2|;$$

$$\epsilon_0 \cdot \mathcal{C}_* \epsilon_0 \leq \mu_1(\epsilon_1-\epsilon_2)^2 + \frac{\kappa_1\kappa_2+\mu_1(f_1\kappa_1+f_2\kappa_2)}{\mu_1+f_1\kappa_2+f_2\kappa_1}(\epsilon_1+\epsilon_2)^2$$
$$\text{if } (\mu_1+f_1\kappa_2+f_2\kappa_1)|\epsilon_1-\epsilon_2| \leq f_1(\kappa_1-\kappa_2)|\epsilon_1+\epsilon_2|;$$

$$\epsilon_0 \cdot \mathcal{C}_* \epsilon_0 \leq \kappa_1(\epsilon_1+\epsilon_2)^2 + \frac{\mu_1\mu_2+\kappa_1(f_1\mu_1+f_2\mu_2)}{\kappa_1+f_1\mu_2+f_2\mu_1}(\epsilon_1-\epsilon_2)^2$$
$$\text{if } (\kappa_1+f_1\mu_2+f_2\mu_1)|\epsilon_1+\epsilon_2| \leq f_1(\mu_1-\mu_2)|\epsilon_1-\epsilon_2|. \tag{23.30}$$

These bounds were first obtained by Gibiansky and Cherkaev (1984) using the translation method in the context of the plate equation, and subsequently by Allaire and Kohn (1993a) first using the Hashin-Shtrikman variational principles and then using the translation method. Both papers also give explicit expressions for the optimal bounds when the moduli of the phases are not well-ordered, that is, when $(\kappa_1-\kappa_2)(\mu_1-\mu_2) < 0$. This case is easily treated using the translation method. Grabovsky (1996) has extended these energy bounds to two-phase composites containing anisotropic phases.

Gibiansky and Cherkaev (1984) and Allaire and Kohn (1993a) have addressed the question of what laminate microgeometries achieve these bounds. There are three different regimes in each of the bounds, and the microstructures attaining the bounds change according to the regime. The first regime of (23.29) corresponds to the Reuss-Hill bound and is achieved by rank-1 laminates with two possible orientations relative to the applied strain ϵ_0. The second regime of (23.29) and the first regime of (23.30) are achieved by rank-1 laminates whose layering direction is an eigenvector of ϵ_0.

The bounds in the third regime of (23.29) and the second regime of (23.30) correspond to the bounds of Zhikov (1988, 1991) and Milton and Kohn (1988) when mapped to bounds

on the energy. These will be discussed in the following section. They are achieved by rank-2 laminates, by assemblages of coated ellipses, and by the Vigdergauz periodic microstructure (Vigdergauz 1994; Grabovsky and Kohn 1995a, 1995b).

Finally, the third regime of (23.30) corresponds to a rank-2 laminate with its directions of lamination matching two of the eigenvectors of $\boldsymbol{\epsilon}_0$. One might wonder if there could be some periodic microgeometry with no fine scale structure (like the Vigdergauz structure discussed in 23.9 on page 481) that could replace this second-rank laminate. By considering the limiting case where one phase is void, Allaire and Aubry (1999) have shown that there is no optimal periodic microgeometry in this regime. This is supported by analysis and numerical calculations of Cherkaev, Grabovsky, Movchan, and Serkov (1998), who consider a periodic microgeometry where there is one simply connected hole per unit cell occupying a fixed but very small area of the unit cell. By examining the polarizability tensor, they investigated what shaped hole minimizes the elastic energy when a fixed average stress $\boldsymbol{\tau}_0$ is applied. When $\det(\boldsymbol{\tau}_0)$ is positive [which corresponds to the second regime in (23.30)] the optimal hole turns out to be elliptical. However, when $\det(\boldsymbol{\tau}_0)$ is negative [which corresponds to the third regime in (23.30)] they find the optimal hole is approximately rectangular and is not as effective at minimizing the energy as a second-rank laminate.

The corresponding three-dimensional elastic energy bounds can be reduced to a form requiring the maximization or minimization over all 3×3 symmetric matrices $\boldsymbol{\eta}$. The analysis simplifies if one assumes that the Lame moduli

$$\lambda_1 = \kappa_1 - 2\mu_1/3 \text{ and } \lambda_2 = \kappa_2 - 2\mu_2/3$$

of both phases are positive. The optimal lower and upper bounds on the elastic energy are those given by Allaire and Kohn (1993b),

$$\begin{aligned}
\boldsymbol{\epsilon}_0 \cdot \boldsymbol{\mathcal{C}}_* \boldsymbol{\epsilon}_0 &\geq (\boldsymbol{\epsilon}_0, \boldsymbol{\mathcal{C}}_2 \boldsymbol{\epsilon}_0) + f_1 \max_{\boldsymbol{\eta}} [2\boldsymbol{\epsilon}_0 \cdot \boldsymbol{\eta} - (\boldsymbol{\eta}, (\boldsymbol{\mathcal{C}}_1 - \boldsymbol{\mathcal{C}}_2)^{-1} \boldsymbol{\eta}) - f_2 g(\boldsymbol{\eta})], \\
\boldsymbol{\epsilon}_0 \cdot \boldsymbol{\mathcal{C}}_* \boldsymbol{\epsilon}_0 &\leq (\boldsymbol{\epsilon}_0, \boldsymbol{\mathcal{C}}_1 \boldsymbol{\epsilon}_0) + f_2 \min_{\boldsymbol{\eta}} [2\boldsymbol{\epsilon}_0 \cdot \boldsymbol{\eta} + (\boldsymbol{\eta}, (\boldsymbol{\mathcal{C}}_1 - \boldsymbol{\mathcal{C}}_2)^{-1} \boldsymbol{\eta}) - f_1 h(\boldsymbol{\eta})],
\end{aligned}$$

where $g(\boldsymbol{\eta})$ and $h(\boldsymbol{\eta})$ are functions of the eigenvalues η_1, η_2, and η_3 of the symmetric matrix $\boldsymbol{\eta}$. Assuming that these are labeled with

$$\eta_1 \leq \eta_2 \leq \eta_3,$$

we have

$$\begin{aligned}
g(\boldsymbol{\eta}) &= \frac{(\eta_1 - \eta_3)^2}{4\mu_2} + \frac{(\eta_1 + \eta_3)^2}{4(\lambda_2 + \mu_2)} \text{ if } \eta_3 \geq \frac{\lambda_2 + 2\mu_2}{2(\lambda_2 + \mu_2)}(\eta_1 + \eta_3) \geq \eta_1, \\
g(\boldsymbol{\eta}) &= \frac{\eta_1^2}{\lambda_2 + 2\mu_2} \text{ if } \eta_1 > \frac{\lambda_2 + 2\mu_2}{2(\lambda_2 + \mu_2)}(\eta_1 + \eta_3), \\
g(\boldsymbol{\eta}) &= \frac{\eta_3^2}{\lambda_2 + 2\mu_2} \text{ if } \eta_3 < \frac{\lambda_2 + 2\mu_2}{2(\lambda_2 + \mu_2)}(\eta_1 + \eta_3),
\end{aligned}$$

and

$$h(\boldsymbol{\eta}) = \frac{1}{\lambda_1 + 2\mu_1} \min\{\eta_1^2, \eta_2^2, \eta_3^2\}.$$

An explicit expression for the optimal upper bound has been found for the case of a two-phase composite where one of the phases is void (Allaire 1994a). It reduces to the expression

obtained earlier using the translation method by Gibiansky and Cherkaev (1987), who also obtained explicit expressions for the optimal lower bound when one of the phases is rigid. In other cases the evaluation of the bounds currently requires a simple numerical calculation. For phases that are not well-ordered, optimal lower bounds on the energy were obtained by Allaire and Kohn (1994). The optimal upper bounds are not yet known.

This idea can be extended further, to obtain bounds on sums of energies when the composite is successively subject to n applied fields, $\boldsymbol{E}_0^{(1)}$, $\boldsymbol{E}_0^{(2)}$,... $\boldsymbol{E}_0^{(n)}$. Specifically, let

$$W_\Sigma = \sum_{i=1}^{n} \boldsymbol{E}_0^{(i)} \cdot \boldsymbol{L}_* \boldsymbol{E}_0^{(i)}$$

denote this sum of energies. Then (23.26) implies the bounds

$$\max_{\{c\}} \sum_{i=1}^{n} W^+(\boldsymbol{E}_0^{(i)}, \{c\}, f_1) \geq W_\Sigma \geq \min_{\{c\}} \sum_{i=1}^{n} W^-(\boldsymbol{E}_0^{(i)}, \{c\}, f_1). \tag{23.31}$$

Again these are optimal bounds (Avellaneda 1987). For example, consider the lower bound, and let $\{c^-\}$ denote a set of positive weights $c^-(\boldsymbol{\xi})$ that attains the minimum in (23.31). Since the structure of the sequential coated laminate that attains the bounds (23.22) does not depend on the choice of $\boldsymbol{E}_0$, it follows that the geometry that attains the bounds when $\{c\} = \{c^-\}$ also attains the lower bound (23.32). For a two-dimensional, two-phase elastic composite where one of the phases is void, Cherkaev, Krog, and Küçük (1998) found a way to obtain an explicit formula for the optimal lower bound on a sum of compliance energies. (To obtain the actual formula it is necessary to correct some minor errors in their analysis.)

23.5. Bounds on the effective tensor that involve only the volume fractions

Naturally the inequalities (23.31) imply bounds on the effective tensor $\boldsymbol{L}_*$. Simpler, but equivalent, bounds on $\boldsymbol{L}_*$ can be obtained from (23.18). Taking n successive choices $\boldsymbol{v}_1, \boldsymbol{v}_2, \ldots, \boldsymbol{v}_n$ of $\boldsymbol{v}$, setting $\boldsymbol{L}_0 = \boldsymbol{L}_2$, using (23.20), and adding the resulting inequalities gives

$$f_1 \sum_{i=1}^{n} \boldsymbol{v}_i \cdot (\boldsymbol{L}_* - \boldsymbol{L}_2)^{-1} \boldsymbol{v}_i \leq \sum_{i=1}^{n} \boldsymbol{v}_i \cdot (\boldsymbol{L}_1 - \boldsymbol{L}_2)^{-1} \boldsymbol{v}_i + f_2 \sum_{\substack{\boldsymbol{\xi} \\ |\boldsymbol{\xi}|=1}} c(\boldsymbol{\xi}) \sum_{i=1}^{n} \boldsymbol{v}_i \cdot \boldsymbol{\Gamma}(\boldsymbol{\xi}) \boldsymbol{v}_i, \tag{23.32}$$

which can be rewritten in the equivalent form

$$f_1 \operatorname{Tr}[\boldsymbol{M}(\boldsymbol{L}_* - \boldsymbol{L}_2)^{-1}] \leq \operatorname{Tr}[\boldsymbol{M}(\boldsymbol{L}_1 - \boldsymbol{L}_2)^{-1}] + f_2 \sum_{\substack{\boldsymbol{\xi} \\ |\boldsymbol{\xi}|=1}} c(\boldsymbol{\xi}) \operatorname{Tr}[\boldsymbol{M}\boldsymbol{\Gamma}(\boldsymbol{\xi})], \tag{23.33}$$

where $\boldsymbol{M}$ is the positive-semidefinite matrix

$$\boldsymbol{M} = \sum_{i=1}^{n} \boldsymbol{v}_i \otimes \boldsymbol{v}_i. \tag{23.34}$$

This inequality is valid for all positive-semidefinite choices of $\boldsymbol{M}$ because any such $\boldsymbol{M}$ is expressible in the form (23.34). The $\boldsymbol{v}_i$ can be chosen to be the eigenvectors of $\boldsymbol{M}$ multiplied

by the square root of the corresponding eigenvalue. Since the attainability criterion implies that (23.18) reduces to an equality for all choices of $\boldsymbol{v}$ when $\boldsymbol{L}_0 = \boldsymbol{L}_2$, and the composite is a sequential coated laminate with a core of phase 1 and a coating of phase 2, it follows that the bound (23.33) is attained for these geometries for all choices of $\boldsymbol{M} \geq 0$.

There are special choices of $\boldsymbol{M}$ for which $\mathrm{Tr}[\boldsymbol{M}\boldsymbol{\Gamma}(\boldsymbol{\xi})]$ is independent of $\boldsymbol{\xi}$. These generate a bound that depends only on f_1 and the moduli $\boldsymbol{L}_1$ and $\boldsymbol{L}_2$. In particular, by taking $\boldsymbol{M} = \boldsymbol{L}_2$ and using the fact that $\mathrm{Tr}[\boldsymbol{L}_2\boldsymbol{\Gamma}(\boldsymbol{\xi})] = \ell$ we see the bound reduces to

$$f_1 \,\mathrm{Tr}[\boldsymbol{L}_2(\boldsymbol{L}_* - \boldsymbol{L}_2)^{-1}] \leq \mathrm{Tr}[\boldsymbol{L}_2(\boldsymbol{L}_1 - \boldsymbol{L}_2)^{-1}] + f_2\ell,$$

in which ℓ is the rank of $\boldsymbol{\Gamma}_1(\boldsymbol{k})$, that is, the dimension of the space onto which $\boldsymbol{\Gamma}_1(\boldsymbol{k})$ projects. This bound is attained whenever the composite is a sequential coated laminate with phase 1 as core and phase 2 as coating. Therefore all such sequential coated laminates are optimal composites whose effective tensors lie on the "lower boundary" of the G-closure at constant volume fraction. Similarly we have the complementary bound,

$$f_2 \,\mathrm{Tr}[\boldsymbol{L}_1(\boldsymbol{L}_1 - \boldsymbol{L}_*)^{-1}] \leq \mathrm{Tr}[\boldsymbol{L}_1(\boldsymbol{L}_1 - \boldsymbol{L}_2)^{-1}] - f_1\ell,$$

which is attained whenever the composite is a sequential coated laminate with phase 2 as core and phase 1 as coating. We see that these too are optimal composites whose effective tensors lie on the "upper boundary" of the G-closure at constant volume fraction.

For example, in a two-phase composite with (possibly anisotropic) component conductivity tensors $\boldsymbol{\sigma}_1$ and $\boldsymbol{\sigma}_2$ having fixed orientation and satisfying $\boldsymbol{\sigma}_1 \geq \boldsymbol{\sigma}_2$, the effective conductivity tensor $\boldsymbol{\sigma}_*$ satisfies the bounds

$$\begin{aligned} f_1 \,\mathrm{Tr}[\boldsymbol{\sigma}_2(\boldsymbol{\sigma}_* - \boldsymbol{\sigma}_2)^{-1}] &\leq \mathrm{Tr}[\boldsymbol{\sigma}_2(\boldsymbol{\sigma}_1 - \boldsymbol{\sigma}_2)^{-1}] + f_2, \\ f_2 \,\mathrm{Tr}[\boldsymbol{\sigma}_1(\boldsymbol{\sigma}_1 - \boldsymbol{\sigma}_*)^{-1}] &\leq \mathrm{Tr}[\boldsymbol{\sigma}_1(\boldsymbol{\sigma}_1 - \boldsymbol{\sigma}_2)^{-1}] - f_1 \end{aligned} \tag{23.35}$$

of Milton and Kohn (1988), which generalize the Murat-Tartar-Lurie-Cherkaev bounds (23.13) and (23.14). In addition, the effective tensor $\boldsymbol{\sigma}_*$ must of course also satisfy the arithmetic and harmonic mean bounds,

$$f_1\boldsymbol{\sigma}_1 + f_2\boldsymbol{\sigma}_2 \geq \boldsymbol{\sigma}_* \geq [f_1\boldsymbol{\sigma}_1^{-1} + f_2\boldsymbol{\sigma}_2^{-1}]^{-1}. \tag{23.36}$$

In fact, the set of bounds (23.35) and (23.36) are optimal (Grabovsky 1993). They completely describe the set of all possible effective tensors $\boldsymbol{\sigma}_*$. It is easy to see that the coated ellipsoid assemblages and the coated sequential laminates saturate either one of the two bounds in (23.35), and it requires a little more work to show that any tensor $\boldsymbol{\sigma}_*$ that is compatible with (23.35) and (23.36) is in fact the effective conductivity tensor of a composite.

For the three-dimensional elasticity problem in a composite with two isotropic phases, the bounds are correlation function independent for any isotropic fourth-order tensor

$$\boldsymbol{M} = \alpha_h\boldsymbol{\Lambda}_h + \alpha_s\boldsymbol{\Lambda}_s \;\text{ with } \alpha_h \geq 0, \;\; \alpha_s \geq 0, \tag{23.37}$$

in which $\boldsymbol{\Lambda}_h$ and $\boldsymbol{\Lambda}_s = \boldsymbol{I} - \boldsymbol{\Lambda}_h$ are the isotropic fourth-order tensors, with elements

$$\{\boldsymbol{\Lambda}_h\}_{ijk\ell} = \tfrac{1}{3}\delta_{ij}\delta_{k\ell}, \quad \{\boldsymbol{\Lambda}_s\}_{ijk\ell} = \tfrac{1}{2}[\delta_{ik}\delta_{j\ell} + \delta_{i\ell}\delta_{kj}] - \tfrac{1}{3}\delta_{ij}\delta_{k\ell} \tag{23.38}$$

that act as projections. The tensor $\boldsymbol{\Lambda}_h$ projects onto the one-dimensional space of matrices proportional to the second-order identity matrix, while $\boldsymbol{\Lambda}_s$ projects onto the five-dimensional space of trace free matrices.

Let us suppose that the phases have bulk moduli κ_1 and κ_2 and shear moduli μ_1 and μ_2, satisfying

$$\kappa_1 \geq \kappa_2, \quad \mu_1 \geq \mu_2.$$

This ensures that the elasticity tensors

$$\mathcal{C}_1 = 3\kappa_1 \mathbf{\Lambda}_h + 2\mu_1 \mathbf{\Lambda}_s \text{ and } \mathcal{C}_2 = 3\kappa_2 \mathbf{\Lambda}_h + 2\mu_2 \mathbf{\Lambda}_s$$

of the two phases are well-ordered with $\mathcal{C}_1 \geq \mathcal{C}_2$. To evaluate $\mathrm{Tr}[M\mathbf{\Gamma}(\boldsymbol{\xi})]$ it suffices to work in a basis where the x_1-axis is chosen aligned with $\boldsymbol{\xi}$. When $\mathcal{C}_2$ is chosen as the reference tensor we see from (23.38) and (9.59) that

$$\begin{aligned}
\mathrm{Tr}[\mathbf{\Lambda}_h \mathbf{\Gamma}(\boldsymbol{\xi})] &= \frac{1}{3\kappa_2 + 4\mu_2}, \\
\mathrm{Tr}[\mathbf{\Lambda}_s \mathbf{\Gamma}(\boldsymbol{\xi})] &= \mathrm{Tr}[\mathbf{\Gamma}(\boldsymbol{\xi})] - \mathrm{Tr}[\mathbf{\Lambda}_h \mathbf{\Gamma}(\boldsymbol{\xi})] = \frac{3(\kappa_2 + 2\mu_2)}{\mu_2(3\kappa_2 + 4\mu_2)},
\end{aligned}$$

implying that

$$\mathrm{Tr}[M\mathbf{\Gamma}(\boldsymbol{\xi})] = \frac{\alpha_h}{3\kappa_2 + 4\mu_2} + \frac{3(\kappa_2 + 2\mu_2)\alpha_s}{\mu_2(3\kappa_2 + 4\mu_2)}.$$

In particular, by setting $M = \mathbf{\Lambda}_h$, we obtain the lower "bulk modulus type bound,"

$$f_1 \,\mathrm{Tr}[\mathbf{\Lambda}_h (\mathcal{C}_* - \mathcal{C}_2)^{-1}] \leq \frac{1}{3(\kappa_1 - \kappa_2)} + \frac{f_2}{3\kappa_2 + 4\mu_2}, \tag{23.39}$$

and by setting $M = \mathbf{\Lambda}_s$, we obtain the lower "shear modulus type bound,"

$$f_1 \,\mathrm{Tr}[\mathbf{\Lambda}_s (\mathcal{C}_* - \mathcal{C}_2)^{-1}] \leq \frac{5}{2(\mu_1 - \mu_2)} + \frac{3(\kappa_2 + 2\mu_2) f_2}{\mu_2(3\kappa_2 + 4\mu_2)}. \tag{23.40}$$

When $\mathcal{C}_1$, $\mathcal{C}_2$, and $\mathcal{C}_*$ are represented as 6×6 matrices as in (2.6), these bounds should be applied with $\mathbf{\Lambda}_h$ and $\mathbf{\Lambda}_s$ represented as the 6×6 matrices,

$$\mathbf{\Lambda}_h = \begin{pmatrix} 1/3 & 1/3 & 1/3 & 0 & 0 & 0 \\ 1/3 & 1/3 & 1/3 & 0 & 0 & 0 \\ 1/3 & 1/3 & 1/3 & 0 & 0 & 0 \\ 0 & 0 & 0 & 0 & 0 & 0 \\ 0 & 0 & 0 & 0 & 0 & 0 \\ 0 & 0 & 0 & 0 & 0 & 0 \end{pmatrix}, \quad \mathbf{\Lambda}_s = \begin{pmatrix} 2/3 & -1/3 & -1/3 & 0 & 0 & 0 \\ -1/3 & 2/3 & -1/3 & 0 & 0 & 0 \\ -1/3 & -1/3 & 2/3 & 0 & 0 & 0 \\ 0 & 0 & 0 & 1 & 0 & 0 \\ 0 & 0 & 0 & 0 & 1 & 0 \\ 0 & 0 & 0 & 0 & 0 & 1 \end{pmatrix},$$

and the trace should be calculated as the usual trace of a 6×6 matrix. When the effective elasticity tensor $\mathcal{C}_*$ is isotropic these reduce to the familiar Hashin-Shtrikman (1963b) lower bounds on the effective bulk modulus κ_* and effective shear modulus μ_*, respectively,

$$\begin{aligned}
\frac{f_1}{3(\kappa_* - \kappa_2)} &\leq \frac{1}{3(\kappa_1 - \kappa_2)} + \frac{f_2}{3\kappa_2 + 4\mu_2}, \\
\frac{5 f_1}{2(\mu_* - \mu_2)} &\leq \frac{5}{2(\mu_1 - \mu_2)} + \frac{3(\kappa_2 + 2\mu_2) f_2}{\mu_2(3\kappa_2 + 4\mu_2)},
\end{aligned} \tag{23.41}$$

which can be rewritten in the equivalent forms

$$\begin{aligned}
\kappa_* &\geq f_1\kappa_1 + f_2\kappa_2 - \frac{f_1 f_2 (\kappa_1 - \kappa_2)^2}{f_2\kappa_1 + f_1\kappa_2 + 4\mu_2/3}, \\
\mu_* &\geq f_1\mu_1 + f_2\mu_2 - \frac{f_1 f_2 (\mu_1 - \mu_2)^2}{f_2\mu_1 + f_1\mu_2 + \mu_2(9\kappa_2 + 8\mu_2)/[6(\kappa_2 + 2\mu_2)]}.
\end{aligned} \tag{23.42}$$

The bulk modulus bound was found independently by Hill (1963) using a different approach [which did not depend on the sign of $(\kappa_1 - \kappa_2)(\mu_1 - \mu_2)$]. For two-dimensional composites (fiber reinforced materials) analogous bounds on the effective elastic moduli were found by Hill (1964) and Hashin (1965b).

Other choices of $\boldsymbol{M}$ of the form (23.37) do not generate any new bounds. They generate bounds that are linear combinations of the above ones, and therefore do not impose any additional constraints on the possible values of $\mathcal{C}_*$. Geometrically, in a 21-dimensional space, where the axes label the different elements of the symmetric 6×6 matrix representing $(\mathcal{C}_* - \mathcal{C}_2)^{-1}$, the inequalities (23.39) and (23.40) each restrict $(\mathcal{C}_* - \mathcal{C}_2)^{-1}$ to lie on one side of a hyperplane. The elastic tensors $\mathcal{C}_*$ of coated laminate materials, with a core of phase 1 and a coating of phase 2, attain both bounds and therefore correspond to points within the 19-dimensional space at the intersection of both hyperplanes. In fact, Avellaneda (1987) has shown that the elastic tensors $\mathcal{C}_*$ of such laminates correspond to points in a 14-dimensional linear space within this 19-dimensional space.

Similar expressions are obtained when $\mathcal{C}_1$ is chosen as a reference tensor, but with the role of $\mathcal{C}_2$ replaced by $\mathcal{C}_1$ and with the signs of the inequalities reversed. We obtain the upper "bulk modulus type bound,"

$$f_2 \operatorname{Tr}[\boldsymbol{\Lambda}_h(\mathcal{C}_1 - \mathcal{C}_*)^{-1}] \leq \frac{1}{3(\kappa_1 - \kappa_2)} - \frac{f_1}{3\kappa_1 + 4\mu_1}, \tag{23.43}$$

and the upper "shear modulus type bound,"

$$f_2 \operatorname{Tr}[\boldsymbol{\Lambda}_s(\mathcal{C}_1 - \mathcal{C}_*)^{-1}] \leq \frac{5}{2(\mu_1 - \mu_2)} - \frac{3(\kappa_1 + 2\mu_1) f_1}{\mu_1(3\kappa_1 + 4\mu_1)}, \tag{23.44}$$

which reduce to the Hashin-Shtrikman (1963b) upper bounds

$$\begin{aligned} \kappa_* &\leq f_1\kappa_1 + f_2\kappa_2 - \frac{f_1 f_2(\kappa_1 - \kappa_2)^2}{f_2\kappa_1 + f_1\kappa_2 + 4\mu_1/3}, \\ \mu_* &\leq f_1\mu_1 + f_2\mu_2 - \frac{f_1 f_2(\mu_1 - \mu_2)^2}{f_2\mu_1 + f_1\mu_2 + \mu_1(9\kappa_1 + 8\mu_1)/[6(\kappa_1 + 2\mu_1)]} \end{aligned} \tag{23.45}$$

when the composite is isotropic. The upper and lower bulk and shear modulus type bounds (23.39), (23.40), (23.43), and (23.44) for elastically anisotropic composites were obtained independently by Zhikov (1988, 1991) and Milton and Kohn (1988).

Hashin and Shtrikman (1963b) noticed that the lower bulk modulus bound coincided with the effective bulk modulus κ_* of the coated sphere assemblage, as given by (7.13). They also noticed that the upper bulk modulus bound is attained by a similar microgeometry, but with the roles of the phases interchanged. Milton (1981b) found that the bulk modulus bound for multiphase materials could also be realized by sphere assemblages in certain parameter regimes. The realizability of the shear modulus bounds for two-phase media with $(\kappa_1 - \kappa_2)(\mu_1 - \mu_2) > 0$ remained an open question until Roscoe (1973) [see also Norris (1985) and Milton (1986)] found that they were attained by a hierarchical microstructure corresponding to the differential scheme with randomly oriented platelike inclusions (see section 10.9 on page 204). Francfort and Murat (1986) found that they were attained by finite-rank laminate microstructures. The reason why these microstructures attain the bounds is simply, first, that the strain field within one phase is constant and, second, that the structures have sufficient symmetry to ensure that they are elastically isotropic (Milton 1986). Figure 23.2 on the next page shows the first stages in the construction of an infinite-rank laminate attaining one of the shear modulus bounds. Interestingly Lukkassen (1999) [see also Braides and Lukkassen

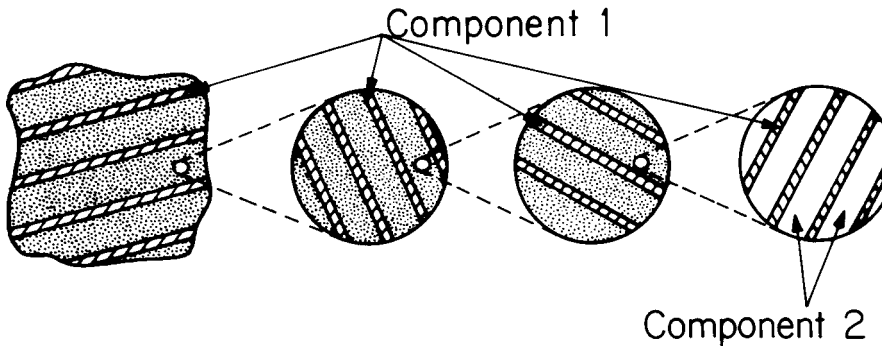

Figure 23.2. The first stages in the construction of an infinite-rank laminate corresponding to the stiffest elastically isotropic material that can be manufactured from two components with bulk moduli $\kappa_1 > \kappa_2$ and shear moduli $\mu_1 > \mu_2$ mixed in fixed proportions f_1 and $f_2 = 1 - f_1$. At each stage in the construction an infinitesimal volume fraction of component 1 is introduced until the desired volume fraction f_1 of phase 1 is reached. The effective moduli κ_* and μ_* of this structure, as calculated using the differential scheme (see section 10.9 on page 204), coincide with the Hashin-Shtrikman bounds. Reprinted with permission from Milton (1986). Copyright 1986, Springer-Verlag.

(2000)] proved that certain reiterated cell structures also attain the bounds. Instead of adding layers with varying orientations at successively larger and larger length scales, one inserts appropriate thin walled cell structures at successively larger and larger length scales. Inserting a thin walled cell structure with, say, cubic cells has the same effect as layering in three orthogonal directions on three widely separated length scales. Gibiansky and Sigmund (2000) found that the shear modulus bounds for multiphase materials could also be realized by hierarchical or finite-rank microstructures in certain parameter regimes. Zhikov (1991) proved that the Hashin sphere assemblage cannot attain the shear modulus bounds.

When both phases and hence the composite are incompressible, the lower and upper "shear modulus type bounds" imply that

$$\sum_{i=1}^{5} \frac{f_2}{2(\mu_{*i} - \mu_2)} \le \frac{5}{2(\mu_1 - \mu_2)} + \frac{3(\kappa_2 + 2\mu_2) f_2}{\mu_2(3\kappa_2 + 4\mu_2)},$$
$$\sum_{i=1}^{5} \frac{f_2}{2(\mu_1 - \mu_{*i})} \le \frac{5}{2(\mu_1 - \mu_2)} - \frac{3(\kappa_1 + 2\mu_1) f_1}{\mu_1(3\kappa_1 + 4\mu_1)}, \tag{23.46}$$

in which the $\mu_{*i}, i = 1, 2, \ldots, 5$ are the five shear moduli of $\mathcal{C}_*$ representing the eigenvalues of $\mathcal{C}_*/2$. Associated with each shear modulus μ_{*i} is a trace free average strain $\boldsymbol{\epsilon}_0^{(i)}$ such that the resulting trace free average stress in the composite is

$$\mathcal{C}_* \boldsymbol{\epsilon}_0^{(i)} = 2\mu_{*i} \boldsymbol{\epsilon}_0^{(i)}.$$

I presented these bounds (23.46) in 1986 at a symposium on nonclassical continuum mechanics in Durham, England. They were also obtained by Lipton (1988, 1992), who proved that in two dimensions they provide a complete set of bounds, characterizing the set of all possible effective elasticity tensors.

As another example, suppose that the composite has cubic symmetry, that is, $\mathcal{C}_*$ takes the form

$$\mathcal{C}_* = 3\kappa_*\mathbf{\Lambda}_h + 2\mu_{*1}\mathbf{\Lambda}_{s1} + 2\mu_{*2}\mathbf{\Lambda}_{s2},$$

where κ_* is the effective bulk modulus, μ_{*1} and μ_{*2} are the two effective shear moduli, and $\mathbf{\Lambda}_{s1}$ and $\mathbf{\Lambda}_{s1}$ are the fourth-order projection tensors with elements

$$\{\mathbf{\Lambda}_{s1}\}_{ijk\ell} = \tfrac{1}{2}[\delta_{ik}\delta_{j\ell} + \delta_{i\ell}\delta_{kj}] - \delta_{ijk\ell}, \quad \{\mathbf{\Lambda}_{s2}\}_{ijk\ell} = \delta_{ijk\ell} - \tfrac{1}{3}\delta_{ij}\delta_{k\ell},$$

where $\delta_{ijk\ell}$ equals one if $i = j = k = \ell$ and is zero otherwise. The tensor $\mathbf{\Lambda}_{s1}$ projects onto the three-dimensional space of trace free matrices with zero diagonal elements while $\mathbf{\Lambda}_{s2}$ projects onto the two-dimensional space of diagonal trace free matrices. The bounds on κ_* remain the same as those given by Hashin and Shtrikman (1963b), while the bounds (23.40) and (23.44) imply that

$$\begin{aligned}
\frac{3f_1}{2(\mu_{*1}-\mu_2)} + \frac{f_1}{(\mu_{*2}-\mu_2)} &\le \frac{5}{2(\mu_1-\mu_2)} + \frac{3(\kappa_2+2\mu_2)f_2}{\mu_2(3\kappa_2+4\mu_2)}, \\
\frac{3f_2}{2(\mu_1-\mu_{*1})} + \frac{f_2}{(\mu_1-\mu_{*2})} &\le \frac{5}{2(\mu_1-\mu_2)} - \frac{3(\kappa_1+2\mu_1)f_1}{\mu_1(3\kappa_1+4\mu_1)}.
\end{aligned} \tag{23.47}$$

Thus a measurement μ_{*1} can give information about μ_{*2}, and vice versa. Other uncoupled bounds on the shear moduli μ_{*1} and μ_{*2} have been obtained by Avellaneda (1987). For composites with transverse isotropy or orthotropic symmetry, various bounds on the moduli have been obtained by Lipton (1991, 1992, 1994) and Lipton and Northrup (1994).

When more than two phases are present, or the phases are not well-ordered, or they are anisotropic, the lower bulk modulus type bound (23.39) generalizes to

$$\begin{aligned}
&\{(3\kappa_0+4\mu_0)\,\mathrm{Tr}[\mathbf{\Lambda}_h(\mathcal{C}_*-\mathcal{C}_0)^{-1}]+1\}^{-1} \\
&\quad \ge \langle\{(3\kappa_0+4\mu_0)\,\mathrm{Tr}[\mathbf{\Lambda}_h(\mathcal{C}(\boldsymbol{x})-\mathcal{C}_0)^{-1}]+1\}^{-1}\rangle,
\end{aligned} \tag{23.48}$$

while the lower shear modulus type bound (23.40) generalizes to

$$\begin{aligned}
&\{2\mu_0(3\kappa_0+4\mu_0)\,\mathrm{Tr}[\mathbf{\Lambda}_s(\mathcal{C}_*-\mathcal{C}_0)^{-1}] \;+\; 6(\kappa_0+2\mu_0)\}^{-1} \\
&\quad \ge \langle\{2\mu_0(3\kappa_0+4\mu_0)\,\mathrm{Tr}[\mathbf{\Lambda}_s(\mathcal{C}(\boldsymbol{x}) \;-\; \mathcal{C}_0)^{-1}]+6(\kappa_0+2\mu_0)\}^{-1}\rangle,
\end{aligned} \tag{23.49}$$

where the isotropic reference elasticity tensor $\mathcal{C}_0$ with bulk modulus $\kappa_0 > 0$ and shear modulus $\mu_0 > 0$ is chosen so that $\mathcal{C}(\boldsymbol{x}) \ge \mathcal{C}_0$ for all $\boldsymbol{x}$. By taking an isotropic reference tensor with $\mathcal{C}_0 \ge \mathcal{C}(\boldsymbol{x})$ for all $\boldsymbol{x}$ one obtains upper bounds that take the same form as (23.48) and (23.49) but with the sign of the inequalities reversed; see Milton (1990) and Zhikov (1991) for further details. We will refer to (23.39), (23.40), (23.48), and (23.49) and the corresponding upper bounds as trace bounds.

When only two isotropic phases are present with non-well-ordered moduli

$$\kappa_2 \ge \kappa_1 > 0, \quad \mu_1 \ge \mu_2 > 0,$$

one recovers the bounds of Hill (1963) and Walpole (1966) by setting $\kappa_0 = \kappa_1$ and $\mu_0 = \mu_2$ in the bounds (23.48) and (23.49), and setting $\kappa_0 = \kappa_2$ and $\mu_0 = \mu_1$ in the corresponding upper bounds. Hill's bulk modulus bounds are given by the inequalities (23.42) and (23.45) and are attained by assemblages of coated spheres. Walpole's shear modulus bounds are given by

$$\begin{aligned}
\mu_* &\ge f_1\mu_1 + f_2\mu_2 - \frac{f_1 f_2(\mu_1-\mu_2)^2}{f_2\mu_1 + f_1\mu_2 + \mu_2(9\kappa_1+8\mu_2)/[6(\kappa_1+2\mu_2)]}, \\
\mu_* &\le f_1\mu_1 + f_2\mu_2 - \frac{f_1 f_2(\mu_1-\mu_2)^2}{f_2\mu_1 + f_1\mu_2 + \mu_1(9\kappa_2+8\mu_1)/[6(\kappa_2+2\mu_1)]}.
\end{aligned} \tag{23.50}$$

For two-dimensional composites (fiber reinforced materials) analogous bounds on the effective elastic moduli were found by Hill (1964) and Walpole (1969). In two dimensions it is still not known whether these bounds of Walpole are attained or not, although Sigmund (2000) has found microgeometries that come close to achieving the bound. In three dimensions Milton (1981a) and Milton and Phan-Thien (1982) have obtained bounds that are always tighter than those of Walpole but which do not include any additional information about the composite microgeometry; see section 26.4 on page 558. Thus the three-dimensional Walpole bounds can never be attained.

Other positive-semidefinite choices of the matrix $\boldsymbol{M}$ are also possible and generate additional bounds. For a two-phase composite with well-ordered tensors $\boldsymbol{L}_1 > \boldsymbol{L}_2 > 0$, a bound that is independent of the correlation functions for a general choice of $\boldsymbol{M}$ can easily be obtained. Following an idea of Khachaturyan (1966, 1983) and Kohn and Lipton (1988), we take the infimum of the right-hand side of (23.33) as the set of positive weights $c(\boldsymbol{\xi})$ are varied over the entire set allowed by (23.22). Clearly the weights should be concentrated in those directions $\boldsymbol{\xi}$ for which $\mathrm{Tr}[\boldsymbol{M}\boldsymbol{\Gamma}(\boldsymbol{\xi})]$ is at a maximum, giving

$$\sup_{\{c\}} c(\boldsymbol{\xi})\,\mathrm{Tr}[\boldsymbol{M}\boldsymbol{\Gamma}(\boldsymbol{\xi})] = r(\boldsymbol{M}), \quad \text{where } r(\boldsymbol{M}) = \max_{\substack{\boldsymbol{\xi} \\ |\boldsymbol{\xi}|=1}} \mathrm{Tr}[\boldsymbol{M}\boldsymbol{\Gamma}(\boldsymbol{\xi})]. \tag{23.51}$$

This generates the lower trace bound

$$f_1\,\mathrm{Tr}[\boldsymbol{M}(\boldsymbol{L}_* - \boldsymbol{L}_2)^{-1}] \le \mathrm{Tr}[\boldsymbol{M}(\boldsymbol{L}_1 - \boldsymbol{L}_2)^{-1}] + f_2 r(\boldsymbol{M}) \tag{23.52}$$

on the effective tensor $\boldsymbol{L}_*$. By taking $\boldsymbol{L}_1$ as the reference tensor, we obtain the corresponding upper trace bound. These generalized trace bounds (Milton and Kohn 1988) have been extended further by Allaire (1994b) to allow for matrices $\boldsymbol{M}$ that are not positive-semidefinite.

23.6. Bounds for two-phase composites with non-well-ordered tensors†

When the moduli $\boldsymbol{L}_1$ and $\boldsymbol{L}_2$ are not well-ordered, that is, when $\boldsymbol{L}_1 - \boldsymbol{L}_2$ is neither positive- nor negative-semidefinite, we cannot set $\boldsymbol{L}_0 = \boldsymbol{L}_1$ or set $\boldsymbol{L}_0 = \boldsymbol{L}_2$ and maintain the inequality $\boldsymbol{L} > \boldsymbol{L}_0$. Consequently, it is necessary to consider other choices of $\boldsymbol{L}_0$. For such values of $\boldsymbol{L}_0$ there is no reason to restrict the choice of polarization fields to those that are zero in phase 2. It is more appropriate to take a trial polarization field that is piecewise constant,

$$\underline{\boldsymbol{P}}(\boldsymbol{x}) = \chi_1(\boldsymbol{x})\boldsymbol{w}_1 + \chi_2(\boldsymbol{x})\boldsymbol{w}_2. \tag{23.53}$$

Then to obtain a bound we need to make three choices, namely, the choice of $\boldsymbol{w}_1$, the choice of $\boldsymbol{w}_2$, and the choice of a reference tensor $\boldsymbol{L}_0$ satisfying

$$\boldsymbol{L}_1 > \boldsymbol{L}_0, \quad \boldsymbol{L}_2 > \boldsymbol{L}_0, \quad \boldsymbol{\Gamma}_1\boldsymbol{L}_0\boldsymbol{\Gamma}_1 \ge 0.$$

This choice can be narrowed in an optimal way, down to the choice of $\boldsymbol{L}_0$ and the field $\boldsymbol{w}_1 - \boldsymbol{w}_2$, once one recognizes that the only difficult term to evaluate in the variational inequality is the nonlocal term

$$\langle \underline{\boldsymbol{P}} \cdot \boldsymbol{\Gamma}_1 \underline{\boldsymbol{P}} \rangle = (\boldsymbol{w}_1 - \boldsymbol{w}_2) \cdot \Big\langle \chi_1 \boldsymbol{\Gamma} \chi_1 (\boldsymbol{w}_1 - \boldsymbol{w}_2) \Big\rangle,$$

which depends only on the difference $\boldsymbol{w} = \boldsymbol{w}_1 - \boldsymbol{w}_2$. So we may as well vary $\boldsymbol{w}_1$ while keeping $\boldsymbol{w}$ fixed to make the variational inequality as tight as possible. This is basically the

same strategy as we employed in section 13.5 on page 278 to find the optimal choice of applied field $\boldsymbol{E}_0$ for a given trial polarization field $\underline{\boldsymbol{P}}$.

Let us begin [following Gibiansky and Milton (1993)] by considering a completely general trial polarization field $\underline{\boldsymbol{P}}(\boldsymbol{x})$, which we express in the form

$$\underline{\boldsymbol{P}}(\boldsymbol{x}) = \boldsymbol{P}_0 + \boldsymbol{P}'(\boldsymbol{x}), \quad \text{where } \langle \boldsymbol{P}' \rangle = 0.$$

Substituting this into the variational inequality (23.17) and placing the nonlocal term on the left-hand side of the equation gives

$$\begin{aligned} \langle \boldsymbol{P}' \cdot \boldsymbol{\Gamma} \boldsymbol{P}' \rangle \geq\ & \boldsymbol{P}_0 \cdot [(\boldsymbol{L}_* - \boldsymbol{L}_0)^{-1} - f_1(\boldsymbol{L}_1 - \boldsymbol{L}_0)^{-1} - f_2(\boldsymbol{L}_2 - \boldsymbol{L}_0)^{-1}]\boldsymbol{P}_0 \\ & -2\boldsymbol{P}_0 \cdot \langle (\boldsymbol{L} - \boldsymbol{L}_0)^{-1} \boldsymbol{P}' \rangle - \langle \boldsymbol{P}' \cdot (\boldsymbol{L} - \boldsymbol{L}_0)^{-1} \boldsymbol{P}' \rangle. \end{aligned} \tag{23.54}$$

The matrix $[(\boldsymbol{L}_* - \boldsymbol{L}_0)^{-1} - f_1(\boldsymbol{L}_1 - \boldsymbol{L}_0)^{-1} - f_2(\boldsymbol{L}_2 - \boldsymbol{L}_0)^{-1}]$ appearing here is clearly negative-semidefinite, as can be seen by substituting $\boldsymbol{P}' = 0$ into this inequality. For simplicity let us assume that it is strictly negative-definite. Then the choice of $\boldsymbol{P}_0$ that maximizes the right-hand side of the above equation is

$$\boldsymbol{P}_0 = [(\boldsymbol{L}_* - \boldsymbol{L}_0)^{-1} - f_1(\boldsymbol{L}_1 - \boldsymbol{L}_0)^{-1} - f_2(\boldsymbol{L}_2 - \boldsymbol{L}_0)^{-1}]^{-1} \langle (\boldsymbol{L} - \boldsymbol{L}_0)^{-1} \boldsymbol{P}' \rangle.$$

Inserting this back in (23.54) gives the bound

$$\begin{aligned} \langle \boldsymbol{P}' \cdot \boldsymbol{\Gamma} \boldsymbol{P}' \rangle \geq & -\langle \boldsymbol{P}' \cdot (\boldsymbol{L} - \boldsymbol{L}_0)^{-1} \boldsymbol{P}' \rangle \\ & + \langle (\boldsymbol{L} - \boldsymbol{L}_0)^{-1} \boldsymbol{P}' \rangle \cdot [f_1(\boldsymbol{L}_1 - \boldsymbol{L}_0)^{-1} + f_2(\boldsymbol{L}_2 - \boldsymbol{L}_0)^{-1} - (\boldsymbol{L}_* - \boldsymbol{L}_0)^{-1}]^{-1} \langle (\boldsymbol{L} - \boldsymbol{L}_0)^{-1} \boldsymbol{P}' \rangle. \end{aligned}$$

In particular, when the trial polarization field is given by (23.53), then

$$\begin{aligned} \boldsymbol{P}'(\boldsymbol{x}) = (\chi_1(\boldsymbol{x}) - f_1)\boldsymbol{w} &= f_2 \boldsymbol{w} \quad \text{in phase 1,} \\ &= -f_1 \boldsymbol{w} \quad \text{in phase 2,} \end{aligned}$$

and it follows that

$$\begin{aligned} \langle (\boldsymbol{L} - \boldsymbol{L}_0)^{-1} \boldsymbol{P}' \rangle &= f_1 f_2 [(\boldsymbol{L}_1 - \boldsymbol{L}_0)^{-1} - (\boldsymbol{L}_2 - \boldsymbol{L}_0)^{-1}]\boldsymbol{w}, \\ \langle \boldsymbol{P}' \cdot (\boldsymbol{L} - \boldsymbol{L}_0)^{-1} \boldsymbol{P}' \rangle &= f_1 f_2 \boldsymbol{w} \cdot [f_2(\boldsymbol{L}_1 - \boldsymbol{L}_0)^{-1} + f_1(\boldsymbol{L}_2 - \boldsymbol{L}_0)^{-1}]\boldsymbol{w}. \end{aligned}$$

Consequently the bound becomes

$$\frac{1}{f_1 f_2} \langle \boldsymbol{w} \cdot \chi_1 \boldsymbol{\Gamma} \chi_1 \boldsymbol{w} \rangle \geq \boldsymbol{w} \cdot \boldsymbol{Y}((\boldsymbol{L}_* - \boldsymbol{L}_0)^{-1}, (\boldsymbol{L}_1 - \boldsymbol{L}_0)^{-1}, (\boldsymbol{L}_2 - \boldsymbol{L}_0)^{-1})\boldsymbol{w},$$

and in view of the identities (19.5) and (19.6) satisfied by the Y-transformation, this simplifies to

$$\frac{1}{f_1 f_2} \langle \boldsymbol{w} \cdot \chi_1 \boldsymbol{\Gamma} \chi_1 \boldsymbol{w} \rangle \geq \boldsymbol{w} \cdot (\boldsymbol{Y}_* + \boldsymbol{L}_0)^{-1} \boldsymbol{w}, \tag{23.55}$$

where $\boldsymbol{Y}_*$ is the Y-tensor given by (19.3).

This bound is clearly equivalent to the bound (19.47) derived directly from the variational principles for the Y-tensor.

We will prove in section 24.10 on page 516 that $\boldsymbol{Y}_* + \boldsymbol{L}_0$ is necessarily positive-semi-definite for all choices of $\boldsymbol{L}_0$ that are quasiconvex and such that $\boldsymbol{L}_1 - \boldsymbol{L}_0$ and $\boldsymbol{L}_2 - \boldsymbol{L}_0$ are

positive-semidefinite. Using this fact and the relation (23.20) we see that (23.55) can be rewritten as

$$\boldsymbol{Y}_* + \boldsymbol{L}_0 \geq [\sum_{\substack{\boldsymbol{\xi} \\ |\boldsymbol{\xi}|=1}} c(\boldsymbol{\xi})\boldsymbol{\Gamma}(\boldsymbol{\xi})]^{-1},$$

where the inverse is to be taken on the space $\mathcal{U}$.

For random composites, this bound can be expressed in terms of the reduced second-order correlation function:

$$\boldsymbol{Y}_* + \boldsymbol{L}_0 \geq \Big[\boldsymbol{\gamma} + \frac{1}{f_1 f_2}\int_{|\boldsymbol{\eta}|=1} \breve{f}_{11}(\boldsymbol{\eta})\boldsymbol{\Gamma}_\infty(\boldsymbol{\eta})\Big]^{-1},$$

and when the composite is geometrically isotropic this simplifies to the bound

$$\boldsymbol{Y}_* + \boldsymbol{L}_0 \geq \boldsymbol{\gamma}^{-1}.$$

Of course, instead of taking just one trial field, we can take a succession of trial fields and add together the resulting inequalities. In the same way that (23.18) implies (23.33), so too does (23.55) imply that the bound

$$\mathrm{Tr}[\boldsymbol{M}(\boldsymbol{Y}_* + \boldsymbol{L}_0)^{-1}] \leq \sum_{\substack{\boldsymbol{\xi} \\ |\boldsymbol{\xi}|=1}} c(\boldsymbol{\xi})\,\mathrm{Tr}[\boldsymbol{M}\boldsymbol{\Gamma}(\boldsymbol{\xi})]$$

is valid for all choices of positive-semidefinite matrices $\boldsymbol{M}$. Again special choices of $\boldsymbol{M}$ lead to bounds that do not depend on the set of constants $c(\boldsymbol{\xi})$. For example, by taking $\boldsymbol{M} = \boldsymbol{L}_0$ we obtain the inequality

$$\mathrm{Tr}[\boldsymbol{L}_0(\boldsymbol{Y}_* + \boldsymbol{L}_0)^{-1}] \leq \ell.$$

For other positive-semidefinite choices of $\boldsymbol{M}$ we can use (23.51) to obtain a bound that does not depend on the correlation functions:

$$\mathrm{Tr}[\boldsymbol{M}(\boldsymbol{Y}_* + \boldsymbol{L}_0)^{-1}] \leq r(\boldsymbol{M}). \tag{23.56}$$

This trace bound reduces to the trace bound (23.52) when $\boldsymbol{L}_1 > \boldsymbol{L}_2$ and $\boldsymbol{L}_0 = \boldsymbol{L}_2$.

23.7. Bounding the complex effective moduli of an isotropic composite of two isotropic phases†

As an example of the application of the bounds in the previous section, let us use them to bound the complex dielectric constant of an isotropic, three-dimensional composite of two isotropic phases. We have seen in section 11.5 on page 234 that the Cherkaev-Gibiansky transformation allows us to express the constitutive law for the complex dielectric equations in the form

$$\begin{pmatrix} \mathrm{Im}(\boldsymbol{e}) \\ \mathrm{Im}(\boldsymbol{d}) \end{pmatrix} = \boldsymbol{\mathcal{L}} \begin{pmatrix} -\mathrm{Re}(\boldsymbol{d}) \\ \mathrm{Re}(\boldsymbol{e}) \end{pmatrix} \text{ with } \boldsymbol{\mathcal{L}} = \begin{pmatrix} [\boldsymbol{\varepsilon}'']^{-1} & [\boldsymbol{\varepsilon}'']^{-1}\boldsymbol{\varepsilon}' \\ \boldsymbol{\varepsilon}'[\boldsymbol{\varepsilon}'']^{-1} & \boldsymbol{\varepsilon}'' + \boldsymbol{\varepsilon}'[\boldsymbol{\varepsilon}'']^{-1}\boldsymbol{\varepsilon}' \end{pmatrix}. \tag{23.57}$$

In a composite comprised of two isotropic phases, with complex dielectric constants $\varepsilon_1 = \varepsilon_1' + i\varepsilon_1''$ and $\varepsilon_2 = \varepsilon_2' + i\varepsilon_2''$, the associated tensors

$$\boldsymbol{\mathcal{L}}_1 = \begin{pmatrix} \boldsymbol{I}/\varepsilon_1'' & \varepsilon_1'\boldsymbol{I}/\varepsilon_1'' \\ \varepsilon_1'\boldsymbol{I}/\varepsilon_1'' & \varepsilon_1''\boldsymbol{I} + (\varepsilon_1')^2\boldsymbol{I}/\varepsilon_1'' \end{pmatrix}, \quad \boldsymbol{\mathcal{L}}_2 = \begin{pmatrix} \boldsymbol{I}/\varepsilon_2'' & \varepsilon_2'\boldsymbol{I}/\varepsilon_2'' \\ \varepsilon_2'\boldsymbol{I}/\varepsilon_2'' & \varepsilon_2''\boldsymbol{I} + (\varepsilon_2')^2\boldsymbol{I}/\varepsilon_2'' \end{pmatrix}$$

are not well-ordered, each having unit determinant. If the composite itself is isotropic, with complex dielectric constant $\varepsilon_* = \varepsilon'_* + i\varepsilon''_*$, one can show [following Gibiansky and Milton (1993)] that the Y-tensor associated with $\boldsymbol{\mathcal{L}}(\boldsymbol{x})$ is

$$\boldsymbol{\mathcal{Y}}_* = \begin{pmatrix} \boldsymbol{I}/y''_\varepsilon & -y'_\varepsilon \boldsymbol{I}/y''_\varepsilon \\ -y'_\varepsilon \boldsymbol{I}/y''_\varepsilon & y''_\varepsilon \boldsymbol{I} + (y'_\varepsilon)^2 \boldsymbol{I}/y''_\varepsilon \end{pmatrix},$$

where

$$y_\varepsilon = y'_\varepsilon + iy''_\varepsilon = -f_2\varepsilon_1 - f_1\varepsilon_2 + \frac{f_1 f_2(\varepsilon_1 - \varepsilon_2)^2}{f_1\varepsilon_1 + f_2\varepsilon_2 - \varepsilon_*}$$

is the complex y-parameter associated with ε_*. (The formula for $\boldsymbol{\mathcal{Y}}_*$ in terms of y_ε is quite similar to the formula for $\boldsymbol{\mathcal{L}}_1$ and $\boldsymbol{\mathcal{L}}_2$ in terms of ε_1 and ε_2, except for the appearance of the minus signs in the off-diagonal blocks.)

Let us take as a reference medium the isotropic tensor

$$\boldsymbol{\mathcal{L}}_0 = \begin{pmatrix} \alpha_1 \boldsymbol{I} & \alpha_2 \boldsymbol{I} \\ \alpha_2 \boldsymbol{I} & \alpha_3 \boldsymbol{I} \end{pmatrix},$$

where the parameters α_1, α_2, and α_3 remain to be chosen. The differential constraints on the fields appearing in the constitutive law (23.57) imply that

$$\boldsymbol{\Gamma}_1(\boldsymbol{\xi}) = \begin{pmatrix} \boldsymbol{I} - \boldsymbol{\xi} \otimes \boldsymbol{\xi} & 0 \\ 0 & \boldsymbol{\xi} \otimes \boldsymbol{\xi} \end{pmatrix}$$

for all unit vectors $\boldsymbol{\xi}$. Consequently, the Γ-operator associated with the reference medium is

$$\boldsymbol{\Gamma}(\boldsymbol{\xi}) = \boldsymbol{\Gamma}_1(\boldsymbol{\xi})[\boldsymbol{\Gamma}_1(\boldsymbol{\xi})\boldsymbol{\mathcal{L}}_0\boldsymbol{\Gamma}_1(\boldsymbol{\xi})]^{-1}\boldsymbol{\Gamma}_1(\boldsymbol{\xi}) = \begin{pmatrix} (\boldsymbol{I} - \boldsymbol{\xi} \otimes \boldsymbol{\xi})/\alpha_1 & 0 \\ 0 & \boldsymbol{\xi} \otimes \boldsymbol{\xi}/\alpha_3 \end{pmatrix},$$

and the quasiconvexity requirement that $\boldsymbol{\Gamma}_1\boldsymbol{\mathcal{L}}_0\boldsymbol{\Gamma}_1$ be positive-semidefinite will be satisfied if and only if α_1 and α_3 are both nonnegative.

With an isotropic tensor $\boldsymbol{\mathcal{M}}$ of the form

$$\boldsymbol{\mathcal{M}} = \begin{pmatrix} w_1^2 \boldsymbol{I} & w_1 w_2 \boldsymbol{I} \\ w_1 w_2 \boldsymbol{I} & w_2^2 \boldsymbol{I} \end{pmatrix},$$

where w_1 and w_2 are arbitrary scalars, a simple calculation shows that

$$\mathrm{Tr}[\boldsymbol{\mathcal{M}}(\boldsymbol{\mathcal{Y}}_* + \boldsymbol{\mathcal{L}}_0)^{-1}] = 3 \begin{pmatrix} w_1 & w_2 \end{pmatrix} \boldsymbol{G}^{-1} \begin{pmatrix} w_1 \\ w_2 \end{pmatrix}, \quad r(\boldsymbol{\mathcal{M}}) = \begin{pmatrix} w_1 & w_2 \end{pmatrix} \boldsymbol{A} \begin{pmatrix} w_1 \\ w_2 \end{pmatrix},$$

in which $\boldsymbol{G}$ and $\boldsymbol{A}$ are the 2×2 matrices

$$\boldsymbol{G} = \begin{pmatrix} \alpha_1 + 1/y''_\varepsilon & \alpha_2 - y'_\varepsilon/y''_\varepsilon \\ \alpha_2 - y'_\varepsilon/y''_\varepsilon & \alpha_3 + y''_\varepsilon + (y'_\varepsilon)^2/y''_\varepsilon \end{pmatrix}, \quad \boldsymbol{A} = \begin{pmatrix} 2/\alpha_1 & 0 \\ 0 & 1/\alpha_3 \end{pmatrix}.$$

Since the bounds (23.56) hold for every choice of w_1 and w_2, we have the matrix inequality $3\boldsymbol{G}^{-1} \le \boldsymbol{A}$. The positive-semidefiniteness of $\boldsymbol{G}$ (which is implied by the positive-semidefiniteness of $\boldsymbol{\mathcal{Y}}_* + \boldsymbol{\mathcal{L}}_0$ when $\boldsymbol{\mathcal{L}}_0$ is quasiconvex and $\boldsymbol{\mathcal{L}}_1 - \boldsymbol{\mathcal{L}}_0$ and $\boldsymbol{\mathcal{L}}_2 - \boldsymbol{\mathcal{L}}_0$ are both positive-semidefinite) allows us to rewrite this as $\boldsymbol{G} \ge 3\boldsymbol{A}^{-1}$ or, equivalently,

$$\begin{pmatrix} 1/y''_\varepsilon - \alpha_1/2 & \alpha_2 - y'_\varepsilon/y''_\varepsilon \\ \alpha_2 - y'_\varepsilon/y''_\varepsilon & y''_\varepsilon + (y'_\varepsilon)^2/y''_\varepsilon - 2\alpha_3 \end{pmatrix} \ge 0.$$

This matrix inequality bears a close resemblance to the constraints

$$\begin{pmatrix} 1/\varepsilon_1'' - \alpha_1 & \varepsilon_1'/\varepsilon_1'' - \alpha_2 \\ \varepsilon_1'/\varepsilon_1'' - \alpha_2 & \varepsilon_1'' + (\varepsilon_1')^2/\varepsilon_1'' - \alpha_3 \end{pmatrix} \geq 0,$$
$$\begin{pmatrix} 1/\varepsilon_2'' - \alpha_1 & \varepsilon_2'/\varepsilon_2'' - \alpha_2 \\ \varepsilon_2'/\varepsilon_2'' - \alpha_2 & \varepsilon_2'' + (\varepsilon_2')^2/\varepsilon_2'' - \alpha_3 \end{pmatrix} \geq 0,$$

which are necessary and sufficient to ensure the positive-semidefiniteness of $\boldsymbol{\mathcal{L}}_1 - \boldsymbol{\mathcal{L}}_0$ and $\boldsymbol{\mathcal{L}}_2 - \boldsymbol{\mathcal{L}}_0$. This resemblance can be made closer by changing basis so that the matrix inequality reads

$$\begin{pmatrix} 2/y_\varepsilon'' - \alpha_1 & y_\varepsilon'/y_\varepsilon'' - \alpha_2 \\ y_\varepsilon'/y_\varepsilon'' - \alpha_2 & y_\varepsilon''/2 + (y_\varepsilon')^2/2y_\varepsilon'' - \alpha_3 \end{pmatrix} \geq 0.$$

In other words, if

$$\boldsymbol{M}(z) = \begin{pmatrix} 1/z'' - \alpha_1 & z'/z'' - \alpha_2 \\ z'/z'' - \alpha_2 & z'' + (z')^2/z'' - \alpha_3 \end{pmatrix}$$

is positive-semidefinite for $z = z'' + iz'' = \varepsilon_1$ and for $z = \varepsilon_2$, then it is also positive-semidefinite for $z = y_\varepsilon/2$. A necessary condition for positive-semidefiniteness is that the determinant be nonnegative, which, assuming that $z'' > 0$, reduces to the inequality

$$(\alpha_1 z'' + \alpha_2^2 - \alpha_1\alpha_3)(1/\alpha_1 - z'') - \alpha_1(z' - \alpha_2/\alpha_1)^2 \geq 0. \tag{23.58}$$

It confines z to a lie inside a disk D centered along the line $z' = \alpha_2/\alpha_1$ and intersecting this line at $z'' = 1/\alpha_1$ and at $z'' = \alpha_3 - \alpha_2^2/\alpha_1$. Conversely, given a disk D intersecting the upper half-plane $z'' > 0$, we can find parameters α_1, α_2, and α_3, with $\alpha_1 > 0$, such that the disk lies below and tangent to the line $z'' = 1/\alpha_1$ (which determines α_1), is centered on the line $z' = \alpha_2/\alpha_1$ (which determines α_2), and intersects this line at $z'' = 1/\alpha_1$ and at $z'' = \alpha_3 - \alpha_2^2/\alpha_1$ (which determines α_3). The idea now is to interpret the constraints and inequalities in terms of the disk D. Since the leading diagonal element of $\boldsymbol{M}(z)$ is positive when $1/\alpha_1'' \geq z'' \geq 0$, the matrix $\boldsymbol{M}(z)$ will be positive-definite if and only if z is in the upper half-plane and inside the disk D. The positivity of α_1 and α_3 is guaranteed provided that the disk D intersects the upper half-plane and does not contain the origin; that is, (23.58) must be violated when $z' = z'' = 0$.

Thus we obtain a geometrical interpretation of the bounds: Any disk D containing the points ε_1 and ε_2 and not containing the origin must necessarily contain the point $y_\varepsilon/2$. (Notice that the disk must necessarily intersect the upper half-plane because ε_1 and ε_2 lie in the upper half-plane.) It follows that $y_\varepsilon/2$ lies inside the region of intersection of all such disks, that is, $y_\varepsilon/2$ must lie in the lens-shaped region bounded on one side by the straight line joining ε_1 and ε_2 and on the other side by the circular arc joining ε_1 and ε_2, which when extended passes through the origin. This bound was first obtained using the analytic method (Milton 1980; Bergman 1980); see figure 27.1 on page 570, where the region $\boldsymbol{\Omega}$ represents this bound.

The advantage of the variational approach is that it can be easily applied to bounding the complex bulk modulus κ_* and complex shear modulus μ_* of an isotropic, three-dimensional composite of two isotropic viscoelastic phases with complex bulk moduli κ_1 and κ_2 and complex shear moduli μ_1 and μ_2. The bounds are best expressed in terms of the y-parameters

$$y_\kappa = -f_2\kappa_1 - f_1\kappa_2 + \frac{f_1 f_2(\kappa_1 - \kappa_2)^2}{f_1\kappa_1 + f_2\kappa_2 - \kappa_*}, \quad y_\mu = -f_2\mu_1 - f_1\mu_2 + \frac{f_1 f_2(\mu_1 - \mu_2)^2}{f_1\mu_1 + f_2\mu_2 - \mu_*}.$$

Gibiansky and Milton (1993) have shown that the bulk y-parameter y_κ lies inside any disk in the complex plane that contains the points $4\mu_1/3$ and $4\mu_2/3$ but which does not contain

the origin and the points $-\kappa_1$ and $-\kappa_2$. To find the best bounds implied by these bounds one should draw the straight line joining $4\mu_1/3$ to $4\mu_2/3$ and the three circular arcs joining $4\mu_1/3$ and $4\mu_2/3$, which when extended pass through the origin, the point $-\kappa_1$, or the point $-\kappa_2$. The outermost pair of these four curves defines the boundary of a lens-shaped region within which y_κ is confined to lie; see figure 23.3. When the arc whose extension passes through

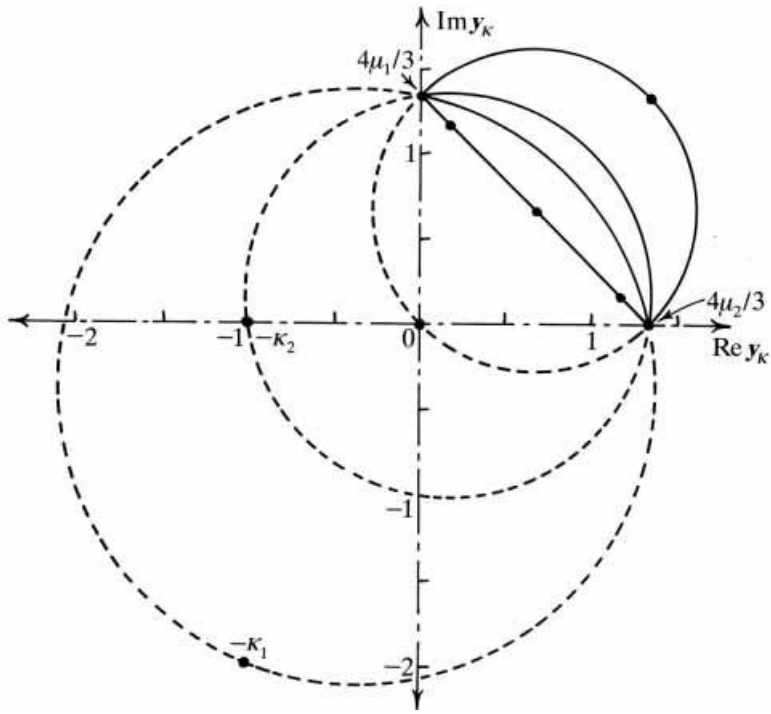

Figure 23.3. The construction of the bounds on y_κ, as described in the text, for a three-dimensional composite of two isotropic phases with complex elastic moduli $(\kappa_1, \mu_1) = (1 + 2i, i)$ and $(\kappa_2, \mu_2) = (1, 1)$. The various points marked as solid dots on the straight line and outermost circular arc correspond to the values of y_κ for particular microgeometries. Reprinted from Gibiansky and Milton (1993).

$-\kappa_1$ (or $-\kappa_2$) is outermost, then this bound is optimal, being attained by doubly coated sphere assemblages. Various points on the straight line and on the circular arc whose extension passes through the origin also correspond to specific microgeometries. When the volume fraction f_1 of phase 1 is unknown one can take the union of the resulting lens-shaped regions in the κ_*-plane as f_1 ranges between 0 and 1. Gibiansky and Lakes (1993) showed that this union is itself lens-shaped and given by a simple geometric construction with κ_1 and κ_2 at the corners of the lens.

Milton and Berryman (1997) have shown that the shear y-parameter y_μ lies inside any disk that does not contain the origin but contains the four points $\gamma(c)\mu_1$, $\gamma(c)\mu_2$, $\gamma(c)\kappa_1/c$, and $\gamma(c)\kappa_2/c$ for some nonnegative value of c, where $\gamma(c) = (8 + 9c)/6(2 + c)$. The region of intersection of all such disks as c varies is not lens-shaped, but an algorithm is provided for constructing it. Bounds on the complex bulk and shear moduli of two-dimensional, two-phase

viscoelastic composites are also available (Gibiansky and Milton 1993; Gibiansky, Milton, and Berryman 1999).

23.8. Using quasiconformal mappings to obtain bounds

Suppose that we have a two-dimensional isotropic composite composed of an isotropic material, phase 0, with conductivity $\sigma_0 \boldsymbol{I}$ occupying a volume fraction f_0 mixed with a polycrystalline material assembled from a crystal having a conductivity tensor with eigenvalues λ_1 and λ_2 such that $\lambda_2 > \lambda_1 > 0$ and $\sigma_0 \geq \sqrt{\lambda_1\lambda_2}$. To obtain a lower bound on the effective conductivity $\boldsymbol{\sigma}_* = \sigma_* \boldsymbol{I}$ of this mixture we follow an argument of Astala and Nesi (2001). Briefly, the quasiconformal mapping introduced in section 8.6 on page 152 is used to map to an equivalent conductivity problem where the conductivity tensor $\boldsymbol{\sigma}'(\boldsymbol{x}')$ is locally isotropic and then the Hashin-Shtrikman bounds are applied to this problem.

The isotropy of the original composite implies the isotropy of the effective tensor $\boldsymbol{\sigma}_*^Q$ associated with the conductivity tensor field $\boldsymbol{\sigma}^Q(\boldsymbol{x}) = \boldsymbol{\sigma}(\boldsymbol{x})/\sqrt{\det \boldsymbol{\sigma}(\boldsymbol{x})}$, and because $\det \boldsymbol{\sigma}_*^Q = 1$ it follows that $\boldsymbol{\sigma}_*^Q = \boldsymbol{I}$. Hence (8.29) implies that $\boldsymbol{\sigma}'_* = \sigma_* \boldsymbol{I}$. After the quasiconformal mapping we see from (8.28) that phase 0 will maintain its conductivity $\sigma_0 \boldsymbol{I}$ while the polycrystalline phase will now have conductivity $\sqrt{\lambda_1\lambda_2}\boldsymbol{I}$. We let f_0' denote the volume fraction occupied by phase 0 after the quasiconformal mapping. Applying the Hashin-Shtrikman lower bound (23.5) to this two-dimensional mixture of two isotropic conducting phases gives

$$\sigma_* \geq \sqrt{\lambda_1\lambda_2} + \frac{2f_0'(\sigma_0 - \sqrt{\lambda_1\lambda_2})\sqrt{\lambda_1\lambda_2}}{2\sqrt{\lambda_1\lambda_2} + (\sigma_0 - \sqrt{\lambda_1\lambda_2})(1 - f_0')}. \tag{23.59}$$

For this bound to be useful we need to find some formula that relates the volume fractions f_0' and f_0. Astala and Nesi (2001) show that there is a maximal area distortion under such K-quasiconformal mappings giving the inequality

$$f_0' \leq f_0^K, \quad \text{where } K = \sqrt{\lambda_2/\lambda_1} > 1. \tag{23.60}$$

Substituting this back into (23.59) produces the bound of Nesi (1996):

$$\sigma_* \geq \sqrt{\lambda_1\lambda_2} + \frac{2f_0^K(\sigma_0 - \sqrt{\lambda_1\lambda_2})\sqrt{\lambda_1\lambda_2}}{2\sqrt{\lambda_1\lambda_2} + (\sigma_0 - \sqrt{\lambda_1\lambda_2})(1 - f_0^K)}, \tag{23.61}$$

which is optimal, being attained by an assemblage of circles with a core of phase 0 and a polycrystalline coating [see equation (7.34)].

The above argument involves a little "cheating," since Astala and Nesi use (23.61) [or more specifically its generalization to anisotropic composites (Milton and Nesi 1999)] to prove (23.60). However the argument shows the usefulness of formulas for the maximal area distortion of quasiconformal mappings for establishing the bound (23.61). In a major advance, Astala (1994) and Erëmenko and Hamilton (1995) obtained bounds on the area distortion associated with a certain large class of quasiconformal mappings: Astala, following a conjecture of Gehring and Reich (1966), found a bound with the optimal exponent K while Eremenko and Hamilton established the bound with the optimal exponent and optimal prefactor, under some normalization condition. Each mapping $\boldsymbol{x}'(\boldsymbol{x}) = (\phi^Q(\boldsymbol{x}), \psi^Q(\boldsymbol{x}))$ in this class is associated with the potentials that solve the conductivity equations (8.25) in a medium containing a single circular disk with conductivity $\boldsymbol{\sigma}^Q(\boldsymbol{x})$ satisfying $\det \boldsymbol{\sigma}^Q(\boldsymbol{x}) = 1$ and having bounded eigenvalues surrounded by a material with conductivity $\boldsymbol{\sigma}^Q(\boldsymbol{x}) = \boldsymbol{I}$ subject to

a uniform applied field at infinity. Nesi (1996) used these bounds to establish (23.61). It is hoped that, at some time in the future, a direct proof of (23.60) will be found, thereby validating the alternative argument of Astala and Nesi presented here.

23.9. Optimal two-dimensional microgeometries: Reduction to a Dirichlet problem†

The microgeometries attaining the two-phase Hashin-Shtrikman conductivity bounds (23.6) and (23.10) or the more general Murat-Tartar-Lurie-Cherkaev bounds (23.13) and (23.14) are certainly not unique. The coated ellipsoid geometries are quite different than the sequential laminate microgeometries, yet they both attain the bound. There is nonuniqueness even within each class of microstructure: There are many ways to pack the coated ellipsoids to fill all space and many possible orderings of the direction of lamination in the sequential laminate that lead to the same effective tensor. In three dimensions the question of what other microgeometries attain these bounds is still unresolved. However, in two dimensions there is a systematic procedure for generating these optimal microstructures. The key idea is to reinterpret the problem as a Dirichlet problem for x_2 (with x_1 being the conjugate harmonic function) on a domain consisting of a periodic array of parallel slits, with appropriately chosen potentials as coordinates, as illustrated in figure 23.4. This approach is commonly used to solve two-dimensional free boundary problems; see, for example, Saffman and Taylor (1958).

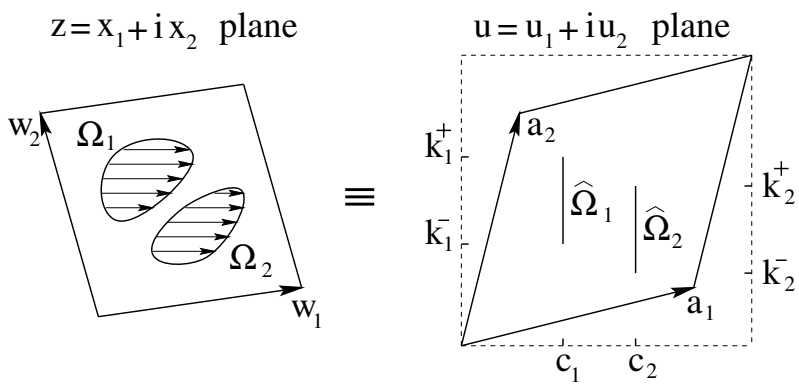

Figure 23.4. Finding a two-dimensional periodic microgeometry attaining the conductivity bounds is equivalent to solving a Dirichlet problem on a domain consisting of a periodic array of parallel slits, with a prescribed potential that varies linearly along each slit. In this example the unit cell contains $m = 2$ inclusions of phase 1, within which the polarization field $\boldsymbol{p}(\boldsymbol{x}) = \boldsymbol{j}(\boldsymbol{x}) - \sigma_2\boldsymbol{e}(\boldsymbol{x})$ is uniform.

Let us look for a two-dimensional conducting composite of two isotropic phases that attains the two-dimensional version of the bounds (23.13):

$$f_1 \sum_{i=1}^{2} \frac{1}{\lambda_i^* - \sigma_2} \leq \frac{2}{\sigma_1 - \sigma_2} + \frac{f_2}{\sigma_2}. \tag{23.62}$$

We suppose that the composite geometry is periodic and such that a given unit cell Ω contains (for example) m inclusions of phase 1, which we label as Ω_j, $j = 1, 2, \ldots, m$. Without loss

of generality let us suppose that phase 2 has conductivity $\sigma_2 = 1$. The attainability criterion tells us that the electric field within phase 1 must necessarily be constant no matter what the direction of the applied field. Let us direct our applied electric field so that the electric field within phase 1 is aligned parallel to the x_1-axis. We then set $z = x_1 + ix_2$ and introduce two complex numbers, $w_1 = w_1' + w_1''$ and $w_2 = w_2' + w_2''$, representing the lattice vectors of periodicity of the microstructure. The electric potential $\phi(z)$ within phase 2 is the sum of a periodic function and a function that is linear in x_1 and x_2, that is, it satisfies the conditions

$$\begin{aligned}
\phi(z + w_1) &= \phi(z) + a_1'(\sigma_1 - 1) + w_1'\alpha \qquad \text{for all } z,\\
\phi(z + w_2) &= \phi(z) + a_2'(\sigma_1 - 1) + w_2'\alpha \qquad \text{for all } z,\\
\phi(z) &= \alpha x_1 + c_j(\sigma_1 - 1) \ \text{ for } z \in \partial\Omega_j \quad \text{for all } j,
\end{aligned}$$

for appropriate choices of the real constants a_1', a_2', $c_1, c_2, \ldots, c_m$ and α where $\partial\Omega_j$ and denotes the boundary of inclusion Ω_j. Here the terms $w_1'\alpha$, $w_2'\alpha$ and the factors of $(\sigma_1 - 1)$ have been introduced to simplify subsequent calculations.

Now, since the current field $\boldsymbol{j}(\boldsymbol{x})$ is divergence free, there exists a continuous potential $\psi(\boldsymbol{x})$ such that $\boldsymbol{j} = \boldsymbol{R}_\perp \nabla\psi$. Within phase 2 this potential satisfies the conditions

$$\begin{aligned}
\psi(z + w_1) &= \psi(z) + a_1''(\sigma_1 - 1) + w_1''\alpha \qquad \text{for all } z,\\
\psi(z + w_2) &= \psi(z) + a_2''(\sigma_1 - 1) + w_2''\alpha \qquad \text{for all } z,\\
\psi(z) &= \alpha\sigma_1 x_2 + d_j(\sigma_1 - 1) \ \text{ for } z \in \partial\Omega_j \quad \text{for all } j,
\end{aligned}$$

for appropriate choices of the real constants a_1'', a_2'', and $d_1, d_2, \ldots, d_m$.

Also, because $\sigma_2 = 1$ the constitutive relation $\boldsymbol{j}(\boldsymbol{x}) = \boldsymbol{\sigma}(\boldsymbol{x})\boldsymbol{e}(\boldsymbol{x})$ within phase 2 reduces to the Cauchy-Riemann equation, $\boldsymbol{R}_\perp \nabla\psi = \nabla\phi$, which implies that $\phi + i\psi$ is an analytic function of $z = x_1 + ix_2$ inside phase 2. The complex potential

$$u(z) = u_1(z) + iu_2(z) = (\phi + i\psi - \alpha z)/(\sigma_1 - 1) \tag{23.63}$$

is also an analytic function of z and satisfies the conditions

$$\begin{aligned}
u(z + w_1) &= u(z) + a_1, \quad u(z + w_2) = u(z) + a_2 \quad \text{for all } z,\\
u_1(z) &= c_j, \quad u_2(z) = \alpha x_2 + d_j \ \text{ for } z \in \partial\Omega_j \quad \text{for all } j,
\end{aligned}$$

where $a_1 = a_1' + ia_1''$ and $a_2 = a_2' + ia_2''$.

Now assume that the function $u(z)$ is univalent [i.e., that $u(z_1) = u(z_2)$ implies $z_1 = z_2$] and consider $z = x_1 + ix_2$ as an analytic function of $u = u_1 + iu_2$. It satisfies

$$\begin{aligned}
z(u + a_1) &= z(u) + w_1, \quad z(u + a_2) = z(u) + w_2 \ \text{ for all } u,\\
x_2(u) &= (u_2 - d_j)/\alpha \ \text{ when } u \in \widehat{\Omega}_j \quad \text{for all } j,
\end{aligned}$$

where $\widehat{\Omega}_j$, for $j = 1, 2, \ldots, m$, is the slit

$$\widehat{\Omega}_j = \{u = iu_1 + iu_2 \mid u_1 = c_j \text{ and } k_j^+ \geq u_2 \geq k_j^-\}$$

parallel to the u_2-axis in the complex u-plane and

$$k_j^+ = \max_{z\in\partial\Omega_j}\{u_2(z)\}, \quad k_j^- = \min_{z\in\partial\Omega_j}\{u_2(z)\}.$$

The function $x_2(u)$ is not periodic. To obtain a periodic harmonic function with prescribed values on the slits we introduce the analytic function

$$g(u) = (a_1' a_2'' - a_1'' a_2')z(u) + (w_1'' \overline{a}_2 - w_2'' \overline{a}_1)u, \tag{23.64}$$

where $\overline{a}_1 = a_1' - i a_1''$ and $\overline{a}_2 = a_2' - i a_2''$. It has an imaginary part

$$g_2(u) = (a_1' a_2'' - a_1'' a_2')x_2(u) - (w_1'' a_2'' - w_2'' a_1'')u_1 + (w_1'' a_2' - w_2'' a_1')u_2,$$

satisfying

$$\begin{aligned} g_2(u + a_1) &= g_2(u), \quad g_2(u + a_2) = g_2(u) \quad \text{for all } u, \\ g_2(u) &= u_2 - e_j \quad \text{when } u \in \widehat{\Omega}_j \quad \text{for all } j, \end{aligned} \tag{23.65}$$

where

$$e_j = d_j(a_1' a_2'' - a_1'' a_2')/\alpha + c_j(w_1'' a_2'' - w_2'' a_1''), \tag{23.66}$$

and we have assumed without loss of generality (by adjusting the magnitude of the applied field if necessary) that

$$\alpha = (a_1' a_2'' - a_1'' a_2')/(1 - w_1'' a_2' + w_2'' a_1'), \tag{23.67}$$

to ensure that the coefficient of u_2 along the slits in (23.65) equals 1. Thus the function $g_2(u)$ is harmonic and periodic in u (with lattice vectors a_1 and a_2) and has prescribed values on the slits $\widehat{\Omega}_j$ for $j = 1, 2, \ldots, m$.

Finding $g_2(u)$ is a Dirichlet problem with the entire complex plane minus the slits as the domain. The solution to such a Dirichlet problem is guaranteed to exist and can be found numerically. After obtaining $g_2(u)$ and the conjugate harmonic function $g_1(u)$, one needs to check that $z(u)$ given implicitly by (23.64) is univalent. If it is, then the values of $g_1(u)$ and $g_2(u)$ around the boundary of each slit provide us with a parameterization of the boundaries of the inclusions Ω_j. The parameterization of the boundary of inclusion Ω_j is

$$\begin{aligned} x_1(u_2) &= \frac{g_1(c_j + i u_2) - u_2(w_1'' a_2'' - w_2'' a_1'') - c_j(w_1'' a_2' - w_2'' a_1')}{a_1' a_2'' - a_1'' a_2'}, \\ x_2(u_2) &= \frac{u_2(1 - w_1'' a_2' + w_2'' a_1') + c_j(w_1'' a_2'' - w_2'' a_1'') - e_j}{a_1' a_2'' - a_1'' a_2'}, \end{aligned} \tag{23.68}$$

as u_2 is varied between k_j^- and k_j^+, where the value of $g_1(c_j + i u_2)$ depends on which side of the slit one is on. The function $u(z)$ gives the potential $\phi(z)$ in the phase 2, through (23.63).

Notice that we are free to vary σ_1 while keeping $u(z)$, the microgeometry, and all other parameters fixed. In this way we see that there is a solution with the electric field constant inside phase 1 and aligned parallel to the x_1-axis for all values of σ_1. By applying the duality transformation of section 3.1 on page 47 we see that there is also a solution with the electric field constant inside phase 1 and aligned parallel to the x_2-axis for all values of σ_1. Finally, by superimposing these solutions we see that the electric field in phase 1 will be constant for all σ_1 and for all directions of the applied field. Thus the effective conductivity tensor of the microstructure will attain the bound (23.62) for all values of $\sigma_1 > \sigma_2 = 1$.

Given a specific solution $g_2(u)$ to the Dirichlet problem one can change the lattice vectors w_1 and w_2 while keeping $g(u)$ and the parameters a_1, a_2, c_j, k_j^+, k_j^-, and e_j fixed. The values of α and the parameters d_j must be adjusted so that (23.67) and the relation

$$d_j = \frac{e_j - c_j(w_1'' a_2'' - w_2'' a_1'')}{1 - w_1'' a_2' + w_2'' a_1'},$$

implied by (23.66), remains valid. According to (23.68), the new boundary $(\tilde{x}_1(u_2), \tilde{x}_2(u_2))$ of inclusion Ω_j is related to the old boundary $(x_1(u_2), x_2(u_2))$ of inclusion Ω_j via a transformation of the form

$$\tilde{x}_1(u_2) = x_1(u_2) + q_j x_2(u_2) + r_j, \quad \tilde{x}_2(u_2) = s_j x_2(u_2) + t_j, \tag{23.69}$$

where the constants q_j, r_j, s_j, and t_j do not depend on u_2. Thus the shape of each inclusion undergoes an affine transformation, which is different than the affine transformation that the unit cell Ω undergoes. In this way one generates other microgeometries attaining the bound, each with a different unit cell of periodicity.

The easiest case to solve is of course when there is just a single slit in the unit cell. In particular, consider the square $1 \geq u_1 \geq -1$, $1 \geq u_2 \geq -1$ as a unit cell with a slit of length 2ℓ, with $\ell < 1$, positioned along the u_2-axis and centered at the origin. We extend this periodically. By symmetry the lines $u_2 = 0$ and $u_2 = 1$ are equipotentials of $g_2(u)$. Without loss of generality we can assume that $g_2(u) = 0$ there and that $g_2(u) = u_2$ along the slit centered at the origin. We take as a domain the strip $1 > u_2 > 0$ cut by the slit regions traced by $u = 2m + iu_2$ as u_2 varies between 0 and ℓ, and as m ranges over all integers. The potential $g_2(u)$ has prescribed values on the boundary of this simply connected domain. In principle we could solve for $g_2(u)$ by using a Schwarz-Christoffel transformation to map the domain to the unit disk and then apply Poisson's formula to solve for the potential and conjugate potential there. In this way we would obtain a periodic array of inclusions with an effective conductivity tensor that attains the bounds and with a single inclusion in each unit cell.

Such a microgeometry has already been found using a different approach by Vigdergauz (1986, 1994). A somewhat simpler treatment was given by Grabovsky and Kohn (1995b), who also gave an alternative parameterization of the inclusion boundary. When the unit cell Ω is square with side length 1 (i.e., when $w_1 = 1$ and $w_2 = i$) they found that the Vigdergauz inclusion boundary depends on two constants m and m_λ that must be chosen with

$$1 > m > 1/2, \quad 1 > m_\lambda > 1/2.$$

For a given choice of these constants the boundary has the parameterization

$$\begin{aligned} x_1(t) &= -\frac{(1-T)}{2(1-hT)K(m)} F(\sqrt{1-t}|m), \\ x_2(t) &= \frac{(1-h)}{2(1-hT)K(m_\lambda)} F(\sqrt{1-M/t}|m_\lambda), \end{aligned}$$

where

$$h = \frac{K(1-m)}{K(m)}, \quad T = \frac{K(1-m_\lambda)}{K(m_\lambda)}, \quad M = \frac{(1-m)(1-m_\lambda)}{mm_\lambda},$$

and

$$F(y|m) = \int_0^y \frac{dt}{\sqrt{(1-t^2)(1-mt^2)}}, \quad K(m) = F(1|m)$$

are the incomplete and complete elliptic integrals of the first kind, respectively. As the parameter t is varied between M and 1, the point $(x_1(t), x_2(t))$ traces along one-quarter of the inclusion boundary. The remaining portions of the inclusion boundary are obtained by reflection. Figure 23.5 on page 486 shows an example of the resulting microgeometry (which I am grateful to Sergey Serkov for computing). The inclusion occupies a volume fraction

$$f_1 = (1-T)(1-h)/(1-hT) = 1-(h+T)/(1-hT)$$

of the unit cell. The choice of m and m_λ ensures that h and T are positive and less than 1. This guarantees that f_1 lies between 0 and 1. The "eccentricity" of the inclusion changes as m and m_λ are varied while keeping f_1 fixed. As f_1 tends to zero, the inclusion shape becomes elliptical. Vigdergauz (1996) has also found the optimal inclusion shape when the inclusions are in rhombic arrays. According to (23.69), this inclusion shape should be related to the one for the square array by an affine transformation. For inclusions in triangular and hexagonal arrays the problem of finding the optimal inclusion shape reduces to a system of algebraic equations, which Vigdergauz (1999b) solves numerically; see also Vigdergauz (1999a).

Another quite different type of two-dimensional microstructure that achieves the bounds was found by Sigmund (2000) and is illustrated in figure 23.6(a) on page 486. For simplicity let us take the unit cell of periodicity Ω to be square with side length 1, which we divide into four rectangular regions:

$$\begin{aligned}
\mathcal{R}_1 &= \{\boldsymbol{x} \mid 0 \le x_1 \le p_1, \quad 0 \le x_2 \le p_2\},\\
\mathcal{R}_2 &= \{\boldsymbol{x} \mid 0 \le x_1 \le p_1, \quad p_2 \le x_2 \le 1\},\\
\mathcal{R}_3 &= \{\boldsymbol{x} \mid p_1 \le x_1 \le 1, \quad 0 \le x_2 \le p_2\},\\
\mathcal{R}_4 &= \{\boldsymbol{x} \mid p_1 \le x_1 \le 1, \quad p_2 \le x_2 \le 1\}.
\end{aligned}$$

We then set

$$\begin{aligned}
\boldsymbol{\sigma}(\boldsymbol{x}) &= \sigma_1 \boldsymbol{I} && \text{when } \boldsymbol{x} \in \mathcal{R}_1,\\
&= \begin{pmatrix} (1-q)\sigma_1 + q\sigma_2 & 0 \\ 0 & \sigma_1\sigma_2/[q\sigma_1 + (1-q)\sigma_2] \end{pmatrix} && \text{when } \boldsymbol{x} \in \mathcal{R}_2,\\
&= \begin{pmatrix} \sigma_1\sigma_2/[(1-q)\sigma_1 + q\sigma_2] & 0 \\ 0 & q\sigma_1 + (1-q)\sigma_2 \end{pmatrix} && \text{when } \boldsymbol{x} \in \mathcal{R}_3,\\
&= \sigma_2 \boldsymbol{I} && \text{when } \boldsymbol{x} \in \mathcal{R}_4,
\end{aligned}$$

where the anisotropic conductivities tensors in the regions $\mathcal{R}_2$ and $\mathcal{R}_3$ can be identified with the effective tensors of laminates of σ_1 and σ_2 layered in proportions $(1-q)$ and q in region $\mathcal{R}_2$ and in proportions q and $(1-q)$ in region $\mathcal{R}_3$.

This conductivity tensor field has been chosen so that the conductivity equations are solved with piecewise constant fields. One solution is

$$\begin{aligned}
\boldsymbol{e}(\boldsymbol{x}) &= \begin{pmatrix} 1 \\ 0 \end{pmatrix} && \text{when } \boldsymbol{x} \in \mathcal{R}_1 \cup \mathcal{R}_2,\\
&= \begin{pmatrix} [(1-q)\sigma_1 + q\sigma_2]/\sigma_2 \\ 0 \end{pmatrix} && \text{when } \boldsymbol{x} \in \mathcal{R}_3 \cup \mathcal{R}_4,\\
\boldsymbol{j}(\boldsymbol{x}) &= \begin{pmatrix} \sigma_1 \\ 0 \end{pmatrix} && \text{when } \boldsymbol{x} \in \mathcal{R}_1 \cup \mathcal{R}_3,\\
&= (\,(1-q)\sigma_1 + q\sigma_2\,) && \text{when } \boldsymbol{x} \in \mathcal{R}_2 \cup \mathcal{R}_4,
\end{aligned}$$

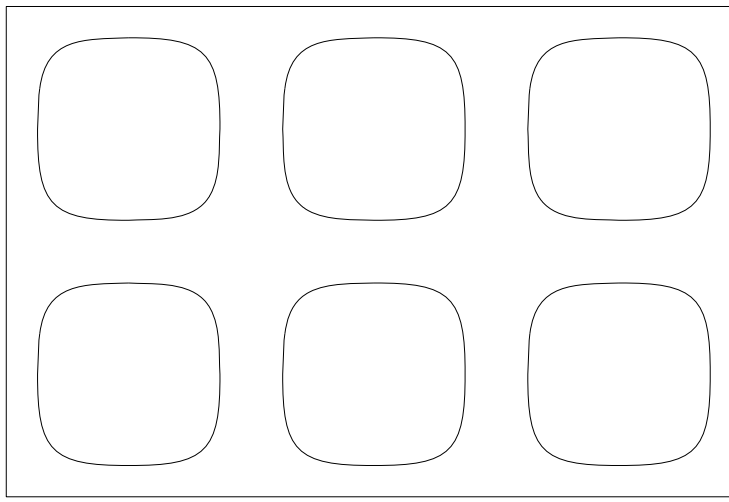

Figure 23.5. The periodic Vigdergauz microstructure.

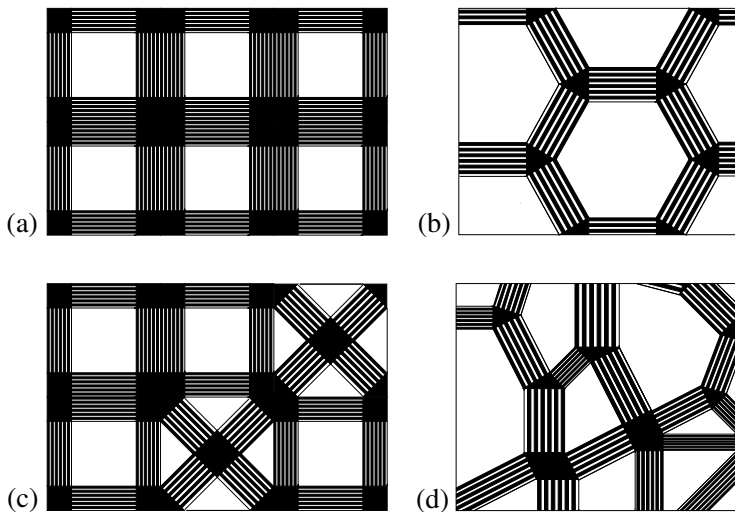

Figure 23.6. Shown in (a) and (b) are the two-dimensional microstructures of Sigmund (2000), which, when periodically extended, have exactly the same effective conductivity as the Hashin-Shtrikman coated circle assemblage. Phase 2 occupies the black regions while phase 1 occupies the remaining regions. Shown in (c) and (d) are generalizations to random microstructures of the type suggested by Sigmund. However, it is not obvious that the structure of (d) can be extended in a statistically homogeneous way. Within each cell in (c) we randomly choose one of the two basic substructures.

and a second independent solution is

$$\begin{aligned}
\boldsymbol{e}(\boldsymbol{x}) &= \begin{pmatrix} 0 \\ 1 \end{pmatrix} && \text{when } \boldsymbol{x} \in \mathcal{R}_1 \cup \mathcal{R}_3, \\
&= \begin{pmatrix} 0 \\ [q\sigma_1 + (1-q)\sigma_2]/\sigma_2 \end{pmatrix} && \text{when } \boldsymbol{x} \in \mathcal{R}_2 \cup \mathcal{R}_4, \\
\boldsymbol{j}(\boldsymbol{x}) &= \begin{pmatrix} 0 \\ \sigma_1 \end{pmatrix} && \text{when } \boldsymbol{x} \in \mathcal{R}_1 \cup \mathcal{R}_2, \\
&= \begin{pmatrix} 0 \\ q\sigma_1 + (1-q)\sigma_2 \end{pmatrix} && \text{when } \boldsymbol{x} \in \mathcal{R}_3 \cup \mathcal{R}_4.
\end{aligned}$$

By taking averages of these fields one sees that the effective conductivity tensor $\boldsymbol{\sigma}_*$ has eigenvalues

$$\begin{aligned}
\lambda_1^* &= \frac{\sigma_2[(1-q)\sigma_1 + q\sigma_2 + p_2 q(\sigma_1 - \sigma_2)]}{(1-q)\sigma_1 + q\sigma_2 + p_1(1-q)(\sigma_2 - \sigma_1)} \\
&= \sigma_2 + \frac{f_1\sigma_2(\sigma_1 - \sigma_2)}{(1-q)\sigma_1 + q\sigma_2 + p_1(1-q)(\sigma_2 - \sigma_1)}, \\
\lambda_2^* &= \frac{\sigma_2[q\sigma_1 + (1-q)\sigma_2 + p_1(1-q)(\sigma_1 - \sigma_2)]}{q\sigma_1 + (1-q)\sigma_2 + p_2 q(\sigma_2 - \sigma_1)} \\
&= \sigma_2 + \frac{f_1\sigma_2(\sigma_1 - \sigma_2)}{q\sigma_1 + (1-q)\sigma_2 + p_2 q(\sigma_2 - \sigma_1)},
\end{aligned}$$

where

$$f_1 = p_1 p_2 + (1-q)p_1(1-p_2) + q(1-p_1)p_2 = p_2 q + p_1(1-q)$$

is the overall volume fraction of phase 1 in the composite when $\mathcal{R}_2$ and $\mathcal{R}_3$ are filled with the laminates.

One can easily check that λ_1^* and λ_2^* attain the bounds (23.62) for all values of q. Moreover, as one would expect, the field inside phase 1 is constant. By taking $q = 1/2$ and $p_1 = p_2$, one obtains a composite with square symmetry with isotropic effective conductivity σ_* attaining the two-dimensional Hashin-Shtrikman bounds. The interesting feature of this microstructure is its simplicity. Sigmund (2000) showed that it can be generalized in various ways, as illustrated in the examples of figures 23.6(b), (c), and (d) on page 486. The common feature in these examples is that each laminated region within the microstructure is rectangular, containing equal proportions of the two phases, and is bounded on the sides by polygonal regions of phase 1 and on the ends by polygonal regions of phase 2. Also, the polygonal regions of phase 1 and the polygonal regions of phase 2 touch only at vertices, not along edges. The field $\boldsymbol{e}(\boldsymbol{x})$ takes a constant value $\boldsymbol{e}_1$ within the polygonal regions of phase 1 and an associated constant value $(\sigma_1 + \sigma_2)\boldsymbol{e}_1/2\sigma_2$ within the polygonal regions of phase 2. Sigmund also showed that there are related microstructures attaining the three-dimensional Hashin-Shtrikman bounds.

23.10. Bounds for cell polycrystals

We saw in sections 22.2 on page 439 and 22.3 on page 441 that there are polycrystals that achieve the classical (Wiener) upper bound on the effective conductivity and the classical (Voigt-Reuss-Hill) bounds on the effective bulk modulus. Thus if we wish to tighten these

bounds, we need to restrict the class of polycrystal microgeometries in some way. A natural class of polycrystalline materials to consider are cell polycrystals, where each crystal orientation in each cell is uncorrelated with the cell shape, the surrounding configuration of cells, and the surrounding configuration of crystal orientations. To derive bounds on the effective tensor, using the Hashin-Shtrikman variational principles we choose a trial polarization field $\underline{\boldsymbol{P}}(\boldsymbol{x})$ that is assumed to be constant within each cell and only correlated with the value that the tensor field $\boldsymbol{L}(\boldsymbol{x})$ takes within that cell; that is, it is independent of the cell shape, the surrounding configuration of cells, and the surrounding configuration of crystal orientations. To evaluate the nonlocal term in the Hashin-Shtrikman variational principle (13.30), we use the fact that $\boldsymbol{\Gamma}$ annihilates constant fields to rewrite it as

$$\langle \underline{\boldsymbol{P}} \cdot \boldsymbol{\Gamma} \underline{\boldsymbol{P}} \rangle = \langle \delta \underline{\boldsymbol{P}} \cdot \boldsymbol{\Gamma} \delta \underline{\boldsymbol{P}} \rangle, \quad \text{where } \delta \underline{\boldsymbol{P}} = \underline{\boldsymbol{P}} - \langle \underline{\boldsymbol{P}} \rangle.$$

The absence of correlations implies that to calculate volume averages we can hold the cell configuration fixed and first do an ensemble average over all realizations of $\underline{\boldsymbol{P}}(\boldsymbol{x})$ sharing that cell geometry; that is, we effectively average over all crystal configurations sharing the same cell geometry. Now the ensemble average of $\{\delta \underline{\boldsymbol{P}}(\boldsymbol{x}_1)\}_a \{\delta \underline{\boldsymbol{P}}(\boldsymbol{x}_2)\}_b$ will be zero unless both points $\boldsymbol{x}_1$ and $\boldsymbol{x}_2$ lie in the same cell. In the same way that the second-order term in (15.15) was derived we see that

$$\langle \delta \underline{\boldsymbol{P}} \cdot \boldsymbol{\Gamma} \delta \underline{\boldsymbol{P}} \rangle = \Big[\int_{\mathbb{R}^d} d\boldsymbol{y}\, g_2(\boldsymbol{y}) \{\boldsymbol{\Gamma}_\infty(\boldsymbol{y})\}_{ba} \Big] \int d\mu(\underline{\boldsymbol{P}}) \{\delta \underline{\boldsymbol{P}}(\boldsymbol{x}_1)\}_a \{\delta \underline{\boldsymbol{P}}(\boldsymbol{x}_2)\}_b,$$

where $\mu(\underline{\boldsymbol{P}})$ is the positive measure characterizing the distribution of values that $\underline{\boldsymbol{P}}$ takes in each cell and $g_2(\boldsymbol{y})$ is the probability that a rod with endpoints at the origin and at $\boldsymbol{y}$ lands with both endpoints in a single cell when translated to a random position in the composite.

Let us make the additional assumption that the cell configuration is geometrically isotropic. Then $g_2(\boldsymbol{y})$ depends only on $|\boldsymbol{y}|$, and by the same reasoning as led to the second-order term in (15.42) we see that

$$\langle \delta \underline{\boldsymbol{P}} \cdot \boldsymbol{\Gamma} \delta \underline{\boldsymbol{P}} \rangle = \int d\mu(\underline{\boldsymbol{P}}) \delta \underline{\boldsymbol{P}}(\boldsymbol{x}_1) \cdot \boldsymbol{\gamma} \delta \underline{\boldsymbol{P}}(\boldsymbol{x}_2) = \langle \underline{\boldsymbol{P}} \cdot \boldsymbol{\gamma} \underline{\boldsymbol{P}} \rangle - \langle \underline{\boldsymbol{P}} \rangle \cdot \boldsymbol{\gamma} \langle \underline{\boldsymbol{P}} \rangle,$$

in which $\boldsymbol{\gamma} = \langle \boldsymbol{\Gamma}(\boldsymbol{n}) \rangle_{\boldsymbol{n}}$, as in (12.35). Substituting this nonlocal term back into the Hashin-Shtrikman variational inequality (13.30) gives

$$\langle \underline{\boldsymbol{P}} \rangle \cdot [\boldsymbol{\gamma} + (\boldsymbol{L}_* - \boldsymbol{L}_0)^{-1}] \langle \underline{\boldsymbol{P}} \rangle \le \langle \underline{\boldsymbol{P}} \cdot [\boldsymbol{\gamma} + (\boldsymbol{L} - \boldsymbol{L}_0)^{-1}]\, \underline{\boldsymbol{P}} \rangle,$$

which holds for all $\boldsymbol{L}_0$ with $\boldsymbol{L} > \boldsymbol{L}_0$, $\boldsymbol{\Gamma}_1 \boldsymbol{L}_0 \boldsymbol{\Gamma}_1 \ge 0$. The trial field $\underline{\boldsymbol{P}}(\boldsymbol{x})$ is now varied to minimize the right-hand side of this inequality while keeping $\langle \underline{\boldsymbol{P}} \rangle$ fixed. By adding the Lagrange multiplier term $-2\langle \underline{\boldsymbol{P}} \rangle \cdot \boldsymbol{v}$ to the right-hand side we see that the minimum occurs when

$$\underline{\boldsymbol{P}}(\boldsymbol{x}) = [\boldsymbol{\gamma} + (\boldsymbol{L} - \boldsymbol{L}_0)^{-1}]^{-1} \boldsymbol{v}.$$

Thus, as assumed, the value of $\underline{\boldsymbol{P}}(\boldsymbol{x})$ is constant within any cell and depends only on the value that $\boldsymbol{L}(\boldsymbol{x})$ takes within that cell. When substituted back in the above inequality this choice of polarization field yields the lower bound

$$[\boldsymbol{\gamma} + (\boldsymbol{L}_* - \boldsymbol{L}_0)^{-1}]^{-1} \ge \langle [\boldsymbol{\gamma} + (\boldsymbol{L} - \boldsymbol{L}_0)^{-1}]^{-1} \rangle. \tag{23.70}$$

Similarly, when $\boldsymbol{L}_0$ is chosen with $\boldsymbol{L}_0 > \boldsymbol{L}$, the variational principle (13.32) yields the upper bound

$$[\boldsymbol{\gamma} + (\boldsymbol{L}_* - \boldsymbol{L}_0)^{-1}]^{-1} \le \langle [\boldsymbol{\gamma} + (\boldsymbol{L} - \boldsymbol{L}_0)^{-1}]^{-1} \rangle. \tag{23.71}$$

These general bounds of Watt and Peselnick (1980), Olson (1991), and Olson and Avellaneda (1992) are based on the pioneering work of Hashin and Shtrikman (1962b, 1963a). In these papers of Hashin and Shtrikman it was unclear what assumptions were being made about the polycrystal microstructure. This was partially clarified by Hashin (1965a) and Beran (1968), page 229.

Let us consider a three-dimensional conducting cell polycrystal, with effective conductivity tensor $\boldsymbol{L}_* = \boldsymbol{\sigma}_*$ having eigenvalues $\lambda_1^* \geq \lambda_2^* \geq \lambda_3^* > 0$, and with local conductivity tensor $\boldsymbol{L}(\boldsymbol{x}) = \boldsymbol{\sigma}(\boldsymbol{x})$ having eigenvalues $\lambda_1 \geq \lambda_2 \geq \lambda_3 > 0$. Choosing an isotropic reference medium with tensor $\boldsymbol{L}_0 = \sigma_0 \boldsymbol{I}$ gives $\boldsymbol{\gamma} = \boldsymbol{I}/3\sigma_0$, and the upper bound (23.70) implies that the inequality

$$\boldsymbol{v} \cdot [\boldsymbol{I}/3\sigma_0 + (\boldsymbol{\sigma}_* - \sigma_0 \boldsymbol{I})^{-1}]^{-1} \boldsymbol{v} \geq \langle \boldsymbol{v} \cdot [\boldsymbol{I}/3\sigma_0 + (\boldsymbol{\sigma} - \sigma_0 \boldsymbol{I})^{-1}]^{-1} \boldsymbol{v} \rangle$$

holds for any choice of the vector $\boldsymbol{v}$. To obtain a bound that is independent of the distribution of crystal orientations, we successively take $\boldsymbol{v} = \boldsymbol{v}_1, \boldsymbol{v}_2$, and $\boldsymbol{v}_3$, where $\boldsymbol{v}_1, \boldsymbol{v}_2$, and $\boldsymbol{v}_3$ are three orthonormal unit vectors, and then we sum the resulting three inequalities. This gives

$$\mathrm{Tr}\{[\boldsymbol{I}/3\sigma_0 + (\boldsymbol{\sigma}_* - \sigma_0 \boldsymbol{I})^{-1}]^{-1}\} \geq \langle \mathrm{Tr}\{[\boldsymbol{I}/3\sigma_0 + (\boldsymbol{\sigma} - \sigma_0 \boldsymbol{I})^{-1}]^{-1}\} \rangle,$$

which, upon taking $\sigma_0 = \lambda_3$, reduces to the lower bound

$$\sum_{i=1}^{3} \frac{\lambda_i^* - \lambda_3}{\lambda_i^* + 2\lambda_3} \geq \sum_{i=1}^{2} \frac{\lambda_i - \lambda_3}{\lambda_i + 2\lambda_3}, \tag{23.72}$$

and similarly from (23.71) we have the upper bound,

$$\sum_{i=1}^{3} \frac{\lambda_i^* - \lambda_1}{\lambda_i^* + 2\lambda_1} \leq \sum_{i=2}^{3} \frac{\lambda_i - \lambda_1}{\lambda_i + 2\lambda_1}. \tag{23.73}$$

In particular, when the polycrystal has an isotropic effective conductivity tensor, so that $\lambda_1^* = \lambda_2^* = \lambda_3^* = \sigma_*$, these bounds simplify to the bounds

$$\lambda_1 \frac{4\lambda_1^2 + 8\lambda_1\lambda_2 + 8\lambda_1\lambda_3 + 7\lambda_2\lambda_3}{16\lambda_1^2 + 5\lambda_1\lambda_2 + 5\lambda_1\lambda_3 + \lambda_2\lambda_3} \geq \sigma_* \geq \lambda_3 \frac{4\lambda_3^2 + 8\lambda_3\lambda_2 + 8\lambda_3\lambda_1 + 7\lambda_1\lambda_2}{16\lambda_3^2 + 5\lambda_3\lambda_2 + 5\lambda_3\lambda_1 + \lambda_1\lambda_2} \tag{23.74}$$

of Hashin and Shtrikman (1963a) on the effective conductivity σ_*. Notice that our derivation did not assume that the cell polycrystal was "equiaxed," that is, the distribution of crystal orientations is uniform in the sense that each crystal orientation is as likely as any other. The important assumptions are, first, that the crystal orientation in each cell is uncorrelated with the cell shape, the surrounding configuration of cells, and the surrounding configuration of crystal orientations, and, second, that the cell configuration is geometrically isotropic.

In naturally occurring polycrystals one might expect some significant correlation between the crystal orientation and cell shape, since the surface energy associated with an interface can depend strongly on the angle of the interface with respect to the crystal axes, which accounts for the characteristic Wulff shape of isolated crystals (Wulff 1901; Taylor 1974; Fonseca 1991; Dobrushin, Kotecký, and Shlosman 1992). Adams, Kinderlehrer, Livshits, Mason, Mullins, Rohrer, Rollett, Saylor, Ta'asan, and Wu (1999) have shown how the correlations between crystal orientations at triple junctions of grain boundaries can be used to determine information about the surface energies of these grain boundaries. Thus there is good reason to question whether these bounds for cell polycrystals apply to real polycrystals.

The bounds (23.74) are not optimal. Tighter bounds, which do not incorporate any additional information about the polycrystal microgeometry, have been obtained by Helsing (1993a, 1993b, 1994) and Pham (1996a). Pham (1998) compared his bounds with the range of effective conductivities achievable in a class of realizable models (corresponding to the effective medium approximation with ellipsoidal grains). Bounds that incorporate higher order statistical information, such as the parameter ζ_1^0 defined by (15.44) appearing in the expansion (15.46), have been obtained by Willemse and Caspers (1979) and Pham (1996b, 2000).

For elasticity Hashin and Shtrikman (1962b), Watt and Peselnick (1980) [see also (Peselnick and Meister 1965) and Peselnick and Meister (1966)], and Watt (1979, 1980, 1986) gave explicit expressions for the bounds (23.70) and (23.71) for polycrystals built from crystals with cubic, hexagonal, trigonal, tetragonal, orthorhombic, and tetragonal symmetries. Watt (1988) found that these bounds are generally, but not always, compatible with measured data on the effective elastic moduli of polycrystals. The discrepancies could be due to correlations between the crystal orientation and grain shape, due to correlations between the crystal orientations of neighboring grains, or due to imperfections at the interface between grains. Pham (1997, 1999) provided bounds for three- and two-dimensional elasticity that are potentially tighter, but which do not incorporate any additional information about the polycrystal microgeometry. He also found substantially tighter bounds, assuming that the cells are spherical (for three-dimensional elasticity) or circular (for two-dimensional elasticity). Beran, Mason, Adams, and Olson (1996) have derived bounds that do not assume that the polycrystal is a cell material, but which require measurements of two-point correlation functions. Using such measurements they found good agreement between their bounds and experimental data for copper.

For piezoelectricity Olson and Avellaneda (1992) give explicit expressions for the bounds (23.70) and (23.71) for polycrystals built from crystals that belong to the orthorhombic 222 class.

References

Adams, B. L., D. Kinderlehrer, I. Livshits, D. E. Mason, W. W. Mullins, G. S. Rohrer, A. D. Rollett, D. M. Saylor, S. Ta'asan, and C.-T. Wu 1999. Extracting grain boundary and surface energy from measurement of triple junction geometry. *Interface Science* 7: 321–337. {*489, 490*}

Allaire, G. 1994b. A remark on trace bounds for elastic composite materials. In G. Bouchitté, G. Buttazzo, and P. Suquet (eds.), *Calculus of Variations, Homogenization and Continuum Mechanics*, pp. 19–28. Singapore / Philadelphia / River Edge, New Jersey: World Scientific Publishing Co. ISBN 981-02-1783-8. {*474, 490*}

Allaire, G. 1994a. Explicit lamination parameters for three-dimensional shape optimization. *Control and Cybernetics* 23(3):309–326. {*467, 490*}

Allaire, G. and S. Aubry 1999. On optimal microstructures for a plane shape optimization problem. *Structural Optimization* 17(2):86–94. {*467, 490*}

Allaire, G. and R. V. Kohn 1993a. Explicit optimal bounds on the elastic energy of a two-phase composite in two space dimensions. *Quarterly of Applied Mathematics* 51(4): 675–699. {*466, 490, 518, 525*}

Allaire, G. and R. V. Kohn 1993b. Optimal bounds on the effective behavior of a mixture of two well-ordered elastic materials. *Quarterly of Applied Mathematics* 51(4):643–674. {*467, 490*}

Allaire, G. and R. V. Kohn 1994. Optimal lower bounds on the elastic energy of a composite made from two non well-ordered isotropic materials. *Quarterly of Applied Mathematics* 52(2):311–333. {*468, 491*}

Astala, K. 1994. Area distortion of quasiconformal mappings. *Acta Mathematica* 173(1): 37–60. {*480, 491*}

Astala, K. and V. Nesi 2001. Area distortion for periodic quasiconformal mappings. *Calculus of Variations and Partial Differential Equations*. Submitted. {*152, 155, 480, 491*}

Avellaneda, M. 1987. Optimal bounds and microgeometries for elastic two-phase composites. *SIAM Journal on Applied Mathematics* 47(6):1216–1228. {*175, 181, 292, 294, 309, 463–465, 468, 471, 473, 491*}

Beran, M. J. 1968. *Statistical Continuum Theories*. New York: Interscience Publishers. xv + 424 pp. ISBN 0-470-06861-2. {*xxv, xxvi, 11, 15, 291, 309, 489, 491*}

Beran, M. J., T. A. Mason, B. L. Adams, and T. Olson 1996. Bounding elastic constants of an orthotropic polycrystal using measurements of the microstructure. *Journal of the Mechanics and Physics of Solids* 44(9):1543–1563. {*490, 491*}

Bergman, D. J. 1976. Variational bounds on some bulk properties of a two-phase composite material. *Physical Review B (Solid State)* 14:1531–1542. {*457, 491, 580, 581, 597*}

Bergman, D. J. 1980. Exactly solvable microscopic geometries and rigorous bounds for the complex dielectric constant of a two-component composite material. *Physical Review Letters* 44:1285–1287. {*452, 453, 478, 491, 569, 577, 588, 597*}

Bornert, M., C. Stolz, and A. Zaoui 1996. Morphologically representative pattern-based bounding in elasticity. *Journal of the Mechanics and Physics of Solids* 44(3):307–331. {*134, 139, 458, 491*}

Braides, A. and D. Lukkassen 2000. Reiterated homogenization of integral functionals. *Mathematical Models and Methods in Applied Science* 10(1):47–71. {*471, 491*}

Cherkaev, A. V., Y. Grabovsky, A. B. Movchan, and S. K. Serkov 1998. The cavity of the optimal shape under the shear stresses. *International Journal of Solids and Structures* 35(33):4391–4410. {*467, 491*}

Cherkaev, A. V., L. A. Krog, and İ. Küçük 1998. Stable optimal design of two-dimensional elastic structures. *Control and Cybernetics* 27(2):265–282. {*432, 434, 468, 491*}

DeLoor, G. P. 1956. Dielectric properties of heterogeneous mixtures. Proefscrift, University of Leiden, Leiden, The Netherlands. 94 pp. Published by Uitgeverij Excelsior, S'Gravenhage, The Netherlands. {*457, 491*}

Dobrushin, R., R. Kotecký, and S. Shlosman 1992. *Wulff Construction. A Global Shape from Local Interaction*. Providence, Rhode Island: American Mathematical Society. x + 204 pp. ISBN 0-8218-4563-2. {*489, 491*}

Erëmenko, A. and D. H. Hamilton 1995. On the area distortion by quasiconformal mappings. *Proceedings of the American Mathematical Society* 123(9):2793–2797. {*480, 491*}

Fonseca, I. 1991. The Wulff theorem revisited. *Proceedings of the Royal Society of London. Series A, Mathematical and Physical Sciences* 432(1884):125–145. {*489, 491*}

Francfort, G. A. and F. Murat 1986. Homogenization and optimal bounds in linear elasticity. *Archive for Rational Mechanics and Analysis* 94(4):307–334. {*174, 182, 471, 492, 501, 504, 525*}

Gehring, F. W. and E. Reich 1966. Area distortion under quasiconformal mappings. *Annales Academia Scientiarum Fennicæ, Series A. I. Mathematica* 388:1–15. {*480, 492*}

Gibiansky, L. V. and A. V. Cherkaev 1984. Design of composite plates of extremal rigidity. Technical Report 914, Ioffe Physicotechnical Institute, Leningrad, USSR. 1–60 pp. English translation in *Topics in the Mathematical Modelling of Composite Materials*, pp. 95–137, ed. by A. Cherkaev and R. Kohn. ISBN 0-8176-3662-5. {*432, 434, 466, 492, 501, 525, 529, 550*}

Gibiansky, L. V. and A. V. Cherkaev 1987. Microstructures of composites of extremal rigidity and exact bounds on the associated energy density. Technical Report 1115, Ioffe Physicotechnical Institute, Leningrad, USSR. 1–52 pp. English translation in *Topics in the Mathematical Modelling of Composite Materials*, pp. 273–317, ed. by A. Cherkaev and R. Kohn. ISBN 0-8176-3662-5. {*174, 175, 182, 468, 492*}

Gibiansky, L. V. and G. W. Milton 1993. On the effective viscoelastic moduli of two-phase media. I. Rigorous bounds on the complex bulk modulus. *Proceedings of the Royal Society of London. Series A, Mathematical and Physical Sciences* 440(1908):163–188. {*397, 412, 475, 477–480, 492*}

Gibiansky, L. V., G. W. Milton, and J. G. Berryman 1999. On the effective viscoelastic moduli of two-phase media: III. Rigorous bounds on the complex shear modulus in two dimensions. *Proceedings of the Royal Society of London. Series A, Mathematical and Physical Sciences* 455(1986):2117–2149. {*480, 492*}

Gibiansky, L. V. and O. Sigmund 2000. Multiphase composites with extremal bulk modulus. *Journal of the Mechanics and Physics of Solids* 48(3):461–498. {*460, 472, 492, 543, 550*}

Grabovsky, Y. 1993. The G-closure of two well-ordered, anisotropic conductors. *Proceedings of the Royal Society of Edinburgh* 123A(3):423–432. {*469, 492*}

Grabovsky, Y. 1996. Bounds and extremal microstructures for two-component composites: A unified treatment based on the translation method. *Proceedings of the Royal Society of London. Series A, Mathematical and Physical Sciences* 452(1947):919–944. {*466, 492, 541, 542, 550, 558, 566*}

Grabovsky, Y. and R. V. Kohn 1995a. Microstructures minimizing the energy of a two phase elastic composite in two space dimensions. I. The confocal ellipse construction. *Journal of the Mechanics and Physics of Solids* 43(6):933–947. {*130, 139, 467, 492*}

Grabovsky, Y. and R. V. Kohn 1995b. Microstructures minimizing the energy of a two phase elastic composite in two space dimensions. II. The Vigdergauz microstructure. *Journal of the Mechanics and Physics of Solids* 43(6):949–972. {*467, 484, 492*}

Hashin, Z. 1965a. Elasticity of random media. *Transactions of the Society of Rheology* 9: 381–406. {*489, 492*}

Hashin, Z. 1965b. On elastic behavior of fiber reinforced materials of arbitrary transverse phase geometry. *Journal of the Mechanics and Physics of Solids* 13:119–134. {*471, 492*}

Hashin, Z. and S. Shtrikman 1962a. A variational approach to the theory of the effective magnetic permeability of multiphase materials. *Journal of Applied Physics* 33:3125–3131. {*113, 116, 140, 271, 279, 287, 347, 350, 353, 457, 458, 460, 493, 574, 586, 598*}

Hashin, Z. and S. Shtrikman 1962b. A variational approach to the theory of the elastic behavior of polycrystals. *Journal of the Mechanics and Physics of Solids* 10:343–352. {*489, 490, 493*}

Hashin, Z. and S. Shtrikman 1963b. A variational approach to the theory of the elastic behavior of multiphase materials. *Journal of the Mechanics and Physics of Solids* 11: 127–140. {*206, 216, 271, 287, 457, 470, 471, 473, 493*}

Hashin, Z. and S. Shtrikman 1963a. Conductivity of polycrystals. *Physical Review* 130(1): 129–133. {*489, 493*}

Helsing, J. 1993a. Higher-order bounds on the conductivity of composites from symmetry considerations. *Proceedings of the Royal Society of London. Series A, Mathematical and Physical Sciences* 443:451–455. {*490, 493*}

Helsing, J. 1993b. Improved bounds on the conductivity of composites by translation in a variational principle. *Journal of Applied Physics* 74(8):5061–5063. {*490, 493*}

Helsing, J. 1994. Improved bounds on the conductivity of composites by interpolation. *Proceedings of the Royal Society of London. Series A, Mathematical and Physical Sciences* 444:363–374. {*490, 493, 569, 598*}

Hill, R. 1963. Elastic properties of reinforced solids: Some theoretical principles. *Journal of the Mechanics and Physics of Solids* 11:357–372. {*77, 90, 247, 268, 272, 287, 471, 473, 493*}

Hill, R. 1964. Theory of mechanical properties of fiber-strengthened materials: I. Elastic behavior. *Journal of the Mechanics and Physics of Solids* 12:199–212. {*75, 77, 87, 90, 471, 474, 493*}

Khachaturyan, A. G. 1966. Some questions concerning the theory of phase transitions in solids. *Fizika Tverdogo Tela.* 8:2709–2717. English translation in *Soviet Phys. Solid State.* 8:2163–2168 (1967). {*252, 268, 295, 311, 474, 493, 672, 696*}

Khachaturyan, A. G. 1983. *Theory of Structural Transformations in Solids*, p. 215. New York / London / Sydney, Australia: John Wiley and Sons. ISBN 0-471-07873-5. {*474, 493*}

Kim, I. C. and S. Torquato 1993. Effective conductivity of composites containing spheroidal inclusions: Comparison of simulations with theory. *Journal of Applied Physics* 74(3):1844–1854. {*40, 44, 465, 493*}

Kohn, R. V. and R. Lipton 1988. Optimal bounds for the effective energy of a mixture of isotropic, incompressible, elastic materials. *Archive for Rational Mechanics and Analysis* 102(4):331–350. {*465, 474, 493*}

Kohn, R. V. and G. W. Milton 1986. On bounding the effective conductivity of anisotropic composites. In J. L. Ericksen, D. Kinderlehrer, R. Kohn, and J.-L. Lions (eds.), *Homogenization and Effective Moduli of Materials and Media*, pp. 97–125. Berlin / Heidelberg / London / etc.: Springer-Verlag. ISBN 0-387-96306-5. {*462, 493*}

Kröner, E. 1977. Bounds for the effective elastic moduli of disordered materials. *Journal of the Mechanics and Physics of Solids* 25:137–155. {*251, 268, 282, 287, 291, 311, 458, 493, 553, 566*}

Lakes, R. 1993. Materials with structural hierarchy. *Nature* 361:511–515. {*5, 16, 479, 494*}

Lipton, R. 1988. On the effective elasticity of a two-dimensional homogenized incompressible elastic composite. *Proceedings of the Royal Society of Edinburgh* 110A(1–2): 45–61. {*472, 494*}

Lipton, R. 1991. On the behavior of elastic composites with transverse isotropic symmetry. *Journal of the Mechanics and Physics of Solids* 39(5):663–681. {*175, 182, 473, 494*}

Lipton, R. 1992. Bounds and perturbation series for incompressible elastic composites with transverse isotropic symmetry. *Journal of Elasticity* 27(3):193–225. {*294, 311, 472, 473, 494*}

Lipton, R. 1994. Optimal bounds on effective elastic tensors for orthotropic composites. *Proceedings of the Royal Society of London. Series A, Mathematical and Physical Sciences* 444(1921):399–410. {*175, 182, 473, 494*}

Lipton, R. and J. Northrup 1994. Optimal bounds on the in-plane shear moduli for orthotropic elastic composites. *SIAM Journal on Applied Mathematics* 54(2):428–442. {*473, 494*}

Lukkassen, D. 1999. A new reiterated structure with optimal macroscopic behavior. *SIAM Journal on Applied Mathematics* 59(5):1825–1842. {*471, 494*}

Lurie, K. A. and A. V. Cherkaev 1985. The problem of formation of an optimal isotropic multicomponent composite. *Journal of Optimization Theory and Applications* 46:571–589. {*118, 140, 460, 494*}

Lurie, K. A. and A. V. Cherkaev 1986. Exact estimates of the conductivity of a binary mixture of isotropic materials. *Proceedings of the Royal Society of Edinburgh. Section A, Mathematical and Physical Sciences* 104(1–2):21–38. {*167, 182, 347, 353, 462, 494, 508, 521, 526*}

Milton, G. W. 1980. Bounds on the complex dielectric constant of a composite material. *Applied Physics Letters* 37(3):300–302. {*124, 140, 452, 454, 478, 494, 569, 570, 577, 588, 599*}

Milton, G. W. 1981a. Bounds on the electromagnetic, elastic, and other properties of two-component composites. *Physical Review Letters* 46(8):542–545. {*397, 399, 412, 474, 494, 553, 566, 577, 599*}

Milton, G. W. 1981b. Concerning bounds on the transport and mechanical properties of multicomponent composite materials. *Applied Physics* A26:125–130. {*118, 141, 459, 460, 471, 494*}

Milton, G. W. 1986. Modeling the properties of composites by laminates. In J. L. Ericksen, D. Kinderlehrer, R. Kohn, and J.-L. Lions (eds.), *Homogenization and Effective Moduli of Materials and Media*, pp. 150–174. Berlin / Heidelberg / London / etc.: Springer-Verlag. ISBN 0-387-96306-5. {*206, 218, 384, 394, 463, 471, 472, 494, 578, 599, 603, 617*}

Milton, G. W. 1990. On characterizing the set of possible effective tensors of composites: The variational method and the translation method. *Communications on Pure and Applied Mathematics (New York)* 43(1):63–125. {*164, 183, 248, 265, 268, 277, 287, 451, 454, 473, 494, 499, 505, 512, 513, 518, 526, 532, 551*}

Milton, G. W. and J. G. Berryman 1997. On the effective viscoelastic moduli of two-phase media. II. Rigorous bounds on the complex shear modulus in three dimensions. *Proceedings of the Royal Society of London. Series A, Mathematical and Physical Sciences* 453(1964):1849–1880. {*479, 495*}

Milton, G. W. and R. V. Kohn 1988. Variational bounds on the effective moduli of anisotropic composites. *Journal of the Mechanics and Physics of Solids* 36(6):597–629. {*172, 183, 280, 287, 462, 466, 469, 471, 474, 495*}

Milton, G. W. and V. Nesi 1999. Optimal G-closure bounds via stability under lamination. *Archive for Rational Mechanics and Analysis* 150(3):191–207. {*207, 218, 480, 495, 646, 669*}

Milton, G. W. and N. Phan-Thien 1982. New bounds on effective elastic moduli of two-component materials. *Proceedings of the Royal Society of London. Series A, Mathematical and Physical Sciences* 380:305–331. {*458, 474, 495, 553, 554, 557, 559, 567*}

Murat, F. and L. Tartar 1985. Calcul des variations et homogénísation. (French) [Calculus of variation and homogenization]. In *Les méthodes de l'homogénéisation: théorie et applications en physique*, pp. 319–369. Paris: Eyrolles. English translation in *Topics in the Mathematical Modelling of Composite Materials*, pp. 139–173, ed. by A. Cherkaev and R. Kohn, ISBN 0-8176-3662-5. {*12, 13, 17, 347, 353, 429, 431, 432, 435, 444, 454, 462, 495, 499, 503, 506, 508, 521, 527, 529, 551*}

Nesi, V. 1996. Quasiconformal mappings as a tool to study certain two-dimensional G-closure problems. *Archive for Rational Mechanics and Analysis* 134(1):17–51. {*124, 141, 152, 156, 480, 481, 495, 646, 669*}

Norris, A. 1985. A differential scheme for the effective moduli of composites. *Mechanics of Materials: An International Journal* 4:1–16. {*203, 206, 218, 471, 495*}

Olson, T. 1991. Overall properties of granular piezoelectrics: Bounds and effective medium approximations. Ph.D. Thesis, Courant Institute, New York University, New York. iii + 57 pp. {*489, 495*}

Olson, T. and M. Avellaneda 1992. Effective dielectric and elastic constants of piezoelectric polycrystals. *Journal of Applied Physics* 71:4455–4464. {*489, 490, 495*}

Peselnick, L. and R. Meister 1965. Variational methods of determining effective moduli of polycrystals: (A) hexagonal symmetry, (B) trigonal symmetry. *Journal of Applied Physics* 36:2879–2884. {*490, 495*}

Peselnick, L. and R. Meister 1966. Variational method of determining effective moduli of polycrystals with tetragonal symmetry. *Journal of Applied Physics* 37:4121–4125. {*490, 495*}

Pham, D. C. 1996a. Conductivity of disordered polycrystals. *Journal of Applied Physics* 80(4):2253–2259. {*490, 495*}

Pham, D. C. 1996b. On macroscopic elastic and conductivity properties of perfectly random cell composites. *International Journal of Solids and Structures* 33(12):1745–1755. {*490, 495, 553, 567*}

Pham, D. C. 1997. Elastic moduli of perfectly random polycrystalline aggregates. *Philosophical Magazine A* 76(1):31–44. {*490, 495*}

Pham, D. C. 1998, November 2. Conductivity of realizable effective medium intergranularly random and completely random polycrystals against the bounds for isotropic

and symmetrically random aggregates. *Journal of Physics: Condensed Matter* 10(43): 9729–9735. {*490, 495*}

Pham, D. C. 1999. Bounds for the effective elastic properties of completely random polycrstals. *Journal of Elasticity* 54(3):229–251. {*490, 496*}

Pham, D. C. 2000. Bounds on the uncertainty of the electrical, thermal, and magnetic properties of completely random cell polycrystals. *Physical Review B (Solid State)* 61 (2):1068–1074. {*490, 496*}

Roscoe, R. 1973. Isotropic composites with elastic or viscoelastic phases: General bounds for the moduli and solutions for special geometries. *Rheologica acta* 12:404–411. {*206, 219, 471, 496, 646, 669*}

Saffman, P. G. and G. Taylor 1958. The penetration of a fluid into a porous medium or Hele-Shaw cell containing a more viscous liquid. *Proceedings of the Royal Society of London. Series A, Mathematical and Physical Sciences* 245:312–329. {*481, 496*}

Sigmund, O. 2000. A new class of extremal composites. *Journal of the Mechanics and Physics of Solids* 48(2):397–428. {*474, 485–487, 496*}

Tartar, L. 1985. Estimations fines des coefficients homogénéisés. (French) [Fine estimations of homogenized coefficients]. In P. Krée (ed.), *Ennio de Giorgi Colloquium: Papers Presented at a Colloquium Held at the H. Poincaré Institute in November 1983*, pp. 168–187. London: Pitman Publishing Ltd. ISBN 0-273-08680-4. {*129, 141, 165, 167, 174, 183, 462, 496, 499, 503, 506, 508, 527, 529, 552, 683, 698*}

Taylor, J. E. 1974. Existence and structure of solutions to a class of nonelliptic variational problems. In *Symposia Mathematica*, pp. 499–508. New York: Academic Press. {*489, 496*}

Torquato, S. 1997. Effective stiffness tensor of composite media. I. Exact series expansions. *Journal of the Mechanics and Physics of Solids* 45(9):1421–1448. {*258, 269, 305, 312, 461, 496*}

Vigdergauz, S. B. 1986. Effective elastic parameters of a plate with a regular system of equal-strength holes. *Inzhenernyi Zhurnal. Mekhanika Tverdogo Tela: MTT* 21:165–169. {*484, 496*}

Vigdergauz, S. B. 1994. Two-dimensional grained composites of extreme rigidity. *Journal of Applied Mechanics* 61(2):390–394. {*467, 484, 496*}

Vigdergauz, S. B. 1996. Rhombic lattice of equi-stress inclusions in an elastic plate. *Quarterly Journal of Mechanics and Applied Mathematics* 49(4):565–580. {*485, 496*}

Vigdergauz, S. B. 1999a. Complete elasticity solution to the stress problem in a planar grained structure. *Mathematics and Mechanics of Solids* 4(4):407–439. {*485, 496*}

Vigdergauz, S. B. 1999b. Energy-minimizing inclusions in a planar elastic structure with macroisotropy. *Structural Optimization* 17(2):104–112. {*485, 496*}

Walpole, L. J. 1966. On bounds for the overall elastic moduli of inhomogeneous systems — I. *Journal of the Mechanics and Physics of Solids* 14:151–162. {*473, 496*}

Walpole, L. J. 1969. On the overall elastic moduli of composite materials. *Journal of the Mechanics and Physics of Solids* 17:235–251. {*199, 205, 219, 474, 496*}

Watt, J. P. 1979. Hashin-Shtrikman bounds on the effective elastic moduli of polycrystals with orthorhombic symmetry. *Journal of Applied Physics* 50:6290–6295. {*490, 496*}

Watt, J. P. 1980. Hashin-Shtrikman bounds on the effective elastic moduli of polycrystals with monoclinic symmetry. *Journal of Applied Physics* 51:1520–1524. {*490, 497*}

Watt, J. P. 1986. Hashin-Shtrikman bounds on the effective elastic moduli of polycrystals with trigonal $(3, \overline{3})$ and tetragonal $(4, \overline{4}, 4m)$ symmetry. *Journal of Applied Physics* 60: 3120–3124. {*490, 497*}

Watt, J. P. 1988. Elastic properties of polycrystalline minerals: comparison of theory and experiment. *Physics and Chemistry of Minerals* 15:579–587. {*490, 497*}

Watt, J. P. and L. Peselnick 1980. Clarification of the Hashin-Shtrikman bounds on the effective elastic moduli of polycrystals with hexagonal, trigonal, and tetragonal symmetry. *Journal of Applied Physics* 51(3):1525–1531. {*489, 490, 497*}

Willemse, M. W. M. and W. J. Caspers 1979. Electrical conductivity of polycrystalline materials. *Journal of Mathematical Physics* 20(8):1824–1831. {*335, 339, 490, 497*}

Willis, J. R. 1977. Bounds and self-consistent estimates for the overall properties of anisotropic composites. *Journal of the Mechanics and Physics of Solids* 25:185–202. {*256, 269, 327, 340, 347, 353, 464, 497*}

Wulff, G. 1901. Zur Frage der Geschwindigkeit des Wachstums und der Auflösung der Krystallflächen. (German) [on questions of speed of growth and dissolution of crystal surfaces. *Zeitschrift für Krystallographie und Mineralogie* 34:449–530. {*489, 497*}

Zhikov, V. V. 1988. Estimates for the trace of an averaged tensor. *Doklady Akademii Nauk SSSR* 299(4):796–800. English translation in *Soviet Math. Dokl.* 37:456–459 (1988). {*462, 466, 471, 497*}

Zhikov, V. V. 1991. Estimates for the homogenized matrix and the homogenized tensor. *Uspekhi Matematicheskikh Nauk = Russian Mathematical Surveys* 46:49–109. English translation in *Russ. Math. Surv.* 46(3):65–136 (1991). {*120, 142, 164, 183, 280, 289, 462, 466, 471–473, 497*}

24

Bounds using the compensated compactness or translation method

One of the most powerful methods for bounding the effective tensors of composites is what has become known as the compensated compactness method or translation method. The method was introduced by Murat and Tartar (Tartar 1979b; Murat and Tartar 1985; Tartar 1985); see in particular theorem 8 of Tartar (1979b), and independently by Lurie and Cherkaev (1982, 1984a). While embodying many of the same ideas, there is a difference between their approaches. For nonlinear media the two approaches give different types of bounds, as discussed in section 25.1 on page 529: the compensated compactness method of Murat and Tartar gives bounds on the average fields, while the approach of Lurie and Cherkaev gives bounds on the energy. Since both approaches yield identical results for linear media, the term translation method [introduced in Milton (1990b)] will be used to encompass both. The name arises because the bounds can be obtained by shifting, that is, translating, the tensor field by a constant tensor and applying the classical bounds. [This approach has the advantage that by applying the same translation, but replacing the classical bounds by tighter correlation function dependent bounds, one generates improved bounds that include more detailed information about the composite microgeometry; see section 26.5 on page 560. It has the disadvantage that one does not see why it is natural to consider bounds on the translated medium in the first place; see section 25.1 on page 529.]

24.1. The translation bound and comparison bound

In chapter 4 on page 59 we encountered the idea of translations. In the applications encountered so far these translations are special tensors $\boldsymbol{T}$ with the property that when we translate the local moduli by a multiple of $\boldsymbol{T}$,

$$\boldsymbol{L}'(\boldsymbol{x}) = \boldsymbol{L}(\boldsymbol{x}) - c\boldsymbol{T},$$

then the effective tensor is also translated by the same multiple of $\boldsymbol{T}$. In other words, the translated material has effective tensor

$$\boldsymbol{L}'_* = \boldsymbol{L}_* - c\boldsymbol{T}, \tag{24.1}$$

in which $\boldsymbol{L}_*$ is the effective tensor of the original material.

For $\boldsymbol{T}$ to have this property, for all choices of $\boldsymbol{L}(\boldsymbol{x})$, it must map fields on the right side of the constitutive equation to fields satisfying the same differential constraints as those fields on the left side of the constitutive equation; that is, it must have the property that

$$\boldsymbol{T}\mathcal{E} \subset \mathcal{J}. \tag{24.2}$$

Since $\boldsymbol{T}$, being a constant operator, acts locally in Fourier space, a necessary and sufficient condition for (24.2) to hold is that

$$\boldsymbol{T}\mathcal{E}_{\boldsymbol{k}} \subset \mathcal{J}_{\boldsymbol{k}} \text{ for all } \boldsymbol{k} \neq 0$$

or, equivalently, that

$$\boldsymbol{\Gamma}_1(\boldsymbol{k})\boldsymbol{T}\boldsymbol{\Gamma}_1(\boldsymbol{k}) = 0 \text{ for all } \boldsymbol{k} \neq 0, \tag{24.3}$$

which is equivalent to the condition (13.19).

The translation method, in its simplest form, rests on a very simple idea, namely, that we can obtain bounds on $\boldsymbol{L}_*$ from elementary bounds on the effective tensor $\boldsymbol{L}'_*$ of the translated medium. The arithmetic mean bound applied to $\boldsymbol{L}'_*$,

$$\boldsymbol{L}_* - c\boldsymbol{T} \leq \langle \boldsymbol{L} - c\boldsymbol{T} \rangle,$$

does not yield any new information; by adding $c\boldsymbol{T}$ to both sides of the above equation, we see that this bound reduces to the arithmetic mean bound on $\boldsymbol{L}_*$. By contrast, the harmonic mean bound applied to $\boldsymbol{L}'_*$ gives the *translation bound*

$$(\boldsymbol{L}_* - c\boldsymbol{T})^{-1} \leq \langle (\boldsymbol{L} - c\boldsymbol{T})^{-1} \rangle, \tag{24.4}$$

which is genuinely new, and depends nonlinearly on the choice of translation $\boldsymbol{T}$. Of course $\boldsymbol{T}$ and the constant c must be chosen so that the harmonic mean bounds are indeed applicable to $\boldsymbol{L}'_*$. This is ensured provided that $\boldsymbol{L}(\boldsymbol{x})$ and $\boldsymbol{T}$ are self-adjoint and c is chosen so that the tensor of the translated medium is positive-semidefinite:

$$\boldsymbol{L}(\boldsymbol{x}) - c\boldsymbol{T} \geq 0. \tag{24.5}$$

Often we are interested in deriving bounds on $\boldsymbol{L}_*$ that do not depend on the volume fractions of the individual phases, or in the case of a polycrystalline material, which do not depend on the distribution of grain orientations. Bounds of this type can be obtained using the translation method from a simple consideration. Since the effective tensor $\boldsymbol{L}'_*$ must be positive-definite whenever $\boldsymbol{L}'(\boldsymbol{x})$ is self-adjoint and positive-definite, it follows that $\boldsymbol{L}_*$ must satisfy the *comparison bound*:

$$\boldsymbol{L}_* - c\boldsymbol{T} \geq 0, \tag{24.6}$$

whenever $\boldsymbol{L}(\boldsymbol{x})$ and $\boldsymbol{T}$ are self-adjoint and c is chosen so that

$$\boldsymbol{L}(\boldsymbol{x}) - c\boldsymbol{T} \geq 0, \quad \text{for all } \boldsymbol{x}. \tag{24.7}$$

Those translations $\boldsymbol{T}$ that are self-adjoint and satisfy (24.3) are precisely those that are associated with quadratic null Lagrangians; see section 13.3 on page 274.

24.2. Upper bounds on the bulk modulus of two-phase composites and polycrystals in two dimensions

As an example of the translation bounds, consider a two-dimensional isotropic composite comprised of two isotropic elastic phases. Let $\kappa_*, \kappa_1, \kappa_2$ and μ_*, μ_1, μ_2 denote the (two-dimensional) bulk and shear moduli of the composite and phases, respectively, and let us suppose that the phases have been labeled so that $\mu_1 \geq \mu_2$. Taking $\boldsymbol{L}(\boldsymbol{x})$ as the compliance

tensor $\boldsymbol{\mathcal{S}}(\boldsymbol{x})$, and $\boldsymbol{T}$ as the translation $\boldsymbol{\mathcal{R}}_\perp$ introduced in section 4.5 on page 66, we find that the translated medium has bulk moduli $\kappa_*', \kappa_1', \kappa_2'$ and shear moduli μ_*', μ_1', μ_2' given by

$$1/\kappa_i' = 1/\kappa_i - 2c, \quad 1/\mu_i' = 1/\mu_i + 2c, \quad \text{for } i = 1, 2, *.$$

The harmonic mean bounds applied to the compliance tensor of the translated medium are equivalent to the arithmetic mean bounds applied to the elasticity tensor of the translated medium and imply that

$$\kappa_*' \le f_1\kappa_1' + f_2\kappa_2', \quad \mu_*' \le f_1\mu_1' + f_2\mu_2'. \tag{24.8}$$

In particular, by taking the limit

$$c \to -\frac{1}{2\mu_1},$$

which is the minimum value allowed, while keeping the moduli $\kappa_1', \kappa_2', \mu_1', \mu_2'$ all nonnegative (μ_1' becomes infinite in this limit), the first bound in (24.8) reduces to

$$\frac{1}{1/\kappa_* + 1/\mu_1} \le \frac{f_1}{1/\kappa_1 + 1/\mu_1} + \frac{f_2}{1/\kappa_2 + 1/\mu_1}.$$

This is precisely the upper Hashin-Shtrikman bound on the effective bulk modulus κ_*. The above derivation follows Gibiansky and Cherkaev (1984) and Francfort and Murat (1986). Coated cylinder assemblages, with a core of phase 2 surrounded by a coating of phase 2, attain the bound.

As an example of the use of the comparison bounds (24.6), let us derive a sharp upper bound on the effective bulk modulus κ_* of a elastically isotropic, two-dimensional polycrystal (Avellaneda and Milton 1989; Rudelson 1989). The compliance tensor takes the form

$$\boldsymbol{\mathcal{S}}(\boldsymbol{x}) = \boldsymbol{R}(\boldsymbol{x})\boldsymbol{R}(\boldsymbol{x})\boldsymbol{\mathcal{S}}_0\boldsymbol{R}^T(\boldsymbol{x})\boldsymbol{R}^T(\boldsymbol{x}),$$

in which $\boldsymbol{\mathcal{S}}_0$ represents the compliance tensor of the pure crystal, while $\boldsymbol{R}(\boldsymbol{x})$ is the field of rotation matrices giving the local crystal orientation. If we take $\boldsymbol{\mathcal{R}}_\perp$ as our translation, then the rotational invariance of $\boldsymbol{\mathcal{R}}_\perp$ implies that the inequality

$$\boldsymbol{\mathcal{S}}(\boldsymbol{x}) - c\boldsymbol{\mathcal{R}}_\perp = \boldsymbol{R}(\boldsymbol{x})\boldsymbol{R}(\boldsymbol{x})(\boldsymbol{\mathcal{S}}_0 - c\boldsymbol{\mathcal{R}}_\perp)\boldsymbol{R}^T(\boldsymbol{x})\boldsymbol{R}^T(\boldsymbol{x}) \ge 0 \tag{24.9}$$

is satisfied if and only if c is chosen so that

$$\boldsymbol{\mathcal{S}}_0 - c\boldsymbol{\mathcal{R}}_\perp \ge 0,$$

and in this case (24.7) implies the bound

$$\boldsymbol{\mathcal{S}}_* - c\boldsymbol{\mathcal{R}}_\perp \ge 0. \tag{24.10}$$

Working in the usual basis where $\boldsymbol{\mathcal{R}}_\perp$, $\boldsymbol{\mathcal{S}}_0$, and $\boldsymbol{\mathcal{S}}_*$ are represented by the matrices

$$\boldsymbol{\mathcal{R}}_\perp = \begin{pmatrix} 0 & 1 & 0 \\ 1 & 0 & 0 \\ 0 & 0 & -1 \end{pmatrix}, \qquad \boldsymbol{\mathcal{S}}_0 = \begin{pmatrix} S_{1111} & S_{1122} & \sqrt{2}S_{1112} \\ S_{1122} & S_{2222} & \sqrt{2}S_{2212} \\ \sqrt{2}S_{1112} & \sqrt{2}S_{2212} & 2S_{1212} \end{pmatrix},$$

$$\boldsymbol{\mathcal{S}}_* = \frac{1}{4}\begin{pmatrix} 1/\kappa_* + 1/\mu_* & 1/\kappa_* - 1/\mu_* & 0 \\ 1/\kappa_* - 1/\mu_* & 1/\kappa_* + 1/\mu_* & 0 \\ 0 & 0 & 2/\mu_* \end{pmatrix},$$

we see that we should choose c as the unique positive root of the cubic polynomial

$$\det(\boldsymbol{\mathcal{S}}_0 - c\boldsymbol{\mathcal{R}}_\perp) = \begin{vmatrix} S_{1111} & S_{1122} - c & \sqrt{2}S_{1112} \\ S_{1122} - c & S_{2222} & \sqrt{2}S_{2212} \\ \sqrt{2}S_{1112} & \sqrt{2}S_{2212} & 2S_{1212} + c \end{vmatrix} = 0, \tag{24.11}$$

to ensure that $\boldsymbol{\mathcal{S}}_0 - c\boldsymbol{\mathcal{R}}_\perp$ is positive-semidefinite. Then from the comparison bound we have

$$\boldsymbol{\mathcal{S}}_* - c\boldsymbol{\mathcal{R}}_\perp = \frac{1}{4}\begin{pmatrix} 1/\kappa_* + 1/\mu_* & 1/\kappa_* - 1/\mu_* - 4c & 0 \\ 1/\kappa_* - 1/\mu_* - 4c & 1/\kappa_* + 1/\mu_* & 0 \\ 0 & 0 & 2/\mu_* + 4c \end{pmatrix} \geq 0,$$

which on diagonalization implies that

$$1/\kappa_* \geq 2c. \tag{24.12}$$

We will see in section 25.3 on page 535 that this bound is in fact optimal, being attained when the polycrystal is a Schulgasser-type circle assemblage, where the crystal has a radially symmetric orientation within each circle.

When the crystal is orthotropic, that is, $S_{1112} = S_{2212} = 0$, the value of c is

$$c = S_{1122} - \sqrt{S_{1111}S_{2222}}.$$

Written in terms of the moduli

$$\begin{aligned} C_{1111} &= \frac{S_{2222}}{S_{1111}S_{2222} - S_{1122}^2}, \quad C_{2222} = \frac{S_{1111}}{S_{1111}S_{2222} - S_{1122}^2}, \\ C_{1122} &= \frac{-S_{1122}}{S_{1111}S_{2222} - S_{1122}^2}, \quad C_{1212} = \frac{1}{4S_{1212}} \end{aligned}$$

of the elasticity tensor $\boldsymbol{\mathcal{C}}_0$ of the crystal, the lower and upper bounds (22.5) and (24.12) on κ_* become

$$\frac{C_{1111}C_{2222} - C_{1122}^2}{C_{1111} + C_{2222} - 2C_{1122}} \leq \kappa_* \leq \left(\sqrt{C_{1111}C_{2222}} + C_{1122}\right)/2. \tag{24.13}$$

Schulgasser (1995) found that these bounds can be used to derive optimal bounds on the effective axial Young's modulus of an axially oriented polycrystal, in effect giving a prescription for constructing the stiffest composite wire constructed from such polycrystals.

The translation method can also be used (Avellaneda, Cherkaev, Gibiansky, Milton, and Rudelson 1996) to bound the effective shear modulus μ_* of two-dimensional polycrystals built from an orthotropic crystal. It yields the optimal bounds

$$\min\{\mu^+, \mu^-\} \leq \mu_* \leq \max\{\mu^+, \mu^-\}, \tag{24.14}$$

where

$$\mu^+ = \frac{C_{1111}C_{2222} - C_{1122}^2}{2C_{1122} - 2C_{2222} + 2\sqrt{C_{2222}[C_{1111} + C_{2222} - 2C_{1122} + (C_{1111}C_{2222} - C_{1122}^2)/C_{1212}]}},$$

$$\mu^- = \frac{C_{1111}C_{2222} - C_{1122}^2}{2C_{1122} - 2C_{1111} + 2\sqrt{C_{1111}[C_{1111} + C_{2222} - 2C_{1122} + (C_{1111}C_{2222} - C_{1122}^2)/C_{1212}]}}.$$

There are microstructures corresponding to every point (κ_*, μ_*) within the rectangle in the (κ, μ)-plane defined by the bounds (24.13) and (24.14). Thus optimal bounds on the effective in-plane Young's modulus and effective in-plane Poisson's ratio follow from (24.13) and (24.14). For sea ice, the bounds are quite tight (Schapery 1997). When the crystal has square symmetry (i.e., $C_{1111} = C_{2222}$) the upper and lower bounds both coincide with the exact formula (4.27) for the effective shear modulus μ_*. The bounds also coincide and equal

$$\mu_* = C_{1212} \quad \text{when} \quad C_{1111}C_{2222} - (C_{1122} + 2C_{1212})^2 = 0, \tag{24.15}$$

which is the two-dimensional analog of the exact result discussed in section 17.4 on page 361.

24.3. Allowing quasiconvex translations

In the above formulation of the translation method we are limited in our choice of translations $\boldsymbol{T}$ to those for which the equality (24.1) holds. If we weaken this equality to an inequality,

$$\boldsymbol{L}'_* \le \boldsymbol{L}_* - c\boldsymbol{T}, \tag{24.16}$$

then the harmonic mean bounds on the translated medium still imply the translation bounds:

$$(\boldsymbol{L}_* - c\boldsymbol{T})^{-1} \le (\boldsymbol{L}'_*)^{-1} \le \langle (\boldsymbol{L}')^{-1} \rangle = \langle (\boldsymbol{L} - c\boldsymbol{T})^{-1} \rangle, \tag{24.17}$$

and the positive-definiteness of $\boldsymbol{L}'_*$ still implies the comparison bounds:

$$\boldsymbol{L}_* - c\boldsymbol{T} \ge \boldsymbol{L}'_* \ge 0.$$

Of course, to ensure that these bounds are applicable, we still require the self-adjointness of both $\boldsymbol{L}(\boldsymbol{x})$ and $\boldsymbol{T}$, and the positive-semidefiniteness of $\boldsymbol{L}(\boldsymbol{x}) - c\boldsymbol{T}$.

It remains to find a suitable class of translations $\boldsymbol{T}$ for which the inequality (24.16) is guaranteed to hold. By comparing the variational expressions for $\boldsymbol{L}'_*$ and $\boldsymbol{L}_* - c\boldsymbol{T}$,

$$\boldsymbol{E}_0 \cdot \boldsymbol{L}'_* \boldsymbol{E}_0 = \min_{\substack{\underline{\boldsymbol{E}} \in \mathcal{U} \oplus \mathcal{E} \\ \langle \underline{\boldsymbol{E}} \rangle = \boldsymbol{E}_0}} \langle \underline{\boldsymbol{E}} \cdot \boldsymbol{L}\underline{\boldsymbol{E}} \rangle - c\langle \underline{\boldsymbol{E}} \cdot \boldsymbol{T}\underline{\boldsymbol{E}} \rangle, \tag{24.18}$$

$$\boldsymbol{E}_0 \cdot (\boldsymbol{L}_* - c\boldsymbol{T})\boldsymbol{E}_0 = \min_{\substack{\underline{\boldsymbol{E}} \in \mathcal{U} \oplus \mathcal{E} \\ \langle \underline{\boldsymbol{E}} \rangle = \boldsymbol{E}_0}} \langle \underline{\boldsymbol{E}} \cdot \boldsymbol{L}\underline{\boldsymbol{E}} \rangle - c\langle \underline{\boldsymbol{E}} \rangle \cdot \boldsymbol{T}\langle \underline{\boldsymbol{E}} \rangle, \tag{24.19}$$

we see that the first expression will certainly be less than the second expression, provided that c is taken to be positive and the inequality

$$\langle \boldsymbol{E} \cdot \boldsymbol{T}\boldsymbol{E} \rangle \ge \langle \boldsymbol{E} \rangle \cdot \boldsymbol{T}\langle \boldsymbol{E} \rangle \tag{24.20}$$

is satisfied for all $\boldsymbol{E} \in \mathcal{U} \oplus \mathcal{E}$, and in particular for $\boldsymbol{E} = \underline{\boldsymbol{E}}$. The latter is equivalent, by definition, to requiring that the quadratic form associated with $\boldsymbol{T}$ be quasiconvex (see chapter 31 on page 671). Consequently, we will call any $\boldsymbol{T}$ satisfying (24.20) a quasiconvex translation, or more precisely, we will call $\boldsymbol{T}$ quasiconvex on $\mathcal{E}$.

The idea of using quasiconvex translations, rather than only translations associated with null Lagrangians, is an important component of the translation method. The idea is due to Tartar (1979b). Murat and Tartar (Tartar 1979a; Murat and Tartar 1985; Tartar 1985) found a simple test to determine if a given translation $\boldsymbol{T}$ is quasiconvex or not. Suppose that we are

given a real field $\boldsymbol{E} \in \mathcal{U} \oplus \mathcal{E}$. By taking $\boldsymbol{E}(\boldsymbol{x})$ so that only one Fourier component is nonzero and real, as in (13.16), we see from (13.15) that a necessary condition for $\boldsymbol{T}$ to be quasiconvex is that, for all $\boldsymbol{k} \neq 0$,

$$\boldsymbol{B} \cdot \boldsymbol{T}\boldsymbol{B} \geq 0 \qquad \text{for all real } \boldsymbol{B} \in \mathcal{E}_{\boldsymbol{k}}. \tag{24.21}$$

Conversely, if this condition holds, then for an arbitrary choice of field $\boldsymbol{E} \in \mathcal{U} \oplus \mathcal{E}$ each term in the sum (13.15) will be positive and hence $\langle \boldsymbol{E} \cdot \boldsymbol{T}\boldsymbol{E} \rangle - \langle \boldsymbol{E} \rangle \cdot \boldsymbol{T} \langle \boldsymbol{E} \rangle$ will be positive. Therefore $\boldsymbol{T}$ is quasiconvex if and only if (24.21) holds for all $\boldsymbol{k} \neq 0$.

For example, if $\mathcal{U} \oplus \mathcal{E}$ is comprised of all periodic matrix-valued real fields $\boldsymbol{E}(\boldsymbol{x})$ such that $\boldsymbol{E} = \nabla \boldsymbol{u}$ for some vector potential $\boldsymbol{u}$, then

$$\mathcal{E}_{\boldsymbol{k}} = \{\boldsymbol{B} \mid \boldsymbol{B} = \boldsymbol{k} \otimes \boldsymbol{b}\},$$

and (24.21) tells us that $\boldsymbol{T}$ is quasiconvex if and only if the quadratic form associated with $\boldsymbol{T}$ is positive on rank-1 matrices.

Thus the translation bounds (24.4) and comparison bounds (24.6) hold when c is positive and $\boldsymbol{T}$ satisfies the quasiconvexity condition

$$\boldsymbol{\Gamma}_1(\boldsymbol{k})\boldsymbol{T}\boldsymbol{\Gamma}_1(\boldsymbol{k}) \geq 0 \ \text{ for all } \boldsymbol{k} \neq 0,$$

which is implied by (24.21).

The translation bound (24.17) can be written in the equivalent form

$$\boldsymbol{E}_0 \cdot \boldsymbol{L}_* \boldsymbol{E}_0 \geq \boldsymbol{E}_0 \cdot [c\boldsymbol{T} + \langle (\boldsymbol{L} - c\boldsymbol{T})^{-1} \rangle^{-1}] \boldsymbol{E}_0, \tag{24.22}$$

which holds for all $\boldsymbol{E}_0$, and thus corresponds to a lower bound on the "energy" $\boldsymbol{E}_0 \cdot \boldsymbol{L}_* \boldsymbol{E}_0/2$.

24.4. A lower bound on the effective bulk modulus of a three-dimensional, two-phase composite

As an example of the use of quasiconvex translations, let us follow Francfort and Murat (1986) and derive a sharp lower bound on the effective bulk modulus of a three-dimensional isotropic composite of two isotropic phases. By assumption, the elasticity tensors of the phases and composite take the forms

$$\boldsymbol{\mathcal{C}}_i = 3\kappa_i \boldsymbol{\Lambda}_h + 2\mu_i \boldsymbol{\Lambda}_s, \quad i = 1, 2, *,$$

in which the κ_i and μ_i for $i = 1, 2, *$ represent the bulk and shear moduli of the two phases and composite, and where $\boldsymbol{\Lambda}_h$ and $\boldsymbol{\Lambda}_s$ are isotropic fourth-order tensors with elements

$$\{\boldsymbol{\Lambda}_h\}_{ijk\ell} = \tfrac{1}{3}\delta_{ij}\delta_{k\ell}, \quad \{\boldsymbol{\Lambda}_s\}_{ijk\ell} = \tfrac{1}{2}[\delta_{ik}\delta_{j\ell} + \delta_{i\ell}\delta_{kj}] - \tfrac{1}{3}\delta_{ij}\delta_{k\ell}.$$

The translation tensor $\boldsymbol{T}$ is taken to have a similar elastically isotropic form:

$$\boldsymbol{T} = 3\kappa_0 \boldsymbol{\Lambda}_h + 2\mu_0 \boldsymbol{\Lambda}_s.$$

Since for elasticity the space $\mathcal{E}_{\boldsymbol{k}}$ consists of those second-order tensors $\boldsymbol{B}$ that can be expressed in the form $\boldsymbol{B} = \boldsymbol{k} \otimes \boldsymbol{b} + \boldsymbol{b} \otimes \boldsymbol{k}$, it follows that the quasiconvexity condition (24.21) is fulfilled if and only if

$$\begin{aligned} \boldsymbol{B} \cdot \boldsymbol{T}\boldsymbol{B} &= \mathrm{Tr}\{(\boldsymbol{k} \otimes \boldsymbol{b} + \boldsymbol{b} \otimes \boldsymbol{k})[2\mu_0(\boldsymbol{k} \otimes \boldsymbol{b} + \boldsymbol{b} \otimes \boldsymbol{k}) + 2\boldsymbol{I}(\kappa_0 - 2\mu_0/3)(\boldsymbol{b} \cdot \boldsymbol{k})]\} \\ &= 4[\mu_0 |\boldsymbol{b}|^2 |\boldsymbol{k}|^2 + (\kappa_0 + \mu_0/3)(\boldsymbol{b} \cdot \boldsymbol{k})^2] \end{aligned}$$

is nonnegative for all choices of the vectors $\boldsymbol{b}$ and $\boldsymbol{k}$. By the Cauchy-Schwartz inequality this is satisfied if and only if

$$\mu_0 \geq 0, \quad \kappa_0 \geq -4\mu_0/3. \tag{24.23}$$

The harmonic mean bounds on the effective bulk modulus of the translated medium imply that

$$(\kappa_* - \kappa_0)^{-1} \leq f_1(\kappa_1 - \kappa_0)^{-1} + f_2(\kappa_2 - \kappa_0)^{-1}, \tag{24.24}$$

and hold provided that the bulk moduli and shear moduli of the phases in the translated medium remain positive, that is, provided that

$$\kappa_i - \kappa_0 \geq 0, \text{ and } \mu_i - \mu_0 \geq 0 \text{ for i} = 1, 2. \tag{24.25}$$

Let us suppose that the phases have been labeled so that $\mu_1 \geq \mu_2$. Then by taking $\mu_0 = \mu_2$ and $\kappa_0 = -4\mu_2/3$, which are the extreme values allowed by the constraints (24.23) and (24.25), we see that (24.24) reduces to the inequality

$$(\kappa_* + 4\mu_2/3)^{-1} \leq f_1(\kappa_1 + 4\mu_2/3)^{-1} + f_2(\kappa_2 + 4\mu_2/3)^{-1},$$

which is exactly the Hashin-Shtrikman-Hill lower bound on the effective bulk modulus κ_*. Francfort and Murat also derived the upper Hashin-Shtrikman-Walpole bulk modulus bound. The Hashin-Shtrikman-Walpole shear modulus bounds were subsequently also rederived using the translation method (Milton 1990a, 1990b).

24.5. Using the idea of embedding to extend the translation method

There is another important ingredient to the translation method of Murat and Tartar and Lurie and Cherkaev. It is the idea of embedding, which enables us to derive bounds on sums of energies rather than just on a single energy, as in (24.22). The key is to reinterpret a sum of energies as a single energy but for a different problem in which a block-diagonal matrix enters the constitutive law.

As an example let us consider the conductivity problem. When the composite is successively subject to n applied electric fields, $\boldsymbol{e}_0^{(1)}$, $\boldsymbol{e}_0^{(2)}$,... $\boldsymbol{e}_0^{(n)}$, the sum of the resulting energies can be reexpressed in the form

$$\sum_{\alpha=1}^{n} \boldsymbol{e}_0^{(\alpha)} \cdot \boldsymbol{\sigma}_* \boldsymbol{e}_0^{(\alpha)} = \boldsymbol{E}_0 \cdot \boldsymbol{\mathcal{L}}_* \boldsymbol{E}_0,$$

where

$$\boldsymbol{E}_0 = \begin{pmatrix} \boldsymbol{e}_0^{(1)} \\ \boldsymbol{e}_0^{(2)} \\ \vdots \\ \boldsymbol{e}_0^{(n)} \end{pmatrix}, \quad \boldsymbol{\mathcal{L}}_* = \begin{pmatrix} \boldsymbol{\sigma}_* & 0 & \ldots & 0 \\ 0 & \boldsymbol{\sigma}_* & \ldots & 0 \\ \vdots & \vdots & \ddots & \vdots \\ 0 & 0 & \ldots & \boldsymbol{\sigma}_* \end{pmatrix}, \tag{24.26}$$

and can be regarded as a single energy of a thermoelectric-type problem with no couplings between the fields. The constitutive relations linking the successive fields,

$$\boldsymbol{j}^{(\alpha)}(\boldsymbol{x}) = \boldsymbol{\sigma}(\boldsymbol{x})\boldsymbol{e}^{(\alpha)}(\boldsymbol{x}), \quad \text{where } \langle \boldsymbol{e}^{(\alpha)} \rangle = \boldsymbol{e}_0^{(\alpha)} \text{ for } \alpha = 1, 2 \ldots, n,$$

can be rewritten as a single thermoelectric-type constitutive law

$$\boldsymbol{J}(\boldsymbol{x}) = \boldsymbol{\mathcal{L}}(\boldsymbol{x})\boldsymbol{E}(\boldsymbol{x}), \quad \text{where } \langle \boldsymbol{E} \rangle = \boldsymbol{E}_0,$$

with fields

$$\boldsymbol{J}(\boldsymbol{x}) = \begin{pmatrix} \boldsymbol{j}^{(1)}(\boldsymbol{x}) \\ \boldsymbol{j}^{(2)}(\boldsymbol{x}) \\ \vdots \\ \boldsymbol{j}^{(n)}(\boldsymbol{x}) \end{pmatrix}, \quad \boldsymbol{E}(\boldsymbol{x}) = \begin{pmatrix} \boldsymbol{e}^{(1)}(\boldsymbol{x}) \\ \boldsymbol{e}^{(2)}(\boldsymbol{x}) \\ \vdots \\ \boldsymbol{e}^{(n)}(\boldsymbol{x}) \end{pmatrix}$$

and a block-diagonal matrix

$$\boldsymbol{\mathcal{L}}(\boldsymbol{x}) = \begin{pmatrix} \boldsymbol{\sigma}(\boldsymbol{x}) & 0 & \dots & 0 \\ 0 & \boldsymbol{\sigma}(\boldsymbol{x}) & \dots & 0 \\ \vdots & \vdots & \ddots & \vdots \\ 0 & 0 & \dots & \boldsymbol{\sigma}(\boldsymbol{x}) \end{pmatrix}$$

entering the constitutive law. We will call $\boldsymbol{J}(\boldsymbol{x})$ and $\boldsymbol{E}(\boldsymbol{x})$ the extended fields and $\boldsymbol{\mathcal{L}}(\boldsymbol{x})$ a supertensor (Gibiansky and Torquato 1993).

The translation bounds on the effective tensor $\boldsymbol{\mathcal{L}}_*$,

$$(\boldsymbol{\mathcal{L}}_* - c\boldsymbol{\mathcal{T}})^{-1} \leq \langle (\boldsymbol{\mathcal{L}} - c\boldsymbol{\mathcal{T}})^{-1} \rangle,$$

provide, through the relation (24.26) between $\boldsymbol{\mathcal{L}}_*$ and $\boldsymbol{\sigma}_*$, a constraint on the possible values that the effective conductivity tensor $\boldsymbol{\sigma}_*$ can take. These translation bounds now correspond to bounds on sums of energies in the same way that (24.17) corresponds to the bound (24.22) on a single energy.

Notice that the translation tensor $\boldsymbol{\mathcal{T}}$ is not required to be block-diagonal. It is only required to be quasiconvex in the sense that the inequality

$$\langle \boldsymbol{E} \cdot \boldsymbol{\mathcal{T}} \boldsymbol{E} \rangle \geq \langle \boldsymbol{E} \rangle \cdot \boldsymbol{\mathcal{T}} \langle \boldsymbol{E} \rangle$$

holds for all periodic fields of the form

$$\boldsymbol{E} = \begin{pmatrix} \boldsymbol{e}^{(1)} \\ \boldsymbol{e}^{(2)} \\ \vdots \\ \boldsymbol{e}^{(n)} \end{pmatrix} \quad \text{with} \quad \nabla \times \boldsymbol{e}^{(\alpha)} = 0 \ \text{ for } \alpha = 1, 2 \dots, n.$$

The constant c must still be positive and such that $\boldsymbol{\mathcal{L}}(\boldsymbol{x}) - c\boldsymbol{\mathcal{T}}$ remains positive-semidefinite for all $\boldsymbol{x}$.

24.6. Bounds on the conductivity tensor of a composite of two isotropic phases

To see how this embedding works, let us follow Lurie and Cherkaev (1982, 1984a) and Murat and Tartar (Murat and Tartar 1985; Tartar 1985) and consider a two-dimensional composite of two isotropic phases with conductivities σ_1 and σ_2 mixed in fixed proportions f_1 and $f_2 = 1 - f_1$. Without loss of generality we assume that the phases have been labeled so that $\sigma_1 > \sigma_2$ and that the coordinates have been chosen so that $\boldsymbol{\sigma}_*$ is diagonal:

$$\boldsymbol{\sigma}_* = \begin{pmatrix} \lambda_1^* & 0 \\ 0 & \lambda_2^* \end{pmatrix}. \tag{24.27}$$

Our objective is to seek bounds that constrain the possible values that the eigenvalue pair $(\lambda_1^*, \lambda_2^*)$ can have. Since we need to apply two different electric fields to measure the effective conductivity tensor, it is natural to take $n = 2$.

A natural choice for $\boldsymbol{\mathcal{T}}$ is then the null Lagrangian,

$$\boldsymbol{\mathcal{T}} = \begin{pmatrix} 0 & -\boldsymbol{R}_\perp \\ \boldsymbol{R}_\perp & 0 \end{pmatrix}, \quad \text{where } \boldsymbol{R}_\perp = \begin{pmatrix} 0 & 1 \\ -1 & 0 \end{pmatrix}, \tag{24.28}$$

which is self-adjoint and maps any pair of curl free fields to a pair of divergence free fields. The translated tensor field

$$\boldsymbol{\mathcal{L}}(\boldsymbol{x}) - c\boldsymbol{\mathcal{T}} = \begin{pmatrix} \sigma_1 & 0 & 0 & c \\ 0 & \sigma_1 & -c & 0 \\ 0 & -c & \sigma_1 & 0 \\ c & 0 & 0 & \sigma_1 \end{pmatrix} \chi_1(\boldsymbol{x}) + \begin{pmatrix} \sigma_2 & 0 & 0 & c \\ 0 & \sigma_2 & -c & 0 \\ 0 & -c & \sigma_2 & 0 \\ c & 0 & 0 & \sigma_2 \end{pmatrix} \chi_2(\boldsymbol{x})$$

is positive-semidefinite for all $\boldsymbol{x}$, provided that the absolute value of c is not greater than σ_2. From the block structure of the matrices

$$\langle (\boldsymbol{\mathcal{L}} - c\boldsymbol{\mathcal{T}})^{-1} \rangle = \frac{f_1}{(\sigma_1^2 - c^2)} \begin{pmatrix} \sigma_1 & 0 & 0 & -c \\ 0 & \sigma_1 & c & 0 \\ 0 & c & \sigma_1 & 0 \\ -c & 0 & 0 & \sigma_1 \end{pmatrix} + \frac{f_2}{(\sigma_2^2 - c^2)} \begin{pmatrix} \sigma_2 & 0 & 0 & -c \\ 0 & \sigma_2 & c & 0 \\ 0 & c & \sigma_2 & 0 \\ -c & 0 & 0 & \sigma_2 \end{pmatrix},$$

$$(\boldsymbol{\mathcal{L}}_* - c\boldsymbol{\mathcal{T}})^{-1} = \frac{1}{(\lambda_1^* \lambda_2^* - c^2)} \begin{pmatrix} \lambda_2^* & 0 & 0 & -c \\ 0 & \lambda_1^* & c & 0 \\ 0 & c & \lambda_2^* & 0 \\ -c & 0 & 0 & \lambda_1^* \end{pmatrix},$$

we see that the translation bounds separate into a pair of uncoupled 2×2 matrix inequalities, one of which implies that the bound

$$\begin{aligned} &\frac{1}{(\lambda_1^* \lambda_2^* - c^2)} \begin{pmatrix} a_1 & a_2 \end{pmatrix} \begin{pmatrix} \lambda_2^* & -c \\ -c & \lambda_1^* \end{pmatrix} \begin{pmatrix} a_1 \\ a_2 \end{pmatrix} \\ &\quad \le \frac{f_1}{(\sigma_1^2 - c^2)} \begin{pmatrix} a_1 & a_2 \end{pmatrix} \begin{pmatrix} \sigma_1 & -c \\ -c & \sigma_1 \end{pmatrix} \begin{pmatrix} a_1 \\ a_2 \end{pmatrix} + \frac{f_2}{(\sigma_2^2 - c^2)} \begin{pmatrix} a_1 & a_2 \end{pmatrix} \begin{pmatrix} \sigma_2 & -c \\ -c & \sigma_2 \end{pmatrix} \begin{pmatrix} a_1 \\ a_2 \end{pmatrix} \end{aligned}$$

holds for all choices of the constants a_1 and a_2.

In the extreme limit where c approaches its maximum allowed value, namely, σ_2, the right-hand side of the above equation approaches infinity unless $a_1 = a_2$. By setting $a_1 = a_2$ we obtain the nontrivial bound

$$\frac{\lambda_1^* + \lambda_2^* - 2\sigma_2}{2(\lambda_1^* \lambda_2^* - \sigma_2^2)} \le \frac{f_1}{\sigma_1 + \sigma_2} + \frac{f_2}{2\sigma_2} \tag{24.29}$$

in the limit as $c \to \sigma_2$. Subtracting $1/\sigma_2$ from both sides of this equation gives

$$\frac{(\lambda_1^* - \sigma_2)(\lambda_2^* - \sigma_2)}{2\sigma_2(\lambda_1^* \lambda_2^* - \sigma_2^2)} \ge \frac{f_1(\sigma_1 - \sigma_2)}{2\sigma_2(\sigma_1 + \sigma_2)},$$

which after taking the inverse of both sides can be seen to be equivalent to (23.62). In particular, for isotropic composites with $\boldsymbol{\sigma}_* = \sigma_* \boldsymbol{I}$ we have $\lambda_1^* = \lambda_2^* = \sigma_*$, and the bounds reduce to the Hashin-Shtrikman lower bound on the effective conductivity σ_*:

$$\frac{1}{\sigma_* + \sigma_2} \le \frac{f_1}{\sigma_1 + \sigma_2} + \frac{f_2}{2\sigma_2}.$$

To obtain an upper bound we need to work with the inverse tensors $\mathcal{L}_*^{-1}$ and $[\mathcal{L}(\boldsymbol{x})]^{-1}$, rather than with $\mathcal{L}_*$ and $\mathcal{L}(\boldsymbol{x})$. But we can still take $\mathcal{T}$ given by (24.28) as our translation since $\mathcal{T}$ also maps any pair of divergence free fields into a pair of curl free fields. The translation bound

$$(\mathcal{L}_*^{-1} - c\mathcal{T})^{-1} \leq \langle(\mathcal{L}^{-1} - c\mathcal{T})^{-1}\rangle$$

now holds provided that the absolute value of c is less than $1/\sigma_1$ and in the extreme limit as c approaches $1/\sigma_1$ implies

$$\frac{1/\lambda_1^* + 1/\lambda_2^* - 2/\sigma_1}{2(1/(\lambda_1^*\lambda_2^*) - 1/\sigma_1^2)} \geq \frac{f_1\sigma_1}{2} + \frac{f_2}{1/\sigma_1 + 1/\sigma_2},$$

which after some algebraic manipulation reduces to the bound

$$f_2 \sum_{i=1}^{2} \frac{1}{\sigma_1 - \lambda_i^*} \leq \frac{2}{\sigma_1 - \sigma_2} - \frac{f_1}{\sigma_1}. \tag{24.30}$$

It was the derivation of the bounds (23.62) and (24.30) by Lurie and Cherkaev (1984a) and Murat and Tartar (Murat and Tartar 1985; Tartar 1985) that generated considerable interest in the translation method. The bounds provided the complete characterization of the G-closure at constant volume fraction. I first heard of Murat and Tartar's results (for d-dimensional composites) at a conference on the macroscopic properties of disordered media that was held in New York in June 1981, and Lurie and Cherkaev's results for two-dimensional composites appeared shortly thereafter (Lurie and Cherkaev 1982). Lurie and Cherkaev's proof used the null Lagrangian (24.28). In 1983, Kohn visited them in Leningrad and told them about the quasiconvex functions introduced by Tartar, which they used in their proof of the three-dimensional conductivity bounds (Lurie and Cherkaev 1986).

Following Murat and Tartar (Murat and Tartar 1985; Tartar 1985) and Lurie and Cherkaev (1986) let us now obtain bounds for three-dimensional conducting composites. Since we now need to apply three different electric fields to measure the effective conductivity, we take $n = 3$. Instead of representing the extended electric field $\boldsymbol{E}(\boldsymbol{x})$ and extended current field $\boldsymbol{J}(\boldsymbol{x})$ as nine component vectors, it proves convenient (Tartar 1979b) to represent them as 3×3 matrices where the columns of $\boldsymbol{E}(\boldsymbol{x})$ are the fields $\boldsymbol{e}^{(1)}(\boldsymbol{x})$, $\boldsymbol{e}^{(2)}(\boldsymbol{x})$, and $\boldsymbol{e}^{(3)}(\boldsymbol{x})$, and the columns of $\boldsymbol{J}(\boldsymbol{x})$ are the fields $\boldsymbol{j}^{(1)}(\boldsymbol{x})$, $\boldsymbol{j}^{(2)}(\boldsymbol{x})$, and $\boldsymbol{j}^{(3)}(\boldsymbol{x})$. Assuming that the composite is isotropic, the tensors of the phases and the composite are then represented as fourth-order tensors $\mathcal{L}_1 = \sigma_1\mathcal{I}$, $\mathcal{L}_2 = \sigma_2\mathcal{I}$, and $\mathcal{L}_* = \sigma_*\mathcal{I}$, in which $\mathcal{I}$ is the fourth-order identity tensor.

The Hashin-Shtrikman lower bound on σ_* is obtained with $c = 1$ and the translation

$$\mathcal{T} = \sigma_2(\mathcal{I} - \boldsymbol{I} \otimes \boldsymbol{I}). \tag{24.31}$$

One can easily check that $\boldsymbol{B} \cdot \mathcal{T}\boldsymbol{B} \geq 0$ for all matrices $\boldsymbol{B} = \boldsymbol{k} \otimes \boldsymbol{b}$, implying that $\mathcal{T}$ is quasiconvex. Both

$$\mathcal{L}_1 - \mathcal{T} = (\sigma_1 - \sigma_2)\mathcal{I} + \sigma_2\boldsymbol{I} \otimes \boldsymbol{I} \quad \text{and} \quad \mathcal{L}_2 - \mathcal{T} = \sigma_2\boldsymbol{I} \otimes \boldsymbol{I} \tag{24.32}$$

are positive-semidefinite. From the translation bound we have

$$\boldsymbol{I} \cdot [(\sigma_* - \sigma_2)\mathcal{I} + \sigma_2\boldsymbol{I} \otimes \boldsymbol{I}]^{-1}\boldsymbol{I} \leq f_1\boldsymbol{I} \cdot [(\sigma_1 - \sigma_2)\mathcal{I} + \sigma_2\boldsymbol{I} \otimes \boldsymbol{I}]^{-1}\boldsymbol{I} + f_2\boldsymbol{I} \cdot [\sigma_2\boldsymbol{I} \otimes \boldsymbol{I}]^{-1}\boldsymbol{I},$$

which when evaluated gives the Hashin-Shtrikman bound

$$\frac{3}{\sigma_* + 2\sigma_2} \leq \frac{3f_1}{\sigma_1 + 2\sigma_2} + \frac{f_2}{\sigma_2}.$$

One can also obtain this bound using the null Lagrangian (6.19).

The Hashin-Shtrikman upper bound on $\boldsymbol{\sigma}_*$ is obtained by working with the inverse tensors $\boldsymbol{\mathcal{L}}_1^{-1}$, $\boldsymbol{\mathcal{L}}_2^{-1}$, and $\boldsymbol{\mathcal{L}}_*^{-1}$ and using the translation

$$\boldsymbol{\mathcal{T}}' = (\boldsymbol{\mathcal{I}} - 2\boldsymbol{I} \otimes \boldsymbol{I})/\sigma_1,$$

with $c = 1$. As yet, no one has derived this bound using null Lagrangians, and so we see that the idea of Tartar (1979b) of using quasiconvex functions rather than just null Lagrangians is a key ingredient for deriving bounds. More generally, if the composite is not isotropic, one obtains by this approach the bounds (23.13) and (23.14).

These bounds are just special cases of the trace bounds encountered in sections 23.5 on page 468 and 23.6 on page 474. In section 24.11 on page 518 we will show how the trace bounds can be recovered in general via the translation method.

24.7. The translation bounds as a corollary of the comparison bounds†

In typical applications the comparison bounds, unlike the translation bounds, do not incorporate information about the volume fractions of the constituents. However, by using the idea of embedding, we can easily incorporate such information in the comparison bounds. As we will see, the resulting bounds turn out to be identical to the translation bounds.

As an example, suppose that we have a quasiconvex translation $\boldsymbol{T}$ such that $\boldsymbol{L}(\boldsymbol{x}) - \boldsymbol{T}$ is positive-definite for all $\boldsymbol{x}$. We begin by supplementing the constitutive equation $\boldsymbol{J} = \boldsymbol{LE}$ with the scalar field equation

$$w(\boldsymbol{x}) = c(\boldsymbol{x})v, \quad \text{where } v = \text{ constant},$$

and where the scalar field $w(\boldsymbol{x})$ is not subject to any differential restrictions. The comparison bounds are applied to the embedded thermoelastic-type problem

$$\begin{pmatrix} \boldsymbol{J}(\boldsymbol{x}) \\ w \end{pmatrix} = \boldsymbol{\mathcal{L}}(\boldsymbol{x}) \begin{pmatrix} \boldsymbol{E}(\boldsymbol{x}) \\ v \end{pmatrix}, \quad \text{where } \boldsymbol{\mathcal{L}}(\boldsymbol{x}) = \begin{pmatrix} \boldsymbol{L}(\boldsymbol{x}) & 0 \\ 0 & c(\boldsymbol{x}) \end{pmatrix},$$

which has an associated effective tensor

$$\boldsymbol{\mathcal{L}}_* = \begin{pmatrix} \boldsymbol{L}_* & 0 \\ 0 & \langle c \rangle \end{pmatrix}.$$

Thus in a two-phase composite, knowledge of $\boldsymbol{\mathcal{L}}_*$ and hence $\langle c \rangle$ allows us to determine the volume fractions of the phases.

Let us take as translation the tensor

$$\boldsymbol{\mathcal{T}} = \begin{pmatrix} \boldsymbol{T} & \boldsymbol{q} \\ \boldsymbol{q}^T & 0 \end{pmatrix},$$

which will be quasiconvex for the extended problem, because $\boldsymbol{T}$ is quasiconvex for the embedded problem. We require that $\boldsymbol{\mathcal{L}}(\boldsymbol{x}) - \boldsymbol{\mathcal{T}}$ be positive-definite for all $\boldsymbol{x}$ or, equivalently, that for all $\boldsymbol{x}$ the associated quadratic form

$$\boldsymbol{P} \cdot (\boldsymbol{L}(\boldsymbol{x}) - \boldsymbol{T})\boldsymbol{P} - 2v\boldsymbol{P} \cdot \boldsymbol{q} + v^2 c(\boldsymbol{x})$$

be positive for all choices of $\boldsymbol{P}$ and v not both zero. By choosing the value

$$\boldsymbol{P} = v(\boldsymbol{L}(\boldsymbol{x}) - \boldsymbol{T})^{-1}\boldsymbol{q},$$

which minimizes the quadratic form, we see that $\boldsymbol{\mathcal{L}}(\boldsymbol{x}) - \boldsymbol{\mathcal{T}}$ is positive-definite when

$$c(\boldsymbol{x}) - \boldsymbol{q} \cdot (\boldsymbol{L}(\boldsymbol{x}) - \boldsymbol{T})^{-1}\boldsymbol{q} > 0. \tag{24.33}$$

Once this constraint is satisfied for all $\boldsymbol{x}$, the comparison bounds imply that $\boldsymbol{\mathcal{L}}_* - \boldsymbol{\mathcal{T}}$ is positive-definite. Equivalently, $\boldsymbol{L}_* - \boldsymbol{T}$ must be positive-definite, and

$$\langle c \rangle > \boldsymbol{q} \cdot (\boldsymbol{L}_* - \boldsymbol{T})^{-1}\boldsymbol{q}, \tag{24.34}$$

where the latter inequality is obtained by following the same argument that leads to (24.33). By selecting $c(\boldsymbol{x})$ so that the left-hand side of (24.33) equals a small positive constant ϵ, we see that (24.34) will be satisfied for all $\epsilon > 0$ if and only if

$$\boldsymbol{q} \cdot (\boldsymbol{L}_* - \boldsymbol{T})^{-1}\boldsymbol{q} \leq \boldsymbol{q} \cdot \langle (\boldsymbol{L}(\boldsymbol{x}) - \boldsymbol{T})^{-1} \rangle \boldsymbol{q}.$$

Since the vector $\boldsymbol{q}$ is arbitrary, this is just the familiar translation bound.

24.8. Embedding in a higher order tensorial problem: A lower bound on the conductivity tensor of a polycrystal

Section 24.5 on page 505 introduced the idea of embedding, whereby a set of conductivity equations that arise as the composite is subject to a sequence of n applied fields are viewed as a single thermoelectric-type problem with no coupling between the n fields. For the special case $n = d$, the equations can also be interpreted as a problem involving second-order tensor fields linked by a fourth-order tensor in the constitutive law. This connection between higher order tensorial problems and thermoelectric-type problems was alluded to in section 6.4 on page 98. There elasticity problems were shown to be equivalent to a subclass of thermoelectric-type problems.

If we consider a three-dimensional composite and let the current fields $\boldsymbol{j}^{(1)}(\boldsymbol{x})$, $\boldsymbol{j}^{(2)}(\boldsymbol{x})$, and $\boldsymbol{j}^{(3)}(\boldsymbol{x})$ form the three columns of a 3×3 matrix-valued field $\boldsymbol{J}(\boldsymbol{x})$ and let the electric fields $\boldsymbol{e}^{(1)}(\boldsymbol{x})$, $\boldsymbol{e}^{(2)}(\boldsymbol{x})$, and $\boldsymbol{e}^{(3)}(\boldsymbol{x})$ form the three columns of a 3×3 matrix-valued field $\boldsymbol{E}(\boldsymbol{x})$, then the constitutive law $\boldsymbol{J} = \boldsymbol{\mathcal{L}}\boldsymbol{E}$ still holds with $\boldsymbol{\mathcal{L}}(\boldsymbol{x})$ being a fourth-order tensor with elements

$$L_{ijk\ell}(\boldsymbol{x}) = \sigma_{ik}(\boldsymbol{x})\delta_{j\ell}.$$

The effect of $\boldsymbol{\mathcal{L}}(\boldsymbol{x})$ acting on a matrix-valued field $\boldsymbol{E}(\boldsymbol{x})$ is simply to multiply $\boldsymbol{E}(\boldsymbol{x})$ on the left by $\boldsymbol{\sigma}(\boldsymbol{x})$.

We are now in a position to forget about the original equations and deal exclusively with the equations

$$\boldsymbol{J}(\boldsymbol{x}) = \boldsymbol{\mathcal{L}}(\boldsymbol{x})\boldsymbol{E}(\boldsymbol{x}), \quad \nabla \cdot \boldsymbol{J}(\boldsymbol{x}) = 0, \quad \nabla \times \boldsymbol{E}(\boldsymbol{x}) = 0, \tag{24.35}$$

in which the divergence and curl act on the first index of the second-order tensor fields $\boldsymbol{J}(\boldsymbol{x})$ and $\boldsymbol{E}(\boldsymbol{x})$. Moreover, having established the mathematical equivalence in a particular coordinate system, we are free to suppose that the fields $\boldsymbol{J}(\boldsymbol{x})$, $\boldsymbol{E}(\boldsymbol{x})$, and $\boldsymbol{\mathcal{L}}(\boldsymbol{x})$ transform as second- and fourth-order tensor fields. In other words, under a rotation of the coordinate system from $\boldsymbol{x}$ to $\boldsymbol{x}' = \boldsymbol{R}\boldsymbol{x}$, where $\boldsymbol{R}$ is a rotation matrix, we are free to suppose that the elements of the tensors undergo the transformations

$$J_{ij}(\boldsymbol{x}) \to \sum_{m,n=1}^{d} R_{mi}R_{nj}J_{mn}(\boldsymbol{x}'), \qquad E_{k\ell}(\boldsymbol{x}) \to \sum_{o,p=1}^{d} R_{ok}R_{p\ell}E_{op}(\boldsymbol{x}'),$$

$$L_{ijk\ell}(\boldsymbol{x}) \to \sum_{m,n,o,p=1}^{d} R_{mi}R_{nj}R_{ok}R_{p\ell}L_{mnop}(\boldsymbol{x}').$$

Such transformation laws are not appropriate to thermoelectric-type equations, but they are appropriate to the equivalent higher order tensorial problem that we are now considering.

This change of viewpoint is not just cosmetic; it also has a real advantage. Translations that would not be regarded as being rotationally invariant from the perspective of the thermoelectric-type equations are sometimes rotationally invariant from the perspective of the higher order tensorial equations. For example, the translation

$$T_{ijk\ell} = \delta_{ij}\delta_{k\ell} - \delta_{i\ell}\delta_{jk}, \tag{24.36}$$

which we encountered in section 6.4 on page 98 (see equation (6.19)) is of this type: It is clearly rotationally invariant when regarded as a fourth-order tensor, but when regarded as a thermoelectric-type tensor its matrix elements under rotation undergo the transformation

$$T_{ijk\ell} \to \sum_{m,n=1}^{d} R_{mi}R_{nk}T_{mjn\ell} = R_{ji}R_{\ell k} - R_{\ell i}R_{jk} \neq T_{ijk\ell}.$$

Clearly $\boldsymbol{\mathcal{T}}$ does not correspond to an isotropic thermoelectric-type tensor.

As we have seen in (24.9), rotationally invariant translations are particularly useful for deriving bounds on the effective tensors of polycrystals. As an example let us take $\boldsymbol{\sigma}(\boldsymbol{x})$ as the conductivity tensor field of a polycrystal:

$$\boldsymbol{\sigma}(\boldsymbol{x}) = \boldsymbol{R}(\boldsymbol{x})\boldsymbol{\sigma}_0\boldsymbol{R}^T(\boldsymbol{x}), \quad \text{where } \boldsymbol{\sigma}_0 = \begin{pmatrix} \lambda_1 & 0 & 0 \\ 0 & \lambda_2 & 0 \\ 0 & 0 & \lambda_3 \end{pmatrix} \text{ with } \lambda_1 \geq \lambda_2 \geq \lambda_3.$$

The associated fourth-order tensor field $\boldsymbol{\mathcal{L}}(\boldsymbol{x})$ also corresponds to a polycrystal:

$$\boldsymbol{\mathcal{L}}(\boldsymbol{x}) = \boldsymbol{R}(\boldsymbol{x})\boldsymbol{R}(\boldsymbol{x})\boldsymbol{\mathcal{L}}_0\boldsymbol{R}^T(\boldsymbol{x})\boldsymbol{R}^T(\boldsymbol{x}), \quad \text{where } \{\boldsymbol{\mathcal{L}}_0\}_{ijk\ell} = \{\boldsymbol{\sigma}_0\}_{ik}\delta_{j\ell} = \lambda_i\delta_{ik}\delta_{j\ell}.$$

Taking $\boldsymbol{\mathcal{T}}$ given by (24.36) as our translation we see that the inequality

$$\boldsymbol{\mathcal{L}}(\boldsymbol{x}) - c\boldsymbol{\mathcal{T}} = \boldsymbol{R}(\boldsymbol{x})\boldsymbol{R}(\boldsymbol{x})(\boldsymbol{\mathcal{L}}_0 - c\boldsymbol{\mathcal{T}})\boldsymbol{R}(\boldsymbol{x})\boldsymbol{R}(\boldsymbol{x}) \geq 0$$

holds if and only if $\boldsymbol{\mathcal{L}}_0 - \boldsymbol{\mathcal{T}} \geq 0$. In the representation where $\boldsymbol{\mathcal{T}}$ is a 9×9 matrix, as in (6.18), the constraint takes the form

$$\boldsymbol{\mathcal{L}}_0 - c\boldsymbol{\mathcal{T}} = \begin{pmatrix} \lambda_1 & 0 & 0 & 0 & -c & 0 & 0 & 0 & -c \\ 0 & \lambda_2 & 0 & c & 0 & 0 & 0 & 0 & 0 \\ 0 & 0 & \lambda_3 & 0 & 0 & 0 & c & 0 & 0 \\ 0 & c & 0 & \lambda_1 & 0 & 0 & 0 & 0 & 0 \\ -c & 0 & 0 & 0 & \lambda_2 & 0 & 0 & 0 & -c \\ 0 & 0 & 0 & 0 & 0 & \lambda_3 & 0 & c & 0 \\ 0 & 0 & c & 0 & 0 & 0 & \lambda_1 & 0 & 0 \\ 0 & 0 & 0 & 0 & 0 & c & 0 & \lambda_2 & 0 \\ -c & 0 & 0 & 0 & -c & 0 & 0 & 0 & \lambda_3 \end{pmatrix} \geq 0. \tag{24.37}$$

By separating this into blocks we see that the inequality holds if and only if

$$\begin{pmatrix} \lambda_1 & -c & -c \\ -c & \lambda_2 & -c \\ -c & -c & \lambda_3 \end{pmatrix} \geq 0 \tag{24.38}$$

and

$$\begin{pmatrix} \lambda_2 & c \\ c & \lambda_1 \end{pmatrix} \geq 0, \quad \begin{pmatrix} \lambda_3 & c \\ c & \lambda_1 \end{pmatrix} \geq 0, \quad \begin{pmatrix} \lambda_3 & c \\ c & \lambda_2 \end{pmatrix} \geq 0. \tag{24.39}$$

By examining the various 2×2 sub-blocks of the 3×3 matrix in (24.38) it is evident that the positivity of this matrix ensures the positivity of the matrices in (24.39). In other words, we need only consider the matrix inequality (24.38). The maximum value of c for which this holds is the unique positive root of the equation

$$\lambda_1\lambda_2\lambda_3 - (\lambda_1 + \lambda_2 + \lambda_3)c^2 - 2c^3 = 0. \tag{24.40}$$

Without loss of generality we can suppose that the coordinates have been chosen so that $\boldsymbol{\sigma}_*$ is diagonal. Then the associated effective tensor $\boldsymbol{\mathcal{L}}_*$ has elements

$$\{\boldsymbol{\mathcal{L}}_*\}_{ijk\ell} = \{\boldsymbol{\sigma}_*\}_{ik}\delta_{j\ell} = \lambda_i^*\delta_{ik}\delta_{j\ell},$$

in which the λ_i^*, for $i = 1, 2, 3$ are the eigenvalues of $\boldsymbol{\sigma}_*$. Clearly when $\boldsymbol{\mathcal{L}}_* - c\boldsymbol{\mathcal{T}}$ is represented as a 9×9 matrix, it takes the same form as the matrix $\boldsymbol{\mathcal{L}}_0 - c\boldsymbol{\mathcal{T}}$ given in (24.37), but with λ_1, λ_2, and λ_3 replaced by λ_1^*, λ_2^*, and λ_3^*. The positivity of $\boldsymbol{\mathcal{L}}_* - c\boldsymbol{\mathcal{T}}$ implied by the comparison bounds then leads directly to the bound

$$\lambda_1^*\lambda_2^*\lambda_3^* - (\lambda_1^* + \lambda_2^* + \lambda_3^*)c^2 - 2c^3 \geq 0, \tag{24.41}$$

derived by Avellaneda, Cherkaev, Lurie, and Milton (1988) using essentially this approach.

In particular, if we consider a isotropic polycrystal, with $\lambda_1^* = \lambda_2^* = \lambda_3^* = \sigma_*$, which is constructed from a uniaxial crystal, with $\lambda_2 = \lambda_3$, then the positive root of the cubic polynomial (24.40) is

$$c = \frac{\lambda_1}{4}\Big[-1 + \sqrt{1 + 8(\lambda_2/\lambda_1)}\,\Big],$$

and the bound (24.41) factorizes and implies

$$\boldsymbol{\sigma}_* \geq 2c = \frac{\lambda_1}{2}\Big[-1 + \sqrt{1 + 8(\lambda_2/\lambda_1)}\,\Big]. \tag{24.42}$$

By comparing the expression with the formula (7.30) we see that the bound is attained when the polycrystal is Schulgasser's assemblage of spheres, each with the crystal oriented so that its axis of conductivity λ_1 is directed radially. Thus his assemblage has the minimum possible effective conductivity. There also exist isotropic polycrystals that attain the bound (24.41) even when the constituent crystal is not uniaxial. These microstructures will be described in section 25.4 on page 537.

The interpretation of $\boldsymbol{\mathcal{T}}$ as a rotationally invariant fourth-order tensor is implicit in the paper of Avellaneda, Cherkaev, Lurie, and Milton (1988). Rotationally invariant eighth-order tensors $\boldsymbol{\mathcal{T}}$ were found to be useful for rederiving the three-dimensional Hashin-Shtrikman-Walpole shear modulus bounds using the translation method (Milton 1990a, 1990b).

24.9. A geometric characterization of translations†

In this section we obtain an alternative characterization of translations that will allow us to generate large classes of useful translations. Furthermore, we will see that finding translations is like fitting a round peg into a square hole, or more precisely, like fitting an ellipsoid into a nonellipsoidal cavity. The interesting translations are operators that are neither positive- nor

negative-definite, but those that have both positive and negative eigenvalues. This suggests that it might be useful to express $\boldsymbol{T}$ in the form

$$\boldsymbol{T} = \boldsymbol{L}_0 - \boldsymbol{\rho},$$

in which $\boldsymbol{L}_0$ is positive-definite and $\boldsymbol{\rho}$ positive-semidefinite. Clearly this decomposition of $\boldsymbol{T}$ is nonunique. Treating $\boldsymbol{L}_0$ as fixed, let us now examine what values $\boldsymbol{\rho}$ can take while still maintaining the quasiconvexity of $\boldsymbol{T}$.

First observe that $\boldsymbol{T}$ will be quasiconvex if and only if for all $\boldsymbol{k} \neq 0$ the inequality

$$\boldsymbol{B} \cdot \boldsymbol{L}_0 \boldsymbol{B} \geq 2\boldsymbol{P} \cdot \boldsymbol{B} - \boldsymbol{P} \cdot \boldsymbol{\rho}^{-1} \boldsymbol{P}$$

holds for all $\boldsymbol{B} \in \mathcal{E}_{\boldsymbol{k}}$ and all $\boldsymbol{P} \in \mathcal{V}$, in which $\mathcal{V}$ denotes the range of $\boldsymbol{\rho}$ and $\boldsymbol{\rho}^{-1}$ is the inverse of $\boldsymbol{\rho}$ on the subspace $\mathcal{V}$. The equivalence of this and (24.21) can be verified by taking the maximum over $\boldsymbol{P} \in \mathcal{V}$ of the right-hand side. Rewriting this inequality as

$$\boldsymbol{P} \cdot \boldsymbol{\rho}^{-1} \boldsymbol{P} \geq 2\boldsymbol{P} \cdot \boldsymbol{B} - \boldsymbol{B} \cdot \boldsymbol{L}_0 \boldsymbol{B},$$

and taking the maximum of the right-hand side over $\boldsymbol{B} \in \mathcal{E}_{\boldsymbol{k}}$, we deduce that $\boldsymbol{T}$ is quasiconvex if and only if, for all unit vectors $\boldsymbol{k}$,

$$\boldsymbol{P} \cdot \boldsymbol{\rho}^{-1} \boldsymbol{P} \geq \boldsymbol{P} \cdot \boldsymbol{\Gamma}(\boldsymbol{k}) \boldsymbol{P} \text{ for all } \boldsymbol{P} \in \mathcal{V}, \quad \text{where } \boldsymbol{\Gamma}(\boldsymbol{k}) = \boldsymbol{\Gamma}_1 (\boldsymbol{\Gamma}_1 \boldsymbol{L}_0 \boldsymbol{\Gamma}_1)^{-1} \boldsymbol{\Gamma}_1. \tag{24.43}$$

This condition is both necessary and sufficient for the quasiconvexity of $\boldsymbol{T}$ (Milton 1990b, 1994). [The above derivation, due to an anonymous referee of my 1994 paper, simplifies the one given in my 1990 paper.]

Although we restricted $\boldsymbol{L}_0$ to be positive-definite, it is clear from this derivation that we only need to assume that $\boldsymbol{L}_0$ is strictly quasiconvex on $\mathcal{E}$. Curiously, equality in (24.21) does not imply equality in (24.43). For example, if $\boldsymbol{T}$ is a null Lagrangian, then (24.21) is satisfied as an equality for all $\boldsymbol{k}$, whereas (24.43) cannot be satisfied as an equality for all $\boldsymbol{k}$ because $\boldsymbol{\Gamma}(\boldsymbol{k})$ depends on $\boldsymbol{k}$, whereas $\boldsymbol{\rho}$ does not.

An important class of translations are those that have only one negative eigenvalue. These can be expressed in the form

$$\boldsymbol{T} = \boldsymbol{L}_0 - \boldsymbol{\rho}, \quad \text{with } \boldsymbol{\rho} = \alpha \boldsymbol{v} \otimes \boldsymbol{v}, \tag{24.44}$$

where α is a positive constant and $\boldsymbol{v}$ is a unit vector satisfying $\boldsymbol{v} \cdot \boldsymbol{v} = 1$. The subspace $\mathcal{V}$ is one-dimensional, consisting of all multiples of $\boldsymbol{v}$, and the condition (24.43) for quasiconvexity reduces to a simple scalar constraint on the constant α,

$$1/\alpha \geq \boldsymbol{v} \cdot \boldsymbol{\Gamma}(\boldsymbol{k}) \boldsymbol{v} \text{ for all } \boldsymbol{k} \neq 0, \tag{24.45}$$

and the largest value of α for which this holds is clearly

$$\alpha = 1/r(\boldsymbol{v} \otimes \boldsymbol{v}), \quad \text{where } r(\boldsymbol{M}) = \max_{\substack{\boldsymbol{\xi} \\ |\boldsymbol{\xi}|=1}} \text{Tr}[\boldsymbol{M} \boldsymbol{\Gamma}(\boldsymbol{\xi})]. \tag{24.46}$$

We will see in section 24.12 on page 519 that translations in this class are useful for deriving the trace bounds that were obtained in sections 23.5 on page 468 and 23.6 on page 474 of the last chapter, from the Hashin-Shtrikman variational inequalities.

What is the geometrical interpretation of (24.43)? Let us suppose that a basis has been chosen for the subspace $\mathcal{V}$. In a space with the elements of the vector representing $\boldsymbol{P}$ as coordinates let us define $\boldsymbol{\Phi}$ and $\boldsymbol{\Psi}(\boldsymbol{k})$ as the solid ellipsoids

$$\boldsymbol{\Phi} = \{\boldsymbol{P} \mid \boldsymbol{P} \in \mathcal{V},\ \boldsymbol{P} \cdot \boldsymbol{\rho}^{-1}\boldsymbol{P} \le 1\}, \qquad \boldsymbol{\Psi}(\boldsymbol{k}) = \{\boldsymbol{P} \mid \boldsymbol{P} \in \mathcal{V},\ \boldsymbol{P} \cdot \boldsymbol{\Gamma}(\boldsymbol{k})\boldsymbol{P} \le 1\},$$

centered at the origin $\boldsymbol{P} = 0$. Depending on the orientation of $\mathcal{V}$, the solid ellipsoid $\boldsymbol{\Psi}(\boldsymbol{k})$ may in fact be more like an elliptical cylinder, with a "cylinder axis" possibly being a multi-dimensional subspace: The "axis" is the subspace $\mathcal{V} \cap \mathcal{J}_{\boldsymbol{k}}$. Let us define $\boldsymbol{\Psi}$ as the region of intersection of these solid ellipsoids or elliptical cylinders:

$$\boldsymbol{\Psi} = \bigcap_{\substack{\boldsymbol{k} \\ |\boldsymbol{k}| = 1}} \boldsymbol{\Psi}(\boldsymbol{k}).$$

In the important case where $\boldsymbol{L}_0 = \sigma_0 \boldsymbol{I}$ and $\mathcal{E}$ is comprised of $d \times m$ matrix-valued fields $\boldsymbol{E}(\boldsymbol{x})$ that are gradients of m-component periodic potentials $\boldsymbol{u}(\boldsymbol{x})$ [so that $\boldsymbol{\Gamma}(\boldsymbol{k}) = \boldsymbol{k} \otimes \boldsymbol{k}/\sigma_0$], we have

$$\boldsymbol{\Psi} = \{\boldsymbol{P} \mid \boldsymbol{P}\boldsymbol{P}^T \le \sigma_0 \boldsymbol{I}\},$$

in which $\boldsymbol{I}$ is the $d \times d$ identity tensor.

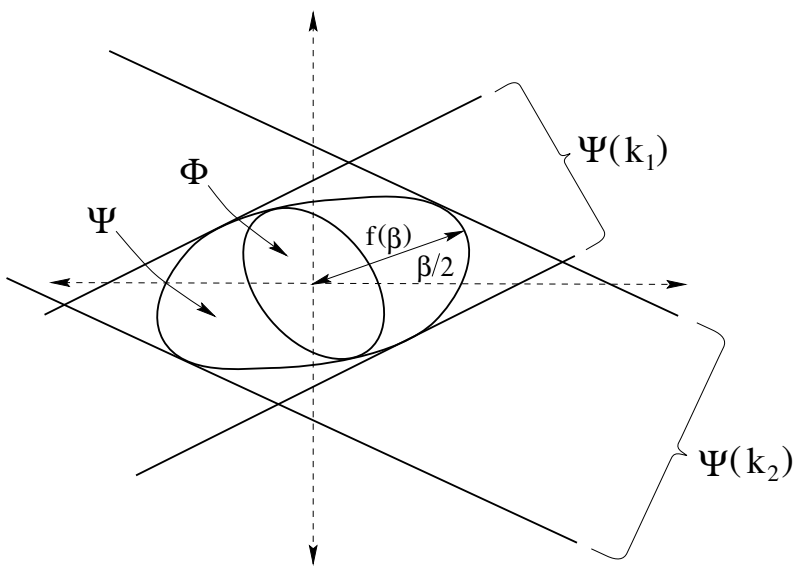

Figure 24.1. Finding translations is like finding ellipsoids $\boldsymbol{\Phi}$ that lie in a nonelliptical cavity $\boldsymbol{\Psi}$, where $\boldsymbol{\Psi}$ is the intersection of the regions $\boldsymbol{\Psi}(\boldsymbol{k})$ as $\boldsymbol{k}$ varies over all unit vectors. Illustrated is the case where $\mathcal{V}$ is two-dimensional and $\mathcal{V} \cap \mathcal{J}_{\boldsymbol{k}}$ is one-dimensional for all $\boldsymbol{k}$, so that $\boldsymbol{\Psi}(\boldsymbol{k})$ degenerates to a strip.

Clearly the inequality (24.43) implies that any $\boldsymbol{P}$ in $\boldsymbol{\Phi}$ necessarily lies in $\boldsymbol{\Psi}$. Due to the quadratic nature of this inequality, the converse is also true. In other words, as illustrated in figure 24.1, $\boldsymbol{T}$ is quasiconvex if and only if $\boldsymbol{\Phi} \subset \boldsymbol{\Psi}$. This is the precise sense in which finding translations is like fitting an ellipsoid into a nonellipsoidal cavity; the ellipsoid is represented by $\boldsymbol{\Phi}$ and the cavity by $\boldsymbol{\Psi}$.

When $\mathcal{V}$ is two-dimensional there is another geometrical interpretation of (24.43) that is due to Smyshlyaev and Willis (1999) and also Smyshlyaev (private communication). If we introduce polar coordinates (r, θ) in the space $\mathcal{V}$ and let $\beta = 2\theta$, then the equation of the boundary of the ellipse $\mathbf{\Phi}$ can be written in the form

$$(b + a_1)r^2 \cos^2(\beta/2) + (b - a_1)r^2 \sin^2(\beta/2) + 2a_2 r^2 \cos(\beta/2) \sin(\beta/2) = 1$$

or, equivalently,

$$1/r^2 = a_1 \cos\beta + a_2 \sin\beta + b.$$

The boundary of the cavity $\mathbf{\Psi}$ is then described by a curve $r = f(\beta)$, as illustrated in figure 24.1 on the facing page, and the constraint that the ellipse lies inside the cavity reduces to the inequality

$$a_1 \cos\beta + a_2 \sin\beta + b \geq 1/[f(\beta)]^2. \tag{24.47}$$

If we introduce coordinates $y_1 = r\cos\beta$ and $y_2 = r\sin\beta$ and plot $1/[f(\beta)]^2$ as a cut cylinder sitting on the unit disk as in figure 24.2, the inequality (24.47) says that the plane

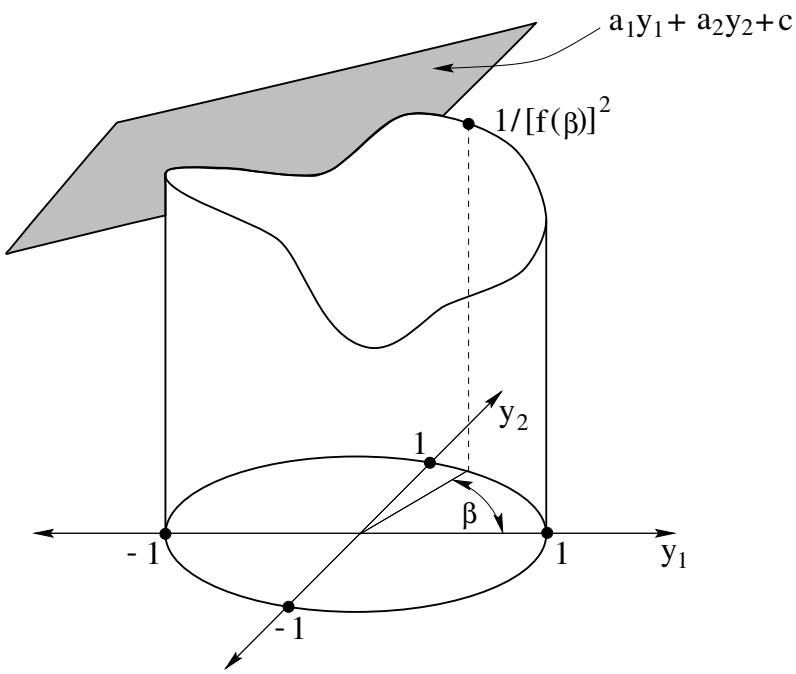

Figure 24.2. When $\mathcal{V}$ is two-dimensional and fixed, finding translations can also be interpreted as a problem of finding planes that lie above a cut cylinder. After Smyshlyaev and Willis (1999).

corresponding to the linear function $a_1 y_1 + a_2 y_2 + b$ lies above the cut cylinder. Moving the plane is equivalent to adjusting $\boldsymbol{\rho}$ (while keeping $\mathcal{V}$ fixed). The nonnegativity of $1/f^2$ guarantees that any plane above the cut cylinder will correspond to a positive-semidefinite matrix $\boldsymbol{\rho}$. Often one expects to find certain special planes that are above the cut cylinder but which touch it at three values of β. These correspond to ellipsoids $\mathbf{\Phi}$ inside the cavity $\mathbf{\Psi}$ that touch the boundary of $\mathbf{\Psi}$ at six points (if they touch at $\boldsymbol{P}$ they will also touch at $-\boldsymbol{P}$).

Depending on the form of f there may only be planes that touch the cut cylinder at two values of β, or there may be planes that touch it at more than three values of β, or possibly infinitely many values of β, as happens when $\boldsymbol{T}$ is a null Lagrangian. The different possibilities are easiest to visualize if one takes the convexification (convex hull) of the cut cylinder. The top surface then has flat sections, corresponding to planes touching the cut cylinder at three or more points, and ruled surfaces with each tie line being identified with a plane touching the cut cylinder at the two endpoints of the tie line, as illustrated in figure 24.3.

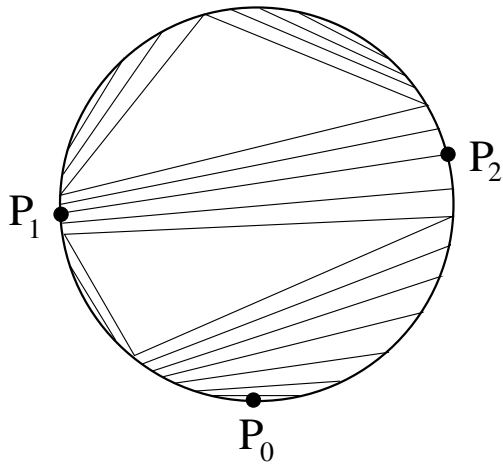

Figure 24.3. The view from above the convexification of the cut cylinder. Shown are two triangular regions, each corresponding to an ellipse touching the cavity walls at six points, and various tie lines, each corresponding to an ellipse touching the cavity walls at four points. There are also tie lines of zero length, such as at $\boldsymbol{P}_0$, each corresponding to an ellipse touching the cavity walls at just two points.

The constraint that $\boldsymbol{L}(\boldsymbol{x}) - c\boldsymbol{T} \geq 0$ can also be given a geometrical interpretation. Without loss of generality, let us suppose that $c = 1$ and $\boldsymbol{L}_0$ has been chosen sufficiently large so that $\boldsymbol{L}_0 \geq \boldsymbol{L}(\boldsymbol{x})$ for all $\boldsymbol{x}$. Then the constraint reads as $\boldsymbol{\rho} \geq \boldsymbol{L}_0 - \boldsymbol{L}(\boldsymbol{x})$ or, equivalently,

$$[\boldsymbol{L}_0 - \boldsymbol{L}(\boldsymbol{x})]^{-1} \geq \boldsymbol{\rho}^{-1}. \tag{24.48}$$

Let us define $\boldsymbol{\Theta}(\boldsymbol{x})$ as the solid ellipsoid

$$\boldsymbol{\Theta}(\boldsymbol{x}) = \{\boldsymbol{P} \mid \boldsymbol{P} \in \mathcal{V},\ \boldsymbol{P} \cdot [\boldsymbol{L}_0 - \boldsymbol{L}(\boldsymbol{x})]^{-1}\boldsymbol{P} \leq 1\}$$

and $\boldsymbol{\Theta}$ as the inclusion that is the union of these ellipsoids,

$$\boldsymbol{\Theta} = \bigcup_{\boldsymbol{x}} \boldsymbol{\Theta}(\boldsymbol{x}).$$

Then the inequality (24.48) states that the ellipsoid $\boldsymbol{\Phi}$ must contain the inclusion $\boldsymbol{\Theta}$. There certainly exists at least one ellipsoid $\boldsymbol{\Phi}$ inside the cavity $\boldsymbol{\Psi}$ yet containing $\boldsymbol{\Theta}$, corresponding to the translation $\boldsymbol{T} = 0$.

24.10. Translation bounds on the Y-tensor

In section 19.1 on page 397 we established a one-to-one correspondence between effective tensors $\boldsymbol{L}_*$ and Y-tensors $\boldsymbol{Y}_*$ in two-phase composites (assuming that $\boldsymbol{L}_1 - \boldsymbol{L}_2$ is nonsingular).

Consequently, in such media the problem of finding constraints on the values that $\boldsymbol{L}_*$ can take is equivalent to that of trying to obtain constraints on the values that $\boldsymbol{Y}_*$ can take. The translation bounds on $\boldsymbol{L}_*$ imply that

$$\boldsymbol{L}_* \geq c\boldsymbol{T} + [f_1(\boldsymbol{L}_1 - c\boldsymbol{T})^{-1} + f_2(\boldsymbol{L}_2 - c\boldsymbol{T})^{-1}]^{-1}, \tag{24.49}$$

and hold provided that

$$\boldsymbol{T} \geq 0 \text{ on } \mathcal{E}, \quad \boldsymbol{L}_1 - c\boldsymbol{T} \geq 0, \quad \boldsymbol{L}_2 - c\boldsymbol{T} \geq 0.$$

Rather than using (24.49) to obtain constraints on the values that the effective tensor $\boldsymbol{L}_*$ can take, it is much easier to work with the equivalent bound on the Y-tensor $\boldsymbol{Y}_*$, which takes a surprisingly simple form:

$$\boldsymbol{Y}_* + c\boldsymbol{T} \geq 0. \tag{24.50}$$

This form of the translation bounds was first obtained by Cherkaev and Gibiansky (1992), assuming that the matrices $\boldsymbol{L}_1$ and $\boldsymbol{L}_2$ commute. This latter restriction was subsequently removed (Milton 1991).

To prove the equivalence of these bounds, without assuming that $\boldsymbol{L}_1$ and $\boldsymbol{L}_2$ commute, we need the following identity, which holds for any matrix $\boldsymbol{A}$:

$$\begin{aligned} f_1\boldsymbol{A} + f_2\boldsymbol{I} - f_1f_2(\boldsymbol{A} - \boldsymbol{I})(f_1\boldsymbol{I} + f_2\boldsymbol{A})^{-1}(\boldsymbol{A} - \boldsymbol{I}) \\ = [(f_1\boldsymbol{A} + f_2\boldsymbol{I})(f_1\boldsymbol{I} + f_2\boldsymbol{A}) - f_1f_2(\boldsymbol{A} - \boldsymbol{I})^2](f_1\boldsymbol{I} + f_2\boldsymbol{A})^{-1} \\ = (f_1 + f_2)^2\boldsymbol{A}(f_1\boldsymbol{I} + f_2\boldsymbol{A})^{-1} = (f_1\boldsymbol{A}^{-1} + f_2\boldsymbol{I})^{-1}. \end{aligned}$$

Upon setting $\boldsymbol{A} = (\boldsymbol{L}_1 - c\boldsymbol{T})(\boldsymbol{L}_2 - c\boldsymbol{T})^{-1}$ and multiplying on the right by $\boldsymbol{L}_2 - c\boldsymbol{T}$, we see that

$$\begin{aligned} [f_1(\boldsymbol{L}_1 - c\boldsymbol{T})^{-1} + f_2(\boldsymbol{L}_2 - c\boldsymbol{T})^{-1}]^{-1} \\ = f_1\boldsymbol{L}_1 + f_2\boldsymbol{L}_2 - c\boldsymbol{T} - f_1f_2(\boldsymbol{L}_1 - \boldsymbol{L}_2)[f_2\boldsymbol{L}_1 + f_1\boldsymbol{L}_2 - c\boldsymbol{T}]^{-1}(\boldsymbol{L}_1 - \boldsymbol{L}_2). \end{aligned} \tag{24.51}$$

To proceed further we assume that $\boldsymbol{L}_1 - \boldsymbol{L}_2$ is nonsingular. Then substitution of (24.51) in (24.49) followed by some straightforward manipulation produces the bound

$$c\boldsymbol{T} - f_2\boldsymbol{L}_1 - f_1\boldsymbol{L}_2 + f_1f_2(\boldsymbol{L}_1 - \boldsymbol{L}_2)(f_1\boldsymbol{L}_1 + f_2\boldsymbol{L}_2 - \boldsymbol{L}_*)^{-1}(\boldsymbol{L}_1 - \boldsymbol{L}_2) \geq 0,$$

which in view of the formula (19.3) for $\boldsymbol{Y}_*$ in terms of $\boldsymbol{L}_*$ reduces to (24.50).

A simpler approach is to directly derive this bound on the Y-tensor. Let $\boldsymbol{E}_1$ be any piecewise constant average value zero field and $\boldsymbol{E}_2$ the corresponding field with zero average value within each phase that solves the Y-tensor problem (19.10). Since $\boldsymbol{E}_1 + \boldsymbol{E}_2 \in \mathcal{E}$, the quasiconvexity of $\boldsymbol{T}$ implies that

$$0 \leq \langle(\boldsymbol{E}_1 + \boldsymbol{E}_2) \cdot \boldsymbol{T}(\boldsymbol{E}_1 + \boldsymbol{E}_2)\rangle = \langle \boldsymbol{E}_1 \cdot \boldsymbol{T}\boldsymbol{E}_1\rangle + \langle \boldsymbol{E}_2 \cdot \boldsymbol{T}\boldsymbol{E}_2\rangle,$$

where the latter identity follows from the orthogonality of $\boldsymbol{E}_2$ and the piecewise constant field $\boldsymbol{T}\boldsymbol{E}_1$, and from the orthogonality of $\boldsymbol{E}_1$ and the field $\boldsymbol{T}\boldsymbol{E}_2$, which has average value zero within each phase. Recalling that $\boldsymbol{L} \geq c\boldsymbol{T}$ and, from (19.12), that $\langle \boldsymbol{E}_1 \cdot \boldsymbol{Y}_*\boldsymbol{E}_1\rangle = \langle \boldsymbol{E}_2 \cdot \boldsymbol{L}\boldsymbol{E}_2\rangle$ and that $\boldsymbol{L} \geq c\boldsymbol{T}$, we are lead to the string of inequalities

$$\langle \boldsymbol{E}_1 \cdot \boldsymbol{Y}_*\boldsymbol{E}_1\rangle \geq \langle \boldsymbol{E}_2 \cdot c\boldsymbol{T}\boldsymbol{E}_2\rangle \geq -\langle \boldsymbol{E}_1 \cdot c\boldsymbol{T}\boldsymbol{E}_1\rangle, \tag{24.52}$$

which clearly imply that $\boldsymbol{Y}_* + c\boldsymbol{T} \geq 0$. Notice that this derivation holds even when $\boldsymbol{L}_1 - \boldsymbol{L}_2$ is singular, and moreover proves that the bound on $\boldsymbol{Y}_*$ applies to multiphase composites and not just two-phase composites, provided that we interpret $\boldsymbol{Y}_*$ and $\boldsymbol{T}$ as operators acting on the space $\mathcal{V}$ of fields that are constant within each phase and which have zero average value.

If we are seeking to find the best bounds on $\boldsymbol{Y}_*$, then, because the bounds (24.52) depend linearly on c, we should either translate as far as possible, that is, increase c to the point where $\boldsymbol{L} - c\boldsymbol{T}$ becomes singular, or choose $c = 0$, which corresponds to no translation at all. By contrast, if one is bounding the energy using (24.22), then the best bound is sometimes obtained with an intermediate value of c, as was emphasized by Allaire and Kohn (1993), correcting a wrong assertion that I had made (Milton 1990b).

24.11. Deriving the trace bounds†

The trace bounds (23.56) can be derived using the translation method. For simplicity, let us consider two-phase composites and take a translation of the form (24.44). The translation bounds, expressed as a constraint on the Y-tensor, imply that

$$\boldsymbol{Y}_* + \boldsymbol{L}_0 \geq \alpha \boldsymbol{v} \otimes \boldsymbol{v}.$$

By taking the inverse of both sides of this equation, and setting α to its extreme value $\alpha = 1/r(\boldsymbol{v} \otimes \boldsymbol{v})$, as in (24.46), we obtain the inequality

$$\boldsymbol{v} \cdot (\boldsymbol{Y}_* + \boldsymbol{L}_0)^{-1} \boldsymbol{v} \leq r(\boldsymbol{v} \otimes \boldsymbol{v}),$$

which corresponds to the trace bound (23.56) with $\boldsymbol{M} = \boldsymbol{v} \otimes \boldsymbol{v}$.

This derivation (Milton 1990b) has a significant advantage over the derivation using the standard Hashin-Shtrikman variational principles: The condition for its validity, that $\boldsymbol{L}(\boldsymbol{x}) - \boldsymbol{T} \geq 0$ or, equivalently, that

$$\boldsymbol{L}_1 - \boldsymbol{L}_0 \geq -\boldsymbol{v} \otimes \boldsymbol{v}/r(\boldsymbol{v} \otimes \boldsymbol{v}), \quad \boldsymbol{L}_2 - \boldsymbol{L}_0 \geq -\boldsymbol{v} \otimes \boldsymbol{v}/r(\boldsymbol{v} \otimes \boldsymbol{v}),$$

allows a wider choice of $\boldsymbol{L}_0$ than is allowed in the derivation using the Hashin-Shtrikman variational principle, which requires that $\boldsymbol{L}_1 - \boldsymbol{L}_0 \geq 0$ and $\boldsymbol{L}_2 - \boldsymbol{L}_0 \geq 0$.

To obtain bounds that correspond to other choices of $\boldsymbol{M} \geq 0$, we embed the problem. Taking

$$\boldsymbol{\mathcal{Y}}_* = \begin{pmatrix} \boldsymbol{Y}_* & 0 & \ldots & 0 \\ 0 & \boldsymbol{Y}_* & \ldots & 0 \\ \vdots & \vdots & \ddots & \vdots \\ 0 & 0 & \ldots & \boldsymbol{Y}_* \end{pmatrix}, \quad \boldsymbol{\mathcal{L}}_i = \begin{pmatrix} \boldsymbol{L}_i & 0 & \ldots & 0 \\ 0 & \boldsymbol{L}_i & \ldots & 0 \\ \vdots & \vdots & \ddots & \vdots \\ 0 & 0 & \ldots & \boldsymbol{L}_i \end{pmatrix} \quad \text{for } i = 1, 2,$$

and a translation

$$\boldsymbol{\mathcal{T}} = \begin{pmatrix} \boldsymbol{L}_0 & 0 & \ldots & 0 \\ 0 & \boldsymbol{L}_0 & \ldots & 0 \\ \vdots & \vdots & \ddots & \vdots \\ 0 & 0 & \ldots & \boldsymbol{L}_0 \end{pmatrix} - \alpha \boldsymbol{V} \otimes \boldsymbol{V}, \quad \text{with } \boldsymbol{V} = \begin{pmatrix} \boldsymbol{v}_1 \\ \boldsymbol{v}_2 \\ \vdots \\ \boldsymbol{v}_n \end{pmatrix} \text{ and } \boldsymbol{V} \cdot \boldsymbol{V} = 1,$$

the bounds $\boldsymbol{\mathcal{Y}}_* + \boldsymbol{\mathcal{T}} \geq 0$, which hold when $\boldsymbol{\mathcal{L}}_1 - \boldsymbol{\mathcal{T}} \geq 0$, $\boldsymbol{\mathcal{L}}_2 - \boldsymbol{\mathcal{T}} \geq 0$, and $\boldsymbol{\mathcal{T}}$ is quasiconvex,

imply that

$$\boldsymbol{V}\cdot\begin{pmatrix}(\boldsymbol{Y}_*+\boldsymbol{L}_0)^{-1} & 0 & \dots & 0\\ 0 & (\boldsymbol{Y}_*+\boldsymbol{L}_0)^{-1} & \dots & 0\\ \vdots & \vdots & \ddots & \vdots\\ 0 & 0 & \dots & (\boldsymbol{Y}_*+\boldsymbol{L}_0)^{-1}\end{pmatrix}\boldsymbol{V}\le\frac{1}{\alpha}. \tag{24.53}$$

To ensure the quasiconvexity of $\boldsymbol{\mathcal{T}}$, the constant α is subject to the restriction, implied by (24.45), that for all $\boldsymbol{k}\neq 0$

$$\frac{1}{\alpha}\ge\boldsymbol{V}\cdot\begin{pmatrix}\boldsymbol{\Gamma}(\boldsymbol{k}) & 0 & \dots & 0\\ 0 & \boldsymbol{\Gamma}(\boldsymbol{k}) & \dots & 0\\ \vdots & \vdots & \ddots & \vdots\\ 0 & 0 & \dots & \boldsymbol{\Gamma}(\boldsymbol{k})\end{pmatrix}\boldsymbol{V}=\mathrm{Tr}[\boldsymbol{M}\boldsymbol{\Gamma}(\boldsymbol{k})],\quad\text{where }\boldsymbol{M}=\sum_{i=1}^{n}\boldsymbol{v}_i\otimes\boldsymbol{v}_i.$$

Clearly the maximum permissible value for α is $\alpha=1/r(\boldsymbol{M})$, where $r(\boldsymbol{M})$ is given by (24.46), and on substituting this into (24.53) we see that this inequality reduces to the general trace bounds [see (23.56)]

$$\mathrm{Tr}[\boldsymbol{M}(\boldsymbol{Y}_*+\boldsymbol{L}_0)^{-1}]\le r(\boldsymbol{M})$$

on the tensor $\boldsymbol{Y}_*$, where now we can choose the vectors $\boldsymbol{v}_i$ so that $\boldsymbol{M}$ is equal to any given positive-semidefinite matrix. (We can relax the constraint that $\boldsymbol{V}\cdot\boldsymbol{V}=1$ or, equivalently, that $\mathrm{Tr}\boldsymbol{M}=1$, because the bounds remain unchanged when we multiply $\boldsymbol{M}$ by a positive constant.) Again the condition for the validity of the bound, that $\boldsymbol{\mathcal{L}}_1-\boldsymbol{\mathcal{T}}\ge 0$ and $\boldsymbol{\mathcal{L}}_2-\boldsymbol{\mathcal{T}}\ge 0$, allows for a wider choice of $\boldsymbol{L}_0$ than is allowed in the derivation using the Hashin-Shtrikman variational principles.

24.12. Mixed bounds

We have seen that finding lower bounds on an effective tensor, such as the effective conductivity tensor $\boldsymbol{\sigma}_*$, corresponds to finding lower bounds on the sum of energies

$$\sum_{\alpha=1}^{n}\boldsymbol{e}_0^{(\alpha)}\cdot\boldsymbol{\sigma}_*\boldsymbol{e}_0^{(\alpha)},$$

in which $\boldsymbol{e}_0^{(1)}$, $\boldsymbol{e}_0^{(2)}$,... $\boldsymbol{e}_0^{(n)}$ denote a succession of n applied electric fields. In a similar fashion, finding upper bounds on $\boldsymbol{\sigma}_*$ corresponds to lower bounds on an appropriate sum of complementary energies,

$$\sum_{\alpha=1}^{p}\boldsymbol{j}_0^{(\alpha)}\cdot\boldsymbol{\sigma}_*^{-1}\boldsymbol{j}_0^{(\alpha)},$$

in which $\boldsymbol{j}_0^{(1)}$, $\boldsymbol{j}_0^{(2)}$,... $\boldsymbol{j}_0^{(p)}$ denote a succession of p applied current fields. Such sets of lower and upper bounds do not always suffice to characterize the set of all possible effective tensors.

To complete the characterization we typically need mixed bounds on $\boldsymbol{\sigma}_*$. These correspond to finding lower bounds on a sum of energies and complementary energies:

$$\sum_{\alpha=1}^{n}\boldsymbol{e}_0^{(\alpha)}\cdot\boldsymbol{\sigma}_*\boldsymbol{e}_0^{(\alpha)}+\sum_{\alpha=1}^{p}\boldsymbol{j}_0^{(\alpha)}\cdot\boldsymbol{\sigma}_*^{-1}\boldsymbol{j}_0^{(\alpha)}.$$

We will see later in section 30.3 on page 647 that knowledge of the best possible lower bound on this sum, for all combinations of nonnegative integers n and p with $n + p \leq m$, and for all possible sets of applied fields $\boldsymbol{e}_0^{(1)}, \boldsymbol{e}_0^{(2)}, \ldots \boldsymbol{e}_0^{(n)} \in \mathcal{U}$ and $\boldsymbol{j}_0^{(1)}, \boldsymbol{j}_0^{(2)}, \ldots \boldsymbol{j}_0^{(n)} \in \mathcal{U}$, provides a complete characterization of the set of all possible effective tensors $\boldsymbol{\sigma}_*$. Moreover, this type of characterization of the G-closure is sufficient not just for conductivity, but also for elasticity, thermoelectricity, piezoelectricity, thermal expansion, and so forth.

So if we seek mixed bounds on the effective conductivity tensor $\boldsymbol{\sigma}_*$, it seems natural to make an additional embedding, taking a tensor field $\boldsymbol{\mathcal{L}}(\boldsymbol{x})$ and effective tensor $\boldsymbol{\mathcal{L}}_*$ given by

$$\boldsymbol{\mathcal{L}}(\boldsymbol{x}) = \begin{pmatrix} \boldsymbol{\sigma}(\boldsymbol{x}) & 0 & \ldots & 0 & 0 \\ 0 & \boldsymbol{\sigma}(\boldsymbol{x}) & \ldots & 0 & 0 \\ \vdots & \vdots & \ddots & \vdots & \vdots \\ 0 & 0 & \ldots & \boldsymbol{\sigma}^{-1}(\boldsymbol{x}) & 0 \\ 0 & 0 & \ldots & 0 & \boldsymbol{\sigma}^{-1}(\boldsymbol{x}) \end{pmatrix}, \quad \boldsymbol{\mathcal{L}}_* = \begin{pmatrix} \boldsymbol{\sigma}_* & 0 & \ldots & 0 & 0 \\ 0 & \boldsymbol{\sigma}_* & \ldots & 0 & 0 \\ \vdots & \vdots & \ddots & \vdots & \vdots \\ 0 & 0 & \ldots & \boldsymbol{\sigma}_*^{-1} & 0 \\ 0 & 0 & \ldots & 0 & \boldsymbol{\sigma}_*^{-1} \end{pmatrix}.$$

We can then apply the comparison or translation bounds to the tensor $\boldsymbol{\mathcal{L}}_*$, with a translation $\boldsymbol{\mathcal{T}}$ that is quasiconvex in the sense that the inequality

$$\langle \boldsymbol{E} \cdot \boldsymbol{\mathcal{T}} \boldsymbol{E} \rangle \geq \langle \boldsymbol{E} \rangle \cdot \boldsymbol{\mathcal{T}} \langle \boldsymbol{E} \rangle$$

holds for all periodic extended fields $\boldsymbol{E}(\boldsymbol{x})$ of the form

$$\boldsymbol{E} = \begin{pmatrix} \boldsymbol{e}^{(1)} \\ \boldsymbol{e}^{(2)} \\ \vdots \\ \boldsymbol{e}^{(n)} \\ \boldsymbol{j}^{(1)} \\ \boldsymbol{j}^{(2)} \\ \vdots \\ \boldsymbol{j}^{(p)} \end{pmatrix} \quad \text{with} \quad \begin{aligned} \nabla \times \boldsymbol{e}^{(\alpha)} &= 0 \ \text{ for } \ \alpha = 1, 2 \ldots, n, \\ \nabla \cdot \boldsymbol{j}^{(\beta)} &= 0 \ \text{ for } \ \beta = 1, 2 \ldots, p. \end{aligned}$$

24.13. Volume fraction independent bounds on the conductivity of a mixture of two isotropic phases

As an elementary example, consider a two-dimensional composite of two isotropic phases with conductivity tensors $\boldsymbol{\sigma}_1 = \sigma_1 \boldsymbol{I}$ and $\boldsymbol{\sigma}_2 = \sigma_2 \boldsymbol{I}$, and let us find bounds on the range of values that the effective tensor $\boldsymbol{\sigma}_*$ takes as the geometry varies over all configurations, with no restriction placed on the volume fractions of the two phases. To do this we apply the comparison bounds, with tensors

$$\boldsymbol{\mathcal{L}}_1 = \begin{pmatrix} \boldsymbol{\sigma}_1 & 0 \\ 0 & \boldsymbol{\sigma}_1^{-1} \end{pmatrix}, \quad \boldsymbol{\mathcal{L}}_2 = \begin{pmatrix} \boldsymbol{\sigma}_2 & 0 \\ 0 & \boldsymbol{\sigma}_2^{-1} \end{pmatrix}, \quad \boldsymbol{\mathcal{L}}_* = \begin{pmatrix} \boldsymbol{\sigma}_* & 0 \\ 0 & \boldsymbol{\sigma}_*^{-1} \end{pmatrix}, \tag{24.54}$$

and a rotationally invariant translation

$$\boldsymbol{\mathcal{T}} = \begin{pmatrix} t_1 \boldsymbol{I} & t_2 \boldsymbol{R}_\perp \\ -t_2 \boldsymbol{R}_\perp & t_3 \boldsymbol{I} \end{pmatrix},$$

with parameters

$$t_1 = \frac{\sigma_1 \sigma_2}{\sigma_1 + \sigma_2}, \quad t_2 = \frac{\sqrt{\sigma_1 \sigma_2}}{\sigma_1 + \sigma_2}, \quad t_3 = \frac{1}{\sigma_1 + \sigma_2},$$

chosen so that $\boldsymbol{\mathcal{L}}_1 - \boldsymbol{\mathcal{T}}$, $\boldsymbol{\mathcal{L}}_2 - \boldsymbol{\mathcal{T}}$, and $\boldsymbol{\mathcal{T}}$ are all singular and positive-semidefinite. Notice that this provides an example of where it is useful to take a positive-semidefinite translation. Without loss of generality, we can assume that the matrix $\boldsymbol{\sigma}_*$ is diagonal with eigenvalues λ_1^* and λ_2^*. Then it is a simple matter to check that the comparison bounds $\boldsymbol{\mathcal{L}}_* - \boldsymbol{\mathcal{T}} \geq 0$ imply that

$$\sigma_1\sigma_2/\lambda_1^* + \lambda_2^* \leq \sigma_1 + \sigma_2, \quad \sigma_1\sigma_2/\lambda_2^* + \lambda_1^* \leq \sigma_1 + \sigma_2. \tag{24.55}$$

These bounds were presented by Tartar (1975) and proved by Raĭtum (1978) [see also Lurie and Cherkaev (1981, 1984a, 1984b)]. They provide a complete characterization of the G-closure (see also section 22.5 on page 446). The first inequality is attained as an equality when $\lambda_1^* = 1/(f_1/\sigma_1 + f_2/\sigma_2)$ and $\lambda_2^* = f_1\sigma_1 + f_2\sigma_2$. Similarly, the second inequality is attained as an equality when $\lambda_1^* = f_1\sigma_1 + f_2\sigma_2$ and $\lambda_2^* = 1/(f_1/\sigma_1 + f_2/\sigma_2)$. Therefore, these are the best possible bounds being attained by simple rank-1 laminates of the two isotropic phases. An alternative way to obtain these inequalities is to recognize, as Lurie and Cherkaev (1984a) did, that the arithmetic mean bound on λ_1^* and the harmonic mean bound on λ_2^* imply that

$$\lambda_1^* - \sigma_2 \leq f_1(\sigma_1 - \sigma_2) \leq \sigma_1 - \sigma_1\sigma_2/\lambda_2^*,$$

which immediately gives the first inequality in (24.55). The second inequality similarly follows from the arithmetic mean bound applied to λ_2^* and the harmonic mean bound applied to λ_1^*.

In three dimensions, Cabib and Dal Maso (1988) have shown that the G-closure consists of all conductivity tensors $\boldsymbol{\sigma}_*$ with eigenvalues $\lambda_1^* \geq \lambda_2^* \geq \lambda_3^*$ satisfying

$$\lambda_1^* - \sigma_2 \leq \frac{\sigma_1 + \sigma_2}{1 + \sigma_2/(\lambda_2^* - \sigma_2) + \sigma_2/(\lambda_3^* - \sigma_2)},$$

and the elementary bounds $\sigma_1 \geq \lambda_1$ and $\lambda_3 \geq \sigma_2$, where σ_1 and $\sigma_2 \leq \sigma_1$ are the conductivities of the two isotropic phases. They obtained these inequalities from the volume fraction dependent bounds of Murat and Tartar (1985) and Lurie and Cherkaev (1986) by taking the union of these bounds as the volume fraction is varied between 0 and 1.

There is still another way to derive the bounds (24.55). Consider the harmonic mean bounds applied to the tensor $\boldsymbol{\mathcal{L}}_*$:

$$\boldsymbol{v} \cdot \boldsymbol{\mathcal{L}}_*^{-1}\boldsymbol{v} \leq f_1\boldsymbol{v} \cdot \boldsymbol{\mathcal{L}}_1^{-1}\boldsymbol{v} + f_2\boldsymbol{v} \cdot \boldsymbol{\mathcal{L}}_2^{-1}\boldsymbol{v}.$$

These bounds will be volume fraction independent if we choose $\boldsymbol{v}$ so that $\boldsymbol{v}\cdot\boldsymbol{\mathcal{L}}_1^{-1}\boldsymbol{v} = \boldsymbol{v}\cdot\boldsymbol{\mathcal{L}}_2^{-1}\boldsymbol{v}$. For the matrices $\boldsymbol{\mathcal{L}}_1$ and $\boldsymbol{\mathcal{L}}_2$ given by (24.54), this identity is satisfied with

$$\boldsymbol{v} = \begin{pmatrix} \sqrt{\sigma_1\sigma_2} \\ 0 \\ 0 \\ 1 \end{pmatrix} \quad \text{and with } \boldsymbol{v} = \begin{pmatrix} 0 \\ \sqrt{\sigma_1\sigma_2} \\ -1 \\ 0 \end{pmatrix},$$

and for these choices of $\boldsymbol{v}$ the harmonic mean bounds are easily seen to be equivalent to the bounds (24.55).

This approach, due to Leonid Gibiansky (private communication, 1990), is easily generalized. In the context of other problems, we can obtain volume fraction independent bounds from the translation bounds by looking for vectors $\boldsymbol{v}$ and constants α such that

$$\boldsymbol{v} \cdot (\boldsymbol{L}(\boldsymbol{x}) - c\boldsymbol{T})^{-1}\boldsymbol{v} \leq \alpha \quad \text{for all } \boldsymbol{x}. \tag{24.56}$$

Once this inequality is satisfied, the translation bounds (24.4) clearly imply that

$$\boldsymbol{v} \cdot (\boldsymbol{L}_* - c\boldsymbol{T})^{-1}\boldsymbol{v} \leq \alpha. \tag{24.57}$$

Of course the constant c and the translation $\boldsymbol{T}$ still must be chosen so that the translation bounds remain valid. One can alternatively derive the bounds (24.57) from the comparison bounds. Without loss of generality let us assume that $\boldsymbol{v}$ is a unit vector with $\boldsymbol{v} \cdot \boldsymbol{v} = 1$. Then the comparison bounds $\boldsymbol{L}_* - c\boldsymbol{T}' \geq 0$ with

$$\boldsymbol{T}' = \boldsymbol{T} + \frac{1}{c\alpha}\boldsymbol{v} \otimes \boldsymbol{v}, \tag{24.58}$$

imply that

$$\boldsymbol{L}_* - c\boldsymbol{T} \geq \frac{1}{\alpha}\boldsymbol{v} \otimes \boldsymbol{v}. \tag{24.59}$$

By taking the inverse of both sides, we arrive at the bounds (24.57). Moreover, the conditions for the validity of the translation bounds guarantee that $\boldsymbol{T}'$ is quasiconvex and that $\boldsymbol{L}(\boldsymbol{x}) - c\boldsymbol{T}' \geq 0$. The quasiconvexity of $\boldsymbol{T}$ clearly implies the quasiconvexity of $\boldsymbol{T}'$, and the inequality (24.56), coupled with the constraint that $\boldsymbol{L}(\boldsymbol{x}) - \boldsymbol{T} \geq 0$, ensures that $\boldsymbol{L}(\boldsymbol{x}) - c\boldsymbol{T}' \geq 0$.

24.14. Bounds correlating different effective tensors

Sometimes we seek bounds that correlate one effective tensor with another effective tensor. Such bounds are called cross-property bounds. For example, one might want to derive bounds correlating the effective bulk modulus and effective conductivity of an isotropic composite material. Then one can utilize measurements of the electrical conductivity to obtain information about the bulk modulus. Bounds of this sort were obtained by Milton (1984), Berryman and Milton (1988), and Torquato (1992). Tighter bounds were obtained by Gibiansky and Torquato (1993, 1995, 1996, 1998) using the translation method. Here we give an example of their approach, which is based on the earlier work of Cherkaev and Gibiansky (1992) correlating effective electrical and magnetic properties of two-phase, two-dimensional composites.

Let us consider a three-dimensional composite of two isotropic phases with conductivities σ_1 and σ_2 and shear moduli μ_1 and μ_2 such that

$$(\sigma_1 - \sigma_2)(\mu_1 - \mu_2) \leq 0. \tag{24.60}$$

We subject the composite to an applied strain and write the elasticity constitutive law in the form

$$\boldsymbol{\tau}(\boldsymbol{x}) = [3\kappa(\boldsymbol{x})\boldsymbol{\Lambda}_h + 2\mu(\boldsymbol{x})\boldsymbol{\Lambda}_s]\nabla\boldsymbol{u}(\boldsymbol{x}), \tag{24.61}$$

in which $\boldsymbol{\Lambda}_h$ and $\boldsymbol{\Lambda}_s$ are the fourth-order tensors given by (23.38), representing the projection onto the one-dimensional space of matrices proportional to the second-order identity tensor and the projection onto the orthogonal five-dimensional space of trace free matrices, respectively. Here $\kappa(\boldsymbol{x})$ is the local bulk modulus, taking the value κ_1 in phase 1 and the value κ_2 in phase 2, while $\mu(\boldsymbol{x})$ is the local shear modulus taking the value μ_1 in phase 1 and the value μ_2 in phase 2. We then subject the composite to a succession of three applied electric fields, and as in section 24.6 on page 506 we let the three resultant current fields $\boldsymbol{j}^{(1)}(\boldsymbol{x})$, $\boldsymbol{j}^{(2)}(\boldsymbol{x})$, and $\boldsymbol{j}^{(3)}(\boldsymbol{x})$ form the columns of a 3×3 matrix-valued field $\boldsymbol{J}(\boldsymbol{x})$ and we let the three resultant electric fields $\boldsymbol{e}^{(1)}(\boldsymbol{x})$, $\boldsymbol{e}^{(2)}(\boldsymbol{x})$, and $\boldsymbol{e}^{(3)}(\boldsymbol{x})$ form the three columns of a 3×3 matrix-valued field $\boldsymbol{E}(\boldsymbol{x})$. Then the constitutive law takes the form

$$\boldsymbol{J}(\boldsymbol{x}) = [\sigma(\boldsymbol{x})\boldsymbol{I}]\boldsymbol{E}(\boldsymbol{x}), \tag{24.62}$$

in which $\boldsymbol{I}$ is the fourth-order identity tensor and $\sigma(\boldsymbol{x})$ is σ_1 in phase 1 and σ_2 in phase 2.

We now embed the equations (24.62) and (24.61) in a larger problem where the constitutive law takes the form

$$\begin{pmatrix} \boldsymbol{\tau} \\ \boldsymbol{J} \end{pmatrix} = (\boldsymbol{\mathcal{L}}_1\chi_1 + \boldsymbol{\mathcal{L}}_2\chi_2)\begin{pmatrix} \nabla \boldsymbol{u} \\ \boldsymbol{E} \end{pmatrix},$$

where

$$\boldsymbol{\mathcal{L}}_i = \begin{pmatrix} 3\kappa_i\boldsymbol{\Lambda}_h + 2\mu_i\boldsymbol{\Lambda}_s & 0 \\ 0 & \sigma_i\boldsymbol{\Lambda}_h + \sigma_i\boldsymbol{\Lambda}_s + \sigma_i\boldsymbol{\Lambda}_a \end{pmatrix} \quad \text{for } i = 1, 2,$$

in which $\boldsymbol{\Lambda}_a = \boldsymbol{I} - \boldsymbol{\Lambda}_h - \boldsymbol{\Lambda}_s$ is the projection onto the three-dimensional space of antisymmetric matrices. The associated effective tensor $\boldsymbol{L}_*$ takes a similar form to $\boldsymbol{L}_i$ but with σ_i, κ_i, and μ_i being replaced by the effective conductivity σ_*, the effective bulk modulus κ_*, and the effective shear modulus μ_*. The associated Y-tensor is

$$\boldsymbol{\mathcal{Y}}_* = \begin{pmatrix} 3y_\kappa\boldsymbol{\Lambda}_h + 2y_\mu\boldsymbol{\Lambda}_s & 0 \\ 0 & y_\sigma\boldsymbol{\Lambda}_h + y_\sigma\boldsymbol{\Lambda}_s + y_\sigma\boldsymbol{\Lambda}_a \end{pmatrix},$$

where the y-parameters

$$\begin{aligned} y_\kappa &= -f_2\kappa_1 - f_1\kappa_2 - \frac{f_1 f_2(\kappa_1 - \kappa_2)^2}{\kappa_* - f_1\kappa_1 - f_2\kappa_2}, \\ y_\mu &= -f_2\mu_1 - f_1\mu_2 - \frac{f_1 f_2(\mu_1 - \mu_2)^2}{\mu_* - f_1\mu_1 - f_2\mu_2}, \\ y_\sigma &= -f_2\sigma_1 - f_1\sigma_2 - \frac{f_1 f_2(\sigma_1 - \sigma_2)^2}{\sigma_* - f_1\sigma_1 - f_2\sigma_2} \end{aligned}$$

are the Y-transformations of the effective bulk and shear moduli and conductivity.

As our translation we take the null Lagrangian

$$\boldsymbol{\mathcal{T}} = \begin{pmatrix} -t_1(2\boldsymbol{\Lambda}_h - \boldsymbol{\Lambda}_s + \boldsymbol{\Lambda}_a) & -t_3(2\boldsymbol{\Lambda}_h - \boldsymbol{\Lambda}_s + \boldsymbol{\Lambda}_a) \\ -t_3(2\boldsymbol{\Lambda}_h - \boldsymbol{\Lambda}_s + \boldsymbol{\Lambda}_a) & -t_2(2\boldsymbol{\Lambda}_h - \boldsymbol{\Lambda}_s + \boldsymbol{\Lambda}_a) \end{pmatrix},$$

where t_1, t_2, and t_3 are scalar parameters and $2\boldsymbol{\Lambda}_h - \boldsymbol{\Lambda}_s + \boldsymbol{\Lambda}_a$ is the familiar null Lagrangian appearing in (24.36), written in terms of the projections $\boldsymbol{\Lambda}_h$, $\boldsymbol{\Lambda}_s$, and $\boldsymbol{\Lambda}_a$. Since these projections project onto orthogonal subspaces, the constraint that $\boldsymbol{\mathcal{L}}_i - \boldsymbol{\mathcal{T}}$ is positive-definite for $i = 1, 2$ or, equivalently, that

$$\begin{pmatrix} (3\kappa_i + 2t_1)\boldsymbol{\Lambda}_h + (2\mu_i - t_1)\boldsymbol{\Lambda}_s + t_1\boldsymbol{\Lambda}_a & t_3(2\boldsymbol{\Lambda}_h - \boldsymbol{\Lambda}_s + \boldsymbol{\Lambda}_a) \\ t_3(2\boldsymbol{\Lambda}_h - \boldsymbol{\Lambda}_s + \boldsymbol{\Lambda}_a) & (\sigma_i + 2t_1)\boldsymbol{\Lambda}_h + (\sigma_i - t_2)\boldsymbol{\Lambda}_s + (\sigma_i + t_2)\boldsymbol{\Lambda}_a \end{pmatrix} \geq 0,$$

decouples into the constraints that

$$\begin{pmatrix} 3\kappa_i + 2t_1 & 2t_3 \\ 2t_3 & \sigma_i + 2t_2 \end{pmatrix} \geq 0, \quad \begin{pmatrix} 2\mu_i - t_1 & -t_3 \\ -t_3 & \sigma_i - t_2 \end{pmatrix} \geq 0, \quad \begin{pmatrix} t_1 & t_3 \\ t_3 & \sigma_i + t_2 \end{pmatrix} \geq 0,$$

for $i = 1, 2$. For these constraints to be satisfied it is necessary and sufficient for the leading element of each matrix to be nonnegative, which demands that

$$0 \leq t_1 \leq \min\{2\mu_1, 2\mu_2\}, \tag{24.63}$$

and for the determinant of each matrix to be positive. This latter constraint requires t_1, t_2, and t_3 to be such that the inequality

$$(3y_1/2 - t_1)(y_2/2 - t_2) - t_3^2 \geq 0 \tag{24.64}$$

is satisfied for the following six values of $\boldsymbol{y} = (y_1, y_2)$:

$$\boldsymbol{y}_{1i} = (-\kappa_i, -\sigma_i), \quad \boldsymbol{y}_{2i} = (4\mu_i/3,\ 2\sigma_i), \quad \boldsymbol{y}_{3i} = (0, -2\sigma_i), \quad i = 1, 2.$$

The desired bound coupling κ_* and σ_* comes from the matrix inequality

$$\begin{pmatrix} 3y_\kappa - 2t_1 & -2t_3 \\ -2t_3 & y_\sigma - 2t_2 \end{pmatrix} \geq 0,$$

which is implied by the positivity of $\boldsymbol{\mathcal{Y}} + \boldsymbol{\mathcal{T}}$. By taking the determinant of this matrix we conclude that the inequality (24.64) is satisfied for

$$\boldsymbol{y} = (y_\kappa,\ y_\sigma).$$

Let Ω_T denote the region in the $\boldsymbol{y}$-plane comprised of all points $\boldsymbol{y} = (y_1,\ y_2)$ satisfying the inequality (24.64). The boundary of this region is a hyperbola. The constraint (24.63) says that the vertical axis of this hyperbola must intersect the y_1-axis between the origin and the minimum value of $4\mu_1/3$ and $4\mu_2/3$. We can think of moving and resizing the region Ω_T as equivalent to varying the parameters t_1, t_2, and t_3. The constraints on Ω_T is that the vertical axis of its hyperbolic boundary lies in the required range and that it contains the six points $\boldsymbol{y}_{hi}$, $h = 1, 2, 3$, $i = 1, 2$. The bounds confine $(y_\kappa,\ y_\sigma)$ to lie inside the region Ω_T. This geometrical interpretation allows one to visually obtain the best bounds by positioning and resizing Ω_T, subject to the preceding restrictions. When the ordering condition (24.60) is satisfied, it is best to position Ω_T so that one branch of the hyperbolic boundary passes through both $\boldsymbol{y}_{21} = (4\mu_1/3,\ 2\sigma_1)$ and $\boldsymbol{y}_{22} = (4\mu_2/3,\ 2\sigma_2)$, while the other branch of the hyperbolic boundary passes through one of the four points $\boldsymbol{y}_{11}, \boldsymbol{y}_{12}, \boldsymbol{y}_{31}$, or $\boldsymbol{y}_{32}$, chosen so that the remaining three points lie inside Ω_T.

Another bound can be obtained by applying quasiconvex translations to the tensor $\boldsymbol{\mathcal{L}}^{-1}$. This bound confines $(y_\kappa,\ y_\sigma)$ to lie to the left of the straight line joining $\boldsymbol{y}_{21} = (4\mu_1/3,\ 2\sigma_1)$ and $\boldsymbol{y}_{22} = (4\mu_2/3,\ 2\sigma_2)$. The prescription for constructing the bounds is therefore the following. For any point $\boldsymbol{w} = (w_1, w_2)$ in the $\boldsymbol{y}$-plane, let Hyp$[\boldsymbol{w}]$ denote the hyperbolic segment in the $\boldsymbol{y}$-plane that joins $\boldsymbol{y}_{21}$ and $\boldsymbol{y}_{22}$, and which when extended passes through $\boldsymbol{w}$. It can be described parametrically by the equations

$$y_1 = 4[\gamma\mu_1 + (1-\gamma)\mu_2]/3 - \frac{16\gamma(1-\gamma)(\mu_1 - \mu_2)^2}{12[\gamma\mu_2 + (1-\gamma)\mu_1] - 9w_1},$$
$$y_2 = 2[\gamma\sigma_1 + (1-\gamma)\sigma_2] - \frac{4\gamma(1-\gamma)(\sigma_1 - \sigma_2)^2}{2[\gamma\sigma_2 + (1-\gamma)\sigma_1] - w_2},$$

with the parameter γ running from 0 to 1. (The points $\boldsymbol{y}_{21}$, $\boldsymbol{y}_{22}$, and $\boldsymbol{w}$ correspond to $\gamma = 1$, $\gamma = 0$, and $\gamma = \infty$, respectively.) Inscribe in the $\boldsymbol{y}$-plane the four segments of hyperbolas:

$$\text{Hyp}[(-\kappa_1, -\sigma_1)], \quad \text{Hyp}[(-\kappa_2, -\sigma_2)], \quad \text{Hyp}[(0, -2\sigma_1)], \quad \text{Hyp}[(0, -2\sigma_2)],$$

and the straight line joining the points $(4\mu_1/3,\ 2\sigma_1)$ and $(4\mu_2/3,\ 2\sigma_2)$. The outermost pair of these five curves is then the desired cross-property bounds on the possible $(y_\kappa,\ y_\sigma)$ pairs. It turns out that the same procedure can be followed for constructing bounds when

$$(\sigma_1 - \sigma_2)(\mu_1 - \mu_2) \geq 0.$$

These arise from mixed bounds on the tensor $\mathcal{L}$.

The points $(y_\kappa,\ y_\sigma)$ on the hyperbolic segments Hyp$[(-\kappa_1, -\sigma_1)]$ and Hyp$[(-\kappa_2, -\sigma_2)]$ correspond to the moduli of assemblages of doubly coated spheres. Therefore, if a bound is described by one of these hyperbolic segments, then that bound is optimal. There are also five points along the line joining the points $(4\mu_1/3,\ 2\sigma_1)$ and $(4\mu_2/3,\ 2\sigma_2)$ that correspond to microgeometries: Assemblages of coated spheres correspond to the endpoints, and the other three points are attained by more complicated microgeometries; see Gibiansky and Torquato (1996) and references therein.

References

Allaire, G. and R. V. Kohn 1993. Explicit optimal bounds on the elastic energy of a two-phase composite in two space dimensions. *Quarterly of Applied Mathematics* 51(4): 675–699. {*466, 490, 518, 525*}

Avellaneda, M., A. V. Cherkaev, L. V. Gibiansky, G. W. Milton, and M. Rudelson 1996. A complete characterization of the possible bulk and shear moduli of planar polycrystals. *Journal of the Mechanics and Physics of Solids* 44(7):1179–1218. {*362, 367, 502, 525, 537, 550*}

Avellaneda, M., A. V. Cherkaev, K. A. Lurie, and G. W. Milton 1988. On the effective conductivity of polycrystals and a three-dimensional phase-interchange inequality. *Journal of Applied Physics* 63(10):4989–5003. {*120, 139, 439, 441, 450, 452, 512, 525, 538, 550, 555, 564*}

Avellaneda, M. and G. W. Milton 1989. Optimal bounds on the effective bulk modulus of polycrystals. *SIAM Journal on Applied Mathematics* 49(3):824–837. {*441, 444, 453, 501, 525, 536, 550*}

Berryman, J. G. and G. W. Milton 1988. Microgeometry of random composites and porous media. *Journal of Physics D: Applied Physics* 21:87–94. {*522, 525, 560, 565*}

Cabib, E. and G. Dal Maso 1988. On a class of optimum problems in structural design. *Journal of Optimization Theory and Applications* 56(1):39–65. {*521, 525*}

Cherkaev, A. V. and L. V. Gibiansky 1992. The exact coupled bounds for effective tensors of electrical and magnetic properties of two-component two-dimensional composites. *Proceedings of the Royal Society of Edinburgh. Section A, Mathematical and Physical Sciences* 122(1–2):93–125. {*397, 399, 411, 450, 453, 517, 522, 525, 614, 617*}

Francfort, G. A. and F. Murat 1986. Homogenization and optimal bounds in linear elasticity. *Archive for Rational Mechanics and Analysis* 94(4):307–334. {*174, 182, 471, 492, 501, 504, 525*}

Gibiansky, L. V. and A. V. Cherkaev 1984. Design of composite plates of extremal rigidity. Technical Report 914, Ioffe Physicotechnical Institute, Leningrad, USSR. 1–60 pp. English translation in *Topics in the Mathematical Modelling of Composite Materials*, pp. 95–137, ed. by A. Cherkaev and R. Kohn. ISBN 0-8176-3662-5. {*432, 434, 466, 492, 501, 525, 529, 550*}

Gibiansky, L. V. and S. Torquato 1993, November 1. Link between the conductivity and elastic moduli of composite materials. *Physical Review Letters* 71(18):2927–2930. {*506, 522, 525*}

Gibiansky, L. V. and S. Torquato 1995. Rigorous link between the conductivity and elastic moduli of fibre-reinforced composite materials. *Philosophical Transactions of the Royal Society of London Series A* 353:243–278. {*522, 526, 561, 565*}

Gibiansky, L. V. and S. Torquato 1996. Connection between the conductivity and bulk modulus of isotropic composite materials. *Proceedings of the Royal Society of London. Series A, Mathematical and Physical Sciences* 452(1945):253–283. {*522, 525, 526*}

Gibiansky, L. V. and S. Torquato 1998. Rigorous connection between physical properties of porous rocks. *Journal of Geophysical Research* 103:23911–23923. {*522, 526*}

Lurie, K. A. and A. V. Cherkaev 1981. *G*-closure of a set of anisotropic conducting media in the case of two-dimensions. *Doklady Akademii Nauk SSSR* 259:328–331. English translation in *Soviet Phys. Dokl.* 26:657–659 (1981). {*428, 429, 435, 447, 453, 521, 526*}

Lurie, K. A. and A. V. Cherkaev 1982. Accurate estimates of the conductivity of mixtures formed of two materials in a given proportion (two-dimensional problem). *Doklady Akademii Nauk SSSR* 264:1128–1130. English translation in *Soviet Phys. Dokl.* 27:461–462 (1982). {*499, 506, 508, 526, 529, 551*}

Lurie, K. A. and A. V. Cherkaev 1984a. Exact estimates of conductivity of composites formed by two isotropically conducting media taken in prescribed proportion. *Proceedings of the Royal Society of Edinburgh. Section A, Mathematical and Physical Sciences* 99(1–2):71–87. {*499, 506, 508, 521, 526, 529, 551*}

Lurie, K. A. and A. V. Cherkaev 1984b. *G*-closure of a set of anisotropically conducting media in the two-dimensional case. *Journal of Optimization Theory and Applications* 42(2):283–304. {*428, 435, 447, 454, 521, 526*}

Lurie, K. A. and A. V. Cherkaev 1986. Exact estimates of the conductivity of a binary mixture of isotropic materials. *Proceedings of the Royal Society of Edinburgh. Section A, Mathematical and Physical Sciences* 104(1–2):21–38. {*167, 182, 347, 353, 462, 494, 508, 521, 526*}

Milton, G. W. 1984. Correlation of the electromagnetic and elastic properties of composites and microgeometries corresponding with effective medium theory. In D. L. Johnson and P. N. Sen (eds.), *Physics and Chemistry of Porous Media: Papers from a Symposium Held at Schlumberger-Doll Research, Oct. 24–25, 1983*, pp. 66–77. Woodbury, New York: American Institute of Physics. ISBN 0-88318-306-4. {*196, 217, 522, 526*}

Milton, G. W. 1990a. A brief review of the translation method for bounding effective elastic tensors of composites. In G. A. Maugin (ed.), *Continuum Models and Discrete Systems*, pp. 60–74. Harlow, Essex, United Kingdom: Longman Scientific and Technical. ISBN 0-582-05121-5. {*505, 512, 526*}

Milton, G. W. 1990b. On characterizing the set of possible effective tensors of composites: The variational method and the translation method. *Communications on Pure and Applied Mathematics (New York)* 43(1):63–125. {*164, 183, 248, 265, 268, 277, 287, 451, 454, 473, 494, 499, 505, 512, 513, 518, 526, 532, 551*}

Milton, G. W. 1991. The field equation recursion method. In G. Dal Maso and G. F. Dell'Antonio (eds.), *Composite Media and Homogenization Theory: Proceedings of the Workshop on Composite Media and Homogenization Theory Held in Trieste, Italy, from January 15 to 26, 1990*, pp. 223–245. Basel, Switzerland: Birkhäuser Verlag. ISBN 0-8176-3511-4, 3-7643-3511-4. {*397, 412, 517, 526, 612, 613, 618, 619, 641*}

Milton, G. W. 1994. A link between sets of tensors stable under lamination and quasiconvexity. *Communications on Pure and Applied Mathematics (New York)* 47(7):959–1003. {*513, 527, 535, 551, 647, 669*}

Murat, F. and L. Tartar 1985. Calcul des variations et homogénísation. (French) [Calculus of variation and homogenization]. In *Les méthodes de l'homogénéisation: théorie et applications en physique*, pp. 319–369. Paris: Eyrolles. English translation in *Topics in the Mathematical Modelling of Composite Materials*, pp. 139–173, ed. by A. Cherkaev and R. Kohn, ISBN 0-8176-3662-5. {*12, 13, 17, 347, 353, 429, 431, 432, 435, 444, 454, 462, 495, 499, 503, 506, 508, 521, 527, 529, 551*}

Raĭtum, U. Ë. 1978. The extension of extremal problems connected with a linear elliptic equation. *Doklady Akademii Nauk SSSR* 243(2):281–283. English translation in *Soviet Math. Dokl.* 19(6):1342–1345 (1978). {*431, 435, 447, 454, 521, 527*}

Rudelson, M. 1989. Phase transitions in solids. Master's Thesis, St. Petersburg Technical University, St. Petersburg, Russia, 1989. {*441, 444, 454, 501, 527*}

Schapery, R. A. 1997. Linear elastic and viscoelastic deformation behavior of ice. *Journal of Cold Regions Engineering* 11(4):271–290. {*503, 527*}

Schulgasser, K. 1995. The stiffest wire. *Journal of Applied Mechanics* 62(4):947–951. {*502, 527*}

Smyshlyaev, V. P. and J. R. Willis 1999. On the relaxation of a three-well energy. *Proceedings of the Royal Society of London. Series A, Mathematical and Physical Sciences* 455 (1983):779–814. {*295, 311, 515, 527*}

Tartar, L. 1975. Problèmes de contrôle des coefficients dans des équations aux dérivées partielles. In A. Bensoussan and J.-L. Lions (eds.), *Control Theory, Numerical Methods and Computer Systems Modelling (Proceedings IRIA 1974)*, pp. 420–426. Berlin / Heidelberg / London / etc.: Springer-Verlag. English translation in *Topics in the Mathematical Modelling of Composite Materials*, pp. 1–8, ed. by A. Cherkaev and R. Kohn. ISBN 0-8176-3662-5. {*426, 429, 431, 435, 447, 454, 521, 527*}

Tartar, L. 1979a. Compensated compactness and applications to partial differential equations. In R. J. Knops (ed.), *Nonlinear Analysis and Mechanics, Heriot-Watt Symposium, Volume IV*, pp. 136–212. London: Pitman Publishing Ltd. ISBN 0-8224-8461-7, 0-273-08461-5. {*59, 72, 275, 276, 288, 503, 527, 529, 552, 676, 677, 684, 698*}

Tartar, L. 1979b. Estimation de coefficients homogénéisés. (French) [Estimation of homogenization coefficients]. In R. Glowinski and J.-L. Lions (eds.), *Computing Methods in Applied Sciences and Engineering: Third International Symposium, Versailles, France, December 5–9, 1977,*, pp. 364–373. Berlin / Heidelberg / London / etc.: Springer-Verlag. English translation in *Topics in the Mathematical Modelling of Composite Materials*, pp. 9–20, ed. by A. Cherkaev and R. Kohn. ISBN 0-8176-3662-5. ISBN 0-387-09123-8. {*155, 156, 162, 183, 274, 289, 499, 503, 508, 509, 527, 529, 552*}

Tartar, L. 1985. Estimations fines des coefficients homogénéisés. (French) [Fine estimations of homogenized coefficients]. In P. Krée (ed.), *Ennio de Giorgi Colloquium: Papers Presented at a Colloquium Held at the H. Poincaré Institute in November 1983*, pp. 168–187. London: Pitman Publishing Ltd. ISBN 0-273-08680-4. {*129, 141, 165, 167, 174, 183, 462, 496, 499, 503, 506, 508, 527, 529, 552, 683, 698*}

Torquato, S. 1992. Connection between the morphology and effective properties of heterogeneous materials. In S. Torquato and D. Krajcinovic (eds.), *Macroscopic Behavior of Heterogeneous Materials from the Microstructure: Presented at the Winter Annual Meeting of the American Society of Mechanical Engineers, Anaheim, California, November 8–13, 1992*, pp. 53–65. New York: American Society of Mechanical Engineers. ISBN 0-7918-1101-8. {*522, 527*}

25

Choosing the translations and finding microgeometries that attain the bounds†

The main difficulty in applying the translation method is in choosing the translation $\boldsymbol{T}$. This is intimately tied with the question of what microgeometries attain a given bound, since one typically wants to choose the translations so that the resulting bounds are attained by at least some microgeometries. This chapter addresses these two issues.

25.1. Other derivations of the translation bounds and their extension to nonlinear problems

The argument leading to the translation bounds (24.17) is appealing because it gives an interpretation of the bounds in terms of the harmonic mean bounds applied to the translated medium. Also, as will be discussed later in section 26.5 on page 560, one immediately sees that tighter correlation function dependent bounds could be used instead of the harmonic mean bounds. However, it is somewhat mysterious as it does not explain why it is natural to consider bounds on the translated medium in the first place. Both the compensated compactness approach (Tartar 1979a, 1979b, 1985; Murat and Tartar 1985; Murat 1987) and the variational approach (Lurie and Cherkaev 1982, 1984 1986; Gibiansky and Cherkaev 1984; Firoozye 1991) provide this insight.

In the compensated compactness approach, which is outlined in theorem 8 in the paper of Tartar (1979b), one seeks to find the possible values of the average field pair $(\langle \boldsymbol{E} \rangle, \langle \boldsymbol{J} \rangle)$ given the differential constraints on the fields and given that the fields satisfy the constitutive relation. This latter constraint can be recast in the form

$$(\boldsymbol{E}(\boldsymbol{x}), \boldsymbol{J}(\boldsymbol{x})) \in \mathcal{K}(\boldsymbol{x}), \quad \text{where } \mathcal{K}(\boldsymbol{x}) = \{(\boldsymbol{A}, \boldsymbol{B}) \mid \boldsymbol{B} = \boldsymbol{L}(\boldsymbol{x})\boldsymbol{A}\},$$

and similarly the effective constitutive law can be recast as

$$(\langle \boldsymbol{E} \rangle, \langle \boldsymbol{J} \rangle) \in \mathcal{K}_*, \quad \text{where } \mathcal{K}_* = \{(\boldsymbol{E}_0, \boldsymbol{J}_0) \mid \boldsymbol{J}_0 = \boldsymbol{L}_* \boldsymbol{E}_0\}.$$

Now suppose that we have identified a quasiconvex function $Q(\boldsymbol{E}, \boldsymbol{J})$, which by definition is such that

$$\langle Q(\boldsymbol{E}, \boldsymbol{J}) \rangle \geq Q(\langle \boldsymbol{E} \rangle, \langle \boldsymbol{J} \rangle) \text{ for all } \boldsymbol{E} \in \mathcal{U} \oplus \mathcal{E} \text{ and } \boldsymbol{J} \in \mathcal{U} \oplus \mathcal{J}. \tag{25.1}$$

This inequality provides a bound on the pair $(\langle \boldsymbol{E} \rangle, \langle \boldsymbol{J} \rangle)$, provided that we can estimate the expression on the left-hand side for fields $\boldsymbol{E}(\boldsymbol{x})$ and $\boldsymbol{J}(\boldsymbol{x})$ satisfying the constitutive law. If we define

$$g(\boldsymbol{x}) = \sup_{(\boldsymbol{E}, \boldsymbol{J}) \in \mathcal{K}(\boldsymbol{x})} Q(\boldsymbol{E}, \boldsymbol{J}), \quad g_* = \sup_{(\boldsymbol{E}_0, \boldsymbol{J}_0) \in \mathcal{K}_*} Q(\boldsymbol{E}_0, \boldsymbol{J}_0), \tag{25.2}$$

then clearly (25.1) implies that

$$\langle g \rangle \geq Q(\boldsymbol{E}_0, \boldsymbol{J}_0) \text{ for all } (\boldsymbol{E}_0, \boldsymbol{J}_0) \in \mathcal{K}_*,$$

and taking the supremum of the right-hand side over $(\boldsymbol{E}_0, \boldsymbol{J}_0) \in \mathcal{K}_*$ gives the compensated compactness bound

$$\langle g \rangle \geq g_*. \tag{25.3}$$

Consider the function

$$Q(\boldsymbol{E}, \boldsymbol{J}) = 2\boldsymbol{J}' \cdot \boldsymbol{E} - \boldsymbol{J} \cdot \boldsymbol{E} + c\boldsymbol{E} \cdot \boldsymbol{T}\boldsymbol{E},$$

where $\boldsymbol{J}'$ is a constant vector. The first term is a null Lagrangian because it is linear in $\boldsymbol{E}$. The second term is also a null Lagrangian because the subspaces $\mathcal{J}$ and $\mathcal{E}$ are orthogonal. Therefore, the whole expression is quasiconvex for $c \geq 0$ provided that $\boldsymbol{T}$ is quasiconvex on $\mathcal{E}$. The resulting formulas for g and g_* are given by the expressions

$$\begin{aligned} g(\boldsymbol{x}) &= \sup_{\boldsymbol{E}}[2\boldsymbol{J}' \cdot \boldsymbol{E} - \boldsymbol{E} \cdot (\boldsymbol{L} - c\boldsymbol{T})\boldsymbol{E}] = \boldsymbol{J}' \cdot (\boldsymbol{L} - c\boldsymbol{T})^{-1}\boldsymbol{J}', \\ g_* &= \sup_{\boldsymbol{E}_0}[2\boldsymbol{J}' \cdot \boldsymbol{E}_0 - \boldsymbol{E}_0 \cdot (\boldsymbol{L}_* - c\boldsymbol{T})\boldsymbol{E}_0] = \boldsymbol{J}' \cdot (\boldsymbol{L}_* - c\boldsymbol{T})^{-1}\boldsymbol{J}', \end{aligned}$$

where we have assumed that $\boldsymbol{L} - c\boldsymbol{T} \geq 0$. The bound (25.3) then becomes

$$\boldsymbol{J}' \cdot \langle (\boldsymbol{L} - c\boldsymbol{T})^{-1} \rangle \boldsymbol{J}' \geq \boldsymbol{J}' \cdot (\boldsymbol{L}_* - c\boldsymbol{T})^{-1}\boldsymbol{J}',$$

which, because $\boldsymbol{J}'$ is arbitrary, is equivalent to the translation bounds (24.17).

Taking Q to be a sum of more general linear and quadratic terms generates the mixed bounds discussed in section 24.12 on page 519. Nonquadratic choices of Q would presumably lead to tighter bounds, but unfortunately this approach is currently limited by our rudimentary knowledge of nonquadratic quasiconvex functions. The beauty of the compensated compactness bounds (25.3) is that they also clearly apply to nonlinear composites (as was evident to Murat and Tartar) once the set $\mathcal{K}(\boldsymbol{x})$ is redefined to be

$$\mathcal{K}(\boldsymbol{x}) = \{(\boldsymbol{A}, \boldsymbol{B}) \mid \boldsymbol{B} = \boldsymbol{F}(\boldsymbol{x}, \boldsymbol{A})\},$$

in which $\boldsymbol{F}(\boldsymbol{x}, \boldsymbol{A})$ is the nonlinear constitutive law at the point $\boldsymbol{x}$. The bounds then restrict the possible values of the average fields $\boldsymbol{E}_0 = \langle \boldsymbol{E} \rangle$ and $\boldsymbol{J}_0 = \langle \boldsymbol{J} \rangle$. In this way quite tight bounds [generalizing the linear bounds (22.12)] were obtained on the possible values of the average current for a prescribed average electric field in nonlinear conducting two-phase composites (Milton and Serkov 2000).

In the variational approach one starts from the variational expression for $\boldsymbol{L}_*$,

$$\boldsymbol{E}_0 \cdot \boldsymbol{L}_*\boldsymbol{E}_0 = \min_{\substack{\underline{\boldsymbol{E}} \in \mathcal{U} \oplus \mathcal{E} \\ \langle \underline{\boldsymbol{E}} \rangle = \boldsymbol{E}_0}} \langle \underline{\boldsymbol{E}} \cdot \boldsymbol{L}\underline{\boldsymbol{E}} \rangle,$$

and replaces the differential constraint that $\underline{\boldsymbol{E}} \in \mathcal{U} \oplus \mathcal{E}$ by the weaker integral corollary that $\underline{\boldsymbol{E}}$ satisfies (24.20). Since the minimum then extends over a larger class of fields, we obtain a lower bound on $\boldsymbol{E}_0 \cdot \boldsymbol{L}_*\boldsymbol{E}_0$:

$$\boldsymbol{E}_0 \cdot \boldsymbol{L}_*\boldsymbol{E}_0 \geq \min_{\substack{\underline{\boldsymbol{E}} \in \mathcal{H} \\ (\underline{\boldsymbol{E}}, \boldsymbol{T}\underline{\boldsymbol{E}}) \geq (\boldsymbol{E}_0, \boldsymbol{T}\boldsymbol{E}_0) \\ \langle \underline{\boldsymbol{E}} \rangle = \boldsymbol{E}_0}} \langle \underline{\boldsymbol{E}} \cdot \boldsymbol{L}\underline{\boldsymbol{E}} \rangle. \tag{25.4}$$

We next introduce a Lagrange multiplier $c \ge 0$ and rewrite (25.4) as

$$\boldsymbol{E}_0 \cdot \boldsymbol{L}_* \boldsymbol{E}_0 \ge \min_{\substack{\underline{\boldsymbol{E}} \in \mathcal{H} \\ \langle \underline{\boldsymbol{E}} \rangle = \boldsymbol{E}_0}} \max_{c \ge 0} \Big\{ \langle \underline{\boldsymbol{E}} \cdot \boldsymbol{L} \underline{\boldsymbol{E}} \rangle - c[\langle \underline{\boldsymbol{E}} \cdot \boldsymbol{T} \underline{\boldsymbol{E}} \rangle - \boldsymbol{E}_0 \cdot \boldsymbol{T} \boldsymbol{E}_0] \Big\}, \tag{25.5}$$

where the maximum over $c \ge 0$ is infinite unless $\langle \underline{\boldsymbol{E}} \cdot \boldsymbol{T} \underline{\boldsymbol{E}} \rangle \ge \boldsymbol{E}_0 \cdot \boldsymbol{T} \boldsymbol{E}_0$. Now for any function $f(x, y)$ of two variables x and y we have

$$\max_{y'} f(x, y') \ge f(x, y) \ge \min_{x'} f(x', y),$$

for all choices of x and y. Taking the minimum over x of the left-hand side and the maximum over y of the right-hand side gives

$$\min_x \max_y f(x, y) \ge \max_y \min_x f(x, y).$$

Applied to (25.5) we see that swapping the order of the maximum over c and the minimum over $\underline{\boldsymbol{E}}$ either leaves unchanged or reduces the right-hand side, and so we have the inequality

$$\boldsymbol{E}_0 \cdot \boldsymbol{L}_* \boldsymbol{E}_0 \ge \max_{c \ge 0} \min_{\substack{\underline{\boldsymbol{E}} \in \mathcal{H} \\ \langle \underline{\boldsymbol{E}} \rangle = \boldsymbol{E}_0}} \Big\{ \langle \underline{\boldsymbol{E}} \cdot \boldsymbol{L} \underline{\boldsymbol{E}} \rangle - c[\langle \underline{\boldsymbol{E}} \cdot \boldsymbol{T} \underline{\boldsymbol{E}} \rangle - \boldsymbol{E}_0 \cdot \boldsymbol{T} \boldsymbol{E}_0] \Big\}. \tag{25.6}$$

Naturally, if this is to provide a useful bound, the minimum over $\underline{\boldsymbol{E}}$ should not be minus infinity, that is, the choice of c should be restricted to those positive values for which $\boldsymbol{L} - c\boldsymbol{T} \ge 0$. Then, by introducing a Lagrange multiplier to take into account the constraint that $\langle \underline{\boldsymbol{E}} \rangle = \boldsymbol{E}_0$, we see that the optimum choice of $\underline{\boldsymbol{E}}$ that minimizes the right-hand side of (25.6) is

$$\underline{\boldsymbol{E}} = (\boldsymbol{L} - c\boldsymbol{T})^{-1} \boldsymbol{v}, \quad \text{where } \boldsymbol{v} = \langle (\boldsymbol{L} - c\boldsymbol{T})^{-1} \rangle^{-1} \boldsymbol{E}_0 \in \mathcal{U}.$$

By substituting this back into (25.6), and recalling that the inequality holds for all choices of $\boldsymbol{E}_0$, we arrive at the inequality

$$\boldsymbol{L}_* \ge c\boldsymbol{T} + \langle (\boldsymbol{L} - c\boldsymbol{T})^{-1} \rangle^{-1}, \tag{25.7}$$

which is clearly equivalent to the translation bound (24.17).

This variational approach is also easily extended to the nonlinear case (Firoozye 1991; Ponte Castañeda 1996; Bhattacharya and Kohn 1997; Nesi, Talbot, and Willis 1999). Starting from the variational principle (13.40) one obtains the nonlinear translation bound

$$W_* \ge cQ + \langle (W - cQ)^\circ \rangle^\circ, \tag{25.8}$$

where the circle superscipts denote Legendre transforms (as in section 13.7 on page 282) and $Q(\boldsymbol{A})$ is any quasiconvex function satisfying

$$\langle Q(\boldsymbol{E}) \rangle \ge Q(\langle \boldsymbol{E} \rangle) \text{ for all } \boldsymbol{E} \in \mathcal{U} \oplus \mathcal{E}. \tag{25.9}$$

Thus, in the nonlinear setting, the variational approach naturally produces bounds on the effective energy potential $W_*(\boldsymbol{E}_0)$, whereas the compensated compactness method naturally produces bounds on the possible average fields, that is, on the derivative of $W_*(\boldsymbol{E}_0)$ with respect to $\boldsymbol{E}_0$ [see equation (13.48)]. The results are different since bounding a function is not the same as bounding the derivative of a function.

Even for linear problems it may prove fruitful to use (25.8) with a nonquadratic Q, but again the problem is to find useful nonquadratic quasiconvex functions. One might ask whether anything is lost by swapping the order of the maximum over c and the minimum over $\underline{\boldsymbol{E}}$ in (25.5), that is, whether the right-hand sides of (25.5) and (25.6) are always equal. In fact nothing is lost, as has been established by Firoozye (1991), in the general nonlinear setting.

25.2. Extremal translations

From the preceding derivation one can see that it is never advantageous to translate by a positive-semidefinite translation $\boldsymbol{T}$. For such choices of $\boldsymbol{T}$ the inequality

$$\langle \underline{\boldsymbol{E}} \cdot \boldsymbol{T}\underline{\boldsymbol{E}} \rangle - \boldsymbol{E}_0 \cdot \boldsymbol{T}\boldsymbol{E}_0 = \langle (\underline{\boldsymbol{E}} - \boldsymbol{E}_0) \cdot \boldsymbol{T}(\underline{\boldsymbol{E}} - \boldsymbol{E}_0) \rangle \geq 0$$

implies that to maximize the right-hand side of (25.6), and thereby produce the best bound, we should take $c = 0$, which corresponds to no translation at all. This makes good sense: When $\boldsymbol{T}$ is positive-semidefinite the constraint $(\underline{\boldsymbol{E}}, \boldsymbol{T}\underline{\boldsymbol{E}}) \geq (\boldsymbol{E}_0, \boldsymbol{T}\boldsymbol{E}_0)$ does not impose any restriction on a field $\underline{\boldsymbol{E}}$ satisfying $\langle \underline{\boldsymbol{E}} \rangle = \boldsymbol{E}_0$. Similar conclusions do not directly extend to the comparison bounds. As was seen in the example of section 24.13 on page 520, it is sometimes advantageous to take translations that are not extremal.

For the same reason, if $\boldsymbol{T}$ can be decomposed into a sum of a quasiconvex operator $\boldsymbol{T}'$ and a nonzero positive-semidefinite operator $\boldsymbol{A}$:

$$\boldsymbol{T} = \boldsymbol{T}' + \boldsymbol{A} \text{ with } \boldsymbol{T}' \geq 0 \text{ on } \mathcal{E} \text{ and } \boldsymbol{A} \geq 0 \text{ on } \mathcal{H} \text{ with } \boldsymbol{A} \neq 0, \tag{25.10}$$

then the translation bounds produced with $\boldsymbol{T}'$ as our translation will be at least as good as those produced with $\boldsymbol{T}$. Therefore to bound $\boldsymbol{L}_*$ using the translation bounds (25.7) we can restrict our choice of $\boldsymbol{T}$ to those quasiconvex operators that cannot be decomposed in this way. We call the translations in this special class extremal (Milton 1990). They have the property that their quasiconvexity is lost whenever a nonzero positive-semidefinite tensor $\boldsymbol{A}$ is subtracted from them.

This definition makes sense only when the subspaces $\mathcal{E}_{\boldsymbol{k}}$ span all of tensor space as $\boldsymbol{k}$ ranges over all unit vectors. Otherwise, the class of extremal translations is empty since we can always subtract from $\boldsymbol{T}$ any multiple of the projection operator that projects onto the space $\mathcal{E}_\perp$, which is the orthogonal complement of the span of these subspaces. In this case we need to modify the definition of an extremal translation, and require that quasiconvexity be lost for nonzero, positive-semidefinite tensors $\boldsymbol{A}$ that have $\mathcal{E}_\perp$ in their nullspace. To avoid these complications let us assume that these subspaces span all tensor space.

In the context of the geometrical characterization of translations given in section 24.9 on page 512, the extremal translations are those $\boldsymbol{T}$ for which $\boldsymbol{\rho}$ cannot be increased without destroying quasiconvexity. When $\boldsymbol{L}_0$ is chosen so that $\boldsymbol{\rho}$ is nonsingular, they correspond to those ellipsoids $\boldsymbol{\Phi}$ that fit tightly in the cavity $\boldsymbol{\Psi}$. They cannot be enlarged and still remain inside. (Here an enlarged ellipsoid is understood as any ellipsoid that contains the original ellipsoid.)

One class of extremal translations are those for which there exist vectors $\boldsymbol{E}_1, \boldsymbol{E}_2, \ldots, \boldsymbol{E}_m$ and associated directions $\boldsymbol{n}_1, \boldsymbol{n}_2, \ldots, \boldsymbol{n}_m$ such that the vectors $\boldsymbol{E}_i$ span the tensor space in which the fields take their values and

$$\boldsymbol{E}_i = \boldsymbol{\Gamma}_1(\boldsymbol{n}_i)\boldsymbol{E}_i, \quad \boldsymbol{E}_i \cdot \boldsymbol{T}\boldsymbol{E}_i = 0 \text{ for all } i.$$

Since $\boldsymbol{T}$ is quasiconvex, and hence positive-semidefinite on $\mathcal{E}_{\boldsymbol{n}_i}$, this latter constraint implies that

$$\boldsymbol{\Gamma}_1(\boldsymbol{n}_i)\boldsymbol{J}_i = 0, \quad \text{where } \boldsymbol{J}_i = \boldsymbol{T}\boldsymbol{E}_i.$$

To see that $\boldsymbol{T}$ is extremal, let us assume on the contrary that $\boldsymbol{T}$ can be expressed in the form (25.10). Since $\boldsymbol{E}_i \cdot \boldsymbol{T}'\boldsymbol{E}_i$ and $\boldsymbol{E}_i \cdot \boldsymbol{A}\boldsymbol{E}_i$ are nonnegative if $\boldsymbol{T}'$ is quasiconvex and $\boldsymbol{A}$ is positive-semidefinite, and since their sum is zero, it follows that $\boldsymbol{E}_i \cdot \boldsymbol{A}\boldsymbol{E}_i$ must be zero, implying that

$$\boldsymbol{A}\boldsymbol{E}_i = 0.$$

As this must hold for all i and as the $\boldsymbol{E}_i$ span all of the relevant tensor space we conclude that $\boldsymbol{A}$ is zero. Therefore $\boldsymbol{T}$ must be extremal. Null Lagrangians are an example of extremal translations in this class. We can take $\boldsymbol{E}_i$ to be any vector in the subspace $\mathcal{E}_{\boldsymbol{n}_i}$ and since, by assumption, these subspaces span of all of tensor space as $\boldsymbol{n}_i$ is varied, we can easily arrange for the set of vectors $\boldsymbol{E}_i$ to span all of tensor space.

Many equations of interest can be expressed in the form

$$\boldsymbol{J} = \boldsymbol{L}\boldsymbol{E}, \quad \boldsymbol{E} = \nabla \boldsymbol{u}, \quad \nabla \cdot \boldsymbol{J} = 0,$$

in which $\boldsymbol{u}$ is an ℓ-component vector while $\boldsymbol{J}$ and $\boldsymbol{E}$ are $d \times \ell$ matrix-valued fields. Examples include conductivity, thermoelectricity, elasticity, and piezoelectricity (see section 6.4 on page 98). In this case the space $\mathcal{E}_{\boldsymbol{k}}$ is comprised of all $d \times \ell$ matrices of the form $\boldsymbol{B} = \boldsymbol{k} \otimes \boldsymbol{b}$, where $\boldsymbol{b}$ is any ℓ-dimensional vector, and the quasiconvexity condition (24.21) is satisfied if and only if

$$(\boldsymbol{k} \otimes \boldsymbol{b}) \cdot \boldsymbol{T}(\boldsymbol{k} \otimes \boldsymbol{b}) \geq 0 \text{ for all } \boldsymbol{k} \text{ and } \boldsymbol{b}. \tag{25.11}$$

If either d or ℓ equals 1, then this condition holds if and only if $\boldsymbol{T}$ is positive-semidefinite, and $\boldsymbol{T} = 0$ is the only extremal translation. If either d or ℓ equals 2, Terpstra (1938) has shown that any tensor $\boldsymbol{T}$ satisfying this constraint can be expressed in the form

$$\boldsymbol{T} = \boldsymbol{T}' + \boldsymbol{A} \text{ with } \boldsymbol{T}' = 0 \text{ on } \mathcal{E}_{\boldsymbol{k}} \text{ for all } \boldsymbol{k} \text{ and } \boldsymbol{A} \geq 0,$$

that is, as the sum of a null Lagrangian and a positive-semidefinite tensor. [See also Serre (1981a, 1981b) and Marcellini (1984).] Thus in two dimensions (with ℓ arbitrary) the only extremal translations for gradient problems are null Lagrangians. This explains why null Lagrangians have proved so useful for generating optimal bounds in two dimensions.

In three dimensions other extremal translations in this class can be constructed by looking for sets of pairs of vectors $\boldsymbol{E}_i$ and $\boldsymbol{J}_i$ for $i = 1, 2, \ldots, m$ and associated directions $\boldsymbol{n}_1, \boldsymbol{n}_2, \ldots, \boldsymbol{n}_m$ such that

$$\boldsymbol{E}_i = \boldsymbol{\Gamma}_1(\boldsymbol{n}_i)\boldsymbol{E}_i, \quad \boldsymbol{\Gamma}_1(\boldsymbol{n}_i)\boldsymbol{J}_i = 0, \tag{25.12}$$

and such that the $\boldsymbol{E}_i$ span all of tensor space. Then the relation $\boldsymbol{J}_i = \boldsymbol{T}\boldsymbol{E}_i$ determines the action of $\boldsymbol{T}$. To ensure that $\boldsymbol{T}$ is self-adjoint we require that $\boldsymbol{E}_i$ and $\boldsymbol{J}_i$ be chosen so that

$$\boldsymbol{J}_i \cdot \boldsymbol{E}_j = \boldsymbol{E}_i \cdot \boldsymbol{J}_j. \tag{25.13}$$

Also, because $\boldsymbol{T}$ is quasiconvex, it follows that for all $\boldsymbol{n}$ and all constants λ,

$$(\boldsymbol{E}_i + \lambda \boldsymbol{J}_i) \cdot \boldsymbol{\Gamma}_1(\boldsymbol{n})\boldsymbol{T}\boldsymbol{\Gamma}_1(\boldsymbol{n})(\boldsymbol{E}_i + \lambda \boldsymbol{J}_i) \geq 0,$$

with equality when $\boldsymbol{n} = \boldsymbol{n}_i$. Expanding this inequality around $\boldsymbol{n} = \boldsymbol{n}_i$ yields the additional identity

$$\boldsymbol{E}_i \cdot \frac{d\boldsymbol{\Gamma}_1(\boldsymbol{n}/|\boldsymbol{n}|)}{d\boldsymbol{n}}\bigg|_{\boldsymbol{n}=\boldsymbol{n}_i} \boldsymbol{J}_i = 0. \tag{25.14}$$

The other identity,

$$\boldsymbol{J}_i \cdot \frac{d\boldsymbol{\Gamma}_1(\boldsymbol{n}/|\boldsymbol{n}|)}{d\boldsymbol{n}}\bigg|_{\boldsymbol{n}=\boldsymbol{n}_i} \boldsymbol{J}_i = 0, \tag{25.15}$$

which follows, is automatically satisfied: Because $\boldsymbol{\Gamma}_1(\boldsymbol{n})$ is positive-definite we have

$$\boldsymbol{J}_i \cdot \boldsymbol{\Gamma}_1(\boldsymbol{n}) \boldsymbol{J}_i \geq 0,$$

with equality when $\boldsymbol{n} = \boldsymbol{n}_i$, and expanding this around $\boldsymbol{n} = \boldsymbol{n}_i$ gives (25.15). Once one has found sets of pairs of vectors $\boldsymbol{E}_i$ and $\boldsymbol{J}_i$ for $i = 1, 2, \ldots, m$ and associated directions $\boldsymbol{n}_1, \boldsymbol{n}_2, \ldots, \boldsymbol{n}_m$ such that the constraints (25.12), (25.13), and (25.14) are satisfied, one still has to check that $\boldsymbol{T}$ defined by $\boldsymbol{J}_i = \boldsymbol{T}\boldsymbol{E}_i$ is quasiconvex.

With $\boldsymbol{T} = \sigma_0 \boldsymbol{I} - \boldsymbol{\rho}$, where σ_0 is chosen sufficiently large so that $\boldsymbol{\rho}$ is positive-definite, we have

$$\boldsymbol{J}_i = \boldsymbol{T}\boldsymbol{E}_i = \sigma_0 \boldsymbol{E}_i - \boldsymbol{\rho}\boldsymbol{E}_i.$$

Hence $\boldsymbol{P}_i = \boldsymbol{J}_i - \sigma_0 \boldsymbol{E}_i$ satisfies

$$(\boldsymbol{\rho}^{-1} - \boldsymbol{\Gamma}_1(\boldsymbol{n}_i)/\sigma_0)\boldsymbol{P}_i = 0. \tag{25.16}$$

Thus the ellipsoid $\boldsymbol{\Phi}$ touches the cavity $\boldsymbol{\Psi}$ at some $\boldsymbol{P}$ proportional to $\boldsymbol{P}_i$. Also, the $\boldsymbol{P}_i$ span all of tensor space because s$\boldsymbol{P}_i = -\boldsymbol{\rho}\boldsymbol{E}_i$ and $\boldsymbol{\rho}$ is nonsingular. Therefore, geometrically, these extremal translations correspond to ellipsoids that touch the cavity walls in a set of "directions" $\boldsymbol{P}_i$ that span tensor space, as illustrated in figure 25.1(a).

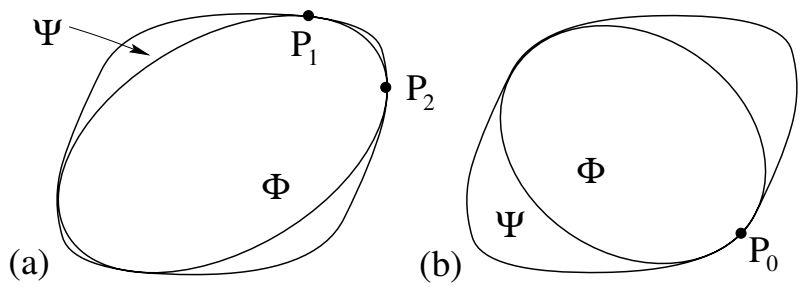

Figure 25.1. Extremal translations may correspond to ellipsoids $\boldsymbol{\Phi}$ that touch the walls of the cavity $\boldsymbol{\Psi}$ at tensors $\boldsymbol{P}_1$, $\boldsymbol{P}_2, \ldots, \boldsymbol{P}_m$, which span all tensor space, as illustrated in (a). Alternatively, they may correspond to ellipsoids $\boldsymbol{\Phi}$ such that the curvatures of the ellipsoid and cavity wall at the points where they touch prevent further enlargement of the ellipsoid, as illustrated in (b).

There are likely other classes of extremal translations. The directions $\boldsymbol{P}_i$ might not span all tensor space, but instead the curvature of the ellipsoid and the curvature of the cavity at the points where the ellipsoid touches the cavity might be such as to prevent enlargement of the ellipsoid, as illustrated in figure 25.1(b). In the context of figure 24.3 on page 516, this corresponds to a tie line of zero length. However, we conjecture that such extremal translations

can be approximated by extremal translations for which the $\boldsymbol{P}_i$ do span all of tensor space. For example, each tie line of zero length in figure 24.3 on page 516 has a neighboring tie line of finite length.

To motivate the conjecture, consider what happens when we replace the quasiconvexity condition (24.43) by the weaker condition that the inequality

$$\boldsymbol{\rho}^{-1} - \boldsymbol{\Gamma}_1(\boldsymbol{k})/\sigma_0 \geq 0 \tag{25.17}$$

holds only for a finite set $\mathcal{S}$ of values, $\boldsymbol{k}_1, \boldsymbol{k}_2, \ldots, \boldsymbol{k}_p$ of $\boldsymbol{k}$. Consider the (possibly empty) set of all $\boldsymbol{P}_i$ and associated $\boldsymbol{n}_i \in \mathcal{S}$ for $i = 1, 2, \ldots, q$ such that (25.16) holds. Let us assume that the subspace $\mathcal{P}$ of tensor space spanned by the $\boldsymbol{P}_i$ has a nonempty orthogonal complement $\mathcal{P}_\perp$. If $\boldsymbol{\Lambda}_\perp$ denotes the projection onto $\mathcal{P}_\perp$, the inequality

$$\boldsymbol{\rho}^{-1} - \boldsymbol{\Gamma}_1(\boldsymbol{k})/\sigma_0 \geq \eta\boldsymbol{\Lambda}_\perp$$

holds for all $\boldsymbol{k} \in \mathcal{S}$ when $\eta > 0$ is chosen less than the lowest nonzero eigenvalue of $\boldsymbol{\rho}^{-1} - \boldsymbol{\Gamma}_1(\boldsymbol{k})/\sigma_0$ as $\boldsymbol{k}$ ranges over $\mathcal{S}$. [For any given $\boldsymbol{k} \in \mathcal{S}$, the matrix $\boldsymbol{\rho}^{-1} - \boldsymbol{\Gamma}_1(\boldsymbol{k})/\sigma_0$ is greater than $\eta(\boldsymbol{I} - \boldsymbol{\Lambda}_{\boldsymbol{k}})$, where $\boldsymbol{\Lambda}_{\boldsymbol{k}}$ is the projection onto the nullspace of $\boldsymbol{\rho}^{-1} - \boldsymbol{\Gamma}_1(\boldsymbol{k})/\sigma_0$ and $\boldsymbol{I} - \boldsymbol{\Lambda}_{\boldsymbol{k}}$ in turn is greater than $\boldsymbol{\Lambda}_\perp$ because it projects onto a larger subspace.] It follows that $\boldsymbol{\rho}^{-1}$ can be decreased while still maintaining the inequality (25.17). Thus in this weakened context the only extremal translations $\boldsymbol{T} = \sigma\boldsymbol{I} - \boldsymbol{\rho}$ are those for which the $\boldsymbol{P}_i$ span all of tensor space. This argument breaks down when $\boldsymbol{k}$ takes an infinity of values because the infimum of the lowest nonzero eigenvalue of $\boldsymbol{\rho}^{-1} - \boldsymbol{\Gamma}_1(\boldsymbol{k})/\sigma_0$ could be zero. As $\mathcal{S}$ is enlarged to include successively more values of $\boldsymbol{k}$, two (or more) pairs $(\boldsymbol{P}_i, \boldsymbol{n}_i)$ and $(\boldsymbol{P}_j, \boldsymbol{n}_j)$ could approach each other. [See section 5 of Milton (1994) for a more complete analysis in a related context, which suggests that extremal translations have an associated tree structure.] The conjecture is that by slightly perturbing $\boldsymbol{T}$ we can avoid such accidental degeneracies while maintaining extremality.

We remark that there are alternative definitions of extremal translations. Since the set of quasiconvex translations with bounded norm $\|\boldsymbol{T}\| \leq k$ is compact and convex [i.e., if $\boldsymbol{T}_1$ and $\boldsymbol{T}_2$ are in the set, then so is $p\boldsymbol{T}_1 + (1-p)\boldsymbol{T}_2$ for all p between 0 and 1], it follows that any $\boldsymbol{T}$ within the set can be expressed as a linear combination with positive weights of the extreme points of the set. These extreme points could be called extremal translations. However we do not adopt this definition, first, because the set of extremal translations defined in this way depends on the choice of norm (as can be seen by considering the set of null Lagrangians), and second, because our definition is the one needed to obtain the relevant translations for application in the translation bounds.

25.3. Attainability criteria for the comparison bounds

When one seeks composites that attain a particular bound the most important clues to the microstructure come from finding the constraints on the field $\boldsymbol{E}(\boldsymbol{x})$ that are both necessary and sufficient to guarantee that the bound will be achieved. Of course, there may not be a single microstructure that supports a field $\boldsymbol{E}(\boldsymbol{x})$ compatible with the constraints, but if such microstructures exist, then the constraints on the fields provide a helpful guide in the search to find the microstructures.

From the variational principles (24.18) and (24.19) it is clear that the comparison bounds will be attained if and only if the field $\boldsymbol{E} \in \mathcal{U} \oplus \mathcal{E}$ lies in the nullspace of both $\boldsymbol{L} - c\boldsymbol{T}$ and $\boldsymbol{\Gamma}_1\boldsymbol{T}\boldsymbol{\Gamma}_1$, that is, if and only if

$$\boldsymbol{L}\boldsymbol{E} = c\boldsymbol{T}\boldsymbol{E}, \quad \boldsymbol{T}\boldsymbol{E} \in \mathcal{U} \oplus \mathcal{J}, \quad \boldsymbol{E} \in \mathcal{U} \oplus \mathcal{E}. \tag{25.18}$$

The first two constraints ensure that $\boldsymbol{J} = \boldsymbol{LE} \in \mathcal{U} \oplus \mathcal{J}$. Given that $\boldsymbol{L}$ is constrained to take values in a set U of given component materials, let us introduce the set of vectors

$$\mathcal{F}_0 = \{\boldsymbol{P} \mid \boldsymbol{LP} = c\boldsymbol{TP} \text{ for some } \boldsymbol{L} \in U\}.$$

Also let us assume, for simplicity of argument, that $\boldsymbol{T}$ is nonsingular. Then from (25.18) we see that the search for microstructures that attain the comparison bound is equivalent to the search for fields $\boldsymbol{E}$ such that

$$\boldsymbol{E}(\boldsymbol{x}) \in \mathcal{F}_0 \text{ for all } \boldsymbol{x} \text{ and } \boldsymbol{E} \in \mathcal{U} \oplus (\mathcal{E} \cap \boldsymbol{T}^{-1}\mathcal{J}). \tag{25.19}$$

These are the attainability criteria for the comparison bounds. The latter differential constraints on $\boldsymbol{E}$ imply that the Fourier components $\widehat{\boldsymbol{E}}(\boldsymbol{k})$ of $\boldsymbol{E}$ satisfy

$$\widehat{\boldsymbol{E}}(\boldsymbol{k}) \in \mathcal{E}_{\boldsymbol{k}} \cap \boldsymbol{T}^{-1}\mathcal{J}_{\boldsymbol{k}} \text{ for all } \boldsymbol{k} \neq 0.$$

For example [following Avellaneda and Milton (1989)], let us consider the lower bound (24.10) on the compliance tensor of a two-dimensional polycrystal. In this context $\mathcal{U} \oplus \mathcal{E}$ is the space of periodic stress fields $\boldsymbol{\tau}(\boldsymbol{x})$. The space $\boldsymbol{J}$ consists of all strain fields that are the symmetrized gradient of some periodic displacement field. Since the translation $\boldsymbol{T} = \boldsymbol{\mathcal{R}}_\perp$ is a null Lagrangian, $\boldsymbol{T}\mathcal{E}$ is contained in $\mathcal{J}$ and consequently $\mathcal{U} \oplus (\mathcal{E} \cap \boldsymbol{T}^{-1}\mathcal{J})$ equals $\mathcal{U} \oplus \mathcal{E}$. When c is chosen as the positive root of the cubic polynomial (24.11) there exists some symmetric matrix $\boldsymbol{v}_0$ such that

$$(\boldsymbol{\mathcal{S}}_0 - c\boldsymbol{\mathcal{R}}_\perp)\boldsymbol{v}_0 = 0,$$

and the set $\mathcal{F}_0$ consists of all 2×2 symmetric matrices $\boldsymbol{P}$ expressible in the form

$$\boldsymbol{P} = a\boldsymbol{R}^T\boldsymbol{v}_0\boldsymbol{R},$$

for some choice of constant a and rotation matrix $\boldsymbol{R}$ satisfying $\boldsymbol{R}^T\boldsymbol{R}$. So the requirement that $\boldsymbol{\tau}(\boldsymbol{x}) \in \mathcal{F}_0$ is fulfilled if the eigenvalues of $\boldsymbol{\tau}(\boldsymbol{x})$ are in the same ratio α as the eigenvalues of $\boldsymbol{v}_0$. The ratio of these eigenvalues is necessarily positive because

$$\det(\boldsymbol{v}_0) = \boldsymbol{v}_0 \cdot \boldsymbol{\mathcal{R}}_\perp\boldsymbol{v}_0/2 = \boldsymbol{v}_0 \cdot \boldsymbol{\mathcal{S}}_0\boldsymbol{v}_0/2c$$

is positive as $\boldsymbol{\mathcal{S}}_0$ is positive-definite and $c > 0$.

Therefore searching for polycrystalline microstructures that attain the bound is equivalent to looking for periodic divergence free stress fields $\boldsymbol{\tau}(\boldsymbol{x})$ that have a constant positive eigenvalue ratio α. To construct a nontrivial field we first consider a stress field that takes the constant value $\boldsymbol{\tau}(\boldsymbol{x}) = \boldsymbol{I}$. We then cut out from the unit cell a circle of radius r_i centered at $\boldsymbol{x} = 0$ and replace the constant stress field with

$$\boldsymbol{\tau}(\boldsymbol{x}) = [\alpha\boldsymbol{I} + (1-\alpha)(\boldsymbol{x} \otimes \boldsymbol{x})/|\boldsymbol{x}|^2]|\boldsymbol{x}|^{\alpha-1}/r_i^{\alpha-1}$$

inside the circle, where the coordinate origin $\boldsymbol{x} = 0$ has been chosen at the center of that circle. One can check that within the circle $\boldsymbol{\tau}(\boldsymbol{x})$ has eigenvalues in the ratio α and is divergence free, deriving from the Airy stress function $\varphi(\boldsymbol{x}) = |\boldsymbol{x}|^{\alpha+1}/[(\alpha+1)r_i^{\alpha-1}]$. Also at the boundary of the circle we have $\boldsymbol{\tau}(\boldsymbol{x}) \cdot \boldsymbol{n} = \boldsymbol{n} = \boldsymbol{I} \cdot \boldsymbol{n}$, when $\boldsymbol{n}$ is normal to the circle boundary. Therefore the stress satisfies the required continuity condition.

One can continue to cut out nonoverlapping circular regions from the unit cell, replacing the constant stress field in each of them according to the above prescription, until the circles

fill all space and one has a periodic stress field with eigenvalues in the desired ratio almost everywhere. Having obtained $\boldsymbol{\tau}(\boldsymbol{x})$, one chooses the crystal orientation so that $\boldsymbol{\tau}(\boldsymbol{x})$ is in the nullspace of $\boldsymbol{\mathcal{S}}(\boldsymbol{x}) - c\boldsymbol{\mathcal{R}}_\perp$. Then $\boldsymbol{\epsilon}(\boldsymbol{x}) = \boldsymbol{\mathcal{S}}(\boldsymbol{x})\boldsymbol{\tau}(\boldsymbol{x}) = c\boldsymbol{\mathcal{R}}_\perp\boldsymbol{\tau}(\boldsymbol{x})$ is automatically the symmetrized gradient of a displacement field. Therefore the bound (24.12) is sharp, being attained by a Schulgasser-type assemblage of circular inclusions.

25.4. Isotropic polycrystals with minimum conductivity constructed from a fully anisotropic crystal

We have already seen in section 24.8 on page 510 that the bound (24.42) on the eigenvalues of the effective conductivity tensor of a three-dimensional polycrystal comprised of uniaxial crystals (with $\lambda_2 = \lambda_3$) is attained when the polycrystal is Schulgasser's sphere assemblage, with the crystal axis oriented radially in each sphere.

When the crystal is not uniaxial, the microstructures that attain the bound (24.41) are not at all trivial, being infinite-rank laminates with the lamination proceeding in a cyclic pattern. The microstructures were first found numerically by Vincenzo Nesi and myself in 1987. First, thousands of multiple-rank laminates were generated randomly, and features were found that characterized those structures which came closest to attaining the bound. Then the random generation process was weighted to favor these desirable features and the program run again. At the next stage more desirable features of the microgeometry became apparent, and the weighting of the random generation process was then modified accordingly. Ultimately, after several further iterations, the optimal microstructure was clearly apparent. Unfortunately, the algorithm was never published, even though an adaptation of it proved useful in finding microstructures that attained the bounds on the possible bulk modulus, shear modulus pairs (κ_*, μ_*) of two-dimensional polycrystals (Avellaneda, Cherkaev, Gibiansky, Milton, and Rudelson 1996).

After the numerical work was completed we realized that the field attainability criteria explained exactly why this cyclic infinite-rank laminate attained the bound (Nesi and Milton 1991). Since the translation $\boldsymbol{\mathcal{T}}$ given by (24.36) is a null Lagrangian, $\mathcal{U} \oplus (\mathcal{E} \cap \boldsymbol{T}^{-1}\mathcal{J})$ equals $\mathcal{U} \oplus \mathcal{E}$. Consequently, the bound $\boldsymbol{\mathcal{L}}_* - c\boldsymbol{\mathcal{T}} \geq 0$ will be sharp, if and only if there exists a square integrable periodic field $\boldsymbol{E} = \nabla \boldsymbol{u}$ that lies in the nullspace of $\boldsymbol{\mathcal{L}}(\boldsymbol{x}) - c\boldsymbol{\mathcal{T}}$ for all $\boldsymbol{x}$, that is, which satisfies

$$\boldsymbol{\sigma}\boldsymbol{E} = c\boldsymbol{\mathcal{T}}\boldsymbol{E}. \tag{25.20}$$

Using the rotational invariance of $\boldsymbol{\mathcal{T}}$ we can rewrite this relation in the form

$$(\boldsymbol{\mathcal{L}}_0 - c\boldsymbol{\mathcal{T}})[\boldsymbol{R}^T(\boldsymbol{x})\boldsymbol{E}(\boldsymbol{x})\boldsymbol{R}(\boldsymbol{x})] = 0. \tag{25.21}$$

Now when c is taken to be the positive root of the cubic (24.40), the operator $\boldsymbol{\mathcal{L}}_0 - c\boldsymbol{\mathcal{T}}$ when represented as a 9×9 matrix as in (24.37) has a null vector of the form

$$(\boldsymbol{\mathcal{L}}_0 - c\boldsymbol{\mathcal{T}}) \begin{pmatrix} s_1 \\ 0 \\ 0 \\ 0 \\ s_2 \\ 0 \\ 0 \\ 0 \\ s_3 \end{pmatrix} = 0. \tag{25.22}$$

To simplify the analysis it is convenient to suppose that this null vector has been normalized so that

$$s_1 + s_2 + s_3 = 1. \tag{25.23}$$

Then on substituting (24.37) into (25.22), we see that

$$s_1 = \frac{c}{c+\lambda_1}, \quad s_2 = \frac{c}{c+\lambda_2}, \quad s_3 = \frac{c}{c+\lambda_3},$$

and having made these identifications (25.23) naturally turns out to be equivalent to the constraint (24.40) on c.

This null vector, when represented as a 3×3 matrix, clearly corresponds to the positive-definite diagonal tensor

$$\boldsymbol{s} = \begin{pmatrix} s_1 & 0 & 0 \\ 0 & s_2 & 0 \\ 0 & 0 & s_3 \end{pmatrix} = c(c\boldsymbol{I} + \boldsymbol{\sigma}_0)^{-1},$$

and (25.21) holds if and only if there exists a scalar field $\alpha(\boldsymbol{x})$ such that

$$\boldsymbol{E}(\boldsymbol{x}) = \alpha(\boldsymbol{x})\boldsymbol{s}(\boldsymbol{x}), \quad \text{where } \boldsymbol{s}(\boldsymbol{x}) = \boldsymbol{R}(\boldsymbol{x})\boldsymbol{s}\boldsymbol{R}^T(\boldsymbol{x}) = c(c\boldsymbol{I} + \boldsymbol{\sigma}(\boldsymbol{x}))^{-1}. \tag{25.24}$$

This implies that $\boldsymbol{E}(\boldsymbol{x})$ must be a symmetric matrix-valued field, its eigenvalues must be in the prescribed ratios $s_1 : s_2 : s_3$, and its eigenvectors must be aligned with the eigenvectors of $\boldsymbol{\sigma}(\boldsymbol{x})$ (Avellaneda, Cherkaev, Lurie, and Milton 1988).

Conversely, given a positive constant c and any periodic symmetric, positive-definite matrix-valued field $\boldsymbol{E}$ that derives from a vector potential $\boldsymbol{u}$, that is, $\boldsymbol{E} = \nabla\boldsymbol{u}$, then there is an associated conductivity tensor field,

$$\boldsymbol{\sigma}(\boldsymbol{x}) = c\{[\boldsymbol{s}(\boldsymbol{x})]^{-1} - \boldsymbol{I}\}, \quad \text{where } \boldsymbol{s}(\boldsymbol{x}) = \frac{\boldsymbol{E}(\boldsymbol{x})}{\mathrm{Tr}[\boldsymbol{E}(\boldsymbol{x})]}, \tag{25.25}$$

such that $\boldsymbol{E}$ solves the equations (25.20) in this medium with conductivity $\boldsymbol{\sigma}(\boldsymbol{x})$. So we can think of the field $\boldsymbol{E}(\boldsymbol{x})$ as determining the conductivity tensor field. Also, since $\langle \boldsymbol{E} \rangle$ lies in the nullspace of $\boldsymbol{\mathcal{L}}_* - c\boldsymbol{\mathcal{T}}$, it is clear that $\langle \boldsymbol{E} \rangle$ determines the effective conductivity tensor $\boldsymbol{\sigma}_*$ through the analogous relation

$$\boldsymbol{\sigma}_* = c\{[\boldsymbol{s}_*]^{-1} - \boldsymbol{I}\}, \quad \text{where } \boldsymbol{s}_* = \frac{\langle \boldsymbol{E} \rangle}{\mathrm{Tr}\langle \boldsymbol{E} \rangle}. \tag{25.26}$$

This effective tensor has the property that

$$\mathrm{Tr}\, \boldsymbol{s}_* = 1, \quad \text{where } \boldsymbol{s}_* = c(c\boldsymbol{I} + \boldsymbol{\sigma}_*)^{-1}. \tag{25.27}$$

In particular, if $\boldsymbol{E}(\boldsymbol{x})$ has its eigenvalues in the prescribed ratios $s_1 : s_2 : s_3$, then the conductivity tensor field (25.25) corresponds to that of a polycrystal constructed from a pure crystal with conductivity $\boldsymbol{\sigma}_0$ and (25.27) implies that the effective conductivity tensor of the polycrystal attains the bound (24.41). In summary, the problem of finding a polycrystal that attains this bound has been reduced to the problem of finding a vector potential $\boldsymbol{u}$ such that $\boldsymbol{E} = \nabla\boldsymbol{u}$ is a positive-semidefinite, symmetric matrix-valued field having the special property that the ratios between the eigenvalues of $\boldsymbol{E}(\boldsymbol{x})$ are independent of $\boldsymbol{x}$ and in the prescribed ratios $s_1 : s_2 : s_3$.

By, if necessary, relabeling the eigenvalues of $\boldsymbol{\sigma}_0$, we may assume that $s_1 \le s_2 \le s_3$. Let us first focus on the special case where $s_2^2 = s_1 s_3$ and consider the symmetric matrix-valued field

$$\boldsymbol{E}(\boldsymbol{x}) = s_1 \begin{pmatrix} s_1 & 0 & 0 \\ 0 & s_2 & 0 \\ 0 & 0 & s_3 \end{pmatrix} \chi_1(x_1) + s_2 \begin{pmatrix} s_3 & 0 & 0 \\ 0 & s_1 & 0 \\ 0 & 0 & s_2 \end{pmatrix} \chi_2(x_1), \tag{25.28}$$

where $\chi_1(x_1) = 1 - \chi_2(x_1)$ is any characteristic function that is periodic in x_1. The jump in this field across any interface,

$$s_1 \begin{pmatrix} s_1 & 0 & 0 \\ 0 & s_2 & 0 \\ 0 & 0 & s_3 \end{pmatrix} - s_2 \begin{pmatrix} s_3 & 0 & 0 \\ 0 & s_1 & 0 \\ 0 & 0 & s_2 \end{pmatrix} = (s_1^2 - s_2 s_3) \begin{pmatrix} 1 & 0 & 0 \\ 0 & 0 & 0 \\ 0 & 0 & 0 \end{pmatrix},$$

is proportional to $\boldsymbol{n} \otimes \boldsymbol{n}$, where $\boldsymbol{n} = (1, 0, 0)$ is the direction in which the field oscillates. This is the compatibility condition appropriate to ensure that $\boldsymbol{E}(\boldsymbol{x})$ can be expressed as the gradient of a vector potential.

Since the field is of the required form (25.24), it corresponds to a polycrystal which attains the bound $\mathrm{Tr}(\boldsymbol{s}_*) = 1$. Specifically, it corresponds to a simple laminate of slices of pure crystal. The associated tensor $\boldsymbol{s}_*$ is determined from (25.26) and (25.28), giving

$$\boldsymbol{s}_* = \frac{1}{f_1 s_1^2 + f_2 s_2 s_3 + s_1 s_2 + s_2^2} \begin{pmatrix} f_1 s_1^2 + f_2 s_2 s_3 & 0 & 0 \\ 0 & s_1 s_2 & 0 \\ 0 & 0 & s_2^2 \end{pmatrix}.$$

It does not correspond to an isotropic effective conductivity tensor $\boldsymbol{\sigma}_*$, but by a judicious choice of volume fractions $f_1 = \langle \chi_1 \rangle$, namely,

$$f_1 = \frac{s_2(s_3 - s_1)}{s_2 s_3 - s_1^2} \quad \text{and} \quad f_1 = \frac{s_2(s_3 - s_2)}{s_2 s_3 - s_1^2},$$

we obtain the uniaxial tensors

$$\boldsymbol{s}_* = \frac{1}{2s_1 + s_2} \begin{pmatrix} s_1 & 0 & 0 \\ 0 & s_1 & 0 \\ 0 & 0 & s_2 \end{pmatrix} \quad \text{and} \quad \boldsymbol{s}_* = \frac{1}{2s_2 + s_1} \begin{pmatrix} s_2 & 0 & 0 \\ 0 & s_1 & 0 \\ 0 & 0 & s_2 \end{pmatrix}.$$

To obtain an isotropic polycrystal that attains the bound we now laminate these two uniaxial crystals together, orienting them so that their crystal axes are aligned with the direction of lamination $\boldsymbol{n}$, which we take to be the unit vector $\boldsymbol{n} = (1, 0, 0)$. The corresponding field $\boldsymbol{E}(\boldsymbol{x})$ (averaged over an intermediate length scale that is larger than the layer width within each uniaxial crystal, yet much smaller than the slices of the uniaxial crystals) takes the form

$$\boldsymbol{E}(\boldsymbol{x}) = s_2 \begin{pmatrix} s_2 & 0 & 0 \\ 0 & s_1 & 0 \\ 0 & 0 & s_1 \end{pmatrix} \chi_1'(x_1) + s_1 \begin{pmatrix} s_1 & 0 & 0 \\ 0 & s_2 & 0 \\ 0 & 0 & s_2 \end{pmatrix} \chi_2'(x_1),$$

where $\chi_1'(x_1) = 1 - \chi_2'(x_1)$ is a characteristic function that is periodic in x_1, with variation on a length scale much larger than the layer width within each uniaxial crystal. By setting the volume fraction

$$f_1' = \langle \chi_1' \rangle = \frac{s_1}{s_1 + s_2},$$

we ensure that $\langle \boldsymbol{E} \rangle$ is proportional to the identity tensor. The corresponding effective conductivity tensor $\boldsymbol{\sigma}_*$, given by (25.26), is then necessarily isotropic and attains the lower bound (24.41). This polycrystal corresponds to an rank-2 laminate of the pure crystal.

Now let us consider the case where $s_2^2 > s_1 s_3$. To construct an isotropic polycrystal with the lowest conductivity we use a cyclic lamination scheme. The basic idea is to introduce an anisotropic seed material with conductivity $\boldsymbol{\sigma}_*$ satisfying (25.27) such that by laminating the seed material with pure crystal, we obtain a composite with effective conductivity tensor sharing the same set of eigenvalues as the original seed material. In other words, we can effectively produce more seed material by laminating the original seed material with the pure crystal. By continuing this process ad infinitum, and sequentially adding more and more pure crystal by lamination on well-separated length scales, we obtain a composite material with the same effective conductivity tensor as the seed material but with the original seed material occupying only an infinitesimal volume fraction of this composite. Replacing this infinitesimal volume of original seed material by pure crystal causes little change to the overall effective conductivity tensor. So we see that the seed material itself can be regarded as a polycrystal, constructed from the pure crystal through a cyclic lamination scheme.

Consider the laminate of seed material and pure crystal. From (25.24) we see that the field $\boldsymbol{E}(\boldsymbol{x})$ in this simple laminate is required to be of the form

$$\boldsymbol{E}(\boldsymbol{x}) = \alpha_1 \begin{pmatrix} s_1 & 0 & 0 \\ 0 & s_2 & 0 \\ 0 & 0 & s_3 \end{pmatrix} \chi_1(x_1) + \alpha_2 \begin{pmatrix} s_3^* & 0 & 0 \\ 0 & s_1^* & 0 \\ 0 & 0 & s_2^* \end{pmatrix} \chi_2(x_1),$$

where α_1 and α_2 are constants and s_1^*, s_2^* and s_3^* denote the eigenvalues of the tensor $\boldsymbol{s}^*$ associated with the effective tensor $\boldsymbol{\sigma}_*$ of the seed material, satisfying $s_1^* + s_2^* + s_3^* = 1$. To ensure that the effective tensor of this laminate has the same eigenvalues as the seed material we impose the constraint that

$$\langle \boldsymbol{E} \rangle = \alpha_1 f_1 \begin{pmatrix} s_1 & 0 & 0 \\ 0 & s_2 & 0 \\ 0 & 0 & s_3 \end{pmatrix} + \alpha_2 f_2 \begin{pmatrix} s_3^* & 0 & 0 \\ 0 & s_1^* & 0 \\ 0 & 0 & s_2^* \end{pmatrix} = \begin{pmatrix} s_1^* & 0 & 0 \\ 0 & s_2^* & 0 \\ 0 & 0 & s_3^* \end{pmatrix}, \tag{25.29}$$

where $f_1 = 1 - f_2 = \langle \chi_1 \rangle$. Thus, lamination with the pure crystal permutes the eigenvalues in a cyclical fashion corresponding to a rotation of the conductivity tensor of the seed material through an angle of 60°.

Next, to ensure that the jump in the field across any interface,

$$\alpha_1 \begin{pmatrix} s_1 & 0 & 0 \\ 0 & s_2 & 0 \\ 0 & 0 & s_3 \end{pmatrix} - \alpha_2 \begin{pmatrix} s_3^* & 0 & 0 \\ 0 & s_1^* & 0 \\ 0 & 0 & s_2^* \end{pmatrix} = \frac{1}{f_1} \begin{pmatrix} s_1^* - \alpha_2 s_3^* & 0 & 0 \\ 0 & s_2^* - \alpha_2 s_1^* & 0 \\ 0 & 0 & s_3^* - \alpha_2 s_2^* \end{pmatrix}$$

is proportional to $\boldsymbol{n} \otimes \boldsymbol{n}$, where $\boldsymbol{n} = (1, 0, 0)$, we impose the additional constraint that

$$\alpha_2 = \frac{s_2^*}{s_1^*} = \frac{s_3^*}{s_2^*}. \tag{25.30}$$

These equations (25.29) and (25.30) have the solution

$$s_1^* = \frac{s_2^2}{s_2^2 + s_2 s_3 + s_3^2}, \quad s_2^* = \frac{s_2 s_3}{s_2^2 + s_2 s_3 + s_3^2}, \quad s_3^* = \frac{s_3^2}{s_2^2 + s_2 s_3 + s_3^2},$$

$$f_2 = 1 - f_1 = \frac{s_2(s_2^2 - s_1 s_3)}{s_3(s_3^2 - s_1 s_2)}, \quad \alpha_2 = \frac{s_3}{s_2}, \quad \alpha_1 = \frac{s_3}{s_2 + s_3}.$$

Having obtained the anisotropic seed material through this cyclic lamination scheme, the next step is to construct an isotropic polycrystal attaining the bound. This is easy because the eigenvalues of the tensor $\boldsymbol{s}_*$ of the seed material satisfy $(s_2^*)^2 = s_1^* s_3^*$. So by applying the previous construction scheme, and laminating the seed material with itself in a rank-2 laminate, we obtain the desired isotropic polycrystal with minimum conductivity.

A similar infinite-rank lamination scheme can be used to construct isotropic polycrystals with minimum conductivity in the case where $s_2^2 < s_1 s_3$.

One can also use the attainability criteria (25.24) to find simple anisotropic rank-1 laminates attaining the bound (24.41). This was done by Nesi (1993), who found a set of equations determining the two orientations that the crystal takes in the laminate relative to the direction of lamination. As the relative thicknesses of the layers is varied, one traces out a trajectory on the surface described by (24.41).

25.5. Attainability criteria for the translation bounds

Now let us examine the translation bounds. For the equality $\langle \boldsymbol{E} \cdot \boldsymbol{T}\boldsymbol{E} \rangle = \langle \boldsymbol{E} \rangle \cdot \boldsymbol{T} \langle \boldsymbol{E} \rangle$ to hold, the field $\boldsymbol{T}\boldsymbol{E}$ must again lie in $\mathcal{U} \oplus \mathcal{J}$ and this implies that the equations

$$\boldsymbol{J}' = \boldsymbol{L}'\boldsymbol{E}', \quad \boldsymbol{J}' \in \mathcal{U} \oplus \mathcal{J}, \quad \boldsymbol{E}' \in \mathcal{U} \oplus \mathcal{E},$$

in the translated medium, with tensor $\boldsymbol{L}' = \boldsymbol{L} - c\boldsymbol{T}$, are solved with fields $\boldsymbol{J}' = \boldsymbol{J} - c\boldsymbol{T}\boldsymbol{E}$ and $\boldsymbol{E}' = \boldsymbol{E}$. To ensure that the harmonic mean bounds on $\boldsymbol{L}'_*$ are sharp, we require that this field $\boldsymbol{J}'$ be constant. In other words, the field $\boldsymbol{E}$ must satisfy the constraints that

$$(\boldsymbol{L} - c\boldsymbol{T})\boldsymbol{E} \in \mathcal{U}, \quad \boldsymbol{T}\boldsymbol{E} \in \mathcal{U} \oplus \mathcal{J}, \quad \boldsymbol{E} \in \mathcal{U} \oplus \mathcal{E}.$$

It is easy to check that these constraints are both necessary and sufficient to ensure that the translation bound is achieved. Given a field $\boldsymbol{v} \in \mathcal{U}$, let us introduce the set of vectors

$$\mathcal{F}_{\boldsymbol{v}} = \{\boldsymbol{P} \mid (\boldsymbol{L} - c\boldsymbol{T})\boldsymbol{P} = \boldsymbol{v} \text{ for some } \boldsymbol{L} \text{ with } \boldsymbol{L}(\boldsymbol{x}) \in U \text{ for all } \boldsymbol{x}\},$$

and assuming, for simplicity, that $\boldsymbol{T}$ is nonsingular, we see that the search for microstructures that attain the translation bound

$$\boldsymbol{v} \cdot (\boldsymbol{L}_* - c\boldsymbol{T})^{-1}\boldsymbol{v} \leq \langle \boldsymbol{v}(\boldsymbol{L} - c\boldsymbol{T})^{-1}\boldsymbol{v} \rangle$$

is equivalent to the search for fields $\boldsymbol{E}$ such that

$$\boldsymbol{E}(\boldsymbol{x}) \in \mathcal{F}_{\boldsymbol{v}} \text{ for all } \boldsymbol{x} \text{ and } \boldsymbol{E} \in \mathcal{U} \oplus (\mathcal{E} \cap \boldsymbol{T}^{-1}\mathcal{J}). \tag{25.31}$$

These are the attainability criteria for the translation bounds. In particular, if $\mathcal{E}_{\boldsymbol{k}} \cap \boldsymbol{T}^{-1}\mathcal{J}_{\boldsymbol{k}}$ happens to be empty for all but a finite set $\boldsymbol{n}_1, \boldsymbol{n}_2, \ldots, \boldsymbol{n}_m$ of unit vectors $\boldsymbol{k}$, then the nonzero Fourier components $\widehat{\boldsymbol{E}}(\boldsymbol{k})$ must be concentrated in these directions. The likely candidates for attaining the bound are multiple-rank laminates laminated in the directions $\boldsymbol{n}_1, \boldsymbol{n}_2, \ldots, \boldsymbol{n}_m$.

This attainability criteria (25.31) was also independently derived (in a less general setting) by Grabovsky (1996) while this book was being written. He applied it to systematize the search for microstructures attaining bounds on the overall elastic energy of a composite comprised of two anisotropic phases, each with fixed orientation, mixed in given proportions. In a certain parameter regime he found that the conditions on the strain field for the translation bound on the energy to be attained implied that this field, when interpreted as a matrix-valued electric field, solved the extended conductivity equations in an associated family of conducting media with two anisotropic phases. It followed that any microstructure attaining the elastic energy bounds in this regime would also necessarily attain the associated conductivity bounds.

25.6. Attainability criteria for the Hashin-Shtrikman-Hill bounds on the conductivity and bulk modulus

In this section, as an example of the application of these attainability criteria, we follow Grabovsky's analysis and consider the Hashin-Shtrikman-Hill lower bound (23.41) on the effective bulk modulus κ_* of a three-dimensional composite comprised of two isotropic phases with bulk moduli κ_1 and κ_2 and shear moduli μ_1 and μ_2 such that $\mu_1 > \mu_2$. We obtained this bound with $c = 1$ and the translation

$$\boldsymbol{T} = -4\mu_2\boldsymbol{\Lambda}_h + 2\mu_2\boldsymbol{\Lambda}_s = -6\mu_2\boldsymbol{\Lambda}_h + 2\mu_2\boldsymbol{\mathcal{I}}.$$

Now the space $\mathcal{E}_{\boldsymbol{k}}$ consists of tensors $\boldsymbol{B}$ that can be expressed in the form $\boldsymbol{B} = \boldsymbol{k}\otimes\boldsymbol{b}+\boldsymbol{b}\otimes\boldsymbol{k}$. If, in addition, $\boldsymbol{TB} \in \mathcal{J}_{\boldsymbol{k}}$, then we have

$$\begin{aligned} 0 &= \boldsymbol{k}\cdot\boldsymbol{TB} = \boldsymbol{k}\cdot[-4\mu_2(\boldsymbol{k}\cdot\boldsymbol{b})\boldsymbol{I} + 2\mu_2(\boldsymbol{k}\otimes\boldsymbol{b}+\boldsymbol{b}\otimes\boldsymbol{k})] \\ &= 2\mu_2[\boldsymbol{b}|\boldsymbol{k}|^2 - \boldsymbol{k}(\boldsymbol{k}\cdot\boldsymbol{b})], \end{aligned}$$

which implies that $\boldsymbol{b}$ must be parallel to $\boldsymbol{k}$. Consequently, in this example $\mathcal{U}\oplus(\mathcal{E}\cap\boldsymbol{T}^{-1}\mathcal{J})$ consists of all periodic strain fields $\boldsymbol{\epsilon}(\boldsymbol{x})$ that are the double gradient of some scalar potential $\psi(\boldsymbol{x})$, that is,

$$\boldsymbol{\epsilon}(\boldsymbol{x}) = \nabla\nabla\psi(\boldsymbol{x}).$$

We also have

$$\boldsymbol{\mathcal{C}}_1 - \boldsymbol{T} = (3\kappa_1+4\mu_2)\boldsymbol{\Lambda}_h + 2(\mu_1-\mu_2)\boldsymbol{\Lambda}_s, \quad \boldsymbol{\mathcal{C}}_2 - \boldsymbol{T} = (3\kappa_2+4\mu_2)\boldsymbol{\Lambda}_h.$$

So with $\boldsymbol{v} = a\boldsymbol{I}$ and $c = 1$ the set $\mathcal{F}_{\boldsymbol{v}}$ contains the matrix $a\boldsymbol{I}/(3\kappa_1+4\mu_2)$ and all matrices that have trace $3a/(3\kappa_2+4\mu_2)$. Thus finding two-phase microstructures that attain the Hashin-Shtrikman-Hill bulk modulus bound is equivalent to looking for periodic double gradients that are constant and proportional to $\boldsymbol{I}$ in some region (which we identify as phase 1) and have constant trace everywhere else (which we identify as phase 2), with the ratio of the trace in the two regions being $(3\kappa_2+4\mu_2)/(3\kappa_1+4\mu_2)$. The associated stress field $\boldsymbol{\tau}(\boldsymbol{x}) = \boldsymbol{\mathcal{C}}(\boldsymbol{x})\nabla\nabla\psi(\boldsymbol{x}) = \boldsymbol{T}\nabla\nabla\psi(\boldsymbol{x})$ will then automatically have zero divergence.

Given $\nabla\nabla\psi(\boldsymbol{x})$ satisfying these conditions we can add to it a constant field proportional to $\boldsymbol{I}$ to adjust the trace ratio to any desired value. In this way we see that microgeometries that attain the bound for one set of moduli κ_1, κ_2, μ_1, and μ_2 will necessarily still attain the bound when these moduli are varied while keeping $\mu_1 > \mu_2$. It is curious that the attainability criteria obtained from the translation bounds differs from the attainability criteria obtained from the Hashin-Shtrikman variational principles, which only requires that the strain field in phase 1 is constant and proportional to $\boldsymbol{I}$ and that the usual differential constraints of the stress and strain are satisfied. Consequently, if in any composite of the two isotropic phases the stress in phase 1 is constant and proportional to $\boldsymbol{I}$, then necessarily $\boldsymbol{\epsilon}(\boldsymbol{x}) = \nabla\nabla\psi(\boldsymbol{x})$ for some potential $\psi(\boldsymbol{x})$.

As a second example, again following Grabovsky (1996), consider the Hashin-Shtrikman lower bound on the effective conductivity σ_* of a three-dimensional composite comprised of two isotropic phases with conductivities σ_1 and σ_2, with $\sigma_1 > \sigma_2$. These were obtained with the translation (24.31). With $\boldsymbol{B} = \boldsymbol{k}\otimes\boldsymbol{b}$ we have $\boldsymbol{\mathcal{T}B} = \sigma_2(\boldsymbol{k}\otimes\boldsymbol{b} - (\boldsymbol{k}\cdot\boldsymbol{b})\boldsymbol{I})$, which satisfies $\boldsymbol{k}\cdot\boldsymbol{\mathcal{T}B} = 0$ only when $\boldsymbol{b}$ is parallel to $\boldsymbol{k}$. So again $\mathcal{U}\oplus(\mathcal{E}\cap\boldsymbol{T}^{-1}\mathcal{J})$ consists of all periodic fields $\boldsymbol{E}(\boldsymbol{x})$ that are the double gradient of some scalar potential $\psi(\boldsymbol{x})$, that is,

$$\boldsymbol{E}(\boldsymbol{x}) = \nabla\nabla\psi(\boldsymbol{x}).$$

Also, with $\boldsymbol{v} = a\boldsymbol{I}$ and $c = 1$ we see from (24.32) that the set $\mathcal{F}_{\boldsymbol{v}}$ contains the matrix $a\boldsymbol{I}/(\sigma_1 + 2\sigma_2)$ and all matrices that have trace a/σ_2. Thus finding two-phase microstructures that attain the Hashin-Shtrikman conductivity bound is equivalent to looking for periodic double gradients that are constant and proportional to $\boldsymbol{I}$ in some region (which we identify as phase 1), and have constant trace everywhere else (which we identify as phase 2), with the ratio of the trace in the two regions being $3\sigma_2/(\sigma_1 + 2\sigma_2)$.

Again by adding a constant field proportional to $\boldsymbol{I}$ to adjust the trace ratio to any desired value we see that microgeometries that attain the bound for one set of moduli σ_1 and σ_2 will necessarily still attain the bound when these moduli are varied while keeping $\sigma_1 > \sigma_2$. Moreover, we see that microgeometries that attain the conductivity bound will necessarily attain the bulk modulus bound, and vice versa, with the extended electric field $\boldsymbol{E}(\boldsymbol{x})$ being the same as the strain field $\boldsymbol{\epsilon}(\boldsymbol{x})$, modulo a proportionality factor and the addition of a constant field proportional to $\boldsymbol{I}$. The coupled conductivity bulk modulus bounds discussed in section 24.14 on page 522 also show that if the effective conductivity attains the Hashin-Shtrikman bound, then the effective bulk modulus attains the Hashin-Shtrikman-Hill bulk modulus bounds, and vice versa.

Attainability criteria can also be useful for proving that certain bounds cannot be attained by any microstructure, and may also suggest a way to improve these bounds. Here we follow an argument of Nesi (private communication) applied to an isotropic two-dimensional composite of three isotropic conducting phases with conductivities $\sigma_1 > \sigma_2 > \sigma_3$. The Hashin-Shtrikman lower bound on the effective conductivity σ_* will be attained if and only if there exists a symmetric matrix-valued field $\boldsymbol{E}(\boldsymbol{x}) = \nabla\nabla\psi(\boldsymbol{x})$ taking values $\boldsymbol{I}/(\sigma_1 + \sigma_3)$ in phase 1, $\boldsymbol{I}/(\sigma_1 + \sigma_3)$ in phase 2, having trace $1/\sigma_3$ in phase 3, and with average value

$$\boldsymbol{E}_0 = (f_1/(\sigma_1 + \sigma_3) + f_2/(\sigma_2 + \sigma_3) + f_3/2\sigma_3)\boldsymbol{I},$$

where without loss of generality we have set $a = 1$. Since the determinant is a null Lagrangian for such fields, we must have $\langle \det \boldsymbol{E}\rangle = \det \boldsymbol{E}_0$ or, equivalently,

$$\frac{f_1}{(\sigma_1 + \sigma_3)^2} + \frac{f_2}{(\sigma_2 + 2\sigma_3)^2} + \langle \chi_3 \det \boldsymbol{E}\rangle = \left[\frac{f_1}{\sigma_1 + 2\sigma_3} + \frac{f_2}{\sigma_2 + 2\sigma_3} + \frac{f_3}{2\sigma_3}\right]^2, \qquad (25.32)$$

where $\chi_3(\boldsymbol{x})$ is the characteristic function of phase 3.

Now Bauman, Marini, and Nesi (2001) have established that any solution $\boldsymbol{E}(\boldsymbol{x})$ of the conductivity equations must be such that $\det \boldsymbol{E}(\boldsymbol{x})$ is zero or takes the same sign as $\det \boldsymbol{E}_0$ almost everywhere in the composite (no matter what the microstructure). Consequently, the Hashin-Shtrikman lower bound for two-dimensional, three-phase composites will be certainly unattainable when

$$\frac{f_1}{(\sigma_1 + \sigma_3)^2} + \frac{f_2}{(\sigma_2 + \sigma_3)^2} > \left[\frac{f_1}{\sigma_1 + \sigma_3} + \frac{f_2}{\sigma_2 + \sigma_3} + \frac{f_3}{2\sigma_3}\right]^2. \qquad (25.33)$$

Using the fact that $\det \boldsymbol{E}(\boldsymbol{x})$ is necessarily positive, Nesi (1995) has obtained a new bound that improves on the Hashin-Shtrikman bound when the above inequality holds. The above inequality is sharp in the limit $\sigma_1 \to \infty$, since in this limit it reduces to the inequality

$$\frac{\sqrt{f_2} - f_2}{\sigma_2 + \sigma_3} \le \frac{f_3}{2\sigma_3},$$

which fails to hold only when the attainability condition (23.8) of Gibiansky and Sigmund (2000) is satisfied.

25.7. A general procedure for finding translations that generate optimal bounds on sums of energies

Let us consider the problem of finding appropriate translations $\mathcal{T}$ for bounding sums of energies, that is, for the embedded problem where the $m \times m$ matrix $\boldsymbol{L}(\boldsymbol{x})$ acts by matrix multiplication on the $m \times n$ matrix-valued extended field $\boldsymbol{E}(\boldsymbol{x})$, the columns of which lie in the subspace $\mathcal{U} \oplus \mathcal{E}$. Thus $\mathcal{T}$ represents a self-adjoint linear operator on the space of $m \times n$ matrices. Associated with $\mathcal{T}$ is the set $G(\mathcal{T})$ that is comprised of all tensors $\boldsymbol{L}$ such that

$$\text{Tr}[\boldsymbol{A}^T \boldsymbol{L} \boldsymbol{A}] \geq \text{Tr}[\boldsymbol{A}^T (\mathcal{T} \boldsymbol{A})],$$

for all $m \times n$ matrices $\boldsymbol{A}$, where $\boldsymbol{L}$ acts on $\boldsymbol{A}$ by matrix multiplication. This set is stable under homogenization. If we are seeking optimal bounds, and in particular bounds that are attained by multiple-rank laminate microgeometries, we would like $\mathcal{T}$ to be such that the boundary $\partial G(\mathcal{T})$ of this set contains many trajectories of lamination. If a tensor $\boldsymbol{L}_0$ is on the boundary, then there is at least one associated matrix $\boldsymbol{E}_0$ such that

$$\boldsymbol{J}_0 \equiv \boldsymbol{L}_0 \boldsymbol{E}_0 = \mathcal{T} \boldsymbol{E}_0. \tag{25.34}$$

Now suppose that $\boldsymbol{L}_0$ is in fact the effective tensor of a multiple-rank laminate material with a piecewise constant tensor field $\boldsymbol{L}(\boldsymbol{x}) \in \partial G(\mathcal{T})$, and suppose that $\boldsymbol{E}_0$ is the average field in this laminate. Then the local field at any given point within the laminate takes the form

$$\boldsymbol{E}(\boldsymbol{x}) = \boldsymbol{E}_0 + \sum_{i=1}^{q} \lambda_i(\boldsymbol{x}) \boldsymbol{E}_i, \tag{25.35}$$

where the functions $\lambda_i(\boldsymbol{x})$ have zero average value and the matrices $\boldsymbol{E}_i$ for $i \geq 1$ are the jumps in the average of the field $\boldsymbol{E}(\boldsymbol{x})$ across the interfaces between the layers. These satisfy the constraint

$$\boldsymbol{\Gamma}_1(\boldsymbol{n}_i) \boldsymbol{E}_i = \boldsymbol{E}_i \ \text{ for } i = 1, 2, \ldots, q, \tag{25.36}$$

in which the $\boldsymbol{n}_i$ are the associated directions of laminations. We also expect that the equation analogous to (25.34) holds locally, that is,

$$\boldsymbol{J}(\boldsymbol{x}) = \boldsymbol{L}(\boldsymbol{x}) \boldsymbol{E}(\boldsymbol{x}) = \mathcal{T} \boldsymbol{E}(\boldsymbol{x}) \ \text{ for all } \boldsymbol{x}. \tag{25.37}$$

Then each matrix

$$\boldsymbol{J}_i = \mathcal{T} \boldsymbol{E}_i, \ \text{ for } i = 1, 2, \ldots, q, \tag{25.38}$$

represents the jump in the average of the field $\boldsymbol{J}(\boldsymbol{x}) = \boldsymbol{L}(\boldsymbol{x}) \boldsymbol{E}(\boldsymbol{x})$ across the interfaces between the layers in direction $\boldsymbol{n}_i$, and therefore must satisfy the constraint

$$\boldsymbol{\Gamma}_1(\boldsymbol{n}_i) \boldsymbol{J}_i = 0 \ \text{ for } i = 1, 2, \ldots, q. \tag{25.39}$$

From (25.37) and because $\boldsymbol{L}(\boldsymbol{x})$ is symmetric we have the matrix identity

$$\boldsymbol{E}(\boldsymbol{x})^T [\mathcal{T} \boldsymbol{E}(\boldsymbol{x})] = [\mathcal{T} \boldsymbol{E}(\boldsymbol{x})]^T \boldsymbol{E}(\boldsymbol{x}).$$

For this to hold for all $\boldsymbol{x}$ it is sufficient that

$$\boldsymbol{E}_i^T [\mathcal{T} \boldsymbol{E}_j] + \boldsymbol{E}_j^T [\mathcal{T} \boldsymbol{E}_i] = [\mathcal{T} \boldsymbol{E}_i]^T \boldsymbol{E}_j + [\mathcal{T} \boldsymbol{E}_j]^T \boldsymbol{E}_i$$

or, equivalently, that

$$\boldsymbol{E}_i^T \boldsymbol{J}_j + \boldsymbol{E}_j^T \boldsymbol{J}_i = \boldsymbol{J}_i^T \boldsymbol{E}_j + \boldsymbol{J}_j^T \boldsymbol{E}_i \text{ for all } i, j = 0, 1, 2, \ldots, q. \tag{25.40}$$

More constraints on these matrices follow from the fact that $\boldsymbol{\mathcal{T}}$ is self-adjoint, implying that

$$\text{Tr}[\boldsymbol{J}_i^T \boldsymbol{E}_j] = \text{Tr}[\boldsymbol{E}_i^T \boldsymbol{J}_j] \text{ for } i, j = 0, 1, 2, \ldots, q. \tag{25.41}$$

Also, because $\boldsymbol{\mathcal{T}}$ is quasiconvex, it follows by direct analogy with (25.14) that

$$\text{Tr}[\boldsymbol{E}_i^T \frac{d\boldsymbol{\Gamma}_1(\boldsymbol{n}/|\boldsymbol{n}|)}{d\boldsymbol{n}}\bigg|_{\boldsymbol{n}=\boldsymbol{n}_i} \boldsymbol{J}_i] = 0. \tag{25.42}$$

This suggests the following approach for finding suitable translations for the comparison bounds: First look for a set of unit vectors $\boldsymbol{n}_i$ for $i = 1, 2, \ldots, q$, and a set of matrices $\boldsymbol{E}_i$ and $\boldsymbol{J}_i$, for $i = 0, 1, 2, \ldots, q$, such that the required algebraic constraints (25.36), (25.39), (25.40), (25.41), and (25.42) are satisfied. Then (25.34) and (25.38) determine the action of $\boldsymbol{\mathcal{T}}$ on the space $\boldsymbol{\mathcal{Q}}$ spanned by the matrices $\boldsymbol{E}_i$. The remaining elements of $\boldsymbol{\mathcal{T}}$ are chosen so that $\boldsymbol{\mathcal{T}}$ is quasiconvex and self-adjoint.

A similar analysis applies when we seek suitable translations for the translation bounds. Within a multiple-rank laminate with effective tensor $\boldsymbol{L}_0$ attaining the bounds the local field $\boldsymbol{E}(\boldsymbol{x})$ again takes the form (25.35) and the associated field $\boldsymbol{J}(\boldsymbol{x})$ is

$$\boldsymbol{J}(\boldsymbol{x}) = \boldsymbol{L}(\boldsymbol{x})\boldsymbol{E}(\boldsymbol{x}) = \boldsymbol{\mathcal{T}}\boldsymbol{E}(\boldsymbol{x}) + \boldsymbol{V}, \tag{25.43}$$

in which $\boldsymbol{V}$ is a constant matrix and $\boldsymbol{L}(\boldsymbol{x})$ is the local symmetric tensor of the laminate. The jumps $\boldsymbol{J}_i$ and $\boldsymbol{E}_i$, for $i = 1, 2, \ldots, q$, in the field again satisfy (25.36), (25.38), and (25.39). Also, the average field $\boldsymbol{J}_0 = \langle \boldsymbol{J} \rangle = \boldsymbol{L}_0\boldsymbol{E}_0$ satisfies

$$\boldsymbol{J}_0 = \boldsymbol{\mathcal{T}}\boldsymbol{E}_0 + \boldsymbol{V}. \tag{25.44}$$

Since $\boldsymbol{L}(\boldsymbol{x})$ is symmetric, we have the matrix identity

$$\boldsymbol{E}(\boldsymbol{x})^T[\boldsymbol{\mathcal{T}}\boldsymbol{E}(\boldsymbol{x}) + \boldsymbol{V}] = [\boldsymbol{\mathcal{T}}\boldsymbol{E}(\boldsymbol{x}) + \boldsymbol{V}]^T \boldsymbol{E}(\boldsymbol{x}),$$

which will be satisfied when the conditions (25.40) are met. Also, because $\boldsymbol{\mathcal{T}}$ is self-adjoint, we have

$$\text{Tr}[\boldsymbol{J}_i^T \boldsymbol{E}_j] = \text{Tr}[\boldsymbol{E}_i^T \boldsymbol{J}_j] \text{ for } i, j = 1, 2, \ldots, q, \tag{25.45}$$

and

$$\text{Tr}[\boldsymbol{J}_i^T \boldsymbol{E}_0] = \text{Tr}[\boldsymbol{E}_i^T (\boldsymbol{J}_0 - \boldsymbol{V})] \text{ for } i = 1, 2, \ldots, q. \tag{25.46}$$

Additionally, the constraint (25.42) must be satisfied because $\boldsymbol{\mathcal{T}}$ is quasiconvex.

Thus to obtain suitable translations for the translation bounds we look for a set of unit vectors $\boldsymbol{n}_i$, for $i = 1, 2, \ldots, q$, and a set of matrices $\boldsymbol{E}_i$ and $\boldsymbol{J}_i$, for $i = 0, 1, 2, \ldots, q$, and a matrix $\boldsymbol{V}$ such that the required constraints (25.36), (25.39), (25.40), (25.45), (25.46), and (25.42) are satisfied. Then (25.44) and (25.38) determine the action of $\boldsymbol{\mathcal{T}}$ on the space $\boldsymbol{\mathcal{Q}}$ spanned by the matrices $\boldsymbol{E}_i$. The remaining elements of $\boldsymbol{\mathcal{T}}$ are chosen so $\boldsymbol{\mathcal{T}}$ is quasiconvex, self-adjoint, and preferably extremal.

For example, consider the three-dimensional conductivity problem. If we are looking for a translation $\boldsymbol{\mathcal{T}}$ for the comparison bounds that is rotationally invariant as a fourth-order tensor, then symmetry considerations and the constraints (25.36) and (25.39) suggest the choice

$$\boldsymbol{E}_0 = \boldsymbol{I}, \quad \boldsymbol{J}_0 = a_1\boldsymbol{I}, \quad \boldsymbol{E}_i = \boldsymbol{n}_i \otimes \boldsymbol{n}_i, \quad \boldsymbol{J}_i = a_2(\boldsymbol{I} - \boldsymbol{n}_i \otimes \boldsymbol{n}_i) \text{ for } i = 1, 2, \ldots, q,$$

where a_1 and a_2 are constants and $\boldsymbol{n}_i$ ranges over all vectors in the reciprocal lattice. The constraint (25.41) forces us to take $a_1 = 2a_2$. The remaining constraints (25.40) and (25.42) are then automatically satisfied and the relation $\boldsymbol{\mathcal{T}}\boldsymbol{E}_i = \boldsymbol{J}_i$ specifies the action of $\boldsymbol{\mathcal{T}}$ on the space $\boldsymbol{\mathcal{Q}}$ of symmetric matrices. Because of rotational invariance, the action of $\boldsymbol{\mathcal{T}}$ on any antisymmetric matrix $\boldsymbol{A}$ must take the form

$$\boldsymbol{\mathcal{T}}\boldsymbol{A} = c\boldsymbol{A},$$

where the constant c is independent of $\boldsymbol{A}$. Thus the action of $\boldsymbol{\mathcal{T}}$ on an arbitrary matrix $\boldsymbol{B}$ takes the form

$$\boldsymbol{\mathcal{T}}\boldsymbol{B} = a_2(2\boldsymbol{I}\,\mathrm{Tr}(\boldsymbol{B}) - \boldsymbol{B} - \boldsymbol{B}^T)/2 + c(\boldsymbol{B} - \boldsymbol{B}^T)/2. \tag{25.47}$$

A calculation similar to the one in section 24.4 on page 504 shows that $\boldsymbol{\mathcal{T}}$ will be quasiconvex for gradients provided that c is chosen with

$$c \geq a_2.$$

By setting $a_2 = c = 1$ we recover the null Lagrangian (24.36) used to obtain lower bounds on the effective conductivity tensor of a polycrystal.

If we are looking for a rotationally invariant translation $\boldsymbol{\mathcal{T}}$ for the translation bounds, the constraint (25.46) will be satisfied provided that we take

$$\boldsymbol{V} = (a_1 - 2a_2)\boldsymbol{I},$$

where we no longer require that $a_1 = 2a_2$. The action of $\boldsymbol{\mathcal{T}}$ on an arbitrary matrix $\boldsymbol{B}$, as determined by (25.44) and (25.38) when $\boldsymbol{B}$ is symmetric, is still given by (25.47).

Notice that we can use the same set of pairs $\boldsymbol{E}_i$ and $\boldsymbol{J}_i$ to construct a translation $\boldsymbol{\mathcal{T}}'$ that is quasiconvex for divergence free fields and such that $\boldsymbol{\mathcal{T}}'\boldsymbol{J}_i = \boldsymbol{E}_i$ for all i. The action of $\boldsymbol{\mathcal{T}}'$ on $\boldsymbol{B}$ takes the form

$$\boldsymbol{\mathcal{T}}'\boldsymbol{B} = (\boldsymbol{I}\,\mathrm{Tr}(\boldsymbol{B}) - \boldsymbol{B} - \boldsymbol{B}^T)/2a_2 + c'(\boldsymbol{B} - \boldsymbol{B}^T)/2.$$

Since $\boldsymbol{\mathcal{T}}'$ is rotationally invariant, it will be quasiconvex for divergence free fields if and only if the quadratic form $\boldsymbol{B} \cdot \boldsymbol{\mathcal{T}}'\boldsymbol{B}$ is nonnegative for all matrices $\boldsymbol{B}$ such that $\boldsymbol{k} \cdot \boldsymbol{B} = 0$ for a fixed choice of the unit vector $\boldsymbol{k}$, say, $\boldsymbol{k} = (0,\ 0,\ 1)^T$. By explicitly calculating the quadratic form with

$$\boldsymbol{B} = \begin{pmatrix} b_{11} & b_{12} & b_{13} \\ b_{21} & b_{22} & b_{23} \\ 0 & 0 & 0 \end{pmatrix},$$

one sees that $\boldsymbol{\mathcal{T}}'$ is quasiconvex if and only if a_2 is negative and c' is nonnegative.

Choosing $a_2 = -1/2$ and $c' = 0$ gives the extremal translation

$$\boldsymbol{\mathcal{T}}'\boldsymbol{B} = \boldsymbol{B} + \boldsymbol{B}^T - \boldsymbol{I}\,\mathrm{Tr}(\boldsymbol{B}),$$

which is not a null Lagrangian. The quadratic form $\boldsymbol{B} \cdot \boldsymbol{\mathcal{T}}'\boldsymbol{B}$ is zero if and only if $\boldsymbol{B}$ has the form

$$\boldsymbol{B} = \alpha(\boldsymbol{I} - \boldsymbol{n} \otimes \boldsymbol{n}) + \beta(\boldsymbol{n}_1^\perp \otimes \boldsymbol{n}_2^\perp - \boldsymbol{n}_2^\perp \otimes \boldsymbol{n}_1^\perp),$$

in which α and β are arbitrary constants while $\boldsymbol{n}_1^\perp$ and $\boldsymbol{n}_2^\perp$ are unit vectors perpendicular to $\boldsymbol{n}$. As $\boldsymbol{n}$ is varied matrices of this form span the space of 3×3 matrices. Therefore $\boldsymbol{\mathcal{T}}'$ is extremal. Also, for fixed $\boldsymbol{n}$, this matrix $\boldsymbol{B}$ satisfies $\boldsymbol{n} \cdot \boldsymbol{B} = 0$, but not all matrices $\boldsymbol{B}$ satisfying $\boldsymbol{n} \cdot \boldsymbol{B} = 0$ can be expressed in the above form. For example, the matrix $\boldsymbol{n}_1^\perp \otimes \boldsymbol{n}$ is not of this form. Therefore, $\boldsymbol{\mathcal{T}}'$ is not a null Lagrangian.

25.8. Translations for three-dimensional elasticity

We can apply this procedure to find candidate rotationally invariant translations for the comparison bound or translation bound for three-dimensional elasticity. The analysis is quite involved, so we will just summarize the results of the search for translations for the comparison bound. The purpose is to provide an example of how the results of the previous section can be applied to a nontrivial problem. Presumably group theory would be a valuable tool in extending and simplifying the approach.

We looked for jumps $\boldsymbol{E}_i$ in the extended strain field with elements $\{\boldsymbol{E}_i\}_{jk\ell m}$ that were linear combinations of

$$n_j n_k n_\ell n_m, \quad n_j n_k \delta_{\ell m} \text{ and, } \quad n_j \delta_{k\ell} n_m + n_j \delta_{km} n_\ell + n_k \delta_{j\ell} n_m + n_k \delta_{jm} n_\ell,$$

and we looked for jumps $\boldsymbol{J}_i$ in the extended stress field with elements $\{\boldsymbol{J}_i\}_{jk\ell m}$ that were linear combinations of

$$\begin{aligned}&(\delta_{jk} - n_j n_k) n_\ell n_m, \quad (\delta_{jk} - n_j n_k)\delta_{\ell m},\\ &\quad \text{and } (\delta_{jm} - n_j n_m)(\delta_{k\ell} - n_k n_\ell) + (\delta_{j\ell} - n_j n_\ell)(\delta_{km} - n_k n_m).\end{aligned}$$

(A more general approach might have been to look for subspaces of fourth-order tensors associated each vector $\boldsymbol{n}$ such that the each subspace is invariant under rotations having $\boldsymbol{n}$ as the rotation axis. Motivated by our experience with the conductivity problem, we confined our attention to the case where each individual tensor is invariant under such rotations. By proceeding in this way it is quite possible that we are missing some useful rotationally invariant translations. Also, instead of considering extended strains, it may have been better to consider extended displacement gradients and associated translations that act on them.) It turns out that there are two types of families of fourth-order tensors $\boldsymbol{E}_i$ and $\boldsymbol{J}_i$ that satisfy the required conditions (25.36), (25.39), (25.40), (25.41), and (25.42).

For the first type of family the jumps in the extended strain field take the form

$$\{\boldsymbol{E}_i\}_{jk\ell m} = n_j n_k n_\ell n_m + b_i n_j n_k \delta_{\ell m}, \tag{25.48}$$

and the associated jumps in the extended stress field take the form

$$\{\boldsymbol{J}_i\}_{jk\ell m} = a(\delta_{jk} - n_j n_k)(n_\ell n_m + b_i \delta_{\ell m}), \tag{25.49}$$

where a is a fixed constant that parameterizes the family while b_i is an arbitrary positive or negative variable that depends on i. (In other words, the possible values of $\boldsymbol{E}_i$ associated with a given unit vector $\boldsymbol{n}_i$ span a two-dimensional subspace.) The pair $\boldsymbol{E}_0$ and $\boldsymbol{J}_0$ can be any fourth-order tensors expressible in the form

$$\begin{aligned}\{\boldsymbol{E}_0\}_{jk\ell m} &= \alpha \delta_{jk}\delta_{\ell m} + \beta(\delta_{j\ell}\delta_{km} + \delta_{jm}\delta_{k\ell}),\\ \{\boldsymbol{J}_0\}_{jk\ell m} &= 2a(\alpha + \beta)\delta_{jk}\delta_{\ell m} - a\beta(\delta_{j\ell}\delta_{km} + \delta_{jm}\delta_{k\ell}),\end{aligned}$$

for some choice of α and β. For this family the fields $\boldsymbol{E}_i$ span the 21-dimensional space $\boldsymbol{\mathcal{Q}}$ comprised of fourth-order tensors $\boldsymbol{\mathcal{B}}$ expressible in the form

$$\boldsymbol{\mathcal{B}} = \boldsymbol{\mathcal{A}} + \boldsymbol{A} \otimes \boldsymbol{I},$$

for some choice of symmetric second-order tensor $\boldsymbol{A}$ and for some choice of fourth-order tensor $\boldsymbol{\mathcal{A}}$ which is completely symmetric, that is, which has elements $A_{jk\ell m}$ with

$$A_{jk\ell m} = A_{kj\ell m} = A_{\ell mjk} = A_{\ell kjm}. \tag{25.50}$$

It is simplest to look for translations that act on the 36-dimensional space of fourth-order tensors $\mathcal{B}$ with elements $B_{jk\ell m}$ satisfying the symmetries

$$B_{jk\ell m} = B_{kj\ell m} = B_{jkm\ell}. \tag{25.51}$$

The 15-dimensional subspace $\mathcal{Q}^{\perp}$ that is the orthogonal complement of $\mathcal{Q}$ is spanned by the irreducible, rotationally invariant, five-dimensional subspace $\mathcal{Q}_1$ comprised of fourth-order tensors $\mathcal{B}$ with elements expressible in the form

$$B_{jk\ell m} = A_{jk}\delta_{\ell m} + 2\delta_{jk}A_{\ell m} - 3(A_{jm}\delta_{k\ell} + A_{j\ell}\delta_{km} + A_{km}\delta_{j\ell} + A_{k\ell}\delta_{jm})/4,$$

for some trace free, symmetric, second-order tensor $\boldsymbol{A}$ with elements A_{jk} (satisfying $A_{hh} = 0$) and the ten-dimensional subspace $\mathcal{Q}_2$ comprised of all tensors $\mathcal{B}$ with elements satisfying

$$B_{jk\ell m} = -B_{\ell mjk}, \quad B_{hh\ell m} = 0,$$

where the sum over the repeated index h is implied. The subspace $\mathcal{Q}_2$ can itself be split into two irreducible rotationally invariant subspaces: The three-dimensional subspace $\mathcal{Q}_3$ comprised of all tensors $\mathcal{B}$ with elements expressible in the form

$$B_{jk\ell m} = A'_{jm}\delta_{k\ell} + A'_{j\ell}\delta_{km} + A'_{km}\delta_{j\ell} + A'_{k\ell}\delta_{jm},$$

for some choice of antisymmetric matrix $\boldsymbol{A}'$ (i.e., with $A'_{mj} = -A'_{jm}$) and the remaining seven-dimensional subspace comprised of all fourth-order tensors $\mathcal{B}$ in $\mathcal{Q}_2$ (with elements $B_{jk\ell m}$ satisfying $B_{jhhm} = 0$) that is the orthogonal complement of $\mathcal{Q}_3$ in the space $\mathcal{Q}_2$. Let $\boldsymbol{\Lambda}_1$, $\boldsymbol{\Lambda}_2$, and $\boldsymbol{\Lambda}_3$ denote the projections onto the subspaces $\mathcal{Q}_1$, $\mathcal{Q}_2$ and $\mathcal{Q}_3$. When these projections are applied to a fourth-order tensor $\mathcal{B}$ satisfying the symmetries (25.51) they produce fourth-order tensors with elements

$$\begin{aligned}
\{\boldsymbol{\Lambda}_1\mathcal{B}\}_{jk\ell m} &= A_{jk}\delta_{\ell m} + 2\delta_{jk}A_{\ell m} - 3(A_{jm}\delta_{k\ell} + A_{j\ell}\delta_{km} + A_{km}\delta_{j\ell} + A_{k\ell}\delta_{jm})/4,\\
\{\boldsymbol{\Lambda}_2\mathcal{B}\}_{jk\ell m} &= (B_{jk\ell m} - B_{\ell mjk})/2 - (B_{jkhh} - B_{hhjk})\delta_{\ell m}/6 + \delta_{jk}(B_{\ell mhh} - B_{hh\ell m})/6,\\
\{\boldsymbol{\Lambda}_3\mathcal{B}\}_{jk\ell m} &= A'_{jm}\delta_{k\ell} + A'_{j\ell}\delta_{km} + A'_{km}\delta_{j\ell} + A'_{k\ell}\delta_{jm},
\end{aligned}$$

where

$$\begin{aligned}
A_{jk} &= 2[2B_{jkhh} + 4B_{hhjk} - 3B_{jhkh} - 3B_{khjh} + 2(B_{ghgh} - B_{gghh})\delta_{jk}]/33,\\
A'_{jk} &= (B_{jhhk} - B_{khhj})/10.
\end{aligned}$$

Associated with the first type of family is the rotationally invariant translation $\mathcal{T}$ that when applied to a fourth-order tensor $\mathcal{B}$ satisfying the symmetries (25.51) produces a fourth-order tensor $\mathcal{T}\mathcal{B}$ with elements

$$\{\mathcal{T}\mathcal{B}\}_{jk\ell m} = a\delta_{jk}B_{hh\ell m} - aB_{jk\ell m} + \{(c_1\boldsymbol{\Lambda}_1 + c_2\boldsymbol{\Lambda}_2 + c_3\boldsymbol{\Lambda}_3)\mathcal{B}\}_{jk\ell m},$$

where the constants a, c_1, c_2, and c_3 need to be chosen so that $\mathcal{T}$ is quasiconvex for strains. One can check that $\boldsymbol{J}_i = \mathcal{T}\boldsymbol{E}_i$. When the constants c_1, c_2, and c_3 are all set equal to zero (and a is taken to be negative to ensure quasiconvexity) the jumps $\boldsymbol{E}_i$ and $\boldsymbol{J}_i = \mathcal{T}\boldsymbol{E}_i$ in the extended fields can be taken to be any pair of fourth-order tensors with elements expressible in the form

$$\{\boldsymbol{E}_i\}_{jk\ell m} = n_j n_k \{\boldsymbol{A}_i\}_{\ell m}, \quad \{\boldsymbol{J}_i\}_{jk\ell m} = a(\delta_{jk} - n_j n_k)\{\boldsymbol{A}_i\}_{\ell m},$$

for some choice of the matrix $\boldsymbol{A}_i$. The pair $\boldsymbol{E}_i$ and $\boldsymbol{J}_i$ given by (25.48) and (25.49) is of this form with $\boldsymbol{A}_i = \boldsymbol{n} \otimes \boldsymbol{n} + b_i \boldsymbol{I}$. If both c_1 and c_2 are zero, but c_3 is not zero, then the jumps $\boldsymbol{E}_i$ and $\boldsymbol{J}_i = \boldsymbol{\mathcal{T}} \boldsymbol{E}_i$ can be taken to be any pair of fourth-order tensors expressible in the above form for some choice of the matrix $\boldsymbol{A}_i$ that has $\boldsymbol{n}$ as its eigenvector. This latter constraint is needed to ensure that $\boldsymbol{\Lambda}_3 \boldsymbol{E}_i = 0$.

For the second type of family the jumps in the extended strain field take the form

$$\{\boldsymbol{E}_i\}_{jk\ell m} = (n_j \delta_{k\ell} n_m + n_j \delta_{km} n_\ell + n_k \delta_{j\ell} n_m + n_k \delta_{jm} n_\ell)/2 - n_j n_k n_\ell n_m + a_1 n_j n_k \delta_{\ell m},$$

and the associated jumps in the extended stress field take the form

$$\begin{aligned} \{\boldsymbol{J}_i\}_{jk\ell m} \;=\; & a_2[(\delta_{jm} - n_j n_m)(\delta_{k\ell} - n_k n_\ell)/2 \\ & + (\delta_{j\ell} - n_j n_\ell)(\delta_{km} - n_k n_m)/2 + a_1(\delta_{jk} - n_j n_k)\delta_{\ell m}], \end{aligned}$$

where a_1 and a_2 are fixed constants that parameterize the family. The pair $\boldsymbol{E}_0$ and $\boldsymbol{J}_0$ can be any fourth-order tensors expressible in the form

$$\begin{aligned} \{\boldsymbol{E}_0\}_{jk\ell m} \;=\; & \alpha \delta_{jk} \delta_{\ell m} + \beta(\delta_{j\ell} \delta_{km} + \delta_{jm} \delta_{k\ell}), \\ \{\boldsymbol{J}_0\}_{jk\ell m} \;=\; & a_2\{[(6a_1^2 + a_1 - 3)\alpha + 6a_1(a_1 + 2)\beta]\delta_{jk}\delta_{\ell m} \\ & + [3(3a_1 + 1)\alpha + 2(-3a_1^2 + a_1 + 3)\beta](\delta_{j\ell}\delta_{km} + \delta_{jm}\delta_{k\ell})/2\}/(3a_1^2 + 2a_1 + 3), \end{aligned}$$

for some choice of α and β.

For this family the fields $\boldsymbol{E}_i$ span the 21-dimensional space $\boldsymbol{\mathcal{P}}$ comprised of fourth-order tensors $\boldsymbol{\mathcal{B}}$ that have elements $B_{jk\ell m}$ expressible in the form

$$B_{jk\ell m} = A_{jk\ell m} + (A'_{jm}\delta_{k\ell} + A'_{j\ell}\delta_{km} + A'_{km}\delta_{j\ell} + A'_{k\ell}\delta_{jm})/2 + a_1 A'_{jk}\delta_{\ell m},$$

for some choice of completely symmetric tensor $\boldsymbol{\mathcal{A}}$ with elements $A_{jk\ell m}$ satisfying (25.50) and for some choice of symmetric second-order tensor $\boldsymbol{A}'$ with elements A_{jk}. The 15-dimensional subspace $\boldsymbol{\mathcal{P}}^\perp$ that is the orthogonal complement of $\boldsymbol{\mathcal{P}}$ is spanned by $\boldsymbol{\mathcal{Q}}_2$ and the rotationally invariant five-dimensional subspace $\boldsymbol{\mathcal{Q}}'_1$ comprised of fourth-order tensors $\boldsymbol{\mathcal{B}}$ with elements expressible in the form

$$\begin{aligned} B_{jk\ell m} \;=\; & (1 + 2a_1)A_{jk}\delta_{\ell m} + (4a_1 - 1)\delta_{jk}A_{\ell m} \\ & - 3a_1(A_{jm}\delta_{k\ell} + A_{j\ell}\delta_{km} + A_{km}\delta_{j\ell} + A_{k\ell}\delta_{jm})/2, \end{aligned}$$

for some trace free, symmetric second-order tensor $\boldsymbol{A}$ with elements A_{jk} (satisfying $A_{hh} = 0$). The projection $\boldsymbol{\Lambda}'_1$ onto the subspace $\boldsymbol{\mathcal{Q}}'_1$ when applied to a fourth-order tensor $\boldsymbol{\mathcal{B}}$ satisfying the symmetries (25.51) produces a tensor with elements

$$\begin{aligned} \{\boldsymbol{\Lambda}'_1 \boldsymbol{\mathcal{B}}\}_{jk\ell m} \;=\; & (1 + 2a_1)A_{jk}\delta_{\ell m} + (4a_1 - 1)\delta_{jk}A_{\ell m} \\ & - 3a_1(A_{jm}\delta_{k\ell} + A_{j\ell}\delta_{km} + A_{km}\delta_{j\ell} + A_{k\ell}\delta_{jm})/2, \end{aligned}$$

where

$$\begin{aligned} A_{jk} = [(1 + 2a_1)B_{jkhh} \;+\; & (4a_1 - 1)B_{hhjk} - 3a_1 B_{jhkh} - 3a_1 B_{khjh} \\ & + \; 2a_1(B_{ghgh} - B_{gghh})\delta_{jk}]/3(11a_1^2 - 4a_1 + 1). \end{aligned}$$

Associated with the second type of family is the rotationally invariant translation $\boldsymbol{\mathcal{T}}$ that when applied to $\boldsymbol{\mathcal{B}}$ produces the tensor $\boldsymbol{\mathcal{T}\mathcal{B}}$ with elements

$$\{\boldsymbol{\mathcal{T}\mathcal{B}}\}_{jk\ell m} = -a_2 B_{jk\ell m} + \{(d_1\boldsymbol{\Lambda}_1' + d_2\boldsymbol{\Lambda}_2 + d_3\boldsymbol{\Lambda}_3)\boldsymbol{\mathcal{B}}\}_{jk\ell m} + \frac{a_2[a_1\delta_{jk}\delta_{\ell m} + (\delta_{j\ell}\delta_{km} + \delta_{jm}\delta_{k\ell})/2][a_1 B_{gghh} + (B_{ghgh} + B_{ghhg})/2]}{3a_1^2 + 2a_1 + 3},$$

where the constants a_1, a_2, d_1, d_2, and d_3 need to be chosen to ensure that $\boldsymbol{\mathcal{T}}$ is quasiconvex for strains. Again one can check that $\boldsymbol{J}_i = \boldsymbol{\mathcal{T}}\boldsymbol{E}_i$.

In a similar way one can construct translations $\boldsymbol{\mathcal{T}}'$ that are quasiconvex for stresses and such that $\boldsymbol{E}_i = \boldsymbol{\mathcal{T}}'\boldsymbol{J}_i$ for all i. The question of what bounds can be generated from these translations has not yet been explored.

References

Avellaneda, M., A. V. Cherkaev, L. V. Gibiansky, G. W. Milton, and M. Rudelson 1996. A complete characterization of the possible bulk and shear moduli of planar polycrystals. *Journal of the Mechanics and Physics of Solids* 44(7):1179–1218. {*362, 367, 502, 525, 537, 550*}

Avellaneda, M., A. V. Cherkaev, K. A. Lurie, and G. W. Milton 1988. On the effective conductivity of polycrystals and a three-dimensional phase-interchange inequality. *Journal of Applied Physics* 63(10):4989–5003. {*120, 139, 439, 441, 450, 452, 512, 525, 538, 550, 555, 564*}

Avellaneda, M. and G. W. Milton 1989. Optimal bounds on the effective bulk modulus of polycrystals. *SIAM Journal on Applied Mathematics* 49(3):824–837. {*441, 444, 453, 501, 525, 536, 550*}

Bauman, P., A. Marini, and V. Nesi 2001. Univalent solutions of an elliptic system of partial differential equations arising in homogenization. *Indiana University Mathematics Journal* 50(2). To appear. {*543, 550*}

Bhattacharya, K. and R. V. Kohn 1997. Elastic energy minimization and the recoverable strains of polycrystalline shape-memory materials. *Archive for Rational Mechanics and Analysis* 139(2):99–180. {*531, 550, 682, 695*}

Firoozye, N. B. 1991. Optimal use of the translation method and relaxations of variational problems. *Communications on Pure and Applied Mathematics (New York)* 44(6):643–678. {*529, 531, 532, 550, 673, 696*}

Gibiansky, L. V. and A. V. Cherkaev 1984. Design of composite plates of extremal rigidity. Technical Report 914, Ioffe Physicotechnical Institute, Leningrad, USSR. 1–60 pp. English translation in *Topics in the Mathematical Modelling of Composite Materials*, pp. 95–137, ed. by A. Cherkaev and R. Kohn. ISBN 0-8176-3662-5. {*432, 434, 466, 492, 501, 525, 529, 550*}

Gibiansky, L. V. and O. Sigmund 2000. Multiphase composites with extremal bulk modulus. *Journal of the Mechanics and Physics of Solids* 48(3):461–498. {*460, 472, 492, 543, 550*}

Grabovsky, Y. 1996. Bounds and extremal microstructures for two-component composites: A unified treatment based on the translation method. *Proceedings of the Royal Society of London. Series A, Mathematical and Physical Sciences* 452(1947):919–944. {*466, 492, 541, 542, 550, 558, 566*}

Lurie, K. A. and A. V. Cherkaev 1982. Accurate estimates of the conductivity of mixtures formed of two materials in a given proportion (two-dimensional problem). *Doklady Akademii Nauk SSSR* 264:1128–1130. English translation in *Soviet Phys. Dokl.* 27:461–462 (1982). {*499, 506, 508, 526, 529, 551*}

Lurie, K. A. and A. V. Cherkaev 1984. Exact estimates of conductivity of composites formed by two isotropically conducting media taken in prescribed proportion. *Proceedings of the Royal Society of Edinburgh. Section A, Mathematical and Physical Sciences* 99(1–2):71–87. {*499, 506, 508, 521, 526, 529, 551*}

Lurie, K. A. and A. V. Cherkaev 1986. Effective characteristics of composite materials and the optimal design of structural elements. *Uspekhi Mekhaniki = Advances in Mechanics* 9(2):3–81. English translation in *Topics in the Mathematical Modelling of Composite Materials*, pp. 175–258, ed. by A. Cherkaev and R. Kohn. ISBN 0-8176-3662-5. {*76, 90, 529, 551*}

Marcellini, P. 1984. Quasiconvex quadratic forms in two dimensions. *Applied Mathematics and Optimization* 11(2):183–189. {*533, 551*}

Milton, G. W. 1990. On characterizing the set of possible effective tensors of composites: The variational method and the translation method. *Communications on Pure and Applied Mathematics (New York)* 43(1):63–125. {*164, 183, 248, 265, 268, 277, 287, 451, 454, 473, 494, 499, 505, 512, 513, 518, 526, 532, 551*}

Milton, G. W. 1994. A link between sets of tensors stable under lamination and quasiconvexity. *Communications on Pure and Applied Mathematics (New York)* 47(7):959–1003. {*513, 527, 535, 551, 647, 669*}

Milton, G. W. and S. K. Serkov 2000. Bounding the current in nonlinear conducting composites. *Journal of the Mechanics and Physics of Solids* 48(6/7):1295–1324. {*530, 551*}

Murat, F. 1987. A survey on compensated compactness. In L. Cesari (ed.), *Contributions to Modern Calculus of Variations*, pp. 145–183. Harlow, Essex, United Kingdom: Longman Scientific and Technical. ISBN 0-470-20378-1 (Wiley), 0-582-99458-6. {*275, 288, 529, 551, 676, 697*}

Murat, F. and L. Tartar 1985. Calcul des variations et homogénísation. (French) [Calculus of variation and homogenization]. In *Les méthodes de l'homogénéisation: théorie et applications en physique*, pp. 319–369. Paris: Eyrolles. English translation in *Topics in the Mathematical Modelling of Composite Materials*, pp. 139–173, ed. by A. Cherkaev and R. Kohn, ISBN 0-8176-3662-5. {*12, 13, 17, 347, 353, 429, 431, 432, 435, 444, 454, 462, 495, 499, 503, 506, 508, 521, 527, 529, 551*}

Nesi, V. 1993. On the G-closure in the polycrystalline problem. *SIAM Journal on Applied Mathematics* 53(1):96–127. {*541, 551*}

Nesi, V. 1995. Bounds on the effective conductivity of two-dimensional composites made of $n \geq 3$ isotropic phases in prescribed volume fraction: The weighted translation method. *Proceedings of the Royal Society of Edinburgh* 125A(6):1219–1239. {*543, 551*}

Nesi, V. and G. W. Milton 1991. Polycrystalline configurations that maximize electrical resistivity. *Journal of the Mechanics and Physics of Solids* 39(4):525–542. {*537, 551, 684, 697*}

Nesi, V., D. R. S. Talbot, and J. R. Willis 1999. Translation and related bounds for the response of a nonlinear composite conductor. *Proceedings of the Royal Society of London. Series A, Mathematical and Physical Sciences* 455(1990):3687–3707. {*531, 552*}

Ponte Castañeda, P. 1996. Variational methods for estimating the effective behavior of non-linear composite materials. In K. Z. Markov (ed.), *Proceedings of the Eighth International Symposium on Continuum Models and Discrete Systems: 11–16 June 1995, Varna, Bulgaria*, pp. 268–279. Singapore / Philadelphia / River Edge, New Jersey: World Scientific Publishing Co. ISBN 981-02-2552-0. {*531, 552*}

Serre, D. 1981a. Condition de Legendre-Hadamard: Espaces de matrices de rang $\neq 1$. (French) [Legendre-Hadamard condition: Space of matrices of rank $\neq 1$]. *Comptes rendus de l'Académie des sciences, Paris* 293(1):23–26. {*533, 552*}

Serre, D. 1981b. Relations d'ordre entre formes quadratiques en compacité par compensation. (French) [Order relations between quadratic forms in compensated compactness]. *Comptes rendus de l'Académie des sciences, Paris* 292(17):785–787. {*533, 552*}

Tartar, L. 1979a. Compensated compactness and applications to partial differential equations. In R. J. Knops (ed.), *Nonlinear Analysis and Mechanics, Heriot-Watt Symposium, Volume IV*, pp. 136–212. London: Pitman Publishing Ltd. ISBN 0-8224-8461-7, 0-273-08461-5. {*59, 72, 275, 276, 288, 503, 527, 529, 552, 676, 677, 684, 698*}

Tartar, L. 1979b. Estimation de coefficients homogénéisés. (French) [Estimation of homogenization coefficients]. In R. Glowinski and J.-L. Lions (eds.), *Computing Methods in Applied Sciences and Engineering: Third International Symposium, Versailles, France, December 5–9, 1977,*, pp. 364–373. Berlin / Heidelberg / London / etc.: Springer-Verlag. English translation in *Topics in the Mathematical Modelling of Composite Materials*, pp. 9–20, ed. by A. Cherkaev and R. Kohn. ISBN 0-8176-3662-5. ISBN 0-387-09123-8. {*155, 156, 162, 183, 274, 289, 499, 503, 508, 509, 527, 529, 552*}

Tartar, L. 1985. Estimations fines des coefficients homogénéisés. (French) [Fine estimations of homogenized coefficients]. In P. Krée (ed.), *Ennio de Giorgi Colloquium: Papers Presented at a Colloquium Held at the H. Poincaré Institute in November 1983*, pp. 168–187. London: Pitman Publishing Ltd. ISBN 0-273-08680-4. {*129, 141, 165, 167, 174, 183, 462, 496, 499, 503, 506, 508, 527, 529, 552, 683, 698*}

Terpstra, F. J. 1938. Die Darstellung biquadratischer Formen als Summen von Quadraten mit Anwendung auf die Variationsrechnung. *Mathematische Annalen* 116:166–180. {*533, 552*}

26

Bounds incorporating three-point correlation functions†

If cross-sectional photographs of a material are available and the microstructure is isotropic, then one can determine the two- and three-point statistics of the material, in addition to the volume fractions of the phases. This section shows how to utilize this information to obtain improved bounds on the effective properties.

26.1. A brief history of bounds incorporating correlation functions

Beran (1965) first recognized that conductivity bounds incorporating three-point correlation functions could be obtained by substituting appropriate trial fields into the classical variational principles. Beran and Molyneux (1966) obtained similar bounds on the effective bulk modulus. For statistically isotropic two-phase cell materials Miller (1969a, 1969b) considered these bounds and found that they reduced to expressions involving the cell shape parameter G given by (15.44). McCoy (1970) used the same approach to obtain bounds on the effective shear modulus. The conductivity, bulk modulus, and shear modulus bounds were tightened and extended to multiphase three- and two-dimensional cell materials by Pham (1996, 1997). Silnutzer (1972) extended the Beran conductivity bounds to fiber-reinforced materials, that is, to two-dimensional composites. Beran and Silnutzer (1971) found simplified expressions for these bounds for two-phase cell materials.

Schulgasser (1976) recognized that the two-dimensional bounds of Silnutzer (1972) could be simplified for any two-phase composite, and not just cell materials, and found that they only depended on a single geometric parameter. A similar simplification was found for the three-dimensional Beran conductivity bounds (Torquato 1980; Milton 1981b; Torquato and Stell 1985), for the Beran-Molyneux bulk modulus bounds, and for the McCoy shear modulus bounds (Milton 1981a). The conductivity and bulk modulus bounds for two-phase composites were found to depend on the parameter ζ_1 defined by (15.31) while the shear modulus bounds depend on ζ_1 and on the additional parameter η_1 defined by (15.36). By taking a better trial field Milton and Phan-Thien (1982) slightly improved the McCoy bounds on the shear modulus. These improved bounds still only incorporated the geometric parameters ζ_1 and η_1. Simplified expressions for the two-dimensional bulk and shear moduli third-order bounds were also found (Milton 1982). Torquato (1991) and Markov and Zvyatkov (1991) give a comprehensive review of all of these bounds and related work.

Bounds depending on higher order point statistics have also been obtained. Elsayed and McCoy (1973) and Elsayed (1974) obtained bounds that included five-point statistics for both two- and three-dimensional cell materials. Dederichs and Zeller (1973) and Kröner (1977) recognized that one could obtain bounds incorporating statistical information up to any given

order. Milton and Phan-Thien (1982) and Phan-Thien and Milton (1982) obtained bounds incorporating four-point statistics that were expressed in terms of a set of geometric parameters. These bounds were evaluated by Helte (1994, 1995) for dispersions of penetrable spheres and compared with the numerical simulations of Kim and Torquato (1992). In the next chapter we present bounds that incorporate a succession of $J+1$ coefficients that appear in the series expansion of the effective conductivity of a two-phase material in powers of the difference $\sigma_1 - \sigma_2$ between the component conductivities. In principle, these coefficients could be calculated from the J-point correlation function characterizing the microstructure, as explained in chapter 15 on page 313. In this chapter we will focus on bounds involving three-point statistics since we believe that these are the most useful bounds.

26.2. Three-point bounds on the conductivity of a two-phase mixture

To see how bounds involving three-point statistics can be derived, consider an isotropic composite of two isotropic conducting phases, with conductivities $\sigma_1 \boldsymbol{I}$ and $\sigma_2 \boldsymbol{I}$. In such a medium the series expansions (14.4) and (14.5) for the effective tensor $\boldsymbol{\sigma}_* = \sigma_* \boldsymbol{I}$ and electric field $\boldsymbol{e}(\boldsymbol{x})$ with $\boldsymbol{L}_0 = \sigma_2 \boldsymbol{I}$ become

$$\begin{aligned}\boldsymbol{\sigma}_* = (f_1\sigma_1 + f_2\sigma_2)\boldsymbol{I} \; &- \; (\sigma_1-\sigma_2)^2 \boldsymbol{\Gamma}_0\chi_1\boldsymbol{\Gamma}_1\chi_1\boldsymbol{\Gamma}_0/\sigma_2 \\ &+ \; (\sigma_1-\sigma_2)^3 \boldsymbol{\Gamma}_0\chi_1\boldsymbol{\Gamma}_1\chi_1\boldsymbol{\Gamma}_1\chi_1\boldsymbol{\Gamma}_0/\sigma_2^2 - \cdots \end{aligned} \tag{26.1}$$

and

$$\boldsymbol{e}(\boldsymbol{x}) = \boldsymbol{e}_0 - (\sigma_1-\sigma_2)\boldsymbol{\Gamma}_1\chi_1\boldsymbol{e}_0/\sigma_2 + (\sigma_1-\sigma_2)^2\boldsymbol{\Gamma}_1\chi_1\boldsymbol{\Gamma}_1\chi_1\boldsymbol{e}_0/\sigma_2^2 - \cdots, \tag{26.2}$$

where $\boldsymbol{e}_0$ is the constant applied field. The form of the expansion for $\boldsymbol{e}(\boldsymbol{x})$ suggests that a suitable first choice of trial electric field might be

$$\underline{\boldsymbol{e}} = \boldsymbol{e}_0 + \alpha\boldsymbol{\Gamma}_1\chi_1\boldsymbol{e}_0,$$

in which α is a constant that can be chosen to optimize the bound. This trial field is surely curl free with average value $\boldsymbol{e}_0$ because $\boldsymbol{\Gamma}_1$ projects onto the space of curl free average zero fields.

Inserting this trial field in the classical variational principle [see (13.10)],

$$\boldsymbol{e}_0\cdot\boldsymbol{\sigma}_*\boldsymbol{e}_0 = \min_{\substack{\underline{\boldsymbol{e}} \\ \nabla\times\underline{\boldsymbol{e}}=0 \\ \langle\underline{\boldsymbol{e}}\rangle=\boldsymbol{e}_0}} \langle\underline{\boldsymbol{e}}\cdot\boldsymbol{\sigma}\underline{\boldsymbol{e}}\rangle = \min_{\substack{\underline{\boldsymbol{e}} \\ \nabla\times\underline{\boldsymbol{e}}=0 \\ \langle\underline{\boldsymbol{e}}\rangle=\boldsymbol{e}_0}} \langle\underline{\boldsymbol{e}}\cdot[(\sigma_1-\sigma_2)\chi_1+\sigma_2]\underline{\boldsymbol{e}}\rangle, \tag{26.3}$$

gives the bound

$$\begin{aligned}\sigma_*|\boldsymbol{e}_0|^2 &\le \min_\alpha\Big[\boldsymbol{e}_0\cdot\langle\boldsymbol{\sigma}\rangle\boldsymbol{e}_0 + 2\alpha(\sigma_1-\sigma_2)\boldsymbol{e}_0\cdot\langle\chi_1\boldsymbol{\Gamma}_1\chi_1\boldsymbol{e}_0\rangle \\ &\qquad +\alpha^2\langle\boldsymbol{e}_0\cdot\chi_1\boldsymbol{\Gamma}_1(\sigma_1\chi_1+\sigma_2\chi_2)\boldsymbol{\Gamma}_1\chi_1\boldsymbol{e}_0\rangle\Big] \\ &\le (f_1\sigma_1+f_2\sigma_2)|\boldsymbol{e}_0|^2 - \frac{(\sigma_1-\sigma_2)^2(\boldsymbol{e}_0\cdot\boldsymbol{\Gamma}_0\chi_1\boldsymbol{\Gamma}_1\chi_1\boldsymbol{\Gamma}_0\boldsymbol{e}_0)^2}{\sigma_2\boldsymbol{e}_0\cdot\boldsymbol{\Gamma}_0\chi_1\boldsymbol{\Gamma}_1\chi_1\boldsymbol{\Gamma}_0\boldsymbol{e}_0 + (\sigma_1-\sigma_2)\boldsymbol{e}_0\cdot\boldsymbol{\Gamma}_0\chi_1\boldsymbol{\Gamma}_1\chi_1\boldsymbol{\Gamma}_1\chi_1\boldsymbol{\Gamma}_0\boldsymbol{e}_0}.\end{aligned} \tag{26.4}$$

The tensors $\boldsymbol{\Gamma}_0\chi_1\boldsymbol{\Gamma}_1\chi_1\boldsymbol{\Gamma}_0$ and $\boldsymbol{\Gamma}_0\chi_1\boldsymbol{\Gamma}_1\chi_1\boldsymbol{\Gamma}_1\chi_1\boldsymbol{\Gamma}_0$ required to evaluate this bound are precisely the second- and third-order terms that appear in the series expansion (26.1) for the effective conductivity tensor $\boldsymbol{\sigma}_*$. By comparing (26.1) with (15.30) we see that

$$\boldsymbol{\Gamma}_0\chi_1\boldsymbol{\Gamma}_1\chi_1\boldsymbol{\Gamma}_0 = f_1 f_2 \boldsymbol{I}/3,$$
$$\boldsymbol{\Gamma}_0\chi_1\boldsymbol{\Gamma}_1\chi_1\boldsymbol{\Gamma}_1\chi_1\boldsymbol{\Gamma}_0 = f_1 f_2(f_2 + 2\zeta_1)\boldsymbol{I}/9,$$

where ζ_1 is the geometric parameter defined by (15.31) that depends on the third-order reduced correlation function associated with $\chi_1(\boldsymbol{x})$.

By substituting these expressions back into (26.4) we obtain the Beran upper bound on the effective conductivity σ_*:

$$\sigma_* \le f_1\sigma_1 + f_2\sigma_2 - \frac{f_1 f_2(\sigma_1 - \sigma_2)^2}{f_2\sigma_1 + f_1\sigma_2 + 2(\zeta_1\sigma_1 + \zeta_2\sigma_2)}, \tag{26.5}$$

in which $\zeta_2 = 1 - \zeta_1$. This is called a third-order bound on the effective conductivity σ_*, because the expansion of the bound in powers of $(\sigma_1 - \sigma_2)$ up to the third order agrees with the series expansion (15.33) of σ_* to the third order. This bound is attainable for five specific values of ζ_1, namely, for $\zeta_1 = 0$, $f_2/4$, f_2, $1 - f_2/4$, and 1 (Avellaneda, Cherkaev, Lurie, and Milton 1988). For other values of ζ_1 it is still an open question as to whether the bound can be improved.

Similarly, by substituting the trial current field

$$\underline{\boldsymbol{j}} = \boldsymbol{j}_0 + \alpha\boldsymbol{\Gamma}_2\chi_1\boldsymbol{j}_0$$

into the dual variational principle (13.12), we obtain the Beran third-order lower bound on the effective conductivity σ_*:

$$1/\sigma_* \le f_1/\sigma_1 + f_2/\sigma_2 - \frac{f_1 f_2(1/\sigma_1 - 1/\sigma_2)^2}{f_2/\sigma_1 + f_1/\sigma_2 + (\zeta_1/\sigma_1 + \zeta_2/\sigma_2)/2},$$

which, after some algebraic manipulation, can be reexpressed in the equivalent form

$$\sigma_* \ge f_1\sigma_1 + f_2\sigma_2 - \frac{f_1 f_2(\sigma_1 - \sigma_2)^2}{f_2\sigma_1 + f_1\sigma_2 + 2(\zeta_1/\sigma_1 + \zeta_2/\sigma_2)^{-1}}. \tag{26.6}$$

This bound is not optimal. Assuming that the components have been labeled so that $\sigma_1 \ge \sigma_2$, one has the tighter bound

$$\sigma_* \ge \sigma_2\left(\frac{(2\sigma_1 + \sigma_2)(\sigma_1 + 2f_1\sigma_1 + 2f_2\sigma_2) - 2f_2\zeta_1(\sigma_1 - \sigma_2)^2}{(2\sigma_1 + \sigma_2)(2\sigma_2 + f_2\sigma_1 + f_1\sigma_2) - 2f_2\zeta_1(\sigma_1 - \sigma_2)^2}\right), \tag{26.7}$$

obtained by Avellaneda, Cherkaev, Lurie, and Milton (1988) using the inequality (7.23) in conjunction with the analytic method, discussed in the next chapter. This bound is the best possible one, being attained when the composite is an assemblage of doubly coated spheres.

The Beran bounds were first compared with experimental measurements of effective thermal conductivities by Corson (1974b). Kim and Torquato (1991, 1992) and Bonnecaze and Brady (1991) compared them with numerical simulations of the effective conductivity of suspensions of hard and overlapping spheres. Roberts and Teubner (1995) and Roberts and Knackstedt (1996) compared them with numerical simulations of the effective conductivity

of media defined by the level cut, or level cuts, of a Gaussian random field. The agreement in all cases was good. Many papers that evaluate ζ_1 for various microstructures, such as those referred to in section 15.6 on page 327, also have graphs of the Beran bounds for particular choices of component conductivities. By taking a more general trial field Prager (1963) obtained bounds that are at least as tight, if not tighter. However, the computation of his bounds requires the three-point correlation function, and not just knowledge of ζ_1.

As Berryman (1982) observed, the bounds (26.5) and (26.6) simplify if we introduce the y-parameter

$$y_\sigma = -f_2\sigma_1 - f_1\sigma_2 + \frac{f_1 f_2(\sigma_1 - \sigma_2)^2}{f_1\sigma_1 + f_1\sigma_1 - \sigma_*} = \frac{\sigma_1\sigma_2[\sigma_*(f_1/\sigma_1 + f_2/\sigma_2) - 1]}{f_1\sigma_1 + f_2\sigma_2 - \sigma_*},$$

in terms of which

$$\sigma_* = f_1\sigma_1 + f_2\sigma_2 - \frac{f_1 f_2(\sigma_1 - \sigma_2)^2}{f_2\sigma_1 + f_1\sigma_2 + y_\sigma}.$$

The parameter y_σ is the scalar form of the conductivity Y-tensor defined by (19.3): In an isotropic conducting material we have $\boldsymbol{Y}_* = y_\sigma \boldsymbol{I}$. The bounds, when expressed in terms of y_σ, reduce to simply

$$2(\zeta_1/\sigma_1 + \zeta_2/\sigma_2)^{-1} \le y_\sigma \le 2(\zeta_1\sigma_1 + \zeta_2\sigma_2). \tag{26.8}$$

In other words, it is simpler to check that y_σ satisfies these inequalities rather than verifying that the effective tensor σ_* satisfies the bounds (26.5) and (26.6).

Notice that the upper and lower bounds coincide when $\zeta_1 = 1$, implying that $y_\sigma = 2\sigma_1$ for all conductivity ratios $\sigma_1/\sigma_2 > 0$. Conversely, if $y_\sigma = 2\sigma_1$ for some positive conductivity ratio $\sigma_1/\sigma_2 \neq 1$, then $\zeta_1 = 1$. Since $y_\sigma = 2\sigma_1$ is the expression for the Hashin-Shtrikman bound (23.6), we deduce that if the two-phase Hashin-Shtrikman bound is attained for one conductivity ratio by a particular microgeometry (such as the coated sphere assemblage), then it is necessarily attained for all conductivity ratios by the same microgeometry. This is a particular feature of the two-phase bounds and does not generalize to the three-phase bounds. The bounds also coincide when $\zeta_1 = 0$, giving $y_\sigma = 2\sigma_2$, which corresponds to the other Hashin-Shtrikman bound.

When $\zeta_1 > 1$ or $\zeta_1 < 0$, the value of the lower bound is bigger than that of the upper bound. Clearly this cannot happen and therefore for any microgeometry ζ_1 must lie between zero and one. A more direct proof of this was given in section 15.6 on page 327.

In section 23.4 on page 465 we saw how bounds that depend on the two-point correlation functions could be used to generate correlation function independent bounds by taking the union of the bounds as the geometric parameters $c(\boldsymbol{\xi})$ vary over all possible combinations. A similar approach can be used to obtain correlation function independent bounds from the third-order Beran bounds. Using the fact that ζ_1 lies between zero and one gives the following correlation function independent bound on y_σ:

$$\min_{\substack{\zeta_1 \\ 0 \le \zeta_1 \le 1}} \quad 2(\zeta_1/\sigma_1 + (1-\zeta_1)/\sigma_2)^{-1} \le y_\sigma \le \max_{\substack{\zeta_1 \\ 0 \le \zeta_1 \le 1}} \quad 2(\zeta_1\sigma_1 + \zeta_2\sigma_2)$$

or, equivalently,

$$2\sigma_2 \le y_\sigma \le 2\sigma_1,$$

where we have assumed that the phases are labeled so that $\sigma_2 \le \sigma_1$. Thus the Hashin-Shtrikman bounds on σ_* can be recovered from the third-order Beran bounds on σ_*. This

could have been anticipated. The nesting property of the bounds discussed in section 13.6 on page 281 implies that for any given microstructure, and hence for any possible ζ_1, the Beran bounds lie inside the Hashin-Shtrikman bounds. Then, since the Hashin-Shtrikman bounds on σ_* are optimal, the union of the Beran bounds as ζ_1 ranges over all possible combinations must necessarily equal the Hashin-Shtrikman bounds.

We can carry the simplification that lead to (26.8) one (trivial) step further and define the new "effective constant"

$$\sigma_*^{(1)} = y_\sigma/2,$$

in terms of which the bounds reduce to

$$(\zeta_1/\sigma_1 + \zeta_2/\sigma_2)^{-1} \le \sigma_*^{(1)} \le \zeta_1\sigma_1 + \zeta_2\sigma_2.$$

So we see that this new "effective constant" satisfies harmonic and arithmetic mean bounds with the nonnegative parameters ζ_1 and $\zeta_2 = 1 - \zeta_1$ now playing the role of the volume fractions f_1 and $f_2 = 1 - f_1$.

26.3. Three-point bounds on the elastic moduli of a two-phase mixture

The same sort of analysis can be applied to bounding the effective bulk modulus κ_* and effective shear modulus μ_* of a three-dimensional, elastically isotropic composite of two isotropic elastic phases with bulk moduli κ_1 and κ_2 and shear moduli μ_1 and μ_2. The third-order bounds on κ_* and μ_* (Beran and Molyneux 1966; Milton and Phan-Thien 1982) when expressed in terms of the y-parameters

$$\begin{aligned} y_\kappa &= -f_2\kappa_1 - f_1\kappa_2 + \frac{f_1 f_2(\kappa_1 - \kappa_2)^2}{f_1\kappa_1 + f_1\kappa_1 - \kappa_*}, \\ y_\mu &= -f_2\mu_1 - f_1\mu_2 + \frac{f_1 f_2(\mu_1 - \mu_2)^2}{f_1\mu_1 + f_1\mu_1 - \mu_*}, \end{aligned} \tag{26.9}$$

reduce to

$$\begin{gathered} 4/3\langle\mu^{-1}\rangle_\zeta \le y_\kappa \le 4\langle\mu\rangle_\zeta/3, \\ \frac{\langle 128/\kappa + 99/\mu\rangle_\zeta + \langle 45/\mu\rangle_\eta}{\langle 30/\mu\rangle_\zeta\langle 6/\kappa - 1/\mu\rangle_\zeta + \langle 6/\mu\rangle_\eta\langle 2/\kappa + 21/\mu\rangle_\zeta} \le y_\mu \le \frac{3\langle\mu\rangle_\eta\langle 6\kappa + 7\mu\rangle_\zeta - 5\langle\mu\rangle_\zeta^2}{6\langle 2\kappa - \mu\rangle_\zeta + 30\langle\mu\rangle_\eta}, \end{gathered} \tag{26.10}$$

where for any quantity h taking values h_1 in phase 1 and h_2 in phase 2 we define

$$\langle h\rangle_\zeta = \zeta_1 h_1 + \zeta_2 h_2, \quad \langle h\rangle_\eta = \eta_1 h_1 + \eta_2 h_2,$$

in which $\zeta_1 = 1 - \zeta_2$ and $\eta_1 = \eta_2 - 1$ are the geometric parameters defined by (15.31) and (15.36). The McCoy (1970) bounds on μ_* can also be expressed in terms of ζ_1 and η_1 but are not quite as tight as the bounds (26.10).

The bounds of Beran and Molyneux and McCoy were compared with experimental measurements of the effective bulk and shear moduli by Corson (1974a). Davis (1991) and Davis, Chen, and Thorpe (1992) used the bounds of Beran and Molyneux and Milton and Phan-Thien [together with the results of Torquato and Lado (1986) and Sen, Lado, and Torquato (1987)

for ζ_1 and η_1] to compute third-order bounds on the effective Young's modulus of a suspension of hard spheres, which they compared with experimental results. They also compared the Beran and Molyneux bounds with finite-element calculations for the effective bulk modulus of cubic and face-centered cubic arrays of spheres. Roberts and Garboczi (1999) compared the third-order effective Young's modulus bounds with numerical simulations of media defined by the level cut, or level cuts, of a Gaussian random field. In all cases the agreement was good. Many of the papers referred to in section 15.6 on page 327 that evaluate ζ_1 and η_1 for various microstructures also give graphs of the third-order elasticity bounds for particular choices of moduli.

The bounds on y_κ coincide when ζ_1 equals one or zero, giving $y_\kappa = 4\mu_1/3$ and $y_\kappa = 4\mu_2/3$, respectively. These values of y_κ correspond to the Hashin-Shtrikman-Hill bounds (23.42) and (23.45) on κ_*. Thus any microgeometry (such as the coated sphere assemblage) that attains the Hashin-Shtrikman conductivity bounds for some positive conductivity ratio $\sigma_1/\sigma_2 \neq 1$ necessarily attains the Hashin-Shtrikman-Hill bulk modulus bounds because the microgeometry must be such that ζ_1 equals one or zero. In other words, an isotropic two-phase microgeometry with an extremal effective conductivity necessarily has an extremal effective bulk modulus. This result is also implied by the results of section 24.14 on page 522 bounding the possible (y_κ, y_σ) pairs. An alternative proof was given by Grabovsky (1996); see section 25.6 on page 542.

The bounds on y_μ coincide when the geometric parameter pair (ζ_1, η_1) equals $(1, 1)$, $(0, 0)$, $(1, 5/21)$, and $(0, 16/21)$, giving

$$y_\mu = \frac{\mu_1(9\kappa_1 + 8\mu_1)}{6(\kappa_1 + 2\mu_1)}, \quad y_\mu = \frac{\mu_2(9\kappa_2 + 8\mu_2)}{6(\kappa_2 + 2\mu_2)},$$
$$y_\mu = \frac{8\mu_2(6\kappa_1 + 7\mu_1) + 15\mu_1\kappa_1}{2(21\kappa_1 + 2\mu_1 + 40\mu_2)}, \quad y_\mu = \frac{8\mu_1(6\kappa_2 + 7\mu_2) + 15\mu_2\kappa_2}{2(21\kappa_2 + 2\mu_2 + 40\mu_1)}.$$

The first pair of these expressions corresponds to the Hashin-Shtrikman bounds (23.42) and (23.45) on the shear modulus μ_* and are attained by sequentially laminated microstructures. It is not known what significance (if any) can be attributed to the second pair of formulas.

The two-dimensional bounds analogous to (26.10) (Silnutzer 1972; Milton 1982; Kublanov and Milton 1991) are given by the formulas

$$1/\langle \mu^{-1} \rangle_\zeta \leq y_\kappa \leq \langle \mu \rangle_\zeta / 3$$
$$[2\langle 1/\kappa \rangle_\zeta + \langle 1/\mu \rangle_\eta]^{-1} \leq y_\mu \leq [2/\langle \kappa \rangle_\zeta + 1/\langle \mu \rangle_\eta]^{-1}, \tag{26.11}$$

in which y_κ and y_μ are defined in terms of the two-dimensional effective bulk and shear moduli κ_* and μ_* via (26.10), and the two-dimensional geometric parameters $\zeta_1 = 1 - \zeta_2$ and $\eta_1 = \eta_2 - 1$ are defined by (15.41). Eischen and Torquato (1993) computed the bounds on the bulk and shear moduli for hexagonal arrays of circular inclusions and found that the bounds agreed well with their numerical simulations of the effective moduli. Again, many of the papers referred to in section 15.6 on page 327 that evaluate ζ_1 and η_1 for various two-dimensional microstructures also give graphs of the third-order elasticity bounds for particular choices of moduli.

26.4. Correlation function independent elasticity bounds: Improving the Hashin-Shtrikman-Hill-Walpole bounds

We saw in the last section how the Hashin-Shtrikman bounds on σ_* could be recovered from the Beran bounds. Applying a similar procedure to the third-order bounds on the bulk

and shear moduli gives bounds that equal or improve on the Hashin-Shtrikman-Hill-Walpole bounds on κ_* and μ_*. One recovers the Hashin-Shtrikman-Hill bounds on the effective bulk modulus by taking the union of the third-order bounds on y_κ as ζ_1 varies between zero and one. To apply a similar procedure to the third-order bounds (26.10) on y_μ requires some knowledge of the possible (ζ_1, η_1) pairs. To obtain this information we use the fact that the third-order lower bound on y_μ must not be greater than the upper bound. In particular, the denominators in the upper and lower bounds,

$$\begin{aligned} 6\langle 2\kappa - \mu\rangle_\zeta + 30\langle\mu\rangle_\eta &= 12\langle\kappa\rangle_\zeta + 6(5\langle\mu\rangle_\eta - \langle\mu\rangle_\zeta), \\ \langle 30/\mu\rangle_\zeta\langle 6/\kappa - 1/\mu\rangle_\zeta &+ \langle 6/\mu\rangle_\eta\langle 2/\kappa + 21/\mu\rangle_\zeta \\ &= \langle 6/\kappa\rangle_\zeta(\langle 2/\mu\rangle_\eta + \langle 30/\mu\rangle_\zeta) + \langle 6/\mu\rangle_\zeta(\langle 21/\mu\rangle_\eta - \langle 5/\mu\rangle_\zeta) \end{aligned}$$

must not change sign as the bulk and shear moduli of the phases range over all positive finite values. By considering the limits where κ_1 and κ_2 are small or large we see that $5\langle\mu\rangle_\eta - \langle\mu\rangle_\zeta$ and $\langle 21/\mu\rangle_\eta - \langle 5/\mu\rangle_\zeta$ must be nonnegative for all positive finite values of μ_1 and μ_2, implying (Milton and Phan-Thien 1982) that the geometric parameter $\eta_1 = 1 - \eta_2$ must always be such that

$$5\zeta_1/21 \le \eta_1 \le 1 - 5\zeta_2/21.$$

Let us assume that the phases have been labeled so that $\mu_1 \ge \mu_2$. Then by letting η_1 range between these limits and $\zeta_1 = 1 - \zeta_2$ range between zero and one, we obtain the correlation function independent lower bound

$$y_\mu \ge \min_{\substack{\zeta_1 \\ 0 \le \zeta_1 \le 1}} \frac{8\langle 6/\mu + 7/\kappa\rangle_\zeta + 15/\mu_2}{2(\langle 21/\mu + 2/\kappa\rangle_\zeta/\mu_2 + 40\langle 1/\mu\rangle_\zeta\langle 1/\kappa\rangle_\zeta)}, \tag{26.12}$$

and the correlation function independent upper bound

$$y_\mu \le \max_{\substack{\zeta_1 \\ 0 \le \zeta_1 \le 1}} \frac{8\mu_1\langle 6\kappa + 7\mu\rangle_\zeta + 15\langle\mu\rangle_\zeta\langle\kappa\rangle_\zeta}{2(\langle 21\kappa + 2\mu\rangle_\zeta + 40\mu_1)} \tag{26.13}$$

of Milton and Phan-Thien (1982). When

$$\kappa_1 - \kappa_2 \ge -\frac{(3\kappa_2 + 8\mu_2)^2}{42\kappa_2^2}\frac{\kappa_1\kappa_2}{\mu_1\mu_2}(\mu_1 - \mu_2) \tag{26.14}$$

the minimum over ζ_1 in the lower bound is attained at the extreme limit $\zeta_1 = 0$ and the bound reduces to

$$y_\mu \ge \frac{\mu_2(9\kappa_2 + 8\mu_2)}{6(\kappa_2 + 2\mu_2)},$$

which is equivalent to the lower Hashin-Shtrikman bound (23.42) on the effective shear modulus μ_*. When

$$\kappa_1 - \kappa_2 \ge -\frac{(3\kappa_1 + 8\mu_1)^2}{42\mu_1^2}(\mu_1 - \mu_2) \tag{26.15}$$

the minimum over ζ_1 in the upper bound is attained at the extreme limit $\zeta_1 = 1$ and the bound reduces to

$$y_\mu \le \frac{\mu_1(9\kappa_1 + 8\mu_1)}{6(\kappa_1 + 2\mu_1)},$$

which is equivalent to the upper Hashin-Shtrikman bound (23.45) on the effective shear modulus μ_*.

In other words, the Hashin-Shtrikman bounds on the effective shear modulus μ_* are valid not only when $\kappa_1 - \kappa_2$ is positive but more generally when the inequalities (26.14) and (26.15) are satisfied. When these conditions are not satisfied the bounds (26.12) and (26.13) are always more restrictive than the well-known bounds (23.50) of Walpole:

$$\frac{\mu_2(9\kappa_1 + 8\mu_2)}{6(\kappa_1 + 2\mu_2)} \le y_\mu \le \frac{\mu_1(9\kappa_2 + 8\mu_1)}{6(\kappa_2 + 2\mu_1)},$$

which apply when $\kappa_1 - \kappa_2$ is negative.

If we know the effective bulk modulus κ_* and $\mu_1 \ne \mu_2$, then we obtain bounds on ζ_1,

$$\zeta_1^+(y_\kappa) \equiv \frac{3y_\kappa/4 - \mu_2}{\mu_1 - \mu_2} \ge \zeta_1 \ge \frac{1/\mu_2 - 4/3y_\kappa}{1/\mu_2 - \mu_1} \equiv \zeta_1^-(y_\kappa),$$

which in turn give improved correlation function independent bounds on the effective shear modulus μ_*:

$$y_\mu \ge \min_{\zeta_1^-(y_\kappa) \le \zeta_1 \le \zeta_1^+(y_\kappa)} \frac{8\langle 6/\mu + 7/\kappa\rangle_\zeta + 15/\mu_2}{2(\langle 21/\mu + 2/\kappa\rangle_\zeta(1/\mu_2) + 40\langle 1/\mu\rangle_\zeta\langle 1/\kappa\rangle_\zeta)},$$

$$y_\mu \le \max_{\zeta_1^-(y_\kappa) \le \zeta_1 \le \zeta_1^+(y_\kappa)} \frac{8\mu_1\langle 6\kappa + 7\mu\rangle_\zeta + 15\langle\mu\rangle_\zeta\langle\kappa\rangle_\zeta}{2(\langle 21\kappa + 2\mu\rangle_\zeta + 40\mu_1)}.$$

Whereas the Hashin-Shtrikman-Hill-Walpole bounds confine (κ_*, μ_*) to lie inside a rectangular box in the (bulk modulus, shear modulus)-plane, these bounds (Berryman and Milton 1988) confine (κ_*, μ_*) to lie within a smaller region within the box. The bounds, while they are currently the best available three-dimensional bounds, are unlikely to be optimal. The analogous two-dimensional bounds are not as tight as the bounds of Cherkaev and Gibiansky (1993), which were derived using the translation method.

26.5. Using the translation method to improve the third-order bounds

The basic bounds (24.4) of the translation method are obtained by applying the harmonic mean bounds to the effective tensor of the translated medium. Of course we can equally well apply other bounds to the effective tensor of the translated medium. As an example, let us follow Gibiansky and Torquato (1995a) and consider a two-dimensional, two-phase elastic composite. We apply the third-order bulk modulus bounds to the translated medium with moduli

$$1/\kappa_1' = 1/\kappa_1 - 2c, \quad 1/\kappa_2' = 1/\kappa_2 - 2c, \quad 1/\kappa_*' = 1/\kappa_* - 2c,$$
$$1/\mu_1' = 1/\mu_1 + 2c, \quad 1/\mu_2' = 1/\mu_2 + 2c, \quad 1/\mu_*' = 1/\mu_* + 2c.$$

By rewriting the relation (26.9) between y_κ and κ_* in the equivalent form

$$1/y_\kappa = -f_2/\kappa_1 - f_1/\kappa_2 + \frac{f_1 f_2(1/\kappa_1 - 1/\kappa_2)^2}{f_1/\kappa_1 + f_1/\kappa_1 - 1/\kappa_*},$$

we see that the translated medium has a bulk y-parameter y'_κ given by

$$1/y'_\kappa = 1/y_\kappa + 2c.$$

The third-order lower bound on y'_κ does not yield any new information, however, the third-order upper bound (26.11) applied to y'_κ implies that

$$1/y_\kappa \geq [\zeta_1/(1/\mu_1 + 2c) + \zeta_2/(1/\mu_2 + 2c)]^{-1} - 2c.$$

This inequality holds for all c such that the moduli of the translated medium are nonnegative. In particular, by taking the limit as $2c$ approaches $1/\kappa_{\max}$, where $\kappa_{\max}$ is the maximum of κ_1 and κ_2, we obtain the bound

$$1/y_\kappa \geq [\zeta_1/(1/\mu_1 + 1/\kappa_{\max}) + \zeta_2/(1/\mu_2 + 1/\kappa_{\max})]^{-1} - 1/\kappa_{\max}$$

of Gibiansky and Torquato (1995a), which improves on the upper bound on y_κ in (26.11). They also improve on the upper bound on y_μ, using a similar approach.

26.6. Third-order bounds from cross-property bounds

Since the parameter ζ_1 arises in the third-order series expansion of σ_* in powers of $\sigma_1 - \sigma_2$, one can consider knowing ζ_1 to be virtually equivalent to knowing the value of σ_* when $\sigma_1 - \sigma_2$ is sufficiently small. (Here we assume that the volume fraction f_1 is given.) Following Gibiansky and Torquato (1995a) this suggests that the third-order bounds correlating the bulk y-parameter y_κ and the parameter ζ_1 could be obtained from the cross-property bounds described in section 24.14 on page 522, which correlate the bulk y-parameter y_κ with the conductivity y-parameter y_σ. These bounds were expressed by introducing Hyp$[(w_1, w_2)]$, the hyperbolic segment in the (y_1, y_2)-plane joining $(4\mu_1/3,\ 2\sigma_1)$ and $(4\mu_2/3,\ 2\sigma_2)$, which when extended passes through the point (w_1, w_2). When $\sigma_1 - \sigma_2$ is small, Hyp$[(w_1, w_2)]$ becomes insensitive to the value of w_2, and to the first order in $\sigma_1 - \sigma_2$ can be described parametrically by the equations

$$y_1 = 4[\gamma\mu_1 + (1-\gamma)\mu_2]/3 - \frac{16\gamma(1-\gamma)(\mu_1 - \mu_2)^2}{12[\gamma\mu_2 + (1-\gamma)\mu_1] - 9w_1}, \quad y_2 = 2[\gamma\sigma_1 + (1-\gamma)\sigma_2],$$

with γ running from zero to one.

The bounds confine the point (y_κ, y_σ) to lie between the outermost of the curves obtained by setting w_1 equal to 0, $-\kappa_1$, $-\kappa_2$, and $-\infty$. Since y_1 increases monotonically as w_1 is increased from $-\infty$ to zero, the bounds are obtained by setting w_1 equal to the extreme values, $-\infty$ and zero, at which

$$y_1 = 4[\gamma\mu_1 + (1-\gamma)\mu_2]/3, \ \text{ and } \ y_1 = 4[\gamma/\mu_1 + (1-\gamma)/\mu_2]^{-1}/3,$$

respectively. Also, when $\sigma_1 - \sigma_2$ is small, we have $y_\sigma \approx 2[\zeta_1\sigma_1 + \zeta_1\sigma_2]$. Therefore, y_2 equals y_σ to the first order in $\sigma_1 - \sigma_2$ when $\gamma = \zeta_1$. Thus in the limit as $\sigma_1 - \sigma_2$ approaches zero the cross-property bounds imply the third-order bounds

$$4[\zeta_1/\mu_1 + \zeta_2/\mu_2]^{-1}/3 \leq y_\kappa \leq 4[\zeta_1\mu_1 + \zeta_2\mu_2]/3,$$

in agreement with (26.10). Gibiansky and Torquato (1995a) used this idea to obtain improved lower ζ_1-dependent bounds on the two-dimensional effective shear modulus μ_*. They utilized the bounds of Gibiansky and Torquato (1995b) coupling μ_* with the effective conductivity σ_*.

26.7. General third-order bounds for a two-phase composite

Let us consider a two-phase composite where the tensor field $\boldsymbol{L}(\boldsymbol{x})$ takes the form

$$\boldsymbol{L}(\boldsymbol{x}) = \boldsymbol{L}_1\chi_1(\boldsymbol{x}) + \boldsymbol{L}_2\chi_2(\boldsymbol{x}), \tag{26.16}$$

in which $\chi_1(\boldsymbol{x}) = 1 - \chi_2(\boldsymbol{x})$ is the characteristic function representing the geometry of phase 1, and the tensors $\boldsymbol{L}_1$ and $\boldsymbol{L}_2$ representing the moduli of the two phases are assumed to be self-adjoint and positive-semidefinite. Motivated by the series expansion (14.5), a suitable choice of trial field is

$$\underline{\boldsymbol{E}} = \boldsymbol{E}_0 + \boldsymbol{\Gamma}\chi_1\boldsymbol{V}, \quad \text{where } \boldsymbol{V} \in \mathcal{U},$$

which clearly satisfies the requirement that it lies in the subspace $\mathcal{U} \oplus \mathcal{E}$ for all self-adjoint choices of the reference medium $\boldsymbol{L}_0$: We only need to ensure that $\boldsymbol{\Gamma}\chi_1\boldsymbol{V}$ exists and do not even need to require that $\boldsymbol{L}_0$ be positive-semidefinite on $\mathcal{E}$. (Taking a trial field such that $\underline{\boldsymbol{E}} - \boldsymbol{E}_0$ lies in the subspace spanned by $\boldsymbol{\Gamma}\chi_1\boldsymbol{V}$ as $\boldsymbol{L}_0$ varies would presumably lead to even tighter bounds.) Substituting the trial field into the variational principle (13.10), optimizing over $\boldsymbol{V}$, and noting that the inequality holds for all choices of $\boldsymbol{E}_0$ gives the bound

$$\boldsymbol{L}_* \le \langle \boldsymbol{L} \rangle - (\boldsymbol{L}_1 - \boldsymbol{L}_2)\boldsymbol{\Gamma}_0\chi_1\boldsymbol{\Gamma}\chi_1\boldsymbol{\Gamma}_0(\boldsymbol{\Gamma}_0\chi_1\boldsymbol{\Gamma}\boldsymbol{L}\boldsymbol{\Gamma}\chi_1\boldsymbol{\Gamma}_0)^{-1}\boldsymbol{\Gamma}_0\chi_1\boldsymbol{\Gamma}\chi_1\boldsymbol{\Gamma}_0(\boldsymbol{L}_1 - \boldsymbol{L}_2), \tag{26.17}$$

in which the inverse is to be taken on the subspace $\mathcal{U}$.

For random, statistically homogeneous media the quantities appearing in this bound can be expressed in terms of correlation functions. The procedure is basically the same as that used in section 15.5 on page 323 to express in terms of correlation functions the quantities $\delta\boldsymbol{L}_*^{(2)}$ and $\delta\boldsymbol{L}_*^{(3)}$ entering the series expansions. From (15.22) we see that

$$\boldsymbol{\Gamma}_0\chi_1\boldsymbol{\Gamma}\chi_1\boldsymbol{\Gamma}_0 = f_1 f_2 \boldsymbol{U}, \tag{26.18}$$

where $\boldsymbol{U}$ is the positive-semidefinite matrix

$$\boldsymbol{U} \equiv \boldsymbol{\gamma} + \frac{1}{f_1 f_2}\int_{|\boldsymbol{\eta}|=1} \breve{f}_{11}(\boldsymbol{\eta})\boldsymbol{\Gamma}_\infty(\boldsymbol{\eta}), \tag{26.19}$$

and by analogy with (15.21) we see that

$$\begin{aligned}
\boldsymbol{\Gamma}_0\chi_1\boldsymbol{\Gamma}\boldsymbol{L}\boldsymbol{\Gamma}\chi_1\boldsymbol{\Gamma}_0 &= \boldsymbol{\Gamma}_0\chi_1\boldsymbol{\Gamma}\boldsymbol{L}_1\chi_1\boldsymbol{\Gamma}\chi_1\boldsymbol{\Gamma}_0 + \boldsymbol{\Gamma}_0\chi_1\boldsymbol{\Gamma}\boldsymbol{L}_2\chi_2\boldsymbol{\Gamma}\chi_1\boldsymbol{\Gamma}_0 \\
&= f_1 f_2 \boldsymbol{\gamma}(f_2\boldsymbol{L}_1 + f_1\boldsymbol{L}_2)\boldsymbol{\gamma} + \boldsymbol{\gamma}(f_2\boldsymbol{L}_1 + f_1\boldsymbol{L}_2)\int_{|\boldsymbol{\eta}|=1} \boldsymbol{\Gamma}_\infty(\boldsymbol{\eta})\breve{f}_{11}(\boldsymbol{\eta}) \\
&\quad + \int_{|\boldsymbol{\eta}|=1} \boldsymbol{\Gamma}_\infty(\boldsymbol{\eta})\breve{f}_{11}(\boldsymbol{\eta})(f_2\boldsymbol{L}_1 + f_1\boldsymbol{L}_2)\boldsymbol{\gamma} \\
&\quad + \int_{|\boldsymbol{\eta}_2|=1}\int_{|\boldsymbol{\eta}_1|=1} \boldsymbol{\Gamma}_\infty(\boldsymbol{\eta}_1)[\boldsymbol{L}_1\breve{f}_{111}(\boldsymbol{\eta}_1,\boldsymbol{\eta}_2) + \boldsymbol{L}_2\breve{f}_{222}(\boldsymbol{\eta}_1,\boldsymbol{\eta}_2)]\boldsymbol{\Gamma}_\infty(\boldsymbol{\eta}_2),
\end{aligned} \tag{26.20}$$

in which $\breve{f}_{11}(\boldsymbol{\eta})$ and $\breve{f}_{111}(\boldsymbol{\eta}_1,\boldsymbol{\eta}_2)$ are the first- and second-order reduced correlation functions associated with $\chi_1(\boldsymbol{x})$ while $\breve{f}_{222}(\boldsymbol{\eta}_1,\boldsymbol{\eta}_2)$ is the third-order reduced correlation functions associated with $\chi_2(\boldsymbol{x})$.

Upon noticing that

$$f_1 f_2 \boldsymbol{U}(f_2\boldsymbol{L}_1 + f_1\boldsymbol{L}_2)\boldsymbol{U} = f_1 f_2 \boldsymbol{\gamma}(f_2\boldsymbol{L}_1 + f_1\boldsymbol{L}_2)\boldsymbol{\gamma}$$
$$+ \boldsymbol{\gamma}(f_2\boldsymbol{L}_1 + f_1\boldsymbol{L}_2)\int_{|\boldsymbol{\eta}|=1} \boldsymbol{\Gamma}_\infty(\boldsymbol{\eta})\breve{f}_{11}(\boldsymbol{\eta}) + \int_{|\boldsymbol{\eta}|=1} \boldsymbol{\Gamma}_\infty(\boldsymbol{\eta})\breve{f}_{11}(\boldsymbol{\eta})(f_2\boldsymbol{L}_1 + f_1\boldsymbol{L}_2)\boldsymbol{\gamma}$$
$$- \int_{|\boldsymbol{\eta}_2|=1}\int_{|\boldsymbol{\eta}_1|=1} \boldsymbol{\Gamma}_\infty(\boldsymbol{\eta}_1)(\boldsymbol{L}_1/f_1 + \boldsymbol{L}_2/f_2)\boldsymbol{\Gamma}_\infty(\boldsymbol{\eta}_2)\breve{f}_{11}(\boldsymbol{\eta}_1)\breve{f}_{11}(\boldsymbol{\eta}_2), \tag{26.21}$$

we see that the bound (26.17) reduces to

$$\boldsymbol{L}_* \le f_1\boldsymbol{L}_1 + f_2\boldsymbol{L}_2 - f_1 f_2(\boldsymbol{L}_1 - \boldsymbol{L}_2)[f_2\boldsymbol{L}_1 + f_1\boldsymbol{L}_2 + \boldsymbol{D}_1\boldsymbol{L}_1 + \boldsymbol{D}_2\boldsymbol{L}_2]^{-1}(\boldsymbol{L}_1 - \boldsymbol{L}_2), \tag{26.22}$$

in which $\boldsymbol{D}_1$ and $\boldsymbol{D}_2$ are higher order tensors: $\boldsymbol{D}_i$ acts linearly on $\boldsymbol{L}_i$ to produce the matrix

$$\boldsymbol{D}_i\boldsymbol{L}_i = \frac{1}{f_1 f_2}\boldsymbol{U}^{-1}\left\{\int_{|\boldsymbol{\eta}_2|=1}\int_{|\boldsymbol{\eta}_1|=1} \boldsymbol{\Gamma}_\infty(\boldsymbol{\eta}_1)\boldsymbol{L}_i\boldsymbol{\Gamma}_\infty(\boldsymbol{\eta}_2)\left[\breve{f}_{iii}(\boldsymbol{\eta}_1,\boldsymbol{\eta}_2) - \frac{\breve{f}_{ii}(\boldsymbol{\eta}_1)\breve{f}_{ii}(\boldsymbol{\eta}_2)}{f_i}\right]\right\}\boldsymbol{U}^{-1}, \tag{26.23}$$

where we have assumed for simplicity that the matrix $\boldsymbol{U}$, given by (26.19), has a well-defined inverse. To obtain (26.23) we have used the identity $\breve{f}_{11}(\boldsymbol{\eta}) = \breve{f}_{22}(-\boldsymbol{\eta})$.

To obtain a lower bound on the effective tensor $\boldsymbol{L}_*$ we can apply the duality principle, making the replacements

$$\boldsymbol{L}_* \to \boldsymbol{L}_*^{-1}, \quad \boldsymbol{L}_i \to \boldsymbol{L}_i^{-1}, \quad \boldsymbol{\gamma} \to \boldsymbol{L}_0 - \boldsymbol{L}_0\boldsymbol{\gamma}\boldsymbol{L}_0, \quad \boldsymbol{\Gamma}_\infty(\boldsymbol{y}) \to -\boldsymbol{L}_0\boldsymbol{\Gamma}_\infty(\boldsymbol{y})\boldsymbol{L}_0,$$

in (26.22) and (26.19) to obtain the bound

$$\boldsymbol{L}_*^{-1} \le f_1\boldsymbol{L}_1^{-1} + f_2\boldsymbol{L}_2^{-1}$$
$$- f_1 f_2(\boldsymbol{L}_1^{-1} - \boldsymbol{L}_2^{-1})[f_2\boldsymbol{L}_1^{-1} + f_1\boldsymbol{L}_2^{-1} + \boldsymbol{D}_1'\boldsymbol{L}_1^{-1} + \boldsymbol{D}_2'\boldsymbol{L}_2^{-1}]^{-1}(\boldsymbol{L}_1^{-1} - \boldsymbol{L}_2^{-1}),$$

in which $\boldsymbol{D}_1'$ and $\boldsymbol{D}_2'$ are higher order tensors: $\boldsymbol{D}_i'$ acts linearly on $\boldsymbol{L}_i^{-1}$ to produce the matrix

$$\boldsymbol{D}_i'\boldsymbol{L}_i^{-1} = \frac{1}{f_1 f_2}(\boldsymbol{L}_0 - \boldsymbol{L}_0\boldsymbol{U}\boldsymbol{L}_0)^{-1}\left\{\int_{|\boldsymbol{\eta}_2|=1}\int_{|\boldsymbol{\eta}_1|=1} \boldsymbol{L}_0\boldsymbol{\Gamma}_\infty(\boldsymbol{\eta}_1)\boldsymbol{L}_0\boldsymbol{L}_i^{-1}\boldsymbol{L}_0\boldsymbol{\Gamma}_\infty(\boldsymbol{\eta}_2)\boldsymbol{L}_0\right.$$
$$\left.\times\left[\breve{f}_{iii}(\boldsymbol{\eta}_1,\boldsymbol{\eta}_2) - \frac{\breve{f}_{ii}(\boldsymbol{\eta}_1)\breve{f}_{ii}(\boldsymbol{\eta}_2)}{f_i}\right]\right\}(\boldsymbol{L}_0 - \boldsymbol{L}_0\boldsymbol{U}\boldsymbol{L}_0)^{-1},$$

where we have assumed that the tensor $\boldsymbol{L}_0 - \boldsymbol{L}_0\boldsymbol{U}\boldsymbol{L}_0$ is nonsingular.

By recalling the relations (19.2) and (19.4) between the effective tensor $\boldsymbol{L}_*$ and the Y-tensor $\boldsymbol{Y}_*$ we see that the third-order bounds on $\boldsymbol{L}_*$ are equivalent to the bounds

$$\boldsymbol{Y}_* \le \boldsymbol{D}_1\boldsymbol{L}_1 + \boldsymbol{D}_2\boldsymbol{L}_2, \quad \boldsymbol{Y}_*^{-1} \le \boldsymbol{D}_1'\boldsymbol{L}_1^{-1} + \boldsymbol{D}_2'\boldsymbol{L}_2^{-1}$$

on $\boldsymbol{Y}_*$. Now (19.12) implies that the Y-tensor $\boldsymbol{Y}_*$ is positive-semidefinite. This allows us to rewrite the bounds on $\boldsymbol{Y}_*$ in the form

$$(\boldsymbol{D}_1'\boldsymbol{L}_1^{-1} + \boldsymbol{D}_2'\boldsymbol{L}_2^{-1})^{-1} \le \boldsymbol{Y}_* \le \boldsymbol{D}_1\boldsymbol{L}_1 + \boldsymbol{D}_2\boldsymbol{L}_2. \tag{26.24}$$

26.8. Third-order bounds for two-phase composites with geometrical isotropy

In a composite with geometrical isotropy all correlation functions associated with the characteristic functions $\chi_1(\boldsymbol{x})$ and $\chi_2(\boldsymbol{x})$ are rotationally invariant, and as we have seen in section 15.6 on page 327 it follows that

$$\breve{f}_{11}(\boldsymbol{\eta}) = \breve{f}_{22}(\boldsymbol{\eta}) = 0, \quad \breve{f}_{111}(\boldsymbol{\eta}_1, \boldsymbol{\eta}_2) = \breve{f}_{111}(u), \quad \breve{f}_{222}(\boldsymbol{\eta}_1, \boldsymbol{\eta}_2) = \breve{f}_{222}(u),$$

where $u = -\boldsymbol{\eta}_1 \cdot \boldsymbol{\eta}_2$. Consequently, the matrix $\boldsymbol{U}$ defined by (26.19) can be identified with the matrix $\boldsymbol{\gamma}$ defined by (12.35). Let us first focus on obtaining bounds for the effective conductivity tensor $\boldsymbol{\sigma}_*$ of a geometrically isotropic two-phase material. For simplicity, let us take an isotropic reference medium with conductivity tensor $\boldsymbol{\sigma}_0 = \sigma_0 \boldsymbol{I}$. Then $\boldsymbol{\gamma} = \boldsymbol{I}/(3\sigma_0)$ and from (15.26), (15.28), and (15.29) we see that

$$\int_{|\boldsymbol{\eta}_2|=1} \int_{|\boldsymbol{\eta}_1|=1} \boldsymbol{\Gamma}_\infty(\boldsymbol{\eta}_1)\boldsymbol{\sigma}_i\boldsymbol{\Gamma}_\infty(\boldsymbol{\eta}_2)\Big[\breve{f}_{iii}(\boldsymbol{\eta}_1, \boldsymbol{\eta}_2) - \frac{\breve{f}_{ii}(\boldsymbol{\eta}_1)\breve{f}_{ii}(\boldsymbol{\eta}_2)}{f_i}\Big] = \frac{f_1 f_2 \zeta_i[\boldsymbol{\sigma}_i + 3\boldsymbol{I}\,\mathrm{Tr}(\boldsymbol{\sigma}_i)]}{45\sigma_0^2},$$

in which ζ_1 is the familiar geometric parameter defined by (15.31). This implies that

$$\boldsymbol{D}_i\boldsymbol{\sigma}_i = \zeta_i[\boldsymbol{\sigma}_i + 3\boldsymbol{I}\,\mathrm{Tr}(\boldsymbol{\sigma}_i)]/5, \quad \boldsymbol{D}_i'\boldsymbol{\sigma}_i = \zeta_i[\boldsymbol{\sigma}_i^{-1} + 3\boldsymbol{I}\,\mathrm{Tr}(\boldsymbol{\sigma}_i^{-1})]/20.$$

So from (26.24) we see that the Y-tensor

$$\boldsymbol{Y}_* = -f_2\boldsymbol{\sigma}_1 - f_1\boldsymbol{\sigma}_2 + f_1 f_2(\boldsymbol{\sigma}_1 - \boldsymbol{\sigma}_2)[f_1\boldsymbol{\sigma}_1 + f_2\boldsymbol{\sigma}_2 - \boldsymbol{\sigma}_*]^{-1}(\boldsymbol{\sigma}_1 - \boldsymbol{\sigma}_2)$$

satisfies the bounds

$$\begin{aligned} \boldsymbol{Y}_* &\geq 20[\zeta_1\boldsymbol{\sigma}_1^{-1} + \zeta_2\boldsymbol{\sigma}_2^{-1} + 3\boldsymbol{I}\,\mathrm{Tr}(\zeta_1\boldsymbol{\sigma}_1^{-1} + \zeta_2\boldsymbol{\sigma}_2^{-1})]^{-1}, \\ \boldsymbol{Y}_* &\leq [\zeta_1\boldsymbol{\sigma}_1 + \zeta_2\boldsymbol{\sigma}_2 + 3\boldsymbol{I}\,\mathrm{Tr}(\zeta_1\boldsymbol{\sigma}_1 + \zeta_2\boldsymbol{\sigma}_2)]/5. \end{aligned}$$

In particular, when the two phases are isotropic, with $\boldsymbol{\sigma}_1 = \sigma_1\boldsymbol{I}$ and $\boldsymbol{\sigma}_2 = \sigma_2\boldsymbol{I}$, these inequalities reduce to the Beran bounds (26.8).

References

Avellaneda, M., A. V. Cherkaev, K. A. Lurie, and G. W. Milton 1988. On the effective conductivity of polycrystals and a three-dimensional phase-interchange inequality. *Journal of Applied Physics* 63(10):4989–5003. {*120, 139, 439, 441, 450, 452, 512, 525, 538, 550, 555, 564*}

Beran, M. J. 1965. Use of the variational approach to determine bounds for the effective permittivity in random media. *Nuovo Cimento* 38:771–782. {*553, 564, 574, 577, 597*}

Beran, M. J. and J. Molyneux 1966. Use of classical variational principles to determine bounds for the effective bulk modulus in heterogeneous media. *Quarterly of Applied Mathematics* 24:107–118. {*553, 557, 564, 589, 597*}

Beran, M. J. and N. R. Silnutzer 1971. Effective electrical, thermal, and magnetic properties of fiber reinforced materials. *Journal of Composite Materials* 5:246–249. {*332, 336, 553, 564*}

Berryman, J. G. 1982. Effective medium theory for elastic composites. In V. K. Varadan and V. V. Varadan (eds.), *Elastic Wave Scattering and Propagation: Based on Presentations made at a Special Session of the Midwestern Mechanics Conference Held at the University of Michigan, Ann Arbor, May 7–9, 1981*, pp. 111–129. Ann Arbor, Michigan: Ann Arbor Science. ISBN 0-250-40534-2. {*397, 399, 411, 556, 565*}

Berryman, J. G. and G. W. Milton 1988. Microgeometry of random composites and porous media. *Journal of Physics D: Applied Physics* 21:87–94. {*522, 525, 560, 565*}

Bonnecaze, R. T. and J. F. Brady 1991. The effective conductivity of random suspensions of spherical particles. *Proceedings of the Royal Society of London. Series A, Mathematical and Physical Sciences* 432:445–465. {*39, 41, 555, 565*}

Cherkaev, A. V. and L. V. Gibiansky 1993. Coupled estimates for the bulk and shear moduli of a two-dimensional isotropic elastic composite. *Journal of the Mechanics and Physics of Solids* 41(5):937–980. {*560, 565, 653, 668*}

Corson, P. B. 1974a. Correlation functions for predicting properties of heterogeneous materials. III Effective elastic moduli of two-phase solids. *Journal of Applied Physics* 45 (7):3171–3179. {*557, 565*}

Corson, P. B. 1974b. Correlation functions for predicting properties of heterogeneous materials. IV Effective thermal conductivity of two-phase solids. *Journal of Applied Physics* 45(7):3180–3182. {*555, 565*}

Davis, L. C. 1991. Third-order bounds on the elastic moduli of metal-matrix composites. *Metallurgical Transactions* 22A:3065–3068. {*557, 565*}

Davis, L. C., J. Chen, and M. F. Thorpe 1992. Predicting the elastic properties of composite materials. In *Proceedings of the American Society for Composites — Seventh Technical Conference, October 13–15, 1992, Keller Conference Center, University Park, Pennsylvania*, pp. 339–348. Lancaster, Pennsylvania: Technomic. ISBN 0-87762-997-8. {*557, 565*}

Dederichs, P. H. and R. Zeller 1973. Variational treatment of the elastic constants of disordered materials. *Zeitschrift für Physik* 259:103–116. {*291, 310, 553, 565*}

Eischen, J. W. and S. Torquato 1993. Determining elastic behavior of composites by the boundary element method. *Journal of Applied Physics* 74:159–170. {*39, 42, 558, 565*}

Elsayed, M. A. 1974. Bounds for the effective thermal, electrical, and magnetic properties of heterogeneous materials using high order statistical information. *Journal of Mathematical Physics* 15(11):2001–2015. {*322, 336, 553, 565*}

Elsayed, M. A. and J. J. McCoy 1973. Effect of fiber positioning on the effective physical properties of composite materials. *Journal of Composite Materials* 7:466–480. {*322, 336, 553, 565*}

Gibiansky, L. V. and S. Torquato 1995a. Geometrical-parameter bounds on the effective moduli of composites. *Journal of the Mechanics and Physics of Solids* 43(10):1587–1613. {*560, 561, 565*}

Gibiansky, L. V. and S. Torquato 1995b. Rigorous link between the conductivity and elastic moduli of fibre-reinforced composite materials. *Philosophical Transactions of the Royal Society of London Series A* 353:243–278. {*522, 526, 561, 565*}

Grabovsky, Y. 1996. Bounds and extremal microstructures for two-component composites: A unified treatment based on the translation method. *Proceedings of the Royal Society of London. Series A, Mathematical and Physical Sciences* 452(1947):919–944. {*466, 492, 541, 542, 550, 558, 566*}

Helte, A. 1994. Fourth-order bounds on the effective conductivity for a system of fully penetrable spheres. *Proceedings of the Royal Society of London. Series A, Mathematical and Physical Sciences* 445:247–256. {*319, 337, 554, 566*}

Helte, A. 1995, September 8. Fourth-order bounds on the effective bulk and shear moduli of random dispersions of penetrable spheres. *Proceedings of the Royal Society of London. Series A, Mathematical and Physical Sciences* 450(1940):651–665. {*554, 566*}

Kim, I. C. and S. Torquato 1991. Effective conductivity of suspensions of hard spheres by Brownian motion simulation. *Journal of Applied Physics* 69(4):2280–2289. {*40, 43, 555, 566*}

Kim, I. C. and S. Torquato 1992. Effective conductivity of suspensions of overlapping spheres. *Journal of Applied Physics* 71(6):2727–2735. {*40, 43, 554, 555, 566*}

Kröner, E. 1977. Bounds for the effective elastic moduli of disordered materials. *Journal of the Mechanics and Physics of Solids* 25:137–155. {*251, 268, 282, 287, 291, 311, 458, 493, 553, 566*}

Kublanov, L. and G. W. Milton 1991. Rigorous estimates for the elastic moduli for a two-dimensional two-phase material. Unpublished manuscript. {*558, 566*}

Markov, K. Z. and K. D. Zvyatkov 1991. Optimal third-order bounds on the effective properties of some composite media, and related problems. *Advances in Mechanics* 14(4): 3–46. {*553, 566*}

McCoy, J. J. 1970. On the displacement field in an elastic medium with random variations of material properties. In A. C. Eringen (ed.), *Proceedings of the Sixth Annual Meeting of the Society of Engineering Science, Held at Princeton University, Princeton, New Jersey, November 11–13, 1968*, pp. 235–254. Gordon and Breach: Gordon and Breach. ISBN 0-677-13780-X. {*553, 557, 566*}

Miller, M. N. 1969a. Bounds for effective bulk modulus of heterogeneous materials. *Journal of Mathematical Physics* 10(11):2005–2013. See erratum: *J. Math. Phys.* 12:1057. {*331, 334, 338, 553, 566*}

Miller, M. N. 1969b. Bounds for effective electrical, thermal, and magnetic properties of heterogeneous materials. *Journal of Mathematical Physics* 10(11):1988–2004. {*320, 331, 334, 338, 553, 566*}

Milton, G. W. 1981a. Bounds on the electromagnetic, elastic, and other properties of two-component composites. *Physical Review Letters* 46(8):542–545. {*397, 399, 412, 474, 494, 553, 566, 577, 599*}

Milton, G. W. 1981b. Bounds on the transport and optical properties of a two-component composite material. *Journal of Applied Physics* 52(8):5294–5304. {*371, 379, 382, 394, 553, 566, 569, 574, 581, 583, 586, 587, 592, 599, 610, 617*}

Milton, G. W. 1982. Bounds on the elastic and transport properties of two-component composites. *Journal of the Mechanics and Physics of Solids* 30(3):177–191. {*322, 330–332, 338, 553, 558, 566, 586, 599*}

Milton, G. W. and N. Phan-Thien 1982. New bounds on effective elastic moduli of two-component materials. *Proceedings of the Royal Society of London. Series A, Mathematical and Physical Sciences* 380:305–331. {*458, 474, 495, 553, 554, 557, 559, 567*}

Pham, D. C. 1996. On macroscopic elastic and conductivity properties of perfectly random cell composites. *International Journal of Solids and Structures* 33(12):1745–1755. {*490, 495, 553, 567*}

Pham, D. C. 1997. Overall properties of planar quasisymmetric randomly inhomogeneous media: Estimates and cell models. *Physical Review E (Statistical Physics, Plasmas, Fluids, and Related Interdisciplinary Topics)* 56(1):652–660. {*553, 567, 586, 600*}

Phan-Thien, N. and G. W. Milton 1982. New bounds on the effective thermal conductivity of N-phase materials. *Proceedings of the Royal Society of London. Series A, Mathematical and Physical Sciences* 380:333–348. {*554, 567*}

Prager, S. 1963. Diffusion and viscous flow in concentrated suspensions. *Physica* 29:129–139. {*556, 567*}

Roberts, A. P. and E. J. Garboczi 1999. Elastic properties of a tungsten-silver composite by reconstruction and computation. *Journal of the Mechanics and Physics of Solids* 47 (10):2029–2055. {*558, 567*}

Roberts, A. P. and M. A. Knackstedt 1996. Structure-property correlations in model composite materials. *Physical Review E (Statistical Physics, Plasmas, Fluids, and Related Interdisciplinary Topics)* 54:2313–2328. {*331, 338, 555, 567*}

Roberts, A. P. and M. Teubner 1995. Transport properties of heterogeneous materials derived from Gaussian random fields: Bounds and simulation. *Physical Review E (Statistical Physics, Plasmas, Fluids, and Related Interdisciplinary Topics)* 51(5):4141–4154. {*331, 338, 555, 567*}

Schulgasser, K. 1976. On the conductivity of fiber reinforced materials. *Journal of Mathematical Physics* 17(3):382–387. {*332, 338, 553, 567*}

Sen, A. K., F. Lado, and S. Torquato 1987. Bulk properties of composite media. II. Evaluation of bounds on the shear modulus of suspensions of impenetrable spheres. *Journal of Applied Physics* 62(10):4135–4141. {*331, 338, 557, 567*}

Silnutzer, N. R. 1972. Effective constants of statistically homogeneous materials. Ph.D. thesis, University of Pennsylvania, Philadelphia. xvi + 267 pp. {*331, 332, 338, 553, 558, 567*}

Torquato, S. 1980. Microscopic approach to transport in two-phase random media. Ph.D. thesis, State University of New York, Stony Brook, Stony Brook, New York. {*553, 567*}

Torquato, S. 1991. Random heterogeneous media: Microstructure and improved bounds on effective properties. *ASME Applied Mechanics Reviews* 44(2):37–76. {*xxv, xxviii, 331, 339, 425, 436, 553, 567*}

Torquato, S. and F. Lado 1986. Effective properties of two-phase disordered composite media: II. Evaluation of bounds on the conductivity and bulk modulus of dispersions of impenetrable spheres. *Physical Review B (Solid State)* 33(9):6428–6435. {*331, 339, 557, 567*}

Torquato, S. and G. Stell 1985. Bounds on the effective thermal conductivity of a dispersion of fully penetrable spheres. *Letters in Applied and Engineering Sciences: An International Journal* 23(3):375–383. {*331, 339, 553, 568*}

27

Bounds using the analytic method

27.1. A brief history of bounds derived using the analytic method

Bergman (1978) recognized that the analytic properties discussed in chapter 18 on page 369 provide a powerful tool for deriving bounds. He rederived the Hashin-Shtrikman bounds and obtained new bounds correlating different properties of composites. A major success of the approach was that it lead to tight bounds on the complex dielectric constant of a two-phase composite (Milton 1979, 1980, 1981a; Bergman 1980, 1982). These bounds are illustrated in figure 27.1 on the next page. [The first available bounds on complex dielectric constants were those of Schulgasser and Hashin (1976), but they were limited to materials with low-loss constituents, that is, with permittivities having small imaginary parts.] These complex dielectric constant bounds have been directly compared with experimental measurements: Niklasson and Granqvist (1984) applied them to bounding the optical properties of composite films; Korringa and LaTorraca (1986) applied them to bounding the complex electrical permittivity of rocks; Golden (1995) applied them to bounding the complex permittivity of sea ice; and Mantese, Micheli, Dungan, Geyer, Baker-Jarvis, and Grosvenor (1996) applied them to bounding the complex dielectric constant and magnetic permeability of composites of Barium Titanate and ferrite. In most cases the experimental measurements were consistent with the bounds. However, it is important to recognize that these bounds apply only in the quasistatic limit where the wavelength of the radiation is much larger than the inhomogeneities of the microstructure; see Aspnes (1982). McPhedran, McKenzie, and Milton (1982); McPhedran and Milton (1990); and Cherkaeva and Golden (1998) applied the bounds in an inverse fashion to obtain quite tight bounds on the volume fraction from measurements of the complex dielectric constant.

Bruno (1991) recognized that for dispersions of well-separated particles in a matrix one could further restrict the class of admissible analytic functions and accordingly obtain tighter bounds. Sawicz and Golden (1995) and Golden (1998) extended these bounds to media with complex dielectric constants. Helsing (1994b) found that the analytic method could improve existing bounds on the conductivity of a certain class of polycrystals. Kantor and Bergman (1984) successfully applied a variant of the analytic method to obtain bounds on elastic moduli. Bruno and Leo (1992) obtained tighter bounds for elastic materials containing well-separated holes or rigid inclusions.

A systematic method for obtaining bounds using the analytic method was found by Milton (1981c). The method generated a whole hierarchy of bounds on the effective permittivity or conductivity of two-phase composites, incorporating as many series expansion coefficients and as many (real or complex) known values of the function as desired. The bounds were

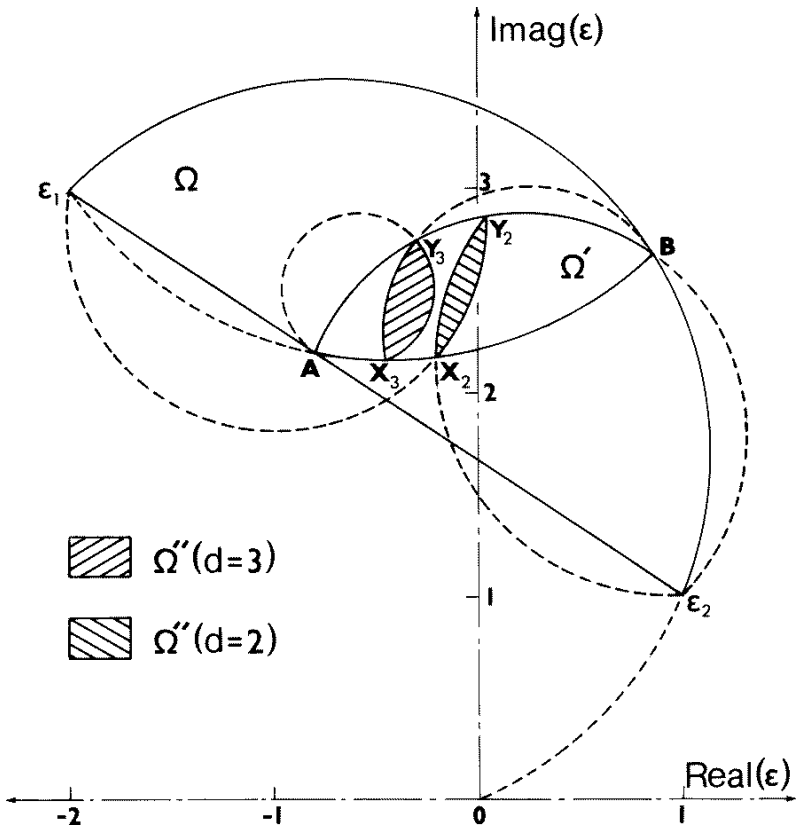

Figure 27.1. The bounds on a diagonal element ε_e (of the complex effective dielectric tensor ε_*) of a composite of two isotropic phases with complex dielectric constants $\varepsilon_1 = -2+3i$ and $\varepsilon_2 = 1+i$. If nothing else is known about the composite, then ε_e is confined to the region $\mathbf{\Omega}$, the boundary of which is traced by the diagonal elements of a laminate microstructure as the volume fraction is varied. If the volume fractions $f_1 = 0.6$ and $f_2 = 1 - f_1 = 0.4$ are known, then ε_e is confined to the region $\mathbf{\Omega}'$, the boundary of which is traced by a diagonal element of the coated elliptical cylinder assemblage as the eccentricity is varied. If one knows f_1 and f_2 and that the composite is isotropic, then ε_e is confined to the region $\mathbf{\Omega}''$, the construction of which is different in two and three dimensions. In two dimensions ($d = 2$) the boundary is traced by the effective dielectric constant of the doubly coated cylinder assemblage as the core material is moved to the outer coating. The circular arcs are determined by their endpoints and by the additional point on their extension. Here A and B are the arithmetic and harmonic averages $f_1\varepsilon_1 + f_2\varepsilon_2$ and $1/(f_1/\varepsilon_1 + f_2/\varepsilon_2)$, X_3 and Y_3 correspond to the Hashin-Shtrikman coated sphere assemblage with phase 1 and phase 2, respectively, as coating, while X_2 and Y_2 correspond to the Hashin-Shtrikman coated cylinder assemblage with phase 1 and phase 2, respectively, as coating. Reprinted with permission from Milton (1980). Copyright 1980, American Institute of Physics.

found to tightly bound numerically generated, effective moduli of periodic lattices of (nonintersecting and intersecting) cylinders and of periodic arrays of spheres (Milton, McPhedran, and McKenzie 1981; McPhedran and Milton 1981). Sangani and Yao (1988a, 1988b) found that the high-order bounds also provided accurate estimates for the conductivity of lattices of cylinders and arrays of spheres containing up to 16 cylinders or spheres in the unit cell. Helsing (1994a) showed how the speed and accuracy of these calculations could be greatly improved. When the moduli of the two phases are real the hierarchy of bounds incorporating just the series expansion coefficients can be generated directly from the classical and Hashin-Shtrikman variational principles by choosing an appropriate sequence of trial fields (Milton and McPhedran 1982). Alternative derivations of this same set of bounds were given by Golden and Papanicolaou (1983), Bergman (1986, 1993), and Tokarzewski (1994). Felderhof (1984) reformulated the bounds to elucidate some of their mathematical structure.

In 1981, Jim Berryman and John Wilkins independently mentioned to me that the bounds in the hierarchy reminded them of bounds on Stieltjes functions. These bounds were rational approximants, known as Padé approximants. Prior to then, Padé approximants and Stieltjes functions had not been discussed in the composite material literature. With knowledge of this connection, many of the bounds (but not those incorporating known complex values of the function) could have been obtained from existing bounds on Stieltjes functions; see in particular Gragg (1968); Baker, Jr. (1969); Field (1976); and the books of Baker, Jr. (1975); and Baker, Jr. and Graves-Morris (1981). Here we will first describe the hierarchy of bounds and then discuss methods of obtaining them. The bounds turn out to be the simplest possible rational functions of the constituent moduli compatible with the available information. The search for bounds thus reduces to the elementary problem of finding these rational approximants.

27.2. A topological classification of rational conductivity functions

Most of the analysis using the analytic method has been directed toward bounding the diagonal element $\sigma_e(\sigma_1, \sigma_2)$ of effective conductivity tensor of a composite of two isotropic phases with conductivities $\sigma_1 \boldsymbol{I}$ and $\sigma_2 \boldsymbol{I}$. For the moment we will ignore the fact that this function satisfies the normalization constraint that $\sigma_e(1, 1) = 1$. In section 18.4 on page 381 we saw that $\sigma_e(\sigma_1, \sigma_2)$ can be approximated by a rational function that is homogeneous of the first degree having finite values of $\sigma_e(1, 0)$ and $\sigma_e(0, 1)$, and with $\sigma_e(\sigma_1, 1)$ having its poles and zeros alternating along the real σ_1-axis with a zero nearest, or at, the origin and a pole nearest, or at, infinity.

Such rational functions can be expressed as the ratio of two polynomials that have no common factor:

$$\sigma_e(\sigma_1, \sigma_2) = \frac{a_0\sigma_2^{k+1} + a_1\sigma_2^k\sigma_1 + a_2\sigma_2^{k-1}\sigma_1^2 + \cdots + a_{k+1}\sigma_1^{k+1}}{b_0\sigma_2^k + b_1\sigma_2^{k-1}\sigma_1 + b_2\sigma_2^{k-2}\sigma_1^2 + \cdots + b_k\sigma_1^k}, \tag{27.1}$$

where b_0 and b_k must both be nonzero to ensure that $\sigma_e(1, 0)$ and $\sigma_e(0, 1)$ are finite. Since we are free to multiply the denominator and numerator by a constant, we can assume without loss of generality that $b_0 = 1$. Rational functions of the form (27.1) can be grouped into four distinct topological types, and within each type the functions can be ranked according to the number r of free parameters that determine the rational function (not counting b_0, which as we have noted can be set equal to 1). Specifically, each function (possibly representing a bound) can be classed as

- type I$[r]$, with r an even number, if $k = r/2$ and the numerator in (27.1) is divisible by $\sigma_1\sigma_2$, that is, $a_0 = 0$ and $a_{k+1} = 0$. The $r = 2k$ free parameters can be taken as

the constants $a_1, a_2, \ldots a_k$ and $b_1, b_2, \ldots, b_k$. One could say that neither phase "percolates" in the sense that conduction is blocked when either phase 1 or phase 2 has zero conductivity, as occurs in a simple laminate when the direction of the applied field $\boldsymbol{e}_0$ is parallel to the direction of lamination $\boldsymbol{n}$. (Thus we have $\sigma_e = 0$ when $\sigma_1 = 0$ or when $\sigma_2 = 0$.)

- type II $[r]$, with r an even number, if $k = r/2 - 1$ and the numerator in (27.1) is not divisible by either σ_1 or σ_2, that is, $a_0 \neq 0$ and $a_{k+1} \neq 0$. The $r = 2k+2$ free parameters in the rational function are $a_0, a_1, \ldots, a_{k+1}$ and $b_1, b_2, \ldots b_k$. One could say that both phases "percolate" in the sense that conduction occurs (for nonnegative values of σ_1 and σ_2) unless both phases have zero conductivity, as occurs in a simple laminate when the direction of the applied field $\boldsymbol{e}_0$ is perpendicular to the direction of lamination $\boldsymbol{n}$.

- type III $[r]$, with r an odd number, if $k = (r-1)/2$ and the numerator in (27.1) is divisible by σ_2 but not by σ_1, that is, $a_0 \neq 0$ and $a_{k+1} = 0$. The $r = 2k + 1$ free parameters in the rational function are $b_1, b_2, \ldots b_k$ and $a_1, a_2, \ldots, a_{k+1}$. One could say that only phase 2 "percolates" in the sense that conduction is blocked when phase 2 has zero conductivity but is not blocked when phase 1 has zero conductivity, as occurs in the Hashin-Shtrikman assemblages of coated spheres with phase 2 as coating and phase 1 as core.

- type IV $[r]$, with r an odd number, if $k = (r-1)/2$ and the numerator in (27.1) is divisible by σ_1 but not by σ_2, that is, $a_0 = 0$ and $a_{k+1} \neq 0$. The $r = 2k + 1$ free parameters in the rational function are $a_0, a_1, \ldots, a_k$ and $b_1, b_2, \ldots b_k$. One could say that only phase 1 "percolates" in the sense that conduction is blocked only when phase 1 has zero conductivity, as occurs in the Hashin-Shtrikman assemblages of coated spheres with phase 1 as coating and phase 2 as core.

Notice that if we swap the labels of the two phases, in effect interchanging the roles of σ_1 and σ_2, functions of type III $[r]$ transform to functions of type IV $[r]$, and vice versa, while functions of type I $[r]$ and type II $[r]$ retain their identity. If instead we make a duality transformation, replacing σ_1, σ_2, and σ_e by their reciprocals $1/\sigma_1$, $1/\sigma_2$, and $1/\sigma_e$ in (27.1), then functions of type I $[r]$ transform to functions of type II $[r]$, and vice versa, while functions of type III $[r]$ and of type IV $[r]$ retain their identity.

In practice it is easiest to recognize the type of a rational function $\sigma_e(\sigma_1, \sigma_2)$ by first setting $\sigma_2 = 1$ (which can be done without loss of generality since the function is homogeneous) and then expressing the resultant function in the form

$$\sigma_e(\sigma_1, 1) = \frac{p(\sigma_1)}{q(\sigma_1)}, \tag{27.2}$$

where $p(\sigma_1)$ and $q(\sigma_1)$ are polynomials with no common factor. The function is of

- type I $[r]$, if $p(\sigma_1)$ and $q(\sigma_1)$ both have degree $r/2$ and $p(0) = 0$.

- type II $[r]$, if $p(\sigma_1)$ has degree $r/2$, $q(\sigma_1)$ has degree $r/2 - 1$, and $p(0) \neq 0$.

- type III $[r]$, if $p(\sigma_1)$ and $q(\sigma_1)$ both have degree $(r-1)/2$ and $p(0) \neq 0$.

- type IV $[r]$, if $p(\sigma_1)$ has degree $(r+1)/2$, $q(\sigma_1)$ has degree $(r-1)/2$, and $p(0) = 0$.

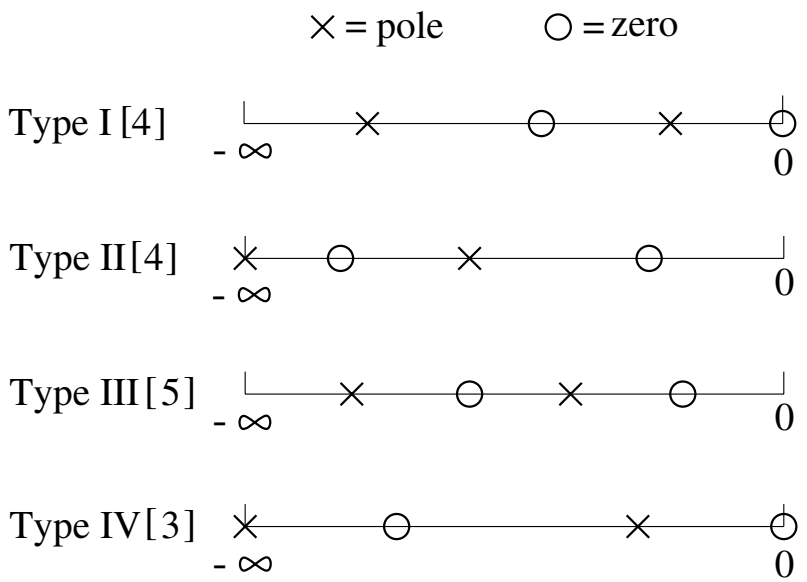

Figure 27.2. The different topological types of rational conductivity functions. Shown are the positions along the negative σ_1-axis of the poles and zeros of the function $\sigma_e(\sigma_1, 1)$.

In other words, as illustrated in figure 27.2, $\sigma_e(\sigma_1, 1)$ has a zero at $\sigma_1 = 0$ if and only if it is of type I or type IV, and has a pole at $\sigma_1 = \infty$ if and only if it is of type II or type IV.

The simplest possible rational functions (i.e., those rational functions having the lowest possible value of r) that are of the appropriate type and which are compatible with what we know about the conductivity function $\sigma_e(\sigma_1, \sigma_2)$ often provide bounds on σ_e. The known information can take various forms: known values of the series expansion coefficients; known values of the conductivity function $\sigma_e(\sigma_1, \sigma_2)$ for various pairs of values of σ_1 and σ_2; the constraint that the function satisfies Keller's relation $\sigma_e(1/\sigma_1, 1/\sigma_2) = 1/\sigma_e(\sigma_1, \sigma_2)$, appropriate to two-dimensional isotropic composites; or the constraint that the function satisfies the identity $\sigma_e(\sigma_1, \sigma_2) = \sigma_e(\sigma_1, \sigma_2)$, appropriate to symmetric materials. Let us first describe the bounds in each of these cases. Then in the last two sections we will describe two ways of proving these bounds. These are approaches that one would naturally attempt. In the next chapter we will describe another powerful approach commonly used to obtain bounds on Stieltjes functions and which is conceptually different.

27.3. Bounds that incorporate a sequence of series expansion coefficients

Suppose that we know a succession of $J + 1$ coefficients $r_0, r_1, \ldots r_J$ that enter the Taylor series expansion for $\sigma_e(\sigma_1, 1)$ in powers of $\sigma_1 - 1$:

$$\sigma_e(\sigma_1, 1) = \sum_{i=0}^{\infty} r_i(\sigma_1 - 1)^i = \sum_{i=0}^{\infty} (-1)^i r_i / s^i, \quad \text{where } s = 1/(1 - \sigma_1). \tag{27.3}$$

In the case of conductivity functions we at least know the value of r_0:

$$r_0 = \sigma_e(1, 1) = 1.$$

However, it may happen that we want to consider problems where even r_0 is unknown, which we will call the $J = -1$ case. When σ_1 and σ_2 are real and positive the simplest rational functions that could form bounds on σ_e and be compatible with the known information are those with no remaining free parameters once their expansion is matched with (27.3) to the J-th order. This imposes $J + 1$ constraints, and to satisfy them the rational function should have $r = J + 1$ parameters.

The most elementary bounds are those that incorporate only the fact that r_0 is positive. In this $J = -1$ case the bounds are

$$U_{-1,0} = 0, \quad V_{-1,0} = \infty,$$

which restrict σ_e to be positive. [Here the first index in the bounds represents the value of J, while the second index will represent the number K of independent known values of the function aside from the possibly known value of $r_0 = \sigma_e(1, 1)$. The letter U signifies a bound that is type I or type III, while the letter V signifies a bound that is of type II or IV (Milton 1981c).] Strictly speaking, $V_{-1,0} = \infty$ is not in the class of rational functions that we are considering, since $V_{-1,0}(1, 0)$ and $V_{-1,0}(0, 1)$ are no longer finite. It can, however, be regarded as the limit of functions that take constant values.

If we do not know any information about the series expansion coefficients other than the value of $r_0 = 1$, then the corresponding bounds in this $J = 0$ case are the elementary bounds

$$U_{0,0} = \sigma_2, \quad V_{0,0} = \sigma_1. \tag{27.4}$$

These are the rational functions of type III [1] and type IV [1] having the required value of r_0.

From only knowledge of the volume fraction f_1 of phase 1 we can determine $r_1 = f_1$, and the corresponding bounds in this $J = 1$ case are the Wiener (1912) arithmetic and harmonic mean bounds,

$$U_{1,0} = [f_1/\sigma_1 + f_2/\sigma_2]^{-1}, \quad V_{1,0} = f_1\sigma_1 + f_2\sigma_2, \tag{27.5}$$

which are the rational functions of type I [2] and type II [2] having the required value of the series expansion coefficients r_0 and r_1.

If in addition we know that the composite is three-dimensional and isotropic, then (14.12) allows us to determine $r_2 = -f_1 f_2/3$. The corresponding bounds in this $J = 2$ case are the Hashin and Shtrikman (1962) bounds,

$$U_{2,0} = \sigma_2 + \frac{3f_1\sigma_2(\sigma_1 - \sigma_2)}{3\sigma_2 + f_2(\sigma_1 - \sigma_2)}, \quad V_{2,0} = \sigma_1 + \frac{3f_2\sigma_1(\sigma_2 - \sigma_1)}{3\sigma_1 + f_1(\sigma_2 - \sigma_1)}, \tag{27.6}$$

which are the rational functions of type III [3] and type IV [3] having the required value of the series expansion coefficients r_0, r_1, and r_2.

Going one step further, if we also know the value of the parameter ζ_1, then (15.33) allows us to determine $r_3 = f_1 f_2(2\zeta_1 + f_2)/9$, and the corresponding bounds in this $J = 3$ case are the Beran (1965) bounds,

$$\begin{aligned} U_{3,0} &= f_1\sigma_1 + f_2\sigma_2 - \frac{f_1 f_2(\sigma_1 - \sigma_2)^2}{f_2\sigma_1 + f_1\sigma_2 + 2(\zeta_1/\sigma_1 + \zeta_2/\sigma_2)^{-1}}, \\ V_{3,0} &= f_1\sigma_1 + f_2\sigma_2 - \frac{f_1 f_2(\sigma_1 - \sigma_2)^2}{f_2\sigma_1 + f_1\sigma_2 + 2(\zeta_1\sigma_1 + \zeta_2\sigma_2)}, \end{aligned} \tag{27.7}$$

derived in section 26.2 on page 554, which are the rational functions of type I [4] and type II [4] having the required values of the series expansion coefficients r_0, r_1, r_2, and r_3.

More generally, for odd values of J the rational functions with no remaining free parameters are those of type I $[J+1]$ and type II $[J+1]$. These rational functions, denoted as $U_{J,0}(\sigma_1, \sigma_2)$ and $V_{J,0}(\sigma_1, \sigma_2)$, are lower and upper bounds on σ_e, respectively. For even values of J the rational functions with no remaining free parameters are those of type III $[J+1]$ and type IV $[J+1]$. These rational functions, denoted as $U_{J,0}(\sigma_1, \sigma_2)$ and $V_{J,0}(\sigma_1, \sigma_2)$, respectively, constitute lower and upper bounds or upper and lower bounds, according to whether the value of $\sigma_1 - \sigma_2$ is positive or negative. These bounds have been graphed or tabulated for various periodic arrays of cylinders and spheres (McPhedran and Milton 1981; Sangani and Yao 1988a, 1988b; Tokarzewski and Telega 1997). Figure 27.3 on the next page shows the bounds for a cubic array of spheres of phase 1 in a matrix of phase 2 at a volume fraction of $f_1 = 0.495$, which is fairly close to the critical volume fraction $f_c = \pi/6$ at which the spheres touch. The bounds converge rapidly as J increases. It should be remarked that, for random composites, the utility of the bounds decreases rapidly as J increases, first because computation of the series expansion coefficient r_i from correlation functions becomes increasingly difficult as i increases, and second because these coefficients need to be known with high accuracy to compute the high-order bounds.

The existence and uniqueness of rational functions of the required type satisfying the required constraints is not obvious but will be established in the course of proving the bounds in section 27.11 on page 592.

Suppose instead that we are interested in bounds on σ_e when σ_1 and σ_2 are complex. Such bounds constrain σ_e to lie in a region of the complex plane, and accordingly the bounds must be curves that enclose this region. To describe a curve we need at least one free parameter to parameterize the points along it. Accordingly, the simplest conceivable rational functions that could form bounds on σ_e are those with a single free remaining parameter once their expansion is matched with (27.3) to the J-th order.

The most elementary bounds are those that incorporate only the fact that r_0 is positive. The bounds in this $J = -1$ case are the rays inscribed by the points

$$\sigma_{b1}(v) = v\sigma_2, \quad \sigma_{b2}(w) = w\sigma_1$$

as the real parameters v and w vary between 0 and ∞. These are the rational functions of type III [1] and type IV [1]. The value of σ_e must lie inside the wedge in the complex plane bounded by these rays, as implied by the wedge bounds (18.7).

If we do not know any information about the derivatives, then the bounds in this $J = 0$ case are the line segment and circular arc inscribed by the points

$$\sigma_{b1}(v) = [v/\sigma_1 + (1-v)/\sigma_2]^{-1}, \quad \sigma_{b2}(w) = w\sigma_1 + (1-w)\sigma_2, \tag{27.8}$$

respectively, as the real parameters v and w vary between 0 and 1. (Here the subscript b signifies that these arcs are bounds.) These are the rational functions of type I [2] and type II [2] having the required value of the leading series expansion coefficient $r_0 = 1$.

An alternative way of describing these bounds is in terms of various points through which the straight line or arc passes. Let $\mathrm{Arc}(z_1, z_2, z_3)$ denote the arc of a circle joining the points z_1 and z_2 that when extended passes through z_3. Such an arc is described by the point

$$z(u) = z_1 + \frac{1-u}{1/(z_2 - z_1) + u/(z_1 - z_3)}$$

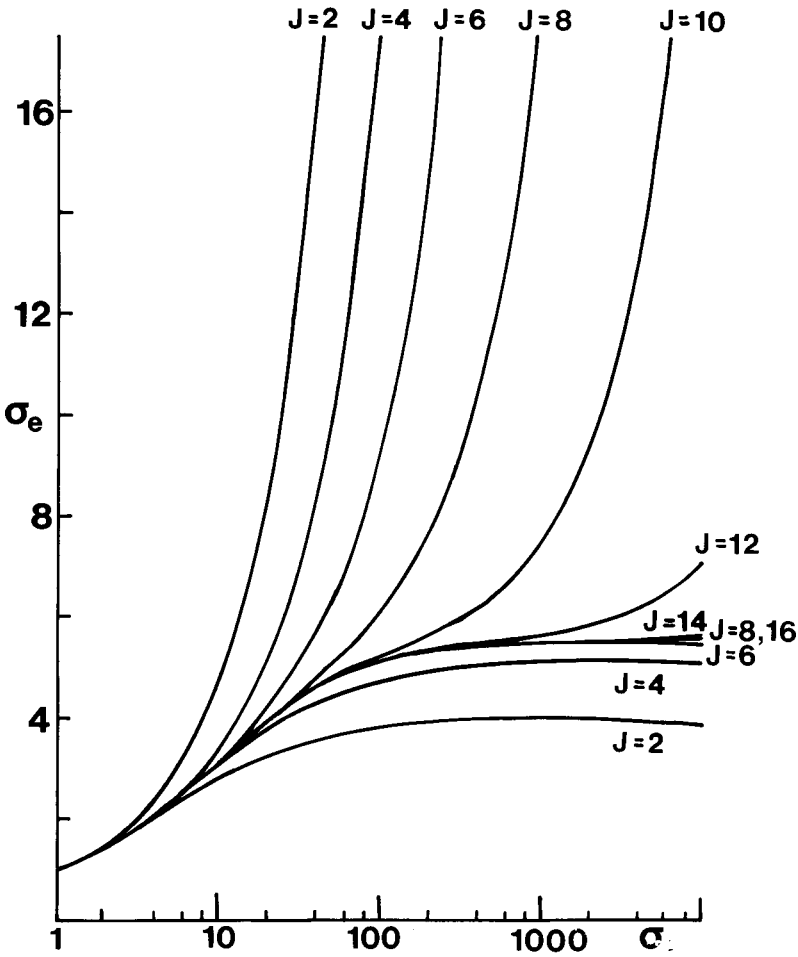

Figure 27.3. Plot of the lower and upper bound hierarchies $U_{J,0}(\sigma_1, 1)$ and $V_{J,0}(\sigma_1, 1)$ for even values of J as a function of σ_1, for a simple cubic lattice of spheres occupying a volume fraction $f_1 = 0.495$. After McPhedran and Milton (1981).

as the real parameter u varies between 0 and 1. Since the circular arc $\sigma_{b1}(v)$ passes through $U_{0,0} = \sigma_2$, $V_{0,0} = \sigma_1$, and the origin, while the straight line $\sigma_{b2}(w)$ passes through $U_{0,0} = \sigma_2$, $V_{0,0} = \sigma_1$, and infinity, we can say that the bounds constrain σ_e to lie within the lens-shaped region bounded by Arc$(U_{0,0}, V_{0,0}, 0)$ and Arc$(U_{0,0}, V_{0,0}, \infty)$. These bounds correspond to the region Ω in figure 27.1 on page 570.

If we know the volume fraction f_1 of phase 1, the bounds in this $J = 1$ case are the circular arcs inscribed by the points

$$\sigma_{b1}(v) = \sigma_2 + \frac{f_1\sigma_2(\sigma_1 - \sigma_2)}{\sigma_2 + vf_2(\sigma_1 - \sigma_2)}, \quad \sigma_{b2}(w) = \sigma_1 + \frac{f_2\sigma_1(\sigma_2 - \sigma_1)}{\sigma_1 + wf_1(\sigma_2 - \sigma_1)} \tag{27.9}$$

as the real parameters v and w vary along the real axis between 0 and 1. These are the rational functions of type III [3] and type IV [3] having the required value of the series expansion

coefficients $r_0 = 1$ and $r_1 = f_1$. Equivalently, we can say that σ_e must be contained in the lens-shaped region bounded by $\mathrm{Arc}(U_{1,0}, V_{1,0}, U_{0,0})$ and $\mathrm{Arc}(U_{1,0}, V_{1,0}, V_{0,0})$. These bounds correspond to the region $\mathbf{\Omega}'$ in figure 27.1 on page 570.

If in addition we know that the composite is three-dimensional and isotropic, the bounds in this $J = 2$ case are the circular arcs inscribed by the points

$$\sigma_{b1}(v) = f_1\sigma_1 + f_2\sigma_2 - \frac{f_1 f_2(\sigma_1 - \sigma_2)^2}{f_2\sigma_1 + f_1\sigma_2 + 2(v/\sigma_1 + (1-v)/\sigma_2)^{-1}},$$
$$\sigma_{b2}(w) = f_1\sigma_1 + f_2\sigma_2 - \frac{f_1 f_2(\sigma_1 - \sigma_2)^2}{f_2\sigma_1 + f_1\sigma_2 + 2(w\sigma_1 + (1-w)\sigma_2)} \tag{27.10}$$

as the real parameters v and w vary along the real axis between 0 and 1. These are the rational functions of type I [4] and type II [4] having the required value of the series expansion coefficients $r_0 = 1$, $r_1 = f_1$, and $r_2 = -f_1 f_2/3$. Equivalently, we can say that σ_e must be contained in the lens-shaped region bounded by $\mathrm{Arc}(U_{2,0}, V_{2,0}, U_{1,0})$ and $\mathrm{Arc}(U_{2,0}, V_{2,0}, V_{1,0})$. These bounds correspond to the shaded region $\mathbf{\Omega}''$ in figure 27.1 on page 570 with $d = 3$. The bounds (27.9) and (27.10) are the complex generalizations of the Wiener and Hashin-Shtrikman bounds (Milton 1979, 1980; Bergman 1980). They reduce to the Wiener and Hashin-Shtrikman bounds when σ_1 and σ_2 are real.

Going one step further, if we also know the value of the parameter ζ_1, then we can say that σ_e must be contained in the lens-shaped region bounded by $\mathrm{Arc}(U_{3,0}, V_{3,0}, U_{2,0})$ and $\mathrm{Arc}(U_{3,0}, V_{3,0}, V_{2,0})$. These bounds are the complex generalization of the Beran (1965) bounds (Milton 1981b). They have been evaluated by Jeulin and Savary (1997) for a variety of random microstructures.

More generally, for odd values of J the rational functions with a single free parameters are those of type III $[J+2]$ and type IV $[J+2]$. As the remaining free parameter is varied, while keeping σ_1 and σ_2 fixed, the value of each of these rational functions traces a circular arc in the complex plane. The two circular arcs meet at the points $U_{J,0}$ and $V_{J,0}$, these being the limits of rational functions of type III $[J+2]$ and type IV $[J+2]$ having the required series expansion coefficients. The lens-shaped region of the complex plane bounded by these two circular arcs contains σ_e.

For even values of J the rational functions with a single free remaining parameter are those of type I $[J+2]$ and type II $[J+2]$. As the remaining free parameter is varied, while keeping σ_1 and σ_2 fixed, the value of each rational function traces out a circular arc. The two circular arcs meet at $U_{J,0}$ and $V_{J,0}$, and the lens-shaped region of the complex plane bounded by these two circular arcs contains σ_e. McPhedran and Milton (1981) and Tokarzewski and Telega (1997) have plotted the lens-shaped regions in the complex plane representing these bounds for periodic arrays of cylinders and spheres.

An equivalent way of expressing the bounds, for both odd and even values of J, is to say that σ_e must be contained in the lens-shaped region bounded by $\mathrm{Arc}(U_{J,0}, V_{J,0}, U_{J-1,0})$ and $\mathrm{Arc}(U_{J,0}, V_{J,0}, V_{J-1,0})$, where $U_{J,0}$ and $V_{J,0}$ are the bounds that are appropriate when σ_1 and σ_2 are real and positive, while $U_{J-1,0}$ and $V_{J-1,0}$ are the bounds that are appropriate when σ_1 and σ_2 are real and positive and only the first J series expansion coefficients are known (i.e., when the value of r_J is not taken into account). Accordingly, as σ_1 and σ_2 become close to being real and positive, the lens-shaped region in the complex plane reduces to the interval on the real axis between $V_{J,0}$ and $U_{J,0}$. In other words, the complex bounds reduce to their real counterparts.

27.4. Relation between the bounds and Padé approximants

If one is familiar with Padé approximants, then it is clear from the preceding description of the bounds that there should be a close relation between them and Padé approximants. This connection has been made explicit, for example, in the papers of Torquato (1985) and Tokarzewski (1994) [see also Milton (1986)].

Given a function $f(z)$ with a power series expansion

$$f(z) = \sum_{i=0}^{\infty} c_i z^i \tag{27.11}$$

around the point $z = 0$, the $[L/M]$ Padé approximant is the rational function

$$[L/M] = \frac{\alpha_0 + \alpha_1 z + \cdots + \alpha_L z^L}{\beta_0 + \beta_1 z + \cdots + \beta_M z^M}, \tag{27.12}$$

in which the $L + 1$ constants α_0,α_1,..α_L and the $M + 1$ constants β_0,β_1,..β_M are chosen so that the expansion of (27.12) in powers of z agrees with the series expansion (27.11) as far as possible. Normally this agreement can be achieved up to and including terms of order z^{L+M}. Since one is free to multiply the numerator and denominator by a constant, without any loss of generality we can suppose that $\beta_0 = 1$. Padé approximants have found many applications in physics, for example, to critical phenomena, to scattering physics, and to electrical circuits as discussed, for example, by Baker, Jr. (1975).

Let us set $z = \sigma_1 - 1$ so that the series expansion (27.3) takes the same form as (27.11). Also recall that rational functions of type II and type III, when expressed in the form (27.2) with $\sigma_2 = 1$, are not subject to the constraint that $p(\sigma_1) = p(1 + z) = 0$. Accordingly,

- the $[L + 1, L]$ Padé approximant to the function $f(z) = \sigma_e(1 + z, 1)$ can be identified with the type II bound $V_{2L+1,0}(1 + z, 1)$;
- the $[L, L]$ Padé approximant to the function $f(z) = \sigma_e(1 + z, 1)$ can be identified with the type III bound $U_{2L,0}(1 + z, 1)$.

Since $U_{J,0}(\sigma_1, \sigma_2)$ and $V_{J,0}(\sigma_1, \sigma_2)$ are homogeneous functions of σ_1 and σ_2, this prescription allows one to recover the bound $V_{J,0}$ for odd values of J and the bound $U_{J,0}$ for even values of J from the relevant Padé approximant. For example, consider a three-dimensional isotropic composite where we know the value of the volume fraction f_1 and consequently the series expansion coefficients $r_0 = 1$, $r_1 = f_1$, and $r_2 = -f_1 f_2/3$. The [1/1] Padé approximate to the function $\sigma_e(1, 1)$ is

$$[1/1] = \frac{3 + (f_2 + 3f_1)z}{3 + f_2 z} = 1 + \frac{3f_1 z}{3 + f_2 z} \approx 1 + f_1 z - (f_1 f_2/3)z^2 + \cdots.$$

Identifying this with $U_{2,0}(1 + z, 1)$, making the substitution $z = \sigma_1/\sigma_2 - 1$, and multiplying the resultant expression by σ_2 gives

$$U_{2,0}(\sigma_1, \sigma_2) = \sigma_2 + \frac{3f_1\sigma_2(\sigma_1 - \sigma_2)}{3\sigma_2 + f_2(\sigma_1 - \sigma_2)},$$

which is in agreement with (27.6).

To recover the type I and type IV bounds from Padé approximates, let us swap the roles of the two phases and then make a duality transformation, in effect letting $1/\sigma_e$, $1/\sigma_2$, and $1/\sigma_1$

play the roles that were played by σ_e, σ_1, and σ_2. Under this combined transformation rational functions of types II and III transform to functions of type I and type IV, and vice versa, and there is a corresponding interchange of bound types. To make this procedure explicit, we first need to expand the function $1/\sigma_e(1, \sigma_2)$ in powers of $1/\sigma_2 - 1$:

$$\frac{1}{\sigma_e(1,\sigma_2)} = \frac{1}{\sigma_2\sigma_e(1/\sigma_2,1)} = \sum_{i=0}^{\infty} r_i' z^i, \quad \text{where now } z = 1/\sigma_2 - 1.$$

By substituting the expansion (27.3) into this expression we see that

$$r_0' = 1/r_0, \quad r_1' = (1 - r_1 r_0')/r_0, \quad r_n' = -\frac{1}{r_0}\sum_{i=0}^{n-1} r_i' r_{n-i} \text{ for } n = 2, 3, \cdots. \tag{27.13}$$

These recursion formulas allow us to determine the series expansion coefficients $r_0', r_1', \ldots r_J'$ from the known coefficients $r_0, r_1, \ldots r_J$. The previous correspondence between Padé approximates and bounds now implies that

- the $[L + 1, L]$ Padé approximant to the function $f(z) = 1/\sigma_e(1, 1/(1 + z))$ can be identified with the function $1/U_{2L+1,0}(1, 1/(1 + z))$;
- the $[L, L]$ Padé approximant to the function $f(z) = 1/\sigma_e(1, 1/(1+z))$ can be identified with the function $1/V_{2L,0}(1, 1/(1 + z))$.

This prescription allows us to recover the bound $U_{J,0}$ for odd values of J and the bound $V_{J,0}$ for even values of J from the relevant Padé approximant. In our example of a three-dimensional isotropic composite, where the volume fraction f_1 is known, we deduce using (27.13) and the known values of $r_0 = 1$, $r_1 = f_1$, and $r_2 = -f_1 f_2/3$ that $r_0' = 1$, $r_1' = f_2$, and $r_2' = -2f_1 f_2/3$. Consequently, the [1/1] Padé approximate to the function $f(z) = 1/\sigma_e(1, 1/(1 + z))$ is

$$[1/1] = \frac{3 + (2f_1 + 3f_2)z}{3 + 2f_1 z} = 1 + \frac{3f_2 z}{3 + 2f_1 z} \approx 1 + f_2 z - (2f_1 f_2/3)z^2 + \cdots.$$

Identifying this with $1/V_{2,0}(1, 1/(1 + z))$, making the substitution $z = \sigma_1/\sigma_2 - 1$, and taking the inverse of the expression and then multiplying it by σ_1 gives

$$V_{2,0}(\sigma_1, \sigma_2) = \sigma_1 + \frac{3f_2\sigma_1(\sigma_2 - \sigma_1)}{3\sigma_1 + f_1(\sigma_2 - \sigma_1)},$$

in agreement with (27.6).

27.5. Bounds incorporating known real or complex values of the function and series expansion coefficients

Besides the $J+1$ known series expansion coefficients, we might know the function $\sigma_e(\sigma_1, \sigma_2)$ for, say, K real positive-valued pairs of σ_1 and σ_2. This imposes K constraints:

$$\sigma_e(\sigma_{1n}, \sigma_{2n}) = \sigma_{en}, \quad \text{for } n = 1, 2, \ldots, K, \tag{27.14}$$

where the $(\sigma_{1n}, \sigma_{2n})$ are the pairs of values of (σ_1, σ_2) at which we know the value of the function, and the σ_{en} are the known values. Such information can typically be obtained from

measurements of a related effective constant, such as the effective diffusivity, effective magnetic permeability, effective thermal conductivity, or effective dielectric constant. It would be useful to repeat these measurements at different temperatures, provided that the structure of the composite does not change. Thus the bounds incorporating this information can be regarded as cross-property bounds.

When σ_1 and σ_2 are real the bounds on σ_e are those rational functions with no remaining free parameters once the $J + K + 1$ constraints are taken into account. For instance, suppose that we only know one value of the function

$$\sigma_e(\sigma_1', \sigma_2') = \sigma_e'.$$

Then the most elementary bounds that do not even take into account the value of r_0 are the $J = -1,\ K = 1$ bounds,

$$U_{-1,1} = \sigma_e'\sigma_2/\sigma_2', \quad V_{-1,1} = \sigma_e'\sigma_1/\sigma_1', \tag{27.15}$$

which are the rational functions of type III [1] and type IV [1] taking the value σ_e' when $\sigma_1 = \sigma_1'$ and $\sigma_2 = \sigma_2'$.

If we take into account the value of $\sigma_e(1, 1) = 1$, then the bounds in this $J = 0,\ K = 1$ case are those of Bergman (1976),

$$U_{0,1} = [u/\sigma_1 + (1-u)/\sigma_2]^{-1}, \quad V_{0,1} = v\sigma_1 + (1-v)\sigma_2, \tag{27.16}$$

where

$$u = \frac{1/\sigma_e' - 1/\sigma_2'}{1/\sigma_1' - 1/\sigma_2'}, \quad v = \frac{\sigma_e' - \sigma_2'}{\sigma_1' - \sigma_2'}. \tag{27.17}$$

These bounds are the rational functions of type I [2] and type II [2] having the required value of the series expansion coefficient $r_0 = 1$ and taking the value σ_e' when $\sigma_1 = \sigma_1'$ and $\sigma_2 = \sigma_2'$. These bounds, together with the decoupling transformation discussed in section 6.2 on page 95, were utilized by Bergman and Fel (1999) to bound the thermoelectric power factor of composites built from two thermoelectric materials. The bounds are achieved when the microstructure is a simple laminate

If in addition we know the volume fraction f_1 of phase 1, then the bounds in this $J = 1$, $K = 1$ case are those of Prager (1969),

$$\begin{aligned} U_{1,1} &= f_1\sigma_1 + f_2\sigma_2 - \frac{f_1 f_2(\sigma_1 - \sigma_2)^2}{f_2\sigma_1 + f_1\sigma_2 + y'\sigma_2/\sigma_2'}, \\ V_{1,1} &= f_1\sigma_1 + f_2\sigma_2 - \frac{f_1 f_2(\sigma_1 - \sigma_2)^2}{f_2\sigma_1 + f_1\sigma_2 + y'\sigma_1/\sigma_1'}, \end{aligned} \tag{27.18}$$

where

$$y' = -f_2\sigma_1' - f_1\sigma_2' + \frac{f_1 f_2(\sigma_1' - \sigma_2')^2}{f_1\sigma_1' + f_2\sigma_2' - \sigma_e'}. \tag{27.19}$$

These are the rational functions of type III [3] and type IV [3] having the required value of the series expansion coefficients $r_0 = 1$ and $r_1 = f_1$ and taking the value σ_e' when $\sigma_1 = \sigma_1'$ and $\sigma_2 = \sigma_2'$.

If we also know that the composite is three-dimensional and isotropic, then the bounds in this $J = 2, K = 1$ case are those of Bergman (1976, 1978),

$$U_{1,2} = f_1\sigma_1 + f_2\sigma_2 - \frac{f_1 f_2(\sigma_1 - \sigma_2)^2}{f_2\sigma_1 + f_1\sigma_2 + 2(u/\sigma_1 + (1-u)/\sigma_2)^{-1}},$$
$$V_{1,2} = f_1\sigma_1 + f_2\sigma_2 - \frac{f_1 f_2(\sigma_1 - \sigma_2)^2}{f_2\sigma_1 + f_1\sigma_2 + 2(v\sigma_1 + (1-v)\sigma_2)}, \tag{27.20}$$

where now

$$u = \frac{2/y' - 1/\sigma_2'}{1/\sigma_1' - 1/\sigma_2'}, \quad v = \frac{y'/2 - \sigma_2'}{\sigma_1' - \sigma_2'},$$

and y' is given by (27.19). These are the rational functions of type I [4] and type II [4] having the required value of the series expansion coefficients $r_0 = 1$, $r_1 = f_1$ and $r_2 = -f_1 f_2/3$ and taking the value σ_e' when $\sigma_1 = \sigma_1'$ and $\sigma_2 = \sigma_2'$.

More generally, for odd values of $J + K$ the rational functions with no remaining free parameters are those of type I $[J + K + 1]$ and type II $[J + K + 1]$. These bounds on σ_e are denoted by $U_{J,K}(\sigma_1, \sigma_2)$ and $V_{J,K}(\sigma_1, \sigma_2)$, respectively. For even values of $J + K$ the rational functions with no remaining free parameters are those of type III $[J + K + 1]$ and type IV $[J + K + 1]$. These bounds on σ_e are denoted by $U_{J,K}(\sigma_1, \sigma_2)$ and $V_{J,K}(\sigma_1, \sigma_2)$, respectively.

This prescription should not be applied blindly, because we need to avoid including redundant information. Since the function $\sigma_e(\sigma_1, \sigma_2)$ is homogeneous, we deduce that $\sigma_e(\lambda\sigma_{1n}, \lambda\sigma_{2n})$ has the value $\lambda\sigma_{en}$ for all choices of λ. To avoid including such information already implied by homogeneity, we should consider only those pairs for which the ratio of σ_{1n} to σ_{2n} takes distinct values. In other words, without loss of generality, we need to assume that

$$\sigma_{1j} > 0, \quad \sigma_{2j} > 0, \quad \sigma_{1j} \neq \sigma_{2j} \quad \text{and} \quad \sigma_{1i}/\sigma_{2i} \neq \sigma_{1j}/\sigma_{2j} \quad \text{for all } i \neq j. \tag{27.21}$$

The question arises as to which expression gives the upper bound and which gives the lower bound. When the ratio σ_1/σ_2 is larger than σ_{1n}/σ_{2n} for all n it is clear that $U_{J,K}$ must be the lower bound and $V_{J,K}$ the upper bound. As we decrease this ratio the character of each bound changes from a lower bound to an upper bound, and vice versa, whenever σ_1/σ_2 passes one of the values σ_{1n}/σ_{2n}, or whenever J is even and σ_1/σ_2 passes unity. This observation allows one to determine the character of each bound for any given value of σ_1/σ_2.

Suppose instead that we are interested in bounds on σ_e when σ_1 and σ_2 are complex. The simplest conceivable rational functions that could form bounds on σ_e are now those with a single free remaining parameter once the $J + K + 1$ constraints are taken into account.

For example, in the $J = 0$, $K = 1$ case, where we take into account only the known values $\sigma_e(\sigma_1', \sigma_2') = \sigma_e'$ and $\sigma_e(1, 1) = 1$, the bounds (Milton 1981c) are the circular arcs inscribed by

$$\sigma_{b1}(v) = \sigma_2 + \frac{v\sigma_2(\sigma_2 - \sigma_1)(1 - \sigma_e'/\sigma_2')}{(\sigma_2/\sigma_2' - \sigma_1/\sigma_1') - v(\sigma_2 - \sigma_1)},$$
$$\sigma_{b2}(w) = \sigma_1 + \frac{w\sigma_1(\sigma_1 - \sigma_2)(1 - \sigma_e'/\sigma_1')}{(\sigma_1/\sigma_1' - \sigma_2/\sigma_2') - w(\sigma_1 - \sigma_2)} \tag{27.22}$$

as the real parameter v varies between $1/\sigma_1'$ and $1/\sigma_e'$ while the real parameter w varies between $1/\sigma_e'$ and $1/\sigma_2'$. These bounds are the rational functions of type III [3] and type IV [3] having the required value of the series expansion coefficient $r_0 = 1$ and taking the value σ_e' when $\sigma_1 = \sigma_1'$ and $\sigma_2 = \sigma_2'$. Now notice that $\sigma_{b1}(v)$ takes the values $U_{0,1}$, $V_{0,1}$, and $U_{-1,1}$ when v equals $1/\sigma_1'$, $1/\sigma_e'$, and ∞, respectively, while $\sigma_{b2}(w)$ takes the values $V_{0,1}$, $U_{0,1}$, and $V_{-1,1}$ when w equals $1/\sigma_2'$, $1/\sigma_e'$, and ∞, respectively. Consequently, we can say that the bounds are the arcs $\mathrm{Arc}(U_{0,1}, V_{0,1}, U_{-1,1})$ and $\mathrm{Arc}(U_{0,1}, V_{0,1}, V_{-1,1})$, where $U_{0,1}$ and $V_{0,1}$ are given by (27.16) while $U_{-1,1}$ and $V_{-1,1}$ are given by (27.15).

If in addition we know the volume fraction f_1, then the bounds are given by the two arcs $\mathrm{Arc}(U_{1,1}, V_{1,1}, U_{0,1})$ and $\mathrm{Arc}(U_{1,1}, V_{1,1}, V_{0,1})$, where $U_{1,1}$ and $V_{1,1}$ are given by (27.18) while $U_{0,1}$ and $V_{0,1}$ are given by (27.16)

More generally, for odd values of $J+K$ the rational functions with a single remaining free parameter are those of type III $[J+K+2]$ and type IV $[J+K+2]$. For even values of $J+K$ the rational functions with a single remaining free parameter are those of type I $[J+K+2]$ and type II $[J+K+2]$. As the free parameter is varied while keeping σ_1 and σ_2 fixed, the values of these rational functions trace out arcs in the complex plane and the value of σ_e must lie inside the lens-shaped region of the complex plane enclosed by these circular arcs. It turns out these arcs are $\mathrm{Arc}(U_{J,K}, V_{J,K}, U_{J-1,K})$ and $\mathrm{Arc}(U_{J,K}, V_{J,K}, V_{J-1,K})$, where $U_{J,K}$ and $V_{J,K}$ are the bounds that are appropriate when σ_1 and σ_2 are real and positive, while $U_{J-1,K}$ and $V_{J-1,K}$ are the bounds that are appropriate when σ_1 and σ_2 are real and positive and only the first J series expansion coefficients are known (i.e., when the value of r_J is not taken into account).

An equivalent way of specifying the bounds is to say that they are given by the two arcs $\mathrm{Arc}(U_{J,K}, V_{J,K}, U_{J,K-1})$ and $\mathrm{Arc}(U_{J,K}, V_{J,K}, V_{J,K-1})$ in which $U_{J,K-1}$ and $V_{J,K-1}$ are the bounds that are appropriate when σ_1 and σ_2 are real and positive and only the first $K-1$ known values of the function are taken into account. In fact it does not matter which known value is ignored in the computation of $U_{J,K-1}$ and $V_{J,K-1}$; the resultant circular arcs are insensitive to this choice.

For example, in the $J=0,\ K=1$ case, notice that $\sigma_{b1}(v)$ given by (27.22) takes the value σ_1 when $v=0$, while $\sigma_{b2}(w)$ takes the value σ_2 when $w=0$. In other words, the bounds can alternatively be characterized as the arcs $\mathrm{Arc}(U_{0,1}, V_{0,1}, U_{0,0})$ and $\mathrm{Arc}(U_{0,1}, V_{0,1}, V_{0,0})$, where $U_{0,1}$ and $V_{0,1}$ are given by (27.16) while $U_{0,0} = \sigma_2$ and $V_{0,0} = \sigma_1$ are as in (27.4).

It may happen that we also have information about the function $\sigma_e(\sigma_1, \sigma_2)$ for, say, I complex-valued pairs of σ_1 and σ_2. This imposes the constraint that

$$\sigma_e(\sigma_{1n}, \sigma_{2n}) = \sigma_{en}, \quad \text{for } n \text{ from } K+1 \text{ to } K+I, \tag{27.23}$$

where the $(\sigma_{1n}, \sigma_{2n})$ are the pairs of values of (σ_1, σ_2) at which we know the value of the function, and the σ_{en} are the known values. By taking complex conjugates we obtain the value of the function at an additional set of I points:

$$\sigma_e(\sigma_{1n}, \sigma_{2n}) = \sigma_{en}, \quad \text{for } n \text{ from } K+I+1 \text{ to } K+2I, \tag{27.24}$$

where

$$\sigma_{1\ell} \equiv \overline{\sigma_{1n}}, \quad \sigma_{2\ell} \equiv \overline{\sigma_{2n}}, \quad \sigma_{e\ell} \equiv \overline{\sigma_{en}} \text{ for } \ell = n + I \text{ from } K+I+1 \text{ to } K+2I,$$

in which the bar denotes complex conjugation. Since the function is homogeneous, knowing its value at a point $(\sigma_{1n}, \sigma_{2n})$ where the ratio of σ_{1n} to σ_{2n} is real is equivalent to knowing its

value at the point $(\sigma_{1n}/\sigma_{2n}, 1)$, and this information can be incorporated into the original set of K known real values. Therefore let us assume not only that (27.21) still holds but also that

$$\mathrm{Im}(\sigma_{1n}/\sigma_{2n}) > 0 \quad \text{for } n = K+1, K+2, \ldots, K+I, \tag{27.25}$$

where the inequality ensures that the information contained in (27.23) is not duplicated by (27.24).

With these definitions the bounds take the same form as before (Milton 1981c). They are the simplest rational functions of the appropriate type that have the required derivatives (27.3) and which pass through the known points given by (27.14), (27.23), and (27.24). Specifically, when σ_1 and σ_2 are real, σ_e lies between $U_{J,K+2I}(\sigma_1, \sigma_2)$ and $V_{J,K+2I}(\sigma_1, \sigma_2)$ while when σ_1 and σ_2 are complex, σ_e lies inside the region bounded by $\mathrm{Arc}(U_{J,K+2I}, V_{J,K+2I}, U_{J-1,K+2I})$ and $\mathrm{Arc}(U_{J,K+2I}, V_{J,K+2I}, V_{J-1,K+2I})$. With a small modification, these bounds also apply to the related problem of bounding the viscoelastic moduli of homogeneous materials at one frequency, given the viscoelastic moduli at several other frequencies (Eyre, Milton, and Lakes 2001).

27.6. Numerical computation of the bounds†

The bounds described in the two previous sections are easily computed by numerically solving a system of linear equations [see, for example, McPhedran and Milton 1981]. To obtain the bounds it is convenient to introduce a new variable,

$$\varrho = \frac{\sigma_1 - \sigma_2}{\sigma_1 + \sigma_2},$$

which has the appealing feature that it transforms to $-\varrho$ when we replace σ_1 and σ_2 by $1/\sigma_1$ and $1/\sigma_2$, or when we swap σ_1 with σ_2. For this reason the bounds for two-dimensional isotropic composites and symmetric materials take a simpler form when expressed in terms of ϱ rather than in terms of, say, the variable $s = \sigma_2/(\sigma_2 - \sigma_1)$. The usefulness of ϱ for these problems motivates its introduction in a general context.

Since $\sigma_e(\sigma_1, \sigma_2)$ is a homogeneous function, we can without any loss of generality suppose that $\sigma_2 = 1$ and consider σ_e as a function of ϱ:

$$\sigma_e(\varrho) \equiv \sigma_e(\sigma_1, 1) = \sigma_e((1+\varrho)/(1-\varrho), 1).$$

The $J+1$ coefficients $r_0, r_1, \ldots\ r_J$ that enter the Taylor series expansion for $\sigma_e(\sigma_1, 1)$ in powers of $\sigma_1 - 1$ translate into known values of the coefficients $q_0, q_1, \ldots\ q_J$ that enter the Taylor series for $\sigma_e(\varrho)$ in powers of ϱ:

$$\sigma_e = \sum_{i=0}^{\infty} q_i \varrho^i. \tag{27.26}$$

Specifically, by substituting $\sigma_1 - 1 = 2\varrho/(1-\varrho)$ into (27.3) and expanding in powers of ϱ we see that

$$q_0 = r_0 \ \text{ and } \ q_n = \sum_{i=1}^{n} \frac{(n-1)!2^i r_i}{(i-1)!(n-i)!} \quad \text{for } n = 1, 2, \ldots, J.$$

Also, the known values of the homogeneous function $\sigma_e(\sigma_1, \sigma_2) = \sigma_e(\sigma_1/\sigma_2, 1)/\sigma_2$ translate into known values of the function $\sigma_e(\varrho)$:

$$\sigma_e(\varrho_n) = g_n \quad \text{for } n = 1, 2, \ldots, K+2I, \quad \text{where } \varrho_n = \frac{\sigma_{1n} - \sigma_{2n}}{\sigma_{1n} + \sigma_{2n}}, \quad g_n = \frac{\sigma_{en}}{\sigma_{2n}}.$$

The bounds are expressed in terms of the rational function

$$g(\varrho) = \frac{p'(\varrho)}{q'(\varrho)}, \tag{27.27}$$

where

$$p'(\varrho) = \sum_{i=0}^{N} \alpha_i \varrho^i \quad \text{and} \quad q'(\varrho) = \sum_{i=0}^{N} \beta_i \varrho^i$$

are polynomials with no common factor but are not necessarily of degree N, since α_N or β_N might be zero. Since we are free to multiply both polynomials by a constant, we can suppose, without loss of generality, that

$$\beta_0 = 1.$$

The associated function $\sigma_2 g((\sigma_1 - \sigma_2)/(\sigma_1 + \sigma_2))$, when regarded as a function σ_1 and σ_2, is of

- type I $[r]$, if $p'(-1) = 0$, $q'(1) \neq 0$, and $N = r/2$;
- type II $[r]$, if $p'(-1) \neq 0$, $q'(1) = 0$, and $N = r/2$;
- type III $[r]$, if $p'(-1) \neq 0$, $q'(1) \neq 0$, and $N = (r-1)/2$;
- type IV $[r]$, if $p'(-1) = 0$, $q'(1) = 0$, and $N = (r+1)/2$.

This places linear constraints on the coefficients α_i and β_i according to the type of bound that we seek. We require that

$$\begin{aligned} p'(-1) &= \sum_{i=0}^{N} \alpha_i (-1)^i = 0 \quad \text{for bounds of type I or III,} \\ q'(1) &= \sum_{i=0}^{N} \beta_i = 0 \qquad\quad \text{for bounds of type II or III.} \end{aligned} \tag{27.28}$$

The constraint that the function passes through the known points places another set of $K + 2I$ linear restrictions on these coefficients:

$$\sum_{i=0}^{N} \beta_i \varrho_n^i g_n = \sum_{i=0}^{N} \alpha_i \varrho_n^i \quad \text{for } n = 1, 2, \ldots, K + 2I, \tag{27.29}$$

while the constraint that the function has the required series expansion coefficients furnishes a further set of $J + 1$ linear restrictions:

$$\begin{aligned} \sum_{i=0}^{n} q_{n-i} \beta_i &= \alpha_n \quad \text{for all } n \text{ such that } 0 \leq n \leq \min\{J, N\}, \\ &= 0 \quad \text{for all } n \text{ such that } N + 1 \leq n \leq J. \end{aligned} \tag{27.30}$$

Obviously, the last case is relevant only when $J > N$, and when $J = -1$ we can forget about the restrictions (27.30) altogether.

If we seek bounds for real values of σ_1 and σ_2, then N should be chosen so that the number of unknown coefficients α_i and β_i, which is $2N+1$ (not counting $\beta_0 = 1$), matches the number of linear restrictions provided by (27.28), (27.29), and (27.30):

$$\begin{aligned} 2N+1 &= J+K+2I+2 \text{ for bounds of type I or II,} \\ &= J+K+2I+1 \text{ for bounds of type III,} \\ &= J+K+2I+3 \text{ for bounds of type IV.} \end{aligned}$$

The set of linear equations can be solved using standard numerical packages, and once the coefficients are found the bound is the function

$$U_{J,K+2I}(\sigma_1,\sigma_2) = \sigma_2 g((\sigma_1-\sigma_2)/(\sigma_1+\sigma_2)) \quad \text{for bounds of type I or III,}$$

or the function

$$V_{J,K+2I}(\sigma_1,\sigma_2) = \sigma_2 g((\sigma_1-\sigma_2)/(\sigma_1+\sigma_2)) \quad \text{for bounds of type II or IV.}$$

If we seek the arcs that bound σ_e when σ_1 and σ_2 are complex, then N should be chosen so that the number of linear restrictions provided by (27.28), (27.29), and (27.30) is $2N$.

27.7. Bounds for two-dimensional isotropic composites†

When the composite is two-dimensional and isotropic the effective conductivity function satisfies Keller's relation,

$$\sigma_e(1/\sigma_1, 1/\sigma_2) = 1/\sigma_e(\sigma_1,\sigma_2), \tag{27.31}$$

implied by (3.6). Rational functions having this property are particularly easy to recognize. They are either of type III or type IV and the polynomials $p(\sigma_1)$ and $q(\sigma_1)$ entering the expression (27.2) for $\sigma_e(\sigma_1, 1)$ satisfy

$$\begin{aligned} p(\sigma_1) &= \sigma_1^k q(1/\sigma_1) \quad \text{for functions of type III,} \\ p(\sigma_1) &= \sigma_1^{k+1} q(1/\sigma_1) \text{ for functions of type IV,} \end{aligned}$$

in which m is the degree of the polynomial $q(\sigma_1)$. In other words, the polynomial $p(\sigma_1)$ has the same set of coefficients as the polynomial $q(\sigma_1)$, but these coefficients appear in reversed order:

$$\begin{aligned} a_{k+1} &= 0 \text{ and } a_i = b_{k-i} \quad \text{for functions of type III,} \\ a_0 &= 0 \text{ and } a_i = b_{k+1-i} \text{ for functions of type IV.} \end{aligned}$$

Now (27.31) implies that $q_0 = r_0 = 1$ and

$$\sigma_e(\varrho)\sigma_e(-\varrho) = 1. \tag{27.32}$$

Accordingly, if we know the value of $g_n = \sigma_e(\varrho_n)$, then we can add

$$\sigma_e(\varrho_{n+1}) = g_{n+1}, \quad \text{where } \varrho_{n+1} = -\overline{\varrho_n}, \quad g_{n+1} = 1/\overline{g_n}, \tag{27.33}$$

to the collection of known values, where we have taken complex conjugates (denoted by the bar) so that $\mathrm{Im}(\varrho_{n+1})$ and $\mathrm{Im}(\varrho_n)$ have the same sign, to be consistent with (27.25). It may happen that $|\sigma_{1n}| = |\sigma_{2n}|$ or, equivalently, that $\mathrm{Re}(\varrho_n) = 0$. In this case, $\varrho_n = -\overline{\varrho_n}$, and we

should not add (27.33) to the collection of known values since it duplicates existing information. Notice that (27.31) implies an exact relation for the complex effective conductivity:

$$|\sigma_e| = |\sigma_1| \text{ when } |\sigma_1| = |\sigma_2|, \tag{27.34}$$

and to be compatible with this we must have $|g_n| = 1$ whenever $|\sigma_{1n}| = |\sigma_{2n}|$.

By substituting the series expansion (27.26) into (27.32) we see that for all even values of n we can calculate the value of the series expansion coefficient q_n in terms of the lower order series expansion coefficients:

$$q_n = \tfrac{1}{2}\sum_{i=1}^{n-1}(-1)^{i+1}q_i q_{n-i} \quad \text{for all even values of } n. \tag{27.35}$$

Due to the relations (27.33) and (27.35), we can assume that both J and K are even integers. Whether I is even or odd depends on whether there is an even or odd number of values of n for which $|\sigma_{1n}/\sigma_{2n}| = 1$.

Let us suppose that we are interested in bounds when σ_1 and σ_2 are real. If we know the volume fraction f_1 of phase 1, then we can determine the value of $q_1 = 2f_1$ and using (27.35) deduce the value of $q_2 = 2f_1^2$. The corresponding bounds in this $J = 2$ case are the bounds of Hashin and Shtrikman (1962),

$$U_{2,0} = \sigma_2\frac{f_1\sigma_1 + f_2\sigma_2 + \sigma_1}{f_2\sigma_1 + f_1\sigma_2 + \sigma_2}, \quad V_{2,0} = \sigma_1\frac{f_1\sigma_1 + f_2\sigma_2 + \sigma_2}{f_2\sigma_1 + f_1\sigma_2 + \sigma_1}, \tag{27.36}$$

which are the rational functions of type III(3) and type IV(3) having the required value of the series expansion coefficients q_0, q_1, and q_2.

If in addition we know the value of the parameter ζ_1, then we can determine the value of $q_3 = 2f_1^3 + 2f_1f_2\zeta_1$ and using (27.35) deduce the value of $q_4 = 2f_1^4 + 2f_1^4 + 4f_1^2f_2\zeta_1$. The corresponding bounds (Milton 1981c, 1982) in this $J = 4$ case are

$$\begin{aligned} U_{4,0} &= \sigma_2\frac{(f_1\sigma_1 + f_2\sigma_2 + \sigma_1)(\sigma_1 + \sigma_2) - f_2\zeta_1(\sigma_1 - \sigma_2)^2}{(f_2\sigma_1 + f_1\sigma_2 + \sigma_2)(\sigma_1 + \sigma_2) - f_2\zeta_1(\sigma_1 - \sigma_2)^2}, \\ V_{4,0} &= \sigma_1\frac{(f_1\sigma_1 + f_2\sigma_2 + \sigma_2)(\sigma_1 + \sigma_2) - f_1\zeta_2(\sigma_1 - \sigma_2)^2}{(f_2\sigma_1 + f_1\sigma_2 + \sigma_1)(\sigma_1 + \sigma_2) - f_1\zeta_2(\sigma_1 - \sigma_2)^2}, \end{aligned} \tag{27.37}$$

which are the rational functions of type III(5) and type IV(5) having the required value of the series expansion coefficients q_0, q_1, q_2, q_3, and q_4.

Torquato and Lado (1988) and Kim and Torquato (1990) have computed these bounds for randomly dispersed impenetrable disks or, equivalently, aligned impenetrable cylinders, and have compared them with numerical simulations. They found that the appropriate bound (the lower bound for highly conducting cylinders and the upper bound for poorly conducting cylinders) provides a remarkably good estimate of the effective conductivity. Torquato and Beasley (1986) calculated the bounds for randomly dispersed penetrable disks, and Helsing (1998) compared them with his numerical results. Torquato, Kim, and Cule (1999) found that their numerical results for the conductivity of random checkerboards are consistent with the bounds. Pham (1997) used the bounds to obtain cell shape independent bounds on the conductivity of planar cell materials.

If instead we are only given one value of the function $\sigma_e(\sigma_1', \sigma_2') = \sigma_e'$, where σ_1' and σ_2' are real, then we can determine the value of $\sigma_e(1/\sigma_1', 1/\sigma_2') = 1/\sigma_e'$ by using (27.33). The

corresponding cross-property bounds (Milton 1981c) in this $J = 0$, $K = 2$ case are

$$U_{0,2} = \sigma_2 \frac{k_1\sigma_1 + k_2\sigma_2 + \sigma_1}{k_2\sigma_1 + k_1\sigma_2 + \sigma_2}, \quad V_{0,2} = \sigma_1 \frac{k_1\sigma_1 + k_2\sigma_2 + \sigma_2}{k_2\sigma_1 + k_1\sigma_2 + \sigma_1}, \tag{27.38}$$

where

$$k_1 = \frac{\sigma_1'[(\sigma_e')^2 - (\sigma_2')^2]}{\sigma_e'[(\sigma_1')^2 - (\sigma_2')^2]}, \quad k_2 = \frac{\sigma_2'[(\sigma_e')^2 - (\sigma_1')^2]}{\sigma_e'[(\sigma_2')^2 - (\sigma_1')^2]}.$$

If we are given the volume fraction f_1 in addition to the known value, then the corresponding bounds in this $J = 2$, $K = 2$ case are

$$\begin{aligned} U_{2,2} &= \sigma_2 \frac{(f_1\sigma_1 + f_2\sigma_2 + \sigma_1)(\sigma_1 + \sigma_2) - \beta_2(\sigma_1 - \sigma_2)^2}{(f_2\sigma_1 + f_1\sigma_2 + \sigma_2)(\sigma_1 + \sigma_2) - \beta_2(\sigma_1 - \sigma_2)^2}, \\ V_{2,2} &= \sigma_1 \frac{(f_1\sigma_1 + f_2\sigma_2 + \sigma_2)(\sigma_1 + \sigma_2) - \beta_1(\sigma_1 - \sigma_2)^2}{(f_2\sigma_1 + f_1\sigma_2 + \sigma_1)(\sigma_1 + \sigma_2) - \beta_1(\sigma_1 - \sigma_2)^2}, \end{aligned} \tag{27.39}$$

where

$$\begin{aligned} \beta_1 &= \frac{(\sigma_1' + \sigma_2')[(f_2\sigma_1' + f_1\sigma_2' + \sigma_1') + 2f_2\sigma_1'(\sigma_1' - \sigma_2')/(\sigma_e' - \sigma_1')]}{(\sigma_1' - \sigma_2')^2}, \\ \beta_2 &= \frac{(\sigma_1' + \sigma_2')[(f_2\sigma_1' + f_1\sigma_2' + \sigma_2') - 2f_1\sigma_2'(\sigma_1' - \sigma_2')/(\sigma_e' - \sigma_2')]}{(\sigma_1' - \sigma_2')^2}. \end{aligned}$$

More generally, when σ_1 and σ_2 are real, the bounds are the simplest rational functions satisfying (27.31) compatible with the known information. One bound is the type III function $U_{J,K+2I}(\sigma_1, \sigma_2)$, while the other bound is the type IV function $V_{J,K+2I}(\sigma_1, \sigma_2)$. In the rational expression (27.27) for these functions the polynomials $p'(\varrho)$ and $q'(\varrho)$ satisfy

$$p'(\varrho) = q'(-\varrho),$$

and consequently their expansion coefficients α_i and β_i are related by

$$\beta_i = (-1)^i\alpha_i \quad \text{for } i = 0, 1, 2, \ldots, N.$$

When σ_1 and σ_2 are complex, the bounds are the simplest possible rational functions with one free parameter that are compatible with the available information, including the constraint (27.31). The most elementary bounds are those that incorporate only the fact that $r_0 = 1$ [which is implied by (27.31) with $\sigma_1 = \sigma_2 = 1$]. The bounds in this $J = K = 0$ case are the circular arcs inscribed by

$$\sigma_{b1}(v) = \sigma_2 \frac{(1 + v)\sigma_1 + (1 - v)\sigma_2}{(1 - v)\sigma_1 + (1 + v)\sigma_2}, \quad \sigma_{b2}(w) = \sigma_1 \frac{(1 + w)\sigma_2 + (1 - w)\sigma_1}{(1 - w)\sigma_2 + (1 + w)\sigma_1} \tag{27.40}$$

as v and w each vary between zero and one.

If in addition we know the volume fraction f_1, then we can deduce the values of $q_1 = 2f_1$ and $q_2 = 2f_1^2$. The bounds in this $J = 2$ case are the circular arcs inscribed by

$$\begin{aligned} \sigma_{b1}(v) &= \sigma_2 \frac{(f_1\sigma_1 + f_2\sigma_2 + \sigma_1)(\sigma_1 + \sigma_2) - f_2v(\sigma_1 - \sigma_2)^2}{(f_2\sigma_1 + f_1\sigma_2 + \sigma_2)(\sigma_1 + \sigma_2) - f_2v(\sigma_1 - \sigma_2)^2}, \\ \sigma_{b1}(w) &= \sigma_1 \frac{(f_1\sigma_1 + f_2\sigma_2 + \sigma_2)(\sigma_1 + \sigma_2) - f_1w(\sigma_1 - \sigma_2)^2}{(f_2\sigma_1 + f_1\sigma_2 + \sigma_1)(\sigma_1 + \sigma_2) - f_1w(\sigma_1 - \sigma_2)^2} \end{aligned} \tag{27.41}$$

as v and w each vary between zero and one (Milton 1980, 1981a). These bounds correspond to the region $\mathbf{\Omega}''$ in figure 27.1 on page 570 with $d = 2$.

In general, when σ_1 and σ_2 are complex, σ_e lies inside the lens-shaped region bounded by $\text{Arc}(U_{J,K+2I}, V_{J,K+2I}, U_{J-2,K+2I})$ and $\text{Arc}(U_{J,K+2I}, V_{J,K+2I}, V_{J-2,K+2I})$. Notice that in the complex case (in contrast to the real case) the constraint (27.31) not only provides additional known function values through (27.33) and additional known terms in the series expansion through (27.35), but also restricts the functional form of the bounds.

An appealing feature of these real and complex bounds for two-dimensional isotropic composites is that they are attained by multicoated cylinder assemblages. This is because of the correspondence between the effective conductivity functions and the microgeometries discussed in section 18.5 on page 383. In particular, the bounds (27.36), (27.38), and (27.40) are attained by assemblages of coated cylinders, while the bounds (27.37), (27.39), and (27.41) are attained by assemblages of doubly coated cylinders. Bergman (1980) mistakenly commented that he did not think that the bounds (27.41) could be attained by assemblages of doubly coated cylinders.

27.8. Bounds for symmetric materials†

When the composite is symmetric, in the sense that interchange of the two phases does not change the effective conductivity tensor, then the function $\sigma_e(\sigma_1, \sigma_2)$ satisfies

$$\sigma_e(\sigma_1, \sigma_2) = \sigma_e(\sigma_2, \sigma_1). \tag{27.42}$$

Rational functions compatible with this relation are either of type I or type II, and the polynomials $p(\sigma_1)$ and $q(\sigma_1)$ entering the expression (27.2) for $\sigma_e(\sigma_1, 1)$ satisfy

$$p(\sigma_1) = \sigma^{k+1} p(1/\sigma_1), \quad q(\sigma_1) = \sigma^k q(1/\sigma_1),$$

in which k is the degree of the polynomial $q(\sigma_1)$. In other words, the polynomials $p(\sigma_1)$ and $q(\sigma_1)$ remain invariant when the order of their coefficients is reversed:

$$a_i = a_{k+1-i} \text{ and } b_i = b_{k-i}.$$

Now (27.42) implies that

$$(1 - \varrho)\sigma_e(\varrho) = (1 + \varrho)\sigma_e(-\varrho). \tag{27.43}$$

Accordingly, if we know the value of $g_n = \sigma_e(\varrho_n)$, then we can add

$$\sigma_e(\varrho_{n+1}) = g_{n+1}, \quad \text{where } \varrho_{n+1} = -\overline{\varrho_n} \text{ and } g_{n+1} = (1 - \overline{\varrho_n})g_n^*/(1 + \overline{\varrho_n}), \tag{27.44}$$

to the collection of known values, where we have taken complex conjugates so that $\text{Im}(\varrho_{n+1})$ and $\text{Im}(\varrho_n)$ have the same sign, again to be consistent with (27.25). It may happen that $|\sigma_{1n}| = |\sigma_{2n}|$ or, equivalently, that $\text{Re}(\varrho_n) = 0$. In this circumstance $\varrho_n = -\overline{\varrho_n}$, and we should not add (27.33) to the collection of known values since it duplicates existing information. Notice that (27.42) implies an exact relation:

$$\arg\sigma_e = (\arg\sigma_1 + \arg\sigma_2)/2 \quad \text{when } |\sigma_1| = |\sigma_2|, \tag{27.45}$$

and to be compatible with this, we must have $2\arg(g_n) = \arg(\sigma_{1n}/\sigma_{2n})$ whenever $|\sigma_{1n}| = |\sigma_{2n}|$.

By substituting the series expansion (27.26) into (27.43) we see that

$$q_n = q_{n-1} \quad \text{for all odd values of } n. \tag{27.46}$$

Due to the relations (27.44) and (27.46) we can assume that K is an even integer and that J is an odd integer. Whether I is even or odd depends on whether there is an even or odd number of values of n for which $|\sigma_{1n}/\sigma_{2n}| = 1$.

Let us suppose that we are interested in bounds when σ_1 and σ_2 are real. If we only know the value of $r_0 = q_0 = 1$, then using (27.46) we determine that $q_1 = 1$ or, equivalently, that $f_1 = 1/2$. The bounds in this $J = 1$ case are the arithmetic and harmonic mean bounds,

$$U_{1,0} = 2\sigma_1\sigma_2/(\sigma_1 + \sigma_2), \qquad V_{1,0} = (\sigma_1 + \sigma_2)/2,$$

which are the rational functions of type I [2] and type II [2] having the required values of q_0 and q_1.

If in addition we know that the composite is three-dimensional and isotropic, then $q_2 = 2/3$ and from (27.46) we deduce that $q_3 = 2/3$ or, equivalently, that $\zeta_1 = 1/2$. The bounds in this $J = 3$ case are the bounds of Beran and Molyneux (1966),

$$U_{3,0} = \frac{6\sigma_1\sigma_2(\sigma_1 + \sigma_2)}{3(\sigma_1 + \sigma_2)^2 - 2(\sigma_1 - \sigma_2)^2}, \qquad V_{3,0} = \frac{3(\sigma_1 + \sigma_2)^2 - (\sigma_1 - \sigma_2)^2}{6(\sigma_1 + \sigma_2)},$$

which are the rational functions of type I [2] and type II [2] having the required values of q_0, q_1, q_2, and q_3. Schulgasser (1977) has established the optimality of the upper bound. The lower bound can be improved. As discussed in section 7.3 on page 118, the optimal lower bound is given by (7.24).

If we do not know that the composite is isotropic but instead know that $\sigma_e(\sigma_1', \sigma_2') = \sigma_e'$, where σ_1' and σ_2' are real, then we can determine the value of $\sigma_e(\sigma_2', \sigma_1') = 1/\sigma_e'$ using (27.33). The corresponding bounds in this $J = 1$, $K = 2$ case are

$$U_{1,2} = \frac{2\sigma_1\sigma_2(\sigma_1 + \sigma_2)}{(\sigma_1 + \sigma_2)^2 - k_1(\sigma_1 - \sigma_2)^2}, \quad V_{1,2} = \frac{(\sigma_1 + \sigma_2)^2 - k_2(\sigma_1 - \sigma_2)^2}{2(\sigma_1 + \sigma_2)},$$

where now

$$k_1 = \frac{(\sigma_1' + \sigma_2')^2 - 2\sigma_1'\sigma_2'(\sigma_1' + \sigma_2')/\sigma_e'}{(\sigma_1' - \sigma_2')^2}, \quad k_2 = \frac{(\sigma_1' + \sigma_2')^2 - 2\sigma_e'(\sigma_1' + \sigma_2')}{(\sigma_1' - \sigma_2')^2}.$$

Elementary bounds on the complex conductivity of symmetric materials are also available (Milton 1981a).

27.9. Reducing the set of independent bounds

Here we will show that the bounds that incorporate the series expansion coefficients r_0, $r_1,\ldots,r_J$ and $K + 2I$ known values of the function can be recovered from the bounds that incorporate $r_0 = \sigma_e(1, 1)$ and a set of $K + 2I + J$ other known values of the function. The additional set of J pairs $(\sigma_{1n}, \sigma_{2n})$ can be taken with $\sigma_{2n} = 1$, for $n = K + 2I + 1$ up to $n = K + 2I + J$, and the key idea, due to Prager (1969), is to take the limit of the bounds as the values σ_{1n} sequentially approach unity for $n = K + 2I + 1$ up to $n = K + 2I + J$. In essence, one can regard knowledge of the series expansion coefficients as being equivalent to

knowledge of the function value at a set of J points $(\sigma_{1n}, \sigma_{2n})$ in the near vicinity of the point $(1, 1)$.

For example, to recover the $J = 1$, $K = 0$ Wiener bounds (27.5) with $r_0 = 1$ and $r_1 = f_1$, we set $\sigma_1' = 1 + z$, $\sigma_2' = 1$ and substitute these values and the series expansion

$$\sigma_e' = 1 + \sum_{i=1}^{\infty} r_i z^i,$$

in the expressions (27.17) for u and v, giving

$$u = \frac{(1+z)\sum_{i=1}^{\infty} r_i z^{i-1}}{1 + \sum_{i=1}^{\infty} r_i z^i}, \qquad v = \sum_{i=1}^{\infty} r_i z^{i-1}.$$

Upon taking the limit $z \to 0$ we see that both u and v approach $r_1 = f_1$. As a consequence, the $J = 0$, $K = 1$ bounds (27.16) reduce to the arithmetic and harmonic mean bounds.

Similarly, to recover the $J = 2$, $K = 0$ Hashin-Shtrikman bounds (27.6) with $r_0 = 1$, $r_1 = f_1$, and $r_2 = -f_1 f_2/3$, we make the same substitution in the expression (27.19) for y'. In the limit as $z \to 0$ we see that

$$y' = -1 - f_2 z - \frac{f_1 f_2}{\sum_{i=2}^{\infty} r_i z^{i-2}}$$

approaches 2. Upon setting $y' = 2$ the $J = 1$, $K = 1$ bounds given by (27.18) reduce to the Hashin-Shtrikman bounds. The $J = 1$, $K = 1$ bounds, in turn, can be recovered in a similar fashion from the $J = 0$, $K = 2$ bounds.

This idea of Prager can be used to generate bounds that incorporate not just the known values of the function, but also the derivatives of the function at the known points when this information is available. Such bounds, incorporating series expansions of the function at two or three different points, have been derived (using a different approach) by Tokarzewski, Bławzdziewicz, and Andrianov (1994); Tokarzewski (1996); and Tokarzewski and Telega (1998). Their bounds, which are related two- and three-point Padé approximants, give tight estimates for the effective conductivity of square arrays of highly conducting cylinders.

27.10. Proving elementary bounds using the method of variation of poles and residues

The method of variation of poles and residues was used by Bergman (1978) to derive some of the elementary bounds. As an example of this method, let us consider the problem of finding bounds when σ_1 and σ_2 are real and positive and the only information that we have is the value of $r_0 = 1$. We can further assume, by rescaling if necessary, that $\sigma_2 = 1$. Rather than examining the function $\sigma_e(\sigma_1, 1)$ we can equally well examine the function

$$F_e(s) = 1 - \sigma_e(1 - 1/s, 1), \quad \text{where } s = 1/(1 - \sigma_1).$$

Now the problem is to bound $F_e(s)$ for a given real value of s with $s < 0$ or $s > 1$. As we have already noted, the conductivity function $\sigma_e(\sigma_1, \sigma_2)$ can be approximated to an arbitrarily high degree of accuracy by a rational function of sufficiently large degree having the required analytic properties. Therefore it suffices to consider bounds on rational functions

$$F_e(s) = \sum_{i=0}^{m} \frac{B_i}{s - s_i},$$

where

$$0 \le s_0 \le s_1 \le \ldots \le s_m < 1, \quad B_i \ge 0 \text{ for all } i, \text{ and } \sum_{i=0}^{m} \frac{B_i}{1 - s_i} \le 1. \tag{27.47}$$

The idea is to take a fixed but large value of m and find the maximum (or minimum) value of $F_e(s)$ as the poles s_i and residues B_i are varied subject to the constraints (27.47) while holding s fixed. The resulting maximum (or minimum) could conceivably depend on m, and we are interested in taking the limit as m tends to infinity. In fact it turns out that the extremum is independent of m and consequently there is no need to take limits.

Since varying the poles s_i and residues B_i corresponds in some rough sense to varying the geometry, this procedure can be compared to finding maximum (or minimum) value of σ_e as the geometry is varied over all configurations. Note, however, that when we are interested in a specific class of composites, such as three-dimensional isotropic composites, it might not be known which combinations of poles and residues correspond to composites in this class and which do not. As a consequence, the bounds obtained might not necessarily be the best possible ones.

The important observation to make is that the quantity $F_e(s)$ to be maximized (or minimized) depends linearly on the $m + 1$ residues B_0, B_1,... B_m, as do the constraints (27.47). Therefore, from the theory of linear programming [see, for example, Dantzig (1998)] we know that it suffices to consider those combinations of residues for which $m + 1$ constraints on the residues are satisfied as equalities. This means that either all of the residues are zero, that is, $F_e(s) = 0$, which corresponds to the bound $\sigma_e = 1 = \sigma_2$, or only one residue, say B_0, is nonzero and $B_0/(1 - s_0) = 1$, that is, $B_0 = (1 - s_0)$. In the latter case, upon taking the maximum or minimum value of

$$F_e(s) = \frac{1 - s_0}{s - s_0} \tag{27.48}$$

as the position s_0 of the pole is varied between 0 and 1, we see that the other bound must be $F_e(s) = 1/s$, which corresponds to $\sigma_e = \sigma_1$. So we conclude that σ_e must lie between σ_1 and σ_2.

If we are interested in elementary bounds on σ_e when σ_1 and σ_2 are complex and $r_0 = 1$, then this is equivalent to finding bounds on $F_e(s)$ for complex values of s. (We can again assume that $\sigma_2 = 1$ by making a rotation in the complex plane and rescaling if necessary.) We now focus on finding the maximum or minimum value of

$$\mathrm{Re}[e^{-i\theta} F_e(s)] = \sum_{j=1}^{m} B_j \,\mathrm{Re}[e^{-i\theta}/(s - s_j)], \tag{27.49}$$

which corresponds to optimizing the component of $F_e(s)$ in a direction at an angle θ to the positive real axis in the complex F_e-plane. Again by the theory of linear programming it suffices to consider functions $F_e(s)$ of the form (27.48). This leaves one free parameter, namely, s_0, which may be varied to obtain bounds on the quantity given by (27.49). As θ is varied these bounds imply that the value of $F_e(s)$ is contained in the convex hull of the set of points generated by (27.48) as s_0 varies between 0 and 1. When translated to bounds on σ_e, this implies that σ_e is confined to the region bounded by the circular arc $\mathrm{Arc}(\sigma_1,\sigma_2, 0)$ and the straight line $\mathrm{Arc}(\sigma_1,\sigma_2, \infty)$.

In principle this method can be extended to incorporate the $J + 1$ known series expansion coefficients $r_0,r_1,\ldots,r_J$ and the $K+2I$ known values of the function. These impose $J+K+2I$

additional linear constraints on the residues B_i, and the theory of linear programming implies that all but $J+K+2I+1$ of the residues can be taken to be zero. This reduces the problem to a finite-dimensional one, but complications arise because the quantity to be optimized depends nonlinearly on the positions of the remaining poles. By allowing variations in their positions one would like to show that approximately half of the remaining $J + K + 2I + 1$ residues can be set equal to zero, but there seems to be no simple way of establishing this within the framework of the method. So let us turn to another approach that is not beset by these difficulties.

27.11. Proving the bounds using the method of variation of poles and zeros

The method of variation of poles and zeros (Milton 1981a, 1981c) is a general method that can be applied to bound any rational function of fixed degree, provided we have some information concerning the location of the poles and zeros of the function. A recent novel application has been to provide a generalization of the well-known Kramers-Kronig relations (Jackson 1975), which for any isotropic material relate the real and imaginary parts of the complex electrical permittivity $\varepsilon(\omega)$ as functions of the frequency ω. (The real and imaginary parts are essentially Hilbert transforms over ω of each other.) The method has been used to obtain bounds on the real part of $\varepsilon(\omega)$ over a frequency interval given measurements of the imaginary part over the same frequency interval and given the real part at a few selected frequencies within this interval (Milton, Eyre, and Mantese 1997). These bounds tighten and reduce to the familiar Kramers-Kronig relations in the limit as the measured frequency interval extends over the entire frequency range, from zero to infinite frequencies. Unfortunately a detailed discussion of these bounds is beyond the scope of this book.

It is convenient to introduce the variable

$$\tau = 1/\varrho = 1 - 2s = \frac{\sigma_1 + \sigma_2}{\sigma_1 - \sigma_2},$$

which (like ϱ but unlike s) has the appealing property that it transforms to $-\tau$ when we replace σ_1 and σ_2 by $1/\sigma_1$ and $1/\sigma_2$ or when we swap σ_1 with σ_2, and has the additional property (like s but unlike ϱ) that negative real values of σ_1/σ_2 correspond to values of τ along a finite interval of the real axis, namely, the interval between -1 and 1. This second property is useful because it means that the poles and zeros of the rational approximate to the function

$$\sigma_e(\tau) \equiv \sigma_e(\sigma_1, 1) = \sigma_e((1+\tau)/(1-\tau), 1) \tag{27.50}$$

are confined to this finite interval. As usual, because of the homogeneity of the function, we have chosen to set $\sigma_2 = 1$.

Since the rational approximate takes the value $r_0 = 1$ at $\tau = \infty$, it has the representation

$$\sigma_e(\tau) = r_0 \frac{(\tau-\tau_1)(\tau-\tau_3)\dots(\tau-\tau_{2m-1})}{(\tau-\tau_2)(\tau-\tau_4)\dots(\tau-\tau_{2m})}, \quad \text{where } r_0 = 1, \tag{27.51}$$

in which the τ_i are the zeros, for odd i, and poles, for even i, of the function. Since the imaginary part of the rational function $\sigma_e(\tau)$ takes the opposite sign as the imaginary part of τ, it follows that the poles and zeros must necessarily be simple and located on the real axis [because $\mathrm{Im}(\sigma_e)$ changes sign around a pole or zero and the number of times it changes sign is determined by the multiplicity of the pole or zero]. Also from this argument we deduce that

the poles must have residues that are real and nonnegative and by continuity of the function $\sigma_e(\tau)$ there must be a zero located between every pair of poles. Finally, because $\sigma_e(\sigma_1, 1)$ takes positive finite values whenever σ_1 is positive, these poles and zeros must be located between -1 and 1, with a pole nearest $\tau = 1$ and a zero nearest $\tau = -1$. In other words, the poles and zeros are real and satisfy the inequalities

$$1 \geq \tau_{2m} \geq \tau_1 \geq \tau_{2m-2} \geq \tau_3 \ldots \geq \tau_{2m-3} \geq \tau_2 \geq \tau_{2m-1} \geq -1, \tag{27.52}$$

where the unusual labeling of indices has been chosen to simplify subsequent formulas.

We remark in passing that when $\sigma_e(\tau)$ is not a rational function the representation that generalizes (27.51) is

$$\log \sigma_e(\tau) = \log r_0 + \int_{-1}^{+1} \frac{d\nu(y)}{\tau - y}, \tag{27.53}$$

where $\nu(y)$ is a positive measure satisfying the constraint

$$0 \leq \int_{-1}^{+1} g(y) d\nu(y) \leq \int_{-1}^{+1} g(y) dy$$

for all smooth positive test functions $g(y)$. In particular, if the measure is smooth and $d\nu(y) = h(y)dy$ for some function $h(y)$, then this condition imposes the constraint that

$$0 \leq h(y) \leq 1 \text{ for all } y.$$

The characteristic function measure $d\nu(y) = h(y)dy$, where

$$\begin{aligned} h(y) &= 1 \text{ if } \tau_{2m-2i} \geq y \geq \tau_{2i+1} \text{ for some } i = 0, 1, 2, \ldots, m-1, \\ &= 0 \text{ otherwise,} \end{aligned}$$

when substituted in (27.53) gives

$$\begin{aligned} \log \sigma_e(\tau) &= \log r_0 + \sum_{i=0}^{m-1} \int_{\tau_{2i+1}}^{\tau_{2m-2i}} \frac{dy}{\tau - y} \\ &= \log r_0 + \sum_{i=0}^{m-1} \log(\tau - \tau_{2i+1}) - \log(\tau - \tau_{2m-2i}), \end{aligned}$$

which corresponds to the logarithm of the rational function (27.51).

Now the object is to find the range of values that σ_e can take, with τ held fixed, as the poles and zeros are varied over all configurations compatible with (27.52) and any other known constraints on the analytic function. We have already observed in section 27.9 on page 589 that it suffices to establish the bounds that incorporate r_0 and a set of $H = K + 2I + J$ known values of the function, since the other bounds can be generated from these bounds. The known values of the function translate into restrictions on the possible positions of the zeros and poles:

$$g_n = r_0 \frac{(t_n - \tau_1)(t_n - \tau_3) \ldots (t_n - \tau_{2m-1})}{(t_n - \tau_2)(t_n - \tau_4) \ldots (t_n - \tau_{2m})}, \quad \text{for } n = 1, 2, \ldots, H, \tag{27.54}$$

where $g_n = \sigma_{en}/\sigma_{2n}$ and $t_n = (\sigma_{1n} + \sigma_{2n})/(\sigma_{1n} - \sigma_{2n})$.

Let us begin by considering the problem of finding bounds on σ_e when σ_1 is real and $\sigma_2 = 1$. The goal is to find the supremum (or infimum) of σ_e as the poles and zeros are varied over all configurations compatible with (27.52) and (27.54) with τ held fixed. Since the set of points $(\tau_1, \tau_2, \ldots, \tau_{2m})$ in $2m$-dimensional parameter space where these constraints are satisfied is a compact set, the supremum (or infimum) of σ_e is surely achieved at some (not necessarily unique) point $(\tau_1', \tau_2', \ldots, \tau_{2m}')$. Now if the position of a pole happens to coincide with the position of a zero, we can cancel this common factor from the numerator and denominator in (27.51) and reduce the degree m by 1. Accordingly, by reducing the value of m as necessary, we can assume that

$$1 \geq \tau_{2m}' > \tau_1' > \tau_{2m-2}' > \tau_3' \ldots > \tau_{2m-3}' > \tau_2' > \tau_{2m-1}' \geq -1. \tag{27.55}$$

The next step is to explore the effect on σ_e when we perturb the positions of the poles and zeros while still maintaining the constraints (27.54).

For simplicity, let us first consider the problem of finding bounds on σ_e for the case $H = 1$, with real positive values of σ_{en}, σ_{1n} and σ_{2n} for $n = 1$. Thus we have $g_1 > 0$ and $|t_1| > 1$. Let us choose τ_1 as our dependent variable to be determined from the constraint (27.54) with $n = 1$. Accordingly we take $(\tau_2, \tau_3, \ldots, \tau_{2m})$ as our set of $2m-1$ independent variables. (There is some freedom in the choice of independent and dependent variables, but we require that τ_{2m} and τ_{2m-1} be kept independent to make it easier to keep track of the constraints $1 \geq \tau_{2m}$ and $\tau_{2m-1} \geq -1$. We took an unusual indexing of the poles and zeros to ensure that the constrained pole and constrained zero are last in the sequence.) The implicit function theorem implies that the equation (27.54) with $n = 1$ has a solution for τ_1 in terms of the independent variables, at least for $(\tau_1, \tau_2, \ldots, \tau_{2m})$ in a neighborhood of the point $(\tau_1', \tau_2', \ldots, \tau_{2m}')$, provided that the partial derivative

$$J = \frac{\partial g_1}{\partial \tau_1} = \frac{-g_1}{t_1 - \tau_1}$$

is nonzero when we set $(\tau_1, \tau_2, \ldots, \tau_{2m})$ equal to $(\tau_1', \tau_2', \ldots, \tau_{2m}')$. Since $g_1 > 0$, $|t_1| > 1$, and $|\tau_1| \leq 1$, it is clear that this condition is always satisfied.

Now let us examine the derivative of σ_e with respect to one of the independent variables, say, τ_i with $i \neq 1$, while keeping the remaining independent variables fixed. By differentiating (27.51) and the constraint (27.54) with respect to τ_i we obtain the pair of equations

$$\begin{aligned} \frac{D\sigma_e}{D\tau_i} + \frac{\sigma_e}{\tau - \tau_1}\frac{D\tau_1}{D\tau_i} &= \frac{(-1)^i \sigma_e}{\tau - \tau_i}, \\ \frac{g_1}{t_1 - \tau_1}\frac{D\tau_1}{D\tau_i} &= \frac{(-1)^i g_1}{t_1 - \tau_i}, \end{aligned}$$

where $D/D\tau_i$ denotes the derivative with respect to τ_i while keeping the remaining independent variables fixed and adjusting τ_1 so that the constraint (27.54) with $n = 1$ remains satisfied. From these equations we see that

$$\frac{D\sigma_e}{D\tau_i} = \frac{(-1)^i \sigma_e (\tau - t_1)(\tau_1 - \tau_i)}{(\tau - \tau_i)(\tau - \tau_1)(t_1 - \tau_i)}. \tag{27.56}$$

The key point is that this derivative is never zero. For a maximum (or minimum) of σ_e to occur at $(\tau_1', \tau_2', \ldots, \tau_{2m}')$ we are left with two possibilities: either the independent variable is constrained, that is, $m = 1$ and $\tau_2' = 1$, or the dependent variable is constrained, that is, $m = 1$

and $\tau_1' = -1$. The remaining parameter, τ_1' or τ_2', is then determined by the constraint (27.54) with $n = 1$. These two possibilities correspond to the bounds $U_{0,1}$ and $V_{0,1}$ given by (27.16).

When σ_1 and hence τ is complex we look for points $(\tau_1', \tau_2', \ldots, \tau_{2m}')$ such that σ_e is at the boundary of its range of possible values. At such points, the derivatives $D\sigma_e/D\tau_i$ and $D\sigma_e/D\tau_j$ (where τ_i and τ_j are two real independent variables), if both nonzero, must be such that

$$\arg\frac{D\sigma_e}{D\tau_i} = \arg\frac{D\sigma_e}{D\tau_j},$$

since otherwise σ_e could be pushed outside the boundary by small variations in τ_i and τ_j. However, from (27.56) we see that the condition can never be satisfied because $\arg(\tau - \tau_i) \neq \arg(\tau - \tau_j)$ when τ is complex and $i \neq j$. Therefore for σ_e to be on the boundary there can be only one unconstrained independent parameter. Either $m = 1$ and the bound is generated as τ_2 is varied (while adjusting the dependent variable τ_1 so that the constraint remains satisfied) or $m = 2$, $\tau_4 = 1$, $\tau_3 = -1$ and the bound is generated as τ_2 is varied (while adjusting τ_1 so that the constraint remains satisfied). These two possibilities correspond to the bounds (27.22) as v and w are varied.

The success of this method hinges on the factorization of the derivative $D\sigma_e/D\tau_i$ into a product of nonzero factors as in (27.56). Remarkably, this factorization carries through even when there are additional constraints on the function of the form (27.54), that is, when $H > 1$.

Let us now examine the general case and choose $(\tau_1, \tau_2, \ldots, \tau_H)$ as our set of H dependent variables to be determined from the H equations (27.54) and $(\tau_{H+1}, \tau_{H+2}, \ldots, \tau_{2m})$ as our set of $2m - H$ independent variables. The implicit function theorem implies that the equations (27.54) have a solution for the dependent variables in terms of the independent ones, at least for $(\tau_1, \tau_2, \ldots, \tau_{2m})$ in a neighborhood of the point $(\tau_1', \tau_2', \ldots, \tau_{2m}')$, provided that the Jacobian

$$J = \begin{vmatrix} \frac{-g_1}{t_1-\tau_1} & \frac{g_1}{t_1-\tau_2} & \frac{-g_1}{t_1-\tau_3} & \cdots & \frac{(-1)^H g_1}{t_1-\tau_H} \\ \frac{-g_2}{t_2-\tau_1} & \frac{g_2}{t_2-\tau_2} & \frac{-g_2}{t_2-\tau_3} & \cdots & \frac{(-1)^H g_2}{t_2-\tau_H} \\ \vdots & \vdots & & \vdots & \\ \frac{-g_H}{t_H-\tau_1} & \frac{g_H}{t_H-\tau_2} & \frac{-g_H}{t_H-\tau_3} & \cdots & \frac{(-1)^H g_H}{t_H-\tau_H} \end{vmatrix} \tag{27.57}$$

is nonzero when we set $(\tau_1, \tau_2, \ldots, \tau_{2m})$ equal to $(\tau_1', \tau_2', \ldots, \tau_{2m}')$.

Aside from the factors of $g_1, g_2, \ldots, g_H$ and the signs of each column, which are easily factored out, this is a Cauchy matrix for which an exact formula is available for the determinant [see, for example, Noble (1969) and Lax (1997)] and we have

$$J = \frac{h\left[\prod_{n=1}^{H} g_n\right]\left[\prod_{n=1}^{H-1} p_n q_n\right]}{\prod_{k=1}^{H}\prod_{\ell=1}^{H}(t_k - \tau_\ell)}, \tag{27.58}$$

where

$$p_n = \prod_{k=n+1}^{H}(t_n - t_k), \quad q_n = \prod_{k=n+1}^{H}(\tau_n - \tau_k)$$

and h is the sign factor

$$\begin{aligned} h &= -1 \text{ if } H = 1 \text{ or } 2 \bmod 4, \\ &= +1 \text{ if } H = 0 \text{ or } 3 \bmod 4, \end{aligned}$$

arising from the minus signs in the columns.

From the inequalities (27.21) and (27.55) it is now clear that the Jacobian as given by (27.58) is nonzero when we set $(\tau_1, \tau_2, \ldots, \tau_{2m})$ equal to $(\tau'_1, \tau'_2, \ldots, \tau'_{2m})$. Now by differentiating (27.51) and (27.54) with respect to the independent variable τ_i, with $i \geq H+1$, we obtain the set of equations

$$\begin{pmatrix} -1 & \frac{-\sigma_e}{\tau-\tau_1} & \frac{\sigma_e}{\tau-\tau_2} & \frac{-\sigma_e}{\tau-\tau_3} & \cdots & \frac{(-1)^H\sigma_e}{\tau-\tau_H} \\ 0 & \frac{-g_1}{t_1-\tau_1} & \frac{g_1}{t_1-\tau_2} & \frac{-g_1}{t_1-\tau_3} & \cdots & \frac{(-1)^H g_1}{t_1-\tau_H} \\ 0 & \frac{-g_2}{t_2-\tau_1} & \frac{g_2}{t_2-\tau_2} & \frac{-g_2}{t_2-\tau_3} & \cdots & \frac{(-1)^H g_2}{t_2-\tau_H} \\ \vdots & \vdots & \vdots & \vdots & & \vdots \\ 0 & \frac{-g_H}{t_H-\tau_1} & \frac{g_H}{t_H-\tau_2} & \frac{-g_H}{t_H-\tau_3} & \cdots & \frac{(-1)^H g_H}{t_H-\tau_H} \end{pmatrix} \begin{pmatrix} D\sigma_e/D\tau_i \\ D\tau_1/D\tau_i \\ D\tau_2/D\tau_i \\ D\tau_3/D\tau_i \\ \vdots \\ D\tau_H/D\tau_i \end{pmatrix} = (-1)^{i+1} \begin{pmatrix} \frac{\sigma_e}{\tau-\tau_i} \\ \frac{g_1}{t_1-\tau_i} \\ \frac{g_2}{t_2-\tau_i} \\ \vdots \\ \frac{g_H}{t_H-\tau_i} \end{pmatrix}, \tag{27.59}$$

where $D/D\tau_i$ denotes the derivative with respect to τ_i while keeping the remaining independent variables fixed and adjusting the dependent variables so that the constraints (27.54) remain satisfied. Using Cramer's rule, the solution to these equations for $D\sigma_e/D\tau_i$ can be expressed as the ratio of two determinants of the form (27.57), and with the aid of the formula (27.58) for such determinants we see that

$$\frac{D\sigma_e}{D\tau_i} = \frac{(-1)^i\sigma_e\left[\prod_{n=1}^H(\tau - t_n)\right]\left[\prod_{n=1}^H(\tau_n - \tau_i)\right]}{(\tau-\tau_i)\left[\prod_{n=1}^H(t_n-\tau_i)\right]\left[\prod_{n=1}^H(\tau-\tau_n)\right]}. \tag{27.60}$$

This derivative is clearly never zero when $(\tau_1, \tau_2, \ldots, \tau_{2m})$ is set equal to $(\tau'_1, \tau'_2, \ldots, \tau'_{2m})$. It follows that for a maximum (or minimum) of σ_e to occur when σ_1 is real there can be no unconstrained independent variables. If H is even, then either $2m = H$ and there are no independent variables, or $2m = H+2$ and the two independent variables must be constrained, that is, $\tau'_{2m} = 1$ and $\tau'_{2m-1} = -1$. If H is odd, then $2m = H+1$ and one variable must be constrained, that is, $\tau'_{2m} = 1$ or $\tau'_{2m-1} = -1$. In either case the rational functions correspond to the upper and lower bounds $U_{0,H}$ and $V_{0,H}$. Similarly, when σ_1 is complex there can be only one unconstrained independent variable when σ_e is at the boundary of its range of possible values because $\arg(\tau - \tau_i)$ and $\arg(\tau - \tau_j)$ are different when $i \neq j$. When some of the t_n and known values $g_n = \sigma_e(t_n)$ are not real but occur in complex conjugate pairs the same arguments apply because the product $\prod_{n=1}^H(t_n - \tau_i)$ remains real. As a consequence, the method of variation of poles and zeros yields all of the bounds discussed in this chapter.

References

Aspnes, D. E. 1982. Bounds on allowed values of the effective dielectric function of two-component composites at finite frequencies. *Physical Review B (Solid State)* 25:1358–1361. {*569, 596*}

Baker, Jr., G. A. 1969. Best error bounds for Padé approximants to convergent series of Stieltjes. *Journal of Mathematical Physics* 10(5):814–820. {*571, 596, 603, 617*}

Baker, Jr., G. A. 1975. *Essentials of Padé Approximants*, pp. 288–291. New York: Academic Press. ISBN 0-12-074855-X. {*370, 392, 571, 578, 596*}

Baker, Jr., G. A. and P. R. Graves-Morris 1981. *Padé Approximants: Basic Theory. Part I. Extensions and Applications. Part II*. Reading, Massachusetts: Addison-Wesley. xviii + 215 pp. ISBN 0-201-13512-4 (part 1), 0-521-30233-1 (part 1), 0-201-13513-2 (part 2), 0-521-30234-X (part 2). {*571, 596*}

Beran, M. J. 1965. Use of the variational approach to determine bounds for the effective permittivity in random media. *Nuovo Cimento* 38:771–782. {*553, 564, 574, 577, 597*}

Beran, M. J. and J. Molyneux 1966. Use of classical variational principles to determine bounds for the effective bulk modulus in heterogeneous media. *Quarterly of Applied Mathematics* 24:107–118. {*553, 557, 564, 589, 597*}

Bergman, D. J. 1976. Variational bounds on some bulk properties of a two-phase composite material. *Physical Review B (Solid State)* 14:1531–1542. {*457, 491, 580, 581, 597*}

Bergman, D. J. 1978. The dielectric constant of a composite material — A problem in classical physics. *Physics Reports* 43(9):377–407. {*341, 352, 370, 371, 376, 377, 379, 382, 387, 390, 392, 569, 581, 590, 597, 603, 617*}

Bergman, D. J. 1980. Exactly solvable microscopic geometries and rigorous bounds for the complex dielectric constant of a two-component composite material. *Physical Review Letters* 44:1285–1287. {*452, 453, 478, 491, 569, 577, 588, 597*}

Bergman, D. J. 1982. Rigorous bounds for the complex dielectric constant of a two-component composite. *Annals of Physics* 138(1):78–114. {*129, 139, 569, 597*}

Bergman, D. J. 1986. The effective dielectric coefficient of a composite medium: Rigorous bounds from analytic properties. In J. L. Ericksen, D. Kinderlehrer, R. Kohn, and J.-L. Lions (eds.), *Homogenization and Effective Moduli of Materials and Media*, pp. 27–51. Berlin / Heidelberg / London / etc.: Springer-Verlag. ISBN 0-387-96306-5. {*451, 453, 571, 597, 603, 604, 617, 638, 641*}

Bergman, D. J. 1993. Hierarchies of Stieltjes functions and their application to the calculation of bounds for the dielectric constant of a two-component composite medium. *SIAM Journal on Applied Mathematics* 53(4):915–930. {*571, 597, 603, 604, 608, 610, 617*}

Bergman, D. J. and L. G. Fel 1999. Enhancement of thermoelectric power factor in composite thermoelectrics. *Journal of Applied Physics* 85(12):8205–8217. {*3, 15, 97, 110, 580, 597*}

Bruno, O. P. 1991. The effective conductivity of strongly heterogeneous composites. *Proceedings of the Royal Society of London. Series A, Mathematical and Physical Sciences* 433(1888):353–381. {*306, 310, 373, 392, 569, 597*}

Bruno, O. P. and P. H. Leo 1992. On the stiffness of materials containing a disordered array of microscopic holes or hard inclusions. *Archive for Rational Mechanics and Analysis* 121(4):303–338. {*372, 373, 392, 569, 597*}

Cherkaeva, E. and K. Golden 1998. Inverse bounds for microstructural parameters of composite media derived from complex permittivity measurements. *Waves in Random Media* 8(4):437–450. {*569, 597*}

Dantzig, G. B. 1998. *Linear Programming and Extensions*. Princeton, New Jersey: Princeton University Press. xvi + 627 pp. ISBN 0-691-08000-3. {*591, 597*}

Eyre, D. J., G. W. Milton, and R. Lakes 2001. Bounds for interpolating complex effective moduli of viscoelastic materials from measured data. *Rheologica acta*. To appear. {*583, 597*}

Felderhof, B. U. 1984. Bounds for the complex dielectric constant of a two-phase composite. *Physica A* 126:430–442. {*571, 597*}

Field, D. A. 1976. Series of Stieltjes, Padé approximants and continued fractions. *Journal of Mathematical Physics* 17:843–844. {*571, 598*}

Golden, K. 1995. Bounds on the complex permittivity of sea ice. *Journal of Geophysical Research (Oceans)* 100(C7):13699–13711. {*569, 598*}

Golden, K. 1998. The interaction of microwaves with sea ice. In G. Papanicolaou (ed.), *Wave Propagation in Complex Media*, pp. 75–94. Berlin / Heidelberg / London / etc.: Springer-Verlag. ISBN 0-387-98309-0. {*569, 598*}

Golden, K. and G. Papanicolaou 1983. Bounds for effective parameters of heterogeneous media by analytic continuation. *Communications in Mathematical Physics* 90(4):473–491. {*11, 12, 15, 248, 268, 370, 376, 393, 571, 598, 603, 617*}

Gragg, W. B. 1968. Truncation error bounds for g-fractions. *Numerische Mathematik* 11: 370–379. {*571, 598*}

Hashin, Z. and S. Shtrikman 1962. A variational approach to the theory of the effective magnetic permeability of multiphase materials. *Journal of Applied Physics* 33:3125–3131. {*113, 116, 140, 271, 279, 287, 347, 350, 353, 457, 458, 460, 493, 574, 586, 598*}

Helsing, J. 1994a. Fast and accurate calculations of structural parameters for suspensions. *Proceedings of the Royal Society of London. Series A, Mathematical and Physical Sciences* 445:127–140. {*39, 42, 210, 216, 571, 598*}

Helsing, J. 1994b. Improved bounds on the conductivity of composites by interpolation. *Proceedings of the Royal Society of London. Series A, Mathematical and Physical Sciences* 444:363–374. {*490, 493, 569, 598*}

Helsing, J. 1998. A high-order accurate algorithm for electrostatics of overlapping disks. *Journal of Statistical Physics* 90(5–6):1461–1473. {*39, 40, 43, 155, 156, 320, 337, 586, 598*}

Jackson, J. D. 1975. *Classical Electrodynamics* (Second ed.). New York / London / Sydney, Australia: John Wiley and Sons. xxii + 848 pp. ISBN 0-471-43132-X. {*224, 228, 243, 592, 598*}

Jeulin, D. and L. Savary 1997. Effective complex permittivity of random composites. *Journal de physique* 7(9):1123–1142. {*577, 598*}

Kantor, Y. and D. J. Bergman 1984. Improved rigorous bounds on the effective elastic moduli of a composite material. *Journal of the Mechanics and Physics of Solids* 32: 41–62. {*248, 268, 569, 598, 603, 617*}

Kim, I. C. and S. Torquato 1990. Determination of the effective conductivity of heterogeneous media by Brownian motion simulation. *Journal of Applied Physics* 68(8):3892–3903. {*40, 43, 586, 598*}

Korringa, J. and G. A. LaTorraca 1986. Application of the Bergman-Milton theory of bounds to the permittivity of rocks. *Journal of Applied Physics* 60:2966–2976. {*569, 598*}

Lax, P. D. 1997. *Linear Algebra*, pp. 222–223. New York: Wiley-Interscience. ISBN 0-471-11111-2. {*595, 598*}

Mantese, J. V., A. L. Micheli, D. F. Dungan, R. G. Geyer, J. Baker-Jarvis, and J. Grosvenor 1996. Applicability of effective medium theory to ferroelectric/ferromagnetic composites with composition and frequency-dependent complex permittivities and permeabilities. *Journal of Applied Physics* 79(3):1655–1660. {*569, 598*}

McPhedran, R. C., D. R. McKenzie, and G. W. Milton 1982. Extraction of structural information from measured transport properties of composites. *Applied Physics A* 29: 19–27. {*569, 599*}

McPhedran, R. C. and G. W. Milton 1981. Bounds and exact theories for the transport properties of inhomogeneous media. *Applied Physics A* 26:207–220. {*39, 44, 317, 331, 333, 337, 571, 575–577, 583, 599*}

McPhedran, R. C. and G. W. Milton 1990. Inverse transport problems for composite media. *Materials Research Society Symposium Proceedings* 195:257–274. {*569, 599*}

Milton, G. W. 1979. Theoretical studies of the transport properties of inhomogeneous media. Unpublished report TP/79/1, University of Sydney, Sydney, Australia. 1–65 pp. Unpublished report. (Available on request from the author). {*370, 394, 569, 577, 599*}

Milton, G. W. 1980. Bounds on the complex dielectric constant of a composite material. *Applied Physics Letters* 37(3):300–302. {*124, 140, 452, 454, 478, 494, 569, 570, 577, 588, 599*}

Milton, G. W. 1981a. Bounds on the complex permittivity of a two-component composite material. *Journal of Applied Physics* 52(8):5286–5293. {*118, 120, 124, 125, 129, 140, 370, 394, 569, 588, 589, 592, 599*}

Milton, G. W. 1981b. Bounds on the electromagnetic, elastic, and other properties of two-component composites. *Physical Review Letters* 46(8):542–545. {*397, 399, 412, 474, 494, 553, 566, 577, 599*}

Milton, G. W. 1981c. Bounds on the transport and optical properties of a two-component composite material. *Journal of Applied Physics* 52(8):5294–5304. {*371, 379, 382, 394, 553, 566, 569, 574, 581, 583, 586, 587, 592, 599, 610, 617*}

Milton, G. W. 1982. Bounds on the elastic and transport properties of two-component composites. *Journal of the Mechanics and Physics of Solids* 30(3):177–191. {*322, 330–332, 338, 553, 558, 566, 586, 599*}

Milton, G. W. 1986. Modeling the properties of composites by laminates. In J. L. Ericksen, D. Kinderlehrer, R. Kohn, and J.-L. Lions (eds.), *Homogenization and Effective Moduli of Materials and Media*, pp. 150–174. Berlin / Heidelberg / London / etc.: Springer-Verlag. ISBN 0-387-96306-5. {*206, 218, 384, 394, 463, 471, 472, 494, 578, 599, 603, 617*}

Milton, G. W., D. J. Eyre, and J. V. Mantese 1997. Finite frequency range Kramers-Kronig relations: Bounds on the dispersion. *Physical Review Letters* 79(16):3062–3065. {*592, 599*}

Milton, G. W. and R. C. McPhedran 1982. A comparison of two methods for deriving bounds on the effective conductivity of composites. In R. Burridge, S. Childress, and G. Papanicolaou (eds.), *Macroscopic Properties of Disordered Media: Proceedings of a Conference Held at the Courant Institute, June 1–3, 1981*, pp. 183–193. Berlin / Heidelberg / London / etc.: Springer-Verlag. ISBN 0-387-11202-2. {*571, 599*}

Milton, G. W., R. C. McPhedran, and D. R. McKenzie 1981. Transport properties of arrays of intersecting cylinders. *Applied Physics* 25:23–30. {*40, 45, 571, 599*}

Niklasson, G. A. and C. G. Granqvist 1984. Optical properties and solar selectivity of coevaporated C*o*–Al_2O_3 composite films. *Journal of Applied Physics* 55:3382–3410. {*569, 599*}

Noble, B. 1969. *Applied Linear Algebra*, pp. 223–224. Upper Saddle River, New Jersey: Prentice-Hall. {*595, 600*}

Pham, D. C. 1997. Overall properties of planar quasisymmetric randomly inhomogeneous media: Estimates and cell models. *Physical Review E (Statistical Physics, Plasmas, Fluids, and Related Interdisciplinary Topics)* 56(1):652–660. {*553, 567, 586, 600*}

Prager, S. 1969. Improved variational bounds on some bulk properties of a two-phase random medium. *Journal of Chemical Physics* 50:4305–4312. {*580, 589, 600*}

Sangani, A. S. and C. Yao 1988a. Bulk thermal conductivity of composites with spherical inclusions. *Journal of Applied Physics* 63(5):1334–1341. {*39, 46, 331, 338, 571, 575, 600*}

Sangani, A. S. and C. Yao 1988b. Transport processes in random arrays of cylinders. I Thermal conduction. *Physics of Fluids* 31(9):2426–2434. {*39, 46, 333, 338, 571, 575, 600*}

Sawicz, R. and K. Golden 1995. Bounds on the complex permittivity of matrix-particle composites. *Journal of Applied Physics* 78(12):7240–7246. {*569, 600*}

Schulgasser, K. 1977. Bounds on the conductivity of statistically isotropic polycrystals. *Journal of Physics C: Solid State Physics* 10:407–417. {*47, 51, 58, 438–440, 454, 589, 600*}

Schulgasser, K. and Z. Hashin 1976. Bounds for effective permittivities of lossy dielectric composites. *Journal of Applied Physics* 47:424–427. {*569, 600*}

Tokarzewski, S. 1994. Inequalities for the effective transport coefficients of two-component composite materials. *Archives of Mechanics = Archiwum Mechaniki Stosowanej* 46(5): 611–623. {*571, 578, 600*}

Tokarzewski, S. 1996. Two-point Padé approximants for the expansions of Stieltjes functions in real domain. *Journal of Computational and Applied Mathematics* 67(1):59–72. {*590, 600*}

Tokarzewski, S., J. Bławzdziewicz, and I. Andrianov 1994. Two-point Padé approximants for formal Stieltjes series. *Numerical Algorithms* 8(2–4):313–328. {*590, 600*}

Tokarzewski, S. and J. J. Telega 1997. *S*-continued fraction method for the investigation of a complex dielectric constant of two-components composite. *Acta Applicandae Mathematicae* 49(1):55–83. {*39, 46, 575, 577, 600*}

Tokarzewski, S. and J. J. Telega 1998. Bounds on effective moduli by analytical continuation of the Stieltjes function expanded at zero and infinity. *Zeitschrift für Angewandte Mathematik und Physik = Journal of Applied Mathematics and Physics* 49(1):137–155. {*590, 600*}

Torquato, S. 1985. Effective Electrical Conductivity of two-phase disordered composite media. *Journal of Applied Physics* 58:3790–3797. {*578, 600*}

Torquato, S. and J. D. Beasley 1986. Effective properties of fiber-reinforced materials. I. Bounds on the thermal conductivity of dispersions of fully penetrable cylinders. *International Journal of Engineering Science* 24(3):415–434. {*333, 339, 586, 600*}

Torquato, S., I. C. Kim, and D. Cule 1999. Effective conductivity, dielectric constant, and diffusion coefficient of digitized composite media via first-passage-time equations. *Journal of Applied Physics* 85(3):1560–1571. {*40, 46, 207, 219, 586, 600*}

Torquato, S. and F. Lado 1988. Bounds on the conductivity of a random array of cylinders. *Proceedings of the Royal Society of London. Series A, Mathematical and Physical Sciences* 417:59–80. {*333, 339, 586, 601*}

Wiener, O. 1912. Die Theorie des Mischkörpers für das Feld des stationären Strömung. Erste Abhandlung die Mittelswertsätze für Kraft, Polarisation und Energie. (German) [The theory of composites for the field of steady flow. First treatment of mean value estimates for force, polarization and energy]. *Abhandlungen der mathematisch-physischen Klasse der Königlich Sächisischen Gesellschaft der Wissenschaften* 32: 509–604. {*574, 601*}

28

Fractional linear transformations as a tool for generating bounds†

The method of variation of poles and zeros discussed in the previous chapter is a powerful tool that can be applied to bound any rational function of fixed degree provided that we have some information on the location of the poles and zeros of that function. For those special classes of analytic functions appropriate to composites there is another approach based on the use of fractional linear transformations. This approach has the advantage that it is easily generalized to matrix-valued analytic functions, and in particular to the matrix-valued conductivity tensor of anisotropic composites. Fractional linear transformations were used by Bergman (1978) as a tool in deriving some of the elementary bounds. In 1980, following remarks of Jim Berryman and John Wilkins (private communication), I became aware of the large body of literature on bounding Stieltjes functions and realized that the fractional linear transformations of Baker, Jr. (1969), among others, provided an alternative proof of many of the bounds discussed in the previous chapter. Independently, Golden and Papanicolaou (1983), Kantor and Bergman (1984), and Bergman (1986, 1993) recognized that one could use fractional linear transformations to generate most of the hierarchies of bounds discussed in the last chapter. Their fractional linear transformations are similar to the ones used by Baker, Jr. (1969); see the appendix in Milton (1986).

The hierarchical structure of the bounds on σ_e, as a nested sequence of intervals on the real line, or as a nested sequence of lens-shaped regions in the complex plane, suggests that there may be some recursive method for deriving the bounds. We will see that certain fractional linear transformations provide a one-to-one correspondence between analytic functions that satisfy the required constraints (imposed by knowledge of the series expansion coefficients) and the larger class of functions that satisfy one less constraint. There is no contradiction here because there are an infinite number of such analytic functions. In some sense the situation is analogous to the way the set of even integers can be bought into one-to-one correspondence with the larger set of all integers through the mapping of halving them.

Affiliated with this correspondence between analytic functions is a correspondence between their associated bounds. We will see that knowledge of the appropriate fractional linear transformations and the elementary bounds (that do not incorporate any series expansion coefficients or known function values) allows us to generate the entire set of bounds.

28.1. Eliminating the constraints imposed by known series expansion coefficients

In this section we follow Golden and Papanicolaou (1983) and Bergman (1986, 1993). Let us revisit the problem of deriving bounds on σ_e for fixed values of σ_1 and σ_2 when one knows the

coefficients $r_0, r_1, \ldots, r_J$ in the series expansion (27.3). We begin by treating the case where only $r_0 = 1$ and $r_1 = f_1$ are known. Without loss of generality, let us assume that $\sigma_2 = 1$. Rather than examining the function $\sigma_e(\sigma_1, 1)$, it proves convenient, as in section 27.10 on page 590 of the previous chapter, to study the function

$$F_e(s) = 1 - \sigma_e(1 - 1/s, 1), \quad \text{where } s = 1/(1 - \sigma_1), \tag{28.1}$$

which has the integral representation

$$F_e(s) = \int_0^1 \frac{d\mu(y)}{s - y}, \tag{28.2}$$

incorporating a positive measure $d\mu(y)$.

By substituting the series expansion (27.3) for $\sigma_e(\sigma_1, 1)$ into the expression (28.1), and noting that $r_0 = 1$, we obtain an expansion for $F_e(s)$ in powers of $1/s$:

$$F_e(s) = \frac{\mu_0}{s} + \frac{\mu_1}{s^2} + \frac{\mu_2}{s^3} + \cdots, \quad \text{where } \mu_i = (-1)^{i+1} r_{i+1}.$$

Also by expanding the denominator in (28.2) in powers of $1/s$ we see that the moments of the measure can be identified with these series expansion coefficients:

$$\int_0^1 y^i d\mu(y) = \mu_i \geq 0 \text{ for all } i.$$

Consequently, knowing the series expansion coefficients $r_1, r_2, \ldots, r_J$ is equivalent to knowing the first J moments of the measure.

One other constraint on the measure follows from the nonnegativity of $\sigma_e(\sigma_1, 1)$ for all nonnegative values of σ_1, and in particular for $\sigma_1 = 0$. This implies that $F_e(1) \leq 1$ or, equivalently, that

$$1 \geq \int_0^1 \frac{d\mu(y)}{1 - y}. \tag{28.3}$$

One immediate consequence of this constraint is an upper bound on the magnitude of the zeroth moment μ_0:

$$\mu_0 = \int_0^1 d\mu(y) \leq \int_0^1 \frac{d\mu(y)}{1 - y} \leq 1.$$

We are ultimately interested in finding the range of values that $F_e(s)$ takes for a fixed value of s as the measure is varied subject to these constraints. Let us define $\mathcal{F}$ as the set of all functions $F_e(s)$ that can be expressed in the form (28.2) for some positive measure $d\mu$ satisfying (28.3), and let us define $\mathcal{F}(\mu_0)$ as the set of those functions in $\mathcal{F}$ with their measure having zeroth moment μ_0.

Now consider the transformation T_1 defined by its action on any function $F_e(s)$:

$$F_e^{(1)}(s) = T_1[F_e(s)] = \left[\frac{1}{\mu_0} - \frac{1}{s F_e(s)}\right] \frac{\mu_0}{1 - \mu_0}, \tag{28.4}$$

where, following Bergman (1986, 1993), the positive post-factor $\mu_0/(1 - \mu_0)$ has been introduced to ensure that the inequality $F_e^{(1)}(1) \leq 1$ holds if and only if $F_e(1) \leq 1$. We want to show that this transformation T_1 provides a one-to-one correspondence between functions in $\mathcal{F}(\mu_0)$ and functions in $\mathcal{F}$.

Our first objective is to establish that $F_e^{(1)}(s)$ necessarily lies in $\mathcal{F}$ when $F_e(s)$ lies in $\mathcal{F}(\mu_0)$. It is immediately clear from the integral representation (28.2) that $F_e(s)$ maps the upper half of the complex plane to the lower half-plane and maps the lower half-plane to the upper half-plane. Indeed, $\mathrm{Im}(s)$ and $\mathrm{Im}[1/(s-y)]$ have opposite signs for all real values of y. The key observation to make is that $sF_e(s)$ also shares this property. This is evident from its integral representation,

$$sF_e(s) = \int_0^1 \frac{d\mu(y)}{1 - y/s}, \tag{28.5}$$

because $\mathrm{Im}(s)$ and $\mathrm{Im}[1/(1-y/s)]$ have opposite signs for all real values of y.

Therefore $F_e^{(1)}(s)$ maps the upper half of the complex plane to the lower half-plane and maps the lower half-plane to the upper half-plane. Also, for real values of s we see from the integral representation that $F_e(s)$ is positive for $s > 1$ and negative for $s < 0$. Consequently, $sF_e(s)$ is nonzero (and positive) for all $s > 1$ and for all $s < 0$. It follows that $F_e^{(1)}(s)$ is analytic for all $s \notin [0, 1]$ and has an expansion

$$F_e^{(1)}(s) = \frac{\mu_0^{(1)}}{s} + \frac{\mu_1^{(1)}}{s^2} + \cdots \tag{28.6}$$

in powers of $1/s$, where

$$\mu_0^{(1)} = \frac{\mu_1}{\mu_0(1-\mu_0)}, \quad \mu_1^{(1)} = \frac{\mu_0\mu_2 - \mu_1^2}{\mu_0^2(1-\mu_0)}. \tag{28.7}$$

Notice that the effect of the transformation T_1 is to shift information in the series expansion: The coefficient μ_i, which enters the series expansion of $F_e(s)$ at order $i+1$, now enters the series expansion of $F_e^{(1)}(s)$ at order i.

From the series expansion (28.6) it is evident that $F_e^{(1)}(s)$ approaches zero (as $1/s$) as s tends to ∞. By applying the Cauchy integral formula as explained in section 18.3 on page 375, we obtain an integral formula

$$F_e^{(1)}(s) = \int_0^1 \frac{d\mu^{(1)}(y)}{s - y}, \tag{28.8}$$

for $F_e^{(1)}(s)$ in terms of a positive measure $d\mu^{(1)}(y)$. Also, from the inequality $1 \geq F_e(1)$ we deduce that $1 \geq F_e^{(1)}(1)$ or, equivalently, that

$$1 \geq \int_0^1 \frac{d\mu^{(1)}(y)}{1 - y}.$$

Therefore $F_e^{(1)}(s)$ lies in $\mathcal{F}$.

Conversely, let us suppose that we are given any function $F_e^{(1)}(s) \in \mathcal{F}$ with a series expansion

$$F_e^{(1)}(s) = \frac{\mu_0^{(1)}}{s} + \frac{\mu_1^{(1)}}{s^2} + \cdots \tag{28.9}$$

in powers of $1/s$. Let $\mu^{(1)}$ denote the measure associated with $F_e^{(1)}(s)$ as in (28.8). Applying the inverse transformation T_1^{-1} to $F_e^{(1)}(s)$ yields the function

$$F_e(s) = T_1^{-1}F_e^{(1)}(s) = \frac{\mu_0}{s - (1-\mu_0)sF_e^{(1)}(s)}. \tag{28.10}$$

Our objective now is to show that this function lies in $\mathcal{F}(\mu_0)$.

From the integral representation (28.8) for $F_e^{(1)}(s)$ we see that

$$sF_e^{(1)}(s) = \int_0^1 \frac{d\mu^{(1)}(y)}{1 - y/s}$$

maps the upper half of the complex plane to the lower half-plane and maps the upper half-plane to the lower half-plane. Because $\mathrm{Im}(s)$ and $-\mathrm{Im}[sF_e^{(1)}(s)]$ always have the same sign and because $1 - \mu_0$ is positive, it follows that $F_e(s)$ defined by (28.10) maps the upper half of the complex plane to the lower half-plane and maps the lower half-plane to the upper half-plane. Also, the integral representation (28.8) tells us that for real values of $s \notin [0, 1]$ $F_e^{(1)}(s)$ is less than $F_e^{(1)}(1)$ and this in turn is less than 1. Therefore the denominator in (28.10) does not vanish for any $s \notin [0, 1]$, implying that $F_e(s)$ is analytic for $s \notin [0, 1]$. By applying the Cauchy integral formula we obtain an integral representation for $F_e(s)$ of the form (28.2) for some positive measure $d\mu(y)$. From the inequality $F_e^{(1)}(1) \leq 1$ we deduce that $F_e(1) \leq 1$, and this implies that the measure satisfies the constraint (28.3). Finally, by substituting the series expansion (28.9) for $F_e^{(1)}(s)$ into (28.10) we see that $F_e(s)$ has an expansion

$$F_e(s) = \frac{\mu_0}{s} + \frac{\mu_0(1-\mu_0)\mu_0^{(1)}}{s^2} + \frac{\mu_0(1-\mu_0)\mu_0^{(2)} + \mu_0(1-\mu_0)^2[\mu_0^{(1)}]^2}{s^3} + \cdots.$$

Therefore $F_e(s)$ defined by (28.5) lies in $\mathcal{F}(\mu_0)$.

This proves that the transformation T_1 provides a one-to-one correspondence between functions in $\mathcal{F}(\mu_0)$ and functions in $\mathcal{F}$. Therefore the problem of finding the range of values that $F_e(s)$ takes when s is held fixed and the function is varied over all candidate functions in $\mathcal{F}(\mu_0)$ is equivalent to the problem of finding the range of values that $F_e^{(1)}(s)$ takes for that value of s as the function is varied over all candidate functions in the larger set $\mathcal{F}$. If $\mathcal{R}$ represents the range of values that $F_e^{(1)}(s)$ takes, then $T_1^{-1}\mathcal{R}$ will represent the range of values that $F_e(s)$ takes.

To find $\mathcal{R}$ we need to use one of the methods discussed in the previous chapter, such as the method of variation of poles and resides described in section 27.10 on page 590. This is easy because there are few constraints on the function. For example, when s is real and greater than 1 (i.e., when $1 = \sigma_2 > \sigma_1 > 0$), $\mathcal{R}$ consists of those real values of $F_e^{(1)}$ satisfying

$$0 \leq F_e^{(1)} \leq 1/s,$$

and $T_1^{-1}\mathcal{R}$ consists of those real values of F_e satisfying

$$\frac{\mu_0}{s} \leq F_e \leq \frac{\mu_0}{s - (1 - \mu_0)}. \tag{28.11}$$

Upon making the substitutions $\mu_0 = f_1$, $s = 1/(1-\sigma_1)$ and $F_e = 1 - \sigma_e$, we see that (28.11) implies the arithmetic and harmonic mean bounds:

$$f_1\sigma_1 + f_2 \geq \sigma_e \geq (f_1/\sigma_1 + f_2)^{-1}.$$

This procedure is easily extended to include higher order series expansion coefficients. For example, let us suppose that the value of the moments μ_0 and μ_1 are known. If $\mathcal{F}(\mu_0; \mu_1)$ denotes the set of those functions in $\mathcal{F}(\mu_0)$ with their measure having first moment μ_1, then from the series expansion (28.6) we see that T_1 provides a one-to-one correspondence between functions in $\mathcal{F}(\mu_0; \mu_1)$ and functions in $\mathcal{F}(\mu_0^{(1)})$.

In the same way that we defined the transformation T_1 through its action on the function $F_e(s) \in \mathcal{F}(\mu_0)$, let us define a transformation T_2 through its action on the function $F_e^{(1)}(s) \in \mathcal{F}(\mu_0^{(1)})$:

$$F_e^{(2)}(s) = T_2[F_e^{(1)}(s)] = \left[\frac{1}{\mu_0^{(1)}} - \frac{1}{sF_e^{(1)}(s)}\right]\frac{\mu_0^{(1)}}{(1-\mu_0^{(1)})}.$$

The preceding analysis shows that T_2 provides a one-to-one correspondence between functions in $\mathcal{F}(\mu_0^{(1)})$ and functions in $\mathcal{F}$. By combining these transformations we see that T_2T_1 provides a one-to-one correspondence between functions in $\mathcal{F}(\mu_0; \mu_1)$ and functions in $\mathcal{F}$. Consequently, for a given value of s, $T_1^{-1}T_2^{-1}\mathcal{R}$ represents the range of values that $F_e(s)$ takes as F_e varies over all functions in $\mathcal{F}(\mu_0; \mu_1)$.

The relation between F_e and

$$F_e^{(2)} = T_2T_1F_e$$

is conveniently expressed as a continued fraction:

$$F_e = T_1^{-1}T_2^{-1}F_e^{(2)} = \frac{\mu_0}{s-(1-\mu_0)sT_2^{-1}F_e^{(2)}} = \cfrac{\mu_0}{s-\cfrac{(1-\mu_0)\mu_0^{(1)}}{1-(1-\mu_0^{(1)})F_e^{(2)}}}. \tag{28.12}$$

To obtain the lower and upper bounds on F_e when s is real and greater than 1, we just need to make the substitutions $F_e^{(2)} = 0$ and $F_e^{(2)} = 1/s$ into this continued fraction. Setting $s = 1/(1-\sigma_1)$ and $F_e = 1-\sigma_e$ in the resultant inequalities gives the bounds $U_{2,0}(\sigma_1, 1)$ and $V_{2,0}(\sigma_1, 1)$.

By repeating this procedure successive moments can be eliminated. When the three moments μ_0, μ_1, and μ_2 are known, the lower and upper bounds on F_e for real $s > 1$ are obtained by making the substitutions $F_e^{(3)} = 0$ and $F_e^{(3)} = 1/s$ into the continued fraction

$$F_e = \cfrac{\mu_0}{s-\cfrac{(1-\mu_0)\mu_0^{(1)}}{1-\cfrac{(1-\mu_0^{(1)})\mu_0^{(2)}}{s-(1-\mu_0^{(2)})sF_e^{(3)}}}},$$

where

$$\mu_0^{(2)} = \frac{\mu_1^{(1)}}{\mu_0^{(1)}(1-\mu_0^{(1)})},$$

and the moments $\mu_0^{(1)}$ and $\mu_1^{(1)}$ are given by (28.7) in terms of μ_0, μ_1, and μ_2. Setting $s = 1/(1-\sigma_1)$ and $F_e = 1-\sigma_e$ in the resultant inequalities gives the bounds $U_{3,0}(\sigma_1, 1)$ and $V_{3,0}(\sigma_1, 1)$.

28.2. Eliminating the constraints imposed by known real values of the function

Let us begin by supposing that we know the value of $\sigma_e' = \sigma_e(\sigma_1', \sigma_2')$ for a pair of positive real conductivities σ_1' and σ_2' with $\sigma_1' \neq \sigma_2'$. This information translates into a known value of the function $F_e(s)$,

$$F_e(s') = F_e', \quad \text{where } F_e' = 1-\sigma_e'/\sigma_2', \;\; s' = \sigma_2'/(\sigma_2'-\sigma_1'). \tag{28.13}$$

The elementary bounds, that σ'_e is positive and lies between σ'_1 and σ'_2, translate into the inequalities

$$F'_e \le 1, \quad 0 \le s' F'_e \le 1. \tag{28.14}$$

Let us define $\mathcal{F}(F'_e, s')$ as the set of all functions $F_e(s)$ satisfying $F_e(s') = F'_e$ that can be expressed in the form (28.2) for some positive measure $d\mu$. Our objective is to find a fractional linear transformation $\widetilde{T}$ such that $\widetilde{T}$ provides a one-to-one correspondence between functions $F_e(s)$ in $\mathcal{F}(F'_e, s')$ and functions $\widetilde{F}_e(s) = \widetilde{T} F_e(s)$ in $\mathcal{F}$.

Here we follow the analysis of Bergman (1993) and consider the transformation

$$\widetilde{F}_e(s) = \widetilde{T} F_e(s) = \left[1 - \frac{(1 - s'/s) F'_e}{[F'_e - F_e(s)]}\right] \frac{1}{\beta}, \tag{28.15}$$

where the factor $1/\beta$ with

$$\beta = (1 - s' F'_e)/(1 - F'_e) = 1 - (s' - 1) F'_e/(1 - F'_e) \tag{28.16}$$

has been introduced to ensure that the inequality $\widetilde{F}_e(1) \le 1$ holds if and only if $F_e(1) \le 1$. The inequalities (28.14) clearly ensure the positivity of β. Also, the positivity of $s' F'_e$ implies that $F'_e > 0$ when $s' > 1$ and that $F'_e < 0$ when $s' < 0$, that is, that $(s' - 1) F'_e$ is positive. Thus β lies between 0 and 1.

The transformation (28.15) looks quite cumbersome, but it is simply a fractional linear transformation of $F_e(s)$. Also, as expected, the transformation $\widetilde{T}$ reduces to T_1 defined by (28.4), in the limit as s' approaches infinity and $F_e(s')$ approaches μ_0/s'. This reflects the fact that knowledge of the zeroth moment μ_0 is equivalent to knowledge of $F_e(s')$ in the asymptotic limit as s' approaches infinity.

Our first objective is to show that $\widetilde{F}_e(s) \in \mathcal{F}$ whenever $F_e(s) \in \mathcal{F}(F'_e, s')$. Since $F_e(s)$ can be approximated arbitrarily closely by a rational function in $\mathcal{F}(F'_e, s')$, it suffices to examine the action of $\widetilde{T}$ on rational functions $F_e(s)$ of the form

$$F_e(s) = \sum_{\alpha=1}^{m} \frac{B_\alpha}{s - s_\alpha},$$

where

$$F_e(s') = \sum_{\alpha=1}^{m} \frac{B_\alpha}{s' - s_\alpha} = F'_e, \quad F_e(1) = \sum_{\alpha=1}^{m} \frac{B_\alpha}{1 - s_\alpha} \le 1, \quad s_\alpha \in [0, 1), \quad B_\alpha \ge 0 \ \forall\, \alpha.$$

Now, assuming that at least one residue B_α is nonzero, $F_e(s)$ is real only when s is real because $\mathrm{Im}[F_e(s)] > 0$ when $\mathrm{Im}[s] > 0$ and $\mathrm{Im}[F_e(s)] < 0$ when $\mathrm{Im}[s] < 0$. Also, $F_e(s)$ for real s is a strictly monotonic decreasing function of s except at the poles s_α of $F_e(s)$. Hence $F_e(s)$ takes the value F'_e only at s' and at $m - 1$ selected points $\widetilde{s}_\alpha$, $\alpha = 1, 2, \ldots, m - 1$ in the interval $(0, 1)$ interlaced between the m poles of $F_e(s)$.

It follows that the only poles of the rational function $\widetilde{F}_e(s)$ are at these points $\widetilde{s}_\alpha$ and possibly at $s = 0$, but not at $s = s'$. In the neighborhood of any one of these points $\widetilde{s}_\alpha$ we have

$$F_e(s) \approx F'_e - A_\alpha (s - \widetilde{s}_\alpha), \quad \widetilde{F}_e(s) \approx \frac{\widetilde{B}_\alpha}{s - \widetilde{s}_\alpha}, \quad \text{where } \widetilde{B}_\alpha = \frac{(s' - \widetilde{s}_\alpha) F'_e}{A_\alpha \widetilde{s}_\alpha \beta}.$$

The monotonicity of $F_e(s)$ implies that $A_\alpha > 0$ and the positivity of $s' F'_e$ implies that $F'_e > 0$ when $s' > 1$ and that $F'_e < 0$ when $s' < 0$, that is, that $(s' - \widetilde{s}_\alpha) F'_e$ is positive. It follows that

the function $\widetilde{F}_e(s)$ has positive residues $\widetilde{B}_\alpha > 0$ at the poles $\widetilde{s}_\alpha$. If $s = 0$ is not a pole of $F_e(s)$, that is, $F_e(0)$ is finite, then $s = 0$ will be pole of $\widetilde{F}_e(s)$. Specifically in the neighborhood of $s = 0$ we have

$$\widetilde{F}_e(s) \approx \frac{\widetilde{B}_0}{s}, \quad \text{where } \widetilde{B}_0 = \frac{F'_e s'}{[F'_e - F_e(0)]\beta}.$$

The monotonicity of $F_e(s)$ implies the positivity of $F'_e - F_e(0)$ and with (28.14) implies the positivity of the residue $\widetilde{B}_0$. If $s = 0$ is a pole of $F_e(s)$, then $\widetilde{F}_e(s)$ will be analytic at $s = 0$.

It is clear from these arguments that all of the poles of $\widetilde{F}_e(s)$ lie in the interval $[0, 1)$ and have positive residues. To check that $\widetilde{F}_e(1) \le 1$ we examine the formula

$$\widetilde{F}_e(1) = 1 - \frac{(s' - 1)F'_e(1 - F_e(1))}{(F_e(1) - F'_e)(1 - s'F'_e)}$$

giving $\widetilde{F}_e(1)$. Monotonicity implies the positivity of $F_e(1) - F'_e$. The elementary bounds (28.14) imply the positivity of $1 - s'F'_e$. Since $1 - F_e(1)$ and $(s' - 1)F'_e$ are also positive, we conclude that $\widetilde{F}_e(1) \le 1$. This establishes that $\widetilde{F}_e(s) \in \mathcal{F}$.

Conversely, let us suppose that we are given any function $\widetilde{F}_e(s)$ in $\mathcal{F}$ and real values of s' and F'_e, with $s' \notin [0, 1]$ and F'_e satisfying (28.14). Applying the inverse transformation $\widetilde{T}^{-1}$ to $\widetilde{F}_e(s)$ yields the function

$$F_e(s) = \widetilde{T}^{-1}\widetilde{F}_e(s) = F'_e - \frac{(1 - s'/s)F'_e}{1 - \beta\widetilde{F}_e(s)}, \tag{28.17}$$

where the factor β given by (28.16) lies between zero and one. Our objective is to show that this function lies in $\mathcal{F}(F'_e, s')$ whenever $\widetilde{F}_e(s)$ lies in $\mathcal{F}$. Again it suffices to consider the action of $\widetilde{T}^{-1}$ on rational functions $\widetilde{F}_e(s)$. Clearly $F_e(s)$ takes the value F'_e at $s = s'$. The poles of $F_e(s)$ are at those points $s = s_\alpha$ where $\widetilde{F}_e(s) = 1/\beta$ and possibly at $s = 0$. Since $1/\beta > 1$ and $\widetilde{F}_e(s) \le 1$ for all s outside the interval $[0, 1)$, it follows that these poles all lie in the interval $[0, 1)$. It is also easy to check that the monotonicity of $\widetilde{F}_e(s)$ implies that these poles have positive residues. From the formula

$$F_e(1) = 1 - \frac{(1 - s'F'_e)(1 - \widetilde{F}_e(1))}{(1 - F'_e)(1 - \beta\widetilde{F}_e(1))},$$

and the positivity of the various factors appearing in it, we deduce that $F_e(1) \le 1$. This establishes that $F_e(s) \in \mathcal{F}(F'_e, s')$ and completes the proof that $\widetilde{T}$ provides a one-to-one correspondence between functions in $\mathcal{F}(F'_e, s')$ and functions in $\mathcal{F}$.

To obtain bounds on $F_e(s)$ that incorporate the known function value $F_e(s') = F'_e$, we first find the appropriate bounds on $\widetilde{F}_e(s)$ and then substitute these bounds into the formula (28.17) for $F_e(s)$ in terms of $\widetilde{F}_e(s)$. For example, when s is real with $s \notin [0, 1]$ we know that $\widetilde{F}_e \in [0, 1/s]$, and this implies that

$$F_e \in [s'F'_e/s, F'_e(s' - 1)/(s - 1 + F'_e(s' - s))]. \tag{28.18}$$

Upon making the substitutions

$$F_e = 1 - \sigma_e/\sigma_2, \;\; s = \sigma_2/(\sigma_2 - \sigma_1), \quad F'_e = 1 - \sigma'_e/\sigma'_2, \;\; s' = \sigma'_2/(\sigma'_2 - \sigma'_1), \tag{28.19}$$

into (28.18) we recover the bounds $V_{0,1}$ and $U_{0,1}$ given by (27.16).

When we have knowledge of the function $F_e(s)$ at two real points $s = s^{(1)} \notin [0, 1]$ and $s = s^{(2)} \notin [0, 1]$ then we introduce the functions

$$\widetilde{F}_e^{(1)}(s) = \widetilde{T}_1 F_e(s) \left[1 - \frac{(1 - s^{(1)}/s) F_e(s^{(1)})}{[F_e(s^{(1)}) - F_e(s)]} \right] \frac{1}{\beta^{(1)}},$$

$$\widetilde{F}_e^{(2)}(s) = \widetilde{T}_2 \widetilde{F}_e^{(1)}(s) = \widetilde{T}_2 \widetilde{T}_1 F_e(s) = \left[1 - \frac{(1 - s^{(2)}/s) \widetilde{F}_e^{(1)}(s^{(2)})}{[\widetilde{F}_e^{(1)}(s^{(2)}) - \widetilde{F}_e^{(1)}(s)]} \right] \frac{1}{\beta^{(2)}},$$

where

$$\beta^{(1)} = [1 - s^{(1)} F_e(s^{(1)})]/[1 - F_e(s^{(1)})], \quad \beta^{(2)} = [1 - s^{(2)} \widetilde{F}_e^{(1)}(s^{(2)})]/[1 - \widetilde{F}_e^{(1)}(s^{(2)})].$$

These relations can then be used to express $F_e(s)$ as a continued fraction involving $\widetilde{F}_e^{(2)}(s)$:

$$F_e(s) = F_e(s^{(1)}) - \cfrac{(1 - s^{(1)}/s) F_e(s^{(1)})}{1 - \beta^{(1)} \widetilde{F}_e^{(1)}(s^{(2)}) + \cfrac{(1 - s^{(1)}/s) \beta^{(1)} \widetilde{F}_e^{(1)}(s^{(2)})}{1 - \beta^{(2)} \widetilde{F}_e^{(2)}(s)}}. \tag{28.20}$$

The problem of bounding $F_e(s)$ is then reduced to the problem of bounding the function $\widetilde{F}_e^{(2)}(s) \in \mathcal{F}$. For example, when s is real and $s \notin [0, 1]$ we have $\widetilde{F}_e^{(2)}(s) \in [0, 1/s]$. The associated bounds on $F_e(s)$ implied by (28.20) when expressed in terms of σ_e, σ_1, and σ_2 reduce to the bounds $V_{0,2}$ and $U_{0,2}$. Of course if we have knowledge of a set of series expansion coefficients and knowledge of a set of function values, then we use transformations like T_1 and T_2 to first eliminate the known series expansion coefficients from consideration, and then we use transformations like $\widetilde{T}_1$ and $\widetilde{T}_2$ to successively eliminate the known function values from consideration. Elementary bounds applied to the resulting function when mapped back give the desired bounds on the original function $F_e(s)$.

When $F_e(s)$ is known at a complex value of s, say, $s = s^{(1)}$, then we immediately know $F_e(s)$ at the complex conjugate value of s:

$$F_e(s^{(2)}) = \overline{F_e(s^{(1)})} \quad \text{for } s^{(2)} = \overline{s^{(1)}},$$

where the bar denotes complex conjugation. Thus knowing $F_e(s)$ at a complex value of s is equivalent to knowing the function at two points. If we apply the single transformation $\widetilde{T}_1$ to $F_e(s)$, then the resulting function $\widetilde{F}_e^{(1)}(s)$ does not lie in $\mathcal{F}$. In particular, $\widetilde{F}_e^{(1)}(s)$ is not real when s is real and greater than 1. However, Bergman (1993) has shown that if we apply the combined transformation $\widetilde{T}_2 \widetilde{T}_1$ to $F_e(s)$, then the resulting function $\widetilde{F}_e^{(2)}(s)$ does lie in $\mathcal{F}$. The transformation $\widetilde{T}_2 \widetilde{T}_1$ provides a one-to-one correspondence between functions in $\mathcal{F}$ having a given value at a complex value of s and functions in $\mathcal{F}$ with no constraints. Using such transformations one can recover the bounds (Milton 1981) discussed in the previous chapter, which incorporate information about the function $F_e(s)$ at an arbitrary number of complex values of s.

28.3. An alternative approach that treats the components on a symmetric basis

The preceding analysis, while it yields the bounds, does not treat the component conductivities σ_1 and σ_2 in a symmetric way. Fractional linear transformations that treat the components in a symmetric way were introduced by Milton and Golden (1985). From the definition (28.1)

of the function F_e, we see that σ_1 is singled out to play a special role. Yet, a quick inspection of formulas like (27.5), (27.7), and (27.16) shows that the bounds $U_{J,K}$ and $V_{J,K}$, with $J+K$ being odd, show no intrinsic bias between the phases. This suggests that there might be some transformation of the conductivity function $\sigma_e(\sigma_1,\sigma_2)$ to a new function $\sigma_e^{(1)}(\sigma_1,\sigma_2)$ that treats the phases on a symmetric basis, preserves the basic analytic properties of the function, and eliminates some of the constraints imposed by the knowledge of a set of series expansion coefficients and by the knowledge of a set of function values. This transformation will then provide a correspondence between the bounds associated with $\sigma_e(\sigma_1,\sigma_2)$ and the bounds associated with $\sigma_e^{(1)}(\sigma_1,\sigma_2)$.

From the previous chapter we know that there is a fundamental topological difference between those functions of type I and type II, which correspond to the bounds $U_{J,K}$ and $V_{J,K}$ with $J+K$ being odd, and the those functions of type III and type IV, which correspond to the bounds $U_{J,K}$ and $V_{J,K}$ with $J+K$ being even. Therefore, if we are to treat the component conductivities in a symmetric way, it makes sense to first look for transformations of $\sigma_e(\sigma_1,\sigma_2)$ that eliminate an even number of constraints.

Let us focus on the case where we know only the expansion coefficients $r_0=1$, r_1, and r_2 in the series (27.3). A natural idea is to try to express the relation (28.12) between F_e and $F_e^{(2)}$ in a form that displays the desired symmetry. By making the substitutions

$$F_e = 1-\sigma_e/\sigma_2, \qquad s=\sigma_2/(\sigma_2-\sigma_1), \qquad F_e^{(2)} = 1-\sigma_e^{(1)}/\sigma_2,$$

where the last identity serves to define $\sigma_e^{(1)}$, we see after some straightforward algebraic manipulation that the relation (28.12) reduces to

$$\sigma_e = w_1\sigma_1 + w_2\sigma_2 - \frac{w_1w_2(\sigma_1-\sigma_2)^2}{w_2\sigma_1+w_1\sigma_2+n\sigma_e^{(1)}}, \tag{28.21}$$

where we have introduced the weights

$$w_1=\mu_0=r_1, \quad w_2=1-\mu_0=1-r_1,$$

and the normalization factor

$$n=(1-\mu_0^{(1)})/\mu_0^{(1)}.$$

In composites, w_1 and w_2 can be identified with the volume fractions f_1 and f_2. These parameters satisfy the constraints

$$w_1+w_2=1, \quad w_1\geq 0, \quad w_2\geq 0, \quad n\geq 0.$$

The relation (28.21) can be inverted to express $\sigma_e^{(1)}$ in terms of σ_e:

$$\sigma_e^{(1)}(\sigma_1,\sigma_2)=\frac{1}{n}\left[-w_2\sigma_1-w_1\sigma_2+\frac{w_1w_2(\sigma_1-\sigma_2)^2}{w_1\sigma_1+w_2\sigma_2-\sigma_e(\sigma_1,\sigma_2)}\right],$$

and this can be regarded as the product of two transformations: a Y-transformation, which when applied to $\sigma_e(\sigma_1,\sigma_2)$ yields the function

$$\begin{aligned} y_\sigma(\sigma_1,\sigma_2)=Y[\sigma_e(\sigma_1,\sigma_2)] &= -w_2\sigma_1-w_1\sigma_2+\frac{w_1w_2(\sigma_1-\sigma_2)^2}{w_1\sigma_1+w_2\sigma_2-\sigma_e(\sigma_1,\sigma_2)} \\ &= \frac{\sigma_1\sigma_2(\sigma_e-\sigma_h)}{\sigma_h(\sigma_a-\sigma_e)}, \end{aligned} \tag{28.22}$$

where

$$\sigma_a = w_1\sigma_1 + w_2\sigma_2 \quad \text{and} \quad \sigma_h = [w_1/\sigma_1 + w_2/\sigma_2]^{-1},$$

and a normalization transformation N, which when applied to $y_\sigma(\sigma_1, \sigma_2)$ yields the function

$$\sigma_e^{(1)}(\sigma_1, \sigma_2) = N[y_\sigma(\sigma_1, \sigma_2)] = y_\sigma(\sigma_1, \sigma_2)/n. \tag{28.23}$$

Now let $\mathcal{S}$ denote the set of functions $\sigma_e(\sigma_1, \sigma_2)$ that are analytic functions of σ_1 and σ_2, except possibly when σ_1/σ_2 is real and nonpositive, and which satisfy the homogeneity property

$$\sigma_e(c\sigma_1, c\sigma_2) = c\sigma_e(\sigma_1, \sigma_2),$$

the Herglotz property

$$\text{Im}(\sigma_e(\sigma_1, \sigma_2)) > 0 \text{ when } \text{Im}(\sigma_1) > 0 \text{ and } \text{Im}(\sigma_2) > 0,$$

and the normalization property

$$\sigma_e(1, 1) = 1.$$

Also let $\mathcal{S}(r_1)$ denote the subset of those functions in $\mathcal{S}$ that have the series expansion coefficient r_1 and let $\mathcal{S}(r_1, r_2)$ denote the subset of those functions in $\mathcal{S}$ that have the series expansion coefficients r_1 and r_2.

We could use the fact that T_2T_1 provides a one-to-one correspondence between functions in $\mathcal{F}(\mu_1, \mu_2)$ and functions in $\mathcal{F}$ to establish that NY provides a one-to-one correspondence between functions in $\mathcal{S}(r_1, r_2)$ and functions in $\mathcal{S}$. There is however a more direct proof based on our knowledge of the bounds on σ_e when σ_1 and σ_2 are complex and both $r_0 = 1$ and $r_1 = w_1$ are given (Milton 1991). As established in the previous chapter, we know that σ_e is confined to the lens-shaped region Ω' in the complex plane bounded by the two circular arcs joining σ_a and σ_h that when extended pass through σ_1 and σ_2, respectively. Now let $\mathcal{Y}$ denote the set of functions $y_\sigma(\sigma_1, \sigma_2)$ that are analytic functions of σ_1 and σ_2, except possibly when σ_1/σ_2 is real and nonpositive, and which satisfy the homogeneity property

$$y_\sigma(c\sigma_1, c\sigma_2) = cy_\sigma(\sigma_1, \sigma_2), \tag{28.24}$$

and the Herglotz property

$$\text{Im}(y_\sigma(\sigma_1, \sigma_2)) > 0 \text{ when } \text{Im}(\sigma_1) > 0 \text{ and } \text{Im}(\sigma_2) > 0.$$

These properties imply, through (18.7), that y_σ is confined to the convex wedge W in the complex plane, bounded on one side by the ray from the origin that passes through σ_1 and on the other side by the ray from the origin that passes through σ_2.

The Y-transformation has the property that it maps Ω' to W, as illustrated in figure 28.1 on the facing page. Indeed, it is a fractional linear transformation of σ_e and therefore maps circular arcs to circular arcs or straight lines. So to find the image under Y of the circular arc that joins σ_a and σ_h and when extended passes through σ_1 it suffices to find the image under Y of the three points σ_a, σ_h, and σ_1. Since these map to $y_\sigma = \infty$, $y_\sigma = 0$ and $y_\sigma = -\sigma_1$, Y clearly maps this circular arc to the ray from the origin that passes through σ_1. Similarly, Y maps the other circular arc to the ray from the origin passing through σ_2. This establishes that Y maps Ω' to W.

An elementary consequence of this result is that if $\sigma_e(\sigma_1, \sigma_2) \in \mathcal{S}(w_1)$, then $Y[\sigma_e(\sigma_1, \sigma_2)]$ necessarily satisfies the Herglotz property, since if σ_1 and σ_2 are in the upper half of the

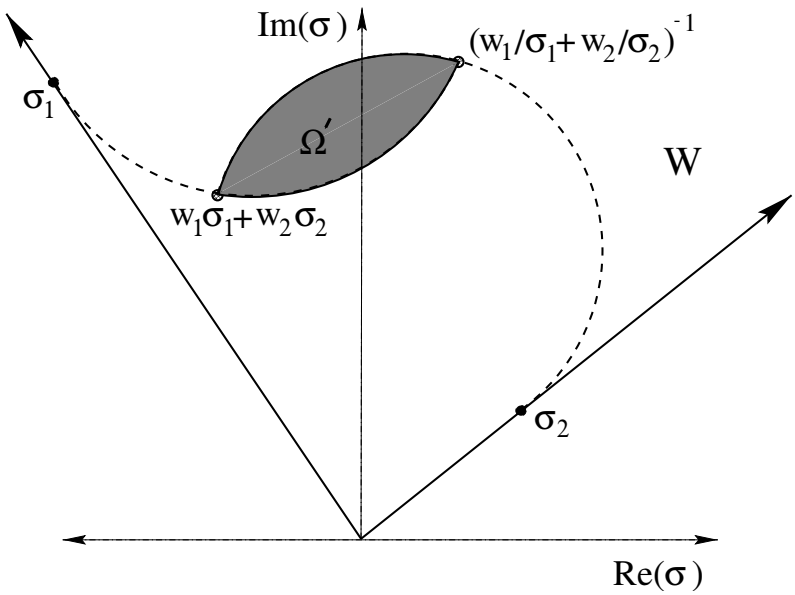

Figure 28.1. When the first-order series expansion coefficient $w_1 = 1 - w_2$ is known, σ_e is confined to the lens-shaped region Ω'. The Y-transformation given by (28.22) maps Ω' onto the wedge W and thus preserves the basic analytic properties of the function. The parameter $y_\sigma = Y(\sigma_e)$ is confined to the wedge W and therefore has a nonnegative imaginary part. After Milton (1991).

complex plane, so too is W. It is also immediately apparent from (28.22) that $Y[\sigma_e(\sigma_1, \sigma_2)]$ satisfies the homogeneity property.

Conversely, if $y_\sigma(\sigma_1, \sigma_2) \in \mathcal{Y}$, then

$$\sigma_e(\sigma_1, \sigma_2) = Y^{-1}[y_\sigma(\sigma_1, \sigma_2)] = w_1\sigma_1 + w_2\sigma_2 - \frac{w_1 w_2(\sigma_1 - \sigma_2)^2}{w_2\sigma_1 + w_1\sigma_2 + y_\sigma(\sigma_1, \sigma_2)} \tag{28.25}$$

necessarily satisfies the Herglotz property, since if σ_1 and σ_2 are in the upper half of the complex plane, so to is Ω' since it is contained in W. It is also immediately apparent that $\sigma_e(\sigma_1, \sigma_2)$ defined by (28.25) satisfies the homogeneity and normalization properties.

This establishes that Y provides a one-to-one correspondence between functions in $\mathcal{S}(r_1)$ and functions in $\mathcal{Y}$. Now let $\mathcal{Y}(n)$ denote those functions $y_\sigma(\sigma_1, \sigma_2)$ in $\mathcal{Y}$ satisfying the normalization $y_\sigma(1, 1) = n$. By substituting the series expansion (27.3) for $\sigma_e(\sigma_1, 1)$ into (28.22) and recalling that $w_1 = r_1$, we see that $y_\sigma(\sigma_1, 1)$ has the expansion

$$y_\sigma = -\left[\frac{r_1(1 - r_1)}{r_2} + 1\right] + \left[\frac{r_1(1 - r_1)r_3}{r_2^2} - r_2\right](\sigma_1 - 1) + \cdots$$

in powers of $\sigma_1 - 1$. It follows that Y provides a one-to-one correspondence between functions in $\mathcal{S}(r_1, r_2)$ and functions in $\mathcal{Y}(n)$ with

$$n = -\left[\frac{r_1(1 - r_1)}{r_2} + 1\right].$$

Since the sets of functions $\mathcal{Y}(n)$ and $\mathcal{S}$ differ only in their normalization, it is immediately clear that N provides a one-to-one correspondence between functions in $\mathcal{Y}(n)$ and functions in $\mathcal{S}$. This completes the proof that NY provides a one-to-one correspondence between functions in $\mathcal{S}(r_1, r_2)$ and functions in $\mathcal{S}$.

28.4. The extension of the fractional linear transformations to matrix-valued analytic functions

The analytic properties of Y-transformations and normalization transformations N for matrix-valued analytic functions were considered by Clark and Milton (1933). Their analysis was restricted to two-dimensional, two-phase conducting composites where the matrix-valued conductivity function $\boldsymbol{\sigma}_*(\sigma_1, \sigma_2)$ satisfies the additional phase interchange analytic constraint, (3.9), which fortunately turns out be preserved by the transformation NY. They also introduced transformations $\widetilde{Y}$ that, like the transformations $\widetilde{T}$ given by (28.15), were useful for eliminating known values of the function. These transformations were particularly well-suited to generating optimal bounds coupling an arbitrary number of effective conductivity tensors (at different conductivity ratios) of two-phase, two-dimensional conducting composites. In particular, they recovered the optimal cross-property bounds coupling the effective electrical permittivity and magnetic permeability tensors that Cherkaev and Gibiansky (1992) had obtained using the translation method.

Here we generalize this approach for eliminating known series expansion coefficients of matrix-valued conductivity functions, allowing for functions that do not necessarily satisfy the phase interchange constraint (3.9). Therefore the ensuing analysis applies to the conductivity functions $\boldsymbol{\sigma}_*(\sigma_1, \sigma_2)$ of both three- and two-dimensional composites. We will see that the relation (28.22) between $y_\sigma(\sigma_1, \sigma_2)$ and $\sigma_e(\sigma_1, \sigma_2)$ has a natural generalization to matrix-valued analytic functions. Let $\mathcal{Y}$ denote those matrix-valued functions $\boldsymbol{Y}_*(\sigma_1, \sigma_2)$ that are analytic, except when σ_1/σ_2 is real and nonpositive, which satisfy the homogeneity property

$$\boldsymbol{Y}_*(c\sigma_1, c\sigma_2) = c\boldsymbol{Y}_*(\sigma_1, \sigma_2),$$

and which satisfy the Herglotz property

$$\mathrm{Im}(\boldsymbol{Y}_*(\sigma_1, \sigma_2)) > 0 \text{ when } \mathrm{Im}(\sigma_1) > 0 \text{ and } \mathrm{Im}(\sigma_2) > 0. \tag{28.26}$$

We now let $\mathcal{S}$ denote those functions $\boldsymbol{\sigma}_*(\sigma_1, \sigma_2)$ in $\mathcal{Y}$ that in addition satisfy the normalization property

$$\boldsymbol{\sigma}_*(1, 1) = 1,$$

and we let $\mathcal{S}(\boldsymbol{R}_1)$ denote those functions in $\mathcal{S}$ that have the series expansion coefficient $\boldsymbol{R}_1$ and we let $\mathcal{S}(\boldsymbol{R}_1, \boldsymbol{R}_2)$ denote those functions in $\mathcal{S}$ that have the series expansion coefficients $\boldsymbol{R}_1$ and $\boldsymbol{R}_2$, where

$$\boldsymbol{R}_1 = \frac{d\boldsymbol{\sigma}_*(\sigma_1, 1)}{d\sigma_1}\bigg|_{\sigma_1=1}, \quad \boldsymbol{R}_2 = \tfrac{1}{2}\frac{d^2\boldsymbol{\sigma}_*(\sigma_1, 1)}{d\sigma_1^2}\bigg|_{\sigma_1=1}.$$

The form of the relation (28.22) suggests that its analog for matrix-valued functions should be the Y-transformation:

$$\begin{aligned}\boldsymbol{Y}_*(\sigma_1, \sigma_2) &= Y(\boldsymbol{\sigma}_*(\sigma_1, \sigma_2)) \\ &= -\boldsymbol{W}_2\sigma_1 - \boldsymbol{W}_1\sigma_2 + (\sigma_1 - \sigma_2)^2(\boldsymbol{W}_1\boldsymbol{W}_2)^{1/2}[\boldsymbol{W}_1\sigma_1 + \boldsymbol{W}_2\sigma_2 - \boldsymbol{\sigma}_*(\sigma_1, \sigma_2)]^{-1}(\boldsymbol{W}_1\boldsymbol{W}_2)^{1/2},\end{aligned} \tag{28.27}$$

where $\boldsymbol{W}_1$ and $\boldsymbol{W}_2$ are the commuting weight matrices

$$\boldsymbol{W}_1 = \boldsymbol{R}_1, \quad \boldsymbol{W}_2 = \boldsymbol{I} - \boldsymbol{R}_1.$$

We will see that these matrices are necessarily positive-semidefinite. This ensures that the matrix $(\boldsymbol{W}_1\boldsymbol{W}_2)^{1/2}$ appearing in (28.27) is real.

To prove that Y provides a one-to-one correspondence between functions in $\mathcal{S}(\boldsymbol{W}_1)$ and functions in $\mathcal{Y}$ it is helpful to set $\sigma_2 = 1$ and to consider the analytic properties of

$$\boldsymbol{F}_* = \boldsymbol{I} - \boldsymbol{\sigma}_*, \quad \boldsymbol{S}_* = \boldsymbol{F}_*^{-1} = (\boldsymbol{I} - \boldsymbol{\sigma}_*)^{-1}, \quad \text{and } \boldsymbol{S}_0 = (\boldsymbol{I} + \boldsymbol{Y}_*)^{-1}$$

as a function of the variable $s = 1/(1 - \sigma_1)$. The fractional linear relation (28.27) between $\boldsymbol{Y}_*$ and $\boldsymbol{\sigma}_*$ reduces to a simple linear relation between $\boldsymbol{S}_*$ and $\boldsymbol{S}_0$:

$$(\boldsymbol{W}_1)^{1/2}\boldsymbol{S}_*(\boldsymbol{W}_1)^{1/2} + (\boldsymbol{W}_2)^{1/2}\boldsymbol{S}_0(\boldsymbol{W}_2)^{1/2} = s\boldsymbol{I}, \tag{28.28}$$

as can be seen by rewriting (28.27) in the form

$$(\boldsymbol{W}_2)^{-1/2}\boldsymbol{S}_0^{-1}(\boldsymbol{W}_2)^{-1/2} = s^{-1}\boldsymbol{I} - s^{-1}[\boldsymbol{I} - s(\boldsymbol{W}_1)^{-1/2}\boldsymbol{S}_0^{-1}(\boldsymbol{W}_1)^{-1/2}]^{-1}, \tag{28.29}$$

taking the matrix inverse of both sides of this equation and applying the matrix identity

$$\boldsymbol{I} - (\boldsymbol{I} - \boldsymbol{A})^{-1} = (\boldsymbol{I} - \boldsymbol{A}^{-1})^{-1},$$

which holds for any matrix $\boldsymbol{A}$ and in particular for $\boldsymbol{A} = s(\boldsymbol{W}_1)^{-1/2}\boldsymbol{S}_0^{-1}(\boldsymbol{W}_1)^{-1/2}$.

Suppose that we are given a function $\boldsymbol{\sigma}_*(\sigma_1, \sigma_2)$ in $\mathcal{S}(\boldsymbol{W}_1)$. From the analytic properties of this function it follows that $\boldsymbol{F}_*$ has an integral representation

$$\boldsymbol{F}_* = \int_0^1 \frac{d\boldsymbol{\mu}(y)}{s - y}, \tag{28.30}$$

in terms of a matrix-valued measure $d\boldsymbol{\mu}(y)$ that is positive-semidefinite for all $y \in [0, 1]$. From the constraint that $\boldsymbol{\sigma}_*(0, 1) \geq 0$ we deduce that $\boldsymbol{F}_*(1) \leq \boldsymbol{I}$ or, equivalently, that

$$\boldsymbol{I} \geq \int_0^1 \frac{d\boldsymbol{\mu}(y)}{1 - y}. \tag{28.31}$$

From the series expansion for (28.30) in powers of $1/s$ we deduce that

$$\boldsymbol{W}_1 = \int_0^1 d\boldsymbol{\mu}(y).$$

This implies that $\boldsymbol{W}_1$ is a positive-semidefinite matrix. By substituting the inequality $1/(1 - y) \geq 1$ into (28.31) we deduce that $\boldsymbol{W}_2 = \boldsymbol{I} - \boldsymbol{W}_1$ is likewise a positive-semidefinite matrix.

From the integral representation (28.30) we see that $\boldsymbol{F}_*$ is nonzero for all $s > 1$ and for all $s < 1$. From the expansion of $\boldsymbol{S}_*$ in powers of $1/s$,

$$\boldsymbol{S}_* = s\boldsymbol{W}_1^{-1} - \boldsymbol{C} + \cdots, \quad \text{where } \boldsymbol{C} = \int_0^1 \boldsymbol{W}_1^{-1} y d\boldsymbol{\mu}(y) \boldsymbol{W}_1^{-1},$$

we see that $\boldsymbol{S}_*(s)$ has a pole at $s = \infty$. Its remaining singularities must be confined to the interval $[0, 1]$. An application of the Cauchy integral formula gives an integral representation for $\boldsymbol{S}_*(s)$:

$$\boldsymbol{S}_* = s\boldsymbol{W}_1{}^{-1} - \boldsymbol{C} + \int_0^1 \frac{d\boldsymbol{\phi}(z)}{z - s}$$

in terms of a matrix-valued measure $d\boldsymbol{\phi}(z)$. This measure is positive-semidefinite for all z because if $\mathrm{Im}(s)$ is positive (negative), then $\mathrm{Im}\,\boldsymbol{F}_e$ is negative-definite (positive-definite), and in this in turn implies that $\mathrm{Im}\,\boldsymbol{S}_*$ is positive-definite (negative-definite). By substituting this integral representation into (28.28) we see that $\boldsymbol{S}_0$ has the integral representation

$$\boldsymbol{S}_0 = \boldsymbol{W}_2{}^{-1/2}\boldsymbol{W}_1{}^{1/2}\left[\boldsymbol{C} + \int_0^1 \frac{d\boldsymbol{\phi}(z)}{s-z}\right]\boldsymbol{W}_1{}^{1/2}\boldsymbol{W}_2{}^{-1/2}, \tag{28.32}$$

from which it is evident that $\mathrm{Im}(\boldsymbol{S}_0) = \mathrm{Im}[(\boldsymbol{I} + \boldsymbol{Y}_*)^{-1}]$ is negative-definite when $\mathrm{Im}(s) = \mathrm{Im}[1/(1-\sigma_1)] > 0$ and positive-definite when $\mathrm{Im}[1/(1-\sigma_1)] < 0$. We conclude that $\mathrm{Im}[\boldsymbol{Y}_*(\sigma_1, 1)]$ is positive-definite when $\mathrm{Im}(\sigma_1) > 0$ and negative-definite when $\mathrm{Im}(\sigma_1) < 0$.

The homogeneity of the function $\boldsymbol{Y}_*(\sigma_1, \sigma_2)$ [which is evident from (28.27)] allows us to state a stronger result:

$$\mathrm{Im}[\sigma_2^{-1}\boldsymbol{Y}_*(\sigma_1, \sigma_2)] > 0\ (<0)\ \text{ when }\ \mathrm{Im}(\sigma_1/\sigma_2) > 0\ (<0). \tag{28.33}$$

Similarly, by interchanging the roles of the two phases, we see that

$$\mathrm{Im}[\sigma_1^{-1}\boldsymbol{Y}_*(\sigma_1, \sigma_2)] > 0\ (<0)\ \text{ when }\ \mathrm{Im}(\sigma_2/\sigma_1) > 0\ (<0). \tag{28.34}$$

To prove that $\boldsymbol{Y}_*(\sigma_1, \sigma_2)$ satisfies the Herglotz property (28.26), let us suppose that we are given two conductivities:

$$\sigma_1 = |\sigma_1|e^{i\theta_1}, \quad \sigma_2 = |\sigma_2|e^{i\theta_2} \ \text{ with } \pi > \theta_1 \geq \theta_2 > 0.$$

The results (28.33) and (28.34) imply that

$$\begin{aligned} \mathrm{Im}[\boldsymbol{Y}_*(\sigma_1, \sigma_2)]\cos\theta_2 - \mathrm{Re}[\boldsymbol{Y}_*(\sigma_1, \sigma_2)]\sin\theta_2 > 0, \\ -\mathrm{Im}[\boldsymbol{Y}_*(\sigma_1, \sigma_2)]\cos\theta_1 + \mathrm{Re}[\boldsymbol{Y}_*(\sigma_1, \sigma_2)]\sin\theta_1 > 0. \end{aligned} \tag{28.35}$$

Multiplying the first equation by $\sin\theta_1 > 0$ and the second by $\sin\theta_2 > 0$ and adding them gives

$$\sin(\theta_1 - \theta_2)\,\mathrm{Im}[\boldsymbol{Y}_*(\sigma_1, \sigma_2)] > 0, \tag{28.36}$$

which implies that $\mathrm{Im}[\boldsymbol{Y}_*(\sigma_1, \sigma_2)] > 0$, because $\theta_1 - \theta_2 \in [0, \pi)$. This proof also goes through with $\theta_2 \geq \theta_1$, but with the sign of the inequalities reversed in (28.35) and (28.36).

From (28.32) and the positivity of the matrix $\boldsymbol{C}$ it is also evident that $\boldsymbol{S}_0$ is positive-definite when s is real and greater than 1. Hence $\boldsymbol{Y}_*(\sigma_1, 1)$ is nonsingular for all real $\sigma_1 \in (0, 1]$. By interchanging the roles of the phases we see that $\boldsymbol{Y}_*(1, \sigma_2)$ must be nonsingular for all real $\sigma_2 \in (0, 1]$. Homogeneity then implies that $\boldsymbol{Y}_*(\sigma_1, 1) = \sigma_1\boldsymbol{Y}_*(1, \sigma_1^{-1})$ is nonsingular for all $\sigma_1 > 0$. Hence $\boldsymbol{Y}_*(\sigma_1, \sigma_2)$ is analytic except when σ_1/σ_2 is real and nonpositive. In conclusion, $\boldsymbol{Y}_*(\sigma_1, \sigma_2)$ given by (28.27) is in the set of functions $\mathcal{Y}$ and so the Y transformation given by (28.27) provides a one-to-one correspondence between matrix-valued functions in $\mathcal{S}(\boldsymbol{R}_1)$ and matrix-valued functions in $\mathcal{Y}$.

If the series expansion coefficient $\boldsymbol{R}_2$ is known, then it follows that the value of the normalization matrix

$$\boldsymbol{N} = \boldsymbol{Y}_*(1, 1) = \boldsymbol{W}_1\boldsymbol{W}_2{}^{1/2}\boldsymbol{R}_2^{-1}\boldsymbol{W}_1\boldsymbol{W}_2{}^{1/2} - \boldsymbol{I}$$

is also known. Now let $\mathcal{Y}(\boldsymbol{N})$ denote the set of functions in $\mathcal{Y}$ that satisfy $\boldsymbol{Y}_*(1, 1) = \boldsymbol{N}$, where $\boldsymbol{N}$ is assumed to be nonsingular. It follows immediately that Y provides a one-to-one

correspondence between matrix-valued functions in $\mathcal{S}(\boldsymbol{R}_1, \boldsymbol{R}_2)$ and matrix-valued functions in $\mathcal{Y}(\boldsymbol{N})$. The matrix-valued analog N of the normalization transformation (28.23) is simply

$$\boldsymbol{\sigma}_*^{(1)} = N[\boldsymbol{Y}_*(\sigma_1, \sigma_2)] = \boldsymbol{N}^{-1/2}\boldsymbol{Y}_*(\sigma_1, \sigma_2)\boldsymbol{N}^{-1/2},$$

and it is clear that this transformation N provides a one-to-one correspondence between matrix-valued functions in $\mathcal{Y}(\boldsymbol{N})$ and matrix-valued functions in $\mathcal{S}$. We conclude that NY provides a one-to-one correspondence between matrix-valued functions in $\mathcal{S}(\boldsymbol{R}_1, \boldsymbol{R}_2)$ and matrix-valued functions in $\mathcal{S}$. Therefore elementary bounds on the functions in $\mathcal{S}$ will generate bounds on the functions in $\mathcal{S}(\boldsymbol{R}_1, \boldsymbol{R}_2)$.

References

Baker, Jr., G. A. 1969. Best error bounds for Padé approximants to convergent series of Stieltjes. *Journal of Mathematical Physics* 10(5):814–820. {*571, 596, 603, 617*}

Bergman, D. J. 1978. The dielectric constant of a composite material — A problem in classical physics. *Physics Reports* 43(9):377–407. {*341, 352, 370, 371, 376, 377, 379, 382, 387, 390, 392, 569, 581, 590, 597, 603, 617*}

Bergman, D. J. 1986. The effective dielectric coefficient of a composite medium: Rigorous bounds from analytic properties. In J. L. Ericksen, D. Kinderlehrer, R. Kohn, and J.-L. Lions (eds.), *Homogenization and Effective Moduli of Materials and Media*, pp. 27–51. Berlin / Heidelberg / London / etc.: Springer-Verlag. ISBN 0-387-96306-5. {*451, 453, 571, 597, 603, 604, 617, 638, 641*}

Bergman, D. J. 1993. Hierarchies of Stieltjes functions and their application to the calculation of bounds for the dielectric constant of a two-component composite medium. *SIAM Journal on Applied Mathematics* 53(4):915–930. {*571, 597, 603, 604, 608, 610, 617*}

Cherkaev, A. V. and L. V. Gibiansky 1992. The exact coupled bounds for effective tensors of electrical and magnetic properties of two-component two-dimensional composites. *Proceedings of the Royal Society of Edinburgh. Section A, Mathematical and Physical Sciences* 122(1–2):93–125. {*397, 399, 411, 450, 453, 517, 522, 525, 614, 617*}

Clark, K. E. and G. W. Milton 1933. Optimal bounds correlating electric, magnetic and thermal properties of two-phase, two-dimensional composites. *Proceedings of the Royal Society of London. Series A, Mathematical and Physical Sciences* 448(1933): 161–190. {*614, 617*}

Golden, K. and G. Papanicolaou 1983. Bounds for effective parameters of heterogeneous media by analytic continuation. *Communications in Mathematical Physics* 90(4):473–491. {*11, 12, 15, 248, 268, 370, 376, 393, 571, 598, 603, 617*}

Kantor, Y. and D. J. Bergman 1984. Improved rigorous bounds on the effective elastic moduli of a composite material. *Journal of the Mechanics and Physics of Solids* 32: 41–62. {*248, 268, 569, 598, 603, 617*}

Milton, G. W. 1981. Bounds on the transport and optical properties of a two-component composite material. *Journal of Applied Physics* 52(8):5294–5304. {*371, 379, 382, 394, 553, 566, 569, 574, 581, 583, 586, 587, 592, 599, 610, 617*}

Milton, G. W. 1986. Modeling the properties of composites by laminates. In J. L. Ericksen, D. Kinderlehrer, R. Kohn, and J.-L. Lions (eds.), *Homogenization and Effective Moduli*

of Materials and Media, pp. 150–174. Berlin / Heidelberg / London / etc.: Springer-Verlag. ISBN 0-387-96306-5. {*206, 218, 384, 394, 463, 471, 472, 494, 578, 599, 603, 617*}

Milton, G. W. 1991. The field equation recursion method. In G. Dal Maso and G. F. Dell'Antonio (eds.), *Composite Media and Homogenization Theory: Proceedings of the Workshop on Composite Media and Homogenization Theory Held in Trieste, Italy, from January 15 to 26, 1990*, pp. 223–245. Basel, Switzerland: Birkhäuser Verlag. ISBN 0-8176-3511-4, 3-7643-3511-4. {*397, 412, 517, 526, 612, 613, 618, 619, 641*}

Milton, G. W. and K. Golden 1985. Thermal conduction in composites. In T. Ashworth and D. R. Smith (eds.), *Thermal Conductivity*, pp. 571–582. New York / London: Plenum Press. ISBN 0-306-41918-1. {*397, 412, 610, 618*}

29

The field equation recursion method†

The fractional linear transformations provide mappings between analytic functions satisfying the homogeneity and Herglotz properties. The field equation recursion method provides mappings at a deeper level, namely, at the level of the underlying Hilbert space. The field equation recursion method has two advantages over the analytic method: First, it has a natural generalization to multiphase composites, and, second, the method provides matrix representations for the relevant operators. Also, with the introduction of additional fields and operators, the method allows one to incorporate the differential constraints on the fields in a direct fashion.

The original papers (Milton 1987a, 1987b) describing the field equation recursion method are difficult to read, but fortunately many of the arguments have since been simplified. It is hoped that the presentation given here will convey the main ideas; see also Milton (1991), where a brief summary is given. We will focus on two-phase composites, since the analysis is simpler and one can immediately see the connection with the analytic method. Another simple case that we could have discussed is the conductivity of a two-dimensional polycrystal, where Clark (1997) has shown that the field equation recursion method leads to an elegant continued fraction expansion of the effective conductivity tensor as a function of the crystal conductivity.

29.1. Associations between operations on analytic functions and operations on subspace collections

The main idea behind the field equation recursion method is that there is some sort of correspondence between operations on $m \times m$ matrix-valued analytic functions $\boldsymbol{L}_*(\lambda_1, \lambda_2, \ldots, \lambda_n)$ satisfying the homogeneity, Herglotz, and normalization properties and operations on what we will call $(3, n)$-subspace collections comprised of sets $(\mathcal{U}, \mathcal{E}, \mathcal{J})$ and $(\mathcal{P}_1, \mathcal{P}_2, \ldots, \mathcal{P}_n)$ of mutually orthogonal subspaces that span the same Hilbert space $\mathcal{H}$:

$$\mathcal{H} = \mathcal{U} \oplus \mathcal{E} \oplus \mathcal{J} = \mathcal{P}_1 \oplus \mathcal{P}_2 \oplus \cdots \oplus \mathcal{P}_n,$$

where $\mathcal{U}$ is m-dimensional. Given a $(3, n)$-subspace collection and given an orthonormal basis of $\mathcal{U}$, the effective tensor [see (12.59)]

$$\boldsymbol{L}_*(\lambda_1, \lambda_2, \ldots, \lambda_n) = \boldsymbol{\Gamma}_0[(\boldsymbol{\Gamma}_0 + \boldsymbol{\Gamma}_2)(\sum_{i=1}^{n} \boldsymbol{\Lambda}_i/\lambda_i)(\boldsymbol{\Gamma}_0 + \boldsymbol{\Gamma}_2)]^{-1}\boldsymbol{\Gamma}_0,$$

represented in a basis $\boldsymbol{u}_1, \boldsymbol{u}_2, \ldots, \boldsymbol{u}_m$ of $\mathcal{U}$ and expressed as a function of the parameters $\lambda_1, \lambda_2, \ldots, \lambda_n$, can be taken as the corresponding analytic function, in which the inverse is

to be taken on the subspace $\mathcal{U} \oplus \mathcal{J}$. It is determined by the basis of $\mathcal{U}$ and, more importantly, by the orientation of the subspace set $(\mathcal{P}_1, \mathcal{P}_2, \ldots, \mathcal{P}_n)$ with respect to the subspace set $(\mathcal{U}, \mathcal{E}, \mathcal{J})$. At present it is still an open (and interesting) question as to whether every matrix-valued analytic function $\boldsymbol{L}_*(\lambda_1, \lambda_2, \ldots, \lambda_n)$ satisfying the homogeneity, Herglotz, and normalization properties can be associated with a $(3, n)$-subspace collection.

The plan is to play with subspace collections rather than with analytic functions. Given a familiar operation on matrix-valued n-variable analytic functions satisfying the homogeneity, Herglotz, and normalization properties, one can look for the associated operation on $(3, n)$-subspace collections, such that their corresponding matrix-valued analytic functions are related by the given familiar operation. Most of the following associations between operations on analytic function and subspace collections are not needed for our subsequent analysis. They are introduced to illustrate the connection between operations on analytic functions and operations on subspace collections.

Suppose that $\boldsymbol{L}_*(\lambda_1, \lambda_2, \ldots, \lambda_n)$ satisfies these properties. Then so does the function

$$\boldsymbol{L}'_*(\lambda_1, \lambda_2, \ldots, \lambda_n) = [\boldsymbol{L}_*(1/\lambda_1, 1/\lambda_2, \ldots, 1/\lambda_n)]^{-1}.$$

The associated operation on the subspace collection is to swap the subspaces $\mathcal{E}$ and $\mathcal{J}$. Similarly, swapping the subspaces $\mathcal{P}_i$ and $\mathcal{P}_j$ is the operation associated with interchanging the variables λ_i and λ_j in the function. Replacing $\mathcal{P}_i$ and $\mathcal{P}_j$ with the single subspace $\mathcal{P}_i \oplus \mathcal{P}_j$ is the operation associated with setting $\lambda_i = \lambda_j$ in the n-variable function to produce an $(n-1)$-variable function.

Also, given some positive integer $k \leq m$ and a $m \times k$ matrix $\boldsymbol{\Lambda}$ such that $\boldsymbol{\Lambda}^T \boldsymbol{\Lambda} = \boldsymbol{I}$, one can construct the $k \times k$ matrix-valued function

$$\boldsymbol{L}'_*(\lambda_1, \lambda_2, \ldots, \lambda_n) = \boldsymbol{\Lambda}^T \boldsymbol{L}_*(\lambda_1, \lambda_2, \ldots, \lambda_n)\boldsymbol{\Lambda}, \tag{29.1}$$

which satisfies the homogeneity, Herglotz, and normalization properties. The associated operation on the subspace collection is as follows. Given the $(3, n)$-subspace collection and an orthonormal basis $\boldsymbol{u}_1, \boldsymbol{u}_2, \ldots, \boldsymbol{u}_m$ for $\mathcal{U}$, construct the vectors

$$\boldsymbol{u}'_i = \sum_{j=1}^{m} \Lambda_{ji} \boldsymbol{u}_j,$$

and let $\mathcal{U}'$ denote the k-dimensional subspace spanned by these vectors. These new vectors will form an orthonormal basis for $\mathcal{U}'$ because $\boldsymbol{\Lambda}^T \boldsymbol{\Lambda} = \boldsymbol{I}$. In the subspace collection we replace $\mathcal{U}$ with $\mathcal{U}'$ and $\mathcal{J}$ with

$$\mathcal{J}' = \mathcal{U}'_\perp \oplus \mathcal{J},$$

where $\mathcal{U}'_\perp$ denotes the orthogonal complement of $\mathcal{U}'$ in the subspace $\mathcal{U}$, that is, $\mathcal{U} = \mathcal{U}' \oplus \mathcal{U}'_\perp$. Given a field $\boldsymbol{u} \in \mathcal{U}'$ we can look in the original subspace collection for the solution to the field equations

$$\boldsymbol{J} = \sum_{i=1}^{n} \lambda_i \boldsymbol{\Lambda}_i \boldsymbol{E} \quad \text{with } \boldsymbol{J} \in \mathcal{U} \oplus \mathcal{J}, \quad \boldsymbol{E} \in \mathcal{U} \oplus \mathcal{E}, \quad \boldsymbol{\Gamma}_0 \boldsymbol{E} = \boldsymbol{u}.$$

Since $\mathcal{U} \oplus \mathcal{J} = \mathcal{U}' \oplus \mathcal{J}'$, this will also represent the solution to the field equations in the new subspace collection. It follows that if $\boldsymbol{L}_*(\lambda_1, \lambda_2, \ldots, \lambda_n)$ is the effective tensor function of the original subspace collection represented in the basis $\boldsymbol{u}_1, \boldsymbol{u}_2, \ldots, \boldsymbol{u}_m$, then $\boldsymbol{L}'_*(\lambda_1, \lambda_2, \ldots, \lambda_n)$

will be the effective tensor function of the new subspace collection represented in the basis $\boldsymbol{u}'_1, \boldsymbol{u}'_2, \ldots, \boldsymbol{u}'_k$.

We can also consider operations on pairs of functions. If the $m \times m$ matrix-valued function $\boldsymbol{L}_*(\lambda_1, \lambda_2, \ldots, \lambda_n)$ and the $\ell \times \ell$ matrix-valued function $\boldsymbol{L}'_*(\lambda_1, \lambda_2, \ldots, \lambda_n)$ both satisfy the homogeneity, Herglotz, and normalization properties, then the $(m+\ell) \times (m+\ell)$ matrix-valued function

$$\boldsymbol{L}''_*(\lambda_1, \lambda_2, \ldots, \lambda_n) = \begin{pmatrix} \boldsymbol{L}_*(\lambda_1, \lambda_2, \ldots, \lambda_n) & 0 \\ 0 & \boldsymbol{L}'_*(\lambda_1, \lambda_2, \ldots, \lambda_n) \end{pmatrix} \tag{29.2}$$

clearly also satisfies the homogeneity, Herglotz, and normalization properties. The associated operation, given a subspace collection $(\mathcal{U}, \mathcal{E}, \mathcal{J})$ and $(\mathcal{P}_1, \mathcal{P}_2, \ldots, \mathcal{P}_n)$ and a subspace collection $(\mathcal{U}', \mathcal{E}', \mathcal{J}')$ and $(\mathcal{P}'_1, \mathcal{P}'_2, \ldots, \mathcal{P}'_n)$, is to form the subspace collection $(\mathcal{U}'', \mathcal{E}'', \mathcal{J}'')$ and $(\mathcal{P}''_1, \mathcal{P}''_2, \ldots, \mathcal{P}''_n)$, where

$$\mathcal{U}'' = \mathcal{U} \oplus \mathcal{U}', \quad \mathcal{E}'' = \mathcal{E} \oplus \mathcal{E}', \quad \mathcal{J}'' = \mathcal{J} \oplus \mathcal{J}', \quad \mathcal{P}''_i = \mathcal{P} \oplus \mathcal{P}' \text{ for all } i.$$

When $\ell = m$, another operation that preserves the homogeneity, Herglotz, and normalization properties is to take the weighted average,

$$\boldsymbol{L}_{*c}(\lambda_1, \lambda_2, \ldots, \lambda_n) = c\boldsymbol{L}_*(\lambda_1, \lambda_2, \ldots, \lambda_n) + (1-c)\boldsymbol{L}'_*(\lambda_1, \lambda_2, \ldots, \lambda_n),$$

where $0 \le c \le 1$. Since the right-hand side can be identified with

$$\boldsymbol{\Lambda}^T \boldsymbol{L}''_*(\lambda_1, \lambda_2, \ldots, \lambda_n)\boldsymbol{\Lambda} \text{ with } \boldsymbol{\Lambda} = \begin{pmatrix} c^{1/2}\boldsymbol{I} \\ (1-c)^{1/2}\boldsymbol{I} \end{pmatrix},$$

where $\boldsymbol{L}''_*(\lambda_1, \lambda_2, \ldots, \lambda_n)$ is given by (29.2) and $\boldsymbol{I}$ is the $m \times m$ identity matrix, we see that weighted averaging can be regarded as a sequence of two operations. Performing the sequence of associated operations on the subspace collections gives the operation associated with weighted averaging.

Another familiar operation that we can do with analytic functions is to make substitutions. Thus if $\boldsymbol{L}_*(\lambda_1, \lambda_2, \ldots, \lambda_n)$ is a $m \times m$ matrix-valued function satisfying the homogeneity, Herglotz, and normalization properties and $\lambda_*(\lambda'_1, \lambda'_2, \ldots, \lambda'_p)$ is a scalar-valued function also satisfying these properties, then

$$\boldsymbol{L}''_*(\lambda'_1, \lambda'_2, \ldots, \lambda'_p, \lambda_2, \ldots, \lambda_n) = \boldsymbol{L}_*(\lambda_*(\lambda'_1, \lambda'_2, \ldots, \lambda'_p), \lambda_2, \ldots, \lambda_n)$$

will be another $m \times m$ matrix-valued function satisfying the homogeneity, Herglotz, and normalization properties. The associated operation on subspace collections is found by considering what happens in an electrical circuit when resistors within a given group (each having the same resistance) are each replaced by a network of resistors.

Specifically, let us suppose that we are given a $(3, n)$-subspace collection $(\mathcal{U}, \mathcal{E}, \mathcal{J})$ and $(\mathcal{P}_1, \mathcal{P}_2, \ldots, \mathcal{P}_n)$ and a $(3, p)$-subspace collection $(\mathcal{U}', \mathcal{E}', \mathcal{J}')$ and $(\mathcal{P}'_1, \mathcal{P}'_2, \ldots, \mathcal{P}'_n)$ in which $\mathcal{U}$ is m-dimensional and $\mathcal{U}'$ is one-dimensional. Let $\boldsymbol{L}_*(\lambda_1, \lambda_2, \ldots, \lambda_n)$ and $\lambda_*(\lambda'_1, \lambda'_2, \ldots, \lambda'_p)$ denote the effective tensor functions associated with these subspace collections. We take as our new $(3, n+p-1)$-subspace collection, $(\mathcal{U}'', \mathcal{E}'', \mathcal{J}'')$ and $(\mathcal{P}''_1, \mathcal{P}''_2, \ldots, \mathcal{P}''_{n+p-1})$, where

$$\mathcal{U}'' = \mathcal{U} \otimes \mathcal{U}', \quad \mathcal{E}'' = (\mathcal{E} \otimes \mathcal{U}') \oplus (\mathcal{P}_1 \otimes \mathcal{E}'), \quad \mathcal{J}'' = (\mathcal{J} \otimes \mathcal{U}') \oplus (\mathcal{P}_1 \otimes \mathcal{J}')$$

are mutually orthogonal subspaces and

$$\begin{aligned}\mathcal{P}_i'' &= \mathcal{P}_1 \otimes \mathcal{P}_i' \quad \text{for } 1 \le i \le p,\\ &= \mathcal{P}_{i+1-p} \otimes \mathcal{U}' \quad \text{for } p+1 \le i \le n+p-1\end{aligned}$$

are mutually orthogonal subspaces. Fields in the Hilbert space

$$\mathcal{H}'' = \mathcal{U}'' \oplus \mathcal{E}'' \oplus \mathcal{J}'' = (\mathcal{H} \otimes \mathcal{U}') \oplus (\mathcal{P}_1 \otimes (\mathcal{E}' \oplus \mathcal{J}'))$$

spanned by these subspaces are represented as a pair $[\boldsymbol{P},\ \boldsymbol{u}']$ added to a linear combination of pairs of the form $[\boldsymbol{P}_1,\ \boldsymbol{P}']$, where $\boldsymbol{P} \in \mathcal{H}$, $\boldsymbol{u}' \in \mathcal{U}'$, $\boldsymbol{P}_1 \in \mathcal{P}_1$, and $\boldsymbol{P}' \in \mathcal{E}' \oplus \mathcal{J}'$.

Now suppose that we are given solutions to the field equations

$$\begin{aligned}\boldsymbol{J} &= \sum_{i=1}^{n} \lambda_i \boldsymbol{\Lambda}_i \boldsymbol{E} \ \text{ with } \boldsymbol{J} \in \mathcal{U} \oplus \mathcal{J},\ \ \boldsymbol{E} \in \mathcal{U} \oplus \mathcal{E},\\ \boldsymbol{J}' &= \sum_{j=1}^{p} \lambda_i' \boldsymbol{\Lambda}_i' \boldsymbol{E}' \ \text{ with } \boldsymbol{J}' \in \mathcal{U}' \oplus \mathcal{J}',\ \ \boldsymbol{E}' \in \mathcal{U}' \oplus \mathcal{E}',\end{aligned}$$

where

$$\lambda_1 = \lambda_*(\lambda_1', \lambda_2', \ldots, \lambda_p')$$

and $\boldsymbol{\Lambda}_i$ and $\boldsymbol{\Lambda}_j'$ are the projections onto $\mathcal{P}_i$ and $\mathcal{P}_j'$. Let us set

$$\begin{aligned}\lambda_i'' &= \lambda_i' \quad \text{for } 1 \le i \le p,\\ &= \lambda_{i+1-p} \quad \text{for } p+1 \le i \le n+p-1.\end{aligned}$$

Then, in the new subspace collection, the fields

$$\boldsymbol{E}'' = [\boldsymbol{E},\ \boldsymbol{\Gamma}_0'\boldsymbol{E}'] + [\boldsymbol{\Lambda}_1\boldsymbol{E},\ \boldsymbol{E}' - \boldsymbol{\Gamma}_0'\boldsymbol{E}'], \quad \boldsymbol{J}'' = [\boldsymbol{J},\ \boldsymbol{\Gamma}_0'\boldsymbol{E}'] + [\boldsymbol{\Lambda}_1\boldsymbol{E},\ \boldsymbol{J}' - \boldsymbol{\Gamma}_0'\boldsymbol{J}']$$

solve the field equation

$$\boldsymbol{J}'' = \sum_{i=1}^{n+p-1} \lambda_i'' \boldsymbol{\Lambda}_i'' \boldsymbol{E}'' \ \text{ with } \boldsymbol{J}'' \in \mathcal{U}'' \oplus \mathcal{J}'',\ \ \boldsymbol{E}'' \in \mathcal{U}'' \oplus \mathcal{E}'',$$

in which

$$\begin{aligned}\boldsymbol{\Lambda}_i'' &= \boldsymbol{\Lambda}_1\boldsymbol{\Lambda}_i' \quad \text{for } 1 \le i \le p,\\ &= \boldsymbol{\Lambda}_{i+1-p}\boldsymbol{\Gamma}_0' \quad \text{for } p+1 \le i \le n+p-1\end{aligned}$$

is the projection onto $\mathcal{P}_i''$. By projecting $\boldsymbol{E}''$ and $\boldsymbol{J}''$ onto the subspace $\mathcal{U}''$ we obtain the fields

$$\boldsymbol{\Gamma}_0''\boldsymbol{E}'' = [\boldsymbol{\Gamma}_0\boldsymbol{E},\ \boldsymbol{\Gamma}_0'\boldsymbol{E}'], \quad \boldsymbol{\Gamma}_0''\boldsymbol{J}'' = [\boldsymbol{\Gamma}_0\boldsymbol{J},\ \boldsymbol{\Gamma}_0'\boldsymbol{E}'] = [\boldsymbol{L}_*(\lambda_1, \lambda_2, \ldots, \lambda_n)\boldsymbol{\Gamma}_0\boldsymbol{E},\ \boldsymbol{\Gamma}_0'\boldsymbol{E}'].$$

Given a basis $\boldsymbol{u}_1, \boldsymbol{u}_2, \ldots, \boldsymbol{u}_m$ for $\mathcal{U}$ and a unit vector $\boldsymbol{u}' \in \mathcal{U}'$ it is natural to take $(\boldsymbol{u}_1, \boldsymbol{u}')$, $(\boldsymbol{u}_2, \boldsymbol{u}'), \ldots, (\boldsymbol{u}_m, \boldsymbol{u}')$ as the basis for $\mathcal{U}''$. With this choice of basis, and by choosing $\boldsymbol{E}'$ so that $\boldsymbol{\Gamma}_0'\boldsymbol{E}' = \boldsymbol{u}'$, it is evident that $\boldsymbol{L}_*(\lambda_*(\lambda_1', \lambda_2', \ldots, \lambda_p'), \lambda_2, \ldots, \lambda_n)$ is the analytic function corresponding to the effective tensor function of the new subspace collection.

A second underlying idea is that there is some sort of correspondence between operations on matrix-valued analytic functions $\boldsymbol{Y}_*(\lambda_1, \lambda_2, \ldots, \lambda_n)$ satisfying the homogeneity and Herglotz properties and operations on what we will call $(2, n+1)$-subspace collections comprised of sets $(\mathcal{E}, \mathcal{J})$ and $(\mathcal{V}, \mathcal{P}_1, \mathcal{P}_2, \ldots, \mathcal{P}_n)$ of mutually orthogonal subspaces that span the same Hilbert space $\mathcal{K}$:

$$\mathcal{K} = \mathcal{E} \oplus \mathcal{J} = \mathcal{V} \oplus \mathcal{P}_1 \oplus \mathcal{P}_2 \oplus \cdots \oplus \mathcal{P}_n.$$

Given a $(2, n+1)$-subspace collection and an orthonormal basis of $\mathcal{V}$, the Y-tensor [see (19.29)]

$$\boldsymbol{Y}_*(\lambda_1, \lambda_2, \ldots, \lambda_n) = \boldsymbol{\Pi}_1[\boldsymbol{\Gamma}_2(\sum_{i=1}^{n} \boldsymbol{\Lambda}_i/\lambda_i)\boldsymbol{\Gamma}_2]^{-1}\boldsymbol{\Pi}_1,$$

represented in a basis $\boldsymbol{v}_1, \boldsymbol{v}_2, \ldots, \boldsymbol{v}_m$ of $\mathcal{V}$ and expressed as a function of the $\lambda_1, \lambda_2, \ldots, \lambda_n$, can be taken as the corresponding analytic function, in which the inverse is to be taken on the subspace $\mathcal{J}$. Again given a familiar operation on matrix-valued, n-variable analytic functions satisfying the homogeneity and Herglotz properties one can look for the associated operation on $(2, n+1)$-subspace collections, such that their corresponding matrix-valued analytic functions are related by the given familiar operation.

For example, suppose that $\boldsymbol{Y}_*(\lambda_1, \lambda_2, \ldots, \lambda_n)$ satisfies these properties. Then so does the function

$$\boldsymbol{Y}'_*(\lambda'_1, \lambda'_2, \ldots, \lambda'_n) = \boldsymbol{Y}_*(c\lambda'_1, \lambda'_2, \ldots, \lambda'_n), \tag{29.3}$$

for any positive real choice of the constant c. The associated operation on the $(2, n+1)$-subspace collection $(\mathcal{E}, \mathcal{J})$ and $(\mathcal{V}, \mathcal{P}_1, \mathcal{P}_2, \ldots, \mathcal{P}_n)$ is a reference transformation. We introduce the linear transformations

$$\psi^+(\boldsymbol{P}) = (\boldsymbol{I} - \boldsymbol{\Lambda}_1)\boldsymbol{P} + c^{1/2}\boldsymbol{\Lambda}_1\boldsymbol{P}, \quad \psi^-(\boldsymbol{P}) = (\boldsymbol{I} - \boldsymbol{\Lambda}_1)\boldsymbol{P} + c^{-1/2}\boldsymbol{\Lambda}_1\boldsymbol{P}$$

on fields $\boldsymbol{P} \in \mathcal{K}$, where $\boldsymbol{\Lambda}_1$ is the projection onto $\mathcal{P}_1$. This definition ensures that, for any two fields $\boldsymbol{P}_1$ and $\boldsymbol{P}_2$ in $\mathcal{K}$, the inner product of $\psi^+(\boldsymbol{P}_1)$ with $\psi^-(\boldsymbol{P}_2)$ is the same as the inner product of $\boldsymbol{P}_1$ and $\boldsymbol{P}_2$, that is,

$$(\psi^+(\boldsymbol{P}_1), \psi^-(\boldsymbol{P}_2)) = (\boldsymbol{P}_1, \boldsymbol{P}_2).$$

Consequently the spaces

$$\mathcal{E}' = \psi^+(\mathcal{E}) \text{ and } \mathcal{J}' = \psi^-(\mathcal{J})$$

are orthogonal because the spaces $\mathcal{E}$ and $\mathcal{J}$ are orthogonal.

Let $(\mathcal{E}', \mathcal{J}')$ and $(\mathcal{V}, \mathcal{P}_1, \mathcal{P}_2, \ldots, \mathcal{P}_n)$ be our new subspace collection. Given a solution to the equations

$$\boldsymbol{E} \in \mathcal{E}, \quad \boldsymbol{J} \in \mathcal{J}, \quad (\boldsymbol{I} - \boldsymbol{\Pi}_1)\boldsymbol{J} = \sum_{i=1}^{n} \lambda_i \boldsymbol{\Lambda}_i \boldsymbol{E}$$

in the original subspace collection, in which $\boldsymbol{\Pi}_1$ is the projection onto $\mathcal{V}$, the fields $\boldsymbol{E}' = \psi^+(\boldsymbol{E})$ and $\boldsymbol{J}' = \psi^-(\boldsymbol{J})$ will be a solution to the equations

$$\boldsymbol{E}' \in \mathcal{E}', \quad \boldsymbol{J}' \in \mathcal{J}', \quad (\boldsymbol{I} - \boldsymbol{\Pi}_1)\boldsymbol{J}' = \sum_{i=1}^{n} \lambda'_i \boldsymbol{\Lambda}_i \boldsymbol{E}'$$

in the new subspace collection with

$$\lambda'_1 = \lambda_1/c, \text{ and } \lambda'_i = \lambda_i \text{ for all } i \geq 2.$$

Since $\mathbf{\Pi}_1 \boldsymbol{E}' = \mathbf{\Pi}_1 \boldsymbol{E}$ and $\mathbf{\Pi}_1 \boldsymbol{E}' = \mathbf{\Pi}_1 \boldsymbol{E}$, it follows that Y-tensor functions of the two subspace collections are related by (29.3), as desired.

It remains an open question as to whether every analytic $m \times m$ matrix-valued function $\boldsymbol{Y}_*(\lambda_1, \lambda_2, \ldots, \lambda_n)$ satisfying the homogeneity and Herglotz properties can be associated with a given $(2, n+1)$-subspace collection.

29.2. Hints of a deeper connection between analytic functions and subspace collections

Given that there are these associations between operations on analytic functions and operations on $(3, n)$-subspace collections, one might wonder if there might be a one-to-one correspondence between matrix-valued analytic functions $\boldsymbol{L}_*(\lambda_1, \lambda_2, \ldots, \lambda_n)$ satisfying the homogeneity, Herglotz, and normalization properties and $(3, n)$-subspace collections. Of particular importance is the question of whether one can uniquely recover the relative orientations of the subspaces from knowledge of the effective tensor function $\boldsymbol{L}_*(\lambda_1, \lambda_2, \ldots, \lambda_n)$. This would allow one to recover matrices representing the operators $\mathbf{\Gamma}_0$, $\mathbf{\Gamma}_1$, $\mathbf{\Gamma}_2$ and $\mathbf{\Lambda}_1, \mathbf{\Lambda}_2, \ldots, \mathbf{\Lambda}_n$, which could subsequently be used to solve coupled field equations.

At present this is still an open (and interesting) question. To provide some evidence, via a counting argument, that one might be able to recover this information, let us consider a $(3, 3)$-subspace collection $(\mathcal{U}, \mathcal{E}, \mathcal{J})$ and $(\mathcal{P}_1, \mathcal{P}_2, \mathcal{P}_3)$ of finite-dimensional subspaces, where $\mathcal{U}$ is one-dimensional, and let $\lambda_*(\lambda_1, \lambda_2, \lambda_3)$ denote the corresponding scalar-valued rational function representing the effective parameter. Let p_1, p_2, and p_3 represent the dimensions of $\mathcal{P}_1$, $\mathcal{P}_2$, and $\mathcal{P}_3$, and let q_1 and q_2 represent the dimensions of $\mathcal{E}$ and $\mathcal{J}$. The total dimension of the Hilbert space is therefore

$$h = p_1 + p_2 + p_3 = 1 + q_1 + q_2.$$

Let us also assume that $\mathcal{H}$ is the smallest space containing $\mathcal{U}$ that is closed under the action of $\mathbf{\Gamma}_1$, $\mathbf{\Lambda}_1$, and $\mathbf{\Lambda}_2$. [If it is not, then we should redefine $\mathcal{H}$ as this space because it is only those fields arising from products of the operators $\mathbf{\Gamma}_1$, $\mathbf{\Lambda}_1$, and $\mathbf{\Lambda}_2$ applied to fields in $\mathcal{U}$ that have a role in determining $\lambda_*(\lambda_1, \lambda_2, \lambda_3)$.] Now consider the subspace

$$[\mathbf{\Lambda}_1(\mathcal{U} \oplus \mathcal{E})] \oplus [\mathbf{\Lambda}_2(\mathcal{U} \oplus \mathcal{E})] \oplus [\mathbf{\Lambda}_3(\mathcal{U} \oplus \mathcal{E})].$$

This clearly contains $\mathcal{U}$ and is closed under the action of $\mathbf{\Lambda}_1$, $\mathbf{\Lambda}_2$, and $\mathbf{\Gamma}_1$ (because it contains $\mathcal{E}$). It therefore must be $\mathcal{H}$ and $\mathbf{\Lambda}_i(\mathcal{U} \oplus \mathcal{E})$, which has dimension of at most $1 + q_1$, must be $\mathcal{P}_i$ for $i = 1, 2, 3$. Therefore we have the inequalities

$$p_1 \leq 1 + q_1, \quad p_2 \leq 1 + q_1, \quad p_3 \leq 1 + q_1,$$

and by summing these we deduce that

$$q_2 \leq 2(1 + q_1).$$

Similarly, by considering the subspace

$$[\mathbf{\Lambda}_1(\mathcal{U} \oplus \mathcal{J})] \oplus [\mathbf{\Lambda}_2(\mathcal{U} \oplus \mathcal{J})] \oplus [\mathbf{\Lambda}_3(\mathcal{U} \oplus \mathcal{J})],$$

which can also be identified with $\mathcal{H}$, we arrive at the inequalities

$$p_1 \leq 1 + q_2, \quad p_2 \leq 1 + q_2, \quad p_3 \leq 1 + q_2, \quad q_1 \leq 2(1 + q_2).$$

Now let us pick some orthonormal basis for the subspace $\mathcal{U} \oplus \mathcal{J}$; let $\boldsymbol{A}_i$ for $i = 1, 2, 3$ denote the $(1+q_2)\times(1+q_2)$ symmetric matrix representing the operator $(\boldsymbol{\Gamma}_0+\boldsymbol{\Gamma}_2)\boldsymbol{\Lambda}_i(\boldsymbol{\Gamma}_0+\boldsymbol{\Gamma}_2)$; and let $\boldsymbol{u}$, with $\boldsymbol{u}\cdot\boldsymbol{u} = 1$, represent the field that spans $\mathcal{U}$. Since the basis is orthonormal, we have

$$\boldsymbol{A}_1 + \boldsymbol{A}_2 + \boldsymbol{A}_3 = \boldsymbol{I}, \tag{29.4}$$

and because $\boldsymbol{\Lambda}_i(\mathcal{U} \oplus \mathcal{J})$ can be identified with $\mathcal{P}_i$, each matrix $\boldsymbol{A}_i$ must have rank p_i. The formula for the effective parameter implies that

$$\lambda_*(\lambda_1, \lambda_2, \lambda_3) = \boldsymbol{u}\cdot[\boldsymbol{A}_1/\lambda_1 + \boldsymbol{A}_2/\lambda_2 + \boldsymbol{A}_3/\lambda_3]^{-1}\boldsymbol{u}.$$

Thus if we express $\lambda_*(\lambda_1, \lambda_2, \lambda_3)$ as a function of $1/\lambda_1$, $1/\lambda_2$, and $1/\lambda_3$, then the denominator of this function can be identified (to within a constant factor) with the polynomial

$$\det[\boldsymbol{A}_1/\lambda_1 + \boldsymbol{A}_2/\lambda_2 + \boldsymbol{A}_3/\lambda_3] = \sum_{a,b,c} \alpha_{abc}/\lambda_1^a\lambda_2^b\lambda_3^c, \tag{29.5}$$

where the sum extends over all integers a, b, and c, with

$$a + b + c = 1 + q_2, \quad 0 \le a \le p_1, \quad 0 \le b \le p_2, \quad 0 \le c \le p_3.$$

If we know $\lambda_*(\lambda_1, \lambda_2, \lambda_3)$, then we should be able to determine this polynomial. From the degree of the polynomial we recover the subspace dimension q_2, and from the maximum powers of $1/\lambda_1$, $1/\lambda_2$, and $1/\lambda_3$ we recover the subspace dimensions p_1, p_2, and p_3. This allows us to also determine $q_1 = p_1 + p_2 + p_3 - 1 - q_2$. Thus all of the subspace dimensions can be recovered from the function $\lambda_*(\lambda_1, \lambda_2, \lambda_3)$.

The matrices $\boldsymbol{A}_1$, $\boldsymbol{A}_2$, and $\boldsymbol{A}_3$ determine the orientation of the subspace $\mathcal{U}\oplus\mathcal{J}$ with respect to the three subspaces $\mathcal{P}_1$, $\mathcal{P}_2$, and $\mathcal{P}_3$. Can we recover these, modulo changes of basis, from the polynomial (29.5)? Each coefficient of the polynomial is a function of the elements of these matrices and provides us with a nonlinear equation for these matrix elements. How many coefficients are there? Without loss of generality let us suppose that the spaces $\mathcal{P}_1$, $\mathcal{P}_2$, and $\mathcal{P}_3$ have been labeled so that $p_1 \ge p_2 \ge p_3$. With a fixed in the regime $0 \le a < 1 + q_2 - p_2$, the constant b can take integer values from $b = 1 + q_2 - a - p_3$ to $b = p_2$, that is, a total of $p_2 + p_3 + a - q_2$ different values. With a fixed in the regime $1 + q_2 - p_2 \le a < 1 + q_2 - p_3$, the constant b can take integer values from $b = 1 + q_2 - a - p_3$ to $b = 1 + q_2 - a$, that is, a total of $p_3 + 1$ different values. Finally, with a fixed in the regime $1 + q_2 - p_3 \le a \le p_1$, the constant b can take integer values from $b = 0$ to $b = 1 + q_2 - a$, that is, a total of $2 + q_2 - a$ different values. Therefore the total number of coefficients in the polynomial is

$$\sum_{a=0}^{q_2-p_2}(p_2 + p_3 + a - q_2) + \sum_{a=1+q_2-p_2}^{q_2-p_3}(p_3 + 1) + \sum_{a=1+q_2-p_3}^{p_1}(2 + q_2 - a) = k + 1,$$

where

$$k = [2(1 + q_2)q_1 - p_1^2 - p_2^2 - p_3^2 + h]/2.$$

These coefficients are not all independent. Since the value of the determinant is 1 when $\lambda_1 = \lambda_2 = \lambda_3 = 1$, we have the relation

$$\sum_{a,b,c} \alpha_{abc} = 1.$$

Thus the number of independent constraints is k.

Now how many independent elements are there in the matrices $\boldsymbol{A}_1$, $\boldsymbol{A}_2$, and $\boldsymbol{A}_3$? A given $(1+q_2)\times(1+q_2)$ symmetric matrix $\boldsymbol{A}_i$ of rank p_i has $p_i(3+2q_2-p_i)/2$ independent elements. However, the identity (29.4) provides $(1+q_2)(2+q_2)/2$ constraints amongst the elements of the three matrices. Therefore the total number of independent elements is

$$\begin{aligned} &p_1(3+2q_2-p_1)/2+p_2(3+2q_2-p_2)/2+p_3(3+2q_2-p_3)/2-(1+q_2)(2+q_2)/2\\ &\quad = k+q_2(1+q_2)/2. \end{aligned}$$

We still have the freedom to change the basis of $\mathcal{U}\oplus\mathcal{J}$ or, equivalently, the freedom to replace each matrix $\boldsymbol{A}_i$ with $\boldsymbol{Q}^T\boldsymbol{A}_i\boldsymbol{Q}$, where $\boldsymbol{Q}^T\boldsymbol{Q}=\boldsymbol{I}$. Since such matrices $\boldsymbol{Q}$ have $q_2(1+q_2)/2$ independent elements, we see that once these degrees of freedom are subtracted, there are precisely k unknowns that determine the orientation of the subspace $\mathcal{U}\oplus\mathcal{J}$ with respect to the three subspaces $\mathcal{P}_1$, $\mathcal{P}_2$, and $\mathcal{P}_3$. Since this exactly matches the number of independent coefficients in the polynomial, one might be tempted to conjecture that knowledge of the polynomial uniquely determines the subspace orientation. An unpublished counterexample of Alexander Movchan and myself shows that this is not true. In general one is left with a discrete set of possible subspace orientations. By considering the numerator of $\lambda_*(\lambda_1,\lambda_2,\lambda_3)$ as a function of λ_1, λ_2, and λ_3, one similarly obtains a discrete set of possible orientations of the subspace $\mathcal{U}\oplus\mathcal{E}$ with respect to the three subspaces $\mathcal{P}_1$, $\mathcal{P}_2$, and $\mathcal{P}_3$. It is hoped that the information gained about the orientations of the subspaces $\mathcal{U}\oplus\mathcal{E}$ and $\mathcal{U}\oplus\mathcal{J}$, coupled with the orthogonality of the three subspaces $\mathcal{U}$, $\mathcal{E}$, and $\mathcal{J}$, is enough to select amongst the different possibilities and determine uniquely the orientation of $\mathcal{U}$, $\mathcal{E}$, and $\mathcal{J}$ with respect to $\mathcal{P}_1$, $\mathcal{P}_2$, and $\mathcal{P}_3$. Whether it is remains an open question.

29.3. The field equation recursion method for two-phase composites

Given that there are some associations between operations on analytic functions and subspace collections, it seems logical to try to find the manipulations of subspace collections that are analogous to the fractional linear transformations of analytic functions found in the previous chapter.

Let us consider a problem where the tensor $\boldsymbol{L}$ takes the form

$$\boldsymbol{L}=\lambda_1\boldsymbol{\Lambda}_1+\lambda_2\boldsymbol{\Lambda}_2,$$

where λ_1 and λ_2 represent the eigenvalues of $\boldsymbol{L}$, and $\boldsymbol{\Lambda}_1$ and $\boldsymbol{\Lambda}_2$ represent projections onto the associated eigenspaces $\mathcal{P}_1$ and $\mathcal{P}_2$, which we assume to be mutually orthogonal and to span $\mathcal{H}$:

$$\mathcal{H}=\mathcal{U}\oplus\mathcal{E}\oplus\mathcal{J}=\mathcal{P}_1\oplus\mathcal{P}_2.$$

We let $\boldsymbol{L}_*$ represent the effective tensor associated with $\boldsymbol{L}$. In particular, $\boldsymbol{L}$ could represent the conductivity tensor

$$\boldsymbol{\sigma}=\sigma_1\chi_1\boldsymbol{I}+\sigma_2\chi_2\boldsymbol{I}$$

of a two-phase composite. In this context $\chi_1\boldsymbol{I}$ and $\chi_2\boldsymbol{I}$ represent projections onto the spaces $\mathcal{P}_1$ and $\mathcal{P}_2$, which are nonzero only inside phase 1 or 2, respectively.

In the analytic method the fundamental object is the function $\boldsymbol{L}_*(\lambda_1,\lambda_2)$, while in the field equation recursion method the fundamental object is the (3, 2)-subspace collection $(\mathcal{U},\mathcal{E},\mathcal{J})$ and $(\mathcal{P}_1,\mathcal{P}_2)$. In the analytic method one might assume, for example, that the first derivative

$$\boldsymbol{W}_1=\boldsymbol{R}_1=\left.\frac{d\boldsymbol{L}_*(\lambda_1,1)}{d\lambda_1}\right|_{\lambda_1=1}$$

of the function $\boldsymbol{L}_*(\lambda_1, \lambda_2)$ is known. Applying the Y-transformation generates a function

$$\begin{aligned}&\boldsymbol{Y}_*(\lambda_1, \lambda_2) = Y[\boldsymbol{L}_*(\lambda_1, \lambda_2)]\\ &= -\boldsymbol{W}_2\lambda_1 - \boldsymbol{W}_1\lambda_2 + (\lambda_1 - \lambda_2)^2(\boldsymbol{W}_1\boldsymbol{W}_2)^{1/2}[\boldsymbol{W}_1\lambda_1 + \boldsymbol{W}_2\lambda_2 - \boldsymbol{L}_*(\lambda_1, \lambda_2)]^{-1}(\boldsymbol{W}_1\boldsymbol{W}_2)^{1/2},\end{aligned} \tag{29.6}$$

satisfying the homogeneity and Herglotz properties, in which $\boldsymbol{W}_2 = \boldsymbol{I} - \boldsymbol{W}_1$. When the second derivative

$$\boldsymbol{R}_2 = \frac{d^2\boldsymbol{L}_*(\lambda_1, 1)}{d\lambda_1^2}\bigg|_{\lambda_1=1}$$

is known, then this information translates into a known value for

$$\boldsymbol{N} = \boldsymbol{Y}_*(1, 1) = -\boldsymbol{I} - \boldsymbol{W}_2^{1/2}\boldsymbol{W}_1^{1/2}\boldsymbol{R}_2^{-1}\boldsymbol{W}_1^{1/2}\boldsymbol{W}_2^{1/2}.$$

One then applies the normalization transformation to generate a function

$$\boldsymbol{L}_*^{(1)}(\lambda_1, \lambda_2) = \boldsymbol{N}^{-1/2}\boldsymbol{Y}_*(\lambda_1, \lambda_2)\boldsymbol{N}^{-1/2}, \tag{29.7}$$

satisfying the homogeneity, Herglotz, and normalization properties.

In the field equation recursion method one performs the analogous sequence of operations on subspace collections. The first step is to generate a (2, 3)-subspace collection $(\mathcal{E}, \mathcal{J})$ and $(\mathcal{V}, \mathcal{P}_1^{(1)}, \mathcal{P}_2^{(1)})$ that span a Hilbert space

$$\mathcal{K} = \mathcal{E} \oplus \mathcal{J} = \mathcal{V} \oplus \mathcal{P}_1^{(1)} \oplus \mathcal{P}_2^{(1)}, \tag{29.8}$$

Then one generates a (3, 2)-subspace collection $(\mathcal{U}^{(1)}, \mathcal{E}^{(1)}, \mathcal{J}^{(1)})$ and $(\mathcal{P}_1^{(1)}, \mathcal{P}_2^{(1)})$ that span a Hilbert space

$$\mathcal{H}^{(1)} = \mathcal{U}^{(1)} \oplus \mathcal{E}^{(1)} \oplus \mathcal{J}^{(1)} = \mathcal{P}_1^{(1)} \oplus \mathcal{P}_2^{(1)}. \tag{29.9}$$

With a suitable choice of the spaces, satisfying the inclusion relations

$$\mathcal{E}^{(1)} \subset \mathcal{E}, \quad \mathcal{J}^{(1)} \subset \mathcal{J}, \quad \mathcal{P}_1^{(1)} \subset \mathcal{P}_1, \quad \mathcal{P}_2^{(1)} \subset \mathcal{P}_2,$$

and with the right choice of basis, the Y-tensor function of the (2, 3)-subspace collection turns out to be $\boldsymbol{Y}_*(\lambda_1, \lambda_2)$, and the effective tensor function of the second (3, 2)-subspace collection turns out to be $\boldsymbol{L}_*^{(1)}(\lambda_1, \lambda_2)$. In other words, the field equation recursion method provides an interpretation for the functions arising in the analytic method and as a direct corollary immediately explains why these functions satisfy the homogeneity and Herglotz properties.

Notice from (29.9) and (29.8) that

$$\mathcal{H} = \mathcal{U} \oplus \mathcal{K}, \quad \mathcal{K} = \mathcal{V} \oplus \mathcal{H}^{(1)},$$

In particular, the space $\mathcal{K}$ is the orthogonal complement of $\mathcal{U}$ in $\mathcal{H}$. In a two-phase composite $\mathcal{K}$ is comprised of all square integrable fields with average value zero. For such a composite we found in chapter 19 on page 397 that it is natural to take $\mathcal{P}_1^{(1)}$ and $\mathcal{P}_2^{(2)}$ as those fields that are nonzero only in phase 1 or phase 2, respectively, and which have average value zero, that is, $\mathcal{P}_1^{(1)}$ and $\mathcal{P}_2^{(2)}$ are comprised of those fields in $\mathcal{P}_1$ and $\mathcal{P}_2$ that are members of $\mathcal{K}$:

$$\mathcal{P}_1^{(1)} = \mathcal{P}_1 \cap \mathcal{K}, \quad \mathcal{P}_2^{(1)} = \mathcal{P}_2 \cap \mathcal{K}.$$

Let us take this as our definition of $\mathcal{P}_1^{(1)}$ and $\mathcal{P}_2^{(2)}$ in the general setting. Then $\mathcal{V}$ is the orthogonal complement of $\mathcal{H}^{(1)} = \mathcal{P}_1^{(1)} \oplus \mathcal{P}_2^{(1)}$ in the space $\mathcal{K}$. In a two-phase composite this space is comprised of those fields that have a constant value in each phase and a zero average value.

The space $\mathcal{V}$ can be equivalently defined as the orthogonal complement of $\mathcal{U}$ in the space spanned by $\boldsymbol{\Lambda}_1\mathcal{U}$ and $\boldsymbol{\Lambda}_2\mathcal{U}$. To justify this assertion we need to prove that

$$\mathcal{U} \oplus \mathcal{V} = \boldsymbol{\Lambda}_1\mathcal{U} \oplus \boldsymbol{\Lambda}_2\mathcal{U}. \tag{29.10}$$

Since

$$\mathcal{H} = (\mathcal{U} \oplus \mathcal{V}) \oplus (\mathcal{P}_1^{(1)} \oplus \mathcal{P}_2^{(1)}),$$

and since the spaces $\mathcal{H}$ and $\mathcal{P}_1^{(1)} \oplus \mathcal{P}_2^{(1)}$ are closed under the action of the self-adjoint operator $\boldsymbol{\Lambda}_1$, it follows that $\mathcal{U} \oplus \mathcal{V}$ must be closed under the action of $\boldsymbol{\Lambda}_1$, implying that

$$\boldsymbol{\Lambda}_1\mathcal{U} \subset \mathcal{U} \oplus \mathcal{V}.$$

Similarly the space $\boldsymbol{\Lambda}_2\mathcal{U}$ must be contained in $\mathcal{U} \oplus \mathcal{V}$, and we conclude that

$$\boldsymbol{\Lambda}_1\mathcal{U} \oplus \boldsymbol{\Lambda}_2\mathcal{U} \subset \mathcal{U} \oplus \mathcal{V}.$$

Now suppose that the sets are not equal. Then there exists some field $\boldsymbol{P}$ in $\mathcal{U} \oplus \mathcal{V}$ that is orthogonal to $\boldsymbol{\Lambda}_1\mathcal{U} \oplus \boldsymbol{\Lambda}_2\mathcal{U}$. It follows that $\boldsymbol{\Lambda}_1\boldsymbol{P}$ is orthogonal to $\boldsymbol{\Lambda}_1\mathcal{U} \oplus \boldsymbol{\Lambda}_2\mathcal{U}$ and in particular orthogonal to $\mathcal{U}$. Therefore $\boldsymbol{\Lambda}_1\boldsymbol{P}$ is in $\mathcal{K}$. Similarly, $\boldsymbol{\Lambda}_2\boldsymbol{P}$ is in $\mathcal{K}$. Consequently we have

$$\boldsymbol{\Lambda}_1\boldsymbol{P} \in \mathcal{P}_1^{(1)}, \quad \boldsymbol{\Lambda}_2\boldsymbol{P} \in \mathcal{P}_2^{(1)}, \text{ implying that } \boldsymbol{P} \in \mathcal{P}_1^{(1)} \oplus \mathcal{P}_2^{(1)}.$$

But as $\mathcal{U} \oplus \mathcal{V}$ is orthogonal to $\mathcal{P}_1^{(1)} \oplus \mathcal{P}_2^{(1)}$, we conclude that $\boldsymbol{P}$ is necessarily zero. This completes the proof of (29.10)

From section 20.4 on page 418 it seems natural to take

$$\mathcal{E}^{(1)} = \mathcal{E} \cap \mathcal{H}^{(1)}, \quad \mathcal{J}^{(1)} = \mathcal{J} \cap \mathcal{H}^{(1)}.$$

In a two-phase conducting composite, $\mathcal{E}^{(1)}$ consists of all curl free electric fields that have a zero average value within each phase, and $\mathcal{J}^{(1)}$ consists of all divergence free current fields that have a zero average value within each phase. The space $\mathcal{U}^{(1)}$ is then taken as the orthogonal compliment of $\mathcal{E}^{(1)} \oplus \mathcal{J}^{(1)}$ in the space $\mathcal{H}^{(1)}$.

The space $\mathcal{U}^{(1)}$ can be equivalently defined as the orthogonal complement of $\mathcal{V}$ in the space spanned by $\boldsymbol{\Gamma}_1\mathcal{V}$ and $\boldsymbol{\Gamma}_2\mathcal{V}$, that is, we have

$$\mathcal{V} \oplus \mathcal{U}^{(1)} = \boldsymbol{\Gamma}_1\mathcal{V} \oplus \boldsymbol{\Gamma}_2\mathcal{V}. \tag{29.11}$$

The proof of this is similar to the proof of (29.10); see also section 20.5 on page 419.

What is the relation between the effective tensor $\boldsymbol{L}_*$ associated with $\mathcal{H}$ and the Y-tensor $\boldsymbol{Y}_*$ associated with $\mathcal{K}$? By direct analogy with (19.17) we have

$$\boldsymbol{L}_* = \boldsymbol{\Gamma}_0\boldsymbol{L}\boldsymbol{\Gamma}_0 - \boldsymbol{\Gamma}_0\boldsymbol{L}\boldsymbol{\Pi}_1[\boldsymbol{\Pi}_1\boldsymbol{L}\boldsymbol{\Pi}_1 + \boldsymbol{Y}_*]^{-1}\boldsymbol{\Pi}_1\boldsymbol{L}\boldsymbol{\Gamma}_0, \tag{29.12}$$

where $\boldsymbol{\Gamma}_0$ is the projection onto $\mathcal{U}$ and $\boldsymbol{\Pi}_1$ is the projection onto $\mathcal{V}$.

To find a more explicit way of representing (29.12) let us suppose that we are given an orthonormal basis $\boldsymbol{u}_1, \boldsymbol{u}_2, \ldots \boldsymbol{u}_m$ of $\mathcal{U}$. We define weight matrices $\boldsymbol{W}_1$ and $\boldsymbol{W}_2$ with matrix elements

$$\{\boldsymbol{W}_1\}_{jk} = (\boldsymbol{u}_j, \boldsymbol{\Lambda}_1\boldsymbol{u}_k), \quad \{\boldsymbol{W}_2\}_{jk} = (\boldsymbol{u}_j, \boldsymbol{\Lambda}_2\boldsymbol{u}_k).$$

These matrices are clearly positive-semidefinite and sum to the identity matrix:

$$\boldsymbol{W}_1 \geq 0, \quad \boldsymbol{W}_2 \geq 0, \quad \boldsymbol{W}_1 + \boldsymbol{W}_2 = \boldsymbol{I}.$$

Now consider the fields

$$\boldsymbol{a}_k = \boldsymbol{\Lambda}_i \boldsymbol{u}_k - \sum_{\ell=1}^{m} \{\boldsymbol{W}_1\}_{k\ell} \boldsymbol{u}_\ell.$$

These span $\mathcal{V}$ but are not orthonormal. They have inner products

$$(\boldsymbol{a}_j, \boldsymbol{a}_k) = \{\boldsymbol{W}_1 \boldsymbol{W}_2\}_{jk}.$$

To avoid mathematical technicalities, let us assume that the fields $\boldsymbol{a}_1, \boldsymbol{a}_2, \ldots, \boldsymbol{a}_m$ are linearly independent, that is, the matrices $\boldsymbol{W}_1$ and $\boldsymbol{W}_2$ are strictly positive-definite. Then the fields

$$\boldsymbol{v}_j = \sum_{k=1}^{m} \{(\boldsymbol{W}_1 \boldsymbol{W}_2)^{-1/2}\}_{jk} \boldsymbol{a}_k = \sum_{k=1}^{m} \{(\boldsymbol{W}_1 \boldsymbol{W}_2)^{-1/2}\}_{jk} [\boldsymbol{\Lambda}_i \boldsymbol{u}_k - \sum_{\ell=1}^{m} \{\boldsymbol{W}_1\}_{k\ell} \boldsymbol{u}_\ell]$$

provide an orthonormal basis for $\mathcal{V}$. From these formulas we see that

$$\begin{aligned}
(\boldsymbol{u}_j, \boldsymbol{\Lambda}_1 \boldsymbol{u}_k) &= \{\boldsymbol{W}_1\}_{jk}, \\
(\boldsymbol{u}_j, \boldsymbol{\Lambda}_2 \boldsymbol{u}_k) &= \{\boldsymbol{W}_2\}_{jk}, \\
(\boldsymbol{u}_j, \boldsymbol{\Lambda}_1 \boldsymbol{v}_k) &= \{(\boldsymbol{W}_1 \boldsymbol{W}_2)^{1/2}\}_{jk}, \\
(\boldsymbol{u}_j, \boldsymbol{\Lambda}_2 \boldsymbol{v}_k) &= -\{(\boldsymbol{W}_1 \boldsymbol{W}_2)^{1/2}\}_{jk}, \\
(\boldsymbol{v}_j, \boldsymbol{\Lambda}_1 \boldsymbol{v}_k) &= \{\boldsymbol{W}_2\}_{jk}, \\
(\boldsymbol{v}_j, \boldsymbol{\Lambda}_2 \boldsymbol{v}_k) &= \{\boldsymbol{W}_1\}_{jk}.
\end{aligned} \tag{29.13}$$

As in section 19.2 on page 399, let us equate each operator with the matrix that represents its action with respect to the basis. Following this convention (29.13) implies that

$$\begin{aligned}
\boldsymbol{\Gamma}_0 \boldsymbol{\Lambda}_1 \boldsymbol{\Gamma}_0 &= \boldsymbol{W}_1, \quad \boldsymbol{\Gamma}_0 \boldsymbol{\Lambda}_2 \boldsymbol{\Gamma}_0 = \boldsymbol{W}_2, \\
\boldsymbol{\Gamma}_0 \boldsymbol{\Lambda}_1 \boldsymbol{\Pi}_1 &= (\boldsymbol{W}_1 \boldsymbol{W}_2)^{1/2}, \quad \boldsymbol{\Gamma}_0 \boldsymbol{\Lambda}_2 \boldsymbol{\Pi}_1 = -(\boldsymbol{W}_1 \boldsymbol{W}_2)^{1/2}, \\
\boldsymbol{\Pi}_1 \boldsymbol{\Lambda}_1 \boldsymbol{\Pi}_1 &= \boldsymbol{W}_2, \quad \boldsymbol{\Pi}_1 \boldsymbol{\Lambda}_2 \boldsymbol{\Pi}_1 = \boldsymbol{W}_1,
\end{aligned} \tag{29.14}$$

and it follows that

$$\begin{aligned}
\boldsymbol{\Gamma}_0 \boldsymbol{L} \boldsymbol{\Gamma}_0 &= \lambda_1 \boldsymbol{W}_1 + \lambda_2 \boldsymbol{W}_2, \quad \boldsymbol{\Gamma}_0 \boldsymbol{L} \boldsymbol{\Pi}_1 = (\lambda_1 - \lambda_2)(\boldsymbol{W}_1 \boldsymbol{W}_2)^{1/2}, \\
\boldsymbol{\Pi}_1 \boldsymbol{L} \boldsymbol{\Pi}_1 &= \lambda_1 \boldsymbol{W}_2 + \lambda_2 \boldsymbol{W}_1.
\end{aligned}$$

With these substitutions the formulas (29.12) relating the effective tensor $\boldsymbol{L}_*$ with the Y-tensor $\boldsymbol{Y}_*$ takes the form

$$\boldsymbol{L}_* = \boldsymbol{W}_1 \lambda_1 + \boldsymbol{W}_2 \lambda_2 - (\lambda_1 - \lambda_2)^2 (\boldsymbol{W}_1 \boldsymbol{W}_2)^{1/2} [\boldsymbol{W}_2 \lambda_1 + \boldsymbol{W}_1 \lambda_2 + \boldsymbol{Y}_*]^{-1} (\boldsymbol{W}_1 \boldsymbol{W}_2)^{1/2},$$

in which $\boldsymbol{Y}_*$ is now the matrix representing the action of the operator $\boldsymbol{Y}_*$ with respect to the basis $\boldsymbol{v}_1, \boldsymbol{v}_2, \ldots, \boldsymbol{v}_m$. Thus the matrix $\boldsymbol{Y}_*$ given by (29.6) represents the action of the operator $\boldsymbol{Y}_*$ associated with the (2, 3)-subspace collection $(\mathcal{E}, \mathcal{J})$ and $(\mathcal{V}, \mathcal{P}_1^{(1)}, \mathcal{P}_2^{(1)})$.

Next, what is the relation between the Y-tensor $\boldsymbol{Y}_*$ associated with $\mathcal{K}$ and the effective tensor $\boldsymbol{L}_*^{(1)}$ associated with $\mathcal{H}^{(1)}$? By direct analogy with (20.29) and (20.28) we have

$$\boldsymbol{Y}_* = \boldsymbol{K}\boldsymbol{L}_*^{(1)}\boldsymbol{K}^T, \quad \text{where } \boldsymbol{K} = -[\boldsymbol{\Pi}_1\boldsymbol{\Gamma}_1\boldsymbol{\Pi}_1]^{-1}\boldsymbol{\Pi}_1\boldsymbol{\Gamma}_1\boldsymbol{\Gamma}_0^{(1)}, \tag{29.15}$$

in which $\boldsymbol{\Pi}_1$ and $\boldsymbol{\Gamma}_0^{(1)}$ are the projections onto the spaces $\mathcal{V}$ and $\mathcal{U}^{(1)}$. To obtain an explicit expression for this relation we introduce the matrices $\boldsymbol{G}_1$ and $\boldsymbol{G}_2$ with matrix elements

$$\{\boldsymbol{G}_1\}_{jk} = (\boldsymbol{v}_j, \boldsymbol{\Gamma}_1\boldsymbol{v}_k), \quad \{\boldsymbol{G}_2\}_{jk} = (\boldsymbol{v}_j, \boldsymbol{\Gamma}_2\boldsymbol{v}_k).$$

These are clearly positive-semidefinite and sum to the identity:

$$\boldsymbol{G}_1 \geq 0, \quad \boldsymbol{G}_2 \geq 0, \quad \boldsymbol{G}_1 + \boldsymbol{G}_2 = \boldsymbol{I}.$$

To avoid mathematical technicalities we assume that these matrices are strictly positive-definite. Then the fields

$$\boldsymbol{u}_j^{(1)} = \sum_{k=1}^{m}\{(\boldsymbol{G}_1\boldsymbol{G}_2)^{-1/2}\}_{jk}[\boldsymbol{\Gamma}_1\boldsymbol{v}_k - \sum_{\ell=1}^{m}\{\boldsymbol{G}_1\}_{k\ell}\boldsymbol{v}_\ell]$$

form an orthonormal basis for $\mathcal{U}^{(1)}$ and we have

$$\begin{aligned}
(\boldsymbol{v}_j, \boldsymbol{\Gamma}_1\boldsymbol{v}_k) &= \{\boldsymbol{G}_1\}_{jk}, \\
(\boldsymbol{v}_j, \boldsymbol{\Gamma}_2\boldsymbol{v}_k) &= \{\boldsymbol{G}_2\}_{jk}, \\
(\boldsymbol{v}_j, \boldsymbol{\Gamma}_1\boldsymbol{u}_k^{(1)}) &= \{(\boldsymbol{G}_1\boldsymbol{G}_2)^{1/2}\}_{jk}, \\
(\boldsymbol{v}_j, \boldsymbol{\Gamma}_2\boldsymbol{u}_k^{(1)}) &= -\{(\boldsymbol{G}_1\boldsymbol{G}_2)^{1/2}\}_{jk}, \\
(\boldsymbol{u}_j^{(1)}, \boldsymbol{\Gamma}_1\boldsymbol{u}_k^{(1)}) &= \{\boldsymbol{G}_2\}_{jk}, \\
(\boldsymbol{u}_j^{(1)}, \boldsymbol{\Gamma}_2\boldsymbol{u}_k^{(1)}) &= \{\boldsymbol{G}_1\}_{jk}.
\end{aligned} \tag{29.16}$$

If we equate operators with the matrices that represent their action with respect to the basis, then (29.16) implies that

$$\begin{aligned}
\boldsymbol{\Pi}_1\boldsymbol{\Gamma}_1\boldsymbol{\Pi}_1 &= \boldsymbol{G}_1, \quad \boldsymbol{\Pi}_1\boldsymbol{\Gamma}_2\boldsymbol{\Pi}_1 = \boldsymbol{G}_2, \\
\boldsymbol{\Pi}_1\boldsymbol{\Gamma}_1\boldsymbol{\Gamma}_0^{(1)} &= (\boldsymbol{G}_1\boldsymbol{G}_2)^{1/2}, \quad \boldsymbol{\Pi}_1\boldsymbol{\Gamma}_2\boldsymbol{\Gamma}_0^{(1)} = -(\boldsymbol{G}_1\boldsymbol{G}_2)^{1/2}, \\
\boldsymbol{\Gamma}_0^{(1)}\boldsymbol{\Gamma}_1\boldsymbol{\Gamma}_0^{(1)} &= \boldsymbol{G}_2, \quad \boldsymbol{\Gamma}_0^{(1)}\boldsymbol{\Gamma}_2\boldsymbol{\Gamma}_0^{(1)} = \boldsymbol{G}_1,
\end{aligned} \tag{29.17}$$

and it follows that the action of $\boldsymbol{K}$ is represented by the matrix

$$\boldsymbol{K} = -\boldsymbol{G}_1^{-1}(\boldsymbol{G}_1\boldsymbol{G}_2)^{1/2} = -\boldsymbol{G}_1^{-1/2}\boldsymbol{G}_2^{1/2},$$

which is symmetric because the matrices $\boldsymbol{G}_1$ and $\boldsymbol{G}_2 = \boldsymbol{I} - \boldsymbol{G}_1$ commute. Introducing the symmetric positive-semidefinite normalization matrix

$$\boldsymbol{N} = \boldsymbol{G}_1^{-1}\boldsymbol{G}_2,$$

we see that the relation (29.15) can be rewritten in the form

$$\boldsymbol{L}_*^{(1)} = \boldsymbol{N}^{-1/2}\boldsymbol{Y}_*\boldsymbol{N}^{-1/2},$$

in agreement with (29.7).

As in the analytic method, one bounds $\boldsymbol{L}_*$ in the field equation recursion method by obtaining elementary bounds on $\boldsymbol{Y}_*$ or $\boldsymbol{L}_*^{(1)}$ and then substituting these elementary bounds into the expression for $\boldsymbol{L}_*$ in terms of $\boldsymbol{Y}_*(\lambda_1, \lambda_2)$ or $\boldsymbol{L}_*^{(1)}$.

29.4. Representing the operators as infinite-dimensional matrices

Not all square integrable fields in $\mathcal{H}$ play a role in determining the function $\boldsymbol{L}_*(\lambda_1, \lambda_2)$. Indeed, we saw in chapter 14 on page 291 that it is only necessary to consider those fields that arise from products of the operators $\boldsymbol{\Gamma}_1$ and $\boldsymbol{\Lambda}_1$ applied to fields in $\mathcal{U}$. In other words we can restrict our attention to the Hilbert space $\mathcal{H}^{(0)}$, which we define as the smallest subspace of $\mathcal{H}$ that contains $\mathcal{U}$ and which is closed under the action of both $\boldsymbol{\Gamma}_1$ and $\boldsymbol{\Lambda}_1$. Let us set

$$\begin{aligned}\mathcal{U}^{(0)} &= \mathcal{U} \cap \mathcal{H}^{(0)} = \mathcal{U}, \quad \mathcal{E}^{(0)} = \mathcal{E} \cap \mathcal{H}^{(0)}, \quad \mathcal{J}^{(0)} = \mathcal{J} \cap \mathcal{H}^{(0)},\\ \mathcal{P}_1^{(0)} &= \mathcal{P}_1 \cap \mathcal{H}^{(0)}, \quad \mathcal{P}_2^{(0)} = \mathcal{P}_2 \cap \mathcal{H}^{(0)}.\end{aligned}$$

Since by definition $\mathcal{H}^{(0)}$ is closed under the action of both $\boldsymbol{\Gamma}$ and $\boldsymbol{\Lambda}$, it follows that

$$\mathcal{H}^{(0)} = \mathcal{U}^{(0)} \oplus \mathcal{E}^{(0)} \oplus \mathcal{J}^{(0)} = \mathcal{P}_1^{(0)} \oplus \mathcal{P}_2^{(0)}.$$

Based on the analysis of the previous section it seems natural to introduce a hierarchy of spaces

$$\mathcal{K}^{(i)} = \mathcal{E}^{(i-1)} \oplus \mathcal{J}^{(i-1)} = \mathcal{V}^{(i)} \oplus \mathcal{P}_1^{(i)} \oplus \mathcal{P}_2^{(i)}$$

and

$$\mathcal{H}^{(i)} = \mathcal{U}^{(i)} \oplus \mathcal{E}^{(i)} \oplus \mathcal{J}^{(i)} = \mathcal{P}_1^{(i)} \oplus \mathcal{P}_2^{(i)},$$

for $i = 1, 2, 3, \ldots$, where

$$\mathcal{P}_1^{(i)} = \mathcal{P}_1 \cap \mathcal{K}^{(i)}, \quad \mathcal{P}_2^{(i)} = \mathcal{P}_2 \cap \mathcal{K}^{(i)}, \quad \mathcal{E}^{(i)} = \mathcal{E} \cap \mathcal{H}^{(i)}, \quad \mathcal{J}^{(i)} = \mathcal{J} \cap \mathcal{H}^{(i)},$$

$\mathcal{V}^{(i)}$ is taken as the orthogonal complement of $\mathcal{P}_1^{(i)} \oplus \mathcal{P}_2^{(i)}$ in the space $\mathcal{K}^{(i)}$, and $\mathcal{U}^{(i)}$ is taken as the orthogonal complement of $\mathcal{E}^{(i)} \oplus \mathcal{J}^{(i)}$ in the space $\mathcal{H}^{(i)}$. Equivalently, $\mathcal{V}^{(i)}$ can be defined as the orthogonal complement of $\mathcal{U}^{(i-1)}$ in the space spanned by $\boldsymbol{\Lambda}_1\mathcal{U}^{(i-1)}$ and $\boldsymbol{\Lambda}_2\mathcal{U}^{(i-1)}$,

$$\mathcal{U}^{(i-1)} \oplus \mathcal{V}^{(i)} = \boldsymbol{\Lambda}_1\mathcal{U}^{(i-1)} \oplus \boldsymbol{\Lambda}_2\mathcal{U}^{(i-1)},$$

and $\mathcal{U}^{(i)}$ can be equivalently defined as the orthogonal complement of $\mathcal{V}^{(i)}$ in the space spanned by $\boldsymbol{\Gamma}_1\mathcal{V}^{(i)}$ and $\boldsymbol{\Gamma}_2\mathcal{V}^{(i)}$,

$$\mathcal{V}^{(i)} \oplus \mathcal{U}^{(i)} = \boldsymbol{\Gamma}_1\mathcal{V}^{(i)} \oplus \boldsymbol{\Gamma}_2\mathcal{V}^{(i)}.$$

We assume that we are given an orthonormal basis $\boldsymbol{u}_1^{(0)}, \boldsymbol{u}_2^{(0)}, \ldots, \boldsymbol{u}_m^{(0)}$ of $\mathcal{U}^{(0)} = \mathcal{U}$. We can then sequentially introduce fields

$$\boldsymbol{v}_j^{(i)} = \sum_{k=1}^{m} \{(\boldsymbol{W}_1^{(i-1)}\boldsymbol{W}_2^{(i-1)})^{-1/2}\}_{jk}[\boldsymbol{\Lambda}_1\boldsymbol{u}_k^{(i-1)} - \sum_{\ell=1}^{m}\{\boldsymbol{W}_1^{(i-1)}\}_{k\ell}\boldsymbol{u}_\ell^{(i-1)}]$$

that form an orthonormal basis for $\mathcal{V}^{(i)}$, in which

$$\begin{aligned}\{\boldsymbol{W}_1^{(i-1)}\}_{jk} &= (\boldsymbol{u}_j^{(i-1)}, \boldsymbol{\Lambda}_1\boldsymbol{u}_k^{(i-1)}), \quad \{\boldsymbol{W}_2^{(i-1)}\}_{jk} = (\boldsymbol{u}_j^{(i-1)}, \boldsymbol{\Lambda}_2\boldsymbol{u}_k^{(i-1)}),\\ \boldsymbol{W}_1^{(i-1)} &\geq 0, \quad \boldsymbol{W}_2^{(i-1)} \geq 0, \quad \boldsymbol{W}_1^{(i-1)} + \boldsymbol{W}_2^{(i-1)} = \boldsymbol{I},\end{aligned}$$

and fields

$$\boldsymbol{u}_j^{(i)} = \sum_{k=1}^{m} \{(\boldsymbol{G}_1^{(i)}\boldsymbol{G}_2^{(i)})^{-1/2}\}_{jk}[\boldsymbol{\Gamma}_1\boldsymbol{v}_k^{(i)} - \sum_{\ell=1}^{m}\{\boldsymbol{G}_1^{(i)}\}_{k\ell}\boldsymbol{v}_\ell^{(i)}]$$

that form an orthonormal basis for $\mathcal{V}^{(i)}$, in which

$$\{\boldsymbol{G}_1^{(i)}\}_{jk} = (\boldsymbol{v}_j^{(i)}, \boldsymbol{\Gamma}_1 \boldsymbol{v}_k^{(i)}), \quad \{\boldsymbol{G}_2^{(i)}\}_{jk} = (\boldsymbol{v}_j^{(i)}, \boldsymbol{\Gamma}_2 \boldsymbol{v}_k^{(i)}),$$
$$\boldsymbol{G}_1^{(i)} \geq 0, \quad \boldsymbol{G}_2^{(i)} \geq 0, \quad \boldsymbol{G}_1^{(i-1)} + \boldsymbol{G}_2^{(i-1)} = \boldsymbol{I}.$$

In this process we assume that the matrices $\boldsymbol{W}_1^{(i-1)}$, $\boldsymbol{W}_2^{(i-1)}$, $\boldsymbol{G}_1^{(i)}$, and $\boldsymbol{G}_2^{(i)}$ are nonsingular for all integers $i \geq 1$ to avoid mathematical technicalities.

These fields $\boldsymbol{u}_j^{(i-1)}$ and $\boldsymbol{v}_j^{(i)}$ for $j = 1, 2, \ldots, m$ and $i = 1, 2, 3, \ldots, \infty$ clearly span a space that contains $\mathcal{U}$ and which is closed under the action of both $\boldsymbol{\Gamma}_1$ and $\boldsymbol{\Lambda}_1$. Moreover, it is clearly the smallest such space with this property, and therefore must be the space $\mathcal{H}^{(0)}$. In other words, these fields constitute an orthonormal basis for $\mathcal{H}^{(0)}$, that is,

$$\mathcal{H}^{(0)} = \mathcal{U}^{(0)} \oplus \mathcal{V}^{(1)} \oplus \mathcal{U}^{(1)} \oplus \mathcal{V}^{(2)} \oplus \mathcal{U}^{(2)} \oplus \mathcal{V}^{(3)} \oplus \cdots.$$

This leads to the question: What matrices represent the operators $\boldsymbol{\Gamma}_1$, $\boldsymbol{\Gamma}_2$, $\boldsymbol{\Lambda}_1$, and $\boldsymbol{\Lambda}_2$ in the new basis? Let $\boldsymbol{\Gamma}^{(i)}$ denote the projection onto $\mathcal{U}^{(i)}$ and let $\boldsymbol{\Pi}_1^{(i)}$ denote the projection onto $\mathcal{V}^{(i)}$. By direct analogy with (29.14) we have

$$\begin{aligned}
\boldsymbol{\Gamma}_0^{(i-1)} \boldsymbol{\Lambda}_1 \boldsymbol{\Gamma}_0^{(i-1)} &= \boldsymbol{W}_1^{(i-1)}, \quad \boldsymbol{\Gamma}_0^{(i-1)} \boldsymbol{\Lambda}_2 \boldsymbol{\Gamma}_0^{(i-1)} = \boldsymbol{W}_2^{(i-1)}, \\
\boldsymbol{\Gamma}_0^{(i-1)} \boldsymbol{\Lambda}_1 \boldsymbol{\Pi}_1^{(i)} &= (\boldsymbol{W}_1^{(i-1)} \boldsymbol{W}_2^{(i-1)})^{1/2}, \quad \boldsymbol{\Gamma}_0^{(i-1)} \boldsymbol{\Lambda}_2 \boldsymbol{\Pi}_1^{(i)} = -(\boldsymbol{W}_1^{(i-1)} \boldsymbol{W}_2^{(i-1)})^{1/2}, \\
\boldsymbol{\Pi}_1^{(i)} \boldsymbol{\Lambda}_1 \boldsymbol{\Pi}_1^{(i)} &= \boldsymbol{W}_2^{(i-1)}, \quad \boldsymbol{\Pi}_1^{(i)} \boldsymbol{\Lambda}_2 \boldsymbol{\Pi}_1^{(i)} = \boldsymbol{W}_1^{(i-1)},
\end{aligned} \tag{29.18}$$

and similarly, by direct analogy with (29.17), we have

$$\begin{aligned}
\boldsymbol{\Pi}_1^{(i)} \boldsymbol{\Gamma}_1 \boldsymbol{\Pi}_1^{(i)} &= \boldsymbol{G}_1^{(i)}, \quad \boldsymbol{\Pi}_1^{(i)} \boldsymbol{\Gamma}_2 \boldsymbol{\Pi}_1^{(i)} = \boldsymbol{G}_2^{(i)}, \\
\boldsymbol{\Pi}_1^{(i)} \boldsymbol{\Gamma}_1 \boldsymbol{\Gamma}_0^{(i)} &= (\boldsymbol{G}_1^{(i)} \boldsymbol{G}_2^{(i)})^{1/2}, \quad \boldsymbol{\Pi}_1^{(i)} \boldsymbol{\Gamma}_2 \boldsymbol{\Gamma}_0^{(i)} = -(\boldsymbol{G}_1^{(i)} \boldsymbol{G}_2^{(i)})^{1/2}, \\
\boldsymbol{\Gamma}_0^{(i)} \boldsymbol{\Gamma}_1 \boldsymbol{\Gamma}_0^{(i)} &= \boldsymbol{G}_2^{(i)}, \quad \boldsymbol{\Gamma}_0^{(i)} \boldsymbol{\Gamma}_2 \boldsymbol{\Gamma}_0^{(i)} = \boldsymbol{G}_1^{(i)},
\end{aligned} \tag{29.19}$$

where we have equated operators with the matrices that represent their action with respect to the basis.

Now, because the subspaces $\mathcal{U}^{(i-1)} \oplus \mathcal{V}^{(i)}$ are closed under the action of the self-adjoint projection operators $\boldsymbol{\Lambda}_1$ and $\boldsymbol{\Lambda}_2$, it follows that $\boldsymbol{\Lambda}_1$ and $\boldsymbol{\Lambda}_2$ couple together only "adjacent pairs" $\mathcal{U}^{(i-1)}$ and $\mathcal{V}^{(i)}$ in the sequence $\mathcal{U}^{(0)}$,$\mathcal{V}^{(1)}$, $\mathcal{U}^{(1)}$,$\mathcal{V}^{(2)}$, $\mathcal{U}^{(2)}$, $\mathcal{V}^{(3)}$, ... of subspaces. From this observation and from (29.18) it follows that $\boldsymbol{\Lambda}_1$ and $\boldsymbol{\Lambda}_2$ are represented by the block-tridiagonal matrices

$$\boldsymbol{\Lambda}_1 = \begin{pmatrix}
\boldsymbol{W}_1^{(0)} & (\boldsymbol{W}_1^{(0)} \boldsymbol{W}_2^{(0)})^{1/2} & 0 & 0 & 0 & \cdots \\
(\boldsymbol{W}_1^{(0)} \boldsymbol{W}_2^{(0)})^{1/2} & \boldsymbol{W}_2^{(0)} & 0 & 0 & 0 & \cdots \\
0 & 0 & \boldsymbol{W}_1^{(1)} & (\boldsymbol{W}_1^{(1)} \boldsymbol{W}_2^{(1)})^{1/2} & 0 & \cdots \\
0 & 0 & (\boldsymbol{W}_1^{(1)} \boldsymbol{W}_2^{(1)})^{1/2} & \boldsymbol{W}_2^{(1)} & 0 & \cdots \\
0 & 0 & 0 & 0 & \boldsymbol{W}_1^{(2)} & \cdots \\
\vdots & \vdots & \vdots & \vdots & \vdots & \ddots
\end{pmatrix}$$

and

$$\boldsymbol{\Lambda}_2 = \begin{pmatrix}
\boldsymbol{W}_2^{(0)} & -(\boldsymbol{W}_1^{(0)} \boldsymbol{W}_2^{(0)})^{1/2} & 0 & 0 & 0 & \cdots \\
-(\boldsymbol{W}_1^{(0)} \boldsymbol{W}_2^{(0)})^{1/2} & \boldsymbol{W}_1^{(0)} & 0 & 0 & 0 & \cdots \\
0 & 0 & \boldsymbol{W}_2^{(1)} & -(\boldsymbol{W}_1^{(1)} \boldsymbol{W}_2^{(1)})^{1/2} & 0 & \cdots \\
0 & 0 & -(\boldsymbol{W}_1^{(1)} \boldsymbol{W}_2^{(1)})^{1/2} & \boldsymbol{W}_1^{(1)} & 0 & \cdots \\
0 & 0 & 0 & 0 & \boldsymbol{W}_2^{(2)} & \cdots \\
\vdots & \vdots & \vdots & \vdots & \vdots & \ddots
\end{pmatrix}.$$

Conversely, an operator $\boldsymbol{\Lambda}_1 = \boldsymbol{I} - \boldsymbol{\Lambda}_2$ that can be expressed in this form for some choice of positive-semidefinite matrices $\boldsymbol{W}_1^{(i)}$ and $\boldsymbol{W}_2^{(i)} = \boldsymbol{I} - \boldsymbol{W}_1^{(i)}$ is necessarily a projection operator.

Similarly, $\boldsymbol{\Gamma}_1$ and $\boldsymbol{\Gamma}_2$ couple together only the adjacent pairs $\mathcal{V}^{(i)}$ and $\mathcal{U}^{(i)}$ in the subspace sequence, and consequently from (29.19) we have

$$\boldsymbol{\Gamma}_1 = \begin{pmatrix} 0 & 0 & 0 & 0 & 0 & \dots \\ 0 & \boldsymbol{G}_1^{(1)} & (\boldsymbol{G}_1^{(1)}\boldsymbol{G}_2^{(1)})^{1/2} & 0 & 0 & \dots \\ 0 & (\boldsymbol{G}_1^{(1)}\boldsymbol{G}_2^{(1)})^{1/2} & \boldsymbol{G}_2^{(1)} & 0 & 0 & \dots \\ 0 & 0 & 0 & \boldsymbol{G}_1^{(2)} & (\boldsymbol{G}_1^{(2)}\boldsymbol{G}_2^{(2)})^{1/2} & \dots \\ 0 & 0 & 0 & (\boldsymbol{G}_1^{(2)}\boldsymbol{G}_2^{(2)})^{1/2} & \boldsymbol{G}_2^{(2)} & \dots \\ \vdots & \vdots & \vdots & \vdots & \vdots & \ddots \end{pmatrix}$$

and

$$\boldsymbol{\Gamma}_2 = \begin{pmatrix} 0 & 0 & 0 & 0 & 0 & \dots \\ 0 & \boldsymbol{G}_2^{(1)} & -(\boldsymbol{G}_1^{(1)}\boldsymbol{G}_2^{(1)})^{1/2} & 0 & 0 & \dots \\ 0 & -(\boldsymbol{G}_1^{(1)}\boldsymbol{G}_2^{(1)})^{1/2} & \boldsymbol{G}_1^{(1)} & 0 & 0 & \dots \\ 0 & 0 & 0 & \boldsymbol{G}_2^{(2)} & -(\boldsymbol{G}_1^{(2)}\boldsymbol{G}_2^{(2)})^{1/2} & \dots \\ 0 & 0 & 0 & -(\boldsymbol{G}_1^{(2)}\boldsymbol{G}_2^{(2)})^{1/2} & \boldsymbol{G}_1^{(2)} & \dots \\ \vdots & \vdots & \vdots & \vdots & \vdots & \ddots \end{pmatrix}.$$

Of course since $\mathcal{U}^{(0)}$ equals $\mathcal{U}$, the operator $\boldsymbol{\Gamma}_0$ is simply

$$\boldsymbol{\Gamma}_0 = \begin{pmatrix} \boldsymbol{I} & 0 & 0 & 0 & 0 & \dots \\ 0 & 0 & 0 & 0 & 0 & \dots \\ 0 & 0 & 0 & 0 & 0 & \dots \\ 0 & 0 & 0 & 0 & 0 & \dots \\ 0 & 0 & 0 & 0 & 0 & \dots \\ \vdots & \vdots & \vdots & \vdots & \vdots & \ddots \end{pmatrix}.$$

29.5. The field equation recursion method for multiphase composites with isotropic components

The field equation recursion method is easily generalized to multiphase composites. Let us consider a problem where the tensor $\boldsymbol{L}$ takes the form

$$\boldsymbol{L} = \sum_{i=1}^{n} \lambda_i \boldsymbol{\Lambda}_i,$$

where the λ_i, for $i = 1, 2, \dots, n$, represent the possibly complex eigenvalues of $\boldsymbol{L}$ and the $\boldsymbol{\Lambda}_i$ represent projections onto the associated eigenspaces $\mathcal{P}_i$, which we assume to be mutually orthogonal and to span $\mathcal{H}$:

$$\mathcal{H} = \mathcal{U} \oplus \mathcal{E} \oplus \mathcal{J} = \mathcal{P}_1 \oplus \mathcal{P}_2 \oplus \cdots \oplus \mathcal{P}_n.$$

In an n-phase composite comprised of isotropic conducting phases we can identify λ_i with the conductivity σ_i of component i, and we can identify $\boldsymbol{\Lambda}_i$ with the projection $\chi_i \boldsymbol{I}$ onto the space of fields $\mathcal{P}_i$ that are nonzero only in phase i.

We introduce the spaces

$$\mathcal{K} = \mathcal{E} \oplus \mathcal{J} = \mathcal{V} \oplus \mathcal{P}_1^{(1)} \oplus \mathcal{P}_2^{(1)} \oplus \cdots \oplus \mathcal{P}_n^{(1)}$$

and

$$\mathcal{H}^{(1)} = \mathcal{U}^{(1)} \oplus \mathcal{E}^{(1)} \oplus \mathcal{J}^{(1)} = \mathcal{P}_1^{(1)} \oplus \mathcal{P}_2^{(1)} \oplus \cdots \oplus \mathcal{P}_n^{(1)},$$

where

$$\mathcal{P}_i^{(1)} = \mathcal{P}_i \cap \mathcal{K}, \quad \mathcal{E}^{(1)} = \mathcal{E} \cap \mathcal{H}^{(1)}, \quad \mathcal{J}^{(1)} = \mathcal{J} \cap \mathcal{H}^{(1)},$$

$\mathcal{V}$ is taken as the orthogonal complement of $\mathcal{P}_1^{(1)} \oplus \mathcal{P}_2^{(1)} \oplus \cdots \oplus \mathcal{P}_n^{(1)}$ in the space $\mathcal{K}$, and $\mathcal{U}^{(1)}$ is taken as the orthogonal complement of $\mathcal{E}^{(1)} \oplus \mathcal{J}^{(1)}$ in the space $\mathcal{H}^{(1)}$.

The space $\mathcal{V}$ can be equivalently defined as the orthogonal complement of $\mathcal{U}$ in the space spanned by $\mathbf{\Lambda}_1\mathcal{U}, \mathbf{\Lambda}_2\mathcal{U}, \ldots \mathbf{\Lambda}_n\mathcal{U}$:

$$\mathcal{U} \oplus \mathcal{V} = \mathbf{\Lambda}_1\mathcal{U} \oplus \mathbf{\Lambda}_2\mathcal{U} \oplus \cdots \oplus \mathbf{\Lambda}_n\mathcal{U}.$$

The proof of this is basically the same as the proof of (29.10).

The space $\mathcal{U}^{(1)}$ can be equivalently defined as the orthogonal complement of $\mathcal{V}$ in the space spanned by $\mathbf{\Gamma}_1\mathcal{V}$ and $\mathbf{\Gamma}_2\mathcal{V}$, as in (29.11).

The formula (29.12) relating the Y-tensor $\boldsymbol{Y}_*$ associated with the $(2, n+1)$-subspace collection $(\mathcal{E}, \mathcal{J})$ and $(\mathcal{V}, \mathcal{P}_1^{(1)}, \mathcal{P}_2^{(1)}, \ldots, \mathcal{P}_n^{(1)})$ to the effective tensor $\boldsymbol{L}_*$ associated with the $(3, n)$-subspace collection $(\mathcal{U}, \mathcal{E}, \mathcal{J})$ and $(\mathcal{P}_1, \mathcal{P}_2, \ldots, \mathcal{P}_n)$ remains valid, with $\mathbf{\Gamma}_0$ still being the projection onto $\mathcal{U}$ and $\mathbf{\Pi}_1$ being the projection onto $\mathcal{V}$.

Finding an explicit expression for this formula requires a representation for the various operators. Since this is a little tedious, the reader not interested in the details can skip to the next section. We start with a basis $\boldsymbol{u}_1, \boldsymbol{u}_2, \ldots \boldsymbol{u}_m$ of $\mathcal{U}$. Since there is no real need to work with orthonormal bases, let us relax this requirement since it simplifies the subsequent analysis. Instead let us assume that we know the $m \times m$ matrix $\boldsymbol{U}$ with elements

$$\{\boldsymbol{U}\}_{ij} = (\boldsymbol{u}_i, \boldsymbol{u}_j),$$

representing the inner products of the basis fields. We define weight matrices $\boldsymbol{W}_1, \boldsymbol{W}_2, \ldots \boldsymbol{W}_n$ with matrix elements

$$\{\boldsymbol{W}_i\}_{jk} = (\boldsymbol{u}_j, \mathbf{\Lambda}_i \boldsymbol{u}_k) \quad \text{for } i = 1, 2, \ldots, n. \tag{29.20}$$

These matrices are clearly positive-semidefinite and sum to the matrix $\boldsymbol{U}$:

$$\boldsymbol{W}_i \geq 0 \text{ for all } i, \quad \sum_{i=1}^{n} \boldsymbol{W}_i = \boldsymbol{U}.$$

To avoid mathematical technicalities let us assume that the weight matrices are strictly positive-definite. This implies that each set of fields $\mathbf{\Lambda}_b \boldsymbol{u}_k$ for $k = 1, 2, \ldots, m$ is linearly independent. We next introduce the set of nm fields

$$\boldsymbol{v}_{bk} = (\boldsymbol{I} - \mathbf{\Gamma}_0)\mathbf{\Lambda}_b \boldsymbol{u}_k = \mathbf{\Lambda}_b \boldsymbol{u}_k - \sum_{\ell=1}^{m} \{\boldsymbol{U}^{-1}\boldsymbol{W}_b\}_{\ell k} \boldsymbol{u}_\ell,$$

parameterized by the indices $b = 1, 2, \ldots, n$ and $k = 1, 2, \ldots, m$. These fields span $\mathcal{V}$, but they are not independent. For any choice of integer h between 1 and n we have

$$\boldsymbol{v}_{hk} = (\boldsymbol{I} - \mathbf{\Gamma}_0)(\boldsymbol{I} - \sum_{b \neq h} \mathbf{\Lambda}_b)\boldsymbol{u}_k = -\sum_{b \neq h} \boldsymbol{v}_{bk}.$$

To remove this degeneracy we take as our basis for $\mathcal{V}$ the $(n-1)m$ fields $\boldsymbol{v}_{bk}$, with b running between 1 and n skipping the value $b = h$, and with k running between 1 and m. These fields have inner products

$$(\boldsymbol{v}_{aj}, \boldsymbol{v}_{bk}) = \{\delta_{ab}\boldsymbol{W}_a - \boldsymbol{W}_a\boldsymbol{U}^{-1}\boldsymbol{W}_b\}_{jk} = \{\boldsymbol{V}\}_{aj,bk}, \tag{29.21}$$

which defines the elements of the $(n-1)m \times (n-1)m$ matrix $\boldsymbol{V}$. This matrix $\boldsymbol{V}$ has an inverse $\boldsymbol{V}^{-1}$ with elements

$$\{\boldsymbol{V}^{-1}\}_{bk,ci} = \{\boldsymbol{W}_h^{-1} + \delta_{bc}\boldsymbol{W}_b^{-1}\}_{ki}.$$

To verify that this is indeed the inverse we calculate the product

$$\begin{aligned}
&\sum_{b\neq h}\sum_{k=1}^{m}\{\delta_{ab}\boldsymbol{W}_a - \boldsymbol{W}_a\boldsymbol{U}^{-1}\boldsymbol{W}_b\}_{jk}\{\boldsymbol{W}_h^{-1} + \delta_{bc}\boldsymbol{W}_b^{-1}\}_{ki} \\
&\quad = \{\boldsymbol{W}_a\boldsymbol{W}_h^{-1} + \delta_{ac}\boldsymbol{I} - \boldsymbol{W}_a\boldsymbol{U}^{-1} - \sum_{b\neq h}\boldsymbol{W}_a\boldsymbol{U}^{-1}\boldsymbol{W}_b\boldsymbol{W}_h^{-1}\}_{ji} \\
&\quad = \{\delta_{ac}\boldsymbol{I} + \boldsymbol{W}_a\boldsymbol{U}^{-1}[\boldsymbol{U} - \boldsymbol{W}_h - \sum_{b\neq h}\boldsymbol{W}_b]\boldsymbol{W}_h^{-1}\}_{ji} = \delta_{ac}\delta_{ji},
\end{aligned}$$

and see that it is indeed the identity, where we have used the fact that the weight matrices sum to the matrix $\boldsymbol{U}$. Our assumption that the weight matrices are strictly positive-definite clearly implies the positive-definiteness of $\boldsymbol{A}^{-1}$ and hence the positive-definiteness of $\boldsymbol{A}$.

For all $c \neq h$ we have

$$\begin{aligned}
(\boldsymbol{u}_j, \boldsymbol{\Lambda}_c\boldsymbol{u}_k) &= \{\boldsymbol{W}_c\}_{jk}, \\
(\boldsymbol{u}_j, \boldsymbol{\Lambda}_c\boldsymbol{v}_{bk}) &= (\boldsymbol{v}_{bk}, \boldsymbol{\Lambda}_c\boldsymbol{u}_j) = \{\boldsymbol{V}\}_{cj,bk}, \\
(\boldsymbol{v}_{aj}, \boldsymbol{\Lambda}_c\boldsymbol{v}_{bk}) &= \sum_{h=1}^{m}\sum_{\ell=1}^{m}\{\boldsymbol{V}\}_{aj,ch}\{\boldsymbol{W}_c^{-1}\}_{h\ell}\{\boldsymbol{V}\}_{c\ell,bk}.
\end{aligned}$$

It follows from this that

$$\begin{aligned}
\boldsymbol{\Gamma}_0\boldsymbol{\Lambda}_c\boldsymbol{\Gamma}_0\boldsymbol{u}_k &= \sum_{i=1}^{m}\{\boldsymbol{U}^{-1}\boldsymbol{W}_c\}_{ik}\boldsymbol{u}_i, \\
\boldsymbol{\Gamma}_0\boldsymbol{\Lambda}_c\boldsymbol{\Pi}_1\boldsymbol{v}_{bk} &= \sum_{i=1}^{m}\{\boldsymbol{U}^{-1}\boldsymbol{V}_c\}_{i,bk}\boldsymbol{u}_i, \\
\boldsymbol{\Pi}_1\boldsymbol{\Lambda}_c\boldsymbol{\Gamma}_0\boldsymbol{u}_k &= \sum_{a\neq h}\sum_{i=1}^{m}\{\boldsymbol{V}^{-1}\boldsymbol{V}_c^T\}_{ai,k}\boldsymbol{v}_{ai} = \sum_{a\neq h}\sum_{i=1}^{m}\{\boldsymbol{I}_c^T\}_{ai,k}\boldsymbol{v}_{ai}, \\
\boldsymbol{\Pi}_1\boldsymbol{\Lambda}_c\boldsymbol{\Pi}_1\boldsymbol{v}_{bk} &= \sum_{a\neq h}\sum_{i=1}^{m}\{\boldsymbol{V}^{-1}\boldsymbol{V}_c^T\boldsymbol{W}_c^{-1}\boldsymbol{V}_c\}_{ai,bk}\boldsymbol{v}_{ai} = \sum_{a\neq h}\sum_{i=1}^{m}\{\boldsymbol{I}_c^T\boldsymbol{W}_c^{-1}\boldsymbol{V}_c\}_{ai,bk}\boldsymbol{v}_{ai},
\end{aligned} \tag{29.22}$$

in which $\boldsymbol{V}_c$ and $\boldsymbol{I}_c$ are $m \times (n-1)m$ matrices with elements

$$\{\boldsymbol{V}_c\}_{j,bk} = \{\boldsymbol{V}\}_{cj,bk}, \quad \{\boldsymbol{I}_c\}_{j,bk} = \delta_{cb}\delta_{jk}. \tag{29.23}$$

To represent the operators $\boldsymbol{L}_*$ and $\boldsymbol{Y}_*$ let us introduce matrices $\boldsymbol{L}_*$ and $\boldsymbol{Y}_*$ such that the matrices $\boldsymbol{L}_*$ and $\boldsymbol{Y}_*$ have elements

$$\{\boldsymbol{L}_*\}_{j,k} = (\boldsymbol{u}_j, \boldsymbol{L}_*\boldsymbol{u}_k), \quad \{\boldsymbol{Y}_*\}_{aj,bk} = (\boldsymbol{v}_{aj}, \boldsymbol{Y}_*\boldsymbol{v}_{bk}), \tag{29.24}$$

where we have used the same symbol to denote the operator and its associated matrix. It follows from these definitions that the action of the operators $\boldsymbol{L}_*$ and $\boldsymbol{Y}_*$ on the basis fields is given by

$$\boldsymbol{L}_*\boldsymbol{u}_k = \sum_{i=1}^{m}\{\boldsymbol{U}^{-1}\boldsymbol{L}_*\}_{ik}\boldsymbol{u}_i, \quad \boldsymbol{Y}_*\boldsymbol{v}_{bk} = \sum_{a\neq h}\sum_{i=1}^{m}\{\boldsymbol{V}^{-1}\boldsymbol{Y}_*\}_{ai,bk}\boldsymbol{v}_{ai}. \tag{29.25}$$

If we equate operators with the matrices that represent their action with respect to the basis, then (29.22) implies that

$$\begin{aligned}
\boldsymbol{\Gamma}_0\boldsymbol{L}\boldsymbol{\Gamma}_0 &= \sum_{i=1}^{n}\boldsymbol{U}^{-1}\boldsymbol{W}_i\lambda_i, \quad \boldsymbol{\Gamma}_0\boldsymbol{L}\boldsymbol{\Pi}_1 = \sum_{a\neq h}(\lambda_a-\lambda_h)\boldsymbol{U}^{-1}\boldsymbol{V}_a,\\
\boldsymbol{\Pi}_1\boldsymbol{L}\boldsymbol{\Gamma}_0 &= \sum_{b\neq h}(\lambda_b-\lambda_h)\boldsymbol{I}_b^T,\\
\boldsymbol{\Pi}_1\boldsymbol{L}\boldsymbol{\Pi}_1 &= \boldsymbol{V}^{-1}[\lambda_h\boldsymbol{V} + \sum_{c\neq h}\boldsymbol{V}_c^T\boldsymbol{W}_c^{-1}\boldsymbol{V}_c(\lambda_c-\lambda_h)] = \boldsymbol{\Upsilon}\boldsymbol{V},
\end{aligned}$$

where $\boldsymbol{\Upsilon}$ is the matrix with elements

$$\{\boldsymbol{\Upsilon}\}_{aj,bk} = \{\lambda_h\boldsymbol{W}_h^{-1} + \delta_{ab}\lambda_b\boldsymbol{W}_b^{-1}\}_{jk}. \tag{29.26}$$

By substituting these into (29.12) and recalling from (29.25) that the matrices $\boldsymbol{U}^{-1}\boldsymbol{L}_*$ and $\boldsymbol{V}^{-1}\boldsymbol{Y}_*$ represent the action of the operators $\boldsymbol{L}_*$ and $\boldsymbol{Y}_*$, we obtain the relation

$$\boldsymbol{U}^{-1}\boldsymbol{L}_* = \sum_{i=1}^{n}\boldsymbol{U}^{-1}\boldsymbol{W}_i\lambda_i - \sum_{a,b\neq h}(\lambda_a-\lambda_h)\boldsymbol{U}^{-1}\boldsymbol{V}_a[\boldsymbol{\Upsilon}\boldsymbol{V} + \boldsymbol{V}^{-1}\boldsymbol{Y}_*]^{-1}\boldsymbol{I}_b^T(\lambda_b-\lambda_h),$$

which can be rewritten as

$$\boldsymbol{L}_* = \sum_{i=1}^{n}\boldsymbol{W}_i\lambda_i - \sum_{a,b\neq h}(\lambda_a-\lambda_h)\boldsymbol{I}_a[\boldsymbol{\Upsilon} + \boldsymbol{V}^{-1}\boldsymbol{Y}_*\boldsymbol{V}^{-1}]^{-1}\boldsymbol{I}_b^T(\lambda_b-\lambda_h), \tag{29.27}$$

in which $\boldsymbol{L}_*$ and $\boldsymbol{Y}_*$ are the matrices defined by (29.24)

To obtain a relation between $\boldsymbol{Y}_*$ and the effective tensor $\boldsymbol{L}_*^{(1)}$ associated with the $(3, n)$-subspace collection $(\mathcal{U}^{(1)}, \mathcal{E}^{(1)}, \mathcal{J}^{(1)})$ and $(\mathcal{P}_1^{(1)}, \mathcal{P}_2^{(1)}, \ldots, \mathcal{P}_n^{(1)})$ we introduce the $(n-1)m \times (n-1)m$ matrices $\boldsymbol{G}_1$ and $\boldsymbol{G}_2$ with elements

$$\{\boldsymbol{G}_1\}_{aj,bk} = (\boldsymbol{v}_{aj}, \boldsymbol{\Gamma}_1\boldsymbol{v}_{bk}), \quad \{\boldsymbol{G}_2\}_{aj,bk} = (\boldsymbol{v}_{aj}, \boldsymbol{\Gamma}_2\boldsymbol{v}_{bk}).$$

satisfying

$$\boldsymbol{G}_1 \geq 0, \quad \boldsymbol{G}_2 \geq 0, \quad \boldsymbol{G}_1 + \boldsymbol{G}_2 = \boldsymbol{V}.$$

We assume that these matrices are strictly positive-definite to avoid mathematical technicalities. Then the fields

$$\boldsymbol{u}_{bk}^{(1)} = (\boldsymbol{I} - \boldsymbol{\Pi}_1)\boldsymbol{\Gamma}_1\boldsymbol{v}_{bk} = \boldsymbol{\Gamma}_1\boldsymbol{v}_{bk} - \sum_{c\neq h}\sum_{\ell=1}^{m}\{\boldsymbol{V}^{-1}\boldsymbol{G}_1\}_{c\ell,bk}\boldsymbol{v}_{c\ell},$$

for $b = 1, 2, \ldots, h-1, h+1, \ldots, n,\ k = 1, 2, \ldots, m$, form a basis for $\mathcal{U}^{(1)}$.

These fields have inner products

$$(\boldsymbol{u}_{aj}^{(1)}, \boldsymbol{u}_{bk}^{(1)}) = \{\boldsymbol{U}^{(1)}\}_{aj,bk}$$

described by the matrix

$$\boldsymbol{U}^{(1)} = \boldsymbol{G}_1 - \boldsymbol{G}_1\boldsymbol{V}^{-1}\boldsymbol{G}_1 = \boldsymbol{G}_1\boldsymbol{V}^{-1}\boldsymbol{G}_2 = \boldsymbol{G}_2\boldsymbol{V}^{-1}\boldsymbol{G}_1,$$

and we have

$$(\boldsymbol{v}_{aj}, \boldsymbol{\Gamma}_1\boldsymbol{v}_{bk}) = \{\boldsymbol{G}_1\}_{aj,bk}, \qquad (\boldsymbol{v}_{aj}, \boldsymbol{\Gamma}_1\boldsymbol{u}_{bk}^{(1)}) = \{\boldsymbol{U}^{(1)}\}_{aj,bk}.$$

This implies that

$$\boldsymbol{\Pi}_1\boldsymbol{\Gamma}_1\boldsymbol{\Pi}_1\boldsymbol{v}_{bk} = \sum_{a\neq h}\sum_{i=1}^{m}\{\boldsymbol{V}^{-1}\boldsymbol{G}_1\}_{ai,bk}\boldsymbol{v}_{ai},$$

$$\boldsymbol{\Pi}_1\boldsymbol{\Gamma}_1\boldsymbol{\Gamma}^{(1)}\boldsymbol{u}_{bk}^{(1)} = \sum_{a\neq h}\sum_{i=1}^{m}\{\boldsymbol{V}^{-1}\boldsymbol{U}^{(1)}\}_{ai,bk}\boldsymbol{v}_{ai}, \quad \boldsymbol{\Gamma}^{(1)}\boldsymbol{\Gamma}_1\boldsymbol{\Pi}_1\boldsymbol{u}_{bk}^{(1)} = \sum_{a\neq h}\sum_{i=1}^{m}\{\boldsymbol{I}\}_{ai,bk}\boldsymbol{v}_{ai}.$$

Hence the action of the operators

$$\boldsymbol{K} = -[\boldsymbol{\Pi}_1\boldsymbol{\Gamma}_1\boldsymbol{\Pi}_1]^{-1}\boldsymbol{\Pi}_1\boldsymbol{\Gamma}_1\boldsymbol{\Gamma}^{(1)} \text{ and } \boldsymbol{K}^T = -\boldsymbol{\Gamma}^{(1)}\boldsymbol{\Gamma}_1\boldsymbol{\Pi}_1[\boldsymbol{\Pi}_1\boldsymbol{\Gamma}_1\boldsymbol{\Pi}_1]^{-1}$$

on the basis are represented by the matrices $-\boldsymbol{G}_1^{-1}\boldsymbol{U}^{(1)}$ and $-\boldsymbol{G}_1^{-1}\boldsymbol{V}$, respectively. To represent the operator $\boldsymbol{L}_*^{(1)}$ we introduce a matrix $\boldsymbol{L}_*^{(1)}$ with elements

$$\{\boldsymbol{L}_*^{(1)}\}_{aj,bk} = (\boldsymbol{u}_{aj}^{(1)}, \boldsymbol{L}_*\boldsymbol{u}_{bk}^{(1)}),$$

where we have used the same symbol to denote the operator and the matrix. The action of the operator $\boldsymbol{L}_*^{(1)}$ on the basis is then represented by the matrix $(\boldsymbol{U}^{(1)})^{-1}\boldsymbol{L}_*^{(1)}$. If we equate operators with the matrices that represent their action with respect to the basis then the operator identity $\boldsymbol{Y}_* = \boldsymbol{K}\boldsymbol{L}_*^{(1)}\boldsymbol{K}^T$ implies that

$$\boldsymbol{V}^{-1}\boldsymbol{Y}_* = \boldsymbol{G}_1^{-1}\boldsymbol{U}^{(1)}[(\boldsymbol{U}^{(1)})^{-1}\boldsymbol{L}_*^{(1)}]\boldsymbol{G}_1^{-1}\boldsymbol{V},$$

which reduces to

$$\boldsymbol{Y}_* = \boldsymbol{V}\boldsymbol{G}_1^{-1}\boldsymbol{L}_*^{(1)}\boldsymbol{G}_1^{-1}\boldsymbol{V}. \tag{29.28}$$

Substituting this back into (29.27) gives a formula,

$$\boldsymbol{L}_* = \sum_{i=1}^{n}\boldsymbol{W}_i\lambda_i - \sum_{a,b\neq h}(\lambda_a - \lambda_h)\boldsymbol{I}_a[\boldsymbol{\Upsilon} + \boldsymbol{G}_1^{-1}\boldsymbol{L}_*^{(1)}\boldsymbol{G}_1^{-1}]^{-1}\boldsymbol{I}_b^T(\lambda_b - \lambda_h), \tag{29.29}$$

linking the matrices $\boldsymbol{L}_*$ and $\boldsymbol{L}_*^{(1)}$.

This procedure can be iterated. At the next stage we introduce the subspace

$$\mathcal{K}^{(2)} = \mathcal{E}^{(1)} \oplus \mathcal{J}^{(1)} = \mathcal{V}^{(2)} \oplus \mathcal{P}_1^{(2)} \oplus \mathcal{P}_2^{(2)} \oplus \cdots \oplus \mathcal{P}_n^{(2)},$$

where

$$\mathcal{P}_c^{(2)} = \mathcal{P}_c \cap \mathcal{K}^{(2)}, \quad \text{for } c = 1, 2, \ldots, n,$$

and $\mathcal{V}^{(2)}$ is taken as the orthogonal complement of $\mathcal{P}_1^{(2)} \oplus \mathcal{P}_2^{(2)} \oplus \cdots \oplus \mathcal{P}_n^{(2)}$ in the space $\mathcal{K}^{(2)}$. We then let $\boldsymbol{Y}_*^{(2)}$ denote the Y-tensor associated with the $(2, n+1)$-subspace collection $(\mathcal{E}^{(1)}, \mathcal{J}^{(1)})$ and $(\mathcal{V}^{(2)}, \mathcal{P}_1^{(2)}, \mathcal{P}_2^{(2)}, \ldots, \mathcal{P}_n^{(2)})$. The matrix representing $\boldsymbol{L}_*^{(1)}$ is linked to the matrix representing $\boldsymbol{Y}_*^{(2)}$ via the formula

$$\boldsymbol{L}_*^{(1)} = \sum_{i=1}^{n} \boldsymbol{W}_i^{(1)} \lambda_i - \sum_{a,b \neq h} (\lambda_a - \lambda_h) \boldsymbol{I}_a^{(1)} [\boldsymbol{\Upsilon}^{(1)} + [\boldsymbol{V}^{(1)}]^{-1} \boldsymbol{Y}_*^{(2)} [\boldsymbol{V}^{(1)}]^{-1}]^{-1} [\boldsymbol{I}_b^{(1)}]^T (\lambda_b - \lambda_h), \tag{29.30}$$

with the matrices $\boldsymbol{W}_i^{(1)}$, $\boldsymbol{V}^{(1)}$, $\boldsymbol{I}_c^{(1)}$, and $\boldsymbol{\Upsilon}^{(1)}$ defined in an analogous way to the matrices $\boldsymbol{W}_i$, $\boldsymbol{V}$, $\boldsymbol{I}_c$, and $\boldsymbol{\Upsilon}$ given by (29.20), (29.21), (29.23), and (29.26).

29.6. Bounds on the energy function of a three-phase conducting composite

As an example of the field equation recursion method, let us apply it to bounding the energy function

$$\sigma_e(\sigma_1, \sigma_2, \sigma_3) = \boldsymbol{e}_0 \cdot \boldsymbol{\sigma}_*(\sigma_1, \sigma_2, \sigma_3) \boldsymbol{e}_0,$$

where $\boldsymbol{e}_0$ is a fixed real unit vector, with $|\boldsymbol{e}_0| = 1$. For real values of σ_1, σ_2, and σ_3 we think of $\sigma_e/2$ as representing the energy dissipation in the composite when it is subject to the applied field $\boldsymbol{e}_0$. For complex values of σ_1, σ_2, and σ_3 we think of σ_e as representing a diagonal element of the effective conductivity tensor $\boldsymbol{\sigma}_*$ in a basis where $\boldsymbol{e}_0$ is chosen as one of the basis vectors. Elementary bounds on σ_e for complex component conductivities were first conjectured by Golden and Papanicolaou (1985) and Golden (1986) and later proved (Bergman 1986; Milton 1987b; Milton and Golden 1990). The field equation recursion method not only established the conjectured bounds but also provided new bounds (Milton 1987b).

The relation between $\sigma_e(\sigma_1, \sigma_2, \sigma_3)$ and $\boldsymbol{\sigma}_*(\sigma_1, \sigma_2, \sigma_3)$ takes the same form as the relation (29.1) between $\boldsymbol{L}'_*(\lambda_1, \lambda_2, \ldots, \lambda_n)$ and $\boldsymbol{L}_*(\lambda_1, \lambda_2, \ldots, \lambda_n)$ with $\boldsymbol{\Lambda} = \boldsymbol{e}_0$. Therefore it is the analytic function associated with the $(3, 3)$-subspace collection $(\mathcal{U}, \mathcal{E}, \mathcal{J})$ and $(\mathcal{P}_1, \mathcal{P}_2, \mathcal{P}_3)$ where $\mathcal{U}$ consists of all constant fields proportional to $\boldsymbol{e}_0$, $\mathcal{E}$ consists of gradients of periodic scalar potentials, $\mathcal{J}$ consists of all divergence free fields $\boldsymbol{j}(\boldsymbol{x})$ such that the average value of $\boldsymbol{e}_0 \cdot \boldsymbol{j}(\boldsymbol{x})$ is zero, and $\mathcal{P}_i$, for $i = 1, 2, 3$, consists of all periodic fields that are nonzero only inside phase i.

The relation (29.27) between σ_e and $\boldsymbol{Y}_*$, with $h = 3$, now takes the form

$$\begin{aligned} \sigma_e &= \sigma_e(\boldsymbol{Y}_*) \\ &= f_1\sigma_1 + f_2\sigma_2 + f_3\sigma_3 - \begin{pmatrix} \sigma_1 - \sigma_3 \\ \sigma_2 - \sigma_3 \end{pmatrix} \cdot [\boldsymbol{\Upsilon} + \boldsymbol{V}^{-1} \boldsymbol{Y}_* \boldsymbol{V}^{-1}]^{-1} \begin{pmatrix} \sigma_1 - \sigma_3 \\ \sigma_2 - \sigma_3 \end{pmatrix}, \end{aligned} \tag{29.31}$$

in which f_1, f_2, and $f_3 = 1 - f_1 - f_2$ are the volume fractions of the phases and $\boldsymbol{\Upsilon}$ and $\boldsymbol{V}^{-1}$ are the 2×2 matrices

$$\boldsymbol{\Upsilon} = \begin{pmatrix} \sigma_1/f_1 + \sigma_3/f_3 & \sigma_3/f_3 \\ \sigma_3/f_3 & \sigma_2/f_2 + \sigma_3/f_3 \end{pmatrix}, \quad \boldsymbol{V}^{-1} = \begin{pmatrix} 1/f_1 + 1/f_3 & 1/f_3 \\ 1/f_3 & 1/f_2 + 1/f_3 \end{pmatrix}.$$

To bound σ_e we require some elementary bounds on $\boldsymbol{Y}_*$. When σ_1, σ_2, and σ_3 are real and positive we know that $\boldsymbol{Y}_*$ must be positive-semidefinite. As $\boldsymbol{Y}_*$ varies over all positive-semidefinite matrices, σ_e given by (29.31) varies over all values in the interval

$$f_1\sigma_1 + f_2\sigma_2 + f_3\sigma_3 \geq \sigma_e \geq [f_1/\sigma_1 + f_2/\sigma_2 + f_3/\sigma_3]^{-1},$$

where the upper and lower limits correspond to $\boldsymbol{Y}_* = \infty \boldsymbol{I}$ and $\boldsymbol{Y}_* = 0$, respectively. Thus the field equation recursion method recovers the standard arithmetic and harmonic mean bounds.

When σ_1, σ_2, and σ_3 are complex and labeled so that

$$\theta_1 = \arg(\sigma_1) \geq \arg(\sigma_2) \geq \arg(\sigma_3) = \theta_3 > \theta_1 - \pi,$$

the matrix $\boldsymbol{Y}_*$ satisfies the wedge bounds,

$$\theta_1 \geq \arg(\boldsymbol{v} \cdot \boldsymbol{Y}_* \boldsymbol{v}) \geq \theta_3, \tag{29.32}$$

for all real two-dimensional vectors $\boldsymbol{v}$. Let $\mathcal{Y}_1$ denote the set of all 2×2 matrices $\boldsymbol{Y}_1$ such that

$$\arg(\boldsymbol{v} \cdot \boldsymbol{Y}_1 \boldsymbol{v}) \geq \theta_3,$$

for all real vectors $\boldsymbol{v}$, and let $\mathcal{Y}_2$ denote the set of all 2×2 matrices $\boldsymbol{Y}_2$ such that

$$\theta_1 \geq \arg(\boldsymbol{v} \cdot \boldsymbol{Y}_2 \boldsymbol{v}),$$

for all real vectors $\boldsymbol{v}$. Then the wedge bounds are equivalent to saying that $\boldsymbol{Y}_*$ lies in the intersection of $\mathcal{Y}_1$ and $\mathcal{Y}_2$. As $\boldsymbol{Y}_*$ varies over all 2×2 matrices in the larger set $\mathcal{Y}_1$, an analysis [the details of which can be found in Milton (1987b)] shows that σ_e ranges over all values inside the circle in the complex plane defined by the inequality

$$\frac{1}{\mathrm{Im}[\sigma_3/(\sigma_3 - \sigma_e)]} \leq \frac{f_1}{\mathrm{Im}[\sigma_3/(\sigma_3 - \sigma_1)]} + \frac{f_2}{\mathrm{Im}[\sigma_3/(\sigma_3 - \sigma_1)]}, \tag{29.33}$$

which is also implied by the bounds (22.25) derived from the variational principles of Cherkaev and Gibiansky (1994). Similarly, as $\boldsymbol{Y}_*$ varies over all 2×2 matrices in the set $\mathcal{Y}_2$, σ_e ranges over all values inside the circle defined by

$$\frac{1}{\mathrm{Im}[\sigma_1/(\sigma_1 - \sigma_e)]} \leq \frac{f_2}{\mathrm{Im}[\sigma_1/(\sigma_1 - \sigma_2)]} + \frac{f_3}{\mathrm{Im}[\sigma_1/(\sigma_1 - \sigma_3)]}. \tag{29.34}$$

The value of σ_e must lie within the lens-shaped region formed by the intersection of these two circles. These are the bounds that Golden and Papanicolaou (1985) and Golden (1986) had conjectured. As $\boldsymbol{Y}_*$ varies over all 2×2 matrices satisfying the wedge bounds (29.32), σ_e takes values inside a subregion of this lens-shaped region. Some portions of the boundary of the subregion coincide with the boundary of the lens-shaped region, as illustrated in the example in figure 29.1 on the following page.

It turns out that the remaining portions of the boundary are generated by rank-1 matrices $\boldsymbol{Y}_*$ with an infinite eigenvalue and varying eigenvector, giving the curve traced out by

$$\begin{aligned} \sigma_e(\phi) \;=\; & f_1\sigma_1 + f_2\sigma_2 + f_3\sigma_3 \\ & - \frac{[\sigma_1 \cos(\phi) + \sigma_2 \sin(\phi) - \sigma_3(\cos(\phi) + \sin(\phi))]^2}{(\sigma_1/f_1)\cos^2(\phi) + (\sigma_2/f_2)\sin^2(\phi) + (\sigma_3/f_3)(\cos(\phi) + \sin(\phi))^2}, \end{aligned} \tag{29.35}$$

as ϕ is varied. The reason these portions of the curve contribute to the bounds is that the mapping $\sigma_e(\boldsymbol{Y}_*)$ given by (29.31) is such that

$$\sigma_e(\mathcal{Y}_1 \cap \mathcal{Y}_2) \neq \sigma_e(\mathcal{Y}_1) \cap \sigma_e(\mathcal{Y}_2).$$

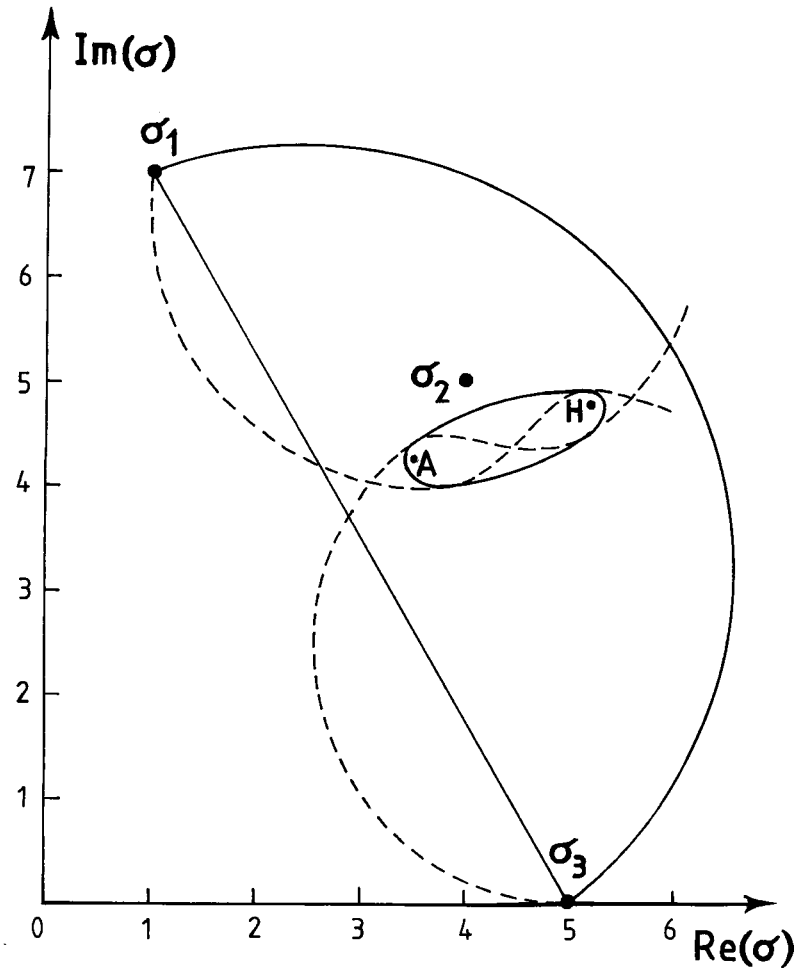

Figure 29.1. Bounds on a diagonal element σ_e of the complex effective conductivity tensor $\boldsymbol{\sigma}_*$ of a composite of three isotropic phases with complex dielectric constants $\sigma_1 = 1 + 7i$, $\sigma_2 = 4 + 5i$, and $\sigma_3 = 5$. If nothing else is known about the composite, then σ_e is confined to the outermost lens-shaped region, the boundary of which is traced by the diagonal elements of a laminate of phases 1 and 3 as the volume fraction is varied. When the volume fractions $f_1 = 1/4$, $f_2 = 1/2$, and $f_3 = 1/4$ are known, then σ_e is confined to the innermost region, bounded by two circular arcs, given by (29.33) and (29.34), and by two portions of the figure eight curve generated by (29.35) as ϕ is varied. The points A and H are the arithmetic and harmonic averages $f_1\sigma_1 + f_2\sigma_2 + f_3\sigma_3$ and $1/(f_1/\sigma_1 + f_2/\sigma_2 + f_3/\sigma_3)$. Reprinted with permission from Milton (1987b). Copyright 1987, Springer-Verlag.

This is a general feature of maps to lower dimensional spaces. For instance, consider the mapping $(x, y) \to (x, 0)$, which projects the (x, y)-plane to the x-axis. The image of both the line $x = y$ and the line $x = -y$ is the entire real axis. Therefore, the intersection of the images is the entire real axis, whereas the image of the intersection of the two lines is just the

point $x = 0$.

Other methods such as the translation method can also be used to bound the tensor $\boldsymbol{Y}_*$. If one seeks the best bounds on σ_e, one should first find the set of tensors $\boldsymbol{Y}_*$ consistent with all of the constraints and then take its image under the mapping $\sigma_e(\boldsymbol{Y}_*)$, rather than taking the intersection of the bounds on σ_e that derive from each constraint taken separately.

References

Bergman, D. J. 1986. The effective dielectric coefficient of a composite medium: Rigorous bounds from analytic properties. In J. L. Ericksen, D. Kinderlehrer, R. Kohn, and J.-L. Lions (eds.), *Homogenization and Effective Moduli of Materials and Media*, pp. 27–51. Berlin / Heidelberg / London / etc.: Springer-Verlag. ISBN 0-387-96306-5. {*451, 453, 571, 597, 603, 604, 617, 638, 641*}

Cherkaev, A. V. and L. V. Gibiansky 1994. Variational principles for complex conductivity, viscoelasticity, and similar problems in media with complex moduli. *Journal of Mathematical Physics* 35(1):127–145. {*221, 234, 237, 243, 264, 267, 271, 276, 277, 286, 639, 641*}

Clark, K. E. 1997. A continued fraction representation for the effective conductivity of a two-dimensional polycrystal. *Journal of Mathematical Physics* 38(9):4528–4541. {*619, 641*}

Golden, K. 1986. Bounds on the complex permittivity of a multicomponent material. *Journal of the Mechanics and Physics of Solids* 34(4):333–358. {*451, 453, 638, 639, 641*}

Golden, K. and G. Papanicolaou 1985. Bounds for effective parameters of multicomponent media by analytic continuation. *Journal of Statistical Physics* 40(5–6):655–667. {*387, 393, 451, 453, 638, 639, 641*}

Milton, G. W. 1987a. Multicomponent composites, electrical networks and new types of continued fraction. I. *Communications in Mathematical Physics* 111(2):281–327. {*248, 268, 397, 412, 619, 641*}

Milton, G. W. 1987b. Multicomponent composites, electrical networks and new types of continued fraction. II. *Communications in Mathematical Physics* 111(3):329–372. {*451, 454, 619, 638–641*}

Milton, G. W. 1991. The field equation recursion method. In G. Dal Maso and G. F. Dell'Antonio (eds.), *Composite Media and Homogenization Theory: Proceedings of the Workshop on Composite Media and Homogenization Theory Held in Trieste, Italy, from January 15 to 26, 1990*, pp. 223–245. Basel, Switzerland: Birkhäuser Verlag. ISBN 0-8176-3511-4, 3-7643-3511-4. {*397, 412, 517, 526, 612, 613, 618, 619, 641*}

Milton, G. W. and K. Golden 1990. Representations for the conductivity functions of multicomponent composites. *Communications on Pure and Applied Mathematics (New York)* 43(5):647–671. {*303, 311, 387, 389, 390, 394, 451, 454, 638, 641*}

30

Properties of the G-closure and extremal families of composites

30.1. An equivalence between G-closure problems with and without prescribed volume fractions

When one is interested in finding bounds that correlate $\boldsymbol{L}_*$ with the volume fractions of the phases, there is a simple trick that reduces this to a problem in which the volume fractions do not explicitly enter. For simplicity, let us consider the problem of bounding the effective tensor $\boldsymbol{\sigma}_*$ of a two-phase composite. The equations

$$\boldsymbol{j}(\boldsymbol{x}) = \boldsymbol{\sigma}(\boldsymbol{x})\boldsymbol{e}(\boldsymbol{x}), \quad \nabla \cdot \boldsymbol{j} = 0, \quad \nabla \times \boldsymbol{e} = 0,$$

where

$$\boldsymbol{\sigma}(\boldsymbol{x}) = \chi_1(\boldsymbol{x})\boldsymbol{\sigma}_1 + \chi_2(\boldsymbol{x})\boldsymbol{\sigma}_2,$$

can be supplemented by a single scalar equation

$$w(\boldsymbol{x}) = \chi_1(\boldsymbol{x})v, \quad v = \text{constant},$$

and rewritten as a single equation

$$\boldsymbol{J}(\boldsymbol{x}) = \boldsymbol{L}(\boldsymbol{x})\boldsymbol{E}(\boldsymbol{x}), \tag{30.1}$$

with

$$\boldsymbol{J}(\boldsymbol{x}) = \begin{pmatrix} \boldsymbol{j}(\boldsymbol{x}) \\ w(\boldsymbol{x}) \end{pmatrix}, \quad \boldsymbol{E}(\boldsymbol{x}) = \begin{pmatrix} \boldsymbol{e}(\boldsymbol{x}) \\ v \end{pmatrix}, \quad \boldsymbol{L}(\boldsymbol{x}) = \chi_1(\boldsymbol{x}) \begin{pmatrix} \boldsymbol{\sigma}_1 & 0 \\ 0 & 1 \end{pmatrix} + \chi_2(\boldsymbol{x}) \begin{pmatrix} \boldsymbol{\sigma}_2 & 0 \\ 0 & 0 \end{pmatrix}.$$

This equation (30.1) resembles a thermoelastic-type problem, but with the conductivity tensor playing the role of the compliance tensor and with no coupling between the fields. By taking averages of the fields $\boldsymbol{J}(\boldsymbol{x})$ and $\boldsymbol{E}(\boldsymbol{x})$ it is evident that the effective tensor associated with the equation (30.1) is

$$\boldsymbol{L}_* = \begin{pmatrix} \boldsymbol{\sigma}_* & 0 \\ 0 & f_1 \end{pmatrix}.$$

Clearly finding bounds that correlate $\boldsymbol{\sigma}_*$ with the volume fraction f_1 is exactly equivalent to finding bounds on the effective tensor $\boldsymbol{L}_*$.

More generally, suppose that the conductivity tensors $\boldsymbol{\sigma}_1, \boldsymbol{\sigma}_2, \ldots, \boldsymbol{\sigma}_n$ of the phases in an n-phase medium depend on some parameter ω, and we are interested in correlating the volume

fractions $f_1, f_2, \ldots, f_n$ with the values $\boldsymbol{\sigma}_*(\omega_1), \boldsymbol{\sigma}_*(\omega_2), \ldots, \boldsymbol{\sigma}_*(\omega_q)$ that the effective tensor $\boldsymbol{\sigma}_*(\omega)$ takes as ω takes q different values $\omega_1, \omega_2, \ldots \omega_q$. Of course since the volume fractions sum to unity, we can regard f_n as being determined from the remaining volume fractions $f_1, f_2, \ldots, f_{n-1}$. The system of equations

$$\begin{aligned} \boldsymbol{j}^{(\alpha)}(\boldsymbol{x}) &= \boldsymbol{\sigma}^{(\alpha)}(\boldsymbol{x})\boldsymbol{e}^{(\alpha)}(\boldsymbol{x}), \quad \nabla \cdot \boldsymbol{j}^{(\alpha)} = 0, \quad \nabla \times \boldsymbol{e}^{(\alpha)} = 0, \quad \text{for } \alpha = 1, 2 \ldots, q \\ w_i(\boldsymbol{x}) &= \chi_i(\boldsymbol{x}) v_i, \quad v_i = \text{constant}, \quad \text{for } i = 1, 2, \ldots, n-1, \end{aligned}$$

where

$$\boldsymbol{\sigma}^{(\alpha)}(\boldsymbol{x}) = \sum_{i=1}^{n} \chi_i(\boldsymbol{x}) \boldsymbol{\sigma}_i(\omega_\alpha),$$

define the effective tensors and volume fractions through the relations

$$\langle \boldsymbol{j}^{(\alpha)} \rangle = \boldsymbol{\sigma}_*(\omega_\alpha) \langle \boldsymbol{e}^{(\alpha)} \rangle, \qquad \langle w_i \rangle = f_i \langle v_i \rangle = f_i v_i. \tag{30.2}$$

This system can be rewritten as a single equation,

$$\boldsymbol{J} = \boldsymbol{L}\boldsymbol{E}, \tag{30.3}$$

incorporating the extended fields

$$\boldsymbol{J}(\boldsymbol{x}) = \begin{pmatrix} \boldsymbol{j}^{(1)}(\boldsymbol{x}) \\ \boldsymbol{j}^{(2)}(\boldsymbol{x}) \\ \vdots \\ \boldsymbol{j}^{(q)}(\boldsymbol{x}) \\ \boldsymbol{w}(\boldsymbol{x}) \end{pmatrix}, \quad \boldsymbol{E}(\boldsymbol{x}) = \begin{pmatrix} \boldsymbol{e}^{(1)}(\boldsymbol{x}) \\ \boldsymbol{e}^{(2)}(\boldsymbol{x}) \\ \vdots \\ \boldsymbol{e}^{(q)}(\boldsymbol{x}) \\ \boldsymbol{v} \end{pmatrix},$$

and a tensor field

$$\boldsymbol{L}(\boldsymbol{x}) = \sum_{i=1}^{n} \chi_i(\boldsymbol{x}) \boldsymbol{L}_i,$$

with block-diagonal component supertensors,

$$\boldsymbol{L}_i = \begin{pmatrix} \boldsymbol{\sigma}_i(\omega_1) & 0 & \ldots & 0 & 0 \\ 0 & \boldsymbol{\sigma}_i(\omega_2) & \ldots & 0 & 0 \\ \vdots & \vdots & \ddots & \vdots & \vdots \\ 0 & 0 & \ldots & \boldsymbol{\sigma}_i(\omega_q) & 0 \\ 0 & 0 & \ldots & 0 & \boldsymbol{K}_i \end{pmatrix},$$

where

$$\boldsymbol{K}_1 = \begin{pmatrix} 1 & 0 & \ldots & 0 \\ 0 & 0 & \ldots & 0 \\ \vdots & \vdots & \ddots & \vdots \\ 0 & 0 & \ldots & 0 \end{pmatrix}, \quad \boldsymbol{K}_2 = \begin{pmatrix} 0 & 0 & \ldots & 0 \\ 0 & 1 & \ldots & 0 \\ \vdots & \vdots & \ddots & \vdots \\ 0 & 0 & \ldots & 0 \end{pmatrix}, \quad \ldots, \quad \boldsymbol{K}_{n-1} = \begin{pmatrix} 0 & 0 & \ldots & 0 \\ 0 & 0 & \ldots & 0 \\ \vdots & \vdots & \ddots & \vdots \\ 0 & 0 & \ldots & 1 \end{pmatrix},$$

and $\boldsymbol{K}_n = 0$.

Also, (30.2) implies that the effective tensor associated with the equation (30.3) is the supertensor

$$\boldsymbol{L}_* = \begin{pmatrix} \boldsymbol{\sigma}_*(\omega_1) & 0 & \dots & 0 & 0 \\ 0 & \boldsymbol{\sigma}_*(\omega_2) & \dots & 0 & 0 \\ \vdots & \vdots & \ddots & \vdots & \vdots \\ 0 & 0 & \dots & \boldsymbol{\sigma}_*(\omega_q) & 0 \\ 0 & 0 & \dots & 0 & \boldsymbol{K}_* \end{pmatrix},$$

where

$$\boldsymbol{K}_* = \begin{pmatrix} f_1 & 0 & \dots & 0 \\ 0 & f_2 & \dots & 0 \\ \vdots & \vdots & \ddots & \vdots \\ 0 & 0 & \dots & f_{n-1} \end{pmatrix},$$

which has the volume fractions as its diagonal elements. Clearly the problem of correlating the volume fractions $f_1, f_2, \dots, f_{n-1}$ and effective tensors $\boldsymbol{\sigma}_*(\omega_1)$, $\boldsymbol{\sigma}_*(\omega_2), \dots, \boldsymbol{\sigma}_*(\omega_q)$ is equivalent to finding the possible values that the effective tensor $\boldsymbol{L}_*$ can take.

30.2. Stability under lamination and the convexity properties of the G-closure

From the analysis of the previous section we see that many bounding problems boil down to the task of characterizing the range GU of values that a suitably defined effective tensor $\boldsymbol{L}_*$ takes as the local tensor field $\boldsymbol{L}(\boldsymbol{x})$ is varied over all periodic functions with

$$\boldsymbol{L}(\boldsymbol{x}) \in U \quad \text{for all } \boldsymbol{x},$$

where U represents the set of tensors of the constituents:

$$U = \{\boldsymbol{L}_1, \boldsymbol{L}_2, \dots, \boldsymbol{L}_n\}.$$

Also from section 12.11 on page 264 we know that problems in which the field $\boldsymbol{L}(\boldsymbol{x})$ and effective tensor $\boldsymbol{L}_*$ are not self-adjoint can be mapped to an equivalent problem in which the field and effective tensor are self-adjoint. Let us therefore suppose that the tensors in GU are self-adjoint. This set GU, the G-closure of U, has the property that

$$G[GU] = GU.$$

In other words, if we build a composite from tensors in GU, then its effective tensor must also lie in GU.

In particular, if we take two tensors $\boldsymbol{A}$ and $\boldsymbol{B}$ in GU and laminate them together in proportions f and $1-f$ with the layers orthogonal to a direction $\boldsymbol{n}$, then the effective tensor $\boldsymbol{A}_*$ must also lie in GU. This stability under lamination implies that GU has certain convexity properties (Francfort and Milton 1994). To see these properties it is helpful to introduce the transformation

$$W_{\boldsymbol{n}}(\boldsymbol{L}) = [\boldsymbol{I} + (\boldsymbol{L} - \boldsymbol{L}_0)\boldsymbol{\Gamma}(\boldsymbol{n})]^{-1}(\boldsymbol{L} - \boldsymbol{L}_0),$$

as in (17.2). From the lamination formula (9.44) we have

$$W_{\boldsymbol{n}}(\boldsymbol{A}_*) = fW_{\boldsymbol{n}}(\boldsymbol{A}) + (1-f)W_{\boldsymbol{n}}(\boldsymbol{B}).$$

So, as f is varied from 0 to 1, $W_{\boldsymbol{n}}(\boldsymbol{A}_*)$ varies along the straight line in tensor space joining $W_{\boldsymbol{n}}(\boldsymbol{A})$ with $W_{\boldsymbol{n}}(\boldsymbol{B})$. This implies that $W_{\boldsymbol{n}}(GU)$ must be a convex set in tensor space for all choices of the unit vector $\boldsymbol{n}$. Specifically, if U consists of $m \times m$ symmetric matrices, then any element of $W_{\boldsymbol{n}}(GU)$ will be a $m \times m$ matrix and we can represent it by a point in an $m(m+1)/2$-dimensional space where the first m coordinates represent the diagonal matrix elements, while the remaining $m(m-1)/2$ coordinates represent the upper off-diagonal elements. The region representing $W_{\boldsymbol{n}}(GU)$ in these coordinates will be convex.

The set GU itself is not necessarily convex, but it does nevertheless have some convexity properties. To see this, suppose that the point $\boldsymbol{B}$ is on the surface of GU and assume that the surface is smooth at $\boldsymbol{B}$. Let $H(\boldsymbol{C})$ denote a scalar-valued parameterization of the surface of GU such that

$$H(\boldsymbol{C}) \geq 0 \text{ if and only if } \boldsymbol{C} \in GU,$$

with equality if and only if $\boldsymbol{C}$ is on the boundary of GU. The parameterization is assumed to be chosen so that the matrix

$$H_{\boldsymbol{B}} = \left.\frac{dH(\boldsymbol{C})}{d\boldsymbol{C}}\right|_{\boldsymbol{C}=\boldsymbol{B}} \neq 0.$$

The matrix then represents the normal to the boundary of GU at $\boldsymbol{B}$. The tensor $\boldsymbol{A}_*$ of the laminate must lie in GU for all choices of $f \in [0, 1]$ and in particular for values of f close to zero. From the lamination formula (9.45) we see that

$$\begin{aligned}\boldsymbol{A}_* &= \boldsymbol{A} + (1-f)[(\boldsymbol{B}-\boldsymbol{A})^{-1} + f\boldsymbol{\Gamma}(\boldsymbol{n})]^{-1} \\ &= \boldsymbol{B} + f[(\boldsymbol{A}-\boldsymbol{B}) - (\boldsymbol{A}-\boldsymbol{B})\boldsymbol{\Gamma}(\boldsymbol{n})(\boldsymbol{A}-\boldsymbol{B})] + \mathcal{O}(f^2),\end{aligned}$$

where

$$\boldsymbol{\Gamma}(\boldsymbol{n}) = \boldsymbol{\Gamma}_1(\boldsymbol{n})[\boldsymbol{\Gamma}_1(\boldsymbol{n})\boldsymbol{A}\boldsymbol{\Gamma}_1(\boldsymbol{n})]^{-1}\boldsymbol{\Gamma}_1(\boldsymbol{n}),$$

in which the inverse is to be taken on the subspace $\mathcal{E}_{\boldsymbol{n}}$ onto which $\boldsymbol{\Gamma}_1(\boldsymbol{n})$ projects. It follows that, to the first order in f,

$$H(\boldsymbol{A}_*) = H(\boldsymbol{B}) + f\,\mathrm{Tr}\{H_{\boldsymbol{B}}[(\boldsymbol{A}-\boldsymbol{B}) - (\boldsymbol{A}-\boldsymbol{B})\boldsymbol{\Gamma}(\boldsymbol{n})(\boldsymbol{A}-\boldsymbol{B})]\} + \mathcal{O}(f^2).$$

Now $H(\boldsymbol{B})$ is zero because $\boldsymbol{B}$ is on the boundary of GU, and the requirement that $\boldsymbol{A}_*$ lies in GU implies that $H(\boldsymbol{A}_*)$ must be nonnegative for all values of f and in particular for values of f close to zero. Hence the bounds

$$\mathrm{Tr}\{H_{\boldsymbol{B}}[(\boldsymbol{A}-\boldsymbol{B}) - (\boldsymbol{A}-\boldsymbol{B})\boldsymbol{\Gamma}(\boldsymbol{n})(\boldsymbol{A}-\boldsymbol{B})]\} \geq 0 \tag{30.4}$$

must hold for all tensors $\boldsymbol{A} \in GU$ (Francfort and Milton 1994). If we have partial knowledge of GU, such as the knowledge of a tensor $\boldsymbol{B} \in \partial GU$ and its associated tangent plane giving $H_{\boldsymbol{B}}$, then (30.4) provides a bound on the rest of GU. In this way Milton and Nesi (1999), generalizing an approach of Roscoe (1973) [see also section 10.9 on page 204], were able to prove a conjecture of Astala and Miettinen (1998) and establish optimal bounds on the conductivity of an anisotropic, two-dimensional composite comprised of an isotropic phase mixed in fixed proportion with an anisotropic polycrystalline phase. The required partial knowledge of GU was provided by the optimal bound (23.61) of Nesi (1996) on the effective conductivity of an isotropic composite.

The relation (30.4) must hold when $\boldsymbol{A}$ is on the surface of GU and is close to $\boldsymbol{B}$. Therefore let us consider a trajectory of matrices $\boldsymbol{A}(t)$ on the surface of GU such that $\boldsymbol{A}(0) = \boldsymbol{B}$. By

twice differentiating the constraint that $H(\boldsymbol{A}(t)) = 0$ and setting $t = 0$ we see that the matrices $\boldsymbol{A}'$ and $\boldsymbol{A}''$ entering the expansion

$$\boldsymbol{A}(t) - \boldsymbol{B} = t\boldsymbol{A}' + t^2\boldsymbol{A}''/2 + \mathcal{O}(t^3) \tag{30.5}$$

satisfy

$$\text{Tr}[H_{\boldsymbol{B}}\boldsymbol{A}'] = 0, \quad \text{Tr}[H_{\boldsymbol{B}}\boldsymbol{A}''] = -\text{Tr}[\boldsymbol{A}'H_{\boldsymbol{BB}}\boldsymbol{A}'], \tag{30.6}$$

where

$$H_{\boldsymbol{BB}} = \left.\frac{d^2H(\boldsymbol{C})}{d\boldsymbol{C}d\boldsymbol{C}}\right|_{\boldsymbol{C}=\boldsymbol{B}}.$$

By substituting (30.5) back into (30.4) and using (30.6) we see that

$$\text{Tr}[\boldsymbol{A}'H_{\boldsymbol{BB}}\boldsymbol{A}']/2 + \text{Tr}\{H_{\boldsymbol{B}}[\boldsymbol{A}'\boldsymbol{\Gamma}(\boldsymbol{n})\boldsymbol{A}']\} \leq 0 \quad \text{for all } \boldsymbol{A}' \text{ such that } \text{Tr}[H_{\boldsymbol{B}}\boldsymbol{A}'] = 0. \tag{30.7}$$

This provides a constraint on the second derivative tensor $H_{\boldsymbol{BB}}$.

Instead of considering GU we could have considered U, and asked when U itself is stable under lamination. Clearly stability under lamination in direction $\boldsymbol{n}$ holds if and only if $W_{\boldsymbol{n}}(U)$ is convex. This convexity is a local condition that can be expressed in terms of the positivity of the curvature of the boundary of $W_{\boldsymbol{n}}(U)$, that is, as a condition that involves only first and second derivatives of the function characterizing the boundary. Therefore a set U, whose boundary is characterized by a function H, will be stable under lamination in direction $\boldsymbol{n}$ if and only if the local condition (30.7) holds for all tensors $\boldsymbol{B}$ on the surface. If the condition also holds for all vectors $\boldsymbol{n}$, then U will be stable under lamination in any direction. This condition (Francfort and Milton 1994) allows one to test the stability under lamination of any set U. Notice that (30.7) bears a close resemblance to the condition (24.43) associated with a translation $\boldsymbol{T}$ being quasiconvex. In fact, knowledge of $H_{\boldsymbol{B}}$ and $H_{\boldsymbol{BB}}$ at a point $\boldsymbol{B}$ on the boundary of a set U (which is stable under lamination) allows one to generate various associated quasiconvex translations $\boldsymbol{T}_{\boldsymbol{B}}$ (Milton 1994). With the aid of the comparison bound (24.6), these translations can often be used to prove that $\boldsymbol{B}$ lies on the boundary of GU. If this can be done for all points $\boldsymbol{B}$ on the surface of U, then U must be stable under homogenization, that is, $GU = U$. This provides an algorithm for showing that certain sets stable under lamination are also stable under homogenization. Sometimes the algorithm will fail because there are sets stable under lamination that are not stable under homogenization, as we will see in section 31.9 on page 690.

30.3. Characterizing the G-closure through minimums of sums of energies and complementary energies

We have seen in section 24.12 on page 519 that the translation method bounds the effective tensor $\boldsymbol{L}_*$ through lower bounds on sums of energies and complementary energies. Here we will show that minimums of sums of energies and complementary energies serve to characterize G-closures in much the same way that Legendre transforms serve to characterize convex sets (Francfort and Milton 1994; Milton 1994; Milton and Cherkaev 1995).

Let us begin by supposing that $\boldsymbol{B}$ is a tensor on that portion of the surface of GU where $H_{\boldsymbol{B}}$ is positive-semidefinite. Then, because $\boldsymbol{\Gamma}(\boldsymbol{n})$ is also positive-semidefinite, it follows that

$$\text{Tr}[H_{\boldsymbol{B}}(\boldsymbol{A} - \boldsymbol{B})\boldsymbol{\Gamma}(\boldsymbol{n})(\boldsymbol{A} - \boldsymbol{B})] = \text{Tr}[H_{\boldsymbol{B}}^{1/2}(\boldsymbol{A} - \boldsymbol{B})\boldsymbol{\Gamma}(\boldsymbol{n})(\boldsymbol{A} - \boldsymbol{B})H_{\boldsymbol{B}}^{1/2}] \geq 0,$$

which in conjunction with (30.4) implies that

$$\mathrm{Tr}[H_{\boldsymbol{B}}\boldsymbol{A}] \geq \mathrm{Tr}[H_{\boldsymbol{B}}\boldsymbol{B}] \text{ for all } \boldsymbol{A} \in GU.$$

In geometrical terms this says that the set GU must lie entirely on one side of the tangent plane

$$\mathcal{P} = \{\boldsymbol{C} \mid \mathrm{Tr}[H_{\boldsymbol{B}}\boldsymbol{C}] = \mathrm{Tr}[H_{\boldsymbol{B}}\boldsymbol{B}]\} \tag{30.8}$$

to the set GU at the point $\boldsymbol{B}$. If this were true for all points $\boldsymbol{B}$ on the boundary of GU, and not just those points where $H_{\boldsymbol{B}}$ is positive-semidefinite, then GU would be convex.

Since the tensor $H_{\boldsymbol{B}}$ is positive-semidefinite we can set

$$H_{\boldsymbol{B}} = \sum_{i=1}^{m} \boldsymbol{h}_i \otimes \boldsymbol{h}_i,$$

where m is the dimension of the matrices in U (i.e., each matrix in U is an $m \times m$ matrix), each $\boldsymbol{h}_i$ is an eigenvector of $H_{\boldsymbol{B}}$, and $\boldsymbol{h}_i \cdot \boldsymbol{h}_i$ is the associated eigenvalue. By substituting this formula for $H_{\boldsymbol{B}}$ into (30.8) and setting $\boldsymbol{A} = \boldsymbol{L}_*$ we see that the minimum in the expression for

$$W_-(\boldsymbol{h}_1, \boldsymbol{h}_2, \ldots, \boldsymbol{h}_m) = \min_{\boldsymbol{L}_* \in GU} \left[\sum_{i=1}^{m} \boldsymbol{h}_i \cdot \boldsymbol{L}_* \boldsymbol{h}_i \right]$$

is achieved when $\boldsymbol{L}_* = \boldsymbol{B}$. Each term $\boldsymbol{h}_i \cdot \boldsymbol{L}_* \boldsymbol{h}_i$ in this sum can be thought of as the "energy" that is stored in the composite when it is exposed to a field with $\langle \boldsymbol{E} \rangle = \boldsymbol{h}_i$. Of course, whether this interpretation makes physical sense or not depends on the nature of the tensors in the set U. If they represent dielectric or elasticity tensors, then $\boldsymbol{h}_i \cdot \boldsymbol{L}_* \boldsymbol{h}_i$ does indeed represent the stored energy. If they represent electrical conductivity tensors, then $\boldsymbol{h}_i \cdot \boldsymbol{L}_* \boldsymbol{h}_i$ represents the energy dissipated into heat.

More generally, when $H_{\boldsymbol{B}}$ is not positive-semidefinite, but has only $k < m$ positive eigenvalues, then we can set

$$H_{\boldsymbol{B}} = H^+_{\boldsymbol{B}} - H^-_{\boldsymbol{B}}, \tag{30.9}$$

where $H^+_{\boldsymbol{B}}$ is positive-semidefinite with rank k and $H^-_{\boldsymbol{B}}$ is positive-semidefinite with rank at most $m - k$. This decomposition can be done in many ways. One way, which ensures that

$$H^+_{\boldsymbol{B}}(\boldsymbol{B} H^-_{\boldsymbol{B}} \boldsymbol{B}) = 0, \tag{30.10}$$

is to first express $\boldsymbol{B}^{1/2} H_{\boldsymbol{B}} \boldsymbol{B}^{1/2}$ in terms of its eigenvalues and eigenvectors,

$$\boldsymbol{B}^{1/2} H_{\boldsymbol{B}} \boldsymbol{B}^{1/2} = \sum_{i=1}^{m} \lambda_i \boldsymbol{v}_i \otimes \boldsymbol{v}_i, \quad \text{where } \boldsymbol{v}_i \cdot \boldsymbol{v}_j = \delta_{ij},$$

with the eigenvalues ordered so that the positive eigenvalues come first,

$$\lambda_i > 0 \text{ for } i \leq k, \quad \lambda_i \leq 0 \text{ for } i \geq k+1.$$

Then (30.9) and (30.10) are satisfied with

$$H^+_{\boldsymbol{B}} = \sum_{i=1}^{k} \lambda_i \boldsymbol{B}^{-1/2} \boldsymbol{v}_i \otimes \boldsymbol{v}_i \boldsymbol{B}^{-1/2}, \quad H^-_{\boldsymbol{B}} = \sum_{i=k+1}^{m} \lambda_i \boldsymbol{B}^{-1/2} \boldsymbol{v}_i \otimes \boldsymbol{v}_i \boldsymbol{B}^{-1/2}.$$

Using (30.9), the inequality (30.4) can be rewritten in the form

$$\begin{aligned}&\mathrm{Tr}\{H^+_{\boldsymbol{B}}[(\boldsymbol{A}-\boldsymbol{B})-(\boldsymbol{A}-\boldsymbol{B})\boldsymbol{A}^{-1/2}\boldsymbol{\Gamma}_1^{\boldsymbol{A}}(\boldsymbol{n})\boldsymbol{A}^{-1/2}(\boldsymbol{A}-\boldsymbol{B})]\}\\&\quad+\mathrm{Tr}\{H^-_{\boldsymbol{B}}[(\boldsymbol{B}\boldsymbol{A}^{-1}\boldsymbol{B}-\boldsymbol{B})-(\boldsymbol{A}-\boldsymbol{B})\boldsymbol{A}^{-1/2}\boldsymbol{\Gamma}_2^{\boldsymbol{A}}(\boldsymbol{n})\boldsymbol{A}^{-1/2}(\boldsymbol{A}-\boldsymbol{B})]\}\geq 0,\end{aligned}$$

where

$$\begin{aligned}\boldsymbol{\Gamma}_1^{\boldsymbol{A}}(\boldsymbol{n})&=\boldsymbol{A}^{1/2}\boldsymbol{\Gamma}(\boldsymbol{n})\boldsymbol{A}^{1/2}=\boldsymbol{A}^{1/2}\boldsymbol{\Gamma}_1(\boldsymbol{n})[\boldsymbol{\Gamma}_1(\boldsymbol{n})\boldsymbol{A}\boldsymbol{\Gamma}_1(\boldsymbol{n})]^{-1}\boldsymbol{\Gamma}_1(\boldsymbol{n})\boldsymbol{A}^{1/2},\\\boldsymbol{\Gamma}_2^{\boldsymbol{A}}(\boldsymbol{n})&=\boldsymbol{I}-\boldsymbol{\Gamma}_1^{\boldsymbol{A}}(\boldsymbol{n})\end{aligned}$$

are the projections onto $\boldsymbol{A}^{1/2}\mathcal{E}_{\boldsymbol{n}}$ and its orthogonal complement $\boldsymbol{A}^{-1/2}\mathcal{J}_{\boldsymbol{n}}$. Since $H^+_{\boldsymbol{B}}$, $H^-_{\boldsymbol{B}}$, $\boldsymbol{\Gamma}_1^{\boldsymbol{A}}(\boldsymbol{n})$, and $\boldsymbol{\Gamma}_2^{\boldsymbol{A}}(\boldsymbol{n})$ are all positive-definite or positive-semidefinite matrices, we deduce that

$$\mathrm{Tr}[H^+_{\boldsymbol{B}}\boldsymbol{A}]+\mathrm{Tr}[H^-_{\boldsymbol{B}}\boldsymbol{B}\boldsymbol{A}^{-1}\boldsymbol{B}]\geq\mathrm{Tr}[H^+_{\boldsymbol{B}}\boldsymbol{B}]+\mathrm{Tr}[H^-_{\boldsymbol{B}}\boldsymbol{B}\boldsymbol{B}^{-1}\boldsymbol{B}]\quad\text{for all }\boldsymbol{A}\in GU.\tag{30.11}$$

Now, because $H^+_{\boldsymbol{B}}$ is positive-semidefinite with rank k and $H^-_{\boldsymbol{B}}$ is positive-semidefinite with rank at most $m-k$, we can set

$$H^+_{\boldsymbol{B}}=\sum_{i=1}^{k}\boldsymbol{h}_i\otimes\boldsymbol{h}_i,\qquad \boldsymbol{B}H^-_{\boldsymbol{B}}\boldsymbol{B}=\sum_{i=k+1}^{m}\boldsymbol{h}_i\otimes\boldsymbol{h}_i,\tag{30.12}$$

where each vector $\boldsymbol{h}_i$ is an eigenvector of $H^+_{\boldsymbol{B}}$ for $i\leq k$ and is an eigenvector of $\boldsymbol{B}H^-_{\boldsymbol{B}}\boldsymbol{B}$ for $i\geq k+1$, and $\boldsymbol{h}_i\cdot\boldsymbol{h}_i$ is the associated eigenvalue. It follows from (30.10) that these eigenvectors are mutually orthogonal,

$$\boldsymbol{h}_i\cdot\boldsymbol{h}_j=0\ \text{ for all } i\neq j.\tag{30.13}$$

By substituting these formulas (30.12) into (30.11) we see that the tensor $\boldsymbol{L}_*=\boldsymbol{B}$ achieves the minimum in the expression for

$$\begin{aligned}&W_-(\boldsymbol{h}_1,\boldsymbol{h}_2,\dots,\boldsymbol{h}_k;\boldsymbol{h}_{k+1},\boldsymbol{h}_{k+2},\dots,\boldsymbol{h}_m)\\&\quad=\min_{\boldsymbol{L}_*\in GU}W(\boldsymbol{h}_1,\boldsymbol{h}_2,\dots,\boldsymbol{h}_k;\boldsymbol{h}_{k+1},\boldsymbol{h}_{k+2},\dots,\boldsymbol{h}_m;\boldsymbol{L}_*),\end{aligned}$$

where

$$W(\boldsymbol{h}_1,\boldsymbol{h}_2,\dots,\boldsymbol{h}_k;\boldsymbol{h}_{k+1},\boldsymbol{h}_{k+2},\dots,\boldsymbol{h}_m;\boldsymbol{L}_*)=\sum_{i=1}^{k}\boldsymbol{h}_i\cdot\boldsymbol{L}_*\boldsymbol{h}_i+\sum_{i=k+1}^{m}\boldsymbol{h}_i\cdot\boldsymbol{L}_*^{-1}\boldsymbol{h}_i\tag{30.14}$$

represents a sum of "energies" and "complementary energies": Each term $\boldsymbol{h}_i\cdot\boldsymbol{L}_*\boldsymbol{h}_i$ or $\boldsymbol{h}_i\cdot\boldsymbol{L}_*^{-1}\boldsymbol{h}_i$ appearing in this sum can be thought of as the "energy" or "complementary energy" that is stored in the composite when it is exposed to a field with $\langle\boldsymbol{E}\rangle=\boldsymbol{h}_i$, for $i\leq k$ or to a field with $\langle\boldsymbol{J}\rangle=\boldsymbol{h}_i$, for $i\geq k+1$.

It follows that the set

$$\begin{aligned}\mathcal{K}(\boldsymbol{h}_1,\boldsymbol{h}_2,\dots,\boldsymbol{h}_k;\boldsymbol{h}_{k+1},\boldsymbol{h}_{k+2},\dots,\boldsymbol{h}_m)=\{\boldsymbol{C}\ \mid\ &W(\boldsymbol{h}_1,\boldsymbol{h}_2,\dots,\boldsymbol{h}_k;\boldsymbol{h}_{k+1},\boldsymbol{h}_{k+2},\dots,\boldsymbol{h}_m;\boldsymbol{C})\\&\geq W_-(\boldsymbol{h}_1,\boldsymbol{h}_2,\dots,\boldsymbol{h}_k;\boldsymbol{h}_{k+1},\boldsymbol{h}_{k+2},\dots,\boldsymbol{h}_m)\}\end{aligned}\tag{30.15}$$

certainly contains GU and has $\boldsymbol{B}$ on its boundary. Also, since this set has the property that

$$\mathcal{K}(\alpha\boldsymbol{h}_1, \alpha\boldsymbol{h}_2, \ldots, \alpha\boldsymbol{h}_k; \alpha\boldsymbol{h}_{k+1}, \alpha\boldsymbol{h}_{k+2}, \ldots, \alpha\boldsymbol{h}_m) = \mathcal{K}(\boldsymbol{h}_1, \boldsymbol{h}_2, \ldots, \boldsymbol{h}_k; \boldsymbol{h}_{k+1}, \boldsymbol{h}_{k+2}, \ldots, \boldsymbol{h}_m),$$

for all $\alpha \neq 0$, without loss of generality we can impose the normalization condition

$$\sum_{i=1}^{m} \boldsymbol{h}_i \cdot \boldsymbol{h}_i = 1. \tag{30.16}$$

Therefore GU can be identified with the region of intersection of the sets

$$\mathcal{K}(\boldsymbol{h}_1, \boldsymbol{h}_2, \ldots, \boldsymbol{h}_k; \boldsymbol{h}_{k+1}, \boldsymbol{h}_{k+2}, \ldots, \boldsymbol{h}_m)$$

as k ranges from 0 to m and as the $\boldsymbol{h}_i$ are varied over all sets of mutually orthogonal vectors satisfying (30.16). In other words, stability under lamination ensures that the set GU has sufficient "convexity" to guarantee that it can be recovered from knowledge of the function $W_-(\boldsymbol{h}_1, \boldsymbol{h}_2, \ldots, \boldsymbol{h}_k; \boldsymbol{h}_{k+1}, \boldsymbol{h}_{k+2}, \ldots, \boldsymbol{h}_m)$. Thus, as illustrated in figure 30.1, minimums of sums of energies and complementary energies serve to characterize G-closures in much the same way that Legendre transforms serve to characterize convex sets.

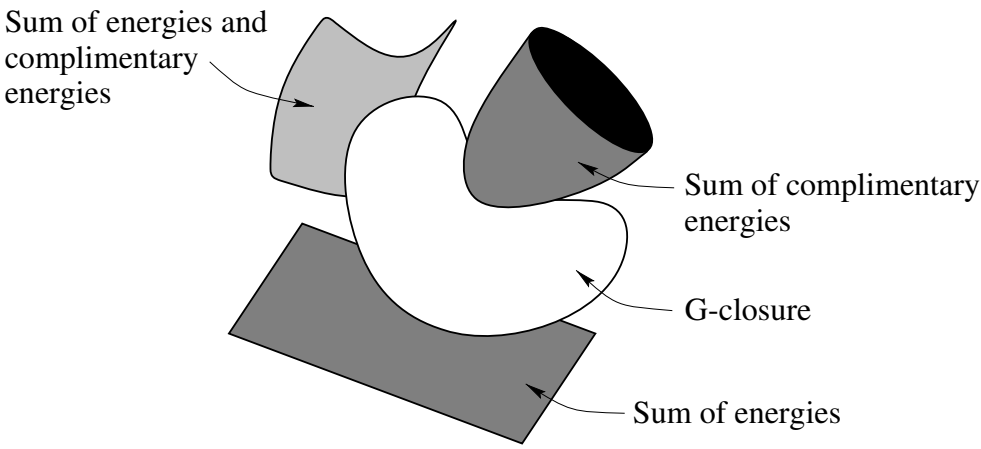

Figure 30.1. G-closures are characterized by minimums of sums of energies and complementary energies. The coordinates here represent the elements of the effective tensor $\boldsymbol{L}_*$. Then a plane represents a surface where a sum of energies is constant, and when this sum takes its minimum value the plane is tangent to the G-closure. The convexity properties of the G-closure guarantee that the surfaces corresponding to the minimums of sums of energies and complementary energies wrap around the G-closure and touch each point on its boundary.

30.4. Characterization of the G-closure by single energy minimizations

The sum of "energies" and "complementary energies" appearing in (30.14) can itself be regarded as a single "energy" of an associated effective tensor. Consider the fields $\boldsymbol{J}^{(i)}(\boldsymbol{x})$ and $\boldsymbol{E}^{(i)}(\boldsymbol{x})$ that solve the equations

$$\boldsymbol{J}^{(i)}(\boldsymbol{x}) = \boldsymbol{L}(\boldsymbol{x})\boldsymbol{E}^{(i)}(\boldsymbol{x}), \quad \boldsymbol{J}^{(i)} \in \mathcal{U} \oplus \mathcal{J}, \quad \boldsymbol{E}^{(i)} \in \mathcal{U} \oplus \mathcal{E},$$

with

$$\langle \boldsymbol{E}^{(i)} \rangle = \boldsymbol{h}_i \quad \text{for } i = 1, 2, \ldots, k,$$
$$\langle \boldsymbol{J}^{(i)} \rangle = \boldsymbol{h}_i \quad \text{for } i = k+1, k+2, \ldots, m.$$

This set of equations can be rewritten as

$$\widetilde{\boldsymbol{J}} = \boldsymbol{\mathcal{L}}\widetilde{\boldsymbol{E}}, \quad \text{with } \widetilde{\boldsymbol{J}} \in \widetilde{\mathcal{U}} \oplus \widetilde{\mathcal{J}}, \quad \widetilde{\boldsymbol{E}} \in \widetilde{\mathcal{U}} \oplus \widetilde{\mathcal{E}}, \quad \langle \widetilde{\boldsymbol{E}} \rangle = \boldsymbol{E}_0,$$

with extended fields

$$\widetilde{\boldsymbol{J}}(\boldsymbol{x}) = \begin{pmatrix} \boldsymbol{J}^{(1)}(\boldsymbol{x}) \\ \vdots \\ \boldsymbol{J}^{(k)}(\boldsymbol{x}) \\ \boldsymbol{E}^{(k+1)}(\boldsymbol{x}) \\ \vdots \\ \boldsymbol{E}^{(m)}(\boldsymbol{x}) \end{pmatrix}, \quad \widetilde{\boldsymbol{E}}(\boldsymbol{x}) = \begin{pmatrix} \boldsymbol{E}^{(1)}(\boldsymbol{x}) \\ \vdots \\ \boldsymbol{E}^{(k)}(\boldsymbol{x}) \\ \boldsymbol{J}^{(k+1)}(\boldsymbol{x}) \\ \vdots \\ \boldsymbol{J}^{(m)}(\boldsymbol{x}) \end{pmatrix}, \quad \widetilde{\boldsymbol{E}}_0 = \begin{pmatrix} \boldsymbol{h}_1 \\ \vdots \\ \boldsymbol{h}_k \\ \boldsymbol{h}_{k+1} \\ \vdots \\ \boldsymbol{h}_m \end{pmatrix}, \tag{30.17}$$

and supertensor

$$\boldsymbol{\mathcal{L}}(\boldsymbol{x}) = \begin{pmatrix} \boldsymbol{L}(\boldsymbol{x}) & \ldots & 0 & 0 & \ldots & 0 \\ \vdots & \ddots & \vdots & \vdots & \ddots & \vdots \\ 0 & \ldots & \boldsymbol{L}(\boldsymbol{x}) & 0 & \ldots & 0 \\ 0 & \ldots & 0 & [\boldsymbol{L}(\boldsymbol{x})]^{-1} & \ldots & 0 \\ \vdots & \ddots & \vdots & \vdots & \ddots & \vdots \\ 0 & \ldots & 0 & 0 & \ldots & [\boldsymbol{L}(\boldsymbol{x})]^{-1} \end{pmatrix},$$

where $\boldsymbol{L}(\boldsymbol{x})$ occurs k times along the block-diagonal of this matrix, and its inverse occurs $m-k$ times. The appropriate definitions of the three orthogonal spaces $\widetilde{\mathcal{U}}$, $\widetilde{\mathcal{E}}$, and $\widetilde{\mathcal{J}}$ should be self-evident from the form of the fields $\widetilde{\boldsymbol{E}}$ and $\widetilde{\boldsymbol{J}}$ in (30.17). For example, $\widetilde{\mathcal{E}}$ consists of all fields $\widetilde{\boldsymbol{E}}(\boldsymbol{x})$ of the form in (30.17), where $\boldsymbol{E}^{(i)} \in \mathcal{E}$ for $i = 1, 2, \ldots, k$ and $\boldsymbol{J}^{(i)} \in \mathcal{J}$ for $i = k+1, k+2, \ldots, m$.

The effective tensor $\boldsymbol{\mathcal{L}}_*$ associated with these equations is clearly

$$\boldsymbol{\mathcal{L}}_* = \begin{pmatrix} \boldsymbol{L}_* & \ldots & 0 & 0 & \ldots & 0 \\ \vdots & \ddots & \vdots & \vdots & \ddots & \vdots \\ 0 & \ldots & \boldsymbol{L}_* & 0 & \ldots & 0 \\ 0 & \ldots & 0 & \boldsymbol{L}_*^{-1} & \ldots & 0 \\ \vdots & \ddots & \vdots & \vdots & \ddots & \vdots \\ 0 & \ldots & 0 & 0 & \ldots & \boldsymbol{L}_*^{-1} \end{pmatrix},$$

and the corresponding "energy" is

$$\begin{aligned} \widetilde{\boldsymbol{E}}_0 \cdot \boldsymbol{\mathcal{L}}_* \widetilde{\boldsymbol{E}}_0 &= \sum_{i=1}^{k} \boldsymbol{h}_i \cdot \boldsymbol{L}_* \boldsymbol{h}_i + \sum_{i=k+1}^{m} \boldsymbol{h}_i \cdot \boldsymbol{L}_*^{-1} \boldsymbol{h}_i \\ &= W(\boldsymbol{h}_1, \boldsymbol{h}_2, \ldots, \boldsymbol{h}_k; \boldsymbol{h}_{k+1}, \boldsymbol{h}_{k+2}, \ldots, \boldsymbol{h}_m; \boldsymbol{L}_*). \end{aligned}$$

Notice that the task of finding $W_-(\boldsymbol{h}_1, \boldsymbol{h}_2, \ldots, \boldsymbol{h}_k; \boldsymbol{h}_{k+1}, \boldsymbol{h}_{k+2}, \ldots, \boldsymbol{h}_m)$ is equivalent to finding the best possible lower bound on the single "energy" $\widetilde{\boldsymbol{E}}_0 \cdot \boldsymbol{\mathcal{L}}_* \widetilde{\boldsymbol{E}}_0$. So the problem of finding bounds on the G-closure is reduced to a family of single energy minimization problems.

30.5. Extremal families of composites for elasticity: Proving that any positive-definite tensor can be realized as the effective elasticity tensor of a composite†

Knowledge of the G-closure GU gives one a precise characterization of what effective tensors can be produced by mixing phases having tensors in the set U. In practice there is a lot of freedom in the choice of the set U, because the moduli of actual materials have an immense range in their magnitudes. Thus it is of interest to study the limit in which the materials in U have widely different properties. For example, given an isotropic positive-definite elasticity tensor $\mathcal{C}_0$, we might consider the associated set

$$U_{\delta\psi} = \{\delta\mathcal{C}_0, \psi\mathcal{C}_0\}$$

containing two elasticity tensors, parametrized by $\psi > \delta > 0$. When δ is very small and ψ is very large these two tensors have widely differing moduli. One important question is whether the union of the associated G-closures,

$$G^+ = \bigcup_{\psi \geq \delta > 0} GU_{\delta\psi},$$

equals the set of all positive-definite fourth-order tensors $\boldsymbol{A}$ satisfying the usual symmetries of elasticity tensors (i.e. $A_{ijk\ell} = A_{jik\ell} = A_{k\ell ij}$). More precisely, given an arbitrary positive-definite tensor $\boldsymbol{A} > 0$ satisfying the usual symmetries of elasticity tensors can one find parameters $\psi \geq \delta > 0$ such that $\boldsymbol{A} \in GU_{\delta\psi}$? Sigmund (1994) provided some numerical evidence indicating that it might always be possible to construct a composite with effective elasticity tensor matching any prescribed positive-definite tensor $\boldsymbol{A}$. Independently, Milton and Cherkaev (1995) established that such a composite can always be constructed, in two and three dimensions. Thus any given tensor that is positive-definite can be realized as the effective elasticity tensor of a mixture of a sufficiently stiff material and a sufficiently compliant material.

We remark that for tensors $\boldsymbol{A}$ that are isotropic the question reduces to the following. Can one make an elastically isotropic composite with effective bulk modulus κ_* and shear modulus μ_* matching any given pair of positive numbers? In particular, can one construct materials where the ratio μ_*/κ_* is very large? Such materials have effective Poisson's ratios

$$\nu_* = [d - 2\mu_*/\kappa_*]/[2\mu_*/\kappa_* + d(d-1)],$$

which are very close to -1. Essentially all materials found in nature have positive Poisson's ratios, and the question of whether materials with negative Poisson's ratio could exist was the subject of debate for a long time.

Experimentally the question was settled when Lakes (1987) and Friis, Lakes, and Park (1988) manufactured polymeric and metallic foams with negative Poisson's ratios. Evidence for negative Poisson's ratios was also found in cracked granites by Homand-Etienne and Houpert (1989). On the theoretical side, Almgren (1985) designed an elastically isotropic structure with rods, hinges, and sliding collars having a Poisson's ratio of -1. Bathurst and Rothenburg (1988) showed that bonded disk assemblages would have a negative Poisson's ratio if the tangential stiffness at the disk contacts exceeds the normal stiffness, but did not show how such contacts could be created. A variety of mechanisms leading to a negative Poisson's ratio were proposed by Lakes (1991). The rigorous analysis of several elastically isotropic microstructures proved conclusively that continuum elastic composite materials can

have a Poisson's ratio arbitrarily close to -1 (Milton 1992; Berlyand and Promislow 1995). One of these microstructures was a multiple-rank laminate and its Poisson's ratio was almost as low as theoretically possible. For a given ratio between the stiffnesses of the constituent phases the Poisson's ratio was close to the theoretical limit implied by the bounds of Cherkaev and Gibiansky (1993); see figure 30.2. A related structure, shown in figure 1.1 on page 3, was found numerically by Sigmund (1995) and subsequently manufactured (Larsen, Sigmund, and Bouwstra 1997).

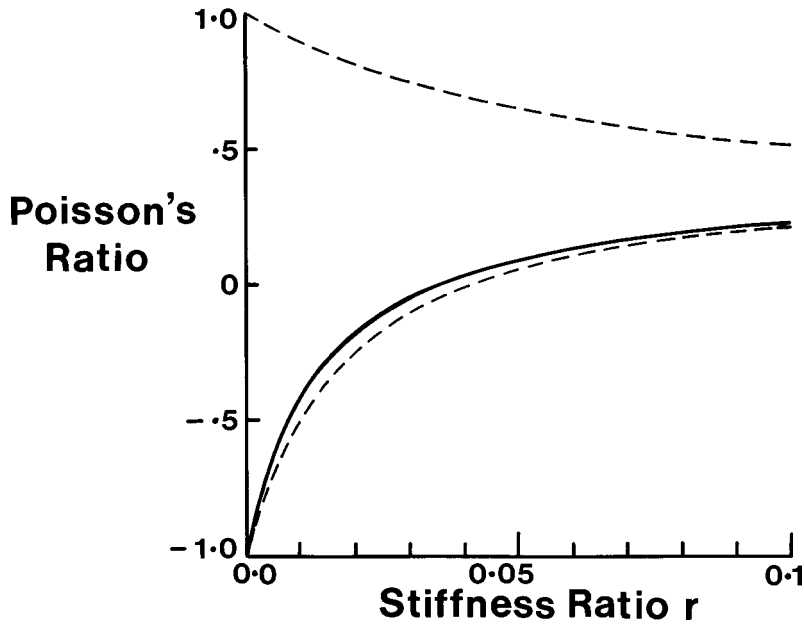

Figure 30.2. The solid line represents the lowest Poisson's ratio obtained within the family of elastically isotropic, multiple-rank laminates generated from materials of the herringbone laminate type illustrated in figure 30.7. (To obtain elastic isotropy the herringbone laminate is layered in equal portions with a reflection of itself about a suitable axis.) The phases have moduli $\kappa_1 = 2/r$, $\mu_1 = 1/r$, $\kappa_2 = 2$, and $\mu_2 = 1$. The broken lines are bounds on the Poisson's ratio, valid for any isotopic microstructure, that follow from the constraints of Cherkaev and Gibiansky (1993) on possible (κ_*, μ_*) pairs. Reprinted with permission from Milton (1992). Copyright 1992, Elsevier Science.

Elastically anisotropic materials with a negative Poisson's ratio were also investigated. Herakovich (1984) showed that graphite-epoxy laminates could have a Poisson's ratio through the thickness as low as -0.21. Kolpakov (1985), Gibson and Ashby (1988), Warren (1990), and Berlyand and Promislow (1995) analyzed, in varying degrees of rigor, inverted honeycomb foams that (because of their anisotropy) can have a Poisson's ratio less than -1. Caddock and Evans (1989) and Alderson and Evans (1992) manufactured anisotropic microporous polymers comprised of microscopic particles connected by fibrils having Poisson's ratios as low as -1.24.

We now address the larger question: What are the possible elasticity tensors of anisotropic composites? We focus on two-dimensional composites and present a rigorous proof, based on the arguments of Milton and Cherkaev (1995), that G^+ includes all positive-definite

tensors satisfying the usual symmetries of elasticity tensors. We first introduce the concept of extremal families of composites. Suppose that we are given k, with $m \geq k \geq 0$, where $m = d(d-1)/2$ is the dimension of the space of symmetric $d \times d$ matrices, and suppose that we have a family of composites, such that for every positive value of a parameter λ and every k-dimensional subspace $\mathcal{V}_k$ of symmetric matrices there is an associated composite in the family with effective tensor $\boldsymbol{\mathcal{C}}_*(\lambda, \mathcal{V}_k)$. This family is defined to be extremal if, given $c > 0$, one can find a $\lambda_k > 0$ such that for every k-dimensional subspace $\mathcal{V}_k$ of symmetric matrices

$$W(\mathcal{V}_k; \boldsymbol{\mathcal{C}}_*(\lambda, \mathcal{V}_k)) < c \quad \text{for all } \lambda > \lambda_k, \tag{30.18}$$

where for any tensor $\boldsymbol{\mathcal{C}}$,

$$W(\mathcal{V}_k; \boldsymbol{\mathcal{C}}) = \operatorname{Tr}(\boldsymbol{\Pi}_k \boldsymbol{\mathcal{C}}) + \operatorname{Tr}(\boldsymbol{\Pi}_k^{\perp} \boldsymbol{\mathcal{C}}^{-1}), \tag{30.19}$$

in which $\boldsymbol{\Pi}_k$ is the fourth-order tensor that projects onto $\mathcal{V}_k$ and $\boldsymbol{\Pi}_k^{\perp} = \boldsymbol{\mathcal{I}} - \boldsymbol{\Pi}_k$ is the fourth-order tensor that projects onto $\mathcal{V}_k^{\perp}$, the $(m-k)$-dimensional orthogonal subspace.

In particular it follows that for any fixed subspace $\mathcal{V}_k$, $W(\mathcal{V}_k; \boldsymbol{\mathcal{C}}_*(\lambda, \mathcal{V}_k))$ must approach zero as λ tends to infinity. To get some idea of what this means consider, for example, the sequence of tensors

$$\boldsymbol{\mathcal{C}}_\lambda = (1/\lambda)\boldsymbol{\Pi}_k + \lambda \boldsymbol{\Pi}_k^{\perp}.$$

For this sequence

$$W(\mathcal{V}_k; \boldsymbol{\mathcal{C}}_\lambda) = (1/\lambda)\operatorname{Tr}(\boldsymbol{\Pi}_k) + (1/\lambda)\operatorname{Tr}(\boldsymbol{\Pi}_k^{\perp}) = k/\lambda + (m-k)/\lambda = m/\lambda$$

tends to zero as λ tends to infinity. For large λ, a material with elasticity tensor $\boldsymbol{\mathcal{C}}_\lambda$ behaves like a very compliant material when it is subject to strains lying in the subspace $\mathcal{V}_k$ but behaves like a very stiff material when it is subject to stresses lying in the subspace $\mathcal{V}_k^{\perp}$.

When $k = 0$, the materials in the extremal family are called nullmode, because for large λ they have no easy modes of deformation. When $k = 1$, the materials in the extremal family are called unimode, because for large λ they have only one easy mode of deformation: They are only easily compliant to strains in the one-dimensional subspace $\mathcal{V}_1$. When $k = 2$, the materials in the extremal family are called bimode, because for large λ they have only two easy modes of deformation: They are compliant to strains in the subspace $\mathcal{V}_2$. In two dimensions ($d = 2$), a simple laminate of the two phases is an example of a bimode material; see figure 30.3 on the facing page. Two other examples of two-dimensional bimode materials are illustrated in figures 30.4 on the next page and 30.5 on page 656. Similarly, for three-dimensional elasticity, the materials in the extremal family with $k = 3, 4, 5$, or 6 are called trimode, quadramode, pentamode, and hexamode, respectively. In three dimensions ($d = 3$) a simple laminate is an example of a trimode extremal material, while an array of stiff cylindrical parallel rods in a soft matrix is an example of a pentamode extremal material.

Given an orthonormal set of tensors $\boldsymbol{v}_1, \boldsymbol{v}_2, \ldots, \boldsymbol{v}_k$ that form a basis for $\mathcal{V}_k$ and given an orthonormal set of tensors $\boldsymbol{v}_{k+1}, \boldsymbol{v}_{k+2}, \ldots, \boldsymbol{v}_m$ that form a basis for $\mathcal{V}_k^{\perp}$ we have

$$\boldsymbol{\Pi}_k = \sum_{i=1}^{k} \boldsymbol{v}_i \otimes \boldsymbol{v}_i, \quad \boldsymbol{\Pi}_k^{\perp} = \sum_{i=k+1}^{m} \boldsymbol{v}_i \otimes \boldsymbol{v}_i.$$

By substituting these back into (30.19) we see that $W(\mathcal{V}_k; \boldsymbol{\mathcal{C}})$ can be equated with a sum of energies and complementary energies:

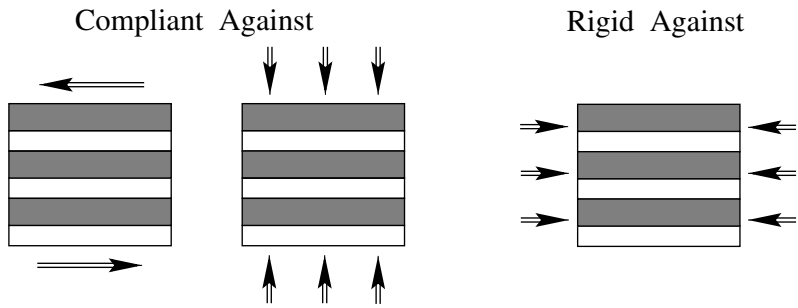

Figure 30.3. A simple laminate of a stiff phase and a compliant phase is an example of a two-dimensional bimode extremal material. The laminate is compliant against two types of loading and stiff against one. It supports a stress with zero determinant. After Milton and Cherkaev (1995).

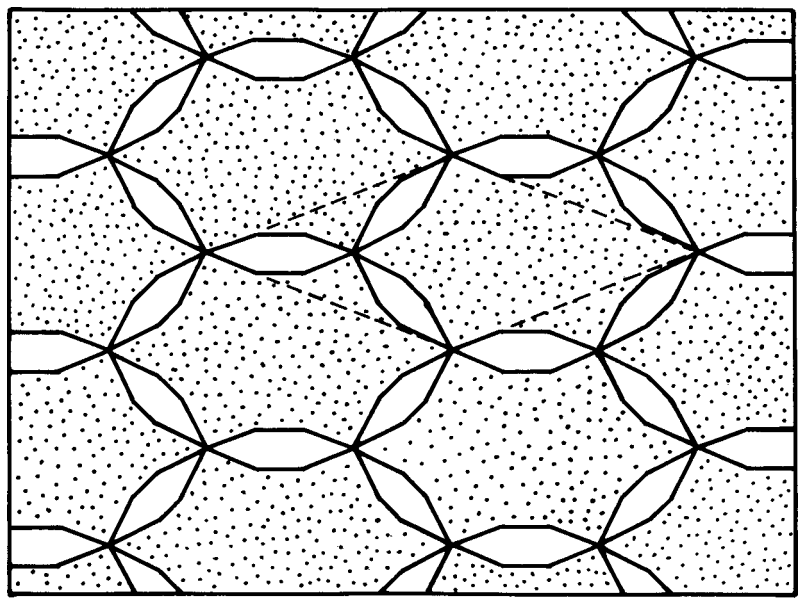

Figure 30.4. The honeycomb array of linkages. It is a two-dimensional bimode material that supports a (compressive) stress with positive determinant. When the dotted material is very compliant the material will remain stiff under an appropriate combination of horizontal and vertical stretching. The unit cell of periodicity is marked by the dashed lines. Reprinted with permission from Milton and Cherkaev (1995). Copyright 1995, ASME.

$$\begin{aligned} W(\mathcal{V}_k; \mathbf{C}) &= \sum_{i=1}^{k} \boldsymbol{v}_i \cdot \mathbf{C}\boldsymbol{v}_i + \sum_{i=k+1}^{m} \boldsymbol{v}_i \cdot \mathbf{C}^{-1}\boldsymbol{v}_i \\ &= W(\boldsymbol{v}_1, \boldsymbol{v}_2, \ldots, \boldsymbol{v}_k; \boldsymbol{v}_{k+1}, \boldsymbol{v}_{k+2}, \ldots, \boldsymbol{v}_m; \mathbf{C}). \end{aligned}$$

If we take any set of orthogonal symmetric matrices $\boldsymbol{h}_i$, such that $\boldsymbol{h}_i$ is proportional to the

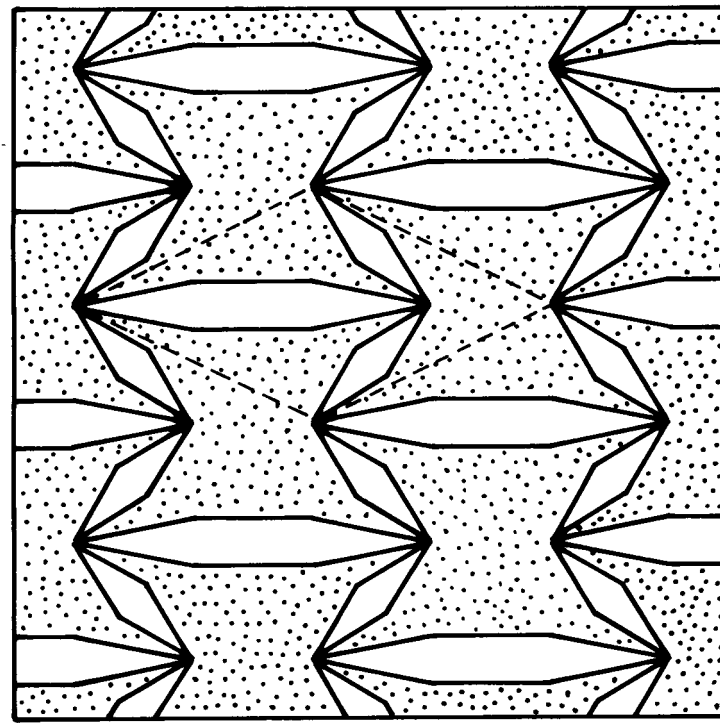

Figure 30.5. The inverted honeycomb array of linkages. It is a two-dimensional bimode material that supports a (shear) stress with negative determinant. When the dotted material is very compliant the material will remain stiff under an appropriate combination of horizontal stretching and vertical compression. Reprinted with permission from Milton and Cherkaev (1995). Copyright 1995, ASME. See also Almgren (1985).

matrix $\boldsymbol{v}_i$ for each i, and such that the normalization condition (30.16) is satisfied, then since the normalization condition implies that $|\boldsymbol{h}_i| \leq 1 = |\boldsymbol{v}_i|$ for all i, it follows that

$$\boldsymbol{h}_i \cdot \boldsymbol{\mathcal{C}}\boldsymbol{h}_i \leq \boldsymbol{v}_i \cdot \boldsymbol{\mathcal{C}}\boldsymbol{v}_i \text{ and } \boldsymbol{h}_i \cdot \boldsymbol{\mathcal{C}}^{-1}\boldsymbol{h}_i \leq \boldsymbol{v}_i \cdot \boldsymbol{\mathcal{C}}^{-1}\boldsymbol{v}_i,$$

for all i and for all positive-definite matrices $\boldsymbol{\mathcal{C}}$. Therefore we have the inequality

$$0 \leq W(\boldsymbol{h}_1, \boldsymbol{h}_2, \ldots, \boldsymbol{h}_k; \boldsymbol{h}_{k+1}, \boldsymbol{h}_{k+2}, \ldots, \boldsymbol{h}_m; \boldsymbol{\mathcal{C}}) \leq W(\boldsymbol{v}_1, \boldsymbol{v}_2, \ldots, \boldsymbol{v}_k; \boldsymbol{v}_{k+1}, \boldsymbol{v}_{k+2}, \ldots, \boldsymbol{v}_m; \boldsymbol{\mathcal{C}}), \tag{30.20}$$

which in particular implies that $W(\boldsymbol{h}_1, \boldsymbol{h}_2, \ldots, \boldsymbol{h}_k; \boldsymbol{h}_{k+1}, \boldsymbol{h}_{k+2}, \ldots, \boldsymbol{h}_m; \boldsymbol{\mathcal{C}}_*(\lambda, \mathcal{V}_k))$ must also approach zero as λ tends to infinity.

Our aim is to look for extremal families of two-phase composites with microgeometries dependent on $\mathcal{V}_k$, and possibly on λ, built from materials with tensors $\psi(\lambda)\boldsymbol{\mathcal{C}}_0$ and $\delta(\lambda)\boldsymbol{\mathcal{C}}_0$, where $\psi(\lambda) \geq \delta(\lambda) > 0$ are appropriately chosen functions of $\lambda > 0$, independent of k and $\mathcal{V}_k$. If we can find such extremal families of composites for all k with $m \geq k \geq 0$, then any positive-definite tensor can be obtained as the effective tensor of a multiple-rank laminate built from materials in these extremal families, and hence G^+ must include all positive-definite tensors.

To see this, suppose that we are given a positive-definite tensor $\mathcal{A}$. Define

$$c = \min_{\boldsymbol{h}_i} W(\boldsymbol{h}_1, \boldsymbol{h}_2, \ldots, \boldsymbol{h}_k; \boldsymbol{h}_{k+1}, \boldsymbol{h}_{k+2}, \ldots, \boldsymbol{h}_m; \mathcal{A}), \tag{30.21}$$

in which the minimum is to be taken over all orthogonal sets of symmetric matrices $\boldsymbol{h}_i$ satisfying the normalization condition (30.16). The value of c is positive (and nonzero) because $\mathcal{A}$ is positive-definite. Choose a fixed value of λ so that the inequality

$$W(\boldsymbol{v}_1, \boldsymbol{v}_2, \ldots, \boldsymbol{v}_k; \boldsymbol{v}_{k+1}, \boldsymbol{v}_{k+2}, \ldots, \boldsymbol{v}_m; \mathcal{C}_*(\lambda, \mathcal{V}_k)) < c \tag{30.22}$$

is satisfied for all k and all sets of orthogonal symmetric $d \times d$ matrices $\boldsymbol{v}_1, \boldsymbol{v}_2, \ldots, \boldsymbol{v}_m$, where $\mathcal{V}_k$ is the subspace spanned by $\boldsymbol{v}_1, \boldsymbol{v}_2, \ldots, \boldsymbol{v}_k$. This is always possible because

$$W(\boldsymbol{v}_1, \boldsymbol{v}_2, \ldots, \boldsymbol{v}_k; \boldsymbol{v}_{k+1}, \boldsymbol{v}_{k+2}, \ldots, \boldsymbol{v}_m; \mathcal{C}_*(\lambda, \mathcal{V}_k)) = W(\mathcal{V}_k; \mathcal{C}_*(\lambda, \mathcal{V}_k)),$$

and from (30.18) we see that the right-hand side is surely less than c when $\lambda > \lambda_k$. Thus it suffices to take

$$\lambda > \max_k \lambda_k,$$

as k ranges from 0 to m.

From (30.20) and (30.22), and because $GU_{\delta(\lambda),\psi(\lambda)}$ contains the effective tensor $\mathcal{C}_*(\lambda, \mathcal{V}_k)$ for all $\mathcal{V}_k$, we have

$$\begin{aligned} &W_-(\boldsymbol{h}_1, \boldsymbol{h}_2, \ldots, \boldsymbol{h}_k; \boldsymbol{h}_{k+1}, \boldsymbol{h}_{k+2}, \ldots, \boldsymbol{h}_m) \\ &\qquad = \min_{\mathcal{C}_* \in GU_{\delta(\lambda),\psi(\lambda)}} W(\boldsymbol{h}_1, \boldsymbol{h}_2, \ldots, \boldsymbol{h}_k; \boldsymbol{h}_{k+1}, \boldsymbol{h}_{k+2}, \ldots, \boldsymbol{h}_m; \mathcal{C}_*) < c, \end{aligned} \tag{30.23}$$

for all k and all orthogonal sets of symmetric matrices $\boldsymbol{h}_i$ satisfying the normalization condition (30.16). Consequently, if we define

$$\begin{aligned} &\mathcal{K}'(\boldsymbol{h}_1, \boldsymbol{h}_2, \ldots, \boldsymbol{h}_k; \boldsymbol{h}_{k+1}, \boldsymbol{h}_{k+2}, \ldots, \boldsymbol{h}_m) \\ &\qquad = \{\mathcal{C} \mid W(\boldsymbol{h}_1, \boldsymbol{h}_2, \ldots, \boldsymbol{h}_k; \boldsymbol{h}_{k+1}, \boldsymbol{h}_{k+2}, \ldots, \boldsymbol{h}_m; \mathcal{C}) \geq c\}, \end{aligned}$$

then (30.15) and (30.23) imply that

$$\mathcal{K}'(\boldsymbol{h}_1, \boldsymbol{h}_2, \ldots, \boldsymbol{h}_k; \boldsymbol{h}_{k+1}, \boldsymbol{h}_{k+2}, \ldots, \boldsymbol{h}_m) \subset \mathcal{K}(\boldsymbol{h}_1, \boldsymbol{h}_2, \ldots, \boldsymbol{h}_k; \boldsymbol{h}_{k+1}, \boldsymbol{h}_{k+2}, \ldots, \boldsymbol{h}_m).$$

It follows that the intersection of the regions $\mathcal{K}'$ as the $\boldsymbol{h}_i$ are varied subject to (30.13) and (30.16) must lie inside the intersection of the regions $\mathcal{K}$, that is, inside $GU_{\delta(\lambda),\psi(\lambda)}$. More precisely, any set closed under lamination that contains the tensors $\mathcal{C}_*(\lambda, \mathcal{V}_k)$ as k varies from 0 to m and as $\mathcal{V}_k$ varies over all k-dimensional subspaces of symmetric $d \times d$ matrices, must at least contain all tensors $\mathcal{C}$ such that the inequality

$$W(\boldsymbol{h}_1, \boldsymbol{h}_2, \ldots, \boldsymbol{h}_k; \boldsymbol{h}_{k+1}, \boldsymbol{h}_{k+2}, \ldots, \boldsymbol{h}_m; \mathcal{C}) \geq c$$

is satisfied for all orthogonal sets of $d \times d$ symmetric matrices $\boldsymbol{h}_i$ satisfying the normalization condition (30.16). In particular, from (30.21) we conclude that $GU_{\delta(\lambda),\psi(\lambda)}$ and hence G^+ contains the tensor $\mathcal{A}$.

It remains to construct the extremal families of composites. An outline of how to do this has been given for both two- and three-dimensional elasticity (Milton and Cherkaev 1995). First we will provide a complete proof for the two-dimensional case, taking

$$\psi(\lambda) = \lambda, \quad \delta(\lambda) = 1/\lambda.$$

The extremal family of nullmode materials is trivial: $\mathcal{V}_0$ is the empty and the family contains the single homogeneous material with elasticity tensor

$$\mathcal{C}_*(\lambda, \mathcal{V}_0) = \psi(\lambda)\mathcal{C}_0 = \lambda\mathcal{C}_0.$$

Similarly, the extremal family of trimode materials is trivial: $\mathcal{V}_3$ is the space of all 2×2 symmetric matrices and the family contains the single homogeneous material with elasticity tensor

$$\mathcal{C}_*(\lambda, \mathcal{V}_3) = \delta(\lambda)\mathcal{C}_0 = \mathcal{C}_0/\lambda.$$

In the next two sections we describe extremal families of unimode and bimode composites. We will see that it suffices to use third-rank laminates to achieve the extremal unimode materials and fourth-rank laminates to achieve the extremal bimode materials.

30.6. An extremal family of unimode materials for two-dimensional elasticity†

This section is a bit technical, but the underlying idea is simple: To show that a particular family of multiple-rank laminates is unimodal we consider each member in the family and construct one trial strain field, designed so that it is nonzero only within the compliant phase, and we construct two independent trial stress fields, designed so that they are nonzero only within the stiff phase. Then the classical variational principles provide an upper bound on the sum of two energies and one complementary energy, which goes to zero as $\lambda \to \infty$, thereby establishing that the family is unimode. Those readers not interested in the details can refer to figures 30.6 on the next page and 30.7 on page 661 and then skip to the next section.

Consider the following second-rank laminate. We take as core material the compliant phase, having tensor $\mathcal{C}_0/\lambda$, and layer it in direction $\boldsymbol{n}$ (where $|\boldsymbol{n}| = 1$) in equal proportions with the stiff phase, having tensor $\lambda\mathcal{C}_0$, and then we slice this laminate in a different direction $\boldsymbol{m} \neq \boldsymbol{n}$ (where $|\boldsymbol{m}| = 1$) and layer it again with an equal proportion of the stiff phase as illustrated in figure 30.6 on the next page. Thus the resulting oblique box laminate, which we will call material A, contains a volume fraction of the compliant phase of $1/4$. Let $\mathcal{C}_A$ denote its effective elasticity tensor. To show that this is a unimode material, we first evaluate the energy associated with a trial strain $\boldsymbol{\epsilon}_1^A(\boldsymbol{x})$, which is zero inside the stiff phase, and inside the compliant phase it takes the value

$$\boldsymbol{w}_1 = \frac{1}{\sqrt{n_1^2m_1^2 + n_2^2m_2^2 + (n_1m_2 + n_2m_1)^2/2}} \begin{pmatrix} n_1m_1 & (n_1m_2 + n_2m_1)/2 \\ (n_1m_2 + n_2m_1)/2 & n_2m_2 \end{pmatrix},$$

which has been chosen so that $|\boldsymbol{w}_1| = 1$ and $\boldsymbol{n}_\perp \cdot \boldsymbol{w}_1\boldsymbol{n}_\perp = \boldsymbol{m}_\perp \cdot \boldsymbol{w}_1\boldsymbol{m}_\perp = 0$, in which $\boldsymbol{n}_\perp$ and $\boldsymbol{m}_\perp$ are unit vectors perpendicular to $\boldsymbol{n}$ and $\boldsymbol{m}$. This latter constraint ensures strain compatibility in the limit where the two laminations are on widely different length scales.

Strictly speaking we should modify the trial strain in a boundary layer to ensure that the trial strain is the symmetrized gradient of a displacement field. However, for any fixed value of $\lambda > 0$ the resulting change in the energy associated with the trial field will be negligible

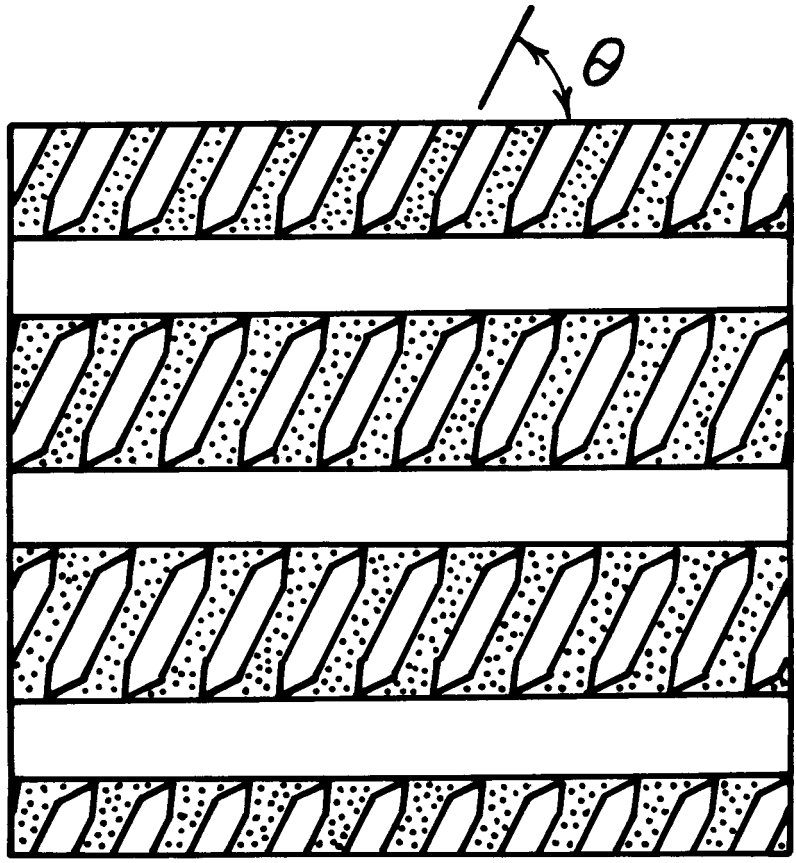

Figure 30.6. A unimode material that is an approximation to the second-rank oblique box laminate discussed in the text. It is compliant under a shearing strain $\boldsymbol{w}_1$ with negative determinant, which can be adjusted so that $|\boldsymbol{w}_1| = 1$. As θ and the orientation of the composite are varied, $\boldsymbol{w}_1$ ranges over all matrices with negative determinant and unit norm. Reprinted with permission from Milton and Cherkaev (1995). Copyright 1995, ASME.

when the two laminations are on sufficiently widely different length scales. The separation between the length scales of successive laminations generally needs to be increased when λ is increased to ensure that the contribution from the boundary layer remains negligible. What is important is that the locally averaged value of the trial strain on one side of an interface must be compatible with the locally averaged value of the trial strain on the other side of the interface.

Since $\boldsymbol{w}_1/4$ is the average of this trial strain, the classical energy minimization principle gives the bound

$$\boldsymbol{w}_1 \cdot \boldsymbol{\mathcal{C}}_A \boldsymbol{w}_1 \leq 4\boldsymbol{w}_1 \cdot \boldsymbol{\mathcal{C}}_0 \boldsymbol{w}_1/\lambda.$$

This inequality means that when λ is large the structure is compliant to strains proportional to $\boldsymbol{w}_1$.

Next we evaluate the complementary energy associated with two trial stress fields $\boldsymbol{\tau}_2^A(\boldsymbol{x})$ and $\boldsymbol{\tau}_3^A(\boldsymbol{x})$. The trial stress $\boldsymbol{\tau}_2^A(\boldsymbol{x})$ is taken to be zero except in the layers of the stiff phase in

direction $\boldsymbol{m}$, where we set it to have the value

$$\boldsymbol{w}_2 = \boldsymbol{m}_\perp \otimes \boldsymbol{m}_\perp,$$

which has been chosen so that $|\boldsymbol{w}_2| = 1$, $\boldsymbol{w}_1 \cdot \boldsymbol{w}_2 = 0$, and $\boldsymbol{w}_2\boldsymbol{m} = 0$. The latter constraint ensures stress compatibility. Since $\boldsymbol{w}_2/2$ is the average of this trial stress, the complementary energy minimization principle gives the bound

$$\boldsymbol{w}_2 \cdot \boldsymbol{\mathcal{C}}_A^{-1}\boldsymbol{w}_2 \le 2\boldsymbol{w}_2 \cdot \boldsymbol{\mathcal{C}}_0^{-1}\boldsymbol{w}_2/\lambda.$$

This inequality means that when λ is large the structure is stiff to stresses proportional to $\boldsymbol{w}_2$.

The trial stress $\boldsymbol{\tau}_3^A(\boldsymbol{x})$ is taken to be zero inside the compliant phase and to have the values

$$\boldsymbol{\tau}_n(\alpha) = \alpha\boldsymbol{n}_\perp \otimes \boldsymbol{n}_\perp, \quad \boldsymbol{\tau}_m(\alpha, \beta) = \alpha\boldsymbol{n}_\perp \otimes \boldsymbol{n}_\perp/2 + \beta\boldsymbol{m}_\perp \otimes \boldsymbol{m}_\perp$$

inside the layers of the stiff phase that are layered in directions $\boldsymbol{n}$ and $\boldsymbol{m}$, respectively. These values have been chosen so that $\boldsymbol{\tau}_n\boldsymbol{n} = 0$ and $\boldsymbol{\tau}_m\boldsymbol{m} = \boldsymbol{\tau}_n\boldsymbol{m}/2$ to ensure stress compatibility in the limit where the two laminations are on widely different length scales. (The average of the trial stress in the region occupied by the first laminate is $\boldsymbol{\tau}_n/2$.) The parameter values

$$\alpha = \frac{2}{\sqrt{1-(\boldsymbol{n}\cdot\boldsymbol{m})^4}}, \quad \beta = \frac{-2(\boldsymbol{n}\cdot\boldsymbol{m})^2}{\sqrt{1-(\boldsymbol{n}\cdot\boldsymbol{m})^4}}$$

are chosen so that the average of the trial stress

$$\boldsymbol{w}_3 = \boldsymbol{\tau}_n(\alpha)/4 + \boldsymbol{\tau}_m(\alpha, \beta)/2 = \alpha\boldsymbol{n}_\perp \otimes \boldsymbol{n}_\perp/2 + \beta\boldsymbol{m}_\perp \otimes \boldsymbol{m}_\perp/2$$

is orthogonal to $\boldsymbol{w}_1$ and $\boldsymbol{w}_2$ and has unit norm $|\boldsymbol{w}_3| = 1$. The complementary energy minimization principle gives the bound

$$\boldsymbol{w}_3 \cdot \boldsymbol{\mathcal{C}}_A^{-1}\boldsymbol{w}_3 \le [\boldsymbol{\tau}_n(\alpha) \cdot \boldsymbol{\mathcal{C}}_0^{-1}\boldsymbol{\tau}_n(\alpha) + 2\boldsymbol{\tau}_m(\alpha, \beta) \cdot \boldsymbol{\mathcal{C}}_0^{-1}\boldsymbol{\tau}_m(\alpha, \beta)]/4\lambda.$$

This inequality means that when λ is large the structure is stiff to stresses proportional to $\boldsymbol{w}_3$.

Letting $\mathcal{W}_1$ denote the one-dimensional subspace of symmetric matrices spanned by $\boldsymbol{w}_1$ we have

$$W(\mathcal{W}_1; \boldsymbol{\mathcal{C}}_A) = \boldsymbol{w}_1 \cdot \boldsymbol{\mathcal{C}}_A\boldsymbol{w}_1 + \boldsymbol{w}_2 \cdot \boldsymbol{\mathcal{C}}_A^{-1}\boldsymbol{w}_2 + \boldsymbol{w}_3 \cdot \boldsymbol{\mathcal{C}}_A^{-1}\boldsymbol{w}_3,$$

and for any fixed unit vectors $\boldsymbol{m} \ne \boldsymbol{n}$ our bounds imply that this energy sum approaches zero as $\lambda \to \infty$. Therefore the material is unimode. However, this class of materials is insufficient to form an extremal family. Since the determinant of the matrix $\boldsymbol{w}_1$ is always negative, we cannot adjust $\boldsymbol{m}$ and $\boldsymbol{n}$ so that $\mathcal{W}_1$ matches an arbitrary prescribed one-dimensional subspace. In particular, since $\mathcal{W}_1$ never contains the identity tensor, we cannot generate negative Poisson's ratio materials that are easily compliant to compressive strains but resistant to shear strains.

To obtain the desired extremal family of unimode materials we reflect the microstructure of material A about the x_2-axis to obtain a material A' and then we layer (on a much larger length scale) equal proportions of the materials A and A' in the direction of the x_1-axis, as illustrated in figure 30.7 on the facing page. Let us call the resulting herringbone laminate material B, and let $\boldsymbol{\mathcal{C}}_B$ denote its effective elasticity tensor. We take a trial strain $\boldsymbol{\epsilon}_1^B(\boldsymbol{x})$ that equals $\boldsymbol{\epsilon}_1^A(\boldsymbol{x})$ inside material A, and which is the reflection of $\boldsymbol{\epsilon}_1^A(\boldsymbol{x})$ inside material A'. (To reflect a two-dimensional stress or strain field about any line parallel to the x_2-axis one just

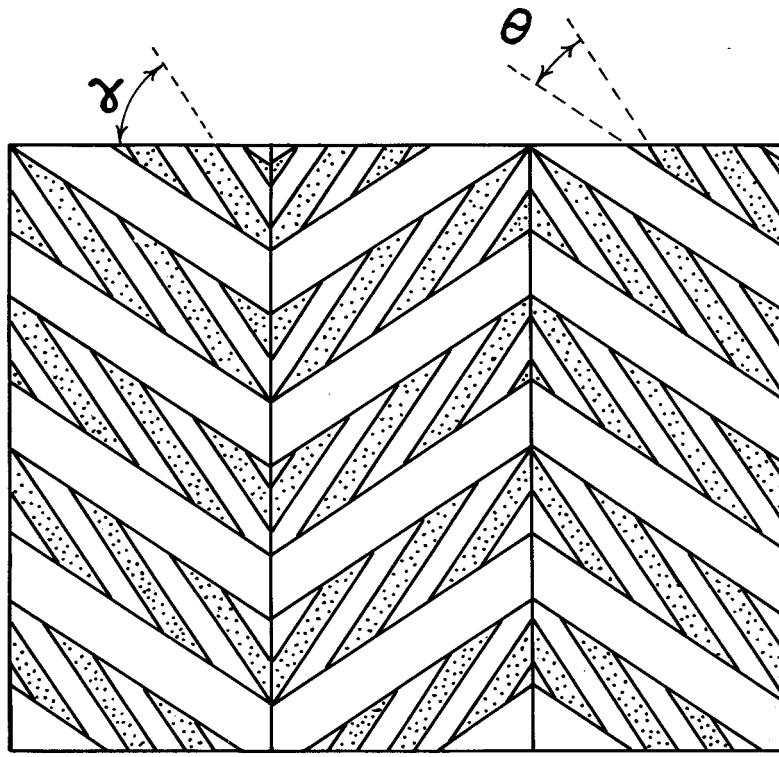

Figure 30.7. A unimode material that is an approximation to the third-rank herringbone laminate discussed in the text. It is compliant under a strain $\boldsymbol{v}_1$, which can be adjusted so that $|\boldsymbol{v}_1| = 1$. As γ, θ, and the orientation of the composite are varied $\boldsymbol{v}_1$ ranges over all matrices, with unit norm. This structure was also used as a building block for constructing an elastically isotropic composite with negative Poisson's ratio. Reprinted with permission from Milton (1992). Copyright 1992, Elsevier Science.

changes the sign of the off-diagonal elements of the stress or strain at the reflected point.) This ensures strain compatibility across the boundary between material A and A' in the limit where the three laminations are on widely different length scales. Thus the trial strain inside material A' is nonzero only inside the stiff phase, where it takes the value

$$\boldsymbol{w}_1' = \frac{1}{\sqrt{n_1^2m_1^2 + n_2^2m_2^2 + (n_1m_2 + n_2m_1)^2/2}} \begin{pmatrix} n_1m_1 & -(n_1m_2 + n_2m_1)/2 \\ -(n_1m_2 + n_2m_1)/2 & n_2m_2 \end{pmatrix}.$$

The average of the trial strain within material B is therefore

$$(\boldsymbol{w}_1 + \boldsymbol{w}_1')/8 = \frac{\boldsymbol{v}_1\sqrt{n_1^2m_1^2 + n_2^2m_2^2}}{4\sqrt{n_1^2m_1^2 + n_2^2m_2^2 + (n_1m_2 + n_2m_1)^2/2}},$$

where

$$\boldsymbol{v}_1 = \frac{1}{\sqrt{n_1^2 m_1^2 + n_2^2 m_2^2}} \begin{pmatrix} n_1 m_1 & 0 \\ 0 & n_2 m_2 \end{pmatrix} \tag{30.24}$$

has been defined so that $|\boldsymbol{v}_1| = 1$. Since $\boldsymbol{\mathcal{C}}_0$ is an isotropic elasticity tensor, it follows that $\boldsymbol{w}_1' \cdot \boldsymbol{\mathcal{C}}_0 \boldsymbol{w}_1' = \boldsymbol{w}_1 \cdot \boldsymbol{\mathcal{C}}_0 \boldsymbol{w}_1$. Hence the classical energy minimization principle gives the bound

$$\boldsymbol{v}_1 \cdot \boldsymbol{\mathcal{C}}_B \boldsymbol{v}_1 \leq \frac{4[n_1^2 m_1^2 + n_2^2 m_2^2 + (n_1 m_2 + n_2 m_1)^2/2] \boldsymbol{w}_1 \cdot \boldsymbol{\mathcal{C}}_0 \boldsymbol{w}_1}{(n_1^2 m_1^2 + n_2^2 m_2^2)\lambda}. \tag{30.25}$$

The trial stress field $\boldsymbol{\tau}_2^B(\boldsymbol{x})$ inside material A' is taken to be a reflection of the trial stress $\boldsymbol{\tau}_2^B(\boldsymbol{x})$ inside material A, where it is chosen to have the same form as the trial stress field $\boldsymbol{\tau}_3^A(\boldsymbol{x})$ with the coefficients α and β replaced by

$$\alpha_2 = \frac{2m_1 m_2}{(n_1 m_2 - n_2 m_1)\sqrt{n_1^2 m_1^2 + n_2^2 m_2^2}}, \quad \beta_2 = \frac{-2n_1 n_2}{(n_1 m_2 - n_2 m_1)\sqrt{n_1^2 m_1^2 + n_2^2 m_2^2}}$$

to ensure stress compatibility across the boundary between materials A and A' (which requires that $\alpha_2 n_1 n_2 + \beta_2 m_1 m_2 = 0$) and to ensure that the average stress

$$\boldsymbol{v}_2 = \frac{1}{2} \begin{pmatrix} \alpha_2 n_2^2 + \beta_2 m_2^2 & 0 \\ 0 & \alpha_2 n_1^2 + \beta_2 m_1^2 \end{pmatrix} = \frac{1}{\sqrt{n_1^2 m_1^2 + n_2^2 m_2^2}} \begin{pmatrix} -n_2 m_2 & 0 \\ 0 & n_1 m_1 \end{pmatrix} \tag{30.26}$$

has unit norm, $|\boldsymbol{v}_2| = 1$. The complementary energy minimization principle then gives the bound

$$\boldsymbol{v}_2 \cdot \boldsymbol{\mathcal{C}}_B^{-1} \boldsymbol{v}_2 \leq [\boldsymbol{\tau}_n(\alpha_2) \cdot \boldsymbol{\mathcal{C}}_0^{-1} \boldsymbol{\tau}_n(\alpha_2) + 2\boldsymbol{\tau}_m(\alpha_2, \beta_2) \cdot \boldsymbol{\mathcal{C}}_0^{-1} \boldsymbol{\tau}_m(\alpha_2, \beta_2)]/4\lambda. \tag{30.27}$$

The trial stress field $\boldsymbol{\tau}_3^B(\boldsymbol{x})$ inside material A' is taken to be minus the reflection of the trial stress $\boldsymbol{\tau}_3^B(\boldsymbol{x})$ inside material A, where it is chosen to have the same form as the trial stress field $\boldsymbol{\tau}_3^A(\boldsymbol{x})$ but now with the coefficients α and β replaced by

$$\alpha_3 = \frac{\sqrt{2} m_2}{n_2(n_1 m_2 - n_2 m_1)}, \quad \beta_3 = \frac{-\sqrt{2} n_2}{m_2(n_1 m_2 - n_2 m_1)},$$

to ensure stress compatibility across the boundary between materials A and A' (which requires that $\alpha_3 n_2^2 + \beta_3 m_2^2 = 0$) and to ensure that the average stress

$$\boldsymbol{v}_3 = \frac{1}{2} \begin{pmatrix} 0 & -(\alpha_3 n_1 n_2 + \beta_3 m_1 m_2) \\ -(\alpha_3 n_1 n_2 + \beta_3 m_1 m_2) & 0 \end{pmatrix}$$

has unit norm, $|\boldsymbol{v}_3| = 1$. The complementary energy minimization principle then gives the bound

$$\boldsymbol{v}_3 \cdot \boldsymbol{\mathcal{C}}_B^{-1} \boldsymbol{v}_3 \leq [\boldsymbol{\tau}_n(\alpha_3) \cdot \boldsymbol{\mathcal{C}}_0^{-1} \boldsymbol{\tau}_n(\alpha_3) + 2\boldsymbol{\tau}_m(\alpha_3, \beta_3) \cdot \boldsymbol{\mathcal{C}}_0^{-1} \boldsymbol{\tau}_m(\alpha_3, \beta_3)]/4\lambda.$$

Notice that $\boldsymbol{v}_1$, $\boldsymbol{v}_2$, and $\boldsymbol{v}_3$ are a set of orthonormal matrices. Let $\mathcal{V}_1$ be the one-dimensional subspace of symmetric matrices spanned by $\boldsymbol{v}_1$. We have established that, for any given $\lambda > 0$, the energy sum

$$W(\mathcal{V}_1; \boldsymbol{\mathcal{C}}_B) = \boldsymbol{v}_1 \cdot \boldsymbol{\mathcal{C}}_B \boldsymbol{v}_1 + \boldsymbol{v}_2 \cdot \boldsymbol{\mathcal{C}}_B^{-1} \boldsymbol{v}_2 + \boldsymbol{v}_3 \cdot \boldsymbol{\mathcal{C}}_B^{-1} \boldsymbol{v}_3$$

is guaranteed to be finite provided that $\boldsymbol{n}$ and $\boldsymbol{m}$ are chosen with

$$n_2 \neq 0, \quad m_2 \neq 0, \quad n_1/n_2 \neq m_1/m_2, \quad n_1 \text{ and } m_1 \text{ are not both zero.}$$

It is convenient to set

$$n_1 = \sin\phi, \quad n_2 = \cos\phi, \quad m_1 = \sqrt{3}/2, \quad m_2 = 1/2. \tag{30.28}$$

Then, as ϕ is varied from $-\pi/6$ to $\pi/6$, the energy sum $W(\mathcal{V}_1; \boldsymbol{\mathcal{C}}_B)$ remains bounded and the ratio

$$r = n_1 m_1 / n_2 m_2 = \sqrt{3}\tan\phi$$

of the eigenvalues of $\boldsymbol{v}_1$ takes all values $r \in [-1, 1]$.

Conversely, if we are given an arbitrary one-dimensional subspace $\mathcal{V}_1$ spanned by a matrix $\boldsymbol{v}_1$, with $|\boldsymbol{v}_1| = 1$, then the ratio r, with $|r| \leq 1$, of the eigenvalue of $\boldsymbol{v}_1$ with the smallest absolute value to the eigenvalue of $\boldsymbol{v}_1$ with the largest absolute value determines ϕ and hence determines the associated microstructure of the unimode material. This unimode material should be rotated so that the interface between materials A and A' is normal to the eigenvector of $\boldsymbol{v}_1$ that corresponds to the eigenvalue with the smallest absolute value. Let $\boldsymbol{\mathcal{C}}_B(\lambda, \mathcal{V}_1)$ denote the effective tensor of the rotated material.

This defines the desired family of unimode materials. Since the upper bound on the sum of energies $W(\mathcal{V}_1; \boldsymbol{\mathcal{C}}_B(\lambda, \mathcal{V}_1))$ is proportional to $1/\lambda$ and remains bounded as $\mathcal{V}_1$ is varied with λ held fixed, there exists some constant M_1, depending only on $\boldsymbol{\mathcal{C}}_0$, such that the sum of energies is less than M_1/λ for all λ and all $\boldsymbol{v}_1$. Therefore it suffices to take $\lambda_1 = M_1/c$ to ensure that for all one-dimensional subspaces $\mathcal{V}_1$,

$$W(\mathcal{V}_1; \boldsymbol{\mathcal{C}}_B(\lambda, \mathcal{V}_1)) < c \text{ for all } \lambda > \lambda_1.$$

Thus this family of unimode materials is extremal.

30.7. An extremal family of bimode materials for two-dimensional elasticity†

The idea underlying this somewhat technical section is again simple: To show that a particular family of multiple-rank laminates is bimodal, we consider each member in the family and construct two independent trial strain fields, designed so that they are nonzero only within the compliant phase, and we construct one trial stress field, designed so that it is nonzero only within the stiff phase. Then the classical variational principles provide an upper bound on the sum of two energies and two complementary energies, which goes to zero as $\lambda \to \infty$, thereby establishing that the family is bimode. We use the unimode materials as building blocks to manufacture bimode materials as suggested by figure 30.8 on the next page. Those readers not interested in the details can skip to the next section.

We first obtain material C, which is a simple laminate of the compliant phase, having tensor $\boldsymbol{\mathcal{C}}_0/\lambda$, and the stiff phase, having tensor $\lambda\boldsymbol{\mathcal{C}}_0$, mixed in equal proportions and layered in the direction of the x_2-axis. We then take materials B and C and layer them together in equal proportions in the direction of the x_1-axis, to form material D with effective tensor $\boldsymbol{\mathcal{C}}_D$.

To show that this fourth-rank laminate is a bimode material, we first evaluate the energy associated with a trial strain $\boldsymbol{\epsilon}_1^D(\boldsymbol{x})$, which represents a vertical shear confined within the simple laminate of material C. It is nonzero only within the compliant phase inside material C, where it takes the value

$$\underline{\boldsymbol{v}}_1 = \frac{1}{\sqrt{2}}\begin{pmatrix} 0 & 1 \\ 1 & 0 \end{pmatrix},$$

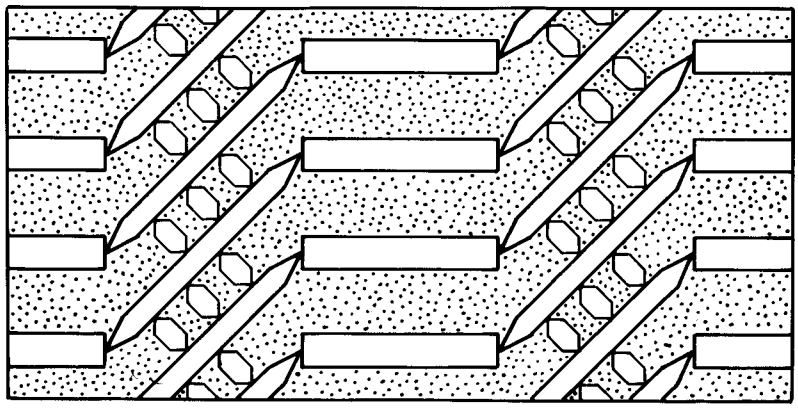

Figure 30.8. A bimode material that is an approximation to a third-rank laminate obtained by laminating the oblique box structure of figure 30.6 with a simple laminate. It supports a stress with positive determinant. A fourth-rank laminate, which is a bimode material and supports any prescribed stress $\underline{\boldsymbol{v}}_3$, can be obtained by replacing the oblique box structure with the herringbone third-rank laminate of figure 30.7. This fourth-rank laminate is the structure that is analyzed in the text. Reprinted with permission from Milton and Cherkaev (1995). Copyright 1995, ASME.

which has been chosen so that $|\underline{\boldsymbol{v}}_1| = 1$. Since the average of this trial strain is $\underline{\boldsymbol{v}}_1/4$, the energy minimization principle gives the bound

$$\underline{\boldsymbol{v}}_1 \cdot \boldsymbol{\mathcal{C}}_D \underline{\boldsymbol{v}}_1 \leq 4\underline{\boldsymbol{v}}_1 \cdot \boldsymbol{\mathcal{C}}_0 \underline{\boldsymbol{v}}_1/\lambda.$$

Next we choose a trial strain $\boldsymbol{\epsilon}_2^D(\boldsymbol{x})$ that inside material B equals the actual strain that would be present with an average strain inside material B equal to $\boldsymbol{v}_1$, as given by (30.24), and inside material C is nonzero only inside the compliant phase, where it takes the value

$$\boldsymbol{\epsilon}_D = \frac{2}{\sqrt{n_1^2m_1^2 + n_2^2m_2^2}} \begin{pmatrix} 0 & 0 \\ 0 & n_2m_2 \end{pmatrix},$$

which has been chosen to ensure strain compatibility with the zero trial strain inside the stiff phase of material C and to ensure compatibility between the average trial strain within material C (which is half the above value) and the average trial strain $\boldsymbol{v}_1$ inside material B.

The overall average of this trial strain is therefore

$$\frac{1}{2\sqrt{n_1^2m_1^2 + n_2^2m_2^2}} \begin{pmatrix} n_1m_1 & 0 \\ 0 & 2n_2m_2 \end{pmatrix} = \frac{\underline{\boldsymbol{v}}_2\sqrt{n_1^2m_1^2 + 4n_2^2m_2^2}}{2\sqrt{n_1^2m_1^2 + n_2^2m_2^2}},$$

where

$$\underline{\boldsymbol{v}}_2 = \frac{1}{\sqrt{n_1^2m_1^2 + 4n_2^2m_2^2}} \begin{pmatrix} n_1m_1 & 0 \\ 0 & 2n_2m_2 \end{pmatrix}$$

has been defined so that $|\underline{\boldsymbol{v}}_2| = 1$. The energy minimization principle then gives the bound

$$\underline{\boldsymbol{v}}_2 \cdot \boldsymbol{\mathcal{C}}_D \underline{\boldsymbol{v}}_2 \leq \frac{4(n_1^2m_1^2 + n_2^2m_2^2)[\boldsymbol{v}_1 \cdot \boldsymbol{\mathcal{C}}_B \boldsymbol{v}_1/2 + \boldsymbol{\epsilon}_D \cdot \boldsymbol{\mathcal{C}}_0 \boldsymbol{\epsilon}_D/4\lambda]}{n_1^2m_1^2 + 4n_2^2m_2^2},$$

and the inequality (30.25) in turn gives a bound on $\boldsymbol{v}_1 \cdot \boldsymbol{\mathcal{C}}_B \boldsymbol{v}_1$.

Finally we take a trial stress field $\boldsymbol{\tau}_3^D(\boldsymbol{x})$ that inside material B equals the actual stress that would be present with an average stress inside material B equal to $\boldsymbol{v}_2$, as given by (30.26), and inside material C is nonzero only inside the stiff phase, where it takes the value

$$\boldsymbol{\tau}_D = \frac{2}{\sqrt{n_1^2 m_1^2 + n_2^2 m_2^2}} \begin{pmatrix} -n_2 m_2 & 0 \\ 0 & 0 \end{pmatrix},$$

which has been chosen to ensure stress compatibility with the zero trial stress inside the compliant phase of material C and to ensure compatibility between the average trial stress within material C (which is half the above value) and the average trial stress $\boldsymbol{v}_2$ inside material B. The overall average of this trial stress is

$$\frac{1}{2\sqrt{n_1^2 m_1^2 + n_2^2 m_2^2}} \begin{pmatrix} -2n_2 m_2 & 0 \\ 0 & n_1 m_1 \end{pmatrix} = \frac{\underline{\boldsymbol{v}}_3 \sqrt{n_1^2 m_1^2 + 4n_2^2 m_2^2}}{2\sqrt{n_1^2 m_1^2 + n_2^2 m_2^2}},$$

where

$$\underline{\boldsymbol{v}}_3 = \frac{1}{\sqrt{n_1^2 m_1^2 + 4n_2^2 m_2^2}} \begin{pmatrix} -2n_2 m_2 & 0 \\ 0 & n_1 m_1 \end{pmatrix}$$

has been defined so that $|\underline{\boldsymbol{v}}_3| = 1$. The complementary energy minimization principle then gives the bound

$$\underline{\boldsymbol{v}}_3 \cdot \boldsymbol{\mathcal{C}}_D^{-1} \underline{\boldsymbol{v}}_3 \leq \frac{4(n_1^2 m_1^2 + n_2^2 m_2^2)[\boldsymbol{v}_2 \cdot \boldsymbol{\mathcal{C}}_B^{-1} \boldsymbol{v}_2/2 + \boldsymbol{\tau}_D \cdot \boldsymbol{\mathcal{C}}_0^{-1} \boldsymbol{\tau}_D/4\lambda]}{n_1^2 m_1^2 + 4n_2^2 m_2^2},$$

and the inequality (30.27) in turn gives a bound on $\boldsymbol{v}_2 \cdot \boldsymbol{\mathcal{C}}_B^{-1} \boldsymbol{v}_2$. Notice that $\underline{\boldsymbol{v}}_1$, $\underline{\boldsymbol{v}}_2$, and $\underline{\boldsymbol{v}}_3$ are a set of orthonormal matrices.

Let $\mathcal{V}_2$ be the two-dimensional subspace of symmetric matrices spanned by $\underline{\boldsymbol{v}}_1$ and $\underline{\boldsymbol{v}}_2$. It is conveniently parameterized by $\underline{\boldsymbol{v}}_3$, which is orthogonal to all matrices in $\mathcal{V}_2$. Again let us choose the same parameter values (30.28) for the unit vectors $\boldsymbol{n}$ and $\boldsymbol{m}$. Then as ϕ is varied between $-\tan^{-1}(2/\sqrt{3})$ and $\tan^{-1}(2/\sqrt{3})$, the energy sum

$$W(\mathcal{V}_2; \boldsymbol{\mathcal{C}}_D) = \underline{\boldsymbol{v}}_1 \cdot \boldsymbol{\mathcal{C}}_D \underline{\boldsymbol{v}}_1 + \underline{\boldsymbol{v}}_2 \cdot \boldsymbol{\mathcal{C}}_D \underline{\boldsymbol{v}}_2 + \underline{\boldsymbol{v}}_3 \cdot \boldsymbol{\mathcal{C}}_D^{-1} \underline{\boldsymbol{v}}_3$$

remains bounded and the ratio

$$\underline{r} = -n_1 m_1 / 2n_2 m_2 = -\sqrt{3}(\tan\phi)/2$$

of the eigenvalues of $\underline{\boldsymbol{v}}_3$ takes all values $\underline{r} \in [-1, 1]$. Since $W(\mathcal{V}_2; \boldsymbol{\mathcal{C}}_D)$ approaches zero as λ tends to infinity, material D is a bimode material.

Conversely, suppose that we are given an arbitrary two-dimensional subspace $\mathcal{V}_2$. We let $\underline{\boldsymbol{v}}_3$ denote the matrix with $|\underline{\boldsymbol{v}}_3| = 1$, which is orthogonal to all matrices in $\mathcal{V}_2$. The ratio $\underline{r}$, with $|r| \leq 1$, of the eigenvalue of $\underline{\boldsymbol{v}}_3$ with the smallest absolute value to the eigenvalue of $\underline{\boldsymbol{v}}_3$ with the largest absolute value determines ϕ and hence determines the associated microstructure of the bimode material. This bimode material should be rotated so that the interface between materials B and C is normal to that eigenvector of $\underline{\boldsymbol{v}}_3$ associated with the eigenvalue having the largest absolute value. Let $\boldsymbol{\mathcal{C}}_D(\lambda, \mathcal{V}_2)$ denote the effective tensor of the rotated material.

This defines the desired family of bimode materials. Since the upper bound on the sum of energies $W(\mathcal{V}_2; \boldsymbol{\mathcal{C}}_D(\lambda, \mathcal{V}_2))$ is proportional to $1/\lambda$ and remains bounded as $\mathcal{V}_2$ is varied with λ held fixed, there exists some constant M_2, depending only on $\boldsymbol{\mathcal{C}}_0$, such that the sum of energies is less than M_2/λ for all λ and all $\boldsymbol{v}_1$. Therefore it suffices to take $\lambda_2 = M_2/c$ to ensure that for all two-dimensional subspaces $\mathcal{V}_2$,

$$W(\mathcal{V}_2; \boldsymbol{\mathcal{C}}_D(\lambda, \mathcal{V}_2)) < c \text{ for all } \lambda > \lambda_2.$$

Thus this family of bimode materials is extremal.

This completes the proof that in two dimensions any positive-definite tensor can be realized as the effective tensor of a two-phase composite assembled from a sufficiently compliant phase and a sufficiently stiff phase. The derivation shows that the subspace $\mathcal{V}_k$, representing the easy modes of deformation of a given multiple-rank laminate, can be determined recursively. Laminating two materials that are easily compliant to strains in subspaces $\mathcal{V}_k^1$ and $\mathcal{V}_\ell^2$, respectively, produces a composite that is easily compliant to strains in a subspace $\mathcal{V}_m^*$. Cherkaev (2000) gives a formula for calculating $\mathcal{V}_m^*$ in terms of $\mathcal{V}_k^1$, $\mathcal{V}_\ell^2$ and the direction of lamination $\boldsymbol{n}$.

30.8. Extremal materials for three-dimensional elasticity

Here we briefly outline the strategy for constructing three-dimensional extremal materials; for more details see Milton and Cherkaev (1995). The first step is to construct the pentamode materials, which, when λ is large, are stiff with respect to a single stress $\boldsymbol{v}_1$ but compliant with respect to any other stress not proportional to $\boldsymbol{v}_1$. These are generalizations of the two-dimensional honeycomb and inverted honeycomb arrays of linkages in figures 30.4 on page 655 and 30.5 on page 656 to three dimensions. Since a structure that is stiff with respect to $\boldsymbol{v}_1$ is also stiff with respect to $-\boldsymbol{v}_1$, we can assume without loss of generality that $\boldsymbol{v}_1$ has at most one negative eigenvalue.

The diamond structure lattice of linkages illustrated in figure 30.9 on the facing page is stiff with respect to hydrostatic compression, that is, to $\boldsymbol{v}_1 = \boldsymbol{I}$, and by making a suitable affine transformation of the structure (but without changing the elasticity tensors of the two phases) one obtains pentamode materials that are stiff with respect to any given positive-definite tensor $\boldsymbol{v}_1$. By moving the point $\boldsymbol{p}$, where the four linkages within the unit cell meet, to the other side of the unit cell and making an appropriate affine transformation one obtains pentamode materials that are stiff with respect to any given tensor $\boldsymbol{v}_1$ with one negative eigenvalue. Pentamode materials that are stiff with respect to any given tensor $\boldsymbol{v}_1$ having zero determinant are obtained as follows. One moves $\boldsymbol{p}$ to the boundary of the unit cell, so three of the four linkages are coplanar, and makes an appropriate affine transformation. The fourth linkage can be removed, if desired, since it can support essentially no stress when λ is large. Then the remaining linkages are in planes, and within these planes they are arranged in the honeycomb and inverted honeycomb arrays of figures 30.4 on page 655 and 30.5 on page 656.

These pentamode materials are used as the basis for constructing the quadramode materials that, when λ is large, are stiff with respect to two independent stresses $\boldsymbol{v}_1$ and $\boldsymbol{v}_2$. We construct the linkages of a pentamode material that is stiff with respect to $\boldsymbol{v}_1$, and we construct the linkages of a pentamode material that is stiff with respect to $\boldsymbol{v}_2$. It is desirable to use very thin linkages in each construction. Then we superimpose these two sets of linkages to obtain a structure of two interpenetrating lattices of linkages, surrounded by a compliant matrix, which, when λ is large, is stiff with respect to $\boldsymbol{v}_1$ and $\boldsymbol{v}_2$ but compliant with respect to any stress not in the space spanned by $\boldsymbol{v}_1$ and $\boldsymbol{v}_2$. We use the freedom in the design of

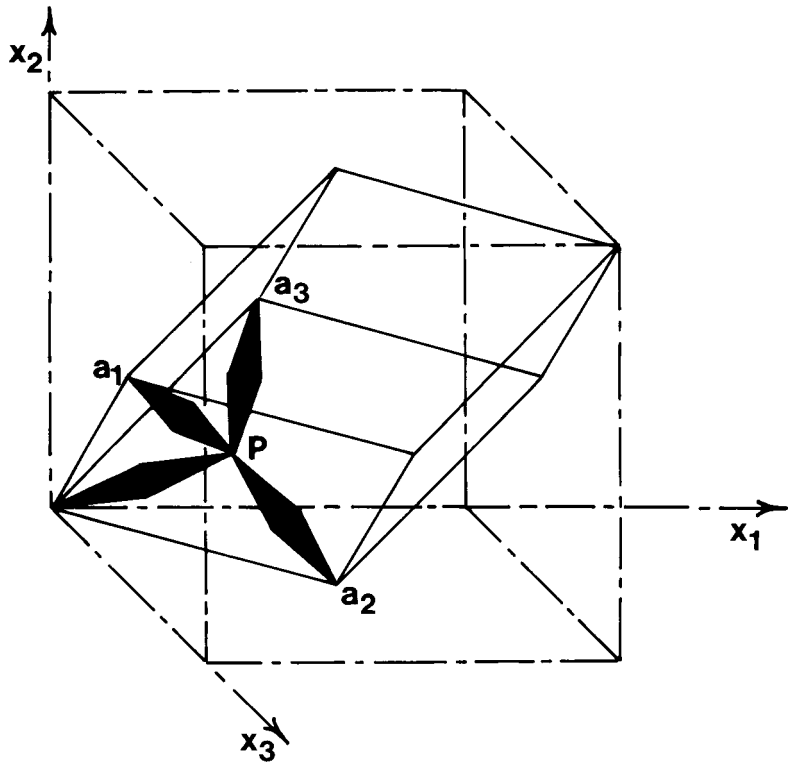

Figure 30.9. The diamond lattice of linkages is a pentamode material that can be used as basis for constructing all of the three-dimensional extremal materials. Shown here are the four linkages inside the primitive unit cell. The cell is outlined by the solid lines and has basis vectors $\boldsymbol{a}_1$, $\boldsymbol{a}_2$, and $\boldsymbol{a}_3$. It sits inside the conventional unit cell of the face-centered cubic lattice, outlined by the broken lines. Depending on which side of the unit cell the point $\boldsymbol{p}$ lies, the material supports a stress with eigenvalues that all have the same sign, or that have mixed signs. Reprinted with permission from Milton and Cherkaev (1995). Copyright 1995, ASME.

the sets of linkages associated with the pentamode material to ensure that the lattices do not intersect. For example, this may require replacing a linkage by a linkage with a hole in it. By superimposing three, four, or five lattices of linkages, one obtains the trimode, bimode, and unimode families of extremal materials, respectively. Of course, the nullmode and hexamode materials are the stiff and compliant phase, respectively. In this way one obtains all of the extremal materials for three-dimensional elasticity.

References

Alderson, K. L. and K. E. Evans 1992, October. The fabrication of microporous polyethylene having a negative Poisson's ratio. *Polymer (Guildford)* 33(20):4435–4438. {*653, 667*}

Almgren, R. F. 1985. An isotropic three-dimensional structure with Poisson's ratio $= -1$. *Journal of Elasticity* 15:427–430. {*652, 656, 667*}

Astala, K. and M. Miettinen 1998. On quasiconformal mappings and 2-dimensional G-closure problems. *Archive for Rational Mechanics and Analysis* 143(3):207–240. {*646, 668*}

Bathurst, R. J. and L. Rothenburg 1988. Note on a random isotropic granular material with negative Poisson's ratio. *International Journal of Engineering Science* 26:373–383. {*652, 668*}

Berlyand, L. and K. Promislow 1995. Effective elastic moduli of a soft medium with hard polygonal inclusions and extremal behavior of effective Poisson's ratio. *Journal of Elasticity* 40(1):45–73. {*653, 668*}

Caddock, B. D. and K. E. Evans 1989. Microporous materials with negative Poisson's ratios: I. Microstructure and mechanical properties. *Journal of Physics D: Applied Physics* 22:1877–1882. {*653, 668*}

Cherkaev, A. V. 2000. *Variational Methods for Structural Optimization*. Berlin / Heidelberg / London / etc.: Springer-Verlag. xxvi + 545 pp. ISBN 0-387-98462-3. {*xxv, xxvi, 352, 353, 426, 434, 666, 668*}

Cherkaev, A. V. and L. V. Gibiansky 1993. Coupled estimates for the bulk and shear moduli of a two-dimensional isotropic elastic composite. *Journal of the Mechanics and Physics of Solids* 41(5):937–980. {*560, 565, 653, 668*}

Francfort, G. A. and G. W. Milton 1994. Sets of conductivity and elasticity tensors stable under lamination. *Communications on Pure and Applied Mathematics (New York)* 47 (3):257–279. {*645–647, 668*}

Friis, E. A., R. Lakes, and J. B. Park 1988. Negative Poisson's ratio polymeric and metallic foams. *Journal of Materials Science* 23:4406–4414. {*652, 668*}

Gibson, L. J. and M. F. Ashby 1988. *Cellular Solids. Structure and Properties*, pp. 72–82. New York: Pergamon. ISBN 0-08-035910-8 (hardback), 0-08-036607-4 (softcover). {*653, 668*}

Herakovich, C. T. 1984. Composite laminates with negative through-the-thickness Poisson's ratios. *Journal of Composite Materials* 18:447–455. {*653, 668*}

Homand-Etienne, F. and R. Houpert 1989. Thermally induced microcracking in granites: characterization and analysis. *International Journal of Rock Mechanics and Mining Sciences and Geomechanics Abstracts* 26:125–134. {*652, 668*}

Kolpakov, A. G. 1985. Determination of the average characteristics of elastic frameworks. *Prikladnaia matematika i mekhanika (Leningrad, R.S.F.S.R.)* 49(6):969–977. {*653, 668*}

Lakes, R. 1987. Foam structures with a negative Poisson's ratio. *Science* 235:1038–1040. {*2, 16, 652, 668*}

Lakes, R. 1991. Deformation mechanisms in negative Poisson's ratio materials: Structural aspects. *Journal of Materials Science* 26:2287–2292. {*652, 668*}

Larsen, U. D., O. Sigmund, and S. Bouwstra 1997. Design and fabrication of compliant micro-mechanisms and structures with negative Poisson's ratio. *Journal of Microelectromechanical Systems* 6:99–106. {*2, 3, 16, 653, 668*}

Milton, G. W. 1992. Composite materials with Poisson's ratios close to -1. *Journal of the Mechanics and Physics of Solids* 40(5):1105–1137. {*2, 16, 653, 661, 668*}

Milton, G. W. 1994. A link between sets of tensors stable under lamination and quasiconvexity. *Communications on Pure and Applied Mathematics (New York)* 47(7):959–1003. {*513, 527, 535, 551, 647, 669*}

Milton, G. W. and A. V. Cherkaev 1995. Which elasticity tensors are realizable? *ASME Journal of Engineering Materials and Technology* 117:483–493. {*647, 652, 653, 655, 656, 658, 659, 664, 666, 667, 669*}

Milton, G. W. and V. Nesi 1999. Optimal G-closure bounds via stability under lamination. *Archive for Rational Mechanics and Analysis* 150(3):191–207. {*207, 218, 480, 495, 646, 669*}

Nesi, V. 1996. Quasiconformal mappings as a tool to study certain two-dimensional G-closure problems. *Archive for Rational Mechanics and Analysis* 134(1):17–51. {*124, 141, 152, 156, 480, 481, 495, 646, 669*}

Roscoe, R. 1973. Isotropic composites with elastic or viscoelastic phases: General bounds for the moduli and solutions for special geometries. *Rheologica acta* 12:404–411. {*206, 219, 471, 496, 646, 669*}

Sigmund, O. 1994. Materials with prescribed constitutive parameters: An inverse homogenization problem. *International Journal of Solids and Structures* 31(17):2313–2329. {*652, 669*}

Sigmund, O. 1995. Tailoring materials with prescribed elastic properties. *Mechanics of Materials: An International Journal* 20(4):351–368. {*653, 669*}

Warren, T. L. 1990. Negative Poisson's ratio in a transversely isotropic foam structure. *Journal of Applied Physics* 67:7591–7594. {*653, 669*}

31

The bounding of effective moduli as a quasiconvexification problem

31.1. Quasiconvexification problems in elasticity theory

Problems of quasiconvexification arise in nonlinear elasticity (Ball 1977) and, in particular, in the study of shape memory materials (Ball and James 1987). We are given a scalar-valued function $W(\boldsymbol{E})$ that is continuous on the space $\mathcal{T}$ comprised of all $d \times \ell$ matrices $\boldsymbol{E}$. The quasiconvexification of W is the function

$$QW(\boldsymbol{E}_0) = \inf_{\substack{\boldsymbol{E}(\boldsymbol{x}) \\ \boldsymbol{E} = \nabla \boldsymbol{u}}} \langle W(\boldsymbol{E}) \rangle = \inf_{\substack{\boldsymbol{E}(\boldsymbol{x}) \\ \boldsymbol{E} = \nabla \boldsymbol{u}}} \frac{1}{|\Omega|} \int_\Omega d\boldsymbol{x} W(\boldsymbol{E}(\boldsymbol{x})), \tag{31.1}$$

where the angular brackets denote averages over a region Ω and the infimum is over all smooth potentials $\boldsymbol{u}(\boldsymbol{x})$ defined in Ω satisfying the affine boundary conditions

$$\boldsymbol{u}(\boldsymbol{x}) = \boldsymbol{x} \cdot \boldsymbol{E}_0 \text{ for all } \boldsymbol{x} \in \partial\Omega. \tag{31.2}$$

It follows from the boundary conditions (31.2) that

$$\langle \nabla \boldsymbol{u} \rangle = \frac{1}{|\Omega|} \int_\Omega d\boldsymbol{x} \nabla \boldsymbol{u}(\boldsymbol{x}) = \boldsymbol{E}_0 + \frac{1}{|\Omega|} \int_\Omega d\boldsymbol{x} \nabla [\boldsymbol{u}(\boldsymbol{x}) - \boldsymbol{x} \cdot \boldsymbol{E}_0] = \boldsymbol{E}_0.$$

Thus $\boldsymbol{E}_0$ can be identified with the average field in the body. When $QW(\boldsymbol{E}_0) = W(\boldsymbol{E}_0)$ the function $W(\boldsymbol{E}_0)$ is said to be quasiconvex.

In three-dimensional elasticity theory $d = \ell = 3$ and $W(\boldsymbol{E})$ is the microscopic elastic energy associated with the deformation $\boldsymbol{E} = \nabla \boldsymbol{u}$, while $QW(\boldsymbol{E}_0)$ is the macroscopic energy when the material is subject to affine boundary conditions. (Here $\boldsymbol{u}$ should not be confused with the displacement, which was represented by $\boldsymbol{u}$ in previous chapters; under the mapping $\boldsymbol{x}'(\boldsymbol{x})$, $\boldsymbol{u}$ should be identified with $\boldsymbol{x}'$ and not with $\boldsymbol{x}' - \boldsymbol{x}$.) Due to the fact, known as the *principle of material frame-indifference*, that the energy does not change when we rotate the body after making the deformation, these functions satisfy

$$W(\boldsymbol{E}\boldsymbol{R}) = W(\boldsymbol{E}), \quad QW(\boldsymbol{E}_0\boldsymbol{R}) = QW(\boldsymbol{E}_0),$$

for all rotation matrices $\boldsymbol{R}$, that is, they are functions of $\boldsymbol{E}\boldsymbol{E}^T$. (The matrices $\boldsymbol{E}\boldsymbol{R}$, $\boldsymbol{E}_0\boldsymbol{R}$, and $\boldsymbol{E}\boldsymbol{E}^T$ appear here, rather than $\boldsymbol{R}\boldsymbol{E}$, $\boldsymbol{R}\boldsymbol{E}_0$, and $\boldsymbol{E}^T\boldsymbol{E}$, because we have chosen to define $\nabla \boldsymbol{u}$ as the matrix having ∇u_1 and ∇u_2 as columns rather than as rows.)

Typically, one expects that the macroscopic energy will be minimized when the displacement is linear, that is, that the infimum in (31.1) will be achieved when $\boldsymbol{u}(\boldsymbol{x}) = \boldsymbol{x} \cdot \boldsymbol{E}_0$

for all points $\boldsymbol{x} \in \Omega$. Accordingly, one has $QW(\boldsymbol{E}_0) = W(\boldsymbol{E}_0)$. However, in some materials an instability develops, and it is energetically favorable for $\boldsymbol{u}(\boldsymbol{x})$ to develop oscillations, usually on length scales that are much shorter than the dimensions of Ω. Then one has $QW(\boldsymbol{E}_0) < W(\boldsymbol{E}_0)$. In particular, suppose that $W(\boldsymbol{E})$ takes its minimum value W_0 when $\boldsymbol{E}\boldsymbol{E}^T$ equals one of a set $\mathcal{S} = \{\boldsymbol{M}_1, \boldsymbol{M}_2, \ldots, \boldsymbol{M}_n\}$ of n matrices. (By adding a constant to the energy we can assume that $W_0 = 0$ without loss of generality.) If $\boldsymbol{u}(\boldsymbol{x})$ satisfying (31.2) can be constructed so that $\nabla\boldsymbol{u}(\boldsymbol{x})(\nabla\boldsymbol{u}(\boldsymbol{x}))^T$ takes values in $\mathcal{S}$ almost everywhere, while $\boldsymbol{E}_0\boldsymbol{E}_0^T \notin \mathcal{S}$, then $QW(\boldsymbol{E}_0) = W_0 < W(\boldsymbol{E}_0)$. The region where $\nabla\boldsymbol{u}(\boldsymbol{x})(\nabla\boldsymbol{u}(\boldsymbol{x}))^T$ takes the value $\boldsymbol{M}_j$ is defined to be phase j and the pattern of phases occupying the region Ω is called the microstructure. One of the most common microstructures is a twinned microstructure where two phases are present in a laminated configuration. This is the theory that Ball and James (1987, 1992) developed to explain phase transitions and microstructures in materials where the energy driving the transition is predominantly elastic; see also Khachaturyan (1966, 1983) and Roytburd (1967, 1968, 1978, 1993), who analyzed the problem of phase transitions in a linear elastic setting, and see Kohn (1991), Ball and James (1992), and Bhattacharya (1993) for a comparison of the nonlinear and linear theories. James and Kinderlehrer (1989), Ball (1996), Müller (1998), and Ball and James (2001) give a more complete account of the nonlinear theory as well as extensive references. Luskin (1996) reviews numerical methods that have been developed for computing the microstructure.

When the function $W(\boldsymbol{E})$ is convex in the sense that the inequality

$$fW(\boldsymbol{E}_1) + (1-f)W(\boldsymbol{E}_2) \geq W(f\boldsymbol{E}_1 + (1-f)\boldsymbol{E}_2) \tag{31.3}$$

is satisfied for all $f \in [0, 1]$ and for all pairs of $d \times k$ matrices $\boldsymbol{E}_1$ and $\boldsymbol{E}_2$, then the inequality

$$\langle W(\boldsymbol{E})\rangle \geq W(\langle \boldsymbol{E}\rangle) \tag{31.4}$$

holds for any field $\boldsymbol{E}(\boldsymbol{x})$, and in particular for $\boldsymbol{E}(\boldsymbol{x}) = \nabla\boldsymbol{u}(\boldsymbol{x})$, where $\boldsymbol{u}(\boldsymbol{x})$ is any potential satisfying the required boundary conditions (31.2). It follows that for convex functions $W(\boldsymbol{E})$ the infimum in (31.1) is attained when $\boldsymbol{u}(\boldsymbol{x}) = \boldsymbol{x} \cdot \boldsymbol{E}_0$, and consequently

$$QW(\boldsymbol{E}_0) = W(\boldsymbol{E}_0).$$

Thus convex functions are quasiconvex. However, convexity is not an appropriate assumption for nonlinear elasticity (Coleman and Noll 1959). If one takes $f_1 = 1/2$, $\boldsymbol{E}_1 = \boldsymbol{I}$, and $\boldsymbol{E}_2 = \boldsymbol{R} = \boldsymbol{E}_1\boldsymbol{R}$, where $\boldsymbol{R}$ is a 180° rotation about some axis, the inequality (31.3) will be violated. The deformation $\boldsymbol{E} = (\boldsymbol{I} + \boldsymbol{R})/2$ corresponds to squeezing the material onto the axis of rotation, which requires an enormous amount of energy, implying that $W(\boldsymbol{E})$ must be much larger than $W(\boldsymbol{I}) = W(\boldsymbol{R})$.

More generally, a function is quasiconvex when the inequality (31.4) holds for every function $\boldsymbol{E}(\boldsymbol{x}) = \nabla\boldsymbol{u}(\boldsymbol{x})$ such that $\boldsymbol{u}(\boldsymbol{x})$ satisfies the affine boundary conditions (31.2). We will see in section 31.3 on page 675 that the affine boundary conditions (31.2) on $\boldsymbol{u}(\boldsymbol{x})$ can be replaced by periodic boundary conditions on $\boldsymbol{E}(\boldsymbol{x}) = \nabla\boldsymbol{u}(\boldsymbol{x})$ with the constraint that $\langle\nabla\boldsymbol{u}\rangle = \boldsymbol{E}_0$. An important class of quasiconvex functions that are not necessarily convex or quadratic are the polyconvex functions introduced by Ball (1977). A function $W(\boldsymbol{E})$ is polyconvex if it can be expressed as a convex function of the elements of $\boldsymbol{E}$, $\det(\boldsymbol{E})$, and all other subdeterminants of $\boldsymbol{E}$, that is, as a convex function of all the null Lagrangians associated with the field $\boldsymbol{E} = \nabla\boldsymbol{u}$. For example, if $W(\boldsymbol{E}) = \Phi(\boldsymbol{E}, \det(\boldsymbol{E}))$, where Φ is convex in its arguments, then by Jensen's inequality and because $\det(\boldsymbol{E})$ is a null Lagrangian, we have

$$\langle W(\boldsymbol{E})\rangle = \langle\Phi(\boldsymbol{E}, \det(\boldsymbol{E}))\rangle \geq \Phi(\langle\boldsymbol{E}\rangle, \langle\det(\boldsymbol{E})\rangle) = \Phi(\langle\boldsymbol{E}\rangle, \det(\langle\boldsymbol{E}\rangle)) = W(\langle\boldsymbol{E}\rangle),$$

which establishes the quasiconvexity of $W(\boldsymbol{E})$.

Now suppose that $\boldsymbol{E}(\boldsymbol{x})$ is a periodic function that oscillates in the direction $\boldsymbol{n}$ taking two values $\boldsymbol{E}_1$ and $\boldsymbol{E}_2$. Specifically, let us suppose that

$$\boldsymbol{E}(\boldsymbol{x}) = \chi(\boldsymbol{n}\cdot\boldsymbol{x})\boldsymbol{E}_1 + [1-\chi(\boldsymbol{n}\cdot\boldsymbol{x})]\boldsymbol{E}_2, \tag{31.5}$$

where $\chi(y)$ is the periodic characteristic function

$$\begin{aligned}\chi(y) &= 1 && \text{for } 0 \le y < f,\\ &= 0 && \text{for } f \le y < 1,\\ &= \chi(y-1) && \text{for all } y.\end{aligned}$$

By taking Fourier transforms it is clear that $\boldsymbol{E}(\boldsymbol{x}) = \nabla\boldsymbol{u}(\boldsymbol{x})$ for some potential $\boldsymbol{u}(\boldsymbol{x})$ if and only if

$$\boldsymbol{E}_1 - \boldsymbol{E}_2 = \boldsymbol{n}\otimes\boldsymbol{v}, \tag{31.6}$$

for some vector $\boldsymbol{v}$. With this choice of $\boldsymbol{E}(\boldsymbol{x})$ the quasiconvexity condition (31.4) reduces to the convexity condition (31.3) with the constraint (31.6). Functions satisfying (31.3) for all matrices $\boldsymbol{E}_1$ and $\boldsymbol{E}_2$ that are rank-1 connected (i.e., such that $\boldsymbol{E}_1 - \boldsymbol{E}_2$ is a rank-1 matrix) are said to be rank-1 convex. Clearly rank-1 convexity is a necessary condition for quasiconvexity. Šverák (1992) showed that rank-1 convexity is not sufficient to guarantee quasiconvexity when $k \ge 3$. A variant of his example of a function that is rank-1 convex but not quasiconvex will be discussed in section 31.8 on page 684.

We will call the field (31.5), where $\boldsymbol{E}_1$ and $\boldsymbol{E}_2$ are rank-1 connected, a simple laminate field. In the same way that one can construct multiple-rank laminates, so too can one construct multiple-rank laminate fields. For example, the electric field $\boldsymbol{e}(\boldsymbol{x})$ solving the equations of conductivity in a multiple-rank laminate is a multiple-rank laminate field. More generally, one constructs a multiple-rank laminate field by taking a multiple-rank laminate and setting the field $\boldsymbol{E}(\boldsymbol{x})$ to have a constant value in each individual layer in such a way as to ensure compatibility across interfaces, with the possible insertion of appropriate boundary layers. Thus the average of $\boldsymbol{E}(\boldsymbol{x})$ on one side of an interface with normal $\boldsymbol{n}$ and the average of $\boldsymbol{E}(\boldsymbol{x})$ on the other side of this interface can differ only by a rank-1 matrix of the form $\boldsymbol{n}\otimes\boldsymbol{v}$. Of course successive laminations must be on widely separated length scales, as usual.

The rank-1 convexification of W is the function $RW(\boldsymbol{E}_0)$ given by the right-hand side of (31.1) when $\boldsymbol{E}(\boldsymbol{x})$ is restricted to range over all periodic multiple-rank laminate gradient fields such that $\langle\boldsymbol{E}(\boldsymbol{x})\rangle = \boldsymbol{E}_0$. Equivalently, it is the largest rank-1 convex function that is less than or equal to $W(\boldsymbol{E}_0)$ for all $\boldsymbol{E}_0$. The convexification of W is the function $CW(\boldsymbol{E}_0)$ given by the right-hand side of (31.1) when $\boldsymbol{E}(\boldsymbol{x})$ ranges over all periodic fields (not just gradients) such that $\langle\boldsymbol{E}(\boldsymbol{x})\rangle = \boldsymbol{E}_0$. Equivalently, it is the largest convex function that is less than or equal to $W(\boldsymbol{E}_0)$ for all $\boldsymbol{E}_0$. The polyconvexification of W is the function $PW(\boldsymbol{E}_0)$ given by the right-hand side of (31.1) when $\boldsymbol{E}(\boldsymbol{x})$ ranges over all periodic fields (not just gradients) such that $\langle Q(\boldsymbol{E}(\boldsymbol{x}))\rangle = Q(\boldsymbol{E}_0)$ for all functions $Q(\boldsymbol{E})$ that are null Lagrangians, that is, the determinant and all other subdeterminants, including the individual elements of $\boldsymbol{E}$. Equivalently, it is the largest polyconvex function that is less than or equal to $W(\boldsymbol{E}_0)$ for all $\boldsymbol{E}_0$. Firoozye (1991) showed that the optimal translation bound $TQ(\boldsymbol{E}_0)$, with null Lagrangians and quadratic quasiconvex functions as translations, is given by the right-hand side of (31.1) when $\boldsymbol{E}(\boldsymbol{x})$ ranges over all periodic fields such that the identity $\langle Q(\boldsymbol{E}(\boldsymbol{x}))\rangle = Q(\boldsymbol{E}_0)$ holds for all null Lagrangians $Q(\boldsymbol{E})$ and, additionally, the inequality $\langle Q(\boldsymbol{E}(\boldsymbol{x}))\rangle \ge Q(\boldsymbol{E}_0)$ holds for all quasiconvex quadratic functions $Q(\boldsymbol{E})$. Of course, the function W is

recovered when one restricts $\boldsymbol{E}(\boldsymbol{x})$ in the right-hand side of (31.1) to be $\boldsymbol{E}_0$. Since the infimum of a function over a set of fields is either reduced or maintained when the set of fields is enlarged, we have the string of inequalities,

$$W(\boldsymbol{E}_0) \geq RW(\boldsymbol{E}_0) \geq QW(\boldsymbol{E}_0) \geq TW(\boldsymbol{E}_0) \geq PW(\boldsymbol{E}_0) \geq CW(\boldsymbol{E}_0), \tag{31.7}$$

which are illustrated in figure 31.1.

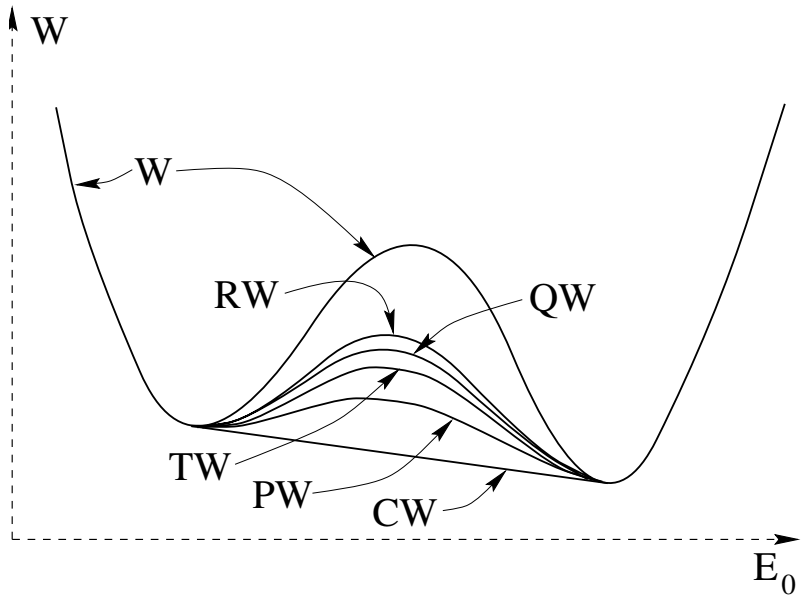

Figure 31.1. A schematic illustration of the relation between the convexification, CW, polyconvexification, PW, translation bound, TW, quasiconvexification, QW, and rank-1 convexification, RW, of a function W. Of course, the horizontal axis should be multidimensional rather than one-dimensional, and in general the function W may have more than two local minima.

31.2. The independence of the quasiconvexified function on the shape and size of the region Ω

The function $QW(\boldsymbol{E}_0)$ is clearly independent of the size of the region Ω, as can be seen by making the change of variable $\boldsymbol{x}' = \lambda\boldsymbol{x}$ in (31.1) and setting $\boldsymbol{u}'(\boldsymbol{x}') = \lambda\boldsymbol{u}(\boldsymbol{x}'/\lambda)$. In fact, $QW(\boldsymbol{E}_0)$ is independent of the shape of Ω, as shown by Ball and Murat (1984) [see also Ball (1996) and Müller (1998)]. The proof uses an idea similar to that used in the construction of the sphere and ellipsoid assemblages in chapter 7 on page 113. Let Ω' be a different shaped region and let $Q'W(\boldsymbol{E}_0)$ denote the quasiconvexification of W with respect to this new region. The first step is to prove that $Q'W(\boldsymbol{E}_0) \leq QW(\boldsymbol{E}_0)$.

For simplicity, let us assume that Ω and Ω' are each smooth and simply connected. For any $\epsilon > 0$ we can find a smooth potential $\boldsymbol{u}_\epsilon(\boldsymbol{x})$ satisfying the boundary conditions (31.2) such that

$$\langle W(\nabla\boldsymbol{u}_\epsilon)\rangle \leq QW(\boldsymbol{E}_0) + \epsilon. \tag{31.8}$$

Now we take our region Ω' and begin by setting the potential $\boldsymbol{u}(\boldsymbol{x})$ equal to $\boldsymbol{x} \cdot \boldsymbol{E}_0$ inside it. Then we carve out from inside Ω' a region with the same shape as Ω but not necessarily of the same size. Inside this region we set

$$\boldsymbol{u}(\boldsymbol{x}) = (1/\lambda)\boldsymbol{u}_\epsilon(\lambda \boldsymbol{x} + \boldsymbol{c}) + \boldsymbol{d},$$

where the scale factor λ and the shifts $\boldsymbol{c}$ and $\boldsymbol{d}$ are selected according to the size and position of the region that we have carved out, so that the potential is continuous at the boundary of the region.

The average of $W(\boldsymbol{u}(\boldsymbol{x}))$ over this region then equals the average of $W(\boldsymbol{u}_\epsilon(\boldsymbol{x}))$ over Ω, which satisfies the bound (31.8). We continue carving out such regions of various sizes ranging to the very small, making sure that they do not intersect each other, until they occupy a proportion p of the total volume of Ω'. This results in a potential $\boldsymbol{u}(\boldsymbol{x})$ with

$$\langle W(\nabla \boldsymbol{u})\rangle \le p[QW(\boldsymbol{E}_0) + \epsilon] + (1-p)W(\boldsymbol{E}_0), \tag{31.9}$$

where the angular brackets now denote an average over Ω'. Strictly speaking, we should smooth the potential near the boundaries of the regions that we have carved out to remove the discontinuities in $\nabla \boldsymbol{u}(\boldsymbol{x})$ that occur there. This can be done with negligible change to $\langle W(\nabla \boldsymbol{u})\rangle$. Since ϵ can be arbitrarily small and since p can be arbitrarily close to 1, (31.9) implies that

$$Q'W(\boldsymbol{E}_0) \le QW(\boldsymbol{E}_0).$$

By switching the roles of Ω and Ω' in the above argument it is evident that the reverse inequality must also hold. Hence $Q'W(\boldsymbol{E}_0)$ must equal $QW(\boldsymbol{E}_0)$.

31.3. Replacing the affine boundary conditions with periodic boundary conditions

For concreteness let us suppose that we are working in a three-dimensional space. Since the shape of Ω does not matter, we can take it to be the cube

$$0 \le x_1 \le h, \quad 0 \le x_2 \le h, \quad 0 \le x_3 \le h,$$

of side length h. Then $\boldsymbol{u}(\boldsymbol{x}) - \boldsymbol{x} \cdot \boldsymbol{E}_0$ satisfies the periodic boundary conditions, being zero on the boundary of the cube. This suggests that we can relax the boundary conditions on $\boldsymbol{u}(\boldsymbol{x})$, allowing potentials $\boldsymbol{u}(\boldsymbol{x})$ such that

$$\boldsymbol{u}'(\boldsymbol{x}) = \boldsymbol{u}(\boldsymbol{x}) - \boldsymbol{x} \cdot \boldsymbol{E}_0 \text{ is } \Omega\text{−periodic.}$$

We need to show that the infimum in (31.1) is not decreased when we admit this larger class of potentials. Let us suppose that we are given any Ω-periodic potential $\boldsymbol{u}'(\boldsymbol{x})$. Our aim is to construct a sequence of associated potentials $\boldsymbol{u}_m(\boldsymbol{x})$ that satisfy the affine boundary conditions (31.2) and are such that

$$\lim_{m\to\infty} \langle W(\nabla \boldsymbol{u}_m)\rangle = \langle W(\nabla \boldsymbol{u})\rangle, \quad \text{where } \boldsymbol{u}(\boldsymbol{x}) = \boldsymbol{x} \cdot \boldsymbol{E}_0 + \boldsymbol{u}'(\boldsymbol{x}).$$

To do this, we pick a large integer p and divide the cube Ω into p^3 subcubes, each with side length h/p. In those cubes that do not touch the boundary of Ω we set

$$\boldsymbol{u}_p(\boldsymbol{x}) = \boldsymbol{x} \cdot \boldsymbol{E}_0 + (1/p)\boldsymbol{u}'(p\boldsymbol{x}). \tag{31.10}$$

The average of $W(\nabla \boldsymbol{u}_p)$ within each of these subcubes is then the same as the average of $W(\nabla \boldsymbol{u})$. In those subcubes that touch the side of Ω we need to make a transition between periodic and affine boundary conditions. This can be done by setting

$$\begin{aligned}\boldsymbol{u}_p(\boldsymbol{x}) \;=\; & \boldsymbol{x}\cdot\boldsymbol{E}_0 \\ & + f\left(\frac{px_1}{h}\right) f\left(\frac{px_2}{h}\right) f\left(\frac{px_3}{h}\right) f\left(\frac{p(h-x_1)}{h}\right) f\left(\frac{p(h-x_2)}{h}\right) f\left(\frac{p(h-x_3)}{h}\right) \frac{\boldsymbol{u}'(p\boldsymbol{x})}{p},\end{aligned}$$

where $f(y)$ is some smooth function of y with

$$f(0) = 0, \quad f(y) = 1 \;\text{ for } y \geq 1.$$

By making the change of variable $\boldsymbol{x}' = p\boldsymbol{x}$ one can check that the average value of $W(\nabla \boldsymbol{u}_p)$ taken over any subcube varies according to whether the subcube touches a vertex, edge, or face of Ω but does not depend on p. Hence the average value of $W(\nabla \boldsymbol{u}_p)$ taken over any subcube has a maximum value W^+ independent of p. It follows that the average value of $W(\nabla \boldsymbol{u}_p)$ taken over all of Ω satisfies the inequality

$$\langle W(\nabla \boldsymbol{u}_p)\rangle \leq \frac{(p-2)^3}{p^3}\langle W(\nabla \boldsymbol{u})\rangle + \frac{p^3-(p-2)^3}{p^3} W^+,$$

in which $(p-2)^3/p^3$ represents the proportion of subcubes which do not touch the side of Ω. Clearly $\langle W(\nabla \boldsymbol{u}_p)\rangle$ approaches $\langle W(\nabla \boldsymbol{u})\rangle$ in the limit as p goes to infinity. Therefore the infimum in (31.1) does not change when the affine boundary conditions on $\boldsymbol{u}(\boldsymbol{x})$ are replaced by the requirement that $\boldsymbol{u}'(\boldsymbol{x}) = \boldsymbol{u}(\boldsymbol{x}) - \boldsymbol{x}\cdot\boldsymbol{E}_0$ be Ω-periodic, that is, by the requirement that $\nabla \boldsymbol{u}(\boldsymbol{x})$ be Ω-periodic.

This result suggests a natural generalization of quasiconvexification, which extends one introduced by Dacorogna (1982) (called $\mathcal{A}$-quasiconvexification) that has been extensively investigated by Fonseca and Müller (1999) and Braides, Fonseca, and Leoni (2000). Given a scalar-valued function W defined on the space of tensors $\mathcal{T}$, we call

$$QW(\boldsymbol{E}_0) = \inf_{\substack{\boldsymbol{E} \in \mathcal{U} \oplus \mathcal{E} \\ \langle \boldsymbol{E}\rangle = \boldsymbol{E}_0}} \langle W(\boldsymbol{E})\rangle$$

the quasiconvexification of W with respect to $\mathcal{E}$. Here, as usual, $\mathcal{U}$ is the space of constant fields and $\mathcal{E}$ is a subspace of Ω-periodic fields having zero average value and satisfying appropriate differential constraints. At each point $\boldsymbol{x}$ the fields in $\mathcal{U}$ and $\mathcal{E}$ take their values in the tensor space $\mathcal{T}$. In a particular representation, $\mathcal{U} \oplus \mathcal{E}$ might contain, for example, the set of all fields $\boldsymbol{E}(\boldsymbol{x})$ given by (12.13) as $\boldsymbol{E}_0$ is varied and $\boldsymbol{U}(\boldsymbol{x})$ ranges over all periodic potentials. Again, a function is said to be quasiconvex if $QW(\boldsymbol{E}_0) = W(\boldsymbol{E}_0)$ for all $\boldsymbol{E}_0$.

The analog of matrices $\boldsymbol{E}_1$ and $\boldsymbol{E}_2$ that are rank-1 connected are matrices such that

$$\boldsymbol{E}_1 - \boldsymbol{E}_2 = \mathcal{E}_{\boldsymbol{n}} \;\text{ for some } \boldsymbol{n},$$

where $\mathcal{E}_{\boldsymbol{n}}$ is the subspace onto which $\boldsymbol{\Gamma}_1(\boldsymbol{n})$ projects. Following Tartar (1979) and Murat (1987) we let Λ denote the set of all such matrices, and we say that $\boldsymbol{E}_1$ and $\boldsymbol{E}_2$ are Λ-connected if their difference is a matrix in Λ. A function $W(\boldsymbol{E})$ is then said to be Λ-convex

if (31.3) holds for all $f \in [0, 1]$ and for all $\boldsymbol{E}_1$ and $\boldsymbol{E}_2$ that are Λ-connected. Again, Λ-convexity is a necessary condition for quasiconvexity. Tartar (1979) showed that Λ-convexity is not sufficient to guarantee quasiconvexity in this generalized sense.

Now suppose that $\nabla \boldsymbol{u}$ takes a finite number of values $\boldsymbol{E}_1, \boldsymbol{E}_2, \ldots, \boldsymbol{E}_n$. Let f_i be the volume fraction of the region where $\nabla \boldsymbol{u}$ takes the value $\boldsymbol{E}_i$. Then we have that

$$\langle W(\nabla \boldsymbol{u}) \rangle - W(\langle \nabla \boldsymbol{u} \rangle) = \left[\sum_{i=1}^{n} f_i W(\boldsymbol{E}_i) \right] - W(\sum_{i=1}^{n} f_i \boldsymbol{E}_i).$$

Notice that the right-hand side only depends on the values $\boldsymbol{E}_i$ and the volume fractions f_i. More generally, the right-hand side depends only on the distribution of values that $\nabla \boldsymbol{u}$ takes. This distribution is called the Young's measure associated with the periodic gradient $\nabla \boldsymbol{u}$. (Strictly speaking, Young's measures are associated with sequences of functions, but for our purposes we ignore the distinction.) In our example, the Young's measure consists of n Dirac delta functions located at the matrices $\boldsymbol{E}_1, \boldsymbol{E}_2, \ldots, \boldsymbol{E}_n$, with masses $f_1, f_2, \ldots, f_n$. If the right-hand side is nonnegative for all $\boldsymbol{E}_0$ and for all Young's measures of periodic gradients, then W is quasiconvex; conversely, if the right-hand side is negative for some Young's measure, then W is not quasiconvex. Thus a characterization of Young's measures of periodic gradients would in principle allow us to identify whether a function W is quasiconvex or not [see, for example, Kinderlehrer and Pedregal (1991)]. Unfortunately, little is known about the possible Young's measures of periodic gradients.

31.4. The equivalence of bounding the energy of multiphase linear composites and quasiconvexification

Kohn (1991) recognized that bounding the energy of a linear composite reduces to a quasiconvexification problem. Suppose that we are given a composite where the tensor field $\boldsymbol{L}(\boldsymbol{x})$ is constrained to take values in a set U. The best possible lower bound $W_-(\boldsymbol{E}_0)$ on the energy

$$\boldsymbol{E}_0 \cdot \boldsymbol{L}_* \boldsymbol{E}_0 = \inf_{\substack{\boldsymbol{E} \in \mathcal{U} \oplus \mathcal{E} \\ \langle \boldsymbol{E} \rangle = \boldsymbol{E}_0}} \langle \boldsymbol{E} \cdot \boldsymbol{L}\boldsymbol{E} \rangle$$

is

$$W_-(\boldsymbol{E}_0) = \inf_{\substack{\boldsymbol{L} \\ \boldsymbol{L}(\boldsymbol{x}) \in U}} \inf_{\substack{\boldsymbol{E} \in \mathcal{U} \oplus \mathcal{E} \\ \langle \boldsymbol{E} \rangle = \boldsymbol{E}_0}} \langle \boldsymbol{E} \cdot \boldsymbol{L}\boldsymbol{E} \rangle. \tag{31.11}$$

Switching the order of the infimums gives

$$W_-(\boldsymbol{E}_0) = \inf_{\substack{\boldsymbol{E} \in \mathcal{U} \oplus \mathcal{E} \\ \langle \boldsymbol{E} \rangle = \boldsymbol{E}_0}} \langle W(\boldsymbol{E}) \rangle, \tag{31.12}$$

where

$$W(\boldsymbol{E}) = \inf_{\boldsymbol{L} \in U} \boldsymbol{E} \cdot \boldsymbol{L}\boldsymbol{E}. \tag{31.13}$$

In other words, the problem of finding the best possible lower bound on the energy of the composite for all applied fields $\boldsymbol{E}_0$ is equivalent to the problem of finding the quasiconvexification of the function $W(\boldsymbol{E})$. In an n-phase composite where the set U consists of the n

tensors $\boldsymbol{L}_1, \boldsymbol{L}_2, \ldots, \boldsymbol{L}_n$, (31.13) implies that the function $W(\boldsymbol{E})$ is the minimum of a set of quadratic wells each centered at $\boldsymbol{E} = 0$:

$$W(\boldsymbol{E}) = \min\{\boldsymbol{E} \cdot \boldsymbol{L}_1\boldsymbol{E}, \boldsymbol{E} \cdot \boldsymbol{L}_2\boldsymbol{E}, \ldots, \boldsymbol{E} \cdot \boldsymbol{L}_n\boldsymbol{E}\}.$$

Thus the problem of bounding the energy of a linear inhomogeneous composite with no restriction placed on the configuration of the phases is equivalent to bounding the energy of a homogeneous nonlinear material. This equivalence is tied with the fact that the following iterative procedure leads to the best possible bound on $\boldsymbol{E}_0 \cdot \boldsymbol{L}_*\boldsymbol{E}_0$. We begin with a trial configuration and a trial field $\boldsymbol{E}(\boldsymbol{x}) \in \mathcal{U} \oplus \mathcal{E}$ that comes close to minimizing the energy for that configuration. Then we improve the configuration by moving the phases to minimize $\boldsymbol{E}(\boldsymbol{x})\boldsymbol{L}(\boldsymbol{x})\boldsymbol{E}(\boldsymbol{x})$ at each point $\boldsymbol{x}$, holding $\boldsymbol{E}(\boldsymbol{x})$ fixed. Then we improve our choice of $\boldsymbol{E}(\boldsymbol{x})$ to reflect the new microgeometry, and so on ad-infinitum. The freedom that we have to move the phases according to the value of $\boldsymbol{E}(\boldsymbol{x})$ means that we are effectively working with a nonlinear homogeneous material with energy $W(\boldsymbol{E})$.

Conversely, subject to some technicalities, quasiconvexification problems can be mapped to essentially equivalent problems of bounding the energy of composites. To see this, consider the thermoelastic-type problem of the form

$$\begin{pmatrix} \boldsymbol{J}(\boldsymbol{x}) \\ \varsigma(\boldsymbol{x}) \end{pmatrix} = \boldsymbol{\mathcal{L}}(\boldsymbol{x}) \begin{pmatrix} \boldsymbol{E}(\boldsymbol{x}) \\ T \end{pmatrix}, \quad \boldsymbol{J} \in \mathcal{U} \oplus \mathcal{J}, \quad \boldsymbol{E} \in \mathcal{U} \oplus \mathcal{E}, \tag{31.14}$$

where $\varsigma(\boldsymbol{x})$ is not subject to any differential constraint, T is constant, and $\boldsymbol{\mathcal{L}}(\boldsymbol{x})$ has the form

$$\boldsymbol{\mathcal{L}}(\boldsymbol{x}) = \begin{pmatrix} \boldsymbol{L}(\boldsymbol{x}) & \boldsymbol{A}(\boldsymbol{x}) \\ [\boldsymbol{A}(\boldsymbol{x})]^T & k(\boldsymbol{x}) \end{pmatrix}.$$

The field $\boldsymbol{\mathcal{L}}(\boldsymbol{x})$ is constrained to take values in some set U. We take an applied field

$$\overline{\boldsymbol{E}}_0 = \begin{pmatrix} \boldsymbol{E}_0 \\ 1 \end{pmatrix}.$$

From the analysis at the beginning of this section it follows that the best possible bound on $\overline{\boldsymbol{E}}_0 \cdot \boldsymbol{\mathcal{L}}_*\overline{\boldsymbol{E}}_0$ can be identified with

$$QF(\boldsymbol{E}_0) = \inf_{\substack{\boldsymbol{E} \in \mathcal{U} \oplus \mathcal{E} \\ \langle \boldsymbol{E} \rangle = \boldsymbol{E}_0}} \langle F(\boldsymbol{E}) \rangle,$$

where

$$F(\boldsymbol{E}) = \inf_{\boldsymbol{\mathcal{L}} \in U} \begin{pmatrix} \boldsymbol{E} \\ 1 \end{pmatrix} \cdot \boldsymbol{\mathcal{L}} \begin{pmatrix} \boldsymbol{E} \\ 1 \end{pmatrix} = \inf_{\boldsymbol{\mathcal{L}} \in U} \boldsymbol{E} \cdot \boldsymbol{L}\boldsymbol{E} + 2\boldsymbol{E} \cdot \boldsymbol{A} + k.$$

In the case where U consists of a set of n tensors $\boldsymbol{\mathcal{L}}_1, \boldsymbol{\mathcal{L}}_2, \ldots, \boldsymbol{\mathcal{L}}_n$, the function $F(\boldsymbol{E})$ is the minimum of a set of arbitrary quadratic wells. We just need to position these wells in the right places, choosing sufficiently many of them, and choosing them to be sufficiently narrow, so that $F(\boldsymbol{E})$ almost matches $W(\boldsymbol{E})$.

Specifically, suppose that a twice differentiable function $W(\boldsymbol{E})$ is given and take U to consist of all tensors of the form

$$\boldsymbol{\mathcal{L}} = \begin{pmatrix} \sigma_0\boldsymbol{I} & W'(\boldsymbol{B})/2 - \sigma_0\boldsymbol{B} \\ [W'(\boldsymbol{B})/2 - \sigma_0\boldsymbol{B}]^T & W(\boldsymbol{B}) - \boldsymbol{B} \cdot W'(\boldsymbol{B}) + \sigma_0\boldsymbol{B} \cdot \boldsymbol{B} \end{pmatrix},$$

as $\boldsymbol{B}$ ranges over a set S in tensor space consisting, say, of tensors $\boldsymbol{B}$ with $|\boldsymbol{B}| < r$, where r is large. Here $W'(\boldsymbol{B}) = dW/d\boldsymbol{B}$ and σ_0 is a fixed large constant that remains to be determined. The form of $\boldsymbol{\mathcal{L}}$ has been chosen so that $F(\boldsymbol{E})$ is simply

$$F(\boldsymbol{E}) = \inf_{\boldsymbol{B} \in S} \sigma_0(\boldsymbol{E}-\boldsymbol{B}) \cdot (\boldsymbol{E}-\boldsymbol{B}) + (\boldsymbol{E}-\boldsymbol{B}) \cdot W'(\boldsymbol{B}) + W(\boldsymbol{B}), \tag{31.15}$$

where the quadratic function appearing in the infimum takes the value $W(\boldsymbol{B})$ and has derivative $W'(\boldsymbol{B})$ at $\boldsymbol{E} = \boldsymbol{B}$. If for $\boldsymbol{E} \in S$ the infimum is achieved at $\boldsymbol{B} = \boldsymbol{E}$, then we can identify $F(\boldsymbol{E})$ with $W(\boldsymbol{E})$. This will be the case if for all $\boldsymbol{B} \in S$

$$\sigma_0(\boldsymbol{E}-\boldsymbol{B}) \cdot (\boldsymbol{E}-\boldsymbol{B}) + (\boldsymbol{E}-\boldsymbol{B}) \cdot W'(\boldsymbol{B}) + W(\boldsymbol{B}) \geq W(\boldsymbol{E}).$$

We choose

$$\sigma_0 > \sup_{\substack{\boldsymbol{E} \in S,\ \boldsymbol{B} \in S \\ \boldsymbol{B} \neq \boldsymbol{E}}} \frac{W(\boldsymbol{E}) - W(\boldsymbol{B}) - (\boldsymbol{E}-\boldsymbol{B}) \cdot W'(\boldsymbol{B})}{(\boldsymbol{E}-\boldsymbol{B}) \cdot (\boldsymbol{E}-\boldsymbol{B})},$$

so this is satisfied for all $\boldsymbol{E} \in S$. The assumption that W is twice differentiable ensures that the expression on the right-hand side remains finite as $\boldsymbol{B}$ approaches $\boldsymbol{E}$.

Outside the set S the function $F(\boldsymbol{E})$ will have quadratic growth as $\boldsymbol{E} \to \infty$. One expects that pointwise $QF(\boldsymbol{E})$ will approach $QW(\boldsymbol{E})$ in the limit as $r \to \infty$, since $F(\boldsymbol{E})$ converges pointwise to $W(\boldsymbol{E})$. In this case the problem of quasiconvexifying a twice differentiable function $W(\boldsymbol{E})$ can regarded as the limit of a sequence of generalized thermoelastic-type composite problems involving energy minimization.

31.5. The link between the lamination closure and Λ-convexification

Given an n-phase composite with component tensors $\boldsymbol{L}_1, \boldsymbol{L}_2, \ldots, \boldsymbol{L}_n$, we have seen that finding the best possible lower bound on the energy

$$\boldsymbol{E}_0 \cdot \boldsymbol{L}_* \boldsymbol{E}_0 = \inf_{\substack{\boldsymbol{E} \in \mathcal{U} \oplus \mathcal{E} \\ \langle \boldsymbol{E} \rangle = \boldsymbol{E}_0}} \langle \sum_{i=1}^{n} \chi_i \boldsymbol{E} \cdot \boldsymbol{L}_i \boldsymbol{E} \rangle,$$

is equivalent to the problem of quasiconvexifying the function

$$W(\boldsymbol{E}) = \min\{\boldsymbol{E} \cdot \boldsymbol{L}_1 \boldsymbol{E}, \boldsymbol{E} \cdot \boldsymbol{L}_2 \boldsymbol{E}, \ldots, \boldsymbol{E} \cdot \boldsymbol{L}_n \boldsymbol{E}\}.$$

Moreover, we have seen in 30.3 on page 647 that knowing the best possible lower bounds on the energy, or on sums of energies and complimentary energies, provides a complete characterization of the G-closure, GU, of the set of tensors $U = \{\boldsymbol{L}_1, \boldsymbol{L}_2, \ldots, \boldsymbol{L}_n\}$.

It turns out that there is also a connection between finding the lamination closure of the set of tensors U and the Λ-convexification of $W(\boldsymbol{E})$. For simplicity, let us assume that the space $\mathcal{U} \oplus \mathcal{E}$ is comprised of periodic functions that are gradients of m-component potentials, that is, $\boldsymbol{E} = \nabla \boldsymbol{u}$ for some potential $\boldsymbol{u}$. Then Λ-convexification is equivalent to rank-1 convexification. Now consider the "1-step lamination process" where we take a set of tensors U, pick a fixed direction $\boldsymbol{n}$, and then laminate each pair of materials in U in volume fractions

varying continuously from 0 to 1, to get a set of tensors U_1. Associated with U and U_1 are energy functions

$$W(\boldsymbol{E}) = \min_{\boldsymbol{L}\in U}\{\boldsymbol{E}\cdot\boldsymbol{L}\boldsymbol{E}\}, \qquad W_1(\boldsymbol{E}) = \min_{\boldsymbol{L}\in U_1}\{\boldsymbol{E}\cdot\boldsymbol{L}\boldsymbol{E}\}.$$

The "1-step lamination process" can then be applied to U_1 with a different choice of the direction $\boldsymbol{n}$ to obtain a set of tensors U_2 having an associated energy function $W_2(\boldsymbol{E})$. By repeating this process, and choosing the direction of lamination randomly at each stage, the set U_j as j tends to infinity ultimately converges to the lamination closure LU of the set U.

We can also consider a "1-step rank-1 convexification process" applied to the energy function $W(\boldsymbol{E})$, where we take a fixed direction $\boldsymbol{n}$ and compute

$$W^1(\boldsymbol{E}) = \min_{\substack{f \\ 0\le f\le 1}} \min_{\boldsymbol{v}} \left[f W(\boldsymbol{E} + (1-f)\boldsymbol{n}\otimes\boldsymbol{v}) + (1-f)W(\boldsymbol{E} - f\boldsymbol{n}\otimes\boldsymbol{v})\right]. \tag{31.16}$$

Thus, given $\boldsymbol{E}$ we can find matrices $\boldsymbol{E}_a$ and $\boldsymbol{E}_b$ [namely, $\boldsymbol{E}_a = \boldsymbol{E} + (1-f)\boldsymbol{n}\otimes\boldsymbol{v}$ and $\boldsymbol{E}_b = \boldsymbol{E} - f\boldsymbol{n}\otimes\boldsymbol{v}$ where f and $\boldsymbol{v}$ achieve the minimum in (31.16)] such that $\boldsymbol{E}_a - \boldsymbol{E}_b$ is rank-1 of the form $\boldsymbol{n}\otimes\boldsymbol{v}$ for some $\boldsymbol{v}$ and such that

$$W^1(\boldsymbol{E}) = fW(\boldsymbol{E}_a) + (1-f)W(\boldsymbol{E}_b), \quad \boldsymbol{E} = f\boldsymbol{E}_a + (1-f)\boldsymbol{E}_b, \tag{31.17}$$

for some value of f with $0 \le f \le 1$. Moreover, $W^1(\boldsymbol{E})$ is the lowest such function with this property. The "1-step rank-1 convexification process" can then be applied to $W^1(\boldsymbol{E})$ with a different choice of the direction $\boldsymbol{n}$ to obtain a function $W^2(\boldsymbol{E})$. By repeating this process, and choosing the direction of lamination randomly at each stage, the function W^j as j tends to infinity ultimately converges to the rank-1 convexification of the function $W(\boldsymbol{E})$. This procedure is known as the Kohn-Strang algorithm for computing the rank-1 convexification (Kohn and Strang 1986).

Our goal is to establish a correspondence between these two "1-step processes" specifically to show that $W^j(\boldsymbol{E}) = W_j(\boldsymbol{E})$ for all j. First we consider the case $j = 1$. Given $\boldsymbol{E}$ we can find matrices $\boldsymbol{E}_a$ and $\boldsymbol{E}_b$ such that (31.17) holds. Also, the definition of $W(\boldsymbol{E})$ implies that there exist tensors $\boldsymbol{L}_a, \boldsymbol{L}_b \in U$ such that

$$W(\boldsymbol{E}_a) = \boldsymbol{E}_a\cdot\boldsymbol{L}_a\boldsymbol{E}_a, \quad W(\boldsymbol{E}_b) = \boldsymbol{E}_b\cdot\boldsymbol{L}_b\boldsymbol{E}_b.$$

By laminating materials a and b with tensors $\boldsymbol{L}_a$ and $\boldsymbol{L}_b$ in direction $\boldsymbol{n}$ in proportions f and $1-f$ we obtain a composite with effective tensor $\boldsymbol{L}_* \in U_1$. Now the field

$$\begin{aligned} \boldsymbol{E}(\boldsymbol{x}) &= \boldsymbol{E}_a \quad \text{in material } a, \\ &= \boldsymbol{E}_b \quad \text{in material } b, \end{aligned} \tag{31.18}$$

can be expressed as the gradient of a potential (because $\boldsymbol{E}_a - \boldsymbol{E}_b = \boldsymbol{n}\otimes\boldsymbol{v}$) and is therefore a perfectly good trial field for substituting into the classical variational principle, giving the inequality

$$\boldsymbol{E}_0\cdot\boldsymbol{L}_*\boldsymbol{E}_0 \le f\boldsymbol{E}_a\cdot\boldsymbol{L}_a\boldsymbol{E}_a + (1-f)\boldsymbol{E}_b\cdot\boldsymbol{L}_b\boldsymbol{E}_b.$$

Also from the definition of $W_1(\boldsymbol{E})$ we have

$$W_1(\boldsymbol{E}_0) \le \boldsymbol{E}_0\cdot\boldsymbol{L}_*\boldsymbol{E}_0.$$

This, coupled with the previous few equations and (31.17), implies that

$$W_1(\boldsymbol{E}_0) \le W^1(\boldsymbol{E}_0).$$

It remains to prove the inequality in the other direction. Given $\boldsymbol{E}_0$ there exists a $\boldsymbol{L}_* \in U_1$ such that

$$W_1(\boldsymbol{E}_0) = \boldsymbol{E}_0 \cdot \boldsymbol{L}_* \boldsymbol{E}_0.$$

Also, since $\boldsymbol{L}_* \in U_1$, there exist tensors $\boldsymbol{L}_a, \boldsymbol{L}_b \in U$ and a volume fraction f such that $\boldsymbol{L}_*$ is the laminate of two materials a and b with tensors $\boldsymbol{L}_a$ and $\boldsymbol{L}_b$ layered in direction $\boldsymbol{n}$ in proportions f and $1-f$. Let $\boldsymbol{E}(\boldsymbol{x})$ be the actual field in the laminate when the average field is prescribed to be $\boldsymbol{E}_0$. The field $\boldsymbol{E}(\boldsymbol{x})$ is piecewise constant, of the form (31.18) with $\boldsymbol{E}_a - \boldsymbol{E}_b = \boldsymbol{n} \otimes \boldsymbol{v}$ for some $\boldsymbol{v}$. Also, the "energy" in the laminate is the sum of the energies in the two phases, that is,

$$\boldsymbol{E}_0 \cdot \boldsymbol{L}_* \boldsymbol{E}_0 = f \boldsymbol{E}_a \cdot \boldsymbol{L}_a \boldsymbol{E}_a + (1-f) \boldsymbol{E}_b \cdot \boldsymbol{L}_b \boldsymbol{E}_b,$$

and because the average of $\boldsymbol{E}(\boldsymbol{x})$ is $\boldsymbol{E}_0$ we have $\boldsymbol{E}_0 = f\boldsymbol{E}_a + (1-f)\boldsymbol{E}_b$. It follows that

$$\begin{aligned} W_1(\boldsymbol{E}_0) &= f \boldsymbol{E}_a \cdot \boldsymbol{L}_a \boldsymbol{E}_a + (1-f) \boldsymbol{E}_b \cdot \boldsymbol{L}_b \boldsymbol{E}_b \\ &\ge f W(\boldsymbol{E}_a) + (1-f) W(\boldsymbol{E}_b) \ge W^1(f\boldsymbol{E}_a + (1-f)\boldsymbol{E}_b) = W^1(\boldsymbol{E}_0), \end{aligned}$$

where the last inequality follows from the definition of W^1. This establishes that $W^1(\boldsymbol{E}) = W_1(\boldsymbol{E})$.

Repetition of the same argument then implies that $W^j(\boldsymbol{E}) = W_j(\boldsymbol{E})$ for all j. Finally, by taking the limit $j \to \infty$ we conclude that the energy function associated with LU equals the rank-1 convexification of the energy function $W(\boldsymbol{E})$ associated with U. This result was also established independently by Allaire and Lods (1999) while this book was being written.

31.6. Quasiconvex hulls and rank-1 convex hulls

Suppose that a periodic gradient field $\nabla \boldsymbol{u}(\boldsymbol{x})$ is such that it takes values in (or arbitrarily close to) a set $\mathcal{K}$, almost everywhere. The quasiconvex hull $Q\mathcal{K}$ of $\mathcal{K}$ is, roughly speaking, the set of all possible values of $\langle \nabla \boldsymbol{u} \rangle$. More precisely, the quasiconvex hull is defined via

$$Q\mathcal{K} \equiv \{\boldsymbol{E} \mid Q(\boldsymbol{E}) \le \sup_{\boldsymbol{E}' \in \mathcal{K}} Q(\boldsymbol{E}') \text{ for all quasiconvex functions } Q\}.$$

Thus if $Q(\boldsymbol{E})$ is quasiconvex and less than a constant c on the set $\mathcal{K}$, then it will also be less than c on the set $Q\mathcal{K}$. Clearly this definition implies that $Q\mathcal{K}$ contains $\mathcal{K}$. Also, if the quasiconvexity requirement on Q is replaced by the stronger condition of convexity, then the resulting set would be $C\mathcal{K}$, the closed convex hull of $\mathcal{K}$. It follows that $Q\mathcal{K}$ is contained in $C\mathcal{K}$.

To find $Q\mathcal{K}$ it suffices to take a single test function $W(\boldsymbol{E})$ that is nonnegative and zero if and only if $\boldsymbol{E} \in \mathcal{K}$; then $Q\mathcal{K}$ is identified with the set of values of $\boldsymbol{E}$ where $QW(\boldsymbol{E}) = 0$. The proof that this set is $Q\mathcal{K}$ follows directly from Theorem 4.10 of Müller (1998), which is partly based on unpublished lectures of Šverák. There it is shown that a matrix $\boldsymbol{E}_0$ is an element of $Q\mathcal{K}$ if and only if there exists a sequence of gradients $\nabla \boldsymbol{u}_j(\boldsymbol{x})$ each having average value $\boldsymbol{E}_0$ (and satisfying affine or periodic boundary conditions) such that the distance between $\nabla \boldsymbol{u}_j(\boldsymbol{x})$ and the set $\mathcal{K}$ approaches zero almost everywhere as $j \to \infty$. In other words, given

$\boldsymbol{E}_0 \in Q\mathcal{K}$, there must exist a gradient $\nabla \boldsymbol{u}(\boldsymbol{x})$ taking values almost everywhere arbitrarily close to the set $\mathcal{K}$, and such that $\langle \nabla \boldsymbol{u} \rangle = \boldsymbol{E}_0$. Again one can see that $Q\mathcal{K}$ contains $\mathcal{K}$ since, given $\boldsymbol{E}_0 \in \mathcal{K}$, the constant gradient field $\nabla \boldsymbol{u} = \boldsymbol{E}_0$ is admissible and $\langle \nabla \boldsymbol{u} \rangle = \boldsymbol{E}_0$.

The rank-1 convex hull $R\mathcal{K}$ of $\mathcal{K}$ is the set of values taken by $\langle \nabla \boldsymbol{u} \rangle$ as $\nabla \boldsymbol{u}(\boldsymbol{x})$ ranges over all laminate fields satisfying the constraint. Equivalently, it is the set of values of $\boldsymbol{E}$ where $RW(\boldsymbol{E}) = 0$.

More generally, if $\boldsymbol{E}(\boldsymbol{x}) \in \mathcal{U} \oplus \mathcal{E}$ is constrained to a take values arbitrarily close to a set $\mathcal{K}$ almost everywhere, the quasiconvex hull is the set of all possible values of $\langle \boldsymbol{E} \rangle$ while the Λ-convex hull is the set of all possible values of $\langle \boldsymbol{E} \rangle$ when $\boldsymbol{E}(\boldsymbol{x})$ is a laminate field.

In the shape memory material problem mentioned in section 31.1 on page 671, the set $\mathcal{K}$ consists of n-components, called wells, where the j-th well for $j = 1, 2, \ldots, n$ consists of the matrices $\boldsymbol{M}_j^{1/2}\boldsymbol{R}$ as $\boldsymbol{R}$ varies over all rotations. Thus $\mathcal{K}$ can be identified with the set of local deformations that cost no elastic energy and the set $Q\mathcal{K}$ represents the set of macroscopic deformations, each of which costs no elastic energy. Since they cost no energy, these deformations are easily produced and are stress free: They are just as preferable as no deformation, and the material looks like it has undergone plastic deformation. However, when the material is heated the elastic energy function changes and consequently one deformation is preferred and the material reverts to its original shape (hence the name shape memory material). This is illustrated schematically in figure 31.2. In contrast to these recoverable deformations, any stress free deformation outside the set $Q\mathcal{K}$ must be associated with plastic yielding (i.e., some slip in the arrangement of atoms) and therefore is not recoverable when the material is heated.

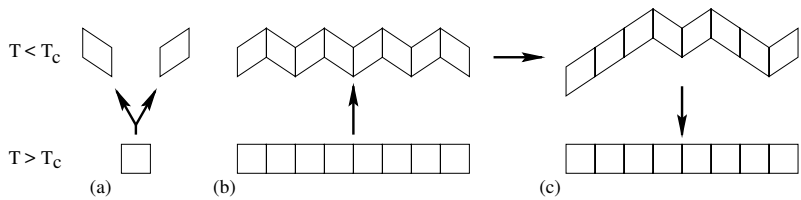

Figure 31.2. Schematic illustration that explains basically why shape memory materials remember their shape. Suppose that a square at high temperature deforms at low temperature to one of two parallelogram "variants" at low temperature as in (a). Then a strip of squares will deform as shown in (b), retaining its overall shape. This zig-zag strip can then be deformed by switching from one variant to the other variant, as in (c) top. When the material is heated, all of the variants revert to squares and the original shape is recovered, as in (c) bottom.

Quasiconvex hulls also arise naturally in the context of bounding the set of recoverable strains of multiphase or polycrystalline shape memory materials [see, for example, Bhattacharya and Kohn (1997)]. Then $\mathcal{K}$ can be identified with the local deformations that cost no elastic energy for at least one choice of phase or crystal orientation and the set $Q\mathcal{K}$ represents the set of macroscopic deformations, each of which costs no elastic energy for at least one microstructure.

Another context in which quasiconvex hulls arise is in bounding yield surfaces in polycrystalline plasticity. The role of the deformation $\nabla \boldsymbol{u}(\boldsymbol{x})$ being replaced by that of the stress $\boldsymbol{\tau}(\boldsymbol{x})$ [see, for example, Kohn and Little (1999)] and the set $\mathcal{K}$ is identified with the set of stresses each of which does not produce any plastic yielding in a crystal grain for at least one choice of crystal orientation. The set $Q\mathcal{K}$ is then the set of possible values of the average

stress when the stress is periodic, divergence free, and takes values in the set $\mathcal{K}$. It provides a bound on the yield surface of the polycrystal. When the average stress lies outside $Q\mathcal{K}$, the local stress field $\boldsymbol{\tau}(\boldsymbol{x})$ must lie outside $\mathcal{K}$ in some region, that is, the material must have undergone plastic yielding in that region. Nontrivial bounds on yield surfaces were first obtained by Ponte Castañeda and DeBotton (1992), Suquet (1993), and Olson (1994).

At first sight the problem of finding the quasiconvex hull looks simple. However, this is far from the truth. The G-closure problem can be recast as a quasiconvex hull-problem. For example, following Tartar (1985), consider three-dimensional conductivity and suppose that the three current fields $\boldsymbol{j}^{(1)}(\boldsymbol{x})$, $\boldsymbol{j}^{(2)}(\boldsymbol{x})$, and $\boldsymbol{j}^{(3)}(\boldsymbol{x})$ and the three electric fields $\boldsymbol{e}^{(1)}(\boldsymbol{x})$, $\boldsymbol{e}^{(2)}(\boldsymbol{x})$, and $\boldsymbol{e}^{(3)}(\boldsymbol{x})$ solve the conductivity equations in a medium with conductivity tensor $\boldsymbol{\sigma}(\boldsymbol{x})$ taking values in a set U. As in section 24.6 on page 506, let $\boldsymbol{j}^{(1)}(\boldsymbol{x})$, $\boldsymbol{j}^{(2)}(\boldsymbol{x})$, and $\boldsymbol{j}^{(3)}(\boldsymbol{x})$ form the columns of a 3×3 matrix-valued field $\boldsymbol{J}(\boldsymbol{x})$ and let $\boldsymbol{e}^{(1)}(\boldsymbol{x})$, $\boldsymbol{e}^{(2)}(\boldsymbol{x})$, and $\boldsymbol{e}^{(3)}(\boldsymbol{x})$ form the columns of a 3×3 matrix-valued field $\boldsymbol{E}(\boldsymbol{x})$. Then the constitutive law takes the form $\boldsymbol{J}(\boldsymbol{x}) = \boldsymbol{\sigma}(\boldsymbol{x})\boldsymbol{E}(\boldsymbol{x})$, where $\boldsymbol{\sigma}(\boldsymbol{x})$ acts on $\boldsymbol{E}(\boldsymbol{x})$ by matrix multiplication. Now define $\widetilde{\mathcal{U}} \oplus \widetilde{\mathcal{E}}$ as the set of all 3×6 matrix-valued fields of the form

$$\widetilde{\boldsymbol{E}}(\boldsymbol{x}) = \begin{pmatrix} \boldsymbol{E}(\boldsymbol{x}) & \boldsymbol{J}(\boldsymbol{x}) \end{pmatrix}, \tag{31.19}$$

where the three columns of $\boldsymbol{E}(\boldsymbol{x})$ are curl free while the three columns of $\boldsymbol{J}(\boldsymbol{x})$ are divergence free. The subspaces $\widetilde{\mathcal{U}}$ and $\widetilde{\mathcal{E}}$ then consist of all fields in $\widetilde{\mathcal{U}} \oplus \widetilde{\mathcal{E}}$ that are respectively constant or which have zero average value.

We take $\widetilde{\mathcal{K}}$ as the set of all values taken by the 3×6 matrix

$$\widetilde{\boldsymbol{V}} = \begin{pmatrix} \boldsymbol{V} & \boldsymbol{\sigma}\boldsymbol{V} \end{pmatrix},$$

as $\boldsymbol{\sigma}$ ranges over all tensors in the set U and as $\boldsymbol{V}$ ranges over all 3×3 matrices. If the field in (31.19) takes values in $\widetilde{\mathcal{K}}$, then clearly the constitutive law

$$\boldsymbol{J}(\boldsymbol{x}) = \boldsymbol{L}(\boldsymbol{x})\boldsymbol{E}(\boldsymbol{x})$$

is satisfied for some choice of the tensor field $\boldsymbol{L}(\boldsymbol{x})$ taking values in U. Therefore, when $\widetilde{\boldsymbol{E}} \in \widetilde{\mathcal{U}} \oplus \widetilde{\mathcal{E}}$, the possible values of

$$\langle \overline{\boldsymbol{E}} \rangle = \begin{pmatrix} \langle \boldsymbol{E} \rangle & \langle \boldsymbol{J} \rangle \end{pmatrix}$$

lie in the set $Q\widetilde{\mathcal{K}}$ comprised of all 3×6 matrices

$$\overline{\boldsymbol{W}} = \begin{pmatrix} \boldsymbol{W} & \boldsymbol{\sigma}_*\boldsymbol{W} \end{pmatrix},$$

as $\boldsymbol{\sigma}_*$ ranges over tensors in the set GU and as $\boldsymbol{W}$ ranges over the tensor space $\mathcal{T}$. Clearly we can determine $Q\widetilde{\mathcal{K}}$ if we know GU. Conversely, if we know $Q\widetilde{\mathcal{K}}$, then the intersection of $Q\widetilde{\mathcal{K}}$ with the set of all 3×6 matrices of the form $(\boldsymbol{I} \;\; \boldsymbol{A})$ gives us the set of all matrices of the form $(\boldsymbol{I} \;\; \boldsymbol{\sigma}_*)$, where $\boldsymbol{\sigma}_* \in GU$. In this way we determine GU.

31.7. Laminate fields built from rank-1 incompatible matrices

Calculating the rank-1 convex hull of a set of matrices is not as simple as one might expect, as was found independently in different contexts by Aumann and Hart (1986); Casadio-Tarabusi (1993); Tartar (1993); and Bhattacharya, Firoozye, James, and Kohn (1994). The underlying idea of introducing an appropriate seed material was also discovered in the (cyclic laminate)

construction of isotropic polycrystals having minimum conductivity amongst all polycrystals formed from a fully anisotropic crystal (Nesi and Milton 1991); see section 25.4 on page 537. Here we follow the example of Tartar (1993) as presented by Müller (1998).

Let $\boldsymbol{u}$ be a two-dimensional, two-component vector field, and suppose that we want to construct a two-dimensional laminate field $\nabla\boldsymbol{u}$ that equals one of the four matrices

$$\boldsymbol{A}_1 = -\boldsymbol{A}_3 = \begin{pmatrix} 1 & 0 \\ 0 & 3 \end{pmatrix}, \quad \boldsymbol{A}_2 = -\boldsymbol{A}_4 = \begin{pmatrix} -3 & 0 \\ 0 & 1 \end{pmatrix},$$

almost everywhere. One cannot laminate $\boldsymbol{A}_i$ with $\boldsymbol{A}_j$ when $j \neq i$ because $\det(\boldsymbol{A}_i - \boldsymbol{A}_j) \neq 0$. Since there are no rank-1 connections between any of these matrices, one might think that $\nabla\boldsymbol{u}$ would have to be constant. However, this is not the case.

It is helpful to consider the restricted space $\mathcal{A}$ of 2×2 diagonal matrices

$$\boldsymbol{E} = \begin{pmatrix} r & 0 \\ 0 & s \end{pmatrix}.$$

Using r and s as coordinates, the matrices $\boldsymbol{A}_1$, $\boldsymbol{A}_2$, $\boldsymbol{A}_3$, and $\boldsymbol{A}_4$ are represent by the points $(1, 3)$, $(-3, 1)$, $(-1, -3)$, and $(3, 1)$, as illustrated in figure 31.3 on the facing page. Rank-1 connected matrices in $\mathcal{A}$ have the same value of r or the same value of s. The key idea is to introduce a seed matrix $\boldsymbol{J}_1 = (1, 1)$ that is rank-1 connected with $\boldsymbol{A}_2$ (and $\boldsymbol{A}_1$). By laminating $\boldsymbol{J}_1$ and $\boldsymbol{A}_2$ together in equal proportions in direction $\boldsymbol{n} = (1, 0)$ one obtains a simple laminate field with average value $\boldsymbol{J}_2 = (-1, 1)$, which is rank-1 connected with $\boldsymbol{A}_3$, as illustrated in figure 31.3 on the next page. By laminating this simple laminate field together with $\boldsymbol{A}_3$ in equal proportions in direction $\boldsymbol{n} = (0, 1)$ one obtains a second-rank laminate field with average value $\boldsymbol{J}_3 = (-1, -1)$, which is rank-1 connected with $\boldsymbol{A}_4$. We now continue the process cyclically, laminating the second-rank laminate field with $\boldsymbol{A}_4$ to obtain a third-rank laminate field with average value $\boldsymbol{J}_4 = (1, -1)$, laminating the third-rank laminate field with $\boldsymbol{A}_1$ to obtain a fourth-rank laminate field with average value $\boldsymbol{J}_1$, and so forth. At each stage the volume fraction occupied by the original seed matrix decreases. Ultimately, in the resulting infinite-rank laminate, illustrated in figure 31.4 on the facing page, the seed material occupies an infinitesimal volume fraction and $\nabla\boldsymbol{u}$ equals one of the four matrices $\boldsymbol{A}_1$, $\boldsymbol{A}_2$, $\boldsymbol{A}_3$, or $\boldsymbol{A}_4$ almost everywhere. Depending at which stage one stops, $\langle\nabla\boldsymbol{u}\rangle$ approaches one of the four matrices $\boldsymbol{J}_1$, $\boldsymbol{J}_2$, $\boldsymbol{J}_3$, or $\boldsymbol{J}_4$. By adding these four matrices to the original set, and then laminating together matrices with the same value of r or the same value of s, one sees that the rank-1 convex hull includes the square $1 \geq r \geq -1$, $1 \geq s \geq -1$ and the four arm segments $[\boldsymbol{J}_i, \boldsymbol{A}_i]$, $i = 1, 2, 3, 4$.

31.8. Example of a rank-1 function that is not quasiconvex†

For functions $W(\nabla\boldsymbol{u})$ of gradients of ℓ-component potentials $\boldsymbol{u}$ in d-dimensions Morrey (1952) conjectured that rank-1 convexity does not imply quasiconvexity when $\ell \geq 2$ or $d \geq 2$. Later Morrey (1966) suggested that rank-1 convexity may in fact be equivalent to quasiconvexity. However, a counterexample which showed that rank-1 convexity does not imply quasiconvexity when $\ell \geq 3$ and $d \geq 2$ was given by Šverák (1992) [see also page 185 of Tartar (1979) for a closely related counterexample]. Whether rank-1 convexity equals quasiconvexity when $d = 2$ and $\ell \geq 2$ remains an open question (Parry 1995; Dacorogna and Haeberly 1996, 1998; Pedregal 1996; Pedregal and Šverák 1998).

The following example of a rank-1 convex function that is not quasiconvex is an adaptation of the example given by Šverák (1992) and of a variant of James and Kohn [discussed

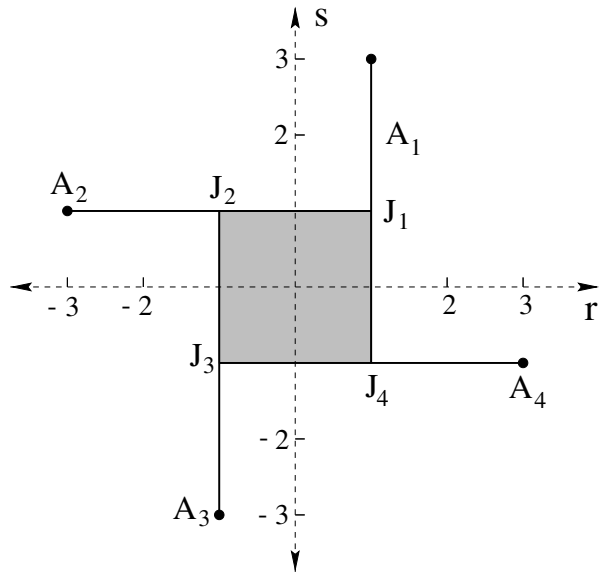

Figure 31.3. Although the four matrices represented by the points $\boldsymbol{A}_1$, $\boldsymbol{A}_2$, $\boldsymbol{A}_3$, and $\boldsymbol{A}_4$ have no rank-1 connections (corresponding to connections by vertical or horizontal lines in this figure) one can nevertheless construct an infinite-rank laminate field such that $\nabla \boldsymbol{u}$ takes one of these four values almost everywhere. The key is to introduce a seed matrix $\boldsymbol{J}_1$ that is laminated with $\boldsymbol{A}_2$, $\boldsymbol{A}_3$, $\boldsymbol{A}_4$, and $\boldsymbol{A}_1$ in cyclic order until the seed matrix occupies an infinitesimal volume fraction.

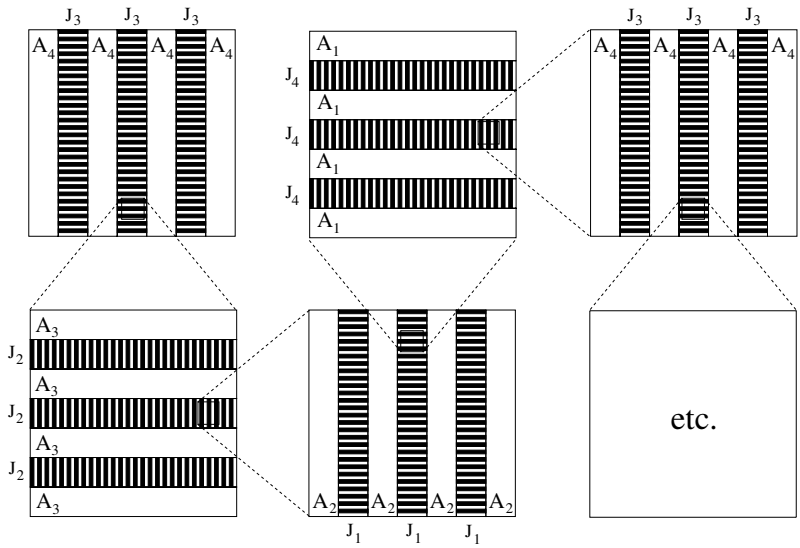

Figure 31.4. The infinite-rank laminate field corresponding to the previous figure. Here $\boldsymbol{J}_3$, $\boldsymbol{J}_2$, $\boldsymbol{J}_1$, and $\boldsymbol{J}_4$ are averages of $\nabla \boldsymbol{u}$ within the corresponding region.

by Pedregal (1996, 1997) and Müller (1998)], which is modified here to lay the basis for constructing a composite with an effective elasticity tensor that cannot be mimicked by a multiple-rank laminate material.

As a warmup exercise, consider the restricted space $\mathcal{A}$ of 3×2 matrices $\boldsymbol{E}$ of the form

$$\boldsymbol{E} = \begin{pmatrix} r & 0 & t \\ 0 & s & t \end{pmatrix},$$

and the function

$$G(\boldsymbol{E}) = (r+1)^2(s+1)^2(t+1)^2. \tag{31.20}$$

The rank-1 matrices within $\mathcal{A}$ are of the form $\lambda \boldsymbol{Y}$, where

$$\boldsymbol{Y} = \begin{pmatrix} 1 & 0 & 0 \\ 0 & 0 & 0 \end{pmatrix}, \quad \boldsymbol{Y} = \begin{pmatrix} 0 & 0 & 0 \\ 0 & 1 & 0 \end{pmatrix} \quad \text{or} \quad \boldsymbol{Y} = \begin{pmatrix} 0 & 0 & 1 \\ 0 & 0 & 1 \end{pmatrix}.$$

Consequently, the function $G(\boldsymbol{E})$ is rank-1 convex on the space $\mathcal{A}$ because $G(\boldsymbol{E} + \lambda \boldsymbol{Y})$ is a quadratic function of λ with a nonnegative coefficient in front of the λ^2 term. More generally, any function is rank-1 convex on $\mathcal{A}$ if and only if it is convex in each variable r, s, and t separately.

Now consider the vector potential

$$\boldsymbol{u} = \big(h(x_1), h(x_2), h(x_1 + x_2 + 2) \big), \tag{31.21}$$

in which $h(y)$ is the periodic sawtooth function

$$\begin{aligned} h(y) &= 3y && \text{for } 0 \le y \le 1, \\ &= 4 - y && \text{for } 1 \le y \le 4, \\ &= h(y-4) && \text{for all } y. \end{aligned} \tag{31.22}$$

Clearly $\boldsymbol{u}$ is periodic with unit cell $0 \le x_1 \le 4$, $0 \le x_2 \le 4$. It is the superposition of three sawtooth waves $(h(x_1), 0, 0)$, $(0, h(x_2), 0)$, and $(0, 0, h(x_1 + x_2 + 2))$ with oscillations along the x_1-axis, x_2-axis, and at 45° to the axes, respectively. When three sawtooth waves oscillating in three different directions are superimposed the gradient of the resulting function typically takes either seven or eight different values. The function $\boldsymbol{u}$ has been chosen so that $\nabla \boldsymbol{u}$ is piecewise constant taking only the seven values,

$$\begin{aligned} &\boldsymbol{A}_1 = \begin{pmatrix} 3 & 0 & -1 \\ 0 & 3 & -1 \end{pmatrix}, \quad \boldsymbol{A}_2 = \begin{pmatrix} -1 & 0 & -1 \\ 0 & 3 & -1 \end{pmatrix}, \quad \boldsymbol{A}_3 = \begin{pmatrix} -1 & 0 & 3 \\ 0 & 3 & 3 \end{pmatrix}, \\ &\boldsymbol{A}_4 = \begin{pmatrix} 3 & 0 & -1 \\ 0 & -1 & -1 \end{pmatrix}, \quad \boldsymbol{A}_5 = \begin{pmatrix} 3 & 0 & 3 \\ 0 & -1 & 3 \end{pmatrix}, \quad \boldsymbol{A}_6 = \begin{pmatrix} -1 & 0 & 3 \\ 0 & -1 & 3 \end{pmatrix}, \\ &\boldsymbol{A}_7 = \begin{pmatrix} -1 & 0 & -1 \\ 0 & -1 & -1 \end{pmatrix}, \end{aligned} \tag{31.23}$$

in the respective regions shown in figure 31.5 on the next page, each occupying volume fractions $f_1, f_2, \ldots, f_7$, where

$$f_1 = f_3 = f_5 = 1/16, \quad f_2 = f_4 = f_6 = 1/8, \quad f_7 = 7/16.$$

The phase of the sawtooth wave $(0, 0, h(x_1 + x_2 + 2))$ has been adjusted so that the matrix

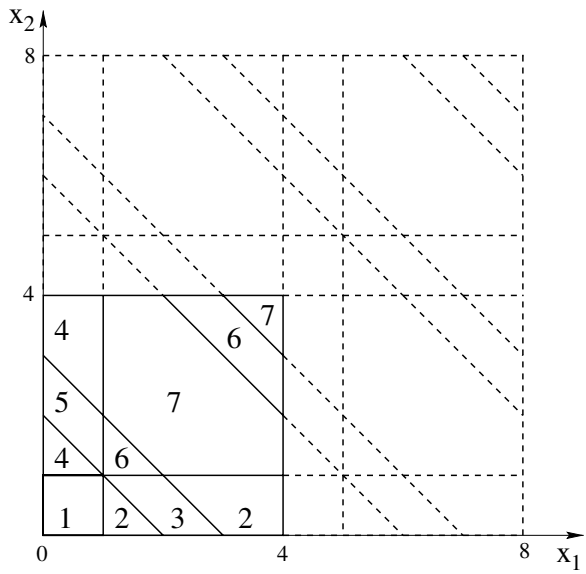

Figure 31.5. The unit cell of periodicity for $\nabla \boldsymbol{u}$, and three neighboring period cells. Shown are the seven different regions within each of which $\nabla \boldsymbol{u}$ is constant, taking the corresponding value given in (31.23). This figure also represents the cross section of a three-dimensional, seven-phase columnar microstructure, discussed in section 31.9 on page 690, whose elasticity tensor cannot be mimicked by a multiple-rank laminate material.

with $r = s = t = 3$ does not appear as a value of $\nabla \boldsymbol{u}$. Each of these matrices $\boldsymbol{A}_i$ lie in the space $\mathcal{A}$ and have $G(\boldsymbol{A}_i) = 0$. Consequently we have

$$\langle G(\nabla \boldsymbol{u}) \rangle = \sum_{i=1}^{7} f_i G(\boldsymbol{A}_i) = 0 < G(\langle \nabla \boldsymbol{u} \rangle) = G(0) = 1,$$

in which $\langle \nabla \boldsymbol{u} \rangle = 0$ because $\boldsymbol{u}$ is periodic. Therefore on the space $\mathcal{A}$ the function $G(\boldsymbol{E})$ is rank-1 convex but not quasiconvex.

One can now see that if a given multiple-rank (possibly infinite-rank) laminate field $\nabla \boldsymbol{u}$ takes the seven values $\boldsymbol{A}_1, \boldsymbol{A}_2, \ldots \boldsymbol{A}_7$ almost everywhere, then the values that $\langle \nabla \boldsymbol{u} \rangle$ can take are quite restricted. We use a result established in lemma 9.9 of Pedregal (1997) that the laminate field can be approximated by a sequence of finite-rank laminate fields $\nabla \boldsymbol{u}^k$, $k = 1, 2, \ldots$, each taking values in the convex hull of the matrices $\boldsymbol{A}_1, \boldsymbol{A}_2, \ldots \boldsymbol{A}_7$ (and having Young's measures converging as $k \to \infty$ to the Young's measure of the given laminate field). Since these finite-rank laminate fields take values in the space $\mathcal{A}$, we have the constraint $G(\langle \nabla \boldsymbol{u}^k \rangle) \leq \langle G(\nabla \boldsymbol{u}^k) \rangle$ arising from rank-1 convexity. Taking the limit $k \to \infty$ gives the constraint $G(\langle \nabla \boldsymbol{u} \rangle) \leq \langle G(\nabla \boldsymbol{u}) \rangle = 0$. On the other hand $\langle \nabla \boldsymbol{u} \rangle$, being an average, must lie in the convex hull of the matrices $\boldsymbol{A}_1, \boldsymbol{A}_2, \ldots \boldsymbol{A}_7$, that is, where $G(\langle \nabla \boldsymbol{u} \rangle) \geq 0$. These constraints force $\langle \nabla \boldsymbol{u} \rangle$ in a multiple-rank laminate field to lie on one of the three surfaces $r = -1$, $s = -1$, or $t = -1$, where $G(\langle \nabla \boldsymbol{u} \rangle) = 0$, and to satisfy the inequalities $3 \geq r \geq -1$, $3 \geq s \geq -1$, and $3 \geq t \geq -1$.

In other words, $\langle \nabla \boldsymbol{u} \rangle$ for a laminate field must lie on one of the three cube surfaces illustrated in figure 31.6 on the following page, while $\langle \nabla \boldsymbol{u} \rangle = 0$ for the potential (31.21). This

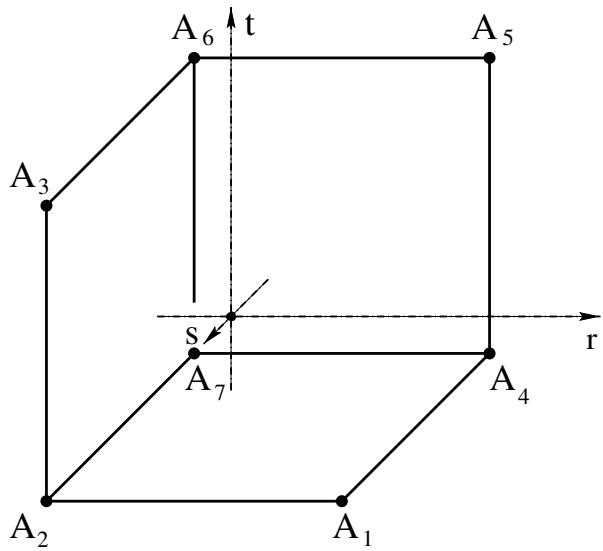

Figure 31.6. If a field $\nabla \boldsymbol{u}$ in a multiple-rank laminate takes the seven values $\boldsymbol{A}_1, \boldsymbol{A}_2, \ldots \boldsymbol{A}_7$ almost everywhere in the material, then the average field $\langle \nabla \boldsymbol{u} \rangle$ must lie on one of the three cube faces illustrated here. By contrast, the microstructure of 31.5 has $\langle \nabla \boldsymbol{u} \rangle = 0$, which lies in the middle of the cube.

provides an example of a set $\mathcal{K}$ of seven matrices for which $R\mathcal{K}$ is not equal to $Q\mathcal{K}$. Another example of a set of eight 6×2 real matrices (or, equivalently, eight 3×2 complex matrices) for which $R\mathcal{K}$ is not equal to $Q\mathcal{K}$ has been found by Šverák and is discussed in the lecture notes of Müller (1998). His example is especially interesting because $Q\mathcal{K}$ equals $R\mathcal{K}$ plus a matrix, which is disconnected from $R\mathcal{K}$.

We are now essentially finished due to an argument of Pedregal (1997). Take $W(\boldsymbol{E})$ as any nonnegative-valued function that is zero at and only at $\boldsymbol{E} = \boldsymbol{A}_i$, $i = 1, 2, \ldots, 7$. Clearly both $RW(\boldsymbol{E})$ and $QW(\boldsymbol{E})$ are nonnegative-valued functions. Also, by taking $\boldsymbol{E}(\boldsymbol{x})$ to be the field $\nabla \boldsymbol{u}$ where $\boldsymbol{u}$ is given by (31.21), the inequality

$$QW(\langle \boldsymbol{E} \rangle) \leq \langle W(\boldsymbol{E}) \rangle = \sum_{i=1}^{7} f_i W(\boldsymbol{A}_i) = 0$$

then implies that $QW(0) = 0$. However, if $RW(0) = 0$, then there would exist a laminate field taking the values $\boldsymbol{A}_1, \boldsymbol{A}_2, \ldots \boldsymbol{A}_7$ almost everywhere, and having $\langle \nabla \boldsymbol{u} \rangle = 0$. But we have seen that this is impossible, implying that $RW(0) > 0$. Consequently, RW is an example of a rank-1 convex function that is not quasiconvex.

To obtain an explicit example requires some extra work. Those readers not interested in the details can skip to the next section. Here we adapt the example of Šverák (1992) to obtain a rank-1 convex function that is not quasiconvex, having quadratic growth as $|\boldsymbol{E}| \to \infty$. (The quadratic growth will be useful in the next section.) First one uses $G(\boldsymbol{E})$ to obtain a function $G_1(\boldsymbol{E})$ that is rank-1 convex and bounded on the set comprised of all 2×3 matrices $\boldsymbol{E}$ with $|\boldsymbol{E}|$ less than r. The radius r needs to be chosen sufficiently large so that each of the seven matrices $\boldsymbol{A}_i$ have $|\boldsymbol{A}_i| < r$. (Thus it suffices to take $r > \sqrt{28}$.) We let $\boldsymbol{\Pi}$ denote the natural

projection onto matrices in the subspace $\mathcal{A}$:

$$\mathbf{\Pi}\begin{pmatrix} a & b & c \\ d & e & f \end{pmatrix} = \begin{pmatrix} a & 0 & (c+f)/2 \\ 0 & e & (c+f)/2 \end{pmatrix}.$$

Then we select some positive number $\epsilon < 1/r^2$ and set

$$G_1(\boldsymbol{E}) = G(\mathbf{\Pi}\boldsymbol{E}) + \epsilon(|\boldsymbol{E}|^2 - r^2) + k|\boldsymbol{E} - \mathbf{\Pi}\boldsymbol{E}|^2.$$

The claim is that k can be chosen positive and large enough to ensure the rank-1 convexity of $G_1(\boldsymbol{E})$ for $|\boldsymbol{E}| \le r$. The rank-1 convexity is ensured if for all rank-1 matrices $\boldsymbol{Y}$ with $|\boldsymbol{Y}| = 1$ and all matrices $|\boldsymbol{E}| \le r$, we have

$$\left.\frac{d^2 G_1(\boldsymbol{E}+\lambda\boldsymbol{Y})}{d\lambda^2}\right|_{\lambda=0} = \left.\frac{d^2 G(\mathbf{\Pi}(\boldsymbol{E}+\lambda\boldsymbol{Y}))}{d\lambda^2}\right|_{\lambda=0} + 2\epsilon + k|\boldsymbol{Y} - \mathbf{\Pi}\boldsymbol{Y}|^2 > \epsilon. \tag{31.24}$$

When k is very large the term involving k will be small only if $\mathbf{\Pi}\boldsymbol{Y} \approx \boldsymbol{Y}$, that is, only if $\boldsymbol{Y}$ being rank-1 is close to one of the matrices in (31.23). But then $G(\mathbf{\Pi}(\boldsymbol{E}+\lambda\boldsymbol{Y}))$ will be close to becoming convex in λ and the term involving the second derivative of G will be either positive or very small and negative. In the limit as $k \to \infty$, the left-hand side of (31.24) approaches 2ϵ, so it is surely greater than ϵ for some finite value of k.

To obtain a function with quadratic growth at infinity, which is rank-1 convex on all 2×3 matrices $\boldsymbol{E}$ but not quasiconvex, we find a convex quadratic function $G_2(\boldsymbol{E})$ that is below $G_1(\boldsymbol{E})$ for $\boldsymbol{E} = \boldsymbol{A}_i$, $i = 1, 2, \ldots, 7$ and for $\boldsymbol{E} = 0$, but which is strictly above $G_1(\boldsymbol{E})$ when $|\boldsymbol{E}| = r$. We take our rank-1 convex function to be

$$\begin{aligned} W(\boldsymbol{E}) &= \max\{G_1(\boldsymbol{E}), G_2(\boldsymbol{E})\} \text{ for } |\boldsymbol{E}| \le r, \\ &= G_2(\boldsymbol{E}) \text{ for } |\boldsymbol{E}| > r. \end{aligned}$$

Then $W(\boldsymbol{E})$ is clearly rank-1 convex for $|\boldsymbol{E}| < r$ and for $|\boldsymbol{E}| = r$ being equal to the convex (and hence rank-1 convex) function $G_2(\boldsymbol{E})$. It is also rank-1 convex for $|\boldsymbol{E}| \le r$ being the maximum of two rank-1 convex functions. It follows that W is rank-1 convex for all 2×3 matrices $\boldsymbol{E}$.

There is a lot of freedom in the choice of the function $G_2(\boldsymbol{E})$. To be specific, we can select radii r_1, r_2, and r_3 with $r > r_1 > r_2 > r_3$ and r_3 such that each of the seven matrices $\boldsymbol{A}_i$ have $|\boldsymbol{A}_i| < r_3$. (Thus it suffices to take $r > r_1 > r_2 > r_3 > \sqrt{28}$.) We then set

$$G_2(\boldsymbol{E}) = c(|\boldsymbol{E}|^2 - r_2^2),$$

where c is chosen sufficiently large to ensure that

$$\begin{aligned} W(\boldsymbol{E}) &= G_1(\boldsymbol{E}) \text{ for } |\boldsymbol{E}| \le r_3, \\ &= G_2(\boldsymbol{E}) \text{ for } |\boldsymbol{E}| \ge r_1. \end{aligned} \tag{31.25}$$

This is guaranteed if we choose

$$c > \max\{M/(r_2^2 - r_3^2), M/(r_1^2 - r_2^2)\}, \quad \text{where } M = \max_{|\boldsymbol{E}| \le r} |G_1(\boldsymbol{E})|. \tag{31.26}$$

Finally, because each of the seven matrices $\boldsymbol{A}_i$ have $|\boldsymbol{A}_i| < r_3$, (31.25) implies that

$$W(\boldsymbol{A}_i) = G_1(\boldsymbol{A}_i) < G(\boldsymbol{A}_i) = 0,$$

as a result of which

$$\langle W(\nabla \boldsymbol{u})\rangle < 0, \quad \text{whereas } W(\langle \nabla \boldsymbol{u}\rangle) = W(0) = 1 - \epsilon r^2.$$

For small values of ϵ we conclude that $\langle W(\nabla \boldsymbol{u})\rangle < W(\langle \nabla \boldsymbol{u}\rangle)$. Thus $W(\boldsymbol{E})$ is rank-1 convex but not quasiconvex.

This example shows that rank-1 convexity is not sufficient to guarantee quasiconvexity; that is, if $\langle W(\nabla \boldsymbol{u})\rangle \geq W(\langle \nabla \boldsymbol{u}\rangle)$ for all periodic functions $\nabla \boldsymbol{u}(\boldsymbol{x})$ that have oscillations in only one direction, then the inequality need not hold if $\nabla \boldsymbol{u}(\boldsymbol{x})$ has oscillations in three directions. Requiring the inequality to hold for functions that have oscillations in three directions leads to additional necessary conditions for quasiconvexity (Pedregal 1996). It is not known what conditions are sufficient to guarantee quasiconvexity, but Kristensen (1999) has shown that they must be nonlocal.

31.9. A composite with an elasticity tensor that cannot be mimicked by a multiple-rank laminate material†

In section 31.4 on page 677 we saw that problems of bounding the energy of multiphase linear composites could be mapped to problems of quasiconvexification and, vice versa. In section 31.5 on page 679 we saw that problems of constructing the lamination closure could be mapped to problems of Λ-convexification of the associated energy function. Thus, since Šverák's example shows that there is a gap between Λ-convexification and quasiconvexification, there should be an associated example where there is a gap between the lamination closure and the G-closure. In principle one could map the function $W(\boldsymbol{E})$ defined in the previous section to an associated problem of bounding the energy of a composite with infinitely many phases. Then one would be essentially finished since if the lamination closure was equal to the G-closure, the rank-1 convexification of $W(\boldsymbol{E})$ would equal its quasiconvexification, which contradicts the results of the previous section. To make the problem more challenging, let us suppose that we want an example in linear elasticity with a relatively small number of phases which does not involve a supplementary field that is constrained to be constant, like T in (31.14). Instead of using T, we recall that when the microstructure is independent of x_3 the strain component ϵ_{33} is constant and thus behaves like T. This is the essential idea: To use ϵ_{33} instead of T.

We consider an elastic material subject to an average strain

$$\boldsymbol{\epsilon}_0 = \begin{pmatrix} 0 & 0 & 0 \\ 0 & 0 & 0 \\ 0 & 0 & 1 \end{pmatrix}, \tag{31.27}$$

with an elasticity tensor $\boldsymbol{\mathcal{C}}(\boldsymbol{x})$ such that the elastic energy takes the form

$$\boldsymbol{\epsilon} \cdot \boldsymbol{\mathcal{C}}\boldsymbol{\epsilon} = W_0(\boldsymbol{E}) + W(\boldsymbol{E}),$$

where $\boldsymbol{\epsilon} = (\nabla \boldsymbol{u} + (\nabla \boldsymbol{u})^T)/2$ and $\boldsymbol{E} = \boldsymbol{D}'\boldsymbol{u}$ is the field

$$\boldsymbol{E} = \boldsymbol{D}'\boldsymbol{u} = \begin{pmatrix} \epsilon_{11} & \partial u_2/\partial x_1 & \epsilon_{13} \\ \partial u_1/\partial x_2 & \epsilon_{22} & \epsilon_{23} \\ \epsilon_{13} & \epsilon_{23} & \epsilon_{33} - 1 \end{pmatrix} = \begin{pmatrix} f_{11} & f_{12} & f_{13} \\ f_{21} & f_{22} & f_{23} \\ f_{31} & f_{32} & f_{33} \end{pmatrix}. \tag{31.28}$$

This serves to define the differential operator $\boldsymbol{D}'$, which when applied to the displacement field $\boldsymbol{u}$ produces the field $\boldsymbol{E}$.

We take large positive constants p and q and set

$$\begin{aligned} W_0(\boldsymbol{E}) &= 2pf_{33} + 2q(f_{21}f_{12} - f_{11}f_{22}) + p \\ &= 2p\epsilon_{33} + 2q[(\partial u_1/\partial x_2)(\partial u_2/\partial x_1) - (\partial u_1/\partial x_1)(\partial u_2/\partial x_2)] - p, \end{aligned} \tag{31.29}$$

which is a null Lagrangian, that is, the identity

$$\langle W_0(\boldsymbol{E})\rangle = W_0(\langle \boldsymbol{E}\rangle)$$

is satisfied for all periodic fields $\boldsymbol{E}$ such that $\boldsymbol{E} = \boldsymbol{D}'\boldsymbol{u}$ for some $\boldsymbol{u}$.

We take $W(\boldsymbol{E})$ as the function

$$W(\boldsymbol{E}) = \sum_{i=1}^{2}\sum_{j=1}^{3} q(1+\delta_{ij})(f_{ij} - f_{33}a_{ij} - a_{ij})^2 + pf_{33}^2, \tag{31.30}$$

where the moduli a_{ij} vary from phase to phase, $a_{21}(\boldsymbol{x}) = a_{12}(\boldsymbol{x}) = 0$ for all $\boldsymbol{x}$, and δ_{ij} equals 1 if $i = j$ and is zero otherwise. When $\epsilon_{33} = 1$, that is, when $f_{33} = 0$, the function $W(\boldsymbol{E})$ is a quadratic well with its minimum at $\boldsymbol{E} = \boldsymbol{A}$, where

$$\boldsymbol{A} = \begin{pmatrix} a_{11} & 0 & a_{13} \\ 0 & a_{22} & a_{23} \\ a_{13} & a_{23} & 0 \end{pmatrix} \tag{31.31}$$

varies from phase to phase. This function $W(\boldsymbol{E})$ has been chosen in such a way that $W_0(\boldsymbol{E}) + W(\boldsymbol{E})$ is a quadratic function of the strain. An explicit calculation (which we omit) shows that

$$\begin{aligned} \boldsymbol{\epsilon}\cdot\boldsymbol{\mathcal{C}}\boldsymbol{\epsilon} &= W_0(\boldsymbol{E}) + W(\boldsymbol{E}) \\ &= q(\epsilon_{11} - \epsilon_{22})^2 + q(\epsilon_{11} - 2\epsilon_{33}a_{11})^2 + q(\epsilon_{22} - 2\epsilon_{33}a_{22})^2 + 4q\epsilon_{12}^2 \\ &\quad + q(\epsilon_{13} - \epsilon_{33}a_{13})^2 + q(\epsilon_{23} - \epsilon_{33}a_{23})^2 + \epsilon_{33}^2[p - 2q(a_{11}^2 + a_{22}^2)]. \end{aligned} \tag{31.32}$$

This serves to define the elasticity tensor $\boldsymbol{\mathcal{C}}(\boldsymbol{x})$ of the material. To ensure that $\boldsymbol{\mathcal{C}}(\boldsymbol{x})$ is positive-definite, we choose p so that the last term in the above expression is positive for all $\epsilon_{33} \neq 0$, that is, we choose p so that in each phase

$$p > 2q(a_{11}^2 + a_{22}^2). \tag{31.33}$$

By considering the energy associated with the average strain (31.27), and using the fact that $W_0(\boldsymbol{E})$ is a null Lagrangian and that $W(\boldsymbol{E})$ is nonnegative, we obtain the following trivial lower bound on the Cartesian element C_{3333}^* of the effective elasticity tensor:

$$C_{3333}^* = \boldsymbol{\epsilon}_0\cdot\boldsymbol{\mathcal{C}}_*\boldsymbol{\epsilon}_0 = \min_{\substack{\boldsymbol{E} = \boldsymbol{D}'\boldsymbol{u} \\ \langle \boldsymbol{E}\rangle = 0}} \langle W_0(\boldsymbol{E}) + W(\boldsymbol{E})\rangle \geq W_0(0) = p.$$

We want to choose $\boldsymbol{A}$ and the constants p and q so that this bound is attained, but not by any laminate microstructure. The bound will be attained if there exists a displacement field $\boldsymbol{u}(\boldsymbol{x})$

such that $\boldsymbol{E} = \boldsymbol{D}'\boldsymbol{u}$ satisfies $\langle \boldsymbol{E} \rangle = 0$ and $W(\boldsymbol{E}) = 0$. From (31.30) we see that $W(\boldsymbol{E})$ is zero if and only if

$$f_{33} = 0 \ \text{ and } \ f_{ij} = a_{ij} \ \text{ for } i = 1, 2 \text{ and } j = 1, 2, 3.$$

Thus the condition for attainability of the bound becomes

$$\langle \boldsymbol{E} \rangle = 0 \ \text{ and } \ \boldsymbol{E} = \boldsymbol{D}'\boldsymbol{u} = \boldsymbol{A} \ \text{ for some } \boldsymbol{u}. \tag{31.34}$$

This is certainly satisfied if the moduli $a_{ij}(\boldsymbol{x})$ are chosen so that

$$\langle \boldsymbol{A} \rangle = 0 \ \text{ and } \ \boldsymbol{A} = \boldsymbol{D}'\boldsymbol{u}_0,$$

for some vector potential $\boldsymbol{u}_0$. In particular, let us take

$$\boldsymbol{u}_0 = \big(h(x_1), h(x_2), x_3 + h(x_1 + x_2 + 2) \big) ,$$

in which $h(y)$ is the periodic function defined in (31.22). Then $\boldsymbol{A} = \boldsymbol{D}'\boldsymbol{u}_0$ is piecewise constant, taking seven values

$$\boldsymbol{A}_i = \begin{pmatrix} r_i & 0 & t_i \\ 0 & s_i & t_i \\ t_i & t_i & 0 \end{pmatrix}, \quad i = 1, 2, 3, \ldots, 7,$$

each corresponding to a different phase, where (referring to figure 31.5 on page 687, in which the numbers represent the value of i indexing each phase)

$$\begin{aligned} (r_i, s_i, t_i) &= (\ 3,\ \ 3, -1) \ \text{ when } i = 1, \\ &= (-1,\ \ 3, -1) \ \text{ when } i = 2, \\ &= (-1,\ \ 3,\ \ 3) \ \text{ when } i = 3, \\ &= (\ 3, -1, -1) \ \text{ when } i = 4, \\ &= (\ 3, -1,\ \ 3) \ \text{ when } i = 5, \\ &= (-1, -1,\ \ 3) \ \text{ when } i = 6, \\ &= (-1, -1, -1) \ \text{ when } i = 7. \end{aligned}$$

These equations, in conjunction with (31.32) and (31.31), give an explicit expression for the (anisotropic) elasticity tensor of each of the seven phases. The composite attains the bound $C_{3333} \geq p$ and has a microstructure that is independent of the x_3 coordinate. By contrast each phase has

$$C_{3333} = p + 2q(r_i^2 + s_i^2 + t_i^2) \geq p + 6q,$$

and therefore does not attain the bound.

It remains to show that the bound is not achievable by any multiple-rank laminate, including laminates that have a microstructure varying in the x_3 direction. First let us define an Λ-matrix (the analog of a "rank-1" matrix) to be any matrix $\boldsymbol{E}$ expressible in the form

$$\boldsymbol{E} = \begin{pmatrix} k_1 v_1 & k_1 v_2 & (k_1 v_3 + k_3 v_1)/2 \\ k_2 v_1 & k_2 v_2 & (k_2 v_3 + k_3 v_2)/2 \\ (k_1 v_3 + k_3 v_1)/2 & (k_2 v_3 + k_3 v_2)/2 & k_3 v_3 \end{pmatrix}, \tag{31.35}$$

for some choice of vectors $\boldsymbol{k} = (k_1, k_2, k_3)$ and $\boldsymbol{v} = (v_1, v_2, v_3)$. We then call two matrices $\boldsymbol{E}_1$ and $\boldsymbol{E}_2$ Λ-connected if the difference $\boldsymbol{E}_1 - \boldsymbol{E}_2$ is a Λ-matrix. We begin by restricting our attention to the subspace $\boldsymbol{\mathcal{A}}$ of 3×3 matrices of the form

$$\boldsymbol{E} = \begin{pmatrix} r & 0 & t \\ 0 & s & t \\ t & t & 0 \end{pmatrix}.$$

The only Λ-matrices in this subspace are of the form $\lambda \boldsymbol{Y}$, where

$$\boldsymbol{Y} = \begin{pmatrix} 1 & 0 & 0 \\ 0 & 0 & 0 \\ 0 & 0 & 0 \end{pmatrix}, \quad \boldsymbol{Y} = \begin{pmatrix} 0 & 0 & 0 \\ 0 & 1 & 0 \\ 0 & 0 & 0 \end{pmatrix} \quad \text{or} \quad \boldsymbol{Y} = \begin{pmatrix} 0 & 0 & 1 \\ 0 & 0 & 1 \\ 1 & 1 & 0 \end{pmatrix},$$

and thus the function $G(\boldsymbol{E}) = (r+1)^2(s+1)^2(t+1)^2$, as in (31.20), is Λ-convex on this subspace and zero when $\boldsymbol{E} = \boldsymbol{A}_i$ for $i = 1, 2, \ldots, 7$.

Therefore, if in a multiple-rank laminate $\boldsymbol{E} = \boldsymbol{D}'\boldsymbol{u}$ takes the seven values $\boldsymbol{A}_1$, $\boldsymbol{A}_2, \ldots, \boldsymbol{A}_7$ almost everywhere in the material, then the values that $\langle \boldsymbol{E} \rangle$ can take are quite restricted. On the one hand, $G(\langle \boldsymbol{E} \rangle)$ must be negative since otherwise the condition $G(\langle \boldsymbol{E} \rangle) \leq \langle G(\boldsymbol{E}) \rangle$ arising from Λ-convexity would be violated. On the other hand, $\langle \boldsymbol{E} \rangle$, being an average, must lie in the subspace $\boldsymbol{\mathcal{A}}$ in the convex hull of the matrices $\boldsymbol{A}_1$, $\boldsymbol{A}_2, \ldots \boldsymbol{A}_7$. These constraints force $\langle \boldsymbol{E} \rangle$ in a multiple-rank laminate microstructure to lie on one of the three surfaces $r = -1$, $s = -1$, or $t = -1$, and to satisfy the inequalities $3 \geq r \geq -1$, $3 \geq s \geq -1$, and $3 \geq t \geq -1$. In other words, $\langle \boldsymbol{E} \rangle$ for a laminate field must lie on one of the three cube surfaces illustrated in figure 31.6 on page 688. In particular, $\langle \boldsymbol{E} \rangle$ cannot be zero. Therefore the conditions (31.34) for attainability cannot be met in any multiple- or infinite-rank laminate.

To find an explicit bound on C_{3333} for multiple- or infinite-rank laminates that is strictly greater than p requires some extra work. Consider any two materials α and β with elasticity tensors $\boldsymbol{\mathcal{C}}_\alpha$ and $\boldsymbol{\mathcal{C}}_\beta$, which we laminate together in direction $\boldsymbol{n}$ in proportions θ and $1 - \theta$, where $0 < \theta < 1$, to form a simple laminate γ with effective tensor $\boldsymbol{\mathcal{C}}_\gamma$. Define

$$W_\rho(\boldsymbol{E}) = \boldsymbol{\epsilon}(\boldsymbol{E}) \cdot \boldsymbol{\mathcal{C}}_\rho \boldsymbol{\epsilon}(\boldsymbol{E}) - W_0(\boldsymbol{E})$$

as the energy function corresponding to material ρ for $\rho = \alpha, \beta$, and γ, where $W_0(\boldsymbol{E})$ is given by (31.29) and

$$\boldsymbol{\epsilon}(\boldsymbol{E}) = (\boldsymbol{E} + \boldsymbol{E}^T + 2\boldsymbol{\epsilon}_0)/2$$

is the strain associated with $\boldsymbol{E}$, in which $\boldsymbol{\epsilon}_0$ is given by (31.27).

Now suppose that we have found a comparison function $W_-(\boldsymbol{E})$ that lies below the energy functions of the materials α and β, that is,

$$W_\alpha(\boldsymbol{E}) \geq W_-(\boldsymbol{E}) \text{ and } W_\beta(\boldsymbol{E}) \geq W_-(\boldsymbol{E}) \text{ for all } \boldsymbol{E}, \tag{31.36}$$

and which is Λ-convex (the analog of "rank-1" convex) in the sense that the inequality

$$W_-(\theta \boldsymbol{E}_1 + (1-\theta)\boldsymbol{E}_2) \leq \theta W_-(\boldsymbol{E}_1) + (1-\theta) W_-(\boldsymbol{E}_2) \tag{31.37}$$

holds for all values of θ between 0 and 1 whenever $\boldsymbol{E}_1$ and $\boldsymbol{E}_2$ are Λ-connected. In the laminate let us set the average value of the field $\boldsymbol{E}$, given by (31.28), to some prescribed value $\boldsymbol{E}_\gamma$. Then $\boldsymbol{E}(\boldsymbol{x})$ is piecewise constant within the laminate taking a value $\boldsymbol{E}_\alpha$ in material α and a value $\boldsymbol{E}_\beta$ in material β, and we have

$$\boldsymbol{E}_\gamma = \theta \boldsymbol{E}_\alpha + (1-\theta)\boldsymbol{E}_\beta, \quad W_\gamma(\boldsymbol{E}_\gamma) = \theta W_\alpha(\boldsymbol{E}_\alpha) + (1-\theta) W_\beta(\boldsymbol{E}_\beta). \tag{31.38}$$

The differential constraints on the field $\boldsymbol{E}(\boldsymbol{x})$ imply that $\boldsymbol{E}_\alpha$ and $\boldsymbol{E}_\beta$ are Λ-connected [with $\boldsymbol{E}_\alpha - \boldsymbol{E}_\beta$ being of the form (31.35) with $\boldsymbol{k}$ matching the direction of lamination $\boldsymbol{n}$]. The inequalities (31.36) and (31.37), together with (31.38), then imply that

$$W_\gamma(\boldsymbol{E}_\gamma) \geq \theta W_-(\boldsymbol{E}_\alpha) + (1-\theta)W_-(\boldsymbol{E}_\beta) \geq W_-(\theta\boldsymbol{E}_\alpha + (1-\theta)\boldsymbol{E}_\beta) = W_-(\boldsymbol{E}_\gamma).$$

Thus the energy function of the laminate γ also lies above the comparison function.

By iterating this argument we see that if the comparison function $W_-(\boldsymbol{E})$ is chosen so that the energy functions $W_\rho(\boldsymbol{E})$ of each of the seven phases lie above it, then the energy function of any multiple-rank laminate (but not necessarily every composite) of the seven phases must also lie above $W_-(\boldsymbol{E})$.

Phase i, for $i = 1, 2, \ldots, 7$, has an energy function given by (31.30) that is a quadratic well, taking the value zero at the well center at $\boldsymbol{E} = \boldsymbol{A}_i$, and which grows rapidly away from the well center when p and q are both very large. The composite of figure 31.5 on page 687, because it attains the bound $C_{3333} \geq p$, has an energy function that is zero at $\boldsymbol{E} = 0$. Therefore, to obtain a bound on C_{3333} for multiple-rank laminates that are strictly greater than p we seek a Λ-convex comparison function $W_-(\boldsymbol{E})$ (with quadratic growth at large $\boldsymbol{E}$) that is negative at $\boldsymbol{E} = \boldsymbol{A}_i$ for $i = 1, 2, \ldots, 7$ yet which is positive at $\boldsymbol{E} = 0$.

Like in section 31.8 on page 684, one procedure is to use $G(\boldsymbol{E})$ to obtain a function $G_1(\boldsymbol{E})$ that is rank-1 convex and bounded on the set comprised of all 3×3 matrices $\boldsymbol{E}$ with $|\boldsymbol{E}|$ less than r. The radius r needs to be chosen sufficiently large so that each of the seven matrices $\boldsymbol{A}_i$ have $|\boldsymbol{A}_i| < r$. (Thus it suffices to take $r > \sqrt{46}$.) We let $\boldsymbol{\Pi}$ denote the natural projection onto matrices in the subspace $\boldsymbol{\mathcal{A}}$:

$$\boldsymbol{\Pi}\begin{pmatrix} a & b & c \\ d & e & f \\ c & f & g \end{pmatrix} = \begin{pmatrix} a & 0 & (c+f)/2 \\ 0 & e & (c+f)/2 \\ (c+f)/2 & (c+f)/2 & 0 \end{pmatrix},$$

and we then select some positive number $\epsilon < 1/r^2$ and set

$$G_1(\boldsymbol{E}) = G(\boldsymbol{\Pi E}) + \epsilon(|\boldsymbol{E}|^2 - r^2) + k|\boldsymbol{E} - \boldsymbol{\Pi E}|^2,$$

where k is chosen positive and large enough to ensure the Λ-convexity of $G_1(\boldsymbol{E})$ for $|\boldsymbol{E}| \leq r$.

We next select radii r_1, r_2, and r_3 with $r > r_1 > r_2 > r_3 > \sqrt{46}$ (so that each of the seven matrices $\boldsymbol{A}_i$ have $|\boldsymbol{A}_i| < r_3$) and set

$$\begin{aligned} W_-(\boldsymbol{E}) &= \max\{G_1(\boldsymbol{E}),\ c(|\boldsymbol{E}|^2 - r_2^2)\} \ \text{ for } |\boldsymbol{E}| \leq r, \\ &= c(|\boldsymbol{E}|^2 - r_2^2) \ \text{ for } |\boldsymbol{E}| > r, \end{aligned}$$

in which c satisfies (31.26). Then $W_-(\boldsymbol{E})$ is clearly rank-1 convex for $|\boldsymbol{E}| \geq r_1$ being equal to the convex (and hence Λ-convex) function $c(|\boldsymbol{E}|^2 - r_2^2)$. It is also Λ-convex for $|\boldsymbol{E}| \leq r$ being the maximum of two Λ-convex functions. Therefore, $W_-(\boldsymbol{E})$ is Λ-convex for all 3×3 matrices $\boldsymbol{E}$. Also, because $W_-(\boldsymbol{E}) = G_1(\boldsymbol{E})$ for $|\boldsymbol{E}| < r_3$ and because each of the seven matrices $\boldsymbol{A}_i$ have $|\boldsymbol{A}_i| < r_3$, it follows that

$$W_-(\boldsymbol{A}_i) = G_1(\boldsymbol{A}_i) < \epsilon(46 - r^2) < 0, \quad \text{whereas } W_-(0) = G_1(0) = 1 - \epsilon r^2 > 0.$$

Having obtained the comparison function $W_-(\boldsymbol{E})$ we select p and q sufficiently large [with $p > 36q$ so that (31.33) is satisfied] to ensure that the energy function of each phase

lies above $W_-(\boldsymbol{E})$. Then the element C^*_{3333} of the effective elasticity tensor of any multiple-rank laminate built from these seven phases satisfies the bound

$$C^*_{3333} \geq p + W_-(0) \geq p + 1 - \epsilon r^2, \tag{31.39}$$

which, for small values of ϵ, is strictly bigger than the value p attained by the composite of figure 31.5 on page 687. The composite achieves an elastic energy that is lower than the energy of any multiple-rank laminate.

In this example the phases have a fixed orientation. It would be interesting to see if it is possible to construct a composite with an effective tensor that cannot be mimicked by a multiple-rank laminate material, in which the phases are allowed to have any orientation.

References

Allaire, G. and V. Lods 1999. Minimizers for a double-well problem with affine boundary conditions. *Proceedings of the Royal Society of Edinburgh. Section A, Mathematical and Physical Sciences* 129(3):439–466. {*681, 695*}

Aumann, R. J. and S. Hart 1986. Bi-convexity and bi-martingales. *Israel Journal of Mathematics* 54(2):159–180. {*683, 695*}

Ball, J. M. 1977. Convexity conditions and existence theorems in non-linear elasticity. *Archive for Rational Mechanics and Analysis* 63(4):337–403. {*671, 672, 695*}

Ball, J. M. 1996. Some recent developments in nonlinear elasticity and its applications to materials science. In P. J. Aston (ed.), *Nonlinear Mathematics and its Applications: A Spring School in Applied Nonlinear Mathematics for Postgraduate Students Held at the University of Surrey on 3–7 April 1995*, pp. 93–119. Cambridge, United Kingdom: Cambridge University Press. ISBN 0-521-57190-1 (hardback), 0-521-57676-8 (paperback). {*672, 674, 695*}

Ball, J. M. and R. D. James 1987. Fine phase mixtures as minimizers of energy. *Archive for Rational Mechanics and Analysis* 100(1):13–52. {*671, 672, 695*}

Ball, J. M. and R. D. James 1992. Proposed experimental tests of a theory of fine microstructure and the two-well problem. *Philosophical Transactions of the Royal Society of London Series A* 338:389–450. {*672, 695*}

Ball, J. M. and R. D. James 2001. *From Microscales to Macroscales in Materials*. In preparation. {*xxv, xxvi, 672, 695*}

Ball, J. M. and F. Murat 1984. $W^{1,p}$-quasiconvexity and variational problems for multiple integrals. *Journal of Functional Analysis* 58(3):225–253. {*674, 695*}

Bhattacharya, K. 1993. Comparison of the geometrically nonlinear and linear theories of martensitic transformation. *Continuum Mechanics and Thermodynamics* 5(3):205–242. {*672, 695*}

Bhattacharya, K., N. Firoozye, R. D. James, and R. V. Kohn 1994. Restrictions on microstructure. *Proceedings of the Royal Society of Edinburgh* 124A(5):843–878. {*683, 695*}

Bhattacharya, K. and R. V. Kohn 1997. Elastic energy minimization and the recoverable strains of polycrystalline shape-memory materials. *Archive for Rational Mechanics and Analysis* 139(2):99–180. {*531, 550, 682, 695*}

Braides, A., I. Fonseca, and G. Leoni 2000. $\mathcal{A}$-quasiconvexity: Relaxation and homogenization. *ESAIM. Control, Optimisation and Calculus of Variations* 5:539–577. {*676, 696*}

Casadio-Tarabusi, E. 1993. An algebraic characterization of quasiconvex functions. *Ricerche di Matematica (Napoli)* 42(1):11–24. {*683, 696*}

Coleman, B. D. and W. Noll 1959. On the thermostatics of continuous media. *Archive for Rational Mechanics and Analysis* 4:97–128. {*672, 696*}

Dacorogna, B. 1982. *Weak Continuity and Weak Lower Semicontinuity of Nonlinear Functionals*. Berlin / Heidelberg / London / etc.: Springer-Verlag. iii + 120 pp. ISBN 3-540-11488-2. {*676, 696*}

Dacorogna, B. and J.-P. Haeberly 1996. Remarks on a numerical study of convexity, quasiconvexity, and rank one convexity. In R. Serapioni and F. Tomarelli (eds.), *Variational Methods for Discontinuous Structures: Applications to Image Segmentation, Continuum Mechanics, Homogenization: Villa Olmo, Como, 8–10 September 1994*, pp. 143–154. Basel, Switzerland: Birkhäuser Verlag. ISBN 0-8176-5273-6 (Basel), 3-7643-5273-6 (Boston). {*684, 696*}

Dacorogna, B. and J.-P. Haeberly 1998. Some numerical methods for the study of the convexity notions arising in the calculus of variations. *Mathematical Modelling and Numerical Analysis = Modelisation mathématique et analyse numérique: M^2AN* 32: 153–175. {*684, 696*}

Firoozye, N. B. 1991. Optimal use of the translation method and relaxations of variational problems. *Communications on Pure and Applied Mathematics (New York)* 44(6):643–678. {*529, 531, 532, 550, 673, 696*}

Fonseca, I. and S. Müller 1999. $\mathcal{A}$-quasiconvexity, lower semicontinuity, and Young measures. *SIAM Journal on Mathematical Analysis* 30(6):1355–1390. {*676, 696*}

James, R. D. and D. Kinderlehrer 1989. Theory of diffusionless phase transitions. In M. Rascle, D. Serre, and M. Slemrod (eds.), *PDE's and Continuum Models of Phase Transitions: Proceedings of an NSF-CNRS Joint Seminar Held in Nice, France, January 18–22, 1988*, pp. 51–84. Berlin / Heidelberg / London / etc.: Springer-Verlag. ISBN 0-387-51617-4. {*672, 696*}

Khachaturyan, A. G. 1966. Some questions concerning the theory of phase transitions in solids. *Fizika Tverdogo Tela.* 8:2709–2717. English translation in *Soviet Phys. Solid State.* 8:2163–2168 (1967). {*252, 268, 295, 311, 474, 493, 672, 696*}

Khachaturyan, A. G. 1983. *Theory of Structural Transformations in Solids*. New York / London / Sydney, Australia: John Wiley and Sons. xiii + 574 pp. ISBN 0-471-07873-5. {*295, 311, 672, 696*}

Kinderlehrer, D. and P. Pedregal 1991. Characterizations of Young measures generated by gradients. *Archive for Rational Mechanics and Analysis* 115(4):329–365. {*677, 696*}

Kohn, R. V. 1991. The relaxation of a double-well energy. *Continuum Mechanics and Thermodynamics* 3(3):193–236. {*293, 295, 311, 672, 677, 696*}

Kohn, R. V. and T. D. Little 1999. Some model problems of polycrystal plasticity with deficient basic crystals. *SIAM Journal on Applied Mathematics* 59(1):172–197. {*682, 696*}

Kohn, R. V. and G. Strang 1986. Optimum Design and Relaxation of Variational Problems, I, II, and III. *Communications on Pure and Applied Mathematics (New York)* 39:113–377. {*426, 431, 435, 680, 697*}

Kristensen, J. 1999. On the non-locality of quasiconvexity. *Annales de l'Institut Henri Poincaré. Analyse non linéaire* 16(1):1–13. {*690, 697*}

Luskin, M. 1996. On the computation of crystalline microstructure. *Acta Numerica* 5:191–257. Cambridge Univ. Press, Cambridge. {*672, 697*}

Morrey, C. B. 1952. Quasiconvexity and the lower semicontinuity of multiple integrals. *Pacific Journal of Mathematics* 2:25–53. {*684, 697*}

Morrey, C. B. 1966. *Multiple Integrals in the Calculus of Variations*, p. 122. Berlin / Heidelberg / London / etc.: Springer-Verlag. {*684, 697*}

Müller, S. 1998. *Variational Models for Microstructure and Phase Transitions*. Leipzig, Germany: Max Planck Institute for Mathematics in the Sciences. 127 pp. {*672, 674, 681, 684, 686, 688, 697*}

Murat, F. 1987. A survey on compensated compactness. In L. Cesari (ed.), *Contributions to Modern Calculus of Variations*, pp. 145–183. Harlow, Essex, United Kingdom: Longman Scientific and Technical. ISBN 0-470-20378-1 (Wiley), 0-582-99458-6. {*275, 288, 529, 551, 676, 697*}

Nesi, V. and G. W. Milton 1991. Polycrystalline configurations that maximize electrical resistivity. *Journal of the Mechanics and Physics of Solids* 39(4):525–542. {*537, 551, 684, 697*}

Olson, T. 1994. Improvements on Taylor's upper bounds for rigid-plastic composites. *Materials Science and Engineering* A175:15–20. {*683, 697*}

Parry, G. P. 1995. On the planar rank-one convexity condition. *Proceedings of the Royal Society of Edinburgh. Section A, Mathematical and Physical Sciences* 125(2):247–264. {*684, 697*}

Pedregal, P. 1996. Some remarks on quasiconvexity and rank-one convexity. *Proceedings of the Royal Society of Edinburgh. Section A, Mathematical and Physical Sciences* 126 (5):1055–1065. {*684, 686, 690, 697*}

Pedregal, P. 1997. *Parameterized Measures and Variational Principles*. Basel, Switzerland: Birkhäuser Verlag. xii + 212 pp. ISBN 3-7643-5697-9. {*686–688, 697*}

Pedregal, P. and V. Šverák 1998. A note on quasiconvexity and rank-one convexity for 2×2 matrices. *Journal of Convex Analysis* 5(1):107–117. {*684, 697*}

Ponte Castañeda, P. and G. DeBotton 1992, August 8. On the homogenized yield strength of two-phase composites. *Proceedings of the Royal Society of London. Series A, Mathematical and Physical Sciences* 438(1903):419–431. {*683, 697*}

Roytburd, A. L. 1967. Orientational and habit relationships between crystalline phases in solid state transformations. *Kristallografiya* 12:567–574. English translation in *Sov. Phys. Crystallography* 12:499–504 (1968). {*672, 697*}

Roytburd, A. L. 1968. Domain structure of crystals formed in a solid phase. *Fizika Tverdogo Tela* 10:2870–2876. English translation in *Sov. Phys. Solid State* 10:2870–2876 (1968). {*672, 697*}

Roytburd, A. L. 1978. Martensitic transformation as a typical phase transformation in solids. *Solid State Physics (New York. 1955)* 33:317–390. {*672, 698*}

Roytburd, A. L. 1993. Elastic domains and polydomain phases in solids. *Phase Transitions* 45:1–33. {*672, 698*}

Suquet, P. 1993. Overall potentials and extremal surfaces of power law or ideally plastic composites. *Journal of the Mechanics and Physics of Solids* 41(6):981–1002. {*683, 698*}

Šverák, V. 1992. Rank-one convexity does not imply quasiconvexity. *Proceedings of the Royal Society of Edinburgh. Section A, Mathematical and Physical Sciences* 120(1–2): 185–189. {*673, 684, 688, 698*}

Tartar, L. 1979. Compensated compactness and applications to partial differential equations. In R. J. Knops (ed.), *Nonlinear Analysis and Mechanics, Heriot-Watt Symposium, Volume IV*, pp. 136–212. London: Pitman Publishing Ltd. ISBN 0-8224-8461-7, 0-273-08461-5. {*59, 72, 275, 276, 288, 503, 527, 529, 552, 676, 677, 684, 698*}

Tartar, L. 1985. Estimations fines des coefficients homogénéisés. (French) [Fine estimations of homogenized coefficients]. In P. Krée (ed.), *Ennio de Giorgi Colloquium: Papers Presented at a Colloquium Held at the H. Poincaré Institute in November 1983*, pp. 168–187. London: Pitman Publishing Ltd. ISBN 0-273-08680-4. {*129, 141, 165, 167, 174, 183, 462, 496, 499, 503, 506, 508, 527, 529, 552, 683, 698*}

Tartar, L. 1993. Some remarks on separately convex functions. In D. Kinderlehrer, R. D. James, M. Luskin, and J. L. Ericksen (eds.), *Microstructure and Phase Transition*, pp. 191–204. Berlin / Heidelberg / London / etc.: Springer-Verlag. ISBN 0-387-94112-6 (New York), 3-540-94112-6 (Berlin). {*683, 684, 698*}

Author index

Abeles, B., 211, 219, 239, 243, *see* GITTLEMAN, J. I., *see* SHENG, P.
Abousleiman (eds.), Y., 33, 41, *see* CHENG, A. H.-D.
Acrivos, A., 39, 45, 191, 214, 331, 339, *see* CHEN, H.-S., *see* SANGANI, A. S., *see* THOVERT, J. F.
Acton, J. R., 191, 220, 252, 270, *see* WILLIS, J. R.
ADAMS, B. L., **318**, **335**, **489, 490**
Adams, B. L., 318, 336, 490, 491, *see* BERAN, M. J., *see* ETINGHOF, P.
AGARWAL, B. D., **xxiv**, **xxvi**
Aharony, A., xxiii, xxviii, *see* STAUFFER, D.
AHLFORS, L. V., **137**, **139**
Aksay, I. A., 4, 18, *see* SIGMUND, O.
ALBERS, W., **4**, **14**
ALDERSON, K. L., **653**, **667**
ALESSANDRINI, G., **152**, **155**
Alexopoulos, A., 188, 191, 214, *see* CHOY, T. C.
ALLAIRE, G., **xxv, xxvi**, **8**, **10**, **13, 14**, **221**, **242**, **426**, **431–433**, **466–468**, **474**, **490, 491**, **518**, **525**, **681**, **695**
ALMGREN, R. F., **652**, **656**, **667**
ALPHUTOVA, N. B., **147**, **155**
AMBEGAOKAR, V., **211**, **213**
Anderson, Jr., H. R., 319, 336, *see* DEBYE, P.
Andrewes, W. J. H., 79, 91, *see* SOBEL, D.
Andrianov, I., 590, 600, *see* TOKARZEWSKI, S.
ANTMAN, S. S., **22**, **40**
ARCHIE, G. E., **202**, **213**
Arie, Y., 211, 219, *see* SHENG, P.
ARMAND, J.-L., **426**, **433**
ASARO, R. J., **254**, **267**
Ashby, M. F., 653, 668, *see* GIBSON, L. J.
ASHCROFT, N. W., **28**, **40**, **223, 224**, **242**
ASPNES, D. E., **569**, **596**
ASTALA, K., **152**, **155**, **480**, **491**, **646**, **668**
ATKIN, R. J., **22**, **38**, **40**
ATTOUCH, H., **13, 14**
Aubry, S., 467, 490, *see* ALLAIRE, G.
AUMANN, R. J., **683**, **695**
AVELLANEDA, M., **4**, **14**, **30**, **40**, **97**, **110**, **120**, **124**, **139**, **163**, **175**, **181, 182**, **197**, **203, 204**, **213**, **221**, **242**, **292**, **294**, **309**, **322**, **335**, **362**, **367**, **370**, **391, 392**, **439**, **441**, **444**, **450**, **452, 453**, **463–465**, **468**, **471**, **473**, **491**, **501, 502**, **512**, **525**, **536–538**, **550**, **555**, **564**
Avellaneda, M., 489, 490, 495, *see* OLSON, T.
AXELL, JØRGEN, **344**, **346**, **352**

BABOS, G., **333**, **335**
BACKUS, G. E., **159**, **162, 163**, **182**
BAKER, JR., G. A., **370**, **392**, **571**, **578**, **596**, **603**, **617**
Baker-Jarvis, J., 569, 598, *see* MANTESE, J. V.
BAKHVALOV, N. S., **8**, **10, 11**, **14**
BALL, J. M., **xxv, xxvi**, **275**, **286**, **671, 672**, **674**, **695**
Banavar, J. R., 40, 46, *see* SCHWARTZ, L. M.
Barnett, D. M., 254, 267, *see* ASARO, R. J.
BARRERA, R. G., **370**, **392**
BATCHELOR, G. K., **19**, **40**, **209**, **213**
BATHURST, R. J., **652**, **668**

NOTE: First authors are given in SMALL CAPS. Subsequent authors are in roman type, and are cross-referenced to first authors.

Page numbers for first authors are in **bold** type, and those for subsequent authors are in roman type.

In the chapter references, each entry is followed by a braced list of page numbers in small *italic* type, showing where in the book the entry is cited, or appears in the references.

BAUMAN, P., **543**, **550**
Beasley, J. D., 331, 333, 339, 586, 600, *see* TORQUATO, S.
BENDSØE, M. P., **426**, **433**
Bendsøe, M. P., 432–435, *see* DIAZ, A., *see* JOG, C. S., *see* ROZVANY, G.
BENSOUSSAN, A., **8**, **10, 11**, **14**, **221**, **242**
BENVENISTE, Y., **96, 97**, **102**, **110**, **135, 136**, **139**
Benveniste, Y., 134, 140, 405, 411, *see* DVORAK, G. J., *see* MILOH, T.
BERAN, M. J., **xxv, xxvi**, **11**, **15**, **291**, **309**, **332**, **336**, **344**, **352**, **489–491**, **553**, **557**, **564**, **574**, **577**, **589**, **597**
BERDICHEVSKII, V. L., **49**, **51**, **57**, **143**, **155**
BERGMAN, D. J., **xxv, xxvi**, **3**, **15**, **34**, **39–41**, **51**, **57**, **65**, **70**, **97**, **110**, **129**, **139**, **213**, **239**, **242**, **341**, **344**, **352**, **370, 371**, **376, 377**, **379, 380**, **382**, **387**, **390**, **392**, **451–453**, **457**, **478**, **491**, **569**, **571**, **577**, **580, 581**, **588**, **590**, **597**, **603, 604**, **608**, **610**, **617**, **638**, **641**
Bergman, D. J., 34, 39, 43, 46, 51, 58, 66, 72, 213, 220, 248, 268, 370, 371, 393, 569, 598, 603, 617, *see* KANTOR, Y., *see* STRELNIKER, Y. M., *see* STROUD, D., *see* TORNOW, M., *see* ZABOLITZKY, J. G.
BERLYAND, L., **207–209**, **213**, **429**, **433**, **653**, **668**
Berlyand, L., 221, 242, *see* AVELLANEDA, M.
BERRYMAN, J. G., **85**, **89**, **163**, **182**, **205**, **213**, **255**, **267**, **317**, **319**, **331**, **336**, **397**, **399**, **411**, **522**, **525**, **556**, **560**, **565**
Berryman, J. G., 479, 480, 492, 495, *see* GIBIANSKY, L. V., *see* MILTON, G. W.
BERS, L., **103**, **110**
BHATTACHARYA, K., **101**, **110**, **531**, **550**, **672**, **682, 683**, **695**
Biggers, J. V., 4, 16, *see* KLICKER, K. A.
BIGONI, D., **135**, **139**
BIOT, M. A., **32**, **41**
BISHOP, J. F. W., **284**, **286**
Bławzdziewicz, J., 590, 600, *see* TOKARZEWSKI, S.
BLOCH, F., **223**, **242**
BOBETH, M., **344**, **353**
BOLOTIN, V. V., **197**, **214**
BONNECAZE, R. T., **39**, **41**, **555**, **565**
Bonnetier, E., 432, 433, *see* ALLAIRE, G.
BORCEA, L., **211**, **214**, **278**, **286**
BORNERT, M., **134**, **139**, **458**, **491**
Botten, L. C., 3, 17, 39, 46, *see* PARKER, A. R., *see* YARDLEY, J. G.
Bouwstra, S., 2, 3, 16, 653, 668, *see* LARSEN, U. D.
Brady, J. F., 39, 41, 555, 565, *see* BONNECAZE, R. T.
BRAIDES, A., **14, 15**, **471**, **491**, **676**, **696**
Brenner, H., 39, 46, *see* ZUZOVSKY, M.
BRIANE, M., **9**, **15**
Briane, M., 8, 10, 14, *see* ALLAIRE, G.
BROPHY, J. J., **414**, **423**
Broutman, L. J., xxiv, xxvi, *see* AGARWAL, B. D.
BROWN, R. J. S., **85**, **89**
Brown, R. J. S., 205, 216, *see* KORRINGA, J.
BROWN, W. F., **279**, **286**, **291**, **310**, **313**, **320**, **329**, **336**
BRUGGEMAN, D. A. G., **159**, **182**, **195**, **201**, **214**, **256**, **267**
Brumberger, H., 319, 336, *see* DEBYE, P.
BRUNO, O. P., **257**, **267**, **298**, **304**, **306**, **310**, **322**, **336**, **372, 373**, **379**, **392**, **569**, **597**
Bruno, O. P., 322, 335, *see* AVELLANEDA, M.
BUDIANSKY, B., **204**, **214**
BURRIDGE, R., **32**, **41**
BURYACHENKO, V. A., **185**, **214**
BUTTAZZO, G., **13**, **15**

CABIB, E., **521**, **525**
CADDOCK, B. D., **653**, **668**
CAFLISCH, R. E., **234**, **242**, **298**, **310**
Callegari, A. J., 202, 218, *see* NORRIS, A.
CALLEN, H. B., **28**, **41**, **236**, **242**
CARGILL III, G. S., **xxiii**, **xxvi**
CARRIER, J., **39**, **41**
CASADIO-TARABUSI, E., **683**, **696**
Caspers, W. J., 335, 339, 490, 497, *see* WILLEMSE, M. W. M.
Chassapis, D., 333, 335, *see* BABOS, G.
Chen, E. P., xxiii, xxvii, *see* SIH, G. C.
CHEN, H.-S., **191**, **214**
CHEN, J., **69, 70**
Chen, J., 188, 210, 214, 216, 557, 565, *see* DAVIS, L. C., *see* JASIUK, I.
CHEN, T., **35**, **41**, **66**, **70, 71**, **96**, **102**, **110, 111**
Chen, Z., 40, 46, *see* TAO, R.
CHENG, A. H.-D., **33**, **41**
CHENG, H., **39–42**, **210**, **214**, **346**, **353**
CHENG, K.-T., **431, 432**, **434**
Cheng, K. T., 433, 435, *see* ROZVANY, G.
Cherednichenko, K. D., 10, 18, *see* SMYSHLYAEV, V. P.
CHERKAEV, A. V., **xxv, xxvi**, **66**, **71**, **221**, **234**, **237**, **243**, **264**, **267**, **271**, **276, 277**, **286**, **352, 353**, **397**, **399**, **411**, **426**, **432**, **434**,

437, **450**, **453**, **467, 468**, **491**, **517**, **522**, **525**, **560**, **565**, **614**, **617**, **639**, **641**, **653**, **666**, **668**
Cherkaev, A. V., 56, 58, 66, 70, 72, 75, 76, 90, 118, 120, 139, 140, 167, 174, 175, 182, 347, 353, 362, 367, 426, 428, 429, 431–435, 439, 441, 444, 447, 450, 452–454, 460, 462, 466, 468, 492, 494, 499, 501, 502, 506, 508, 512, 521, 525, 526, 529, 537, 538, 550, 551, 555, 564, 647, 652, 653, 655, 656, 658, 659, 664, 666, 667, 669, *see* ARMAND, J.-L., *see* AVELLANEDA, M., *see* GIBIANSKY, L. V., *see* LURIE, K. A., *see* MILTON, G. W.
CHERKAEVA, E., **569**, **597**
CHEW, W. C., **xxiii**, **xxvi**
CHOY, T. C., **188**, **191**, **214**
CHRISTENSEN, R. M., **xxiv**, **xxvi**, **68**, **71**, **205**, **214**, **230**, **233**, **243**
CHRISTIANSSON, H., **64**, **69**, **71**, **333**, **336**
CIARLET, P. G., **22**, **26**, **42**
CIORANESCU, D., **11**, **15**
CLARK, K. E., **387**, **392**, **614**, **617**, **619**, **641**
Cleary, M. P., 32, 45, *see* RICE, J. R.
Clouet, J.-F., 221, 242, *see* AVELLANEDA, M.
Clyne, T. W., xxiii, xxiv, xxvii, *see* HULL, D.
Cohen, M. H., 202, 219, *see* SEN, P.
COLEMAN, B. D., **672**, **696**
CONCA, C., **221**, **243**
Conca, C., 221, 242, *see* ALLAIRE, G.
CORSON, P. B., **555**, **557**, **565**
CRASTER, R. V., **154, 155**
CRESWICK, R. J., **212**, **214**
CRIBB, J. L., **75**, **79**, **90**
Cule, D., 40, 46, 207, 219, 586, 600, *see* TORQUATO, S.
Currie, J. C., 275, 286, *see* BALL, J. M.

DACOROGNA, B., **676**, **684**, **696**
DAL MASO, G., **13–15**
Dal Maso, G., 521, 525, *see* CABIB, E.
DANTZIG, G. B., **591**, **597**
DAVIS, L. C., **40**, **42**, **210**, **214**, **557**, **565**
Davis, L. C., 69, 70, *see* CHEN, J.
DAVIS, P. J., **210**, **215**
DAY, A. R., **40**, **42**, **66**, **68**, **71**, **377**, **392, 393**
Day, A. R., 40, 42, 46, 69, 71, *see* GARBOCZI, E. J., *see* SNYDER, K. A.
DE GIORGI, E., **12, 13**, **15**
Debenedetti, P. G., xxiii, xxviii, *see* TORQUATO, S.
DeBotton, G., 683, 697, *see* PONTE CASTAÑEDA, P.
DEBYE, P., **319**, **336**
DEDERICHS, P. H., **251**, **267**, **291**, **310**, **553**, **565**
Dederichs, P. H., 291, 312, *see* ZELLER, R.
DEEG, W. F., **255**, **267**
DELL'ANTONIO, G. F., **248**, **267**, **371**, **373**, **387**, **393**
DELOOR, G. P., **457**, **491**
Derrick, G. H., 39, 44, *see* MCKENZIE, D. R.
Detournay, E., 33, 41, *see* CHENG, A. H.-D.
DeVries, M. S., 40, 42, *see* GARBOCZI, E. J.
DIAZ, A., **432**, **434**
Diener, G., 344, 353, *see* BOBETH, M.
DJORDJEVIĆ, B. R., **188**, **215**
Djordjević, B. R., 377, 395, *see* THORPE, M. F.
DOBRUSHIN, R., **489**, **491**
Dougherty, J. P., 4, 15, 16, *see* HARSHÉ, G.
DOYLE, W. T., **39**, **42**
DRUCKER, D. C., **284**, **287**
DUFOUR, R., **153**, **155**
DUNDURS, J., **66**, **71**
Dungan, D. F., 569, 598, *see* MANTESE, J. V.
Dunn, K.-J., 40, 41, *see* BERGMAN, D. J.
DUNN, M. L., **255**, **267**
DVORAK, G. J., **75**, **90**, **405**, **411**
DYKHNE, A. M., **47**, **49, 50**, **57**, **59, 60**, **64**, **71**

Eberl, K., 34, 46, *see* TORNOW, M.
EINSTEIN, A., **2**, **15**
EISCHEN, J. W., **39**, **42**, **558**, **565**
ELSAYED, M. A., **322**, **336**, **553**, **565**
ENGLAND, A. H., **107**, **111**
ERËMENKO, A., **480**, **491**
ESHELBY, J. D., **252**, **254–256**, **267**
ETINGHOF, P., **318**, **336**
Evans, K. E., 653, 667, 668, *see* ALDERSON, K. L., *see* CADDOCK, B. D.
EYRE, D. J., **40**, **42**, **303**, **308**, **310**, **583**, **597**
Eyre, D. J., 592, 599, *see* MILTON, G. W.

Fabre, S., 153, 155, *see* DUFOUR, R.
FANNJIANG, A., **22**, **42**, **265**, **267**, **277, 278**, **287**
Farach, H. A., 212, 214, *see* CRESWICK, R. J.
FARADAY, M., **2**, **15**
Fedorov, A. V., 75, 76, 90, 175, 182, 431, 432, 435, *see* LURIE, K. A.
Fel, L. G., 3, 15, 97, 110, 580, 597, *see* BERGMAN, D. J.
FELDERHOF, B. U., **239**, **243**, **571**, **597**
Felderhof, B. U., 239, 243, 377, 393, *see* HINSEN, K.
FENG, S., **197**, **213**, **215**
Feng, S., 197, 213, 219, *see* SCHWARTZ, L. M.
FIELD, D. A., **571**, **598**

Figari, R., 248, 267, 371, 373, 393, *see* DELL'ANTONIO, G. F.
FINKEL'BERG, V. M., **191**, **215**
FINLAYSON, B. A., **278**, **287**
Firoozye, N., 683, 695, *see* BHATTACHARYA, K.
FIROOZYE, N. B., **295**, **310**, **529**, **531, 532**, **550**, **673**, **696**
FISHER, M. E., **212**, **215**
FLAHERTY, J. E., **49**, **57**, **210**, **215**
Fleck, N. A., 271, 288, *see* SMYSHLYAEV, V. P.
FOKIN, A. G., **248**, **267**, **291**, **298**, **310**
FONSECA, I., **489**, **491**, **676**, **696**
Fonseca, I., 676, 696, *see* BRAIDES, A.
FOSTER, R. M., **370**, **393**
Fox, N., 22, 38, 40, *see* ATKIN, R. J.
FRANCFORT, G. A., **47**, **57**, **77**, **90**, **174, 175**, **182**, **447–449**, **453**, **471**, **492**, **501**, **504**, **525**, **645–647**, **668**
Francfort, G. A., 432, 433, *see* ALLAIRE, G.
FRANK, D. J., **40**, **42**, **212**, **215**
FRICKE, H., **194**, **215**
FRIIS, E. A., **652**, **668**
FRISCH, H. L., **320**, **336**
FUCHS, R., **370**, **393**
Fuchs, R., 370, 392, *see* BARRERA, R. G.
FUNG, Y. C., **22**, **25, 26**, **30**, **42**

GARBOCZI, E. J., **40**, **42**, **69**, **71**, **197**, **215**
Garboczi, E. J., 40, 42, 46, 66, 68, 71, 197, 215, 558, 567, *see* DAY, A. R., *see* FENG, S., *see* ROBERTS, A. P., *see* SNYDER, K. A.
GASSMANN, F., **85**, **90**
GAUTESEN, A. K., **207**, **215**
GEHRING, F. W., **480**, **492**
GELFAND, I. M., **223**, **243**
GÉRARD, P., **293**, **310**
Geyer, R. G., 569, 598, *see* MANTESE, J. V.
GIBIANSKY, L. V., **4**, **15**, **70, 71**, **81**, **90**, **163**, **174, 175**, **182**, **359**, **367**, **397**, **412**, **432**, **434**, **444**, **453**, **460**, **466**, **468**, **472**, **475**, **477–480**, **492**, **501**, **506**, **522**, **525, 526**, **529**, **543**, **550**, **560, 561**, **565**
Gibiansky, L. V., 221, 234, 237, 243, 264, 267, 271, 276, 277, 286, 362, 367, 397, 399, 411, 437, 450, 453, 502, 517, 522, 525, 537, 550, 560, 565, 614, 617, 639, 641, 653, 668, *see* AVELLANEDA, M., *see* CHERKAEV, A. V.
GIBSON, L. J., **653**, **668**
GILLETTE, G. J., **317, 318**, **323**, **336**
GITTLEMAN, J. I., **239**, **243**
GOLDEN, K., **11, 12**, **15**, **207**, **211**, **215**, **248**, **268**, **370**, **376**, **387**, **393**, **451**, **453**, **569**, **571**, **598**, **603**, **617**, **638, 639**, **641**
Golden, K., 207, 213, 303, 311, 322, 336, 379, 387, 389, 390, 392, 394, 397, 412, 451, 454, 569, 597, 600, 610, 618, 638, 641, *see* BERLYAND, L., *see* BRUNO, O. P., *see* CHERKAEVA, E., *see* MILTON, G. W., *see* SAWICZ, R.
GOODMAN, J., **432**, **434**
Gosz, M., 66, 72, *see* MORAN, B.
GRABOVSKY, Y., **130**, **139**, **305**, **310**, **355**, **358–363**, **365–367**, **432**, **434**, **466, 467**, **469**, **484**, **492**, **541, 542**, **550**, **558**, **566**
Grabovsky, Y., 467, 491, *see* CHERKAEV, A. V.
GRAGG, W. B., **571**, **598**
Granqvist, C. G., 569, 599, *see* NIKLASSON, G. A.
Grant, A. R., 377, 392, 393, *see* DAY, A. R.
Graves-Morris, P. R., 571, 596, *see* BAKER, JR., G. A.
GREENGARD, L., **39**, **42**, **188**, **215**, **333**, **337**
Greengard, L., 39–42, 210, 214, *see* CARRIER, J., *see* CHENG, H.
GREER, R. T., **3**, **15**
GRIMMETT, G., **xxiii**, **xxvii**
Grosvenor, J., 569, 598, *see* MANTESE, J. V.
GUBERNATIS, J. E., **291**, **311**

Haber, R. B., 432, 434, *see* JOG, C. S.
Haeberly, J.-P., 684, 696, *see* DACOROGNA, B.
Halperin, B. I., 211, 213, 215, *see* AMBEGAOKAR, V., *see* FENG, S.
Hamilton, D. H., 480, 491, *see* ERËMENKO, A.
HARMAN, T. C., **97**, **111**
HARSHÉ, G., **4**, **15, 16**
Harshé, G., 4, 14, 30, 40, *see* AVELLANEDA, M.
Hart, S., 683, 695, *see* AUMANN, R. J.
HASHIN, Z., **xxiv**, **xxv**, **xxvii**, **7**, **16**, **84**, **90**, **113**, **116, 117**, **139, 140**, **206**, **216**, **233**, **243**, **247**, **268**, **271, 272**, **279**, **287**, **347**, **350**, **353**, **457, 458**, **460**, **470, 471**, **473**, **489, 490**, **492, 493**, **574**, **586**, **598**
Hashin, Z., 80, 81, 83, 91, 569, 600, *see* ROSEN, B. W., *see* SCHULGASSER, K.
Hass, K. C., 210, 214, *see* DAVIS, L. C.
HE, Q.-C., **66**, **71**, **87**, **90**
Hejazi, M., 40, 45, *see* NEMAT-NASSER, S.
HELSING, J., **39, 40**, **42, 43**, **51**, **53**, **55**, **57**, **70**, **72**, **105, 106**, **111**, **155, 156**, **197**, **210**, **216**, **320**, **331**, **333**, **337**, **490**, **493**, **569**,

571, **586**, **598**
Helsing, J., 39, 42, 69, 71, 333, 336, 337, *see* CHRISTIANSSON, H., *see* GREENGARD, L.
HELTE, A., **319**, **337**, **554**, **566**
Helte, A., 197, 216, *see* HELSING, J.
HERAKOVICH, C. T., **653**, **668**
Hermans, J. J., 187, 218, *see* PETERSON, J. M.
Herrmann, G., 188, 216, *see* HONEIN, E.
Herrmann, H. J., 212, 218, *see* NORMAND, J.-M.
HETHERINGTON, J. H., **188**, **216**, **378**, **393**
Hetherington, J. H., 188, 215, 377, 395, *see* DJORDJEVIĆ, B. R., *see* THORPE, M. F.
HILL, R., **75**, **77**, **87**, **90**, **204**, **216**, **247**, **268**, **271–273**, **281**, **287**, **442**, **453**, **471**, **473, 474**, **493**
Hill, R., 284, 286, *see* BISHOP, J. F. W.
HINSEN, K., **239**, **243**, **377**, **393**
HOMAND-ETIENNE, F., **652**, **668**
HONEIN, E., **188**, **216**
Honein, T., 188, 216, *see* HONEIN, E.
Honig, J. M., 97, 111, *see* HARMAN, T. C.
HORI, M., **291**, **311**, **320**, **331, 332**, **337**
Hori, M., xxiii, xxiv, xxvii, 7, 17, *see* NEMAT-NASSER, S.
HORNUNG, U., **40**, **43**
HOU, T. Y., **40**, **43**
Houpert, R., 652, 668, *see* HOMAND-ETIENNE, F.
HU, G. K., **69**, **72**
Hughes, T. J. R., 22, 44, *see* MARSDEN, J. E.
HULL, D., **xxiii, xxiv**, **xxvii**
Hwang, K. C., 69, 72, 73, *see* ZHENG, Q.-S.

IKEDA, T., **29**, **43**
INGEBRIGTSEN, K. A., **103**, **111**
IWAKUMA, T., **40**, **43**
Iwakuma, T., 40, 45, *see* NEMAT-NASSER, S.

JACKSON, J. D., **185**, **216**, **224**, **228**, **243**, **369**, **393**, **592**, **598**
JAMES, R. D., **672**, **696**
James, R. D., xxv, xxvi, 671, 672, 683, 695, *see* BALL, J. M., *see* BHATTACHARYA, K.
JASIUK, I., **188**, **216**
Jasiuk, I., 66, 68, 72, *see* OSTOJA-STARZEWSKI, M., *see* THORPE, M. F.
JEFFREY, D. J., **187**, **191**, **216**
JEULIN, D., **577**, **598**
Jeulin, D., 332, 333, 337, *see* LE COËNT, A.
JOANNOPOULOS, J. D., **xxiii**, **xxvii**
JOG, C. S., **432**, **434**
Jones, R. B., 239, 243, *see* FELDERHOF, B. U.
JOSLIN, C. G., **333**, **337**
Jouve, F., 432, 433, *see* ALLAIRE, G.

KACHANOV, M., **188**, **216**
Kaganova, I. M., 47, 57, *see* DYKHNE, A. M.
KALAMKAROV, A. L., **426**, **434**
KANTOR, Y., **39**, **43**, **248**, **268**, **370, 371**, **393**, **569**, **598**, **603**, **617**
KAPITZA, P. L., **134**, **140**
KAWOHL, B., **432**, **434**
KELLER, J. B., **47**, **49**, **58**, **207, 208**, **210**, **216**
Keller, J. B., 32, 39, 41, 45, 47, 49, 57, 58, 210, 215, 218, 223, 244, *see* BURRIDGE, R., *see* FLAHERTY, J. E., *see* NEVARD, J., *see* NUNAN, K. C., *see* ODEH, F.

KELLOGG, O. D., **124**, **132**, **140**
KERNER, E. H., **117**, **140**, **199**, **204**, **216**
KESTEN, H., **xxiii**, **xxvii**
KHACHATURYAN, A. G., **252**, **268**, **295**, **311**, **474**, **493**, **672**, **696**
KHRUSLOV, E. YA., **9**, **16**
Kikuchi, N., 433, 435, *see* BENDSØE, M. P., *see* SUZUKI, K.
KIM, I. C., **40**, **43, 44**, **465**, **493**, **554, 555**, **566**, **586**, **598**
Kim, I. C., 40, 46, 207, 219, 331, 339, 586, 600, *see* THOVERT, J. F., *see* TORQUATO, S.
KINDERLEHRER, D., **677**, **696**
Kinderlehrer, D., 489, 490, 672, 696, *see* ADAMS, B. L., *see* JAMES, R. D.
KIRKPATRICK, S., **197**, **211**, **216**
KLICKER, K. A., **4**, **16**
Klitzing, K. v., 34, 46, *see* TORNOW, M.
Knackstedt, M. A., 331, 338, 555, 567, *see* ROBERTS, A. P.
KNEER, G., **254**, **268**
KOHLER, W., **248**, **268**
KOHN, R. V., **293**, **295**, **311**, **426**, **431**, **435**, **462**, **465**, **474**, **493**, **672**, **677**, **680**, **682**, **696, 697**
Kohn, R. V., 47, 58, 130, 139, 172, 183, 207, 219, 280, 287, 295, 310, 432–434, 462, 466–469, 471, 474, 484, 490–492, 495, 518, 525, 531, 550, 682, 683, 695, *see* ALLAIRE, G., *see* BHATTACHARYA, K., *see* FIROOZYE, N. B., *see* GOODMAN, J., *see* GRABOVSKY, Y., *see* LEVY, O., *see* MILTON, G. W., *see* SHENG, P.
KOLOSOV, G. V., **107**, **111**

Kolpakov, A., 209, 213, *see* BERLYAND, L.
KOLPAKOV, A. G., **653**, **668**
Kolpakov, A. G., 426, 434, *see* KALAMKAROV, A. L.
KONDRATIEV, V. A., **101**, **111**
KORÁNYI, A., **390**, **393**
KORRINGA, J., **205**, **216**, **254**, **268**, **569**, **598**
Korringa, J., 85, 89, *see* BROWN, R. J. S.
Kotecký, R., 489, 491, *see* DOBRUSHIN, R.
KOZLOV, S., **155, 156**
KOZLOV, S. M., **11, 12**, **16**, **207**, **210**, **217**
Kozlov, S. M., xxv, xxviii, 8, 11, 13, 18, 47, 58, 200, 207, 208, 211, 213, 215, 220, *see* BERLYAND, L., *see* GOLDEN, K., *see* ZHIKOV, V. V.
KRISTENSEN, J., **690**, **697**
Krog, L. A., 432, 434, 468, 491, *see* CHERKAEV, A. V.
KRÖNER, E., **251**, **268**, **282**, **287**, **291**, **311**, **458**, **493**, **553**, **566**
Krumhansl, J. A., 291, 311, *see* GUBERNATIS, J. E.
KUBLANOV, L., **558**, **566**
Küçük, İ, 432, 434, 468, 491, *see* CHERKAEV, A. V.
KUNIN, I. A., **254**, **268**
Kunze, K., 318, 335, *see* ADAMS, B. L.

Lado, F., 331, 333, 338, 339, 557, 567, 586, 601, *see* SEN, A. K., *see* TORQUATO, S.
Lai, D., 35, 41, 66, 71, *see* CHEN, T.
LAKES, R., **2–5**, **16**, **230**, **243**, **479**, **494**, **652**, **668**
Lakes, R., 583, 597, 652, 668, *see* EYRE, D. J., *see* FRIIS, E. A.
LAM, J., **39**, **44**
LANDAU, L. D., **21**, **33**, **44**
LANDAUER, R., **2**, **16**, **185**, **193**, **217**
Langer, J. S., 211, 213, *see* AMBEGAOKAR, V.
LARSEN, U. D., **2, 3**, **16**, **653**, **668**
LAST, B. J., **213**, **217**
LaTorraca, G. A., 569, 598, *see* KORRINGA, J.
LAX, P. D., **595**, **598**
LE COËNT, A., **332, 333**, **337**
LEHTO, O., **153**, **156**
LEKHNITSKII, S. G., **107**, **111**
Leo, P. H., 257, 267, 372, 373, 392, 569, 597, *see* BRUNO, O. P.
Leoni, G., 676, 696, *see* BRAIDES, A.
LEVIN, V. M., **80**, **90**
LEVY, O., **47**, **58**, **242, 243**
Levy, O., 97, 110, *see* BERGMAN, D. J.
Li, Z.-Y., 242, 243, *see* LIU, X.-Y.
LIFSHITZ, E. M., **28**, **44**, **61**, **72**
Lifshitz, E. M., 21, 33, 44, *see* LANDAU, L. D.
Lin, I.-H., 254, 268, *see* KORRINGA, J.
Lions, J.-L., 8, 10, 11, 14, 221, 242, *see* BENSOUSSAN, A.
LIPTON, R., **135**, **140**, **175**, **182**, **188**, **217**, **294**, **311**, **346**, **353**, **370**, **394**, **472, 473**, **494**
Lipton, R., 465, 474, 493, *see* KOHN, R. V.
Little, T. D., 682, 696, *see* KOHN, R. V.
LIU, C., **40**, **44**, **377**, **394**
LIU, X.-Y., **242, 243**
Livshits, I., 489, 490, *see* ADAMS, B. L.
Lo, K. H., 205, 214, *see* CHRISTENSEN, R. M.
Lobb, C. J., 40, 42, 212, 215, *see* FRANK, D. J.
Lods, V., 681, 695, *see* ALLAIRE, G.
LOVE, J. D., **188**, **217**
Lu, W., 39, 45, *see* SANGANI, A. S.
LUKKASSEN, D., **471**, **494**
Lukkassen, D., 471, 491, *see* BRAIDES, A.
LURIE, A. I., **22**, **44**
LURIE, K. A., **56**, **58**, **66**, **70**, **72**, **75, 76**, **90**, **118**, **140**, **167**, **175**, **182**, **347**, **353**, **428, 429**, **431, 432**, **435**, **447**, **450**, **453, 454**, **460**, **462**, **494**, **499**, **506**, **508**, **521**, **526**, **529**, **551**
Lurie, K. A., 66, 71, 120, 139, 426, 432–434, 439, 441, 444, 450, 452, 453, 512, 525, 538, 550, 555, 564, *see* ARMAND, J.-L., *see* AVELLANEDA, M., *see* CHERKAEV, A. V., *see* GIBIANSKY, L. V.
LUSKIN, M., **672**, **697**
LYSNE, P. C., **370**, **394**

MA, H., **40**, **44**, **377**, **394**
MACKENZIE, J. K., **205**, **217**
Majda, A. J., 370, 391, 392, *see* AVELLANEDA, M.
MANSFIELD, E. H., **134**, **140**
MANTESE, J. V., **569**, **598**
Mantese, J. V., 592, 599, *see* MILTON, G. W.
MARCELLINI, P., **533**, **551**
Marini, A., 543, 550, *see* BAUMAN, P.
MARINO, A., **153**, **156**
Markenscoff, X., 66, 71, *see* DUNDURS, J.
MARKOV, K. Z., **xxv**, **xxvii**, **2**, **16**, **185**, **191**, **217**, **346**, **353**, **553**, **566**
MARSDEN, J. E., **22**, **44**
Mason, D. E., 489, 490, *see* ADAMS, B. L.
Mason, T. A., 490, 491, *see* BERAN, M. J.
MASON, W. P., **29**, **44**
MATHERON, G., **47**, **58**, **320**, **337**, **346**, **353**
MATTHEWS, F. L., **xxiv**, **xxvii**, **1**, **16**

MAXWELL GARNETT, J. C., **3**, **16**, **239**, **243**
MAXWELL, J. C., **2**, **16**, **132**, **140**, **159**, **165–167**, **183**, **252**, **268**
Mazliak, L., 9, 15, *see* BRIANE, M.
MCCARTHY, J. F., **40**, **44**
MCCOY, J. J., **553**, **557**, **566**
McCoy, J. J., 291, 309, 317, 318, 322, 323, 336, 553, 565, *see* BERAN, M. J., *see* ELSAYED, M. A., *see* GILLETTE, G. J.
MCKENZIE, D. R., **39**, **44**
McKenzie, D. R., 3, 17, 39, 40, 44, 45, 116, 141, 239, 244, 377, 381, 394, 569, 571, 599, *see* MCPHEDRAN, R. C., *see* MILTON, G. W., *see* PARKER, A. R., *see* PERRINS, W. T.
MCLAUGHLIN, R., **206**, **217**
MCPHEDRAN, R. C., **39**, **44**, **188**, **210**, **217**, **239**, **244**, **306**, **311**, **317**, **331**, **333**, **337**, **377**, **381**, **394**, **569**, **571**, **575–577**, **583**, **599**
McPhedran, R. C., 3, 17, 39, 40, 44–46, 116, 141, 239, 241, 244, 390, 394, 571, 599, *see* MCKENZIE, D. R., *see* MILTON, G. W., *see* NICOROVICI, N. A., *see* PARKER, A. R., *see* PERRINS, W. T., *see* YARDLEY, J. G.
Meade, R. D., xxiii, xxvii, *see* JOANNOPOULOS, J. D.
Meister, R., 490, 495, *see* PESELNICK, L.
MENDELSON, K. S., **47, 48**, **58**
Mermin, N. D., 28, 40, 223, 224, 242, *see* ASHCROFT, N. W.
MEYERS, N. G., **200**, **204**, **217**
MICHEL, J. C., **40**, **44, 45**, **298**, **303**, **308, 309**, **311**
Micheli, A. L., 569, 598, *see* MANTESE, J. V.
MICHELL, J. H., **66**, **72**
Miettinen, M., 646, 668, *see* ASTALA, K.
Miksis, M. J., 234, 242, *see* CAFLISCH, R. E.
MILGROM, M., **93–96**, **111**, **118**, **140**, **147**, **156**
MILLER, C. A., **331**, **333**, **338**
MILLER, M. N., **320**, **331**, **334**, **338**, **553**, **566**
Mills, R. L., 254, 268, *see* KORRINGA, J.
MILNE-THOMSON, L. M., **38**, **45**
MILOH, T., **134**, **140**
Miloh, T., 135, 136, 139, *see* BENVENISTE, Y.
MILTON, G. W., **2**, **16**, **35**, **40**, **45**, **61**, **64**, **72**, **81**, **91**, **105**, **111**, **118**, **120**, **124, 125**, **129**, **136**, **138**, **140, 141**, **147**, **154**, **156**, **164**, **172**, **183**, **196, 197**, **202**, **206, 207**, **217, 218**, **248**, **265**, **268**, **277**, **280**, **287**, **303**, **311**, **322**, **330–332**, **338**, **370, 371**, **379**, **382**, **384**, **387**, **389, 390**, **394**, **397**, **399**, **412**, **451, 452**, **454**, **458–460**, **462, 463**, **466**, **469**, **471–474**, **478–480**, **494, 495**, **499**, **505**, **512, 513**, **517, 518**, **522**, **526, 527**, **530**, **532**, **535**, **551**, **553, 554**, **557–559**, **566, 567**, **569–571**, **574**, **577, 578**, **581**, **583**, **586–589**, **592**, **599**, **603**, **610**, **612, 613**, **617–619**, **638–641**, **646, 647**, **652, 653**, **655, 656**, **658, 659**, **661**, **664**, **666–669**
Milton, G. W., 39, 40, 42–44, 51, 53, 55, 57, 66, 70–72, 85, 89, 105, 106, 111, 120, 139, 175, 182, 210, 217, 228, 230, 239, 241, 244, 303, 305, 308, 310, 317, 331, 333, 337, 338, 355, 359–363, 365–367, 387, 390, 392, 394, 397, 412, 439, 441, 444, 447–450, 452, 453, 462, 475, 477–480, 492, 493, 501, 502, 512, 522, 525, 536–538, 550, 551, 554, 555, 558, 560, 564–567, 569, 571, 575–577, 583, 597, 599, 614, 617, 645–647, 668, 684, 697, *see* AVELLANEDA, M., *see* BERRYMAN, J. G., *see* CHERKAEV, A. V., *see* CLARK, K. E., *see* EYRE, D. J., *see* FRANCFORT, G. A., *see* GIBIANSKY, L. V., *see* GRABOVSKY, Y., *see* HELSING, J., *see* KOHN, R. V., *see* KUBLANOV, L., *see* MCPHEDRAN, R. C., *see* NESI, V., *see* NICOROVICI, N. A., *see* PHAN-THIEN, N., *see* SØLNA, K.
Mioduchowski, A., 132, 141, *see* RU, C.-Q.
Mityushev, V., 429, 433, *see* BERLYAND, L.
Molyneux, J., 291, 309, 553, 557, 564, 589, 597, *see* BERAN, M. J.
MORAN, B., **66**, **72**
MORREY, C. B., **684**, **697**
Morse, S., 194, 215, *see* FRICKE, H.
MORTOLA, S., **154**, **156**
Moskalenko, V. N., 197, 214, *see* BOLOTIN, V. V.
Mossino, J., 153, 155, *see* DUFOUR, R.
MOULINEC, H., **40**, **45**, **306**, **308**, **311**
Moulinec, H., 40, 44, 45, 298, 303, 308, 309, 311, 333, 338, *see* MICHEL, J. C., *see* SUQUET, P.
Moura, M., 39, 42, 188, 215, *see* GREENGARD, L.
MOVCHAN, A. B., **69**, **72**,

186, **188**, **218**
Movchan, A. B., 39, 43, 44, 51, 53, 55, 57, 70, 72, 105, 106, 111, 135, 139, 147, 155, 156, 210, 217, 467, 491, *see* ALPHUTOVA, N. B., *see* BIGONI, D., *see* CHERKAEV, A. V., *see* HELSING, J., *see* MCPHEDRAN, R. C., *see* MILTON, G. W.
Movchan, N. V., 186, 218, *see* MOVCHAN, A. B.
MÜLLER, S., **14**, **16**, **672**, **674**, **681**, **684**, **686**, **688**, **697**
Müller, S., 676, 696, *see* FONSECA, I.
Mullins, W. W., 489, 490, *see* ADAMS, B. L.
MURAT, F., **10**, **12, 13**, **17**, **59**, **72**, **250**, **269**, **275, 276**, **287, 288**, **347**, **353**, **429**, **431, 432**, **435**, **444**, **454**, **462**, **495**, **499**, **503**, **506**, **508**, **521**, **527**, **529**, **551**, **676**, **697**
Murat, F., 47, 57, 174, 175, 182, 447, 453, 471, 492, 501, 504, 525, 674, 695, *see* BALL, J. M., *see* FRANCFORT, G. A.
MUSKHELISHVILI, N. I., **107**, **111**

NAN, C.-W., **4**, **17**
Nazarov, S. A., 147, 155, *see* ALPHUTOVA, N. B.
NEMAT-NASSER, S., **xxiii, xxiv**, **xxvii**, **7**, **17**, **40**, **45**
Nemat-Nasser, S., 40, 43, *see* IWAKUMA, T.
NESI, V., **120**, **124**, **141**, **152**, **156**, **480, 481**, **495**, **531**, **537**, **541**, **543**, **551, 552**, **646**, **669**, **684**, **697**
Nesi, V., 152, 155, 207, 218, 387, 393, 480, 491, 495, 543, 550, 646, 669, *see* ALESSANDRINI, G., *see* ASTALA, K., *see* BAUMAN, P., *see* DELL'ANTONIO, G. F., *see* MILTON, G. W.
NEVARD, J., **47**, **58**
Newnham, R. E., 4, 15, 16, *see* HARSHÉ, G., *see* KLICKER, K. A.
NGUETSENG, G., **8**, **10**, **17**
NICOROVICI, N. A., **239**, **241**, **244**, **390**, **394**
Nicorovici, N. A., 3, 17, 39, 46, *see* PARKER, A. R., *see* YARDLEY, J. G.
NIKLASSON, G. A., **569**, **599**
NOBLE, B., **595**, **600**
NOH, T. W., **200**, **218**
Noll, W., 672, 696, *see* COLEMAN, B. D.
NORMAND, J.-M., **212**, **218**
NORRIS, A., **32**, **45**, **85**, **91**, **202, 203**, **206**, **218**, **471**, **495**
NORRIS, J. R., **277**, **288**
Northrup, J., 473, 494, *see* LIPTON, R.
NUNAN, K. C., **39**, **45**, **210**, **218**

O'BRIEN, R. W., **210**, **218**
O'Brien, R. W., 209, 213, *see* BATCHELOR, G. K.
Obnosov, Y.. V., 154, 155, *see* CRASTER, R. V.
OBNOSOV, Y. V., **143**, **154**, **156**, **207**, **218**
ODEH, F., **223**, **244**
OGDEN, R. W., **22**, **45**
OLDROYD, J. G., **256**, **269**
OLEINIK, O. A., **11**, **17**, **101**, **111**
Oleinik, O. A., xxv, xxviii, 8, 11, 13, 18, 47, 58, 101, 111, 200, 220, *see* KONDRATIEV, V. A., *see* ZHIKOV, V. V.
Olhoff, N., 431–435, *see* CHENG, K.-T., *see* ROZVANY, G.
OLSON, T., **489, 490**, **495**, **683**, **697**
Olson, T., 97, 110, 163, 182, 490, 491, *see* AVELLANEDA, M., *see* BERAN, M. J.
OLVER, P. J., **147**, **156**
Olver, P. J., 275, 286, *see* BALL, J. M.
Ong, T., 433, 435, *see* ROZVANY, G.
Orlandi, E., 248, 267, 371, 373, 393, *see* DELL'ANTONIO, G. F.
OSBORN, J. A., **132**, **141**
OSTOJA-STARZEWSKI, M., **66**, **72**

Palais, R., 432, 434, *see* CHERKAEV, A. V.
Panasenko, G. P., 8, 10, 11, 14, *see* BAKHVALOV, N. S.
PAPANICOLAOU, G., **11, 12**, **17**, **248**, **269**
Papanicolaou, G., 8, 10–12, 14, 15, 22, 42, 211, 214, 221, 234, 242, 248, 265, 267, 268, 277, 278, 287, 370, 376, 387, 393, 451, 453, 571, 598, 603, 617, 638, 639, 641, *see* BENSOUSSAN, A., *see* BORCEA, L., *see* CAFLISCH, R. E., *see* FANNJIANG, A., *see* GOLDEN, K., *see* KOHLER, W.
Park, J. B., 652, 668, *see* FRIIS, E. A.
PARKER, A. R., **3**, **17**
PARRY, G. P., **684**, **697**
PEDREGAL, P., **275**, **288**, **684**, **686–688**, **690**, **697**
Pedregal, P., 677, 696, *see* KINDERLEHRER, D.
PERRINS, W. T., **39**, **45**, **116**, **141**
Perrins, W. T., 188, 217, 239, 244, 306, 311, *see* MCPHEDRAN, R. C.
Persson, L., 8, 17, *see* PERSSON, L.-E.
PERSSON, L.-E., **8**, **17**
PESELNICK, L., **490**, **495**
Peselnick, L., 489, 490, 497, *see* WATT, J. P.
PETERSON, J. M., **187**, **218**
PHAM, D. C., **490**, **495, 496**,

553, **567**, **586**, **600**
PHAN-THIEN, N., **331**, **338**, **554**, **567**
Phan-Thien, N., 458, 474, 495, 553, 554, 557, 559, 567, *see* MILTON, G. W.
Pitaevskii, L. P., 28, 44, 61, 72, *see* LIFSHITZ, E. M.
PITTMAN, E. D., **xxiii**, **xxvii**
POISSON, S. D., **2**, **17**, **252**, **269**
Poladian, L., 210, 217, *see* MCPHEDRAN, R. C.
POLDER, D., **198**, **218**
PÓLYA, G., **186**, **218**
PONTE CASTAÑEDA, P., **271**, **284–286**, **288**, **531**, **552**, **683**, **697**
Poole, Jr., C. P., 212, 214, *see* CRESWICK, R. J.
POSTMA, G. W., **163**, **183**
PRAGER, S., **556**, **567**, **580**, **589**, **600**
Prager, S., 317, 319, 339, *see* WEISSBERG, H. L.
Promislow, K., 653, 668, *see* BERLYAND, L.
Pukánszky, L., 390, 393, *see* KORÁNYI, A.

Radchik, A. V., 143, 156, 377, 394, *see* REUBEN, A. J.
RAĬTUM, U. Ë., **431**, **435**, **444**, **447**, **454**, **521**, **527**
RAITUMS, U., **13**, **17**
RAITUMS, U. E., **431**, **435**
Rawlings, R. D., xxiv, xxvii, 1, 16, *see* MATTHEWS, F. L.
RAYLEIGH, L., **2**, **17**, **39**, **45**
REED, M., **223**, **244**
Reich, E., 480, 492, *see* GEHRING, F. W.
Reitich, F., 257, 267, 304, 310, *see* BRUNO, O. P.
REUBEN, A. J., **143**, **156**, **377**, **394**
REUSS, A., **271**, **288**, **442**, **454**
Reyna, L., 432, 434, *see* GOODMAN, J.
RICE, J. R., **32**, **45**
Rikvold, P. A., 331, 338, *see* STELL, G.
Rintoul, M. D., 135, 142, *see* TORQUATO, S.
ROBERTS, A. P., **331**, **338**, **555**, **558**, **567**
Rohrer, G. S., 489, 490, *see* ADAMS, B. L.
ROKHLIN, V., **39**, **45**
Rokhlin, V., 39, 41, 42, *see* CARRIER, J., *see* CHENG, H., *see* GREENGARD, L.
Rollett, A. D., 489, 490, *see* ADAMS, B. L.
ROSCOE, R., **206**, **219**, **471**, **496**, **646**, **669**
ROSEN, B. W., **80, 81**, **83**, **91**
Rothenburg, L., 652, 668, *see* BATHURST, R. J.
ROYTBURD, A. L., **672**, **697, 698**
ROZVANY, G., **433**, **435**
RU, C.-Q., **132**, **135**, **141**
RUDELSON, M., **441**, **444**, **454**, **501**, **527**
Rudelson, M., 362, 367, 502, 525, 537, 550, *see* AVELLANEDA, M.
RUDIN, W., **372**, **390**, **394, 395**
Runge, R. J., 205, 216, *see* KORRINGA, J.
Ruzin, I. M., 64, 71, *see* DYKHNE, A. M.

SAFFMAN, P. G., **481**, **496**
Sage, D. S., 305, 310, 355, 358, 360, 363, 365–367, *see* GRABOVSKY, Y.
Saint Jean Paulin, J., 11, 15, *see* CIORANESCU, D.
Samuelsson, K., 39, 40, 43, *see* HELSING, J.
SANCHEZ-PALENCIA, E., **xxiii**, **xxvii**, **8**, **17**, **134**, **141**, **221**, **244**
SANDERS, J. V., **3**, **17**
Sandler, R., 433, 435, *see* ROZVANY, G.
SANGANI, A. S., **39**, **45, 46**, **331**, **333**, **338**, **571**, **575**, **600**
Savary, L., 577, 598, *see* JEULIN, D.
SAWICZ, R., **390**, **395**, **569**, **600**
Saylor, D. M., 489, 490, *see* ADAMS, B. L.
SCAIFE, B. K. P., **19**, **46**, **193**, **219**
Scala, C., 202, 219, *see* SEN, P.
SCHAPERY, R. A., **503**, **527**
SCHEIDEGGER, A. E., **xxiii**, **xxvii**
Schiavone, P., 132, 141, *see* RU, C.-Q.
SCHULGASSER, K., **47**, **49**, **51**, **58**, **81**, **84**, **91**, **96**, **111**, **118–122**, **141**, **159**, **183**, **332**, **338**, **438–440**, **454**, **502**, **527**, **553**, **567**, **569**, **589**, **600**
SCHWARTZ, L. M., **40**, **46**, **197**, **213**, **219**
SEN, A. K., **331**, **338**, **557**, **567**
SEN, P., **202**, **219**
Sen, P. N., 197, 213, 215, 219, *see* FENG, S., *see* SCHWARTZ, L. M.
Serkov, S. K., 69, 72, 135, 136, 138, 139, 141, 188, 218, 467, 491, 530, 551, *see* BIGONI, D., *see* CHERKAEV, A. V., *see* MILTON, G. W., *see* MOVCHAN, A. B.
SERRE, D., **533**, **552**
Shafiro, B., 188, 216, *see* KACHANOV, M.
Shamaev, A. S., 11, 17, 101, 111, *see* OLEINIK, O. A.
SHENG, P., **xxiii**, **xxvii**, **207**, **211**, **219**
Sheng, P., 40, 44, 46, 202, 218, 377, 394, *see* MA, H., *see* NORRIS, A., *see* TAO, R.
Shermergor, T. D., 291, 310, *see* FOKIN, A. G.
SHKLOVSKIĬ, B. I., **65**, **72**
Shlosman, S., 489, 491, *see* DOBRUSHIN, R.
Shtrikman, S., 93, 95, 96, 111,

113, 116, 140, 147, 156, 206, 216, 271, 279, 287, 347, 350, 353, 457, 458, 460, 470, 471, 473, 489, 490, 493, 574, 586, 598, *see* HASHIN, Z., *see* MILGROM, M.
Sievers, A. J., 200, 218, 377, 392, 393, *see* DAY, A. R., *see* NOH, T. W.
SIGMUND, O., **3, 4**, **17, 18**, **474**, **485–487**, **496**, **652, 653**, **669**
Sigmund, O., 2, 3, 16, 460, 472, 492, 543, 550, 653, 668, *see* GIBIANSKY, L. V., *see* LARSEN, U. D.
SIH, G. C., **xxiii**, **xxvii**
SILNUTZER, N. R., **331, 332**, **338**, **553**, **558**, **567**
Silnutzer, N. R., 332, 336, 553, 564, *see* BERAN, M. J.
Simon, B., 223, 244, *see* REED, M.
Smith, G. B., 143, 156, 377, 394, *see* REUBEN, A. J.
SMITH, J. C., **205**, **219**
SMITH, W. A., **4**, **18**
SMYSHLYAEV, V. P., **10**, **18**, **271**, **288**, **295**, **311**, **515**, **527**
SNYDER, K. A., **40**, **46**
Snyder, K. A., 40, 42, 66, 68, 71, *see* DAY, A. R.
SOBEL, D., **79**, **91**
SØLNA, K., **228**, **230**, **244**
Song, P. H., 200, 218, *see* NOH, T. W.
Sosnina, E. G., 254, 268, *see* KUNIN, I. A.
SPAGNOLO, S., **12, 13**, **18**
Spagnolo, S., 153, 156, *see* MARINO, A.
Stara, J., 432, 434, *see* KAWOHL, B.
STAUFFER, D., **xxiii**, **xxviii**
Stauffer, D., 213, 220, *see* ZABOLITZKY, J. G.
Steffé, Sergio, 154, 156, *see* MORTOLA, S.
STELL, G., **331**, **338**
Stell, G., 317, 331, 333, 337, 339, 553, 568, *see* JOSLIN, C. G., *see* TORQUATO, S.
Stolz, C., 134, 139, 458, 491, *see* BORNERT, M.
STONER, E. C., **132**, **141**
STORER, J. E., **370**, **395**
STRALEY, J. P., **93**, **95**, **112**, **212**, **219**, **370**, **395**
STRANG, G., **413**, **423**
Strang, G., 426, 431, 435, 680, 697, *see* KOHN, R. V.
STRELNIKER, Y. M., **34**, **46**, **51**, **58**
Strelniker, Y. M., 34, 41, 46, 51, 57, *see* BERGMAN, D. J., *see* TORNOW, M.
STROUD, D., **66**, **72**, **197**, **219**, **379**, **395**
Stroud, D., xxv, xxvi, *see* BERGMAN, D. J.
SUQUET, P., **284**, **288**, **333**, **338**, **683**, **698**
Suquet, P., 40, 44, 45, 286, 288, 298, 303, 306, 308, 309, 311, *see* MICHEL, J. C., *see* MOULINEC, H., *see* PONTE CASTAÑEDA, P.
SUZUKI, K., **433**, **435**
Svanstedt, N., 8, 17, *see* PERSSON, L.-E.
ŠVERÁK, V., **673**, **684**, **688**, **698**
Šverák, V., 684, 697, *see* PEDREGAL, P.
Swart, P. J., 4, 14, *see* AVELLANEDA, M.
Szegő, G., 186, 218, *see* PÓLYA, G.
Szeto, W., 433, 435, *see* ROZVANY, G.

Ta'asan, S., 489, 490, *see* ADAMS, B. L.
TALBOT, D. R. S., **271**, **285**, **288**
Talbot, D. R. S., 135, 140, 531, 552, *see* LIPTON, R., *see* NESI, V.
Tam, W. Y., 40, 44, 377, 394, *see* MA, H.
TAO, R., **40**, **46**
TARTAR, L., **10**, **12, 13**, **18**, **59**, **72**, **129**, **141**, **155, 156**, **162**, **164, 165**, **167**, **174**, **177**, **183**, **274–276**, **288, 289**, **292–294**, **311, 312**, **426**, **429**, **431, 432**, **435, 436**, **444, 445**, **447**, **454, 455**, **462**, **496**, **499**, **503**, **506**, **508, 509**, **521**, **527**, **529**, **552**, **676, 677**, **683, 684**, **698**
Tartar, L., 10, 12, 13, 17, 77, 90, 175, 182, 347, 353, 429, 431, 432, 435, 444, 454, 462, 495, 499, 503, 506, 508, 521, 527, 529, 551, *see* FRANCFORT, G. A., *see* MURAT, F.
Taya, M., 255, 267, *see* DUNN, M. L.
Taylor, G., 481, 496, *see* SAFFMAN, P. G.
TAYLOR, G. I., **3**, **18**, **234**, **244**
TAYLOR, J. E., **489**, **496**
Taylor, J. E., 433, 435, *see* ROZVANY, G.
Telega, J. J., 39, 46, 575, 577, 590, 600, *see* TOKARZEWSKI, S.
TERPSTRA, F. J., **533**, **552**
Teubner, M., 331, 338, 555, 567, *see* ROBERTS, A. P.
Thompson, D. D., 205, 216, *see* KORRINGA, J.
THORPE, M. F., **66**, **68**, **72**, **188**, **219**, **377**, **395**
Thorpe, M. F., 40, 42, 66, 68–71, 188, 191, 197, 210, 213–216, 219, 377, 378, 392, 393, 557, 565, *see* CHEN, J., *see* CHOY, T. C., *see* DAVIS, L. C., *see* DAY, A. R., *see* DJORDJEVIĆ, B. R., *see* FENG, S., *see* GARBOCZI, E. J., *see* HETHERINGTON, J. H., *see* JASIUK, I., *see* SCHWARTZ, L. M.

Thouless, D. J., 213, 217, *see* LAST, B. J.
THOVERT, J. F., **331**, **339**
TIMOSHENKO, S., **22**, **26**, **46**
Ting, L., 234, 242, *see* CAFLISCH, R. E.
TOKARZEWSKI, S., **39**, **46**, **571**, **575**, **577, 578**, **590**, **600**
TOLAND, J. F., **284**, **289**
Tonning, A., 103, 111, *see* INGEBRIGTSEN, K. A.
TORNOW, M., **34**, **46**
TORQUATO, S., **xxiii**, **xxv**, **xxviii**, **40**, **46**, **135**, **142**, **207**, **219**, **258**, **269**, **305**, **312**, **317**, **331**, **333**, **339**, **425**, **436**, **461**, **496**, **522**, **527**, **553**, **557**, **567, 568**, **578**, **586**, **600, 601**
Torquato, S., 3, 4, 15, 17, 18, 39, 40, 42–44, 70, 71, 81, 90, 163, 182, 331, 333, 338, 339, 346, 353, 425, 436, 465, 493, 506, 522, 525, 526, 554, 555, 557, 558, 560, 561, 565–567, 586, 598, *see* CHENG, H., *see* EISCHEN, J. W., *see* GIBIANSKY, L. V., *see* KIM, I. C., *see* MILLER, C. A., *see* SEN, A. K., *see* SIGMUND, O., *see* THOVERT, J. F., *see* YEONG, C. L. Y.
Truskett, T. M., xxiii, xxviii, *see* TORQUATO, S.
Tsukrov, I., 188, 216, *see* KACHANOV, M.

Valentini, M., 135, 139, *see* BIGONI, D.
VAN BEEK, L. K. H., **185**, **219**
VAN DER POEL, C., **205**, **219**
Van Santen, J. H., 198, 218, *see* POLDER, D.
VAN WIJNGAARDEN, L., **234**, **244**
Vanninathan, M., 221, 243, *see* CONCA, C.
Varadhan, S., 11, 12, 17, 248, 269, *see* PAPANICOLAOU, G.
Vernescu, B., 135, 140, *see* LIPTON, R.
VIGDERGAUZ, S. B., **467**, **484, 485**, **496**
Virtanen, K. I., 153, 156, *see* LEHTO, O.
VOIGT, W., **271**, **289**, **442**, **455**
Vucans, J., 155, 156, *see* KOZLOV, S.

WALPOLE, L. J., **199**, **205**, **219**, **255**, **269**, **473, 474**, **496**
WANG, B., **255**, **269**
WARREN, T. L., **653**, **669**
WATT, J. P., **489, 490**, **496, 497**
Weiss, D., 34, 46, *see* TORNOW, M.
WEISSBERG, H. L., **317**, **319**, **339**
Weng, G. J., 69, 72, *see* HU, G. K.
WIENER, O., **574**, **601**
WILCOX, C. H., **223**, **244**
WILLEMSE, M. W. M., **335**, **339**, **490**, **497**
WILLIS, J. R., **xxv**, **xxviii**, **185**, **191**, **200**, **220**, **252**, **254–256**, **258**, **269, 270**, **284**, **289**, **291**, **312**, **327**, **340**, **347**, **353**, **464**, **497**
Willis, J. R., 191, 217, 271, 284, 285, 288, 289, 295, 311, 515, 527, 531, 552, *see* MARKOV, K. Z., *see* NESI, V., *see* SMYSHLYAEV, V. P., *see* TALBOT, D. R. S., *see* TOLAND, J. F., *see* PONTE CASTAÑEDA, P.
Winn, J. N., xxiii, xxvii, *see* JOANNOPOULOS, J. D.
Wittum, G., 432, 434, *see* KAWOHL, B.
Woinowsky-Krieger, S., 26, 46, *see* TIMOSHENKO, S.
WOOD, A. B., **89**, **91**
Wright, S. I., 318, 335, *see* ADAMS, B. L.
Wu, C.-T., 489, 490, *see* ADAMS, B. L.
Wu, H., 40, 44, 377, 394, *see* LIU, C.
WU, T. T., **205**, **220**
Wu, X.-H., 40, 43, *see* HOU, T. Y.
WULFF, G., **489**, **497**
Wyller, J., 8, 17, *see* PERSSON, L.-E.

Yao, C., 39, 46, 331, 333, 338, 571, 575, 600, *see* SANGANI, A. S.
YARDLEY, J. G., **39**, **46**
YEONG, C. L. Y., **425**, **436**
Yonezawa, F., 332, 337, *see* HORI, M.
Yosifian, G. A., 11, 17, 101, 111, *see* OLEINIK, O. A.

ZABOLITZKY, J. G., **213**, **220**
Zaoui, A., 134, 139, 458, 491, *see* BORNERT, M.
ZELLER, R., **291**, **312**
Zeller, R., 251, 267, 291, 310, 553, 565, *see* DEDERICHS, P. H.
Zhang, B., 40, 44, 377, 394, *see* MA, H.
ZHENG, Q.-S., **69**, **72, 73**
ZHIKOV, V. V., **xxv**, **xxviii**, **8**, **11**, **13**, **18**, **47**, **58**, **120**, **142**, **164**, **183**, **200**, **220**, **280**, **282**, **289**, **462**, **466**, **471–473**, **497**
ZUZOVSKY, M., **39**, **46**
Zvyatkov, K. D., 553, 566, *see* MARKOV, K. Z.

Subject index

$\mathcal{A}$-quasiconvexification, 676
acoustic tensor, 174, 233
acoustic waves
  bubbly fluid, 3, 89, 233
  poroelastic media, 33
adjoint equation effective tensor, 263
affine boundary conditions, 671, 675
affine transformation, 145, 327
Airy stress function, 24, 27, 67
Allaire-Kohn energy bounds, 466
analytic properties, 369–391, 569
analyticity in frequency, 225
antiplane elasticity, 37
  planar elasticity link, 105
antiplane elasticity equations, *see* conductivity, equations
antiplane viscoelasticity, 106
approximations
  average field, 198
  differential, 201
  effective medium, 195
  testing validity, 425
arc, Arc(z_1, z_2, z_3), 575
Archie's law, 202
attenuation length, 226, 228
Avellaneda bounds, 464
average field approximations, 198
  nonrealizability, 199
average fields, bounds on, 426, 444, 529, 530
Backus formulas, 163
bending moments, 27
bending of plates, *see* elasticity, two-dimensional
Beran bounds, 553, 555, 564, 574, 577
Beran-Molyneux bounds, 553, 557, 589
Bergman bounds, 581
Bergman-Milton bounds, 452, 478, 569, 577
bimetal strip argument, 79
bimode materials, 654, 663, 667
Bloch waves, 223, 231
Bloch's theorem, 223
block-tridiagonal matrices, 632
bones, 5
boundary integral equation, 39
bounds
  and quasiconvexification, 677
  arithmetic mean, 273, 426, 437, 469, 500, 557, 574, 606, 639
  assemblages, 458
  attainability criteria, 535–543
  average fields, 426, 444, 499, 529, 530
  bulk modulus, 470, 471, 500, 504, 542
  bulk modulus type, 470, 471, 473
  comparison, 500, 503, 509, 535
  complex conductivity, 575, 581, 587, 591, 639
complex dielectric constant, 450, 476, 569, 570
complex elastic moduli, 478
conductivity-elasticity, 522, 542
correlating function values, 579, 589, 607, 614
correlating moduli, 522
correlating quantities, 428, 587
correlation function dependent, 458, 465, 476, 490, 499, 553–564, 574, 577, 586
cross-property, 458, 522, 561, 580, 587, 607, 614
cylinder suspensions, 429
effective tensor, 468
elastic energy, 465
elasticity tensor, 470, 471
energy, 499, 518, 531, 677
examples, 426
field variance, 346
harmonic mean, 273, 426, 437, 469, 500, 557, 574, 606, 639
hierarchy, 569, 603
incompressible two-phase media, 472
interdependence, 589
mixed, 519
multiphase conductivity, 437, 457, 638

multiphase elasticity, 472, 473
non-well-ordered materials, 473, 474
nonlinear composites, 286, 530
numerical computation, 583
Poisson's ratio, 653
polarizability, 188
polycrystal conductivity, 426, 439, 480, 489, 569, 646
polycrystal elasticity, 441, 490, 500, 536
polycrystal energy, 426
Reuss-Hill, 444
series expansion dependent, 573, 579, 586, 589, 603
shear modulus, 470, 471, 473, 502
shear modulus type, 470–473
sums of energies, 468, 505, 519, 544, 647, 679
trace, 473, 474, 476, 509, 518
translation, 500, 503, 504, 509, 530, 531
two-dimensional conductivity, 446, 481, 585
two-phase conductivity, 458, 481, 506, 520, 542, 554, 564, 569–596, 603–617
two-phase elasticity, 465, 470, 473, 542, 557, 558, 569
types I–IV, 571
using quasiconformal mappings, 480
utility, 425
via fractional linear transformations, 603–617
viscoelasticity, 452, 478, 583
Voigt-Hill, 442
Voigt-Reuss, 442
volume fraction, 569
well-ordered materials, 462
y-parameters, 478, 524, 556–558, 560
Y-tensor, 411, 475, 516, 519, 563, 564, 641
Brownian motion simulations, 40
Bruggeman's unsymmetrical effective medium theory, 201
Bruno bounds, 569
bubbly fluid, 3, 89
bulk modulus κ, 23

Cauchy integral formula, 376, 381, 605, 615
Cauchy sequence, 299
Cauchy-Schwartz inequality, 505
cell materials, 320, 331–333, 553, 586
cell polycrystals, 322, 335, 487
cell problem, 10
cell shape parameters, 322, 331, 332, 334, 553
cellular materials, *see* perforated structures
chain property, 366
characteristic functions, 49
characteristic polynomial, 107
chattering sequences, 430
checkerboard
conductivity, 49, 207, 377
elasticity, 207
magnetotransport, 65
nonlinear, 282
random, 207, 586
three-dimensional, 207
see also symmetric materials
Cherkaev-Gibiansky transformation, 234, 450, 476
Cherkaev-Gibiansky variational principles, 276, 639
classical energy minimization principle, 273, 282, 659
classical variational principles, 271, 403, 571
Clausius-Mossotti formula, *see* Maxwell formula
CLM theorem, 66
coarse graining, 212
coated ellipsoids, *see* ellipsoid assemblages
coated laminates, *see* laminates, coated
coated spheres, *see* sphere assemblages
coercivity condition, 300
coherent potential approximation, *see* effective medium approximation
columnar microstructures, *see* fibrous composites
comparison bound, 500, 503, 509
attainability, 535
compensated compactness bound, 530
compensated compactness method, 275, 499–525, 529–550
compensating terms, 325
complementary classical variational inequality, 283
complementary energy minimization principle, 273, 284, 660
complex conductivity equations, 227
complex dielectric constant, 3, 224
complex dielectric tensor, 224
complex elasticity tensor, 231
complex equations and thermoelectricity, 237
complex equations reformulated, 234
complex magnetic permeability tensor, 224
complex permittivity, *see* complex dielectric constant
complex-valued tensors, 295
compliance tensor, 23, 371
composite not mimicked by a laminate, 690
composites
examples, 1
extremal, 652
optimal, 5, 177, 469, 481

random, 11, 315
concentration factor tensors, 405
conductivity
cream, 194
equations, 19, 40
fibrous composites, 33, 87
fused glass beads, 202
hopping, 211
tensor, 5
tensors, nonsymmetric, 22
conductivity function, 383
classification, 571
degree, 385
eliminating values, 607
types, 571
conductivity threshold, 196
conformal transformations, 143
constant shear modulus materials, 77
constitutive relation, 5, 23
constitutive relation, reduced, 52
continued fraction expansions, 384, 397, 406, 607, 610, 619
convection enhanced diffusion, *see* magnetotransport
convex functions, 283, 672
convexification, 673
correlation functions, 313–335
one-point, 315
two-point, 315
three-point, 314, 319, 553
four-point, 318, 320
cell materials, 320
geometrical interpretation, 317
penetrable spheres, 319
polycrystals, 318
reduced, 323, 328
symmetry properties, 317
correspondence principle, 233
coupled equations, 28, 35, 93, 237, 264, 342, 356, 362
two-dimensional, 101
covariance property
effective tensor, 94, 356
fundamental matrix, 104
Cramer's rule, 596
critical exponents, 211
cross-property bounds, 458, 522, 561, 580, 587, 607, 614
cross-property relations, 80, 355
curvature tensor, 27
curvilinear transformation, 149, 297
cylinder arrays, 39, 116, 241, 333, 377, 390, 429, 575, 590
cylinder assemblages, 116, 429, 501, 570, 588
cylinder suspension, 429, 586

Darcy's law, 6
dead-leaves model, 332
decoupling transformation, 95, 97, 580
defect compliance tensor, 69
demagnetizing factors, *see* depolarizing factors
depolarization tensors, 129, 255
depolarizing factors, 128, 132, 187
dielectric equations, *see* conductivity, equations
differential approximation, *see* differential scheme
differential constraints, 5, 249
differential scheme
attractor, 203
conductivity, 201
elasticity, 206, 471
generalized, 177, 203
realizability, 202
diffusion equations, *see* conductivity, equations
dilute suspension
dielectric constant, 188–195
elastic moduli, 256
ellipsoids, 252
dimension reduction, 20, 297
dipole moment, 185, 188
Dirichlet problem, 481
displacement field, 22
Drude model, 224
duality
conductivity, 47, 356
elasticity, 51, 53
magnetotransport, 51
nonlinear conductivity, 47
principle, 262, 398, 407
pyroelectricity, 51
transformation, 48, 60, 212

eddy currents, 39
effective conductivity tensor, 6
effective constitutive relation, 6
effective dielectric constant, 191
effective dielectric tensor, 188
effective medium approximation
as attractor, 203
conductivity, 195
elasticity, 204, 256
ellipsoidal grains, 256
polycrystals, 197
realizability, 196
y-parameters, 397
effective tensor
adjoint equation, 263
analytic properties, 369–391
generalized, 260
monotonicity, 274
resistor network, 418
series expansions, 291–309, 313–335
solutions for, 261
eigenstress, 31, 405
eigenstress concentration factor tensors, 405
Einstein summation convention, 313
elastic energy minimizing hole, 467
elastic moduli
fibrous composites, 25, 26, 35, 86
elastic waves, 230–233
elasticity
analyticity, 371
equations, 22
nonlinear, 22, 87, 671
planar, antiplane link, 105
tensor, 22
two-dimensional, 24
elasticity as coupled equations, 98
electrical circuits
active network, 415

passive network, 415
see also resistor network
electrical conductivity equations, *see* conductivity, equations
electrochemical potential, 28
electromagnetic signal propagation, 228
electromagnetic waves, 222–230
electrostatic resonances, *see* resonances, electrostatic
ellipsoid assemblages
conductivity, 124, 129, 144, 148, 377, 462, 570
elasticity, 130, 467
ellipsoid suspension, 252
ellipsoidal coordinates, 124
ellipticity condition, 9, 298
embedding, 355, 505, 510, 520
energy functions, 381
energy sum as single energy, 650
ensemble average, 12
entropy, 31
equiaxed polycrystal, 489
equivalent inclusions, 240
equivalent media, 59
Eshelby's solution, 252
Euler-Lagrange equation, 282
exact relations, 75–110, 304, 332, 355–366
candidates for, 358
limited statistics, 363
necessary conditions, 357, 365
sufficient conditions, 359
exactly solvable geometries, 113–181, 295
extended fields, 506, 508, 544, 547, 644
extremal composites, 652
extremal materials, 658, 663
extremal translations, 532, 545

fast Fourier transform, 40
fast multipole method, 39, 331
fast variable, 8
fibrous composites, 25, 33, 35, 86, 87, 97, 102
field decomposition, 248
field equation recursion method, 619–641
fields
distributions, 346
series expansions, 291–309
solutions for, 261, 298
uniqueness, 299
variance, 344
fields in terms of analytic functions, 106
finite difference scheme, 40
finite element methods, 40
Floquet's theorem, 223
flow in porous media equations, *see* conductivity, equations
fluid suspensions, bulk modulus, 88
fluidity threshold, 204
Fourier methods, 40
fractional linear transformations, *see* transformations, fractional linear
Francfort-Murat formula, 174
fundamental matrix, 103

G-convergence, 12
G-closure, 429, 643, 679, 683, 690
characterization, 520, 647, 650, 679
constant volume fraction, 431, 462, 508, 643
convexity properties, 645
three-dimensional conductivity, 450, 521
two-dimensional conductivity, 446, 521
Γ-operators, 245, 247, 250, 257, 314
conductivity, 161, 189
elasticity, 168, 174
piezoelectricity, 170
representation, 631
thermoelasticity, 170
thermoelectricity, 170
Γ-convergence, 12
Γ-realizing sequence, 14
gap resistance, 209
Gassman equations, 86
Gaussian random field, 331, 556, 558
geometric isotropy, 327
geometric parameter η_1, 330–333, 553, 557
geometric parameter ζ_1, 329–333, 398, 553, 555, 557, 574, 577, 586
geometrical isotropy, 294, 333, 488, 564
Gibiansky-Cherkaev energy bounds, 466
Gibiansky-Cherkaev formulas, 174, 175
Gibiansky-Sigmund microstructures, 460
Gibiansky-Torquato bounds, 522
Golden-Papanicolaou bounds, 451, 639
group velocity, 228

H-convergence, 12
H-measures, 293, 295, 327
Hall coefficient, 21, 60, 344
Hashin coated spheres, *see* sphere assemblages
Hashin formula, 84
Hashin-Shtrikman bounds, 116, 207, 282, 347, 399, 458, 460, 470–472, 480, 481, 487, 489, 501, 507–509, 542, 556, 558, 569, 574, 577, 590
realizability, 206
Hashin-Shtrikman coated spheres, *see* sphere assemblages
Hashin-Shtrikman formula, 115, 239
Hashin-Shtrikman variational principles, 140, 181, 216, 271, 278–283, 285, 287, 309, 353, 409, 410, 457, 461, 462, 466, 488, 491, 493, 513, 518, 519, 542, 571, 598
Hashin-Shtrikman-Hill bounds, 505, 542, 558
Hashin-Shtrikman-Hill-Walpole

bounds, 558
Hashin-Shtrikman-Walpole bounds, 505, 512
heat equation, 22
heat lens problem, 432
Helmholtz decomposition, 248
Herglotz property, 374, 385, 612, 614, 616, 619
hexamode materials, 654
high-contrast media, 40, 207
Hilbert space decomposition, 248
Hill bounds, 471, 473, 505, 542, 558
Hill relations, 87
Hill's formula, 78, 332, 356, 364
homogeneity property, 8, 212, 345, 372, 612, 614, 619
homogenization
  Bloch wave, 221
  G-convergence, 12
  Γ-convergence, 12
  H-convergence, 12
  higher order, 10
  intuitive viewpoint, 7
  nonlinear elasticity, 14
  periodic, 8
  random media, 11
  stability under, 359, 365, 544
hopping conductivity, 211
hyperbolic segment, Hyp$[(w_1, w_2)]$, 524

imperfect interface, 134
incidence matrix, 413
infinite volume limit, 12
infinitely interchangeable materials, 322
inner product, 248, 299
integral equation, 39
integral representations, 346, 375, 387, 391, 605, 615, 616
interphase region, 134
iterated dilute limit approximation, 201

Jacobian, 595

K-quasiconformal mappings, 152
Kapitza resistance, 134
Keller's relation, 48, 573, 585
Khachaturyan's solution, 252
Kirchoff's law, 415
Kohn-Strang algorithm, 680
Korn inequalities, 101
Kramers-Kronig relations, 592

Lagrange multiplier, 531
Lagrangian, null, 67, 274, 503, 507, 513, 516, 530, 533, 546, 672, 691
Λ-connected, 676, 693
Λ-convexification, 679
Λ-convexity, 676, 693
Lame modulus λ, 23
laminate fields, 673, 683
laminates, 159–181
  coated, 165, 171, 173, 256, 294, 462, 463, 467, 471
  conductivity, 162, 165, 174, 382, 570, 572
  cyclic, 537, 540, 541, 683
  elasticity, 163, 167, 174, 471
  general formula, 164, 172, 645, 646
  herringbone, 653, 660, 661
  infinite-rank, 471, 537
  mimicking ellipsoids, 256
  multicoated, 383
  multiple-rank, 159, 164, 544
  oblique box, 658, 659
  optimal, 351
  ordinary differential, 175
  partial differential, 177
  perturbing lamination directions, 351
  piezoelectricity, 167
  randomly generated, 537
  signal propagation, 229
  thermoelectricity, 97, 167
  Y-tensor, 407
lamination closure, 679, 690
lamination closure and Λ-convexification, 679
lamination trajectories, 544
lamination, stability under, 357, 645, 647
Laplace equation
  solution in terms of analytic functions, 110
layered material, *see* laminates
Legendre polynomials, 328, 330
Legendre transforms, 236, 283, 531, 647, 650
lens-shaped region, 576, 603
Levin formula, 80
linear elasticity, *see* elasticity
linear programming, 591
linkage array
  diamond lattice, 666, 667
  honeycomb, 655, 666
  inverted honeycomb, 656, 666
Lippmann-Schwinger equation, 251
Lipton bounds, 473
local averaging, 7
local field, 189
Lorenz-Lorentz formula, *see* Maxwell formula
Lurie-Cherkaev bounds, 347, 462, 508, 521

macroscale, 7
magnetism equations, *see* conductivity, equations
magnetoelectric effect, 4, 30
magnetostrictive materials, 4, 30, 97
magnetotransport, 21, 33, 51, 124
  relation to conductivity, 33, 87, 344
  relation to thermoelectricity, 264
Maxwell formula, 192–194, 239, 243, 306, 457
Maxwell's equations, 222
Maxwell-Garnett formula, *see* Maxwell formula
McCoy bounds, 553, 557
mean-field formula, 6
measure $\boldsymbol{\mu}$, 376, 388, 391
  constraints on, 379, 389, 604
mechanical stress concentration factor tensor, 405
mesoscale, 7

microlocal defect measures, 293
microscale, 7
microstructure reconstruction, 425
microstructure-independent relations, *see* exact relations
Milgrom-Shtrikman relation, 96
minimizing sequence, 282
moments of measure $\boldsymbol{\mu}(y)$, 379
momentum conservation, 230
monotone function, 309
monotonicity of effective tensor, 274
Mortola-Steffé conjecture, 154
multigrid methods, 40
multiple-scale analysis, 10
Murat-Tartar bounds, 347, 462, 508, 521

nearly touching inclusions, 40, 209
negative Poisson's ratio material, 2, 4, 652, 660, 661
Nesi bound, 480, 646
neutral inclusion assemblage, 136, 138
neutral inclusions, 134, 240
neutral surface, 26
nonlinear elasticity, 22, 87
nonlinear thermal expansion, 81
nonlinear variational inequalities, 282
norm of field, 248
norm of linear operator, 299
normalization condition, 650
normalization factors, 611
normalization matrix, 423, 616, 630
normalization property, 374, 385, 614, 619
normalization transformation, 413, 612, 614, 617, 627
normalizing function, 259, 324
null Lagrangian, 67, 274, 503, 507, 513, 516, 530, 533, 546, 672, 691
nullmode materials, 654
numerical methods, 38, 306

Onsager's principle, 28
opals, 3
operator representations, 631
optimal composites, *see* composites, optimal
optimization
  average temperature, 430
  elastic energy, 432
  heat flow, 432
  nonconvex, 430
  plate elasticity, 432
  structural, 425, 429, 446
  torsional rigidity, 432

Padé approximants, 571, 578, 590
pair correlation function, 191
partial differential microstructures, 181
penetrable disk model, 320, 333, 586
penetrable sphere model, 319, 331, 554
pentamode materials, 654, 666
percolation threshold, 196, 205, 211
perforated structures, 11
periodic homogenization, *see* homogenization, periodic
perturbation solutions
  nonlinear media, 308
  other, 341–352
  see also series expansions
phase boundary shift, 347
phase interchange identities
  conductivity, 49, 118, 385
  elasticity, 53, 57, 70
  piezoelectricity, 102
phase interchange inequalities
  conductivity, 120
  elasticity, 70
phase transitions, 672
phase velocity, 228
piezoelectricity
  bounds, 490
  equations, 28, 342
  relation to elasticity, 35
  see also coupled equations
piezoelectrics, 4, 29, 96
plane strain, 25, 37
plane stress, 25
plate equations
  bending, 26, 466
  conductivity, 20
plate with holes, 40, 66, 67
Poisson's equation, 189
Poisson's ratio, ν, 23, 68, 213, 652
polarizability
  bounds, 188
  circle pairs, 188
  crystal sphere, 187
  elastic, 188, 191, 254
  ellipse, 187
  hole, 188
  inclusion, 185, 188
  nonlinear, 242
  piezoelectric, 255
  poroelastic, 255
  sphere, 187
  sphere pairs, 187, 191
  tensor, 186
polarization charge density, 188
polarization field, 145, 171, 186, 457
  equation for, 251
pole and residue variation method, 590
pole and zero variation method, 592
pole lines, 390
Pólya-Szegő matrix, *see* polarizability tensor
polyconvex functions, 672
polyconvexification, 673
polycrystals
  analyticity, 371
  bulk modulus, 69, 76
  cell, 322, 335, 487
  conductivity, 50, 387, 619
  conductivity bounds, 426, 439, 446, 450, 489, 510, 569, 646
  conductivity maximizing, 439
  conductivity minimizing, 512, 537
  correlation functions, 318

effective medium approximation, 197
elasticity, 99
elasticity bounds, 441, 490, 500, 536
equiaxed, 489
Hall coefficient, 60
piezoelectricity bounds, 490
plasticity, 682
series expansions, 335
shear modulus, 55, 56, 69, 361
sphere assemblage, 121
thermoelasticity, 83
polydisk representation formula, 389
polynomial applied field, 254
Ponte Castañeda bounds, 285
poroelasticity, 30, 84
see also thermoelasticity
Postma formulas, 163
power dissipation, 225, 232
Prager bounds, 580
product properties, 4, 30
projections, $\mathbf{\Lambda}_h$, $\mathbf{\Lambda}_s$, 371, 469
pyroelectric effect, 5
pyroelectric equations, 33, 51
pyroelectricity, relation to conductivity, 33, 87

quadramode materials, 654, 666
quasiconformal mappings, 152, 480
quasiconvex function, 529, 671
quasiconvex hulls, 681
quasiconvex tensors, 302
quasiconvex translations, 503
quasiconvexification, 671–695
generalization, 676
quasiconvexity, 359
conditions for, 673, 677, 690
quasiconvexity test, 503, 513
quasistatic limit, 221, 370, 569

Radon transforms, 327
random media, 11, 315
rank constancy assumption, 250
rank-1 connected, 673
rank-1 convex, 673
rank-1 convex function not quasiconvex, 684
rank-1 convex hull not quasiconvex, 688
rank-1 convex hulls, 681, 683
rank-1 convexification, 673, 679
rank-1 positivity, 504
rank-1 tensor fluctuations, 77
rational approximants, 571
Rayleigh's method, 39
recoverable deformations, 682
reduced correlation functions, 323, 328
reference tensor, 171, 278, 457
reference transformations, 172
reflection transformation, 447
relaxations, partial, 433
relaxed problem, 431
renormalization group theory, 212
representation formulas, 370, 375, 382
representations of operators, 631
resistance, gap, 209
resistivity tensor, 21
resistor network, 40, 197, 209, 370, 377, 413
effective tensor, 418
resonances
electrostatic, 39, 238, 381
localized, 238
resonant solutions, 380
Reuss-Hill bound, 444, 487
Ricatti equation, 121, 127, 176
rigidity threshold, 205
Rosen-Hashin formulas, 80, 81, 83
ruled surface, 516

saddle-point variational principles, 277
Schulgasser formula, 84
Schulgasser inequality, 120
Schulgasser sphere assemblage, 121, 512
Schulgasser-type circle assemblage, 502, 537
Schur complement, 236
sea ice, 1, 569
seed material, 540, 683
self-consistency assumption, 196, 198
self-consistent estimates, 198
series expansions
bounds incorporating, 573, 579, 586, 589, 603
conductivity, 329, 335, 586
convergence, 298–306
correlation functions, 313–335
elasticity, 330, 331
eliminating terms, 603, 610
numerical computation, 306
second-order, 292
thermoelasticity, 294
truncated, 306
with fast convergence, 302–309
shape factors, *see* cell shape parameters
shape memory materials, 671, 682
shear matrix $\boldsymbol{\mu}$, 38
shear modulus μ , 23
shear viscosity, 2, 19, 234
Sigmund microstructures, 485, 486
single oscillator model, 224, 369
slow variable, 8
sound waves, *see* acoustic waves, *see* elastic waves
spaces $\mathcal{E}_{\boldsymbol{k}}$, $\mathcal{J}_{\boldsymbol{k}}$, and $\mathcal{T}$, 246
specific heat
constant strain, 31
constant stress, 31, 79, 82
spectral broadening, 239
spectral measure, 380
sphere arrays, 2, 39, 208, 331, 377, 558, 571, 575, 576
sphere assemblages, 134, 166, 238, 239
bulk modulus, 116, 471, 473, 525, 558
bulk viscosity, 233
conductivity, 115, 144, 194, 330, 350, 459, 525, 558, 570, 572
multicoated, 117, 460
Schulgasser's, 121
shear modulus, 205, 472
thermoelectricity, 97

sphere suspension, 2, 189–194, 256, 331, 377, 555, 558
spheroid suspension, 205
spring network, 40, 197
stability under homogenization, 359, 365, 544
stability under lamination, 357, 645, 647
Stieltjes functions, 379, 380, 571, 573, 603
strain field, 22
stress field, 22
stress invariance, 66
structural hierarchy, 5
structural optimization, 425, 429, 446
subspace collections, 406, 619, 626
  and analytic functions, 619, 624
  operations on, 620
sum rules, 379
supertensor, 506, 644
suspension of ellipsoids, *see* ellipsoid suspension
suspension of spheres, *see* sphere suspension
suspension, dilute, *see* dilute suspension
Šverák's example, 673, 684, 690
swelling due to humidity, 81
Swiss cheese models, 213
symmetric materials, 49, 55, 69, 102, 123, 573, 588
Szẽgo kernel, 389

Talbot-Willis variational inequality, 285, 286
Tartar's formula, 165, 174, 177
tendons, 5
tensorial properties, 99
thermal conduction equations, *see* conductivity, equations
thermal expansion
  negative, 3
  nonlinear, 81
  tensor, 30, 79, 82
thermal expansion coefficient
  link with bulk modulus, 80
thermoelastic-type problem, 33, 86, 509, 643, 678
thermoelasticity
  equations, 30, 356, 364
  relation to elasticity, 35
  relation to Y-tensor, 403
  series expansions, 294
thermoelectric
  equations, 28, 237, 342
  figure of merit, 97
  power factor, 4, 97, 580
thermoelectric coefficients, 96
thermoelectricity
  relation to complex conductivity, 237
  relation to magnetotransport, 264
  see also coupled equations
thin films, conductivity, 20
threshold
  conductivity, 196, 207
  fluidity, 204
  percolation, 196, 205
  rigidity, 205
tie line, 516
touching spheres, 210
trace bounds, 473, 474, 476, 509, 518
trajectory method, 387
transformations
  affine, 145, 327
  Cherkaev and Gibiansky's, 234
  curvilinear, 149, 297
  decoupling, 95, 97, 580
  fractional linear, 59, 63, 102, 413, 603–617, 619
  Legendre, 236
  normalization, 413, 612, 614, 617, 627
  quasiconformal, 152
  reference, 172
  reflection, 447
  Y, 398, 611, 614, 627
translation bound, 500, 503, 504, 509, 530, 531
  attainability, 541
  nonlinear, 531
translation method, 462, 466, 499–525, 529–550, 560
translations, 59–70, 373
  as exact relations, 356
  conductivity, 65, 506, 510, 545
  coupled equations, 97, 100
  elasticity, 66, 500, 504, 547
  extremal, 532, 545
  finding them, 544
  geometrical characterization, 512, 532
  one negative eigenvalue, 513
  quasiconvex, 503, 647
  quasiconvexity test, 503, 513
trimode materials, 654, 667
twinned microstructure, 672
two-phase media
  conductivity bound, 458, 460, 461, 481, 506, 520, 542, 554, 564, 569–596, 603–617
  elastic energy bounds, 465
  elastic moduli bounds, 470, 471, 500, 504, 542, 557, 558, 569
  Hall coefficient, 61
  specific heat, 81, 83
  thermal expansion coefficient, 80
  thermal expansion tensor, 82
  thermoelectric coefficients, 96
  Y-tensor, 397

uniform field relations, 75, 144, 361
unimode materials, 654, 658, 667
universality, 211

Vandermonde determinant, 96
variance of fields, 344
Vigdergauz microstructure, 467, 484, 486
viscoelasticity, 230
Voigt-Hill bound, 442, 487
Voigt-Reuss bounds, 442, 487

Walpole bounds, 473, 505, 558
wavelength, 226, 228

waves, elastic, *see* elastic waves
waves, electromagnetic, *see* electromagnetic waves
weak convergence, 10
weak limit, 11
weakly continuous bilinear forms, 276
weakly continuous functions, 275
weakly coupled equations, 342
wedge bounds, 374, 375, 575, 639
weight matrices, 615, 628, 634
weights, 611
well-ordered materials, 462
well-separated distributions, 191
well-separated spheres, 189, 205
well-stirred distributions, 191
Wheatstone bridge, 413
Wiener bounds, 487, 574, 577, 590, 601
Willis bounds, 464
Wood's formula, 89
Wulff shape, 489

y-parameter
  y_κ, 523, 557
  y_μ, 523, 557
  y_σ, 399, 556
Y-tensor, 397–411, 413–423, 556, 627, 630, 638
  bounds, 411, 475, 516, 519, 563, 564, 641
  electrical circuit, 417
  formula for, 406
  laminates, 407
  multiphase media, 399
  polarization problem, 408
  problem, 401, 406
  two-phase media, 397
  variational principle, 401
Y-transformation, 398, 611, 614, 627
yield surface bounds, 682
Young's measure, 677, 687
Young's modulus, E, 23, 66, 68

zero lines, 390